SILICA FUME CONCRETE IN HOT AND TEMPERATE ENVIRONMENTS

By

AZMI SAMI SAID AL-EESA, B.Sc., M.Sc.

A Thesis submitted in accordance

with the requirements for the degree of

DOCTOR OF PHILOSOPHY

Department of Civil Engineering

Loughborough University of Technology

May 1990

بسم الله الرحمن الرحيم

" وقل ربي زدني علما "

(صدق الله العظيم)

IN THE NAME OF GOD, THE MERCIFUL AND THE BENEFICIAL

"AND SAY, MY LORD; INCREASE MY KNOWLEDGE"

(THE HOLY QURAN)

الاهـــداء

الى كل من بذل الدم الزكي دفاعا عن ارض وعراق العراق العظيم

الى زوجتي التي منحتني الدعم و العون

الى ابنائي الاعزاء احمد و مصطفى الذين اعطو الحياة معاني كثيرة

الى ابي و امي الذين وهبوني الحياة و الدعم

DEDICATION

I wish to dedicate this work to:

the memory of all the Iraqi martyrs who sacrificed themselves for the sake of our great country;

my faithful wife who continues to give me love, support and encouragement;

my sons Ahmad and Mustafa who have given more meaning to life; and

my father and mother who gave me all the support and encouragement throughout my life.

ABSTRACT

This investigation deals with the influence of hot and temperate curing environments on the hardened properties of concrete and mortar mixes. Condensed silica fume was blended with OPC as a potential alternative cementitious material to plain OPC for use in the hot Iraqi climate, in an attempt to find a cement combination that would overcome some of the durability problems experienced when using a plain OPC concrete in such an environment. Throughout the investigation two curing environments were used: the first simulating the UK temperate climate and the second simulating the hot Iraqi climate. Temperature and humidity were varied to simulate day and night time.

The first stage of the experimental study was the development of a mix design method capable of producing an OPC-CSF cement concrete of a medium workability and a specific 28-days compressive strength ranging between 25 to 55 MPa, both with and without superplasticizer. Three grades of concrete strength were chosen (25, 40 and 55 MPa) and the effect of four cement replacement levels (5, 10, 15 and 20%) of silica fume on concrete compressive strength was assessed. Test results showed that CSF was relatively more effective in lean mixes than in rich ones. Compressive strength of CSF concrete increased with increasing CSF percentages for both normal and superplasticized mixes up to an optimum levels of 10-15% and 15-20%, respectively. The amount of OPC (kg/m^3) necessary to bring a change in compressive strength of 1MPa was also determined and the theoritical blend proportions of OPC-CSF necessary to produce 28-day compressive strength equivalent to the plain OPC mixes were determined from the produced data above. The theoretical blend proportions were examined experimentally and the data were used to establish the relationship between strength and water/cementitious ratio for the blend mixes with and without superplasticizer. Results showed that this basic relationship had changed quantitatively but not qualitatively when CSF was used. A

cost study using current OPC and CSF material costs was performed in an attempt to determine the most economic blend proportions.

A total of eleven different concrete mixes were selected to study the effect of curing environment (hot and temperate), initial curing time (0, 1, 3 and 7 days) and curing method (water and polythene sheeting) on the compressive strength, permeability and absorption properties of the CSF concretes. Tests were carried out at 3, 7, 14, 28, 56, 90 and 180 days of age. In addition five different mortar mixes were used to examine the effect of curing environment (temperate and hot) on the permeability, pore size distribution and durability to magnesium sulphate attack.

Test results showed that hot Iraqi curing environment was favourable to the early-age strength, absorption and permeability of plain OPC mixes. However, the later-age properties were significantly lower than those obtained for concretes cured in a temperate UK environment. The early and later-age strength and more importantly the permeability, absorption and durability properties of CSF mixes were all improved by the hotter curing environment. Consequently, the later age permeability and absorption of CSF mixes were much lower than the plain OPC ones, and the strength and durability properties of CSF mixes were all higher. The improvement in compressive strength and durability and the reduction in permeability and absorption properties of CSF mixes increased with increasing CSF percentages.

The effect of curing time under both temperate and hot climate on the compressive strength, permeability and absorption properties helps to define the critical curing period (period beyond which effects on hardened properties become insignificant) for both plain OPC and CSF mixes. This critical curing period seems to depend on the type of cement as well as the curing environment. For plain OPC mixes a critical curing period of 3 days was found under both temperate and hot environment. For the CSF blend mixes critical curing periods for the temperate and hot environment

were found to be 3 and 1 day respectively. Results also reveal the importance of curing specimens immediately after casting for one day. Research work has also confirmed the superiority of water curing over polythene sheeting in a temperate environment for the rich plain OPC and CSF mixes. However, there was no significant difference between water and polythene for lean mixes.

The reduction in permeability and absorption properties of CSF mixes cured in a both temperate and hot environments is thought to be due to the changes in the pore structure brought about by the use of silica fume. Combining CSF with OPC was found to increase the percentages and volume of fine pores at the expense of coarse pores. This effect may be described as a "refining" effect.

Finally, the performance of CSF mortar mixes cured in a temperate and hot environment and their resistance to magnesium sulphate attack was significantly better than the plain OPC ones.

CONTENTS

ACKNOWLEDGEMENTS

The author would like to express his sincere appreciation to his supervisors, Dr S. Austin and Dr P. Robins, for their advice, continuous support and encouragement throughout the duration of research.

The author also wishes to thank the technical staff of the Department of Civil Engineering.

Grateful thanks are also extended for the financial support provided by the Iraqi Government.

The author extends his appreciation to Mrs Eileen Kearins for her excellent standard of typing.

Finally, the author would like to recognise with deep appreciation the understanding and encouragement given by his wife during the course of his study.

ABBREVIATIONS

OPC	Ordinary Portland Cement
CSF	Condensed silica fume
C_3S	Tricalcium silicate
C_2S	Dicalcium silicate
C_3A	Tricalcium aluminate
C_4AF	Tetracalcium aluminoferrite
C-S-H	Calcium silicate hydrate
$CaSO_4.H_2O$	Gypsum
$C_3A.3CSH_{32}$	Ettringite
$3C_3A.CSH_{12}$	Monosulphate
M = MgO	Magnesium Oxide
C = CaO	Calcium Oxide
S = SiO_2	Silicon Dioxide
A = Al_2O_3	Aluminium Oxide
F = Fe_2O_3	Ferric Oxide
Na = Na_2O	Sodium Oxide
K = K_2O	Potassium Oxide
H = H_2O	Water
$MgSO_4.7H_2O$	Magnesium Sulphate
W/C	Water/Cement Ratio
W/C+CSF	Water/Cement + Condensed Silica Fume) ratio
μ	Micrometre 1 x 10^{-6}

CHAPTER ONE
INTRODUCTION

1.1 General

Concrete is one of the most common construction materials due to its low cost and wide range of applications.However, in Iraq it has often been used without imposing suitable standards for quality control. Many small concrete structures have been built without imposing limits on water/cement ratio, cement content or workability. Reinforcing steel which had already been corroded after being left exposed for long periods has often been used. Most importantly, curing has often been overlooked by contractors who paid little attention to it and budgeted small amounts of the total contract value for it. In Iraq, as well as the other Middle Eastern Countries, there are two aspects of the environment from which concrete deterioration can arise: these are the climate and the geology. As far as the latter is concerned, a complex variety of salts exist in both soils and ground water. The principal chemical compounds involved are calcium, magnesium and sodium sulphates and chlorides. The presence of these harmful salts can cause two problems:external attack of concrete elements in contact with them, and internal attack arising from contamination of the aggregate, mix water or on the reinforcment. As far as the climate is concerned high temperatures and low humidities can accelerate the rate of water evaporation and drying of fresh mixes at early ages which in turn can adversely affect the strength and durability properties of the mature concrete. Therefore, strength, durability and other characteristics are critically dependent on the curing after the concrete has been placed and compacted and during the first few days following casting.

The Iraqi environment problem is, however, more complex in the situation of substructure concrete elements. Due to the concurrent presence of high chloride and sulphate levels in the soils and ground water. In such a situation the use of sulphate resistant cement (low C_3A content)

usually provides adequate protection against sulphate attack, but would not significantly reduce the corrosion of steel due to chlorides.

The use of pozzolans such as pulverized fuel ash (PFA) as a cementitious material is quite common in Europe and America. However, there is an increasing interest in the use of condensed silica fume (CSF) as a partial cementitious replacement material. Research shows that with the use of CSF under temperate environment conditions, many aspects of concrete can be favourably influenced, some by physical effects associated with the very fine particle sizes, and others by the pozzolanic reaction. The rate and extent of hydration are among the physical effects associated with the particle sizes of pozzolans. Strength, permeability, resistance to alkali silica expansion and sulphate attack are the main properties associated with the pozzolanic and cementitious reactions. However, the performance and behaviour of CSF concrete and mortar mixes under severe curing environments (hot and dry) compared to the cooler temperate curing environments has not been investigated thoroughly.

Durability of concrete is not an intrinsic property of concrete and therefore it is not easy to define or measure. Broadly speaking durability is an attribute of concrete which is related to its ability to resist attack from the environment in which it is placed, to maintain its appearance and to continue to function in the manner for which it was designed. Deleterious attacks from the environment need fluids either as a transport means or as a reaction medium. Since permeability and absorption can affect and control the rate and the degree of ingress of fluids and ions, they have an important bearing on the durability and the vulnerability of concrete to different kinds of attack. Accordingly a great deal of emphasis had been paid in this research work on measuring permeability and absorption. Previous experience and research work shows that concrete surfaces are considered the most vulnerable and weakest part of concrete since many types of attack (mechanical and chemical) start from the

surface. Therefore it is vital for concrete durability to have a sound surface with low permeability characteristics.

Recently, more attention has been paid to the use and development of non-destructuve permeability and absorption test methods which can be used for assessing durability. These tests do not give an absolute value for permeability but rather time and rate of flow and absorption. None of these parameters can easily be converted to a true intrinsic permeability value. However, it seems reasonable to expect that these parameters can be related to durability, although there is at present very limited data available on these test methods. Since they have the advantage of assessing the concrete surface ("surfacecrete") and concrete subsurface ("subsurfacecrete") permeability and absorption properties, efforts were made in this research work to use these non-destructive absorption and permeability tests for assessing durability. The major problem associated with these test methods which can limit their usefulness and make comparison difficult is the moisture content of tested specimens. This is because moisture can affect the permeability of concrete and mortars by blocking the capillary pores as the degree of saturation increases. Consequently concrete specimens used in this research work were conditioned by oven drying to a constant weight, (0.1% change in weight over 24 hours of drying). In addition, tests for true air and water permeability together with the pore size distribution were conducted on mortar specimens.

Permeability of concretes, mortars and pastes is not a simple function of their bulk porosity but depends also on the size, distribution and the continuity of pores. Therefore it is the pore size distribution, the volume of the harmful capillary coarse pores available and the importance of eliminating continuous pores are more important in relation to the control of permeability other than the total porosity. Further more total porosity cannot describe pore characteristics since at the same strength it may vary widely. This reveals that distribution of the pores rather

than the total porosity which would have an important role on the strength of concrete and mortar mixes.

1.2 Aims of the research

There are seven aims in this research.

1. To review the current state of knowledge on silica fume modified concrete and concreting in hot climates.
2. Hence to design a cohesive experimental programme that targets areas requiring further research work.
3. To produce a mix design method capable of producing plain OPC and OPC-CSF concrete mixes with equivalent medium workability and compressive strength at 28-days of age.
4. To study the effect of age, curing methods (water and polythene sheeting), temperate and hot environment, condensed silica fume content, initial curing duration and the use of superplasticizer on the absorption and permeability properties of plain OPC and OPC-CSF concrete mixes with equivalent 28 day compressive strength by means of five non-destructive test methods. These tests are Figg air and water permeability, Egg air permeability, Initial Surface Absorption and water absorption at 30 minutes.
5. To study the effect of age, temperate and hot curing environments, CSF content and superplasticizer on the intrinsic air and water permeability and the pore structure of five mortar mixes.
6. To determine the resistance of plain OPC and CSF mortar mixes to magnesium sulphate attack conducted by alternate soaking and drying, the most common condition of attack in hot environments.
7. To make recommendations on the use of condensed silica fume concrete in Middle Eastern climates and more specifically in Iraq.

1.3 Introduction to the thesis

This thesis can be divided into seven parts, which address the seven aims of the research programme.

1. Current Knowledge

Chapters 2, 3 and 4 examine the background of the subject. More specifically, Chapter 2 provides a general illustration on the use of CSF and its effect on the fresh and hardened properties of concrete, mortars and paste. The chapter also identifies the areas where knowledge is lacking.

Chapter 3 contains general information about concreting operations in hot climates, dealing first with the main climatic factors. The chapter also focuses on the effect of hot environments on the properties of fresh and hardened concrete. Chapter 4 provides a description of curing methods and curing materials used in practice.

2. Experimental Programme

Chapter 5 and 6 describe a pre-research hypothesis and the test methods used in the experimental programme. More specifically, Chapter 5 focuses on the mechanism of hydration of plain OPC and OPC-CSF mixture. It also illustrates the general problem with concrete structures in the Middle East. The chapter also contains a description of the research model which aims to give an explanation of the strength and durability characteristics of plain and CSF concrete mixes used in temperate and hot environments.

Chapter 6 describes the experimental tests used in the investigation together with the methods of mixing preparation, curing and conditioning. The chapter also gives a brief introduction to the Iraqi climate and the means used to simulate it in the laboratory.

3. Mix Design

Chapter 7 gives details of the development of a mix design method capable of producing an OPC-CSF concrete mix of a specific 28 day compressive strength and medium workability.

4. Properties of CSF Concrete

Chapter 8 discusses strength results together with the absorption and permeability results collected from five non-

destructive test methods. It also details the statistical relationships between these test methods.

5. Properties of CSF Mortars

Chapter 9 discusses the true air and water permeability and pore size distribution test results on mortar specimens. It also details the relationship between permeability and pore structure.

6. Sulphate Resistance of CSF Mortars

Chapter 10 details the resistance of plain and CSF mortars to sulphate attack.

7. Recommendations

Chapter 11 consists of the conclusions of the experimental work and makes recommendations on the use of silica fume concrete in Middle East countries as well as areas for further research.

CHAPTER TWO
CONDENSED SILICA FUME
CONCRETE: BACKGROUND

2.1 Introduction

The escalating cost of energy in the manufacture of Portland cement has led to the search for industrial by-products requiring little or no pyro-processing. One such material is silica fume or CSF. CSF is a by-product from the reaction of high-purity quartz with coal in electric arc furnaces in the manufacture of ferro-silicon and silicon metal. The fume, which contains between 85 and 98 percent silicon dioxide, and consists of extremely fine spherical glassy particles, is collected by filtering the gases escaping from the furnace.

For the specific surface area of silica fume, values as high as 20,000 m^2/kg have been reported. When compared to a natural pozzolan or a fly ash, silica fume appears to be as a very unique product because of its peculiarities noted above.

The addition of silica fume favourably influences many aspects of concrete some by physical effects associated with small particles which have generally a finer particle size distribution than does Portland cement, and others by pozzolanic and cementitious reactions resulting in certain desirable physical effects. Concrete mix proportion, rheological behaviour of plastic concrete, and degree of hydration of Portland cement are among the physical effects associated with the particle size of silica fume. Strength, permeability, resistance to thermal cracking, alkali silica reaction and chemical attack are the main effects associated with the pozzolanic and cementitious reactions.

This chapter will review the use of silica fume in pastes, mortars and concrete and will cover its effects on the fresh and hardened properties. Finally an evaluation and discussion on the research work so far will be made to identify the gaps in knowledge on which the current research work was made.

2.2. Fresh properties of concrete and mortars incorporating silica fumes

2.2.1 Colour

Condensed silica fume (1) varies considerably in colour depending upon; a) its source, i.e. whether it is from a ferrosilicon or silicon furnace, b) the carbon content and c) to a lesser extent the iron content. The colour can vary from a very dark grey when silicon is produced in an open electric arc furnace without a heat recovery system to a whitish colour when produced in a furnace equipped for heat recovery.

Fresh concrete incorporating condensed silica fume is generally darker grey in colour than fresh conventional concrete, particularly so for concrete incorporating higher percentages of condensed silica fume.

2.2.2 Workability and water demand

Condensed silica fume has very fine particles with high surface area. Accordingly its use as an admixture or as a replacement ingredient in the cement can increase the amount of mixing water necessary to maintain a specific workability. Nevertheless (2,3,), experience in U.K. and abroad has shown that a well designed mix containing less than 300 kg/m^3 of OPC and less than 10% of silica fume will not significantly increase the amount of mixing water. Richer concrete mixes with high silica fume dosage may become sticky. Therefore, either the use of plasticising agents or increasing the amount of mixing water becomes advisable to reduce the energy required for moving and compacting. Carrette and Malhotra (4) found that the increase in water demand is almost directly proportional to the amount of silica fume added (Figure 2.1). The water demand increases approximately 1 litre per kilogram of added silica fume (5).

This increase in water demand can be overcome with the use of water reducer or superplasticizer admixtures and to a lesser degree by reducing the fine aggregate content of a mix. The effect of silica fume, cement content and plasticizer dosage on the water demand of concrete has been

studied by Loland and Hustad (6). After a comparison of water demand values at cement content of 100 kg/m³ and 250 kg/m³ they reported that in all mixes containing plasticizer and silica fume, water demand decreased at all dosages of silica fume. This reduction was because of the dispersing action of the plasticizer. Similar conclusion may be drawn from Sellevold and Radjy's work (7).

Better results can be achieved by the incorporation of superplasticizer which is a better dispersant than the normal plasticizer. However, it has been claimed (5) without substantial published data that lignosulphonated-based water reducers can be more efficient in reducing water demand in condensed silica fume concrete than superplasticizers. Moreover, the use of high dosage of lignosulphonate-based water reducers can cause serious delays in the setting of fresh concrete.

2.2.3 Bleeding

Concrete incorporating condensed silica fume shows reduced bleeding because of the changes in its rheological properties. These changes are to be expected because condensed silica fume has a high affinity for water resulting in very little water left in the mix for bleeding. Moreover, silica fume particles attach themselves to adjacent cement particle and reduce the channels for bleeding.

Loland and Hustad (6) quantitatively evaluated the bleeding and segregation aspect of a large number of concrete mixes, concluding that bleeding was greatly reduced in concrete incorporating condensed silica fume. In his investigation of the bleeding of fresh concrete Maag (8) also found that in concrete with condensed silica fume as a cement replacement, a large reduction in bleeding resulted. This was true for mixtures with and without water reducing admixtures. Similar conclusions were drawn by Burge (9) on light weight concrete. Data shown in Figure 2.2 indicates that incorporating various percentages of condensed silica fume results in a significant reduction in bleeding.

2.2.4 Setting time

Setting time of Portland cement concrete can be measured by determining the resistance to penetration by needles of a given bearing area (BS.4550 Section 3.6)(10).

Data on setting time of concrete incorporating silica fume are sparse. Swamy (11) cited that according to the few published investigations the addition of silica fume in small amounts to ordinary concrete mixes can alter the setting time slightly.

Data published by Pistilli et al (12) showed that the presence of 24 kg/m^3 silica fume in a concrete mixture containing 237 kg/m^3 Portland cement increases the initial and the final setting time by 26 min and 29 min respectively. Moreover, these initial and final setting times were increased by 47 min and 45 min respectively in a concrete mixture containing 297 kg/m^3 Portland cement.

2.2.5 Plastic shrinkage

The principal cause of plastic shrinkage in Portland cement concrete is understood to be the excessively rapid rate of evaporation of the water from the surface of the concrete and the inability or lack of bleed water to quickly replace the evaporating surface water (13). As soon as the surface becomes dry menisci for a capillary pressure developed on the surface of fresh concrete. Once the magnitude of this capillary pressure exceeds the tensile strength of fresh concrete, plastic shrinkage cracks could form. The magnitude of capillary pressure depends on the size of menisci. The smaller the size (i.e. small solid particle size or large surface area) the larger the capillary pressure. Thus, all chemical and mineral admixtures which can reduce bleeding of fresh concrete and have fine particles and high surface area can increase concrete plastic shrinkage and make it more prone to cracks.

The problem of plastic shrinkage cracking can become very serious under severe curing conditions of high temperature, low humidity and high wind velocity, as they favour faster water evaporation. According to investigations

reported from Norway, the most likely period for plastic shrinkage cracks to appear is the time when concrete is about to set (about 15 to 30 minutes after the specimens are cast) (5).

Merashi et al (14) found that the time when the rate of evaporation exceeds the rate of bleeding which corresponds to the sheen disappearance from the surface, is very critical. Earlier disappearance of the sheen would result in more severe cracking as the mix would not have enough time to set and develop sufficient tensile strength. Delay in the time of disappearance of the sheen means less cracking.

2.2.6 Hydration and reactions in the cement-silica fume-water system

Silica fume containing 80 to 95% SiO_2 has a high surface area. It can be used with cement to improve strength and other properties. The strength development, physical and mechanical properties are related to the hydration kinetics in the cement-silica fume mixture. Silica fume, as well as increasing the rate of hydration of C_3S, combines with lime formed as a reaction product in cement hydration. The hydration of silica fume and plain OPC cement is not easy to follow but the sequence of hydration can be followed and estimated from determining:

a. heat of hydration;
b. calcium hydroxide formation; and
c. non evaporable water.

a) Heat of hydration

Conduction calorimetry, which measures the rate of heat development during the hydration of a cementitious material is one of the methods used for following hydration and the effect of silica fume on cement hydration.

The rate of heat development in cement paste (15) containing 0,10,20 & 30% silica fume is plotted in Figure 2.3.

The earlier peak below 1 hour is generally attributed to the alumina reaction. The second broad hump occurring in

the cement paste (reference) shows a peak effect at about 6 to 7 hours and this is caused by C_3S hydration. Addition of silica fume changes the profile of the curves. An intense peak appears at about 5 hours and another sharp, intense peak at about 6 to 10 hours. The greater the amount of added silica fume the larger the intensities of these peaks. The earlier peak can be associated with the C_3S hydration which occurs at an earlier time than in the mix containing no silica fume. This signifies acceleration of C_3S hydration. The acceleration of C_3S hydration by the effect of silica fume has been demonstrated by Kurdowski and Nocun-Wozelik (16) who mixed amorphous silica with C_3S at a C_3S/SiO_2 molar ratio of 0.4 to 3.33 and followed the rate of heat evolution up to 24 hours as shown in Figure 2.4. A hump with a peak at about 8 hours occurs with C_3S containing no SiO_2. At a C_3S/SiO_2 molar ratio of 3.33 the initial peak (below 60 minutes) and the second peak are intensified, suggesting acceleration effects.

The more prominent second peak occurring in the paste containing silica fume (Figure 2.3), may be due to the reaction of $Ca(OH)_2$ (formed from OPC hydration) with silica fume. The intensity of this peak increases as the SiO_2 fume content is increased. The total amount of heat developed is increased by the increasing amounts of silica fume incorporated. Similar conclusion may be drawn from the work of Wu and Young (17).

b) <u>Calicum hydroxide formation and consumption</u>

The sequence of hydration of cement and silica fume mixture can be followed by determining the amount of calcium hydroxide formed or consumed at different times.

Cheng-yi and Feldman (15) studied the effect of 30% of both silica fume (21 x 20^3 m^2/kg) and a relatively coarsely ground silica (passing 100 mesh; 75 micrometre) on the production of lime based on ignited weight. Results are plotted in Figure 2.5. The three curves are similar up to 8 hours, but at later periods cement paste containing no additives shows higher $Ca(OH)_2$ contents. This would indicate

that both silica fume and ground silica interact with $Ca(OH)_2$ formed during hydration to produce C-S-H (18). The results also suggest that silica fume of greater surface area reacts more efficiently with $Ca(OH)_2$.

c. Non evaporable water

The determination of the non evaporable water content is another method of following hydration. The non-evaporable water includes all the water combined chemically with $Ca(OH)_2$, and the silicate and aluminate phases. Figure 2.6 compares the non-evaporable water content in cement hydration with 0, 10, and 30% silica fume prepared at water/cement and silica fume ratios of 0.25 and 0.45. The designations of all the mixes are shown the Figure. Cheng-yi and Feldman (15) found that the non-evaporable waters in all silica fume mixes are lower than in the plain mixes. This may be explained by the consumption of $Ca(OH)_2$ by silica fume with the formation of a C-S-H product containing less hydrated water than in that formed during normal hydration of cement.

2.3 Hardened properties of concrete incorporating silica fume

The hardened concrete properties of greatest interest are strength, modulus of elasticity, drying shrinkage, creep, permeability and other durability related properties. In general, strength properties of concrete are important as they are related to the structure of hardened cement paste and are relatively easy to determine. However, because strength sometimes correlates poorly with other durability related properties, there are instances when durability and permeability, more specifically, may become the governing criteria.

2.3.1 Compressive strength

The effect of silica fume on the strength of concrete depends largely on whether it has been used as an addition to Portland cement or as a partial substitution for the Portland cement in a reference concrete mixture. Most researchers

agree that when silica fume is used as a direct replacement for Portland cement, there is no significant change in compressive strength at early ages (4,7,19,20). Results reported by Malhotra (19) are typical of such research. When silica fume is used as a direct replacement for Portland cement, there is little or no change in compressive strength at early ages (1 to 3 days) for concrete with high W/C+CSF ratio, regardless of the percentage of silica fume used. This would indicate that the pozzolanic effect of silica fume requires some minimum amount of $Ca(OH)_2$ formation. However at lower W/C+SF ratio and higher percentages of incorporated silica fume, there is a marked increase in strength at 3 days (Figure 2.7). Thus at lower W/C+CSF ratios the products formed by the pozzolanic reaction are more efficient than higher W/C+CSF. This effect was noticed both in air-entrained and non air-entrained concrete.

If silica fume is used as an addition, there is no deleterious effect on early age strength (1 and 2 days). A noticeable strength increase is recorded during the 3 to 28 days moist curing period (7,21) as shown in Figure 2.8. Pistilli et al's (12) results agree with the above. In their work 24 kg/m^3 of silica fume was added to the concrete mixture containing 297 kg/m^3 ASTM type I Portland cement. No differences in the strength of either the reference concrete or the silica fume concrete at test ages of 1 and 2 days were recorded. However, there was an increase in strength of above 10% and 20% at 7 and 28 days respectively. A disparity reported by Popovic et al (22), was that the addition of silica fume up to 10% does not significantly influence early age strength. Higher percentages of silica fume up to 20% can cause a strength loss at early ages. The 28 days strength of both silica fume mixes were higher than the reference Portland cement mix.

As mentioned already, the water demand of silica fume concrete is directly proportional to the amount of silica fume if the slump of concrete is maintained constant by increasing the water content rather than by using a superplasticizer. In such instances, the increase in the

strength of silica fume concrete over that of the control concrete is only observed at lower W/C ratios and at longer ages. An example is shown in Figure 2.9. However, by keeping the W/C+SF ratio constant and compensating any loss in slump by using superplasticizer, the compressive strength of silica fume concrete was higher than that of the control (Figure 2.10). This was observed regardless of the age and the percentage of silica fume used (4).

Considerable work has been done in Norway on the relative strength of silica fume and OPC concretes. This property has been variously called the activity index, substitution index, cement equivalent index or efficiency index. (K). The efficiency index has been calculated based on the reduction in the amount of Portland cement (by replacing it with condensed silica fume) versus the amount of silica fume) added to achieve the same strength level as in the reference Portland cement mix (23).

According to the information gathered by Jahren (24) the value of the efficiency index varies greatly as shown in Figure 1.11, and depends on many factors. These factors include;

a. dosage of condensed silica fume;
b. carry condition (higher with wet curing);
c. age (higher at early ages);
d. cement content (higher with low cement content);
e. type and dosage of plasticizer or super-plasticizer; and
f. type of cement.

Tables 1 to 3 provide strength test data from a ready-mixed concrete producer of silica fume concrete for different maximum size aggregate (23). The compressive strength values at 9, 14, and 28 days, together with the percentage of silica fume used and slump of fresh concrete, are shown in the tables. The so-called efficiency factor increases with increasing cement content of concrete mixture. With lean concrete mixture (200 to 250 kg/m^3 Portland cement content)

researchers (12 & 25) have reported that the use of silica fume has a relatively better effect on strength than is the case with normal or rich concrete mixtures (i.e. > 300 kg/m³ Portland cement content). Pistilli et al's data (12) shows that with 24 kg/m³ of silica fume, the strength increases approximately 6.9 to 13.8 MPa with lean mixes and 3.4 to 6.9 MPa with rich mixes at 28 and 120 days respectively.

Typical relationships between compressive strength and water/cement ratio at 28 days were demonstrated by Sellevold and Radjy (7) for concrete containing different percentages of silica fume (Figure 2.12). Swamy (11) cited Loland & Hustad's conclusion from their data that the relationship between compressive strength of concrete and elastic modulus or tensile strength is more or less the same for concretes both with and without silica fume.

Wolsiefer (26) investigated the engineering properties of a high strength concrete containing 594 kg/m³ type I Portland cement and 90 kg/m³ of silica fume. The water/ cementitious materials ratio was 0.22 with the use of a superplasticizer. He reported that this concrete gave a compressive strength of 111 MPa at 28 days. Bache (27) used large dosages of superplasticizer to maintain the water/ cementitious ratio of a Portland cement and silica fume mixture in the range 0.13 to 0.15. He was able to produce laboratory specimens with about 250 MPa compressive strength.

Recently Carrette et al (28) investigated the effect of air curing after 2 days of moist curing on the long term (up to 2 years) compressive and tensile strength. Results show a reduction in strength between the age of 91 days and two years. Aitcin disagrees with this (29). His strength study was based on a core sample taken from a field concrete where both CSF and non-CSF concrete were used.

2.3.2 Drying shrinkage

Withdrawal of adsorbed water from the surface of gel particles of concrete stored in unsaturated air causes drying shrinkage. The drying shrinkage of concrete is affected by the volume fraction of the cement paste, the aggregate

content, maximum size and stiffness, water to cement ratio and water content. Also the conditioning of the test specimens before the beginning of drying shrinkage seriously affects the test results.

Several investigators have reported data on unrestrained shrinkage of standard concrete specimens at a relative humidity of 50 to 60%, but test results are generally difficult to compare because of the different mix proportions and different curing periods used before drying shrinkage measurements (6,30).

Johansen (30) performed shrinkage measurements on concrete prisms that were exposed to a drying environment (50% relative humidity) immediately after demoulding and after 28 days moist curing. The condensed silica fume content ranged from 0 to 25% and W/C+SF ratio ranged from 0.37 to 1.06. Some mixes contained water reducers. It was concluded that for concrete with W/C+SF ratio < 0.6, no significant differences in shrinkage existed between the reference concrete and condensed silica fume concrete containing up to 10% silica fume. Concrete containing 25% silica fume and no water reducer showed higher shrinkage values.

Loland & Hustad (6) have reported shrinkage data on condensed silica fume concrete with varying W/C+SF and containing up to 20% silica fume. The conditioning of test specimens consisted of 7 days of moist curing followed by drying shrinkage at 60% relative humidity. The general conclusion was that the shrinkage of the condensed silica fume concrete was comparable to that of the reference concrete.

Data by Carette and Malhotra (4) indicated that the drying shrinkage of condensed silica fume concrete after 28 days of moist curing is generally comparable to that of the control concrete regardless of the W/C materials ratio. Figure 2.13 shows drying shrinkage of concrete with a W/C+SF ratio of 0.4; the coarse and fine aggregates were limestone and natural sand and the concrete was made using a naphthalene-based superplasticizer. The drying shrinkage of

control concrete and that incorporating 15% silica fume are comparable while concrete containing 30% silica fume shows slightly lower shrinkage values at 420 days (31).

Results by other researchers on the shrinkage of silica fume mortars are somewhat contradictory. Bagers (32) drying shrinkage results show that shrinkage values after exposure to 40% relative humidity for six months, increase with silica fume content at any W/C ratio and increases with W/C at 8 or 16% silica fume. No chemical admixture was used in these mixes. Other researchers (33), however, have measured shrinkage at a W/C ratio of about 0.4 and found that with 2.4% superplasticizer by weight of cement, shrinkage was substantially less in the presence of silica fume.

Recently Ravindrarajah et al (34) examined the effect of adding 8% of silica fume by weight of OPC on the drying shrinkage of mortars. They found that silica fume addition reduced drying shrinkage provided the specimens were water cured for a long period before they were allowed to dry.

2.3.3 Creep

Very few published data on the effect of incorporating silica fume on creep are available. However, it is expected that the creep of a silica fume concrete will be lower than the corresponding Portland cement concrete. This is probably because of the higher ultimate strength of concrete with the silica fume.

Wolsiefer (26) has produced limited data on concrete incorporating silica fume. Creep measurements were made after 7 days and every month after that up to 1 year. Results show that the percentage differences at 7 and 28 days were 30.4 and 28.8 percent in favour of high-strength concrete with the admixture.

Buil and Acker (35) evaluated the creep of Portland cement and a 25% silica fume concrete. The ratio of water/ cementitious materials was about 0.41. Superplasticizer was used to maintain workability in the silica fume concrete mixes. Specimens were cured for 28 days, then some specimens were loaded in an unsealed condition (for drying creep)

whereas the others were sealed before loading (for basic creep). The 1-year creep data reveal that basic creeps were similar in both concretes; however the drying creep for the silica fume concrete was lower than that of the reference. The 28 day compressive strengths of plain and silica fume concrete were 53 MPa and 76 MPa respectively.

2.3.4 Permeability

Concrete permeability is regarded as an important property as it determines its resistance to attack not only by aggressive media, but also by pure water. That concrete survives aqueous environments at all is attributable to the low equilibrium solubility of the hydrated components and the low rate of mass transfer in well compacted and cured concrete (36).

Incorporation of supplementary cementing materials such as natural pozzolans, fly ash and slags in concrete considerably influences its permeability (37). Significant decreases in permeability are often attributed to the influence of pozzolans on the fine pore structure and interfacial effects. Condensed silica fume which is a much more efficient pozzolanic material than natural pozzolans and fly ashes, greatly reduces the permeability of concrete (9, 38).

Only a limited amount of work has been carried out on the permeability of silica fume, Portland cement paste, mortars and concrete. Gjorv (39) reported the results of water permeability tests performed on concrete in which the cement content varied from 100 to 500 kg/m^3. In concrete incorporating 100 kg/m^3 cement and 10% condensed silica fume permeability decreased to about 4.0 x 10^{-10} m/sec from 1.6 x 10^{-7} m/sec. The permeability of concrete containing 100 kg/m^3 cement and 20% silica fume was the same as that of concrete containing a cement content of 250 kg/m^3 without silica fume. Gjorv's results fall in line with previous findings in which the most significant effect of silica fume was obtained at lower cement contents. At a cement content of 400 to 500 kg/m^3 water permeability was in the range of 10^{-14}

to 10^{-15} m/sec for concrete with or without silica fume. This indicates that at higher cement content silica fume has only a slight effect on permeability. Gjoru's finding was confirmed recently by Hustad et al (177).

Maage (40) found that the water permeability efficiency factor of a concrete moist cured for more than 6 months varied between 2 and 16 depending on curing conditions and strength grade.

2.3.5 Porosity and pore structure

Various studies have shown that the addition of silica fume, even in moderate quantities, can have a very significant effect on hydration of Portland cement (41, 42 & 43). It is to be expected, therefore, that silica fume will also have a major effect on the pore structure, although published data is limited.

Four different techniques can be used to determine bulk porosity in the body of cement paste or mortar. These are mercury porosimetry, helium pycnometry, methanol exchange and adsorption and the (P.T.I) Porosity method. The mercury porosimetry method is used to classify and determine the distribution of the pores as well as the bulk quantity. This method was found to give reliable results (44). Helium pycnometry gives measurements of the solid volume excluding all the accessible pores available. This accurate solid volume can be used to calculate the bulk porosity using the following equation;

$$P = (1 - \frac{Dd}{SG}) \times 100$$

where P = porosity in percent

Dd = dry density

SG = specific gravity

This method is known to give relatively accurate bulk porosity, whereas the P.T.I. porosity method, which uses water to fill up all the accessible pores, may not be accurate because firstly it involves selection of the right fluid density as hydration proceeds and the size of the pores diminishes. Secondly, capillary tension effects can cause pore structure alteration when water is removed from the pore

structure by drying. Thus unless the capillary tension effect can either be prevented or reduced, the results of this method are doubtful, but the problem can be overcome by exchanging the pore water with a polar liquid of lower surface tension such as methanol. Day (45) suggested a short exchange time may be necessary as Portland cement may react chemically during the exchange process which causes some doubt upon the value of subsequent pore structure assessment. However, Parrott's (46) results show little differences in the total porosity between samples before and after methanol exchange.

Feldman & Huang (47) examined the effect of blending 10 & 30% silica fume on the pore structure of Portland cement using mercury intrusion porosimetry. They found that the total porosities were 16.81; 14.4, and 10.08 percent with 0, 10 and 30 percent of silica fume respectively (Figure 2.14).

The curves on the graph are of decreasing slope and are concave to the pore-size axis for 0% silica fume, becoming increasingly convex with increasing silica fume content and longer curing times. The threshold pore-diameter (diameter at which the slope of the volume-diameter-curve increases abruptly) of the curves decreases with increasing silica fume content. The same trend was observed for a W/C+SF ratio of 0.45. For specimens containing silica fume, the slopes of the curves at maximum intrusion pressure increase with time, attaining maximum value between 14 and 90 days. The slope is greatest where the $Ca(OH)_2$ content is low, as shown in Figure 2.15; those curves for mixes without silica fume where the $Ca(OH)_2$ content is high are relatively low and constant in slope.

The convex shape of the curves at high pressure is believed due to the breaking of the pore structure by mercury. This is because the $Ca(OH)_2$-CSH interface and the $Ca(OH)_2$ crystals themselves (which provide the pathway for mercury migration through the pores (48)) are replaced by CSH-CSH interfaces. This makes access to many of the pores by mercury during mercury intrusion only possible by rupture of the structure (49).

Huang and Feldman (43) also studied the pore structure of Portland cement. Silica fume mortars (sand/binder = 2.25) containing 0, 10 & 30% silica fume at W/C+SF ratios of 0.45 & 0.60 were used. Results for plain cement show that the volume of mercury intruding into the specimens decreases with curing time over the full range of pore sizes. The pore-size distribution result for 10 & 30% silica fume mortars show at diameter smaller than 60nm & 30 nm, the total intruded volume decreases as the curing time increases. Moreover, in the range of 100 to 300 nm, the total pore volume is greater in many cases for the specimens cured for longer periods.

A research group concluded that with silica fume, the pozzolanic reaction and the formation of the discontinuous structure commences after only 3 days of curing. The formation and development of pore structure between 3 and 14 days, especially in the 100 to 1000 nm size range may be the result of the $Ca(OH)_2$ concentrated around sand grains forming a structure involving dissolution of some of the $Ca(OH)_2$ and then the formation of C-S-H by reaction between silica fume and $Ca(OH)_2$. The abrupt increases in intruded volume suggest that in this region of mercury pressure, rupture of the pore structure may occur (50).

Changes in pore distribution curves in mortar blends containing silica fume are more marked than in paste blends. This is especially true for the variations in the large pore-size range caused by the formation of discontinuous pores, due partly to the removal of lime accumulated at the sand-paste interface and partly to the reaction of lime with silica fume within the matrix.

The threshold value (the point where mercury intrudes at the maximum rate) of pore size for mercury intrusion in mortar blends and paste blends are quite different. In mortar blends the threshold value increases and becomes less abrupt with silica fume addition, while in paste blends it decreases.

Pore structure studies on pastes containing silica fume made at constant consistency with 0, 5, and 15% silica fume addition and cured for 15 days have also been out (51).

Increased pore volume in the 10^{2} to 10^{4} nm pore size range with increased silica fume content was observed (51). Similarly increased pore volume in the 5 x 10^{2} to 5 x 10^{3} nm range was observed on field concretes made at W/C of 0.56 to 1.0 with 15% silica fume addition (44).

2.3.6 Chloride diffusion

Gautefall (52) investigated the diffusivity of chloride ions in hardened cement paste. Both ordinary Portland cement and blended cement wih 10% fly ash was used. Condensed silica fume was used as a cement replacement of up to 15% by weight of cement. The water/cement + silica fume ratio was varied between 0.5 to 0.9. Results show that the addition of silica fume can decrease chloride diffusion markedly. This effect was more distinct for ordinary Portland cement than for blended cement. Recently Grimaldi et al (53) stated that the effect of silica fume on chloride diffusion has to be linked with carbonation and vice versa.

Aitcin (29) in a report based on a field exposure after 4 to 6 years, stated that silica fume field concrete exhibits very low chloride ions diffusion. It was almost in the range of latex modified or polymer impregnated concrete. This trend was confirmed by Berke (54).

Gautefall et al (55) concluded from their study on a cement paste that using silica fume as a cement replacement reduces the effective diffusion coefficient of chloride.

Maage (40) found that the chloride diffusion efficiency factor of silica fume pastes cured for more than 6 months varied between 5 and 19 depending on silica fume quantity and water/cement + silica fume ratio.

2.3.7 Carbonation and steel corrosion

In a well made, well-compacted and well cured concrete, reinforcing steel should not corrode because of the high alkalinity of the pore solution in concrete (pH>13). The high alkalinity of concrete results in the formation of a protective oxide film (passive film) on the surface of the

reinforcement. Under certain conditions of service, this protective film may be destroyed. This can occur either when the pH of concrete is reduced to about 11.0 or due to the presence of chlorides. The former situation is due to atmospheric carbon dioxide reacting with calcium hydroxide in the cement paste to form calcium carbonate.

If the passive film is destroyed, the corrosion of the reinforcing or other embedded steel begins. Rusting is an electrochemical process that requires a flow of electrical current for the chemical corrosion reactions to proceed. These electrochemical reactions take place when two dissimilar metals come into contact with oxygen and moisture. Under normal conditions iron becomes the anode and the other metal becomes the cathode with the oxidation taking place at the former site and the reduction of oxygen taking place at the latter site. The anodic and cathodic reactions take the following form:

anodic reaction : $Fe \rightarrow Fe^{2+} + 2e^-$

cathodic reaction : $2H_2O + O_2 + 4e^- \rightarrow 4OH^-$

the overall reaction takes the form: $2Fe + 2H_2O + O_2 \rightarrow 2Fe(OH)_2$

The ferrous hydroxide $Fe(OH)_2$ is further spontaneously oxidized to hydrated ferric oxide, $Fe_2O_3.nH_2O$.

Once the corrosion of the reinforcing steel starts, the rate of corrosion is primarily controlled by the rate of oxygen transport through the concrete and the electrical resistivity of the concrete. In the case of steel corrosion, a separate cathodic metal is not essential as separate parts of a reinforcing bar can develop an anodic-cathodic galvanic cell.

Vennesland and Gjorv (56) and Gjorv (39) have reported on the effect of up to 20% condensed silica fume by weight of cement on the rate of carbonation, electrical resistivity and rate of oxygen transport through water saturated concrete. They concluded that the rates of oxygen transport and carbonation are slightly reduced. The electrical resistivity of the concrete, in which the cement was replaced by 20% of silica fume, was increased by up to 190 to 1600% for cement contents ranging from 100 to 400 kg/m^3, respectively. Thus,

it would appear that silica fume does not increase the corrosion potential of steel reinforcement. Recently Berke (54) found that silica fume can increase concrete electrical resistivity to over 30,000 ohm-cm. Generally concretes having electrical resistivity over 30,000 ohm-cm do not exhibit evidence of severe corrosion (57).

2.3.8 Alkali-aggregate reactions

It was reported by Stanton (58) that chemical reactions involving aggregates in concrete can result in serious damage by causing abnormal expansion and cracking. The reaction referred to by Stanton is known as the alklai-silica reaction, involving a reaction between alkalis (Na_2O and k_2O) from the cement with hydroxyl and certain siliceous constituents that may be present in the aggregate. The principle products are distinctive gelatinous hydrates which expand as water is absorbed, exerting pressure on the surrounding mortar. Also certain carbonate rocks participate in reactions with alkalis which can produce detremental expansion and cracking. The expansive alkali-carbonate reaction was originally recognised by Swenson and Gillott (59). According to their theory, the reaction involves the release of entrapped active clay minerals that absorb water directly and swell.

The most effective method of controlling the expansive alkali-aggregate reaction is to reduce the total alkali content of the concrete below a critical limit. This method, however, is not always economic. Another method which has shown promise is to blend an approved mineral admixture with the high alkali cement.

Silica fume has been tested as one of the mineral admixtures for the above purpose. Oberholster and Westra (60) monitored the expansion of mortar prisms (ASTM, C441-69), made with incorporation of 5 to 30% of different pozzolanic admixtures including silica fume. The expansion results after 555 days are shown in Figure 2.16 in which all the admixtures show a decrease in expansion, being silica fume. Assuming 0.1% expansion as the criterion for allowable

expansion (ASTM C227), a 10% replacement by silica fume would be required.

Olafson (61) used crushed pyrex as the reactive aggregate suggested in ASTM methods C227 and C441. His work reveals that using pozzolans of a high surface area such as silica fume can lower the quantity required necessary to contain the reaction. Perry & Gillott (62) have also shown the effectiveness of silica fume in controlling alkali silica reactions using pyrex as a reactive aggregate. In addition, they tested a very reactive opal according to ASTM C227 except that temperatures of 25° and 50°C were used as well as the standard 38°C. The amount of silica fume ranged from 0 to 40% by weight of cement. The results of experiments performed at 50°C are shown in Figure 2.17. The expansion of the mortar bar increased when 5% cement was replaced by silica fume but eliminated at replacement levels of 20% or more. Evidence presented in this work indicated, however, that superplasticizer of the sulphonated naphthalene formaldehyde type increase expansion of the mortar bar containing 0-10% silica fume, whereas lignosulphonated admixtures decrease expansion. The reduction in the latter case was probably due to air entrainment by the admixture.

The precise mechanism by which the alkali-aggregate reaction produces expansion as well as how this expansion is reduced in the presence of pozzolans are not fully understood. However, hypotheses concerning the mechanism by which pozzolans provide resistance to alkali-aggregate reactions are generally centred on the type of C-S-H formed during hydration of cement. When the CaO/SiO_2 ratio of the C-S-H formed is approximately 12 or lower, this product will have an increased capacity for accommodating Na_2O and k_2O in its structure. During normal hydration without the mineral admixture this ratio is about 1.5 (63).

2.3.9 Resistance to sulphates

Several studies have been made on the effectiveness of silica fume in mortars and concrete in improving resistance to attack by aggressive agents (5, 22, 64, 65, 66, 68).

Observation on the modifications of the pore structure with resultant effects on permeability, and the chemical combination of $Ca(OH)_2$ would all suggest that silica fume additions enhance chemical resistance of mortars and concrete.

Aitcin (1) reported that in 1952, Bernhardt in Norway was the first to publish limited data on the sulphate resistance of concrete exposed to 10% $NaSO_4$ solution. The conclusion was that the sulphate resistance was improved when 10 to 15% of Portland cement was replaced by the condensed silica fume.

Swamy (11) cited Fiskka's investigation of the long-term performance of concrete specimens exposed to alum shale water containing 5 g/l SO_3 and with 2.8 pH. Measurements of the change in volume after 20 years of exposure indicated that the most resistant concrete was made of Portland cement in which 15% of the cement had been replaced by silica fume. Sellevold (5) attributed the superior performance of silica fume concrete to the refined pore structure of the matrix, lower content of calcium hydroxide, and an increased amount of aluminium incorporated in the hydrates, thus reducing the amount of alumina available for ettringite production.

The relative chemical resistance of low W/C concretes, containing either styrene butadiene latex or silica fume, has been compared when exposed to the following solutions: 1% HCl, 1.1% H_2SO_4, 1% lactic acid and 5% acetic acid, 5% ammonium sulphate and 5% sodium sulphate (66). The investigation revealed that except for ammonium sulphate solution, concrete incorporating silica fume generally showed better resistance to the aggressive solutions. The poor performance of silica fume concrete in ammonium sulphate solution was attributed by the fact that ammonium salts are able to decompose the C-S-H which is the principal solid phase in the hydrated Portland cement paste. Also, it may enhance the formation of expansion-producing ettringite.

Silica fume addition also improves the durability of mortars to sulphate attack. This was confirmed by results obtained by immersing mortars prepared at W/C of 0.6 in a 10%

$Na_2SO_4.10H_2O$ solution. Flexural strength changes, as a ratio of the values with respect to those stored in water, are presented in Figure 2.18. Ordinary and blended Portland cement mortars with added silica fume exhibit better durability than sulphate-resisting cement (22).

Mather (65) monitored the durability of mortar bars made at water/cement ratio of 0.48 and sand/cement ratio of 2.75 by measuring their expansion in a 4-1 Na_2SO_4 solution. Among the ten different pozzolans examined, silica fume was ranked the best.

Recently Berke (54) examined the resistance of silica fume concrete to salt crystallization. The test was performed by immersing specimens in chemical solution for 7 days and drying them for the next seven days in an oven, each immersing and drying was represented as a cycle. Results show that silica fume improved the resistance of concrete. The greater the amount of silica fume used the better is the resistance.

Yamato et al's chemical resistance tests using 5% H_2SO_4, 5% HCl and 10% Na_2SO_4 confirm the improvement in resistance offered by the use of silica fume. (69).

2.4 Summary, evaluation and significance of research work

2.4.1 Introduction

This review has shed light on the properties of paste, mortar and concrete incorporating silica fume. The pozzolanic reaction between silica fume and calcium hydroxide liberated by cement hydration produces new calcium hydrate products which fill the large pores and eventually refine the pore structure. This pore refinement increases the strength and reduces the permeability of concrete.

2.4.2 Workability

Due to the high surface area and fineness of silica fume, Portland-silica fume mixtures were found to require more water to produce mortars and concrete of a given consistency. This can be avoided by the addition of water reducing agents, but at increased cost.

2.4.3 Curing and environmental conditions

The research work so far has highlighted the effect of incorporating silica fume on the properties of Portland-silica fume mortars and concrete under controlled curing environment of temperature and humidity such as 20°C + 70% R.H or 20°C moist curing. The effect of initial curing and more realistic environment conditions on strength, permeability and durability in general has not been thoroughly investigated.

Most of the research work on the use of silica fume in concrete has been under temperate environment conditions. The behaviour of concrete and mortar incorporating silica fume under environments simulating those of Middle Eastern sites conditions has not yet been investigated to the author's knowledge. Hence, a research study is needed to investigate the influence of such environments on the different properties of silica fume concrete.

2.4.4 Pore structure

The effect of curing environment and duration on the durability properties of plain and silica fume concrete has to be linked to the pore structure. Unfortunately, there has been very little reported on the influence of silica fume on this relationship. This area of work clearly requires further study.

2.4.5 Mix design approach

Portland cement-silica fume concrete and mortars used in nearly all of the research work were produced by either adding the silica fume as an admixture to the designed quantity of cement in the reference OPC mix or by direct weight for weight replacement of reference OPC in the range 10 to 40% by weight of cement. The author believes that it is necessary to consider silica fume and Portland cement as two cement components within the concrete being designed for both strength at a given age and workability, as in normal concrete practice. As far as the strength is concerned, the problems associated with using SF as an admixture are;

1) The concrete possesses a greater early, and late age strength than that specified by the structural engineer. Thus concrete structure will have unnecessary large sections and elements.
2) Because of the high unit weight cost of silica fume in comparison to Portland cement, the unit cost of concrete per cubic metre will considerably be much greater especially when high percentages are used.

Using silica fume as a direct replacement for Portland cement is, apart from the high early age strength which will be similar to or slightly lower than the reference OPC strength, accompanied by the problems mentioned above. Hence, it is important to develop a simple mix design method for proportioning silica fume concrete which also takes into account material costs. When evaluating the effect of silica fume incorporation on durability, the comparison between plain OPC and Portland-silica fume concrete will usually be most meaningful when they are designed to produce the same target strength and workability. We then need to examine how different combination of the two cement components (each of which satisfies the strength and workability requirements) influence unit costs, durability, resistance to degradation and repair cost throughout the service life of the element. On the basis of the above a certain cement combination might then be preferred.

2.4.6 Quality control

Compressive strength is widely used as a quality control test. It is a good test for engineers to verify the mix proportions and to assess the ability of the structure to carry the design loads. It is also useful for engineers during the construction period to know when to remove formwork. Nevertheless, more information is required to establish whether this test alone is sufficient from the viewpoint of curing control and durability.

2.4.7 Efficiency factor

Silica fume producers and researchers normally present an efficiency factor based on the compressive strength after 28 days of curing in water at 20°C. In this situation, factors around 2 to 5 are reported by many researchers. However, building owners are interested in the silica fume efficiency factor under more realistic curing and environmental conditions. Moreover, they are more interested in the durability efficiency factor than the strength efficiency factors. Further work is required to furnish this former factor as very limited information is available.

Table 2.1
RESULTS OF COMPRESSIVE STRENGTH TESTS AT 7, 14, AND 28 DAYS FOR CONCRETES MADE WITH AND WITHOUT CONDENSED SILICA FUME — 10 mm MSA (20) (23)

10 mm MSA (in brackets: control mixes)

		20 MPa		25 MPa		30 MPa		35 MPa	
Cement (kg/m³)		200	(268)	227	(310)	255	(360)	273	(400)
Silica fume (kg/m³)		24.0	—	27.2	—	28.1	—	27.3	—
Silica fume (%)		12.0	—	12.0	—	11.0	—	10.0	—
Compressive strength (MPa)	7 days	13.4	(15 8)	17.8	(19.8)	21.0	(24.7)	24.5	(27.2)
	14 days	18.1	(19.2)	23.6	(23.5)	27.5	(28.5)	32.8	(33.4)
	28 days	23.5	(22.0)	30.4	(26.4)	35.7	(33.2)	41.4	(37.2)
Slump (mm)		75—125		70—125		65—110		65—110	
Efficiency factor		2.9		3.5		4.3		5.3	

Note: MSA — Maximum size aggregates; specimen size = 150 × 300-mm cylinders.

Table 2.2
RESULTS OF COMPRESSIVE STRENGTH TESTS AT 7, 14, AND 28 DAYS FOR CONCRETES MADE WITH AND WITHOUT CONDENSED SILICA FUME — 14 mm MSA (20) (23)

14 mm MSA (in brackets: control mixes)

		20 MPa		25 MPa		30 MPa		35 MPa	
Cement (kg/m³)		186	(250)	200	(282)	245	(341)	273	(386)
Silica fume (kg/m³)		22.3	—	24.0	—	27.0	—	27.3	—
Silica fume (%)		12.0	—	12.0	—	11.0	—	10.0	—
Compressive strength (MPa)	7 days	14.1	(16.6)	17.9	(18.9)	23.1	(26.8)	28.1	(27.8)
	14 days	18.1	(17.4)	20.6	(23.0)	31.9	(33.2)	34.1	(32.6)
	28 days	24.6	(22.0)	27.9	(26.0)	36.4	(34.0)	40.8	(36.8)
Slump (mm)		75—125		80—125		70—130		65—110	
Efficiency factor		3.5		3.7		4.2		5.2	

Note: Specimen size = 150 × 300-mm cylinders.

Table 2.3
RESULTS OF COMPRESSIVE STRENGTH TESTS AT 7, 14, AND 28 DAYS FOR CONCRETES MADE WITH AND WITHOUT CONDENSED SILICA FUME — 20 mm MSA (20) (23)

20 mm MSA (in brackets: control mixes)

		20 MPa		25 MPa		30 MPa		35 MPa	
Cement (kg/m³)		182	(245)	195	(277)	240	(336)	273	(395)
Silica fume (kg/m³)		21.8	—	21.5	—	26.4	—	27.3	—
Silica fume (%)		12.0	—	11.0	—	11.0	—	10.0	—
Compressive strength (MPa)	7 days	14.9	(18.0)	18.6	(22.0)	23.4	(27.1)	27.1	(31.0)
	14 days	19.2	(20.4)	25.1	(26.6)	27.5	(30.0)	33.8	(35.2)
	28 days	26.7	(24.1)	33.2	(29.5)	34.6	(34.5)	40.2	(37.6)
Slump (mm)		80—135		60—130		65—120		60—105	
Efficiency factor		3.6		3.9		4.1		5.0	

Note: Specimen size = 150 × 300-mm cylinders.

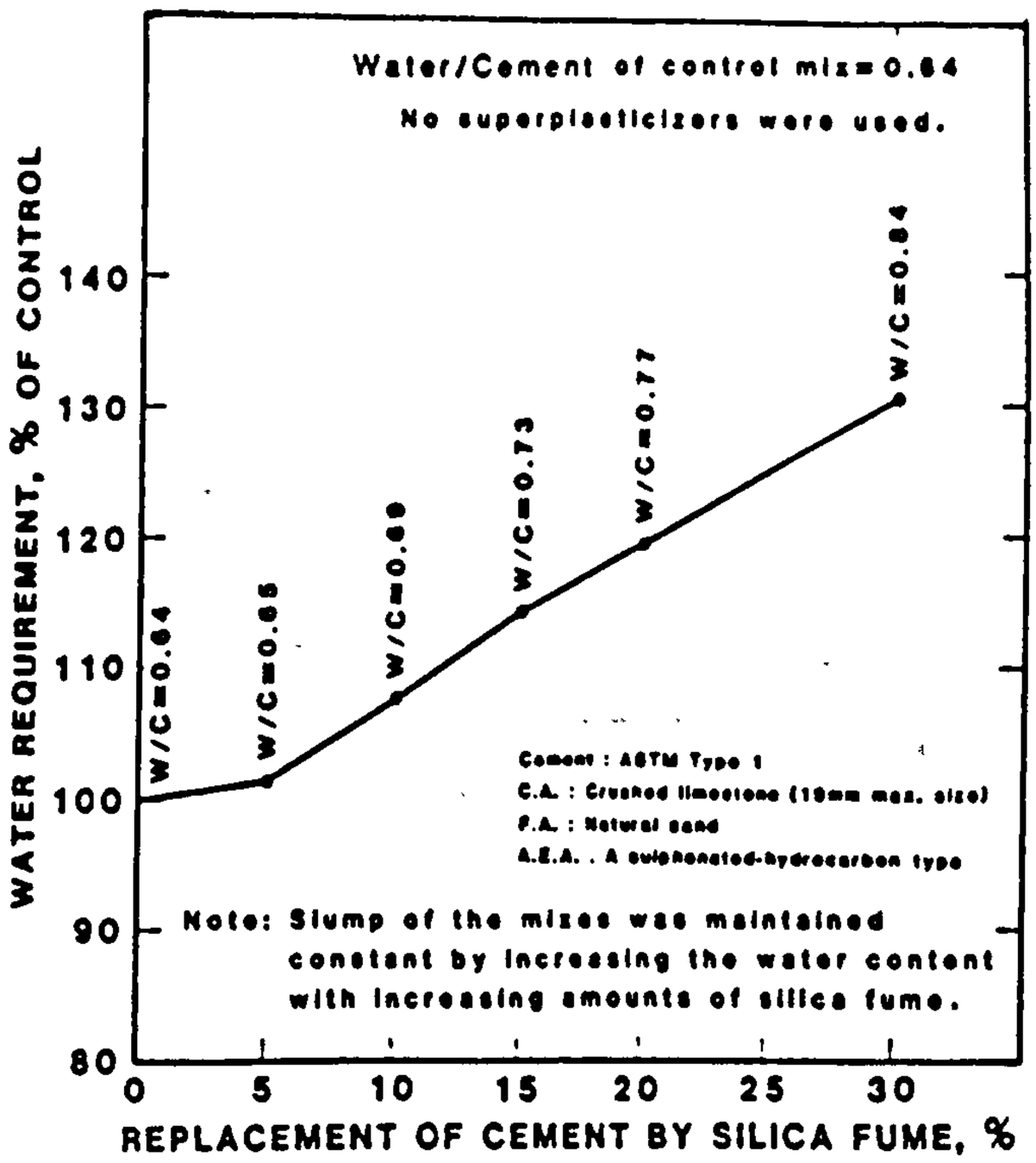

Figure 2.1 Relation between water requirement and dosage of silica fume for concrete with a W/(C + SF) of 0.64. (4).

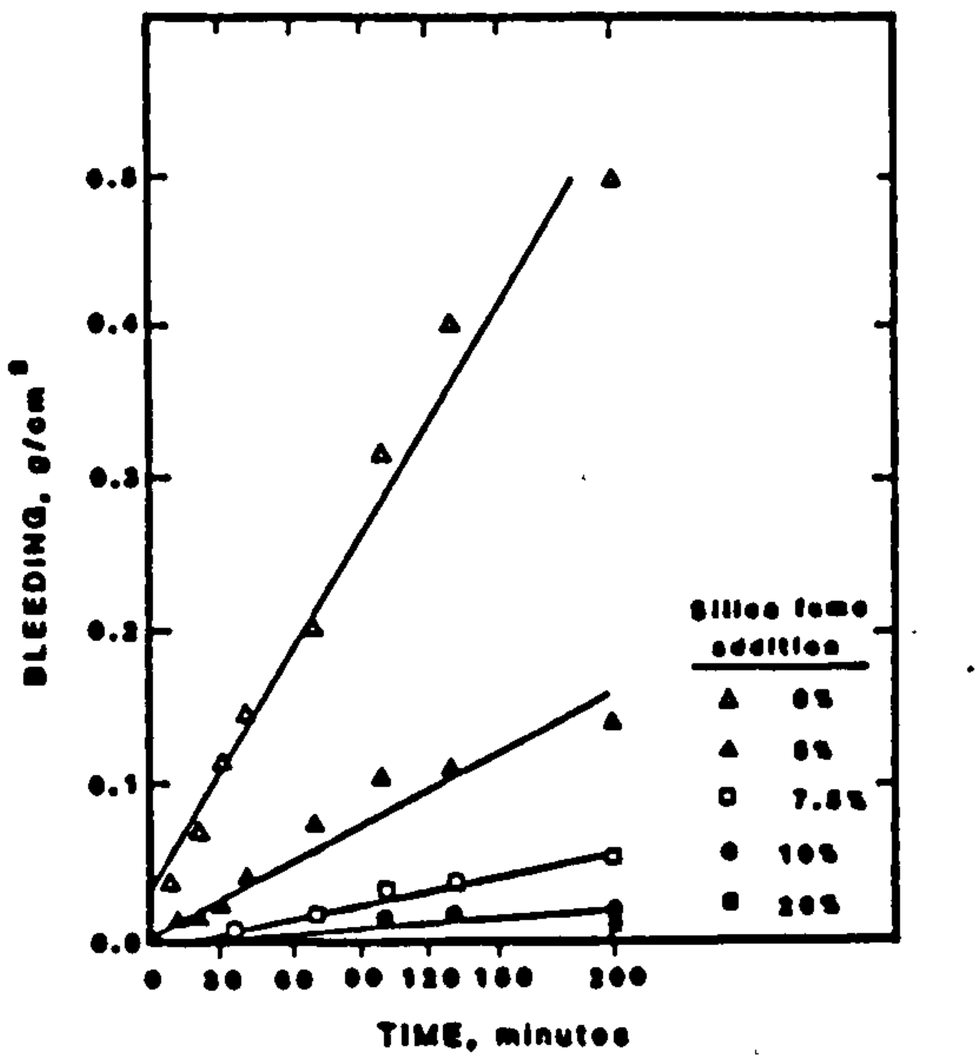

Figure 2.2 Bleeding rate of lightweight silica fume concrete (9)

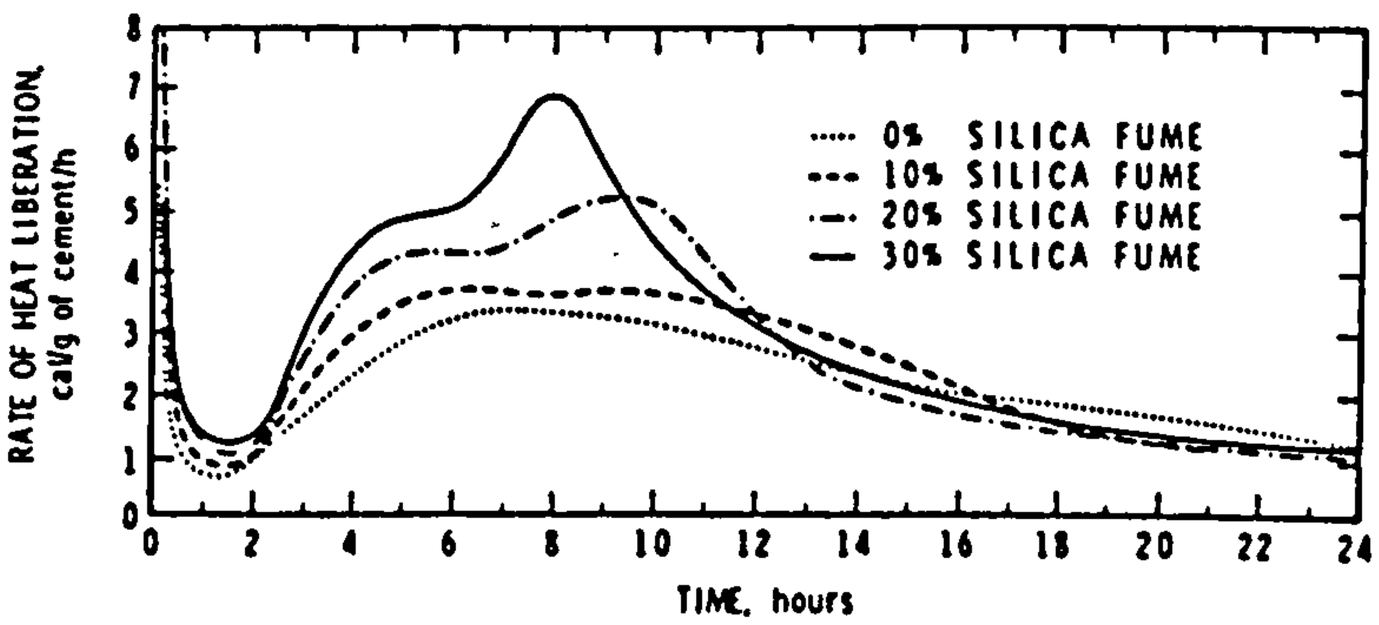

Figure 2.3 Change in rate of heat evolution of C/S fume pastes with time (15)

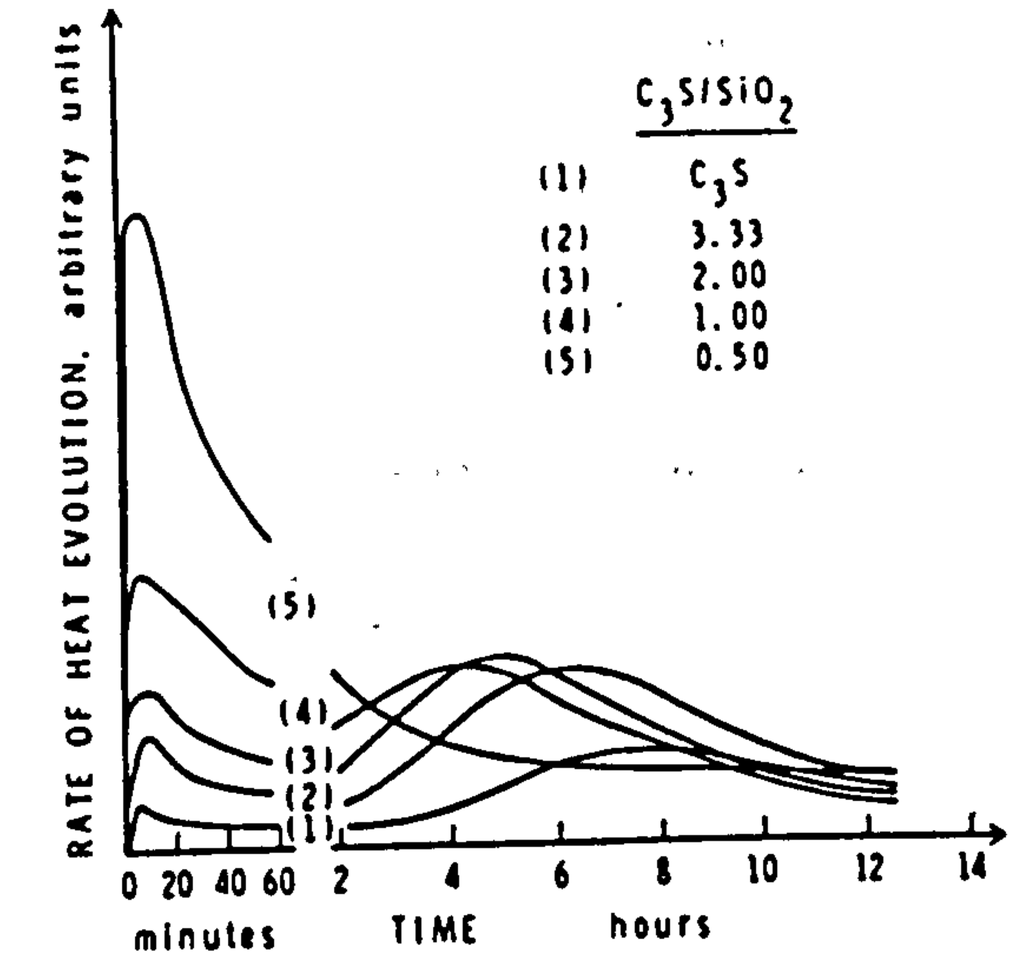

Figure 2.4 Heat evolution curves for samples of C,S containing silica (16)

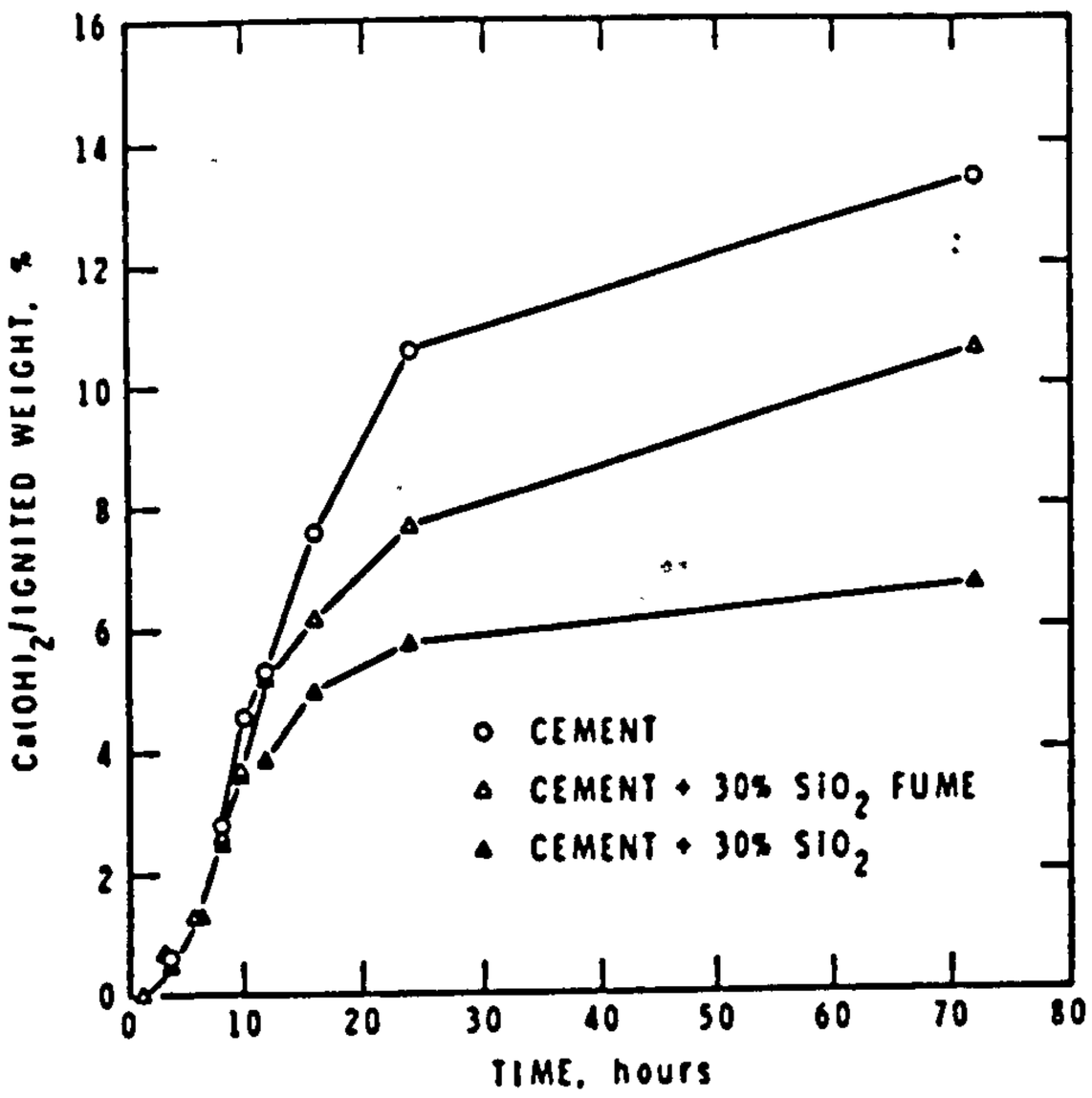

Figure 2.5 Change in $Ca(OH)_2$ content at early times for cement and cement blends. (15)

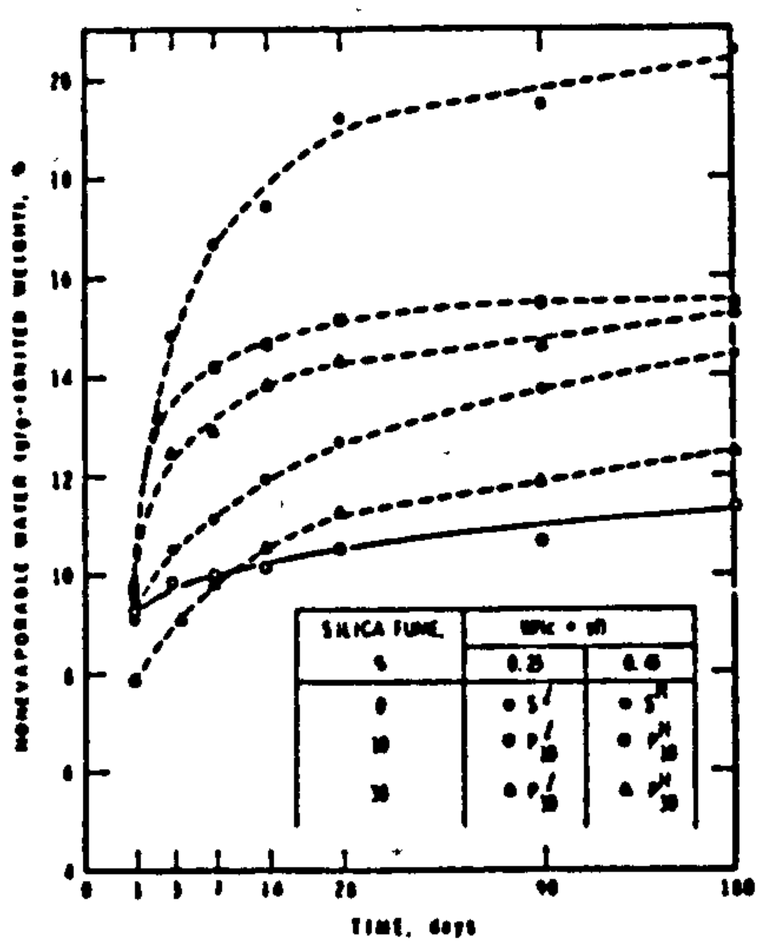

Figure 2.6 Change in non-evaporable water content with time for various silica fume-cement mixtures (15)

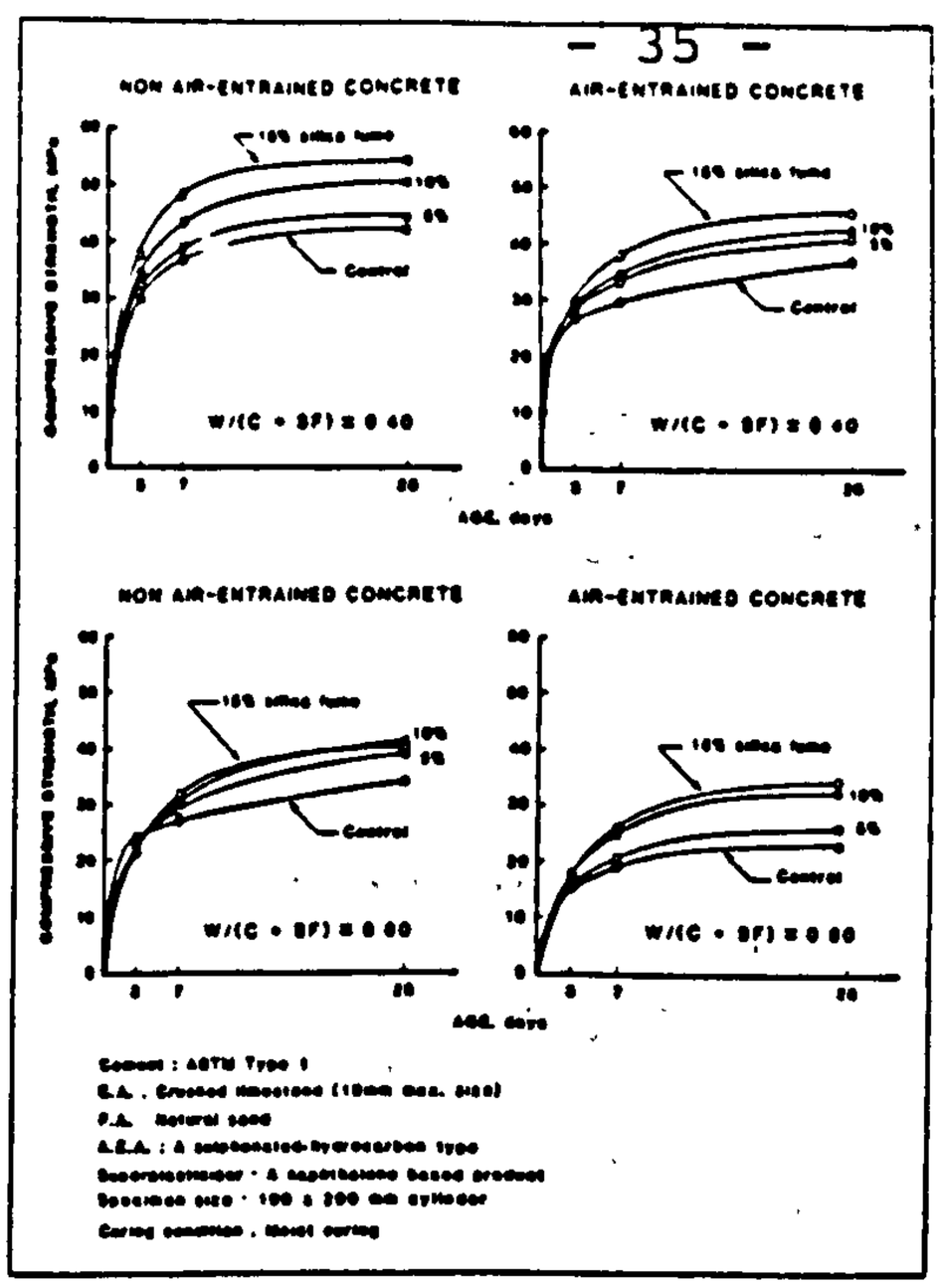

Figure 2.7 Relation between compressive strength and age for silica fume concrete made with W/(C + SF) of 0.40 and 0.60 (19)

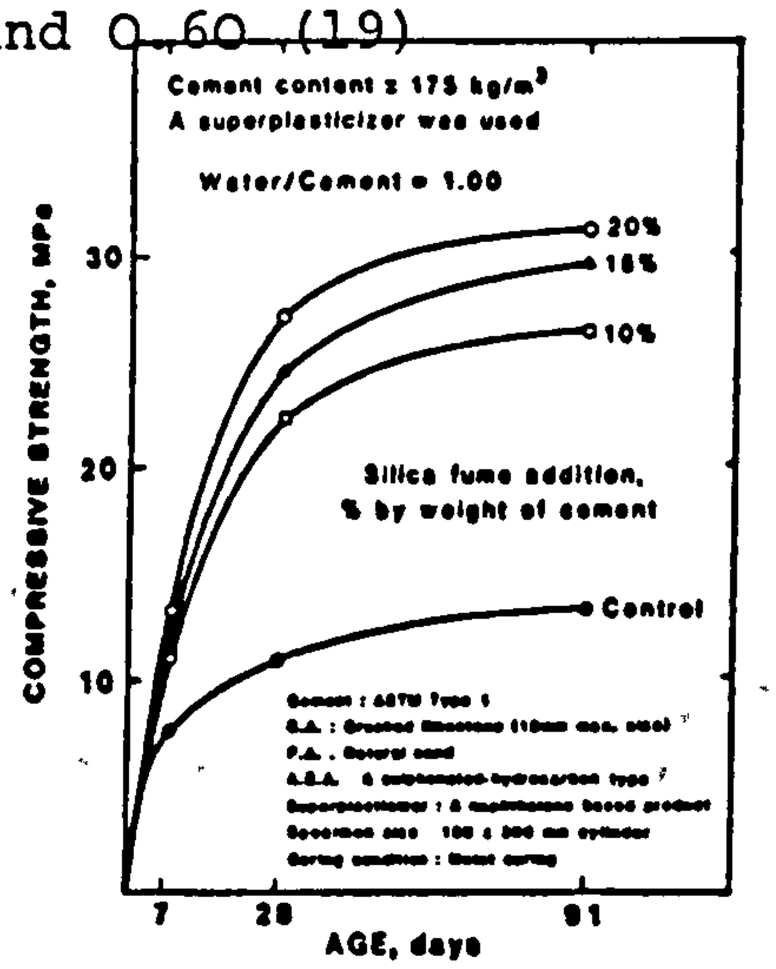

Figure 2.8 Relation between compressive strength and age for concrete incroporating various percentages of silica fume as an addition to cement (21)

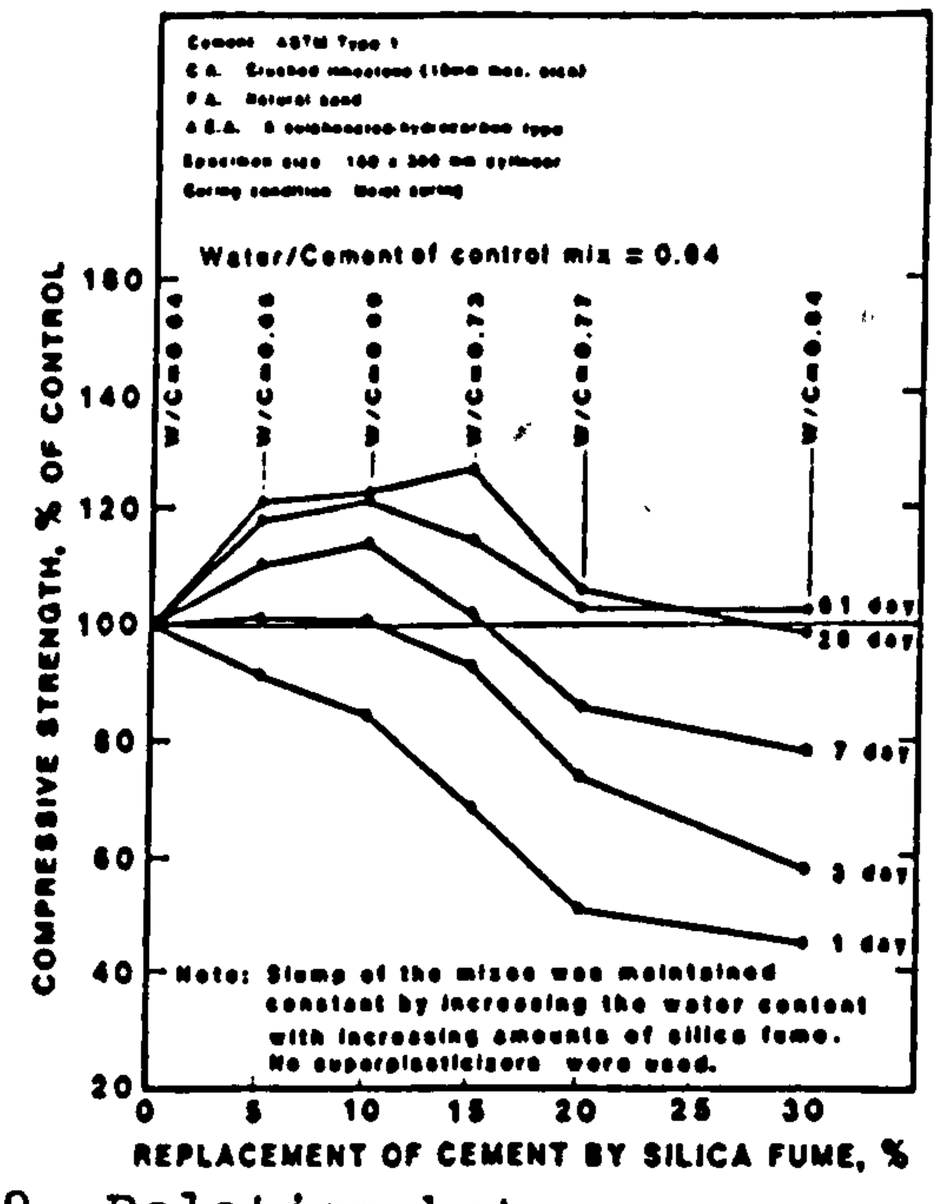

Figure 2.9 Relation between compressive strength of concrete and dosage of silica fume (W/C) 0.64 (4)

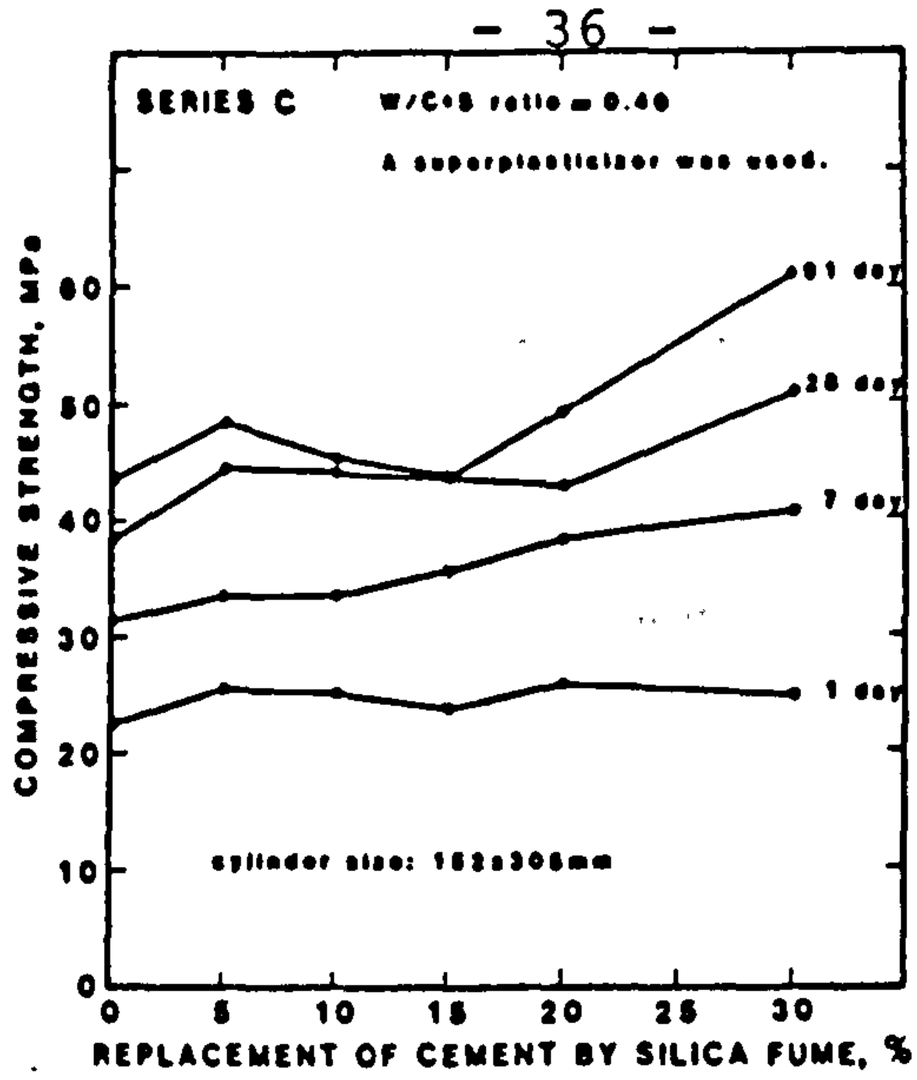

Figure 2.10 Effect of replacement of cement by silica fume on compressive strength for Series C. (4)

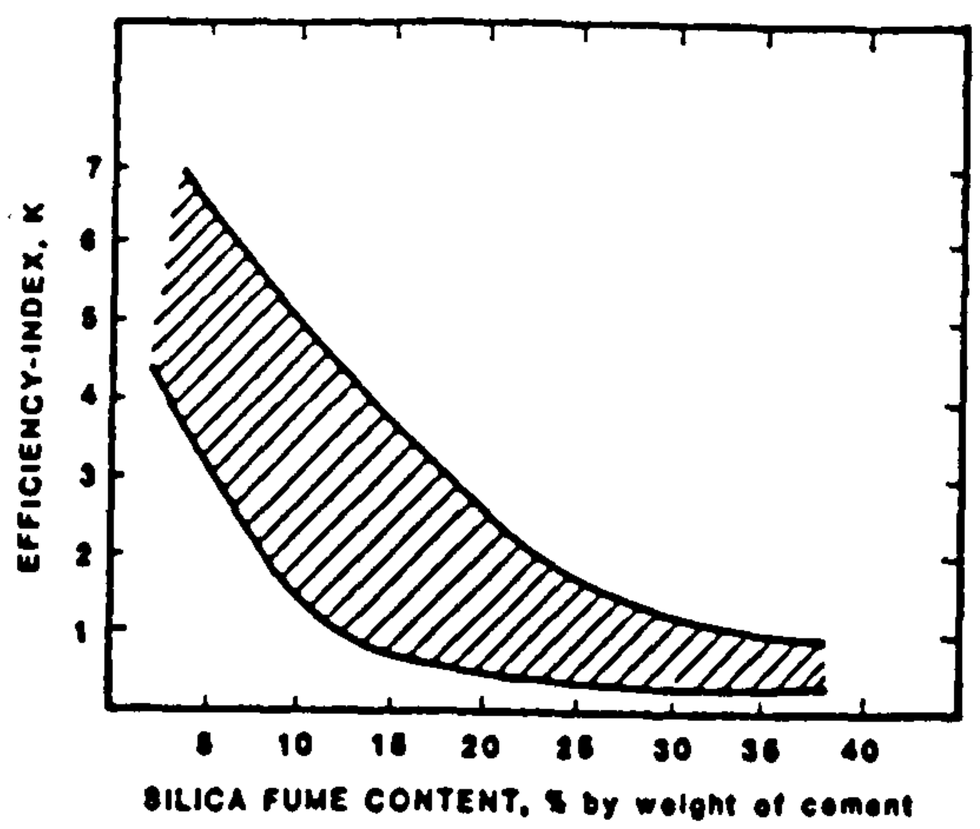

Figure 2.11 A generalized relation between efficiency index and silica fume content of concrete (24)

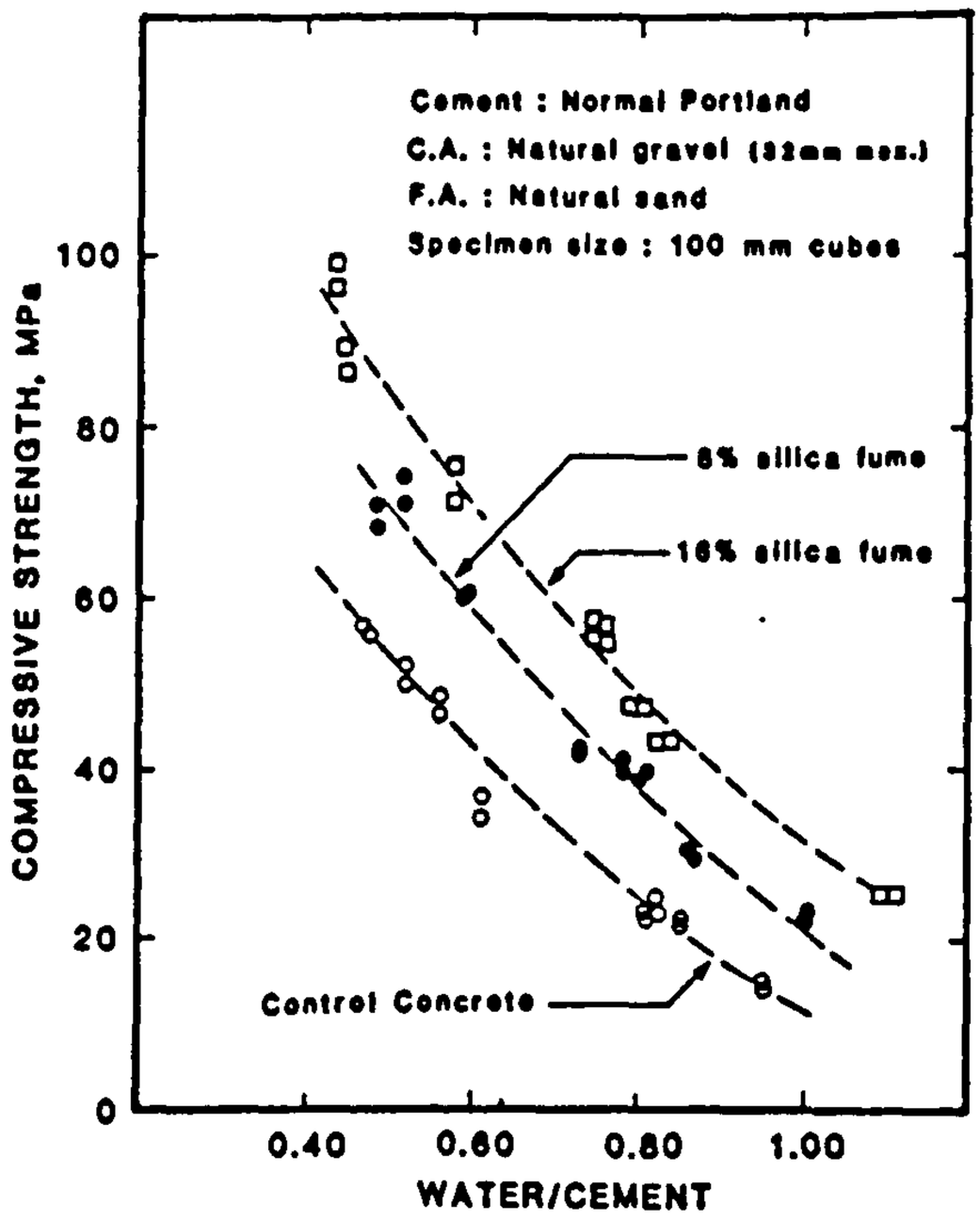

Figure 2.12 Relation between compressive strength of silica fume concrete and W/X ratio. (7)

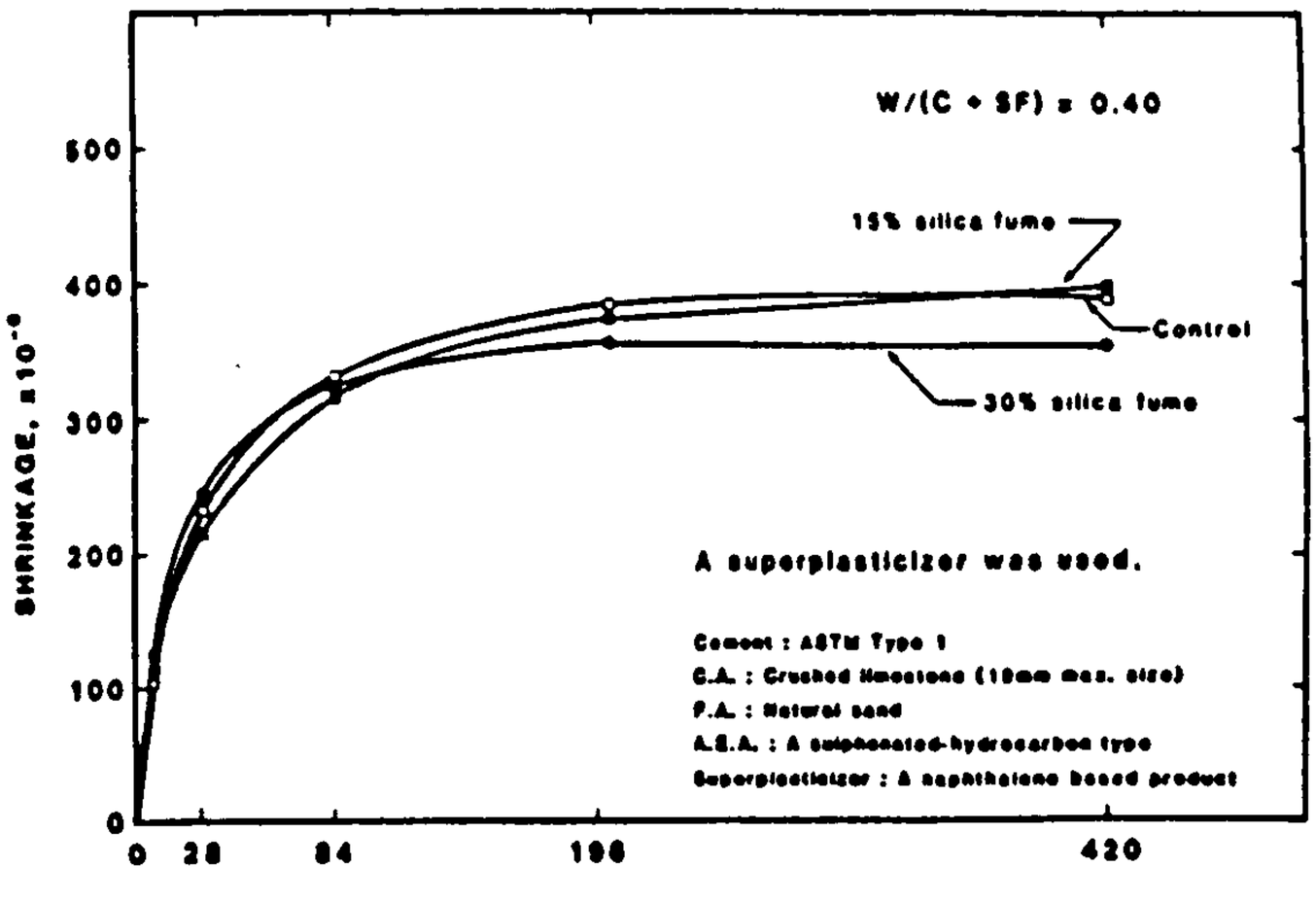

Figure 2.13 Relation between shrinkage and duration of drying for concrete W/(C + SF) 0.40. (31)

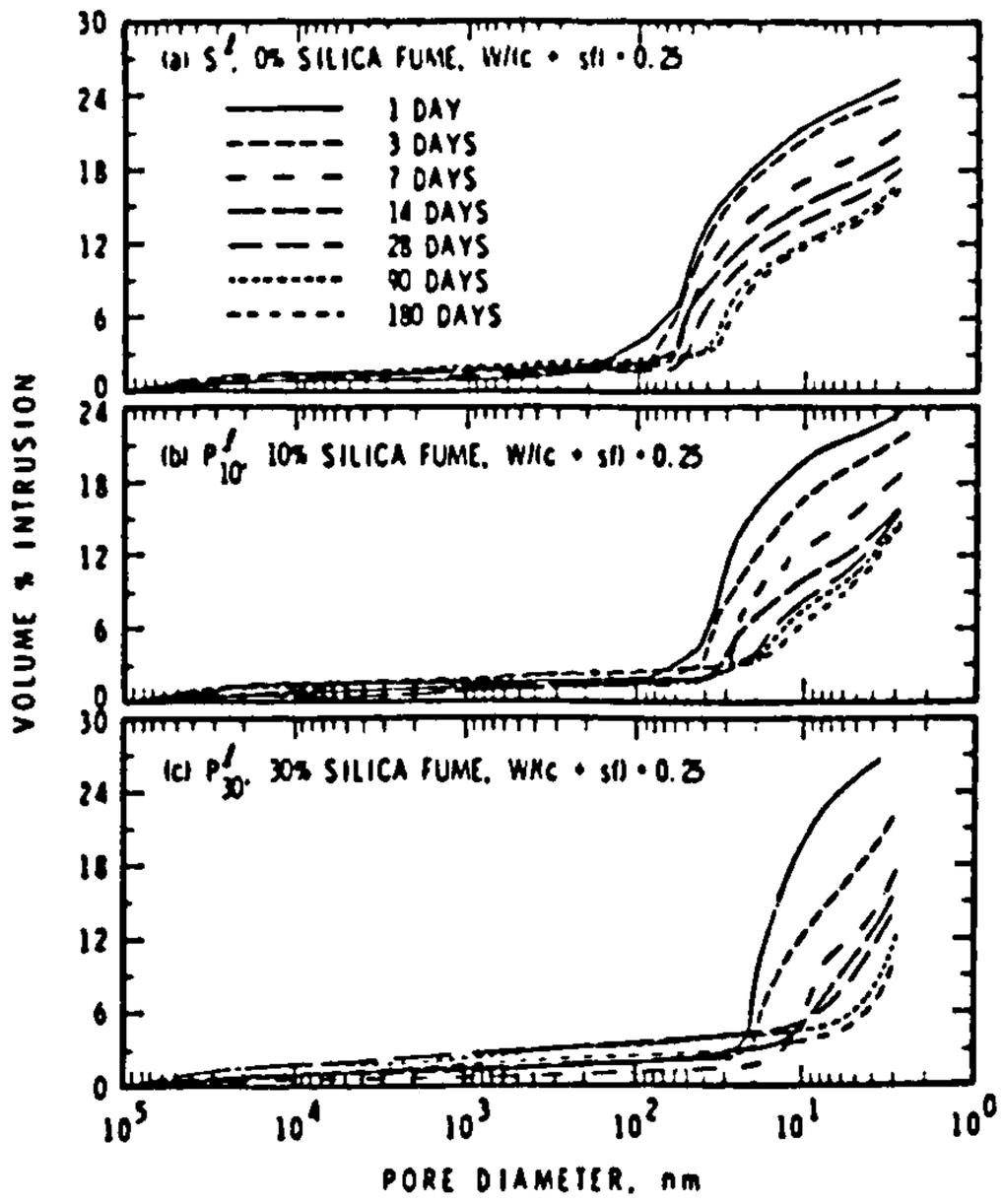

Figure 2.14 Pore-size distribution curves of cement pastes with different silica fume contents W/(C + SF) - 0.25 (a) 0% silica fume, (b) 10% silica fume (c) 30% silica fume (47)

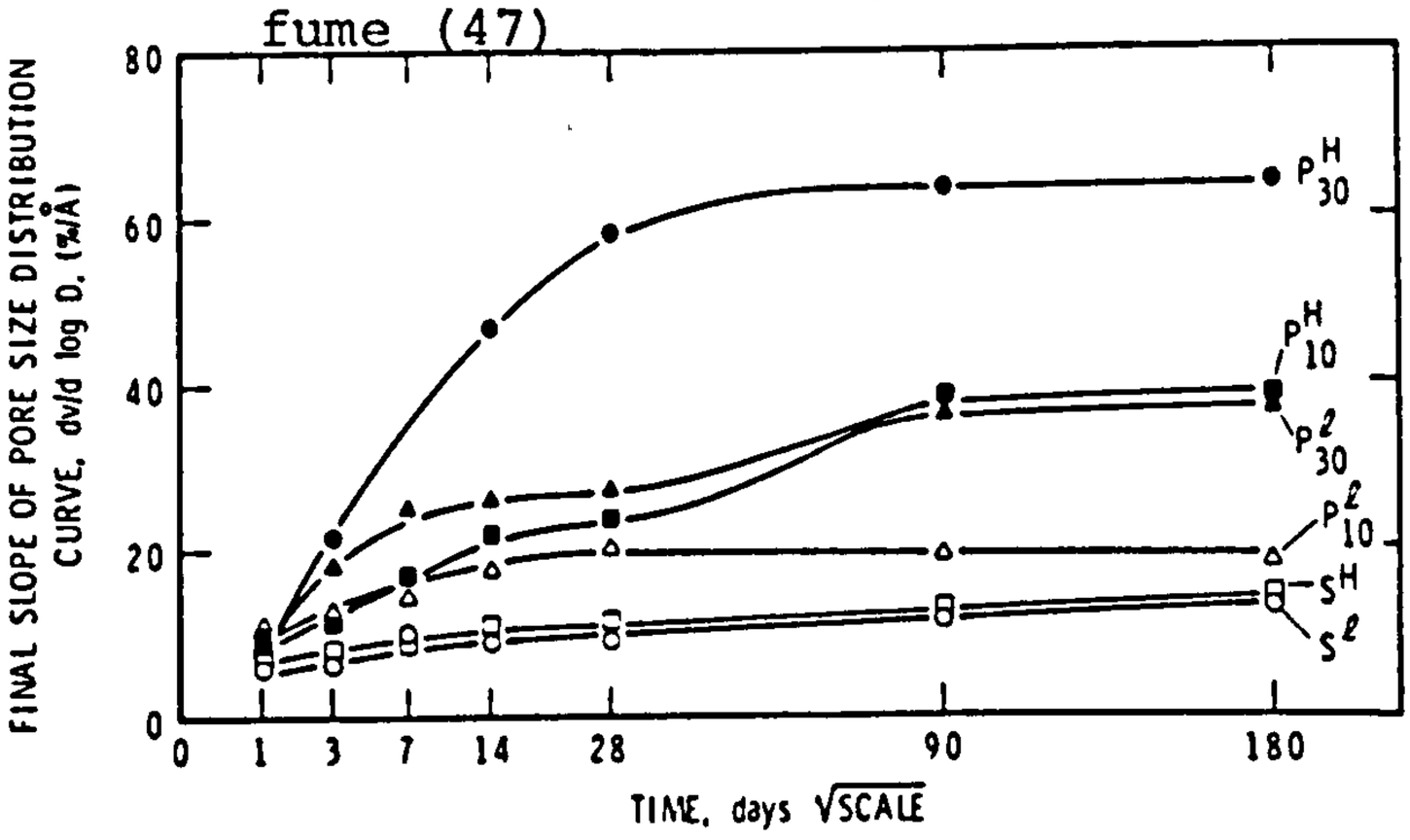

Figure 2.15 Slope of mercury intrusion curve at maximum pressure and $Ca(OH)_2$ content vs. hydration time for silica fume blends. (47)

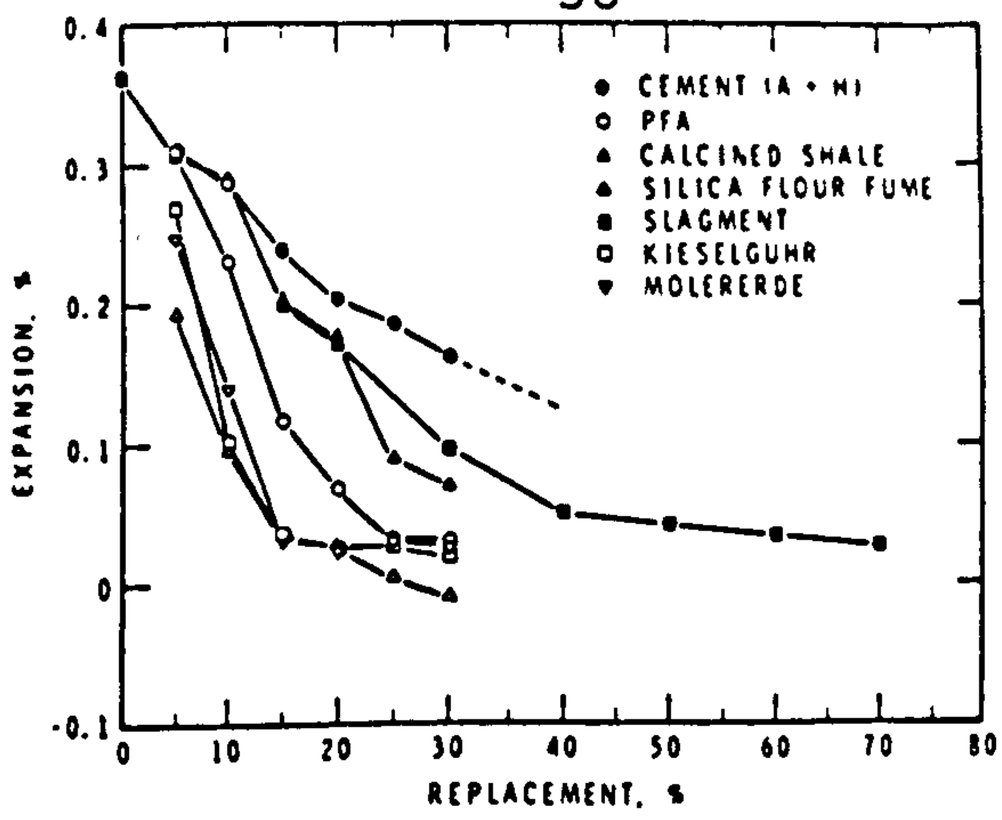

Figure 2.16 Effect of replacing cement H (0.97% Na_2O) with increasing amounts of cement A (0.16% Na_2O) or various mineral admixtures on the linear expansion of mortar prisms stored at 38°C for 555 days. (60)

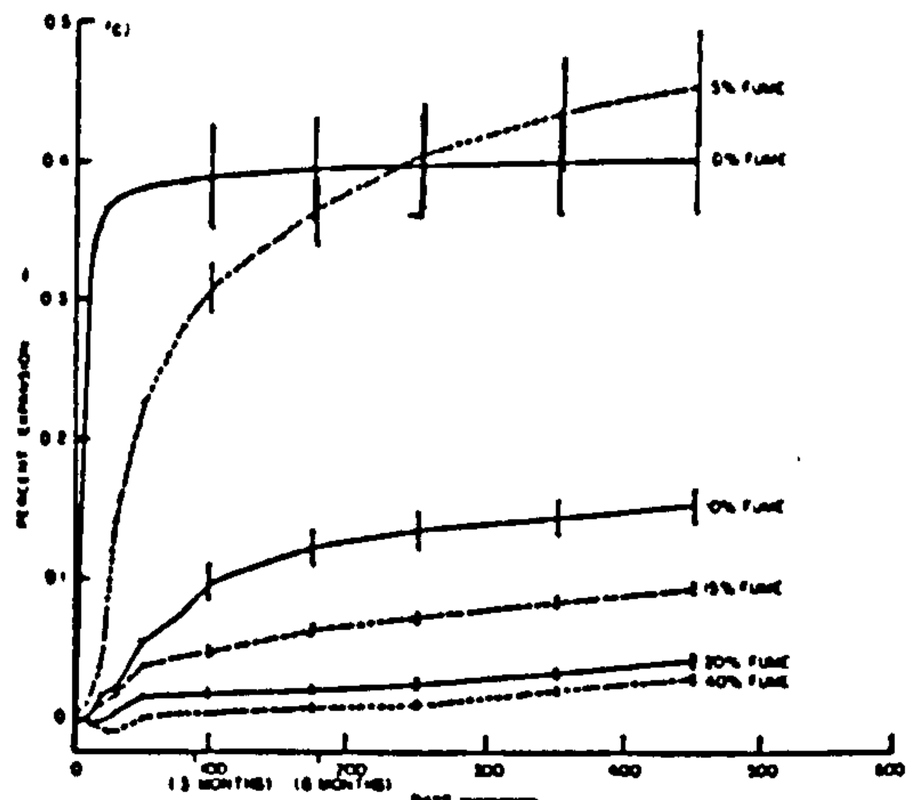

Figure 2.17 Expansion of mortar bars containing 4% opal and increasing amounts of silica fume (50°C, 100% RH (62)

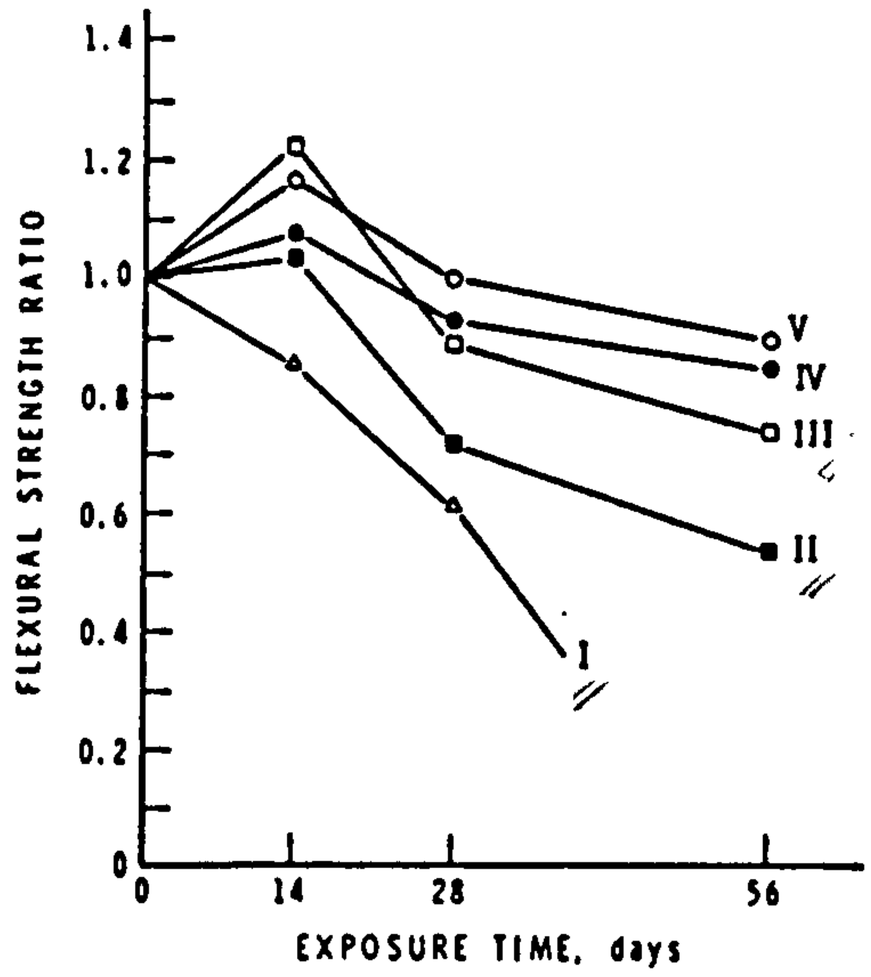

Figure 2.18 Ratio of flexural strength of corroded to uncorroded mortars with various additives, as a function of exposure time in Na_2SO_4 solution. (i) Portland Cement, (ii) No. I + 45% slag, (iii) sulfate resisting cement (iv) I + 10% silica fume (v) No.II + 10% silica fume (22)

CHAPTER THREE

HOT WEATHER CONCRETING

3.1 Introduction

In recent years there has been a rapidly expanding construction programme in the Middle East. However, it has unfortunately become apparent that defects are present in most classes of concrete ranging from unsightly blemishes to serious failures. Problems in the Middle East mainly arise in three categories: climate, geology and workmanship (69). Details of these categories are given in Table (3.1).

This chapter will focus on the effect of Middle Eastern climatic conditions in terms of temperature and humidity on the fresh and hardened properties of concrete together with the effect of soil and goundwater on the performance and durability of concrete. The necessary precautions that should be considered during mixing, transporting, placing and curing of concrete are also considered.

3.2 Hot weather elements

3.2.1 Air temperature

In hot countries, the temperature often rises to 50°C in the shade mainly during the months of May, June, July and August. The mean maximum temperature in the summer day time can be as high as 45°C and the mean minimum in the night time can be 25°C. Thus a variation in the ambient temperature of up to 20°C can occur within 24 hours, which when combined with exposure to about 11 hours of direct sunlight, can cause several problems. High ambient temperatures can raise the temperature of concrete ingredients to an unacceptable level. On mixing, concrete temperature will be high enough to cause quick stiffening which prevent satisfactory compaction and result in a porous permeable concrete. High ambient temperature can increase the rate of surface evaporation giving rise to possible risk of plastic shrinkage cracks.

3.2.2 Relative humidity

The term relative humidity is defined as the ratio of water vapour available to the amount of water needed to reach saturation. The lower the relative humidity, the higher the capacity of air to absorb moisture from available sources including concrete. Shirley (70) reported that a decrease in relative humidity from 90% to 50% without change in any other conditions will increase fivefold the rate of evaporation of water from the exposed surfaces.

3.2.3 Solar radiation

Solar radiation can affect the properties of concrete because it heats up the concrete ingredients, reinforcements, formwork and construction equipment. Eventually it can result in rapid loss of workability, rapid hydration and stiffening. During hardening, solar radiation can cause further evaporation of water from the exposed surfaces, giving rise to a possible risk of plastic shrinkage cracks.

3.2.4 Wind velocity

The effect of high winds on both fresh and hardened concrete should not be underestimated. An increase in wind speed results in an increase in the rate of water evaporation leading to a reduction in concrete workability and difficulty in compaction. Shirley (70) reported that water evaporation at a wind velocity of 15 and 40 km/hour is 4 to 9 times that in still air. The exposed surfaces of hardened concrete may also be attacked by salts deposited by the wind. Salts carried by winds can also be deposited on the aggregate resulting in a high salt content within the concrete unless precautions are taken.

3.2.5 Overnight temperature

In general the temperature will drop during night time and this drop is more pronounced in areas remote from the sea. The drop in temperature has both beneficial and harmful effects on the concrete and its ingredients. Stored materials will lose some of the heat gained during the day as

will the mixing plant, but the reduction in temperature may seriously affect the unprotected concrete in the early stages of hardening. The concrete at this time is immature and will develop little resistance to induced stresses. If the concrete is unprotected, its surface will lose heat to the cool night time environment and contract. In mass concreting, the concrete surface will cool down and contract during the night more rapidly than the inner core, which will induce tensile stresses in the surface which may lead to cracking.

3.3 Effect of hot weather on the properties of fresh concrete

3.3.1 Introduction

Scanlon (71) has summarised the following effects often exhibited by fresh mortars and concrete cured in a hot climate:

a. Increased water demand for a required consistency;
b. Increased rate of slump loss;
c. Increased rate of setting;
d. Increased tendency for plastic shrinkage cracking; and
e. Increased difficulty in controlling entrained air content.

A number of papers on these effects have been published. Unfortunately, the conclusions are often conflicting. This may result from the fact that only a few papers have been concerned with the combined effects of ambient humidity, wind velocity and radiation on the properties of fresh concrete. For example, surface water evaporation (which may cause plastic shrinkage cracks when its rate exceeds the rate of bleeded water) is different for the same piece of concrete conditioned under hot-humid and hot-dry environments. The rate of surface water evaporation under a hot-dry environment is higher than a hot-humid one. Consequently, the tendency to have surface plastic shrinkage cracks is higher under hot-dry than the hot-humid environment.

3.3.2 Rate of evaporation

High rates of evaporation of water from concrete are enhanced by high concrete temperature, high ambient air temperature, low relative humidity and high wind speed (72). Figure 3.1 shows the combined effect of the above factors on the rate of surface evaporation. According to the American Concrete Institute (ACI) precautionary measures are mandatory when evaporation rate exceeds 0.98 kg/m^3 hours to prevent plastic shrinkage cracks and loss of strength in the concrete near the surface. Such precautions may include: casting at a lower environmental temperature, erecting wind breakers, reducing the time between production and placement and providing adequate curing.

The effect of different environment conditions on the rate and amount of evaporation from fresh mortar and concrete surfaces was investigated by Berhane (73). The results showed that in a hot humid climate, evaporation is 3½ times lower than in a hot moderate climate and 7½ times lower than in a hot dry environment (Figure 3.2). Moreover the higher the W/C ratio, the higher the amount and rate of evaporation measured for the first 24 hours after casting as shown in Figure 3.3.

Shalon and Ravina (74) found the water evaporation controlled by the combined effect of both temperature and humidity together under hot climates. Their water evaporation measurements on 12 cm thick specimens showed that evaporation at 20°C/45% R.H and 40°C/70% R.H. is practically the same, while at 30°C/20% R.H. evaporation is considerably higher than at 40°C/70°R.H.

3.3.3 Setting time

Cement hydration, like many other chemical reactions is accelerated by heat and the rate of hydration is likely to double for every 10°C increase in temperature (75). Thus high temperatures accelerate the setting of concrete as shown in Figure 3.4, where an increase in temperature from 15°C to 30°C halved the time of initial set (76).

The American Concrete Institution (77) stated that both temperature and cement type effect concrete setting time as shown in Figure 3.5.

The influence of high temperature on the setting time of cement was confirmed by Berhane (73) who studied the effect of temperature on the heat of hydration. He found that the heat generated at early ages was greater at elevated temperatures than at normal temperatures and, since setting time and the heat of hydration are closely related, this agrees with the earlier findings of the American Concrete Institute.

One way to counteract the rapid setting caused by elevated temperatures is to use set-retarding admixtures in concrete, whose efficiency depends on the compatability of the cement and admixture.

For example, set-retarders appear more effective with cement that has lower alkali and (C_3A content (78)).

3.3.4 Workability

The process of compacting concrete consists of the elimination of any entrapped air bubbles and in doing so, two types of friction have to be overcome. These are the internal friction between the individual particles and the external friction between the concrete and the surface of the mould. Since the internal friction is an intrinsic property of the mix, workability may be defined as "the property of concrete which determines the amount of useful internal work necessary to produce full compaction". (79).

Due to the fact that hot environments increase the evaporation rate of water and decrease the setting time of cement, workability of the concrete is likely to be impaired in a hot dry environment. It has been reported by Klieger (80), Shirley (70) and Orr (81) that the temperature of freshly mixed concrete has a significant effect on workability and the amount of water necessary to maintain slump. Klieger reported that an increase of 11°C in concrete temperature may be expected to decrease the slump by 2.5cm. Moreover, the amount of water necessary to increase slump by

25 mm at 50°C was found to be 33% greater than that at 20°C. (Figure 3.6). Similar results were reported by Shirley and Orr. It is interesting to note that Klieger (80) found the workability of ASTM type III cement (high early strength) mixes to be unaffected by the high concrete and ambient temperature up to 50°C, whereas the same conditions show a significant effect on the workability of ASTM type I & II cement mixes. Klieger could not give an explanation of the above behaviour.

Throughout their experimental work carried out in the Negev desert to investigate the effect of hot environment in terms of air temperature and humidity, on different properties of concrete, Shalon & Ravina (74) monitored the workability of concrete by measuring the slump and V.B time. They found that temperatures up to 40°C at relative humidities ranging between 20% and 70% have no measurable effect upon the slump value and only little effect upon the V.B value. The effect was considerable only at 50°C and relative humidity of 20°, though not at 50°C and 45% R.H. Moreover, they found that slump remained almost constant for about 20 minutes under the rather severe environmental conditions of 50°C and 40% R.H. Their findings have thus not confirmed the generality of the established opinion by Klieger (80) and Shirley (70). They nevertheless suggested that, although they used a similar type of cement to that of Klieger, the cement composition which is known to influence setting rate, could have been different. Sample size could be another factor in explaining such behaviour. It is understood that Shalon & Ravina's samples (74) were bigger than those used by Klieger (80).

The increased rate of concrete slump loss can be counter-balanced by softening its consistency during or after delivery by the addition of a suitable material. Such material can be water, water reducing admixture, cement paste or any combination of these. This procedure is called retempering (78).

Retempering with water is not the best practice because it increases the original W/C ratio and reduces the

quality of concrete (36). Nevertheless, it may be tolerable because of its simplicity, provided that the increased W/C ratio is still below the specified limit. Using an initial slump higher than the required final slump to compensate for expected slump loss when prolonged delays are encountered is not advisable. Experiments have shown that the retempering of concrete will result in a higher total W/C ratio when there is initially a higher slump value than when there is a lower slump value (82).

A better result can be obtained by retempering with superplasticizer. It was reported by Ramakrishnan et al (83) that the slump of retempered concrete both with and without superplasticizer decreased about equally with time. Nevertheless, large increases in slump can be maintained for several hours by repeated retempering with superplasticizers (Figure 3.7), without impairing strength. Ramakrishnan also drew the following conclusions:

(a) The slump loss is proportional to the initial slump level. The total span during which concrete could be kept workable is however, longer for concrete with higher slump;

(b) About 60 to 80 percent of the slump of control and retempered control concrete is lost in 60 to 90 minutes;

(c) The ability of the superplasticizer to keep the concrete workable is reduced as the number of retemperings is increased;

(d) Repeated dosage of superplasticizer causes a loss in entrained air; and

(e) The properties of hardened retempered concretes such as compressive strength are not adversely affected.

Malhotra's (84) work supports the conclusions drawn by Ramakrishnan. Moreover, he found that both the size and character of the changes in concrete properties caused by such retempering with superplasticizer are a function of the type of superplasticizer used. Contrary to the findings reported by Ramakrishnan and Malhotra in which both conventional and superplasticized concrete slump decreased

about equally with time, Ravina (85) and Previte (82) found that slump loss in superplasticized concrete is higher than with the control concrete made without any admixtures.

The high rates of workability loss and the use of additional water to restore workability (the most common practice in the Middle East) can be considered to be amongst the most important problem facing concreting in the Middle East. This is because the addition of extra water will result in an increase in water/cement ratio leading to a reduction in the strength and, most important, the durability of concrete.

3.3.5 Heat of hydration

The measurement of heat evolution is particularly suitable for the investigation of the early stages of hydration. The effect of curing temperature on the intensity of hydration, reflected by the heat of hydration, can be seen in Figure 3.8, which shows that changes in the hydration process appear at a temperature of about 25°C (76).

The initial temperature of concrete ingredients can contribute to the final temperature of fresh concrete and eventually influences both the rate of cement hydration and liberated heat. The higher the initial concrete temperature, the greater the heat released by cement hydration and the greater will be the peak temperature within the concrete body. As an approximation role it may be assumed that rate of a chemical reaction is approximately doubled for every 10°C increase in the temperature of the reactants. And a reduction of 1°C in the temperature of fresh concrete can reduce the peak temperature by 1.5°C (79).

High rate of initial cement hydration and liberated heat can increase the rate of setting and reduce the time necessary for proper compaction. Eventually this can result in a low strength due to both high porosity due to improper compaction and early cessation of cement hydration caused by the precipitation of hydration products in the vicinity around cement particle forming an encapsulating layer preventing the continuation of cement hydration.

3.3.6 Bleeding

Bleeding can be defined as the tendency for water to rise to the surface of freshly placed concrete, due to the settlement of solid constituents. This results from the inability of the constituent materials in the concrete to hold all the mixing water while they settle down. (36).

The bleeding capacity of concrete and its rate depends upon the following:

(a) The physical properties and chemical composition of the cement;

(b) Physical properties of fine aggregate (especially those smaller than a 150 rm (No-100) BS sieve));

(c) Aggregate/cement ratio;

(d) Specific gravity of the solids;

(e) Viscosity of water and its quantity available;

(f) Depth of concrete; and

(g) The temperature of concrete.

As a result of bleeding the W/C ratio in the top portion of the concrete increases which tends to produce porous, weak and non-durable concrete. Also water rising to the top surface of concrete may carry with it the fine particles of unhydrated cement and the very fine particles of sand which weaken the top portion and form a weak film, called "laitance". If laitance is formed at the top surface of a slab a porous and dusty surface will result.

In hot weather, the rate of the evaporation of water from the surface of concrete is increased by high ambient temperature, low humidity, high wind velocity and sometimes by the direct sun rays. Hence the rate of bleeding becomes less but the total bleeding capacity is probably unaffected (36). Attention therefore, needs to be paid to controlling the bleeding rate and capacity.

3.3.7 Early age volume changes and cracking

Early (86, 87) volume changes in freshly mixed concrete are due to absorption by dry aggregate, bleeding, cement hydration and finally thermal changes. Furthermore,

volume changes are affected by the ambient conditions such as high temperatures and low relative humidity.

The main factor is the bleeding of free water which starts very shortly after the concrete has been placed and continues until further compaction is prevented by aggregate interference or by setting of concrete. This change in volume is called "plastic shrinkage", since it takes place while concrete is still in its plastic condition. Under normal climatic conditions, this type of shrinkage does not necessarily impair the quality and durability of concrete. However, excessive plastic shrinkage is usually associated with hot weather concreting and may result in cracks. These cracks appear when water evaporation from the freshly placed concrete is greater than the rate at which the concrete can bleed water to the surface (86). ACI stated that when the rate of evaporation is expected to exceed 0.98 kg/m^2/hour, plastic shrinkage cracks are likely to appear. Therefore, precautionary measures to reduce that rate should be considered.

Most of the researchers agree that the rate of evaporation of water from the surface of fresh concrete is the most important factor influencing plastic shrinkage cracks. This is confirmed by Ravia & Shalon (88) who have studied this phenomenon under hot weather conditions, However, they reported that plastic shrinkage cracking is not a direct function of water loss, evaporation rate or shrinkage, but is a function of the tensile stresses and strength of fresh concrete mortar. i.e. plastic shrinkage cracks occur only when the tensile stresses produced by shrinkage exceed the tensile strength of the fresh mortars or concrete. Moreover, plastic shrinkage cracks did not appear under severe evaporation conditions in semiplastic mortars, while plastic and wet mortars of the same dry mix cracked severely. This was because the former mix showed the lowest shrinkage and highest tensile strength.

The above authors (74) investigated the effect of early exposure to sun versus shade on plastic shrinkage cracking. They found that slabs cast and exposed in the

shade (evening casts) developed more cracks than those cast and exposed in the sun. Van Dijk (89) confirmed these findings. He reported that concrete cracked when tested with infra-red lamps off, did not crack when the lamps were on. The reason was that strength increased under the infra-red lamp more than the stresses generated by shrinkage.

3.4 Effect of hot weather on the properties of hardened concrete

3.4.1 Compressive strength

At normal temperature about 20% of cement hydrates in 2-3 hours, while at 40°C, 30 to 40% may hydrate in 2 hours (90). The rapid increase of the initial rate of hydration due to high curing temperature can lead to the expectation that the early age strength will consequently be higher, a trend most researchers agree upon (77, 80, 91, 92). Figure 3.9 shows clearly the effect of curing temperature on the one day compressive strength of Portland cement concrete (91). As the temperature increased, there was an increase in the one day compressive strength, a trend also confirmed by Price (92), Klieger (80) and Verbeck & Helmuth (91).

In spite of the above stated general agreement on the effect of high curing temperature on the early age strength, there is some disagreement as to the effect of both curing and fresh concrete temperature on the compressive strength at later ages. There seem to be two main schools of opinion. The first believe in the continuing beneficial effect of high curing temperature on the late-age as well as the early-age strength. This school is supported by Albassia and Alam (93). Berhane (94) and Jaegerman and Gluklich (95). The second school considers high curing temperatures to be harmful to the late-age strength, and is supported by Shalon & Ravina (74), Klieger (80), PCA Bulletin (96), Bloem (97), Grynor et al (98), Verbeck & Helmuth (91), Ridgley (99) and Price (92).

Albassia and Alam (93) studied the compressive strength of concrete prepared and cured under controlled hot environment of 45°C and a field hot environment of 40°C in

comparison to a moderate lab condition of 24°C. Results showed that concrete cured in a hot environment can have at least the same strength at 28 days as that cured under moderate temperature. Consequently they concluded that costly precautions would not be necessary for hot weather.

Berhane (94) found that the effect of elevated curing temperature on the late-age strength of mortar depend on the period of curing under a hot environment. These data showed that the strength of mortar cast and exposed to hot humid environment for 24 hours is increased at early-age. However, this did not defect the late-age strength as shown in Figure 3.10. Although prolonged exposure to hot-humid environments up to 28 days adversely affected the late-age strength, Figure 3.11, there is an indication that mortars or concrete exposed to a hot-humid climate for its life might attain a strength equal to or even higher than that cured under normal conditions.

Jaegerman and Gluklick (95) investigated the effect of exposure of fresh concrete to high evaporation (in a wind-tunnel, mostly at 40°C/30% R.H. and 20 km/hr W.V) on its properties. Exposure varied from 1 to 22 hours, after which all specimens were water cured at 20°C up to 28 days, and then stored at 20°C and 50% R.H. until it was tested. Results indicated that specimens exposed to evaporation beyond 3.5 hours shows a reduction in strength in the order of 10-25%. No further significant reduction in strength was observed within the interval of 3.5 to 22 hours of evaporation.

Shalon and Ravina (74) studied the effect of mix and curing temperature on the 56 day compressive strength of concrete. Concretes with mix temperatures of between 30-40°C were water-cured for seven days on site then left uncovered for seven more days on site before transfer to the laboratory where they were left uncovered. The temperature and relative humidity of the laboratory was 20°C and 70% R.H.

Also similar concretes were water cured for seven days in the laboratory and then kept uncovered until testing.

They found that the strength of those concretes kept initially on site were 8-15% lower than those continuosuly kept in the laboratory.

Klieger (80) found that the accelerating effect of high temperatures above 23°C on the early-age strength gain will, however, reduce the late strength of the concrete (Figure 3.12). Moreover, he reported that there is an optimum casting and curing temperature for strength development. For cement ASTM type I and II without accelerator this optimum is 12.5°C. For cement ASTM type III without accelerator the optimum is 5°C. Using calcium chloride as an accelerator, this optimum temperature appears somewhat lower. Similar results have been reported in PCA Bulletin (96) and Bloem (97).

Grynor et al (98) investigated the effect of raising concrete temperature from 18°C to 35°C on the strength of plain, plasticized and PFA modified concrete. The work extended to measure the effect of temperature on the amount of cement and water necessary to provide a certain workability and compressive strength. They found that increasing the concrete temperature from 18 to 35°C had a harmful effect on the 28-day compressive strength of plain concrete. However, using plasticizing agent or PFA can reduce that effect, (see Figure 3.13). The cement content necessary to restore the strength was increased by 4/7 kg/m^3.

Helmuth and Verbeck (91) reported results of concrete cast at different temperature ranging from 13 to 46°C, moist cured at the casting temperature for the first 24 hours, and then kept at the same temperature for 28 days. Their results emphasise the harmful effect of high curing temperature on the late-age strength. Ridgley (99) found that the compressive strength of concrete at 28 days manufactured in Lagos at an average temperature of 30°C and relative humidity of 70-87% was 15% lower than that of similar concrete moist cured at 23°C.

Price (92) found that concrete cast, sealed and maintained in a temperature range between 4 to 40°C for two

hours, shows a progressive loss in strength with the increase of mixing tmeperature, Figure 3.14.

The literature indicates the agreement among all the researchers working in this field on the beneficial effect of curing temperature on the early-age strength. However they disagree on the late-age strength. This disagreement can be partially attributed to the fact that the cement composition used by various researchers could have been different resulting in a totally different strength development behaviour.

3.4.2 Drying shrinkage and creep

It is worthwhile mentioning shrinkage and creep of the hardened concrete as both of these deformation mechanisms are based on drying and other moisture movements and also because they play an important role in the cracking of concrete which is difficult to remedy.

Drying shrinkage of concrete is caused principally by the loss of water and the consequent contraction of hardened cement gel. Since moisture loss is the underlying cause of drying shrinkage, the relationship between the two is of interest. Figure 3.15 shows a typical shrinkage-weight loss curve for cement paste; five approximately linear domains are observed. Domains (1) and (2) have been attributed to the loss of water from capillary pores. Domain (3) represents loss of adsorbed water from the surfaces of C-S-H particles. Domain (4) results from the loss of water that contributes to the structure of C-S-H. And domain (5) is due to the decomposition of C-S-H. (100).

Among the factors that influence the shrinkage of concrete and mortars are the water content, W/C ratio, aggregate content, curing regime and curing time, and specimen geometry. As far as the magnitude and rate of drying shrinkage is concerned, it is the last two factors which dominate the rate of drying shrinkage.

Drying conditions relate to both the temperature and humidity of the curing environment. The effect of these two factors is well illustrated by Figures 3.16 & 3.17, which

show that the higher the curing temperature and the lower the relative humidity, the faster the rate of drying shrinkage. In this study the initial rate of shrinkage was found to affect the ultimate shrinkage magnitude. The faster the initial rate of shrinkage, the lower the magnitude of shrinkage at later times.

In hot-dry environments where a high air temperature is coupled with low air humidity, it might be expected that the initial rate of drying shrinkage will be high and consequently yield a lower total shrinkage.

Grynor et al (98) examined the effect of raising concrete temperature from 18 to 35°C on the different properties of concrete. They found that raising concrete temperature leading to greater mixing water had no effect on drying shrinkage.

The influence of temperature on creep has become of increased interest in connection with the use of concrete in the construction of prestressed concrete nuclear pressure vessels. Neville (36) reported that the rate of creep increases with temperature up to about 70°C when at least for a 1:7 mixture with W/C ratio of 0.6, it is approximately 3.5 times higher than that at 21°C. Between 70 and 96°C the rate drops to 1.7 times the rate at 21°C.

3.4.3 Permeability

Permeability of concrete plays an important role in durability as it controls the rate of entry of moisture that may contain aggressive chemicals and the movement of water during heating or freezing. Thus permeability can be regarded as a direct measure of durability.

Neville (36) suggested that the importance of eliminating continuous capillary pores might be regarded as a necessary condition for a concrete to be classified as good. Thus it is not the bulk porosity inside the concrete body that is important, but the size, distribution and continuity of the pores.

Concrete permeability is influenced by many factors such as, degree of hydration, W/C ratio, aggregate, curing

type and duration, the properties of cement used and curing environment. As far as this review is concerned, the effect of hot environment on concrete and mortar permeability will be discussed with reference to the limited work in this field, which has concentrated on the consistency and strength of concrete.

The effect of temperature (27 and 60°C) on the permeability of Portland cement pastes was studied by Goto and Roy (101). They found that the permeability of specimens cured at 60°C was greater than those cured at 27°C. This was found to hold true for all the W/C ratios they used, i.e. 0.35 & 0.45, see Figure 3.18. This behaviour was explained as being due to the increase of coarse pores generated by the effect of high curing temperature.

High permeabilities caused by high curing temperatures were explained by Bakker (102). He stated that temperature affects both the amount of gel formed and its locality and therefore it influences the permeability. At a temperature of 20°C, the hydration products of an OPC paste are well dispersed resulting in a more effective closure of the capillaries and a lower permeability, see Figure 3.19.

3.4.4 Porosity and pore structure

Porosity and, more importantly, its distribution in hardened cement paste and mortars have been widely investigated in the last fifteen years as strong evidence of their influence on some cement mechanical properties has been demonstrated. The structure of hardened cement paste is generally held to consist of two types of pores, namely capillary and gel pores. Capillary pores are classified as having a diameter of the order of 13 A° whereas gel pores are much smaller; between 0.0015 to 0.002 rm in diameter (36). Recently Winslow and Diamond (103) described the pore structure of hardened cement paste (using the mercury intrusion porosimetry) as being composed of a threshold diameter (a diameter below which intrusion proceeds at a high rate and which is determined by the diameter below which the differentiated volume starts increasing sharply) and several

families of pores. The latter are described as macro or capillary porosity, micro or C-S-H gel porosity and mesoporosity (porosity between particulate hydration products). Macroporosity is composed of pores greater than a few thousands Angstroms microporosity is composed of pores narrower than a few hundred Angstroms.

The quantity of these pores in the cement matrix is influenced by many factors such as degree of hydration, W/C ratio, type of cementitious material used, age, curing and environmental conditions in terms of temperature and humidity. As far as this review is concerned, the effect of temperature and relative humidity on the bulk porosity and pore size distribution will be discussed.

Groto and Roy (101) examined the effect of curing temperature (27 & 60°C) on the porosity of Portland cement pastes. They used two methods namely evaporated water and mercury intrusion porosimetry. They found that the total porosity (measured by the evaporated water method) of the samples cured at 60°C was less than those cured at 27°C (Figure 3.20). Yet the mercury porosimetry method revealed that capillary porosity was increased from 36% to 56% of the total porosity as the curing temperature was increased from 27 to 60°C. Moreover, on the pore size distribution Figure 3.21, one peak at 75-140 A° range and no pores larger than 4300 A° in radius was found in specimens cured at 27°C. While the sample cured at 60°C had two peaks at 75-140 A° and at 1400-2300 A°.

The increase in the percentage of the coarse pores as a result of high curing temperature was explained by Bakker (102) as follows: at lower curing temperatures, the hydration products of Portland cement are better dispersed, resulting in a more complete blocking of the capillary pores (since hydration products occupy a volume more than twice the original volume of the cement paste (36)) than at higher temperatures.

The effect of curing temperature (29, 55, 71, and 84°C) on the pore size distribution of cement slurries at very young ages (from few minutes to one day of hydration)

has been investigated by Parcevaux (104). Results show that up to the setting time, the curing temperature is of little influence on cement pore size distribution except when it exceeds 80°C. Above 80°C, cement hydration proceeds at a higher rate and gives rise to macropores (capillary pores).

3.5 Hot weather concreting precautions

Hot weather poses special problems in concreting operations. Among these are greater mixing water demand; rapid drying resulting in reduced strength and cracking; stiffening of concrete mix before it can be properly consolidated; difficulty in controlling entrained air content and finishing difficulties caused by rapid drying. Those problems can be minimized by taking the following precautions (55, 56, 74, 79, 96, & 97).

3.5.1 Precautions during mixing

1. Control the temperature of concrete: This can be achieved by controlling the temperature of its ingredients. The effect of these ingredients on the final concrete temperature depends on their initial temperature, their specific heat and their quantity. A mathematical (88) approach using equations for estimating fresh concrete temperature can be utilized, which shows that a reduction in concrete temperature of 1°C requires a reduction of either cement temperature about (8°C), mixing water temperature about (4°C) or the aggregate temperature about (2°C). The aggregate and mixing water exerted the most pronounced effect on the temperature of concrete. Mixing water (70,87) has the greatest effect on concrete temperature since it has a specific heat about 4½ to 5 times that of cement and aggregate. The use of cool mixing water is very effective. Figure 3.22 shows the effect of mixing water at 7°C on the reduction of concrete temperature. The use of ice as a part of mixing water is the most effective in reducing concrete temperature since on melting alone

it takes up heat at the rate of 80 Cal/gm (Figure 3.23).

Aggregate also has a significant effect on concrete temperature since it represents the greatest portion of concrete. Thus measures should be taken to minimize its temperature. Different means can be used for this purpose, including providing shade and wetting the stock pile with water (70, 87).

Although cement temperature has little effect on concrete temperature, the maximum reasonable limit of cement temperature is around 75°C to avoid flash set.

2. The concrete should be mixed at the coolest possible temperature.
3. Mixing time should be kept to the minimum necessary for ensuring adequate concrete quality. This is because concrete can be heated up by the operation of mixing.
4. Mixers should be kept cool by painting them with white paint and spraying them from time to time with cold water.

3.5.2 Precaution during delivery and placing

1. The haul delivery distance and time should be the shortest possible. This is because a delay in placing freshly mixed concrete affects its workability and strength.
2. Use plasticizing and/or set-retarders admixtures where concrete is required to be transported for long distances.
3. Transport should be organized so that delay in the supply of concrete will not result in the formation of unwanted construction joints.
4. The waiting time to unload should be the shortest possible.
5. The placement should be ready for concrete as soon as it arrives. This means;
   a. The placing equipment must have adequate capacity.

b. The vibration equipment and labour should be adequate to consolidate the concrete quickly after placing.
c. Maintaining the rate of placement in difficult areas.
d. Arrangements should be made in advance to secure a standby crane or pump quickly in the event of equipment breakdown.

6. The placement should preferably take place during the coolest part of the day.
7. Concrete must be placed in its final position where it is required. The nearer the concrete is placed in its final position, the less the effort required for finishing will be, and the less the chance of segregation.
8. The cast layers should be shallower than those cast under moderate conditions to ensure good compaction and response to vibration and good bond with the layer below.
9. It is important to make sure that concrete is not placed in the forms faster than it can be properly consolidated.

Specification requirements (105, 106) indicate that the concrete should be placed within thirty minutes of discharge from the mixer and also that the concrete temperature when discharged should be within the range 5°C to 32°C.

3.5.3 Precaution during curing and protection

Since hot weather leads to more rapid setting and drying of concrete, curing and protection are far more critical than under cool weather conditions. The most substantial gain in strength and other desirable properties of concrete take place in the first few days immediately following the placing of fresh concrete. Thus the following should be provided where possible:

1. Immediate curing, as soon as the finishing operation is complete.

2. If membrane curing is used, the white-pigmented type is preferred to reflect the heat.
3. Use insulation during evening and night in environments where the temperature is expected to drop considerably at night.
4. Shade is preferable to protect the concrete from the direct sun rays and winds.
5. Whatever the method used for curing concrete in hot weather, it must satisfy the following basic requirements:
   a. It is necessary to ensure that the capillary water is either retained or replaced to enable the chemical reactions to continue.
   b. Curing must be maintained continuously for a time sufficient enough so that the concrete hardens to a degree that permits its safe use.

3.6 Summary and discussion of research work

There are many problems associated with concreting and concrete performance in the hot Middle East climates. High temperature results in increased water demand for workability, and also accelerates setting with the possibility of poor compaction and cold joints. Once the concrete is placed a high initial placing temperature accelerates the rate of hydration resulting in high early temperature rise. This, in turn, can increase the occurrence of early thermal cracking and whilst accelerating the early strength gain, may impair properties in the long-term. In terms of durability, the increased water and placing problems can lead to concrete with high permeability, resulting in the rapid ingress of salts or carbon dioxide, leading to corrosion of reinforcement.

The experimental data leads to the suggestion that there seems to be a curing temperature which may be considered as an optimum with regard to the late age strength. This temperature is found to be influenced somewhat by the cement type. For ASTM Type I and II Portland cement this temperature is 13°C; for type III it is 4°C (80).

However, other researchers (93) conclude that the maximum temperature may vary between 20-40°C.

The findings and conclusions of different researchers upon the effect of temperature on concrete long-term properties seem contradictory.

The research work, however, seems to lack the following:

1. Most of the experimental work was performed in laboratories on control specimens which were prepared and cured under controlled conditions. Such conditions are different from those on a typical construction site where the concrete is exposed to varying temperature daily. Therefore, unless the laboratory conditions are so controlled as to reasonably simulate the actual atmospheric conditions of hot weather, the results may be doubtful.
2. Curing is a term referring to the procedures for promoting cement hydration. The procedures consist of a control of temperature and of the moisture movement from and into the concrete. The availability of water (which is either replaced from outside or retained inside the concrete) is essential for the continuation of the hydration process. The hydration is known to cease if the relative humidity inside the capillary pores of concrete drops to below 80° (67). Temperature on the other hand is known to accelerate the hydration processes and reactions. Therefore, the curing period necessary to achieve certin strength and durability levels under hot environments need to be examined as there is a lack of information on this particular aspect.
3. Permeability has an important bearing on the vulnerability of concrete to chemical attack. Moreover, in the case of reinforced concrete, permeability of the concrete cover to water and air can control the corrosion of steel. Therefore, permeability can be considered as a key element in the durability of concrete. Unfortunately, there is

neither much information on the effect of hot environments nor the curing period on the permeability of concrete and mortars.

4. The majority of research work carried out has been devoted to the effect of high temperatures on compressive strength. Although the test for compressive strength of concrete is widely used as a quality control test, it is the increase in cement strength over the last 35 years (which results in a reduction in cement content necessary to achieve a certain strength) which brings into doubt the applicability of using this test, i.e. compressive strength, as a measure of durability and an indication of the efficiency of curing. This problem obviously can be aggravated in the Middle East by the effects of high tmeperature, low relative humidity and high wind velocity. Thus, investigation on the correlation between the compressive strength and the other durability related properties is very important and needs the attention of researchers.

5. In hot Middle Eastern countries, where the average temperature is often over 35°C during several months of the year, the inclusion of pozzolanic materials such as silica fume may show advantageous results in terms of strength and durability compared to plain Portland cement. Thus, information on how simulated hot environments and curing time can affect the short and long term properties of these modified concretes needs to be investigated urgently.

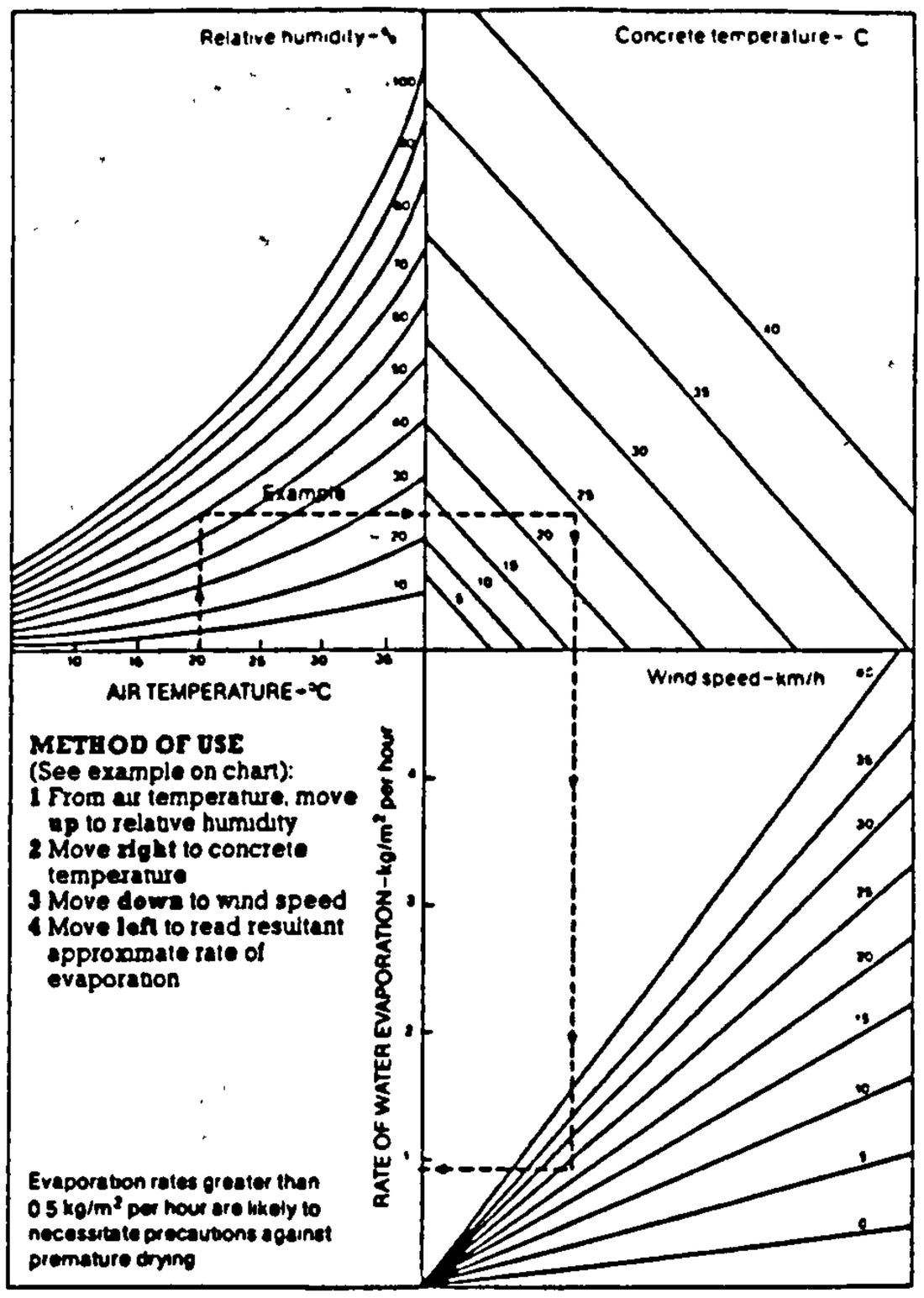

Figure 3.1 Effects of concrete and air temperatures, relative humidity, wind velocity on the rate of evaporation of surface moisture from concrete. (72)

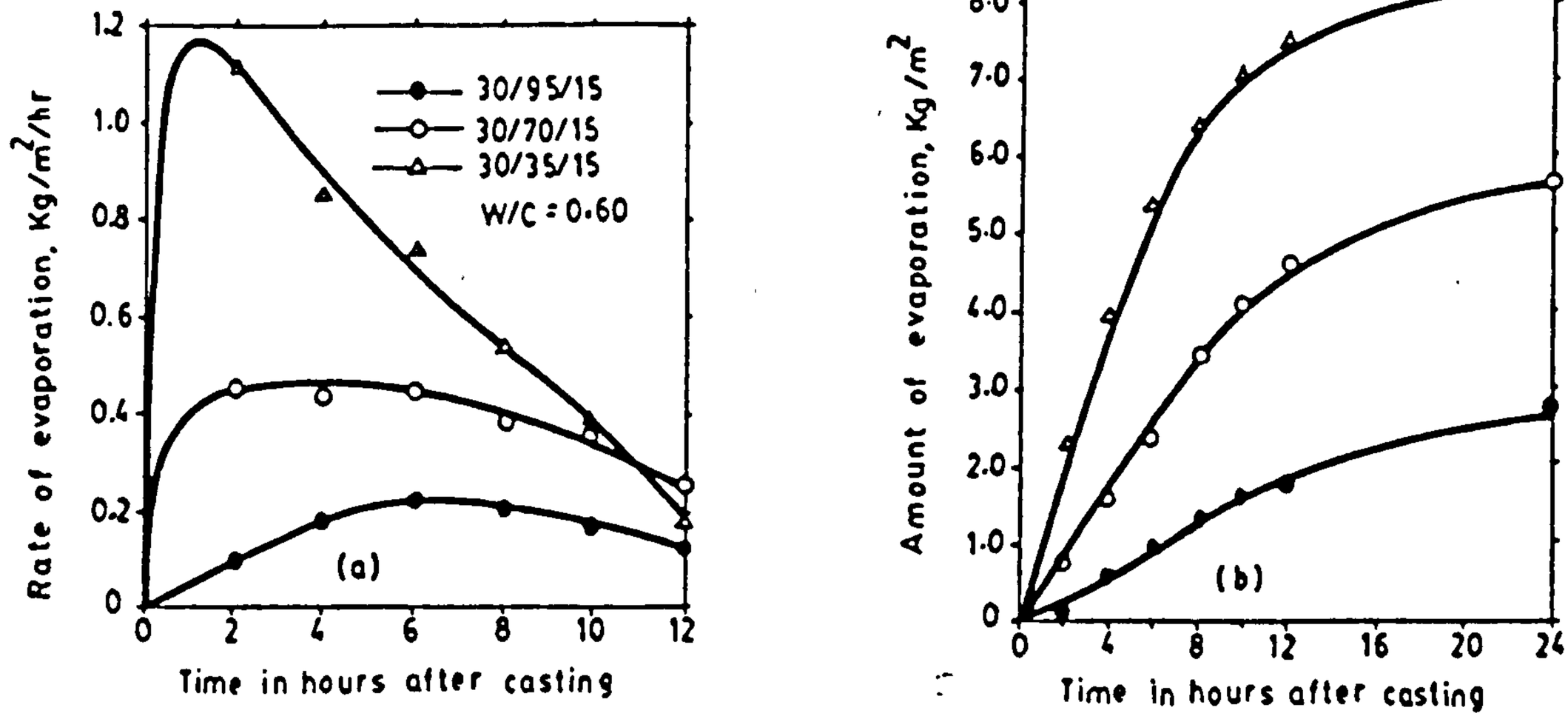

Figure 3.2 Effect of relative humidity on loss of water from fresh mortar. (a) Rate of evaporation and (b) amount of evaporation (73).

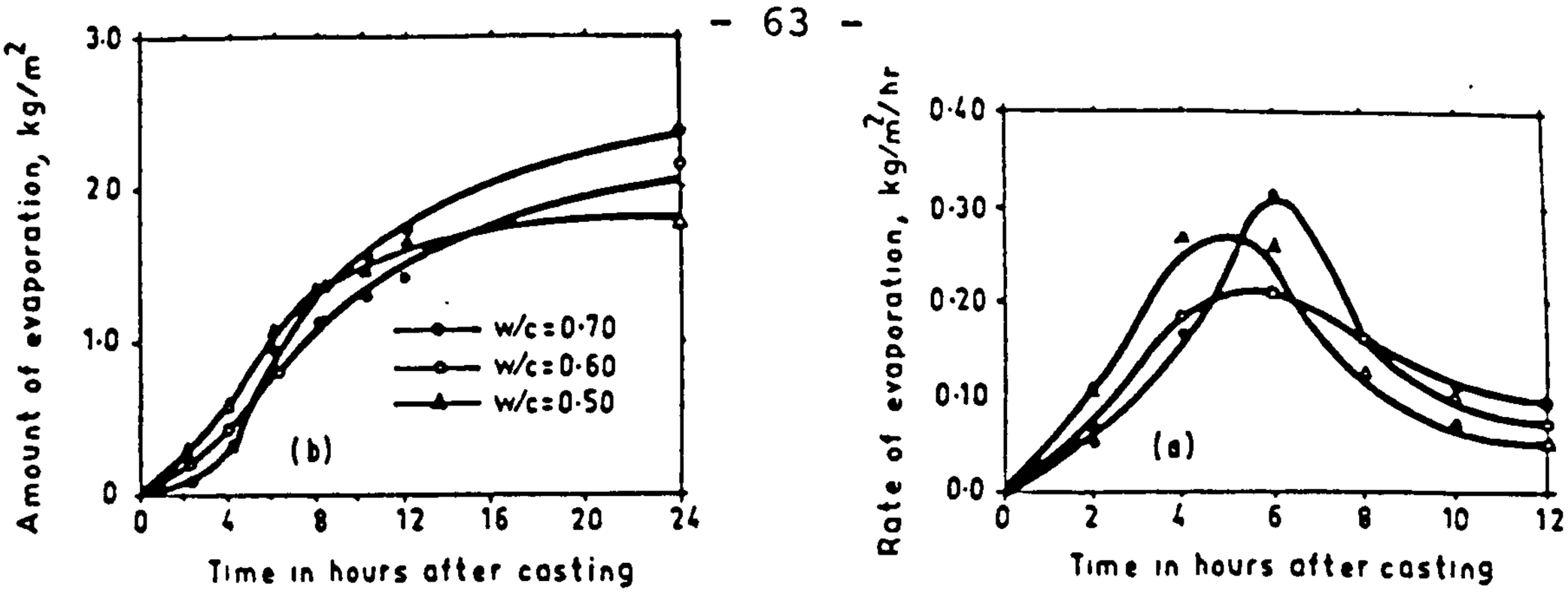

Figure 3.3 Evaporation-time relationship for different mortar mixes cast under and exposed to 40/95/0. (a) Rate of evaporation and (b) amount of evaporation (73)

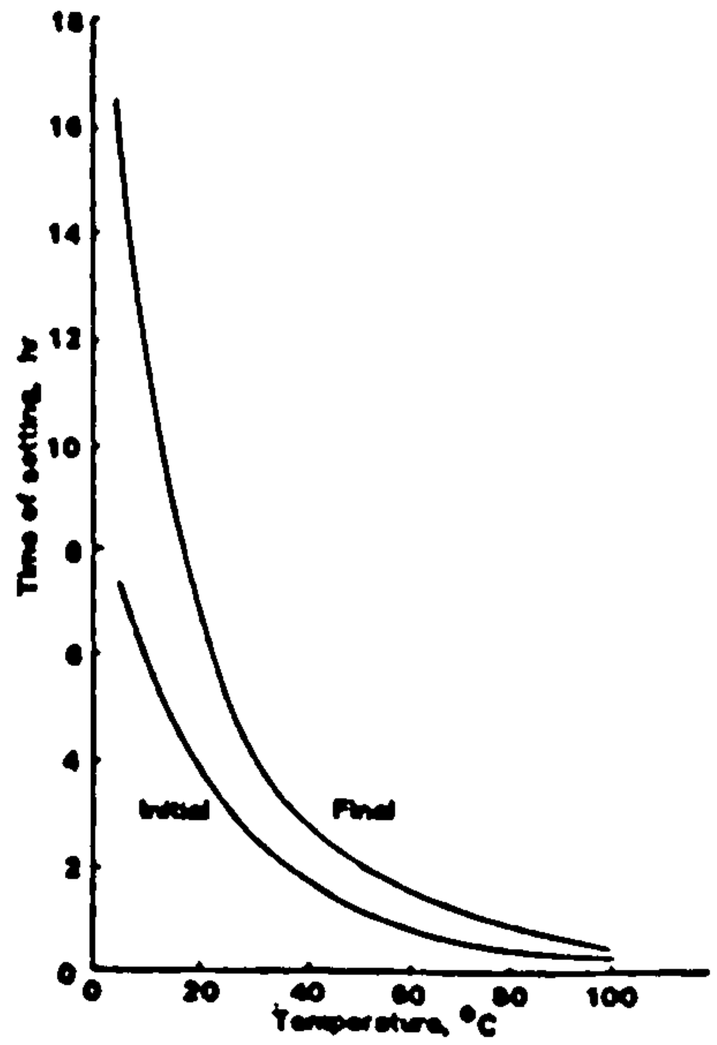

Figure 3.4 Effect of temperature on initial and final sets of Portland Cement mortar (mix proportion, 1:3 by weight. (76)

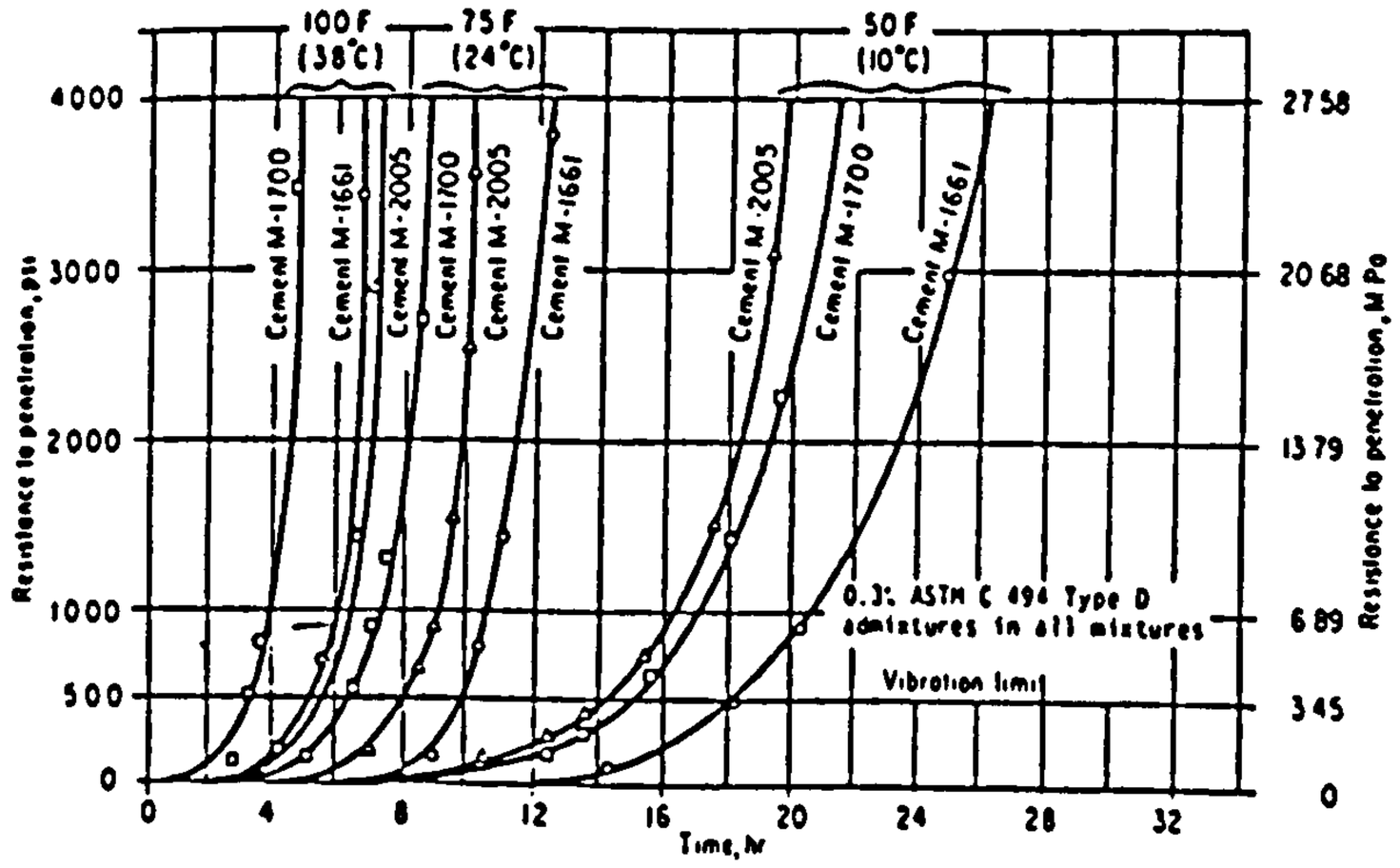

Figure 3.5 Temperature and brand of cement influence hardening characteristics of concrete mortars (77)

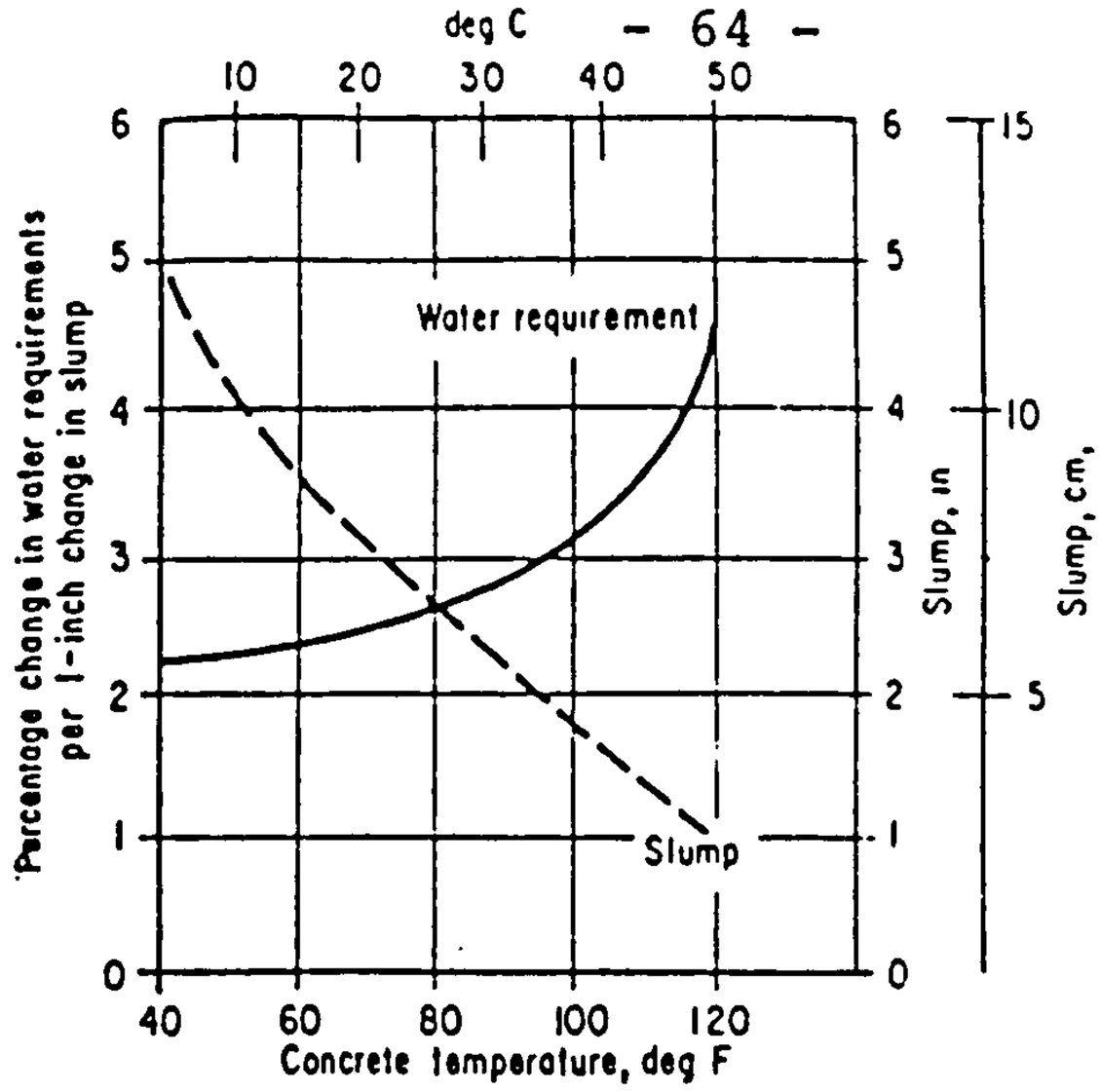

Figure 3.6 Effect of concrete temperature on slump and on water required to change slump (80)

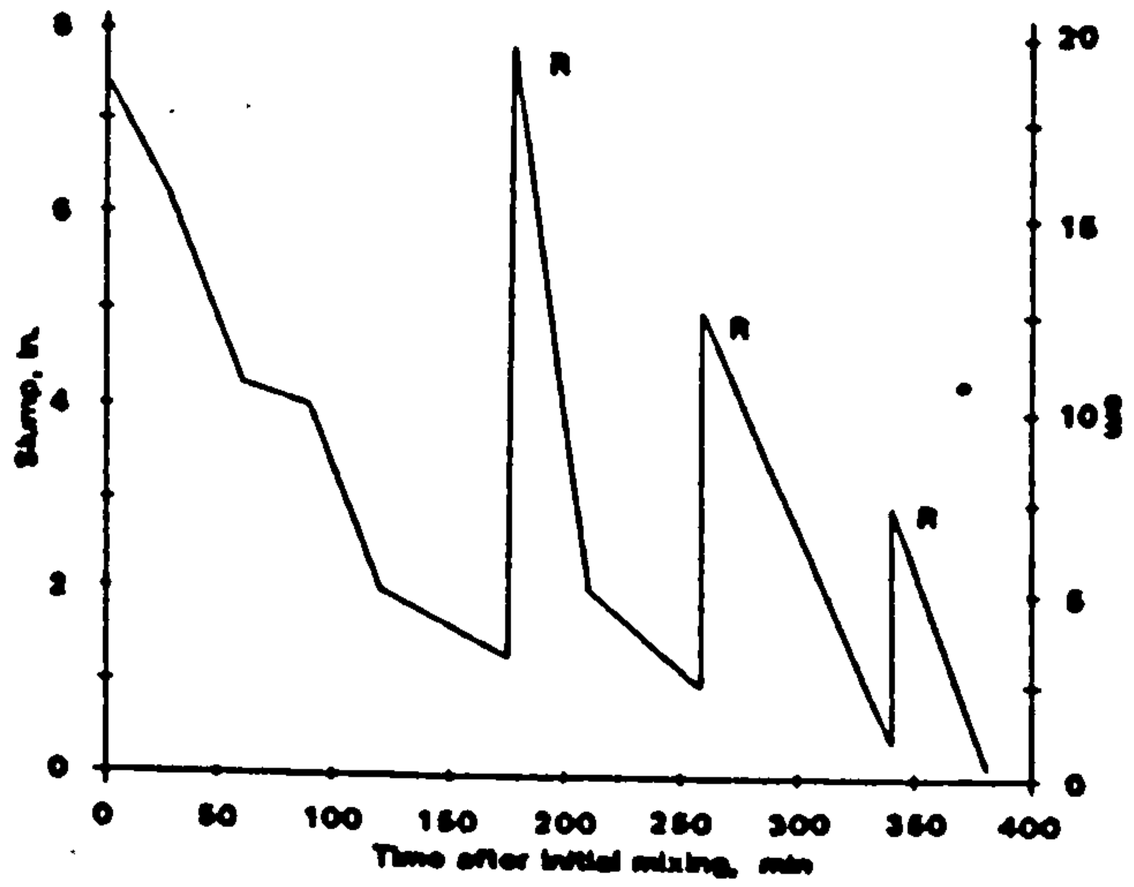

Figure 3.7 Slump-time retempering study. (83)

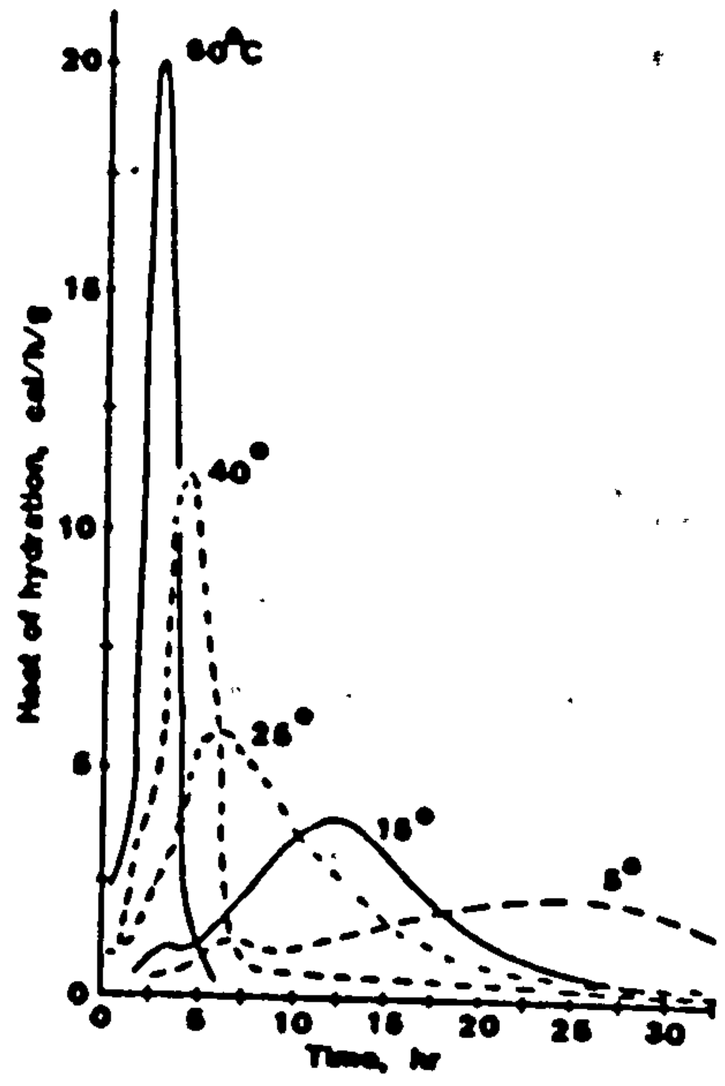

Figure 3.8 Hydration of tricalcium silicates: effect of temperature (76)

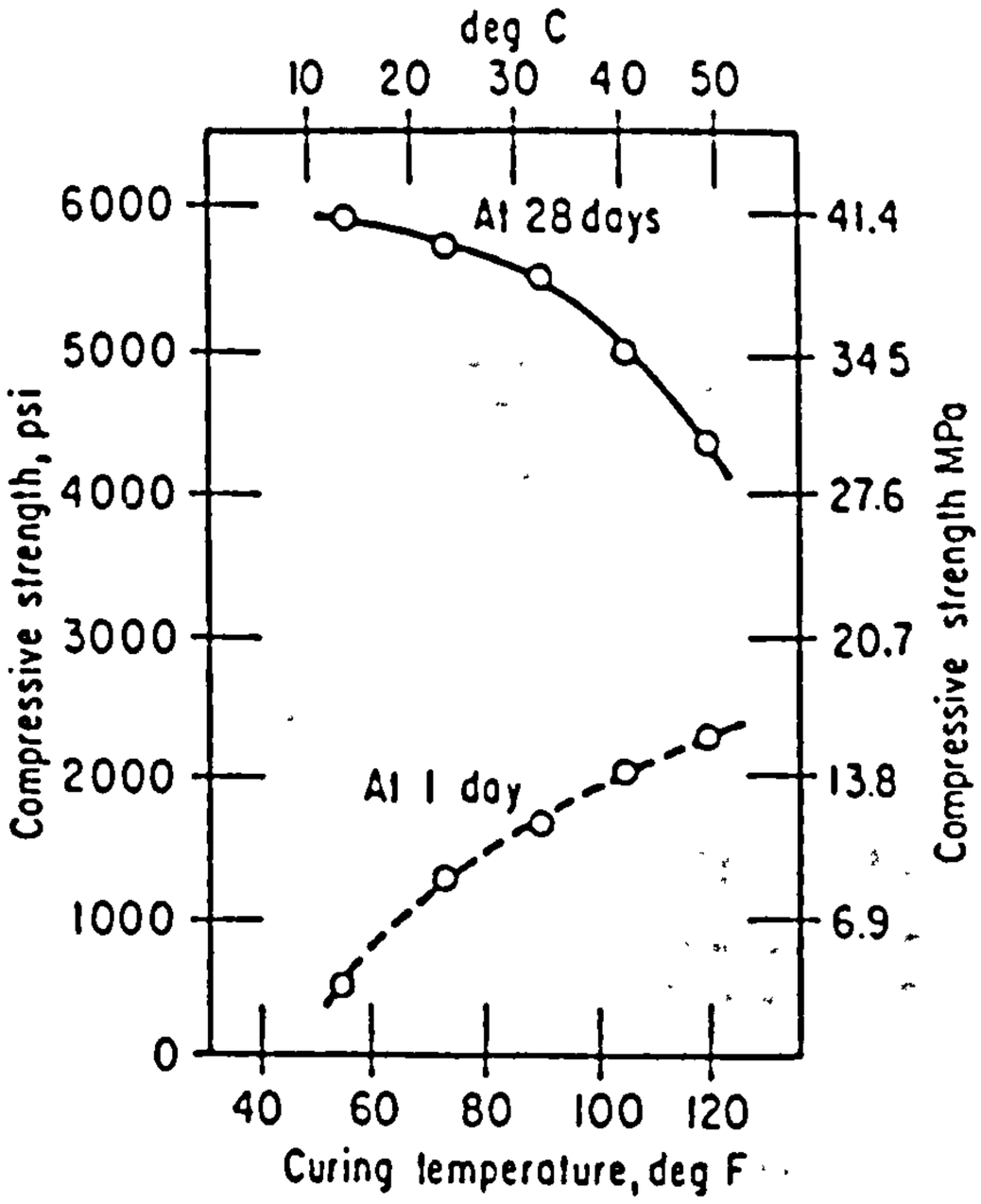

Figure 3.9 One-day strength increases with increasing curing temperature but 28-day strength decreases with increasing curing temperature (91)

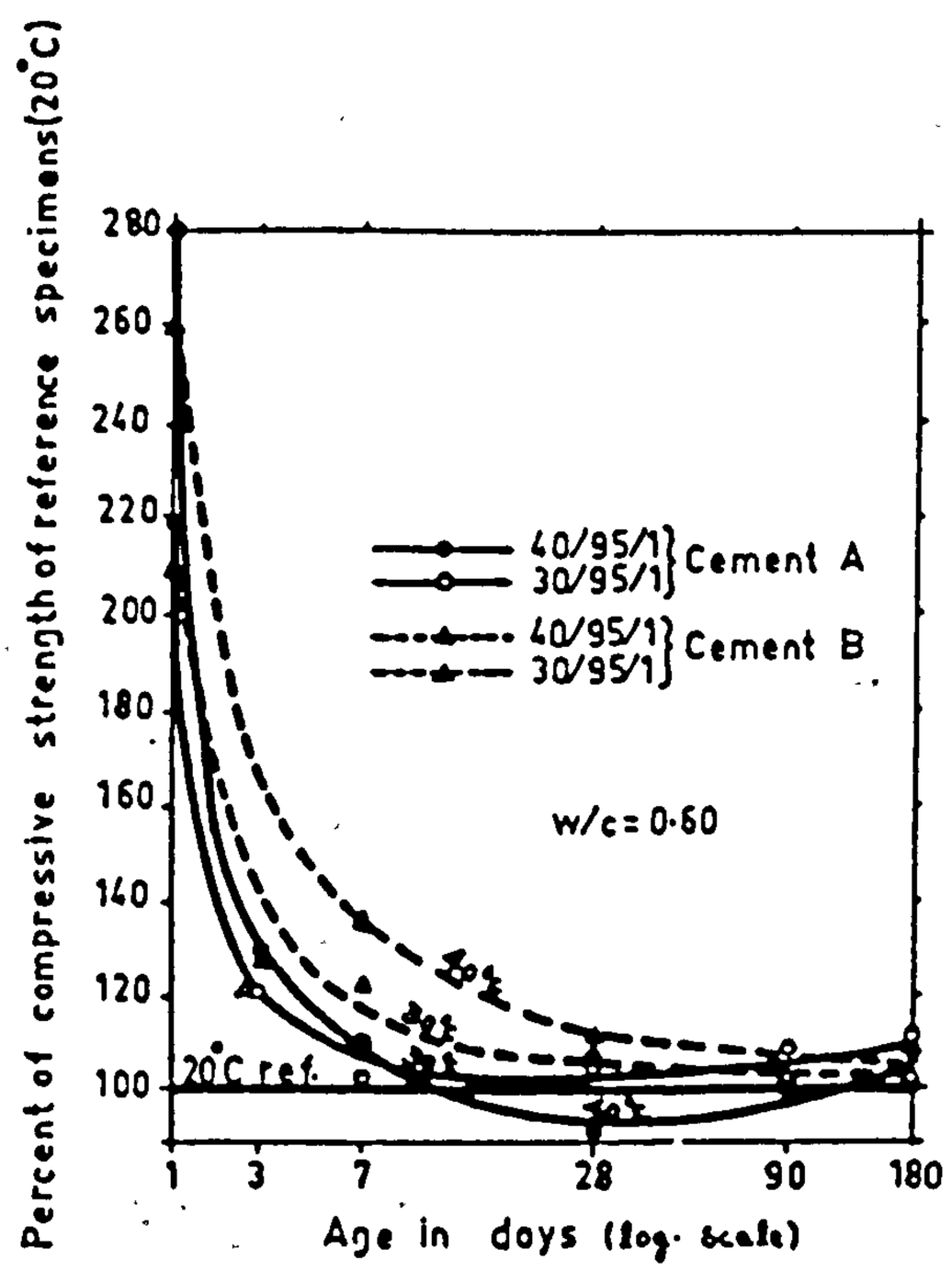

Figure 3.10 Effect of 24 hours exposure to hot-humid environment on the compressive strength of mortar made with Cement A and B. (94)

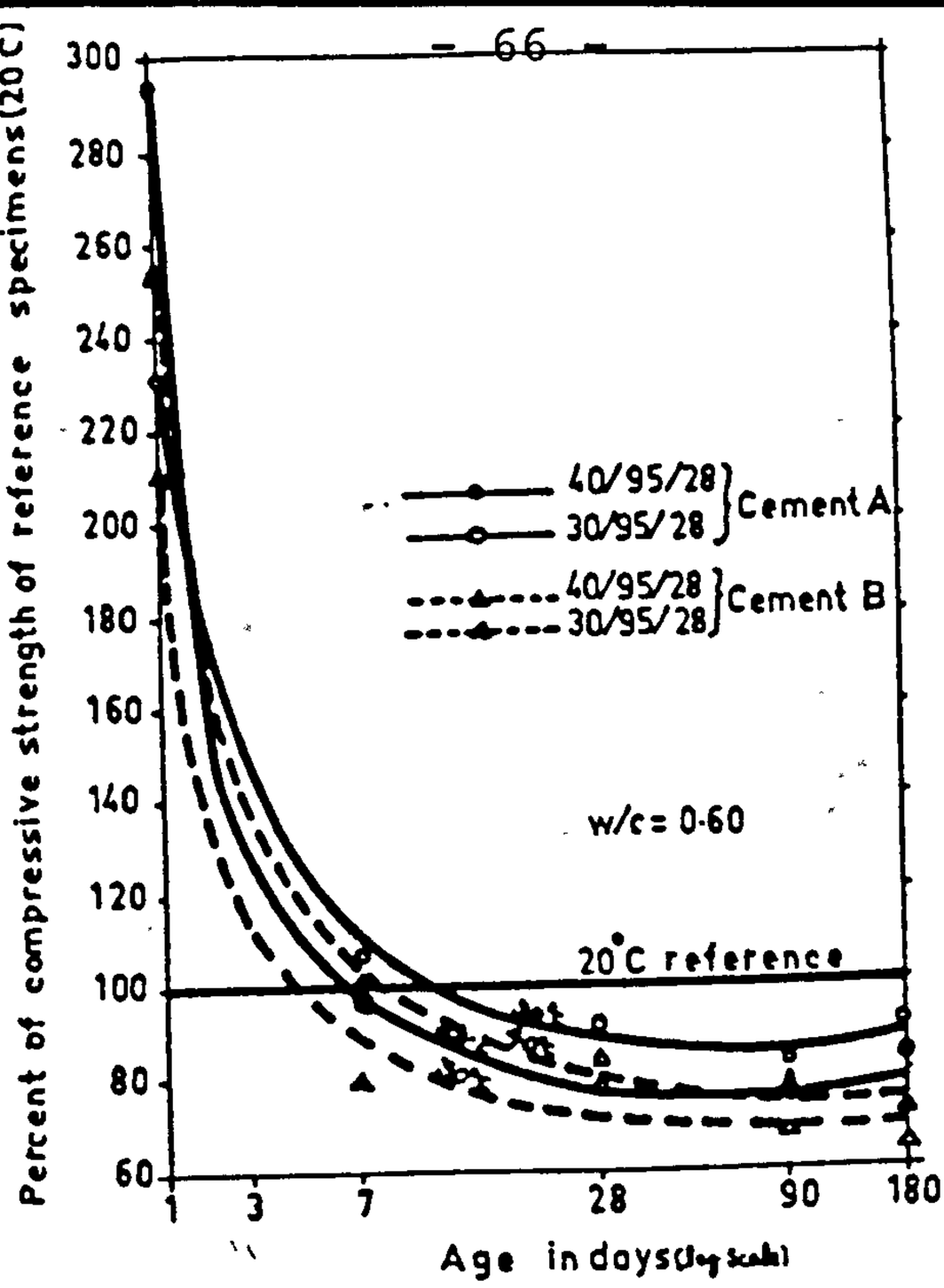

Figure 3.11 Effect of 28 days exposure to hot-humid environment on the compressive strength of mortar made with Cement A and B. (94)

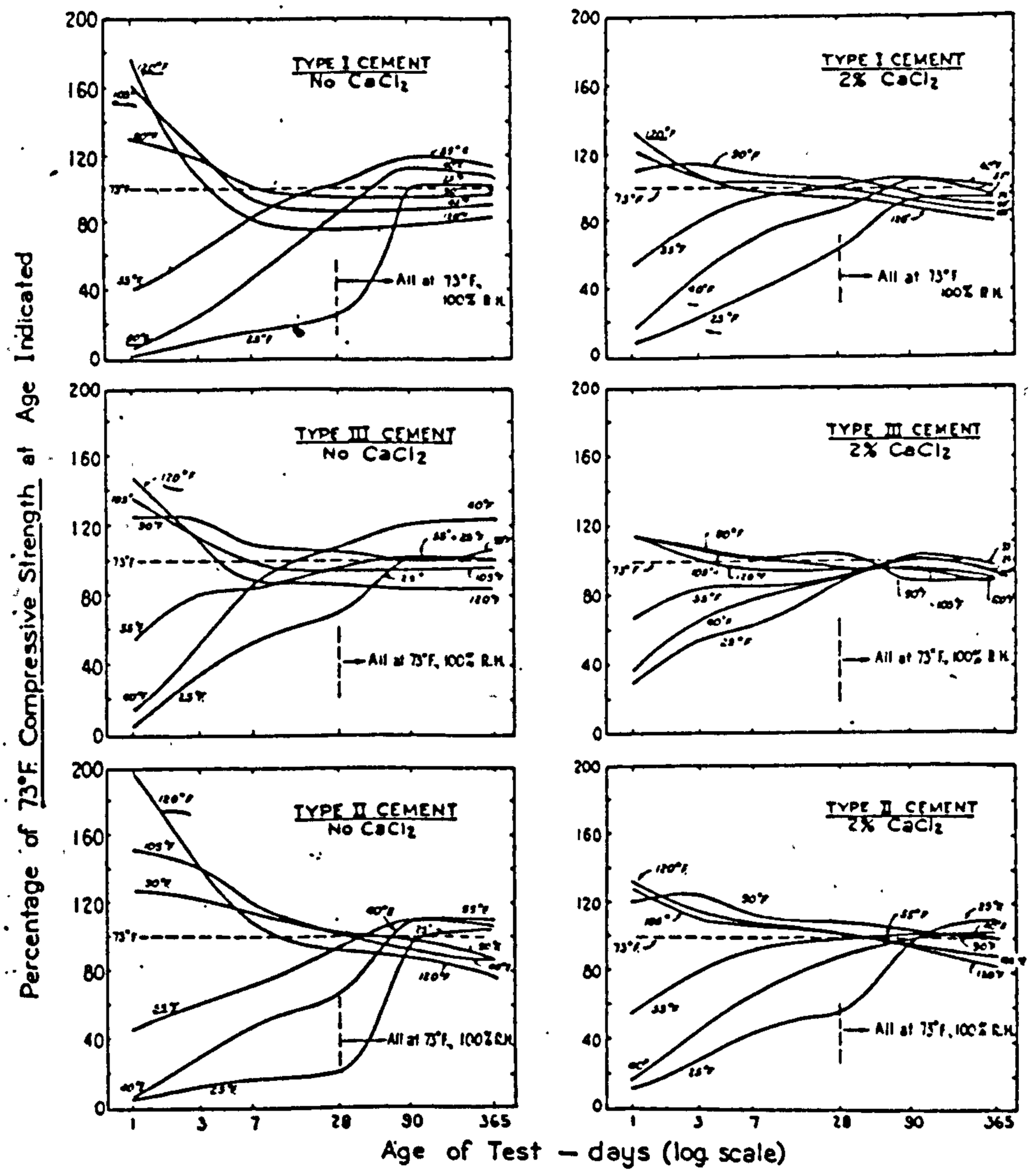

Figure 3.12 Effect of temperature on compressive strength of concretes made with different types of cement with and without an accelerator (80)

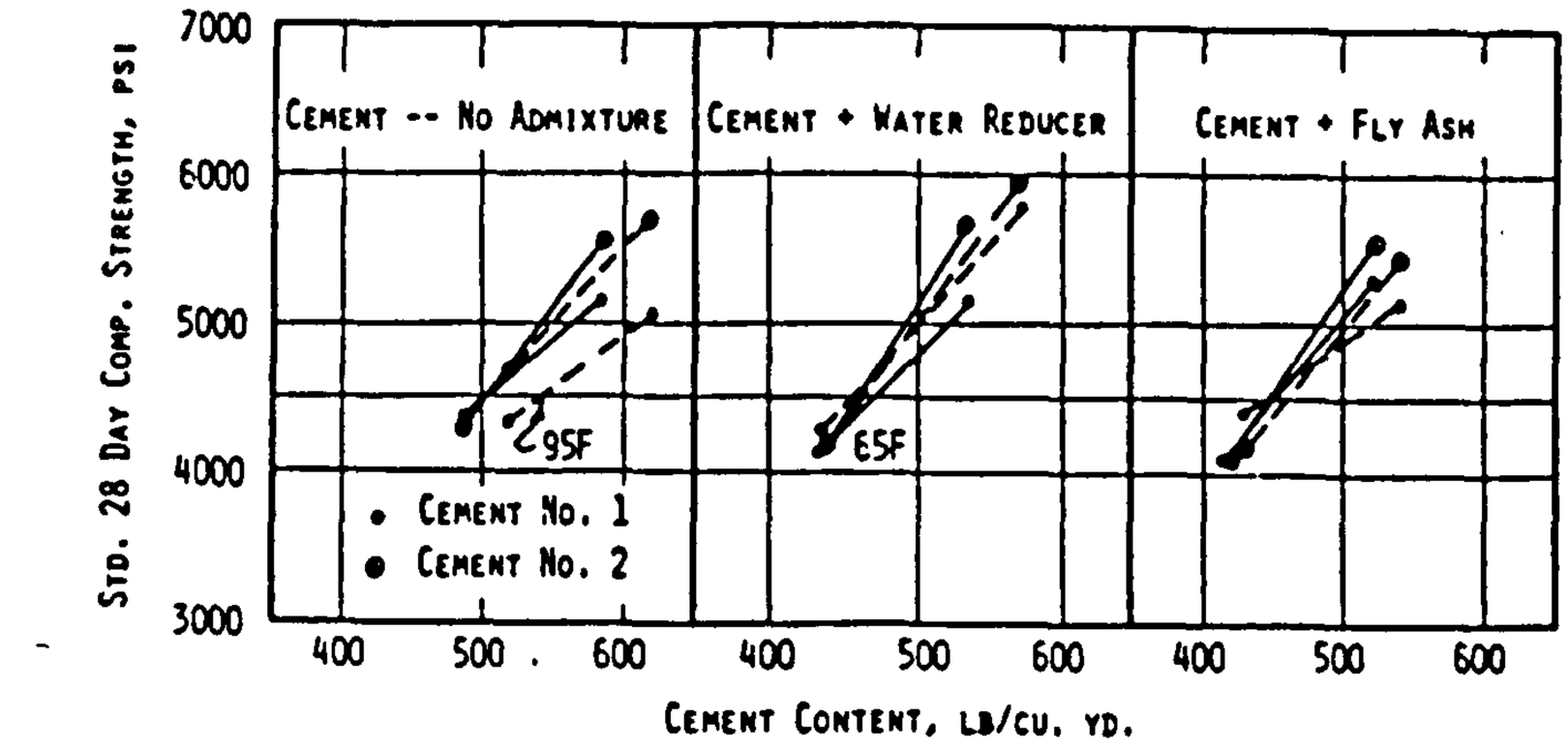

Figure 3.13 Example of interpolation of strength data-20 min delivery time. (98)

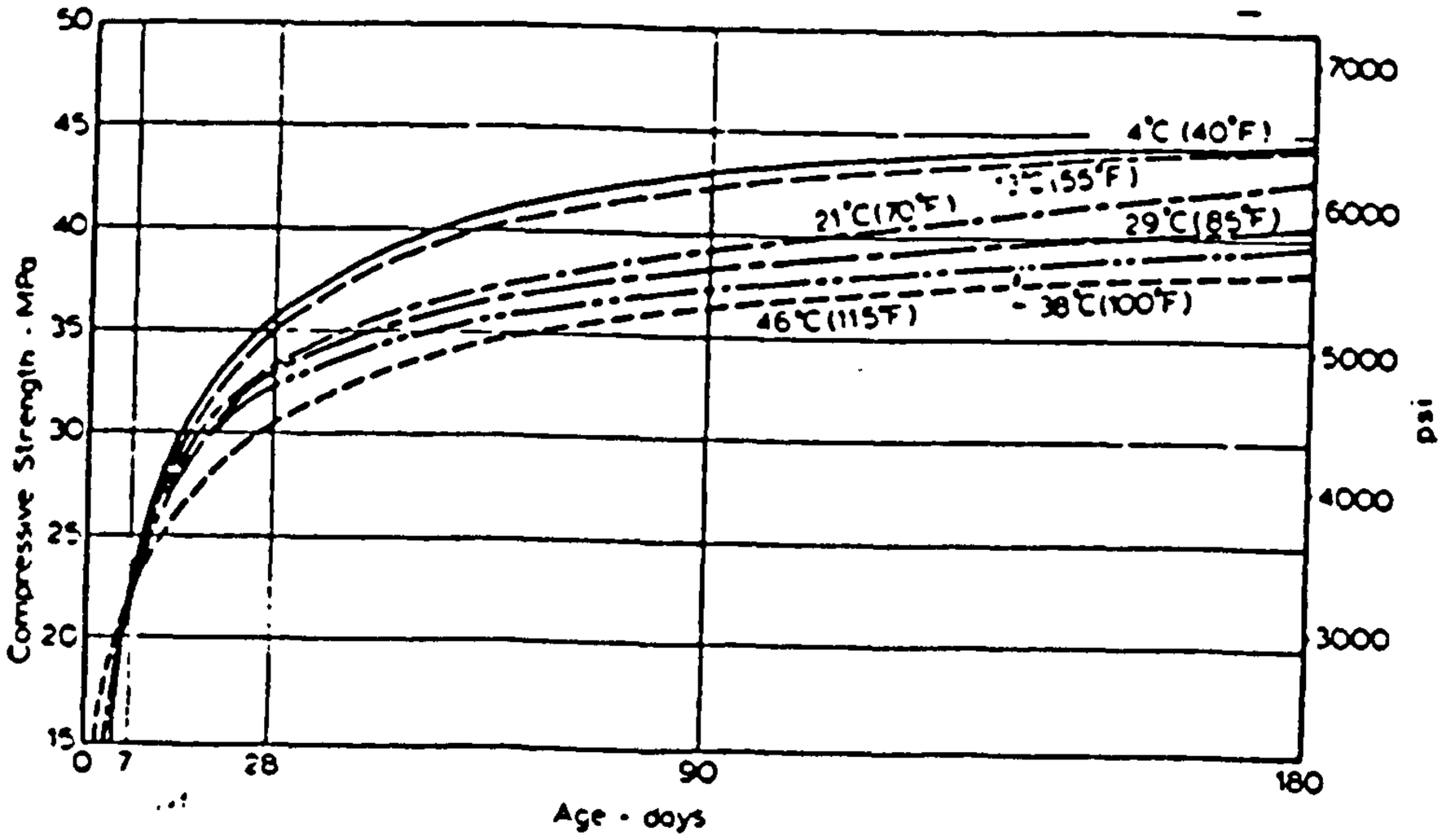

Figure 3.14 Effect of temperature during the first two hours after casting on the development of strength (92)

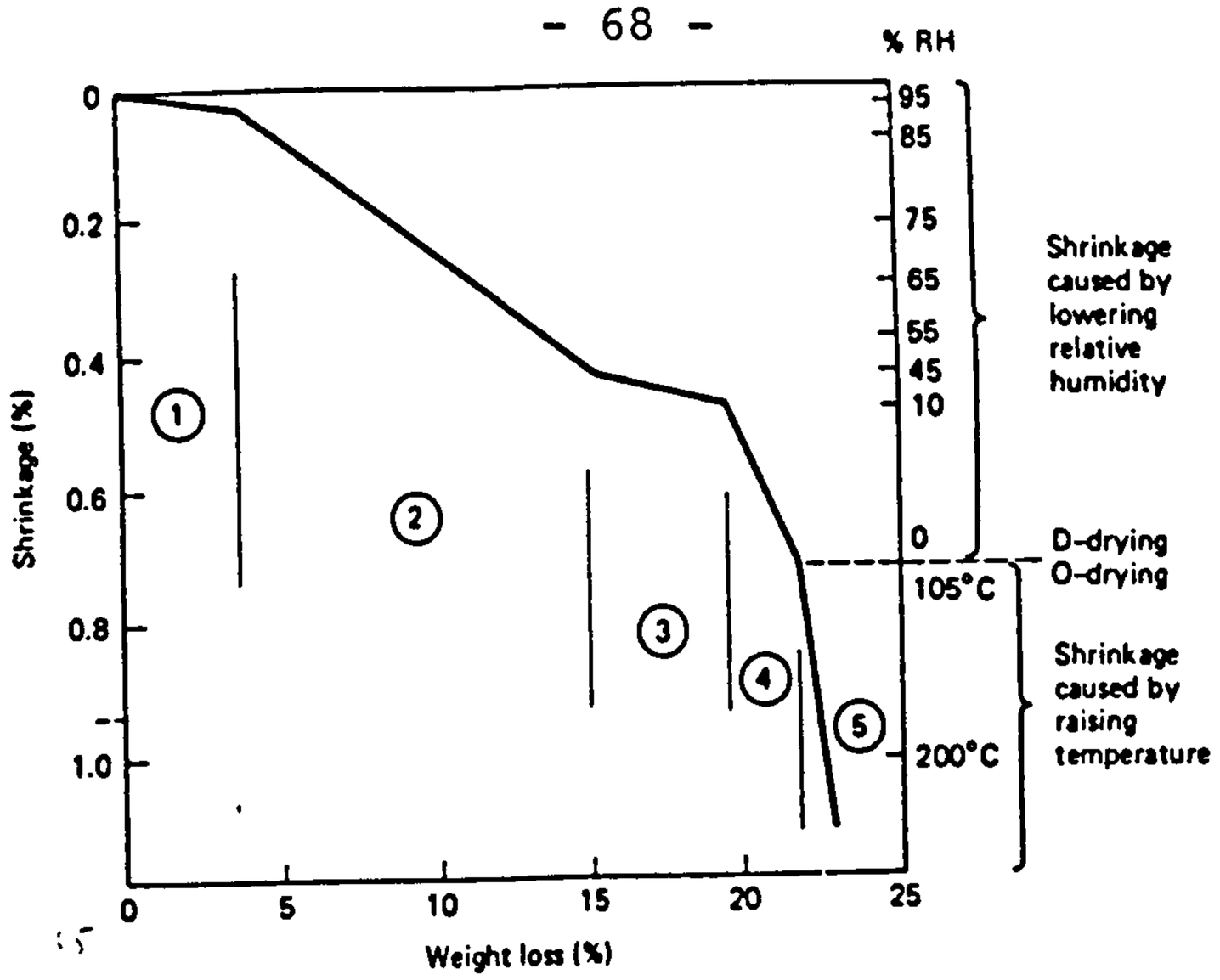

Figure 3.15 Shrinkage - moisture loss relationships in pure cement pastes during drying, (100)

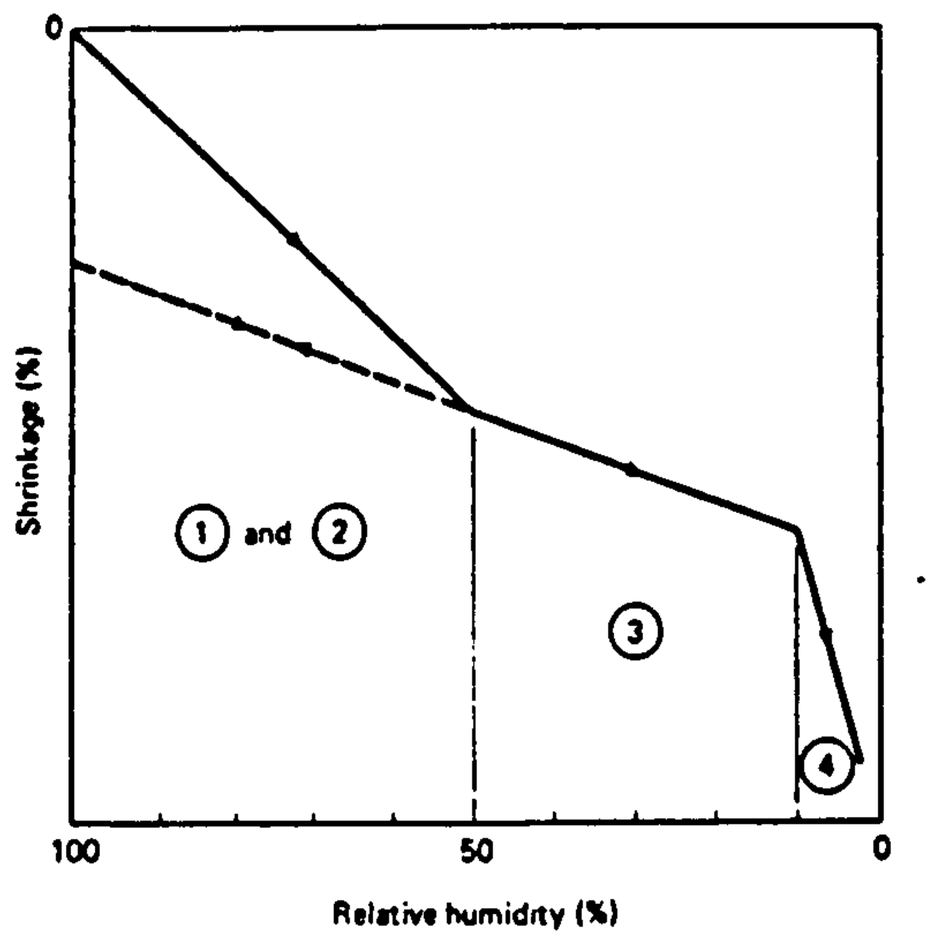

Figure 3.16 Shrinkage of cement paste as a function of relative humidity. (100)

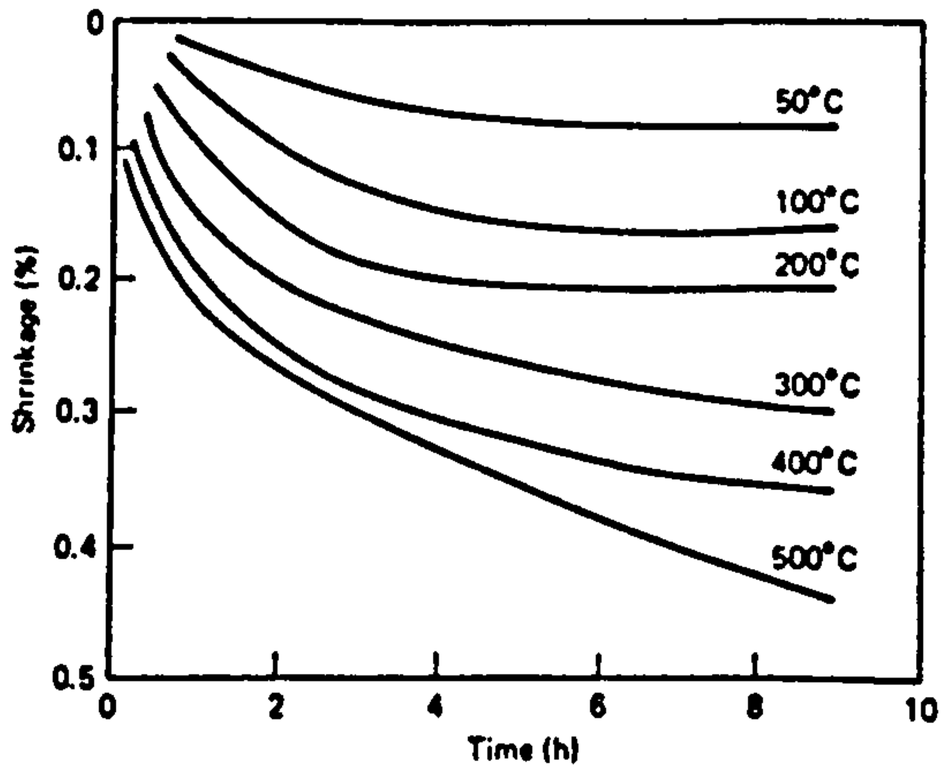

Figure 3.17 Effect of temperature on magnitude and rate of shrinkage. (From N.G. Zoldners, in Temperature and Concrete. SP-25. American Concrete Institute Detroit, Mich., pp.1-31). (100)

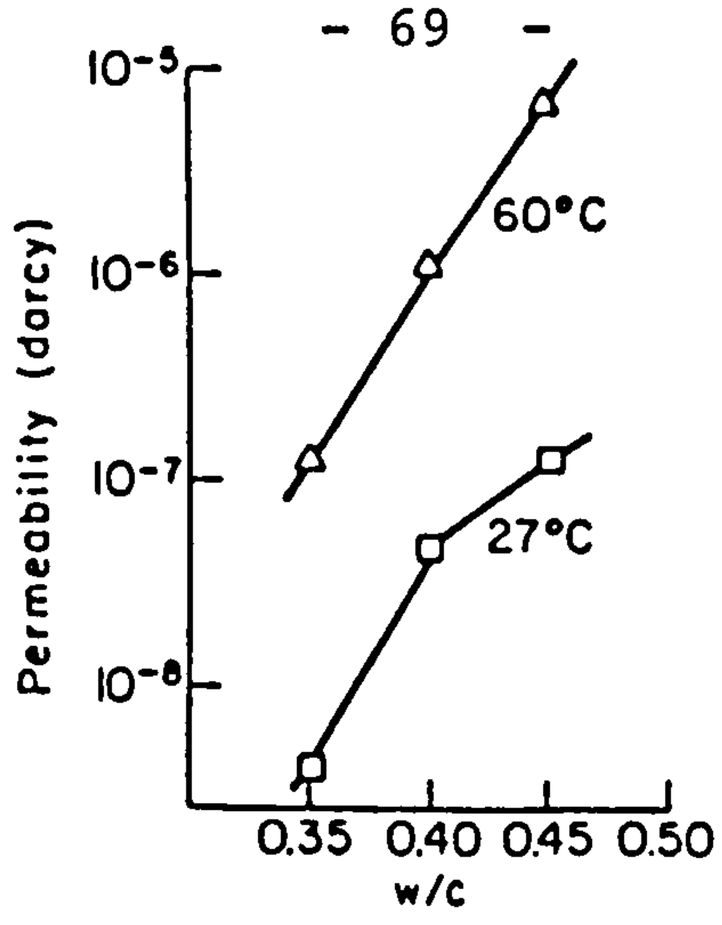

Figure 3.18 Relationship between permeability and W/C ratio (101)

Figure 3.19 Influence of locality of precipitation of the same amount of gel on the sealing effects in a pore (102)

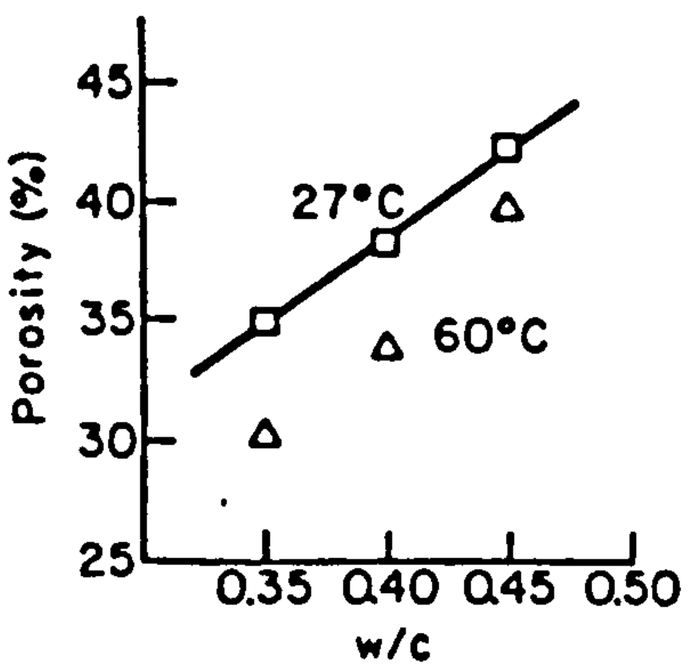

Figure 3.21 Pore size distribution of hardened cement paste (101)

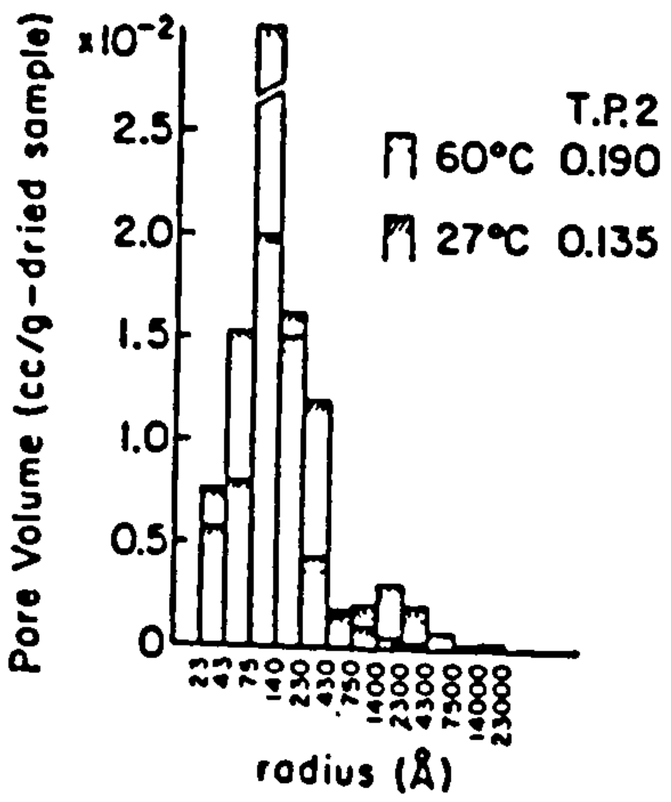

Figure 3.20 Relationship between porosit and W/C ratio (101)

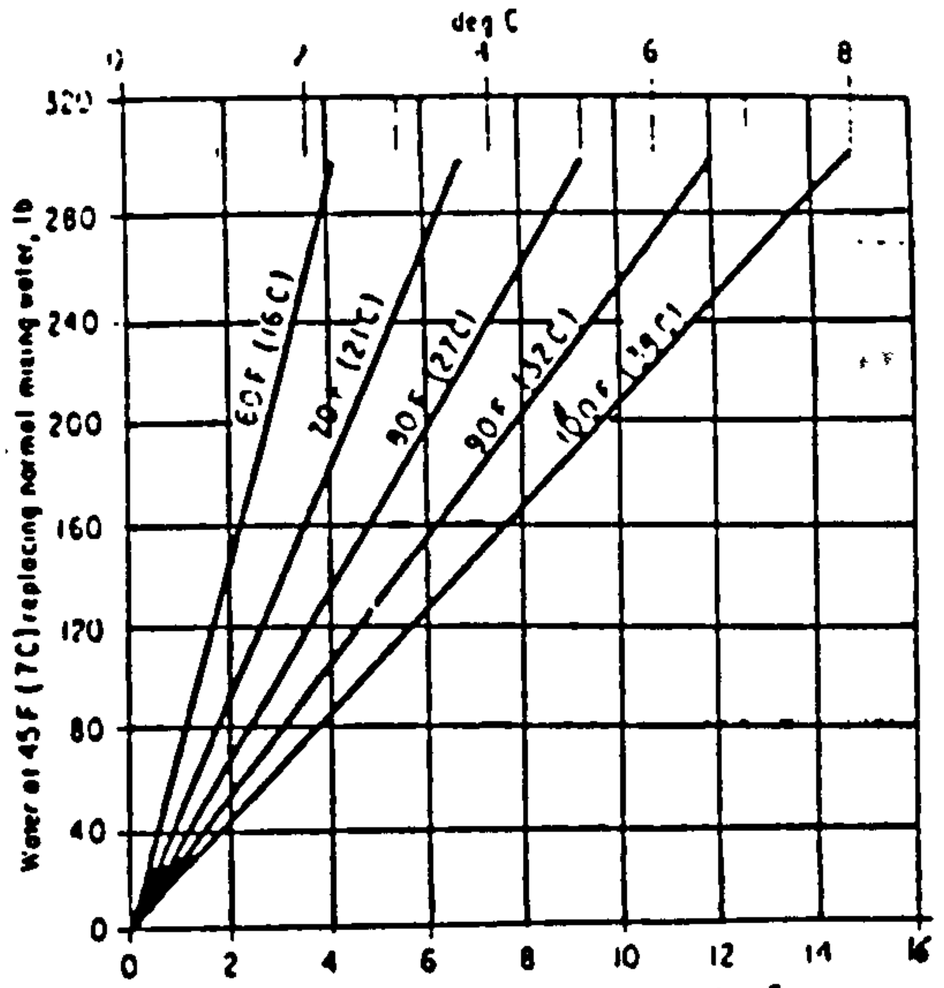

Figure 3.22 Effect of cooled mixing water on concrete temperature (77)

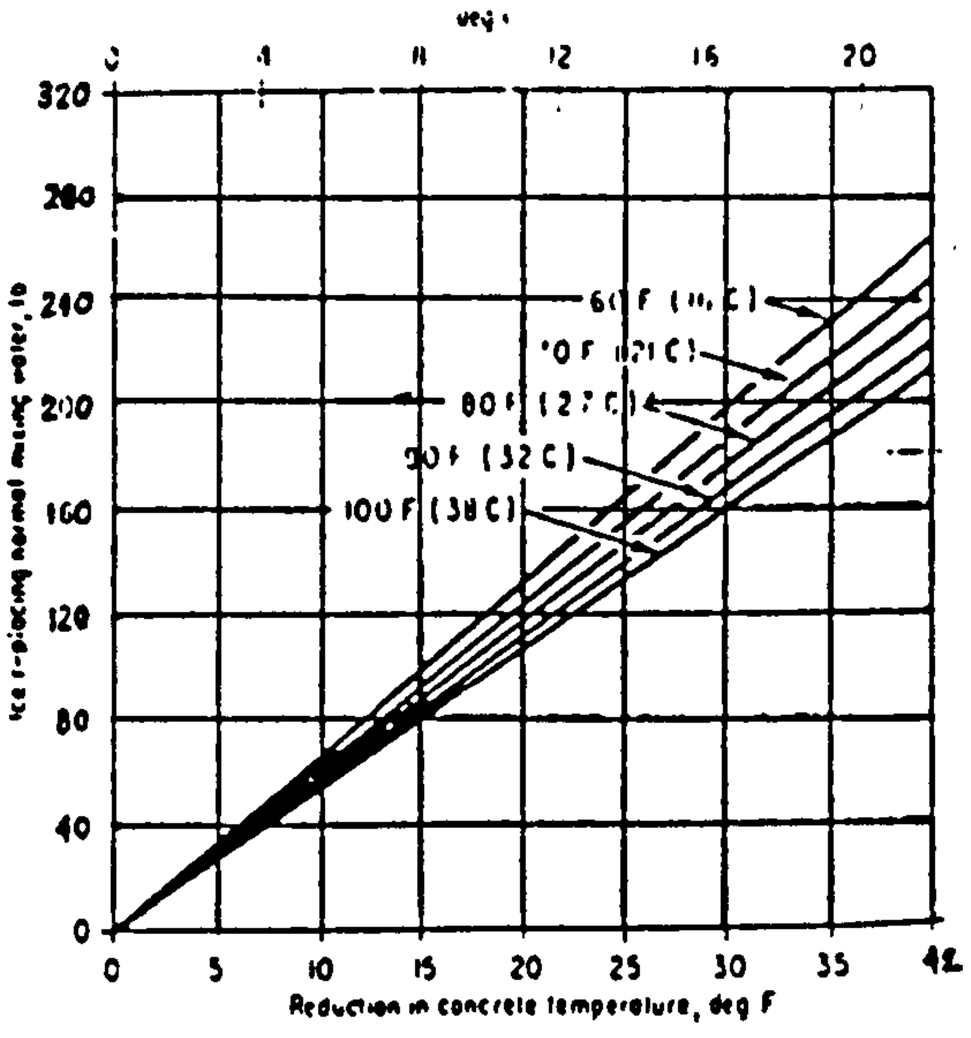

Figure 3.23 Effect of ice in mixing water on concrete temperature (77)

Climate and environment	*Extremely arid or arid with:* High ratio of evaporation to precipitation Intense solar radiation (minimum cloud cover) Rapidly fluctuating humidity (up to 70% variation in one day) Rapidly varying, very high temperatures (up to 20°C variation in a day at coast — somewhat greater inland)
Geology and materials	High, salty water table at coastline — sabkha formation. Zone IV Concentration of ground flows and evaporation cause salt to form — salinas, playas. Zone IV Recent to Tertiary age rocks usually make poor aggregates[a, m]
Workmanship and others	Enormous rate of growth of construction 1970 — 1980 Influx of inexperienced professionals and artisans High rate of spending on individual projects (such as £300 M per year) requiring rapid implementation and foreshortened construction schedules Poor workmanship and practice

Table 3.1 Factors affecting durability of concrete in the Middle East (69)

CHAPTER FOUR

CURING OF CONCRETE AND CURING METHODS

4.1 Introduction

Curing can be defined as the process of maintaining a satisfactory moisture content and favourable temperature in the concrete during the period immediately following placement so that hydration of cement may continue until the desired properties are developed to a sufficient degree to meet the requirements of the service (108). Thus the potential strength, performance and durability can only be achieved if the concrete is properly cured for an adequate period within the initial stage after casting. The importance of curing is illustrated in Figure 4.1 (109).

Concrete can be cured either by accelerated methods including steam and electrical curing, or by normal curing methods, including moisture or sealing. On construction sites normal curing methods are invariably used, and it is on these methods the emphasis is placed in this chapter. The principal factors controlling curing are:

moisture,
temperature, and
time.

4.1.1 Moisture

The chemical reaction between Portland cement and water starts when the two substances are combined together. The precise mechanism by which hydrating cement gains strength and other properties is still incompletely understood. However, it is known that cement gel is the precipitated product formed during hydration. And that it is precipitated into the capillary water-filled spaces. (36). Hence the answer to the question when does hydration stop depends on curing practice which should keep concrete and mortars as nearly saturated as possible until the original capillary water-filled spaces have become filled with hydration products.

Powers (110) has shown that Portland cement virtually stops hydrating when concrete dries to the point where the

internal relative vapour pressure falls below about 0.80 of the saturation pressure (or about 80 percent internal relative humidity). The hydration rate for relative vapour pressure between 0.3 and 0.80 is relatively low (see Figure 4.2) and is negligible below 0.3.

The vapour pressure of the capillaries can be reduced internally by the chemical uptake of water by the hydration process, a phenomenon called self-dessication (111). Powers and Brownyard (112) found that for sealed concrete specimens, hydration would cease when the chemically combined water became equal to about half the initial mixing water. Moreover, the maximum cement hydration would not occur for water/cement ratios less than about 0.5. Thus, self-dessication is important in sealed concrete when the water/cement ratio is less than 0.5.

Moisture losses and vapour pressure reduction other than the chemical uptake of water occur by evaporation. Water evaporation which was caused by the low relative humidity of the environment surrounding the concrete mass was found to affect the top few millimetre of concrete cover. Tests at Penn State University by Carrier & Cady (113) indicated that for moderately severe field exposure, drying at a point of 25 mm below the surface at 28 days is not sufficient to cause cessation of hydration.

Abrams and Orals (114) found from subjecting concrete slabs (900 x 900 x 150 mm), cured initially in fog for 7 days, to a drying environment of 75% and 35% Relative Humidity that only a very thin layer of the upper surface of concrete was shown to dry very rapidly to below 80% relative humidity the point when hydration ceases (see Figure 4.3). The author concluded that curing is only important for the top few millimetres. However, moisture loss by evaporation not only affects the continuity of the hydration process but also early volume changes and cracking. Early volume changes due to bleeding are usually not serious since significant stresses cannot develop in plastic concrete. However, high early evaporation losses can cause plastic and drying

shrinkage cracks. Plastic shrinkage cracks are usually good indicators of inadequate early curing.

Therefore, the curing objective is not just keeping the concrete saturated or nearly saturated for the benefits of continuing hydration, but to eliminate or even control as much as possible the moisture loss by evaporation.

4.1.2 Temperature

High concrete and environment temperatures accelerate the rate of hydration and consequently influence the locality of the hydration products within the matrix body. Also high temperatures, if not uniform throughout the curing mass, may cause physical disruption. If large variations occur before the concrete has developed sufficient strength to resist the resulting thermal stresses, cracking occurs. Flash set, excessive shrinkage and random cracking are also related to high early temperature. High curing temperatures improve the early-age strength. Although the conclusions about the effect of high curing temperatures are conflicting, the majority agree that the late-age strength is lower than that cured at lower temperatures. Therefore it is important to reduce the temperature of fresh concrete in hot weather.

Although the main criterion is to maintain the concrete temperature in the range of 5 to 71°C (115), the optimum curing temperature is usually considered to be about 32°C (115). The Transportation Research Board (108) states that for pavements the temperature of concrete should be in the range of 16 to 32°C under hot weather conditions. ACI Committee 305 (77) recommended that, for best assurance of good results with concrete placing in hot weather, the temperature of concrete should be limited to between 24°C and 38°C.

4.1.3 Time

Since hydration is relatively rapid for the first few days after fresh concrete is placed, it is important for the curing to start as soon as the concrete is placed and compacted. If the concrete is allowed to dry during its

early stages of hardening it is more likely to exhibit visual defects and to have suspect long-term strength and durability. It is also important that there be no interruption in the curing during the early period. (116) As shown in Figure 4.4, if curing water is denied for a period sufficient to allow curing concrete to dry, it never again regains the strength of continuously moist cured concrete, even after a long period of subsequent moist curing. This is probably because the continuity of capillaries which carry the water from outside to the location of unhydrated cement particles (see Figure 4.5) is broken and cuts off the water access paths. This continuity is never again fully regained by the addition of moisture (117). However, Waters (118) found that, except in cases where an early development of strength is required, it is not necessary to keep concrete wet after the initial curing period, as the curing can be performed at any time. Thus if the concrete is allowed to become dry for a period and is then re-wetted, it will continue to increase in strength as though the dry period had never existed (see Figure 4.6).

The duration of curing is difficult to estimate exactly, since concrete is made with an extremely wide range of properties and placed under widely varying atmospheric conditions (119). All concretes benefit from long curing, but long curing is often inconvenient and sometimes costly. Since the theoretical purpose of curing is to enable concrete to reach its design strength in a given time, the necessary period of continuous curing should be specified by the engineer on the basis of results from test tubes or cylinders. However, various arbitrary curing periods are specified by different authorities. For example, the American Concrete Institute (115) recommends that when the daily mean ambient temperature is above 5°C and normal Portland cement (Type I) is used, curing should be continuous for a minimum of 7 days, or for the necessary duration to attain 70 percent of the specified compressive or flexural strength, whichever is shorter. If rapid hardening cement (Type III) is used, the curing duration may be as short as 3

days. And when pozzolans are used as part of cementing materials, the minimum continuous curing should be 21 days.

British Standard BS 8110 (120) specifies a minimum curing period depending on the type of cement, the ambient conditions and the temperature of concrete. The appropriate period is given in Table (4.1).

4.2 Methods of curing

Various materials and methods for curing concrete are available. However, the principle involved and the target are the same; to ensure the maintenance of a satisfactory moisture content and temperature so that desired properties may develop.

The two systems of securing a satisfactory moisture content are:

1. The continuous or frequent application of water; and
2. The prevention of excessive loss of water from the concrete.

Selecting an appropriate curing method and material is largely dependent on:

1. Site conditions;
2. Size, shape and position of concrete element;
3. The availability of labour;
4. Cost and economic consideration;
5. Aesthetic appearance; and
6. Subsequent surface treatments (e.g. paint).

No matter which method is selected, it should be applied on the formed surface within a maximum of half an hour after removing the formwork, otherwise it should be applied immediately.

4.3 Continuous or frequent application of water

Site experience shows that this method is far better than the second curing method which involves preventing evaporation. However, the problems with this approach, which have been described by Carrier (117), Blackledge (121) and Keeley (122) are:

1. Plastic shrinkage cracks can commence within 10 minutes of completion of a section of concrete. Often it is not posible to apply water for at least an hour.
2. The application of cool water to the surface of newly struck concrete can cause thermal shock or excessively steep thermal gradients. Thus curing water should not be more than about 11°C cooler than the concrete.
3. The concrete surface must be kept continuously damp for the required curing period, otherwise more harm than good can result.
4. Intermittent wetting in the first 2 or 3 days of placing is likely to result in surface cracking.

It is therefore essential (especially in hot weather) to specify curing into two stages. These include an initial surface covering for the first 60 minutes to prevent excessive evaporation, followed by water curing.

Where the appearance of concrete is important, the water must be free of harmful substances that may stain or discolour the concrete. The methods of water curing are:

a. ponding
b. fog spraying or sprinkling
c. burlab, cotton mats, or rugs
d. earth, sand, sawdust, straw or hay.

4.3.1 Ponding

Ponding is applicable for horizontal slabs, floors or pavements. A small dyke is set up around the perimeter of newly placed concrete area, and the water is pumped into the pond. This method is very efficient and is specially recommended for the cases where the formation of shrinkage cracks is expected. On the other hand, this method is very messy.

4.3.2 Fog spraying or sprinkling

In this method water is forced out through a nozzle. This method is applicable to horizontal or vertical surfaces. It is very efficient, but it is costly. Care should be taken to avoid erosion especially on vertical surfaces. On hot or

windy days, spraying or sprinkling will be started 3-2 hours after finishing of concrete. In this method, continuation is paramount, so that the surface of concrete will never dry out. When the temperature is more than 15°C, especially in the first three days, it is recommended to sprinkle water every 3 hours during the day time, and once or more during the night time. In any case, the sprinkling should be a minimum three times in 24 hours (123).

4.3.3 Burlap, cotton mats or rugs

In this method the entire surface of concrete (vertical or horizontal) is covered by burlap, or cotton mats or rugs and then wetted by spraying water. It must be kept wet throughout the curing period. Double thicknesses may be advantageous to extend the elapsed time between sprayings. At the edge of the strips overlapping should be avoided and protected against the wind.

Burlap should be of heavy weight (to hold water better) and should be thoroughly rinsed before it is used in order to remove soluble substances and make it more absorbent. Cotton mats and rugs hold water longer than burlap, but are at some disadvantage due to their bulk weight and expense.

4.3.4 Earth, sand, sawdust, straw or hay

This method is usable on horizontal surfaces where the appearance of concrete is not important, since discolouration and stains often occur on the surface of the concrete. If earth is used, it should be free of particles larger than 25 mm. The thickness of the earth, sand, straw or hay will be about 150 mm. Sawdust, straw or hay should be protected against the wind. These materials should be wetted by spraying of water at intervals of approximately 1.5 times of the duration for which these materials retain the moisture well (123).

4.4 Prevention of excessive loss of water

In this method materials are used to seal the moisture in the concrete. It is not as efficient as the first method, but still it is sufficient for all normal concreting works (121). However, it may not be advisable on concrete having a water/cement ratio of less than 0.5 (122, 111).

4.4.1 Plastic sheets

Plastic sheets are an effective moisture barrier when the surface is covered carefully. ASTM C171 specifies the minimum thickness of the sheet as 0.1mm. Plastic sheets are available in black, clear or white colours. Normally, black sheets are preferred in winter time, and white in hot weather. Clear is not recommended during summer times since it does not provide good shading. Care is required to provide several centimetres overlapping at the edge of the strips which should be protected against the wind. When the appearance of the concrete is important, the use of the plastic sheets is not recommended. Moisture condensing on the underside of the smooth plastic creates an uneven distribution of water in the concrete, and results in a mottled appearance. Wrinkling of the sheet should also be avoided to prevent discolouration. On hot days, it is recommended to flood the concrete surface with water under the plastic sheet. This also helps to reduce the adverse effect of the plastic sheet on the appearance of concrete.

4.4.2 Bituminous paper

Bituminous paper is composed of two sheets of paper cemented together with a bituminous adhesive and reinforced with fibre. They provide a moisture barrier and do not require a periodical addition of water. They also offer some protection against the frost. The edges of the paper should overlap for several centimetres and be secured against the wind.

4.4.3 Liquid membrane curing compounds

Liquid membrane curing compounds are of three types (119): those with a heavy synthetic resin (plastic) base; those with a wax base; and those with a combination of wax and resin base. Resin based compounds are more expensive, but they do not leave any residue on the surface of concrete after about 28 days, or if there is any residue, it can be removed easily. Wax based compounds are difficult to move, but since they are gummy, they tend to hold dirt and other litter.

Curing compounds can be clear, white, grey or even black. Clear compounds are recommended for architecturally attractive surfaces. Since the residue can be removed easily any type of painting is applicable. Clear compound is not a good shading against the sun, therefore, the temperature of concrete rises in hot weather. The Transportation Research Board (108) states that clear compounds should not be used when the ambient temperature exceeds 27°C.

White or grey compounds are specially recommended in hot weather since they reflect most of the heating rays, and help to reduce the temperature of the concrete. White pigmented compound acts as a shading material and may reduce the temperature of concrete up to 4°C (124). Black compound absorbs the heat and increases the temperature of concrete. Thus, it must be avoided in hot weather.

Compounds should be applied as soon as the bleeding stops and the water sheen on the surface of concrete disappears. If the surface has lost water and becomes dry before the application of the curing compounds, the compound will be absorbed by the concrete and will not form a surface film. In this case, the best thing to do is to fog down the concrete surface and then apply the compound.

However, if the application is too early, the standing water will prevent the formation of a continuous film free of pinholes or voids. When the evaporation rate exceeds 1 $kg/m^2/hour$, it may be difficult to estimate whether the bleeding has stopped or not. If the rate of bleeding is lower than the rate of evaporation the concrete surface may

be dry, but the bleeding may still be going on. In this case, one of the following can occur;

1. Evaporation may be stopped effectively, but continuing bleeding results in a layer of water forming below the compound film which promotes scaling.
2. Evaporation may be stopped temporarily, but continuing bleeding may result in map cracking of the membrane.

Therefore, to avoid any of these failures, it is recommended that firstly the evaporation must be minimised by shading or by use of othr methods, and then bleeding should be observed.

On formed surfaces, the compound should be applied either immediately or within half an hour of removing the form. (121). Curing compound can be applied either by hand or power sprayer at about 0.5 to 0.7 MPa pressure (115). In very small jobs, the compound can also be applied with a wide soft brush or paint roller. The usual coverage range of one coat is about 0.2 to 0.25 litre/m^2 (124, 115, 119, 121). However, research into the effect of coverage rate (0.25 and 0.06 litre/m^2) on the moisture content reveals the importance of properly sealing the concrete surface rather than increasing the thickness of the compound film. If clear compound is used it is recommended that each coat is applied in two coats to provide a complete coverage. The first coat should have a rate of coverage equal to half of the standard rate of coverage. The second coat should be applied in perpendicular direction to the first one.

The major benefits of surface applied membranes have been summarized by Keeley (122) as follows:

1. The speed at which they can be applied, i.e. in the first 5 minutes after completion to prevent the occurance of plastic shrinkage cracks;
2. They are continuous in spite of protrusions through a slab or kicker, and
3. They involve a single application and therefore do not require continuous maintenance.

4.5 Benefits of proper curing

It is generally thought that proper curing has the following positive effect on the properties of concrete (119, 125).

4.5.1 Compressive strength

It has been reported (119) that the compressive strength of properly cured concrete is increased by 80 to 100 percent, over that which has not been cured at all. Birt (125) reported that a laboratory specimen exposed to dry air from the time it is made, is only 42 percent as strong as a specimen continuously moist cured at six months age. Tensile strength is also increased by proper curing and this will increase concrete's resistance to cracking and surface crazing.

4.5.2 Abrasion resistance

ACI Committee 210 (126) states that curing is one of the important factors that improves the abrasion resistance of concrete. It is also stated that a surface cured for 7 days is nearly twice as wear resistance as one cured for only 3 days. Thus, a properly cured concrete surface will wear well, whereas a poorly cured concrete surface abrade rapidly.

4.5.3 Shrinkage

Proper curing controls the evaporation of bleeded water from concrete surface. This will eliminate the appearance of plastic shrinkage cracks in the first 15-30 minutes. Proper continuous curing controls the evaporation of water from hardened concrete and eventually reduces any excessive drying shrinkages that may take place reducing the risk of cracking (109).

4.5.4 Thermal cracks

Proper curing assists in the control of temperature gradient within the mass concrete which would otherwise precipitate the development of thermal movement cracks.

4.5.5 Impermeability

The more prolonged the hydration of the cement the more cement gel is produced in the capillary pores, as hydration can only take place in capillary water-filled spaces. The produced gel blocks and disconnects the capillary pores (a matter depending on concrete temperature and rate of hydration) and consequently improves the water-tightness resistance to chemical attack and freezing and thawing of concrete.

4.5.6 Appearance

Poor curing can enhance water evaporation and cause deficiency of moisture in the concrete surface region, which will stop the hydration of cement. These unhydrated cementing materials at the surface of OPC concrete and mortars will be apparent as dust which can be brushed away from the surface resulting in a rough surface usually of an irregular pattern.

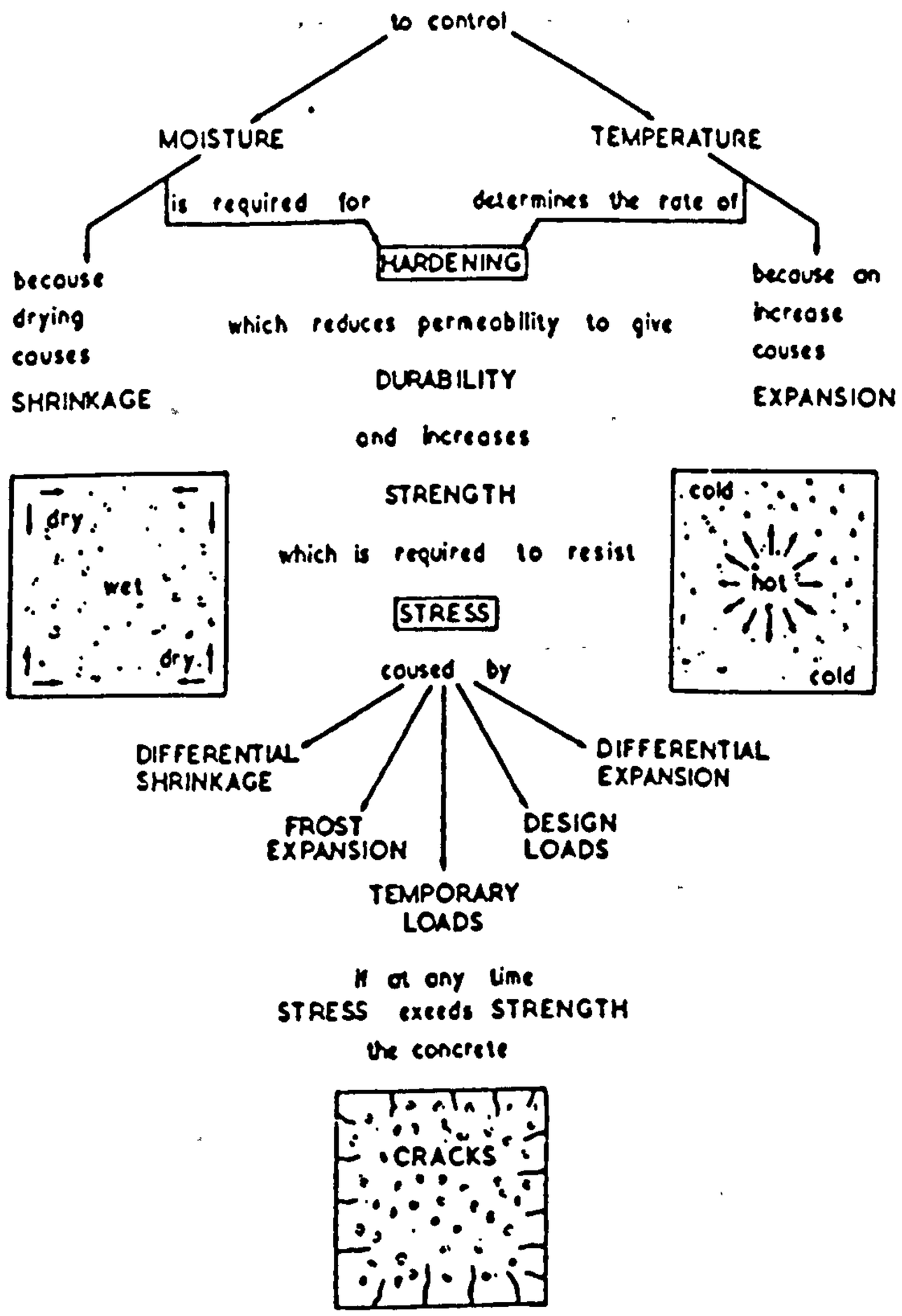

Figure 4.1 Importance of curing (109)

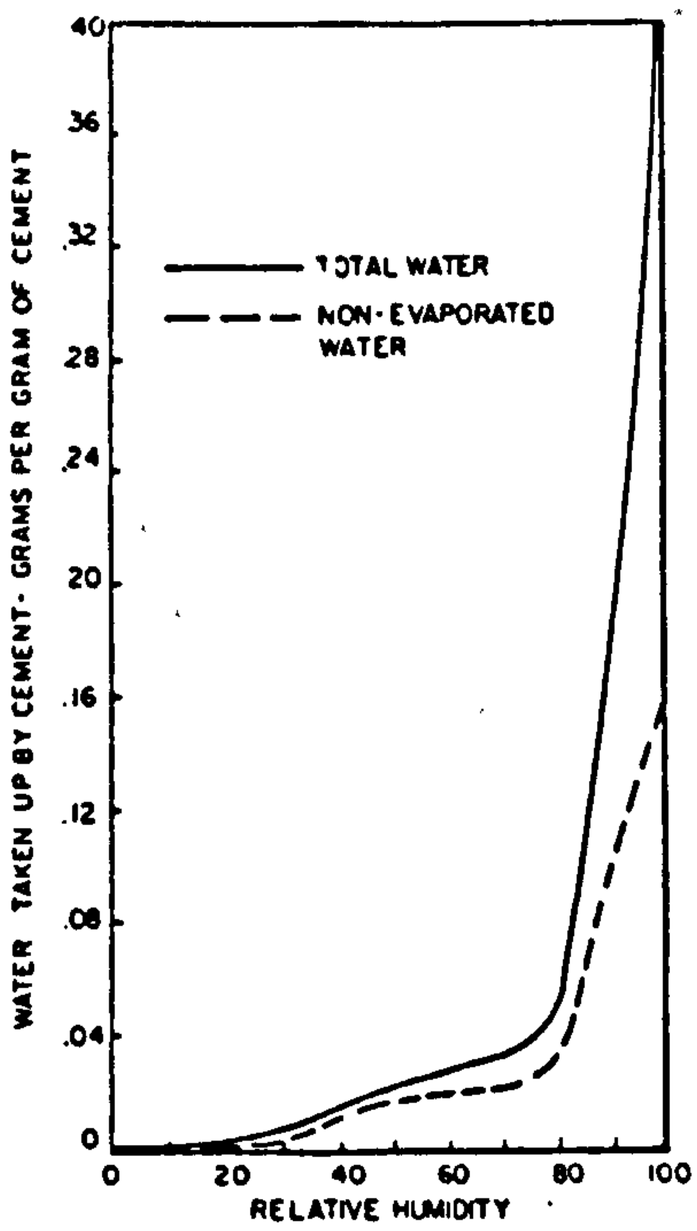

Figure 4.2 Amounts of water taken up by dry cement exposed to water vapour 6 months (110)

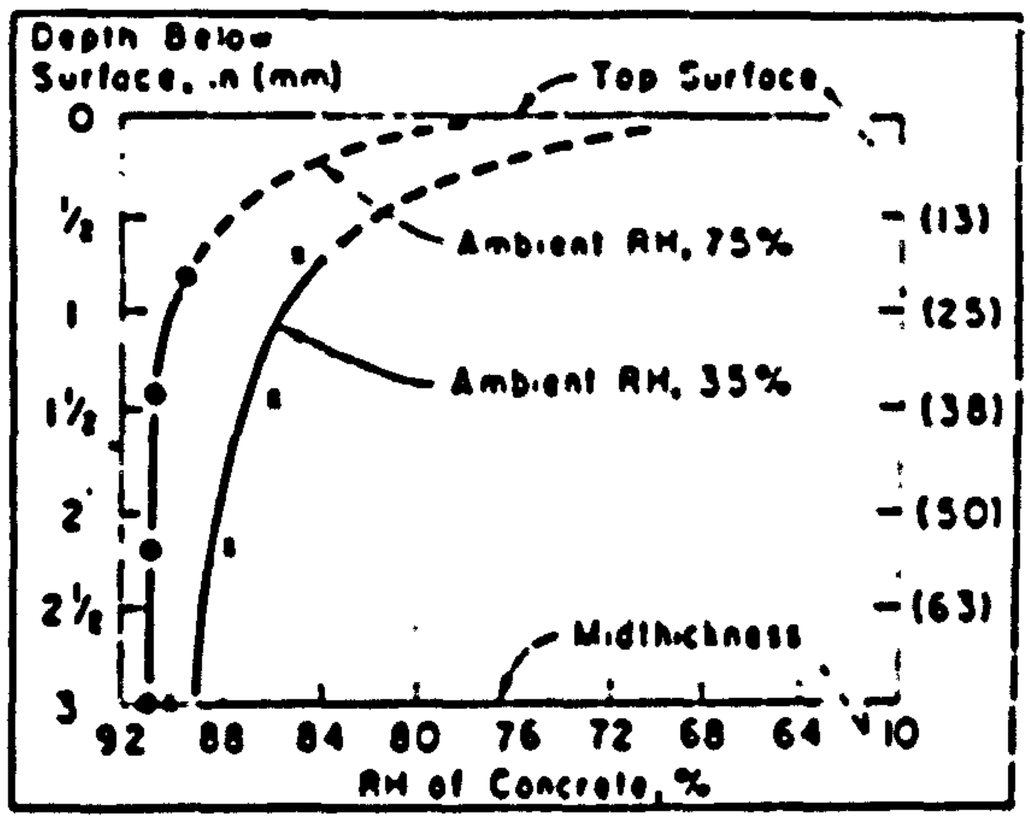

Figure 4.3 Humidity gradient within 6in slab (114)

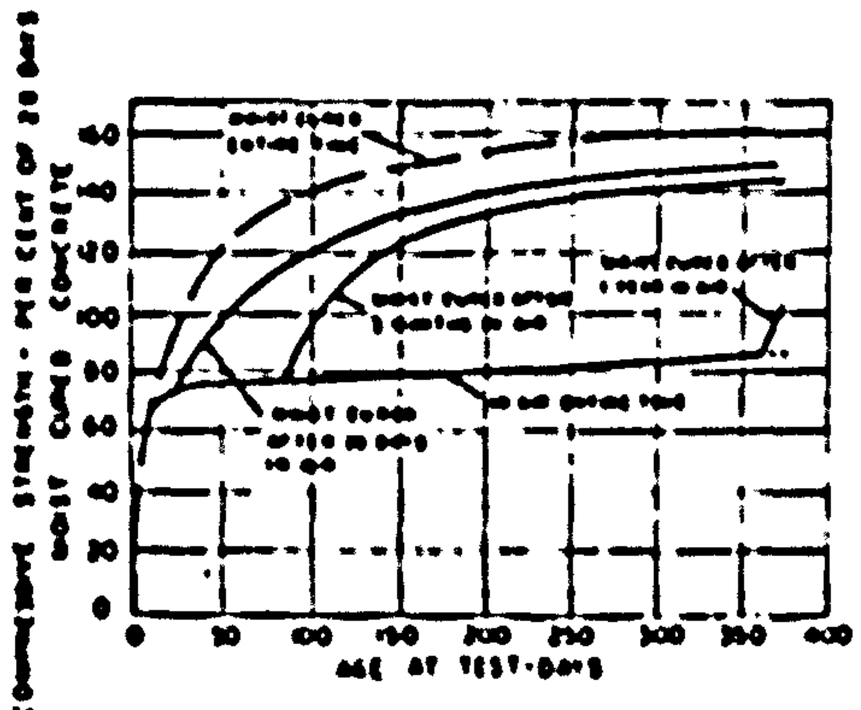

Figure 4.4 Strength of concrete increases whilst moisture and unhydrated cement are still available. (116)

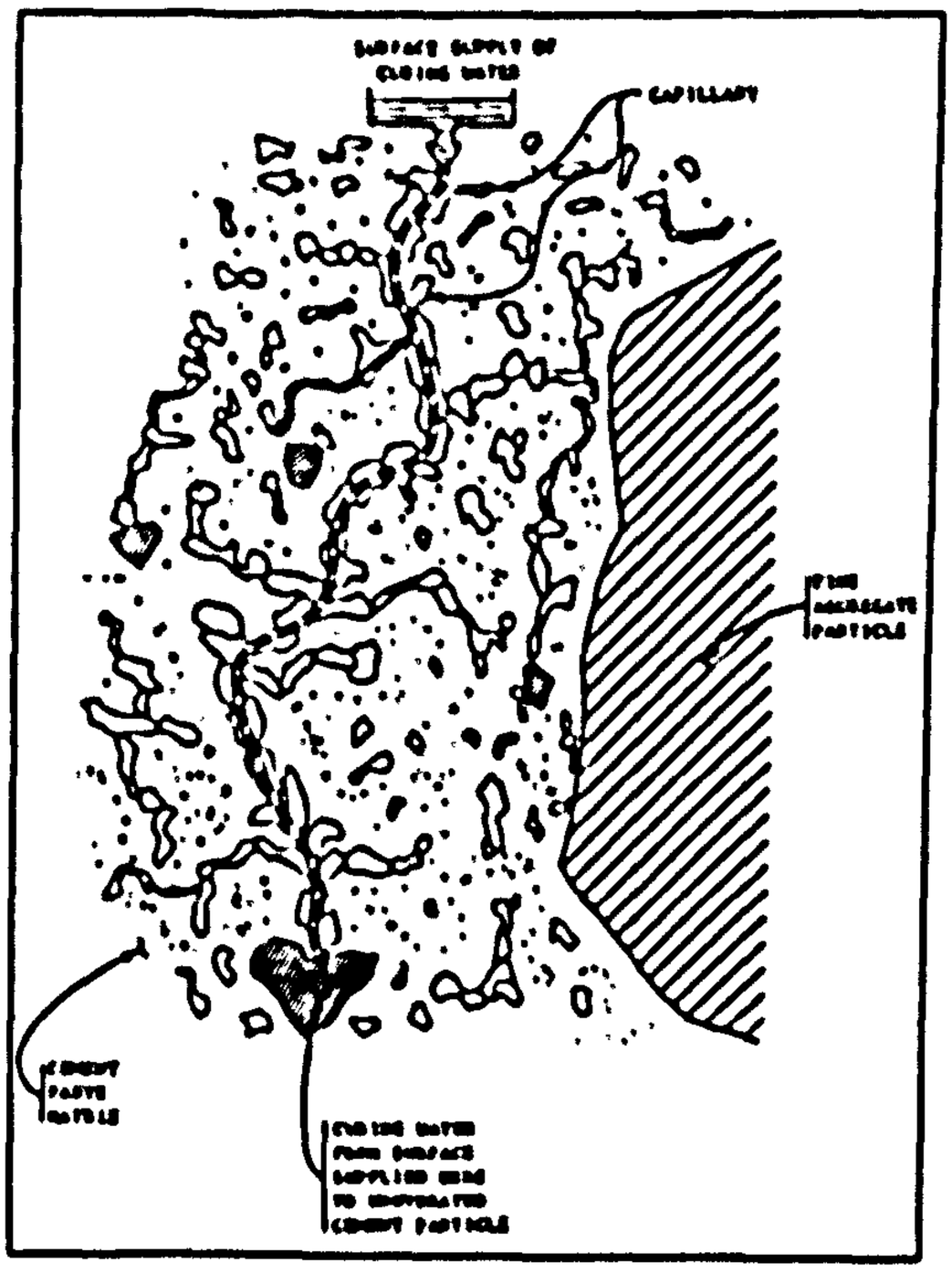

Figure 4.5 Sketch of curing water gaining access to unhydrated cement (117)

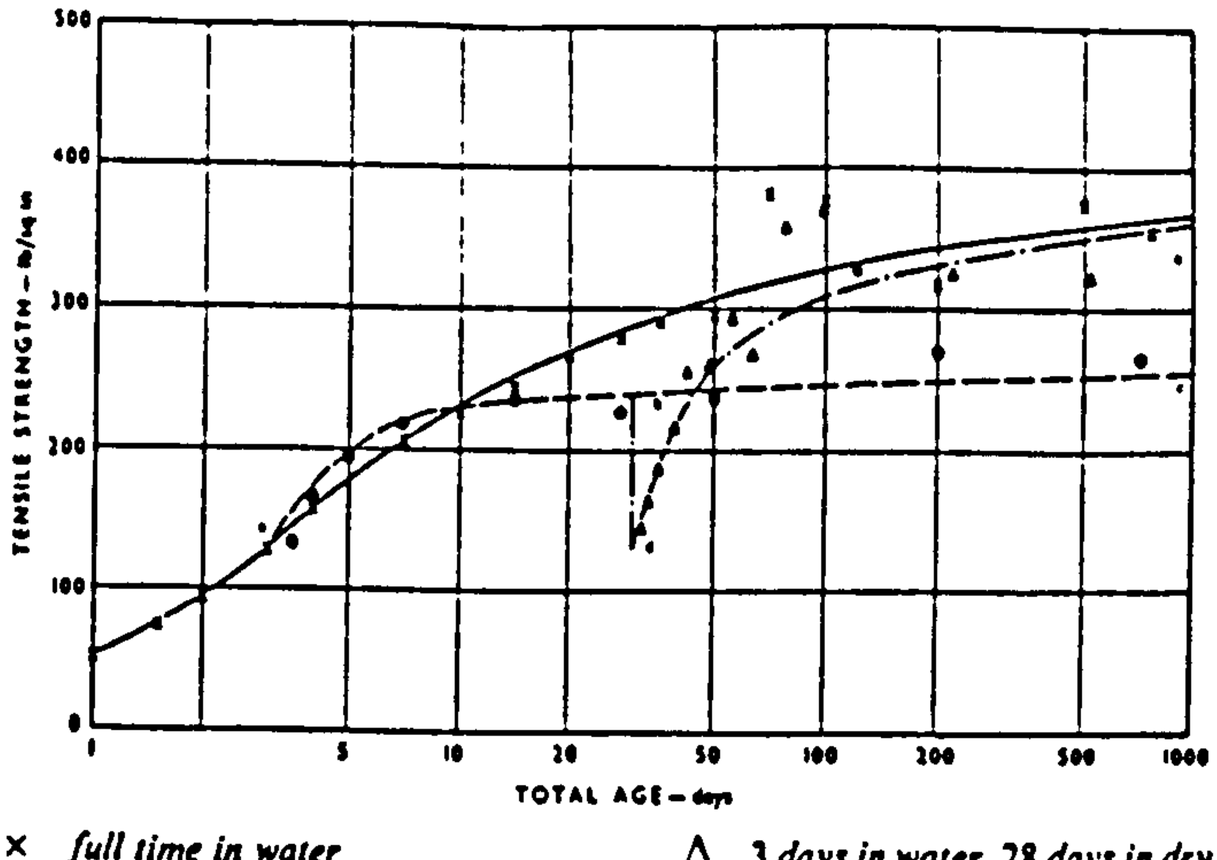

Figure 4.6 The effect of allowing concrete to dry before it has fully cured (118)

Type of cement	Ambient conditions after casting	Minimum periods of curing and protection		
		Average surface temperature of concrete		
		5 °C to 10 °C	Above 10 °C	t (any temperature between 5 °C and 25 °C)
OPC, RHPC, SRPC	Average	Days 4	Days 3	Days $\frac{60}{t+10}$
	Poor	6	4	$\frac{80}{t+10}$
All except RHPC, OPC and SRPC and all with g.g.b.f.s or p.f.a.	Average			
	Poor	10	7	$\frac{140}{t+10}$
All	Good	No special requirements		

NOTE 1. Abbreviations for the type of cement used are as follows:
OPC: ordinary Portland cement (see BS 12);
RHPC: rapid-hardening Portland cement (see BS 12);
SRPC: sulphate-resisting Portland cement (see BS 4027).

NOTE 2. Ambient conditions after casting are as follows:
good: damp and protected (relative humidity greater than 80 %; protected from sun and wind);
average: intermediate between good and poor;
poor: dry or unprotected (relative humidity less than 50 %; not protected from sun and wind).

Table 4.1 Minimum periods of curing and protection (120)

CHAPTER FIVE

PRE-RESEARCH MODEL AND HYPOTHESIS

5.1 Introduction

This research work was aiming to review the current state of knowledge upon which a cohesive experimental program would be built that targeted areas requiring further work. The durability and performance of CSF concrete under moderate temperate and more severe hot curing environments was identified as the main area which had not been investigated thoroughly. Hot curing environments were found harmful to most of the engineering properties of mature plain concrete. More specifically a high curing temperature was found to impair the durability and performance of mature plain concrete. In this research OPC-CSF mixtures formulated from combining OPC with CSF is proposed as a modified cementitious material that can be used in a hot curing environment for both superstructural and substructural concrete elements. In this chapter a microstructural model of OPC and OPC-CSF mixture sbased on the chemical and physical properties of both OPC and CSF is described. This model was used for the prediction and explanation of the engineering properties of plain and modified OPC-CSF concrete and mortars under both temperate and hot curing environments.

5.2 Hot climate concreting problems

It becomes quite clear from Chapter 3 that the problems of concreting and concrete performance in hot climates are many fold. High curing temperature can impair the long-term property development of the concrete, such as strength and permeability which represent the key to concrete durability.

The hot climate problem is, however, more complex when we have come to talk about the construction of substructure in Middle Eastern environments. The problem is then usually characterised by the concurrent presence of high chloride and sulphate concentration in soils and ground water. Substructural concrete in the Middle East is concurrently subjected to sulphate attack and chloride-induced steel corrosion. In such situations, the use of sulphate resistant

cement (low C_3A content) usually provides adequate protection against sulphate attack, but would fail to decelerate embedded steel corrosion. This is because up to 8% of C_3A in cement is preferentially consumed by the 4 to 5% gypsum typically added to regulate the time of setting. Since the sulphate resistant cement is limited to a maximum 5% C_3A, it is clear that the available C_3A will not be adequate to convert chlorides expected to permeating foundations through the ingress and seepage of chloride-contaminated groundwater. Only normal Portland Cement (ASTM Type I) with a C_3A content around 12% will have enough aluminate to be effective for chloride removal, but would fail to decelerate sulphate attack.

A potentially useful approach in the Middle Eastern conditions would be to generally specify, for both sub-structure and superstructure, the use of ordinary (high C_3A content) Portland Cement with a suitable admixture to provide sulphate resistance which at least has a resistance equivalent to sulphate resistant cement. Such a cement would be expected to stand against the deleterious late-age effects of high curing temperature on strength and permeability and simultaneously resist sulphate attack and chloride-induced reinforcement corrosion.

There are strong indications that such a cement can be formulated by blending Ordinary Portland Cement (high C_3A content) with a pozzolanic material of proper characterisation. Silica fume is one of the possible pozzolanic materials that could be used to formulate a new modified cementitious material.

The chemical composition of silica fume varies with the type of metal or alloy that is produced in the furnace, but for a given production this chemical composition is found to be very constant because of the purity of the raw materials used in the process. When compared to natural pozzolans or fly ash, condensed silica fume appears to be a unique product because of its high silica content, constant chemical composition, very low impurity content, its vitreous state and extreme fineness.

5.3 Portland Cement model

5.3.1 Hydration products of Portland Cement

The setting and hardening of concrete is the result of the chemical and physical processes that take place between cement and water. An adequate understanding of the chemistry of hydration is necessary for full appreciation of the properties of cement and concretes.

The hydration of cement has been investigated by many workers and the process is now well documented (127) (128). The main components of Portland Cement, C_3S. C_2S, C_3A & C_4AF, react with water to produce complex hydrates.

During the course of the hydration of C_3S and C_2S with water, calcium hydroxide is split off and a calcium silicate hydrate gel is formed. At complete hydration the reaction can be presented approximately be presented by the following equation:

$$2(3CaO.SiO_2) + 6H_2O = 3CaO.2SiO_2.3H_2O + 3Ca(OH)_2$$

tricalcium silicate — water — C-S-H — calcium hydroxide

$$2(2CaO.SiO_2) + 4H_2O = 3CaO.2SiO_2.3H_2O + Ca(OH)_2$$

dicalcium silicate — water — C-S-H — calcium hydroxide

The composition of the calcium silicate hydrate gels produced during the hydration of the anhydrous silicates changes during the period of the reaction and it also varies with the temperature. The immediate product formed in the paste on mixing has a C:S ratio near to 3. This forms a coating on the C_3S surfaces and retard the reaction. After a few hours, dissolution or splitting of this initial product results in an acceleration of the hydration and the formation of CSH(I) consisting of poorly crystallised plates and a C:S molar ratio of 0.8 to 1.5. This is followed by the formation of a third stable product CSH(II) with a fibrous structure and molar ratio of 1.5 to 2. The crystallised hexagonal plates of $Ca(OH)_2$ grow with time.

Finely ground C_3A reacts very rapidly with water, though apparently less so in a saturated lime solution. The hydration of C_3A involves reactions with sulphate ions which

are supplied by the dissolution of gypsum. The reaction is presented by the following equation:

$(CaO)_3.Al_2O_3 + 3CaSO_4.2H_2O + 26H_2O \longrightarrow (CaO)_6.Al_2(SO_4)_3.32H_2O$

Tricalcium aluminate — gypsum — water — Ettringite

Ettringite is a stable hydration product only while there is an ample supply of sulphate available. If the sulphate is all consumed before the C_3A has completely hydrated, then Ettringite transforms to monosulfoaluminate which contains less sulphate. The reaction is presented below:

$2(CaO)_3.Al_2O3 + (CaO)_6.Al_2(SO_4)_3.32H_2O + 4H_2O = 3(CaO)_4Al_2SO_4.12H_2O$

Tricalcium aluminate — ettringite — water — monosulfoaluminate

When monosulfoaluminate is brought into contact with a new source of sulphate ions, then etrringite can be formed once again. The reaction is presented below.

$(CaO)_4Al_2SO_4\,12H_2O + 2CaSO_4.2H_2O + 16H_2O = (CaO)_6.Al_2(SO_4)_3.32H_2O$

monosulfoaluminate — gypsum — water — ettringite

The potential formation of ettringite is the basis for sulphate attack of Portland Cement when exposed to an external supply of sulphate ions. The above hydration products may crystallise in a number of different forms all belonging to cubic crystal systems.

Tetracalcium aluminoferrite (C4AF) forms the same sequence of hydration products as does C_3A. The reaction is slower. The hydration reactions of C_4AF is presented by the following equations:

$(CaO)_4.Al_2O_3.Fe_2O_3 + 3CaSO_4.2H_2O + H_2O = (CaO)_6.Al_2(SO_4)_3.32H_2O$

Tetracalcium aluminoferrite — gypsum — water — Ettringite

$CaO.Fe_2O_3.3H_2O$
amorphous hydrate of iron

5.3.2 Physical structure of hydrated portland cement

Although the properties of the hydration products will clearly influence the properties of the hydrated cement paste, the behaviour of hardened cement paste cannot be properly understood without an appreciation of how the hydration products fit together to form the cementing matrix. A microstructural model of plain cement paste is described in this study based on the previous knowledge for the purpose of predicting and explaining the physical behaviour and properties of plain OPC concrete mixes. The model is illustrated schematically in Figures 5.1 & 5.2. According to this model, hydration of OPC take place at the time when cement particles come into contact with water. In a temperate curing environment, the hydration proceeds at a normal rate, hydration products accumulating in the water-filled spaces. At the final stage of hydration the hardened cement paste consist of unhydrated cement particles, crystallised hexagonal plates of calcium hydroxide and ettringite grown in the open spaces available (avoiding contact with other solid particles), a poorly crystallised assembly of CSH(I) plates formed initially, and a crystallised CSH(II) with a fibrous structure and intra-crystallite capillary and gel pores.

In a hot curing environment the proposed model shown in Figure 5.2 suggests that at early-ages, high curing temperature will accelerate the hydration of OPC particles. This acceleration will reduce the time necessary for proper diffusion and uniform precipitation of hydration products. As a result, a high concentration of the hydration products will build up in the vicinity of the hydrated OPC grains. High temperature also affects the morphology and structure of C-S-H gel, yielding a short-fibred C-S-H which will restrict the development of a long-fibred gel. At late ages the hydrated C-S-H gel which built up in the vicinity of cement particles will be converted by the effect of heat to a crystalline, dense low surface area product which will form an encapsulating layer with the course of time, retarding any subsequent hydration. The whole process described above will

draw the picture of the final hydrated cement structure which will be a poor interconnected crystalline low surface area with coarse capillary pores.

The model described above is expected to influence the physical properties of a cement matrix (namely strength, permeability and porosity, and sulphate resistance) in the following manner:

5.3.2.1 Strength

Since calcium silicate hydrates make up the bulk of the paste matrix (one-half to two-thirds of the volume of the hydrated paste), it is reasonable to assume that it has the dominant effect on strength. Thus, strength of hardened OPC cement paste is mainly dependent on the formation, quantity and volume of the final high surface area CSH gel with a fibrous structure produced from the hydration of C_3S and C_2S. The CSH is expected to make up about one-half to two-thirds of the volume of the hydrated paste. During hydration CSH fibres radiate from the hydrating surface of OPC grains outward into the surrounding pore space. During the late hydration stage these fibres are developed forming a reticular network binding the cement grains together and cement grains with aggregate particles. The physical and chemical bond developed between the intergrowing crystals and the crystals with aggregate are the main source of strength in the hardened cement mix.

According to the model a high curing temperature may affect the morphology and structure of CSH gels yielding a dense low surface area and short fibred CSH gel and this may limit the formation of a reticular network of CSH gels. Retardation and cut-off any subsequent hydration may also restrict the development of an intergrowing structure. Therefore the chemical and physical bond forces between the intermeshing structure is expected to be lower than those developed in a temperate curing environment. Consequently late-age strength produced in a hot curing environment is expected to be lower than that produced in a temperate curing environment.

5.3.2.2 Porosity and permeability

Porosity is one of the basic properties of hardened cement paste. The amount and distribution of porosity between capillary and gel pores changes considerably as hydration proceeds; the capillary spaces are filled up by the hydration products, results in a decrease in the capillary volume. The reverse is true for gel pores. However, since the volume of the hydrated solid is greater than the volume of the unhydrated cement, the total porosity of the system decreases with the continuing of hydration. The above is expected to be the case under temperate curing environment. However, in a hot curing environment the model suggests that at early ages hydrated gels deposited in the capillary water-filled spaces at higher rates result in a decrease in porosity. However, at later-age the formation of dense gel around OPC grains will retard any subsequent hydration as suggested by the described model. Consequently, porosity and the volume of coarse pores is expected to be higher than that produced in a temperate curing environment. Porosity dominates the permeability of a cement paste matrix. Pastes with high capillary porosities have high permeabilities, as fluids flow easily through the larger pores. Accordingly, the permeability of cement paste matrix cured in a hot curing environment is expected to be higher than that cured in a temperature curing environment.

5.3.2.3 Sulphate attack

To describe the behaviour of a plain OPC matrix under sulphate attack we have to understand first the reactions involved and the common mechanism of destruction in temperate and hot curing environments. This will be illustrated by considering a specific case of magnesium sulphate. Under temperate conditions, destructuve expansion is believed to be the common mechanism of destruction. The expansion of plain cement matrices due to sulphate attack has been attributed to three major deleterious sulphate reactions, involving the formation of ettringite and gypsum (129, 130, 131, 132 & 133).

In the first case the sulphate ions react with calcium aluminate hydrate to form calcium sulphaluminate products (ettringite) as follows:

$3(CaO)_4.Al_2SO_4.12H_2O + 7MgSO_4.7H_2O = CaO)_6.Al_2(SO_4)_3.32H_2O$

(C4ASH12) magnesium sulphate (C6ASH32)

$+6Al(OH)_3 + 7Mg(OH)_2 + 5H_2O$

aluminium hydroxide magnesium hydroxide water

This reaction is considered an expansive process since the volume of ettringite produced is 2.27 greater than the volume of the reactants. However, there is some uncertainty as to the actual physical mode of destruction by ettringite.

Although the "sulphate attack" phenomenon is generally attributed to the formation of ettringite, it is observed that ettringite is also the primary source of strength in many cements. Therefore, a question can be raised whether there are two kinds of ettringite, one expansive and the other cementitious, or whether there is only one ettringite which can respond differently depending upon conditions. The former type of behaviour is supported by Mehta (134), who categorized ettringite crystals into two types, one cementitious and the other expansive.

Type 1 ettringite crystals are large lathlike crystals, 10-100 microns long and several microns thick, formed under conditions of low hydroxyl ion concentration which for instance, prevails during hydration of supersulphated or rapid hardening cements. Since hydrated cements containing considerable amounts of large etrringite crystals show high strength but no expansion, he proposed that Type 1 ettringite crystals are not expansive.

Type 2 ettringite crystals are small rod-like crystals, typically 1-2 microns long and 0.1-0.2 microns thick, formed under conditions of high hydroxyl ions concentrations which, for instance, exists during the hydration of normal Portland Cements. Large amounts of these crystals were found in concrete which had deteriorated due to sulphate attack, and Type 2 crystals can be either expansive

or a source of strength, depending on the environmental conditions such as stiffness of the cement paste and the type and concentration of ions in the attacking medium. Mehta's experimental observations showed that this micro-crystalline ettringite is capable of absorbing amounts of water on its surface, thereby causing considerable volume changes.

The second destructive reaction of magnesium sulphate involves the replacement of calcium hydroxide $Ca(OH)_2$ in mortars by gypsum ($CaSO_4 2 H_2O$) as follows:

$Ca(OH)_2$ +	$MgSO_4.7 H_2O$ --→	$CaSO_4 2H_2O$ +	$Mg(OH)_2$ +	$5H_2O$
calcium hydroxide	magnesium sulphate	gypsum	magnesium hydroxide	water

This reaction is expansive since gypsum occupies more volume than calcium hydroxide. The respective molecular volume of $Ca(OH)_2$ and $CaSO_4.2H_2O$ are 33.2 and 74.3 cm^3.

The third reaction involved in the attack process is the subsequent formation of ettringite from the reaction of gypsum with the calcium aluminate hydrate, as follows:

$$(CaO)_3.Al_2O_3.12H_2O + 3CaSO_4.2H_2O + 14H_2O = (CaO)_6.Al_2(SO_4)_3.32H_2O$$

C_3AH_{12} gypsum water ettringite

There is also a further expansive process, in addition to the expansion reactions between sulphate and the products of hydration described above. This is associated with the growth of salt crystals in the capillary pores as the concrete is alternately wetted and dried. The resulting internal forces can build up quickly and salt crystallisation is perhaps the most serious expansion process in hot climates.

5.4 OPC-CSF Model

5.4.1 Hydration of CSF-OPC cement

Condensed silica fume as a pozzolanic material possesses little or no cementitious value in itself when mixed with water. The pozzolanic reaction takes place between silicous, or silicous aluminous fractions of CSF with calcium hydroxide in the presence of moisture to form compounds possessing cementitious properties.

The hydration reaction of cement and CSF can be considered separately, although to a certain extent they occur simultaneously. In fact the pozzolanic reaction can take place only after the hydrolysis of C_3S has formed calcium hydroxide.

As regards the pozzolanic reaction, since the components mainly involved are SiO_2, AL_2O_3, Fe_2O_3 and C_mO, the cementitious reaction products are similar to the products of portland cement hydration. The main reaction products are calcium silicate hydrates (C-S-H) which are produced after the silica of the pozzolan reacts with the calcium hydroxide.

Hydration mechanism of CSF-Portland cement can best be investigated by considering the individual reactions between the pozzolan and the hydration of portland cement compound namely C_3S. Ogawa et al (135) proposed a schematic explanation of the C_3S-pozzolana reaction which is shown in Figure 5.3. The specific details of the mechanism are as follows. Calcium ions dissolved from C_3S are captured by collision to the negatively charged pozzolana grains and are adsorbed on the surfaces. On contact with water, surfaces of pozzolana grain are protonically attacked by H_3O^+, formed by the dissociation of water. It brings a gradual dissolution of Na^+ and K^+...etc., resulting in a silicon rich amorphous layer on the surfaces. Dissolved Na^+ and k^+ accelerate the dissociation of water, intensifying the protonic attack of water and accelerate the dissolution of SiO_4^{4-} which combines with Ca^{2+} and increases the thickness of layer.

Due to osmotic pressure generated by the difference of concentration of ions, such as alkalies and SiO_4^{4-}, between

the inside and outside of the layers, the layer swells gradually.. When the osmoitic pressure attains a certain pressure, the film is broken and SiO_4^{4-} diffuses outside through the openings to meet Ca^{+}. The condition of precipitation being satisfied, C-S-H precipitates on the surface of the outer hydrates of C_3S. The solution near the outer surfaces of the destroyed film becomes poorer in Na^{+} and K^{+} than on the inside and Ca^{2+} is adsorped on the film resulting in the precipitation of C-S-H. The hydration proceeds according to the repetition of above mentioned cycle. When alkali concentration is low, such as in CSF, destruction of the amorphous Si rich film enables Ca^{2+} to move into the inside of the film from the openings and to precipitate C-S-H onto the surface of pozzolana grain.

5.4.2 Physical structure of hydrated OPC-CSF

As stated earlier, the properties of the hydration products will clearly influence the properties of the hydrated OPC-CSF matrix. However, the behaviour of hardened OPC-CSF paste matrix cannot be properly understood without an appreciation of how the hydration products fit together to form the cementing matrix. A microstructural model of OPC-CSF paste matrix has been built in this study based on OPC-CSF hydration mechanism and previous knowledge for the purpose of predicting and explaining the physical behaviour and properties of OPC-CSF matrices.

The proposed model shown schematically in Figure 5.1 & 5.2 suggests that initially, due to the high surface area and fineness of CSF particles, each cement particle will be surrounded by hundreds of CSF particles. Thus the portland cement flocs are stably dispersed by the physical effect of CSF particles in the plastic concrete. This will expose a greater surface area of portland cement to normal hydration than that without CSF. Thus for a fixed quantity of cement the inclusion of CSF may result in a more efficient utilization of the available material and more uniform matrix structure. The high surface area of CSF on the other hand will accelerate the early age hydration rate of calcium

silicate by both adsorbing large amounts of Ca^{2+} ions on its surface, lowering their concentration in the liquid phase and increasing the sites which are favourable to the precipitation of C-S-H.

The hydration of calcium silicate will result in the formation of $Ca(OH)_2$ and calcium silicate hydrate C-S-H(II) fibres which agglomerate on its surface and the surfaces of CSF particles. Calcium hydroxide begins to form discrete hexagonal crystals in the pore solution of the OPC cement matrix, while in the CSF modified matrix it reacts with the CSF particles producing a secondary C-S-H(II). Due to the low molar ratio of C:S (less than 1.0) in the C-S-H near the CSF particle, compared to that in pure OPC which is around 3.0, this secondary C-S-H(II) is expected to be denser and contain even finer pores compared to the C-S-H(II) gel produced by C_3S hydration. This secondary C-S-H will be precipitated on the surface of CSF grains as shown in Figure 5.1. The continuation of hydration brought about by the presence of silica fume (see Section 5.4.1) will result in more and more precipitation of C-S-H(II) gel in the capillary spaces. Eventually C-S-H development dominates the CSF modified matrix, forming a matrix of C-S-H gel growing outward and inward from the cementitious grains, forming a more rigid high surface area structure compared to that produced in the normal OPC mixture itself.

In a hot environment, high curing temperature will initially accelerate the hydration of both cement particles and the $Ca(OH)_2$ with CSF (pozzolanic reaction). Because of the high surface area, silica fume will provide more sites which are favourable to the precipitation of C-S-H gel. Thus the presence of CSF can improve the diffusion of the hydrated products away from the cement grain allowing uniform precipitation. On the other hand, CSF will motivate the continuation of OPC grain hydration as a result of diffusion. This hydration continuation will furnish the matrix with more C-S-H gel fibres, which will result at late-age in a well interconnected high surface area and dense matrix with a high percentage of fine gel pores. The late-age microstructure is

expected to be comparable to that produced under temperate conditions. Thus high curing temperature is expected to accelerate the build up of the early age matrix microstructure without affecting the late-age one.

According to this model the inclusion of CSF in concrete and mortar as a cementitious material is expected to improve the engineering properties such as strength, permeability, pure size distribution and sulphate resistance under both environments in the following manner.

5.4.2.1 Compressive Strength

At early ages the accelerated hydration of C_3S by the physical effect of CSF and curing temperature, will increase the concentration of C-S-H gel and $Ca(OH)_2$ in the pore solution. This will in turn accelerate the pozzolanic reaction between lime and CSF particles. This acceleration for both reactions will result in an early age strength improvement. At later-ages the improvement in strength of CSF mixes over the plain OPC ones can be explained by the model described earlier, *i.e.* the improvement in strength is a result of:

(i). The conversion of $Ca(OH)_2$ to C-S-H gel; and

(ii). C-S-H gels formed by both calcium silicate and the pozzolanic reaction intergrow into a rigid network increasing the surface area of the hydration products and the physical and chemical bond between the intergrowing crystals.

5.4.2.2 Permeability and pore size distribution

One of the most important expected improvements from the inclusion of CSF is the decrease in permeability of concrete and mortar mixes. Due to the accelerated hydration process of both calcium silicate and pozzolana at early ages permeability is expected to fall dramatically especially under hot environments.

According to the model described, a reduction in permeability can be attributed to the change in pore size distribution and more specifically to the ability of CSF to

increase the volume and percentages of fine pores at the expense of the coarse capillary pores *i.e.* pore refining. Because hydration can only take place in the capillary water-filled spaces, then the persue of hydration caused by the pozzolanic reaction between generated calcium hydroxide and CSF particles will result in the formation of a fine, dense secondary C-S-H gel deposited in the capillary pores. Eventually, this process will result in a very fine and probably discontinuous pore structure. And since the flow of fluids and gases can only be facilitated by an interconnected network of capillary pores, permeability is expected to fall in CSF mixes.

5.4.2.3 Sulphate attack resistance

To understand the improvement in sulphate resistance caused by the partial substitution of OPC by CSF, we have to understand first the reactions involved and mechanism of destruction.

There are two main deletrious sulphate reactions that can take place. These reactions are:

(i). The reaction of sulphate ions with calcium aluminate hydrate to form calcium sulphaluminate products (Ettringite). This reaction is an expansive process which under appropriate conditions can cause cracking; and

(ii). the replacement of $Ca(OH)_2$ in concrete by gypsum ($CaSO_4-2H_2O$). Formation of gypsum can lead to the deterioration of concrete by two processes: expansion, because gypsum occupies more volume that calcium hydroxide, and also as gypsum is leached, leaving a porous concrete with high permeability.

Beside these two deletrious reactions, the more common sulphate destruction process experienced in hot countries is the build up of sulphate salt crystals in the capillary pores by the frequent wetting and drying of concrete elements which can eventually disrupt the concrete.

Thus the potential improvement in sulphate resistance offered by CSF can be explained by the dilution of C_3A

content and the conversion of the most vulnerable hydration product $Ca(OH)_2$ to a stable C-S-H product. On the top of that is the reduction in permeability (key to durability) which reduces the ingress of sulphate solution and sulphate ions from outside, which is responsible for the improvement in sulphate resistance.

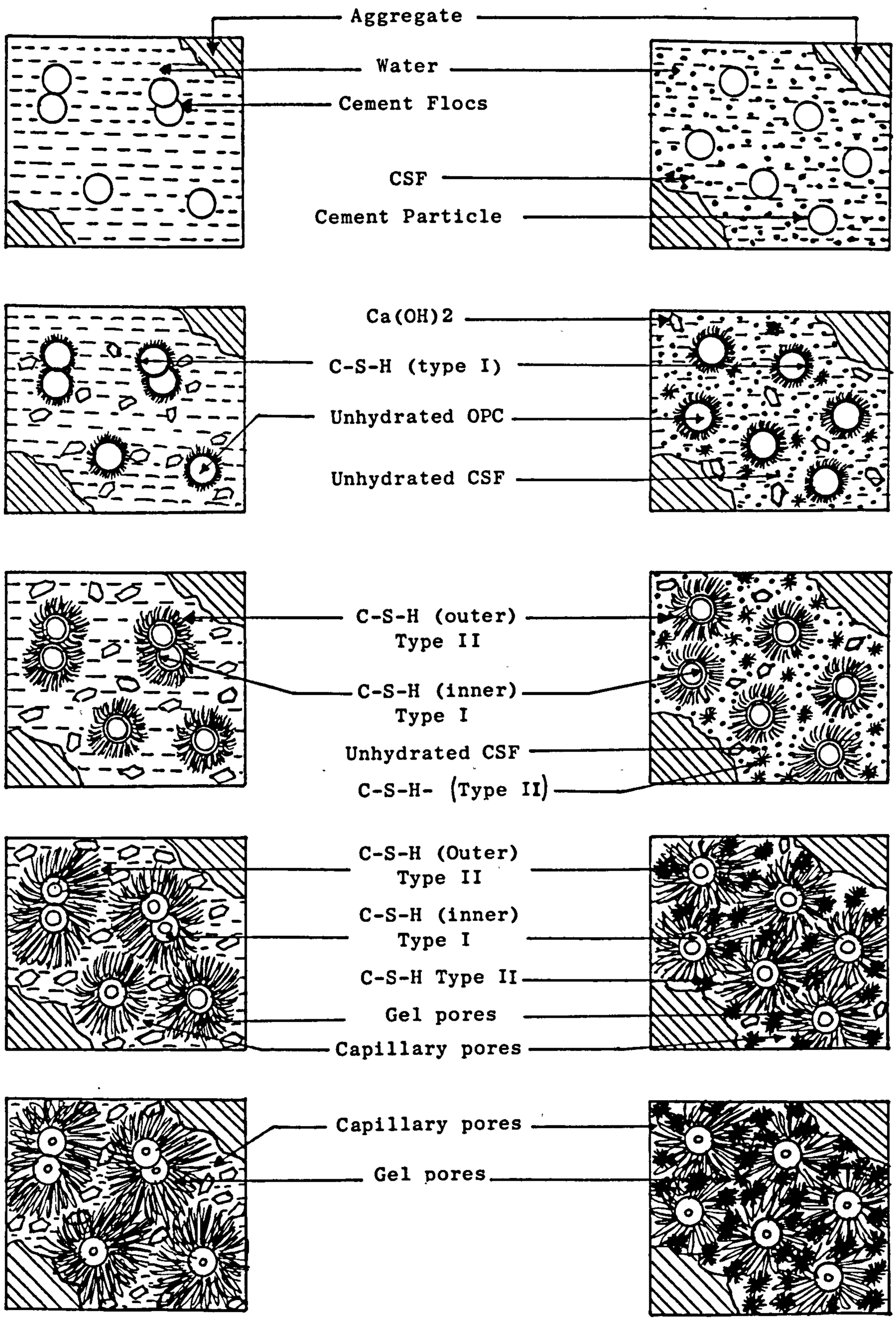

FIGURE 5.1 Schematic model describes the OPC and CSF reactions and microstructural development under temperate curing environment.

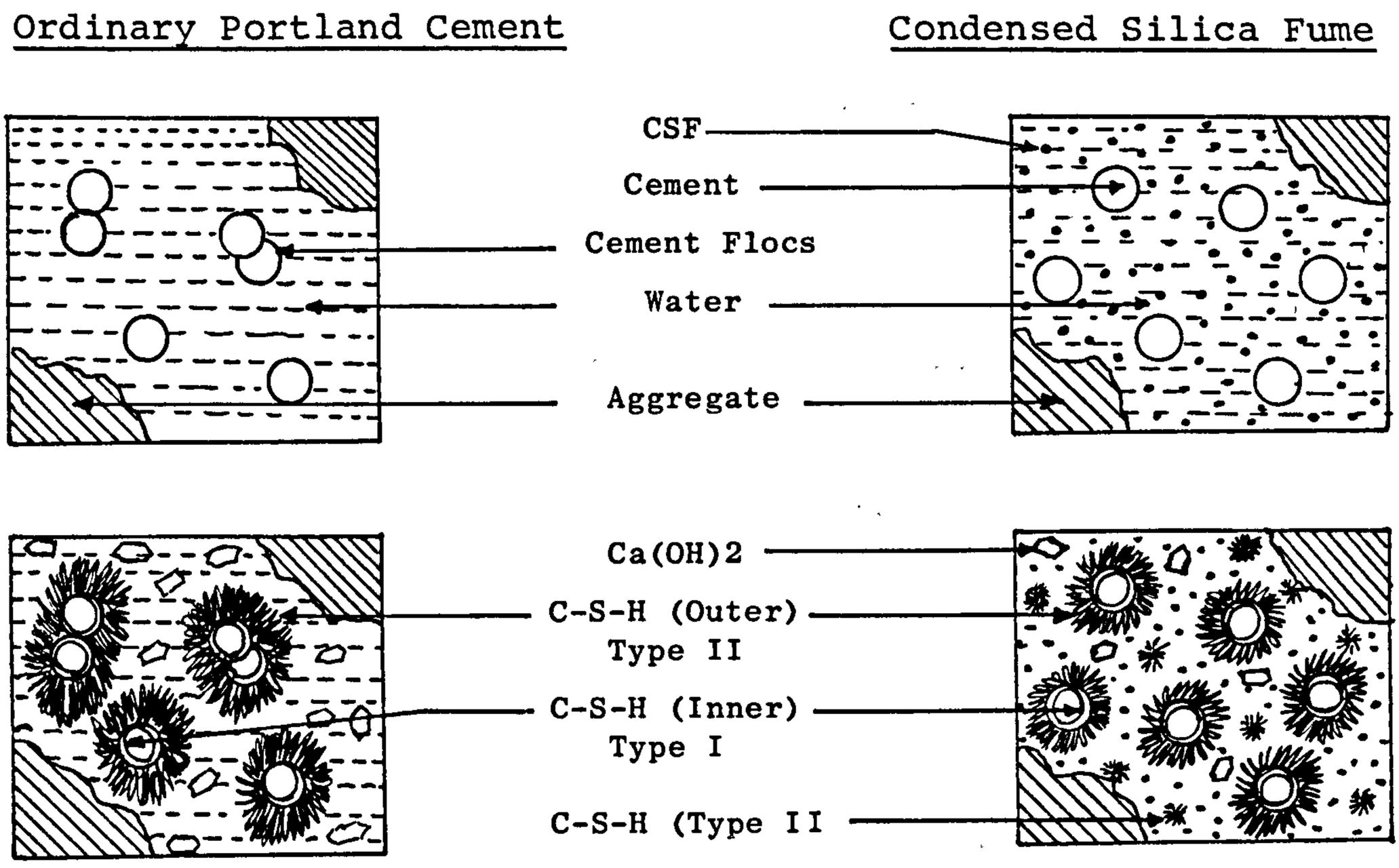

FIGURE 5.2 Schematic model describes the OPC and CSF reactions and microstructural development under hot curing environment.

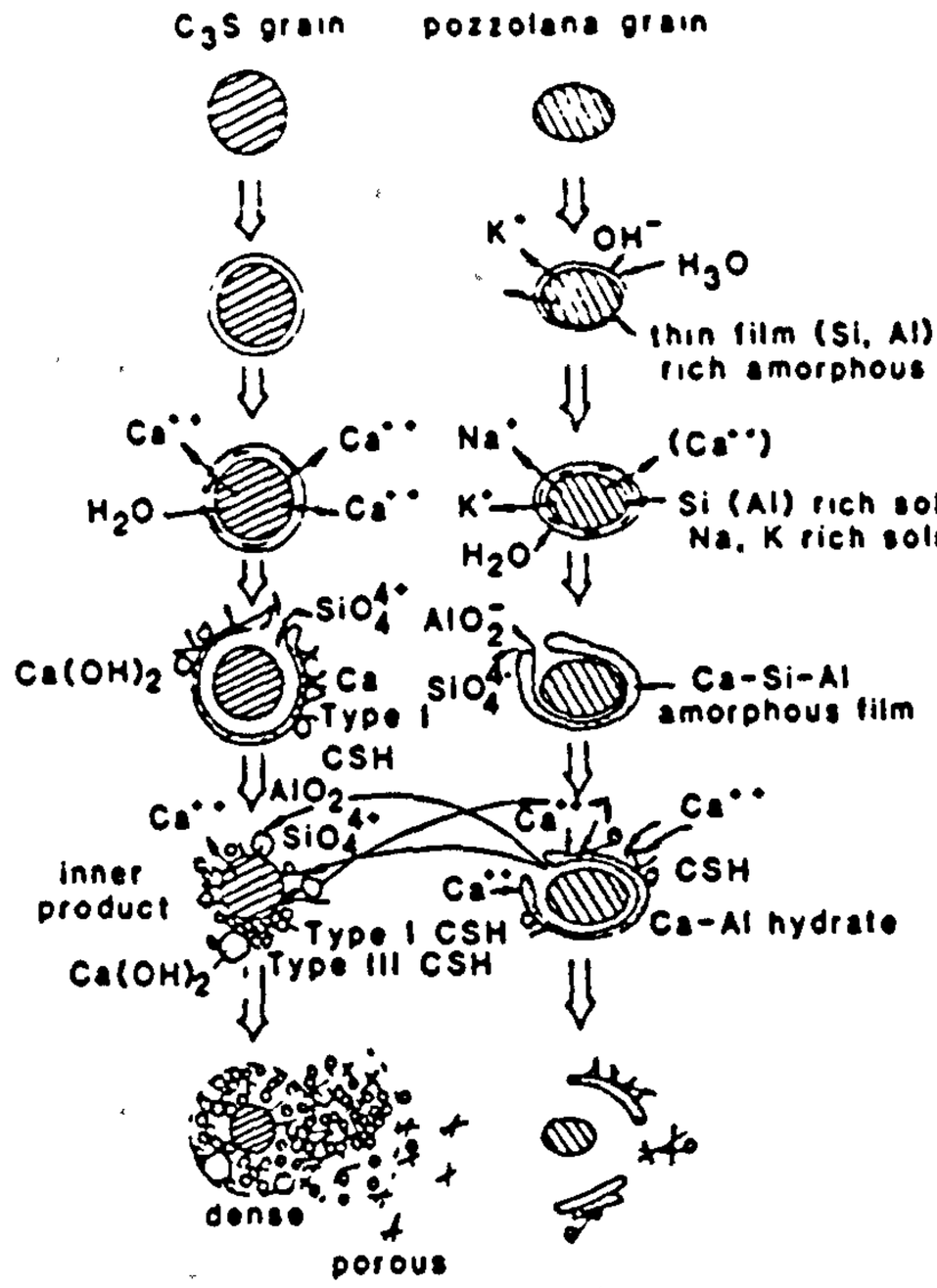

Figure 5.3 Schematic development of the C_3S-pozzolana reaction (135)

CHAPTER SIX

MATERIAL CURING AND TEST METHOD USED

6.1 Introduction

This chapter contains a description of the concrete and mortar ingredients, curing materials and environments used, with a full description of the test used throughout the experimental work. This chapter also contains a description of the facilities used to furnish the desired environmental conditions, namely an environmental room and cabinet.

6.2. Materials

6.2.1 Ordinary Portland Cement (OPC)

The Ordinary Portland Cement was supplied by Castle Cement. It conformed with requirements of BS121 (136). The chemical composition and some physical properties of the cement are given in Table (6.1).

6.2.2 Condensed silica fume (CSF)

The condensed silica fume was supplied by Elkem. Its chemical composition and some if its physical properties are given in Table (6.2). The major chemical constituent is silicon dioxide: its amount varies from 86 to 94 percent.

6.2.3 Aggregate

a. Fine aggregate (sand):-

The fine aggregate was river sand obtained from deposit in North Nottinghamshire. Sieve analysis was carried out on a representative sample in accordance with BS812:1975 (137). The analysis showed that the sand fell in Zone M as specified by BS882:1983 (138). The sieve analysis is given in Table (6.3). The water absorption and specific gravities are given in Table 6.3. The sand was dried prior to batching.

b. Coarse aggregate

The coarse aggregate was river gravel with a maximum size of 20 and 10 millimetres. It was obtained from a deposit in Hemington. The specific gravities and water

absorption are given in Table 6.4. The gravel was also dried before batching.

6.2.4 Superplasticizer

The use of CSF as an admixture or as replacement ingredient in a percentage of ≥10% by weight of cement can result in concrete and mortar mixes with low workability. Workability level can be restored either by increasing the amount of mixing water or using superplasticizer admixture. Both approaches were employed in this research work. A melamine-formaldehyde based superplasticizer in a fluid form was used. The trade name of this superplasticizer is Conplast M1.

This type of superplasticizer, which is based on a higher molecular weight, is said to be a very effective dispersant as it does not affect the surface tension and will not cause air entrainment (139). The amount of superplasticizer was defined as that necessary to restore a medium workability (3-6 vebe seconds) in silica fume concrete and mortar mixes without adjusting the amount of mixing water. This amount was achieved in the laboratory.

6.3 Batching, mixing and casting

6.3.1 Concrete mixes

Batching of concrete. CSF aggregate and water was done by weight. Mixing of plain Portland cement concrete was performed by loading the ingredients according to BS 1881: Part 125 (140) in a Liner cum-flow mixer type 'O' which had a capacity of 0.043 cubic metres. The ingredients were mixed for 2 minutes. As soon as mixing was completed, the concrete was placed into 100 mm cube moulds. The moulds were half filled before vibrating started. The second half was filled after the compaction of the first half and during the progress of vibration. The top surface was levelled off and smoothed using a float.

Silica fume has a very high surface area (15-20 m^2/g, see Table 6.2). Its average particle size is 0.16 micron. Because of this, silica fume was found to generate a

significant amount of dust at the time of mixing. This will obviously deduct from its designed quantity. Moreover, intimate dispersion of silica fume in concrete drastically improves the performace of the binder phase and increases its bonding action with aggregate. Jahren (24) recommended adding CSF in the mixing process as early as possible to ensure proper wetting and thorough dispersion of the fine particles. Thus to make the most of silica fume, dusting and dispersion should be considered critically at the mixing stage.

To reduce CSF dusting at the mixing stage and to improve dispersion, mixing of CSF concrete was performed by loading the ingredients in the following sequence:

Gravel-CSF-water-mix-cement-mix-sand-water-mix.

Mixing time was extended to 3 minutes. Tazaw et al (141) found that using this sort of mixing sequence in which mixing water is divided into two portions and added to the ingredients at different mixing stages which they call 'double mixing' produces superior properties of CSF mixes such as strength, pore distribution and drying shrinkage than conventional mixing in which all water is added at one time. The necessary superplasticizer amount designed to secure workability without adding extra water was added to the mixing water just before starting the mixing process.

6.3.2. Mortar mixes

All plain OPC and CSF mortars were mixed in a Hobart mixer which had a capacity of 25 litres. The ingredients were loaded in the following order; half the sand, then the cement then the second half of sand and water immediately before mixing. Mixing time was 2 minutes. As soon as mixing was completed, mortar was placed into cylinder moulds (100 mm in diameter and 220 mm in depth). The mortar specimens were compacted in four layers.

The CSF mortar mixes were performed by loading the ingredients in the following sequence:

half the sand quantity/silica fume/water/mix/cement/mix - the second half of sand/water/mix. The whole mixing time was

extended to 3 minutes. Casting was carried out the way described above. The required amount of superplasticizer found necessary to secure workability in CSF mixes containing ≥10% of silica fume was added to the mixing water just before the start of the mixing process.

6.4 Initial curing and environmental conditioning

Once all the steel moulds were filled with compacted concrete, or mortar , they were covered with polythene sheets. One third of the moulds were transferred to be conditioned in a room which simulated a hot Iraqi climate. The temperature and humidity cycles during the 24 hours are given in Table (6.5). The other two thirds of the moulds were left to be conditioned under temperate laboratory conditions. The temperature and humidity during the 24 hours are given in Table (6.5). All the specimens were demoulded after 24 hours.

After demoulding the first one third of specimens conditioned in a simulated hot climate they were initially cured by wrapping them with two layers of polythene sheet. Specimens were cured for 0,1,3 and 7 days after which they were left exposed to the environment until they were tested.

After demoulding the second two thirds of specimens, conditioned in a temperate laboratory condition, were divided into two halves. The first half was initially cured in water at a temperature of 20±1 C° for 7 days after which they were taken out and left exposed to the temperate environment until testing. The second half of specimens were initially cured by wrapping them with two layers of polythene sheet, and then leaving them under the temperate environment condition. The specimens were cured for 0,1,3 and 7 days after which they were left exposed totally to the environment until they had been tested. The initial curing methods and environmental conditioning are summarised graphically in Figure 6.1.

6.5 Iraqi weather conditions

6.5.1 Introduction

Iraq is an almost landlocked country lying between six countries. The country has a very short coastline on the

Arabian Gulf. Most of the country is flat and low-lying and has a low plateau in the west and central regions. The northern part is mountainous.

Researchers (142, 143, 144) have divided the country into three climatic regions: north, central and south. However, it has been found that there is no great difference in summer temperatures from the south to the north, see Tables (6.6, 6.7 & 6.8).

The country has a very harsh climate with a marked contrast between the extremely hot, sunny and dry summers, and a cooler winter during which some rain falls. The country experiences some of the highest temperatures anywhere in the world.

6.5.2 Temperature

The temperature in the country often rises to 50°C in the southern area with May, June, July and August being the hottest months of the year. The mean maximum temperature in the summer can be as high as 40°C while the mean minimum temperature is 20°C. When this high ambient temperature is combined with about 11 hours of sunshine, it is understandable that the surface temperature of concrete and formwork can be much higher. Furthermore, a variation in the ambient temperature of up to 20°C can occur within 24 hours which may cause severe thermal stresses in concrete especially when it is young.

6.5.3 Humidity

The term relative humidity is defined as the ratio of water vapour available to the amount of water needed to reach saturation. Consequently a rise in temperature is always accompanied by a reduction in relative humidity (assuming no extra water is added).

Apart from the southern part of Iraq, the mean maximum relative humidity in the summer can be about 35% while the mean minimum is 15%. The relative humidity in the south is much higher as it is affected by the Arabian Gulf. The mean maximium is about 60% and the mean minimum is about 35%.

6.6 Environmental Room

It was difficult to fit moulded specimens into the available climatic cabinet whose shelves were designed to hold a maximum of 50 kg. Therefore these moulds were cured for the first 24 hours in an environmental room in which a typical Iraqi hot climate was simulated.

Heating and cooling of the room was achieved by means of two units, each of which can provide a temperature between 5 to 30°C and relative humidity between 25 to 80%. Thus to achieve the upper limit of temperature, illustrated in the previous section (*i.e.* 40°C), the two units were run simultaneously during the heating cycle. To achieve the lowest limits of relative humidity (*i.e.* 15% R.H.), the hot air was pushed into a drying unit which used silica gel as a moist absorbent material to remove the moisture from the air and return it to the room.

The heating and cooling units mentioned above are:

a. **Air conditioning unit:-** This unit was supplied with an external floor mounted fan with variable speed to circulate air at up to 28-31 m^3/min. This unit had a fully integrated control system to provide hot and dehumidified environments by means of multistep electric heaters. Temperate and humidified environments were accomplished by circulating chilled air through the ceiling and wall panels.

b. **Water cooled condensing unit:-** This unit had up to two and a half tons refrigeration capacity and it operated a water chiller. Cooling was achieved by circulating chilled water through coils clipped to the false wall and ceiling panels. Heating was achieved by means of the condensing unit which operated a heat exchanger. Water was heated up by this unit and circulated through the coils above.

The environmental room was programmed to operate on two main cycles simulating the typical day and night temperature and humidity occurring in Iraq (see Section 6.4). Each cycle lasted for 10 hours, providing the programmed

temperature and humidity. The remaining four hours were used by the system for changing the environmental consistently from one to the other as shown in Figure (6.2). Although the average temperature and humidity inside the room are within the designed ones, they are not even inside the room. This was because the cool and hot air was not circulating efficiently inside.

6.7 Environmental cabinet

A Fisons climatic cabinet type FE1000H/MP/R40-IND was also used to simulate the Iraqi hot climate, see section (6.5). This cabinet was used beside the room as it can provide well controlled temperature and humidity cycles with minimum trouble. The cabinet can provide a control temperature in the range of -40 to 100°C. Its interior dimension is 990 x 1000 x 980 mm.

6.7.1 Principle of operation

The cabinet interior was divided into working and treatment chambers. Air is conditioned in the treatment chamber and continuously recirculated through the working chamber in an air flow system designed to create turbulent flow. The temperature and relative humidity of the air are maintained at the conditions set by the operator via a micro processor programmer.

6.7.2 Temperature

Accurate, repeatable temperature level is achieved by continuously balancing heat loss with intermittent modulated heating, controlled by electronic controllers.

a. Heating

One or more 'Inconel' sheathed electrical heating elements are sited in the treatment area. These heat up the air to achieve the required temperature.

b. **Cooling**

The range of conditions over which the cabinet operates, involves the use of two modes of cooling, Direct and Indirect. Both use a common refrigerator system.

The direct mode uses a finned aluminium cooling coil (evaporator coil) situated in the treatment chamber to extract heat from the circulating air.

The indirect mode uses the same refrigerator but extracts heat from another heat exchanger. This one is situated in a tank of coolant (glycol/water) solution. The coolant solution is continuously pumped through an indirect cooling coil situated in the treatment chamber. This coil in turn extracts heat from the cabinet air but a surface temperature much closer to that of the air. Thus its dehumidifying effect can be very small, enabling control of high humidity levels.

6.7.3 Relative humidity

Relative humidity could be increased and controlled by two humidification systems. These are:

a. **Atomisation:-** finely atomised water is sprayed on to the heating elements in the treatment chamber to produce water vapour which is absorbed by the air in the cabinet.

b. **Vapour phase generation:-** Water vapour produced in the upg is introduced into the treatment chamber and is absorbed by the air.

Dehumidification was achieved using either of the cooling systems to remove water vapour from the air in the working chamber.

6.8 Test philosophy

The most serious causes of durability related problems with concrete are chemical attack, abrasion or wear, corrosion of reinforcing steel and the presence of reactive aggregate. In all cases the susceptibility of the concrete to deteriorate and the rate of deterioration are directly related to the permeability and pore size distribution.

These two properties are related to each other and any change in one will simultaneously change the other.

Permeability and porosity are dependent on the degree and extent of cement hydration. Hydration can only take place in the capillary water filled pores and proceeds when the vapour pressure (moisture content) within the concrete mass is maintained at over 80 percent. Thus hydration is affected by the initial curing and environment conditions in terms of temperature and humidity. However, researchers have reported that curing can only affect a very thin layer of the exposed surface and it happens that curing ceases, only the top few millimetres cover (about 12mm) was found to dry out very rapidly to below 80% relative humidity.

From the above discussion, it is clear that the properties of the concrete surface and sub-surface are of great importance to concrete durability and performance because:

deterioration usually starts from the surface;

curing is of great importance to the first few millimetres of the surface of concrete; and

concrete cover can offer potential protection to the embedded reinforcement and inhibit its corrosion. The latter is a problem of great importance in the Middle East.

Interest was then expressed in reliable testing methods that can examine the permeability of surface and sub-surface concrete. Also interest was expressed in testing methods that have application on site and require less preparation efforts and reasonable testing time. Consequently I chose to use five test methods associated with air and water permeability. These were the Figg relative air and water permeability tests (145), the British standard water absorption and Initial surface water absorption tests (146), and a relative air permeability test developed recently at Loughborough called the Egg test (147).

True water and air permeability methods are tedious and time consuming and it was decided to perform limited work

using these testing methods in a way to examine their correlation with the Insitu testing methods.

Permeability is not a simple function of its porosity but depends also on the size, distribution and continuity of the pores. Therefore, it was decided to examine the effect of curing method, time and environment on the pore size distribution of mortars. Attempts to correlate this property with the permeability were also intended. The literature survey had shown that mercury porosimetry used by different researchers yields reliable data and a suitable apparatus was available. This method was used in the testing program.

An attempt was also made to monitor the deterioration of mortars due to chemical attack. Accelerated laboratory tests were derived consisting of both continuous immersion in a magnesium sulphate solution and alternate soaking and drying. Details of the tests are given later in the chapter.

6.9 Details of test carried out

6.9.1 Compressive strength

The test for compressive strength was carried out in accordance with BS 1881: Part 116 (148), using 100mm cubes. The results recorded were the average of five samples.

6.9.2 Relative air permeability test (Figg test method)

a. Apparatus and test procedure

The first relative air permeability test used in this research work was the one developed by Figg (145, 149) and named after him. The test involved drilling a hole 10mm in diameter and 40mm deep into the sample. A silicon rubber plug is inserted in the outer 20mm of the hole leaving the remaining 20mm as a cavity, see Plate 6.1. A hypodermic needle is then inserted through the rubber plug and the permeability assessed by attaching a digital manometer and a hand vacuum pump to the other end of the needle (see Figure 6.3 and Plate 6.2). A vacuum pressure of 55 KN/m^2 is created in the hole by means of a vacuum pump and the time taken for the pressure to drop 5 KN/m^2, *i.e.* from 55 to 50, is measured. A typical relationship between pressure drop and

time is shown in Figure 6.4. The longer the time taken for the pressure to drop the less permeable the sample. Results of this test will be recorded as the time taken for the pressure to drop by 1 KN/m^2 or simply the inverse of the slope of the line in Figure 6.4.

One of the problems noticed with this method is the silicon rubber seal. With some of the initially tested specimens, it was noticed that the pressure dropped from 55 to 50 kPa faster than expected. The assumed reason was a leakage in the area between the rubber seal and the needle or the concrete. Thus, as a precaution, water was spread on the tested hole area. This procedure was employed on all the subsequent specimens.

Figg air permeability results can vary with specimen size. A specimen of at least a 100mm diameter core or a 100 x 100mm cube can be used for this test (150). Site experience using this in Hong Kong showed that time taken for pressure drop by 5 kpa using 100 x 100mm cubes is higher than that from using 70 x 70mm cubes. However, no difference was noticed between 100 x 100mm and 150 x 150mm cubes (151).

b. **Sample preparation**

The test was performed on 100mm concrete cubes. Concrete specimens were left in a well ventilated oven at 105 ± 5°C to dry out until constant weight was achieved. Constant weight was taken to be not more than 0.1% weight change over a 24 hour drying period. The concrete cubes were then removed from the oven and placed in polythene bags and left over night to cool down. Holes (10mm dia. x 40mm long) were drilled in the centre of the top-as-cast face. The criticism highlighted by Montgomery (152) is that drilling may cause localised microcracking which may affect test results. To reduce the risk of having such microcracks, drilling was accomplished over three stages using 3, 7 and 10mm drills respectively. The hole was then cleaned thoroughly using a compressed air gun. Once the holes were clear an 11mm diameter by 3mm thick foam plastic plug was

inserted into each hole at a depth of about 20mm. Silicon rubber was then poured into the holes and left to set.

6.9.3 Egg test

a. Apparatus and test procedure

The test measures the relative air permeability of concrete skin. It was developed at Loughborough University Civil Engineering Department, by Ray Hudd (153).

This test method is based on the Figg test, and uses its apparatus. The Egg was made by pouring silicon rubber on a brass cube (which had a hypodermic needle fixed in place by soldering and placed onto a 100mm glass dish.

The test is carried out by sticking the 'Egg' on the concrete surface by means of water grease and the air permeability was assessed by attaching the digital manometer and the hand vacuum pump to the other end of the needle (see plate (6.3)), applying a vacuum pressure of 55 kPa and then measuring the time needed for the pressure to drop 5 kPa. A linear relationship has been found by Hudd between pressure drop and time (153). The longer the time taken for the pressure to drop the less permeable the sample is. Results of this test will be recorded as the time taken for pressure to drop 5 kpa.

The test was performed on two vertical faces of each 100mm cube. The results represent the average of six readings.

b. Preparation of specimens

No specific preparation was required. However, the specimen conditioning was identical to that described in section (6.9.2).

6.9.4 The relative water permeability test (Figg method)

a. Apparatus and test procedure

The relative water permeability test used in this investigation was that suggested by Figg (145) and named after him. The apparatus consists of a fine canula connected to a syringe, and inserted via an adaptor block into a

manometer tube. The adaptor block is fitted to an aluminium frame, with a capillary tube fixed on the side of it.

To carry out the test a 21 gauge hypodermic needle is pushed through the silicon rubber plug until it protrudes just below the foam plastic plug. See Plate 6.4. The bore of the needle is checked for freedom from obstruction by rodding with brass wire. After that the two tubes are connected to the needle which will give a water-tight connection to the small cavity in the concrete. Water is then forced into the hole from the syringe via the caula. Once the concrete hole is full, the water overflows through the manometer tube to the adaptor block, and then along the capillary tube. One minute after the first contact with water, the water meniscus is brought to a zero position in the capillary tube and the stopcock is closed. The time in seconds for the meniscus to travel a distance of 50mm is taken as a measure of the water permeability of concrete.

b. **Specimen preparation**

Details of the specimen preparation were given in section (6.9.2).

6.9.5 Initial surface water absorption (ISAT test method)

a. **Apparatus and test procedure**

The initial surface water absorption test (ISAT) measures the rate of flow of water per unit area. The test was first suggested by Levitt (154) and standardised by the British Standard Institution (147) for testing roof tiles. The test measures the rate of water flow per unit area.

The apparatus is shown in Figure 6.5 and Plate 6.5, and consists of a 90mm by 90mm cap, a capillary tube and a reservoir funnel connected together with flexible tubing. The reservoir is set up to apply a water head of (200 ± 20mm) over the concrete surface. The cap was sealed against the concrete surface by means of a greased rubber gasket. Clamps were used to hold the cap in position and to ensure good sealing by pushing the rubber gasket against the concrete surface.

The test is started once the water in the reservoir is allowed to touch the concrete surface, filling the cap and overflowing the flexible tubing connected to the cap outlet and then along the capillary tube. According to the British standard, water flow into concrete can be measured using the capillary tube after 10, 30, 60 and 120 minutes after the water first contacts concrete surface. Because of the number of test specimens, the flow was recorded only after 10 minutes from the start of the test. Water flow in the capillary tube was recorded in centimetres per minute. The recorded distance was then converted to ml/m^2/sec by multiplying it by the previously calculated conversion factor.

The calculation of a conversion factor depends on the cap contact area with the specimen (A1) and the capillary tube section area (A2). The conversion factor can then be calculated using the following equation:

$$0.01 \text{ ml/m}^2\text{/sec} = 6 \times 10^{-4} \times \frac{A1}{A2} \quad \text{(centimetres)} \qquad \ldots\ldots(6.1)$$

The ISAT in this investigation was performed on two faces of each 100mm cube. The results represent the average of six readings.

The problem found with this test method is the formation of air locks in the cap and/or the capillary tube. This air lock was preventing either the cap and the tube or the capillary tube from properly filling up with water. The cap air lock was overcome by disconnecting the outlet tube until the cap was full. The capillary tube airlock was overcome by sucking the air from the other open end.

b. <u>Specimen preparation</u>

The test was carried out on 100mm concrete cubes. The test were carried out on the same specimens prepared for Figg testing method. Therefore, the specimen drying and conditioning is identical to that illustrated in section (6.9.2).

6.9.6 Water absorbtion

The test for water absorption was performed in accordance with BS 881: Part 5 (146), using 100mm concrete cubes instead of the 75mm cylinders specified in the standard.

According to the test procedure, specimens were put in a ventilated drying oven (105 ± 5°C) for 72 ± 2 hours before the testing age, i.e. for a concrete tested at 28 days of age, drying of specimens should be started at an age of 24 days. The specimens were then removed from the oven and placed in an airtight polythene bag for 24 ± ½ hour for room temperature conditioning. After that specimens were weighed and completely immersed in a water tank for 30 ± ½ minute, (the water has to be 25 ± 5mm above the top face of the specimens). The measured water absorption is simply calculated as the increase in weight resulted from absorption divided by the dry weight of specimens. The recorded results are the average of four specimens.

6.9.7 Mercury porosimetry

a. The technique

This technique, introduced by Ritter & Darke (155), is based on the fact that a non-wetting fluid can enter the pores of a solid under an applied pressure. Assuming that all the pores are cylinders of uniform radius, the amount of work required to force the liquid into a pore of radius (r) and length (ℓ) is proportional to the increased surface exposed to that liquid at the pore wall; hence

$$W1 = 2\pi r l.\gamma \cos\theta \quad \ldots\ldots\ldots\ldots\ldots\ldots \quad (6.2)$$

where:

W1 = work required to force the liquid into a pore of radius r and length l

r = radius of cylindrical pore

γ = surface tension of liquid

l = length of pore

θ = contact angle between solid surface and fluid surface.

For a non-wetting liquid the mercury where θ is greater than 90°, the amount of work needed to force a volume of mercury (V) into a pore under external pressure (P) can be written

$$W2 = PV = P.\pi r^2 l \quad \ldots\ldots\ldots \quad (6.3)$$

at equilibrium $W1 = W2$

Thus

$$P = \frac{-2\gamma \cos\theta}{r} \quad \ldots\ldots\ldots \quad (6.4)$$

Equation (6.4) is known as the Washburn (156) equation and shows that the pressure required for the mercury to fill a capillary is inversely proportional to the radius of that capillary.

This method has been reviewed in detail by Orr (157) and Diamond (158). It involves evacuating the gases from the pores and then forcing mercury into the sample by systematically increasing the pressure on the mercury. Both the volume of mercury intruded and the pressure to achieve the intrusion are measured. From these data the cumulative pore volume against pore diameter or a pore size distribution curve is plotted. The assumption of cylindrical pore geometry and some other assumptions are the main sources of error in this technique. In the following section some important sources of error are explained.

b. <u>Type of pores</u>

Ritter & Drake (155) in 1945, pointed out that the assumption of cylindrical pore geometry is an important source of error. They reported that the extrusion curve does not coincide with the intrusion curve. This was attributed to mercury being trapped in the ink-bottle pores of the samples. This type of pore has an entry radius smaller than that of the pore itself and will not be intruded until the pressure is high enough to force mercury to pass through the narrow neck. The total volume of mercury intruded through these kind of pores is attributed to the radius of the neck which is smaller than the true radius of pore. Obviously this will shift the pore size distribution curve to the finer pores which does not represent the true curve.

In addition there are some pores which have an entry smaller than the minimum pore diameter which can be measured or they are completely isolated. Such pores cannot be measured by mercury intrusion porosimetry.

c. **Contact angle**

Ritter & Drake (155) also measured the contact angle between mercury and a variety of materials. They found that it varies between 135° and 142°. Later Orr (157) reported the contact angle between mercury and a large variety of materials ranging from 112° to 142°, with 130° being the most frequent value.

Winslow & Diamond (159) used hardened cement paste and measured the contact angle at two different drying conditions. They found a contact angle of 117° and the mercury surface tension of 484 dyne/cm for oven-dried specimens. They found that the contact angle will vary according to drying conditions. It is interesting that it is generally considered that the contact angle may vary with the applied pressure but recently it has been shown (160) that for relatively hard materials such as porous alumina this is not the case. The results also showed no evidence of sample damage at high pressure which gave validity to the mercury intrusion technique.

For the present work a fixed value of 130° was used for all the specimens as a compromise value most frequently used by research workers in the field.

d. **Apparatus and test procedure**

The instrument used in this investigation was the Micromeritics Autopore 9310. See Plate 6.6. This instrument is capable of generating 207 MPa pressure. It calculates pores volume of a porous material and their distribution in the range 300 to 0.006m.

The instrument consists of three stations for sample analysis of both macro and micro pore sizes. In the first two low pressure stations, the samples were pressurized up to 0.17 MPa and the mercury intrusion volume was measured. In

the third high pressure station, samples were pressurized up to 207 MPa and the volume of mercury introduced were also measured concurrently. The volume of mercury forced into the pores of a sample by an applied pressure which represents the reduction in mercury height in the pentrometer capillary stem is measured by the change in electrical capacitance of a cylindrical coaxial capacitor formed by an outer metallic shield around the pentrometer stem and the inner capillary of mercury. The instrument uses three capacitance transducers to measure the capacitance change. Two of these are used in the low pressure test run, the third is mounted in the high pressure chamber and makes electrical contact to the pentrometer through a high pressure insulator.

In the low pressure procedure, moderate vacuum conditions are created. Pressure is increased from vacuum levels in the low pressure manifold, *i.e.* preparation chamber, by use of a solenoid valve which permits dry air to be admitted and then elevates the pressure up to 0.21 MPa. Pressure measurement is provided between 0-0.21 MPa by a pressure transducer mounted on the manifold assembly.

High pressure generation is accomplished in the Pore Sizer 9310 with a ram generator driven by a ball screw which is in turn driven by a small, universal type gear motor. The control allows precise setting of desired pressure with ease. Figure 6.7 shows the high pressure system. The system is integral with a hydraulic fluid reservoir.

The instrument is integrated with an IBM compatible computer. All the information about the sample and the pentrometers must be fed manually and saved by the software. Although the low pressure operation is done manually, all the information created during this operation is logged by the computer and saved. The high pressure operation is run automatically and controlled by the computer. In addition to saving all the information created during the low and high pressure operation, the software is capable of analyzing true data presenting results.

Samples to be tested are housed in a sample holder which is much like a dilamatometer and is called a

pentrometer. This is illustrated in Figure 6.6 which shows a pentrometer assembly.

A mechanical vacuum pump is also provided and attached to the instrument to meet the vacuum requirements.

e. Sample preparation and test procedure

Cylindrical cores 25mm in diameter and 70mm in length were taken from mortar cylinders of 100mm in diameter and 70mm long (cut down from 110mm). Samples for the pore sizer were small discs 25mm in diameter by about 10-12mm in thickness cut from the 25 x 70mm cores.

The samples were dried in a well ventilated oven at 105°C for 24 hours. The sample should be free of volatile materials such as adsorbed water or other compounds with high vapour pressure. These materials evaporate during the vacuum procedure and prolong the time required to achieve the desired vacuum reading before mercury intrusion. Each dry sample was weighed and loaded into a pentrometer which was sealed and weighed again. Two pentrometers would be prepared simultaneously and inserted into the low pressure ports. Appropriate information relating to weights, contact angle, surface tension, table of pressure, etc was then entered by the keyboard for each of the pentrometers, and the analysis then started. The machine automatically evacuates the samples. When the pressure reaches 50 μm or has stabilized below that, mercury filling is then started. A manual low pressure measurement is then started by increasing the pressure manually in stages and taking a record of the intrusion at each stage up to 0.17 MPa. Pentrometers were taken out at the end of the low pressure operation and weighed. They were then loaded in the high pressure chamber and appropriate information is then entered again and the high pressure analysis started. The machine automatically increases the pressure in the increments entered in the pressure table and pressurizes the sample up to 207 MPa. The pressure can be checked in the high-pressure analysis through the terminal. After completion of the high-pressure run the samples were automatically depressurized and returned to

ambient pressure. The data from the low pressure file is combined with high-pressure data, and the report is printed automatically.

f. **Type of results**

The mercury intrusion porosimetry test produces many results that help to describe the pore structure of cement pastes or mortars. The direct parameters given by the machine are: total porosity, total pore surface area, median pore diameter by pore volume, median pore diameter by surface area and the average pore diameter. These four parameters are calculated from the pore size distribution by use of the pore volume and the pore surface area.

(i) **Pore surface area (PSA)**

The pore surface area is directly related to the number of pores in the matrix. Hence, at a constant porosity, the greater the pore surface area, the higher the number of small pores;

(ii) **Median pore diameter by surface area (MPD-A)**

The median pore diameter by area relates to the number of small pores present in the cement matrix, the smaller the median pore diameter the greater the number of small pores (see Figure 6.8);

(iii) **Median pore diameter by pore volume (MPD-V)**

The median pore diameter by volume relates to the relative volume of smaller pores. The greater this value is the greater the volume of larger pores (see Figure 6.9) and;

(iv) **Average pore diameter (APD)**

The average pore diameter (APD) is a parameter that takes into account both the porosity and the pore surface area by use of the following equation:-

$$APD = \frac{4\ (Porosity)}{Pore\ surface\ area} \qquad \ldots\ldots\ldots (6.5)$$

Thus the higher the pore surface area and the lower the porosity, the smaller the (APD).

6.9.8 True air permeability

a. Apparatus and test procedure

The apparatus used to measure the air permeability of mortars was built in the laboratory based on equipment used by Lovelock (161). The air permeator is shown in Figure 6.10 and Plate (6.7). The apparatus was designed initially to measure Nitrogen, Oxygen, hydrogen, carbon dioxide and helium as well as compressed air permeability. The gas outflow can be measured using either the gas rotameters or the water bubble flow manometer. The gas rotameters must, however, be suitably calibrated for the gas being used. The apparatus consists of a Hassler type pressure cell, see Figure 6.11. Two sizes of cells were available for testing specimens; 21mm diameter by 50mm long and 50mm diameter by 100mm long. The Hassler cell consists of a plastic sleeve which is squeezed against the specimens using air from a high pressure gas cylinder. This seal allows only longitudinal flow to occur when the lower pressure inlet gas passes through the sample. To accomplish this a minimum of 100 psi differential between the outside sleeve pressure and the pressure at the inflow face of the sample should be used.

The sealing system was tested prior to the start of loading and testing specimens, by loading an impermeable steel cylinder in place of the specimens. Using a sealing air pressure of 500 psi and an inflow air pressure of 0.55 MPa no passing flow was recorded after 3 days.

After achieving the above test, mortar specimens 21mm diameter by 50mm long were loaded in the Hassler cell. A sealing pressure of 3.45 MPa was applied. An inflow air pressure of 0.21 MPa was applied on the specimens face. The specimens were allowed to equilibriate for 15 minutes before recording the air flow from the water bubble flow manometer. Rate of gas flow (cm^3/sec) can be measured either by recording the water flow in the manometer in a fixed time or the time for a fixed flow. Initial tests showed that it was

more accurate to record the time for a fixed water flow of 15 cm^3 in the water manometer. The gas flow was stopped, sealing pressure released and the sample dimensions were taken using vernier calipers.

The calculation of air permeability is based on Darcy's law for isothermal steady state flow of gas through a porous media. Thus the relationship between the flow rate Q (cm^3/sec) and differential pressure (P_2^2-1) was investigated to identify the pressure range under which the flow is laminer. This relationship is shown in Figure 6.12. the data consistenyly fitted a straight line relationship. Thus any pressure in the above tested range can give a laminer air flow throughout the specimens. However, experience shows that the lower the pressure the more accurate the results will be.

The calculation of air permeability from test data involves a special case of Darcy's law for isothermal steady state flow of gas through a porous media (162).

The basic equation is:

$$V = \frac{K}{\mu} \cdot \frac{dp}{dl} \qquad \text{.....(6.6)}$$

flow velocity = $\frac{\text{Permeability}}{\text{Gas viscosity}}$ x pressure gradient

The above equation is generally used to calculate the liquid permeability. Because of the compressibility of gas, the flow of air must be measured on the basis of mass rather than volume. Therefore both sides of equation (1) are multiplied by the density of the gas, ρ.

$$\rho V = \frac{k.\rho}{\mu} \cdot \frac{dp}{dl} \qquad \text{.....(6.7)}$$

where ρV = mass velocity

But:

$$\rho V = \frac{Qb}{A} \cdot \rho b \qquad \text{.....(6.8)}$$

where:

ρb = gas density at pressure, Pb

Qb = gas flow at pressure, Pb

A = cross-sectional area of sample

If the gas is "Ideal", the flow is isothermal:

$$\rho \; \rho b \cdot \frac{P}{Pb} \qquad \ldots\ldots\ldots\ldots\ldots\ldots (6.9)$$

where

P = Outlet pressure

Pb = Inlet pressure

Putting (6.8) and (6.9) into (6.7)

$$\frac{Qb}{A} = \frac{k}{\mu} \cdot \frac{P}{Pb} \cdot \frac{dp}{dl} \qquad \ldots\ldots\ldots\ldots\ldots\ldots (6.10)$$

Integrating (6.10) can give

$$\frac{Q}{A} = \frac{k.(P_1^2-P_2^2)}{2.\mu.L.P_2} \qquad \ldots\ldots\ldots\ldots\ldots\ldots (6.11)$$

which leads to

$$K = \frac{2.\mu.Q.L.P_2}{(P_1^2-P_2^2) \cdot A} \qquad \ldots\ldots\ldots\ldots\ldots\ldots (6.12)$$

where:

P_1 = Inlet pressure (atmosphere)

P_2 = Outlet pressure (atmosphere)

K = Permeability (cm/sec)

Q = Rate of gas flow (cm^3/sec)

L = Length of sample (cm)

μ = Viscosity of gas (temperature dependent)

If P_2 = 1 atmosphere

then:

$$K = \frac{2.\mu.Q.L}{(P_1^2-1) \cdot A} \qquad \ldots\ldots\ldots\ldots\ldots\ldots (6.13)$$

b. **Specimen preparation**

Sample preparation entailed drilling cores (21mm diameter) with a Pillar drill using Dromus B soluble oil as the coolant. The mortar cylinder (100mm diameter) from which the above cores were taken was fixed in a vice to ensure stability and safety during drilling. Cores were removed and mounted in a 'Cutrock' cutter machine having a diamond face cutting disc of 10cm diameter. The cutter was used to give a core of approximately 50mm in length. The cores were then labelled, washed and dried in a ventilated oven at 105 ± 5°C for two days, after which they were transferred to a dessicator and allowed to cool down.

6.9.9 Water permeability

a. **Apparatus and test procedure**

The water permeability apparatus used was built initially by Newsome (163). This was then modified by Hudd (153) as the only inconvenience was the long time it took for specimen preparation and setting. The apparatus is shown schematically in Figure 6.13 and plate (6.8). Water flow was recorded each 24 hours by measuring the fall in water height taking place in a perspex tube (16.39mm internal diameter) attached to the cell, see Figure 6.13. Specimens were loaded into the cell and tested for 14 days.

The calculation of water permeability from the test data was based on Darcy's law:

$$-\frac{dq}{dt} = k.\ \frac{\Delta h}{L}\ .\ A \qquad \ldots\ldots\ldots\ldots\ldots\ldots\ (6.14)$$

where

$\frac{dq}{dt}$ = flow rate (m^3/sec)

k = coefficient of permeability (m/sec)

Δh = head drop (m)

L = specimen length (m)

A = specimen cross sectional area (m^2)

But

$P = \rho . g . \Delta h$

$$\therefore \Delta h = \frac{P}{\rho \cdot g} \qquad \ldots\ldots\ldots\ldots\ldots \quad (6.15)$$

where

P = inlet pressure (N/m^2)

ρ = water density (1000 kg/m^3)

g = gravity acceleration (9.81 m/S^2)

And

$$\frac{dq}{dt} = \frac{h.a}{t} \qquad \ldots\ldots\ldots\ldots\ldots \quad (6.16)$$

where

h = height drop of water column (m)

a = cross sectional area of inlet tube ($\simeq 2.11 \times 10^{-4}\ m^2$)

t = time for height drop, h. (seconds)

Putting 6.15 & 6.16 into 6.14

$$\therefore \quad k = \frac{L.h.a.\rho.g}{A \,.\, t.\, P} \qquad \ldots\ldots\ldots (6.17)$$

b. **Preparation of specimens**

100mm diameter by 25mm thick mortar discs were cut from the centre of 100mm diameter by 220mm long cylinders. The discs were washed and then dried in a vertical oven at 105 ± 5°C for two days after which they were taken out and stored in a well sealed polythene bag for conditioning.

To seal the edges of these mortar discs and to ensure that water can only pass through the specimens, epoxy resin was cast around the edge. Epoxy resin was cast by placing the mortar discs into a plastic piece of pipe having an internal diameter of 110mm and then pouring the resin into the gap around the specimen. (See Plate 6.9). The resin was left to harden for 24 hours when the specimens were taken out and loaded into the permeability cell for testing.

To improve the bond between the resin and the specimen edge it was roughened by brushing with a wire brush. All the loose particles and dust was cleaned using compressed air before casting the resin.

6.9.10 Chemical attack

Most knowledge on the durability of different types of concrete towards aggressive sulphate solution has been derived from laboratory experiments. Yet limited attempts have been made to study the performace of actual structures in service.

According to Markestade (164) and Mielenz (165) for a laboratory test to be of a reliable and practical value for both the manufacturers and the consumer of cement, it should yield reliable and reproducible information, correlate well with the field experience and be applicable to a wide variety of cement.

To achieve this, the accelerated laboratory testing should take into account the type and nature of the attack (weakening by leaching, disruption by volume change due to crystallisation etc), the corresponding type of laboratory exposure and the criteria to evaluate the attack.

These are the temperate and the simulated IRAQI hot weather.

In consideration of the first two points, two types of attack are possible in the environments under consideration in this research (temperate and simulated Iraqi hot climate. The first is the formation of gypsum and ettringite that results from the reaction between sulphate and hydrated lime and calcium aluminate respectively, these two reactions being accompanied by a considerable expansion and disruption of concrete at advanced stages. This type of attack can take place in either environment. The second type of attack is the deposition of sulphate salt crystals in the capillary pores. The alkali water entering the concrete may evaporate and deposit salts in the pores. The growing crystals resulting from alternate wetting and drying may eventually fill the pores and develop pressure sufficient to disrupt concrete. This type of disintegration is most likely to take place in hot climates where the fluids present inside the concrete element can be evaporated by the effect of high temperature and low relative humidity.

Therefore the following two laboratory exposure conditions were selected to simulate these forms of attack.

6.9.10.1 Continuous immersing in sulphate solution

The problem with this type of test is that both the solution pH and sulphate ions vary with time. This can detract from its usefulness in several ways:

(i) The validity introduced by variation of sulphate ions can make comparison of result difficult;

(ii) The pH value rapidly approaches the values determined by the solubility products of calcium hydroxide. Thus, the solution pH values which are obtained during tests of this type tend to be three to five orders of magnitude of those ordinarily encountered in actual service; and

(iii) The progressively diminishing supply of sulphate ions prolong the time required to reach a reasonable failure criterion.

Mehta and Gjorv (166) proposed an accelerated continuous immersing test method which is capable of evaluating the resistance of cement to ettringite and gypsum type of sulphate attack. The method involved immersion of small specimens in a sulphate solution. The pH of the solution was maintained in the range of 6.0 to 7.0 by frequent addition of one normal H_2SO_4 to the solution. The reason behind maintaining the pH in this range and more important below 9.0 was not only to prevent the possibility of carbonate incrustation on the surface of specimens, which will later on insulate the concrete from corrosive media, but also to replenish the hydrogen ions and sulphate ions which were used up as a result of chemical reaction between the sulphate solution and cement paste. This test method was employed in this investigation.

6.9.10.2 Alternate soaking and drying of specimens

This test method used was proposed by the Bureau of Reclamation (167). It involves soaking concrete or mortar specimens in a sulphate solution at about 23°C for 16 hours

and then drying them in an oven at 50°C for 8 hours. This accelerated test is suitable if concrete is expected to be exposed and serve in the Middle East where high temperature and low humidities occur.

6.9.11 Failure criteria

In consideration of the failure criteria for evaluations, this mainly depends on the nature and type of attack. Ettringite and gypsum formation can result in expansion and disruption of specimens. Salts crystallisation can result initially in increased weight followed by disruption and weight loss. Therefore monitoring changes in volume and weight represent the appropriate measures for evaluating the attack. The number of days required to register a 25% change in weight is often accepted as a failure criterion, whereas expansion of 0.5% of mortar specimens can be considered as a failure.

6.9.12 Specimen preparation

Mortars were cast and vibrated in 40 x 40 x 160mm moulds. Half of the specimens were left in the laboratory and half were conditioned in the environmental cabinet. All the specimens were covered by polythene sheets for the first 24 hours. After demoulding, specimens were wrapped with polythene sheet and left in the environment for 6 days. Polythene sheets were taken off after 7 days leaving the specimens exposed to the environment for another 7 days. At the age of 14 days specimens were cut to get 40 x 40 x 40mm cubes. Specimens were divided into two groups each consisting of four specimens. The first continuously immersed in a 5% $MgSO_4$ solution and the second alternately soaked in a similar solution for 16 hours and oven dried for 8 hours. The pH of the solution was monitored and kept in the range of 6-7 by frequent addition of one normal H_2SO_4. The sulphate solution was stirred by using diaphragm pumps located outside the immersion tank. The above arrangement is shown in Plate (6.10).

Table 6.1 - Chemical and physical properties of ordinary Portland Cement

OXIDES	PERCENTAGES (%)
SiO_2	21.14
Al_2O_3	4.63
Fe_2O_3	2.74
Ca O	64.84
SO_3	2.80
MgO	1.27
K_2O	0.64
Na_2O	0.13
L.O.I.	1.10
Insol Res	0.25
Na_2O Eqivalents	0.55
C35	55.3
C_2S	18.9
C_3A	7.6
C_4AF	8.3
Specific gravity	3150 kg/m^3
Specific surface area	360-380 m^2/kg

Table 6.2 Chemical and physical properties of silica fume

OXIDES		PERCENTAGES
SiO_2	---------→	86-94
SiC	---------→	0.1-0.8
C (total)	---------→	0.4-1.3
Fe_2O_3	---------→	0.2-2.5
AL_2O_3	---------→	0.2-2.0
CaO	---------→	0.1-0.7
MgO	---------→	0.3-3.5
Na_2O	---------→	0.2-1.5
K_2O	---------→	0.5-3.0
P	---------→	0.03-0.07
S	---------→	0.1-0.3
TiO_2	---------→	0.002-0.2
Mn	---------→	0.1-0.2
Pb	---------→	.001-0.05
Zn	---------→	.006-0.08
L.O.i	---------→	0.8-2.5

Specific surface area = 15-20 m^2/g

Average particle size = 0.16 micron

size distribution:

+ 10 microns	1.5%
+ 5 microns	7%
+ 1 micron	10%
+ 0.5 microns	19%

Table 6.3 Sand sieve analysis and specific gravity

Sieve size	weight retained	Percentages Retained	Passing	B.S.882 limits % Passing for (M) Lower	Upper
10.0 mm	NIL	NIL	100	-	-
5.00 mm	16	1.6	98.4	89	100
2.36 mm	175	17.5	80.9	65	100
1.18 mm	163	16.3	64.6	45	100
600 µm	99	9.9	54.7	25	80
300 µm	314	31.4	23.3	5	48
150 µm	215	21.5	1.8	-	-
PAN	18	1.8		-	-

Specific gravity (oven dry)	2.62
Specific gravity (saturated surface dry)	2.53
Specific gravity (apparent)	2.66
Water absorption (%)	0.64
Bulk density (oven dry)	
uncompacted	1572 kg/m³
compacted	1687 kg/m³

Table 6.4 Physical properties of coarse aggregate

Max. coarse aggregate size	S.G. Oven dry	S.G. saturated surface dry	S.G. apparent	Water1 absorption %
20 mm	2.53	2.55	2.59	1.0
10 mm	2.52	2.66	2.57	2.12

Table 6.5 **Temperature and humidity of the environment conditions**

Environment	Description
Hot	Temperature and humidity were designed to simulat the day and night IRAQI environment. Temperature and humidity of day and night were 40°C, 15% R.H. and 20°C, 35% R.H. respectively.
Temperate	The temperature and humidity of this environment were the ones available in the laboratory. The temperature and humidity of day and night were 20°C, 40% R.H. and 18°C, 45% R.H.

Table 6.6 Temperature, humidity and precipitation in the North (143)

Temperature °F					Temperature °C				Relative humidity	Precipitation			
Highest recorded		Average daily		Lowest recorded	Highest recorded	Average daily		Lowest recorded	All hours	Average monthly		Average no. days with 0.04 in + (1 mm +)	
		max.	min.			max.	min.		%	in	mm		
J	72	53	35	16	22	12	2	−9	80	1.6	41	6	J
F	72	58	38	18	22	14	3	−8	73	0.8	20	5	F
M	91	70	42	24	33	21	6	−4	65	0.3	8	3	M
A	103	80	52	37	39	27	11	3	61	0.8	20	4	A
M	105	92	61	46	41	33	16	8	45	0.1	3	0.7	M
J	111	99	70	45	44	37	21	7	36	0	0	0.1	J
J	114	105	78	67	46	41	26	19	29	0	0	0	J
A	113	104	76	68	45	40	24	20	38	0	0	0	A
S	111	97	68	48	44	36	20	9	39	0	0	0	S
O	97	86	56	43	36	30	13	6	48	0.2	5	2	O
N	90	72	46	25	32	22	8	−4	51	1.5	38	5	N
D	68	58	37	17	20	14	3	−8	60	0.9	23	4	D

Table 6.7 Temperature, humidity and precipitation in the CENTRE (143)

Temperature °F					Temperature °C				Relative humidity		Precipitation			
Highest recorded		Average daily		Lowest recorded	Highest recorded	Average daily		Lowest recorded	0600 hours	1500 hours	Average monthly		Average no. days with 0.04 in + (1 mm +)	
		max.	min.			max.	min.		%	%	in	mm		
J	77	60	39	18	25	16	4	−8	84	51	0.9	23	4	J
F	86	64	42	23	30	18	6	−5	78	42	1.0	25	3	F
M	90	71	48	27	32	22	9	−3	73	36	1.1	28	4	M
A	104	85	57	37	40	29	14	3	64	34	0.5	13	3	A
M	112	97	67	51	44	36	19	11	47	19	0.1	3	1	M
J	119	105	73	58	48	41	23	14	34	13	0	0	0	J
J	121	110	76	62	49	43	24	17	32	12	0	0	0	J
A	120	110	76	64	49	43	24	18	33	13	0	0	0	A
S	116	104	70	51	47	40	21	11	38	15	0	0	0	S
O	107	92	61	39	42	33	16	4	49	22	0.1	3	1	O
N	94	77	51	29	34	25	11	−2	70	39	0.8	20	3	N
D	79	64	42	20	26	18	6	−7	84	52	1.0	25	5	D

Table 6.8 Temperature, humidity and precipitation in the South (143)

Temperature °F					Temperature °C				Relative humidity		Precipitation			
Highest recorded		Average daily		Lowest recorded	Highest recorded	Average daily		Lowest recorded	0500 hours	1600 hours	Average monthly		Average no. days with 0.04 in + (1 mm +)	
		max.	min.			max.	min.		%	%	in	mm		
J	81	64	45	24	27	18	7	−4	89	62	1.4	36	5	J
F	87	68	48	28	31	20	9	−2	87	55	1.1	28	4	F
M	95	75	55	36	35	24	13	2	81	49	1.2	31	3	M
A	105	85	63	47	41	29	17	8	76	43	1.2	31	3	A
M	114	95	76	48	46	35	24	9	65	40	0.2	5	0.7	M
J	115	100	81	69	46	38	27	21	60	41	0	0	0	J
J	123	104	81	72	51	40	27	22	58	35	0	0	0	J
A	120	105	78	68	49	41	26	20	56	32	0	0	0	A
S	116	102	72	58	47	39	22	14	62	32	0	0	0	S
O	114	94	64	45	46	34	18	7	67	36	0	0	0	O
N	98	80	57	38	37	27	14	3	83	52	1.4	36	2	N
D	85	69	48	29	29	21	9	−2	89	62	0.8	20	3	D

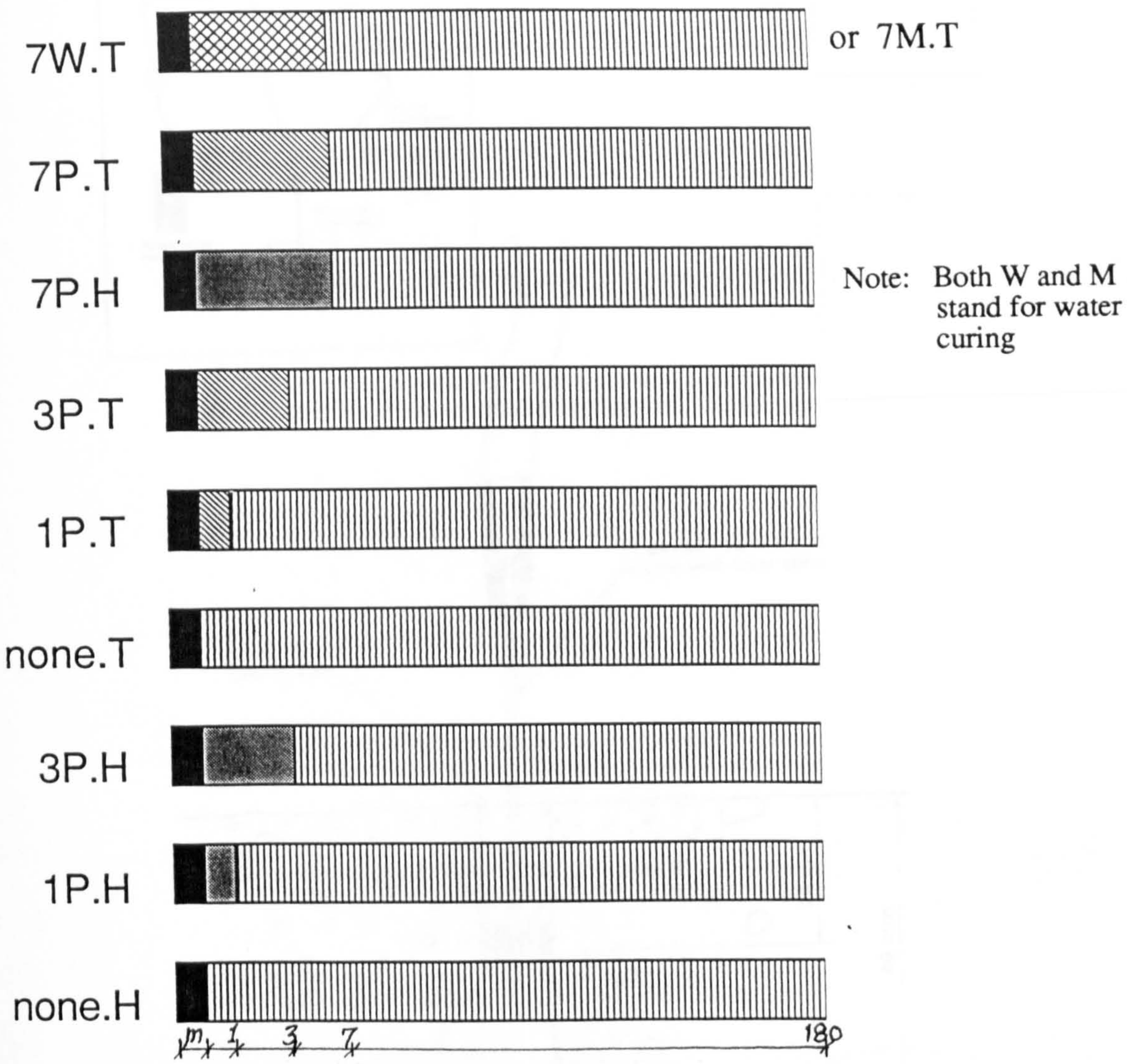

In this figure, T and H stand for temperate and hot environment conditioning respectively; P and W stand for polythene and water initial curing respectively; m stands for mould curing in the first 24 hours; 7, 3, 1 and none stand for the period of initial curing.

Figure 6.1 Initial curing and environmental conditioning used for concrete and mortar specimens.

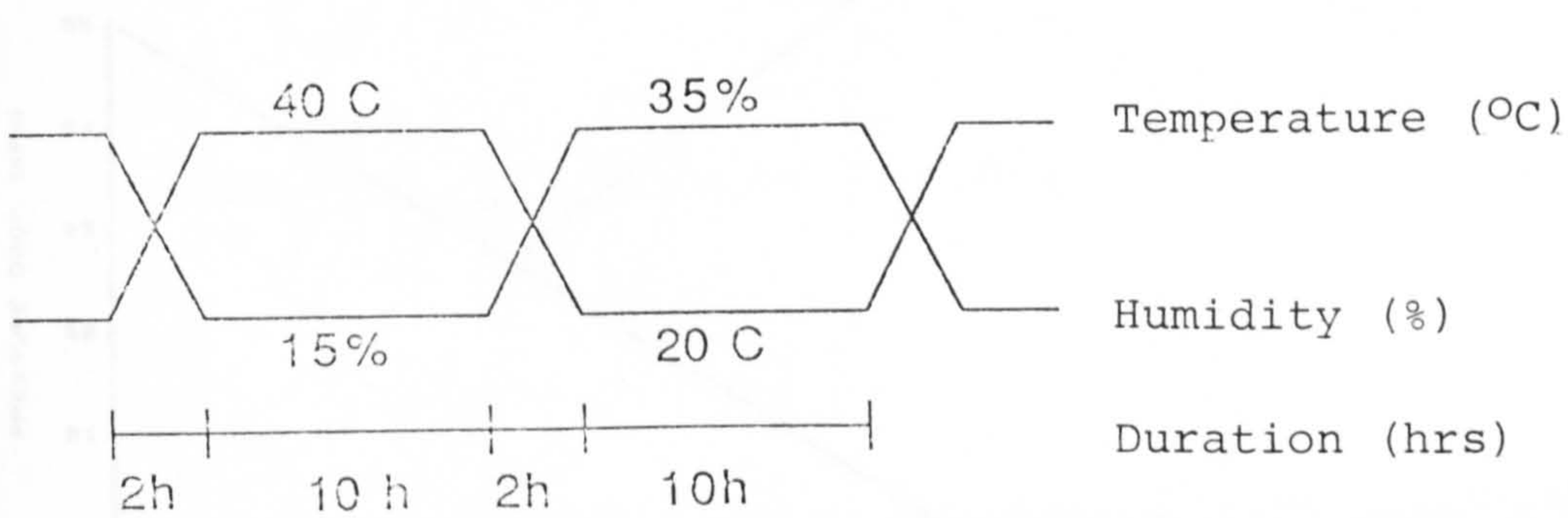

Figure 6.2 Temperature and humidity cycles with their duration during the simulated day and night IRAQI environment.

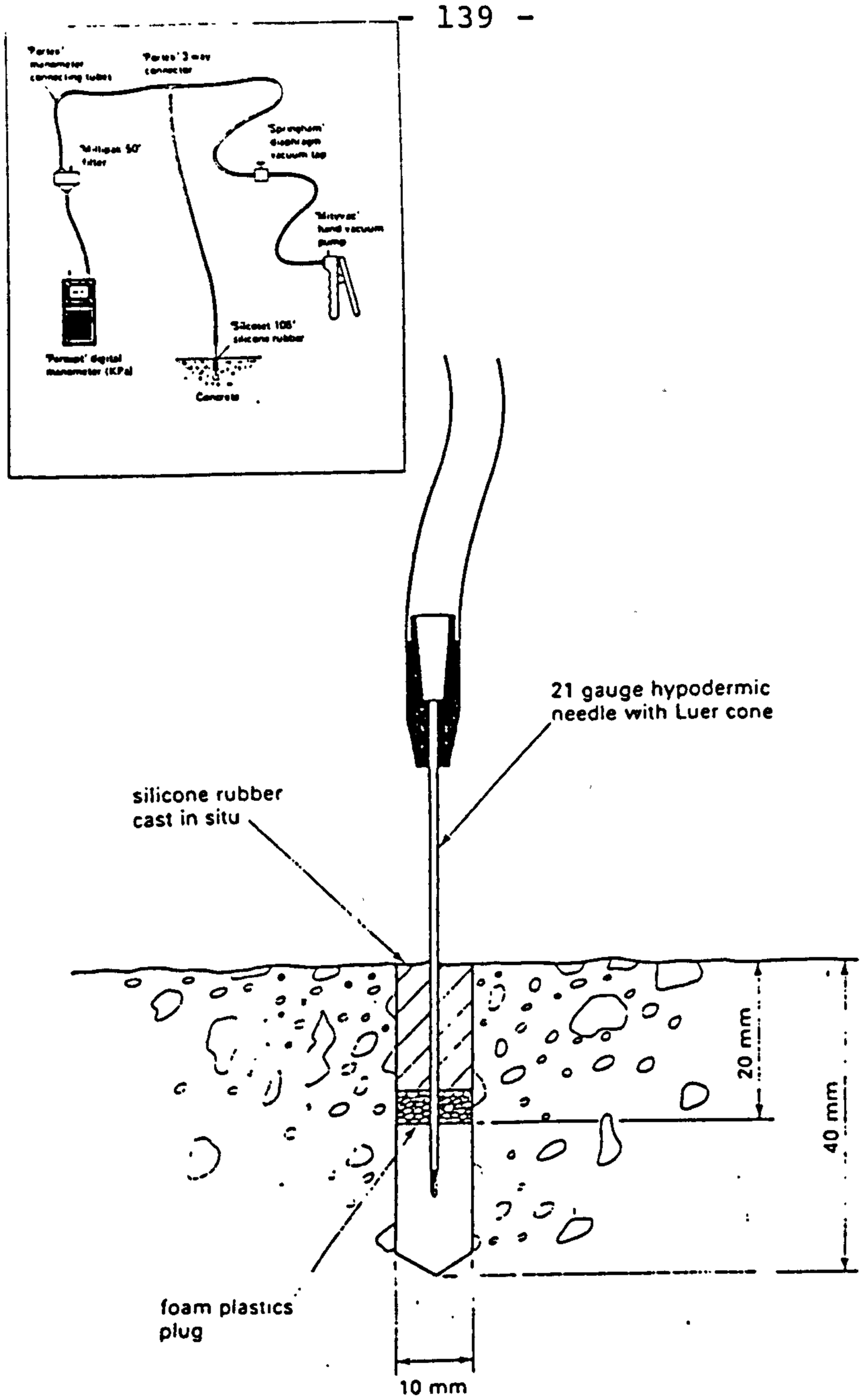

Figure 6.3 Figg Apparatus

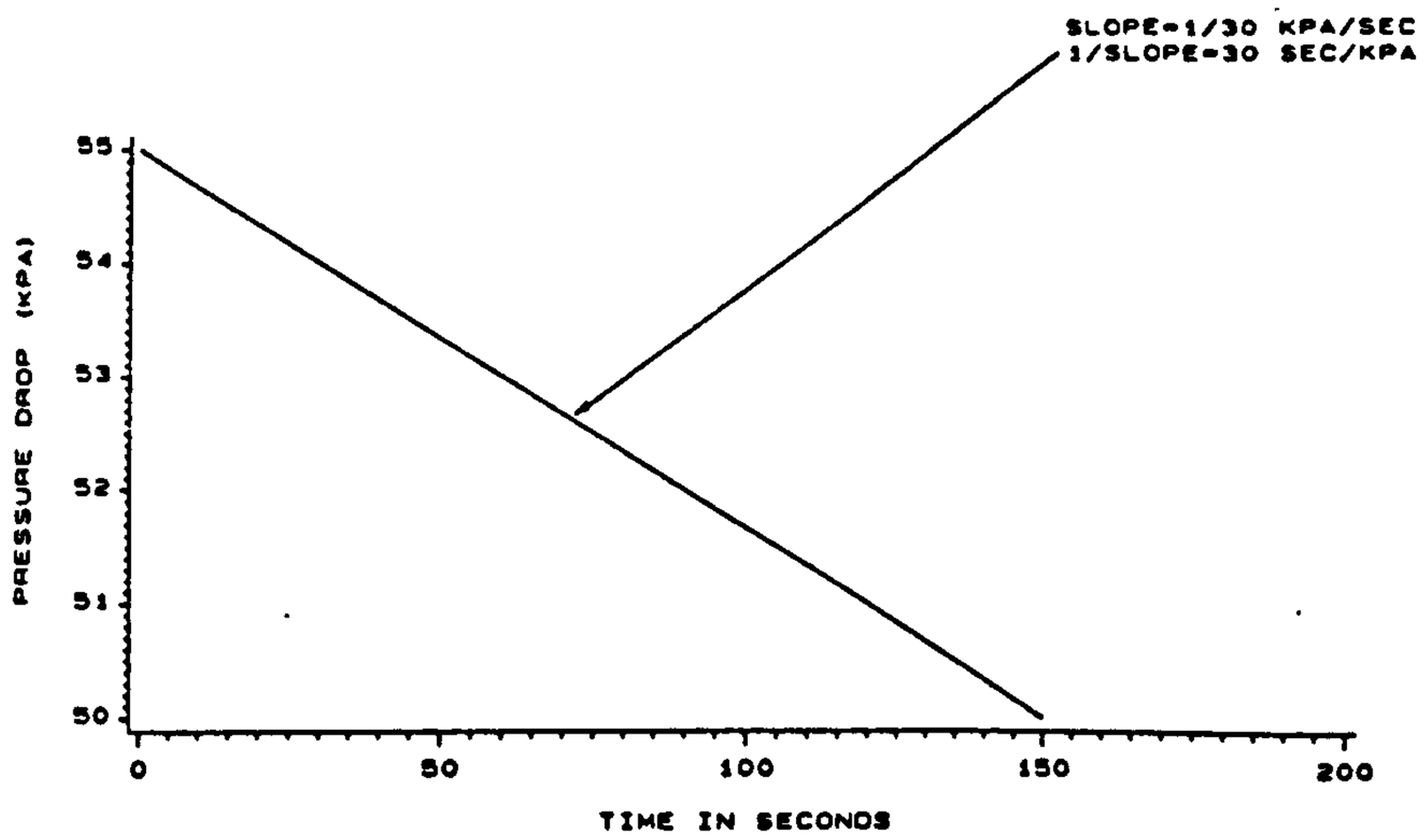

Figure 6.4 The Figg relationship between pressure drop and time (145)

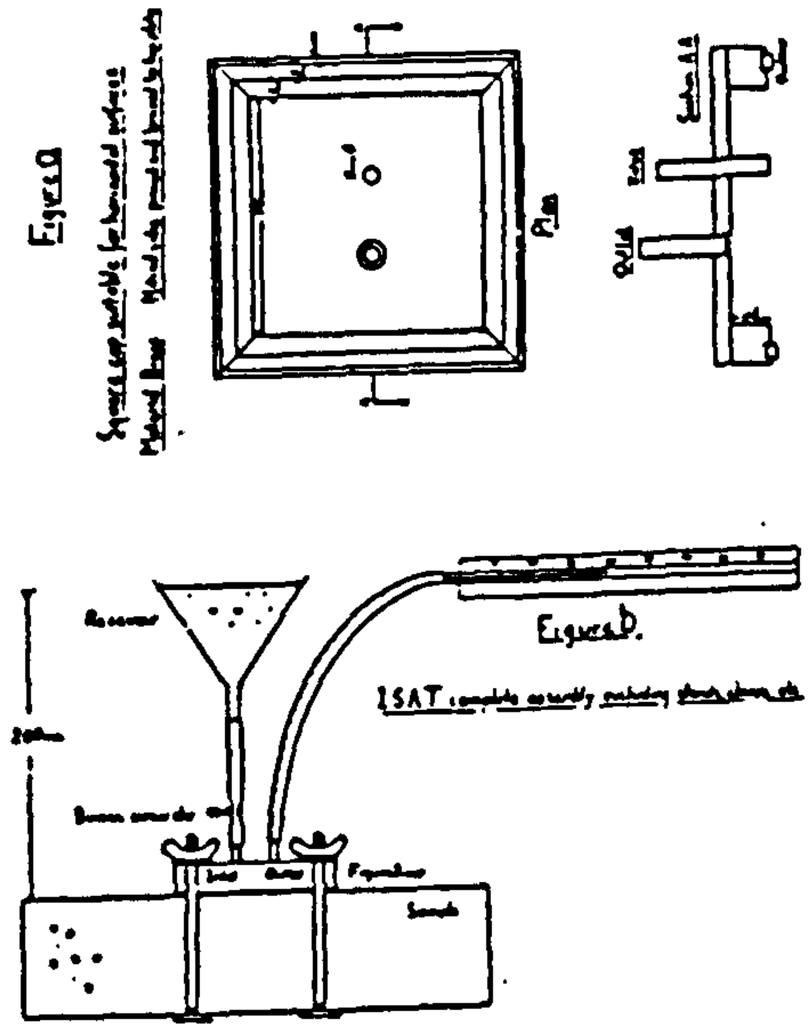

Figure 6.5 ISAT Apparatus (146)

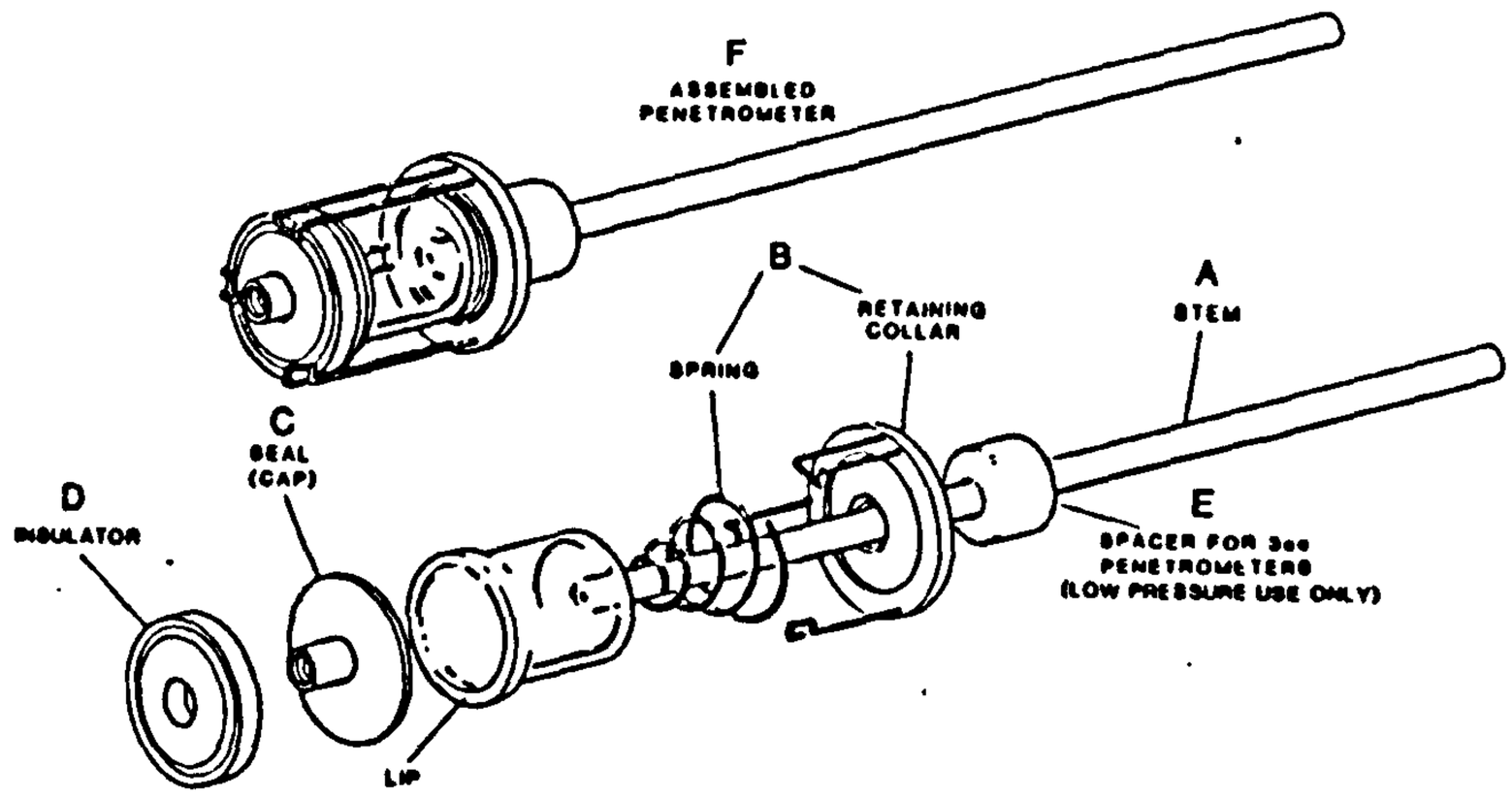

Figure 6.6 Penetrometer Assembly

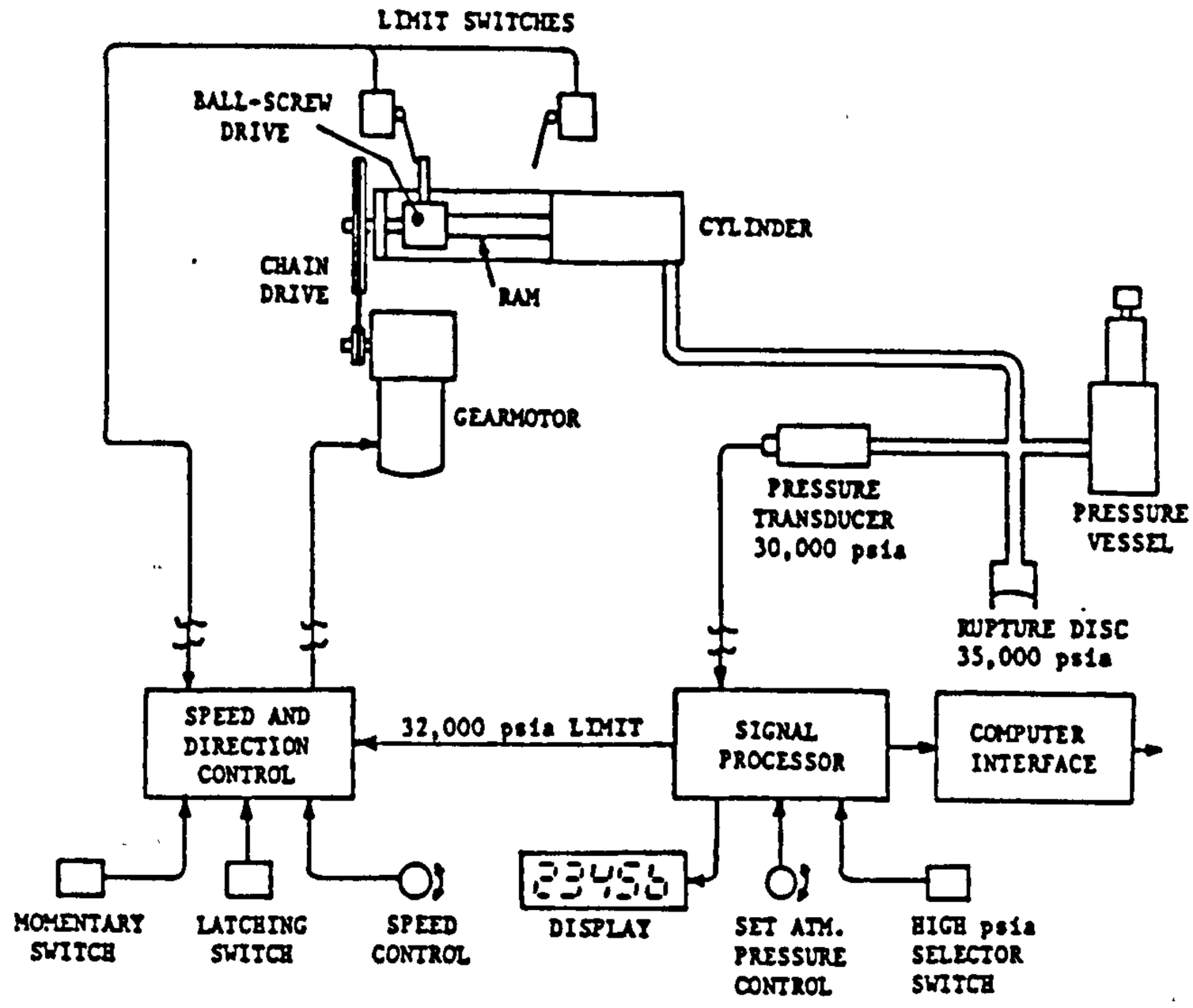

Figure 6.7 Block diagram of high pressure generation and control system

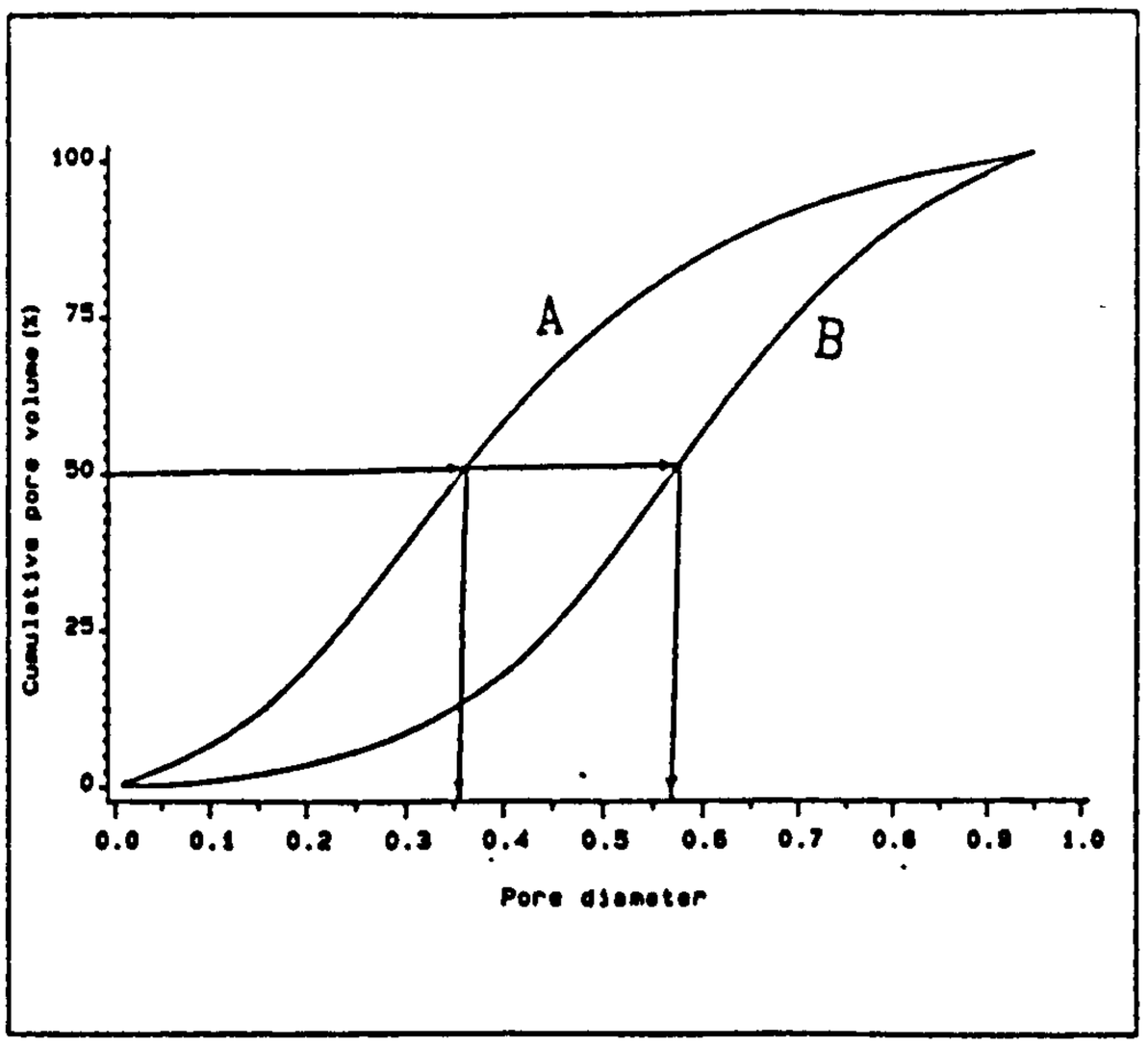

Figure 6.8 Median pore diameter by pore volume (mix A and B have the same pore volume, but mix A has greater volume of smaller pores)

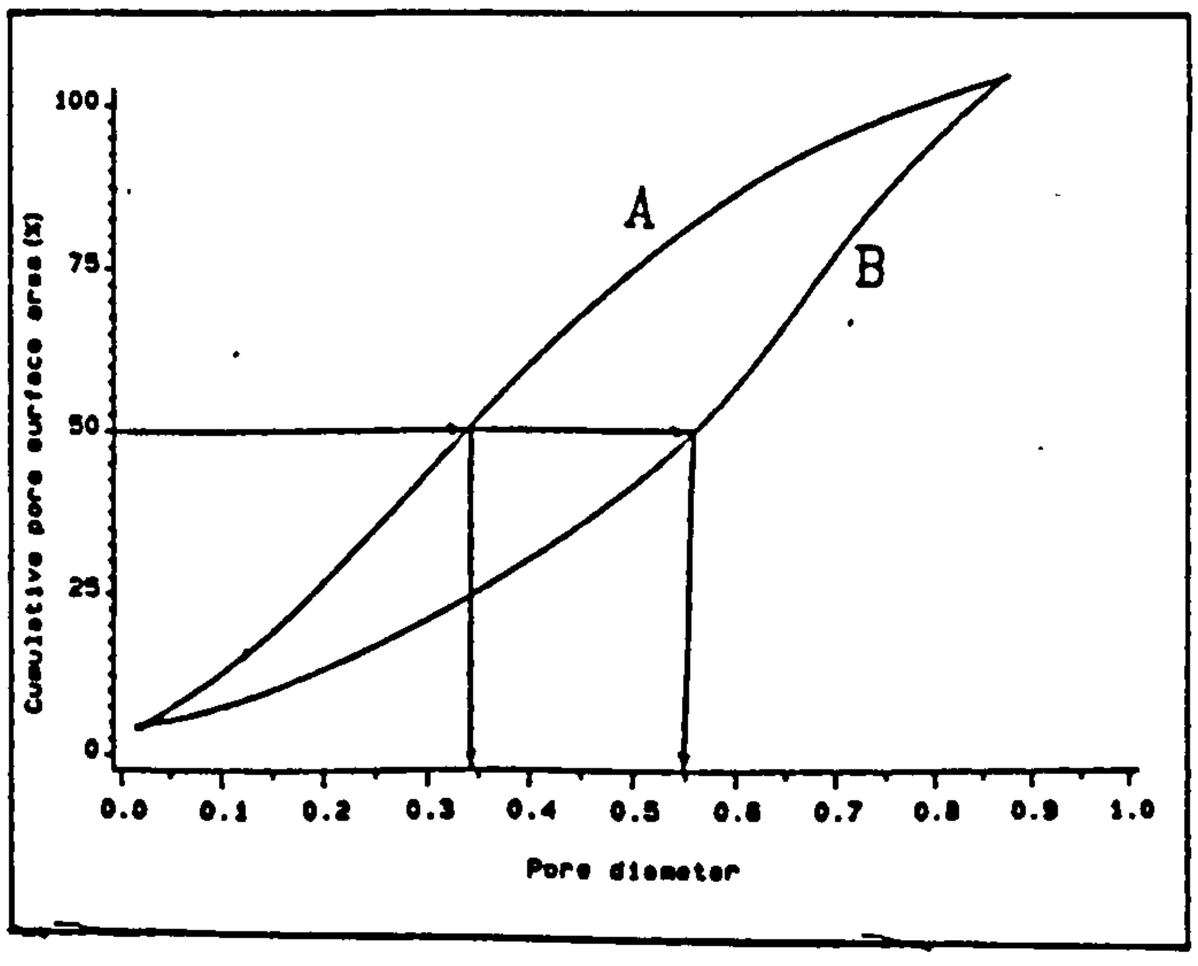

Figure 6.9 Median pore diameter by pore surface area (mix A and B have the same pore volume, but mix A has greater volume of smaller pores).

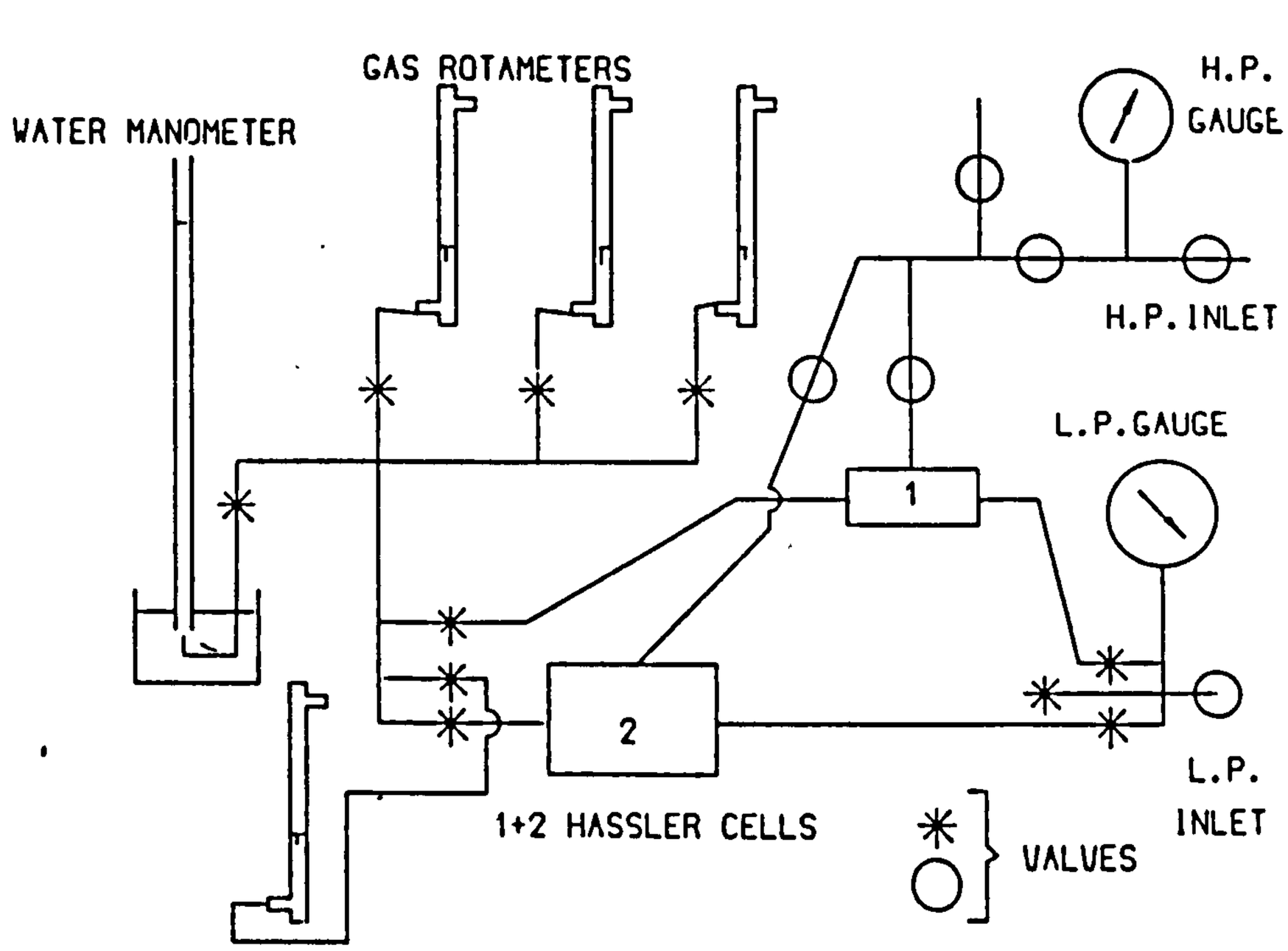

Figure 6.10 Air permeameter

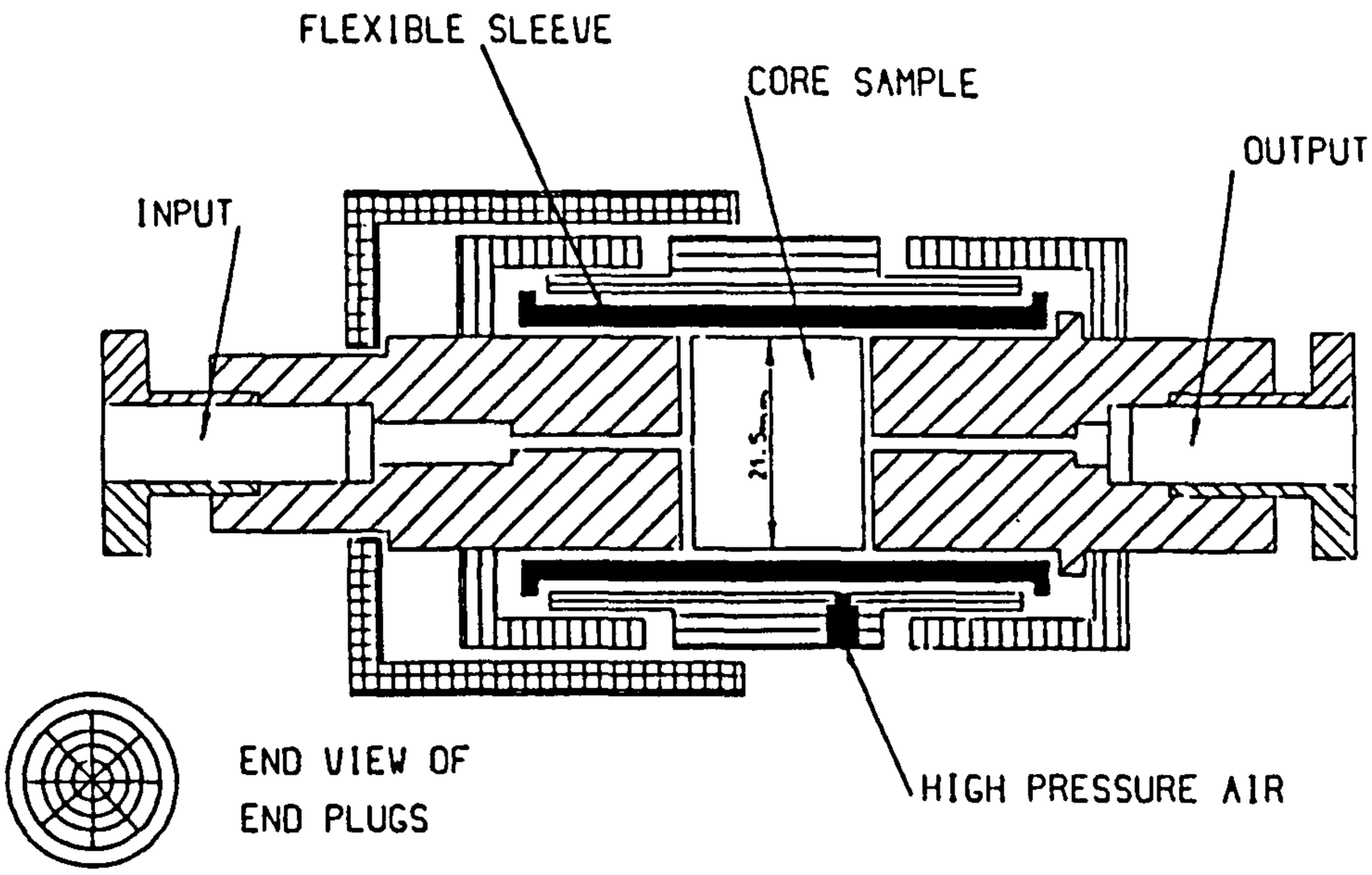

Figure 6.11 The Hassler-type permeability cell

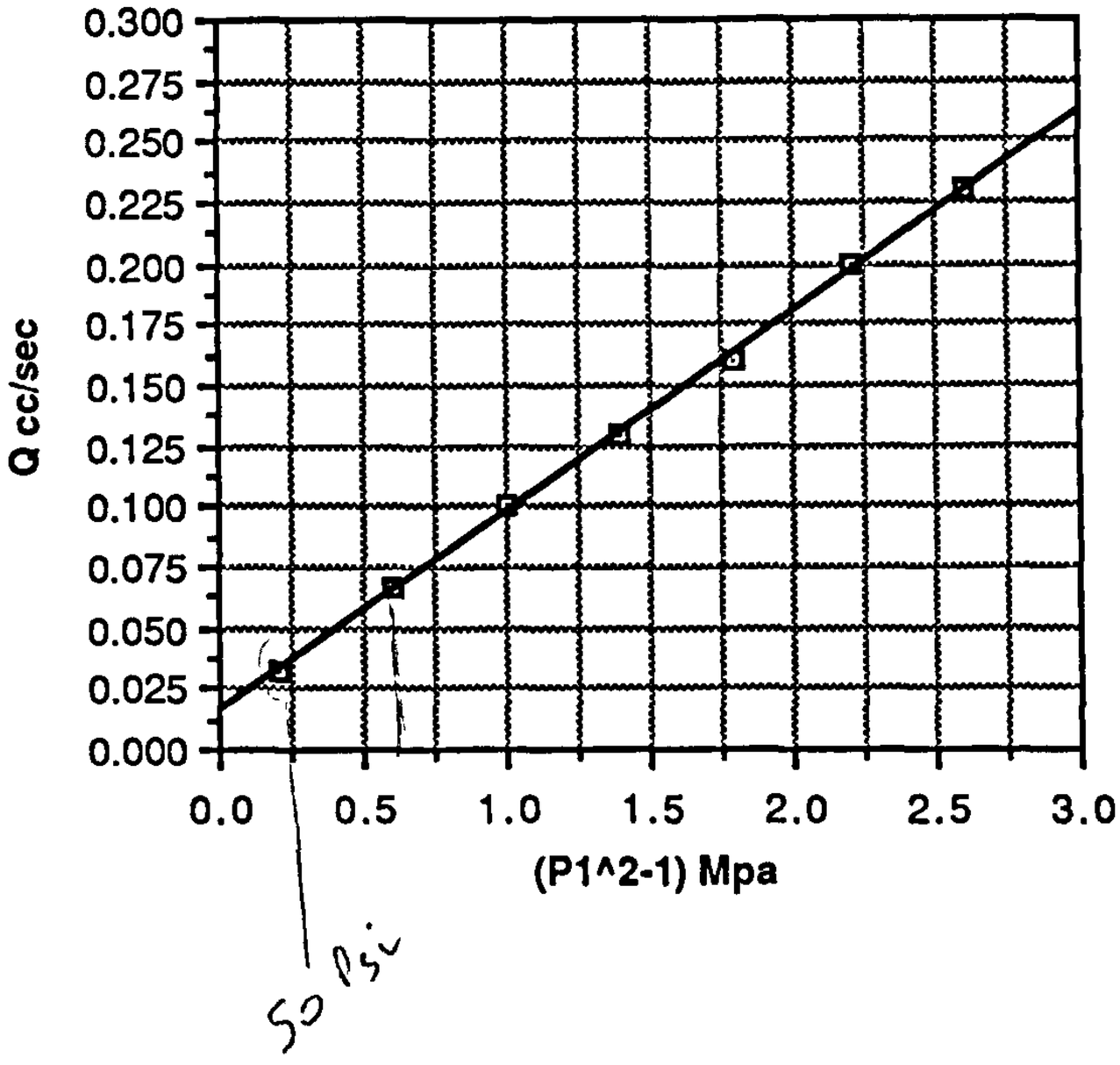

Figure 6.12 Typical regression line showing the relationship between flow rate and (P_1^2-1)

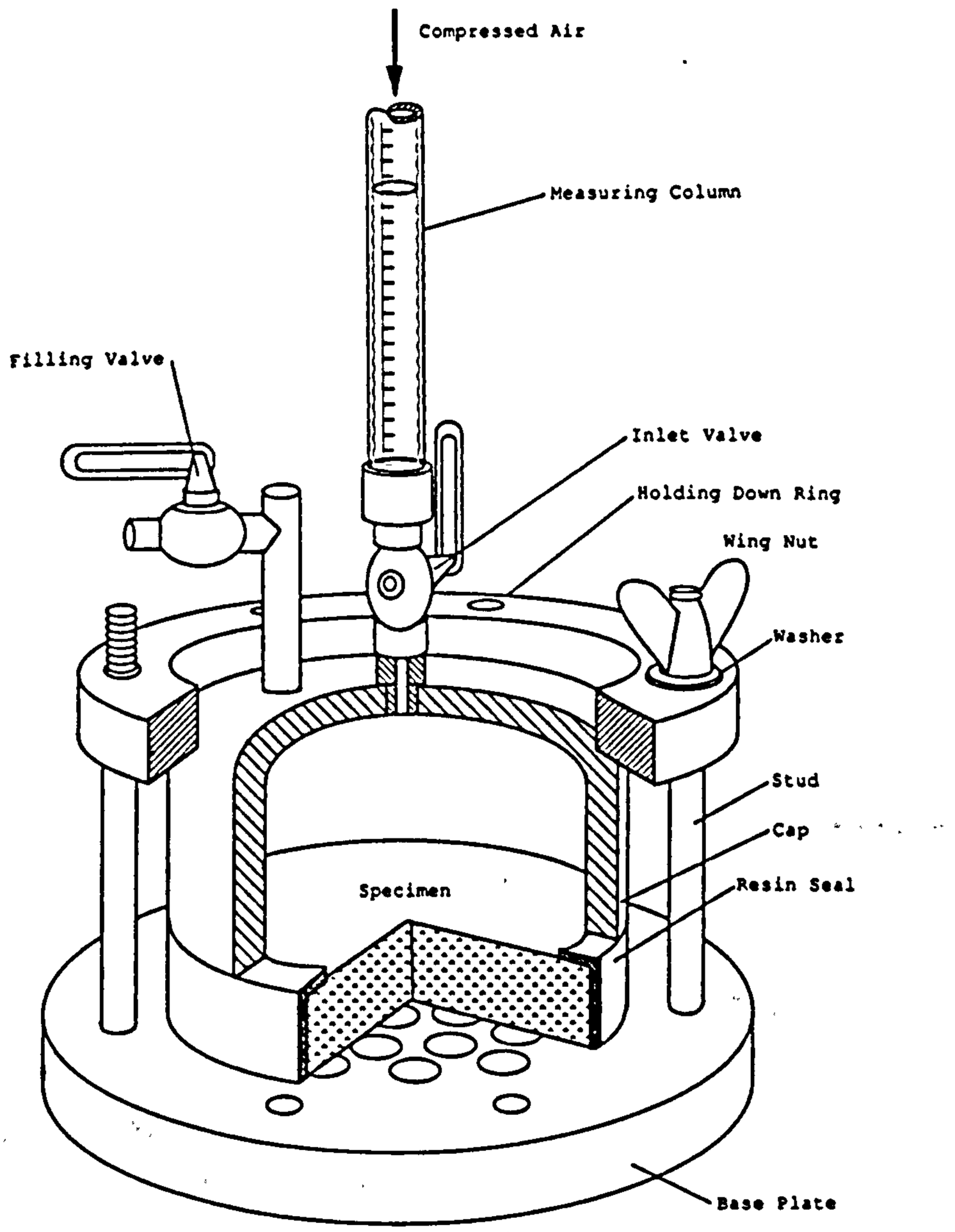

Figure 6.13 Cut-away drawing of water permeability cell

Plate 6.1 Figg test hole details

Plate 6.2 Figg air permeability test apparatus

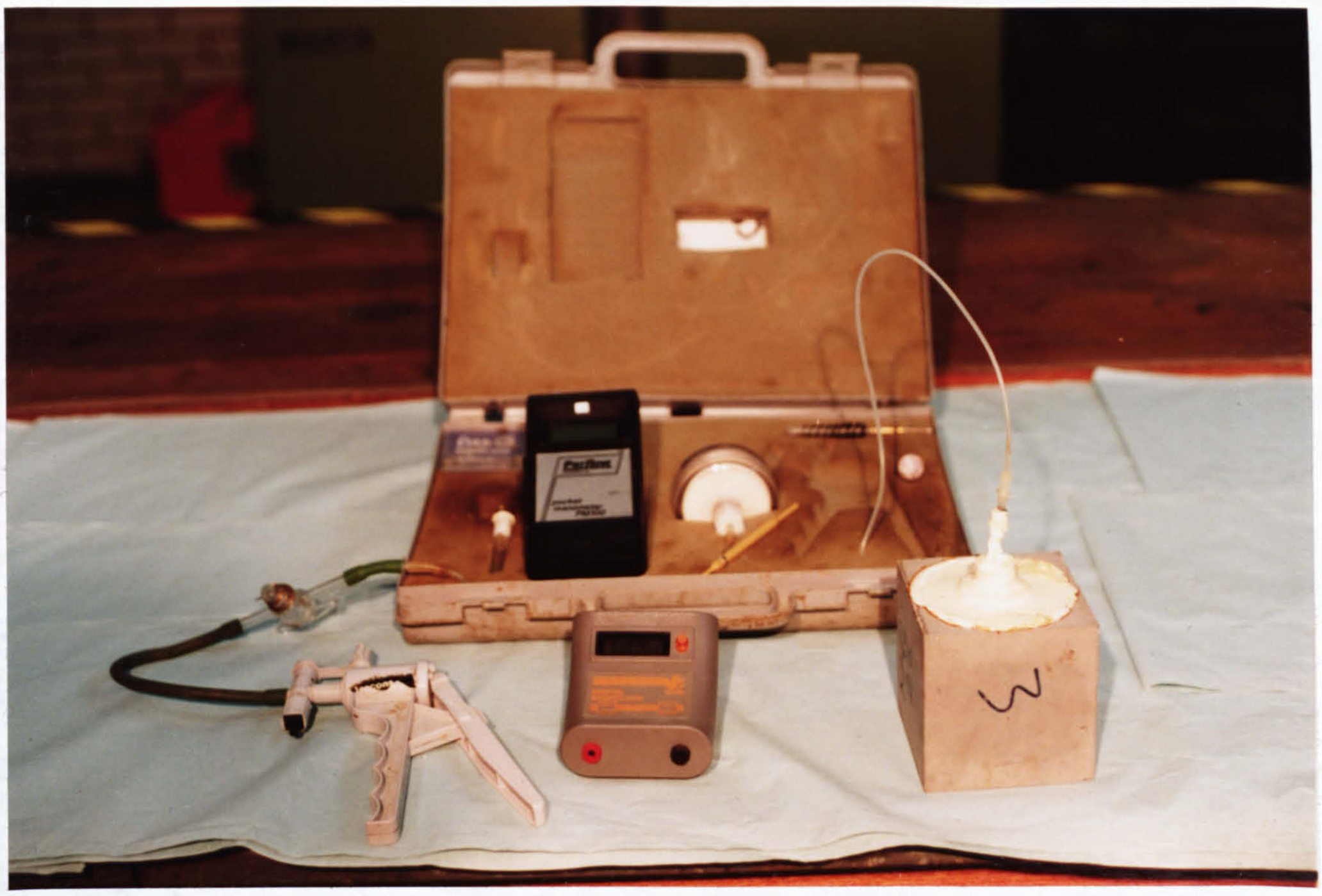

Plate 6.3 Egg air permeability test apparatus

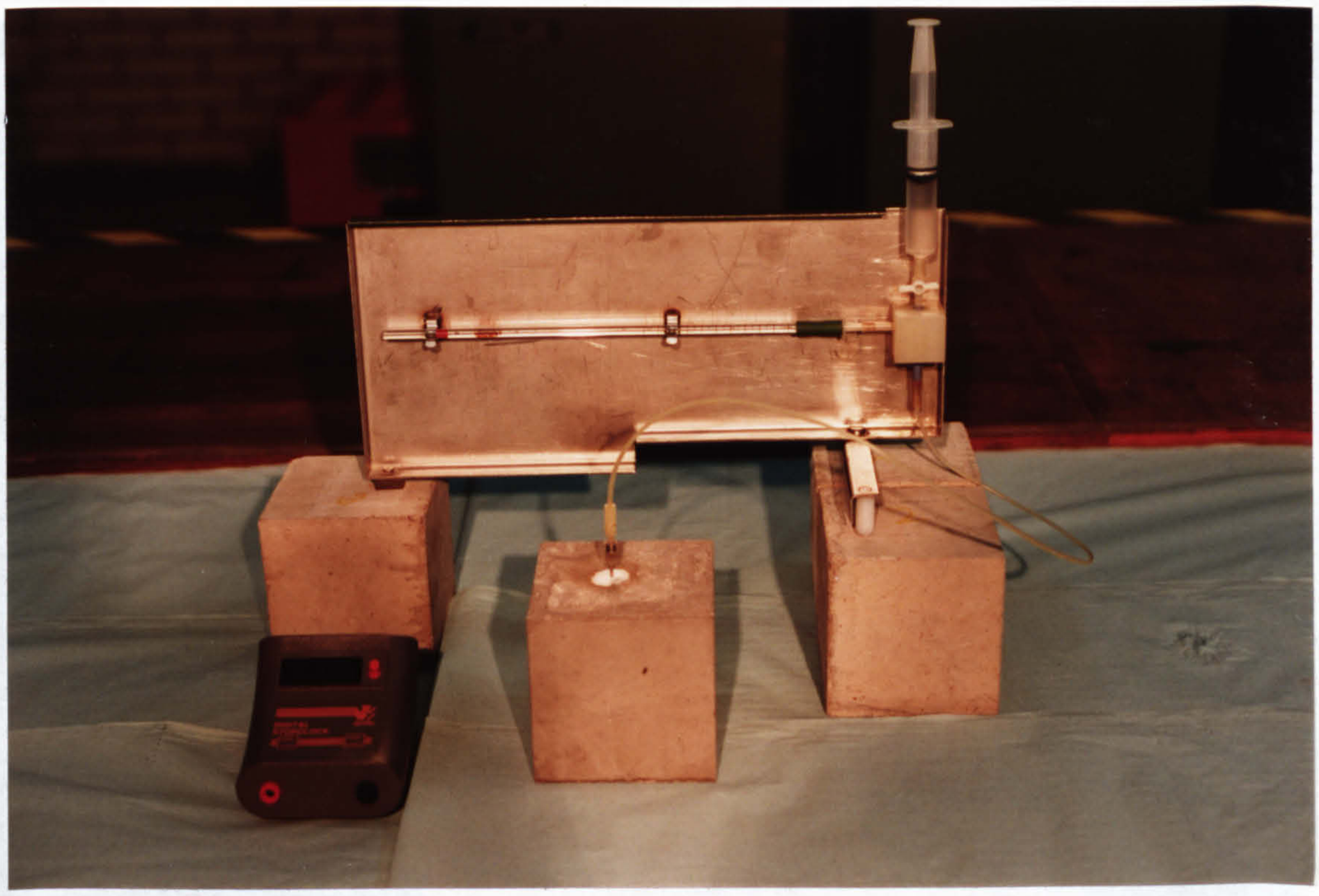

Plate 6.4 Figg water permeability test apparatus

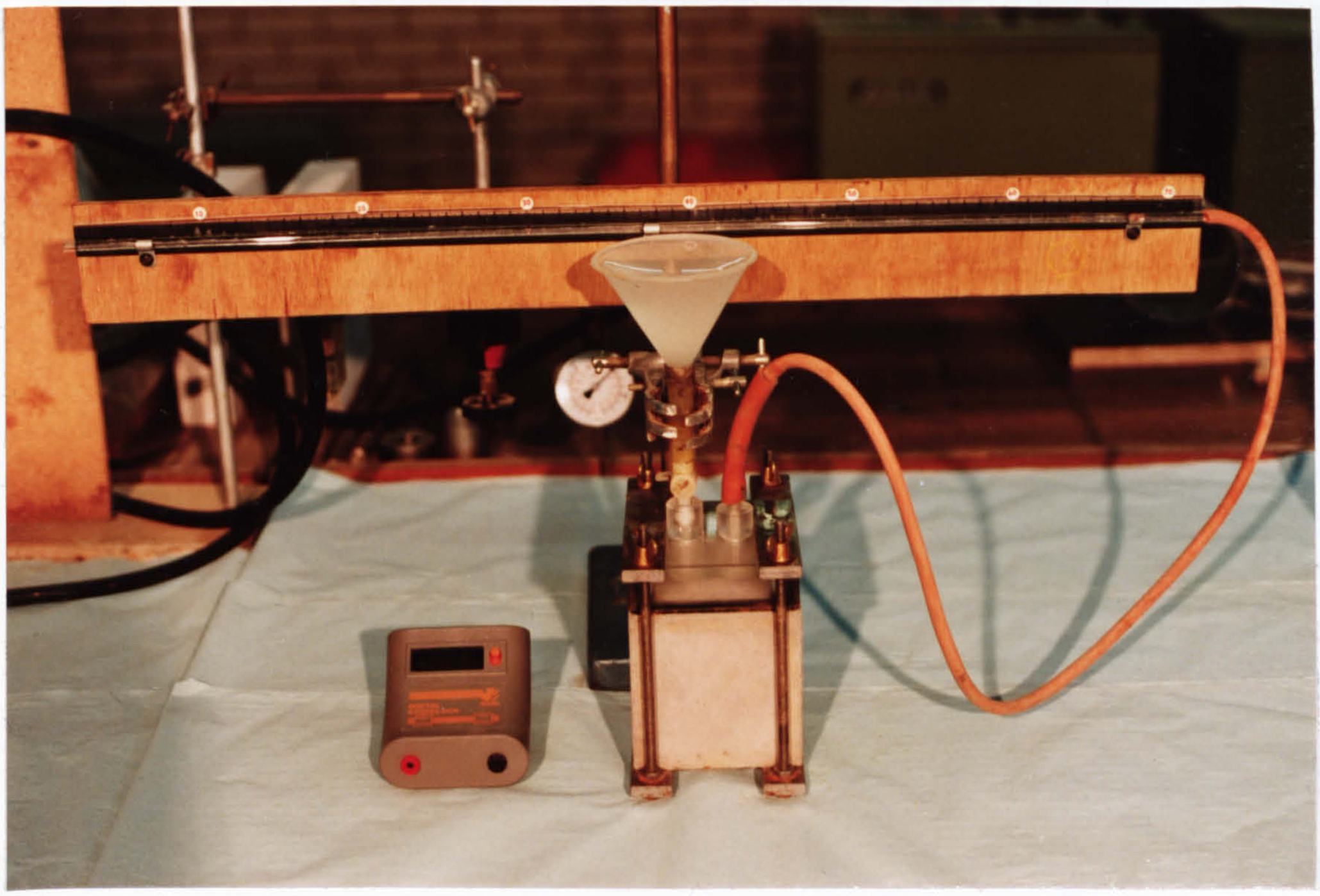

Plate 6.5 ISA test apparatus

Plate 6.6 Pore size distribution test apparatus

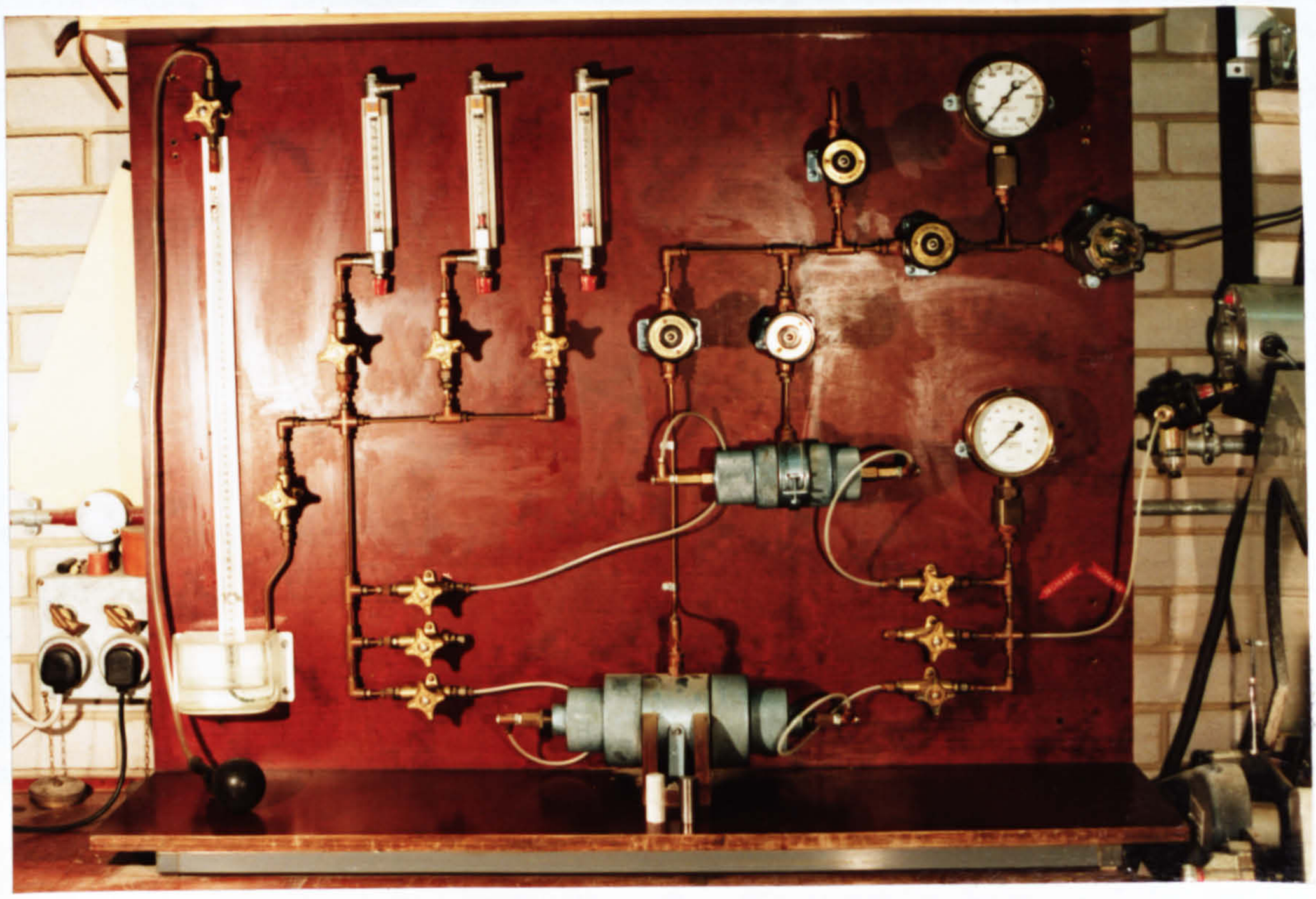

Plate 6.7 Air permeability apparatus

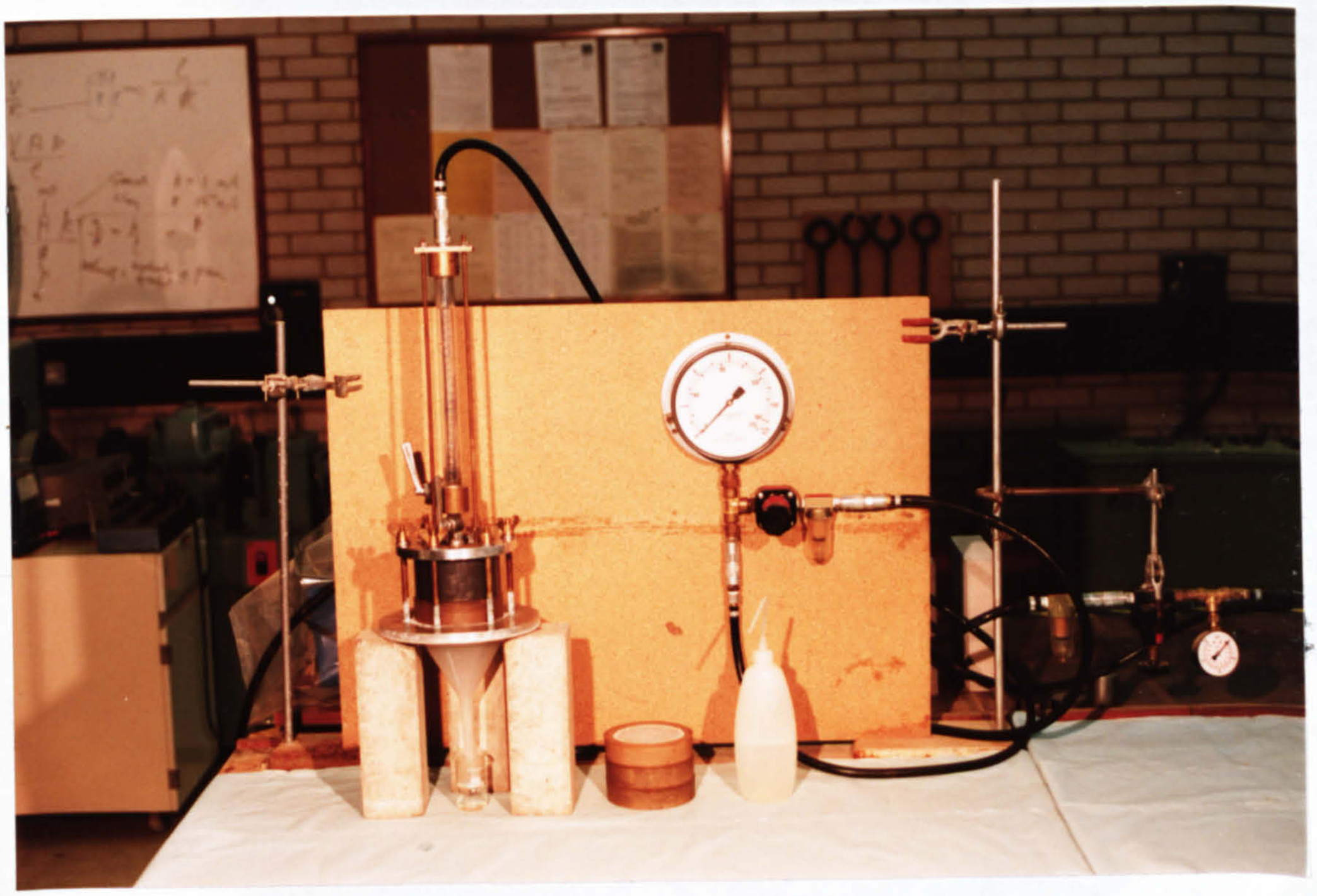

Plate 6.8 Water permeability apparatus

Plate 6.9 Preparation of test specimen for water permeability

Plate 6.10 Apparatus used in the controlled environment sulphate attack test

CHAPTER SEVEN

DEVELOPMENT OF MIX DESIGN METHOD

7.1 Introduction

The most common method of proportioning silica fume in concrete is to simply substitute silica fume for Portland cement on a one-for-one basis by weight. Silica fume concrete proportioned by this method will nearly always have a comparable strength with a control OPC mix at early ages, (1 to 3 days), and higher strengths at 28 days and onwards. This high strength coupled with the relatively high unit cost of the silica fume compared to OPC may lead many designers and contractors to conclude that proportioning silica fume concrete on the above simple substitution basis is not economical. Therefore it is important to have a mix design rationale which is able to proportion silica fume concrete for workability, strength and economy.

A method is presented here for proportioning a blended silica fume and OPC cement to produce concrete of comparable workability and 28 days compressive strength to a reference plain OPC concrete mix. The method was developed after an extensive experimental programme.

Initially the effect of simple substitution of CSF for OPC on a one-for-one basis by weight on the workability and compressive strength at 3, 7 and 28 days was examined experimentally and discussed. The amount of OPC(kg/m^3) necessary to bring a change in the 28-day compressive strength of 1 MPa was also determined and the theoretical OPC-CSF blend proportions necessary to give a compressive strength comparable to the plain OPC mix were determined. The theoretical OPC-CSF blends were examined experimentally for the purpose of verification the theoretical blend proportions. The yielded experimental data produced were used to establish the relationship between compressive strength and water/cementitious ratio both with and without the use of superplasticizer. The current ingredient costs were used to establish the optimum replacing percentages of CSF.

The experimental work consists of three mix series: A, B & C. Full description of these three series are given in the Chapter.

7.2 Materials

The chemical and physical properties of OPC and CSF used are detailed in Chapter 6. All aggregate were dried before batching.

7.3 Curing

After casting and compacting, concrete specimens were covered with polythene sheeting securely held on the top casting for the first 24 hours. After 24 hours the concrete specimens were demoulded and cured continuously in water tanks at a temperature of 20±2°C for 27 days.

7.4 Workability

A medium workability in terms of 30-60mm slump, 3-6 seconds V.B. time or 0.8-0.9 compaction factor was specified for this experimental work (36).

Silica fume in a concrete mix tends to make it appear sticky and dry due to the high surface area and fineness of silica fume. However, because of the spherical and smooth nature of silica fume particles, silica fume concrete tends to be more workable with vibration, a phenomenon called "thixotropy". Static workability test methods are not well suitable for measuring the consistency of thixotropic mixes. Therefore, the use of a dynamic workability test such as VeBe and compaction factor which puts more energy into the concrete and simulates site conditions was considered to be more appropriate than the static slump test method. To prove this point, workability of silica fume mixes were measured by means of static slump test and the dynamic VeBe and compaction factor tests.

7.5 Series A: Assessment of plain OPC concrete mixes

In this series experimental work was carried out to establish the relationship between water/cement ratio and 28

days compressive strength of plain OPC mixes that can fit the specific concrete ingredients available in the laboratory. The effect of partial subtracting of OPC from the designed OPC concrete mixes on the 28-days compressive strength was also examined aiming to identify the amount of OPC (kg/m^3) necessary to bring a change of 1 MPa in the 28-days strength.

7.5.1 Mixes

Nine target strengths were chosen to cover a compression strength range from 20 MPa to 60 MPa. The initial concrete ingredients, proportions and quantities needed to produce the strength levels were derived from the existing mix design practice (DOE and Concrete Society) (168).

7.5.2 Workability

A medium workability of 30-60mm slump was designed and achieved in all the mixes. Because the aggregates were dried before batching, the free water content was adjusted during mixing to allow for the aggregate water absorption by a quantity equivalent to 30 minutes of absorption. As a result, the water content is lower than would be the case had full absorption of water by the aggregate been possible; this behaviour can be attributed aggregate particles becomes quickly coated with cement paste which prevents further ingress of water necessary for saturation. Table 7.1 shows that the free water/cement ratios are comparable to the net water/cement ratio calculated on the basis of aggregate moisture content at 30 minute absorption. Test data falls in line with Nevilles (36) prediction of behaviour.

7.5.3 Relationship between water/cement ratio, compressive strength

OPC concrete mixes designed initially using the DOE, and Concrete Society method were cast, cured and tested at 28 days of age. After a few adjustments to the cement content of the concrete mixes whose compressive strength was not meeting the target strengths, the 28 days compressive

strengths aimed at were achieved. Data was then used to establish the relationship between water/cement ratio and 28-day compressive strength shown in Figure 7.1.

7.5.4 Relationship between strength and OPC quantity

According to the W/C ratio, compressive strength relationship, adjusting the compressive strength of any concrete mix requires adjusting its W/C ratio which can be achieved by adjusting the cement content. To quantify the amount of OPC necessary for strength adjustment, the relationship between the compressive strength in terms of MPa units and the adjusting percentage of OPC must be established. To establish this relationship, three designed concrete mixes of a target mean strength 25, 40 and 55 MPa were chosen from the strength range to represent lean, medium and rich mixes. Concrete mixes were made by subtracting a certain percentage of OPC ranging from 5 to 20%, by weight of OPC, from the reference concrete mixes. Concrete specimens (100 x 100mm cube) were tested at 28 days. The test data shows that there is a linear relationship between the compressive strength in terms of MPa units and the percentage by weight of OPC need to be adjusted (see Figure 7.2). Thus a change in the compressive strength of OPC concrete mix of 1 MPa requires adjusting the cement content by 2.5 percent for the aggregate and cement source used in this experimental programme.

7.6 Series B: Assessment of silica fume concrete mixes

In this series the effect of partial substituting of OPC with CSF on consistency and compressive strength was assessed.

7.6.1 Mixes

Three referenced plain OPC concrete mixes were chosen from the nine mixes designed in series A. These mixes were concrete grades C25, C40 and C55. These three mixes were chosen as each of them can represent a certain concrete group and grade, i.e. they cover the range from lean to rich mixes

and the strength area where most of site concrete applications fall.

Silica fume concrete mixes were established on the basis of simple (one-for-one) substitution of OPC in the plain mix by 5, 10, 15 and 20% by weight of OPC.

7.6.2 Workability

CSF is composed of very fine vitreous silica particles. The surface area of CSF is much greater than portland cement. This high fineness and surface area is advantageous when considering the pozzolanic reaction in hardened concrete. However, this is not the case when the properties of fresh concrete are considered.

The use of CSF in concrete was generally found to increase the water content necessary to maintain a medium workability. This effect can be counteracted by the use of superplasticizer admixtures. In this research work two approaches were used for controlling workability. In the first mixing water was increased and in the second a super plasticizer commercially known as "CONPLAST M1" was used. The admixture was used in a sufficient quantity to secure the workability level without changing the initial mixing watr content.

The effect of CSF on concrete workability is illustrated below:

1. In the lean and normal concrete mixes containing 230 and 300kg of cement per cubic metre, silica fume can replace up to 10% by weight of OPC without requiring extra water. However, in rich concrete mixes containing 400 kg of OPC per cubic metre, silica fume can only replace 5 percent of OPC without reducing the workability.
2. The increase in W/C+CSF ratio to maintain a medium workability was found to be almost linearly related to the amount of CSF (see Figures 7.3 & 7.5), i.e. it appears that the water demand increase is independent of the amount of cement in the mix. This agrees with the findings of Carette & Malhotra (4). However the

test results disagreed with those reported by Loland and Hustad (6).

3. The increase in water content required to produce a medium workability is dependent on the W/C ratio in the reference plain mix and CSF quantity. Figure (7.5) shows the percentage increase in mixing water necessary to secure medium workability in CSF mixes in terms of CSF percentage and W/C ratio. The curves are based on a medium workability measured by means of the V.B. test method.

4. As mentioned earlier, superplasticizer admixture (CONPLAST MI) was used to counteract any extra water required from the use of CSF. Test results showed that a dosage of 12.5 to 16 percent by weight of condensed silica fume was found necessary depending on the CSF dosage, (see Figure 7.6). Test results show that these dosages are the same for all three concrete grades. Therefore, the superplasticizer dosage is also independent of concrete grade and OPC content and is only dependent on the CSF dosage.

5. Silica fume concrete mixes in which workability was secured by using superplasticizer were found to lose their workabilities with time. The higher the percent of CSF used and the lower the W/C ratio in the reference plain mix the shorter is the time for the workability to reduce.

6. As expected the dynamic VeBe and compaction factor tests which puts more energy into the concrete and simulate site conditions were more appropriate for measuring the workability of silica fume than the static slump test. Results shown in Table 7.2 show that with increasing silica fume content slump values fall down and become out of the limits which specified for medium workability (i.e. 30-60mm). whereas the dynamic workability test results and in specific the VeBe results were all within the specified limit (i.e. 3-6 sec).

7.6.3 Bleeding, cohesiveness and segregation

Although the effect of silica fume on the bleeding, cohesiveness and segregation was not measured, it was noticed throughout the experiment work that silica fume can improve cohesiveness and reduce the tendency to segregation and bleeding. In fact silica fume concrete was vibrated for up to 30 minute without a sign of segregation or reduction in compressive strength. This effect of silica fume can be explained as follows.

Due to the high fineness and high surface area, each grain of cement will be surrounded by hundreds of silica fume particles. This will increase the number of contact points between the fine particles (per unit weight of cementitious material) and consequently increase the cohesiveness.

The presence of ultra-fine silica fume particles will increase and lengthen the internal paths taken by the water molecules to reach the surface. Consequently this will reduce the rate of internal liquid flow in the mix. Thus bleeding will be reduced significantly.

The cement grains and silica fume particle will be bound together initially by internal friction. This friction is dependent on the contact points between the cementitious (OPC & CSF) particles themselves and between cementitious particles and aggregate particles. The greater the number of contact points, the higher is the internal friction. Thus silica fume will prevent and reduce the tendency to segregation by this mechanism. The observation reported above agree with those reported by Loland and Hujstand (6), Maag (8) and Burge (9).

7.6.4 Compressive strength with workability obtained by adding extra water

The compressive strength of the fifteen CSF concrete mixes was measured at 3, 7, and 28 days. Five 100 x 100 mm cubes were tested for each mix and age. The effect of the inclusion of CSF, as a cementitious material partially replacing OPC, on compressive strength can be described as follows:

Unlike PFA concrete, the early age (3-7 days) compressive strength of CSF concrete is higher than the control OPC concrete at replacment ranging from 5 to 15% by weight of OPC in the lean concrete mix (Grade C25) and 5 to 10% in the medium and rich concrete mixes (Grade C40 & C55), see Figure 7.7. This behaviour can be attributed to the fact that each cement particle will be surrounded by hundreds of CSF particles and the Portland cement flocs will be stabley dispersed by the physical nature of CSF particles. This will obviously expose a greater surface area of OPC to normal hydration than that without CSF, which will increase the rate of initial hydration. Silica fume on the other hand can accelerate the early age hydration of OPC by adsorbing Ca^{2+} ions on the CSF particle surfaces lowering their concentration in the liquid phase. However, at higher replacement (20% by weight of OPC) the early age compressive strength of CSF concrete mixes lags behind the control OPC mixes. This may be attributed by the fact that using CSF in a high percentage can increase the density and thickness of the layer of the CSF particle around each cement particle will narrow the channels for water perculation and increase the necessary time for water molecule to perculate the OPC particles. This will obviously decelerate the initial rate of OPC hydration and result in lower early-age strength.

At 28 days of age, substituting the OPC in the control rich and medium control plain mixes with CSF for up to 10 & 15% respectively by weight of OPC was found to improve the compressive strength. At higher replacement levels (i.e. 20%), however, there was a marked reduction in compressive strength. In lean concrete mixes, the results show that OPC can be replaced by CSF for up to 20% without having a reduction in strength below that of the control plain OPC (see Figure 7.7).

Results of this study also indicate that for rich, medium and lean concrete mixes, the optimum levels of cement replacement based on increasing the compressive strength are 5, 9 and 11 percent respectively (see Figure 7.8).

The improvement in the 28 day compressive strength of CSF concrete mixes was brought about by the pozzolanic reaction that took place after 3 to 7 days. This reaction helps to convert the unstable $Ca(OH)_2$, a product which contributes little to compressive strength, to more stable calcium silicate hydrates (C-S-H) which are mainly responsible for concrete strength. The reduction in the compressive strength of medium and rich CSF concrete mixes in which high percentages of CSF were used, can be explained by the following effects.

The chemical reaction is stopped by either the consumption of all available $Ca(OH)_2$ before using all the available reactive silica, or both the matrix structure and the hydration reaches a saturation limit. Whichever is the case it will leave any excess CSF as an inert filler causing a decrease in strength proportional to its concentration.

It is well known that W/C ratio is inversely related to compressive strength. High CSF content or replacing percentage results in a high water content and high W/C + CSF ratio. Therefore, it is quite probable that the increase in W/C + CSF ratio above a certain limit will result in a reduction in compressive srength.

The combined effect of these two penomenon is believed to be responsible for the reduction in the compressive strength of CSF concrete and is illustrated graphically in Figure 7.9.

Test results show that CSF is more effective in lean mixes than rich mixes. For example the improvement in the 28-day compressive strength brought about by replacing OPC with 10% of silica fume is 45%, 35% and

13% in the lean, medium and rich mixes respectively. In the author's opinion, the high effectiveness of silica fume in lean concrete mixes has two causes. Firstly it increases the effective volume of paste in the mix, brought about by the high fineness of silica fume. CSF can fill the voids available (the fine particle may be securely held in the paste by molecular attraction), thus increasing the average thickness of the paste surrounding the aggregate particles and providing a strong bond of paste to aggregate particles, thereby increasing concrete strength in mixes having a deficiency of paste without silica fume. When this component is coupled with the pozzolanic reaction taking place between $Ca(OH)_2$ and SiO_2. the improvement in compressive strength of lean concrete mixes seems to be very distinctive when compared to rich mixes.

7.6.5. Compressive strength with workability obtained by superplasticizer

The compressive strength of eight concrete mixes was measured at 3, 7 and 28 days. Five 100 x 100 mm cubes were tested for each specific concrete mix and age. The effect of inclusion of CSF and superplasticizer on the compressive strength of concrete can be summarized as follows.

The relationship between compressive strength and age are presented in Figures 7.10. It is clear from the figure that the use of superplasticizer to restore the medium workability without adding extra water improves both early and late age compressive strength of CSF concrete mixes compared with those mixes in which workability was restored by adding extra water (see Figure 7.7). This improvement may be due to maintaining the water/cement + CSF ratio which is effectively lower than in the comparable mixes discussed in Section 7.6.4. Moreover, theimprovement in strength may result from the more uniform dispersion of cement and CSF particles paste. This

will result in a more uniform distribution of hydration products and consequently a well densified matrix and good bond between the aggregate and the matrix.

The variation in the relative 28-days strength with CSF replacing percentages is shown in Figure (7.11). Results indicate that with superplasticizer the optimum levels of cement replacement based on the 28 day compressive strength are 12.5, 14 & 16% in the rich, medium and lean concrete mixes.

7.7 Series C: Establishment of mix design procedure

7.7.1 Introduction

In this series the information yielded from series A & B was used to establish the theoretical blend proportions of CSF and OPC necessary to give a comparable consistency and 28-day compressive strength both with and without superplasticizer. The proportions were calculated based on the assumption of combining the individual effects on the compressive strength of both simple substitution of OPC with CSF in the CSF concrete mixes (Series B) and the partial subtracting of OPC from the control plain OPC mix. The resultant strength of CSF concrete mixes would be equivalent to the strength of the control OPC mix. This requirement was tested experimentally by setting a range of three mixes for each specific concrete grade and CSF percentage, again with and without superplasticizer. In the range of these three mixes the theoretical quantity of OPC was increased and decreased by 3 percent. The information produced helped to confirm the above requirement and also establish the efficiency and economy of CSF concrete.

7.7.2 Compressive strength, Water/OPC+CSF ratio relationship

The compressive strength of five 100 x 100mm cubes was measured at 28 day of age. The statistical analysis performed show that the coefficient of variation of test result are within 10%.Results show that in most of the

designed concrete mixes, the average compressive strengths closely matched the required target strengths. The data were used to establish the relationship between compressive strength and W/OPC + CSF ratio with and without superplasticizer, as shown in Figure 7.12 and 7.13. The statistical fitting equation and correlation factor for each set of data are given in Tables (7.3 and 7.4). Results show that the basic inverse relationship between strength and W/C ratio can change quantitatively, but not qualitatively when silica fume is used, i.e. using a certain percentage of silica fume can result in a shift of the strength verses W/cementitious ratio to a higher level, but not a change in the configuration of the curve.

Figure 7.12 shows that the curves which represent the CSF replacement percentages are close to each other at low W/C+CSF ratios and widen up at higher W/C+CSF ratios. This was because silica fume was more effective in lean mixes than in rich mixes. Consequently the improvement in compressive strength caused by increasing CSF content from 5 to 20% in lean mixes were effective whereas in rich mixes the above improvements were not very effective. The Figure also shows that the position of the curves representing CSF replacements percentages were increasing in the order of 5, 20, 10 and 15%. The position of 20% CSF curve came inbetween 5 and 10% CSF curves. This was because compressive strength of CSF mixes was increased with the increase of CSF content up to an optimum level of 10% to 15% after which it fell down. The reason for this was explained earlier. The use of superplasticizer resulted in shifting the curves to a higher level compared to those in which extra water was used. This shifting was due to the reduction in water content caused by the use of superplasticizer.

7.7.3 Cost effectiveness

The compressive strength experimental data show that silica fume improve early-age and late-age strength by the pozzolanic reaction between the active silica and the lime liberated from cement hydration. However, the economies of

using silica fume as a partial cementing material depends upon the relative cost of the silica fume to portland cement, the efficiency of silica fume, the compressive strength requirement and the admixtures used.

Figures 7.14 and 7.15 show the relationships between the CSF percentage and the variation in the cost of a cubic metre of concrete. Calculations were made on the basis of Spring 1990 UK and foreign current prices

OPC	£55 / tonne
CSF	£100 - 220 / tonne
Sand	£14.50 / tonne
Gravel	£12.50 / tonne
Superplasticizer	£ 0.70 / a litre.

The curves are established on the basis of three different relative costs of silica fume to OPC. The figures show that in situations where workability was secured by adding extra water, the economic range of CSF percentages depend on the efficiency of CSF, richness of the control mix or strength level, and the relative cost of CSF to OPC. Based on the lowest relative cost of CSF to OPC, of to 1.8, CSF can be economically substituted for OPC in the control mix by up to a percentage ranging from 12.5 to 18 percent, depending on the strength of the control concrete mix. The lower the richness the higher is the efficiency of CSF and the economical substituting percentages. This economical CSF substituting percentages becomes rather limited at the highest relative CSF to OPC cost, of 4, ranging from 8% in the rich mix to 9% in the lean mix. This is because the increase in the unit weight cost of CSF was coupled with the decrease in the efficiency of moderate and high percentage of CSF in the rich mixes compared to the lean mixes.

In a situation where workability was obtained by using superplasticizer, the economic substituting percentages range of CSF was lower than those obtained above. This was because any additional saving in OPC quantity and cost of cementitious material caused by using superplasticizer was diminished by the added high extra cost of superplaticizer.

Therefore, it is economically better to add extra water than using superplasticizer.

Although the unit price of silica fume is much higher than the current UK cement prices test results shown in Figure 7.14 and 7.15 reveal that silica fume concrete can be produced at a lower cost than with Portland Cement alone when the maximum cementitious efficiency of silica fume can be utilised. However the capital cost of any equipment needed to store and batch silica fume may add on the cost of producing silica fume concrete and therefore it must also be considered.

The relationship between 28-day compressive strength and the optimum CSF percentages (by weight of OPC in the control plain mix) for each relative CSF to OPC costs was derived from Figure 7.14 and 7.15. These relationships helped to identify the most economical CSF percentage which can provide the minimum cost of the OPC & CSF blend with and without the use of superplasticizer and are shown in Figures 7.16 and 7.17.

7.7.4 Efficiency factor

The activity of silica fume compared to Portland cement can be expressed in terms of a factor called the efficiency factor (K)(23). To identify the efficiency factor of CSF the 28-day compressive strength data obtained from Series C were used to calculate the amount of OPC necessary to produce an equivalent strength in both plain OPC and the modified OPC-CSF blend concrete. The ratio of the reduced amount of OPC versus the amount of CSF represents the efficiency factor of CSF. Thus value may be calculated from the following formula;

$$K = \frac{C_1 - C_2}{CSF}$$

C_1 = OPC kg/m³ in the control mix

C_2 = OPC kg/m³ in the CSF concrete mix of a comparable 28-day strength

CSF = weight of CSF in kg/m³

Figure 7.18 and 7.19 show the variation of CSF efficiency at different replacement levels with or without the use of superplasticizer. The figures show clearly that the CSF efficiency factor decreases with the increase of CSF replacing percentages. The use of superplasticizer helps to increase the efficiency, but, the trend is unchanged. The figures also show that the efficiency factor ranges from 1 to 5. These figures are in line with general experience reported by Jahren (24).

7.7.5 Procedure for proportioning

The present OPC-CSF mix design method proposed, based partly on the existing mix design method proposed by DOE and Concrete Society (168) together with strength versus water/cement + silica fume ratio, percent increase in water content versus W/C ratio, dosage of superplasticizer versus CSF% and the optimum CSF% by weight of OPC versus compressive strength curves produced as part of the experimental work.

The mix design method procedure is illustrated by the following steps and shown also by the flow chart (Figure 7.22).

STEP 1: Deals with the free water content.
Select the free water content from data in Table 7.5 based on workability and aggregate type and maximum size.

STEP 2: Deals with the CSF content.
I. Select from Figure 7.1 the water/cement ratio required for a given 28-day compressive strength
II. Calculate the amount of cement content using w/C ratio and free water content from Stept 1.
Cement content = free water content ÷ W/C ratio
III. Select the silica fume proportions to be used (from economic consideration) based on compressive strength, relative CSF/OPC cost and the option for securing workability, using either Figure 7.16 or 7.17.

IV. Calculate the amount of CSF (kg/m³) using its percentage by weight of OPC and OPC content

CSF content = CSF % x OPC (kg/m³)

STEP 3: Deals with the adjusting of water content.

This step should be considered in case workability is secured by adding extra water and the selected CSF percentage is ≯ 10%.

I. Determine the percentage increase in free mixing water from Figure 7.5 based on W/C ratio and CSF% from Step 2.

II. Adjusted water content = water content (Step 1) x % increase

STEP 4: Deals with superplasticizer content.

This step should be considered in case workability is secured by using superplasticizer and the selected CSF percentage is > 10%. Determine the doage of superplasticizer by weight of silica fume using Figure 7.6.

STEP 5: Deals with the OPC content.

I. Get the water/cement + silica fume ratio using either Figure 7.12 or 7.13 based on compressive strength and workability option.

II. Calculate the amount of OPC + CSF using the adjusted water content if workability is secured by adding extra water (Step 3) or the free water content (Step 1) if workability is secured by superplasticizer -

OPC + CSF = water content ÷ W/C + CSF ratio

III. Calculate the amount of OPC by subtracting the amount CSF (Step 2) from the amount of OPC + CSF.

STEP 6: Deals with the aggregate content.

I. Determine concrete density using Figure 7.20.

II. Hence, Aggregate content = concrete density - (water content + cement content + CSF content)

III. Select the proportion of fine aggregate using Figure 7.21, hence fine aggregate content equals to total aggregate content x fine proportion.

IV. Coarse aggregate content = total aggregate content - fine aggregate content.

7.7.6 **Example problem 1**

Design a 28-day, 40 MPa silica fume concrete with 3-6 sec VeBe time, 20mm uncrushed aggregate, no water reducing agent and relative CSF/OPC cost of 2.9.

STEP 1: From data in Table 7.5, the free water content is 180 kg/m³.

STEP 2: I. Using Figure 7.1, the W/C ratio is 0.61.

II. Cement content = 180/0.61 = 295 kg/m³

III. From Figure 7.16 the economical CSF percentage is 6

IV. CSF content = 295 x 0.06 = 18 kg/m³.

STEP 3: No adjustment required to water content as CSF% less than 10%.

STEP 4: I. Using Figure 7.12, W/C + CSF ratio = 0.78.

II. OPC + CSF = 180/0.78 = 230 kg/m³

III. OPC = 230 - 18 = 212 kg/m³.

STEP 5: I. Using Figure 7.20, concrete density = 2375kg/m³

II Aggregate content = 2375 - (180 + 212 + 18) = 1803 kg/m³

III. For a medium zone sand, sand proportion = 38%. hence fine aggregate content = 1803 x 0.38 = 685 kg/m³

IV. Coarse aggregate = 1803 - 685 = 1118 kg/m³

7.7.7 **Example Problem 2**

Design a 28-day, 60 MPa silica fume concrete with 3-6 VeBe time, 20mm maximum uncrushed aggregate, water reducing admixture and relative CSF/OPC cost of 1.8.

STEP 1: From data in Table 7.5, the free water content is 180 kg/m³.

STEP 2: I. Using Figure 7.1 the W/C ratio is 0.42.

II. Cement content = 180/0.42 = 430 kg/m³.

III. From Figure 7.17, CSF% is 5.5%.

IV. Silica fume content = 430 x 0.055 = 24 kg/m³.

STEP 4: No superplasticizer required as the CSF% is less than 10%

STEP 5: I. Using Figure 7.13, W/C + CSF ratio = 0.58

II. OPC + CSF = 180/0/0.58 = 310 kg/m^3

III. OPC content = 310-24 = 286 kg/m^3.

STEP 6: I. Using Figure 7.20, concrete density = 2375 kg/m^3

II. Aggregate content = 2375 - (180 + 286 + 24) = 1885 kg/m^3

III. For a medium zone sand, sand proportion = 35% hence fine aggregate content = 1885 x 0.35 = 650 kg/m^3

IV. Coarse aggregate content = 1885 - 660 = 1225 kg/m$_3$

Free W/C ratio	Used W/C ratio	Net W/C ratio
0.75	0.84	0.75
0.67	0.74	0.66
0.60	0.67	0.59
0.55	0.58	0.52
0.50	0.55	0.50
0.42	0.47	0.43
0.39	0.43	0.39
0.36	0.42	0.37

Note: The net W/C ratios were calculated on the basis of aggregate absorption after 30 minutes

Table 7.1: Comparison between the Free, Used and Net W/C ratios

Concrete mixes	Slump (mm) 30 - 60	V.B. (Sec) 3 - 6	C.F. (%) 0.8 - 0.9
C25/0	55		
C25/5	25	4	0.86
C25/10	10	5.6	0.79
C25/15	15	3.5	0.82
C25/20	10	4.6	0.75
C40/1	40		
C40/5	15	4.8	0.82
C40/10	20	3.6	0.88
C40/15	10	5.2	0.78
C40/20	15	4.5	0.83
C55/0	45		
C55/5	15	5.3	0.84
C55/10	30	3.7	0.91
C55/15	20	4.9	0.84
C55/20	10	5.1	0.73

Table 7.2: **Workability of plain and CSF concrete mixes measured by slump, V.B. and compacting factor**

Table 7.3 Statistical fitting equations and correlation coefficients for different CSF percentages (workability secured by adding extra water)

CSF %		
5	$y = 152.10 - 200 x + 71.4 x^2$	R = 0.96
10	$y = 128.1 - 144.5 x + 45.2 x^2$	R = 0.98
15	$y = 123.6 - 133.2 x + 39.56 x^2$	R = 0.95
20	$y = 139.6 - 170.5 x + 57.5 x^2$	R = 0.96

Table 7.4 Statistical fitting equations and correlation coefficient for different CSF percentages (workability secured by superplasticizer)

5	$y = 152.1 - 200 x + 71.4 x^2$	R = 0.98
10	$y = 128.1 - 144.5 x + 45.2 x^2$	R = 0.99
15	$y = 138.5 - 161.9 x + 54.6 x^2$	R = 0.96
20	$y = 134.7 - 157.9 x + 53.4 x^2$	R = 0.95

Table 7.5 Approximate free-water contents (kg/m³) required to give various levels of workability (168)

Slump (mm)		0-10	10-30	30-60	60-180
V-B(s)		>12	6-12	3-6	0-3
Maximum size of aggregate (mm)	**Type of aggregate**				
10	Uncrushed	150	180	205	225
	Crushed	180	205	230	250
20	Uncrushed	135	160	180	195
	Crushed	170	190	210	225
40	Uncrushed	115	140	160	175
	Crushed	155	175	190	205

Note: When coarse and fine aggregates of different types are used, the free-water content is estimated by the expression

$$\frac{2}{3} W_f + \frac{1}{3} W_c$$

where W_f = free-water content appropriate to type of fine aggregate

and W_c = free-water content appropriate to type of coarse aggregate.

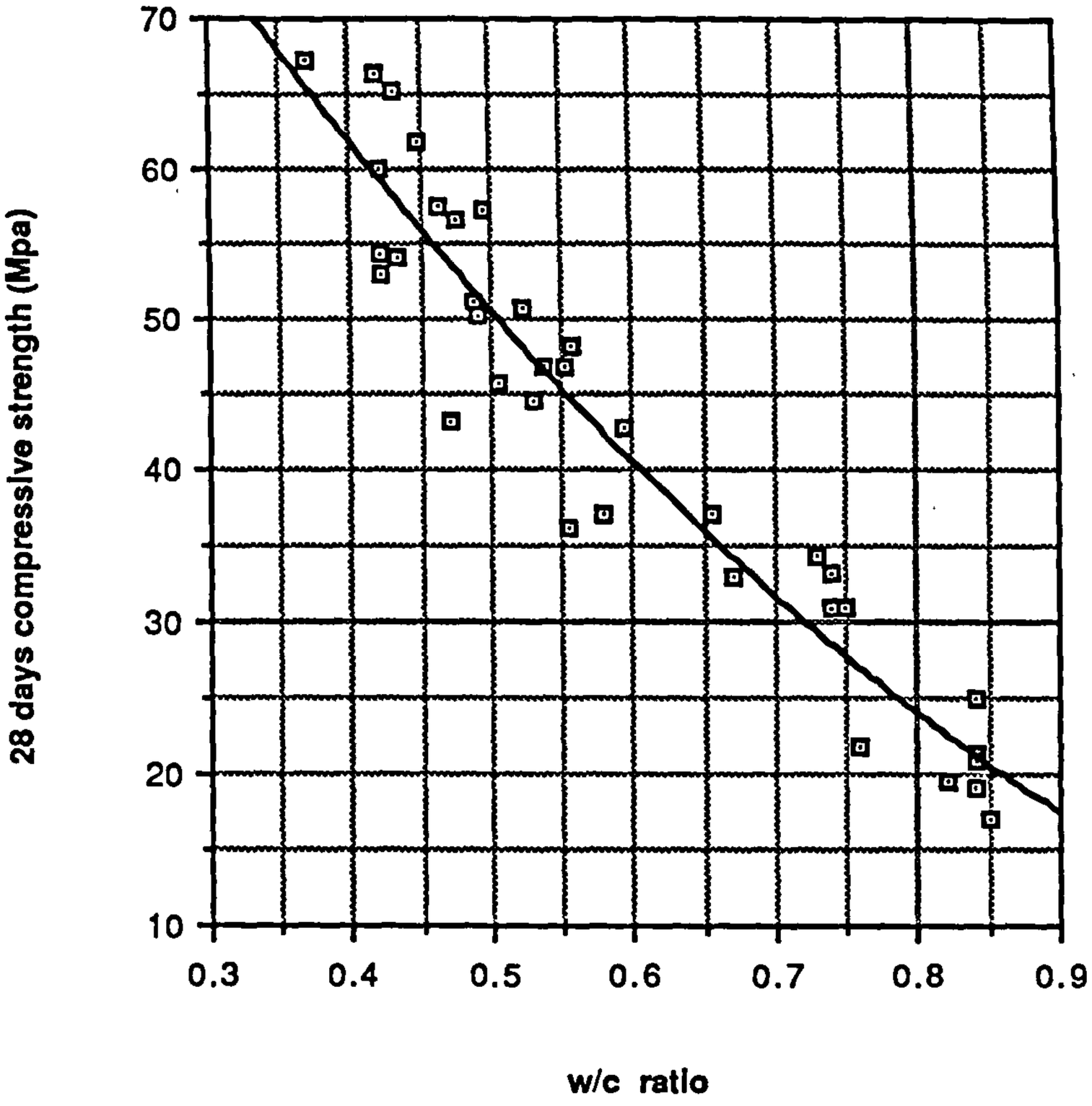

Figure 7.1 Relationship between 28 day compressive strength and W/C ratio of plain OPC mixes

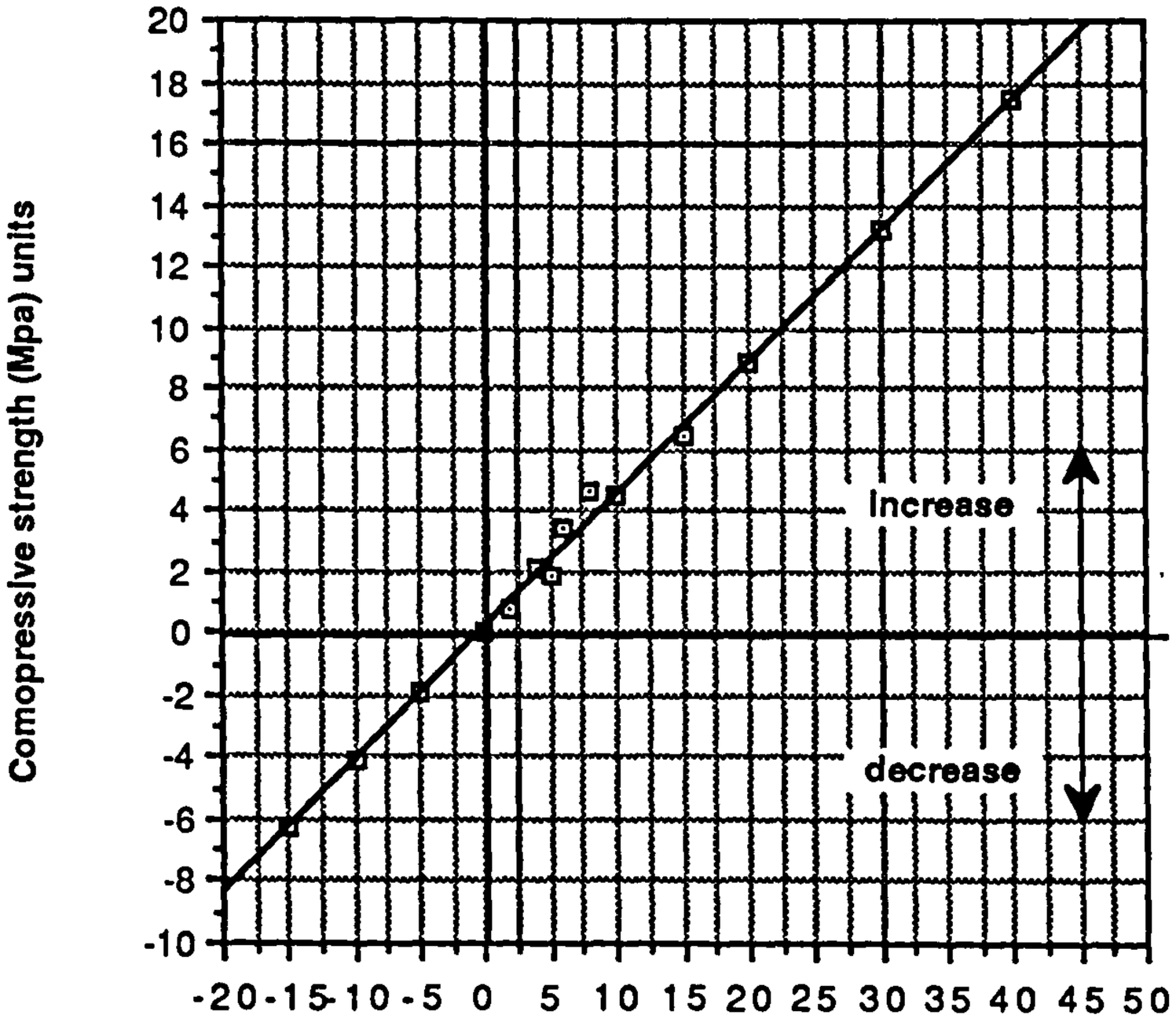

Figure 7.2 Relationship between compressive strength and % of cement

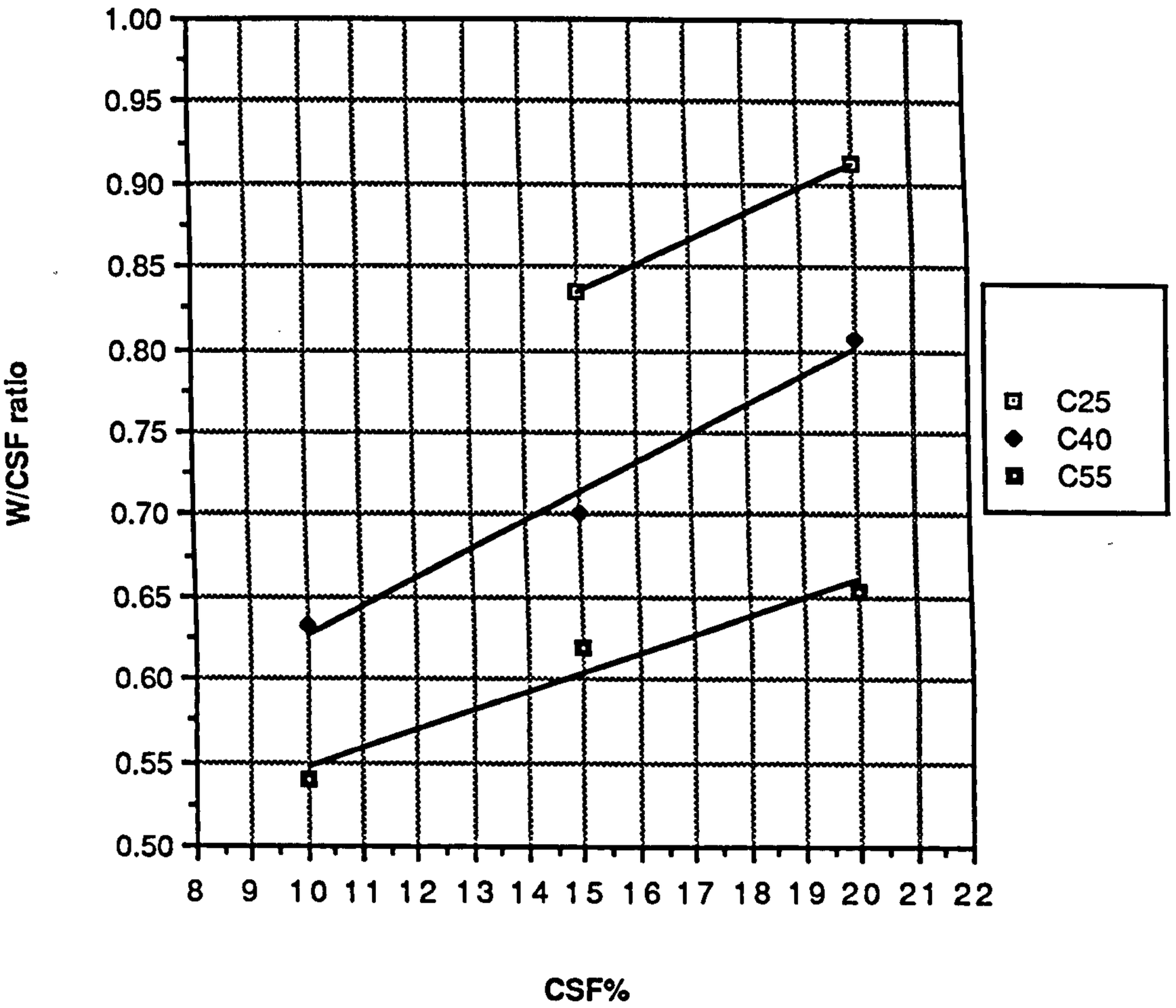

Figure 7.3 Relationship between CSF% and W/C + CSF ratio

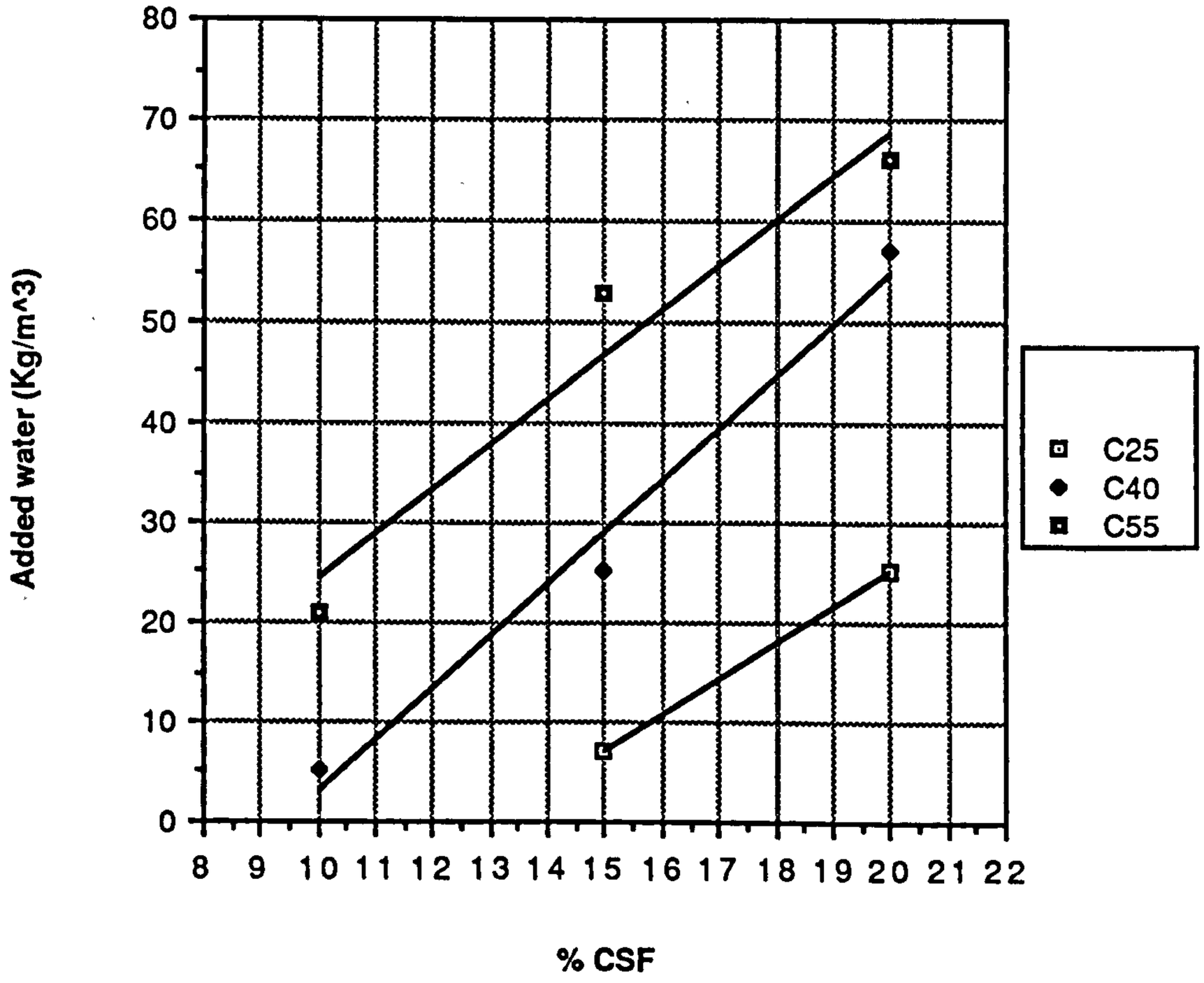

Figure 7.4 Relationship between CSF% and necessary added water to secure medium workability

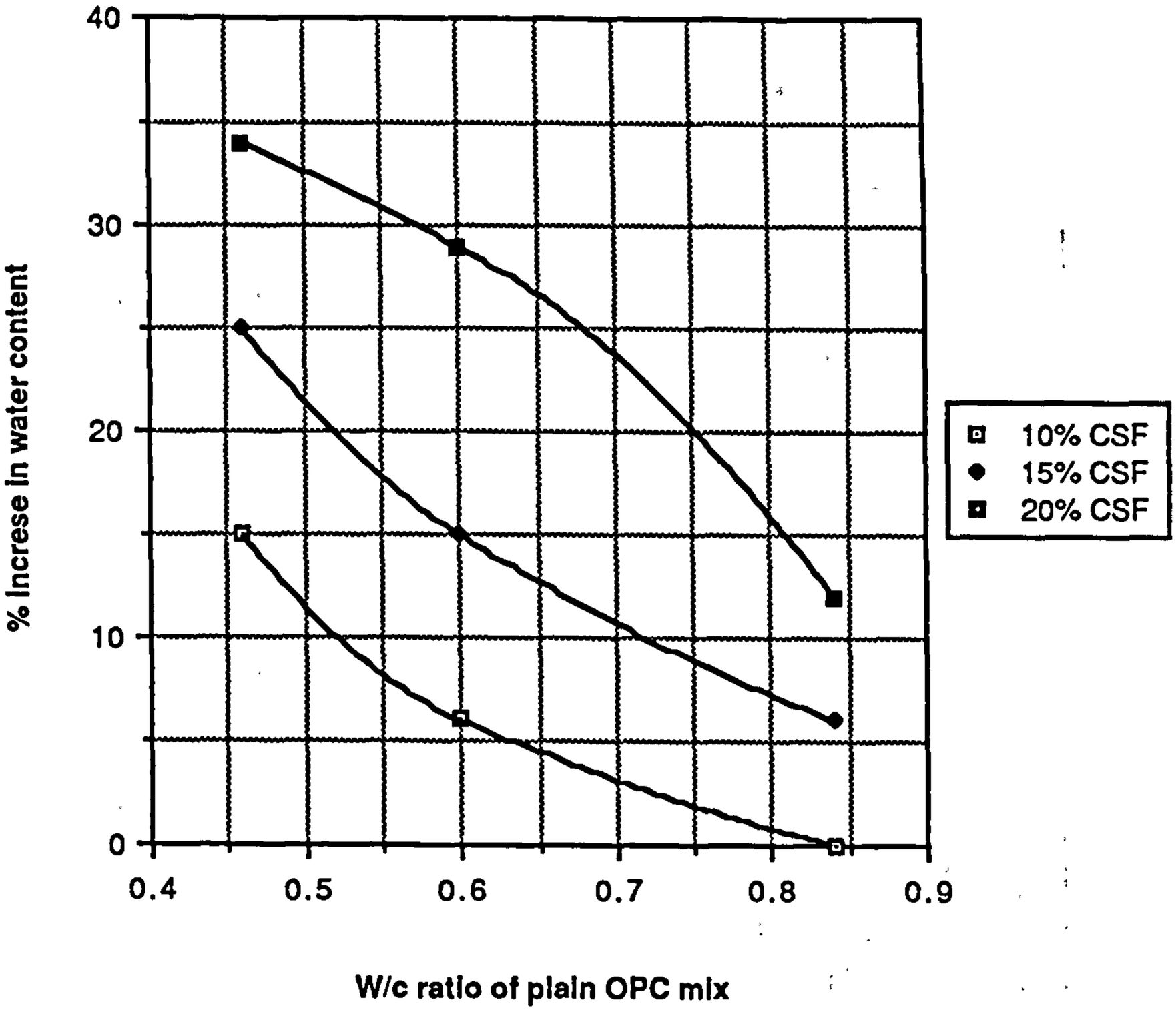

Figure 7.5 Relationship between W/C ratio and the percentage increase in water content necessary to restore workability

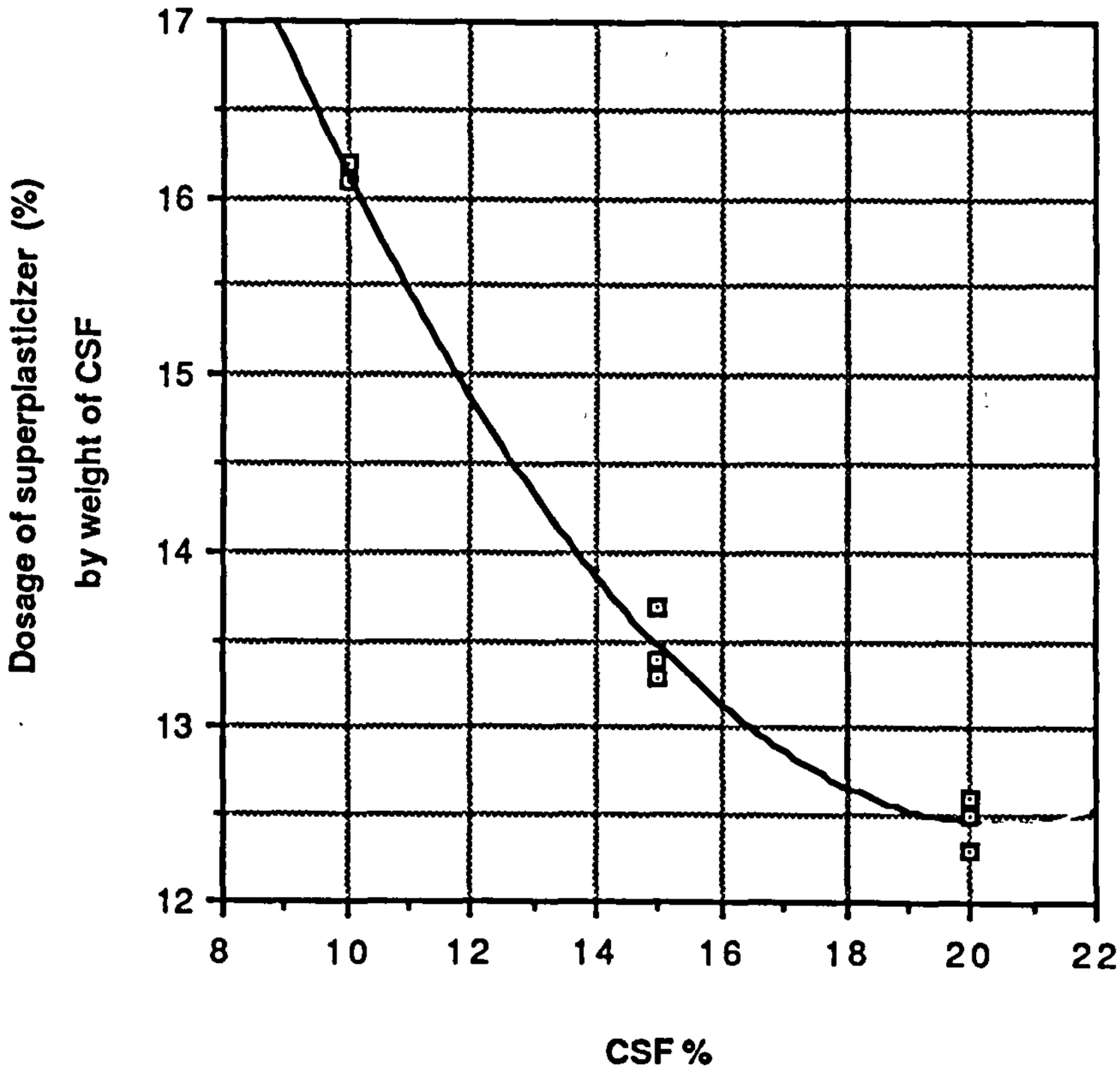

Figure 7.6 Relationship between CSF% and dosage of superplasticizer necessary to restore workability without adding extra water

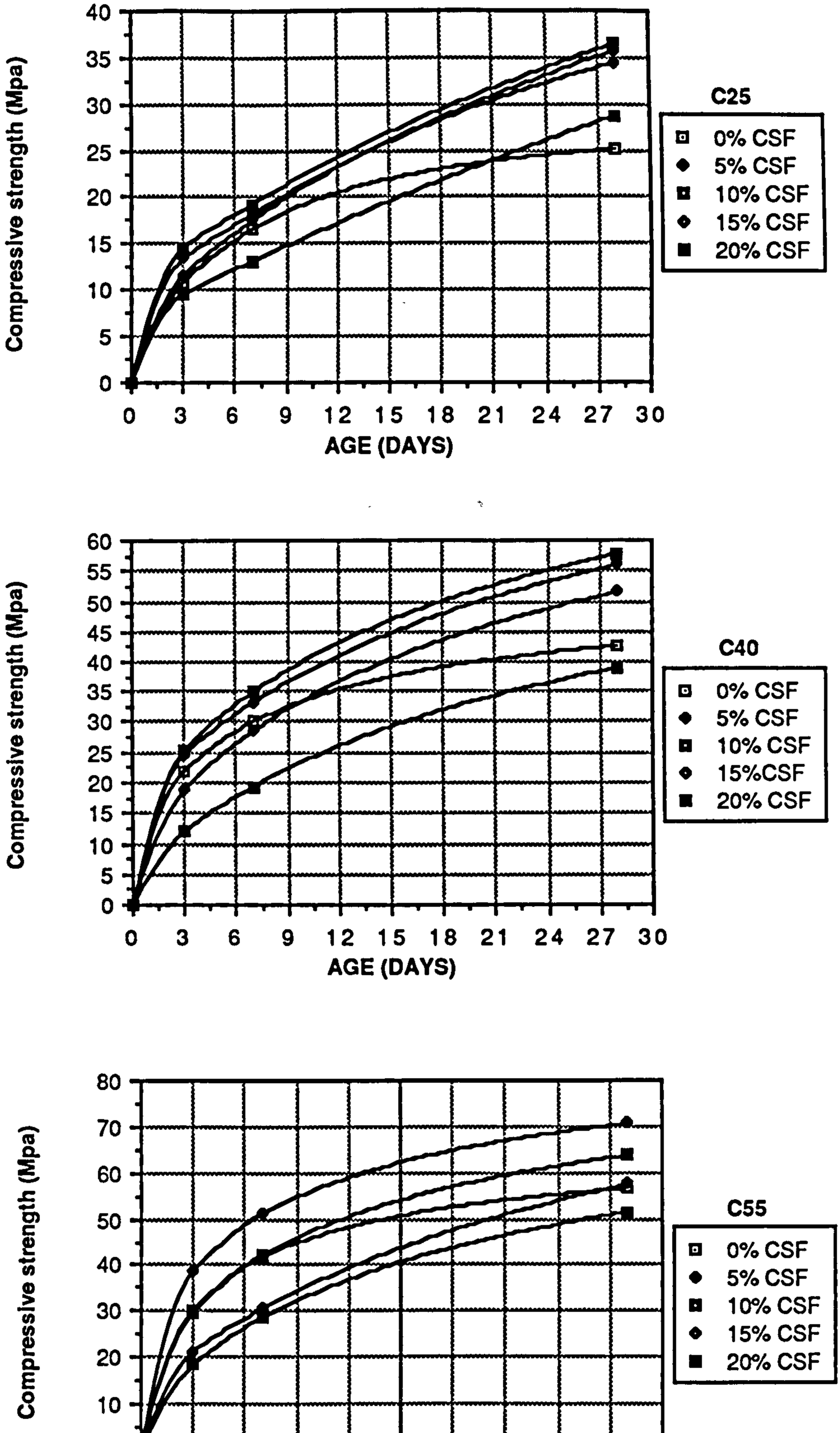

Figure 7.7 Effect of age on compressive strength of plain OPC and CSF concrete mixes of different grades (workability obtained by adding extra water)

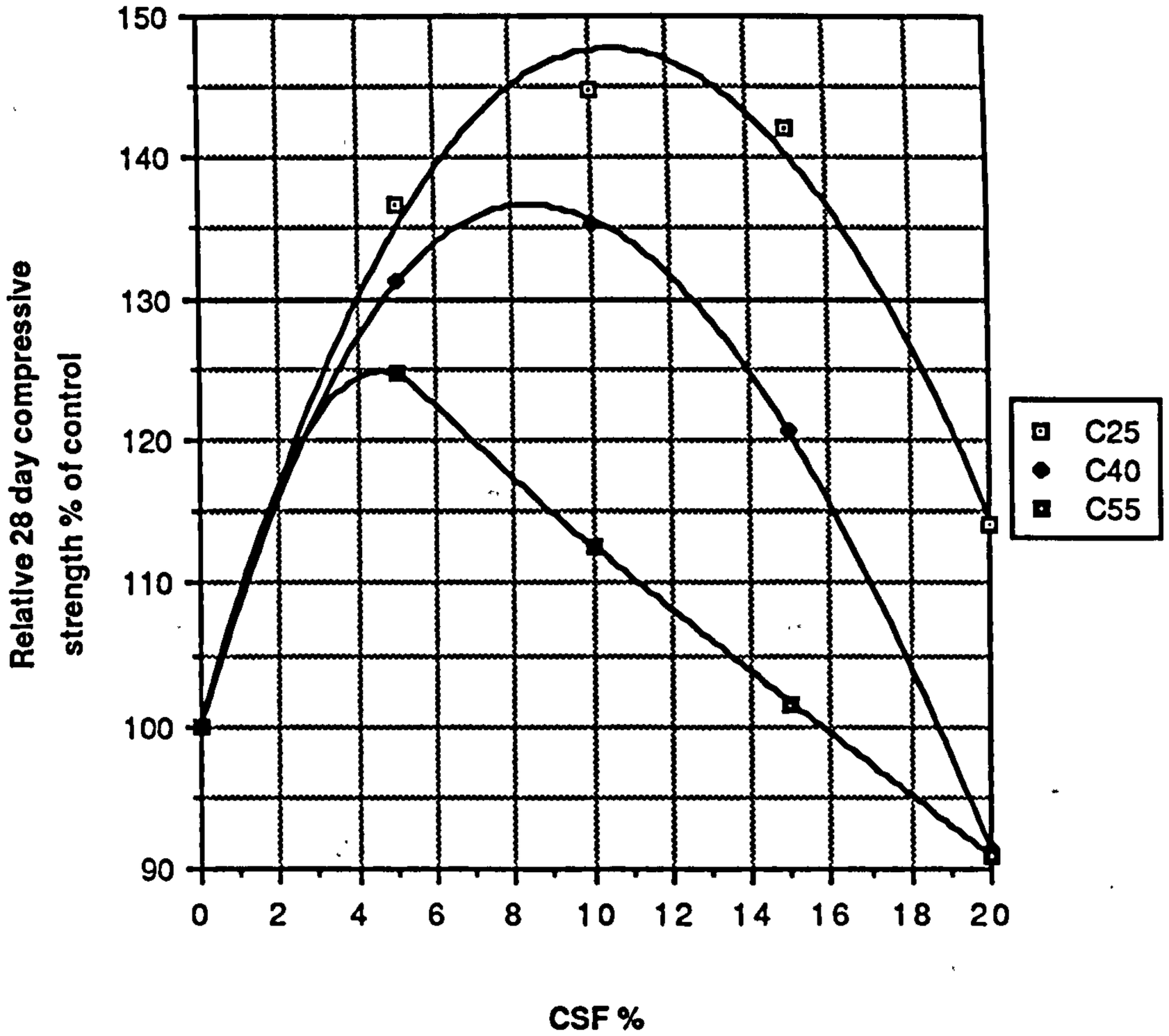

Figure 7.8 Relationship between CSF% and relative 28-day strength for different concrete mixes (workability secured by adding water)

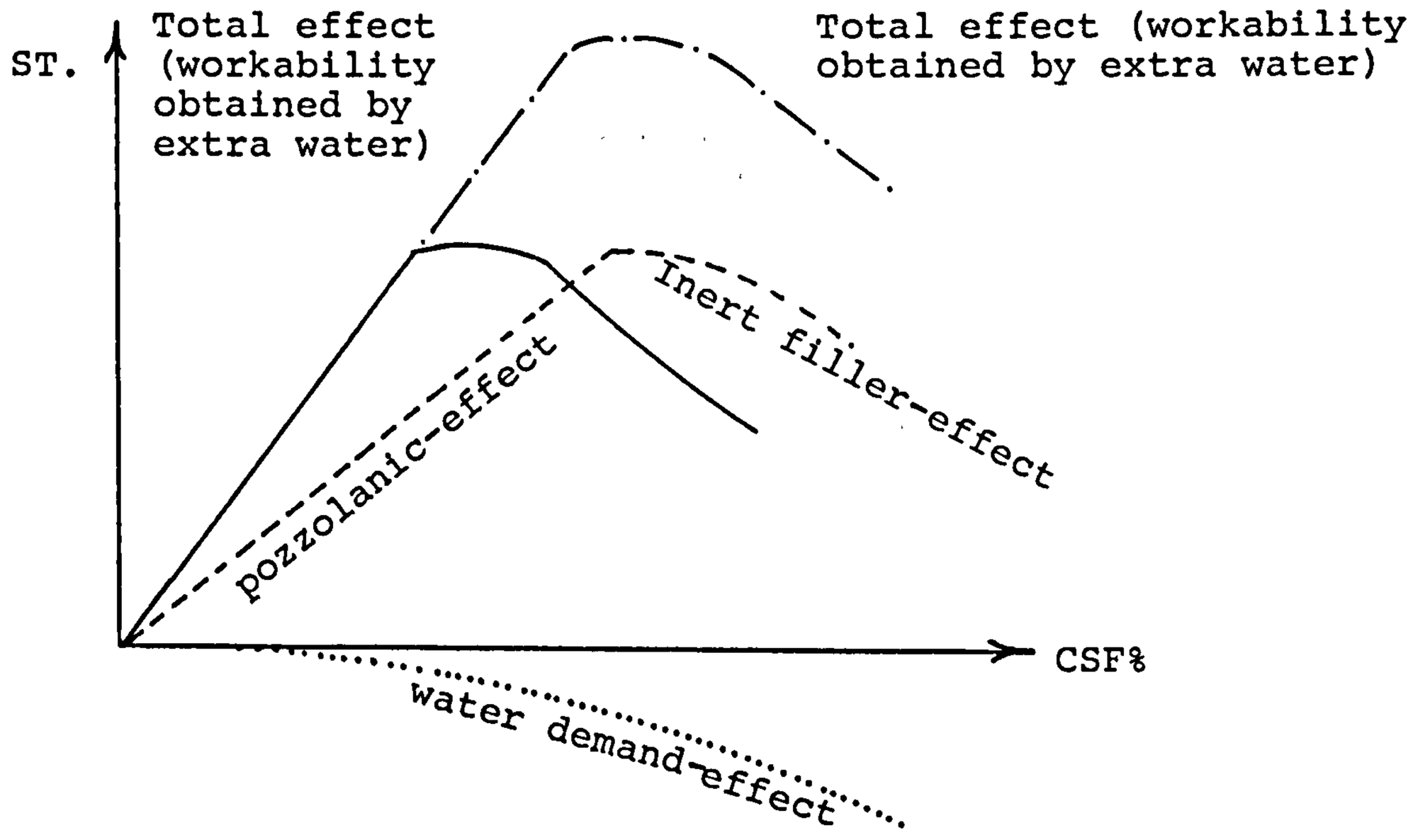

Figure 7.9 Effect of CSF on strength

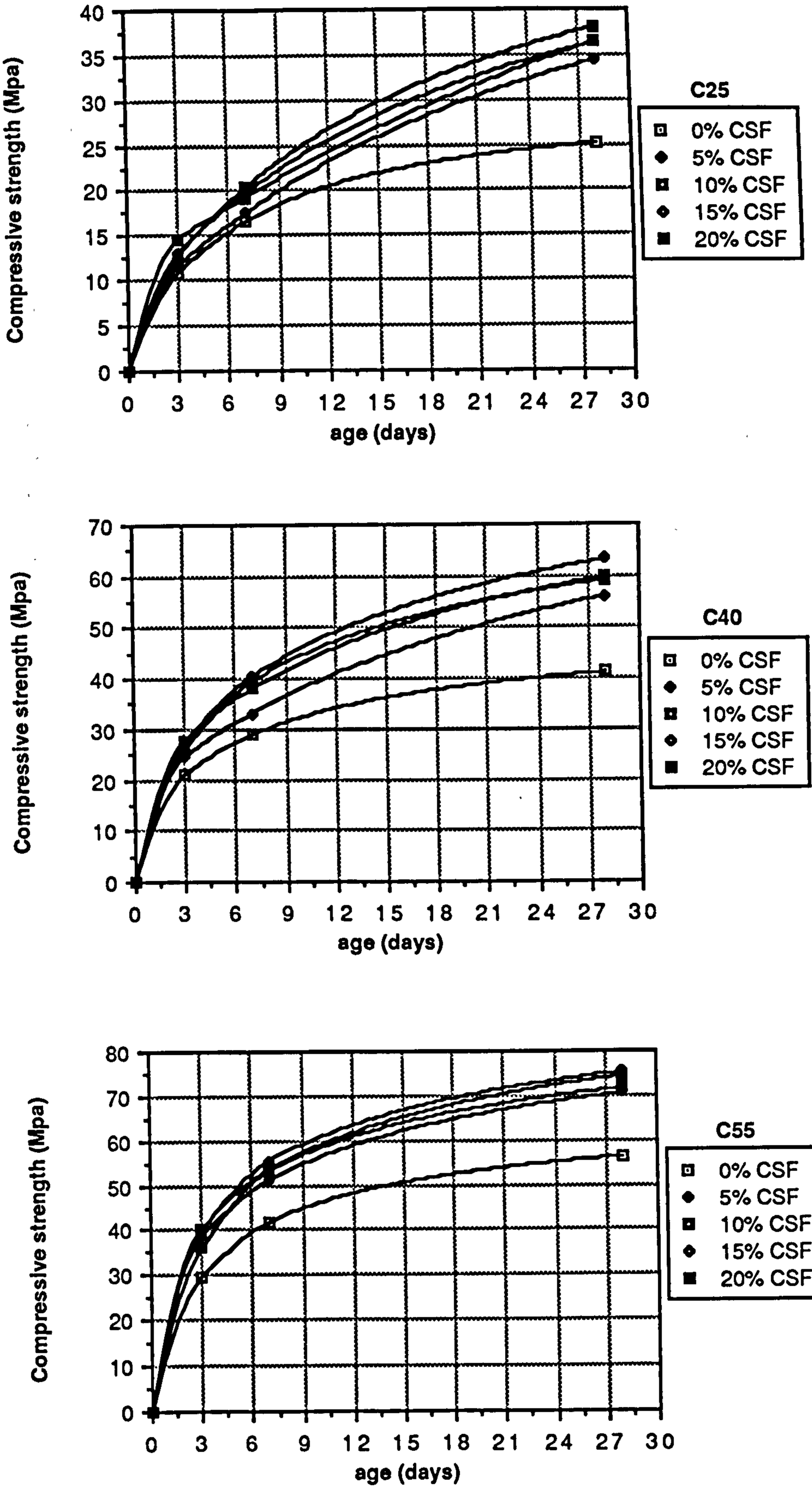

Figure 7.10 Effect of age on compressive strength of plain OPC and CSF mixes of different grades Workability obtained by superplasticizer)

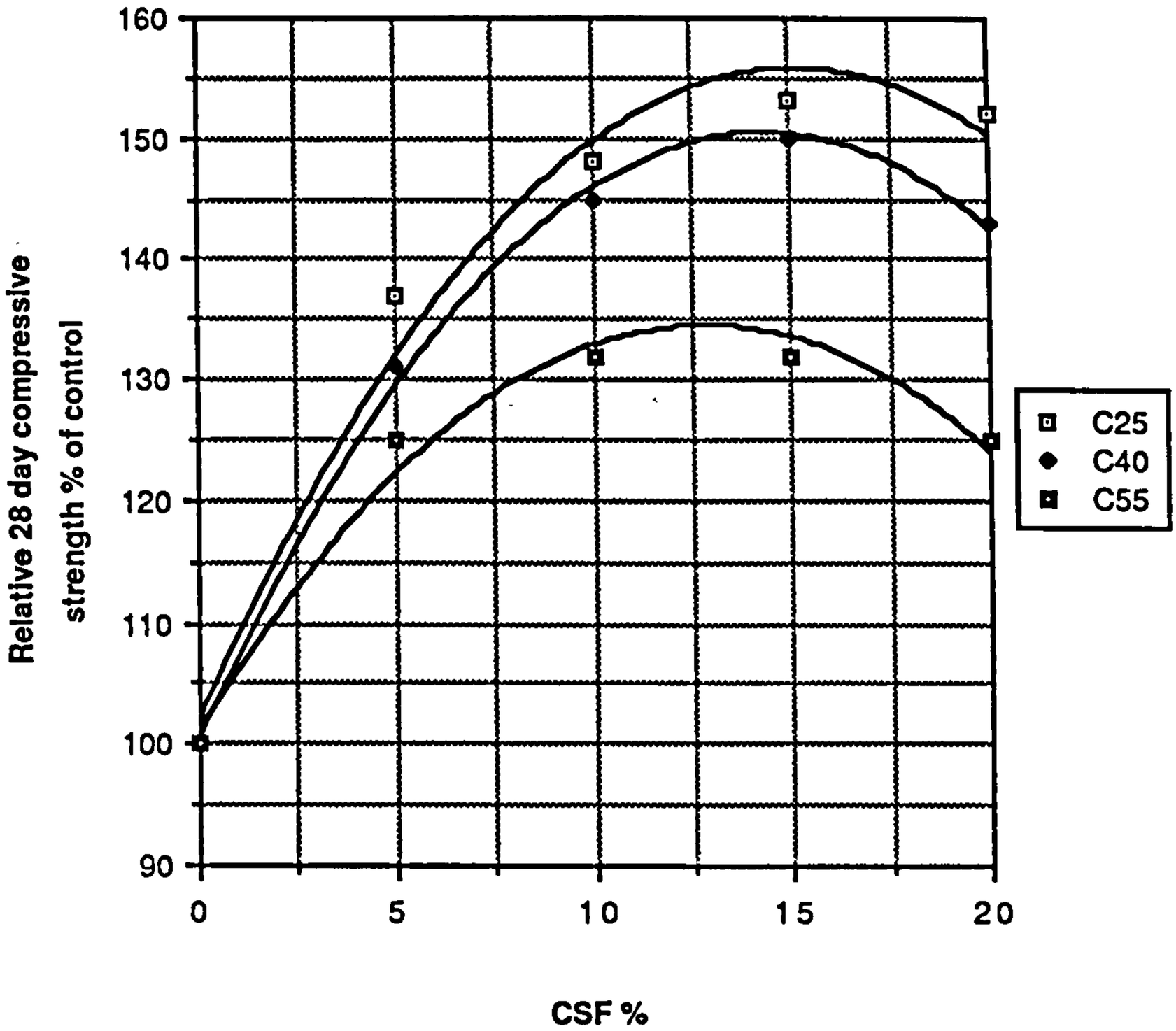

Figure 7.11 Relationship between CSF% and relative 28-day strength (workability secured by superplasticizer)

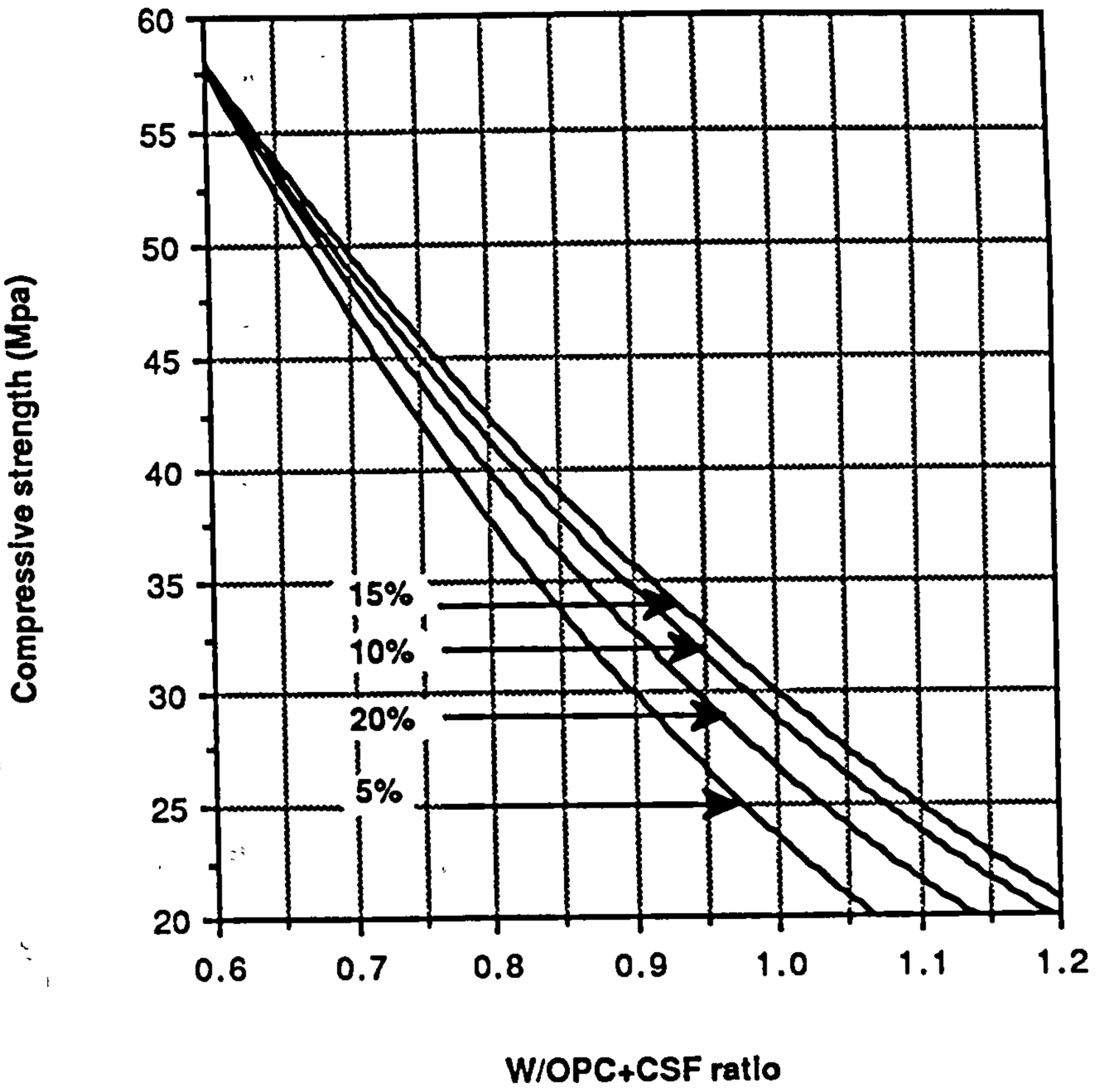

Figure 7.12 Relationship between compressive strength and W/C + CSF ratio of CSF mixes (workability obtained by adding extra water)

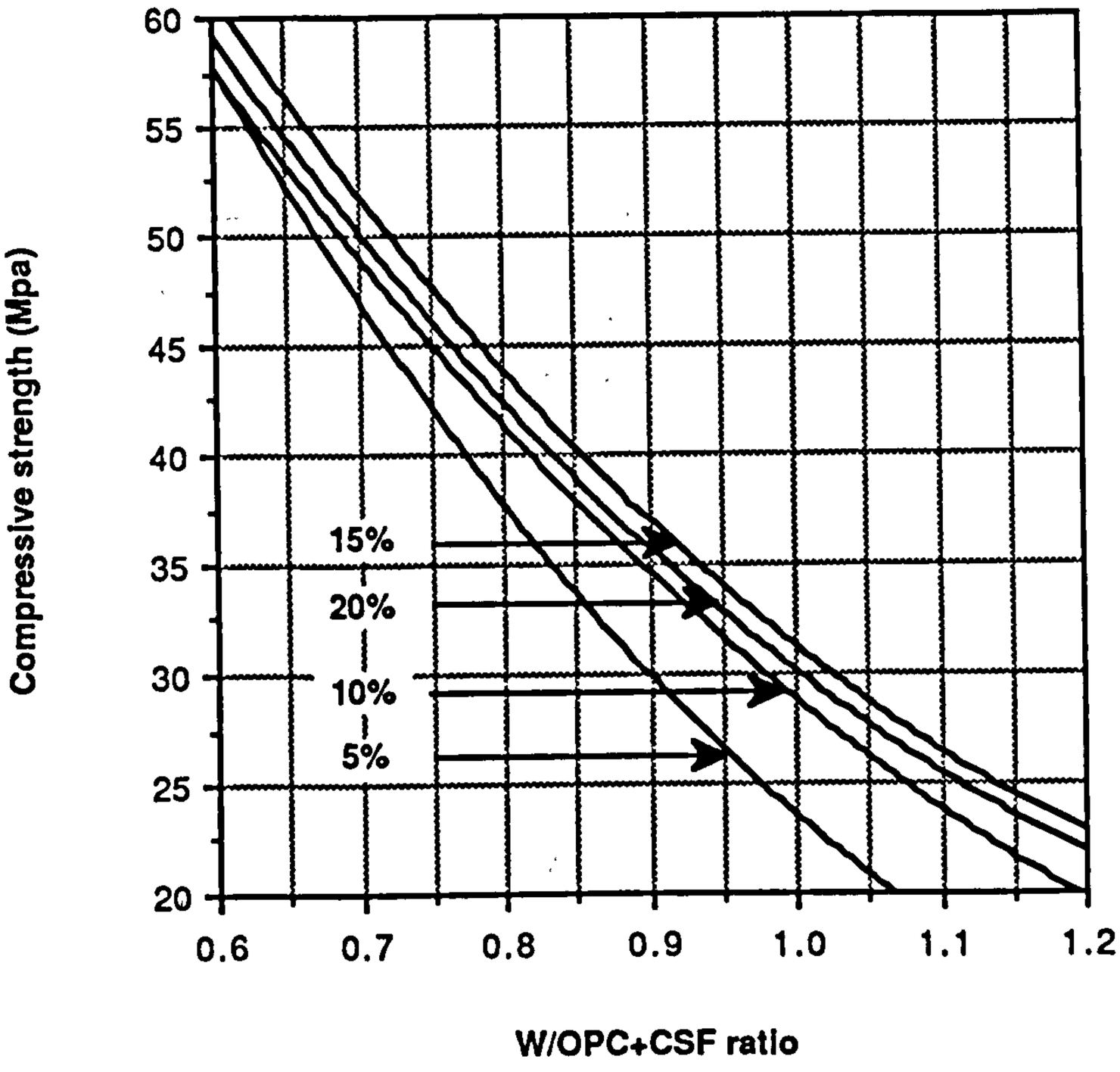

Figure 7.13 Relationship between compressive strength and W/C + CSF ratio for CSF mixes (workability obtained by superplasticizer)

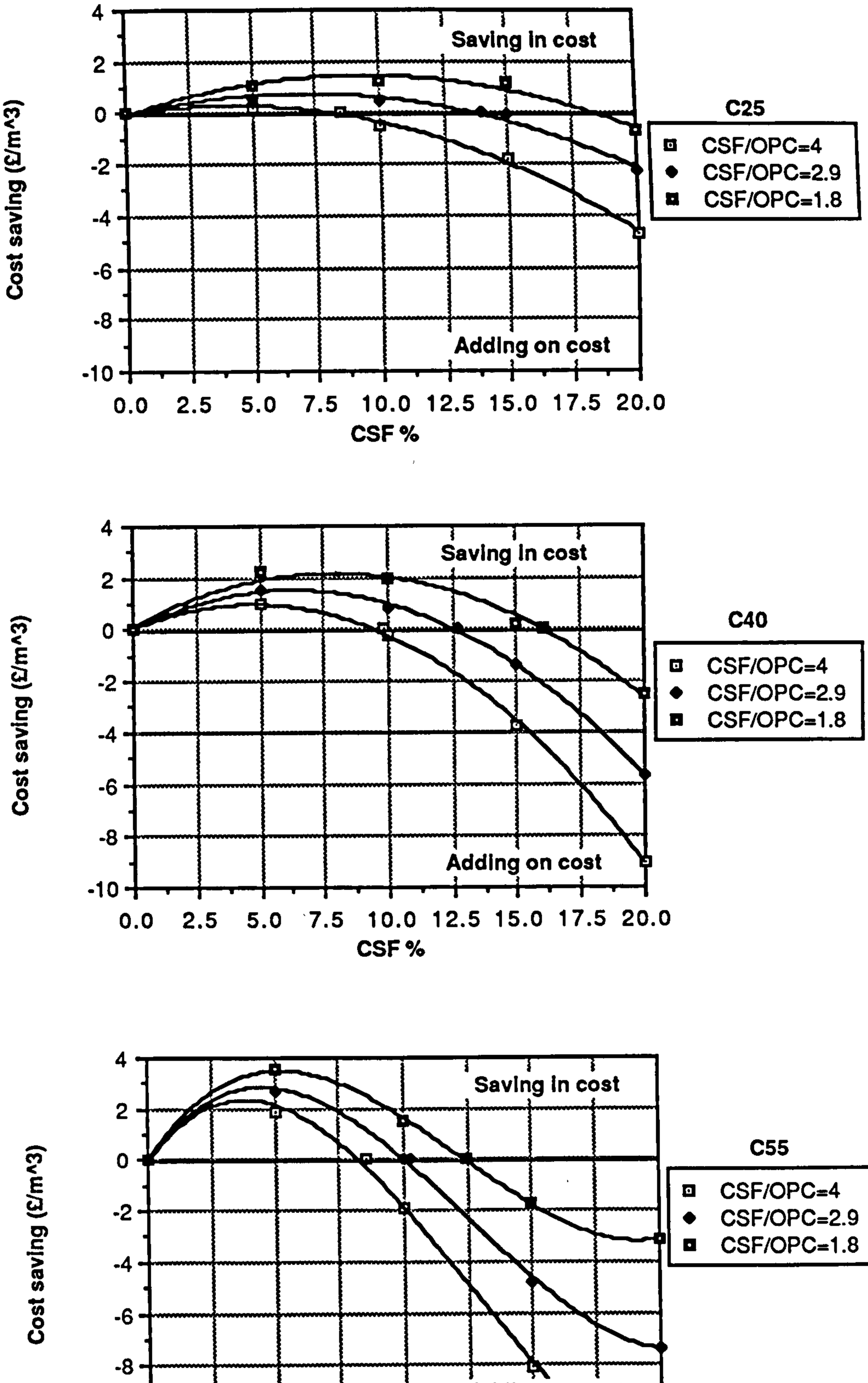

Figure 7.14 Relationship between CSF% and saving in cost per cubic metre (workability obtained by adding extra water)

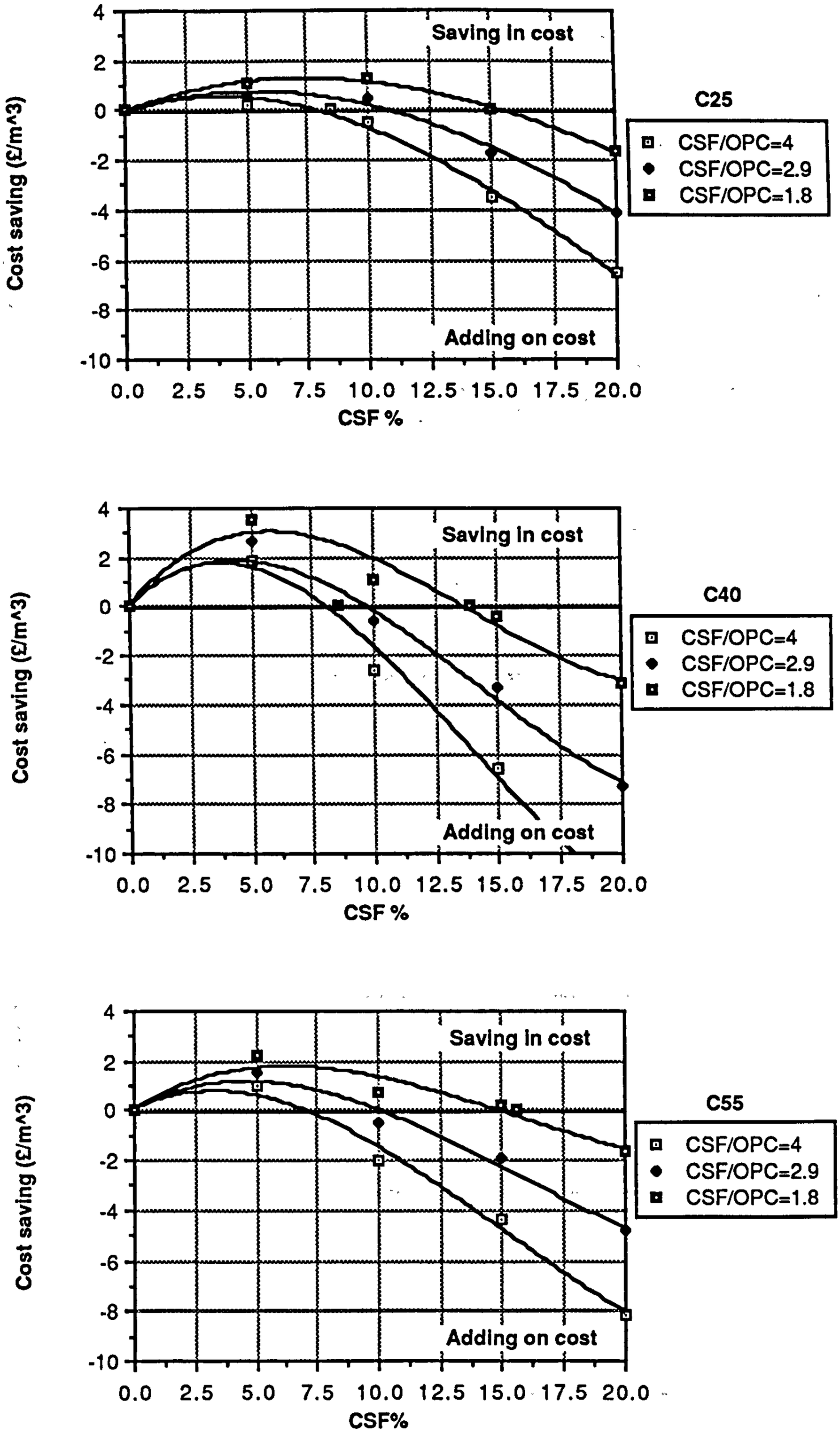

Figure 7.15 Relationship between CSF% and saving in cost per cubic metre (workability secured by super-plasticizer)

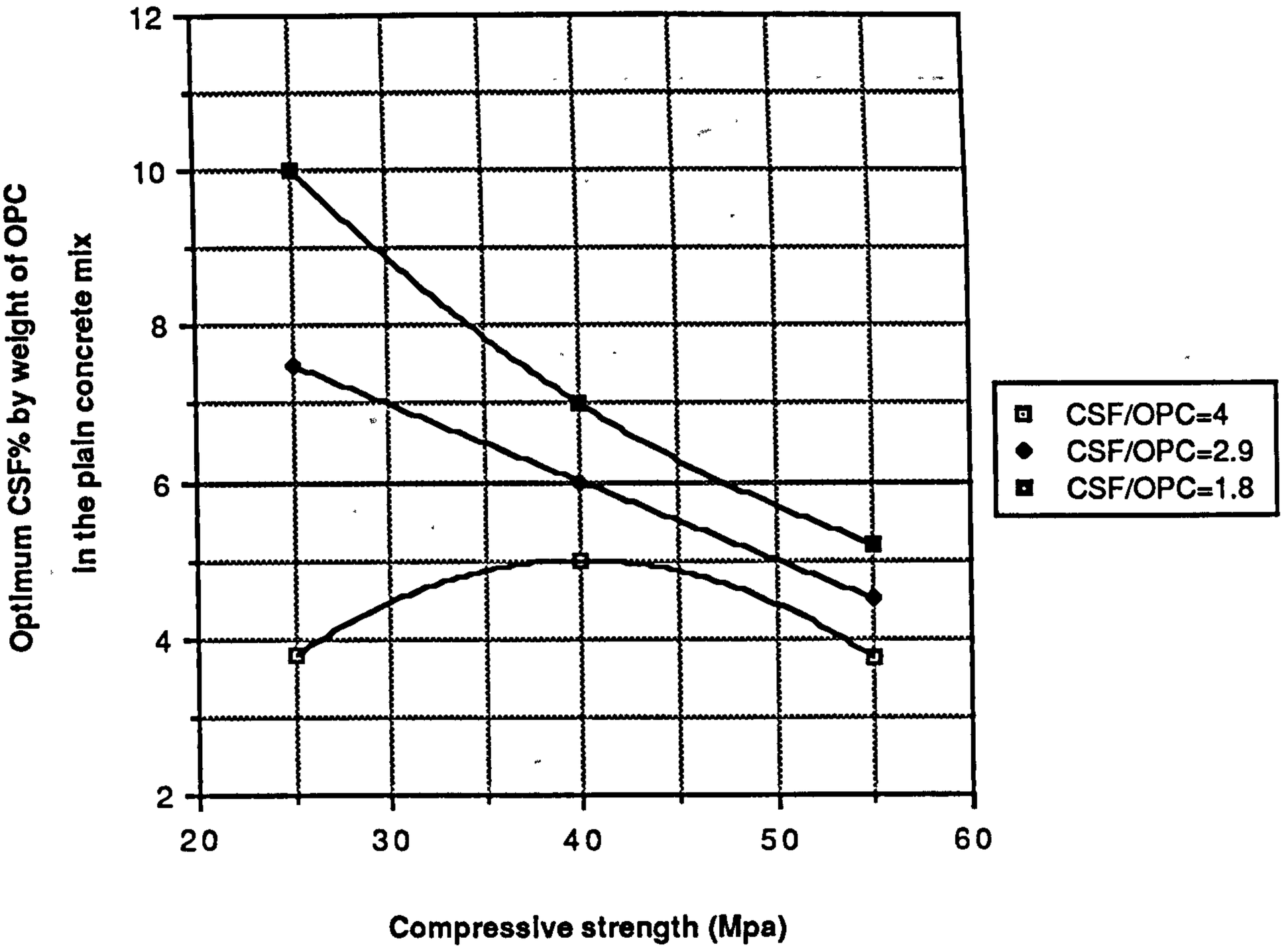

Figure 7.16 Relationship between compressive strength and the most economic CSF% (without super-plasticizer)

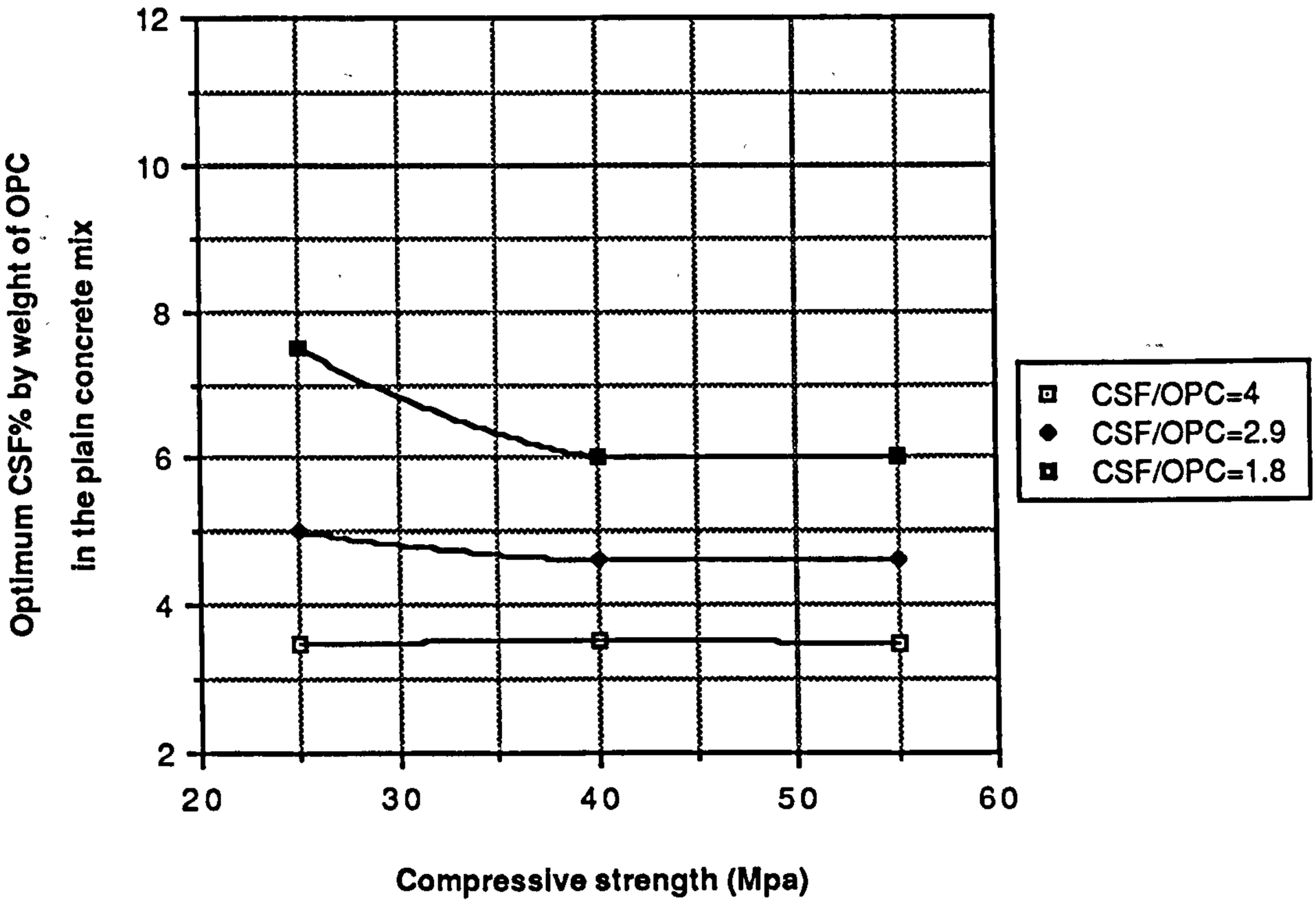

Figure 7.17 Relationship between compressive strength and the most economic CSF% (with superplasticizer)

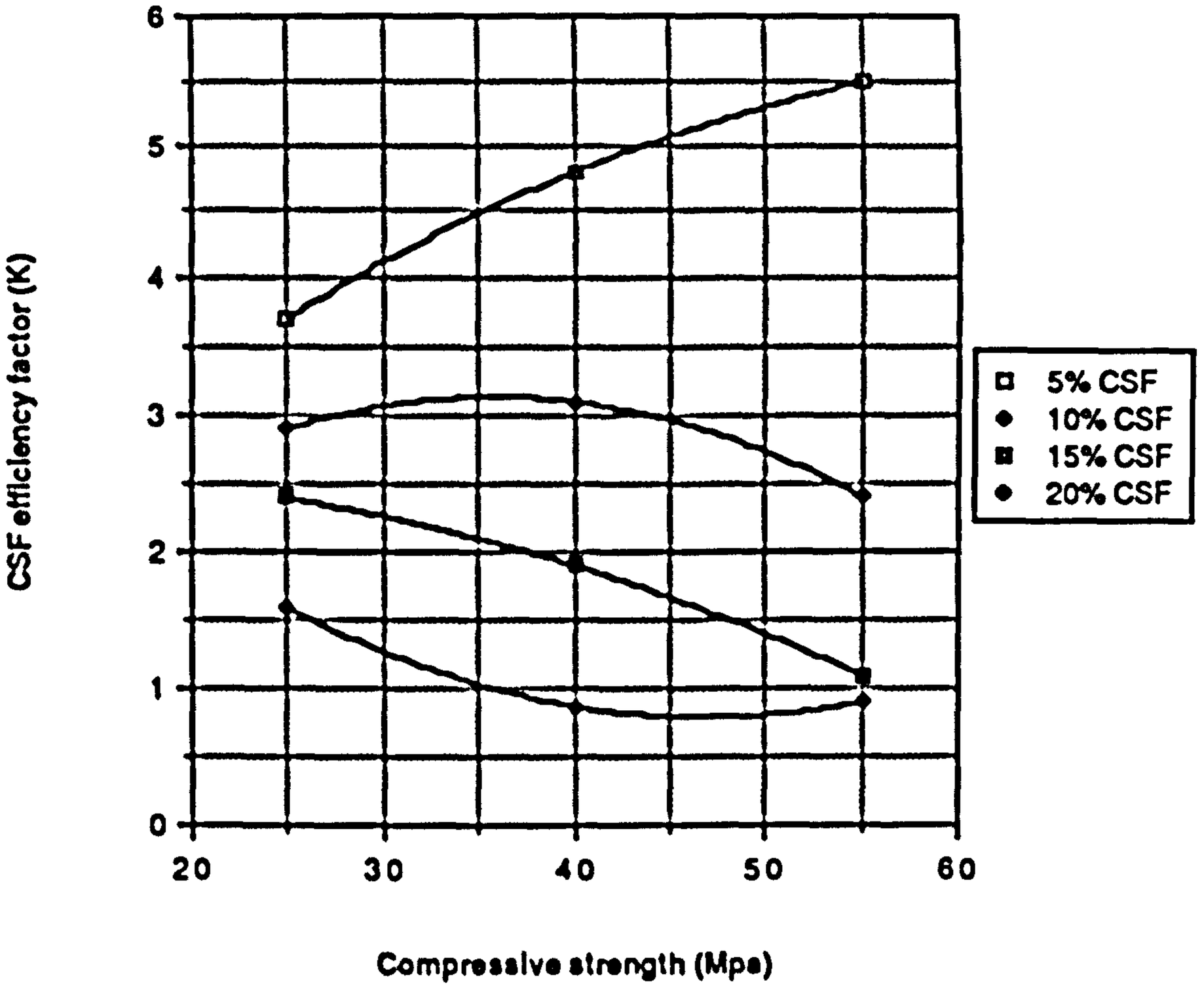

Figure 7.18 Relationship between compressive strength and CSF efficiency factor (workability obtained by adding extra water)

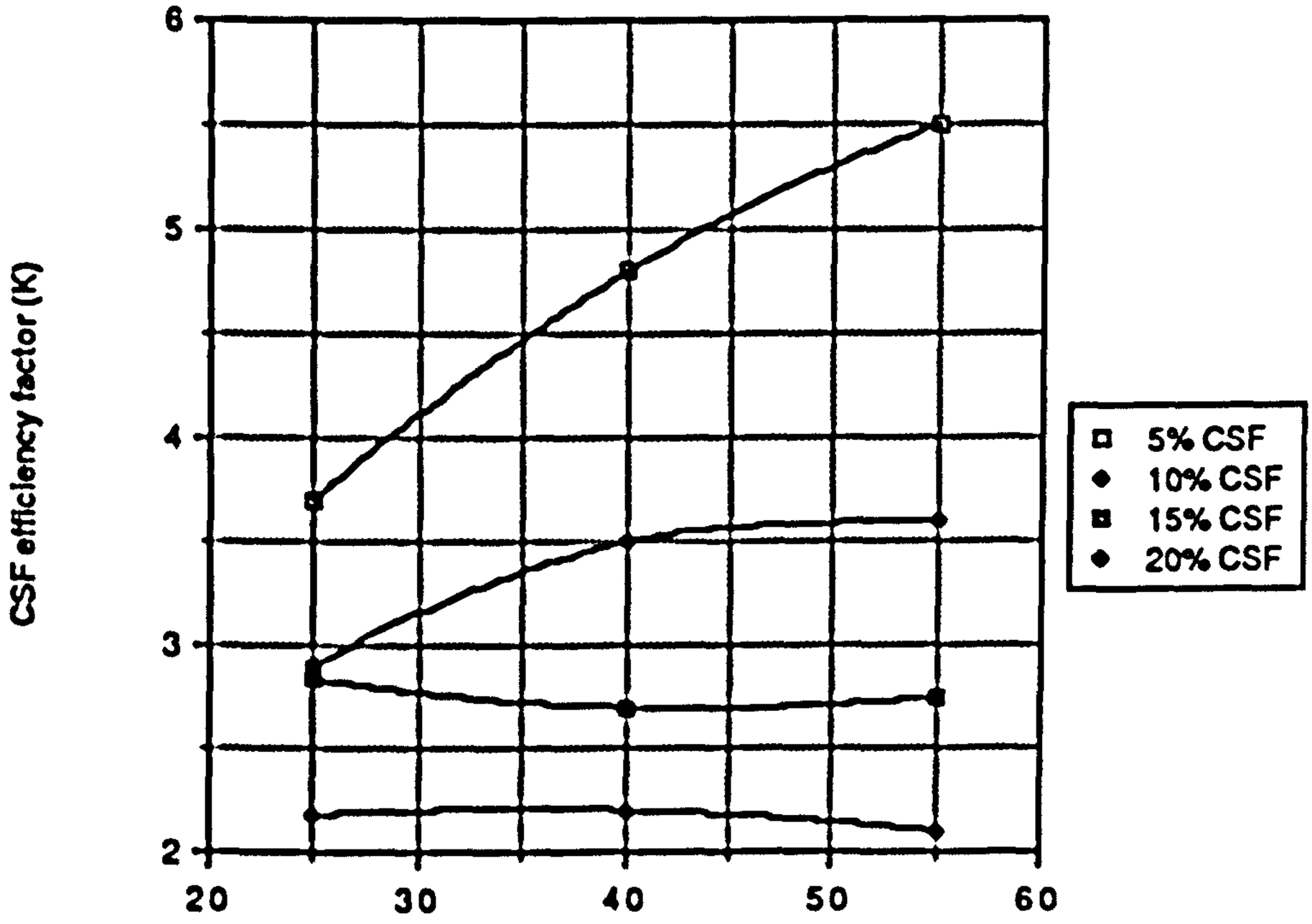

Figure 7.19 Relationship between compressive strength and CSF efficiency factor (workability obtained by superplasticizer)

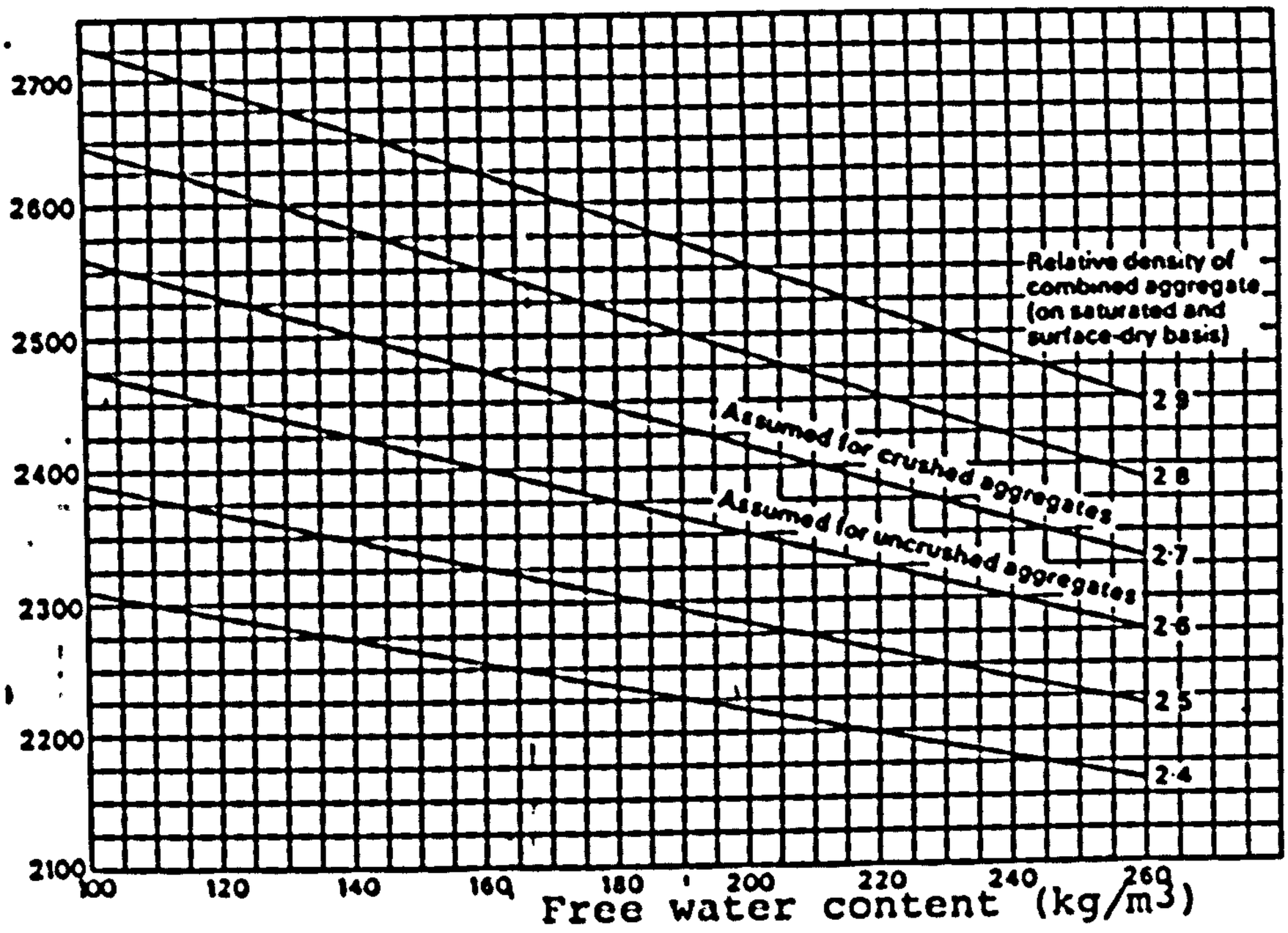

Figure 7.20 Estimated wet density of fully compacted concrete (168)

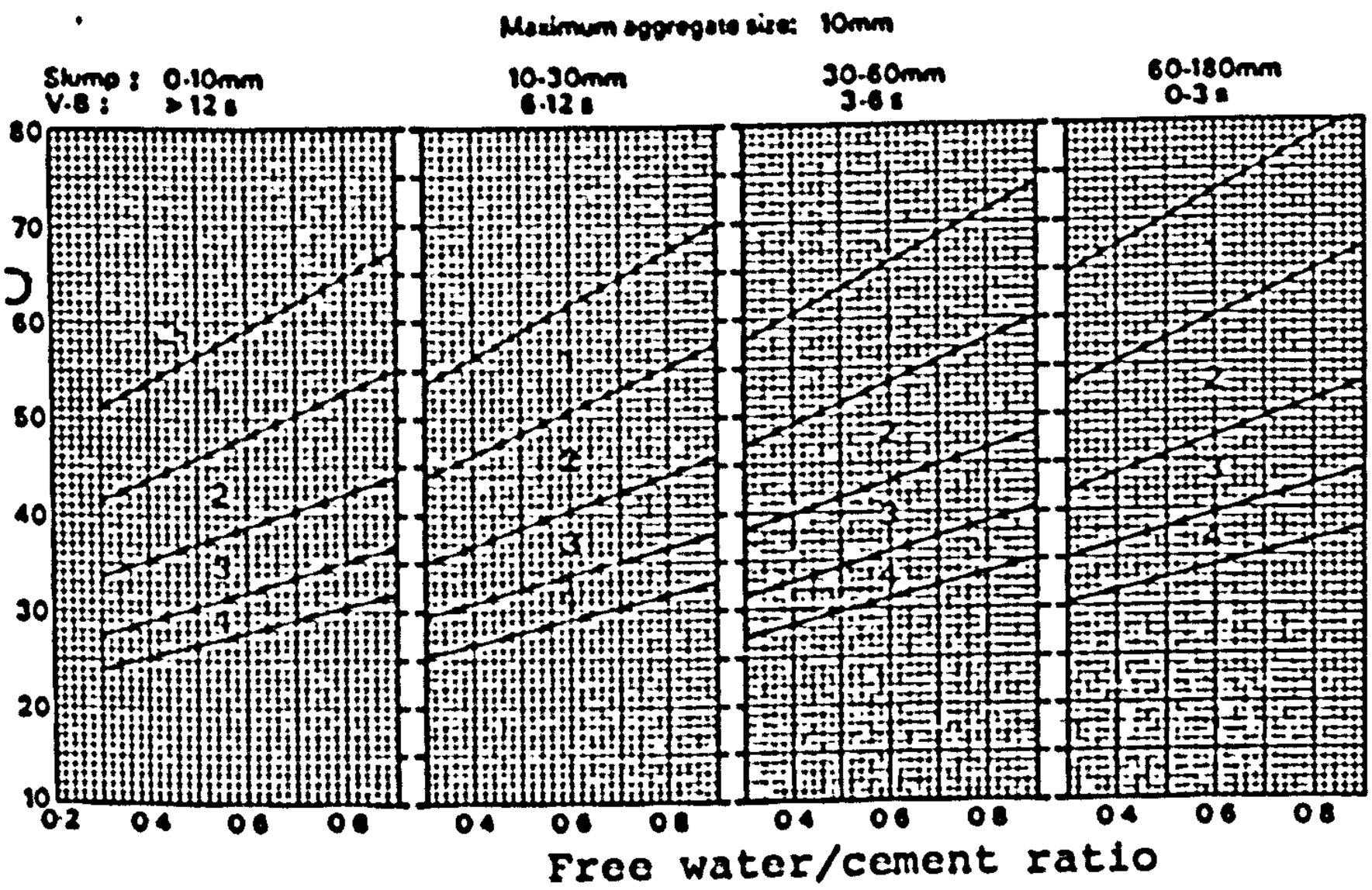

Figure 7.21 Recommended proportions of fine aggregate for BS 882 grading zones 1, 2, 3 and 4 (168)

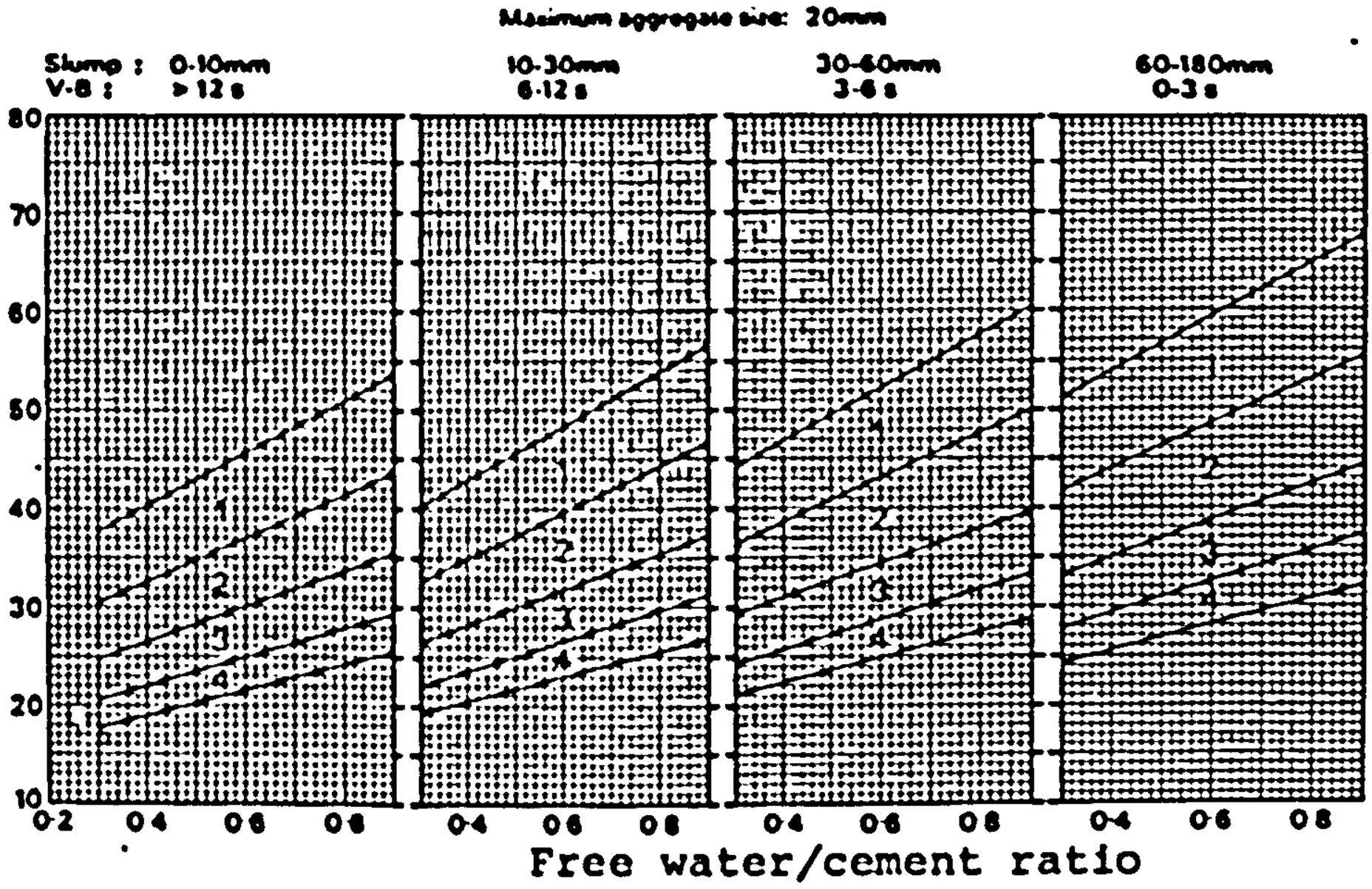

Figure 7.21 (continued)

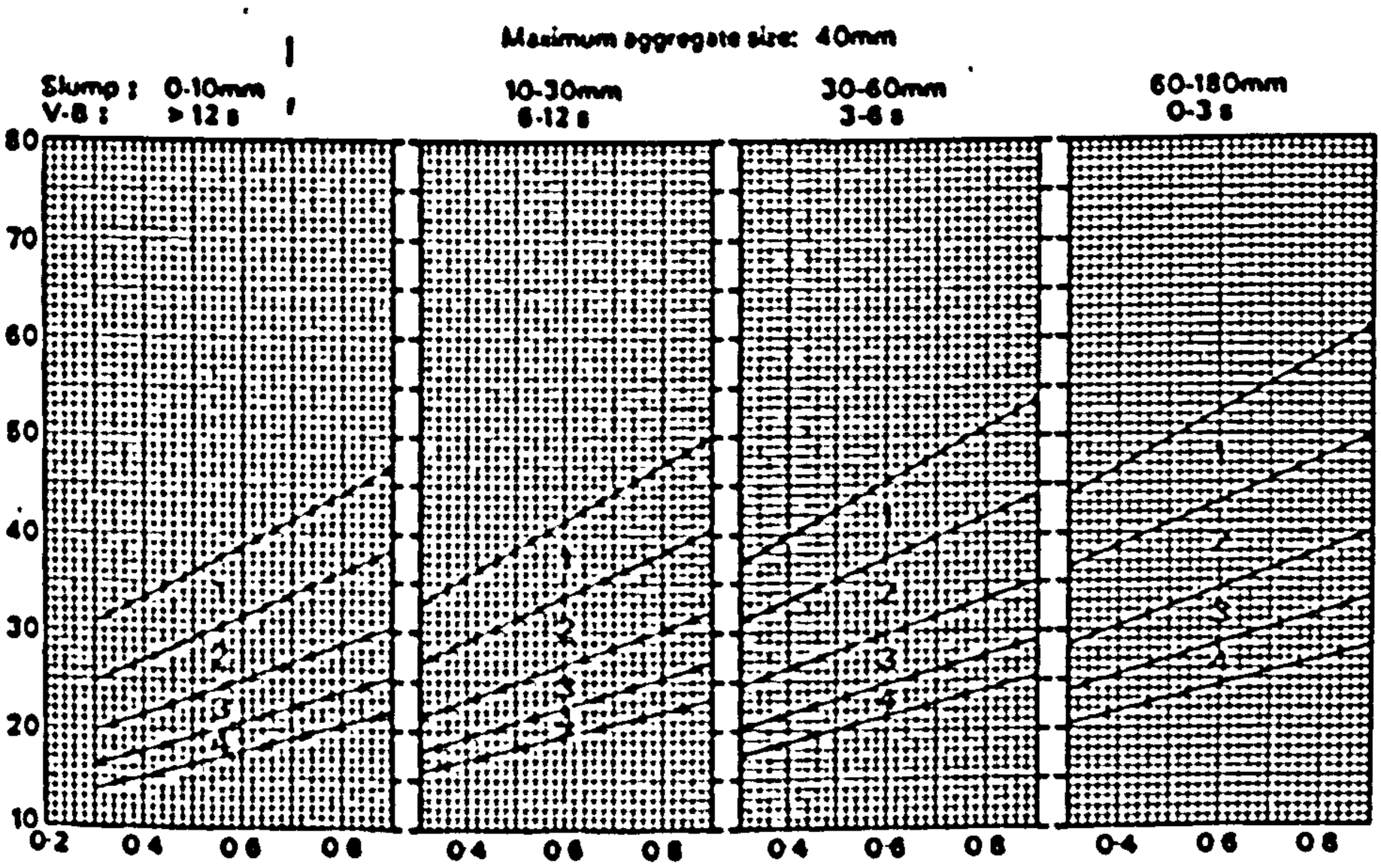

Figure 7.21 (continued)

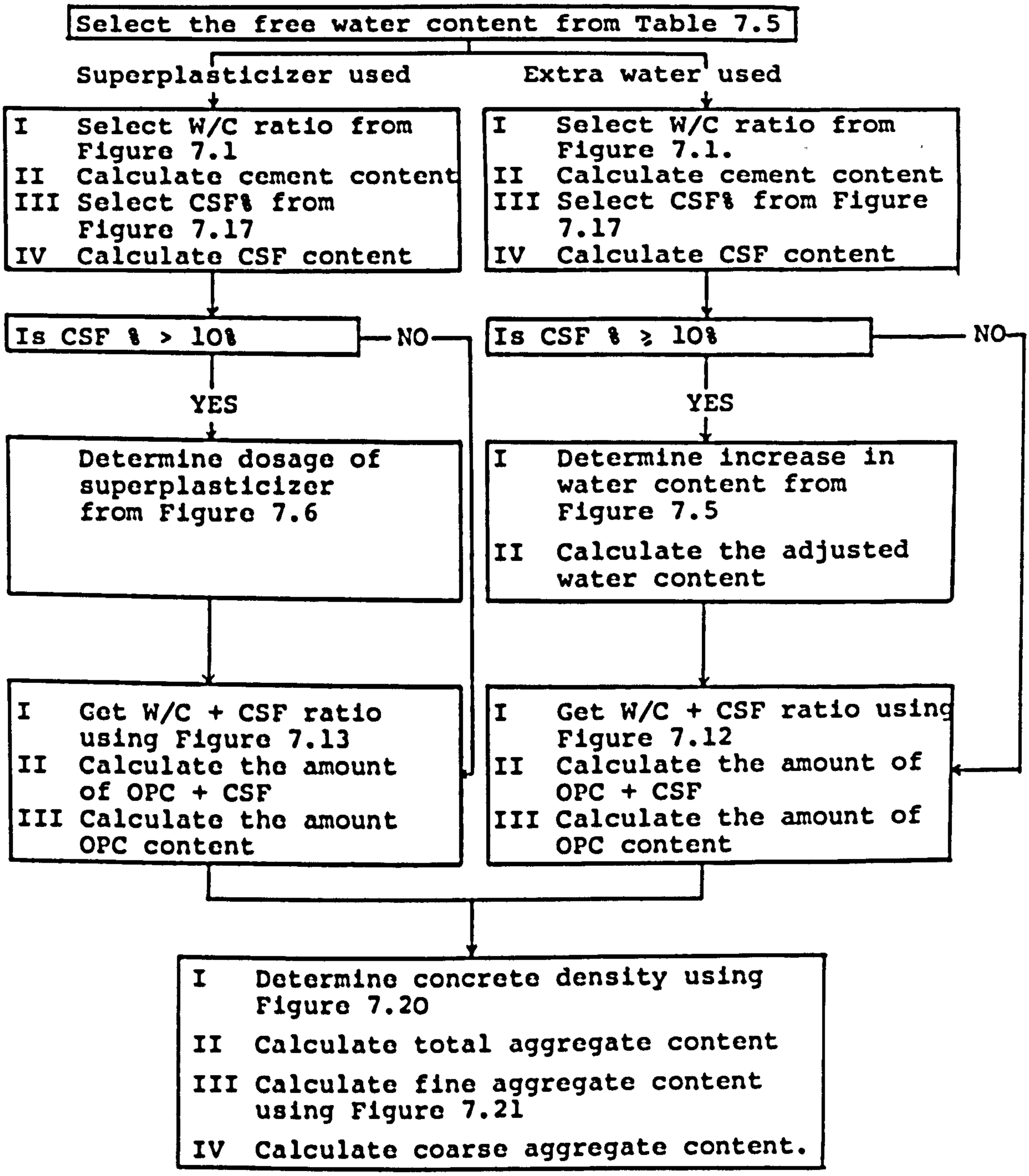

Figure 7.22: Mix Design Flow Chart

CHAPTER EIGHT

EFFECT OF CURING METHOD, TIME AND ENVIRONMENT ON THE STRENGTH AND PERMEABILITY PROPERTIES OF A PLAIN AND CONDENSED SILICA FUME CONCRETE

8.1 Introduction

The work described in this Chapter was designed to assess the effect of initial curing method, time and curing environments on the strength and durability related properties of both plain and silica fume concrete mixes. In addition to the effect of curing and environmental conditions, the concrete mixes are designed to study the effect of cement content and different levels of OPC replacement by silica fume. Finally, the effect on the above mentioned properties of controlling the workability by either adding extra water or using superplasticizer was also investigated. The effect of all the different variables on the properties of the concrete mixes were evaluated at 3, 7, 14, 28, 56, 90 and 180 days of age.

8.2 Mix proportions

The mix proportions used throughout this test programme are shown in Table 8.1. These mixes were designed as described in Chapter seven to have an equivalent compressive strength at 28 days of age. They were selected from among the mixes employed in the previous testing programme, designed to establish a mix design method, based on efficiency and economy. Moreover, consideration was given assessing the effect of controlling the workability by either adding extra water or using superplasticizer on the strength and durability properties. Mixing was carried out as described previously in Chapter six, and with each mix type the following specimens were cast:

1. (72) 100 x 100mm cubes to assess the effect of two initial curing method (polythene and water) and two environmental conditions (temperate and hot) on the compressive strength.

2. (60) 100 x 100mm cubes to assess the effect of variables in (1) on the Figg air, Fig water and Egg air permeability and ISAT.
3. (60) 100 x 100mm cubes to assess the effect of variables in (1) on water absorption.
4. (120) 100 x 100mm cubes to assess the effect of initial curing time (0, 1 and 3 days) under two environments (temperate and hot) on the durability properties in two and three. This short program was carried out to cover mix (C40/0) and (C40/10).

A total of 2352 cubes were tested in the test program described in this Chapter.

8.3 Initial curing and environmental conditioning

Concrete specimens were subjected to one of the seven different initial curing/environmental conditions described in Chapter six and shown in Figure 6.1.

8.4 Tests carried out

The following tests were carried out at age of 3, 7, 14, 28, 56, 90 and 180 days on the specimens cast:

1. Compression strength
2. Figg relative air permeability.
3. Egg relative air permeability
4. Figg relative water permeability
5. ISAT
6. Water absorption.

These tests were performed following the procedure described earlier in Chapter six.

8.5 Results and discussion

8.5.1 Compressive strength

Results of compressive strength test on plain OPC and CSF concrete mixes are shown graphically in Figures 8.1 to 8.10. The statistical analysis performed on the test result shows that the coefficient of variation between test results of nominally identical specimens is within 10%.

Due to the similarity in the pattern of compressive strength results trend between the three concrete grades C25, C40 and C55, discussion will be based on the test results of concrete mixes grade C10.

8.5.1.1 Effect of age

The effect of age on the compressive strength is shown graphically in Figure 8.1. Test results of all concrete mixes (plain OPC and CSF) show that compressive strength increases with age. The rate of strength gain is high at early ages and gradually decreases at later ages. CSF concrete mixes show lower compressive strength at early ages (3 and 7 days) compared to the reference plain OPC mixes. The higher the CSF content the lower is the early-age strength. This behaviour is possibly caused by the CSF physical effect viewed as a "densifying effect" in the sense that the extremely fine CSF particles tend to accommodate themselves in the empty spaces between two cement grains. Hundreds of CSF particles were found between two cement grains (169). These CSF particles may possibly prevent water percolation reaching cement grains, thus slowing down the early age hydration and resulting in a lower early age strength. Since all concrete mixes (plain & CSF) were designed on the basis of comparable workability and 28-days compressive strength under standard continuous water curing, it is interesting to see them, regardless of the curing method, reaching the same strength at 28-days under temperate conditioning environment. Results of all CSF concrete mixes show that their compressive strength continues to increase at a higher rate compared to the reference plain OPC mix. This higher rate of strength gain is believed to be initially caused by the physical properties of CSF particles. The physical effect of the CSF particles can be explained by their high ability to disperse cement flocs which eventually result in exposing higher surface area of OPC to normal hydration than that without the CSF effect. The CSF dispersing ability is a result of its extreme fineness and large surface area compared with portland cement. This dispersion will

accelerate the hydration of OPC particles and in turn accelerate the pozzolanic reaction taking place between the calcium hydroxide produced by OPC hydration and CSF. The overall acceleration of both reactions may quite possibly be responsible for the high rate of strength gain in CSF concrete mixes.

At later-ages (180 days) CSF concrete mixes attained compressive strength values higher than the reference plain OPC mix. This high late-age compressive strength is predominantly due to the formation of more strength dependent cementitious reaction products, i.e. C-S-H. A secondary factor contributing to this high late-age strength could be the changes that take place in the structure of the cementitious products formed during the pozzolanic reaction, i.e. the increase in the crystallinity and density of the secondary C-S-H produced by the pozzolanic reaction. Moreover, C-S-H gels produced by both calcium silicate and pozzolanic reactions intergrow into a rigid network increasing the physical and chemical bond between the intergrowing crystals. Finally, calcium hydroxide crystals found to grow preferentially around aggregate particles in the plain OPC mixes (170) were replaced by C-S-H in the CSF mixes. This improves the bond between paste matrix and aggregate and increases the strength fraction derived from the aggregate-cement paste matrix bond.

Similar results were observed for the plain and CSF concrete mixes grade C25 & C55 (see Figures A1.1 and A1.2 in Appendix 1).

8.5.1.2 Effect of curing method

(1) Plain OPC mixes

The effect of the water and polythene curing method on compressive strength of plain OPC concrete mixes grade C25, C40 & C55 is shown in Figure 8.2. At early ages (3 and 7 days), results show that concrete specimens cured by sealing them with polythene sheets for seven days yielded a comparable compressive strength to those water cured. This shows clearly that partial drying by self dessication had

very small effect on the hydration rate of cementitious material at early-ages. Moreover, polythene sealing at early ages helps to retain the moisture inside the concrete specimens. This was undoubtedly beneficial to the early age hydration and strength gain. At 28-days, although the compressive strength of polythene cured specimens was lower than those water cured, the difference between them was statistically insignificant. At later-ages (180 days) the compressive strength of polythene cured specimens was generally lagging behind the water cured ones. Such behaviour and trend has been reported and explained before by Powers (110). He suggested that hydration can only take place in the capillary water filled spaces where the relative water vapour pressure is above 80-90% of saturation pressure. Therefore the amount and rate of hydration of cementitious material is restricted by the partial drying caused by evaporation and/or self-desiccation. Partial drying starts affecting the polythene cured specimens from the beginning, whereas, it affects the water cured ones only after 7 days. Therefore the relative capillary water vapour pressure is expected to fall down faster in the polythene cured specimens than in the water cured ones. Eventually reaction rate and final compressive strength may be relatively lower in the polythene cured specimens.

The difference in the later-age compressive strength between the polythene and water cured concrete specimens was found to be a function of W/C ratio, cement content and paste matrix volume. The lower the W/C ratio and the higher the cement content and paste volume the greater will be the difference in compressive strength (Figure 8.2). This behaviour can possibly be explained by the fact that the plain concrete mixes were designed for equivalent workability and water content. Therefore partial drying by evaporation and self-dessication is expected to result in a relatively higher amount of unhydrated cement particles in the rich mix (concrete grade C55) compared to the lean mix (concrete grade C25). The higher the relative amount of unhydrated cement

left in the matrix the more porous and less dense it is and the lower the compressive strength is.

(11) CSF mixes

Due to similarity in test results between the concrete grade C25, C40 and C55, discussion will be based on the test results of concrete grade C40. Test results of concrete grade C25 and C55 are shown graphically in Figures A1.3 & A1.4. in Appendix 1.

The effect of curing method on the compressive strength of CSF concrete mixes grade C40 is shown in Figure 8.3. Test results shown in this figure indicate that the effect of polythene and water curing on the compressive strength of CSF mixes is similar to that previously seen with plain OPC mixes, i.e. at early-ages the compressive strength of polythene cured specimens was similar to that of those cured under water. At later-ages the compressive strengths of polythene cured specimens lagged behind the identical specimens cured under water. The reasons for this behaviour have been discussed earlier.

Test results also show that the effect of polythene curing on compressive strength in comparison to water curing is only noticeable in concrete mixes grades C40 & C55. The compressive strengths of polythene and water cured concrete mixes grade C25 were comparable (see Figure A1.3 Appendix 1).

8.5.1.3 Effect of curing environment

(1) OPC concrete

The effects of simulated Iraqi hot and U.K. temperate environments on the compressive strength of plain concrete mixes grade C25, C40 & C55 are shown in Figure 8.4. Results show that hot curing environments increase the early-age (3 & 7 days) compressive strength. However, at later-ages (28-180 days) the situation was found to reverse. Specimens cured under temperate environments exhibited later-age compressive strength in excess of those cured under hot environments. This trend has been found and reported by many researchers. For example Klieger (80) showed that OPC concretes cured for

seven days at 45°C before curing at 20°C to an age of 28 days were about 15% weaker than similar samples cured for 28 days at 20°C. Other researchers such as Shalon and Ravina (74), PCA Bulletin (96), Bloem (97), Gynor et al (98), Verbeck & Helmuth (91), Ridgley (99) and Price (92) have also reported a similar trend (see Chapter 3). However, these late-age test results disagree with other researchers who believe in the continuing beneficial effect of high curing temperature on the late-age as well as the early-age compressive strength. For example Abassia and Alam (93) studied the effect of a controlled hot environment of 45°C and a field hot environment of 40°C on compressive strength in comparison to moderate lab conditions of 24°C. Their results showed that concrete cured in a hot environment can have at least the same strength at 28 days as that cured under moderate temperature. This trend was also supported by other researchers such as Berhane (94) & Jaegerman and Gluklich (95).

The possible explanation for this behaviour is given by the model illustrated in Chapter 5. The model suggests that high curing temperature accelerates the early-age hydration and strength gain. However, because of their low solubility and low diffusibility, the cement hydration products cannot diffuse to any significant distance from the surface of the hydrating cement within the relatively shorter time allowed by rapid hydration. Consequently a high concentration of the hydration products builds up in the vicinities immediately surrounding cement grains. These hydration products may be converted by the effect of heat to crystalline, dense, low surface area product forming an encapsulating layer. In the course of time this encapsulating layer is expected to retard any subsequent hydration. Secondly,, the hydration process accelerated by high curing temperature may cause the rapid formation of short-fibred calcium silicate hydrate as suggested by the model (see Chapter 5). These short fibres may restrict the development of long-fibres and result in a poorly interconnected structure.

Under temperate curing environments, there is ample time for the hydration products to diffuse and precipitate away from the hydrated cement grains. This can allow longer hydration to take place and a uniform precipitation of hydration products. Eventually the compression strength of concrete specimens under such temperate environments is expected to be higher than that of those cured under hot environments.

Results show that the harmful effect of high curing temperature on the later-age compressive strength is a function of W/C ratio, cement content and paste matrix volume (see Figure 8.5). In fact hot curing environments have been found to have higher later-age detrimental effect on the compressive strength of rich mixes than on that of lean mixes. For example the late age (180 days) compressive strength of concrete mixes grade C25 (W/C = 0.8), C40 (W/C = 0.63) and C55 (W/C = 0.46) cured under hot environment were about 10, 13 and 19% weaker respectively than similar specimens cured under temperate environment. A possible explanation for this behaviour suggests that under temperate curing environments cement hydration rate is higher in the rich mixes than in the lean mixes. With a high curing temperature, the hydration rate of rich concrete mixes will increase still further.

This can result in a higher precipitation rate of hydration products in the vicinity close to the hydrating cement particles. The hydration process is expected to last for a shorter time in the rich mixes than in the lean mixes. Eventually the relative amount of unhydrated cement particles left in matrix will be higher in the rich mixes than in the lean ones. The higher the relative amount of unhydrated cement particle the poorer the paste matrix and the higher the detrimental effect of high curing temperature on late-age compressive strength.

(ii) CSF mixes

Due to similarity in test results of the three concrete grades C25, C40 & C55, discussion will be based on

test results of CSF concrete mixes grade C40. The effect of curing temperature on the compressive strength of CSF concrete mixes grade C25 & C55 is shown graphically in Figures A1.5 & A1.6 in Appendix 1.

The effect of curing temperature on the compressive strength of CSF concrete mixes grade C40 is shown in Figure 8.6. The CSF concrete specimens cured under elevated curing temperature showed a different trend from the plain OPC concrete mixes. It is quite obvious from Figure 8.6 that curing CSF concrete specimens under hot environments is favourable to both early and late-age strength. For example the increases in compressive strength of mix C40/10/7P.H above mix C40/10/7P.T at 3, 7, 28, 90 and 180 days are 72, 47, 20, 21, and 25 percent respectively. A possible explanation for this behaviour is offered by the model illustrated in Chapter 5. The model suggests that high curing temperature initially accelerates the hydration of OPC particles, which consequently accelerates the pozzolanic reaction between $Ca(OH)_2$ produced by OPC hydration and CSF. The high surface area of silica fume has the advantage of providing more sites favourable to the precipitation of C-S-H gels, and thus the presence of high surface area CSF will improve the dissipation of hydration products away from the cement grains, allowing relatively uniform precipitation of hydration products. On the other hand the presence of CSF has the effect of promoting the continuation of OPC grain hydration. Thus hydration of both OPC and $Ca(OH)_2$ with CSF will continue at a higher rate for a relatively longer time compared with the reference plain OPC cured under the same environment. Since hydration can only take place in the capillary water filled pores, hydration of CSF concrete mixes is expected to last longer than that of the reference plain OPC mix due to the physical effect of CSF in the fresh paste matrix followed by its chemical effect in the mature matrix. These two effects help retain the necessary moisture for hydration inside the matrix and prevent any pronounced water evaporation likely to take place under the effect of high curing temperature. The CSF physical effect can be viewed as

a "densifying effect" in the sense that the extremely fine CSF particles added tend to accomodate themselves in the empty spaces between cement grains. Hundreds of CSF particles have been found to be positioned between two cement grains (Figure 8.7). The presence of these fine particles between cement grains can narrow or even close some of the water flow channels in the fresh state. The CSF chemical effect can be viewed as the "pozzolanic effect" explained earlier. The high volume and surface area of C-S-H may fine the capillary pores or even block them. The combination of these two effects is expected to reduce the amount of free capillary water lost to the outside by evaporation and hence allow hydration to continue for a longer period.

8.5.1.4 Effect of CSF content

Due to similarity in test results between the three concrete grades C25, C40 and C55, discussion will be based on CSF concrete grade C40. Test results for the other concrete grade are shown graphically in Figures A1.7 & A1.8 in Appendix 1.

The effect of CSF content on the development of compressive strength of concrete grade C40 is shown in Figure 8.8. Test results indicate that regardless of the curing method and environment, the later-age compressive strength of CSF concrete is higher the higher the CSF content up to 10%. The same trend was noticed in concrete mixes grade C25 and C55. At a replacing percentage of 15% by weight of OPC, CSF concrete mixes (C40/15/7WT) & (C40/15/7P.T) exhibited compressive strength lower than concrete mixes (C40/10/7W.T) and (C40/10/7P.T) in which only 10% of CSF was used. This was attributed to the presence of surface cracks noticed on the specimens of CSF concrete mixes C40/15/7W.T and C40/15/7P.T. These surface cracks may counteract any improvements expected to take place in the core. These surface cracks were drying shrinkage cracks. Since moisture loss is the underlying cause of drying shrinkage, high water content demanded by the high CSF content concrete mix (C40/15) seems to increase comparatively the amount of

moisture loss by evaporation and eventually the magnitude of drying shrinkage. This can be proved by comparing CSF concrete mix (C40/15) in which workability was secured by adding extra water and CSF concrete mix (C40/155) in which workability was secured by using superplasticizer without altering the amount of mixing water. Surface cracks noticed in the former mix did not appear in the latter.

This confirms that higher moisture loss from concrete mix C40/15 compared to C40/155 resulted in a comparatively higher surface drying shrinkage magnitude. This surface drying shrinkage was restrained by the core. Consequently induced tensile stresses were set up in the surface region. According to Neville (36), these induced tensile stresses must exceed the tensile strength to cause surface cracks (see Figure 8.9). Nevertheless, it is important to report that specimen geometry can play an important role in the drying shrinkage rate and magnitude. Specimen geometry relates to both size and shape of concrete elements. Thus it can be well defined by the volume-to-surface area ratio. The smaller the ratio, the higher is the water loss from the surface and the greater are the drying shrinkage magnitude and induced tensile stresses. Thus it is possible that the specimen size used (100mm cubes) enhances drying shrinkage and increases the probability of having these surface cracks.

The surface cracks noticed in the CSF concrete mixes (C40/15/7W.T) & (C40/15/7P.T) cured under the temperate environment were not present in the identical mix (C40/15/7P.H) cured under a hot environment. The possible reasons for this behaviour are listed below:

1. High curing temperature increases the rate of moisture loss from the concrete surface and thus increases the initial rate of drying shrinkage taking place. This initial rate of drying shrinkage has its effect on the ultimate shrinkage magnitude. The faster the initial rate of drying shrinkage, the lower the magnitude of shrinkage at late time. Thus, it seems that high curing temperatures enhance the initial rate of shrinkage and yield a lower ultimate shrinkage value.

2. High curing temperature accelerates the rate of hydration and improves the tensile strength of CSF concrete mixes.
3. At the time that the concrete surface is subjected to tensile stresses, the wet core is subjected to compressive stresses under which concrete will creep. This creep is expected to relieve the induced surface tensile stresses gradually. High curing temperature up to 70°C were found to enhance creep of concrete specimens according to Neville (36).

The combined effect of the above three elements may reduce the magnitude of shrinkage and induced tensile stresses and on the other hand increase the tensile strength of CSF specimens.

In spite of not having any surface drying shrinkage cracks on the surface of CSF concrete specimens (C40/15) cured under hot environment, the improvement in compressive strength achieved from increasing the CSF content from 10 to 15 percent is negligible. The optimum CSF content based on compressive strength test results appear to be around 10 percent.

8.5.1.5 Effect of superplasticizer

As described earlier, the workability of CSF concrete mixes were obtained by two means: either by increasing water content or by using a superplasticizer admixture. The effect of using superplasticizer on the compressive strength of CSF mixes cured by different methods and environments in comparison with the identical mix in which workability was secured by adding extra water is shown in Figure 8.10. Compressive strength test results show the superiority of superplasticized concrete mixes over the non-superplasticized ones. It is obvious from the Figure that using superplasticizer has the effect of increasing the rate of cementitious material hydration which consequently results in a higher later-age-strength. This higher rate of hydration may possibly be caused by the good dispersion of cementitious particles brought about by the use of superplasticizer.

Moreover, there is an inverse relationship between strength and water/cementitious ratio. Therefore, the increase in compressive strength of superplasticized concrete mixes may also possibly be caused by the lower water/cementitious ratio of superplasticized mixes compared with the non-superplasticized ones.

8.5.1.6 Effect of initial curing duration

The effect of initial polythene curing duration on the compressive strength of plain OPC (C40/0) and CSF (C40/10) concrete mixes was examined under both temperate and hot environments. The initial curing duration lasted for 0, 1, 3 and 7 days. Results are presented graphically in Figures 8.11 and 8.12.

With regard to the influence of curing duration on the compressive strength of plain OPC concrete mixes cured under temperate environment, results seem to agree with those of Popovics (171). Test results from this study indicate that initial curing duration up to seven days had a significant effect on the strength. The 180-days compressive strengths of uncured, one, and three days cured OPC concrete cubes were 48%, 29% and 13% weaker respectively than the 7 days cured samples. Thus results indicate that under temperate environment, longer initial curing duration results in a significant compressive strength gain. Under hot curing environments, results show that initial curing duration up to 3 days can significantly effect the strength gain. For example, the 180-days compressive strengths of uncured, one and three days cured OPC concrete cubes were 50%, 29% and 5% weaker respectively than the 7 days cured specimens. Thus results indicate the existence of a critical initial curing period of 3 days under hot environment.

The CSF concrete mix (C40/10) result shows that there was no significant difference in compressive strength between specimens cured initially for 3 to 7 days under temperate environment. Moreover curing these identical specimens

initially beyond one day under hot environment brings about no significant change in the compressive strength from thosecured initially for 3 and 7 days. Thus results indicate the existence of a critical initial curing period of 3 days and 1 day under temperate and hot curing environments respectively, for this silica fume concrete mix.

Test results for both plain OPC and CSF indicate that CSF concrete is less sensitive to the initial curing duration than plain OPC. Once more the physical effect of CSF (viewed as a "densifying effect" in the fresh state) and the chemical effect (viewed as a "pozzolanic effect" in the mature hardened state) described earlier and helped in retaining the moisture necessary for pursuing hydration inside the paste matrix thus reducing water evaporation caused by the effect of high temperature. As a result of this behaviour, sensitivity to the initial curing duration is expected to be reduced in the CSF concrete mixes compared to the plain OPC ones.

Finally, the sharp change in compressive strength results caused by one day curing reveals the importance of curing concrete specimens initially for the first day after casting.

8.6 Permeability and absorption related properties

Permeability and absorption tests were carried out on plain OPC and CSF concrete specimens cured by water and polythene under temperate and hot environments. These tests are listed in 8.4 and described in Chapter 6.

The general trend of test results show that permeability and absorption properties of both plain and CSF concrete mixes can be divided into two groups. The first concerns the permeability properties of subsurface concrete or "subsurfacecrete". The second concerns the permeability and absorption properties of surface concrete or "surfacecrete". Accordingly presentation and discussion of test results will focus on the effect of curing method and environment, CSF content and initial curing duration on the

permeability and absorption properties of the subsurfacecrete and surfacecrete.

8.6.1 Permeability of subsurfacecrete

The air and water permeability of plain OPC and CSF subsurfacecrete was examined by means of the Figg air and water test method described in Chapter six. The statistical analysis performed on the test result shows that the coefficient of variation between test results of nominally identical specimens is within 20% and 15% for the Figg air and water permeability test results respectively.

Due to similarity in test results between the three concrete grades C25, C40 and C55, discussion will be based on the test results of concrete mixes grade C40 with reference to the other grades in case of differences.

8.6.1.1 Effect of age

The effect of age on the Figg air and water subsurfacecrete permeability of plain and CSF concrete mixes is shown in Figures 8.13 and 8.24.

In all plain and CSF concrete mixes, air and water permeability decreases with age. The rate of reduction in subsurfacecrete permeability is high at early ages and gradually decreases at later-ages; this behaviour was expected. Subsurfacecrete air and water permeability is directly related to the permeability of the paste matrix, and therefore it varies with the progress of hydration. As hydration progresses with time, hydrated gel gradually builds up inside the original capillary water filled spaces. This reduces their sizes or even block them depending on the degree of hydration and locality of hydration products. Since air and water flow more easily through coarse capillary pores than through fine ones air and water permeability will be lower in mature specimens than the immature ones.

Results on all CSF concrete mixes show that the subsurfacecrete air and water permeability continue to decrease at a higher rate when compared to the plain OPC mixes. This higher rate of reduction in air and water

permeability may possibly be caused by the physical effect i.e. "densifying effect", and the chemical effect, i.e. "pozzolanic effect", of CSF explained earlier.

Similar results were found when testing CSF concrete mixes grade C25 & C55, (see Figures A1.9, A1.10, A1.17 and A1.18 in Appendix 1).

8.6.1.2 Effect of curing method

i. Plain OPC concrete

The effect of water and polythene curing method on the Figg air and water permeability is shown in Figures 8.14 and 8.25. Generally, test results show that the subsurfacecrete air and water permeability of polythene cured specimens is higher than that of those cured by water. The difference in air and water permeability between the polythene and water cured concrete specimens was found insignificant in lean and medium concrete mixes grades C25 & C40. The above difference was found noticeable in rich concrete mix grade C55. This reveals that partial drying by self-dessication is only effective in rich concrete mixes which have a W/C ratio below 0.5. Such a finding was reported by Powers (110). He found that hydration of sealed cured specimens can proceed to the point where the non-evaporable water has become about one-half the original water content. The capillaries will have become empty and hydration will have ceased. Therefore full hydration of cement in a sealed specimen cannot occur unless the original water content is at least double the non-evaporable water. His test results show that for an average cement the value of the non-evaporable water/cement ratio is about 0.25. Therefore full hydration of a sealed cured specimen can occur if the water/cement ratio is about 0.5.

ii CSF concrete

The effect of the water and polythene curing method on the air and water permeability of CSF concrete specimen is similar to that noticed with plain OPC concrete specimens. Generally the air and water permeability of polythene cured

specimens is higher than that of those cured by water. See Figures 8.15 & 8.26. Results also show that the rate of reduction in air and water permeability of polythene cured specimens is lower than that of water cured. These lower rates and higher permeabilities of the polythene cured specimens compared with the water cured ones can possibly be explained by the fact that partial drying by self-dessication will lower the water vapour pressure inside the capillary pores. This may consequently lower the chemical activity of the water causing a comparatively lower rate of hydration which means a lower rate of permeability reduction resulting eventually in higher permeabilities. Test results show that the deviation between the permeability (air and water) of water and polythene cured specimens are marginal in concrete mixes grade C25 and C40. However, in richer CSF concrete mixes (grade C55) the deviation described above is more noticeable, compared to the lean mixes (See Figures A1.11, A1.12, A1.19 and A1.20 in Appendix 1.) One possible explanation for this behaviour is that the amount of OPC and CSF left unreacted in the paste matrix by the effect of the low rate of hydration is comparatively higher in the rich mixes than in the lean ones. Thus hydration products produced under such circumstances will comparatively not be sufficient to produce a fine discontinuous pore system. Deviation in air and water permeability between the water and polythene cured specimens will be higher in the rich mixes than in the lean mixes.

8.6.1.3 Effect of curing environment

i Plain OPC concrete

The effect of curing temperature on the Figg air and water subsurfacecrete permeability is shown in Figures 8.16 and 8.27. Results show that generally high curing temperature reduces the early age permeability. At late-ages, air and water permeability were higher in specimens cured under hot environments than in those cured in a temperate one. Higher late-age air and water permeabilities caused by the high curing temperature may possibly be

explained by the poor diffusion and non-uniform precipitation of hydration products produced at early-ages, which consequently may retard any subsequent hydration at later-ages. Therefore the amount of gel produced by cement hydration under high temperature will be lower than that produced under temperate environment. Since these gel products are deposited in the capillary water filled spaces, the paste matrix of concrete specimens cured under hot environment may contain a coarser and better interconnected capillary pore system than that established in the paste matrix of the identical specimens cured under temperate environments. This explanation agrees with the possible microstructure changes brought about by the effect of high curing temperature suggested by the established model (see Chapter 5).

Test results indicate that the degree to which high curing temperature may affect the subsurfacecrete air and water permeability seems to be a function of W/C ratio, cement content and paste matrix volume. (See Figures 8.17 & 8.28). The higher the cement content, the greater is the harmful effect of hot curing on air and water permeabilities. For example the late-age (180 days) air and water permeabilities of concrete grades C55, C40 & C25 were increased by 19, 15 and 7 percent and 18, 16 and 11 percent respectively. Thus high curing temperatures seem to have a negligible detrimental effect on the subsurfacecrete air and water permeability of lean OPC mixes. However, the same curing temperature had a more pronounced detrimental effect on the air and water permeability of the richer concrete mixes. One possible explanation of this behaviour is as follows: since the three concrete mixes have a comparable water content, temperature is expected to have a more or less comparable effect on water evaporation. Therefore the relative amount of unhydrated cement left in the paste matrix is expected to be higher in the rich mixes than in the lean mixes. This rich paste matrix is expected to have a relatively coarser pore system than the lean one.

ii CSF concrete mix

Due to similarity in test results between the three concrete grades, discussion will be based on concrete grade C40. Test results of other concrete grades are shown graphically in Figures A1.13, A1.14, A1.21, and A1.22 in Appendix 1.

The effect of curing temperature on the subsurfacecrete air and water permeabilities of concrete grade C40 is shown in Figures 8.18 and 8.29. Results show that an advantageous behaviour, as far as the hot Iraqi environment is concerned, was seen when CSF was partially substituted for OPC. Figg air and water permeability results of CSF concrete mixes show a different trend from those of COP concrete mixes. High curing temperature reduces the air and water permeability at early and later-ages. For example the subsurfacecrete air permeability of concrete mix C40/15/7P.H was lower than that of C40/15/7P.T by 64 and 23 percent at 14 and 180 days. The subsurfacecrete water permeability of CSF mix C40/15/7P.H was lower than that of mix C40/15/7P.T by 66 & 26% at 14 and 180 days. Explanation for this behaviour is offered by the model described in Chapter 5 which suggests that at early ages high curing temperature will accelerate the ordinary hydration of OPC and the pozzolanic hydration taking place between $Ca(OH)_2$ and CSF. Hydration products produced by both reactions will accumulate in the capillary pores reducing their size and blocking some of the air and water flow channels depending on their quantity and precipitation locality. This will eventually reduce the air and water permeabilities at early-age. Because of their extreme surface area, CSF particles will provide more sites which are favourable to the precipitation of C-S-H gels. This can obviously improve the diffusion of hydration products away from cement grains, allowing on one hand a uniform precipitation of hydration products and on the other hand the continuation of hydration of both OPC and CSF particle. The uniform precipitation will offer better pore segmentation which will consequently narrow down or even block some of the air and water flow channels.

The continuation of hydration has the effect of furnishing the matrix with more C-S-H which will improve the pore refining and segmentation process. Finally a CSF paste matrix cured under a hot environment is expected to have a higher percentage of fine gel pores at later-ages than those cured under a temperate environment.

8.6.1.4 Effect of CSF content

Due to similarity in test results between concrete grades C25, C40 & C55, discussion will be based on test results of concrete grade C40 shown in Figures 8.19 & 8.30. Test results of concrete grade C25 & C55 are shown graphically in Figure A1.15, A1.16, A1.23 and A1.24 in Appendix 1.

Results show that regardless of the curing method and environment, Figg air an water subsurfacecrete permeabilities were decreased with increasing percentage of CSF. What is clear from Figures 8.19 and 8.30 is that CSF is far more effective in reducing the air and water permeabilities under a hot curing environment compared to the temperate environment. This high reduction in air and water permeabilities was accomplished as a result of two counteracting effects of high curing temperature on the late-age permeability of reference plain OPC and CSF mixes. At that time curing temperature increases the late-age air and water permeabilities in the reference plain OPC mixes it decreases them in the CSF concrete mix. As a result the difference in air and water permeabilities between OPC and CSF mixes is increased, i.e. there is a very significant reduction in the CSF air and water permeabilities.

Results also show that CSF is more effective in reducing the air and water permeabilities in the lean mixes compared to the rich mixes (see Figures 8.20 & 8.31). This behaviour can be explained by the fact that hydration products (gel products) occupy a volume of approximately 2.1 times that of unhydrated cement grains (36) (this space includes gel pores). Thus for cement grains totalling one cubic centimetre, not less than 2.1 cubic centimetres of

water filled spaces are required in the fresh paste simply to provide room necessary for housing hydration products. A simple calculation illustrated in Appendix (2) shows that this amount of water per unit volume of cementitious material corresponds to 1.6 gram of cementitious material per gram of water. Therefore the amounts of water filled spaces necessary for full hydration required in the fresh mixes (C25/10) and (C55/10) are 145 and 259 kg respectively. Comparing these amounts with the actual mixing water used reveals that there is ample room in the lean mix (C25/10) for housing all hydration products even if the maximum degree of hydration is achieved. However, in the rich mix there is not enough room for housing all the hydration products. Consequently the hydration reaction will reach a saturation level and stop before hydrating all the OPC & CSF grains, i.e. the full benefit from all the CSF grains will not be attained.

8.6.1.5 Effect of superplasticizer

The effect of securing the workability in concrete mix C40/15 by either adding extra water or using superplasticizer on the Figg air and water permeability is shown in Figures 8.21 & 8.32 respectively. Test results reveal the superiority of superplasticized CSF concrete mix over the non-superplasticized one, i.e. Figg air and water permeability of superplasticized CSF mixes was lower than the non-superplasticized under the effect of different curing methods and environment. These lower permeabilities are possibly caused by the combined effect of superplasticizer on the dispersion of cementitious particles and the water/cementitious ratio. Good dispersion of cementitious products can result in a good and uniform distribution of hydration products resulting from both OPC and CSF hydration. This uniform deposition of hydration products can result in a more efficient blocking of the air and water flow channels, resulting in lower permeabilities. A lower W/C + CSF ratio can help in reducing the percentages of the coarse capillary pores. Therefore the use of superplasticizer can have a

significant effect on the paste matrix pore structure. In other words superplasticizers have an effect on the fraction of the fine gel pore and the coarse capillary pores, i.e. superplasticizer may increase the fraction of the former at the expense of the latter.

8.6.1.6 Effect of initial curing duration

The effects of the initial curing duration period on the Figg air and water subsurfacecrete permeabilities of plain OPC (C40/0) and CSF (C40/10) concrete mixes cured under both temperate and hot environment are shown in Figures 8.22, 8.23, 8.33 and 8.34 respectively.

i Plain OPC

Under temperate curing environment, results shown in Figures 8.22 & 8.33 indicate that increasing the initial curing duration up to 7 days produces lower air and water permeabilities. Results of this nature are expected, since a longer curing period results in a greater degree of hydration. This higher degree of hydration has the effect of reducing the total porosity and increases the probability of the pores being either blocked or narrowed down. This trend has been found by other researchers including Nyame (172), who shows that the decrease in permeability of plain OPC mixes was improved with long curing period and hydration. A similar effect was also reported by Goto and Roy (101).

Under the effect of hot environment, results indicate that curing specimens initially up to 3 days can effectively reduce air and water permeabilities. However, extending curing duration for another four days does not bring about any effective reduction in the air and water permeability. This is obviously caused by the high rate of reaction resulting from higher curing temperature. Results, therefore, suggest that a critical initial curing duration of 3 days exists when conditioning OPC mixes under a hot environment.

ii CSF mixes

Under a temperate curing environment results show no significant difference in air and water subsurfacecrete permeabilities between identical CSF concrete mixes cured initially for 3 and 7 days. Results of curing CSF mixes under hot environments indicate that a critical curing period of one day exists, i.e. curing CSF concrete specimens initially for a period longer than one day does not reduce the air and water subsurfacecrete permeabilities significantly.

Results indicate that CSF concrete mixes cured under both environments show less sensitivity to the initial curing duration compared to the plain OPC mix. This behaviour is believed to be caused by the CSF physical and chemical effect viewed as a "densifying effect" and a "pozzolanic effect" respectively. These two effects have been illustrated previously. The two effects helped in retaining the moisture inside the CSF specimens and reduced the effect of water evaporation enhanced by high curing temperature.

8.6.2 Permeability and absorption properties of subsurface

The air permeability and water absorption of plain OPC and CSF surface-crete was examined by Egg air permeability, initial surface absorption (ISA) and water absorption test method described in Chapter six. The statistical analysis performed on the test results from all these methods shows that the coefficient of variation between test results of nominally identical specimens is within 10%.

There was general similarity in the test result trend between concrete mixes grades C25, C40 and C55. Thus discussion will be based on the test results of concrete mixes grade C40.

8.6.2.1 Effect of age

The effect of age on the Egg air, absorption and ISAT results of plain OPC and CSF concrete mixes are shown in Figures 8.35, 8.46 and 8.57 respectively.

Apart from concrete mix (C40/15) whose behaviour will be discussed later the effect of age on the surfacecrete permeability and absorption properties is similar to that on the subsurfacecrete permeabilities. Therefore the previous discussion holds true in this section,

Similar test results were accomplished from examining plain and CSF concrete mixes grade C25 and C55, (see Figures A1.25, A1.26, A1.33, A1.34, A1.41, and A1.42 in Appendix 1).

8.6.2.2 Effect of curing method

i Plain OPC concrete

The effect of the water and polythene curing methods on the permeability and absorption properties of surfacecrete is shown in Figures 8.36, 8.47 and 8.58. Test results in general reflect the superiority of water curing over the polythene curing in reducing the air permeability and water absorption of surfacecrete. Unlike the subsurfacecrete air and water permeability results, the surfacecrete air permeability and absorption results show that lean OPC concrete (C25) is more sensitive to the effect of water and polythene curing than the richer concrete mixes (C40 & C55). For example the later-age (180 days) initial surface absorption of concrete mixes (C25/0), (C40/0) and (C55/0) cured by polythene was higher than of those cured under water by 18%, 13% and 8% respectively. The probable reason behind this behaviour seems related to the rate of OPC hydration and drying by evaporation taking place in the surface region. The hydration process and its rate is a function of cement content, fineness and temperature. As far as the content is concerned the higher the cement content the higher the rate of hydration. Thus hydration rate is higher in the rich concrete mix (C55/0) than in the lean mix (C25/0). Consequently a higher amount of gel will be deposited in the surfacecrete capillary pores of rich mixes which helps either

to block or narrow them down in a comparatively shorter time. Surface free water evaporation from the capillary pores will be lower in the rich mixes compared with the lean mixes. Since hydration can only take place in the capillary water filled spaces, hydration is expected to cease sooner in the lean mixes, leaving the surface with a coarser and probably better interconnected pores compared with the rich mixes.

ii CSF concrete mixes

The effect of water and polythene curing on the air permeability and water absorption properties of CSF concrete mixes grade C40 is shown in Figures 8.37, 8.48 & 8.59.

Test results of all CSF concrete mixes show that water cured specimens have lower permeabilities and water absorption values than those cured with polythene sheets. However, the difference in air permeability and absorption results between the water and polythene cured specimens is not significant. This behaviour may once again be attributed to the physical and chemical effects of CSF described earlier. Thus the presence of CSF reduces the rate and amount of water loss by evaporation from the capillary pores in the surface region, allowing for more and longer hydration to take place. Results may also indicate that the similarity in permeability and absorption test results between the water and polythene cured specimens reflect the similarity in pore volume and distribution in the surface region between identical CSF concrete specimens cured by water and polythene.

Similar results were achieved from testing CSF concrete mixes grades C25 and C55. Test results are shown in Figures A1.27, A1.28, A1.35, A1.36, A1.43 and A1.44 in Appendix 1.

8.6.2.3 Effect of curing environment

i OPC mixes

The effect of curing environments (hot and temperate) on the air permeability and absorption properties of surfacecrete mixes grade C25, C40 and C55 is shown in Figures

8.38, 8.49 & 8.60. Test results show that a hot curing environment has adversely affected the surfacecrete air permeability and absorption properties of plain OPC concrete specimens. The magnitude of this later-age adverse affect was found again to be a function of W/C ratio, cement content and paste matrix volume. The reason for this behaviour has been explained previously. An attempt was made to compare the later-age harmful effect of high curing temperature on the subsurfacecrete permeabilities and the surfacecrete permeability and absorption properties on the basis of calculating the percentage increase in later-age permeability and absorption caused by high curing temperature. Results indicate that the surfacecrete permeability and absorption are more harmfully affected by high curing temperature than the subsurfacecrete permeabilities. For example the later-age subsurfacecrete air permeabilities of concrete mix (C55/0) cured under a hot environment were higher than those cured under a temperate environment by 19 percent. However, surfacecrete initial surface absorption of the same identical mix was increased by 26 percent. This trend was expected since high curing temperature accelerates water evaporation from the surface layer more than the subsurface layer. Therefore, hydration tends to cease in the surface region sooner than in the subsurface region leaving concrete surface or surfacecrete with higher total porosity compared to the subsurfacecrete in which hydration is expected to last for a longer period. This agrees with the findings of Abrams and Orals (114). They concluded that drying caused by surface water evaporation can only affect a thin layer of concrete skin. Once again the effect of high curing temperature on permeability and absorption was found to be a function of W/C ratio and cement paste matrix volume, see Figures 8.39, 8.50 and 8.61. This behaviour has been explained earlier.

ii CSF concrete mixes

The effect of curing temperature on the surfacecrete permeability and absorption properties of concrete mixes grade C40 is shown in Figure 8.40, 8.51 and 8.62. Test

results of other concrete grades C25 & C55 are shown graphically in Figures A1.29, A1.30, A1.37, A1.38, A1.45 and A1.46 in Appendix 1.

Unlike the permeability and absorption properties of plain OPC concrete mixes, CSF concrete mixes show a completely different trend. Test results indicate that hot curing temperature was favourable to both early and late-age surfacecrete permeability and absorption properties. The reason for this behaviour has been given previously.

8.6.2.4 Effect of CSF content

The effect of CSF content on the surfacecrete air permeability and absorption properties of concrete grade C40 is shown in Figures 8.41, 8.52 and 8.63. Results of other concrete grades are shown graphically in Figures A1.31, A1.32, A1.39, A1.40, A1.47, and A1.48 in Appendix 1.

Under temperate environments test results indicate that increasing CSF content up to 10% by weight of OPC was accompanied by a reduction in the surfacecrete air permeability and water absorption. The higher the percentages of CSF used up to 10%, the lower are the surfacecrete air permeability and absorption values. However, the beneficial effects noticed above from using CSF were ruined when CSF content was increased to 15%. The surfacecrete air permeability and water absorption of CSF mix (C40/15/7W.T) and (C40/15/7P.T) are higher than for CSF mixes (C40/10/7W.t) and (C40/10/7P.T). This increase in air permeabilities and water absorptions was due to the presence of drying shrinkage surface cracks. The presence of these surface cracks obviously counteracts any improvement possibly brought by increasing CSF content. The possible reason for these surface cracks has been explained earlier. Surprisingly, the surface cracks noticed in the high CSF content mix (C40/15) cured under a temperate environment did not appear when the same identical concrete specimens were cured under hot environments. The possible reasons behind this behaviour has been discussed earlier. However, the reduction in surfacecrete air permeability and water

absorption brought about by increasing CSF content from 10 to 15 percent was marginal.

Test results also show that CSF is more effective in lean mixes than rich mixes (see Figure 8.42, 8.58 & 8.64). This behaviour has been explained earlier.

8.6.2.5 Effect of superplasticizer

The effect of using superplasticizer to secure the workability in CSF concrete mix (C40/15) without the need for adding extra water on the surfacecrete air permeability, absorption and ISA is shown in Figures 8.43, 8.54 and 8.65 respectively.

Under a temperate curing environment, test results shown graphically indicate that the use of superplasticizer reduces the permeability and absorption properties very significantly compared to those in which workability was secured adding extra water. The reason behind that is that the surface drying shrinkage cracks noticed in concrete mix (C40/15) did not appear in mix (C40/155). This may possibly indicate that the drying shrinkage which took place in concrete specimens of mix (C40/155) is lower than that which took place in concrete specimens of mix (C40/15). The decrease in the drying shrinkage magnitude of superplasticized CSF concrete mixes was due to the reduced water content and the increased degree of hydration and the amount of formed hydrated gel.

Under a hot curing environment, results also reveal the superiority of superplasticized concrete mixes in reducing the surfacecrete permeability and absorption properties compared to the non-superplasticized. The reason behind this behaviour has been given earlier.

8.6.2.6 Effect of initial curing duration

1. OPC concrete

The effects of different initial curing duration on the surfacecrete air permeability and absorption properties are shown in Figures 8.44, 8.55 and 8.66.

In a temperate environments, the results show that increasing the initial curing duration for up to 7 days results in lower surfacecrete air permeabilities and water absorption values. Results therefore are similar in trend to those of subsurfacecrete air and water permeabilities in which no clear critical curing period is noticed. These results agree with those confirmed by Payne and Dransfield (175). Similar results were also found when the same identical concrete specimens were conditioned under hot environments i.e. longer initial curing duration up to 7 days had resulted in lower absorption and permeability.

ii. CSF mixes

The effect of initial curing duration on the air permeability and absorption properties of CSF mixes under hot and temperate environments is shown in Figures 8.50, 8.56 and 8.67.

Under both temperate and hot environments, test results show that curing concrete specimens for up to three days can significantly affect surfacecrete air permeability and water absorption. However, no significant difference in the surfacecrete air permeability and water absorption was noticed between the identical concrete specimens cured for 3 and 7 days. Thus results suggest that a critical curing duration of 3 days exists.

Results indicate that CSF concrete mixes cured under hot and temperate environments show less sensitivity to the initial curing duration compared to the plain OPC mixes. This behaviour has been explained earlier.

8.7 General discussion

8.7.1 Variability of test result

The statistical analysis performed on test results of different durability related properties, i.e. permeability and absorption properties, indicate that the coefficient of variation of Egg air permeability, absorption and ISA test results were all within 5 to 10%. Whereas the coefficient of variation of Figg air and water permeability were within 20

and 15 percent respectively. This was despite all the care taken during the fabrication of test holes (see Chapter 6). These high coefficients of variation may be attributed to the following:

1. Inaccuracy in controlling the depth of the testing hole.
2. Inaccuracy in controlling the depth of the sealed part of the hole.

Considering the effect of initial curing duration on the coefficient of variation of test results, statistical analysis performed on the compressive strength and ISAT results shows that the longer the initial curing duration the lower the coefficient of variation. For example the coefficient of variation of ISAT varied from 7 percent at 7 days curing to 13% at no curing.

8.7.2 Correlation between compressive strength and permeability and absorption related properties

The typical relationship between compressive strength and Figg water and water absorption under temperate and hot curing environments is shown graphically in Figures 8.68, 8.69, 8.70 & 8.71 respectively. Other relationships are also shown graphically in Figures A1.49 to A1.54 in Appendix 1.

Figures show that for each CSF replacing percentage, there exists an individual inverse relationship between strength and permeability and absorption. However, there was not a unique relationship which can represent all these mixes collectively. What is clear and interesting from these relationships is that different concrete mixes which have exactly the same compressive strength, can exhibit significantly different permeabilities and absorption properties.

Similarly concrete mixes with significantly different compressive strength can exhibit similar permeabilities and absorption properties. Therefore if it is assumed that concrete quality and durability are related to the permeability and absorption properties, then concrete

strength cannot give a true indication of concrete quality or durability.

8.7.3 Relationsip between permeability and absorption properties

The statistical analysis carried out to investigate the correlation between different permeability and absorption properties shows that these tests are highly correlated. The coefficients of correlation between these test methods are given in Table (8.2). The statistical analysis conducted on the relationship between different permeability and absorption properties shows that they are better related by a polynomial function than a linear function. This is confirmed typically by the graphical relationship between permeability and absorption properties shown in Figures 8.72-8.75. However a linear relationship was only noticed between ISAT and absorption (under temperate curing) and between Figg air and Egg air permeability (under hot curing) (See Figures A1.62 and A1.64 in Appendix 1). The other relationships are presented graphically in Figures A1.55 to A1.70 in Appendix 1.

8.7.4. Importance of curing

Test results show that surfacecrete needs more curing attention and longer duration than the subsurfacecrete. This confirms that curing is more important for the top few millimetres. This was confirmed also by Abrams and Orals (114). The above finding and the conclusion based upon it sounds logical since the properties of surfacecrete are very important for the durability and performance of concrete and reinforced concrete structure. This is because during construction and service life of the building, surfacecrete is likely to be subjected to different mechanical and chemical influences and often greater working loads than the subsurfacecrete. For these reasons the surfacecrete should be of the highest quality possible.

8.7.5 Quality control and compliance testing for concrete

The present quality control and compliance testing of concrete is usually measured either by prescription i.e. by mix proportions, or by performance, i.e. by testing the compressive strength of separately manufactured cubes. Test results gathered from measuring the compressive strength and permeability with the absorption properties of different concrete mixes shows that compressive strength cannot give a true indication of concrete quality. Moreover, this test method cannot differentiate between the properties of surfacecrete (believed to be more important and relevant to concrete quality and durability) and the subsurfacecrete. Therefore customer quality control and compliance testing should be based not only on compressive strength but on at least one other test method that can be used on site and in laboratory and which has a high repeatability value. This test method is aimed at differentiating between proper and improper curing regime and duration. A comparison between the simple techniques used in this research work indicates that the ISA test can be used for quality control as well as the cube strength. Thus ISAT can be used for verifying the curing regime and period while compression strength can be used for verifying the mix proportions. A proposed graphical mean is presented in Figure 8.76, and may be used for verification of both mix proportions and curing regime and duration. Therefore two sets of concrete specimens can be prepared and cured simultaneously with the actual structure. The first set can be tested for strength to verify mix proportions. The second set can be tested by ISAT to verify curing regime and duration.

Mix No.	Mix Ref.	Concrete Grade	Cement kg/m^3	Water kg/m^3	CSF kg/m^3	Sand kg/m^3	10 mm gravel kg/m^3	20 mm gravel kg/m^3
1	25/0	C25	230	185	0	780	385	770
2	25/5		190	185	12			
3	25/10		170	195	24			
4	40/0	C40	300	185	0	660	390	780
5	40/5		225	185	16			
6	40/10		205	190	31			
7	40/15		210	210	46			
8	40/15S		175	185	46			
9	55/0	C55	400	185	0	590	380	760
10	55/5		300	185	20			
11	55/10		310	215	40			

Table 8.1 Mix proportions for plain and CSF concrete mixes

	Polythene temperate					Polythene hot					
	Figg Air	Figg Water	Egg Air	Water Absorption	ISAT	Figg Air	Figg Water	Egg Air	Water Absorption	ISAT	CSF %
Figg Air		0.97	0.98	0.95	0.97		0.99	0.98	0.96	0.98	0
		0.94	0.97	0.91	0.91		0.95	0.98	0.86	0.85	5
		0.91	0.94	0.86	0.90		0.94	0.96	0.85	0.72	10
		1.00	*0.11	0.96	*0.19		0.99	0.99	1.00	1.00	15
		1.00	1.00	1.00	1.00		0.99	1.00	1.00	1.00	155
Figg Water			0.99	0.99	0.99			0.99	0.99	0.99	0
			0.97	0.98	0.97			0.98	0.95	0.92	5
			0.98	0.97	0.97			0.99	0.94	0.83	10
			*0.07	0.98	*0.20			1.00	0.99	1.00	15
			1.00	1.00	1.00			1.00	1.00	1.00	155
Egg Air				0.99	0.97				0.97	1.00	0
				0.96	0.96				0.92	0.94	5
				0.98	0.96				0.94	0.84	10
				0.93	*0.27				1.00	1.00	15
				1.00	1.00				1.00	1.00	155
Water Absorp -tion					0.99					0.98	0
					1.00					0.97	5
					1.00					0.94	10
					*0.44					0.98	15
					1.00					0.98	155
ISAT											0
											5
											10
											15
											155

TABLE 8.2: Correlation coefficients of a polynominal relation between the permeability and absorption test used.

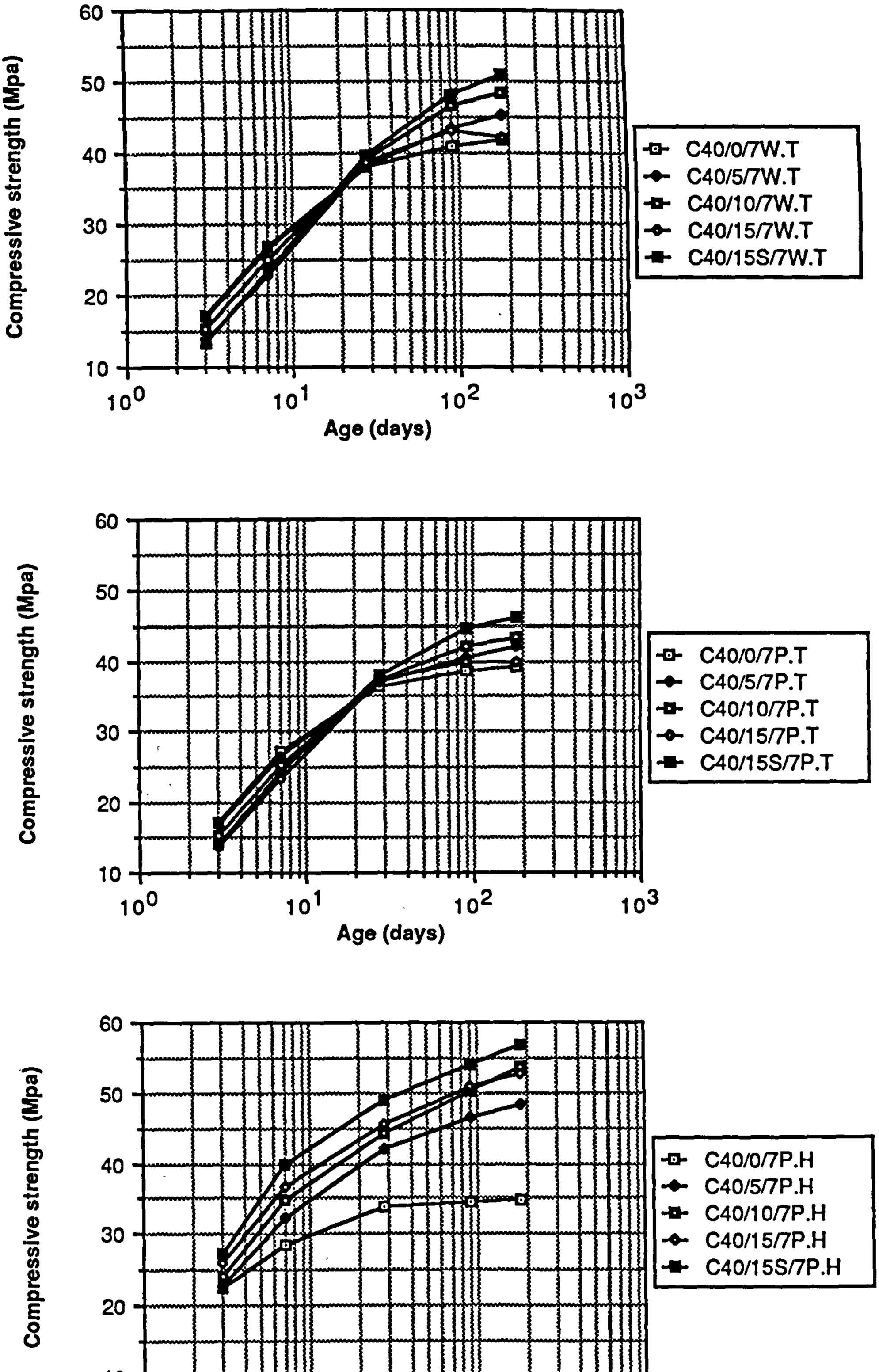

Figure 8.1 Relationship between age and compressive strength of plain anc CSF concrete mixes grade C40

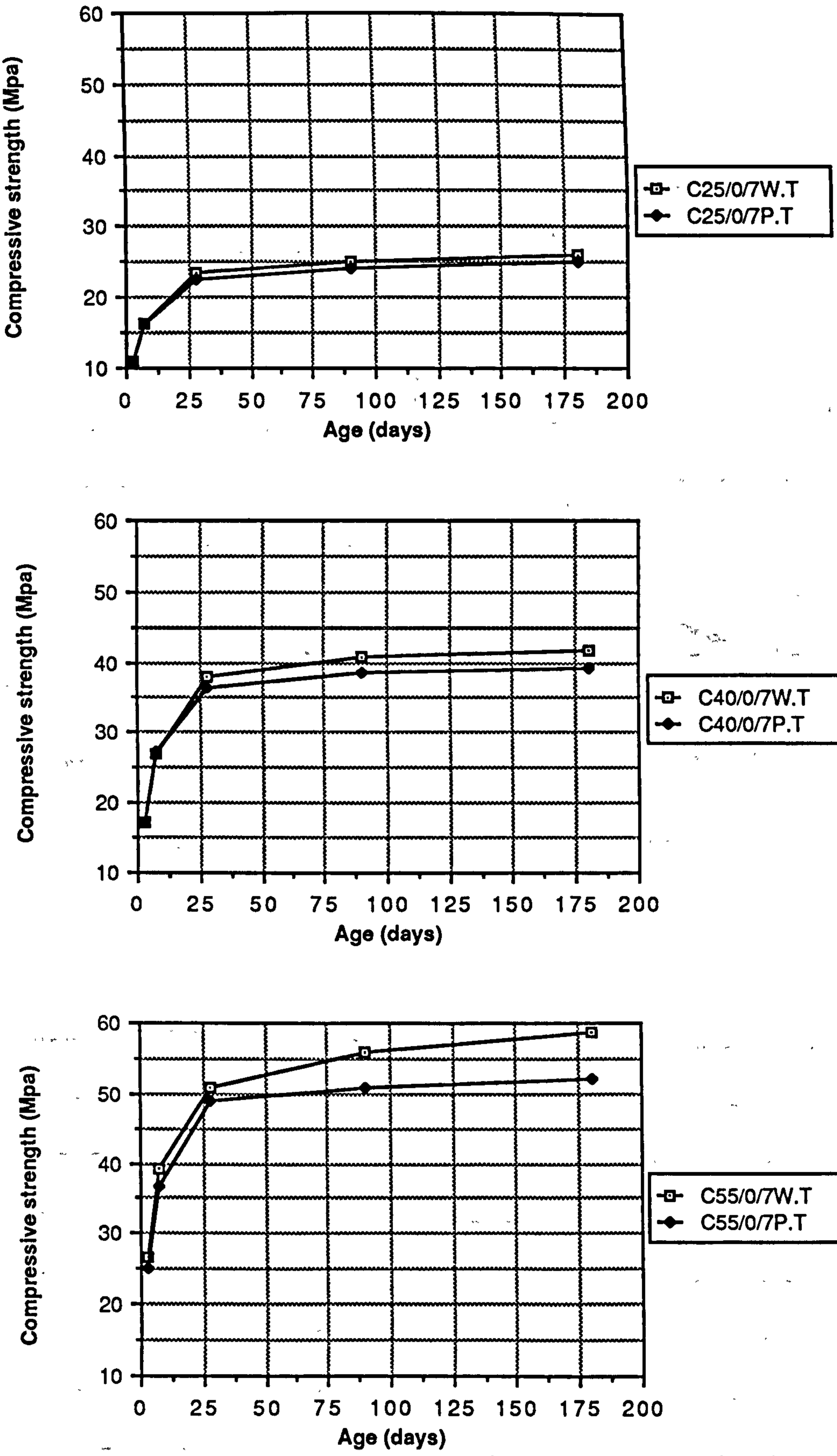

Figure 8.2 The effect of water and polythene curing on the compressive strength of plain concrete mixes

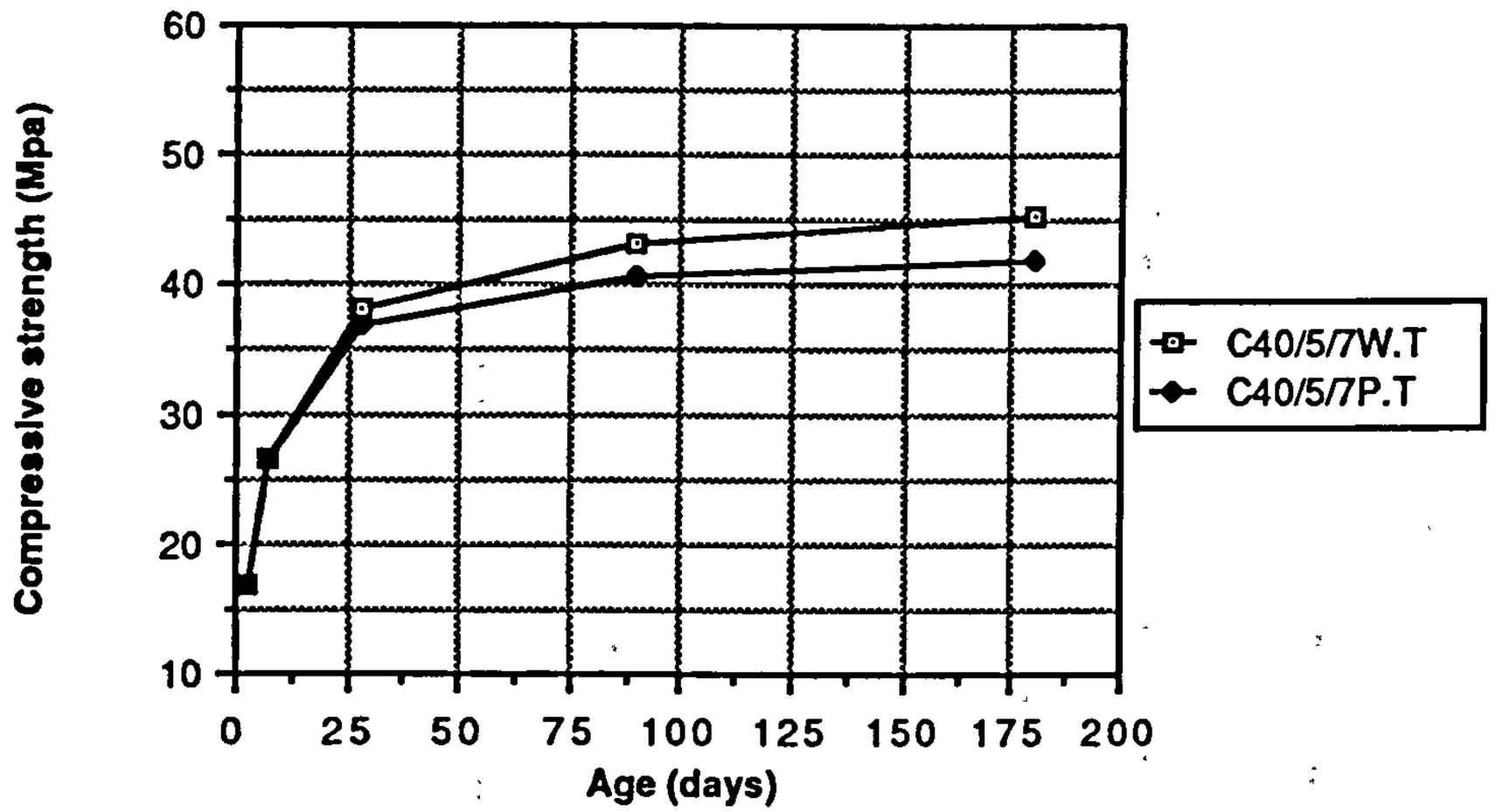

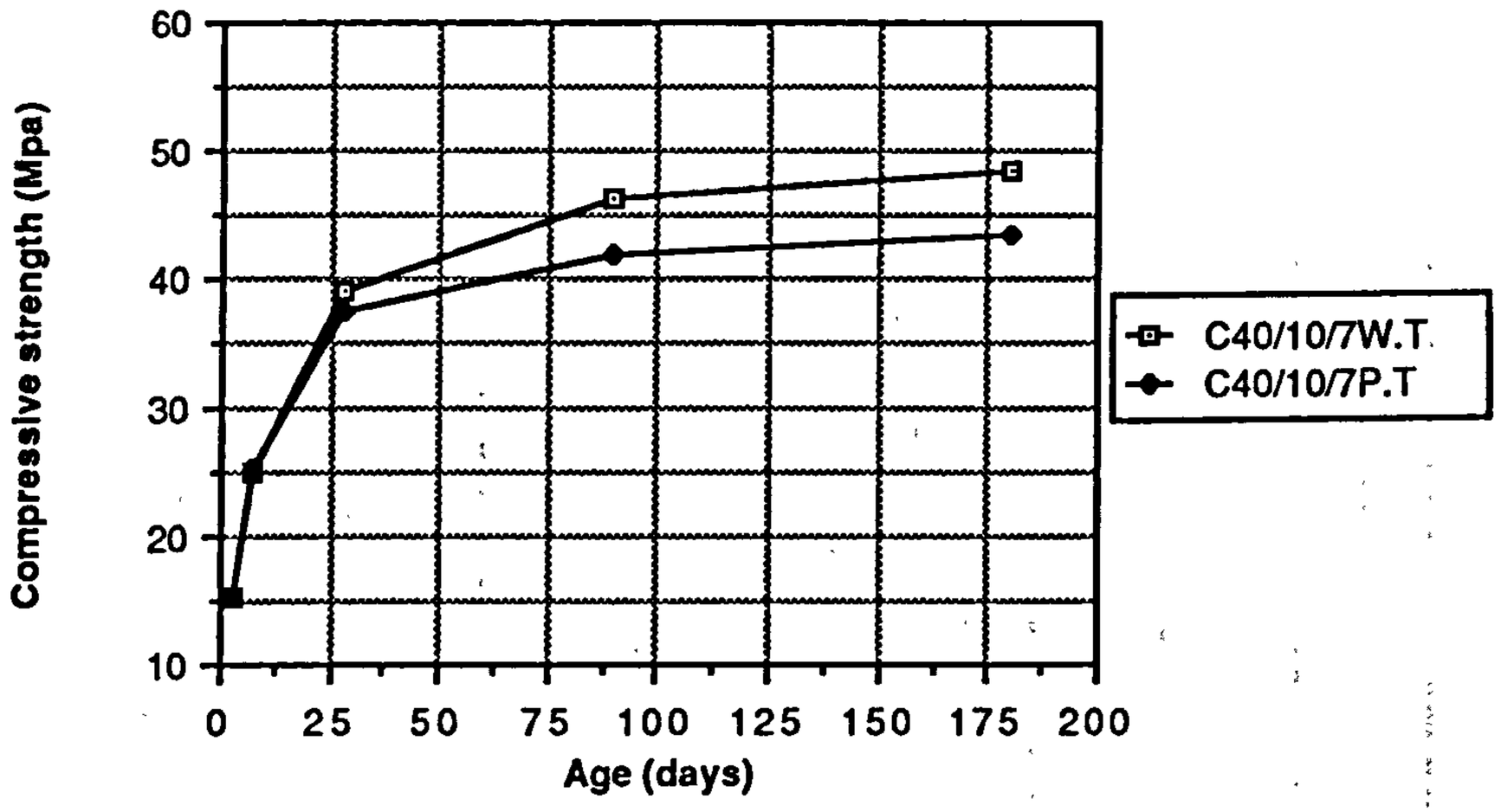

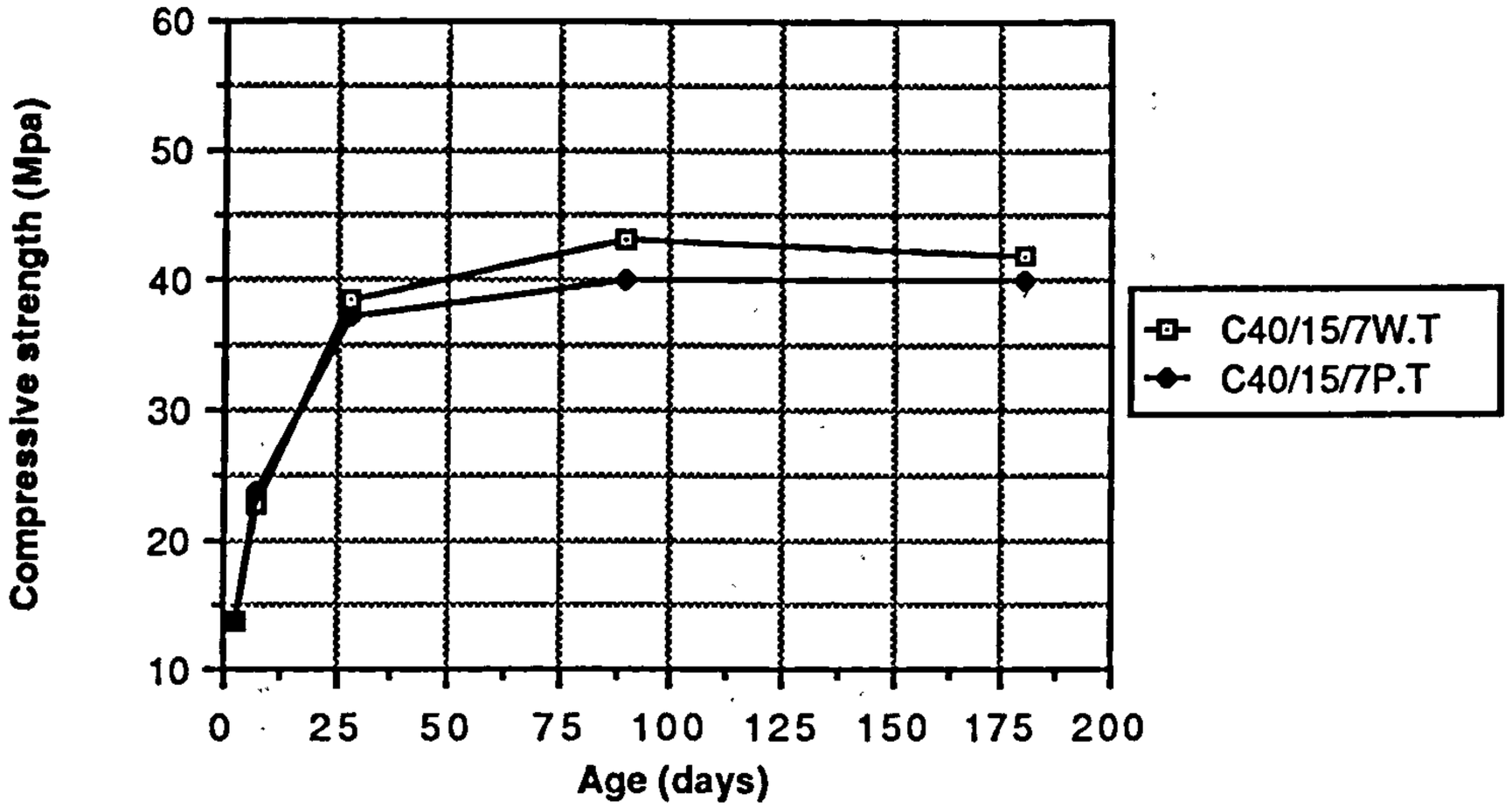

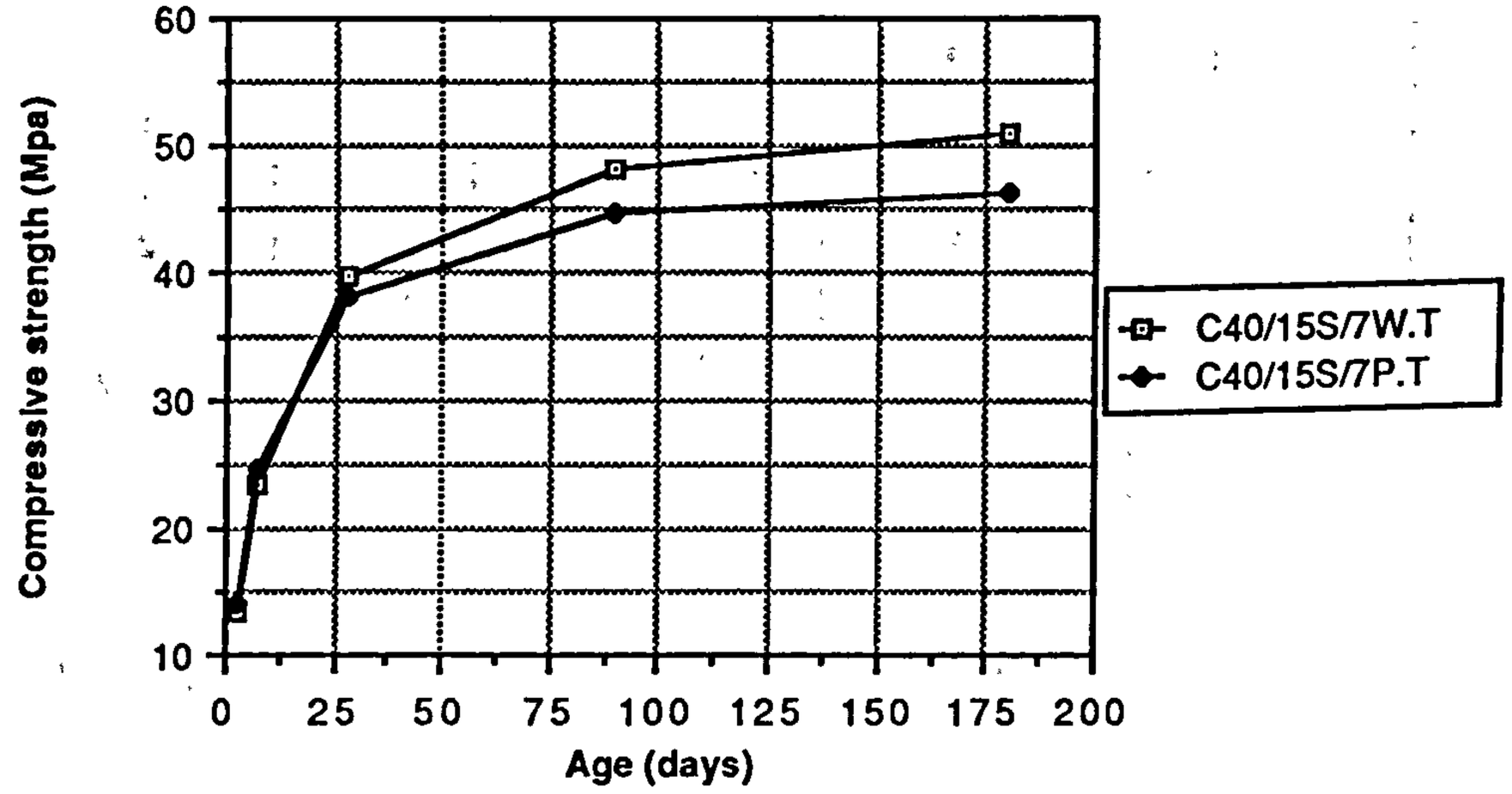

Figure 8.3 Effect of water and polythene curing on the compressive strength of CSF mixes

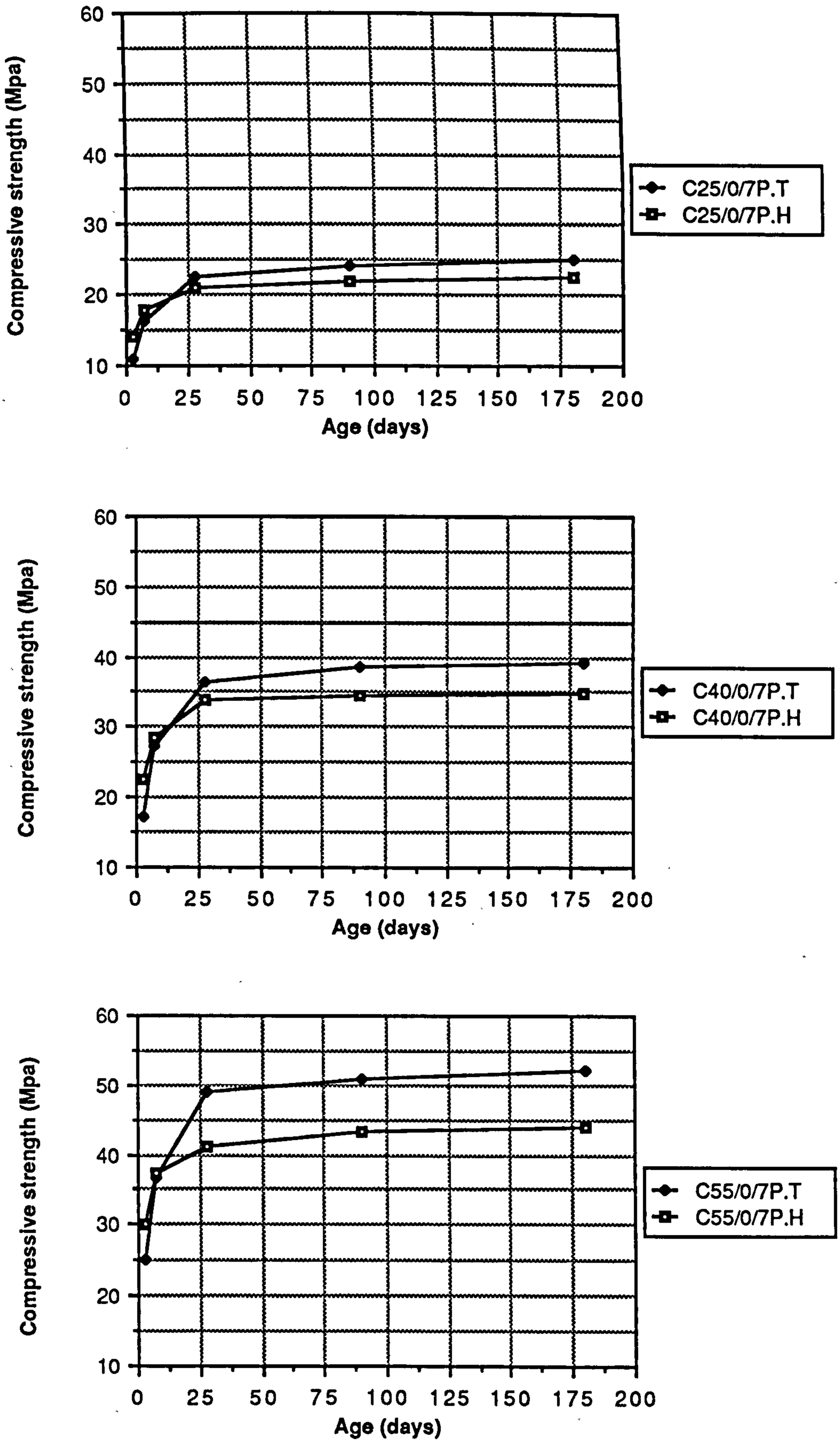

Figure 8.4 Effect of temperate and hot curing on the compressive strength of plain OPC mixes

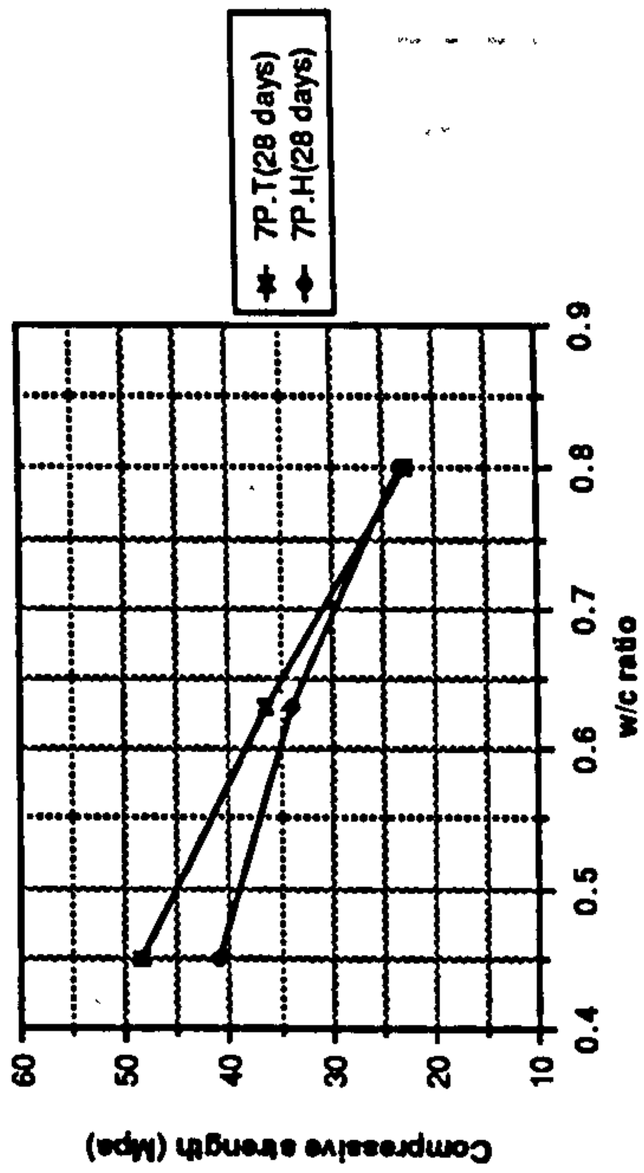

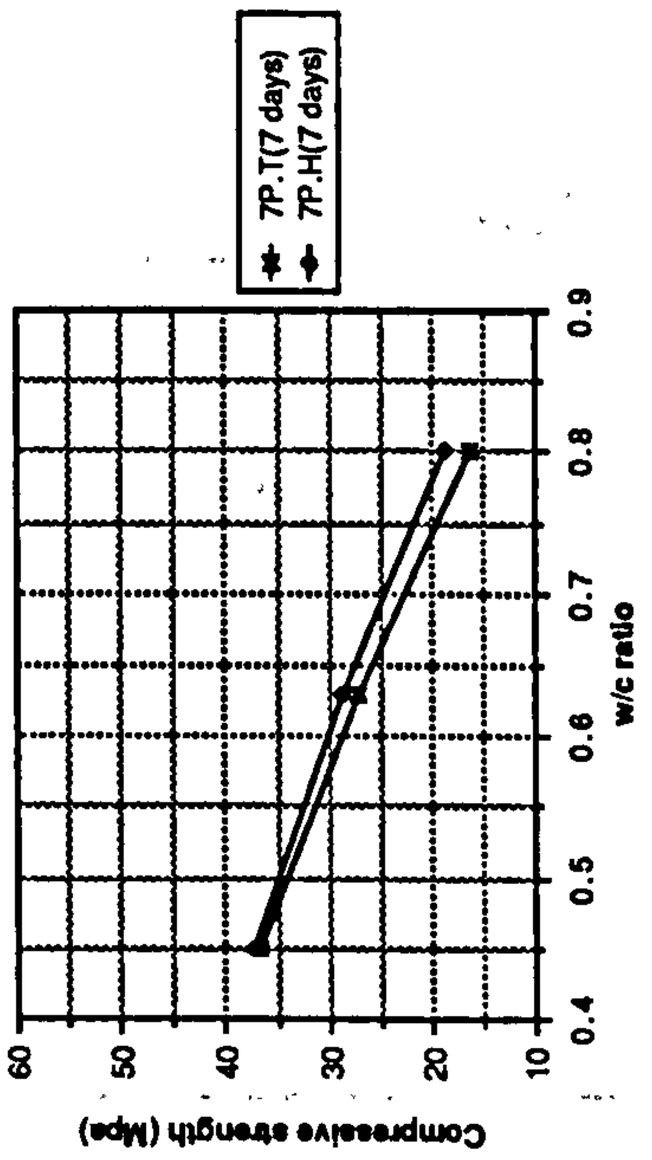

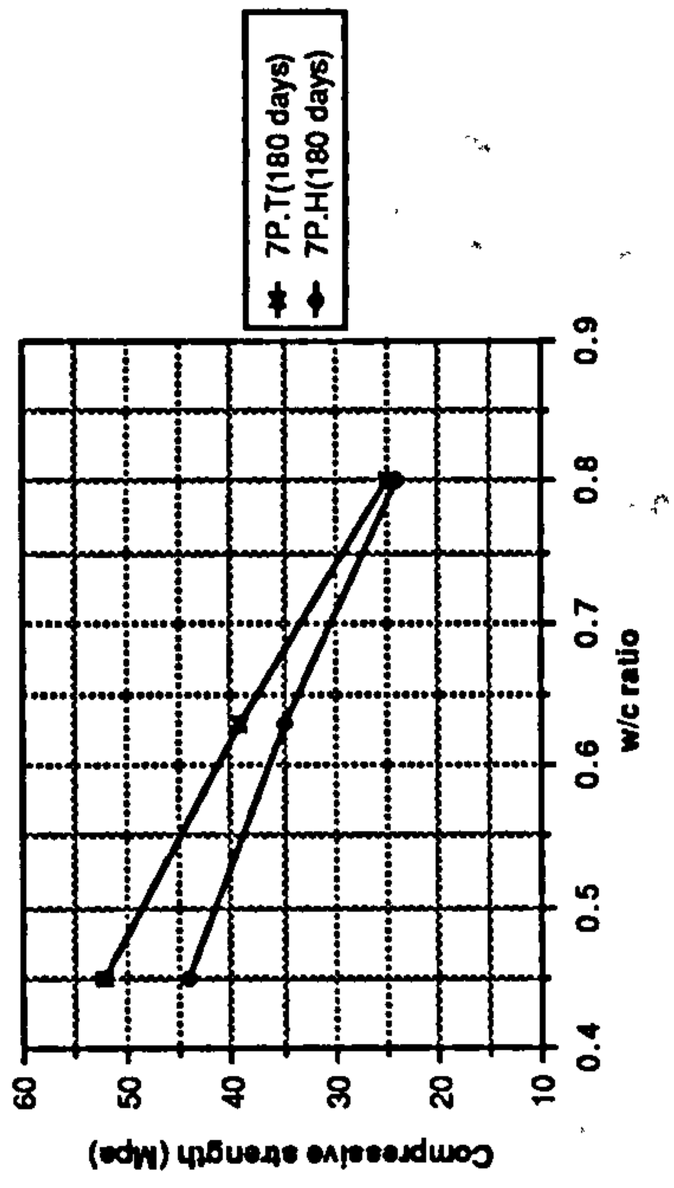

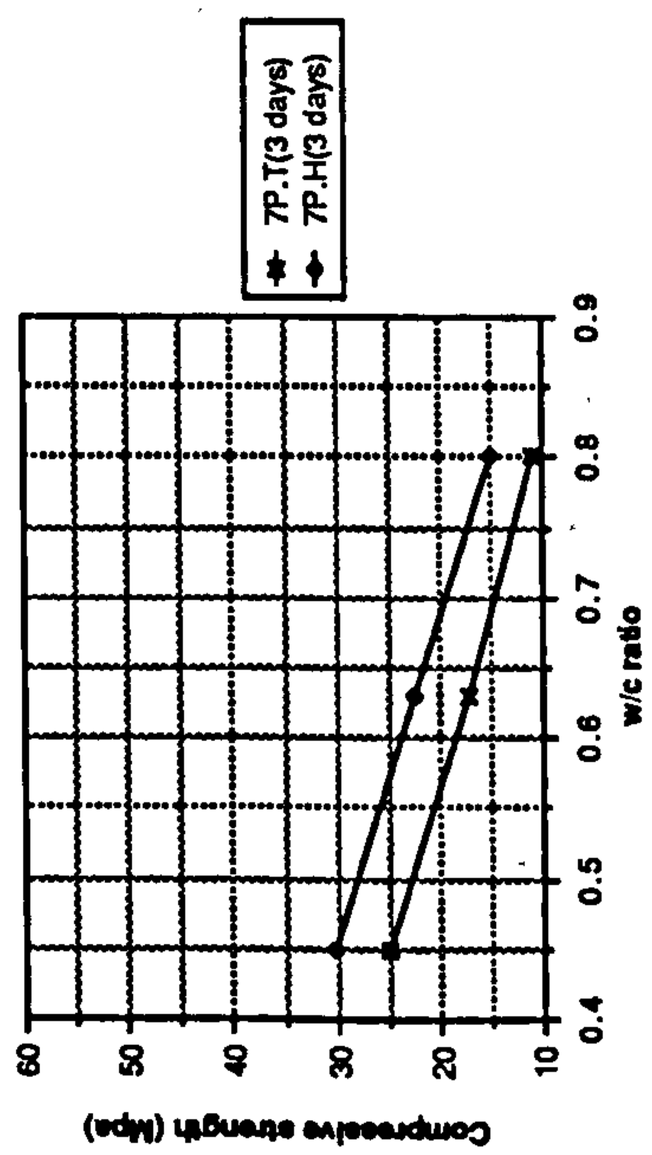

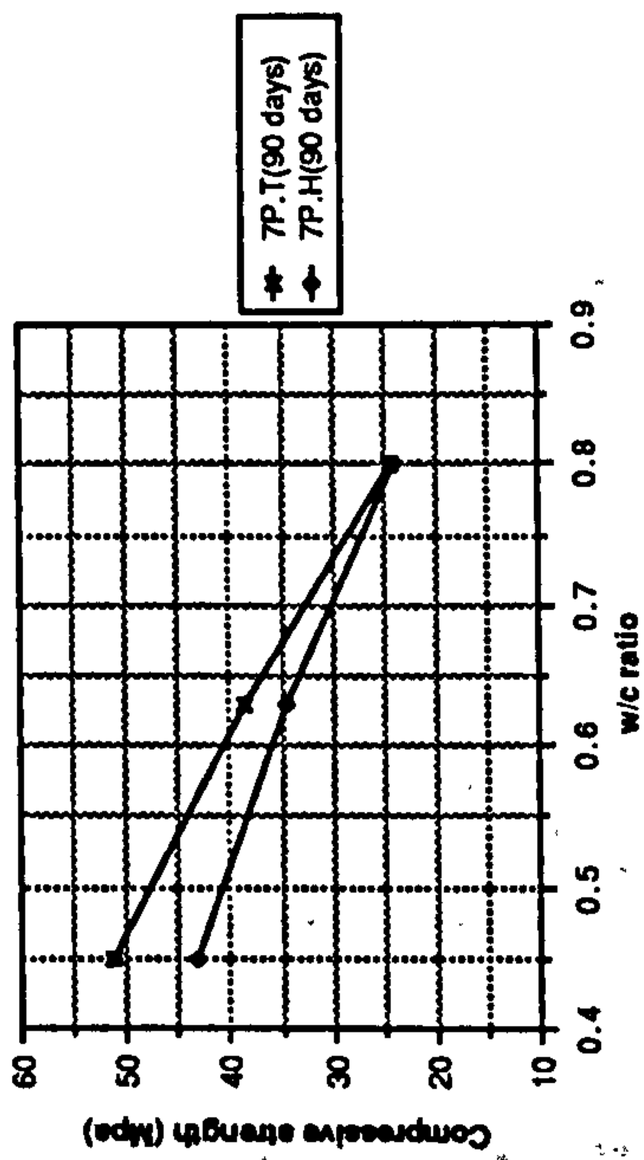

Figure 8.5 Effect of W/C ratio on the compressive strength of plain OPC mixes cured under temperate and hot environment

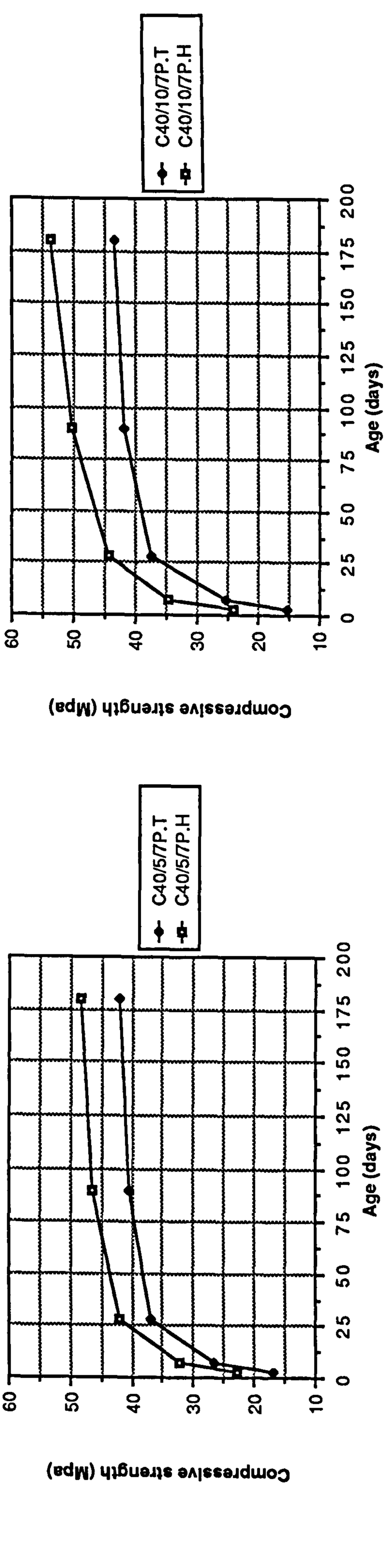

Figure 8.6 Effect of temperate and hot curing on the compressive strength of CSF mixes

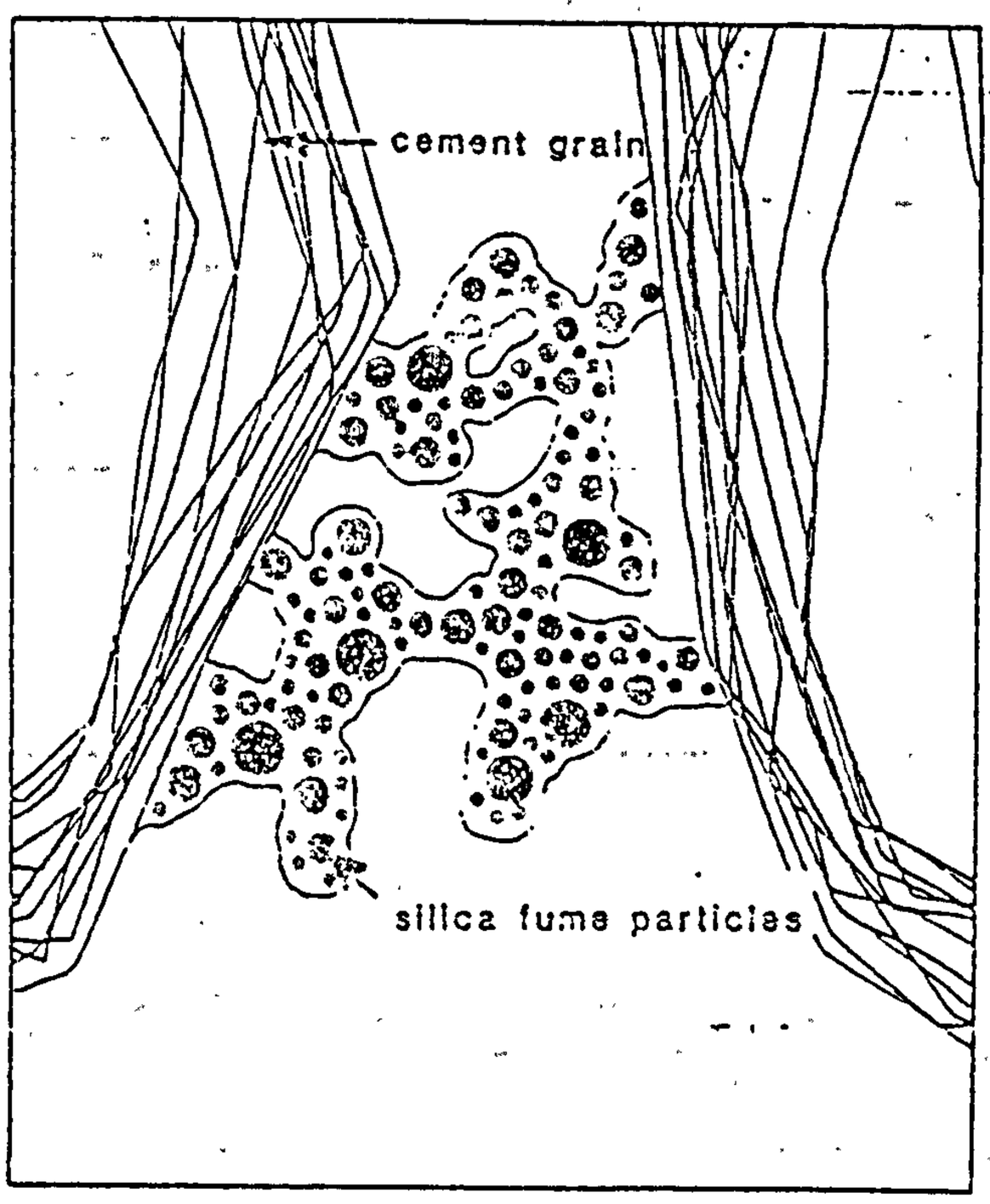

Figure 8.7 Mechanism of bleeding reduction in cement paste by silica fume addition

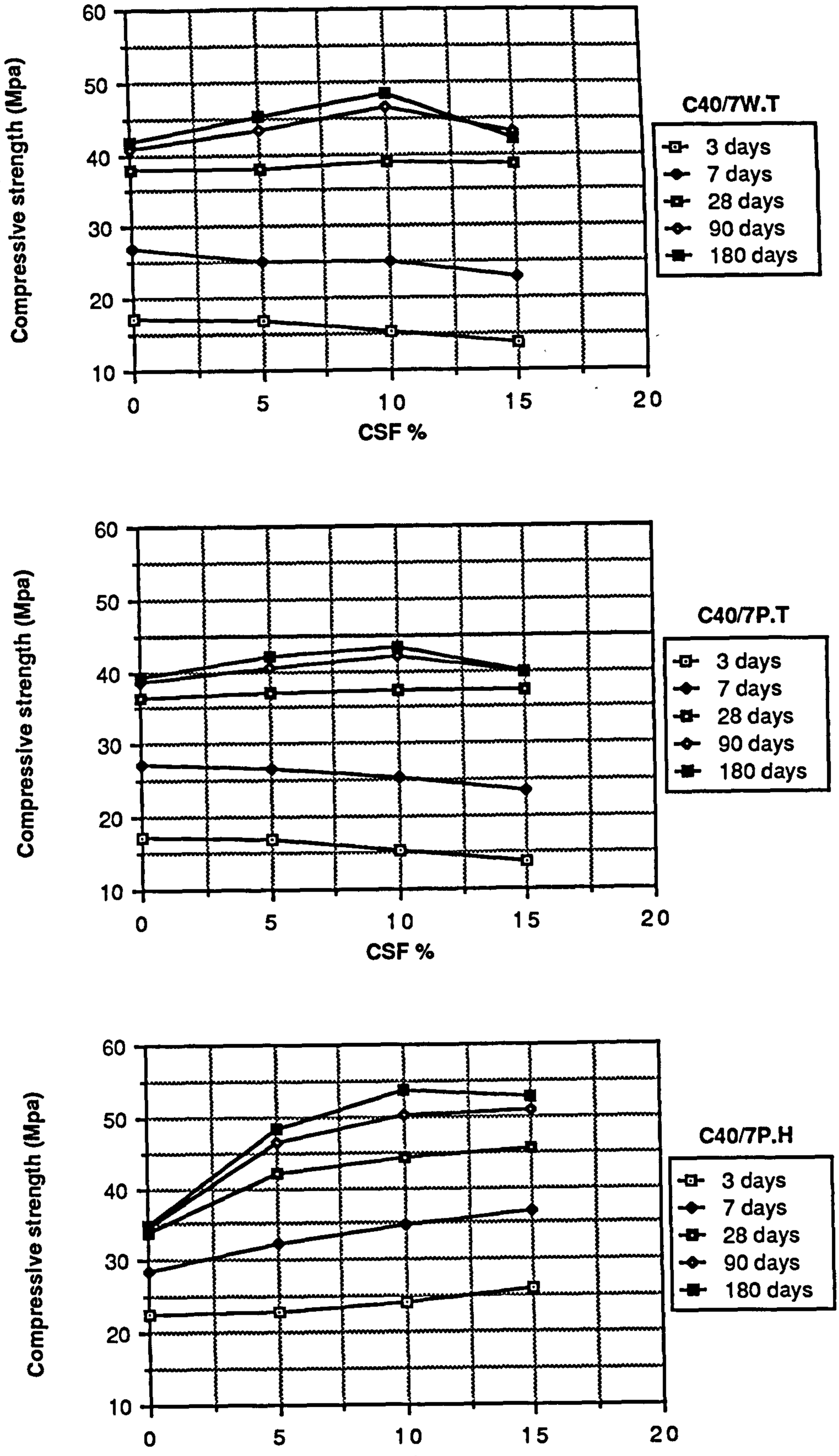

Figure 8.8 Effect of CSF content on the compressive strength

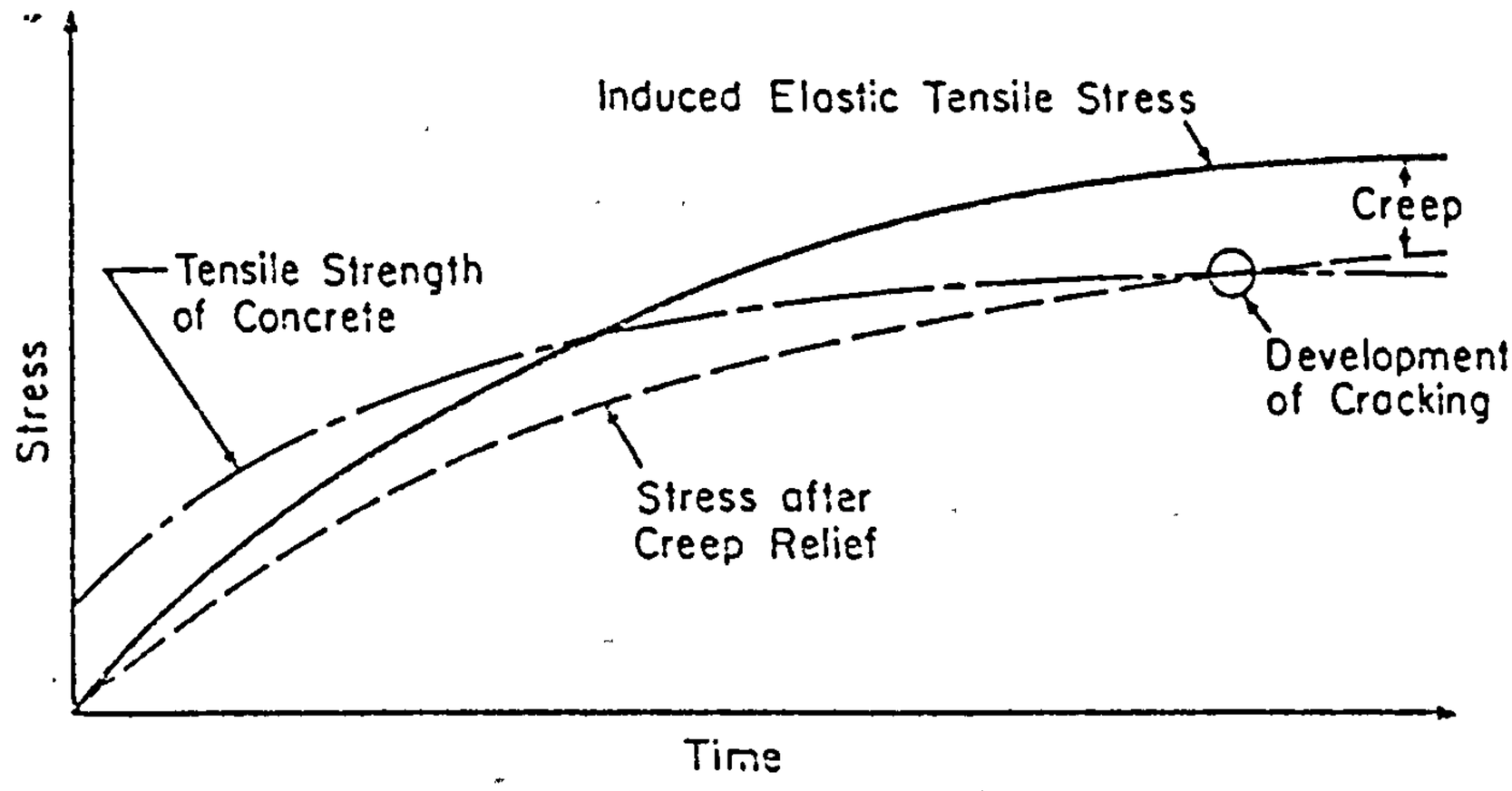

Figure 8.9 Schematic pattern of crack development when tensile stress due to restrained shrinkage is relieved by creep (36)

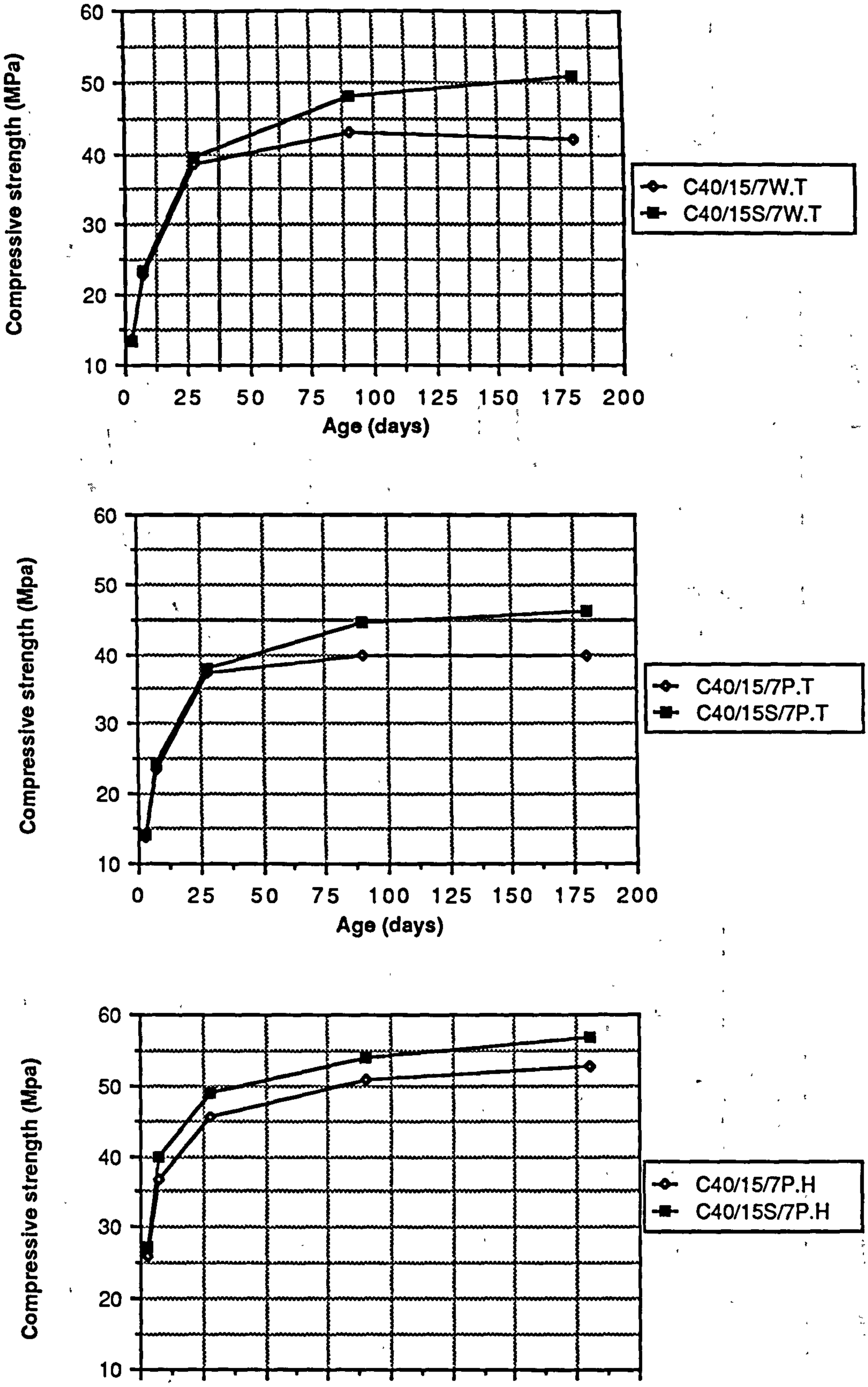

Figure 8.10 Effect of superplasticizer on the compressive strength

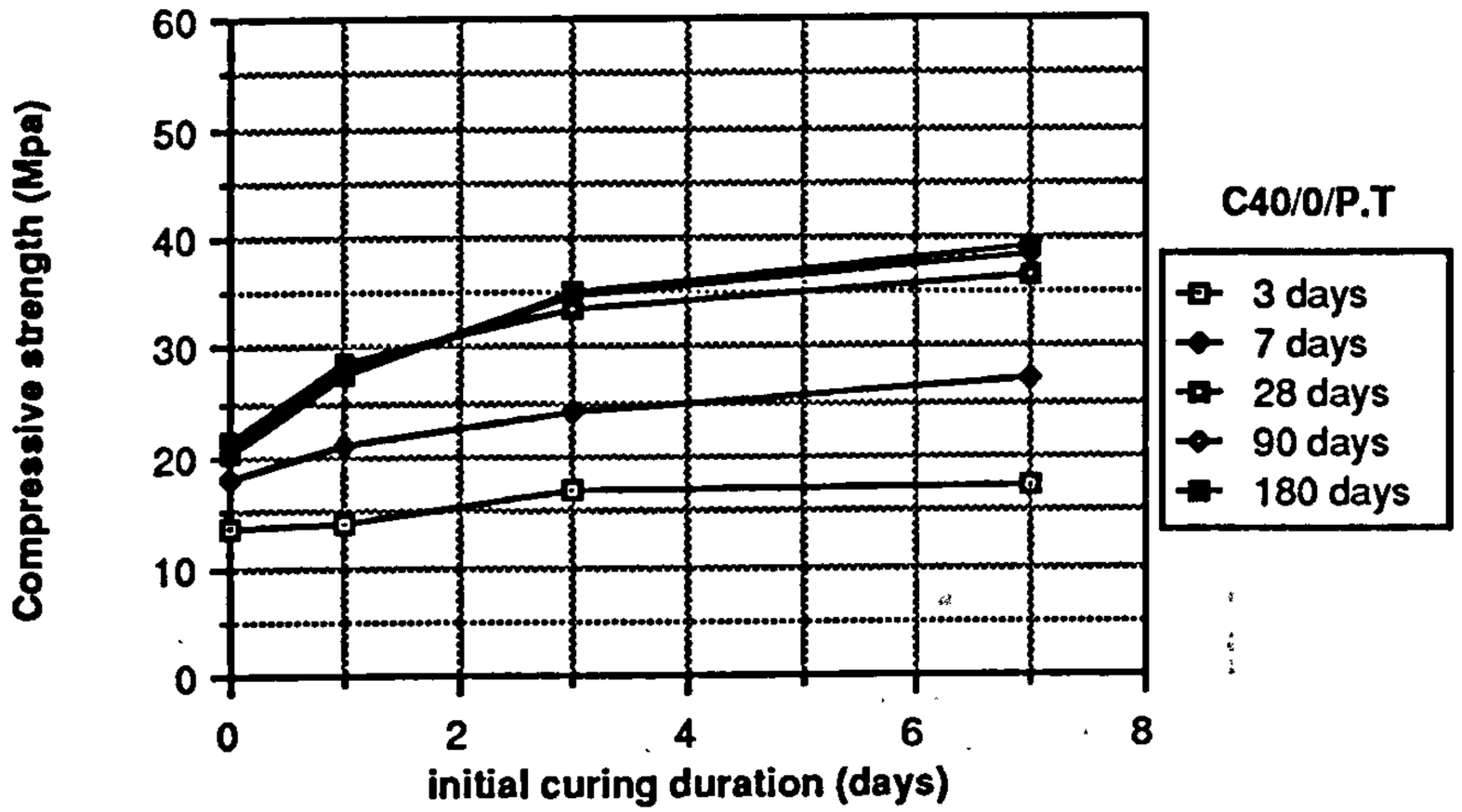

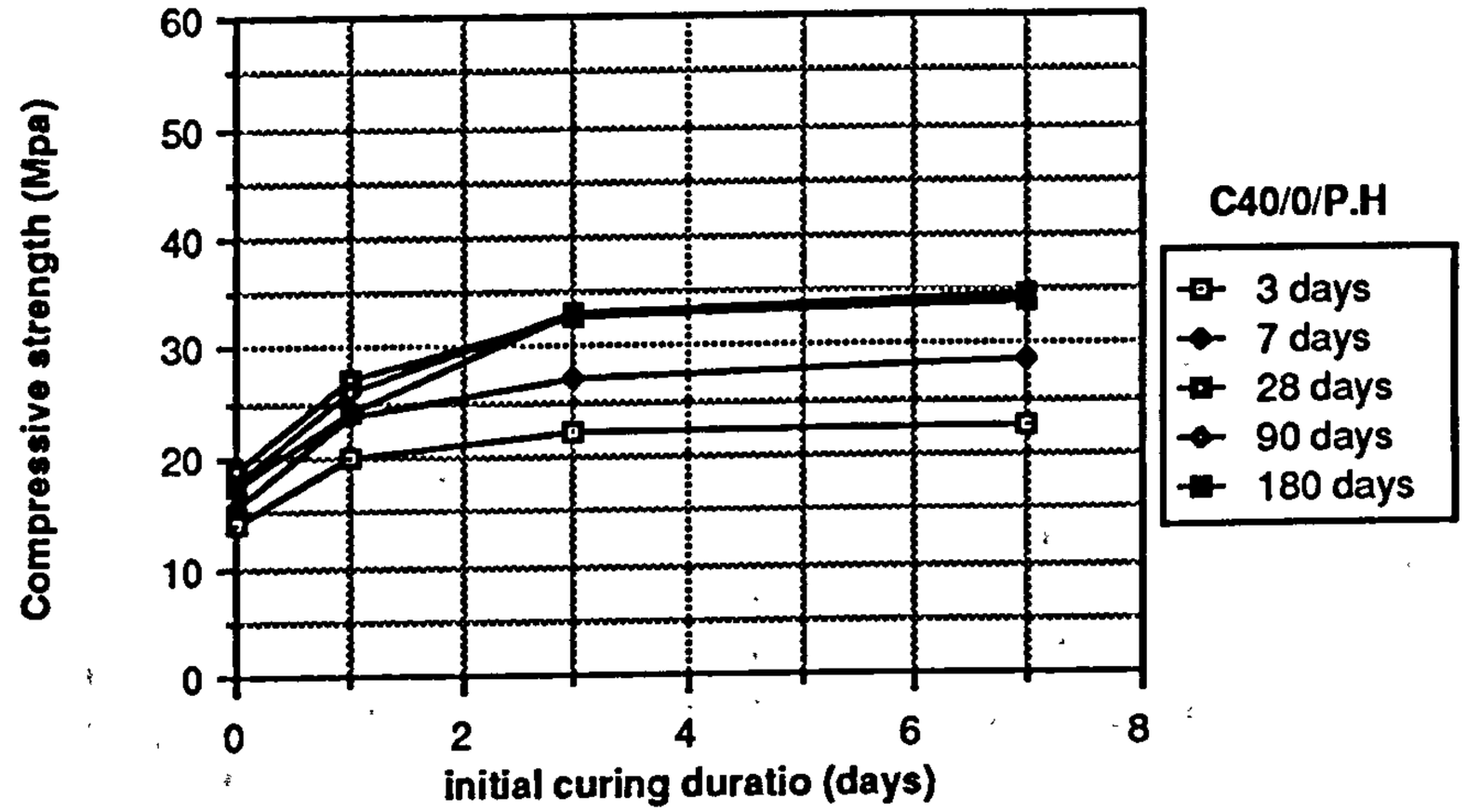

Figure 8.11 Effect of initial curing duration on the compressive strength of plain OPC mixes

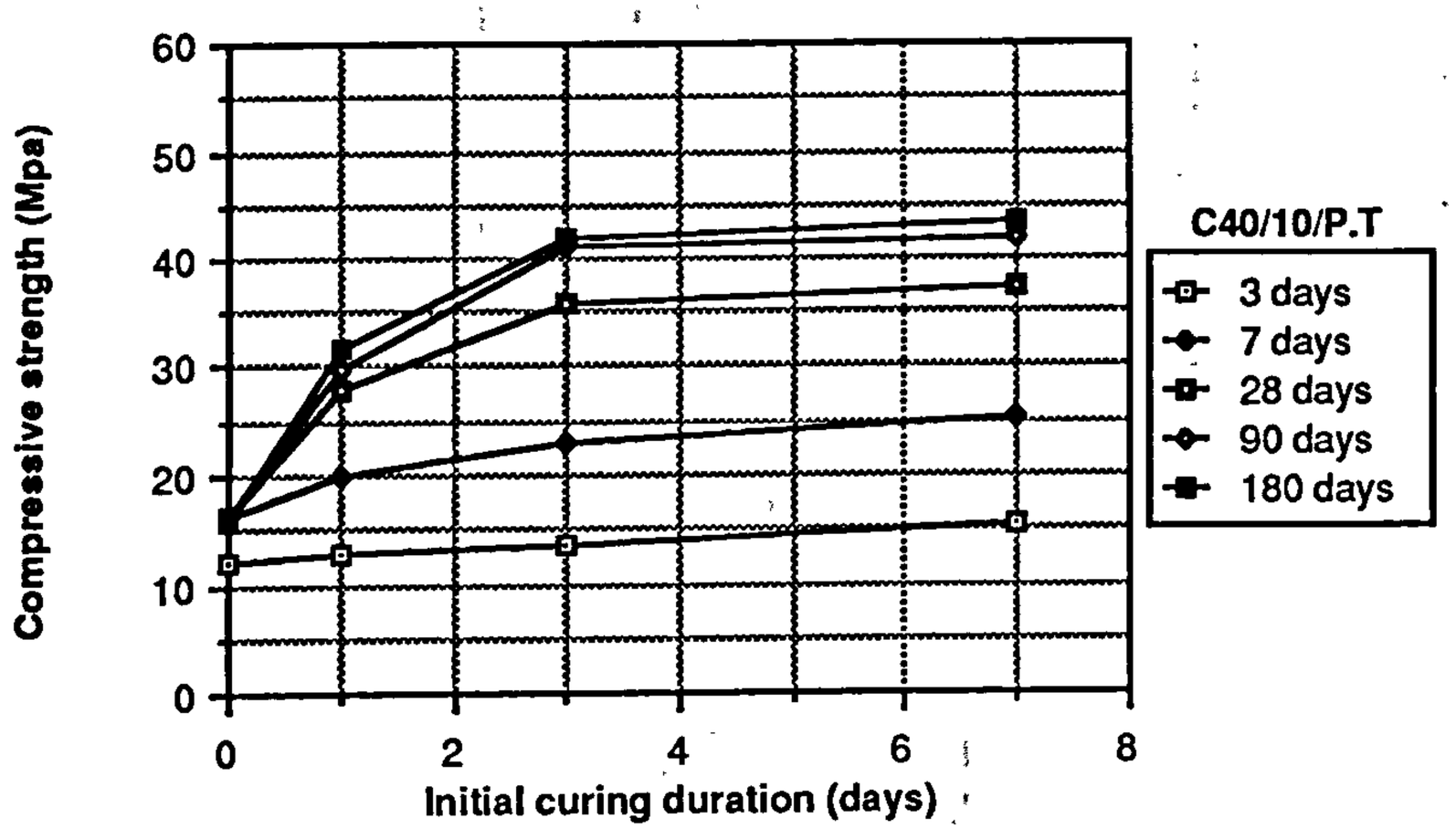

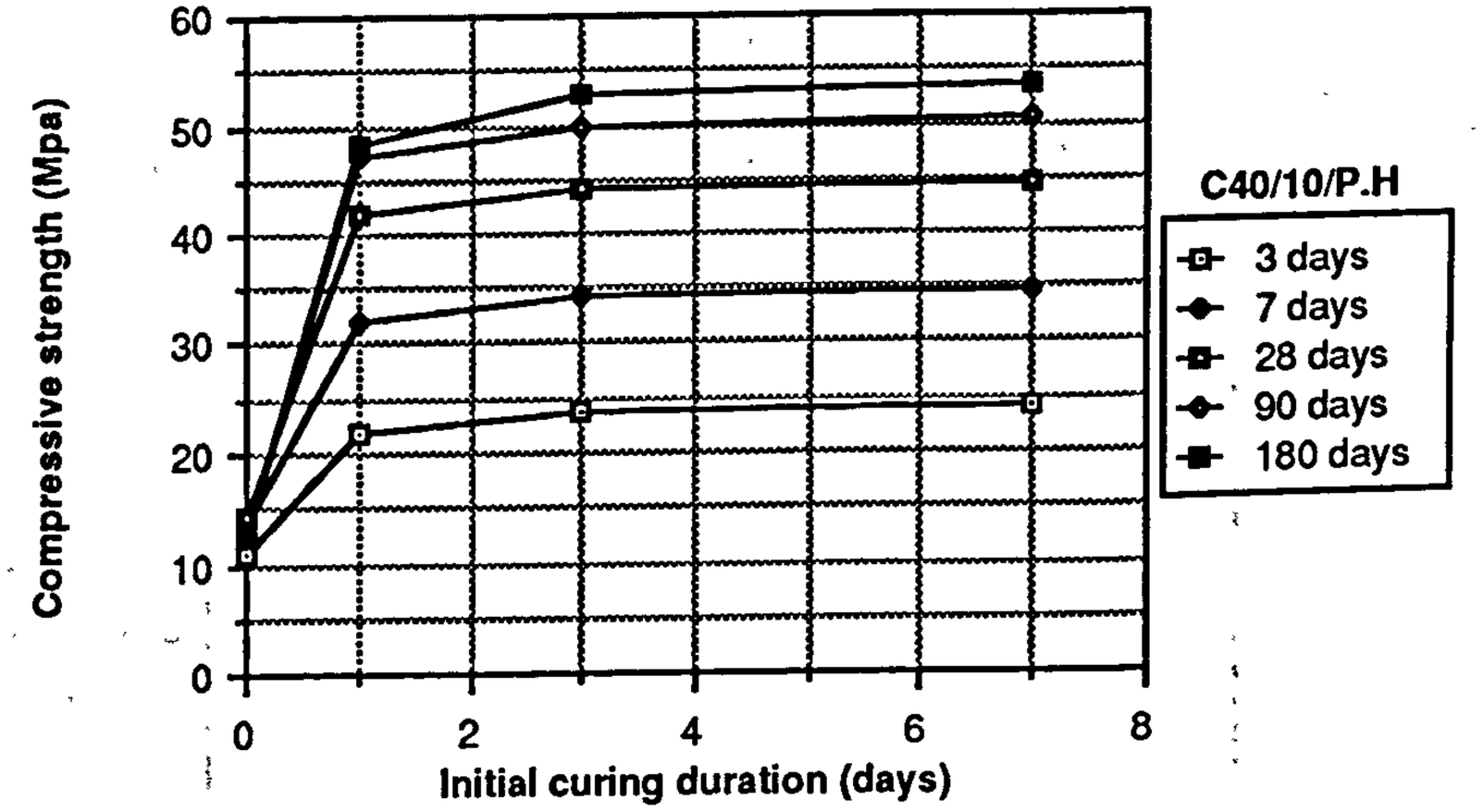

Figure 8.12 Effect of initial curing duration on the compressive strength of CSF concrete mixes

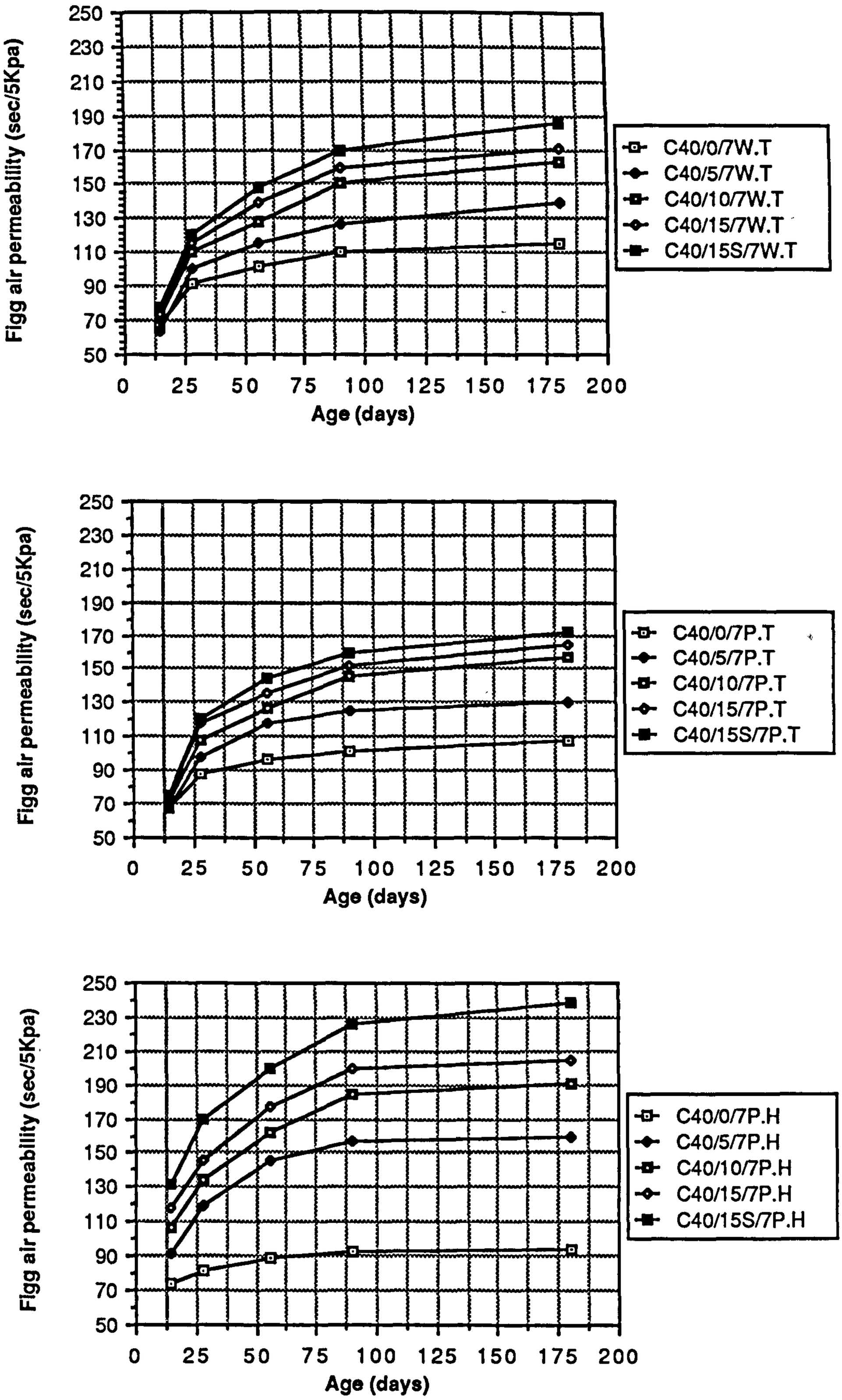

Figure 8.13 Effect of age on the Figg air permeability of plain and CSF concrete mixes

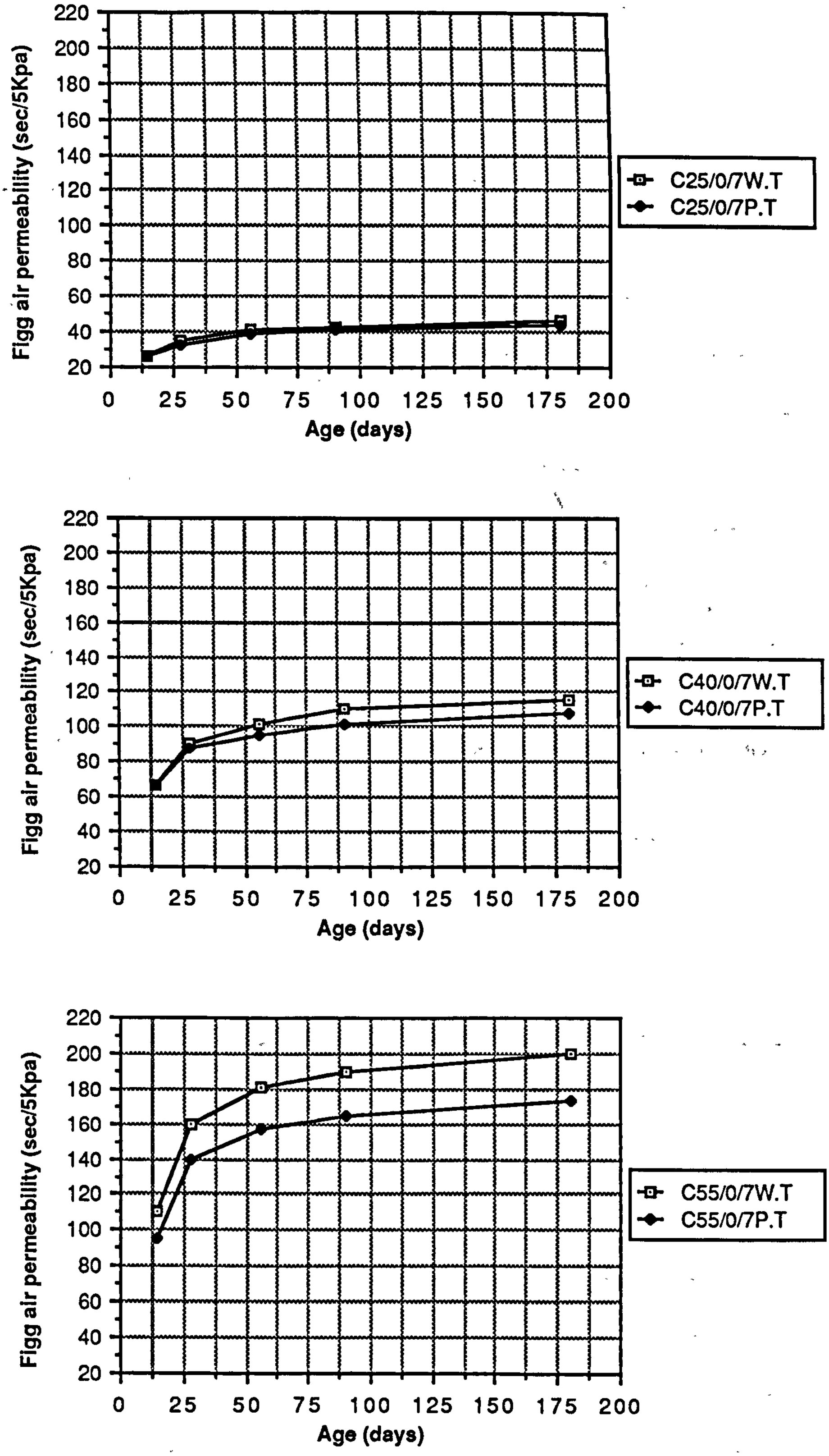

Figure 8.14 Effect of water and polythene curing on the Figg air permeability of plain OPC mixes

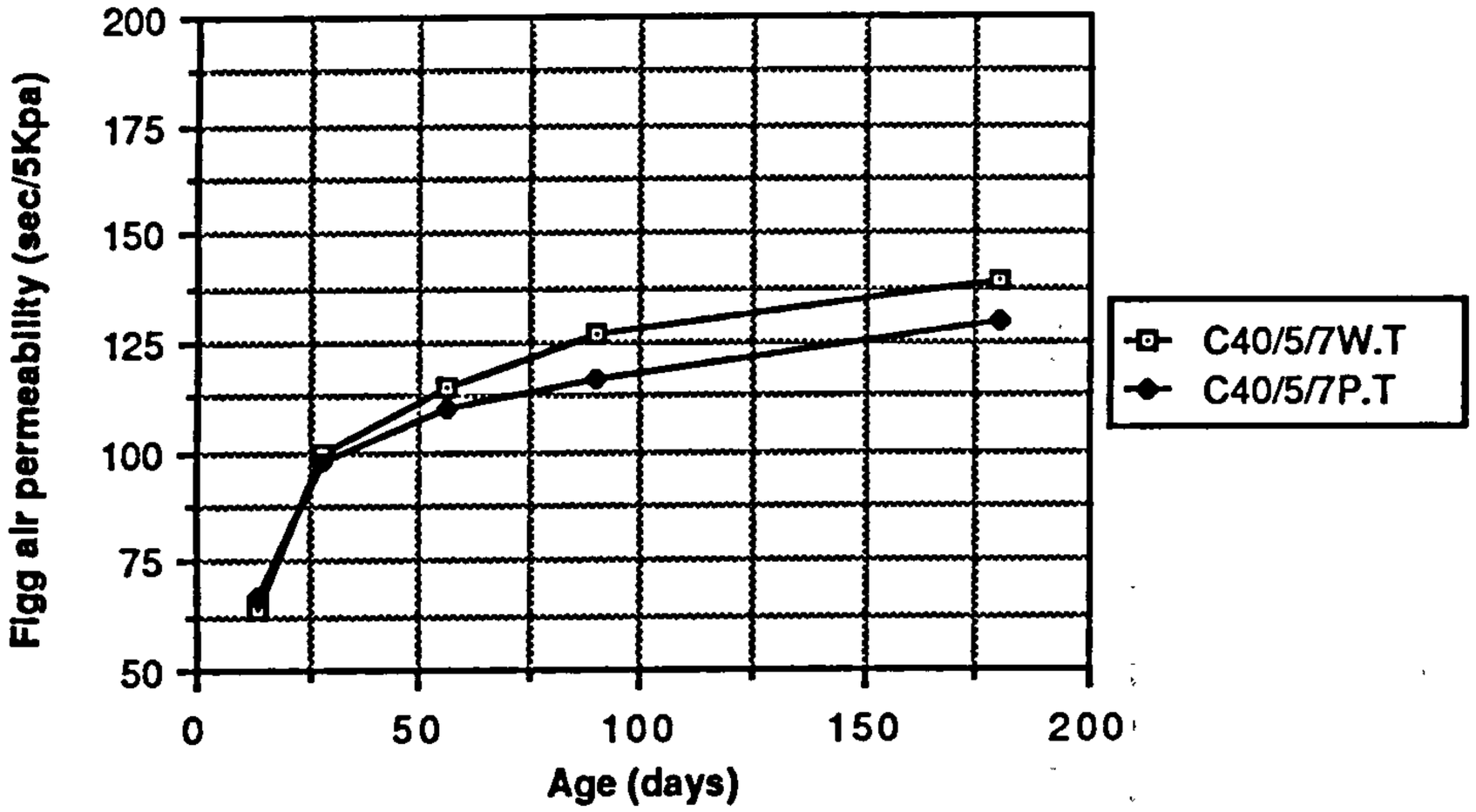

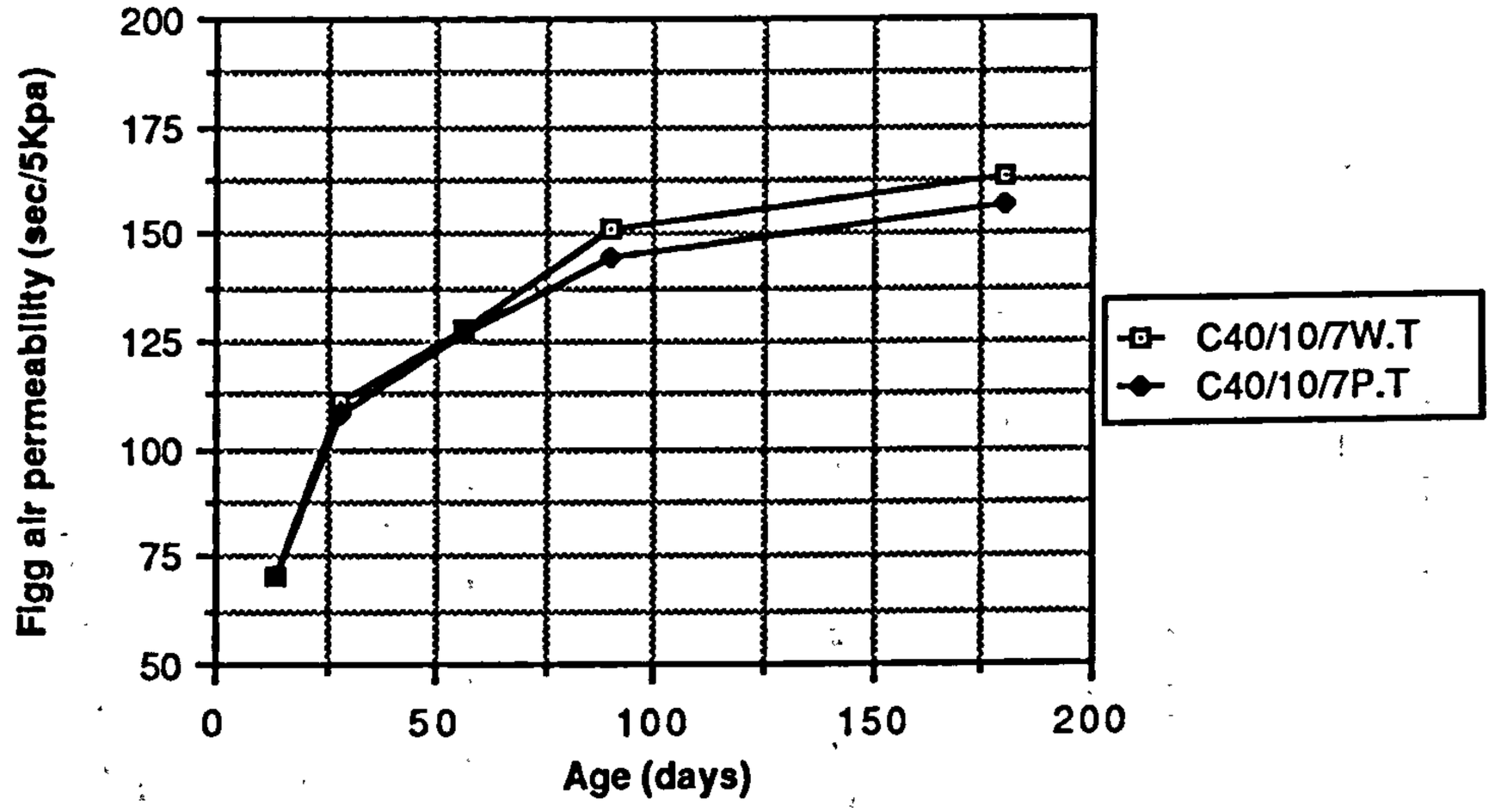

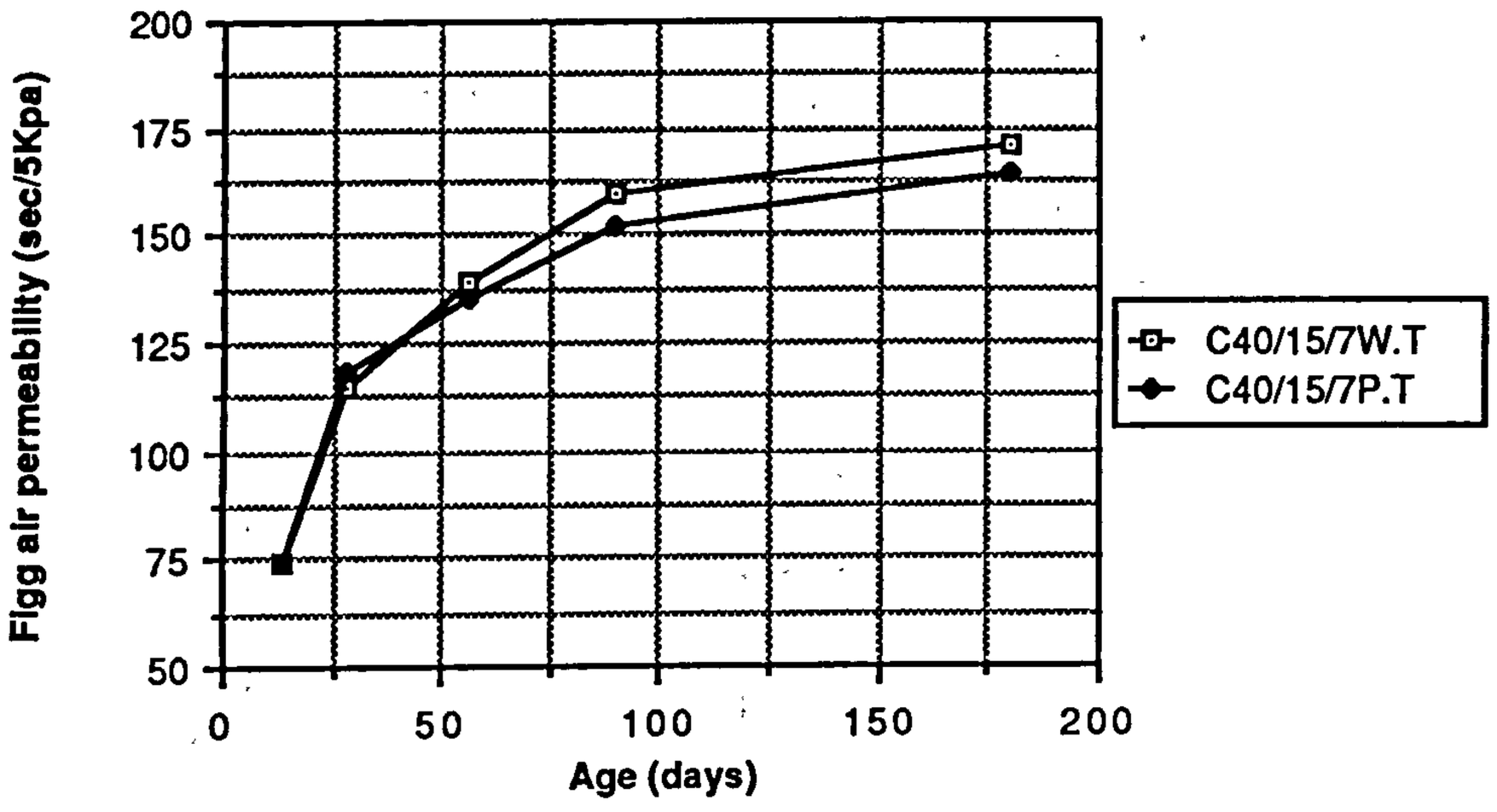

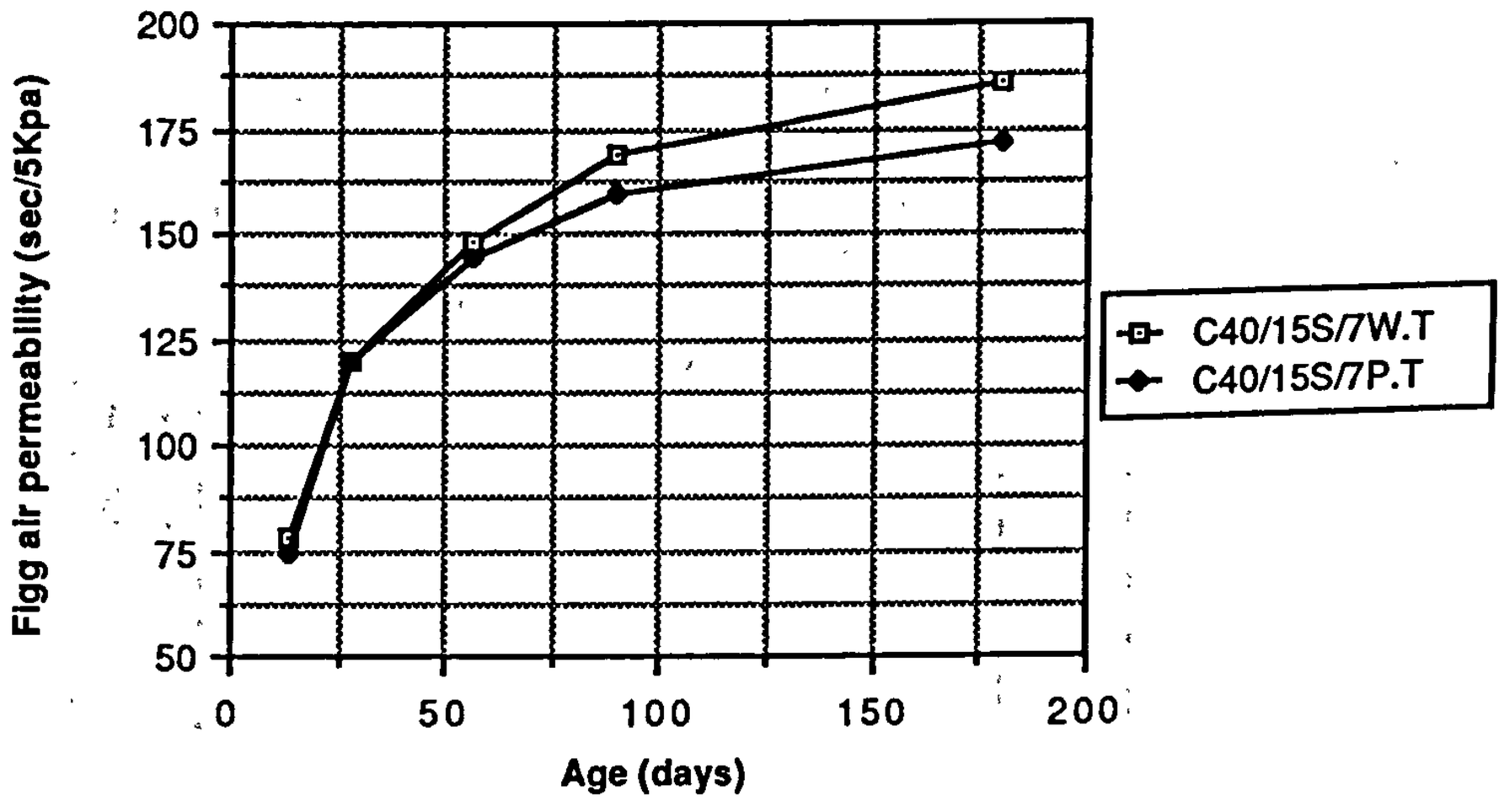

Figure 8.15 Effect of water and polythene curing on the Figg air permeability of CSF concrete mixes

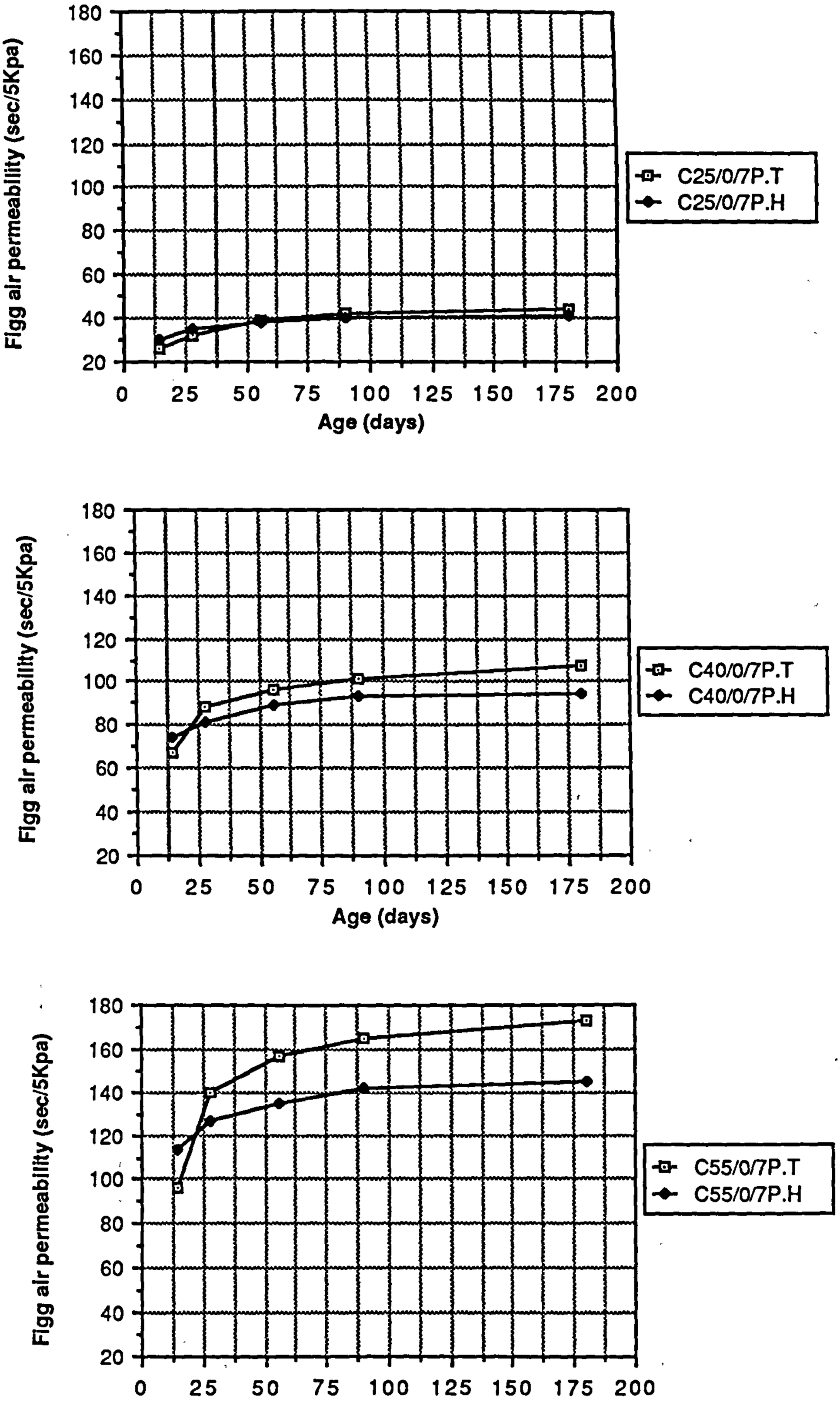

Figure 8.16 Effect of temperate and hot curing on the Figg air permeability of plain OPC mixes

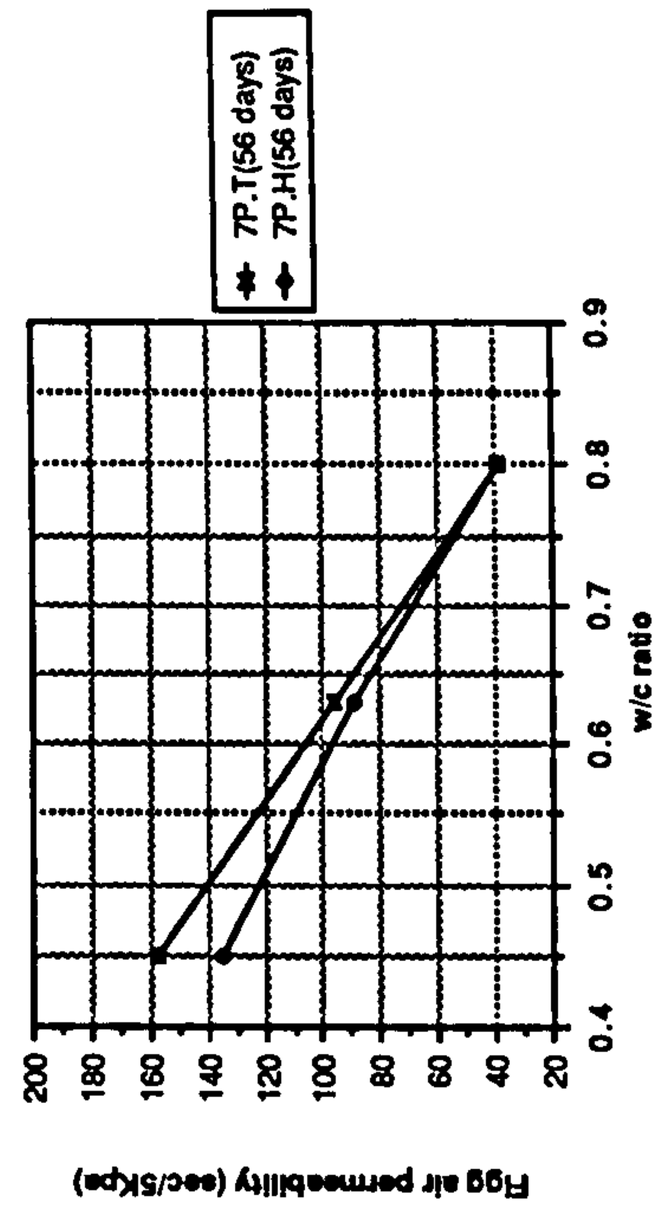

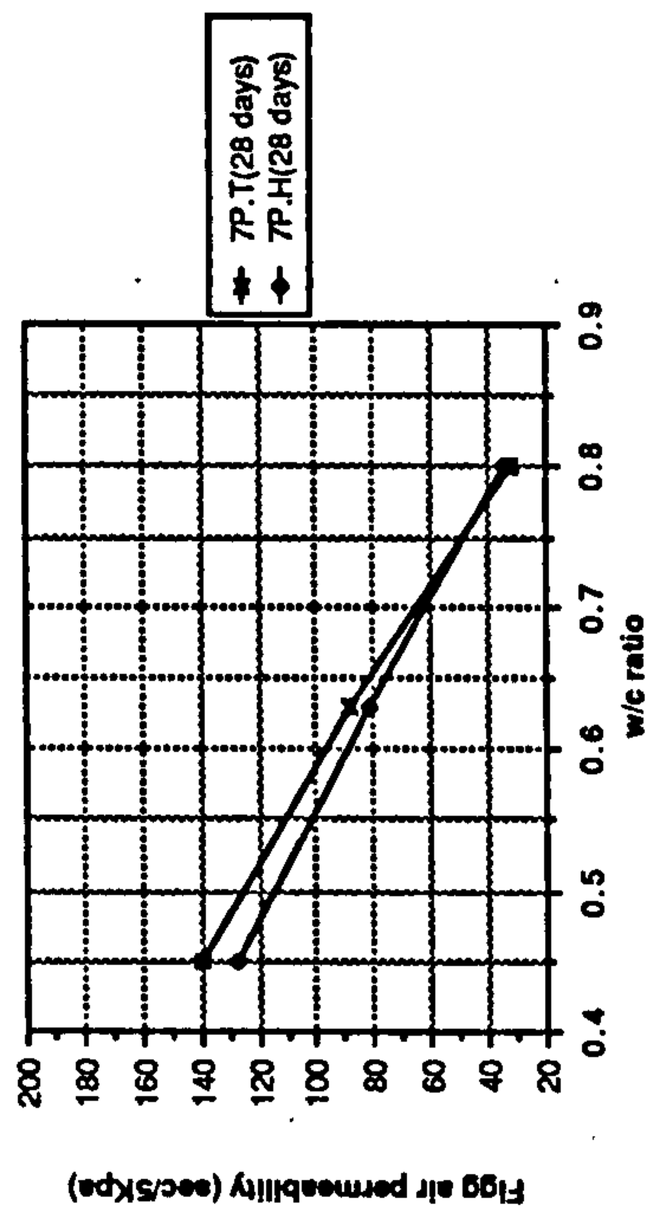

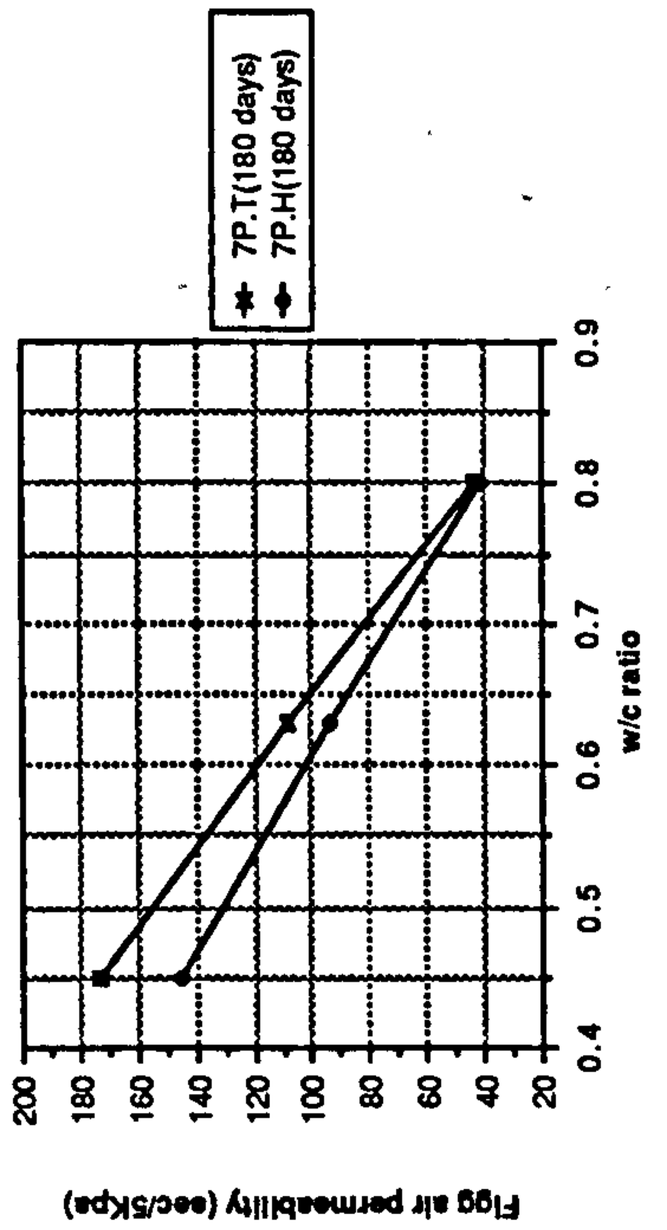

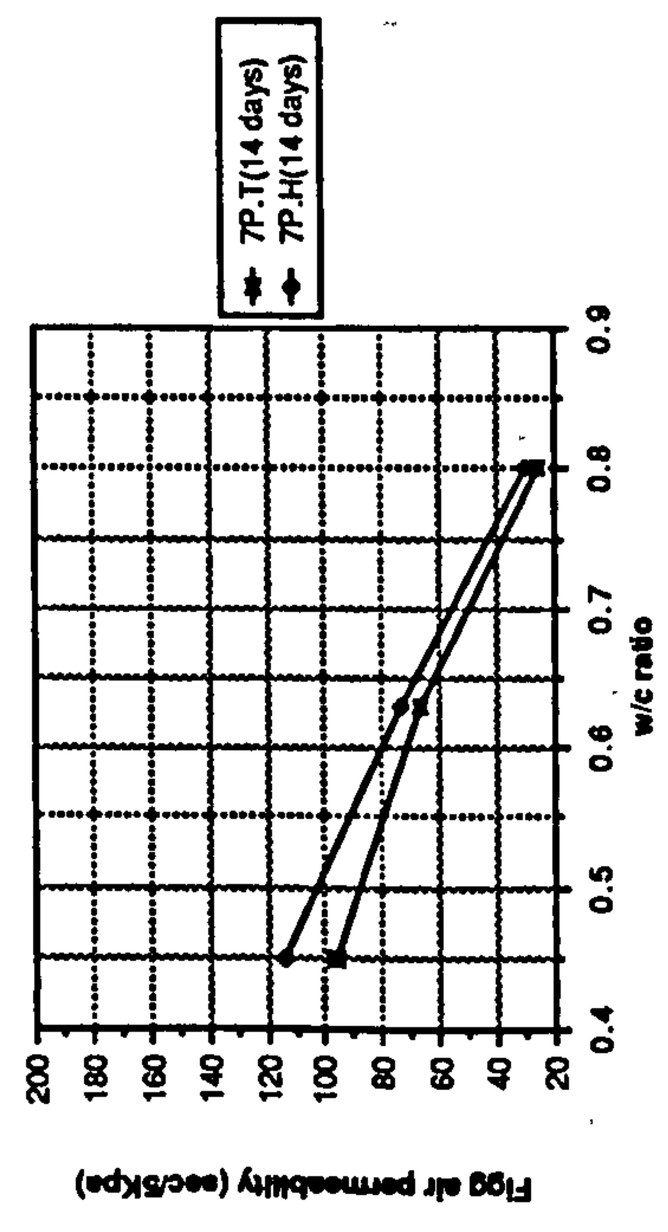

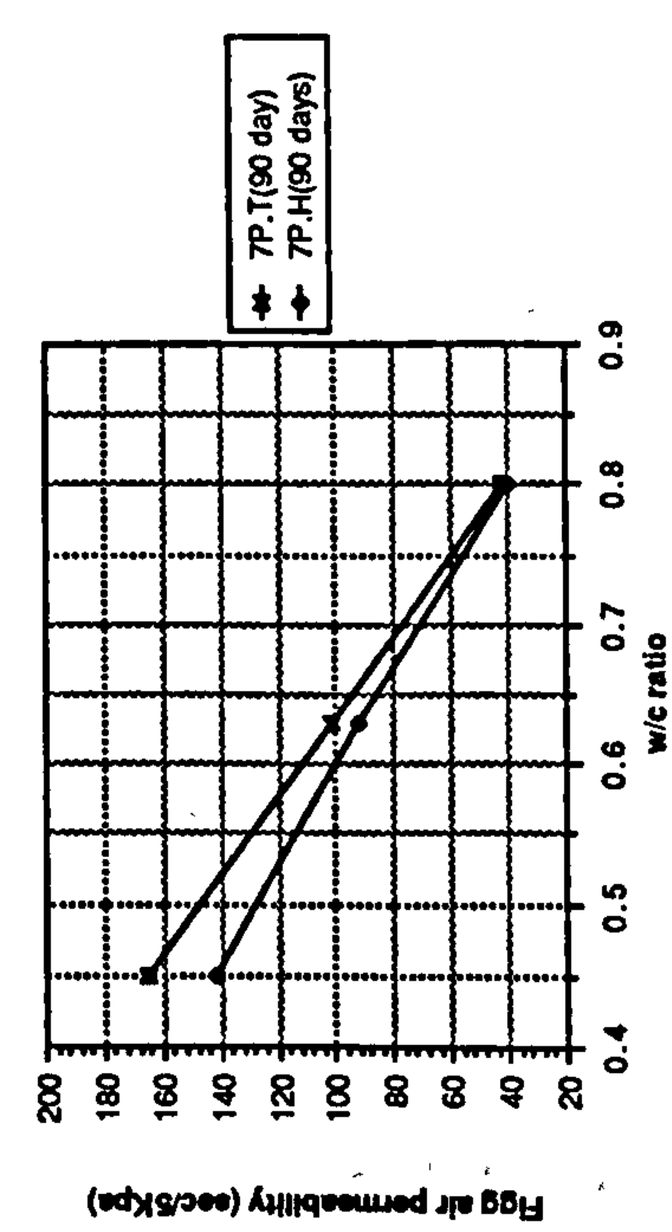

Figure 8.17 The effect of W/C ratio on the Figg air permeability of plain OPC mixes

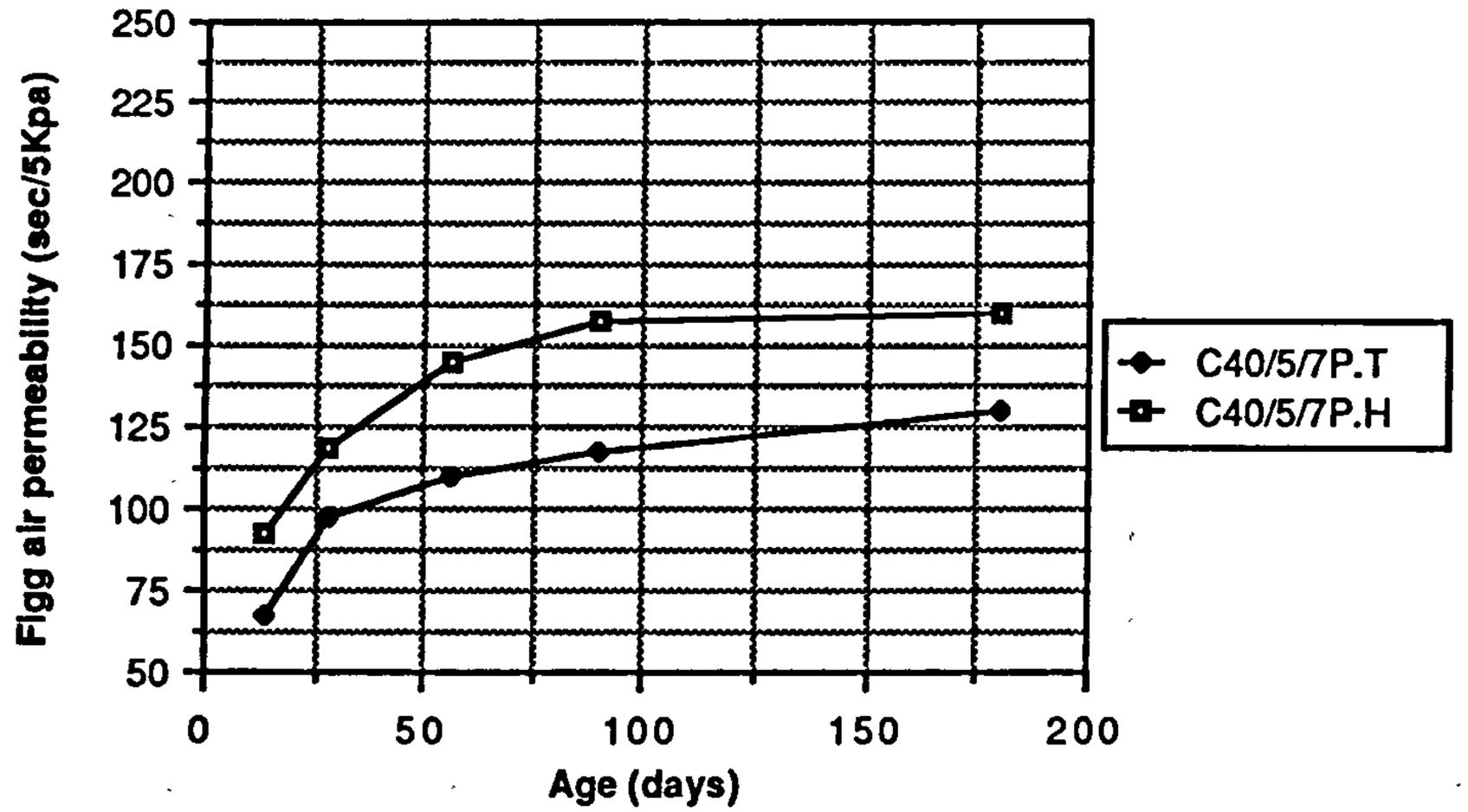

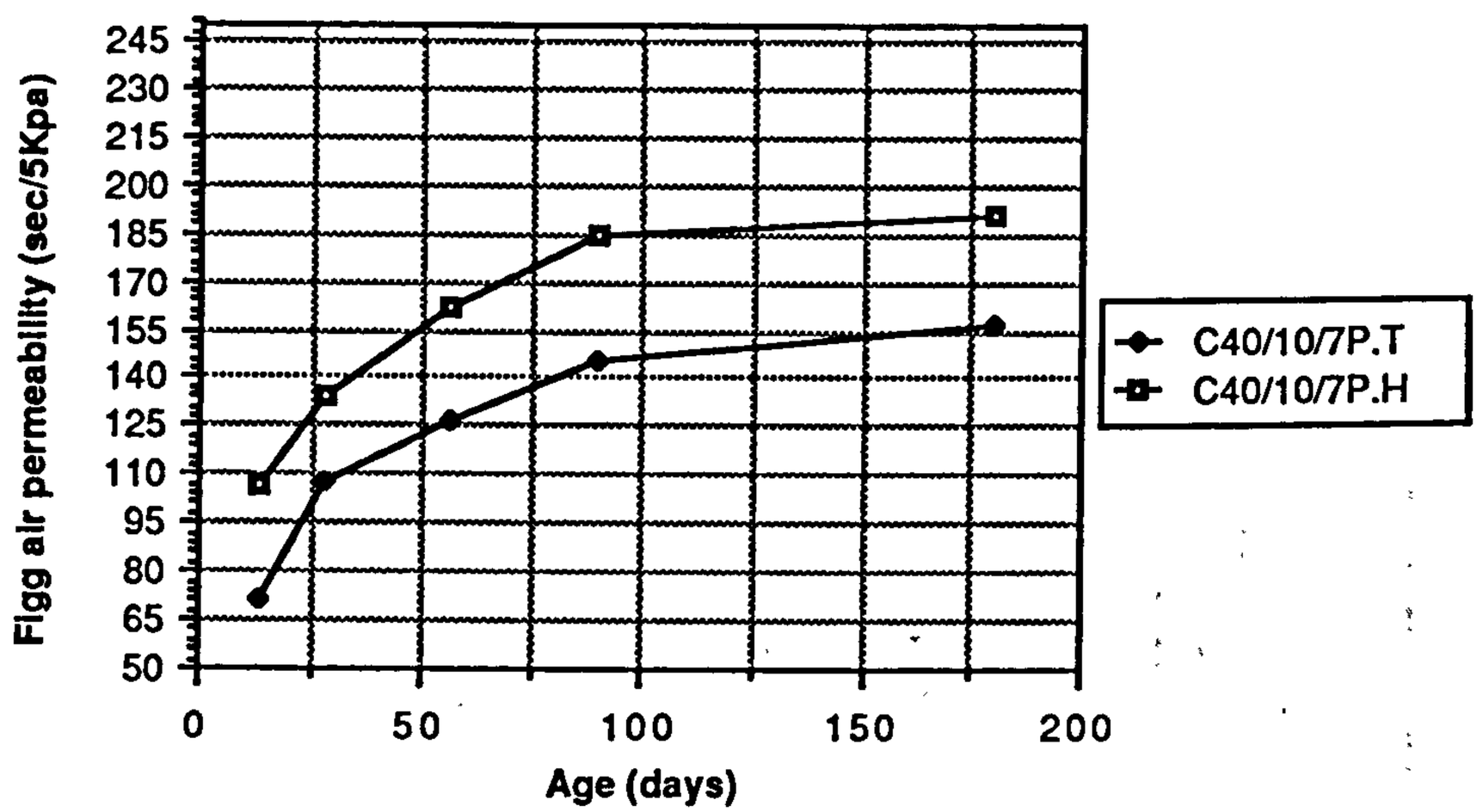

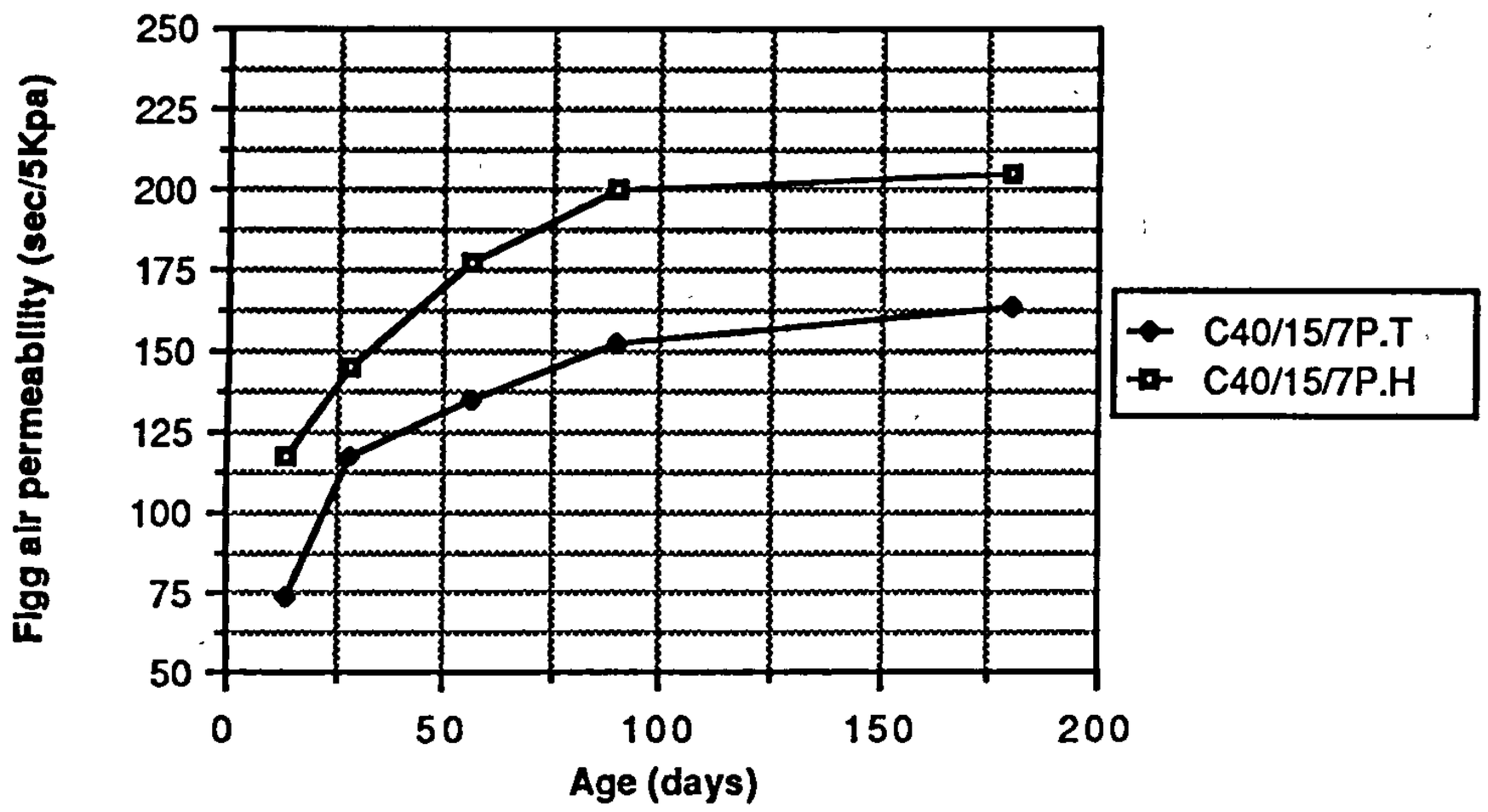

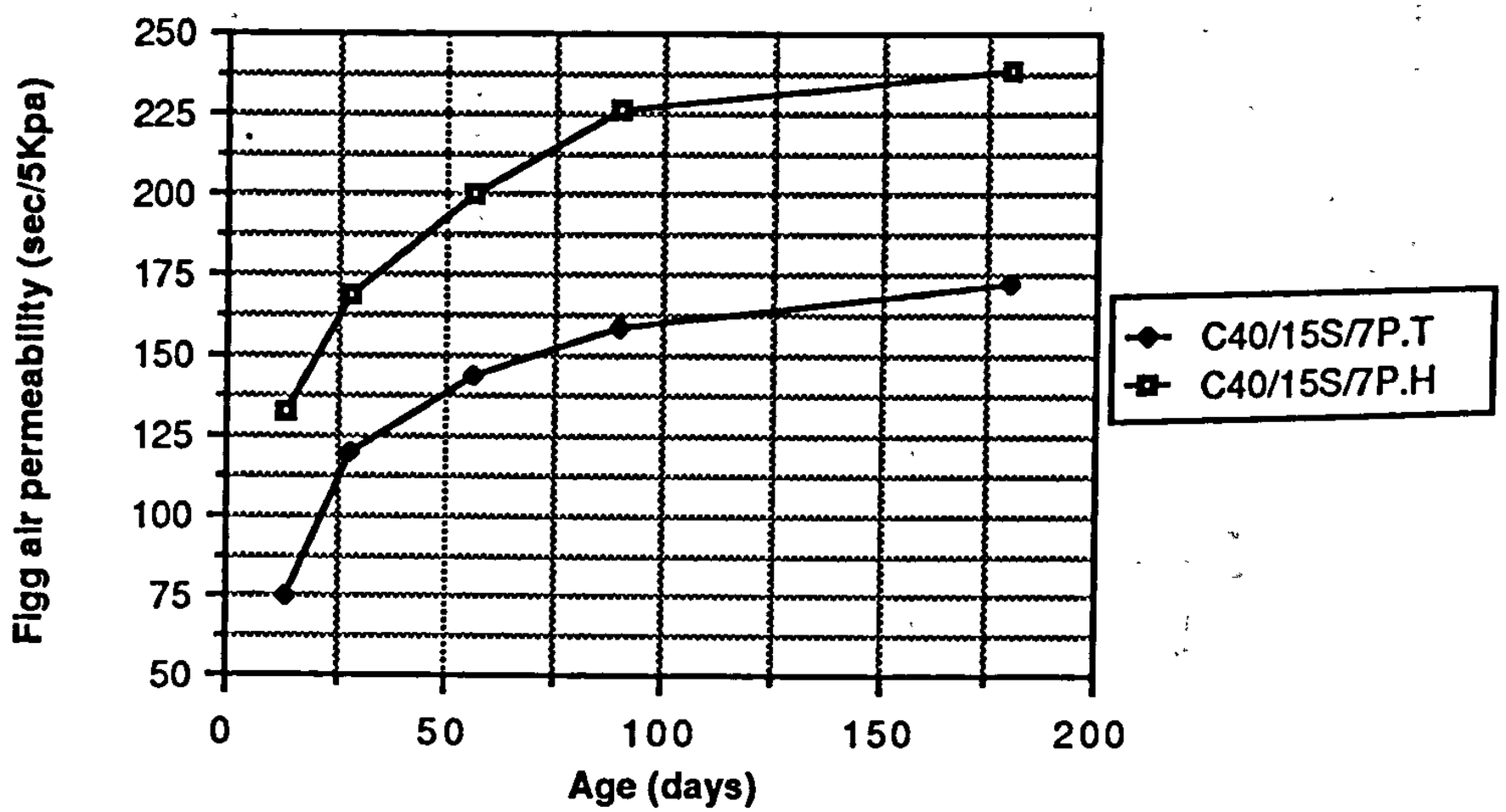

Figure 8.18 Effect of temperate and hot curing on the Figg air permeability of CSF concrete mixes

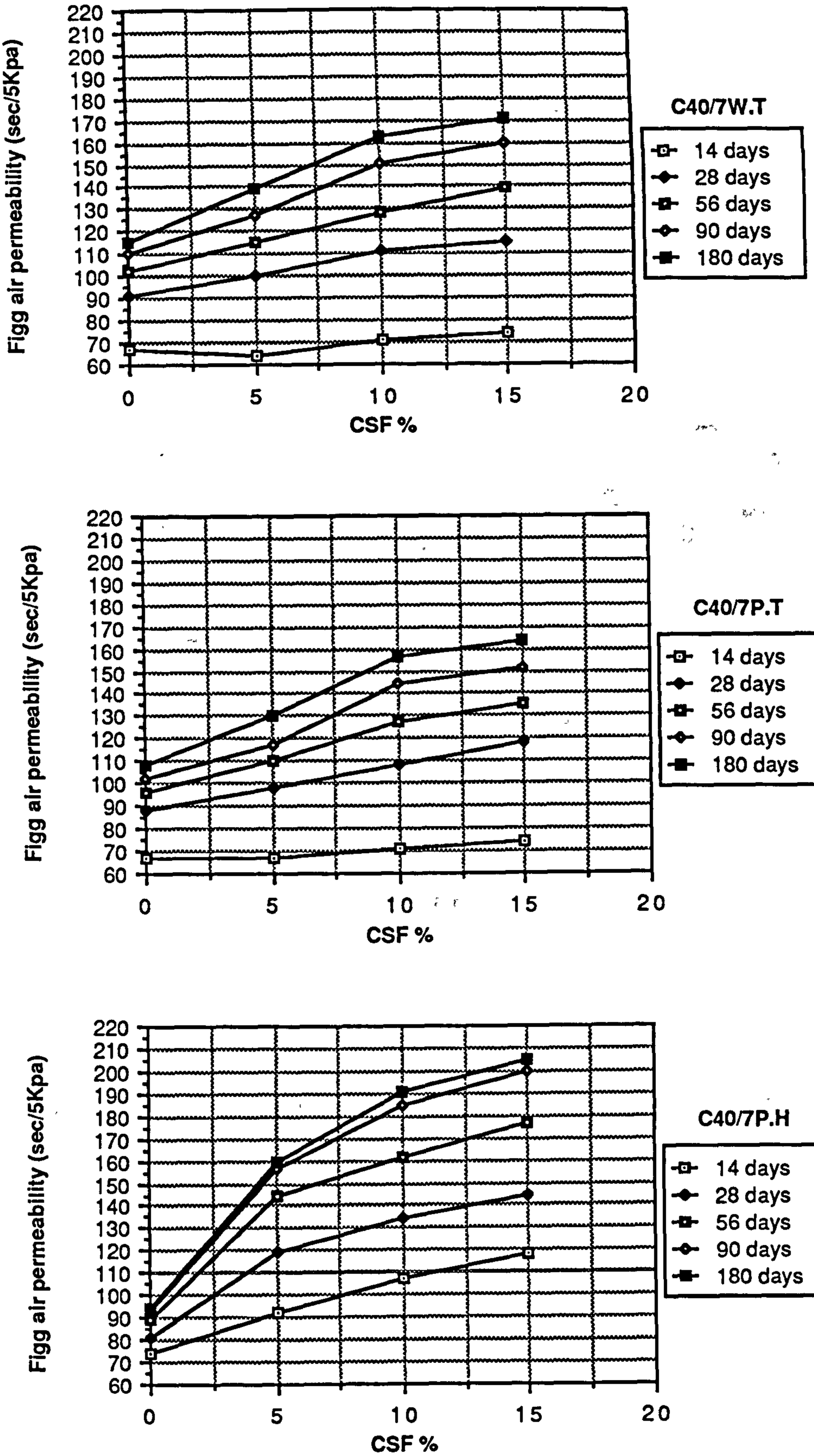

Figure 8.19 The effect of CSF content on the air permeability of CSF mixes

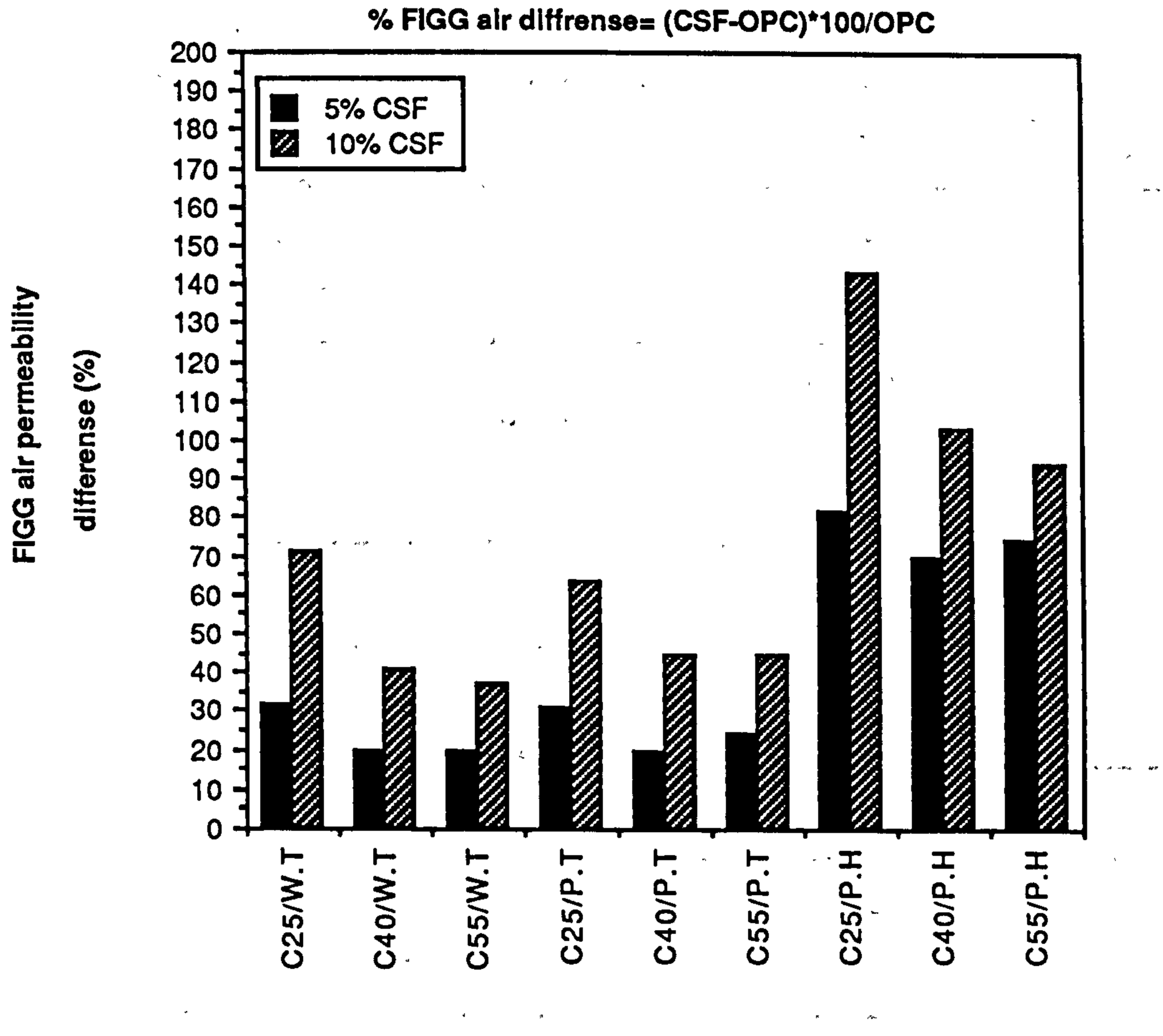

Figure 8.20 Percent reduction in Figg air permeability caused by CSF addition in lean, medium and rich concrete mixes

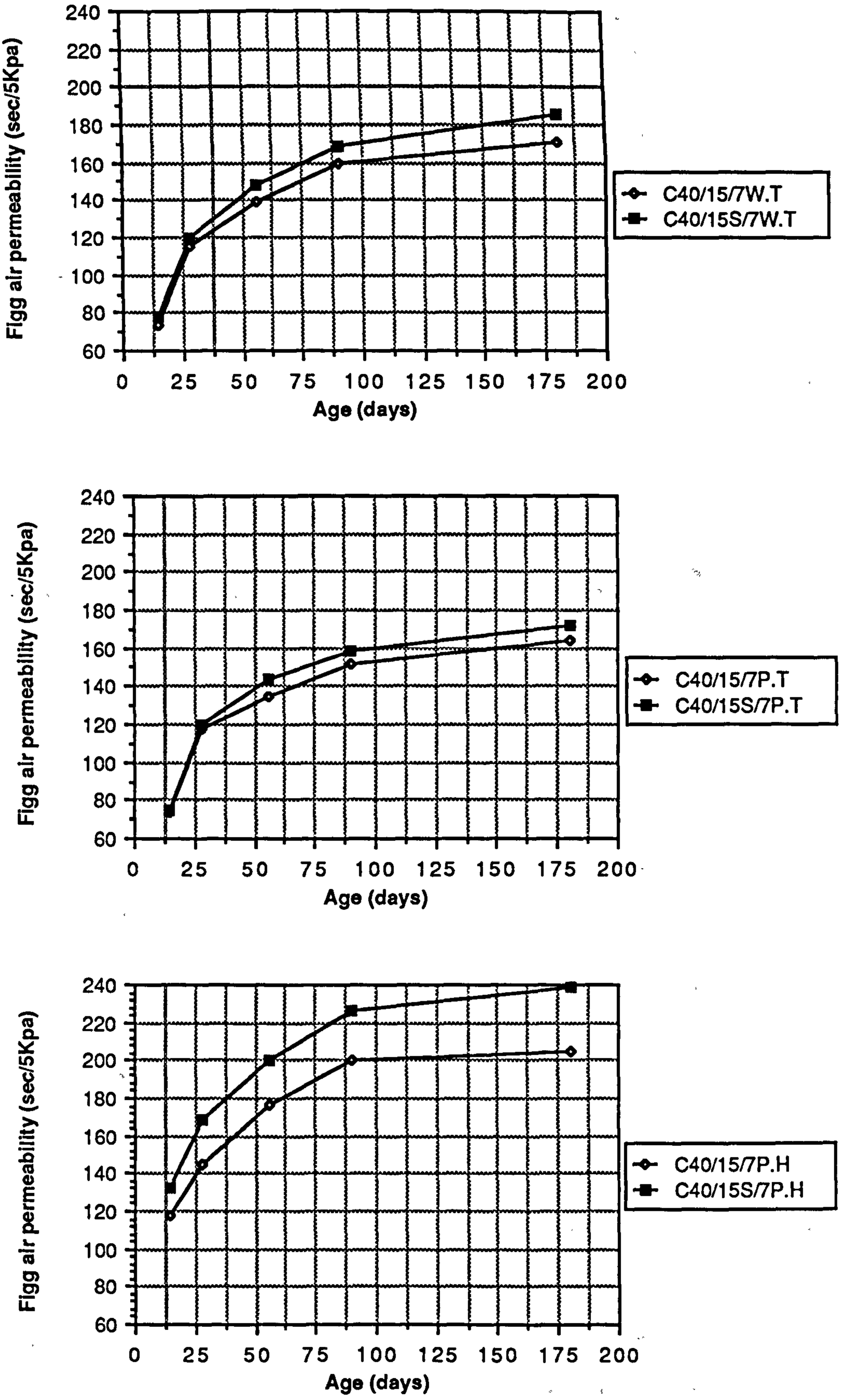

Figure 8.21 Effect of superplasticizer on the Figg air permeability of CSF mixes

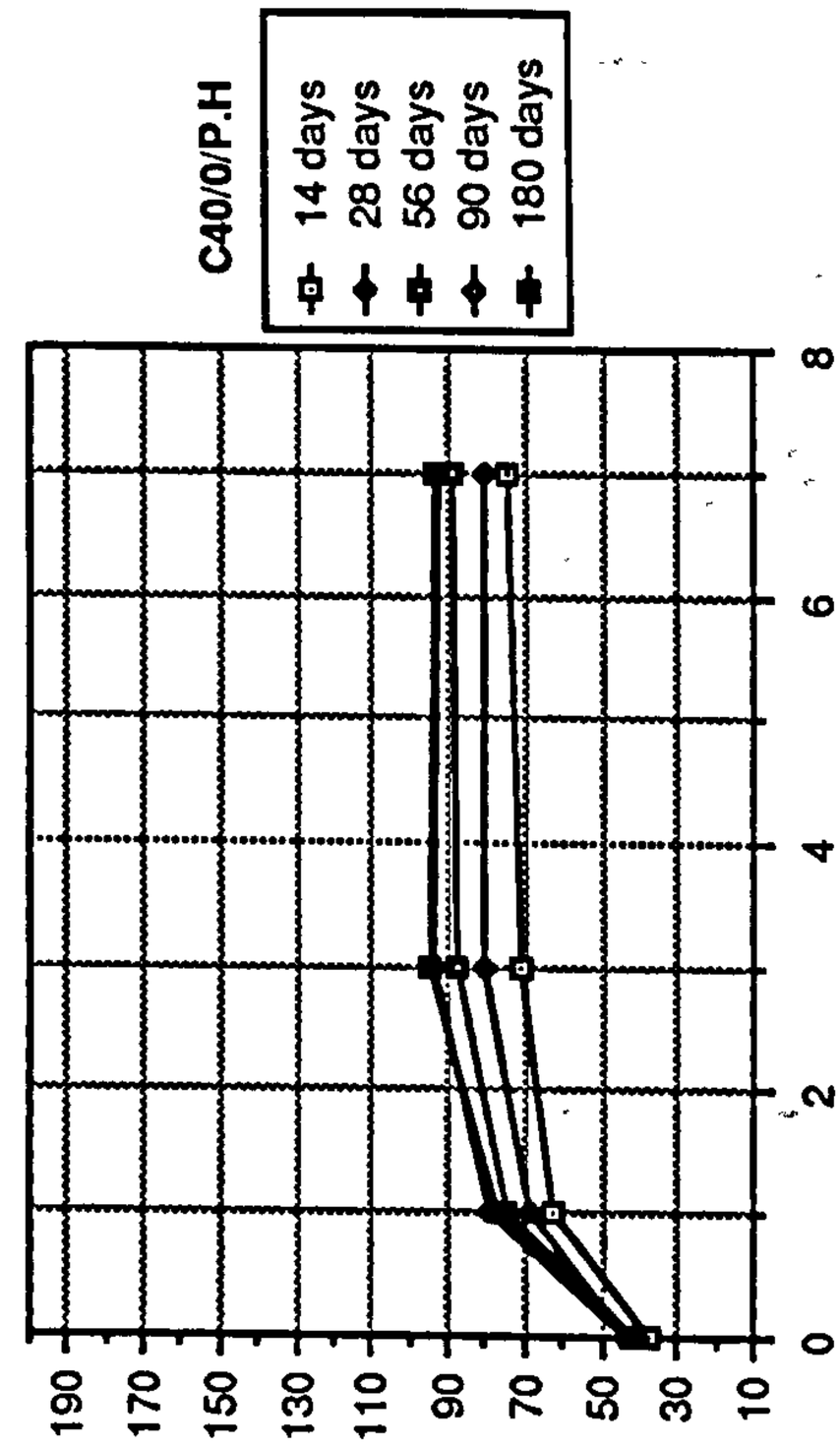

Figg air permeability of plain OPC

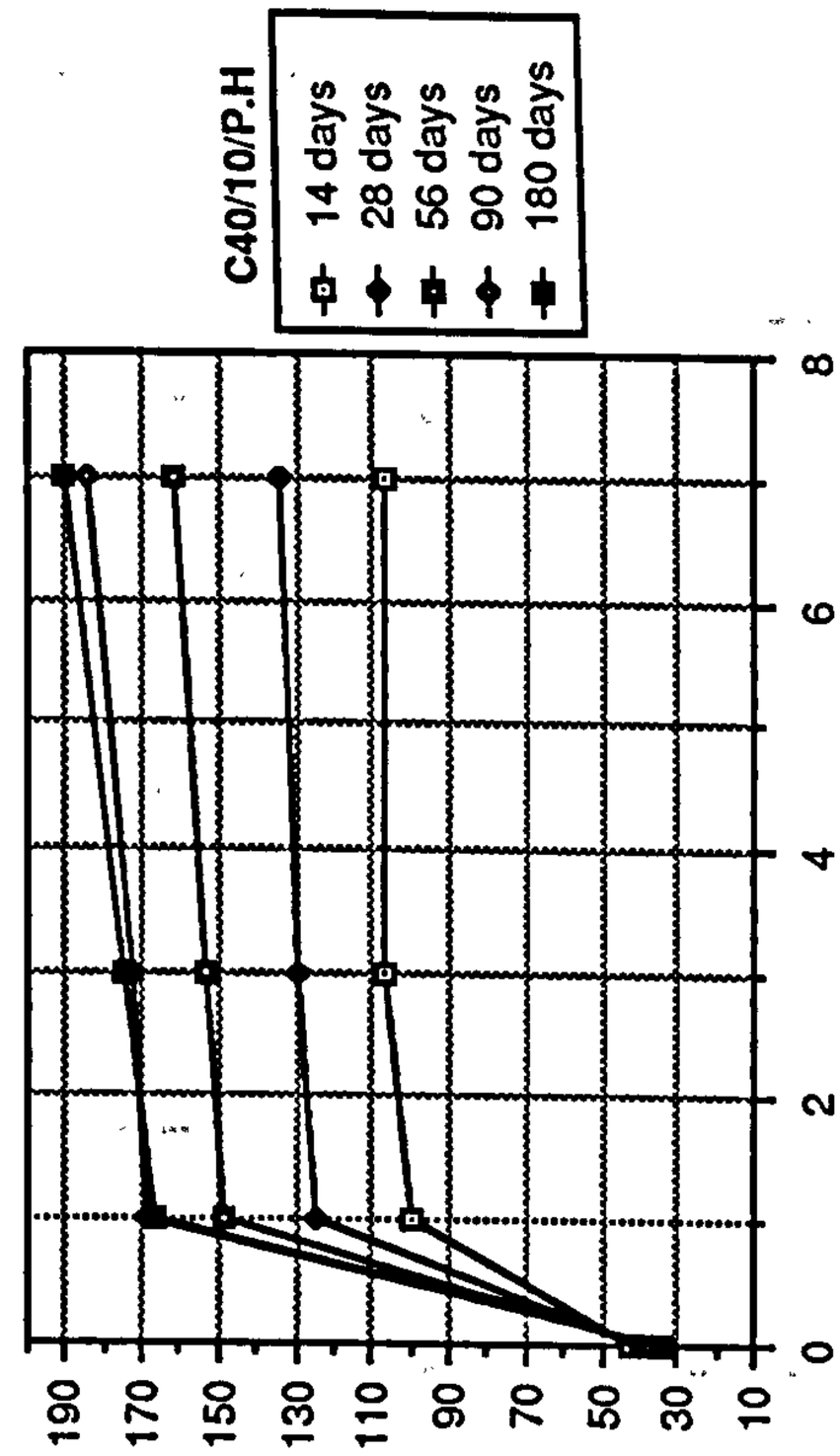

Figg air permeability of CSF

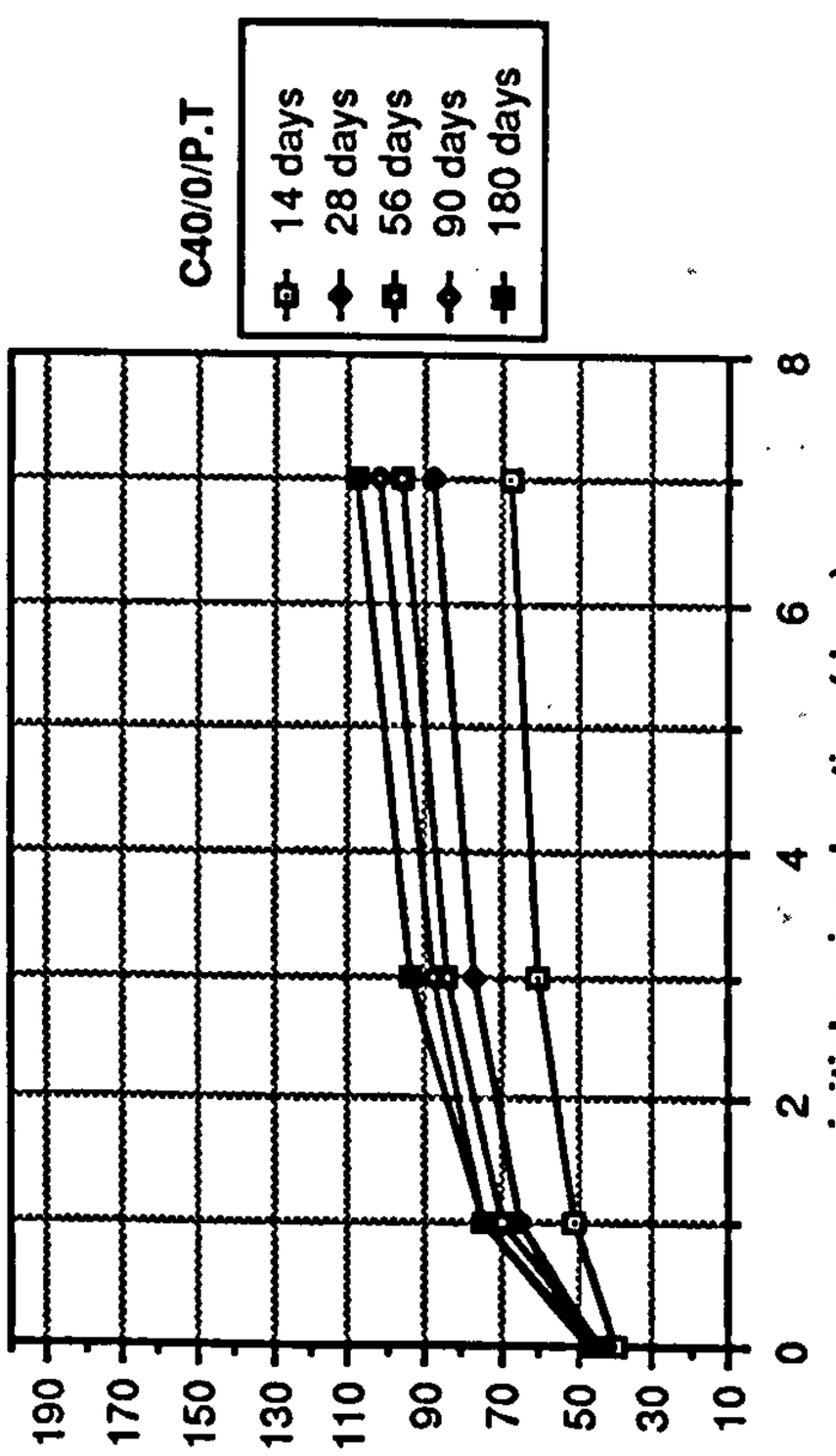

Figure 8.22 Effect of initial curing duration on

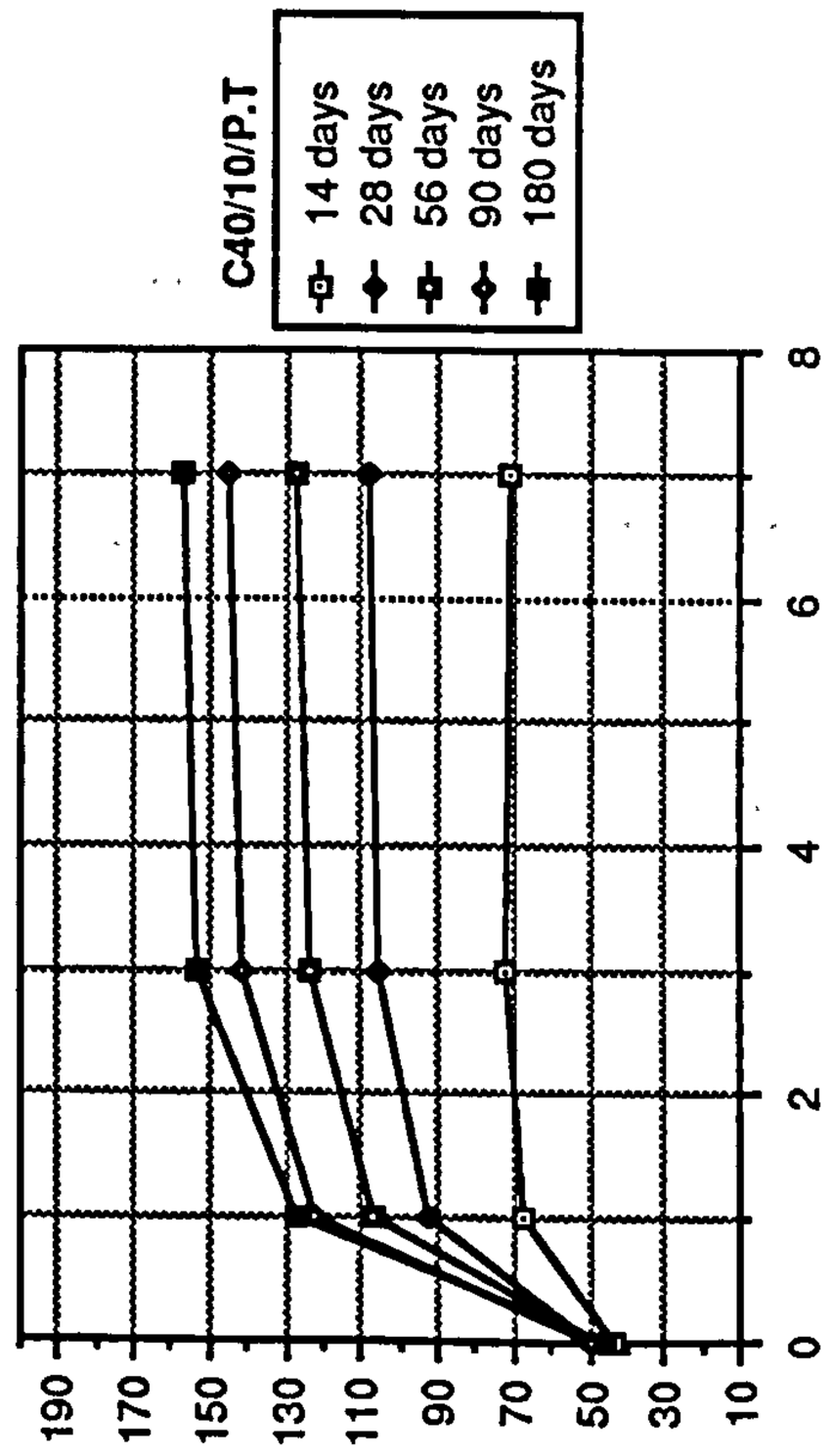

Figure 8.23 Effect of initial curing duration on

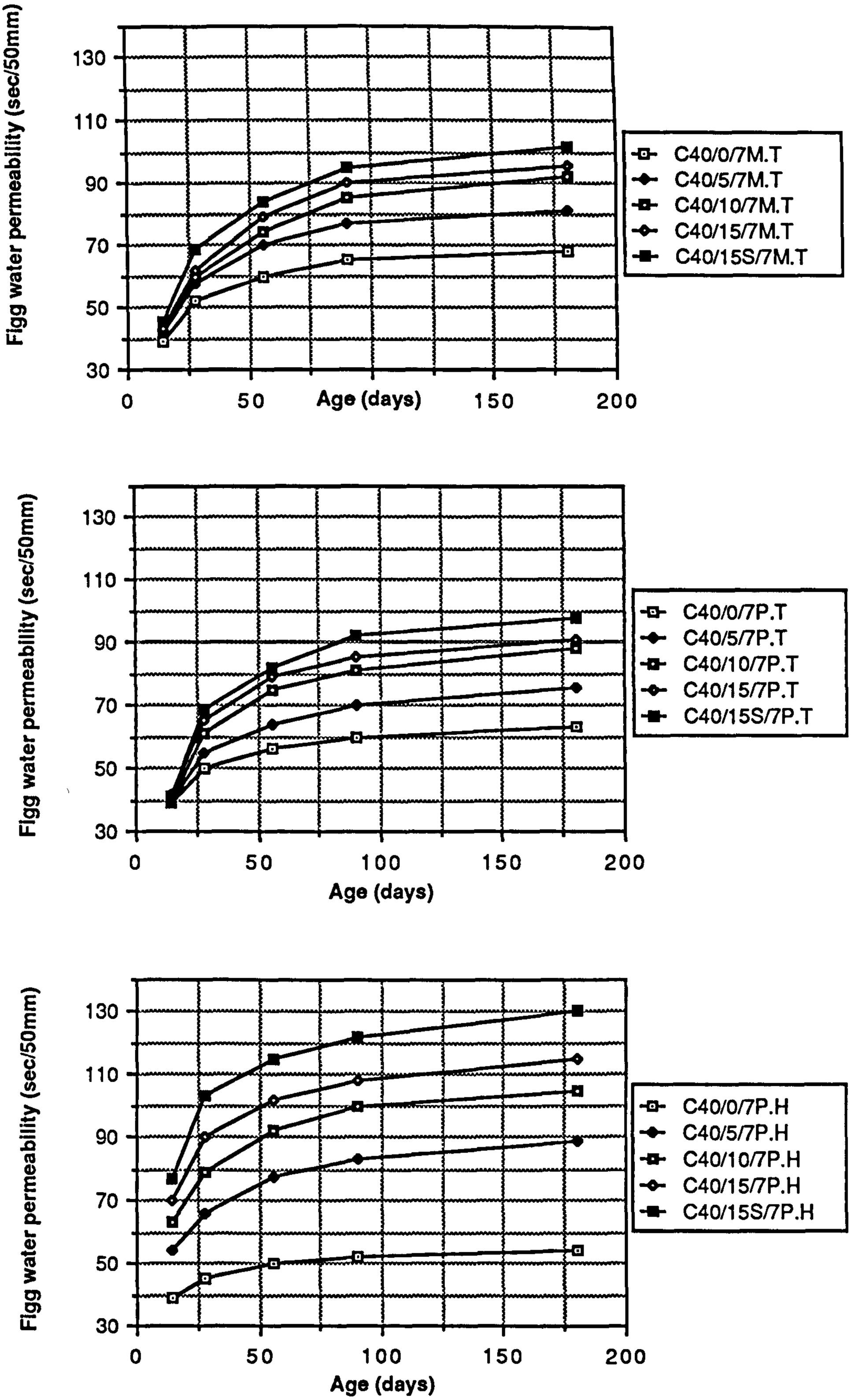

Figure 8.24 Effect of age on Figg water permeability of plain and CSF concrete mixes

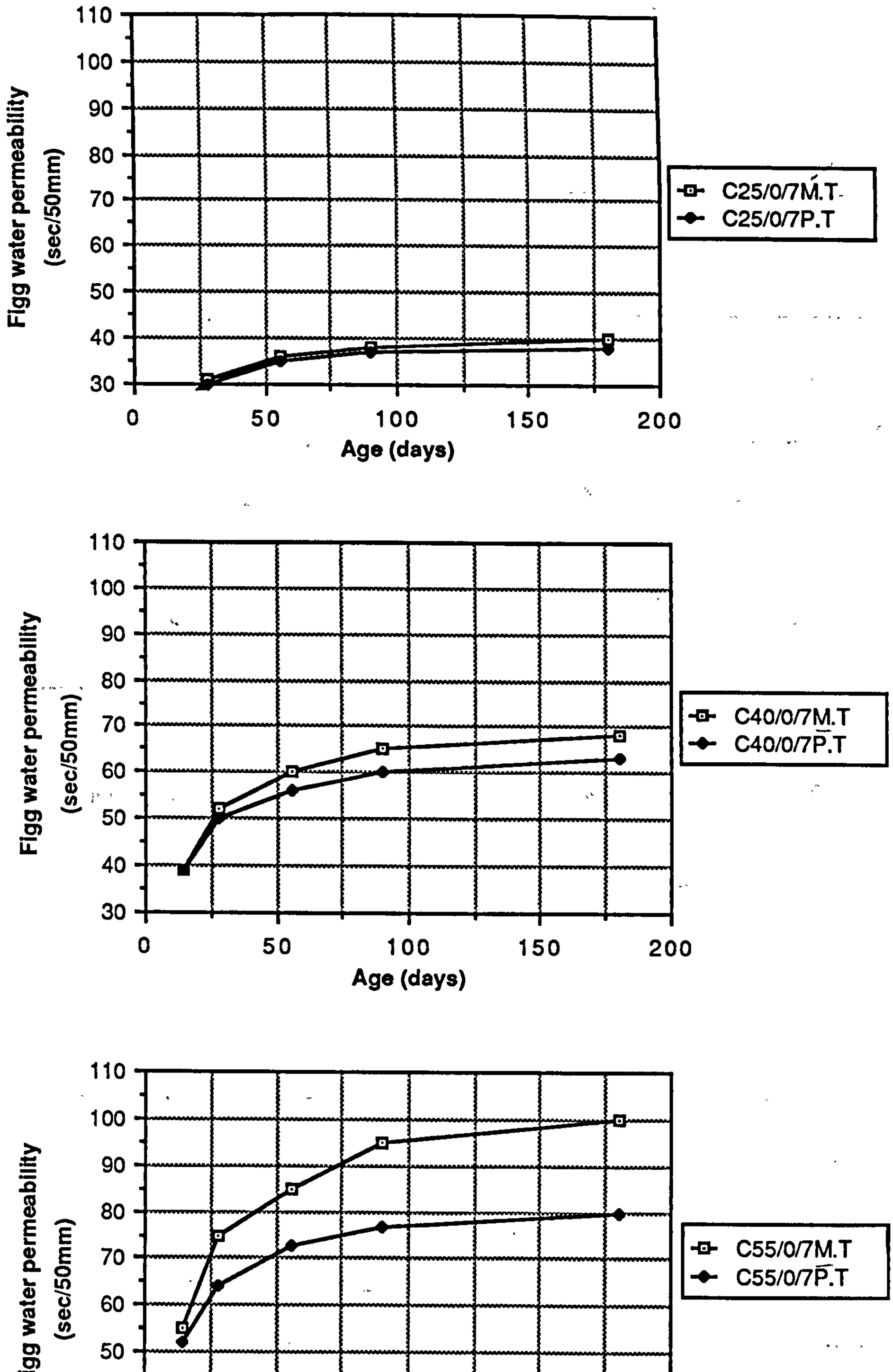

Figure 8.25 Effect of water and polythene curing on the Figg water permeability of plain OPC mixes

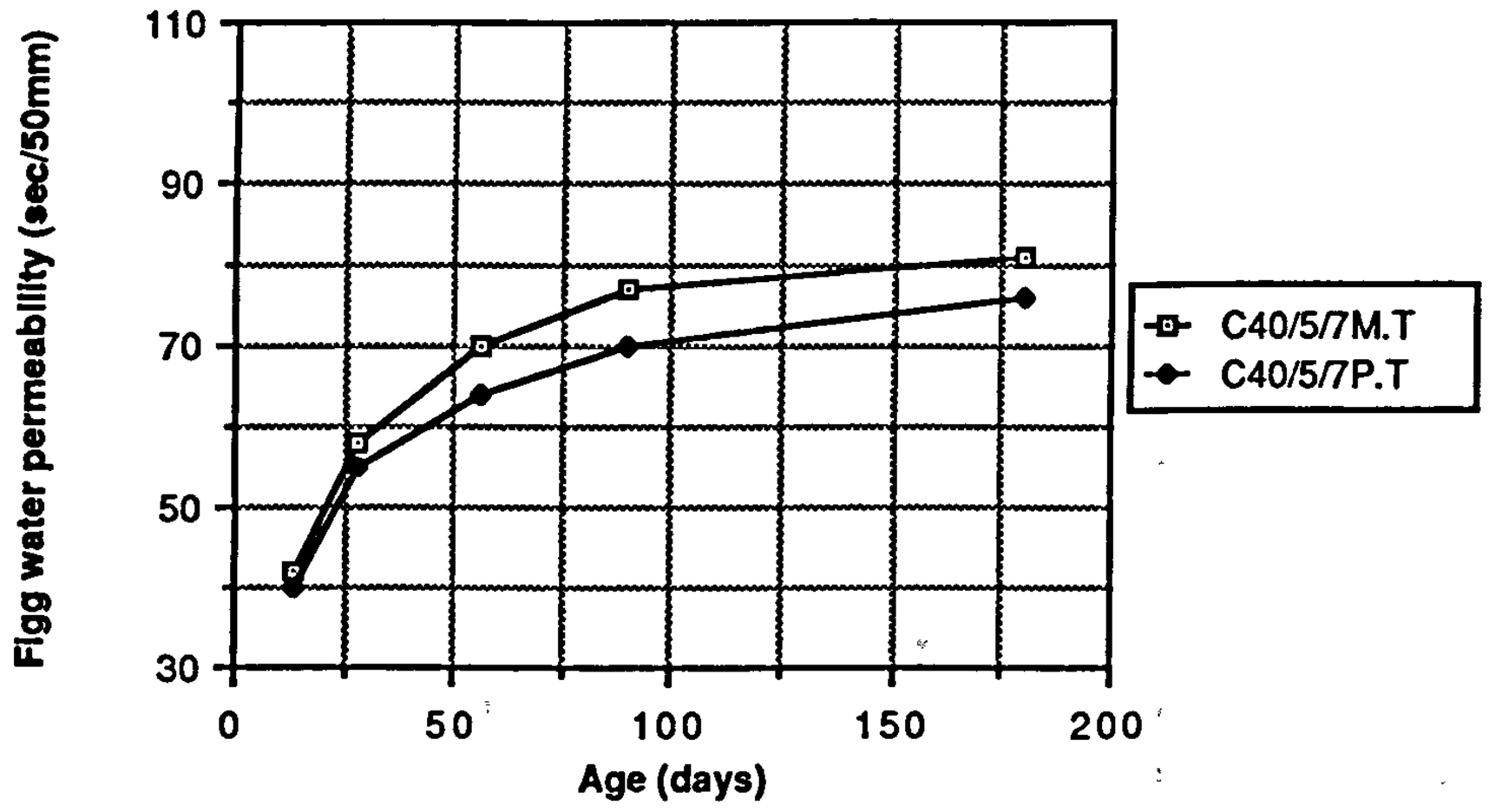

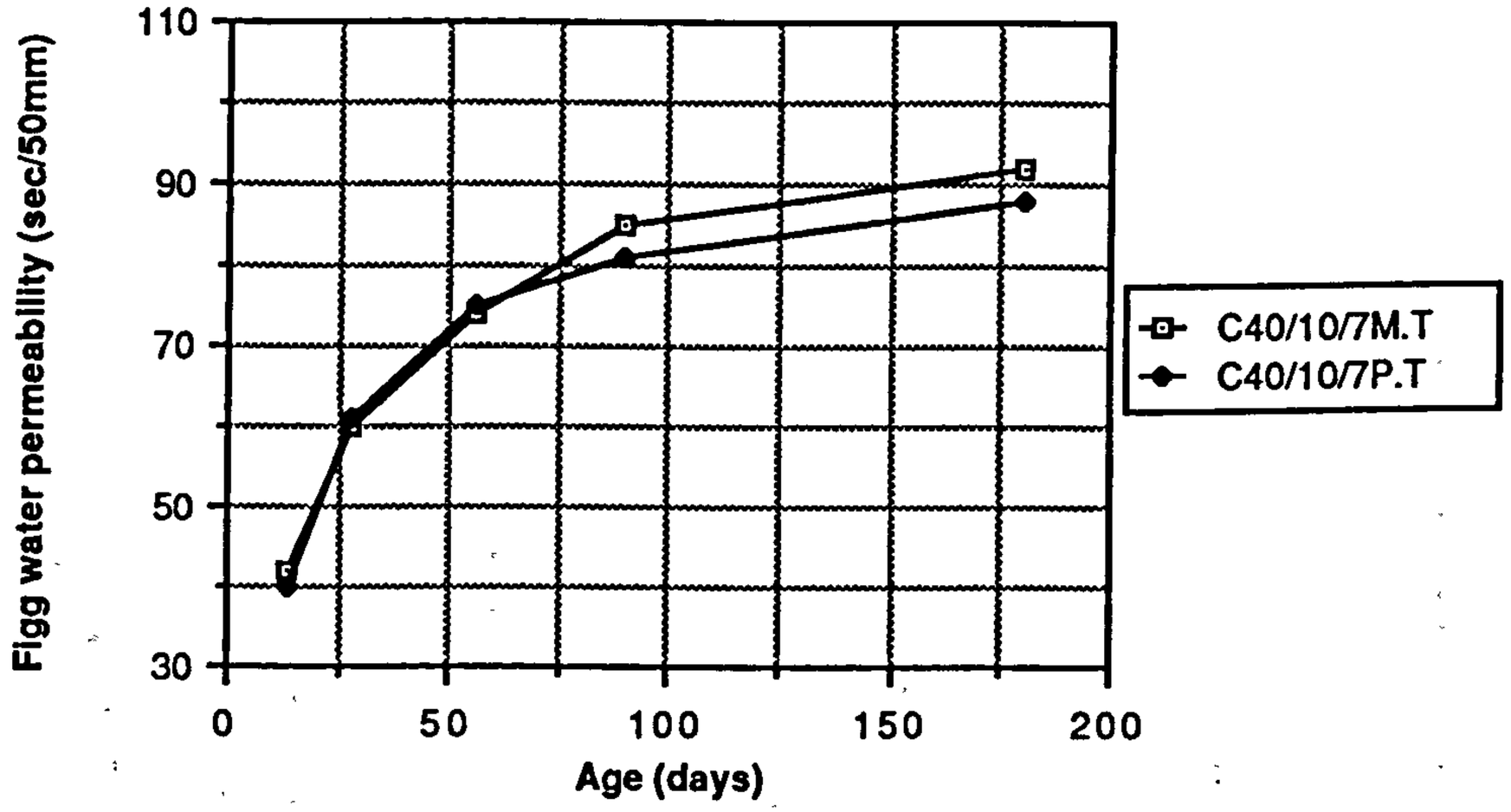

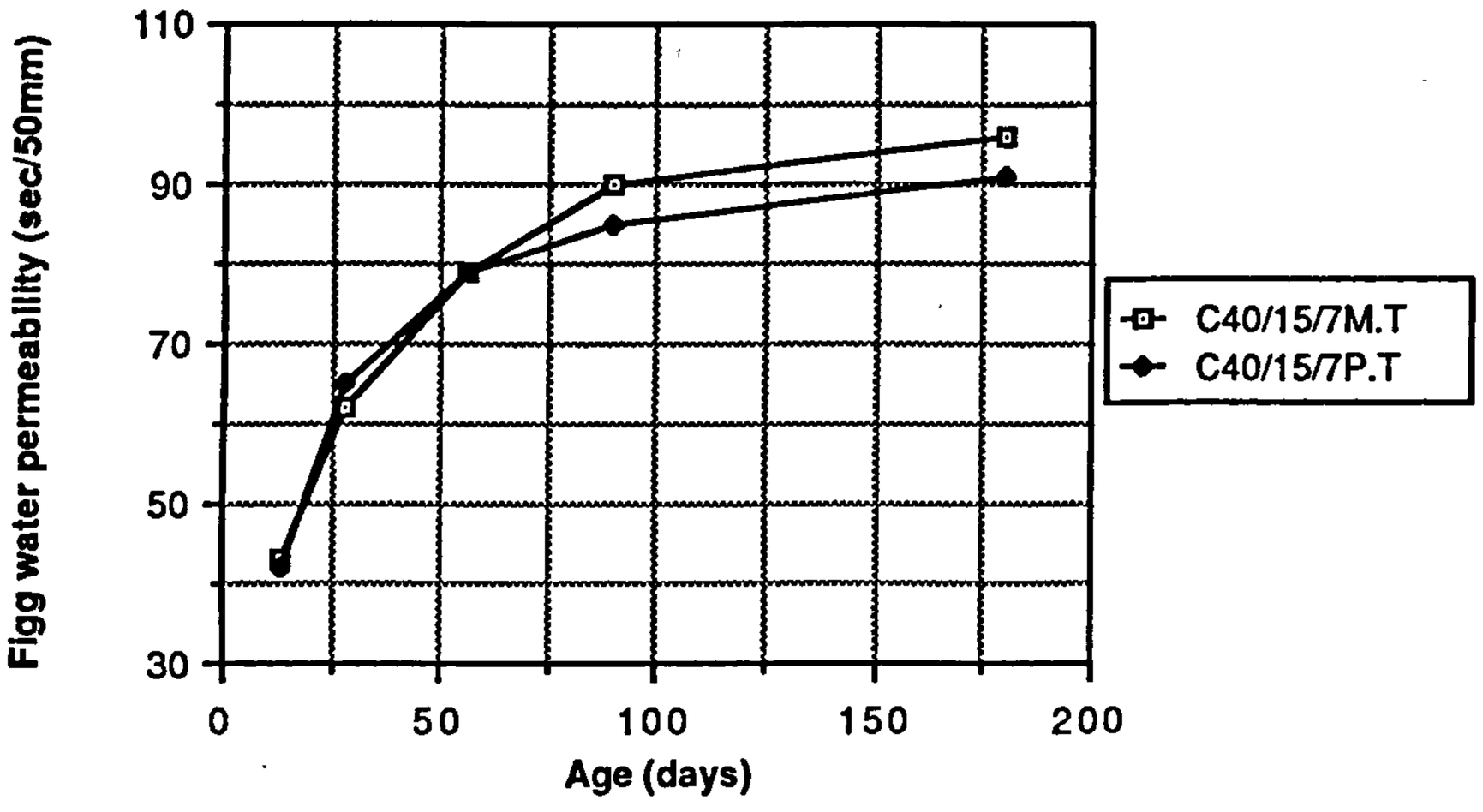

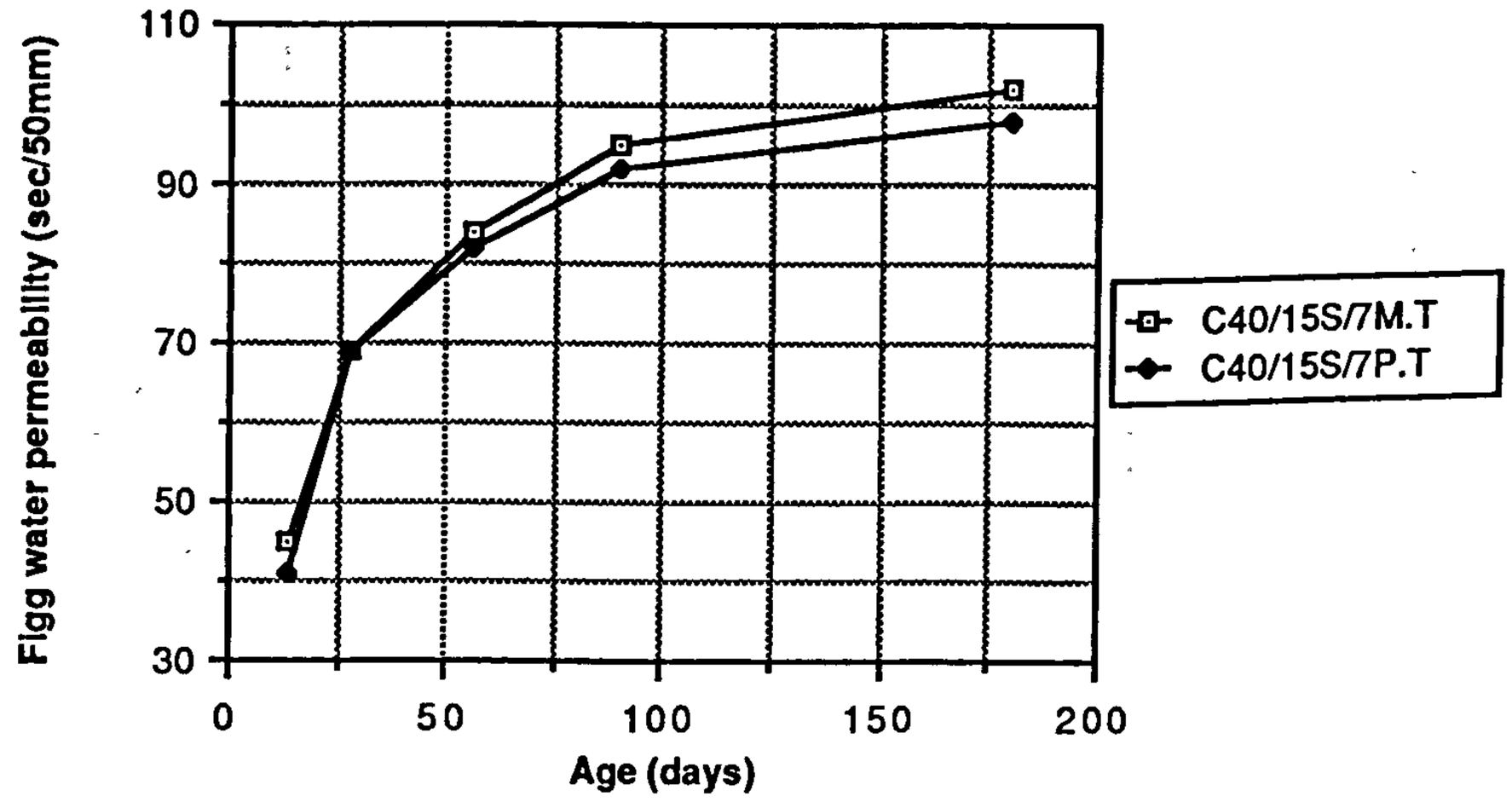

Figure 8.26 Effect of water and polythene curing on the Figg water permeability of CSF mixes

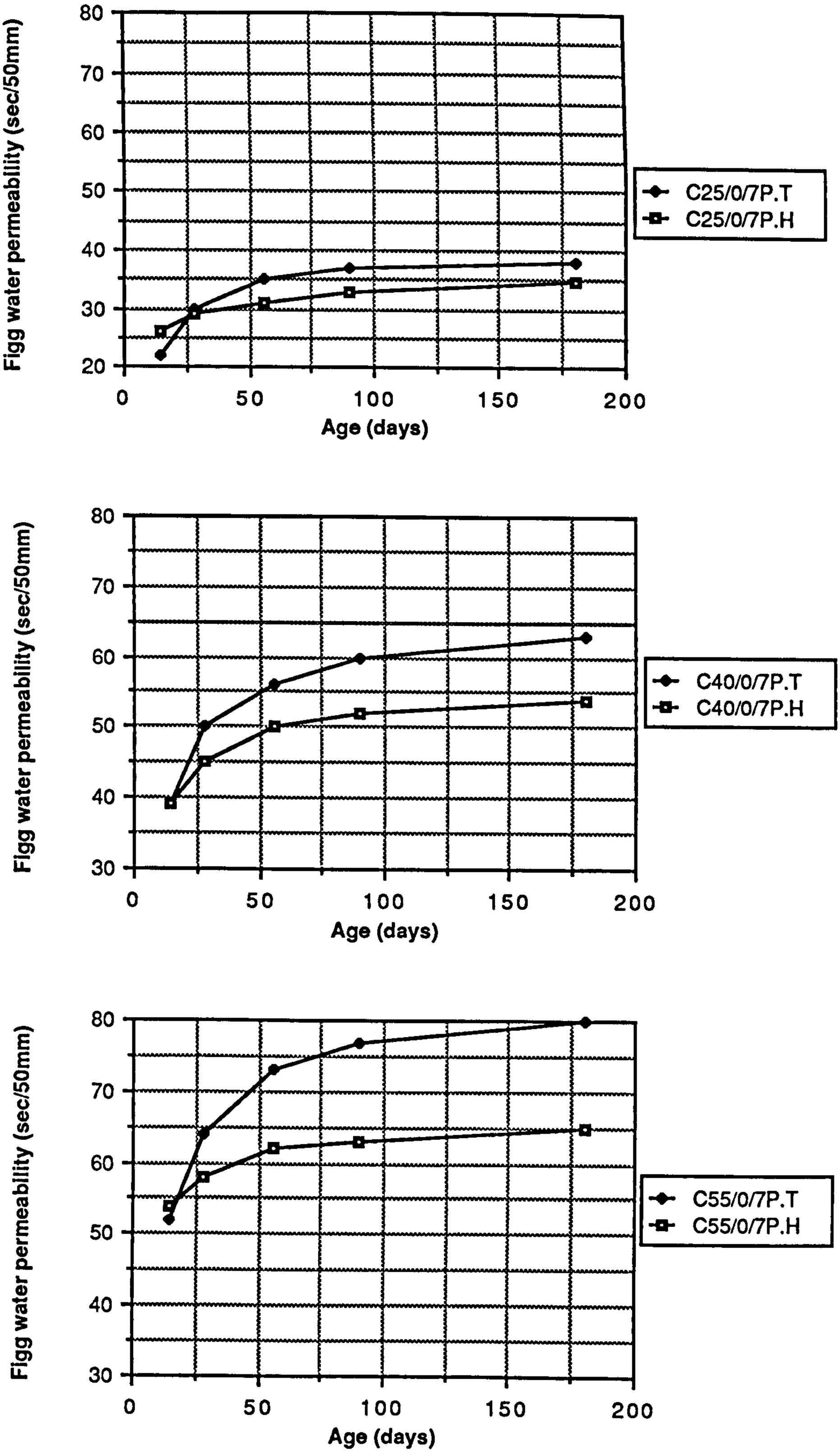

Figure 8.27 Effect of temperate and hot curing environment on the Figg water permeability

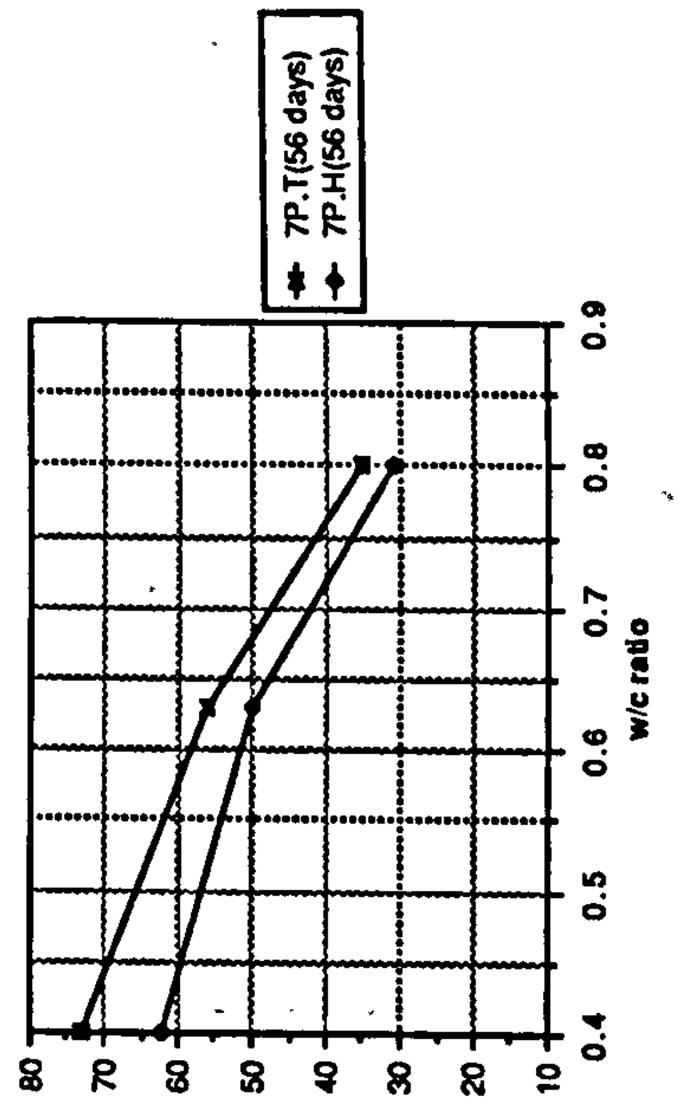

Figure 8.28 The effect of W/C ratio on the Figg water permeability of plain OPC mixes

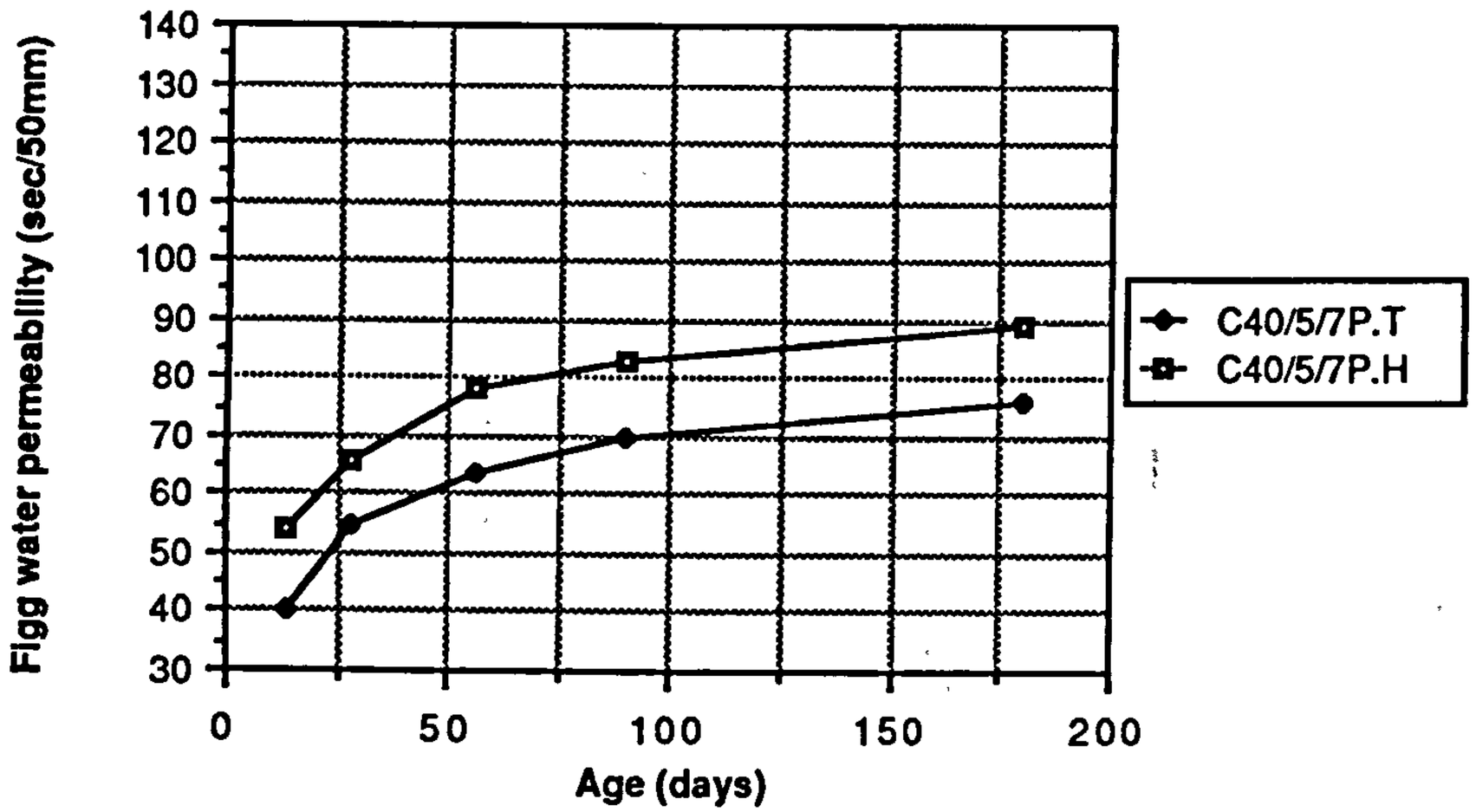

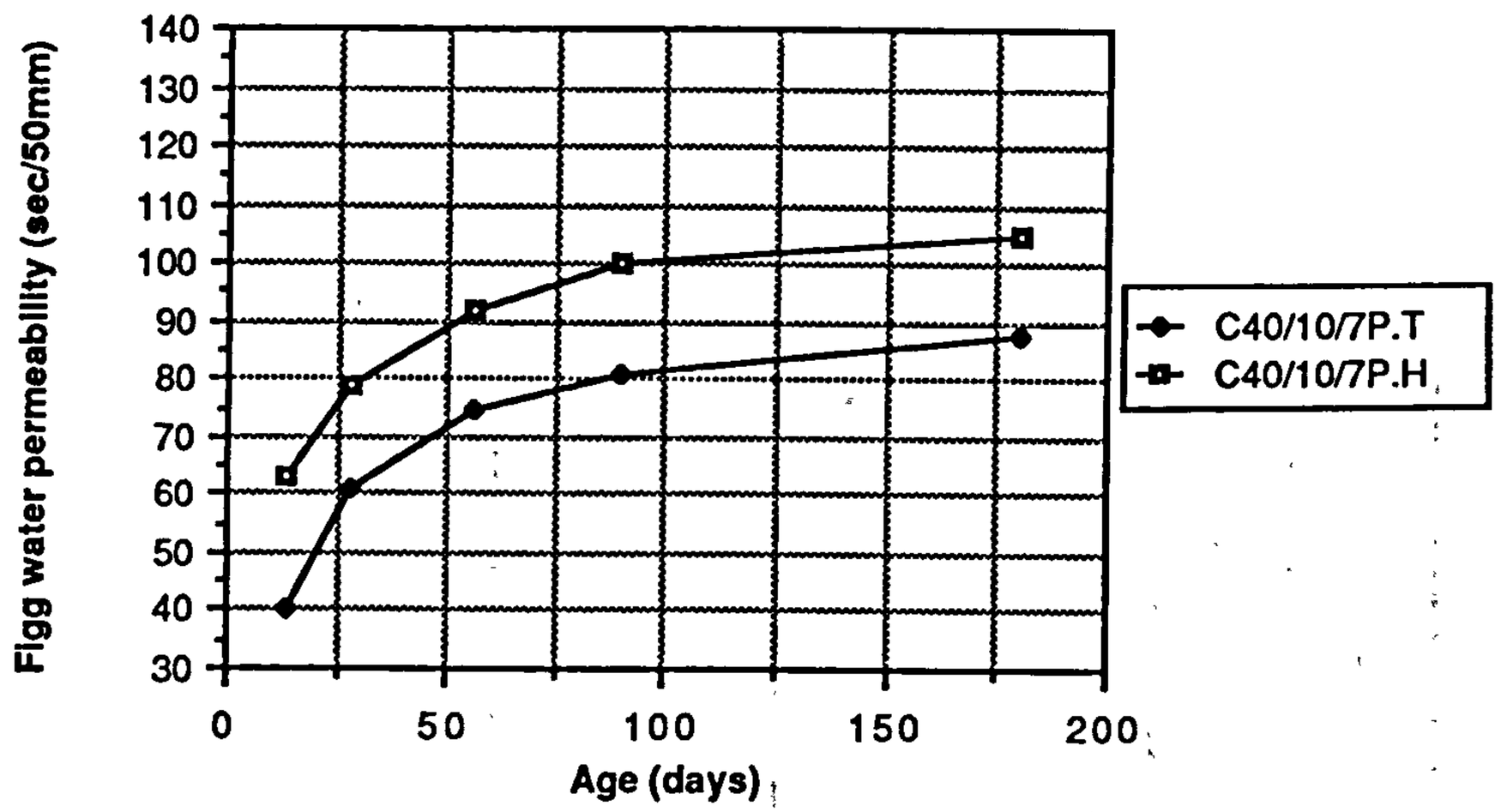

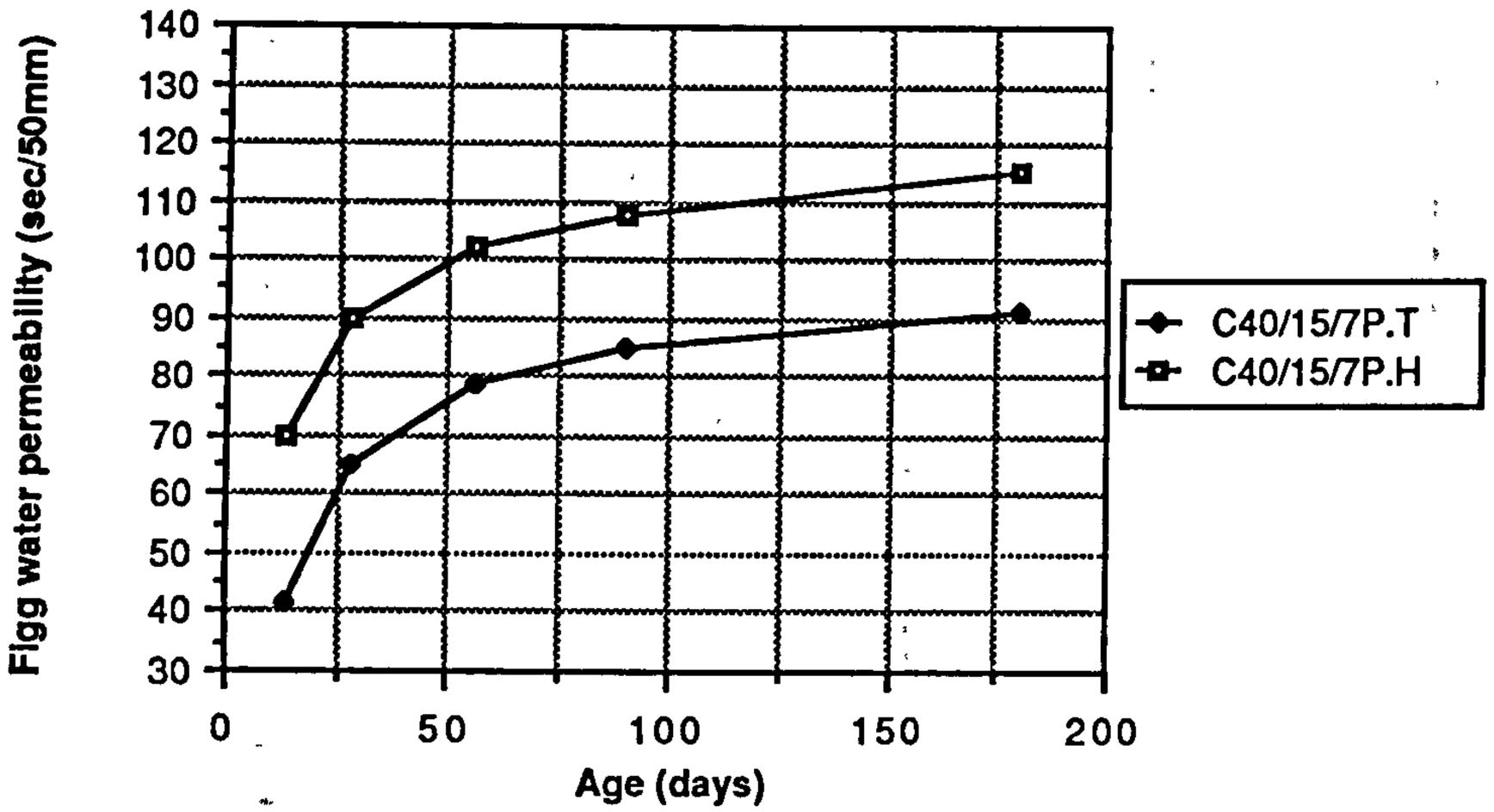

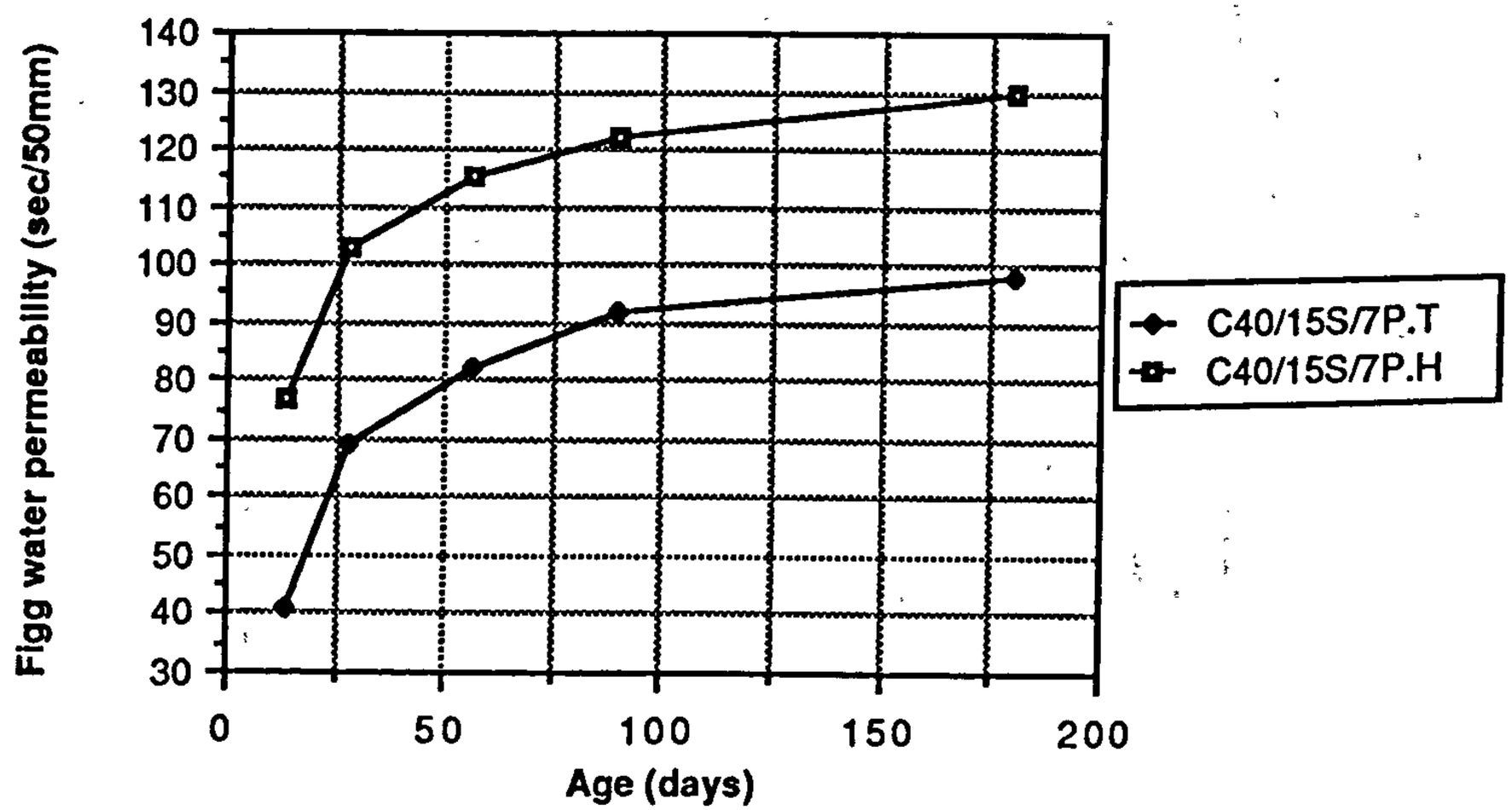

Figure 8.29 The effect of temperate and hot curing on the Figg water permeability of CSF mixes

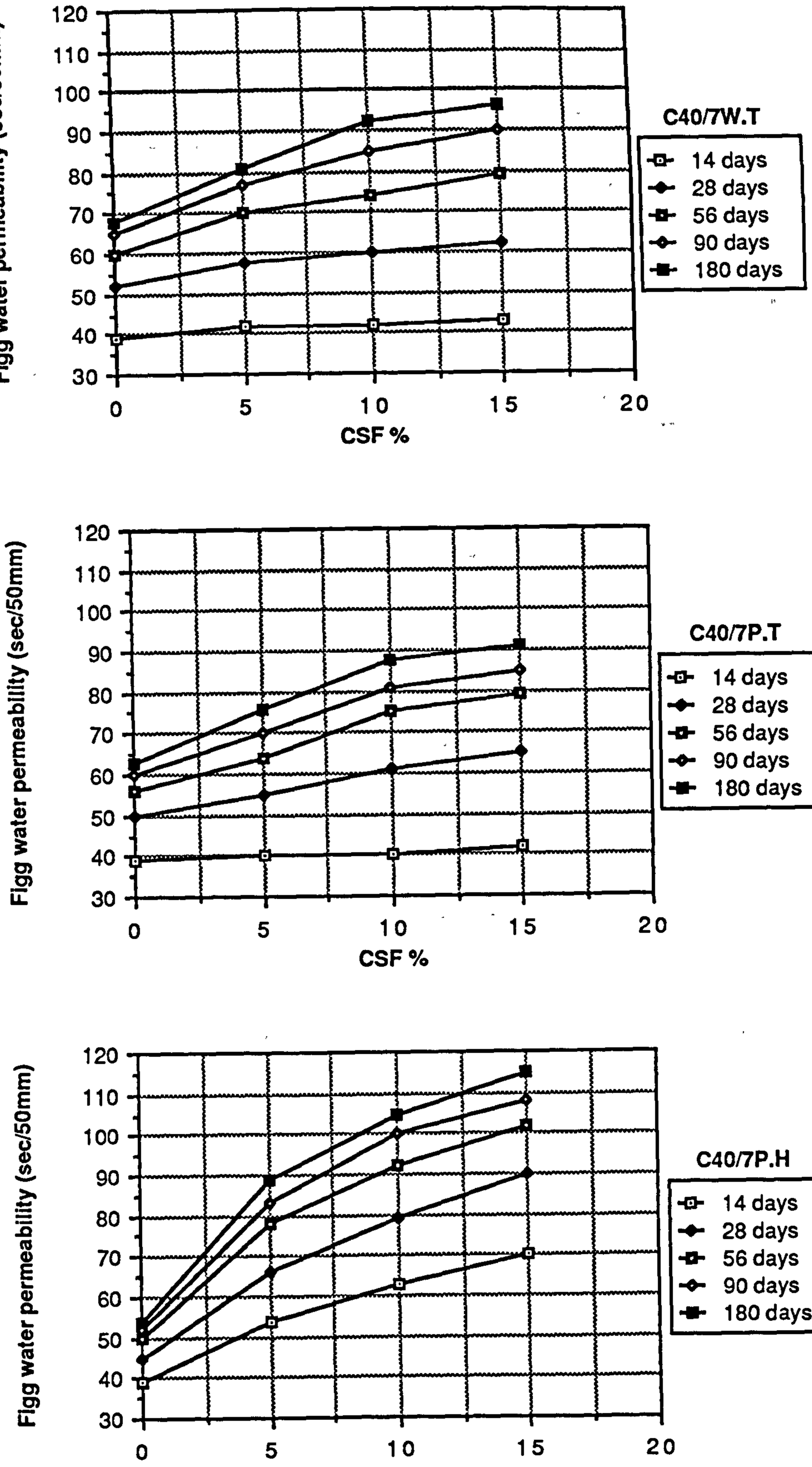

Figure 8.30 The effect of CSF content on the Figg water permeability

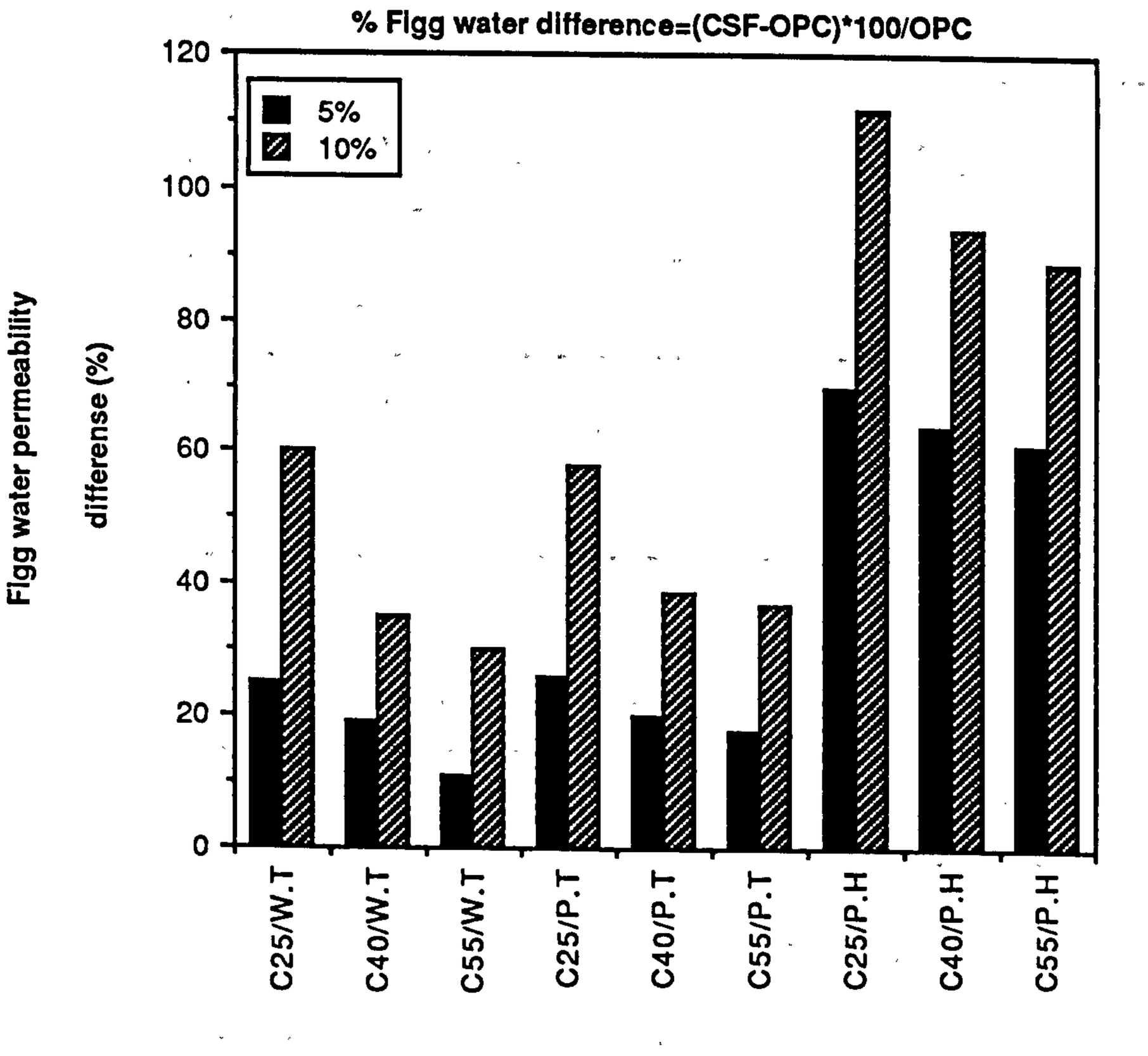

Figure 8.31 Percent reduction in water permeability caused by CSF addition to lean, medium and rich mixes

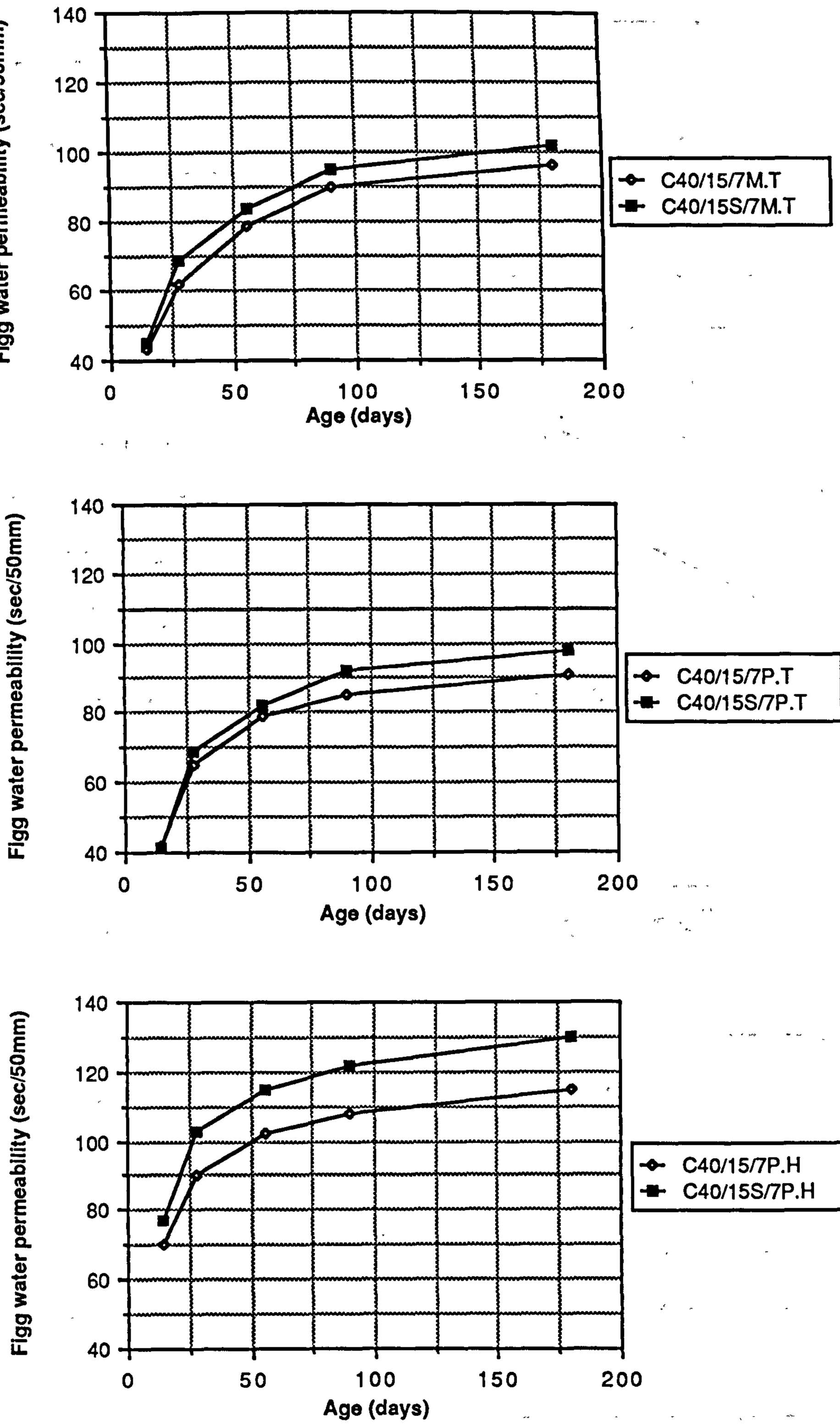

Figure 8.32 Effect of superplasticizer on the Figg water permeability of CSF concrete mixes

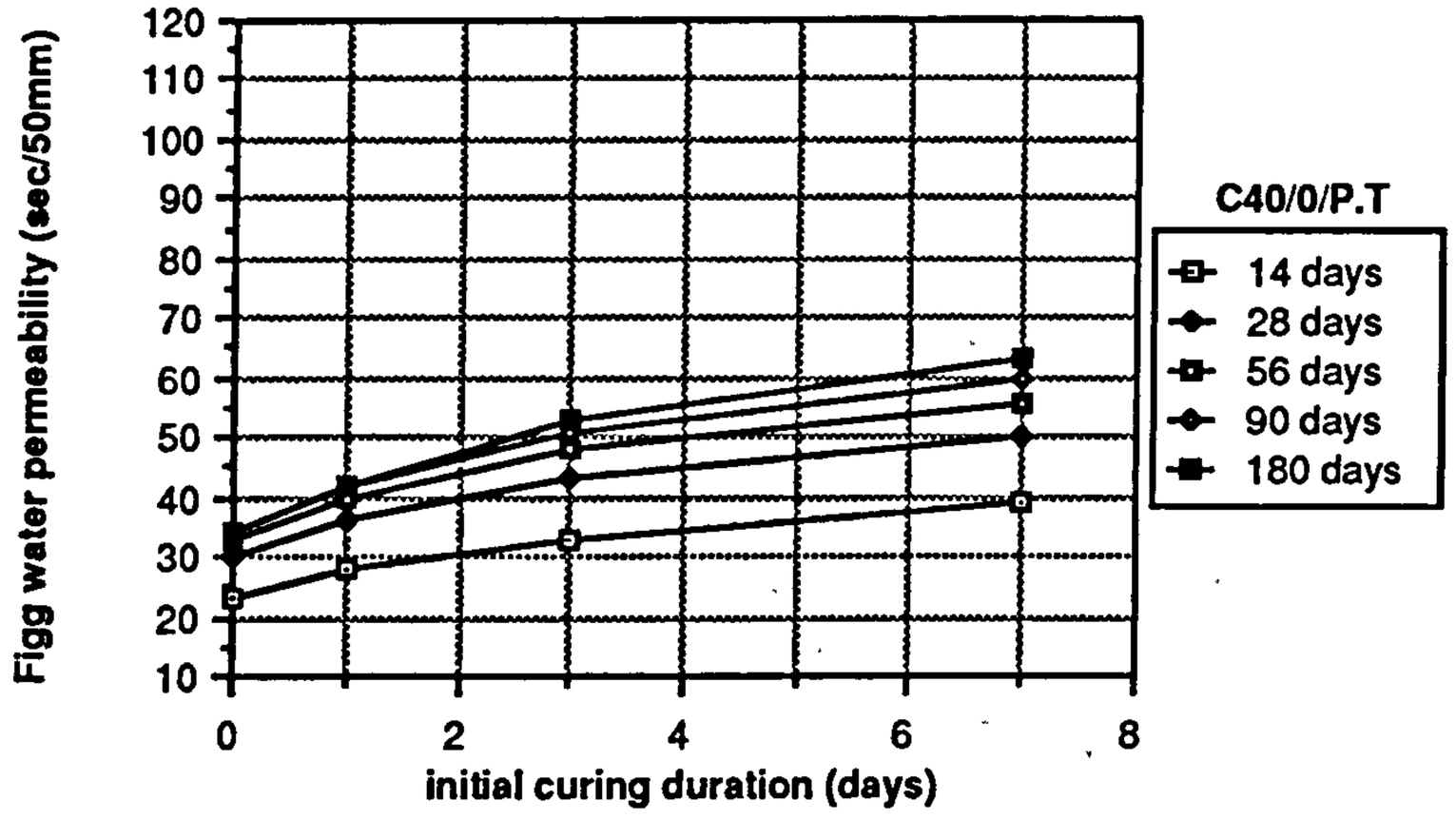

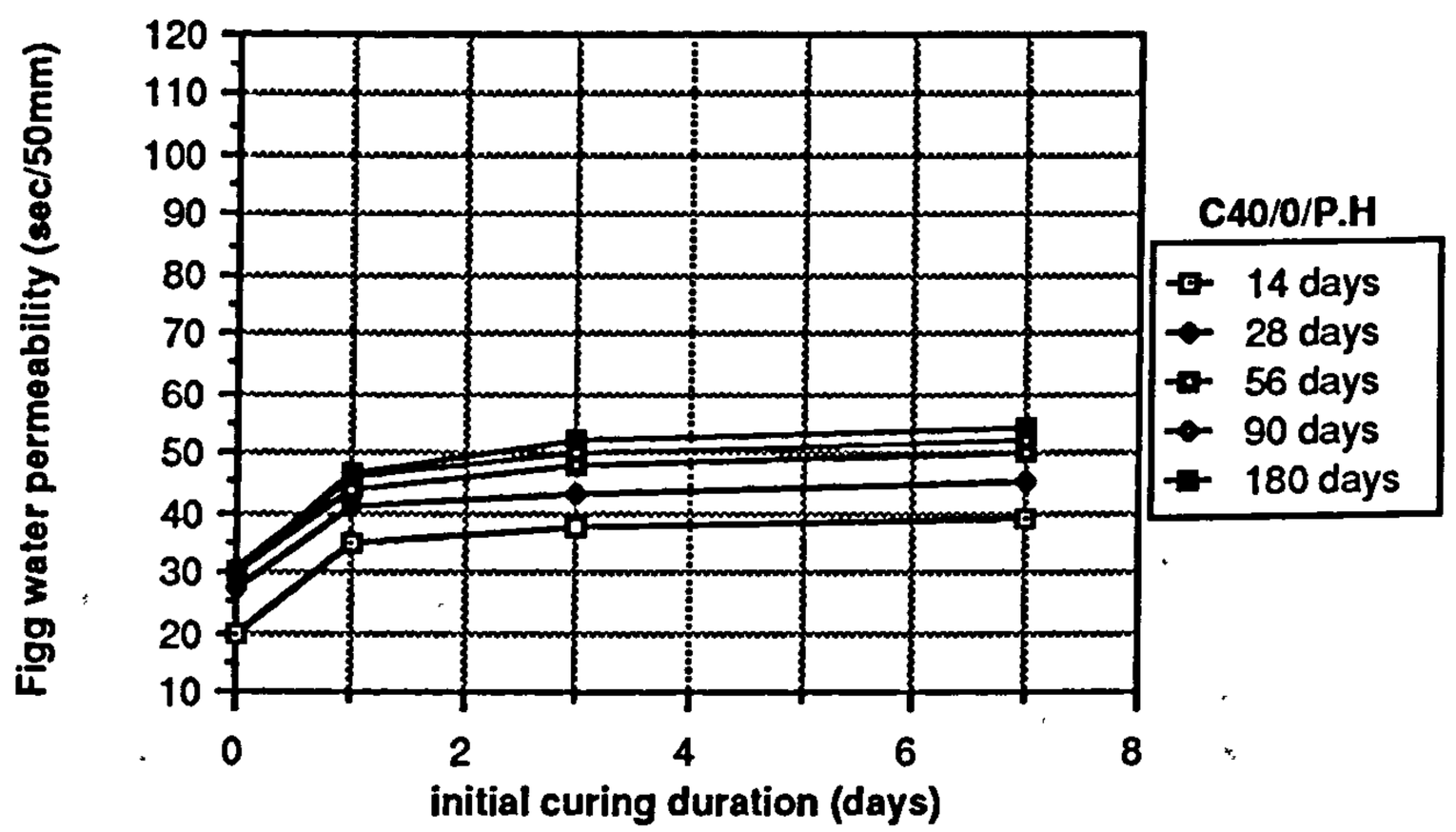

Figure 8.33 Effect of initial curing duration on the Figg water permeability of plain OPC mixes

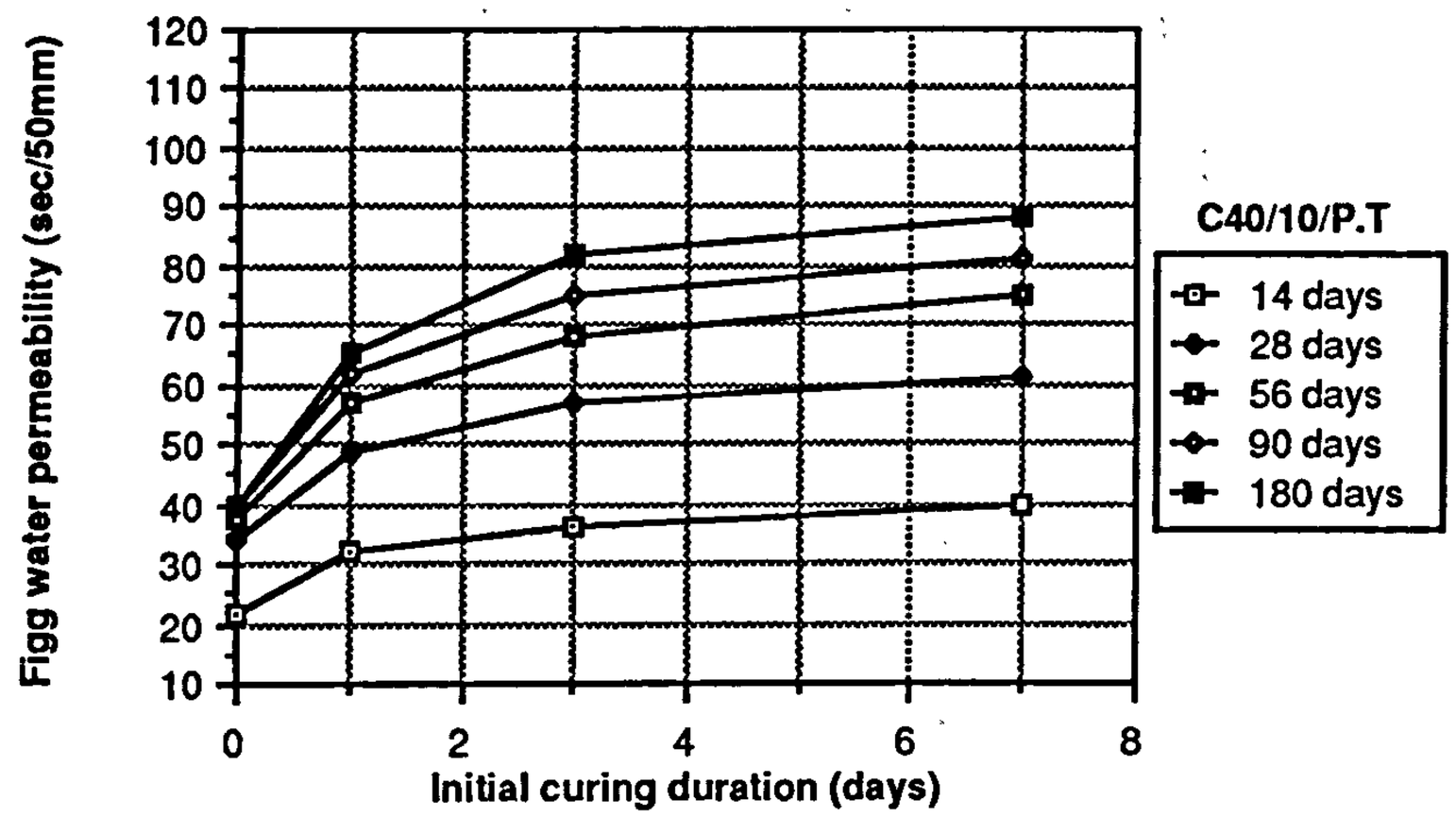

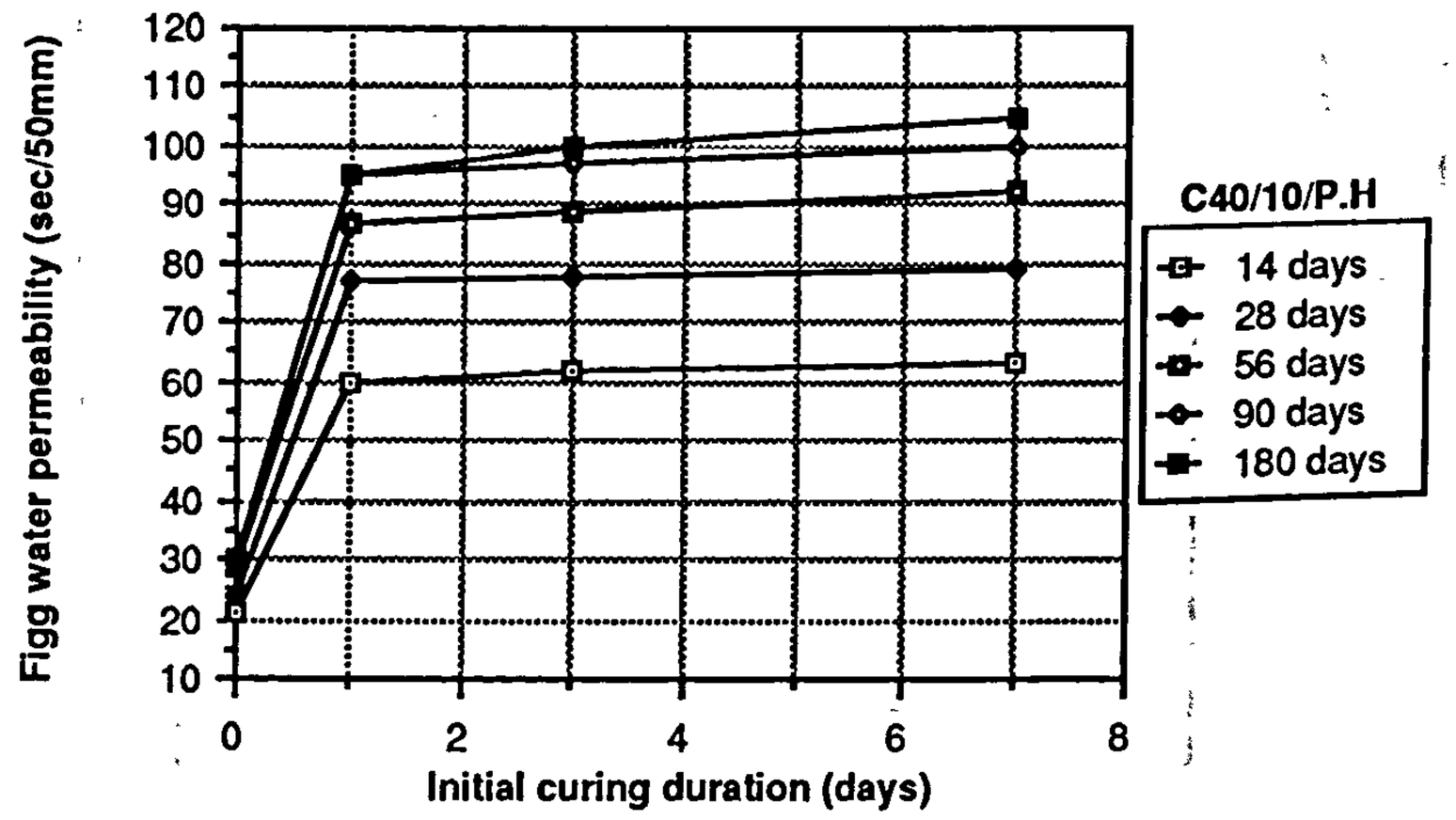

Figure 8.34 Effect of initial curing duration on the Figg water permeability of CSF mixes

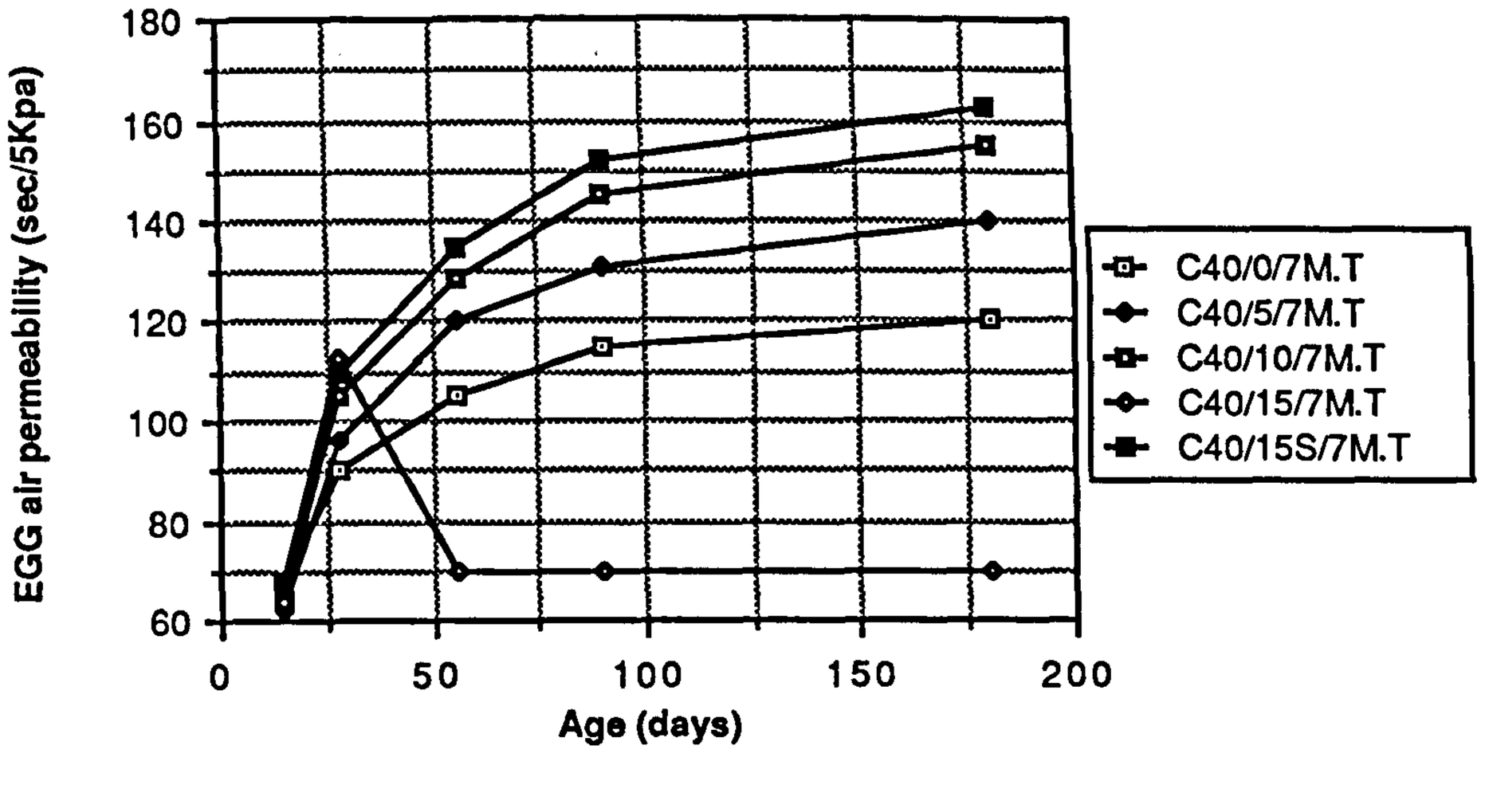

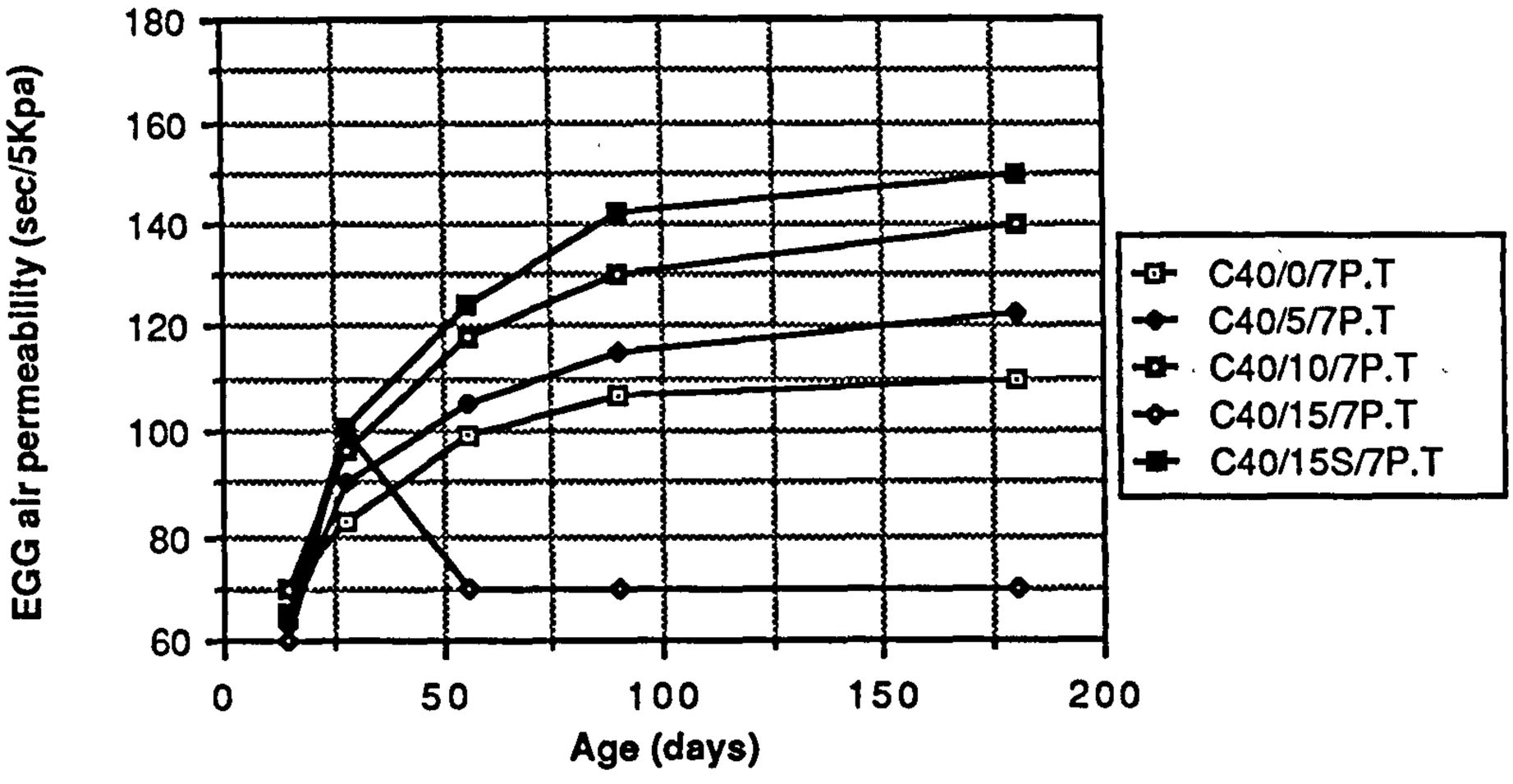

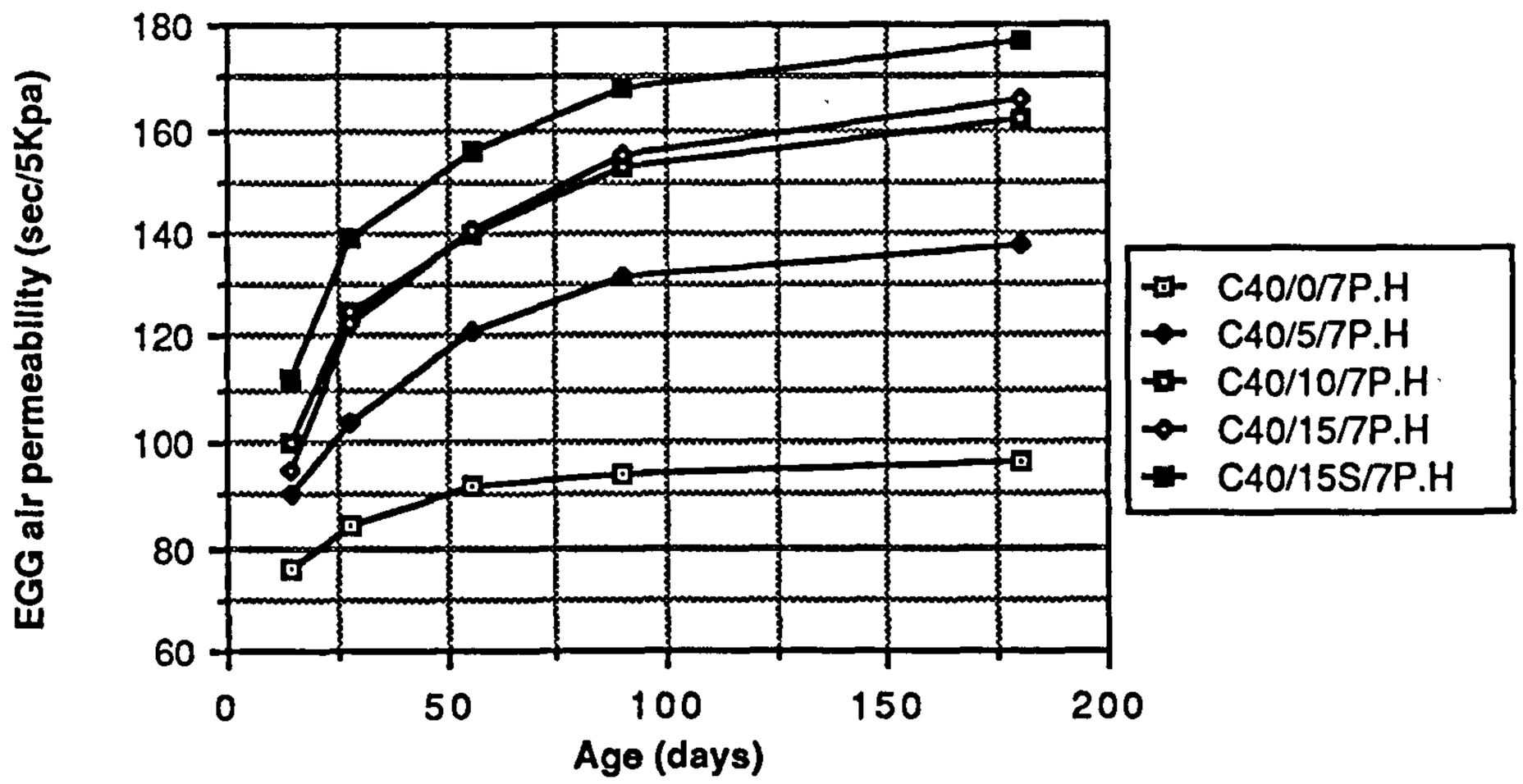

Figure 8.35 Effect of age on the Egg air permeability of plain and CSF mixes

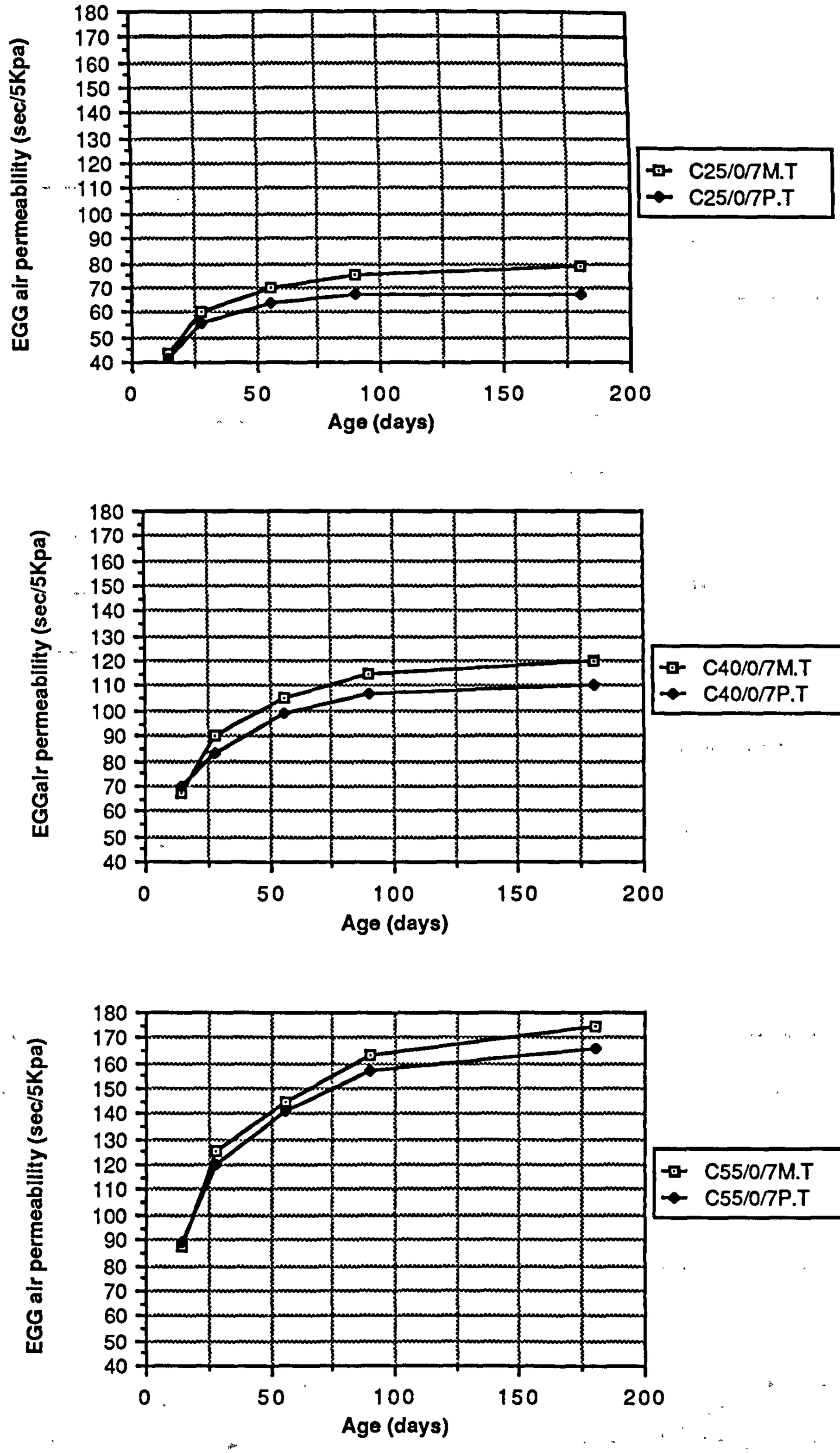

Figure 8.36 Effect of water and polythene curing on the Egg air permeability of plain OPC mixes

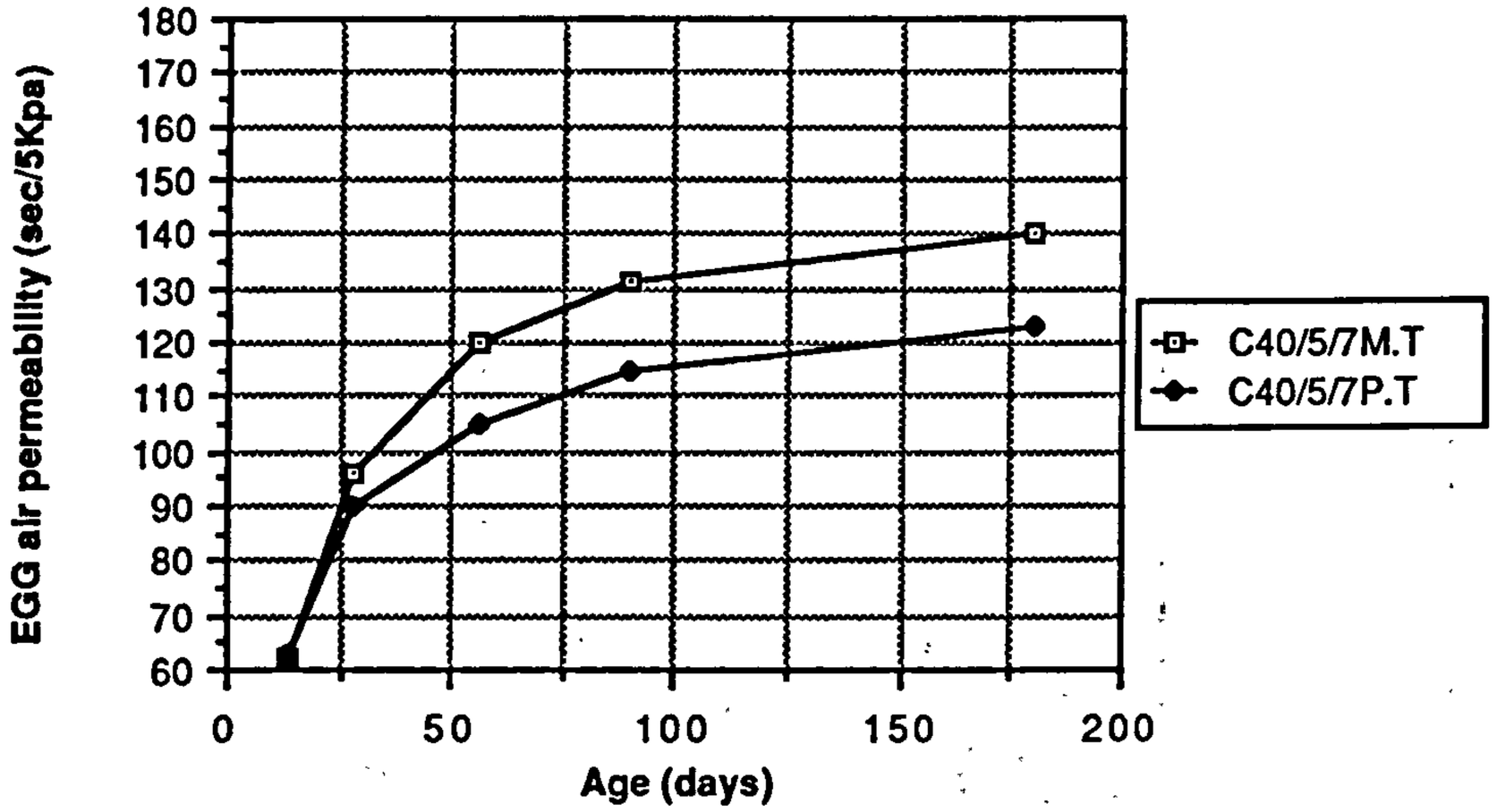

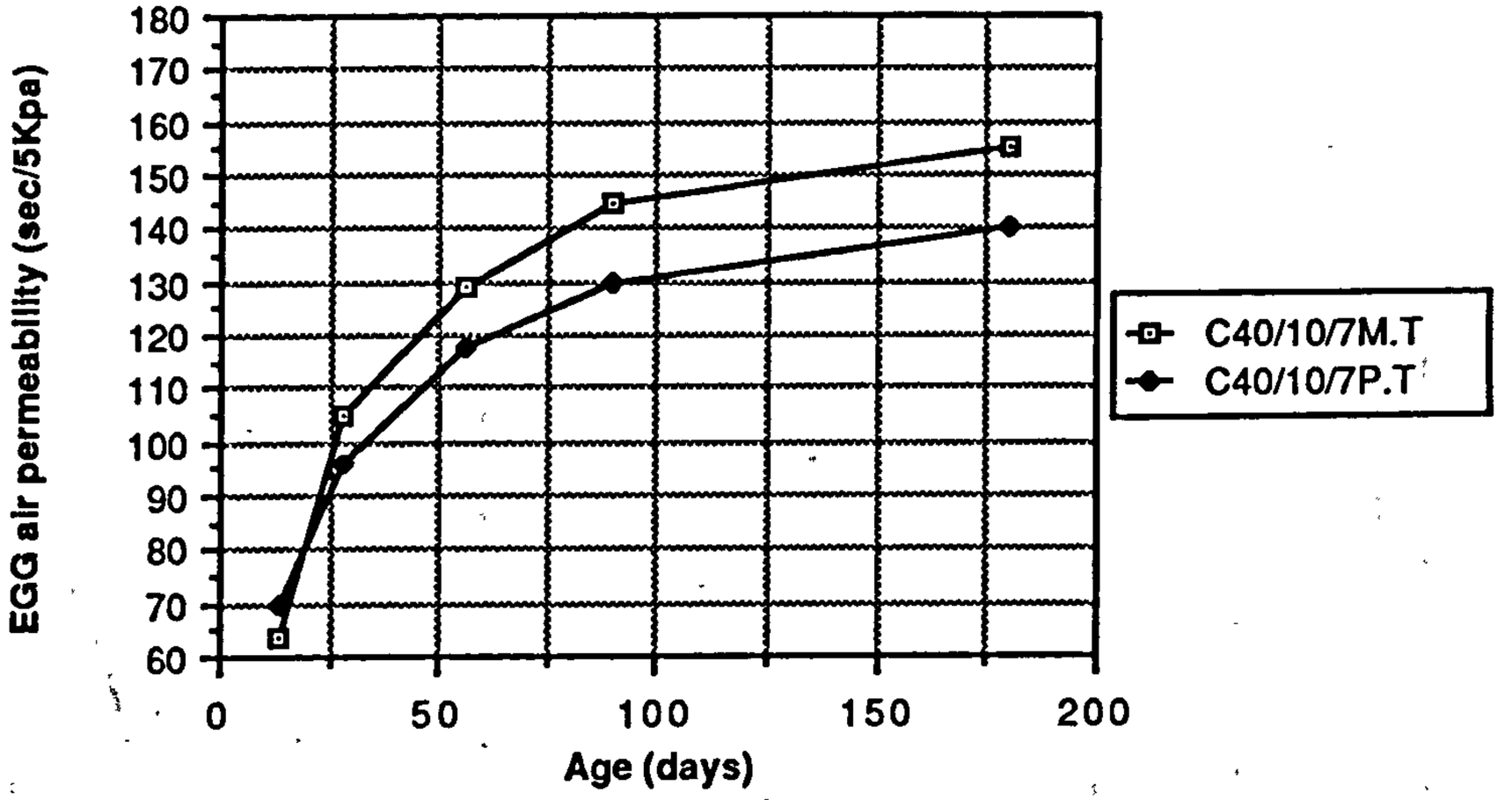

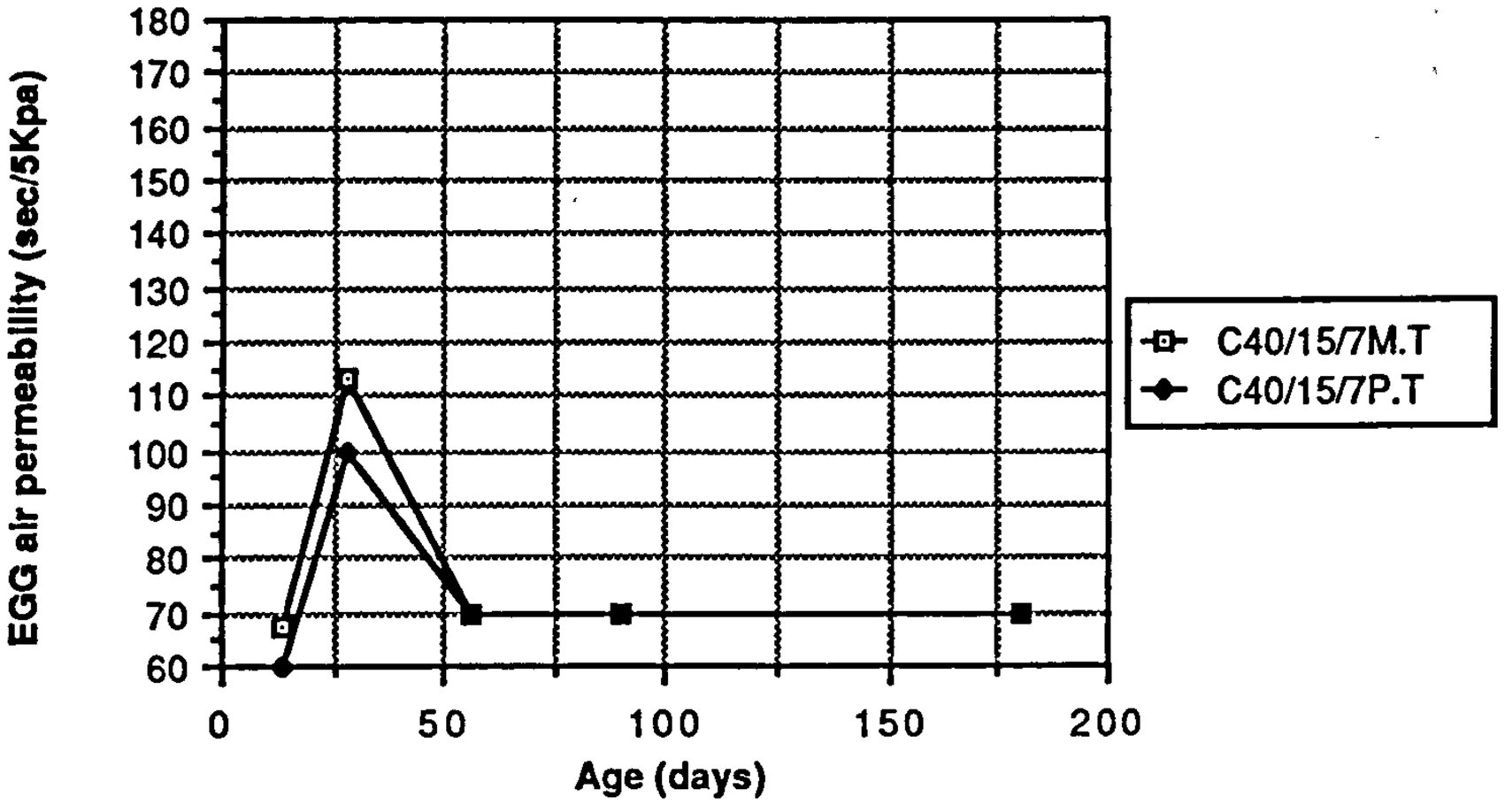

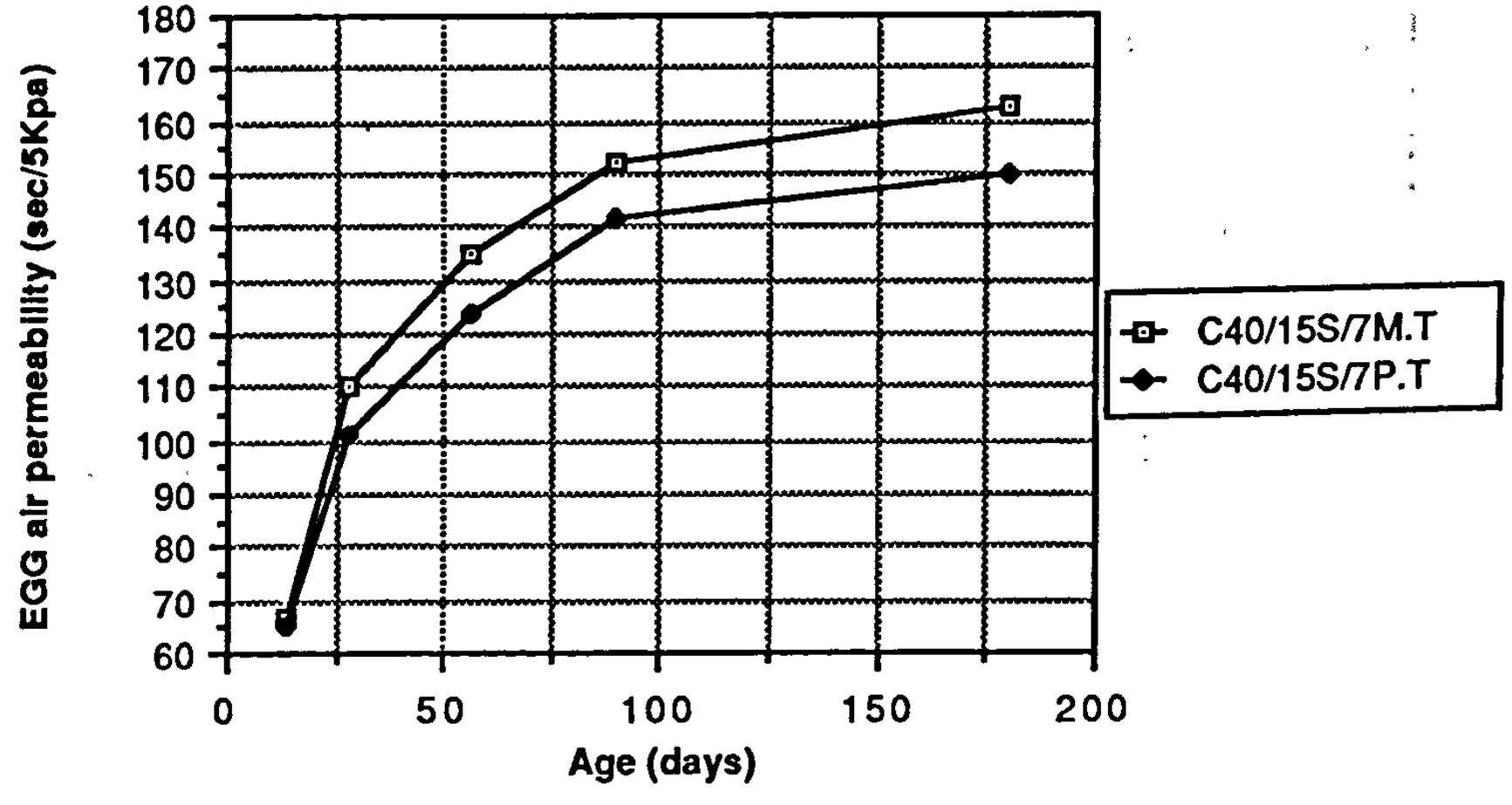

Figure 8.37 Effect of water and polythene curing on the Egg air permeability of CSF mixes

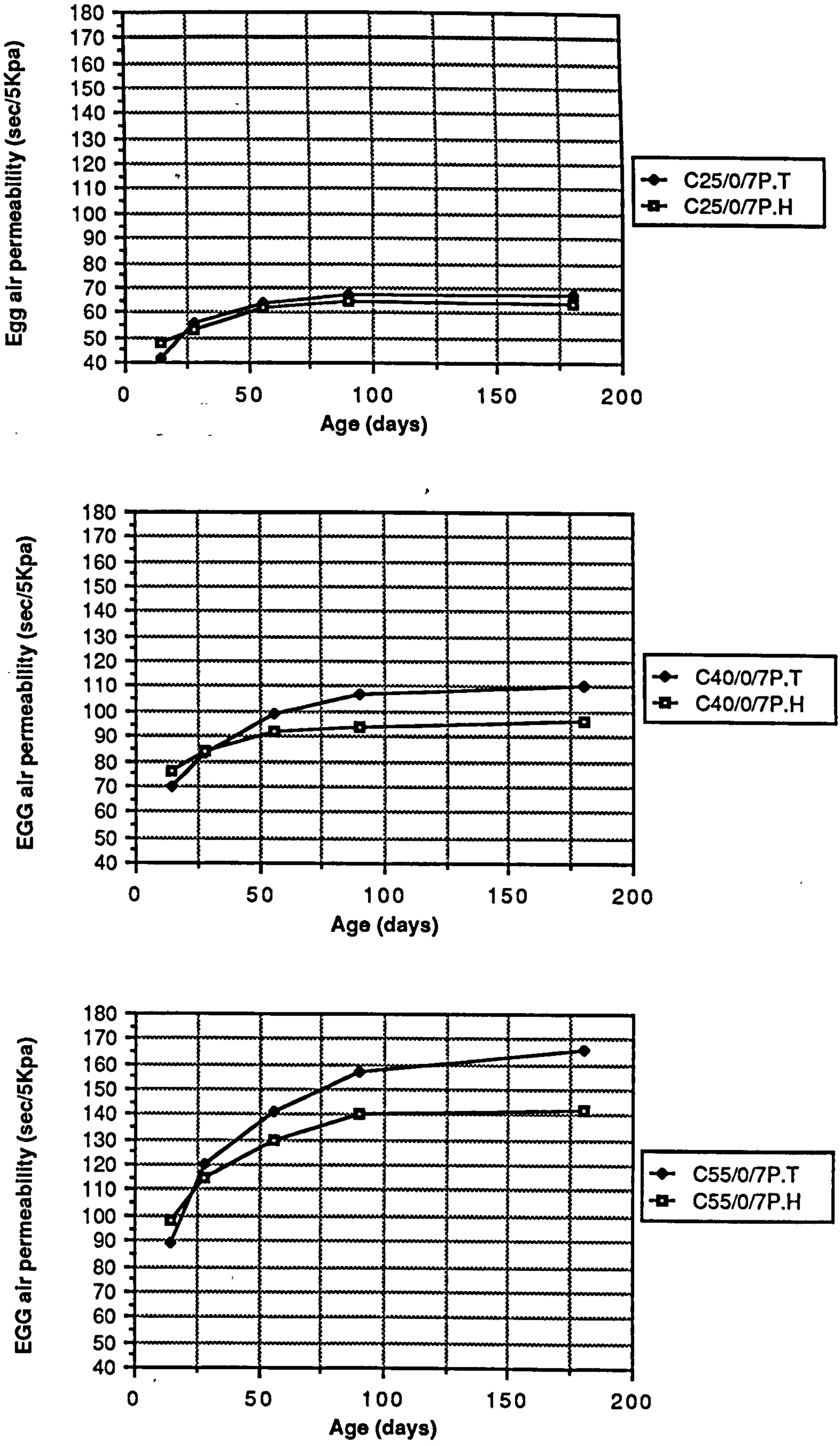

Figure 8.38 Effect of temperature and hot climate on the Egg air permeability of plain OPC mixes

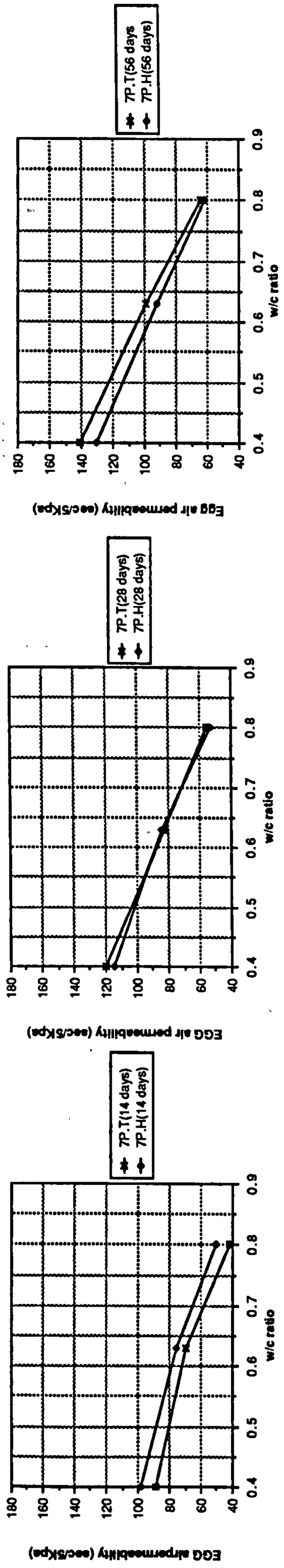

Figure 8.39 Effect of W/C ratio on the Egg air permeability of plain OPC mixes

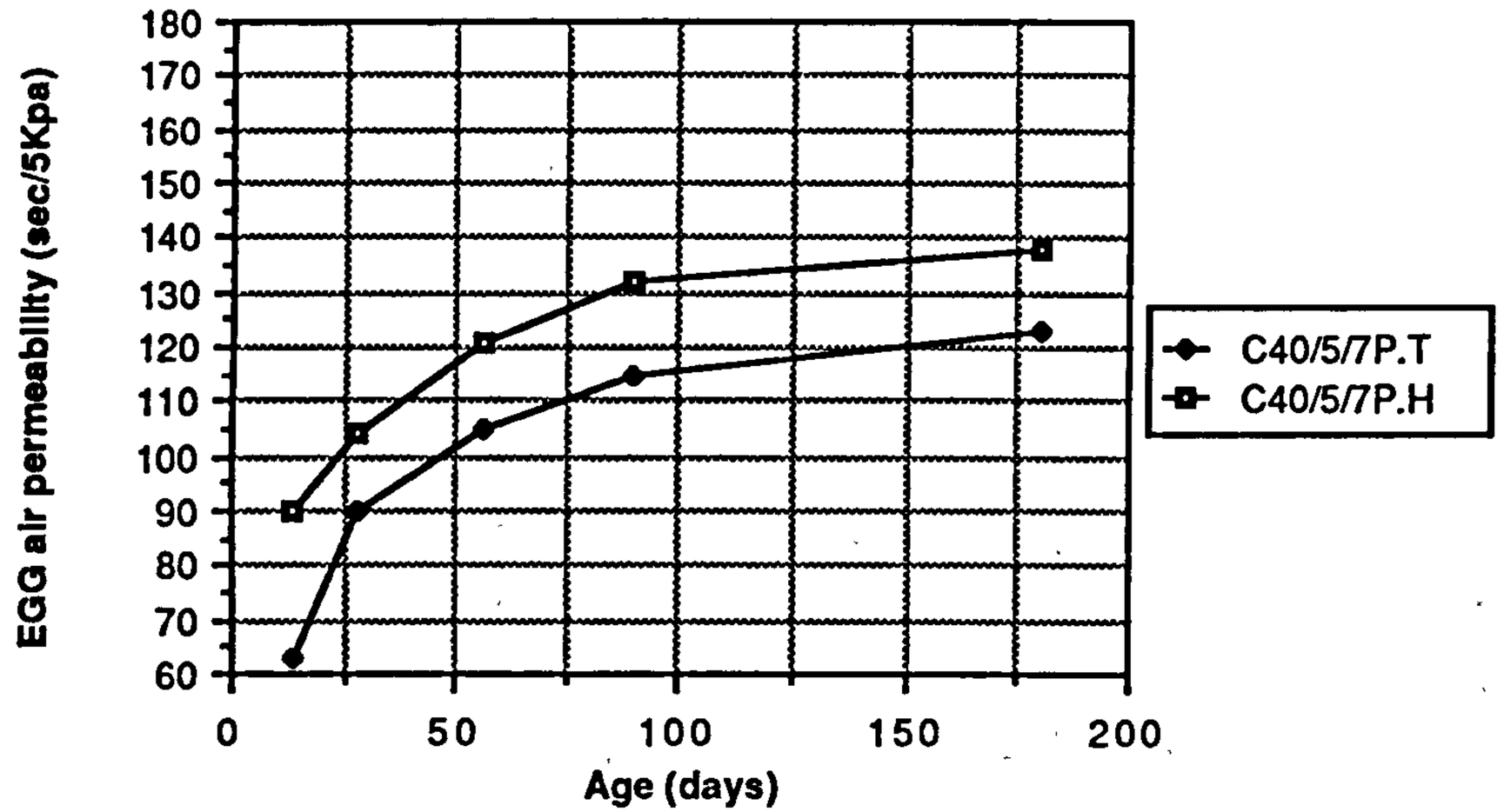

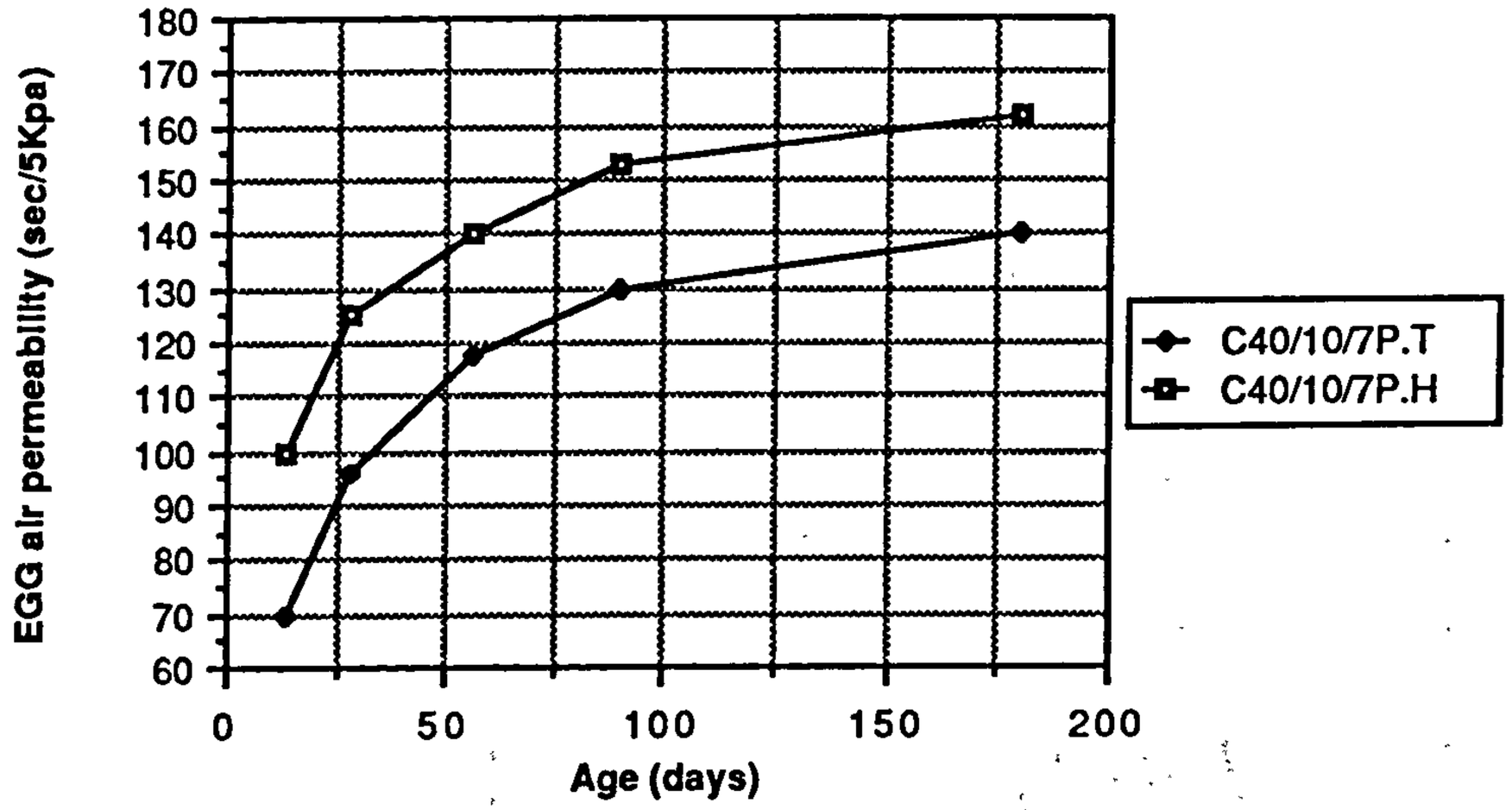

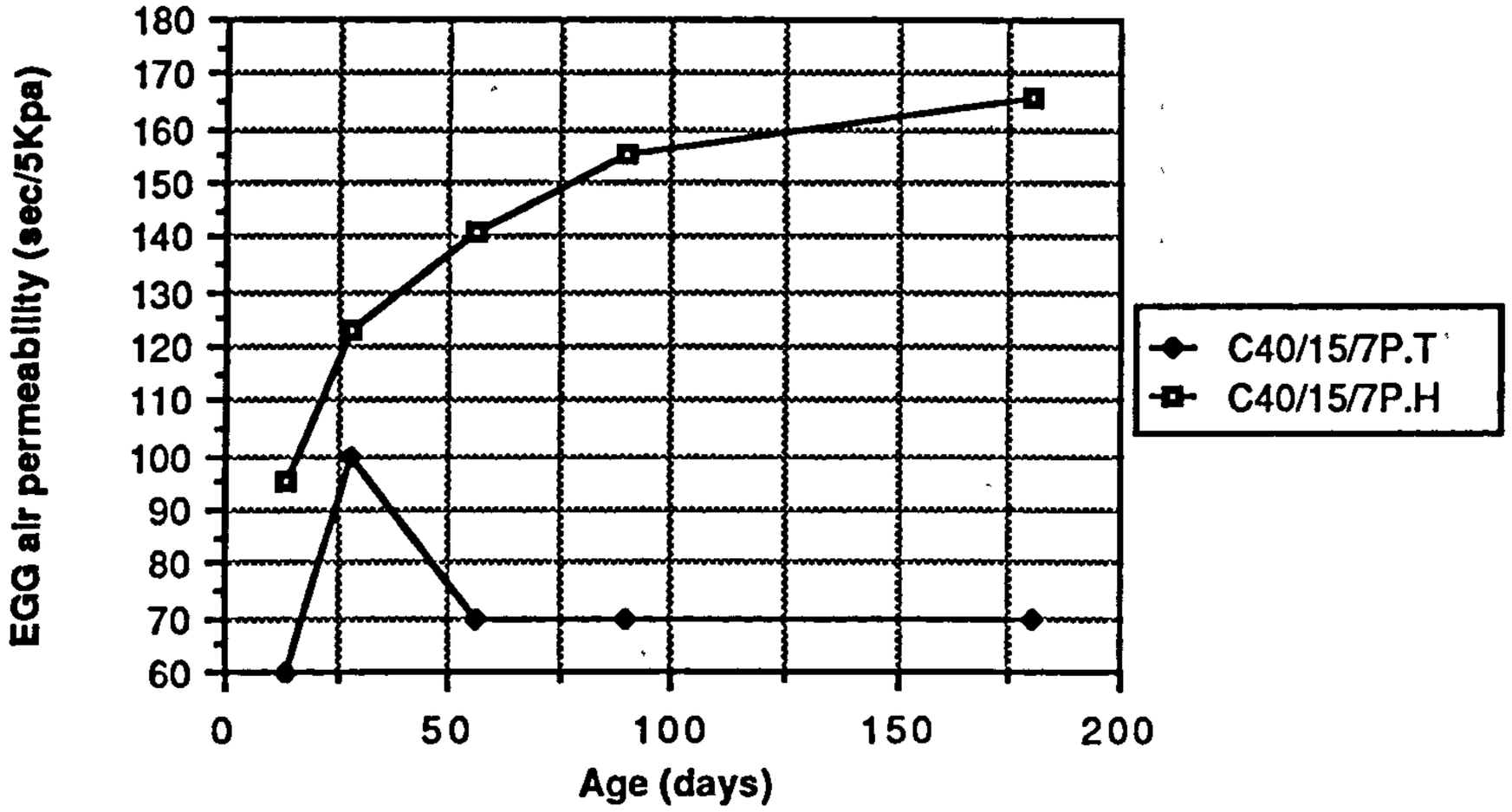

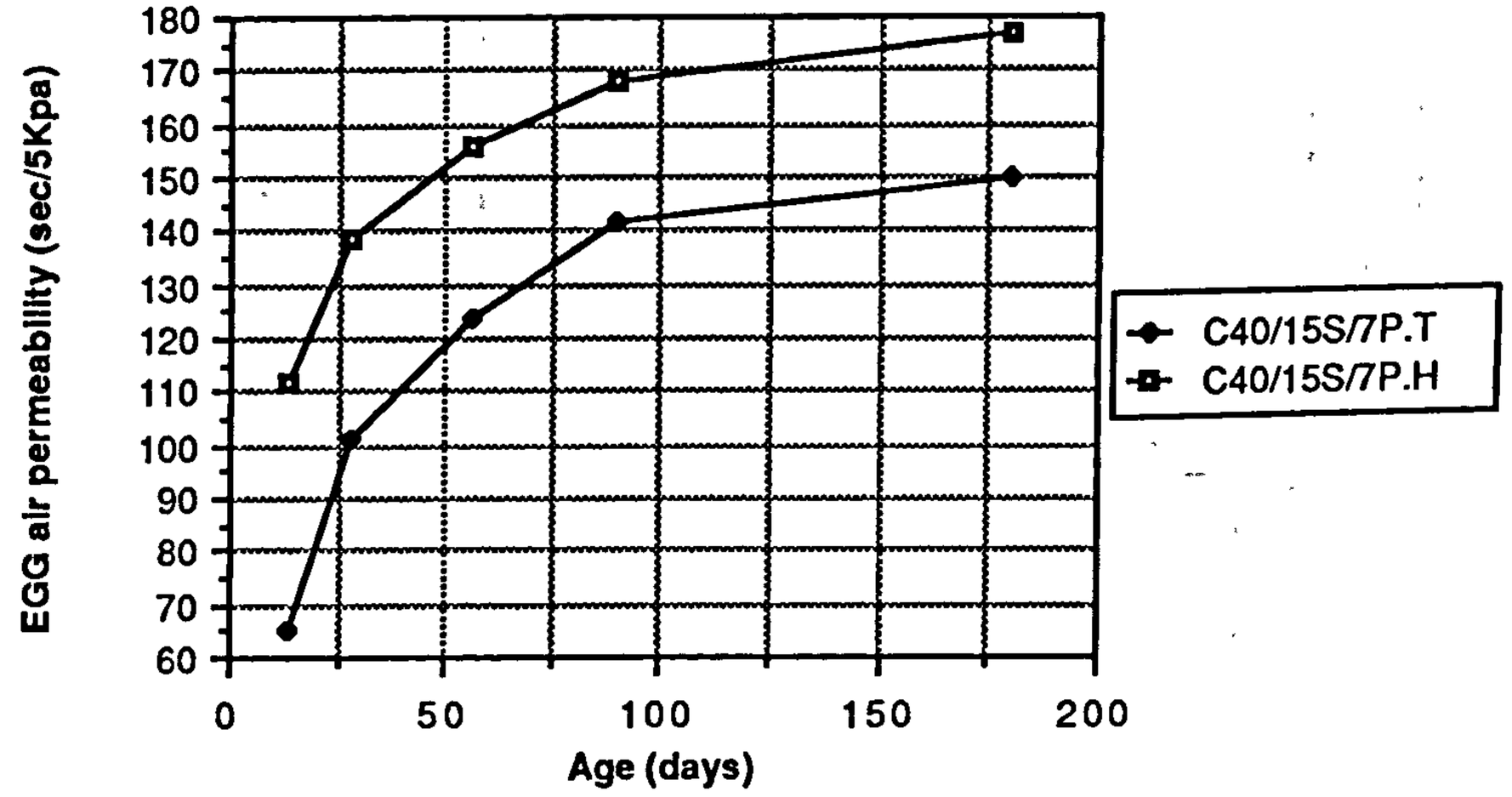

Figure 8.40 Effect of temperate and hot curing on the Egg air permeability of CSF mixes

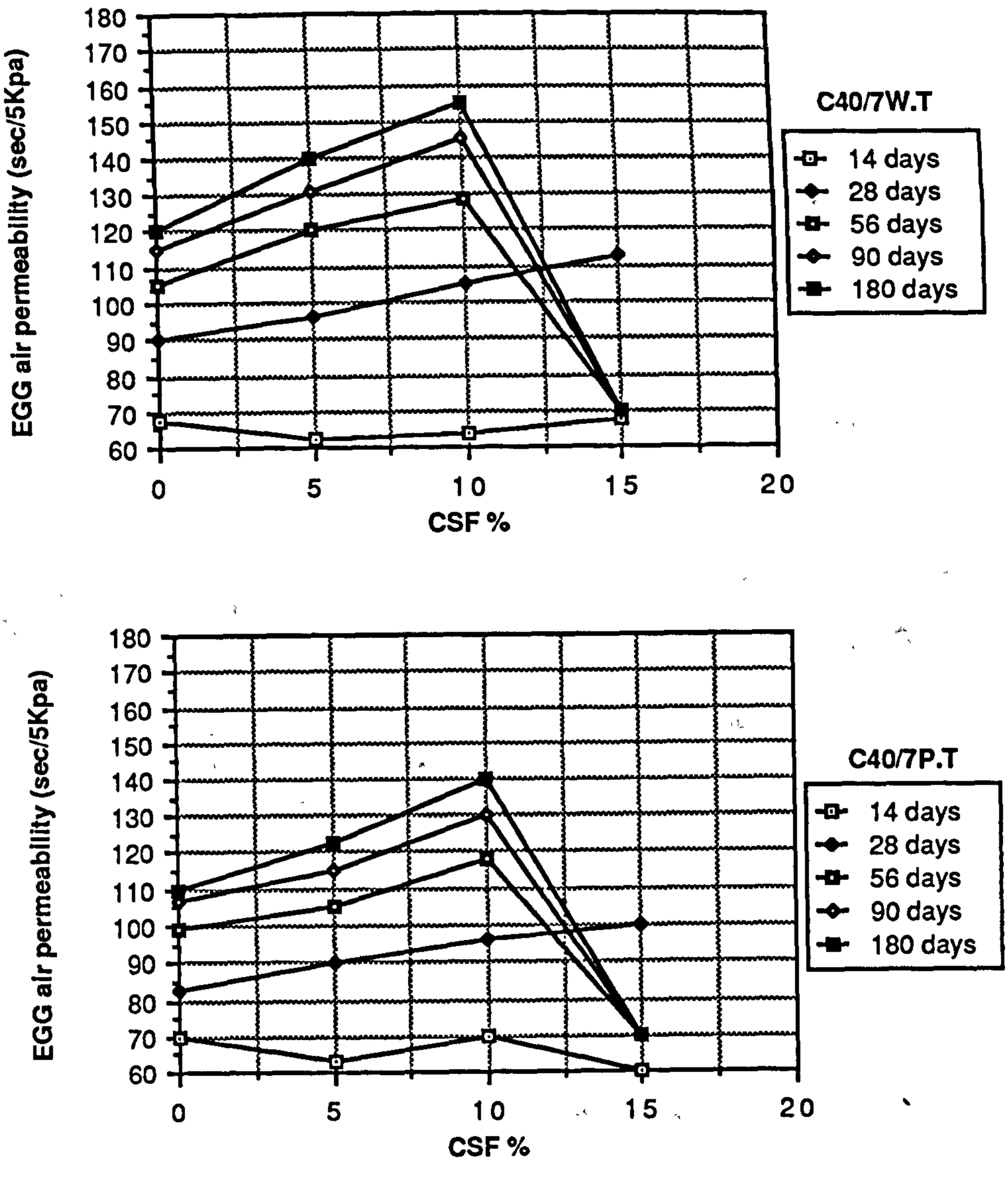

Figure 8.41 Effect of CSF content on the Egg air permeability of CSF mixes

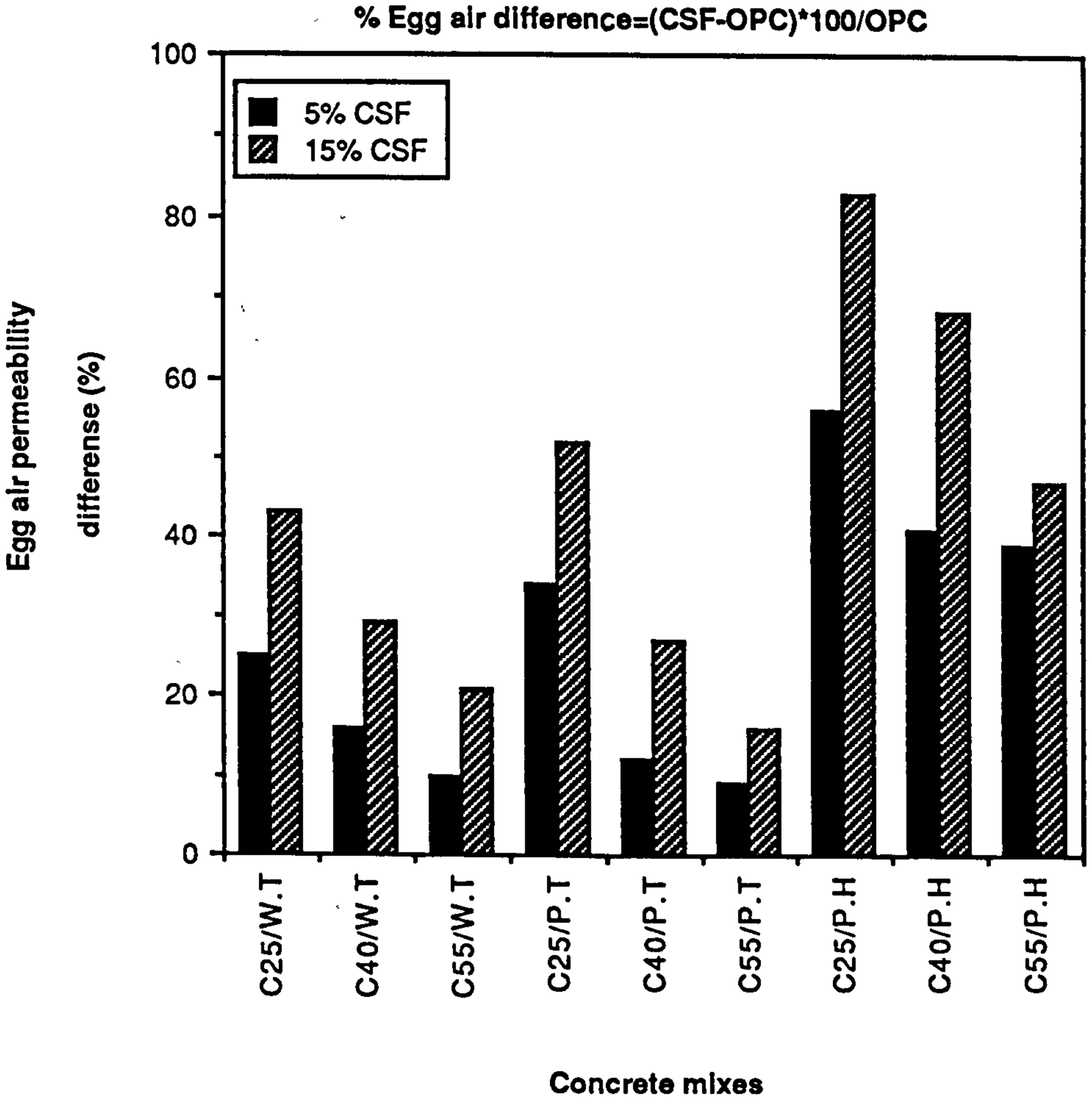

Figure 8.42 Percent reduction in Egg air permeability caused by addition of CSF to lean, medium and rich concrete mixes

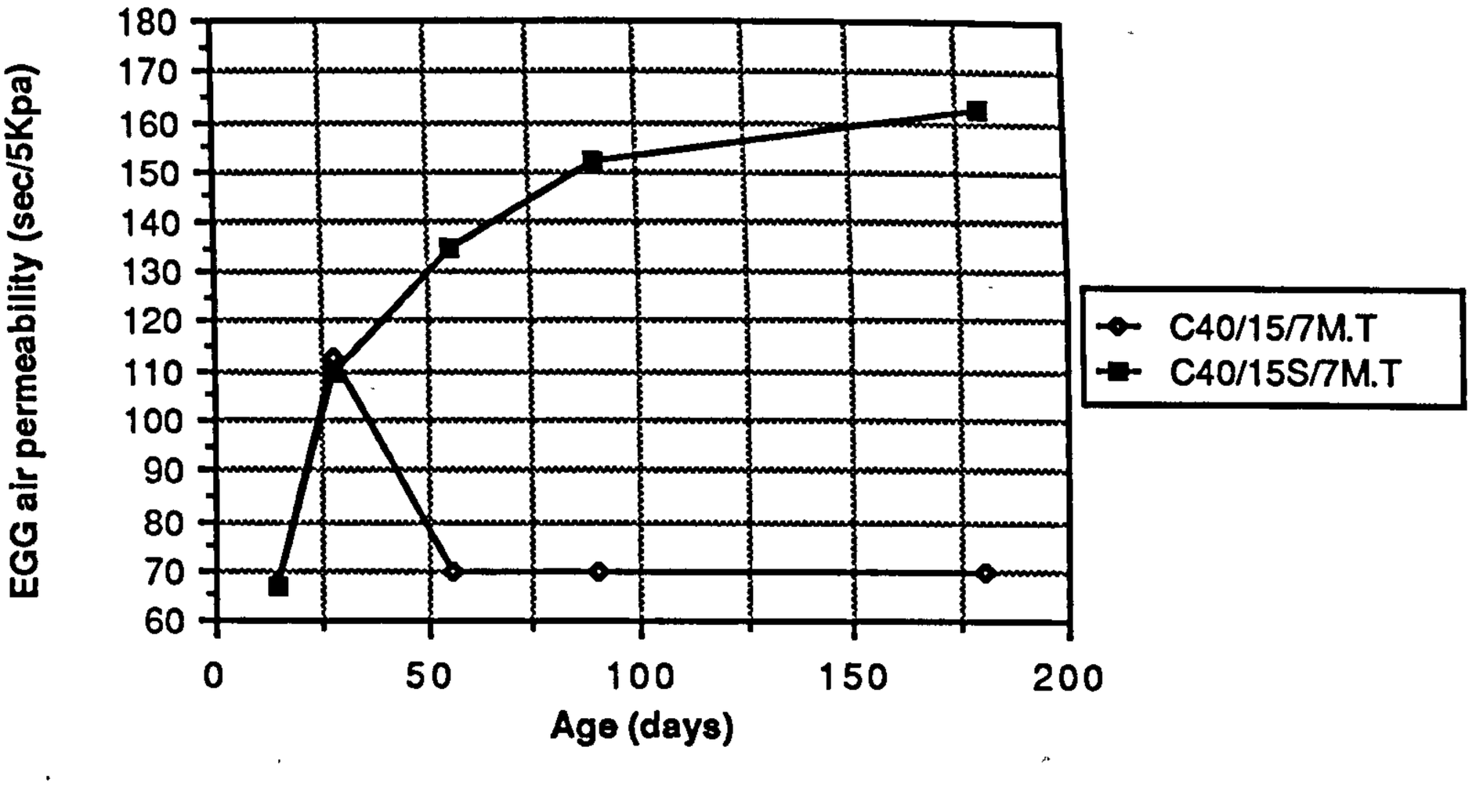

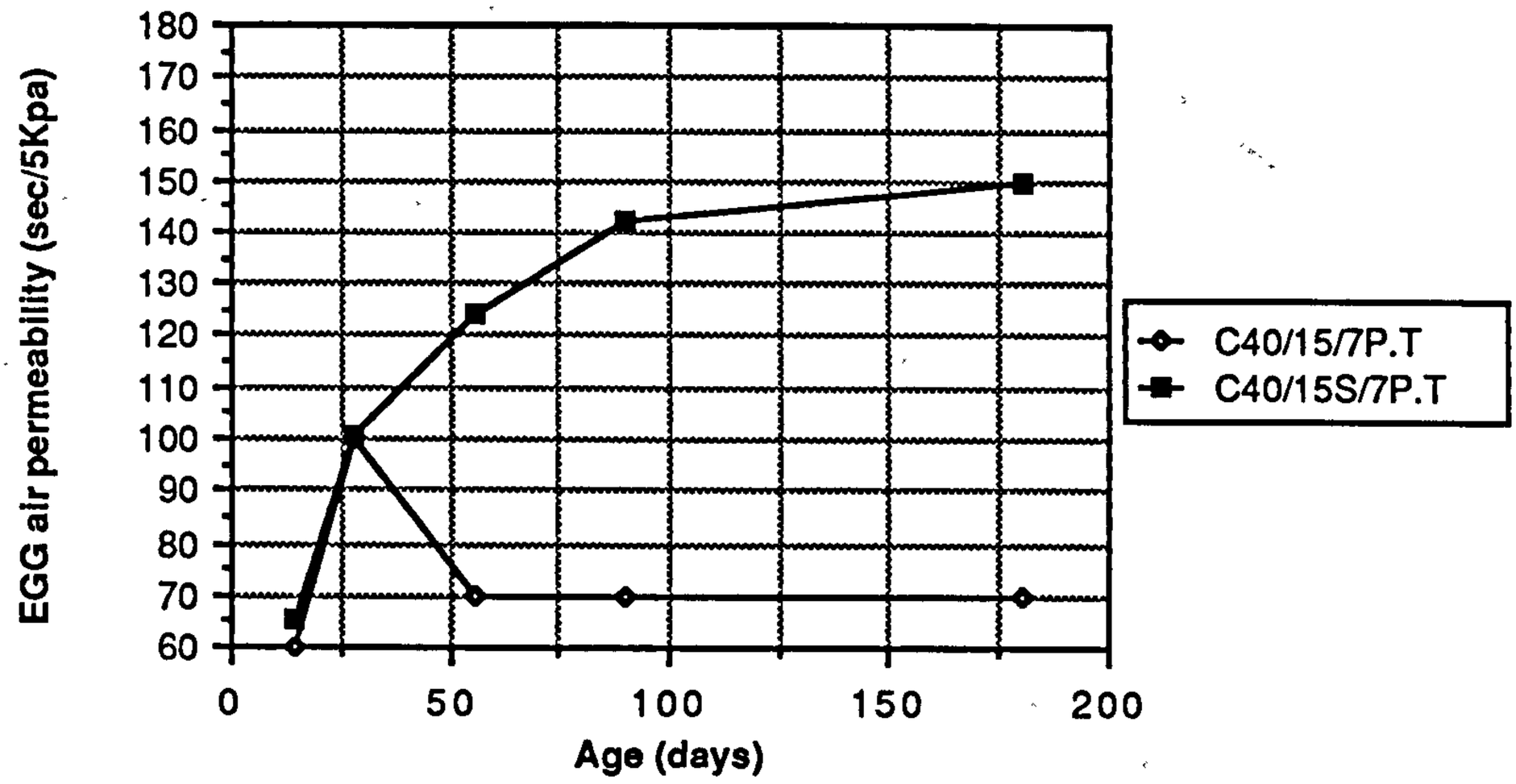

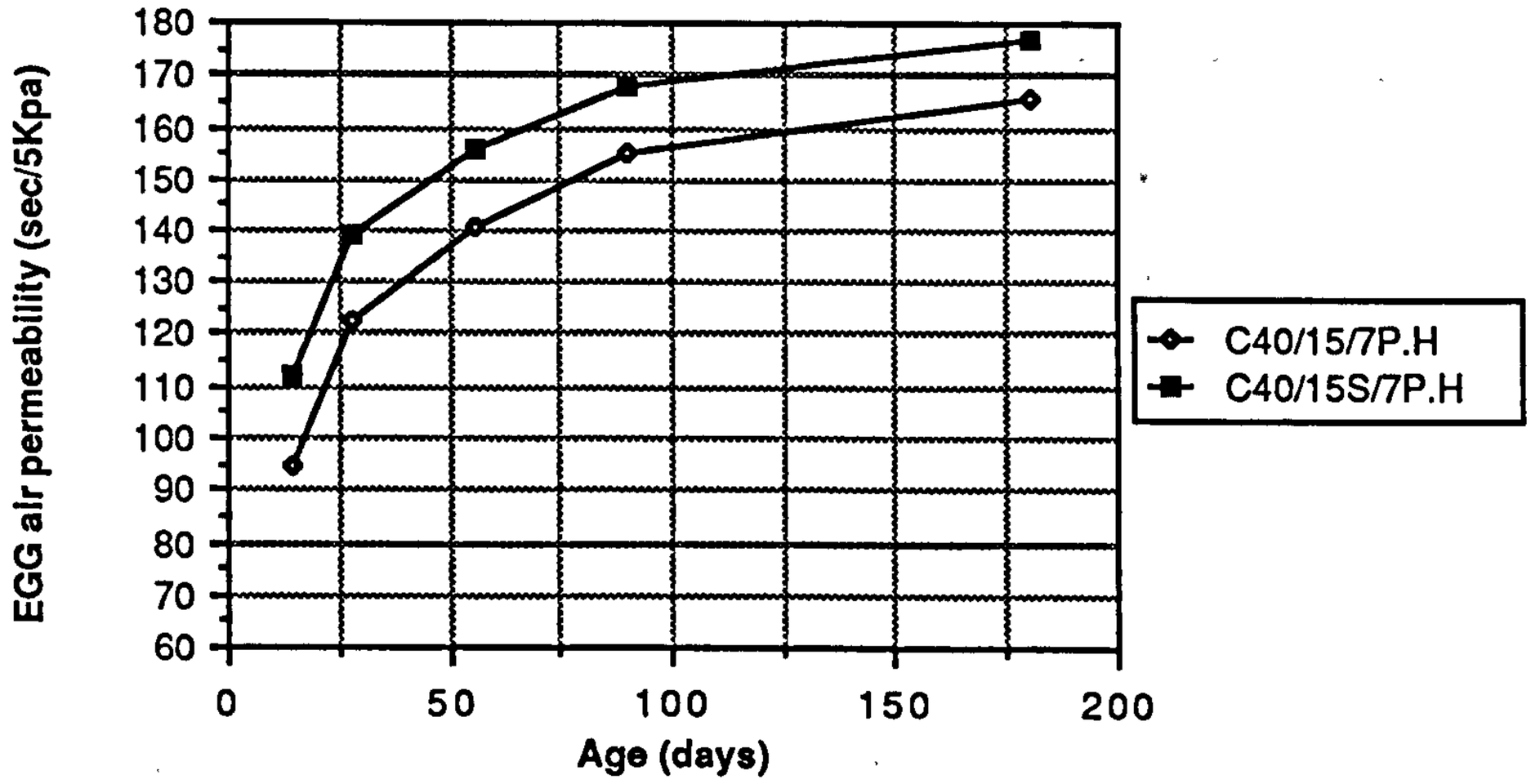

Figure 8.43 Effect of superplasticizer on the Egg air permeability of CSF mixes

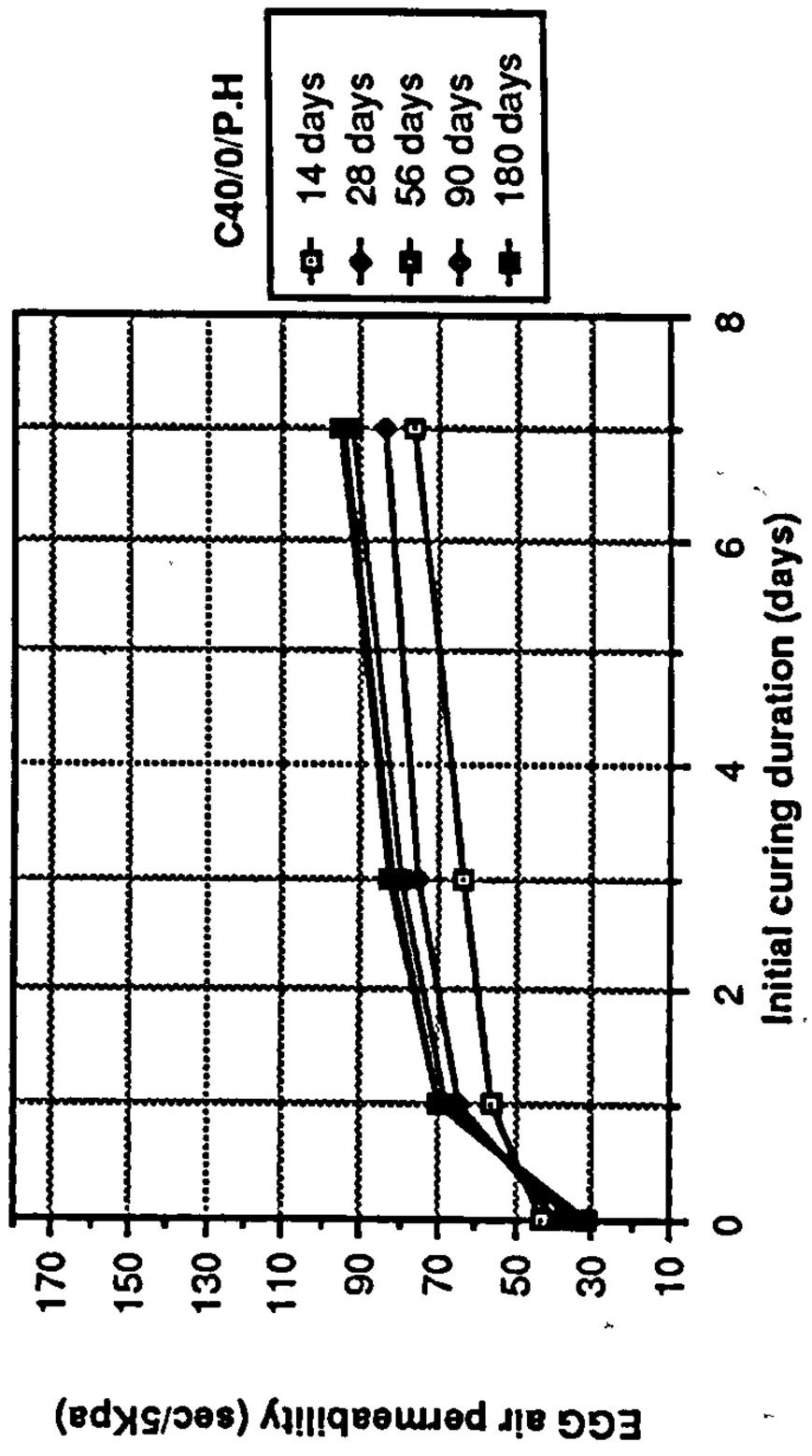

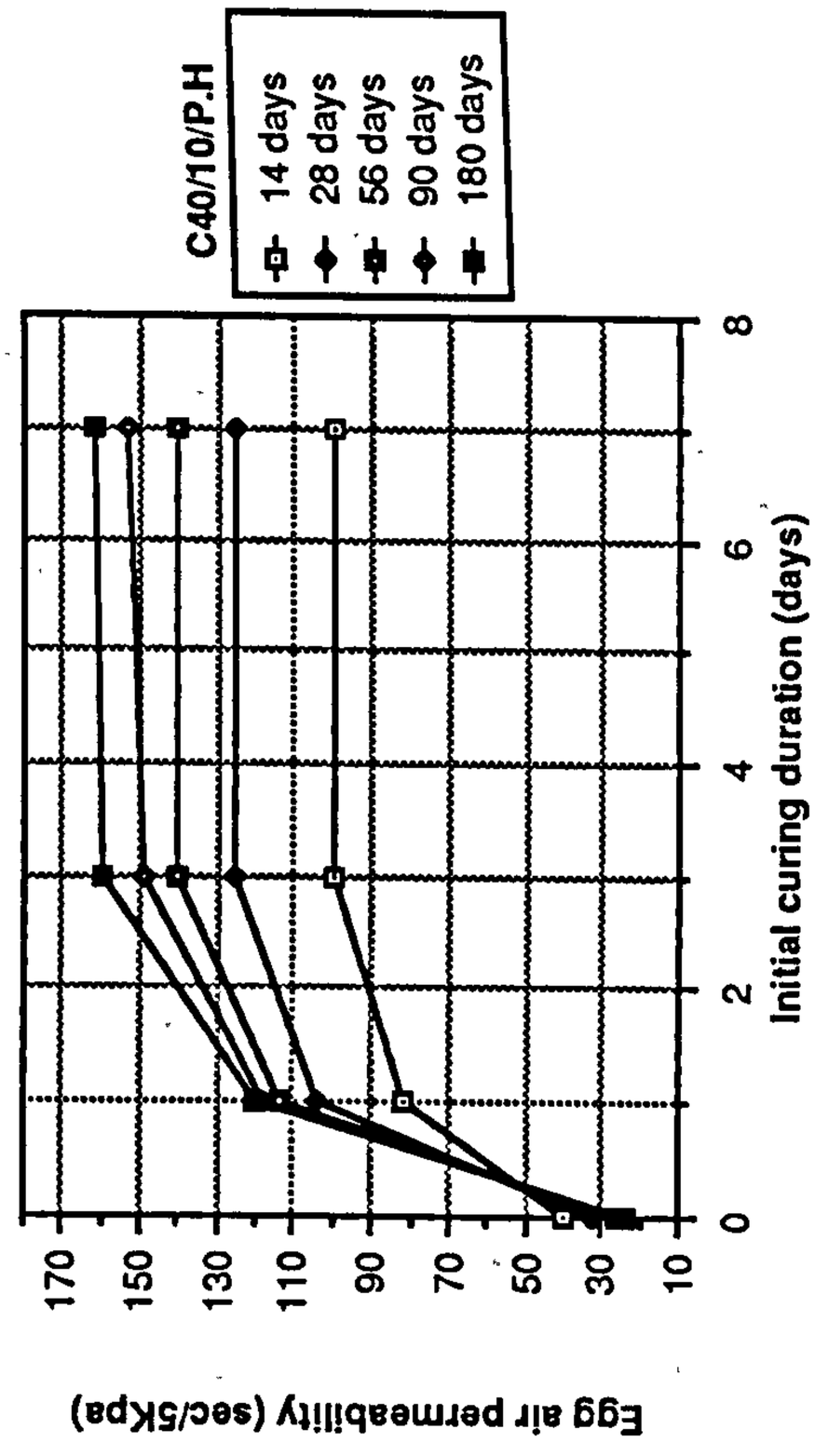

Figure 8.44 Effect of initial curing on Egg air permeability of plain OPC

Figure 8.45 Effect of initial curing duration on Egg air permeability of CSF

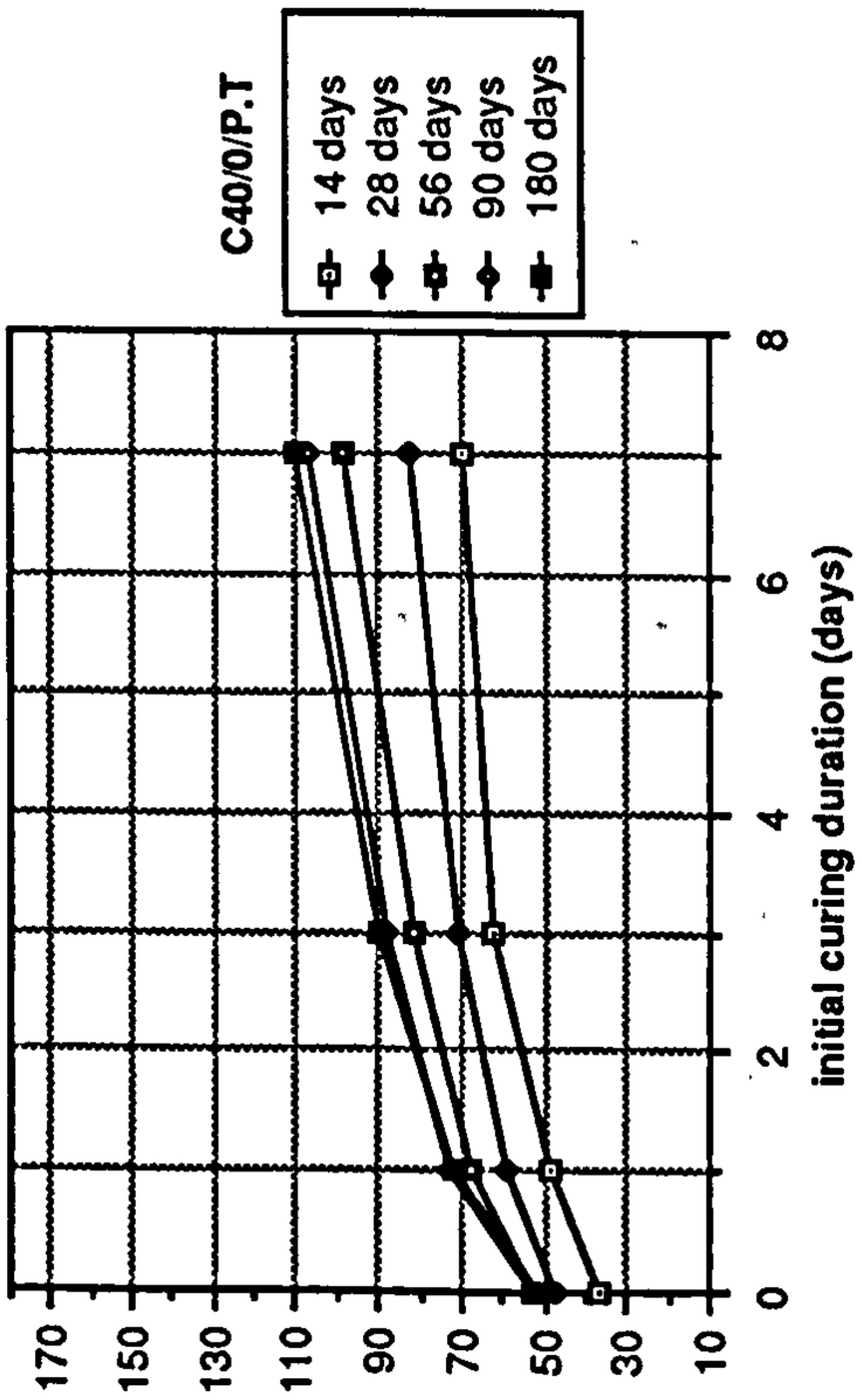

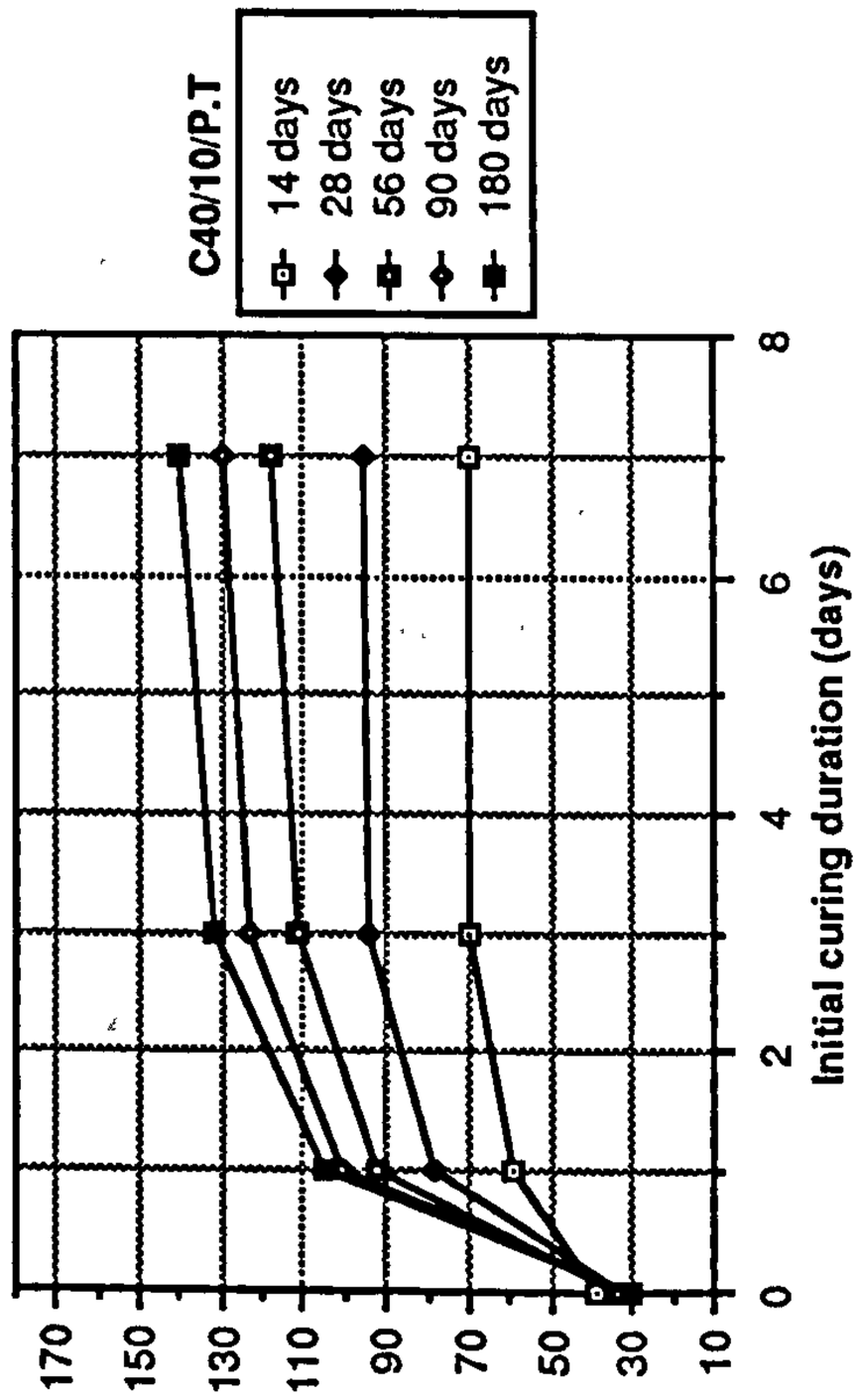

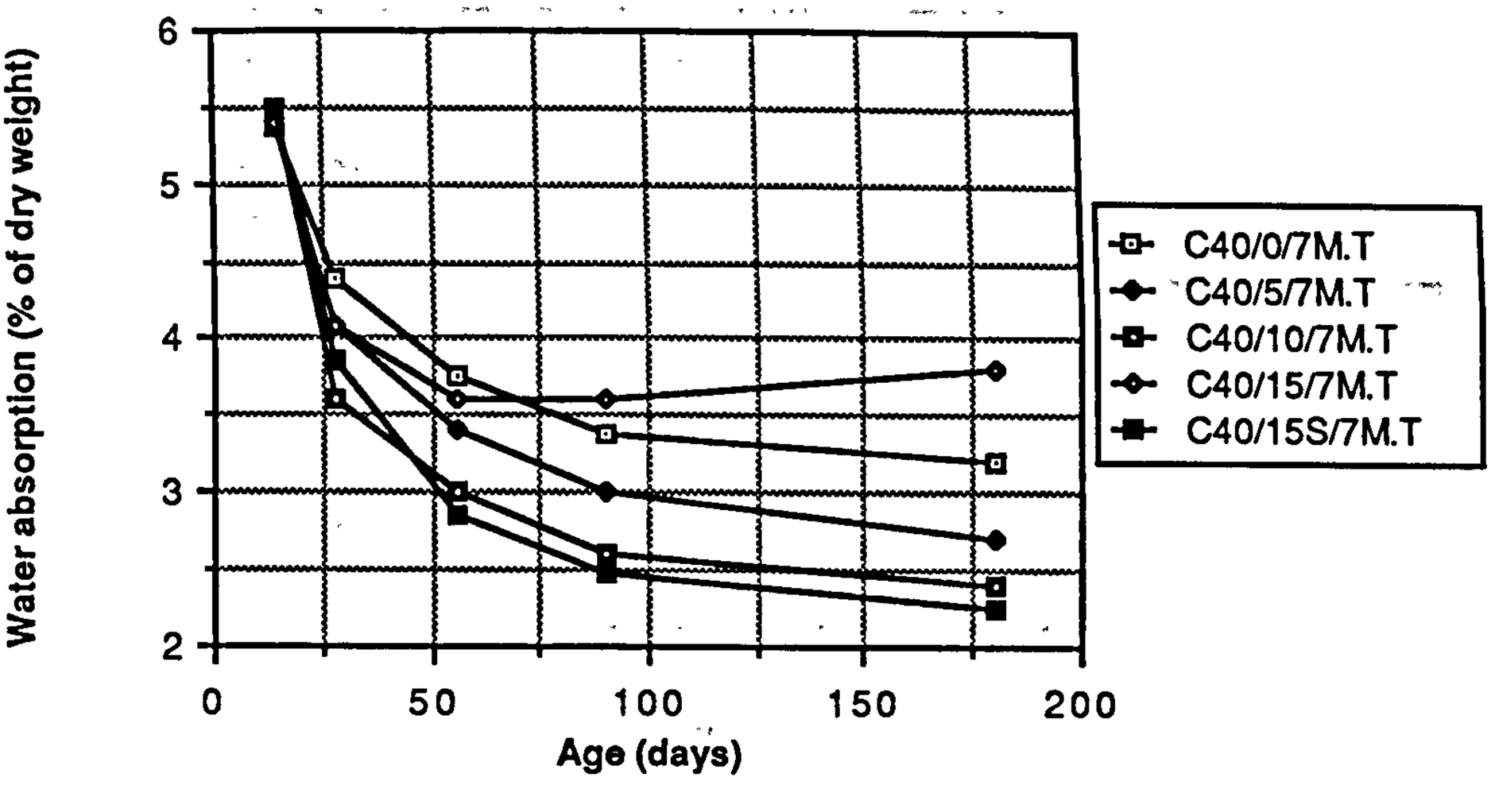

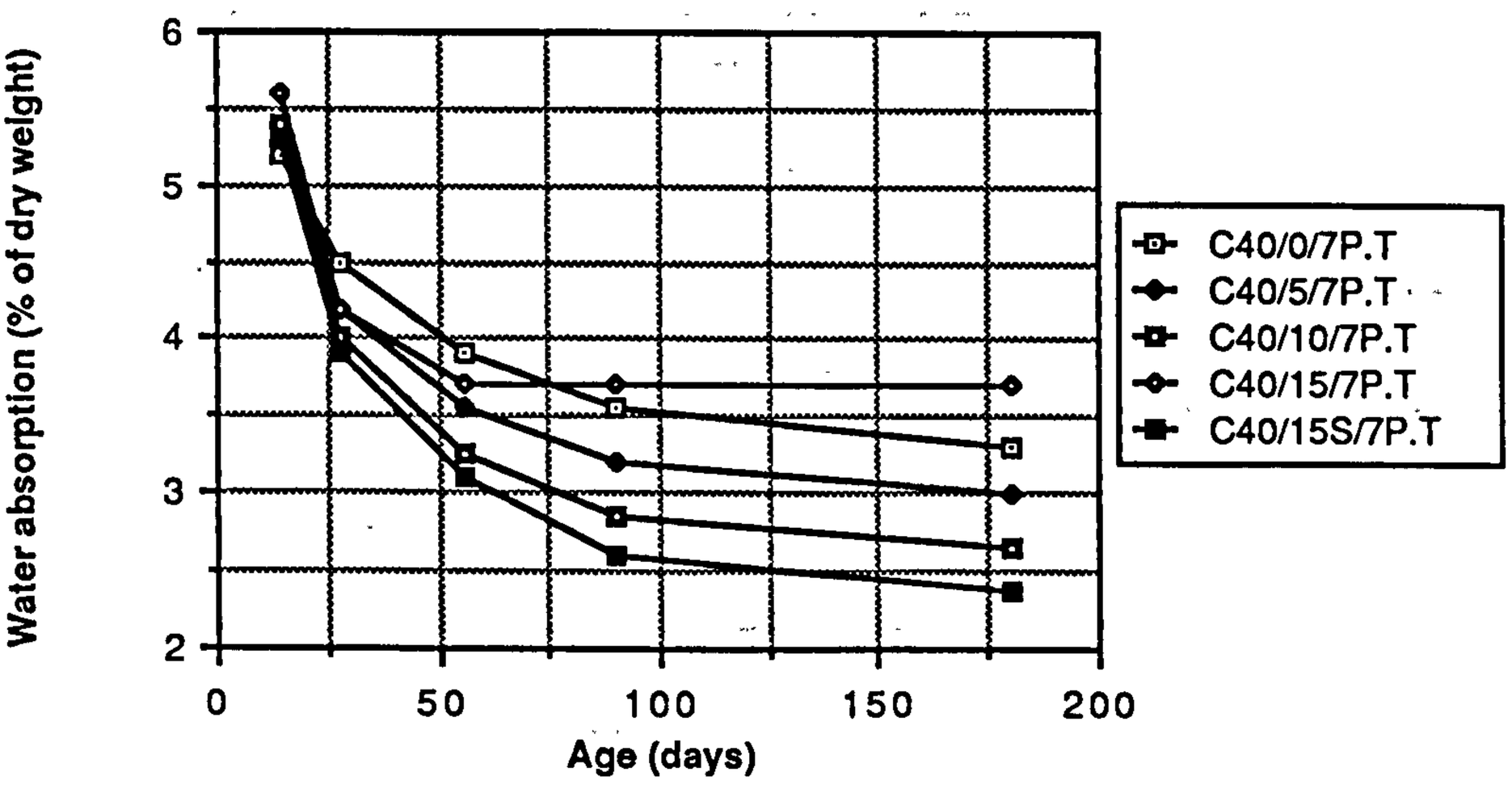

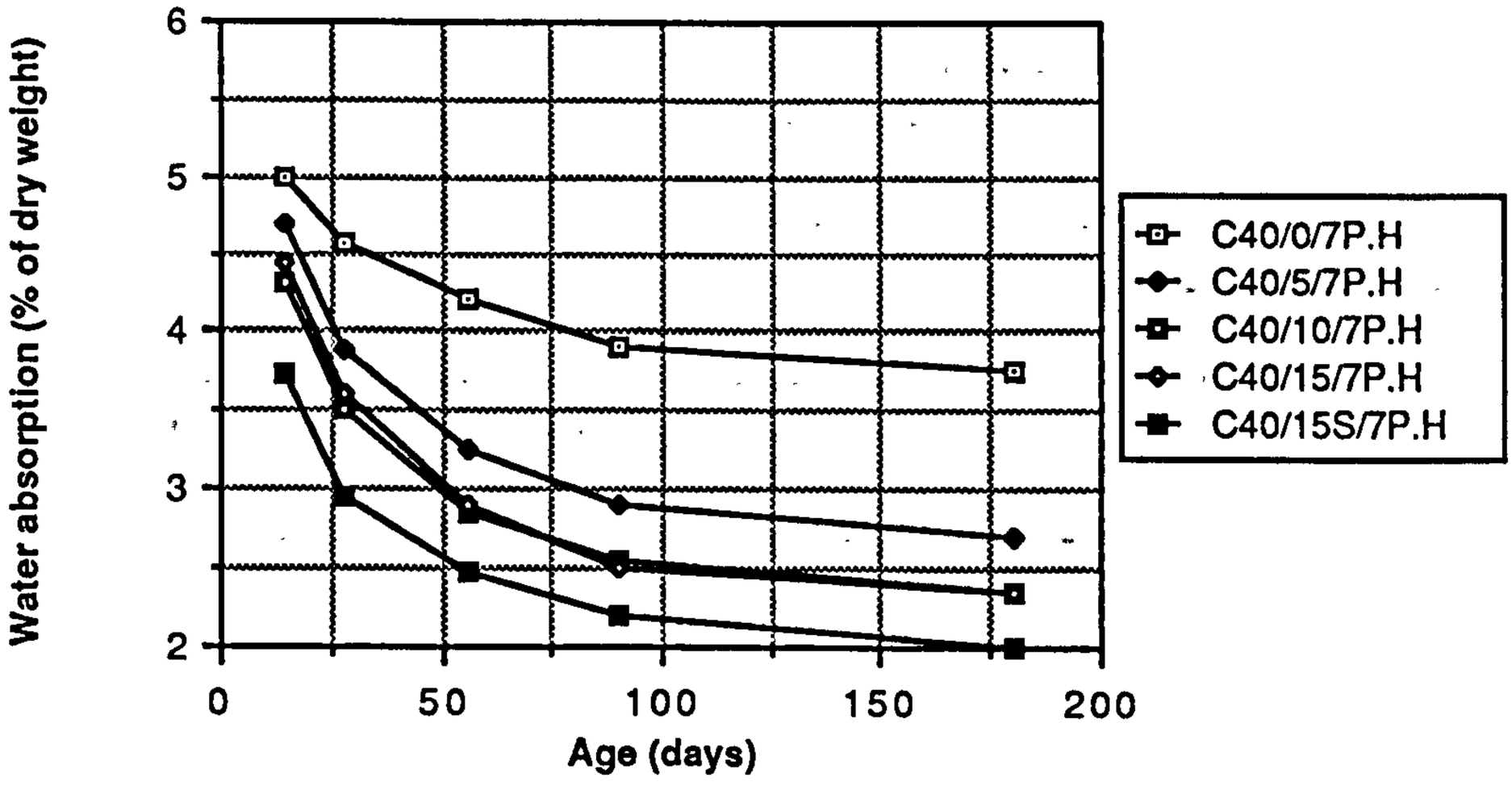

Figure 8.46 Effect of age on water absorption of plain and CSF mixes

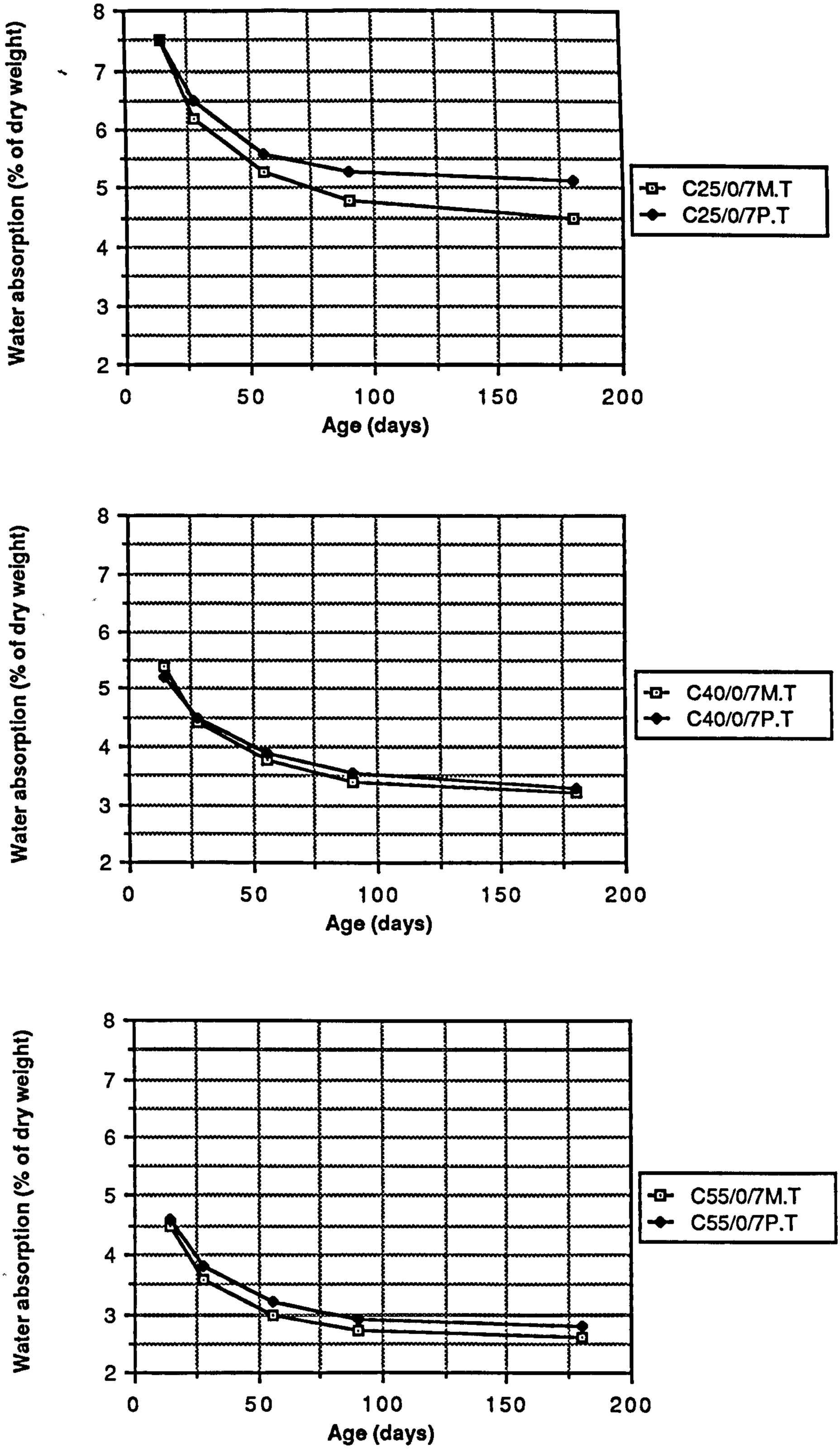

Figure 8.47 Effect of water nad polythene curing on water absorption of plain OPC mixes

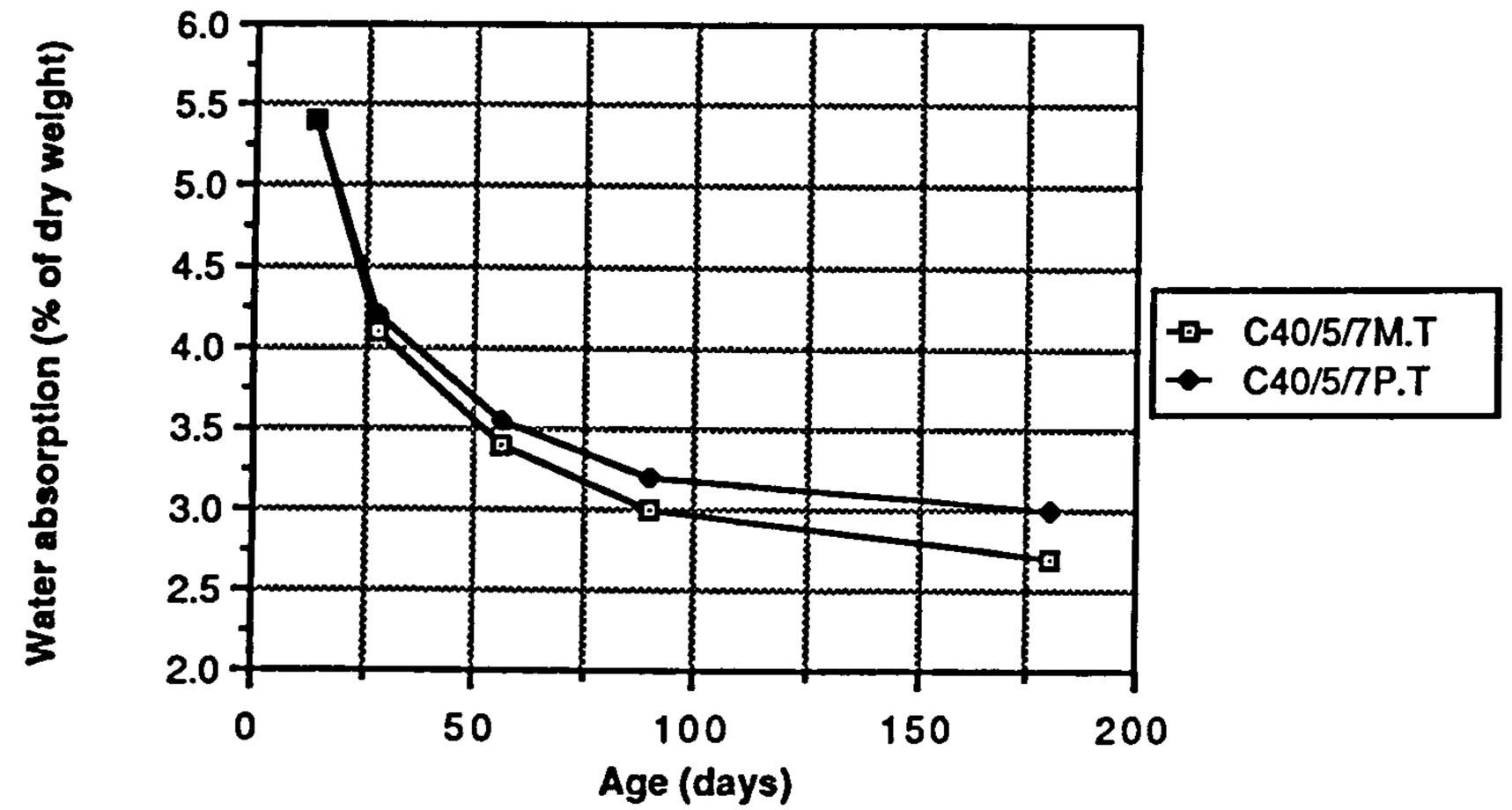

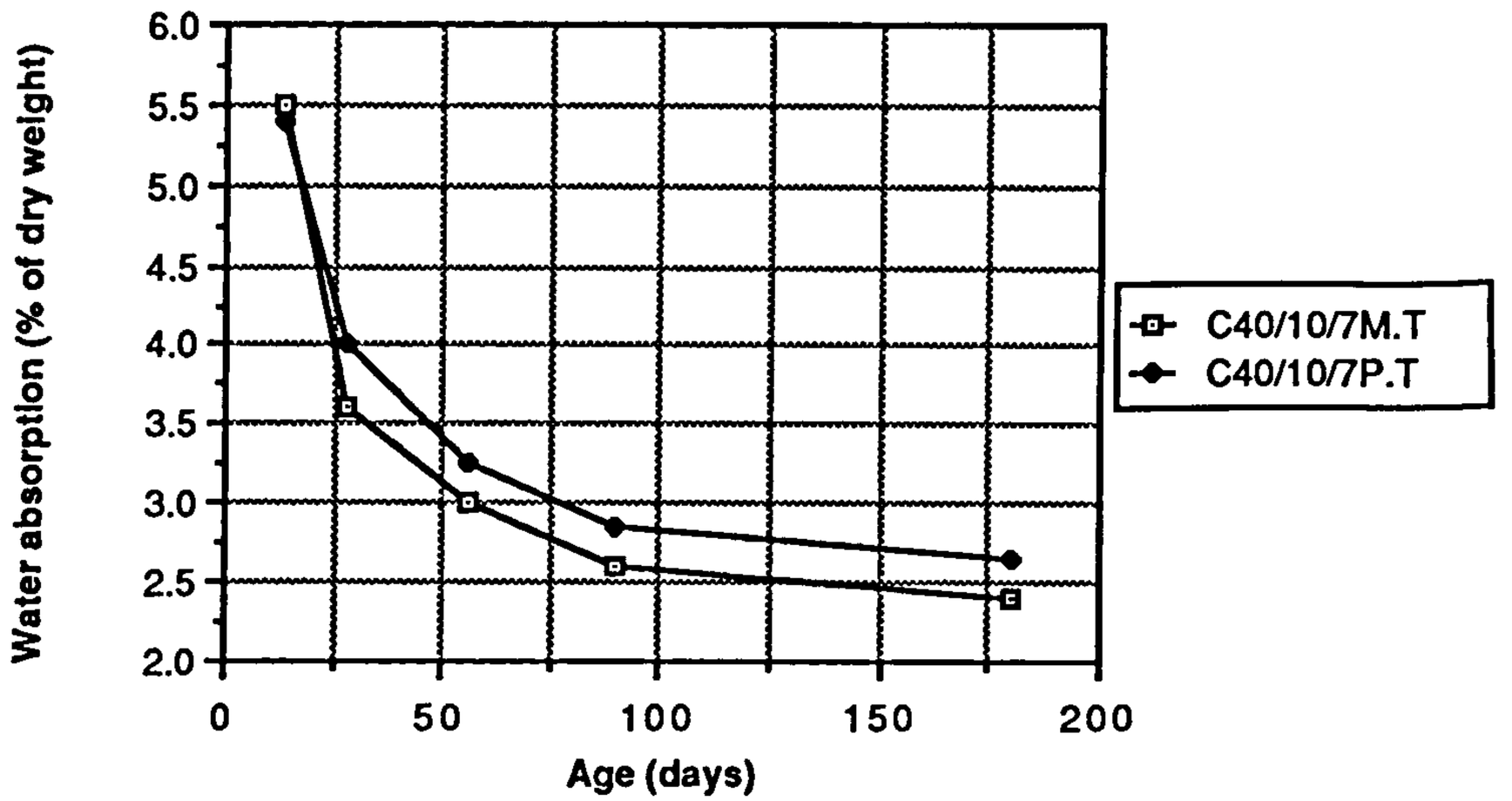

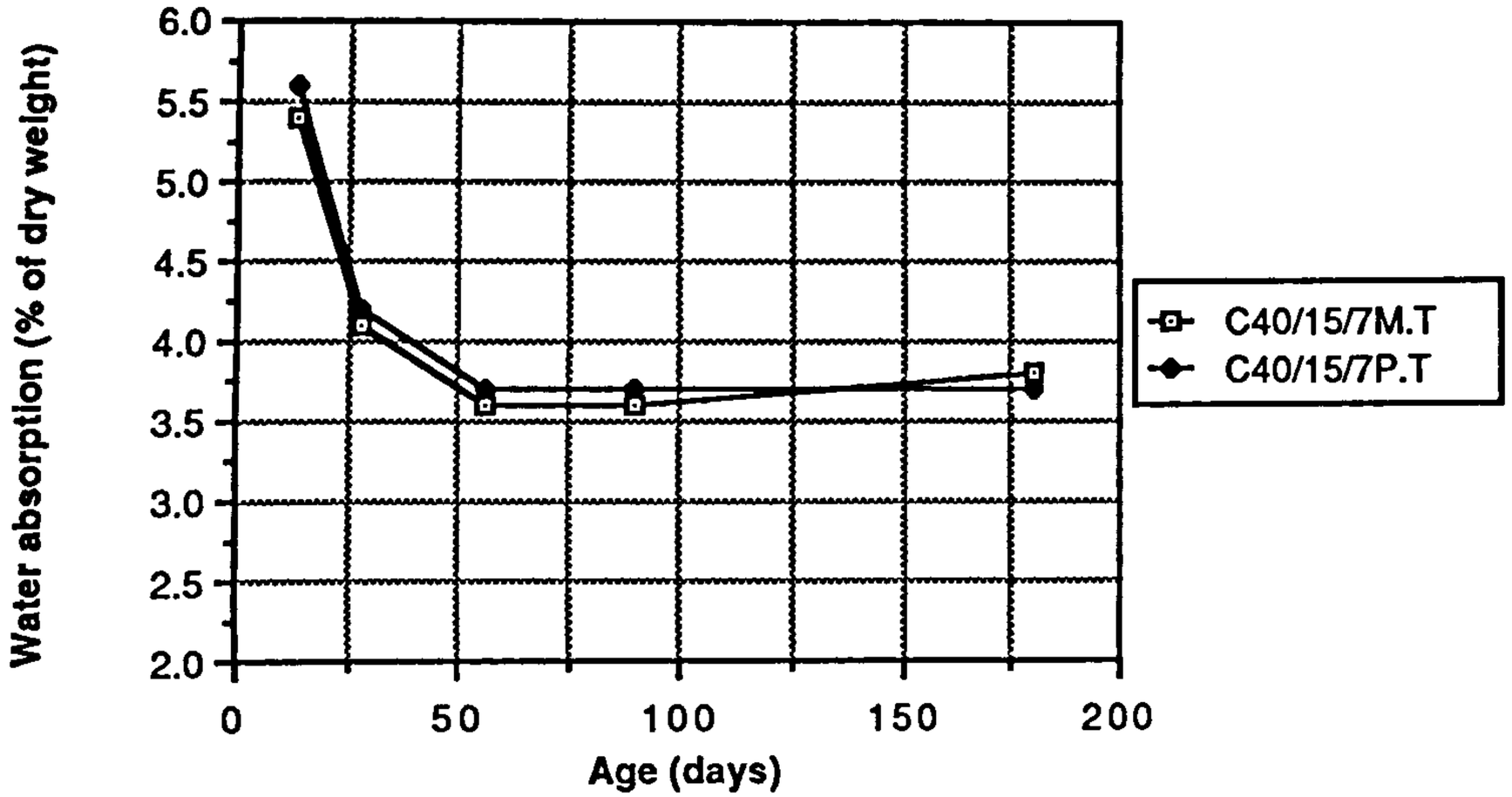

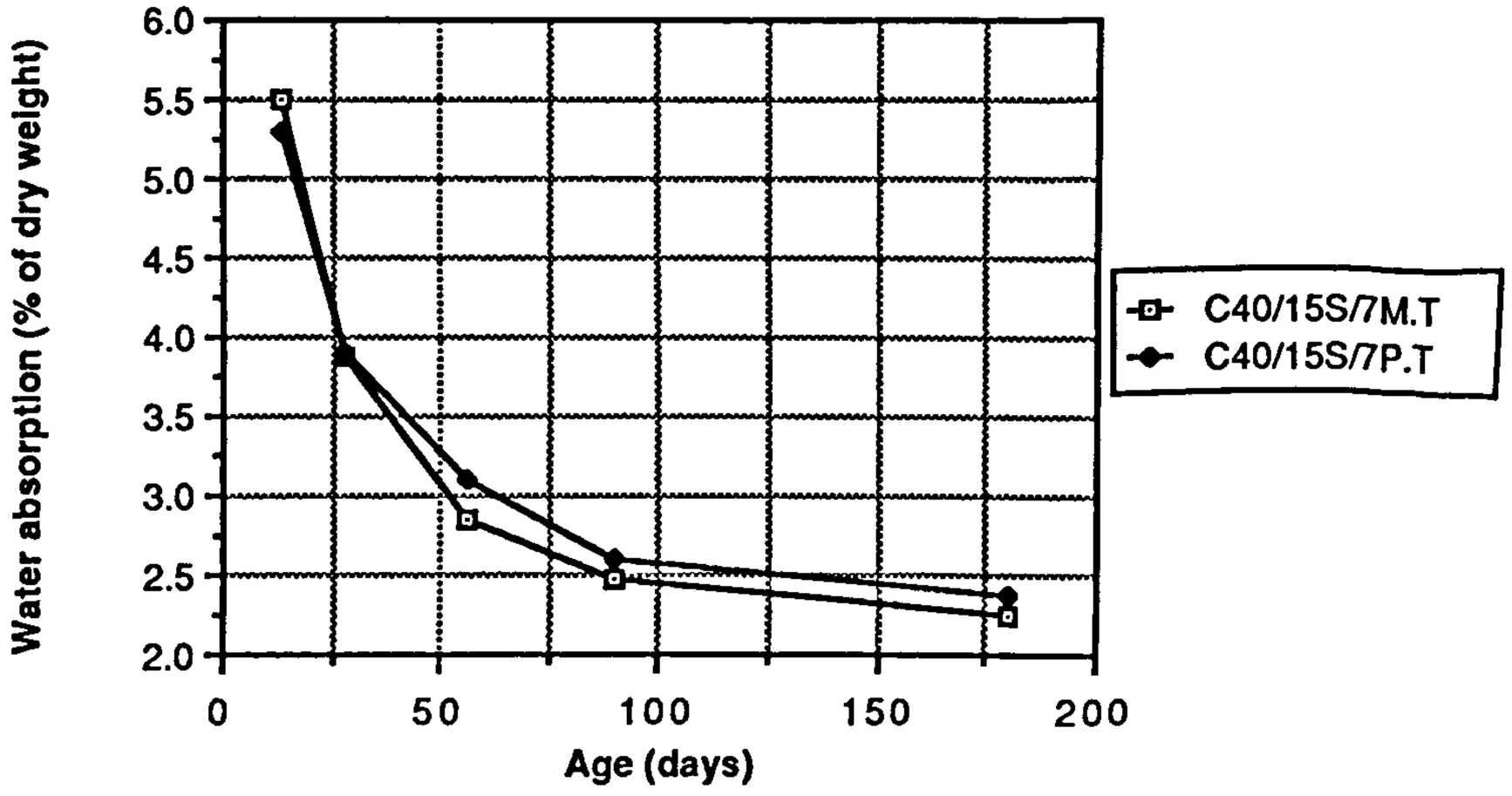

Figure 8.48 Effect of water and polythene curing on water absorption of CSF mixes

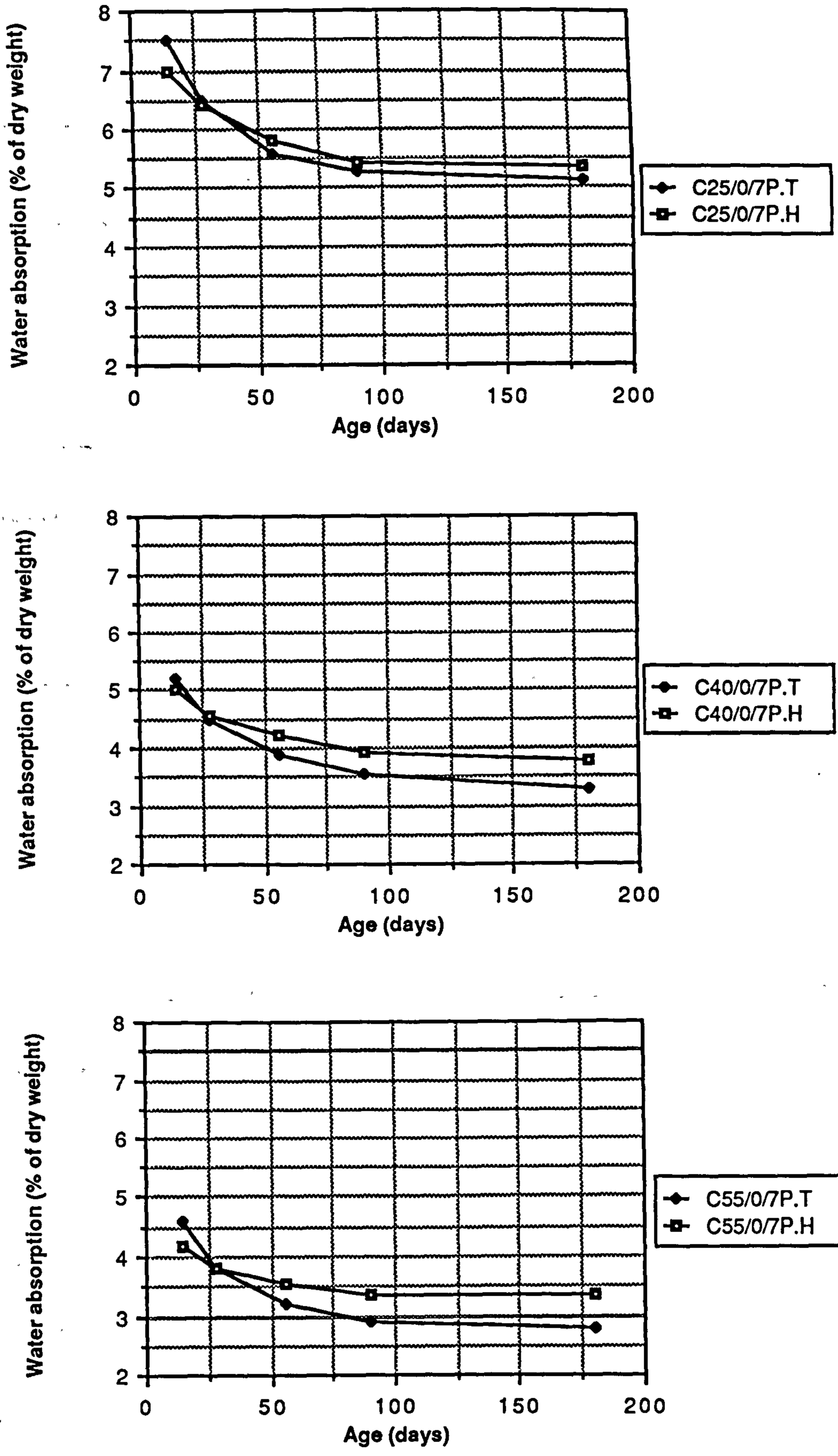

Figure 8.49 Effect of temperate and hot curing on water absorption of plain OPC mixes

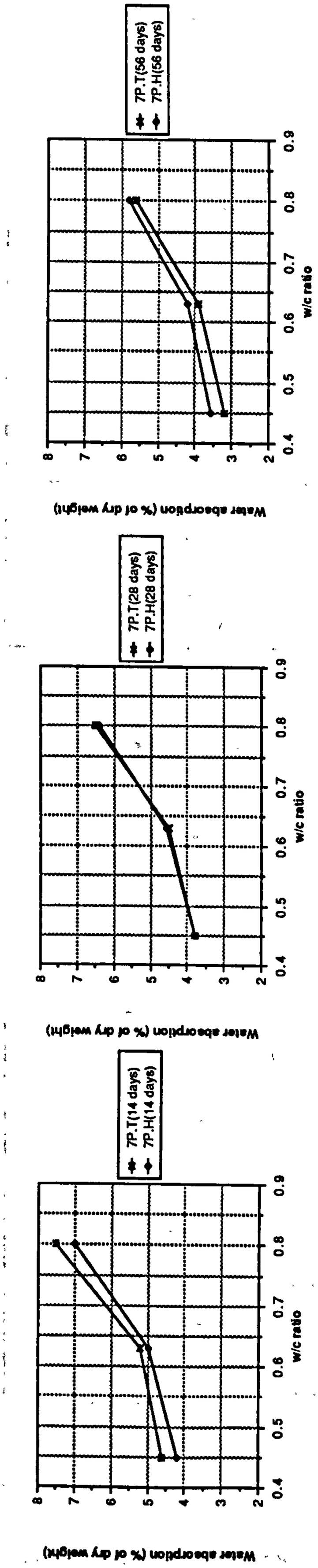

Effect of W/C ratio on water absorption of plain OPC mixes

Figure 8.50

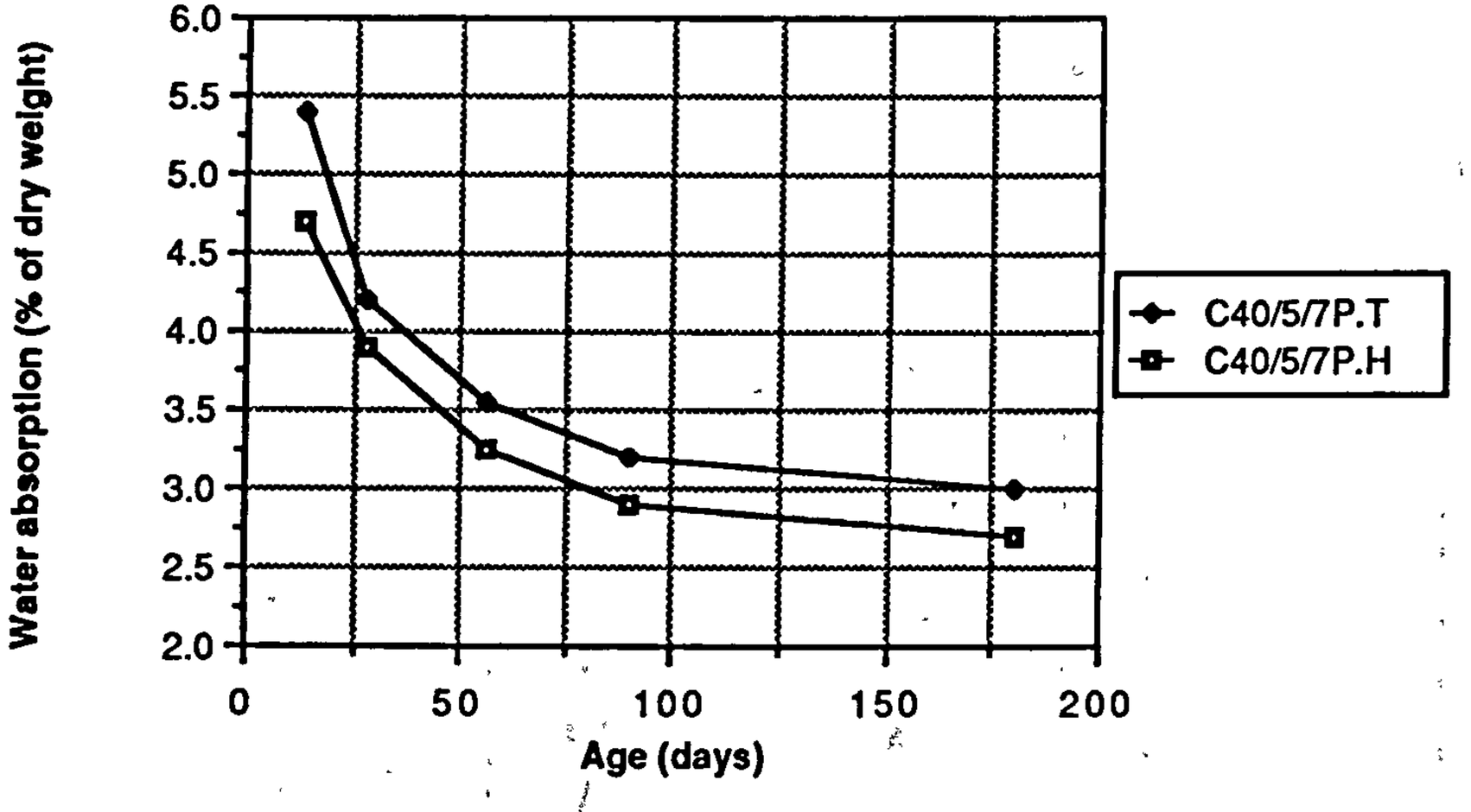

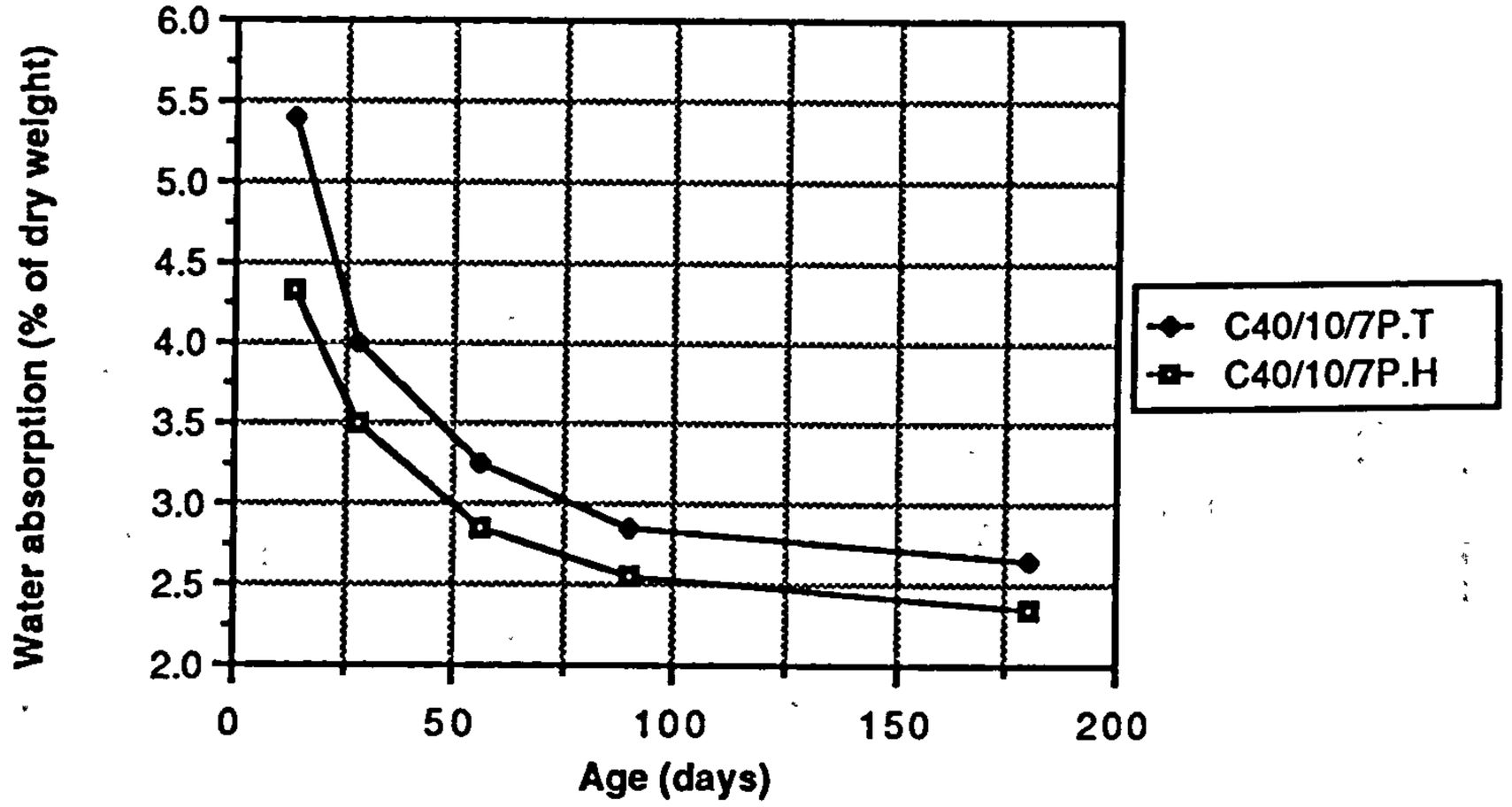

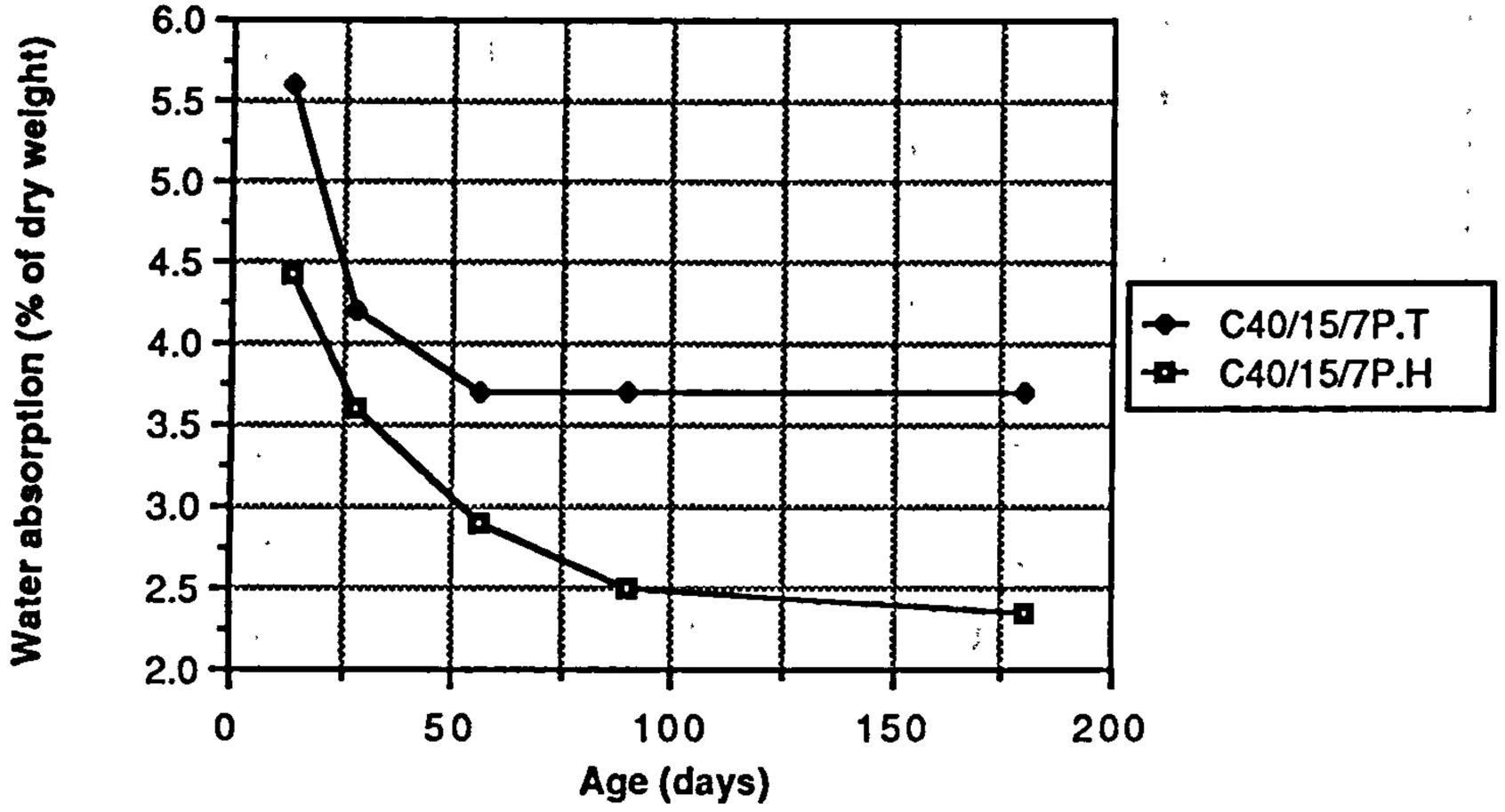

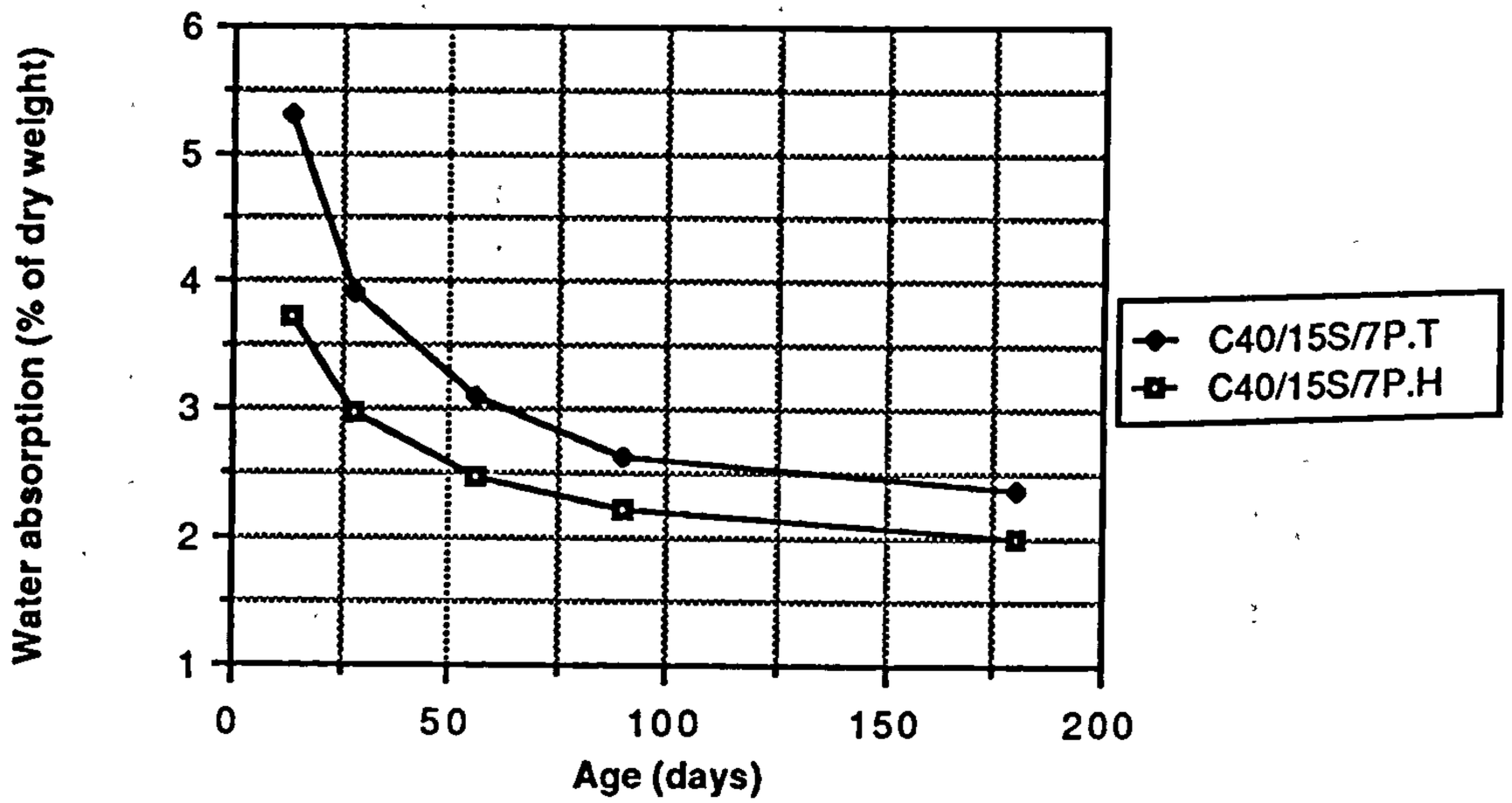

Figure 8.51 Effect of temperate and hot curing environment on water absorption of CSF mixes

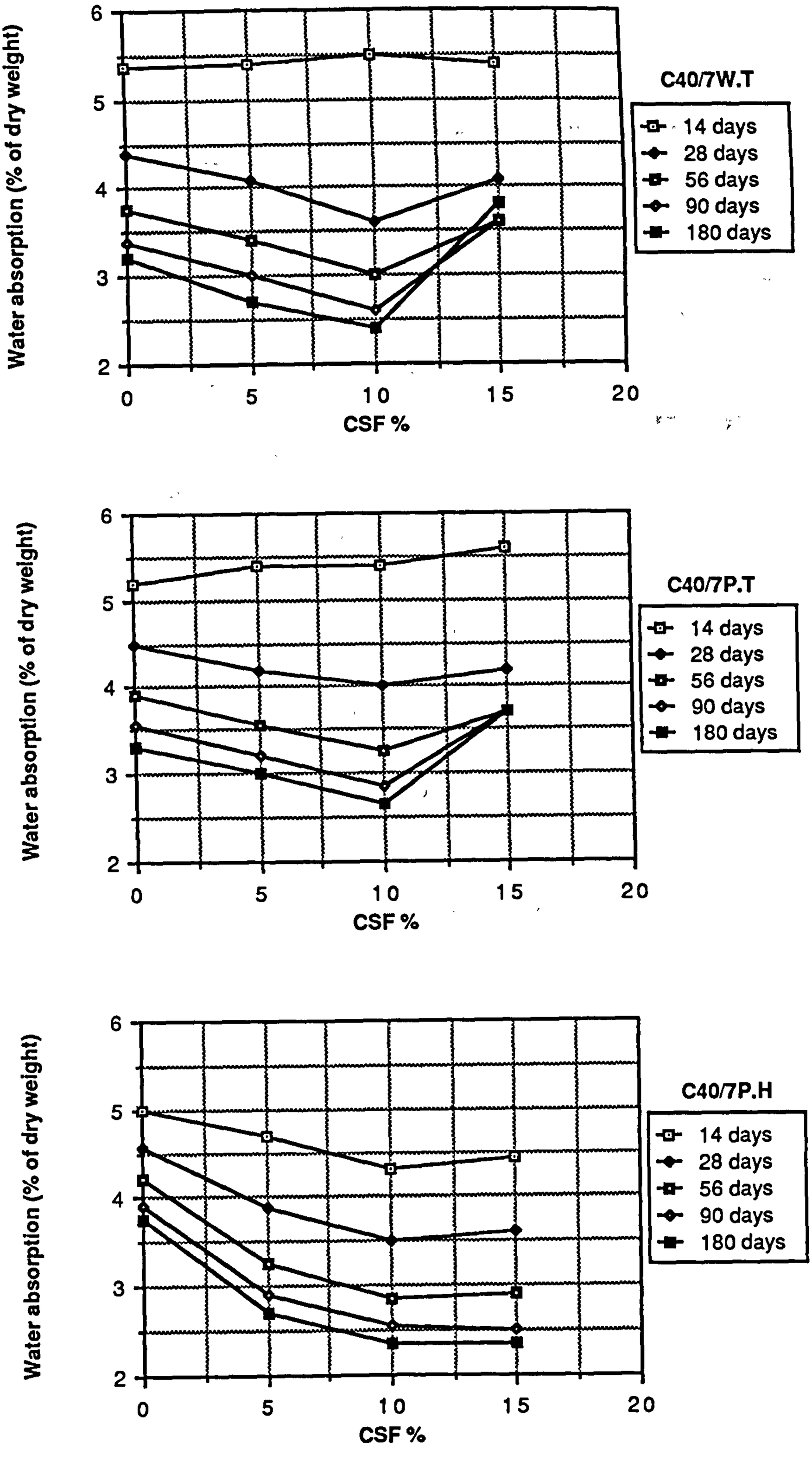

Figure 8.52 Effect of CSF content on water absorption

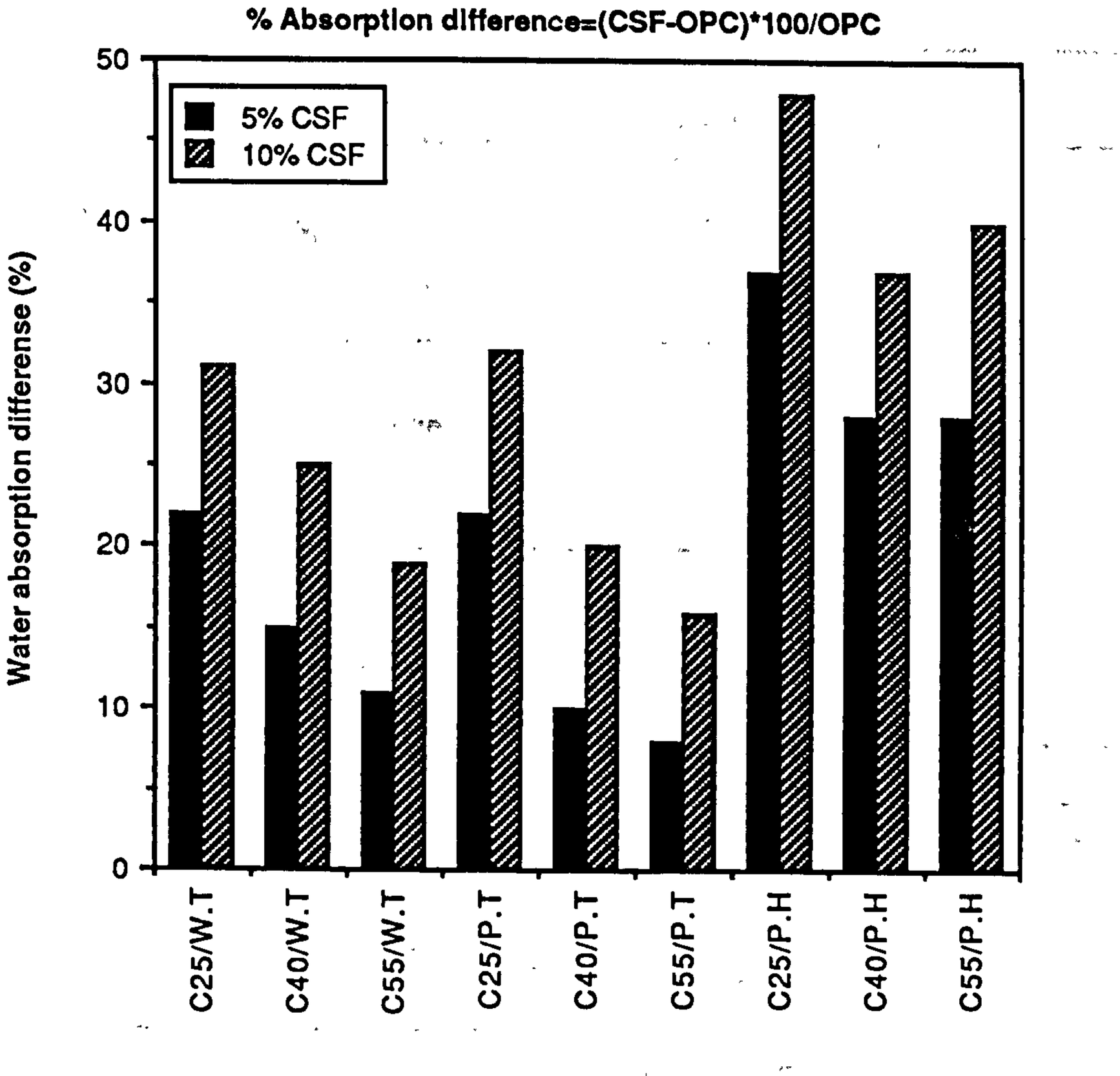

Figure 8.53 Percent reduction in water absorption caused by adding CSF to lean, medium and rich mixes

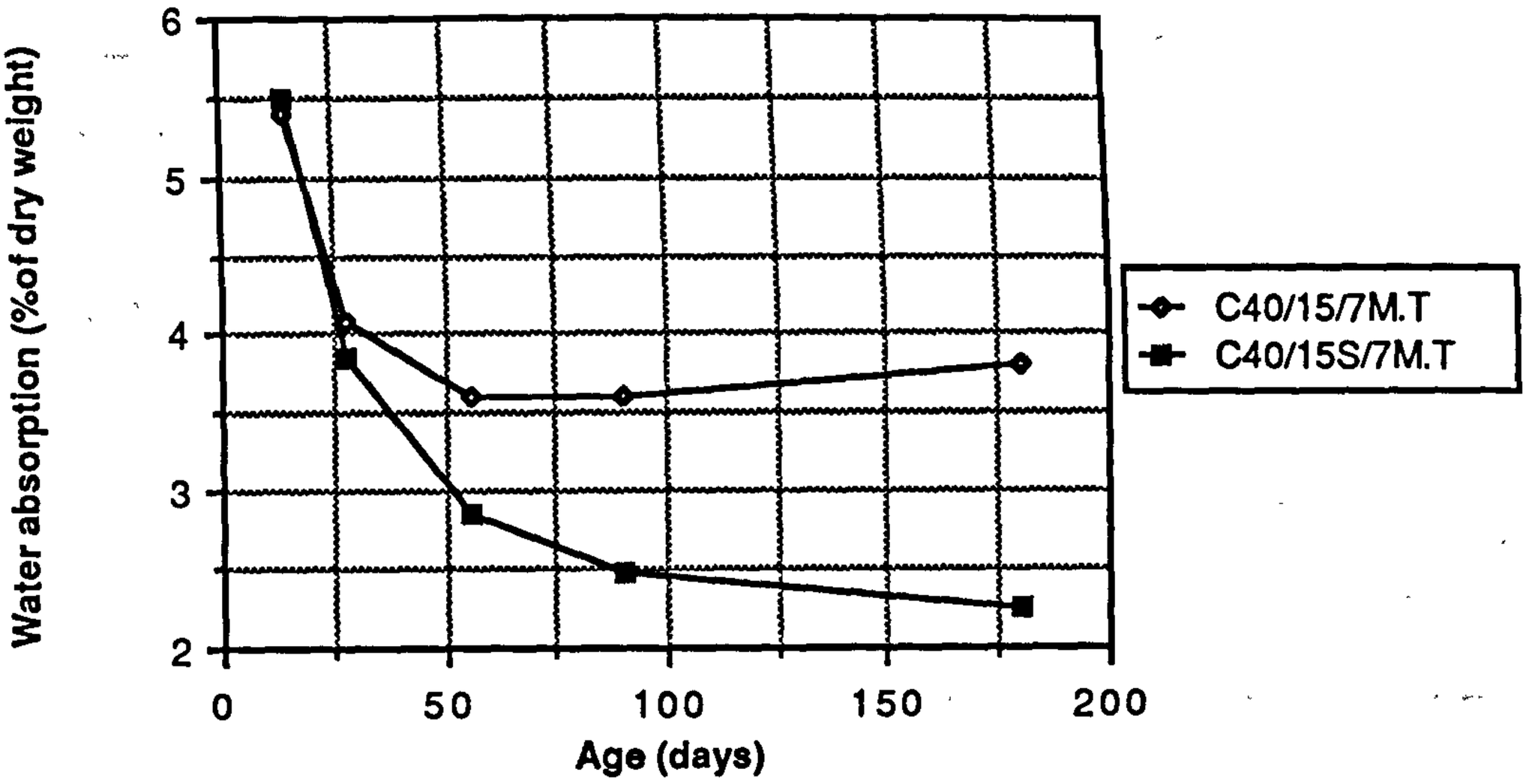

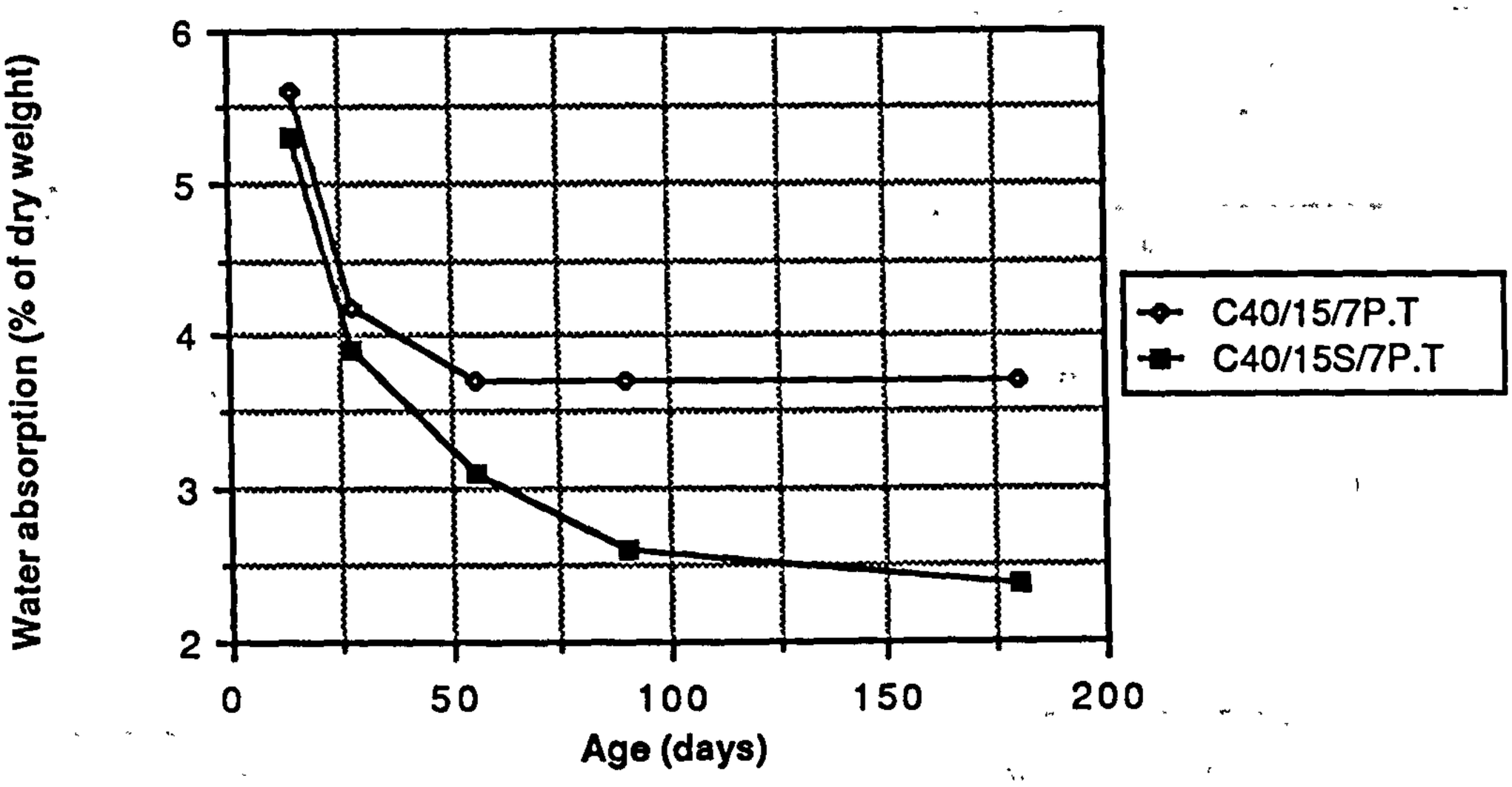

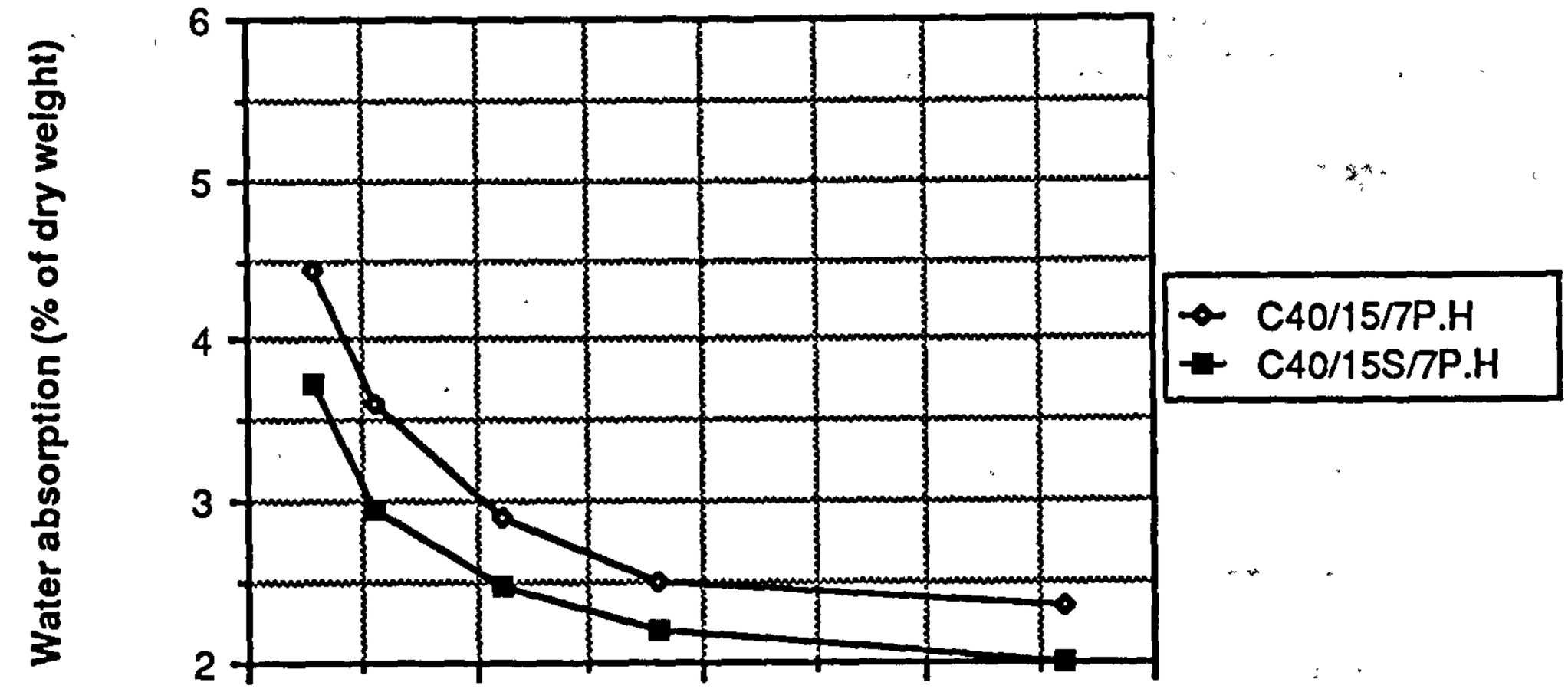

Figure 8.54 Effect of superplasticizer on water absorption of CSF mixes

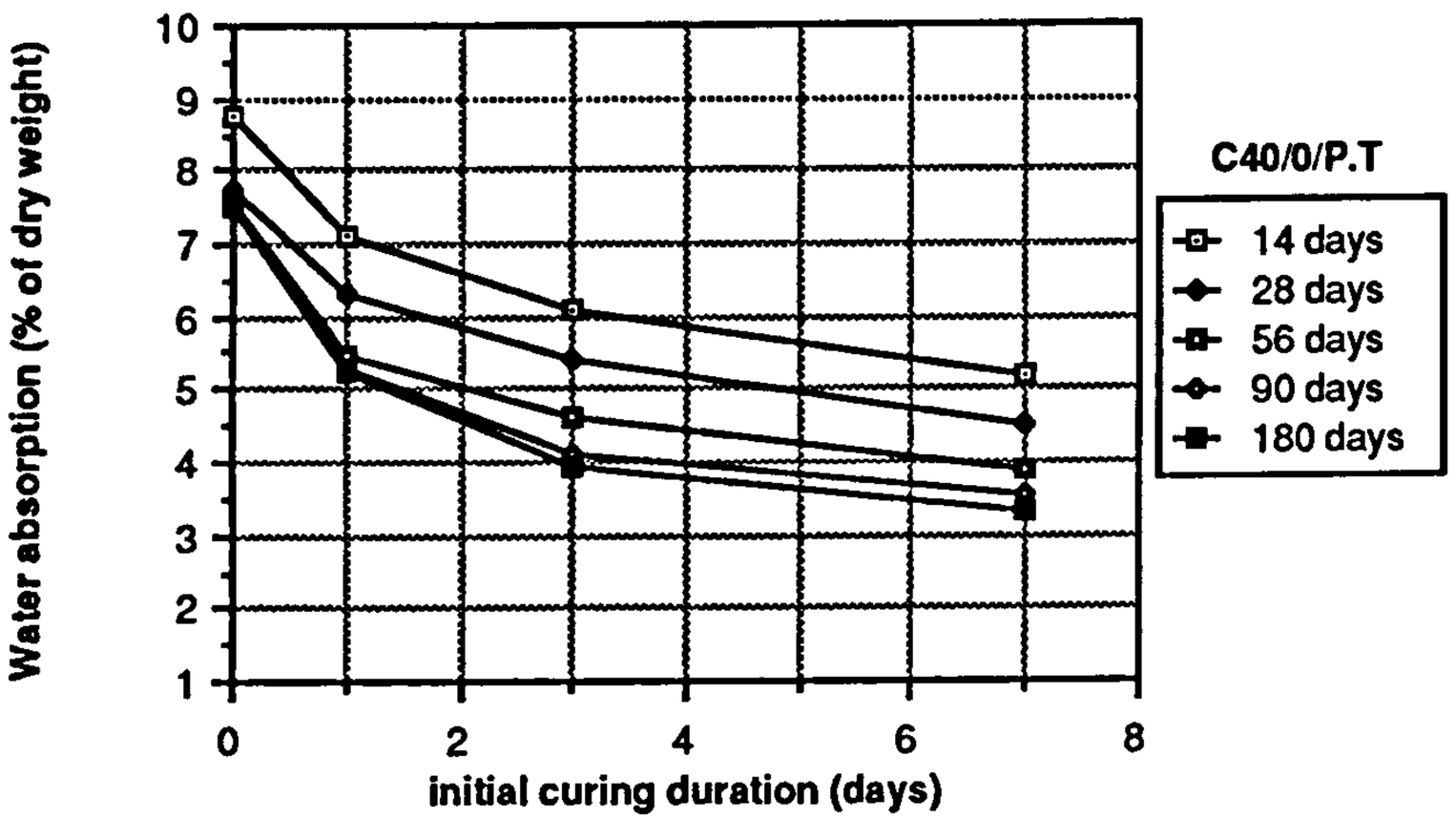

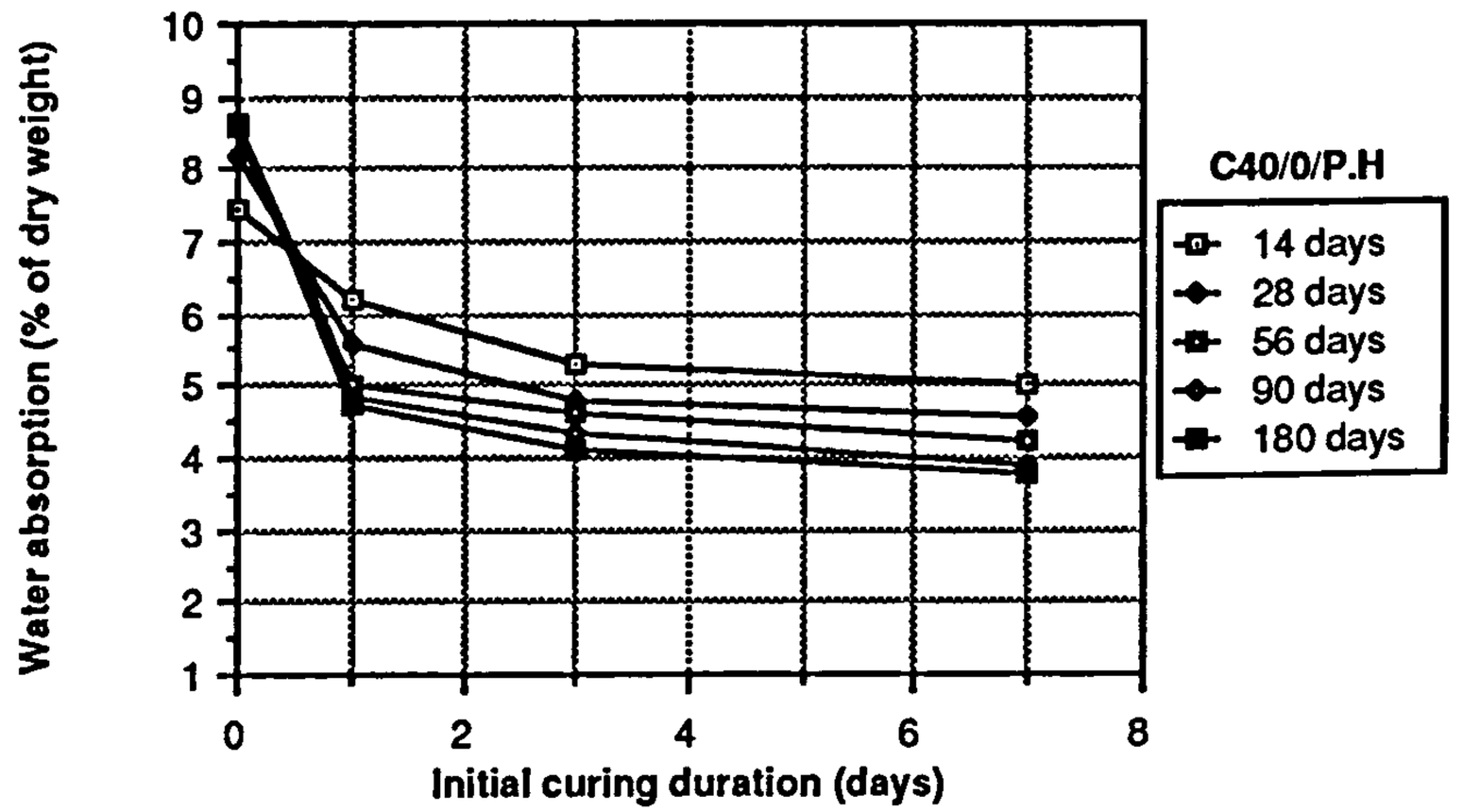

Figure 8.55 Effect of initial curing duration on water absorption of OPC

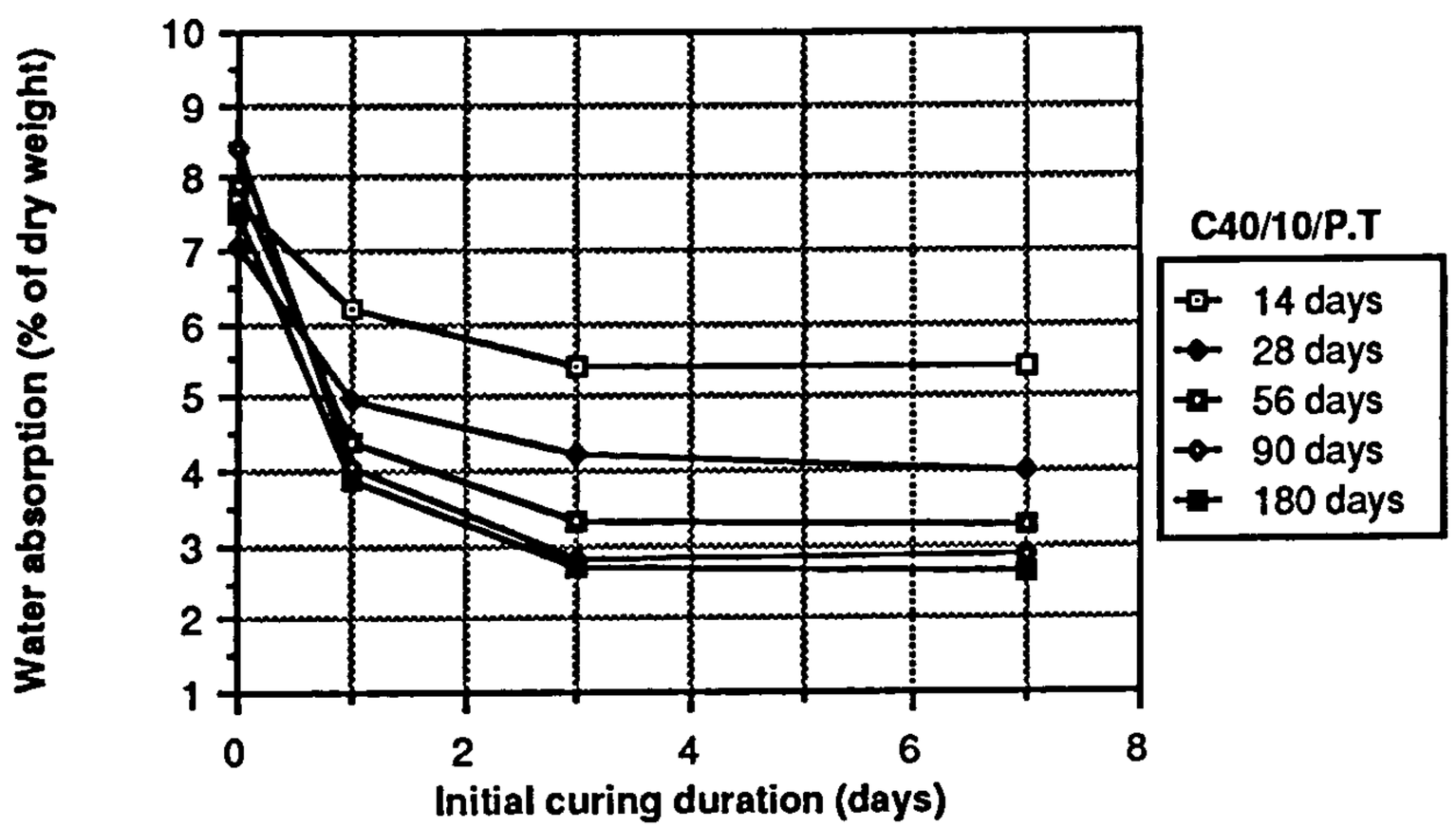

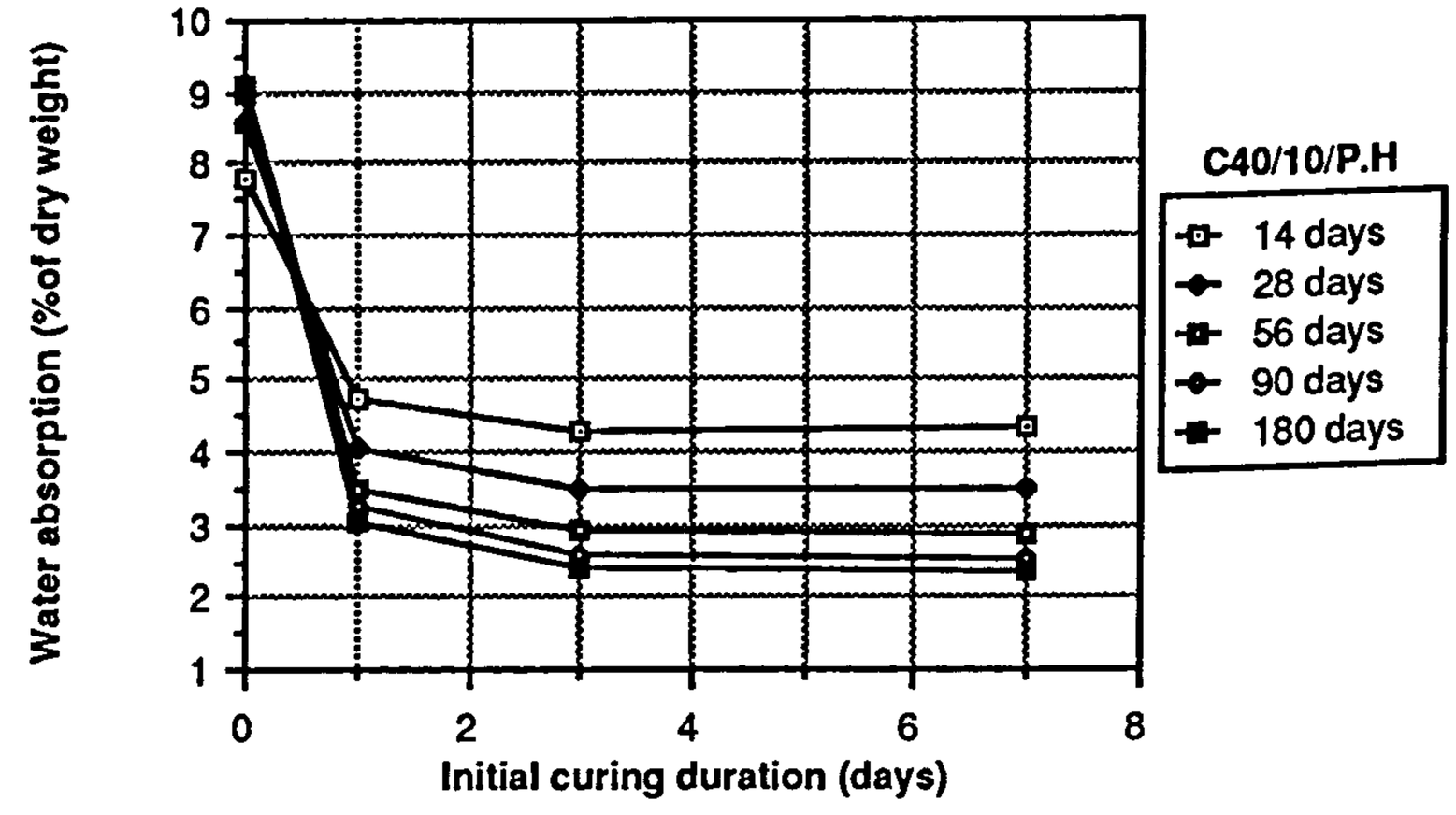

Figure 8.56 Effect of initial curing on water absorption of CSF

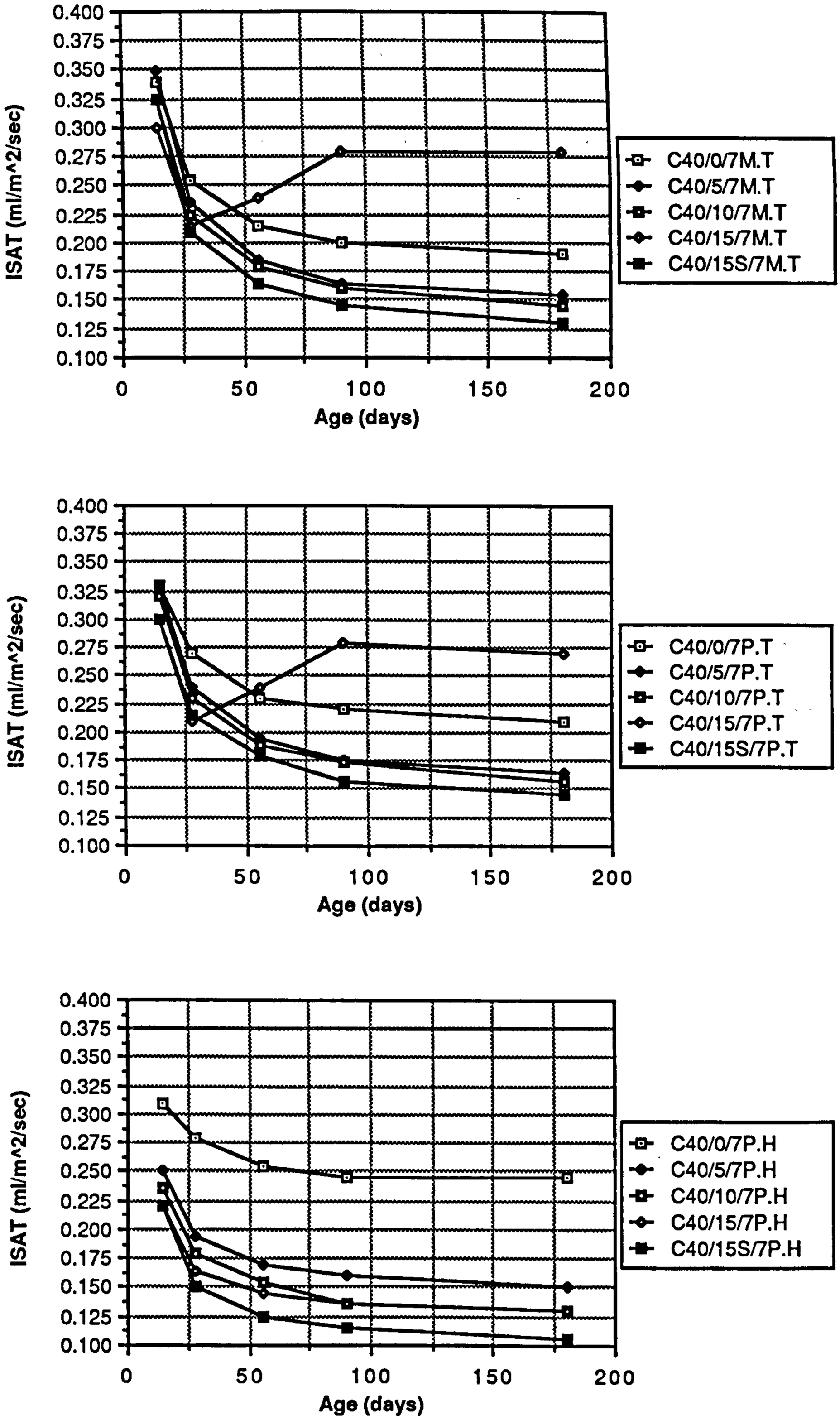

Figure 8.57 Effect of age on ISAT of plain and CSF mixes

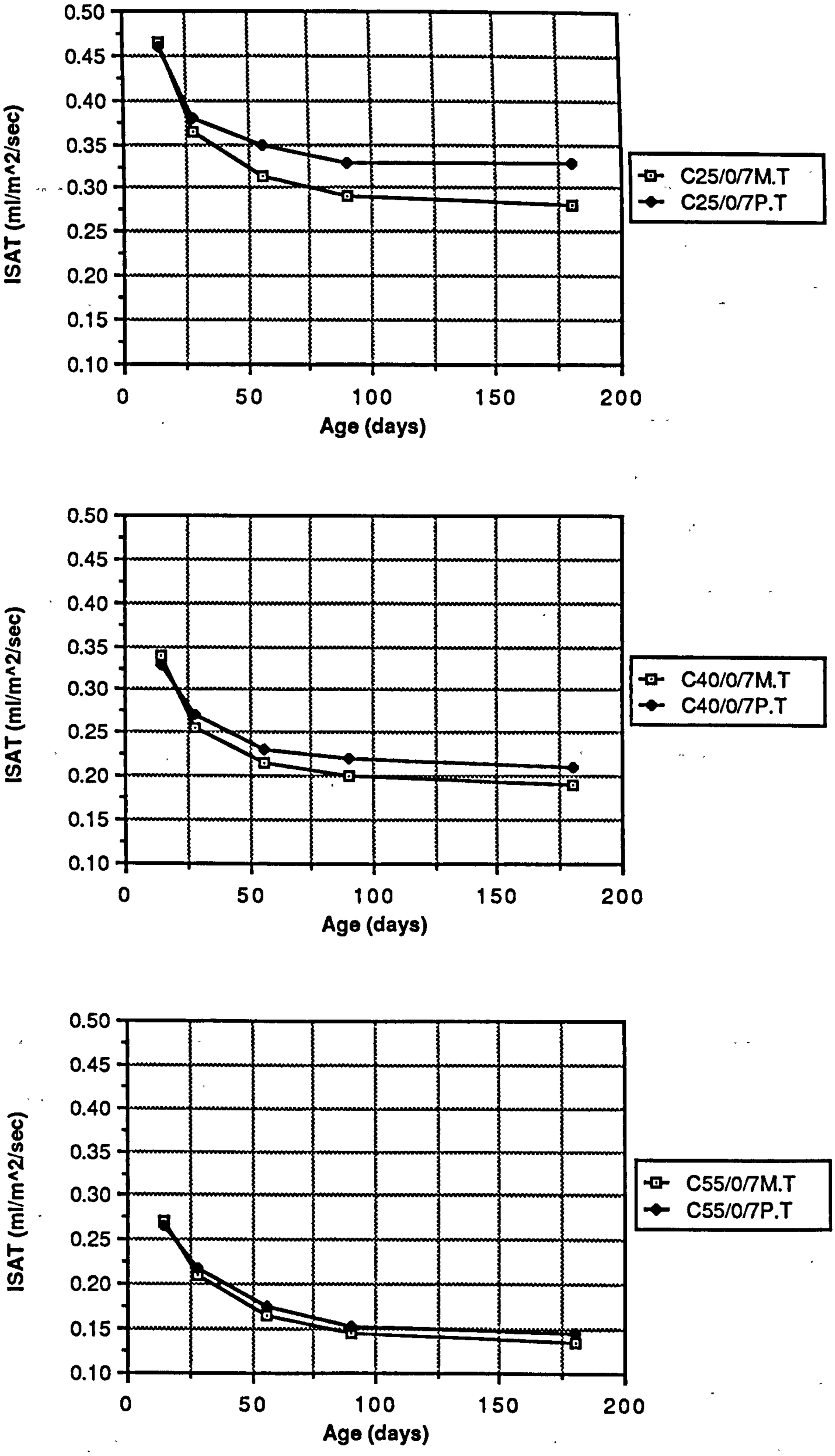

Figure 8.58 Effect of water and polythene curing on ISAT of plain OPC mixes

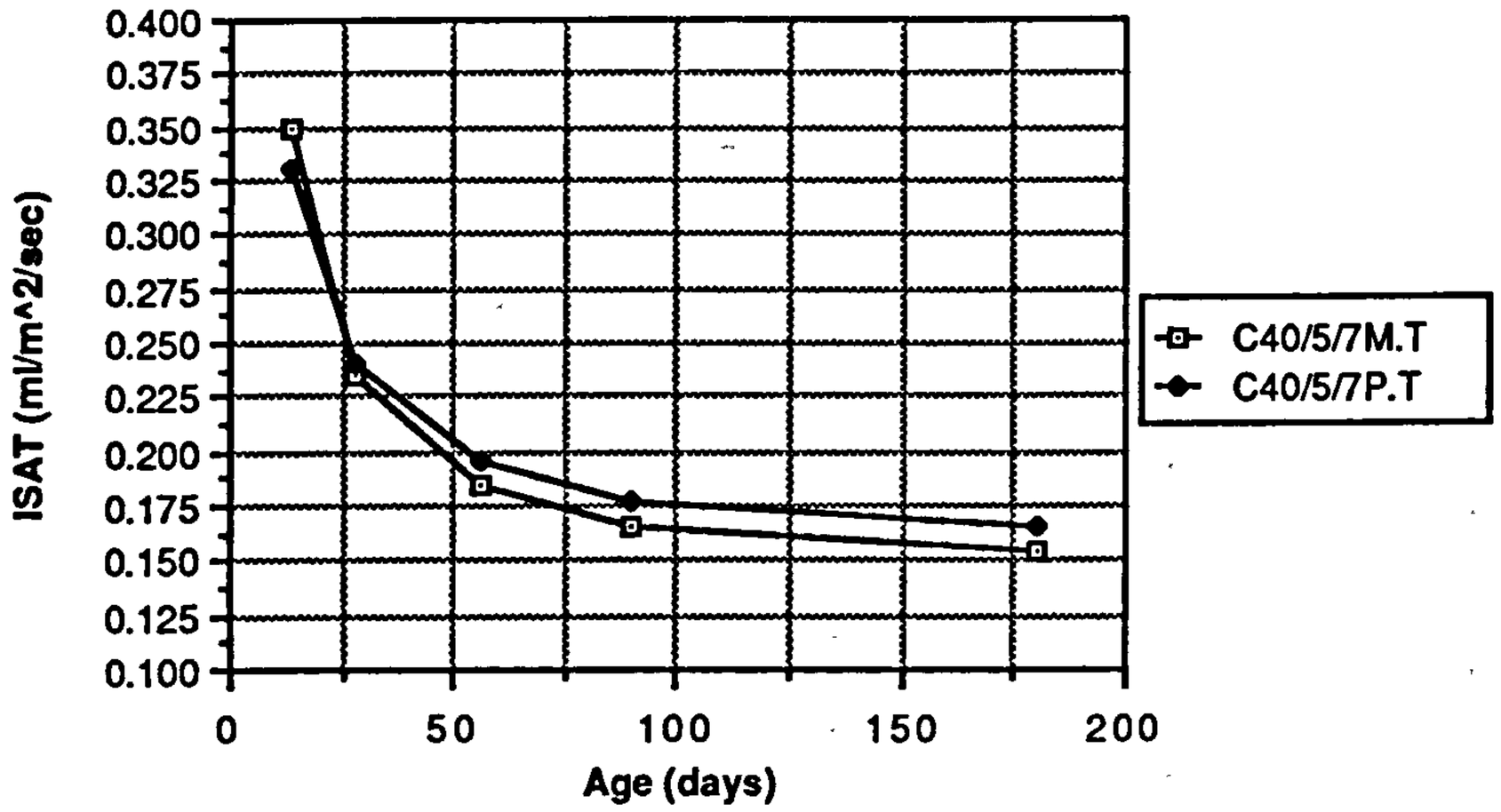

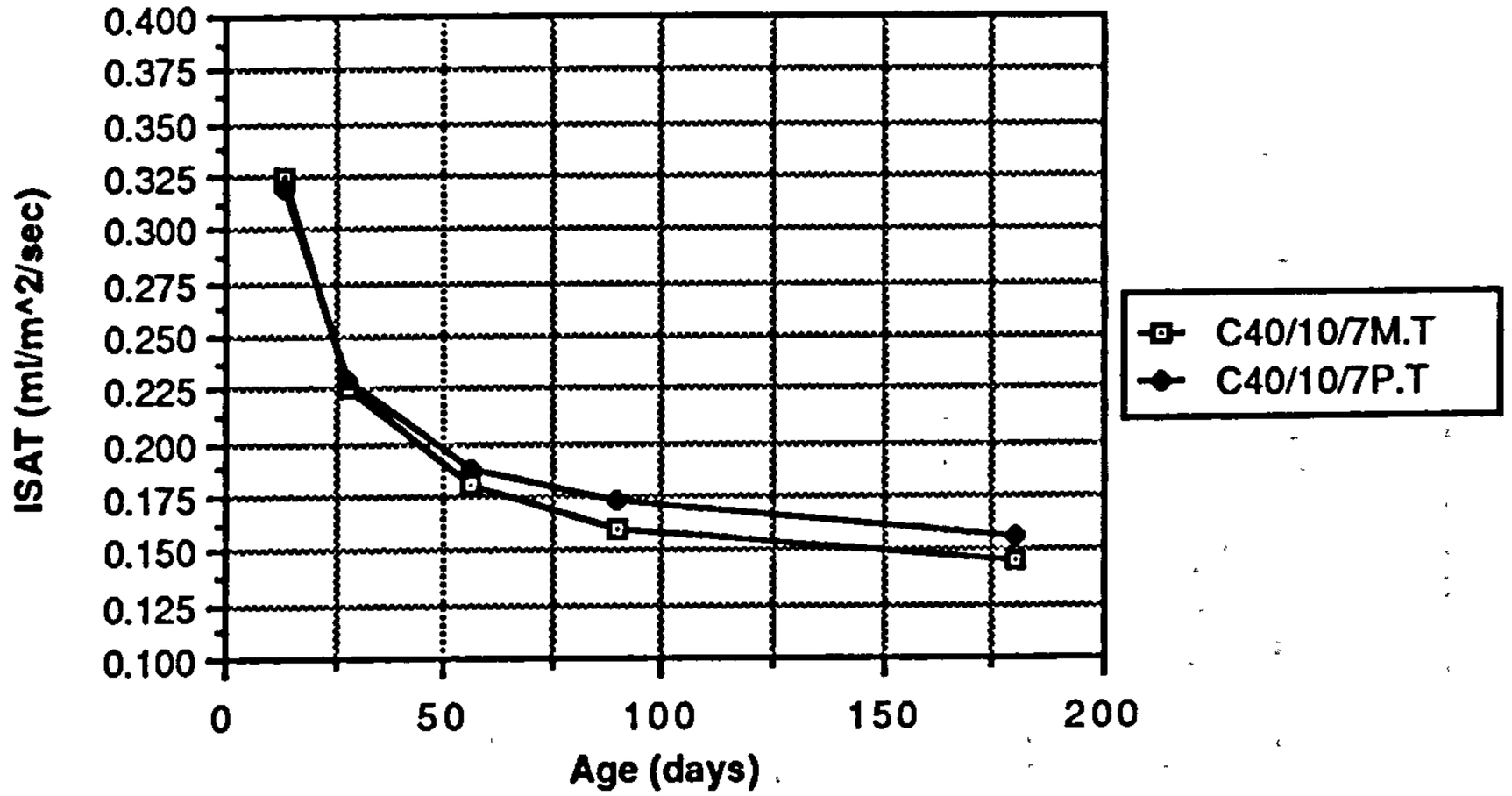

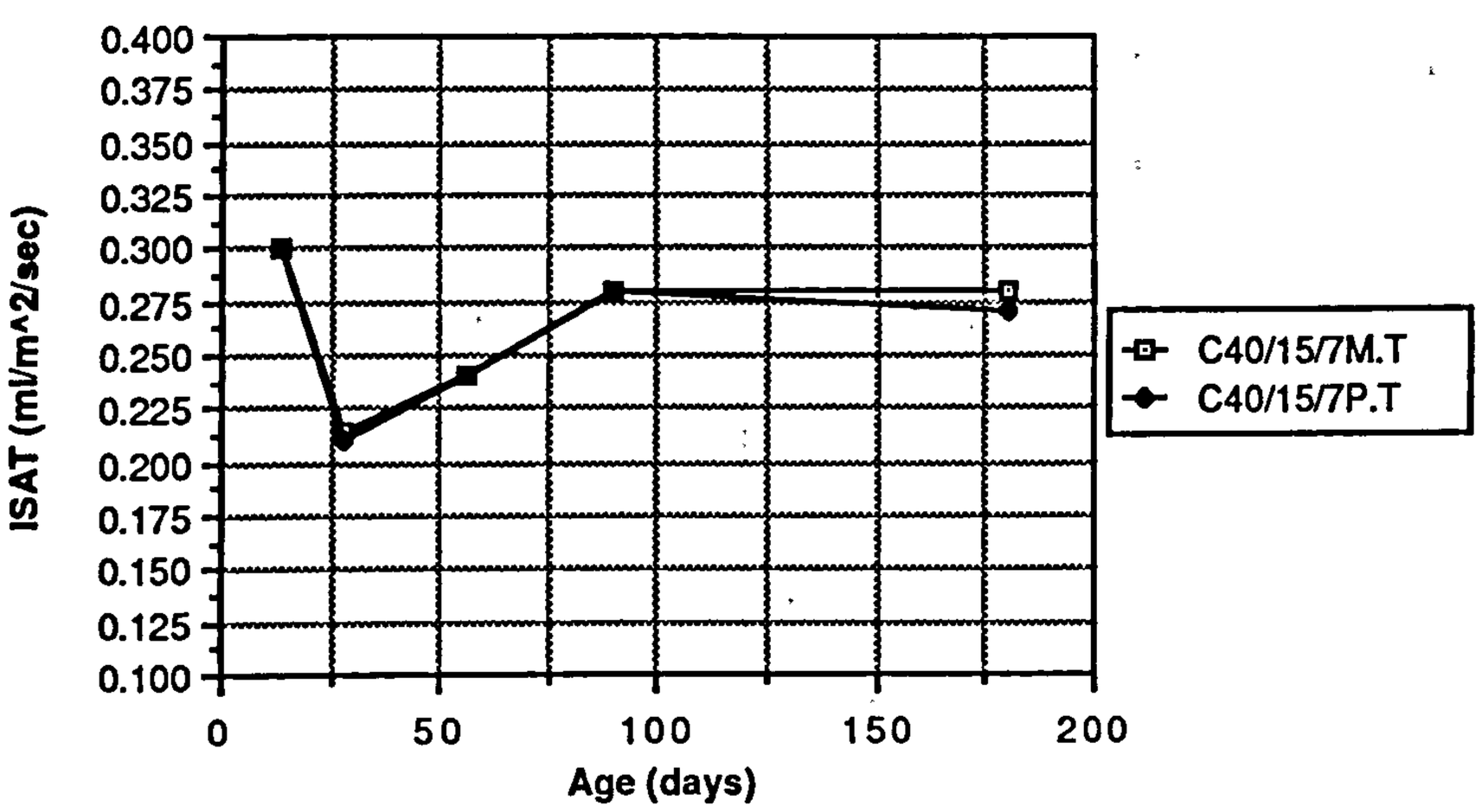

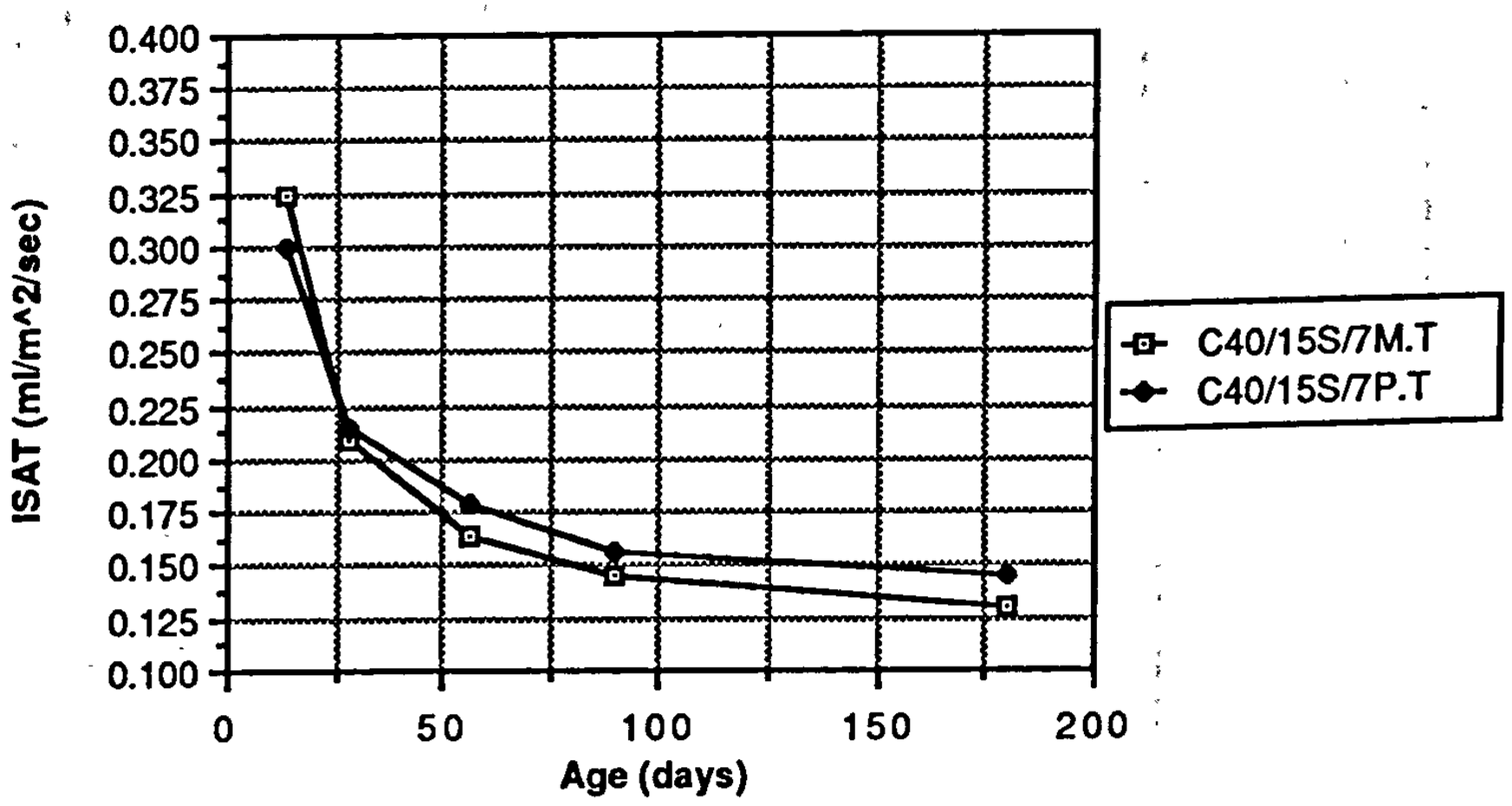

Figure 8.59 Effect of water and polythene curing on ISAT of CSF mixes

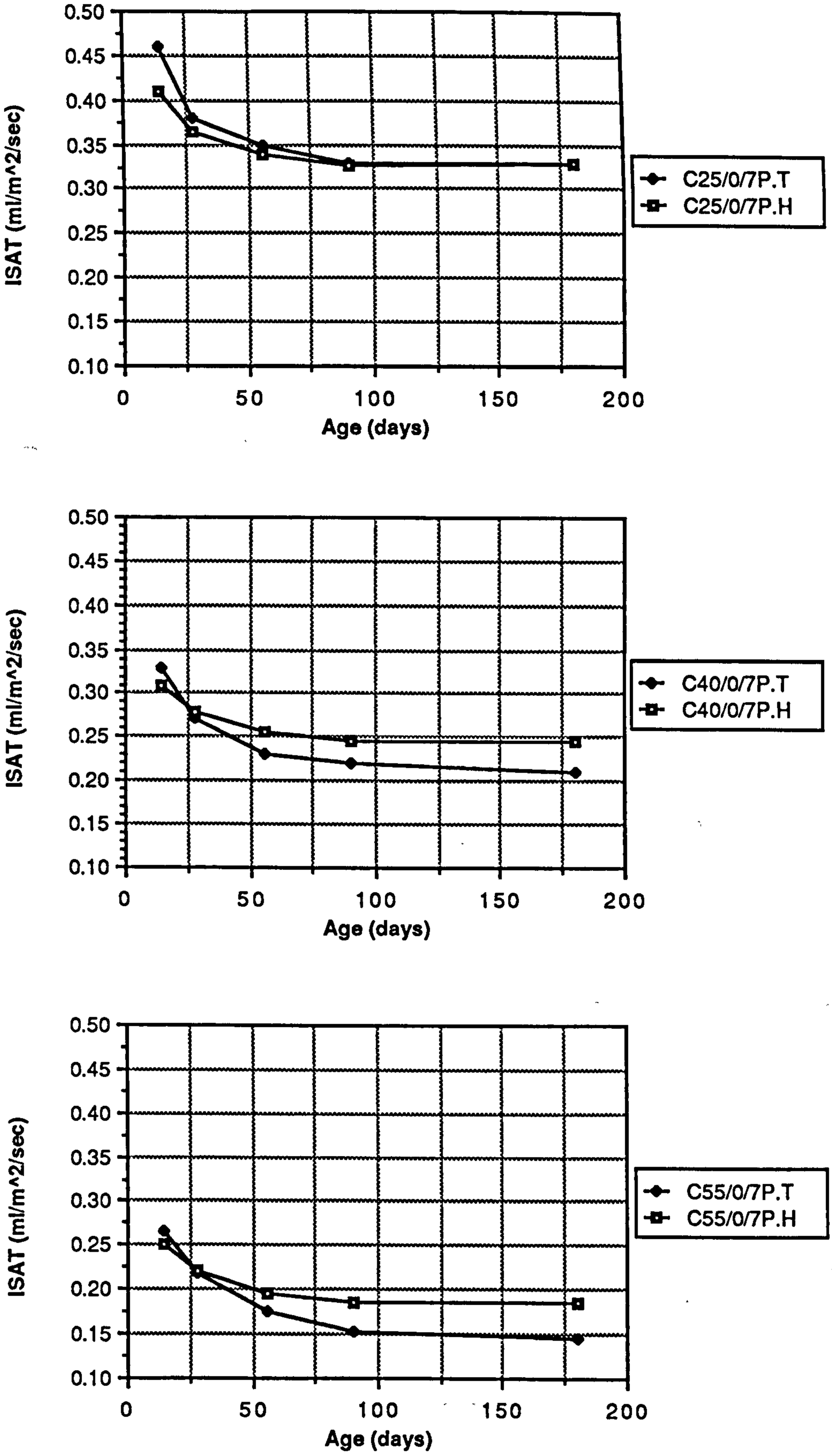

Figure 8.60 Effect of temperate and hot curing on ISAT of plain OPC concrete mixes

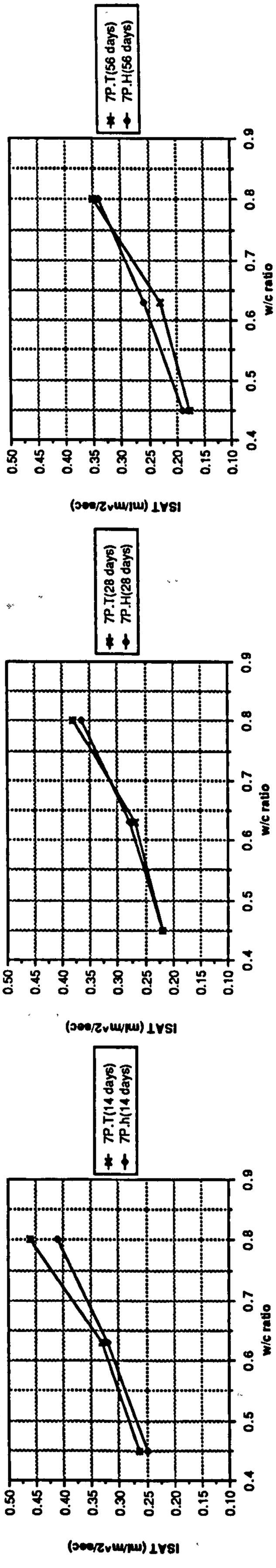

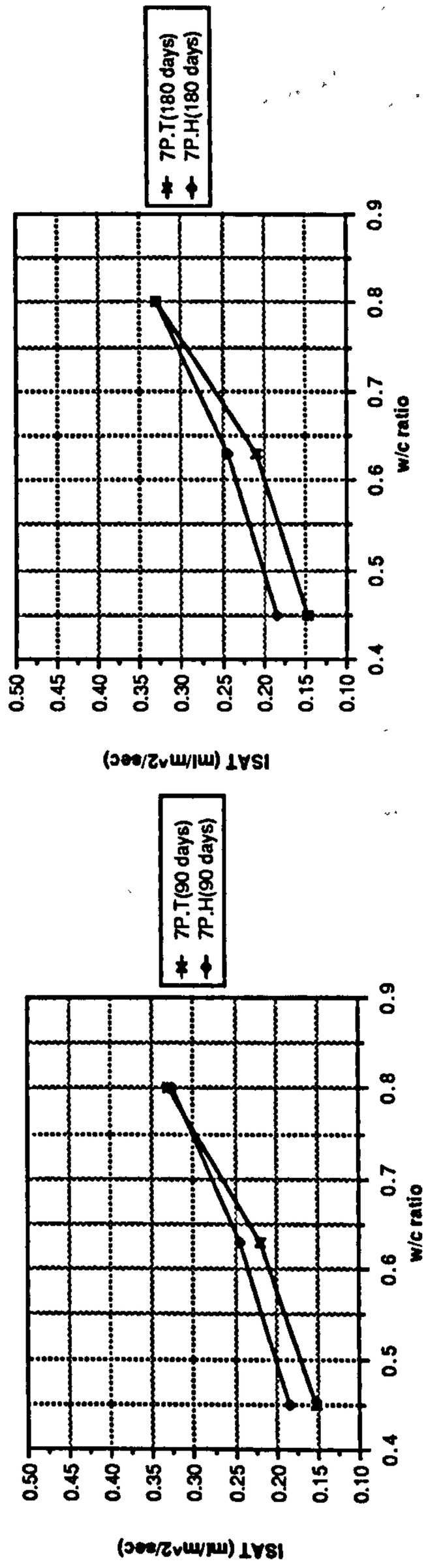

Figure 8.61 Effect of W/C ratio on ISAT of plain OPC mixes

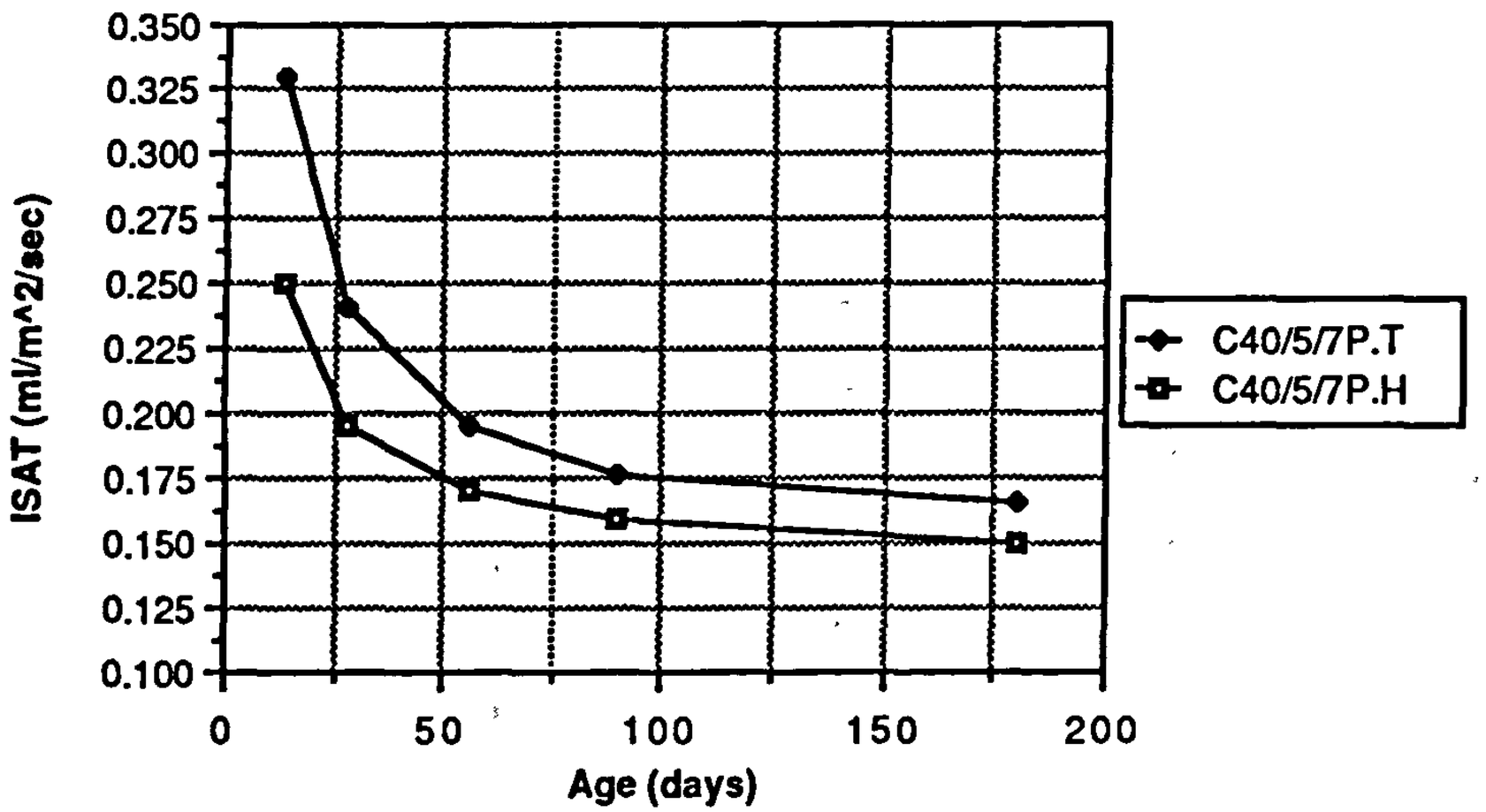

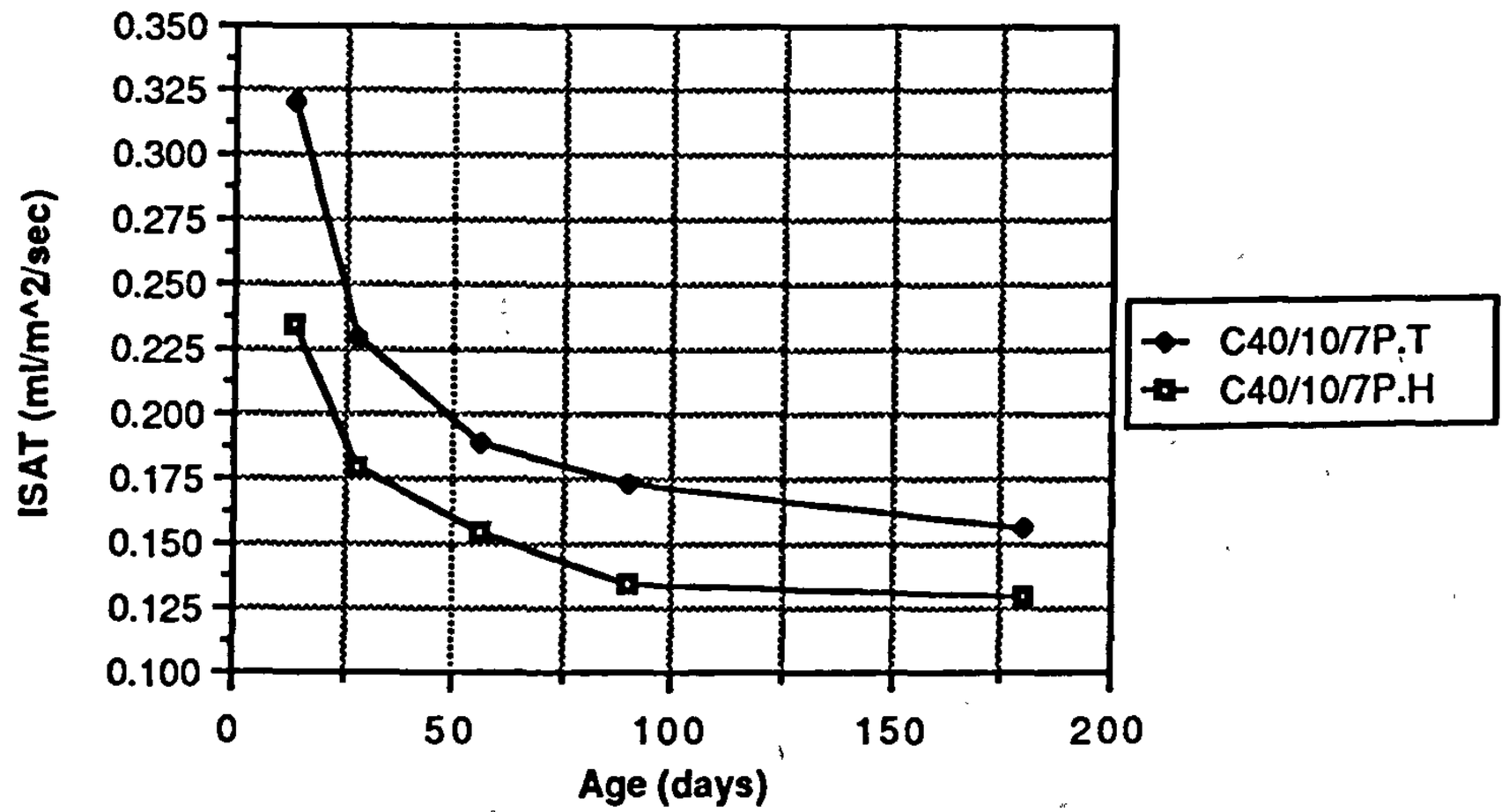

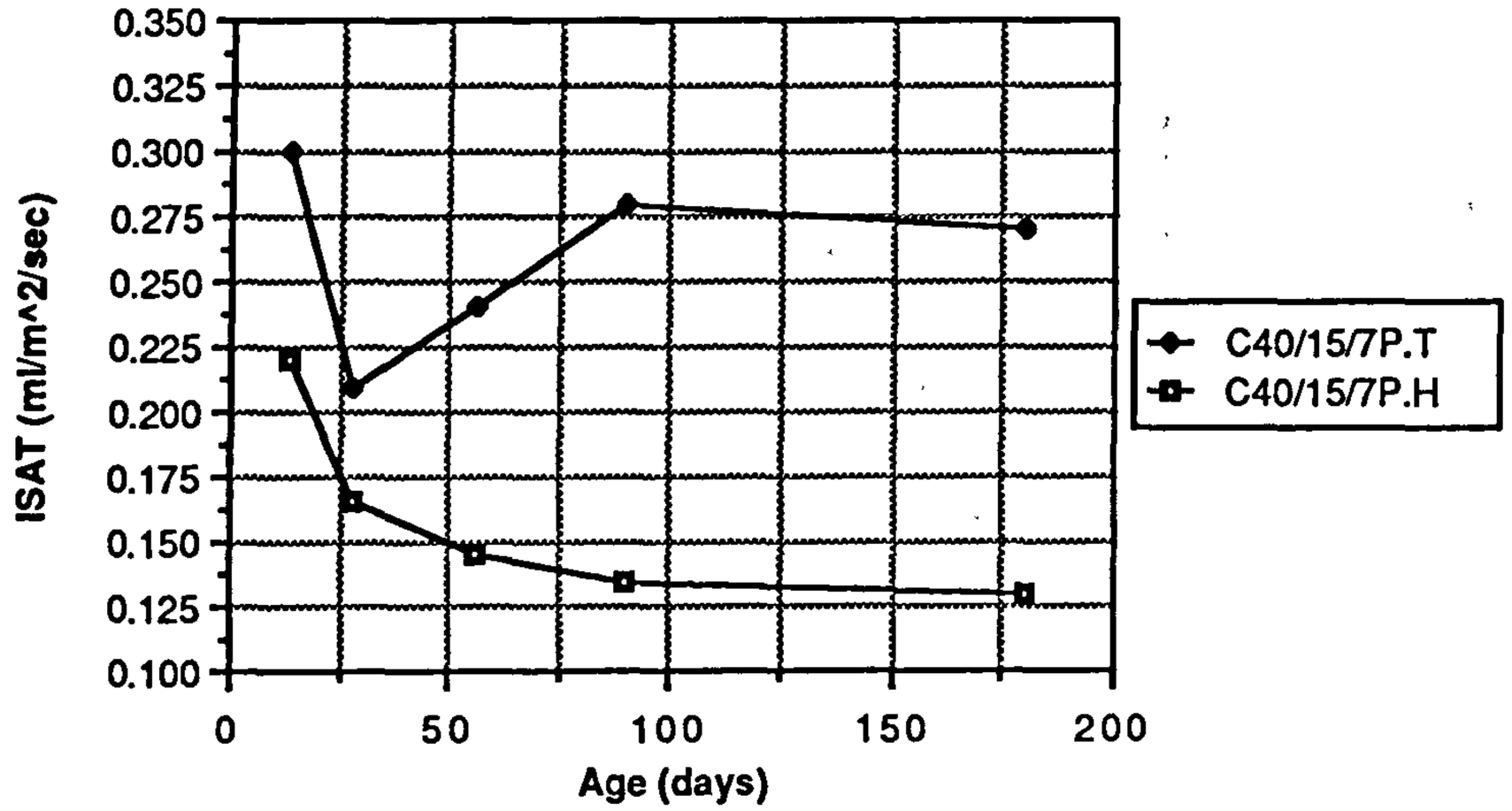

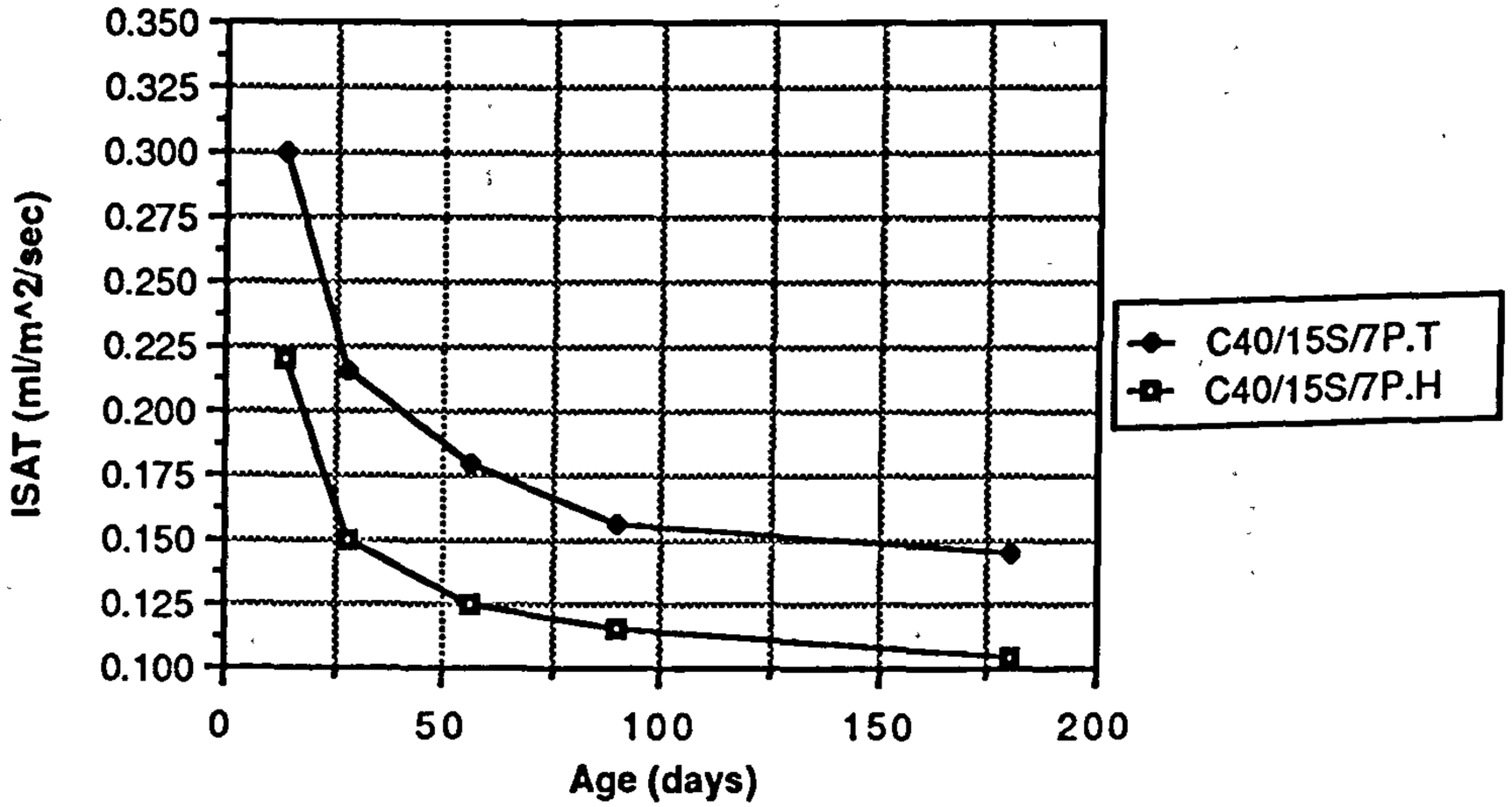

Figure 8.62 Effect of temperate and hot curing on ISAT of CSF mixes

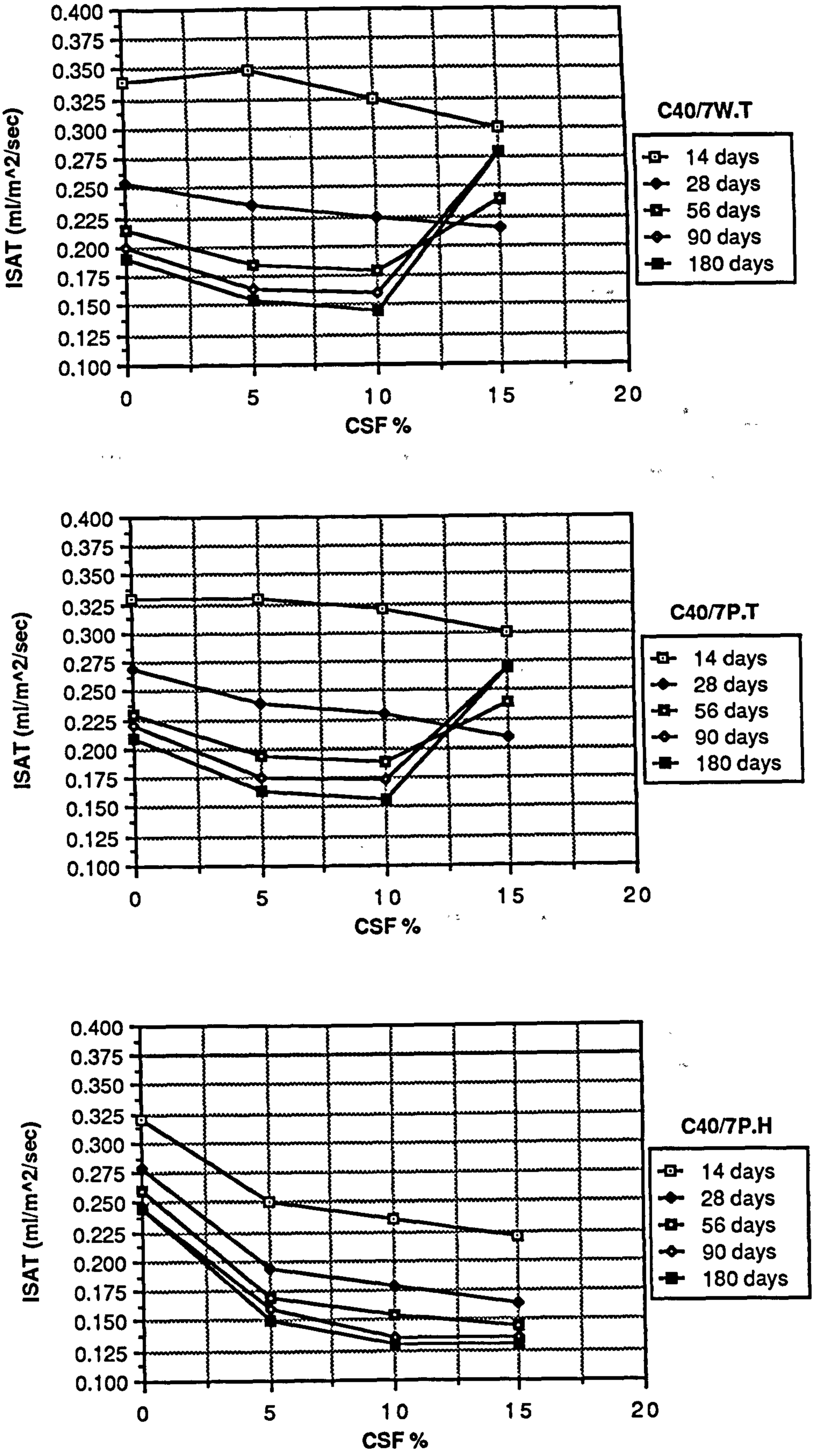

Figure 8.63 Effect of CSF content on ISAT

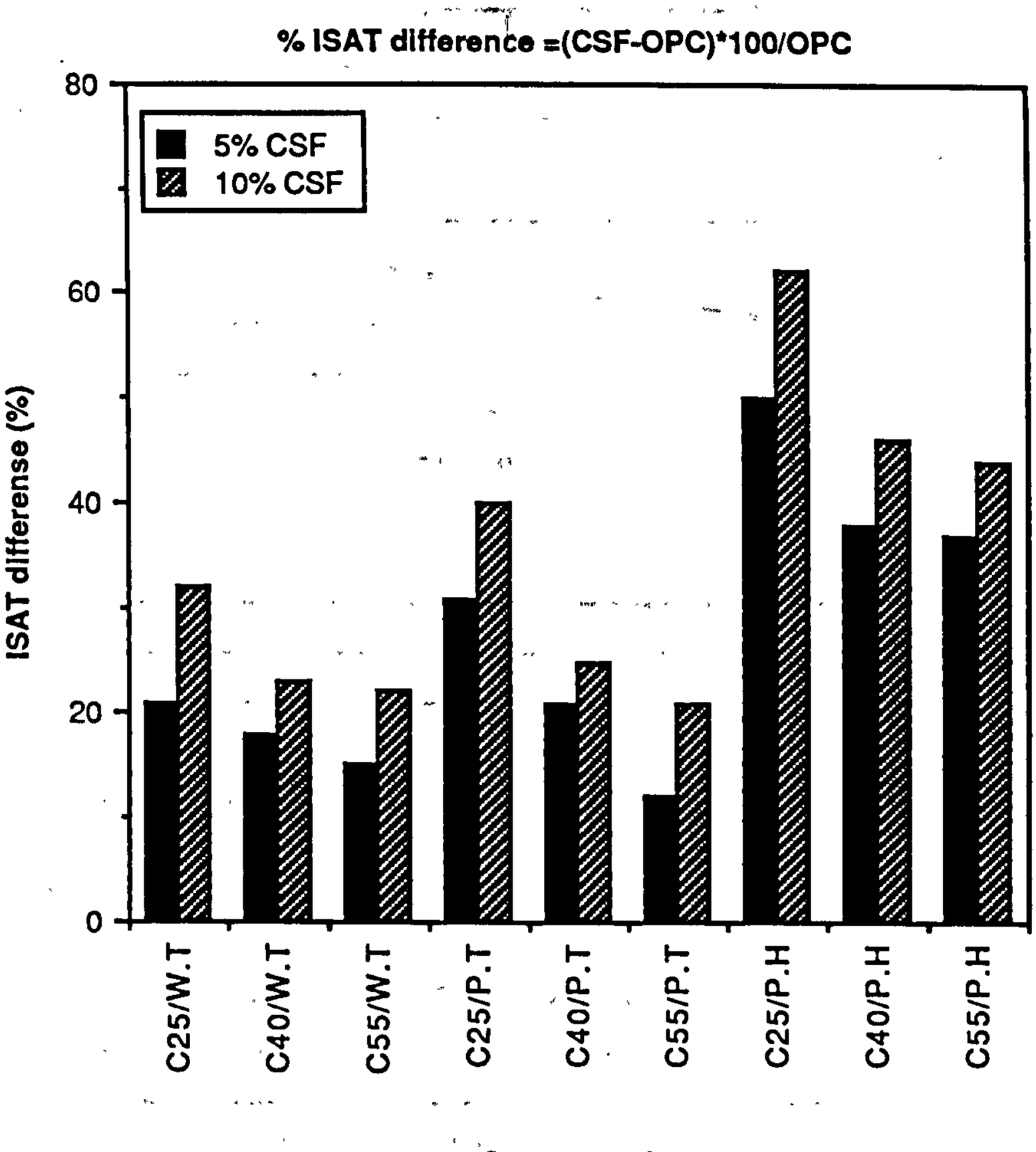

Figure 8.64 Percent reduction on ISAT caused by adding CSF to lean, medium and rich concrete mixes

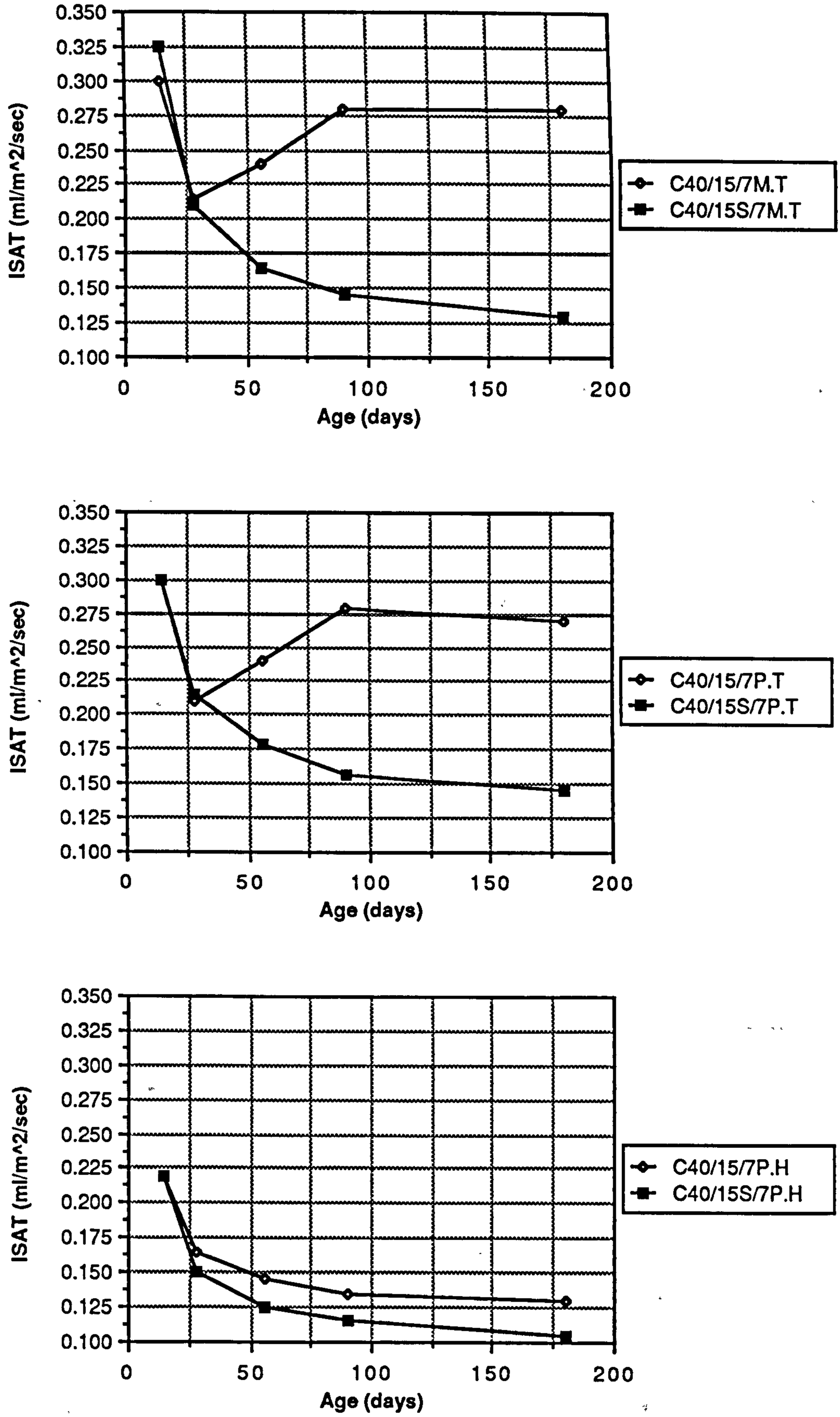

Figure 8.65 Effect of superplasticizer on ISAT

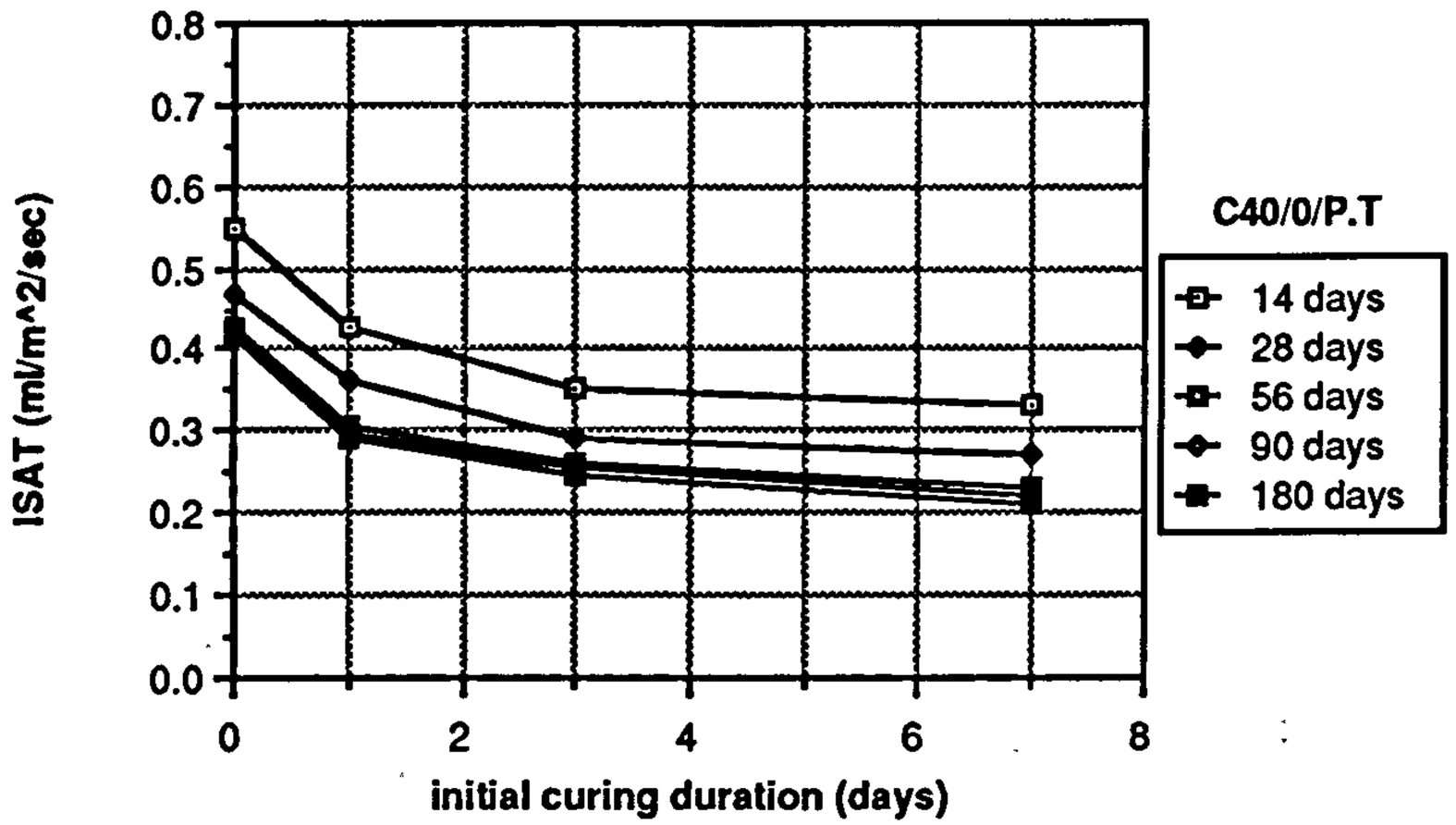

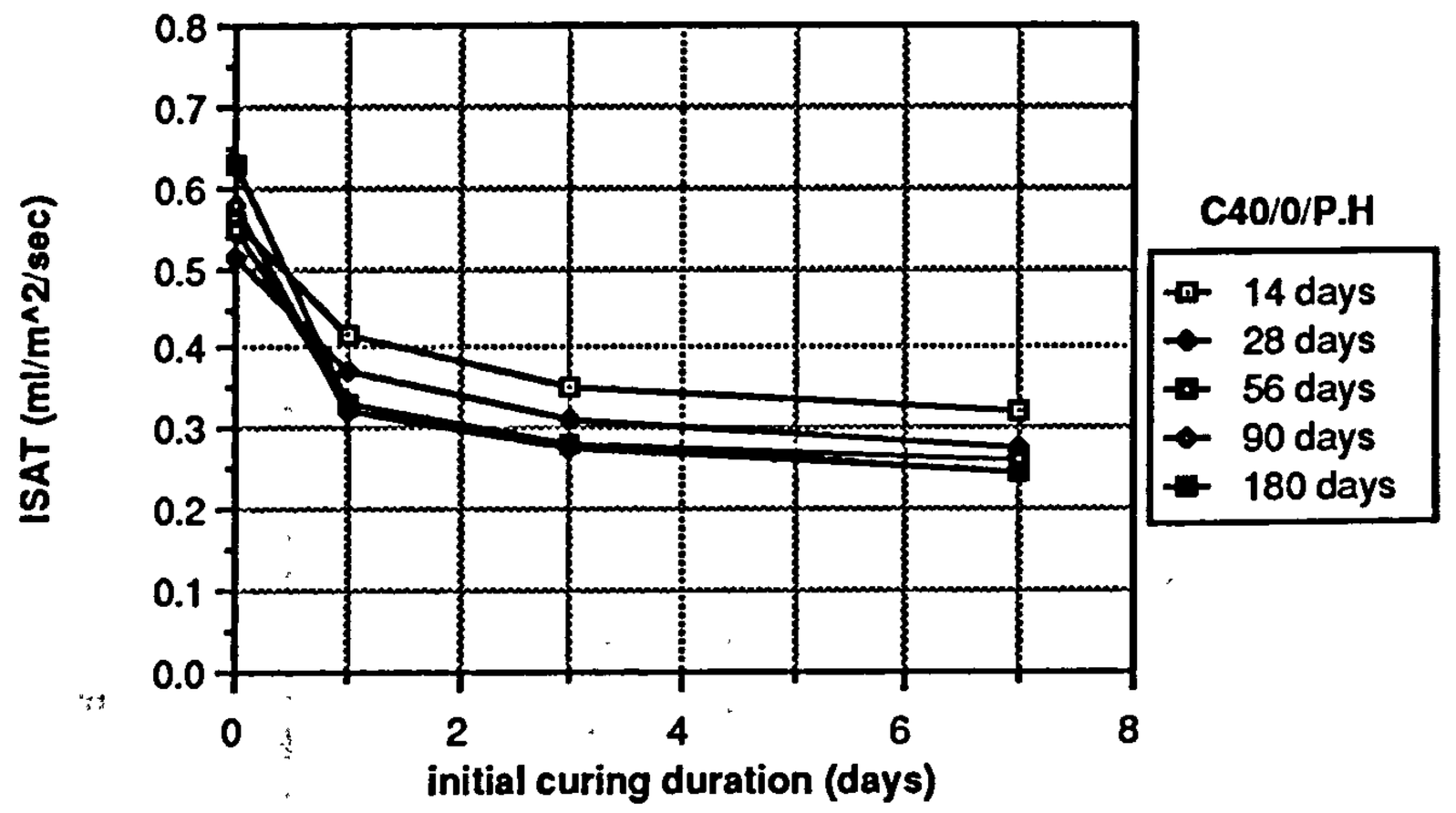

Figure 8.66 Effect of initial curing duration on ISAT of plain OPC

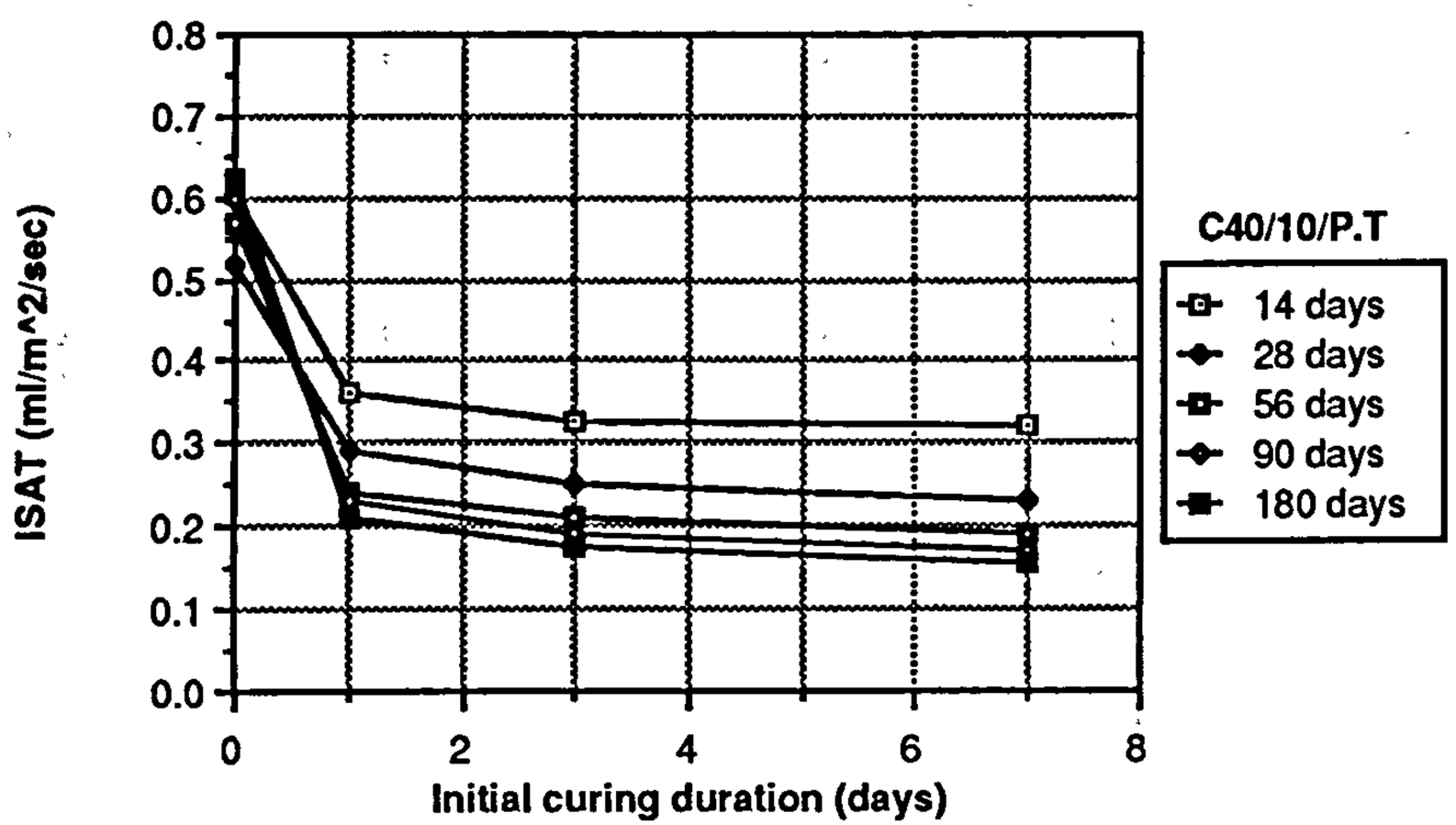

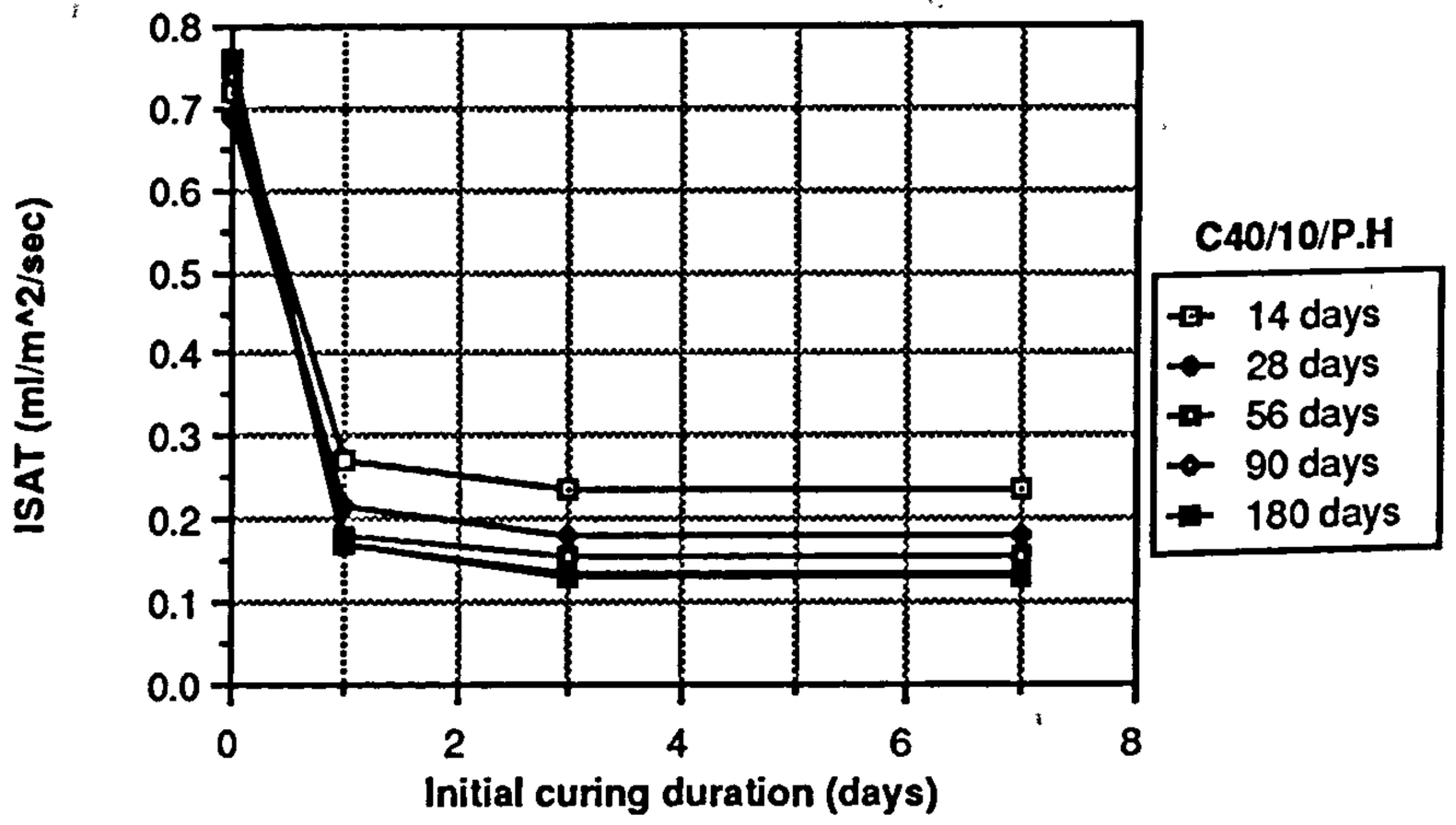

Figure 8.67 Effect of initial curing duration on ISAT of CSF mixes

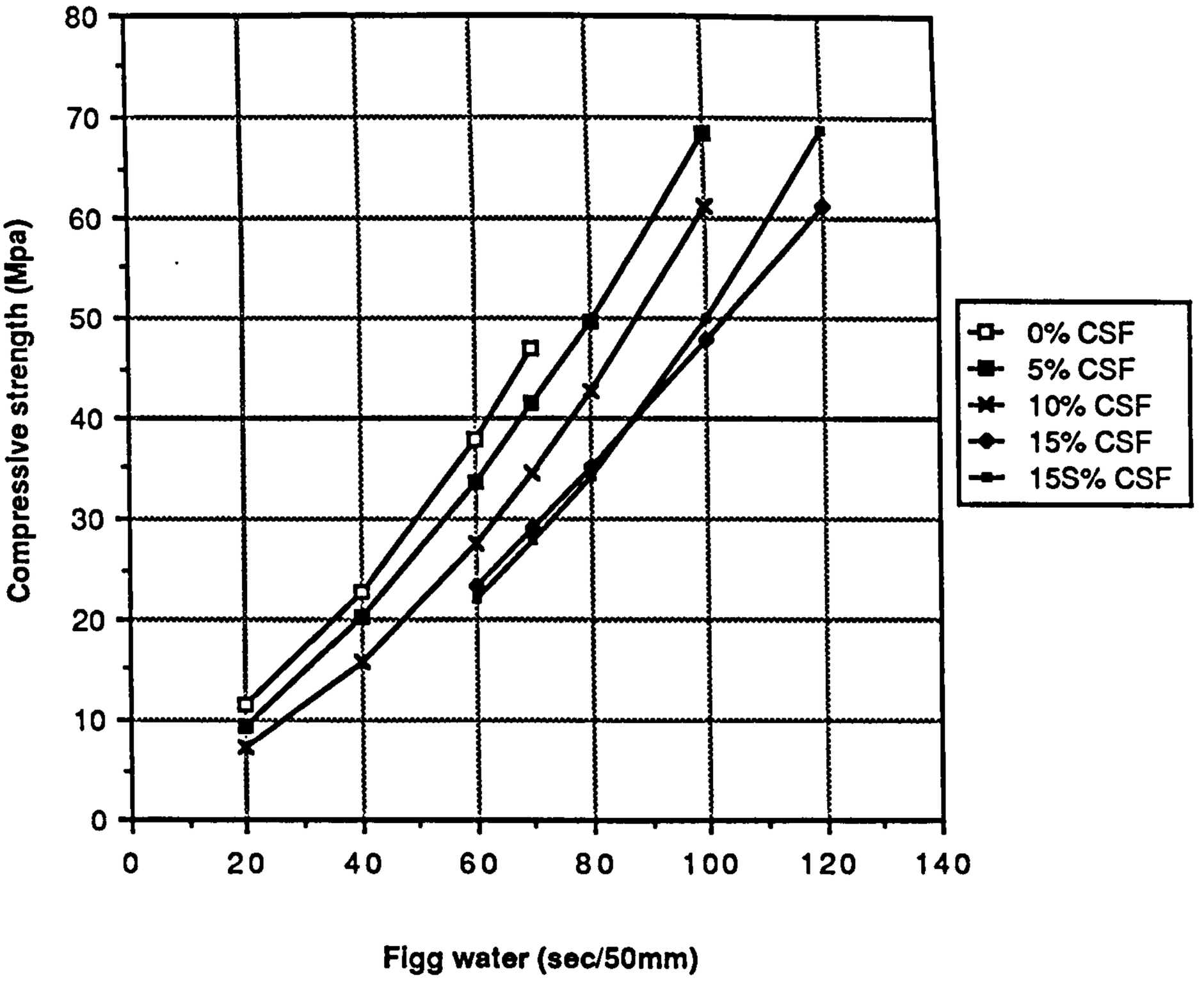

Figure 8.68 Relationship between compressive strength and Figg water (Temperate curing)

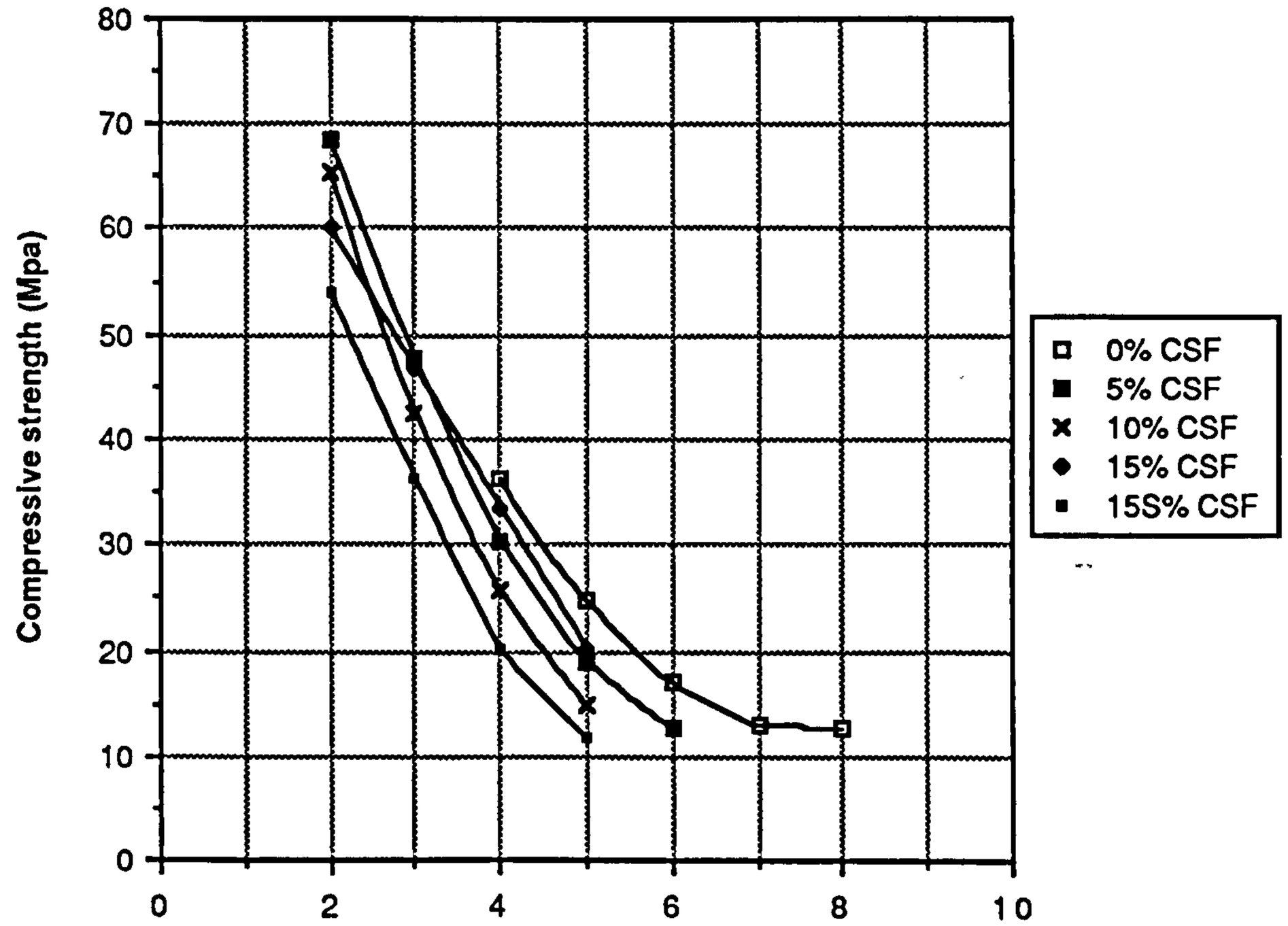

Figure 8.69 Relationship between compressive strength and water absorption (Temperate curing)

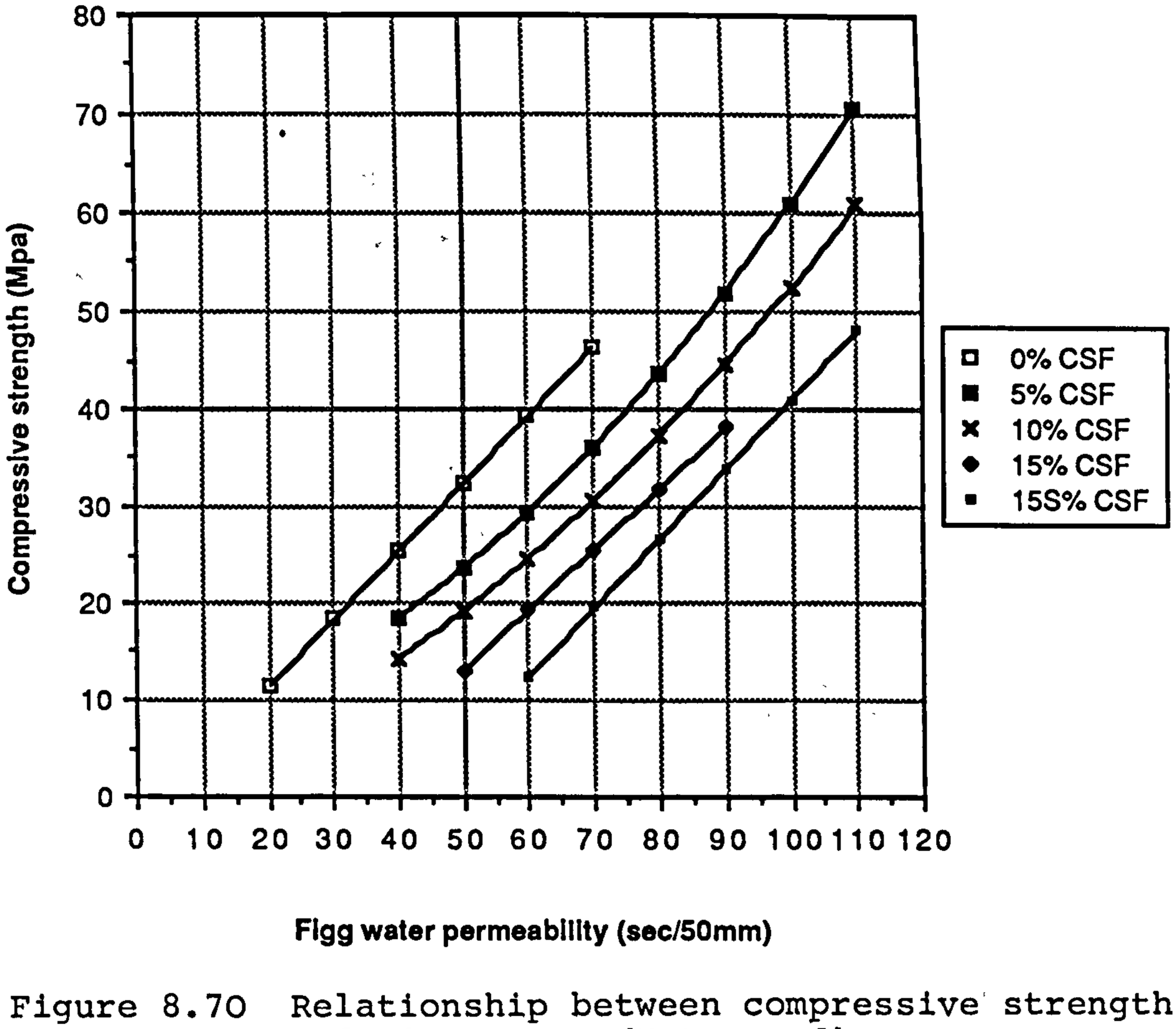

Figure 8.70 Relationship between compressive strength and Figg water (Hot cured)

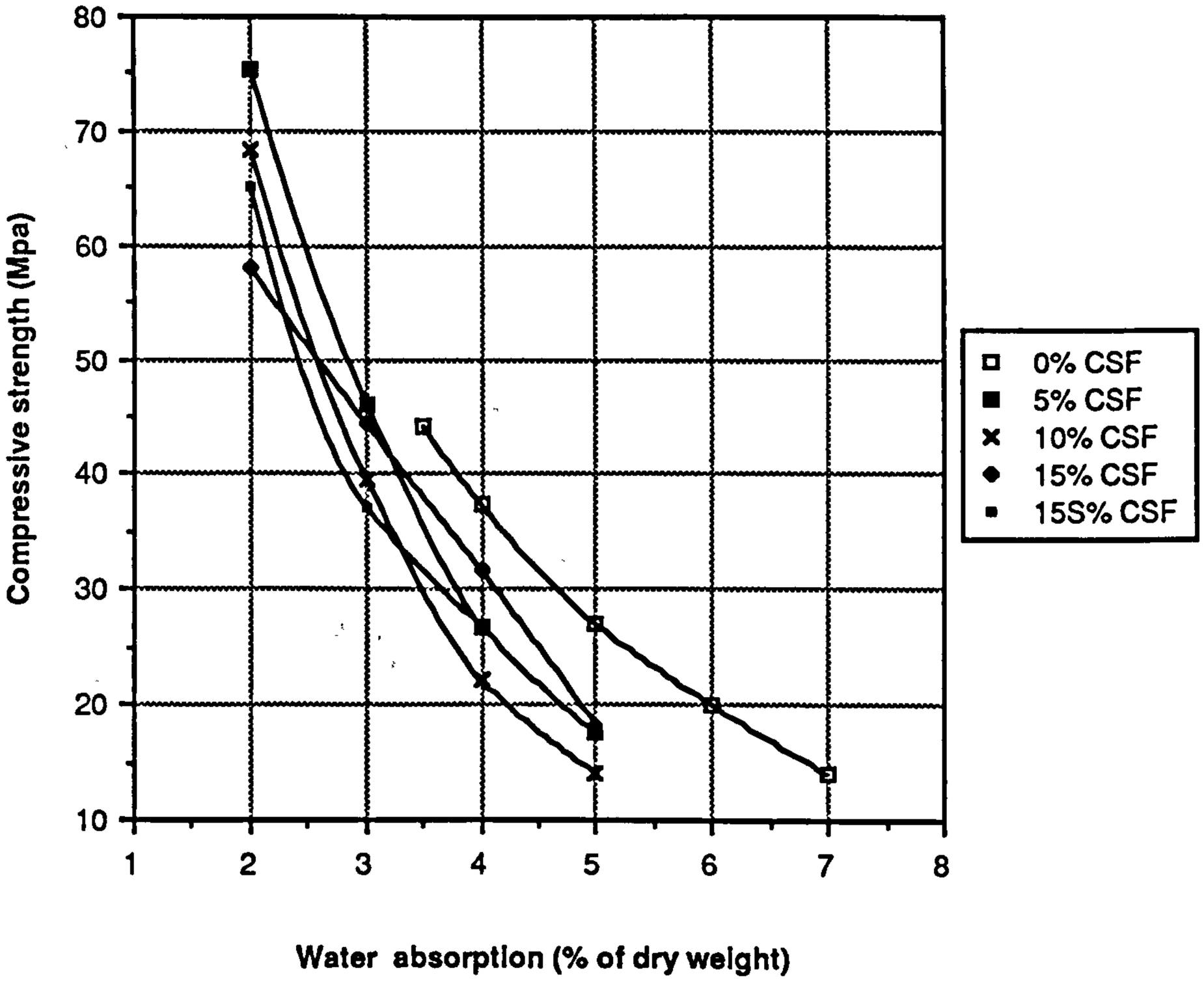

Figure 8.71 Relationship between compressive strength and water absorption (Hot cured)

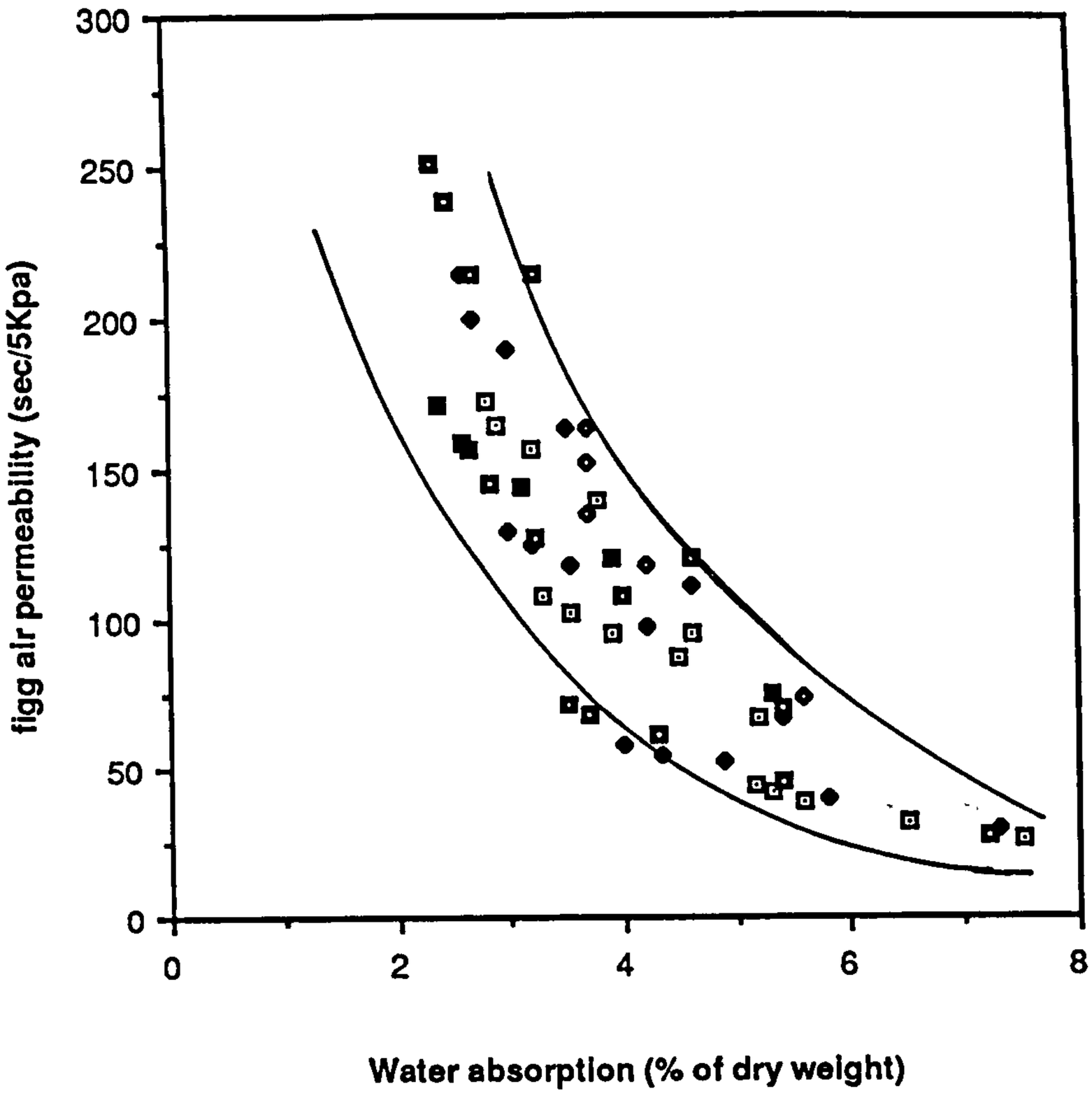

Figure 8.72 Relationship between Figg air permeability and water absorption (Temperate curing)

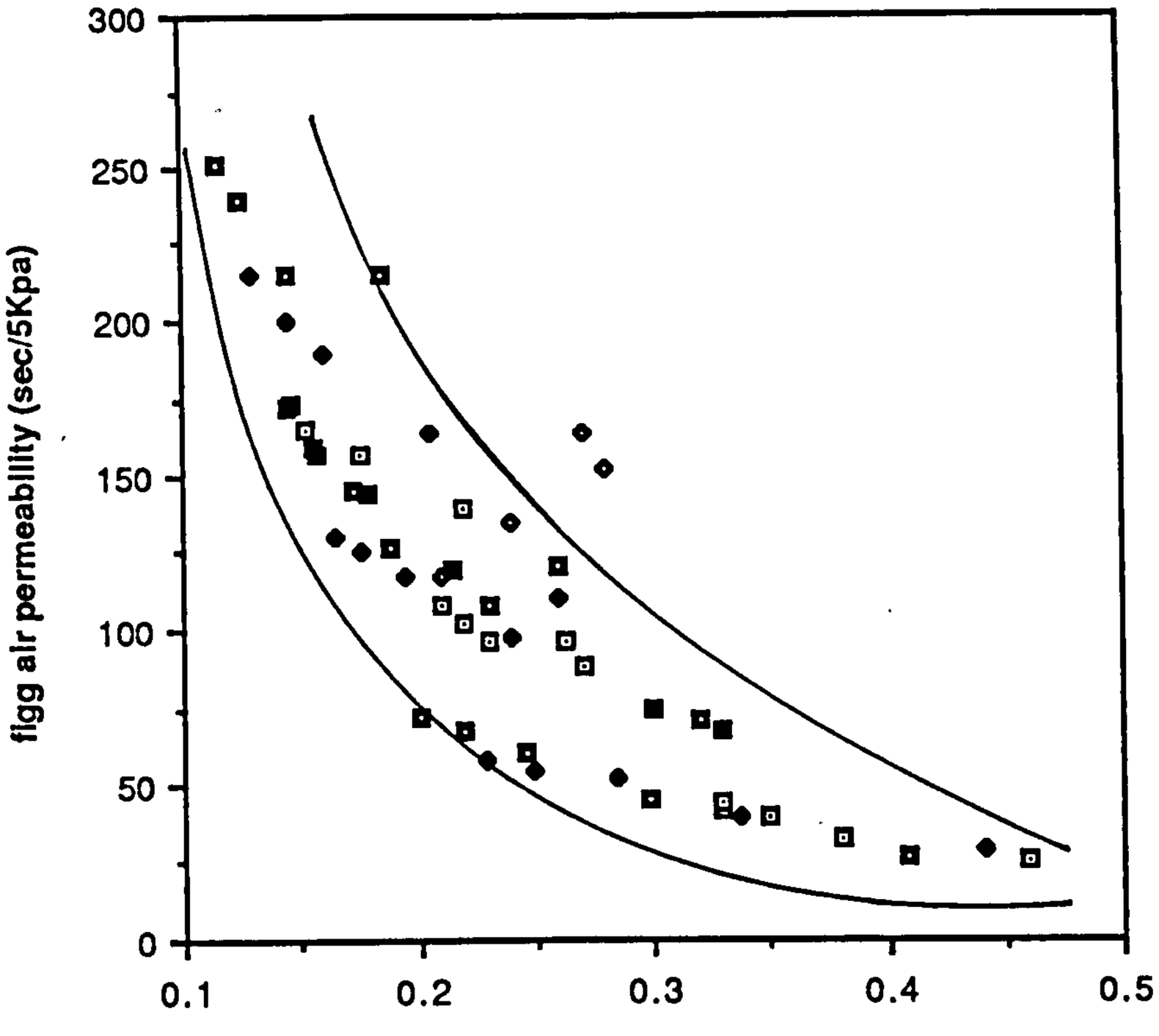

Figure 8.73 Relationship between Figg air permeability and ISAT (Temperate curing)

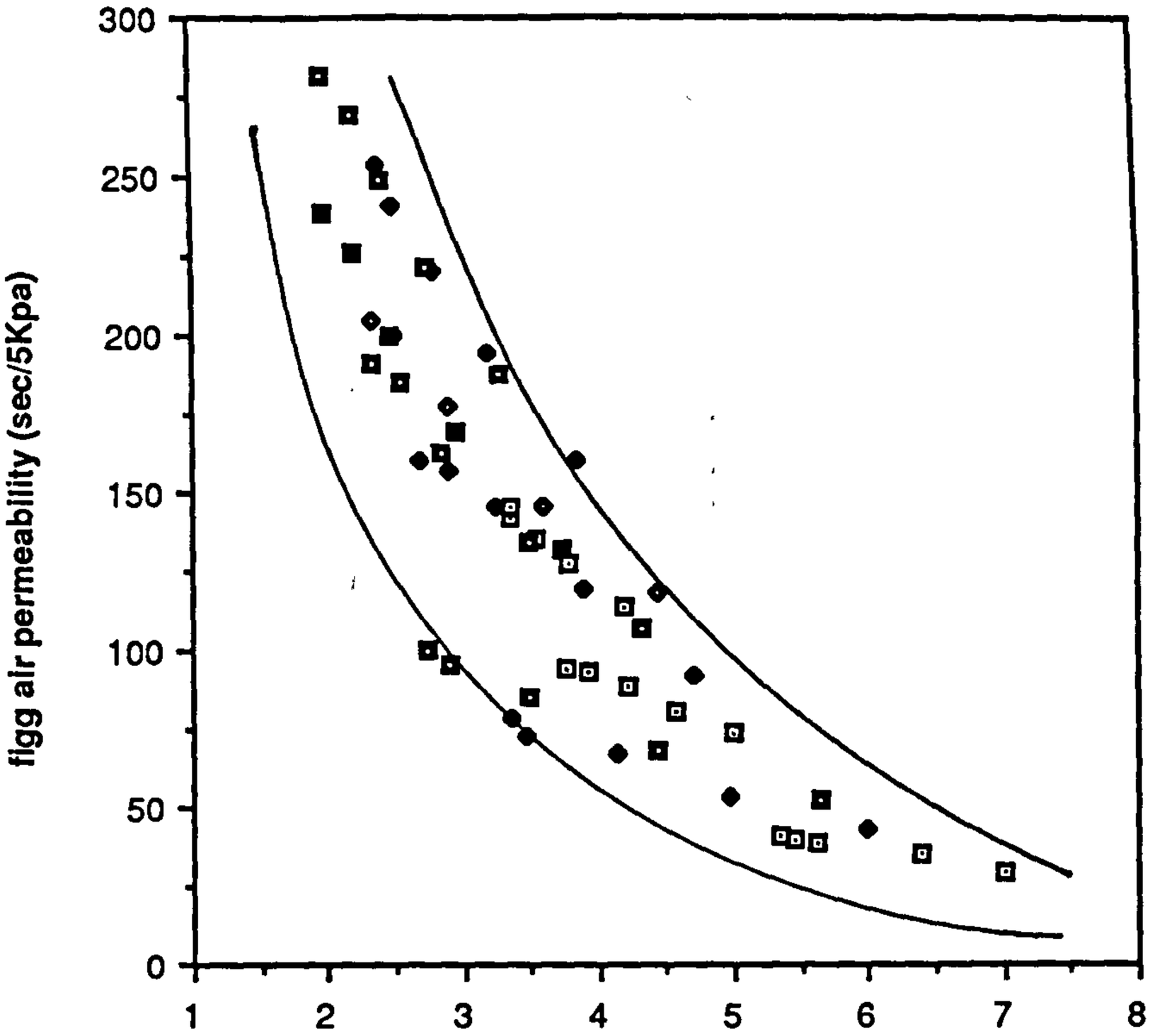

Figure 8.74 Relationship between Figg air permeability and water absorption (Hot curing)

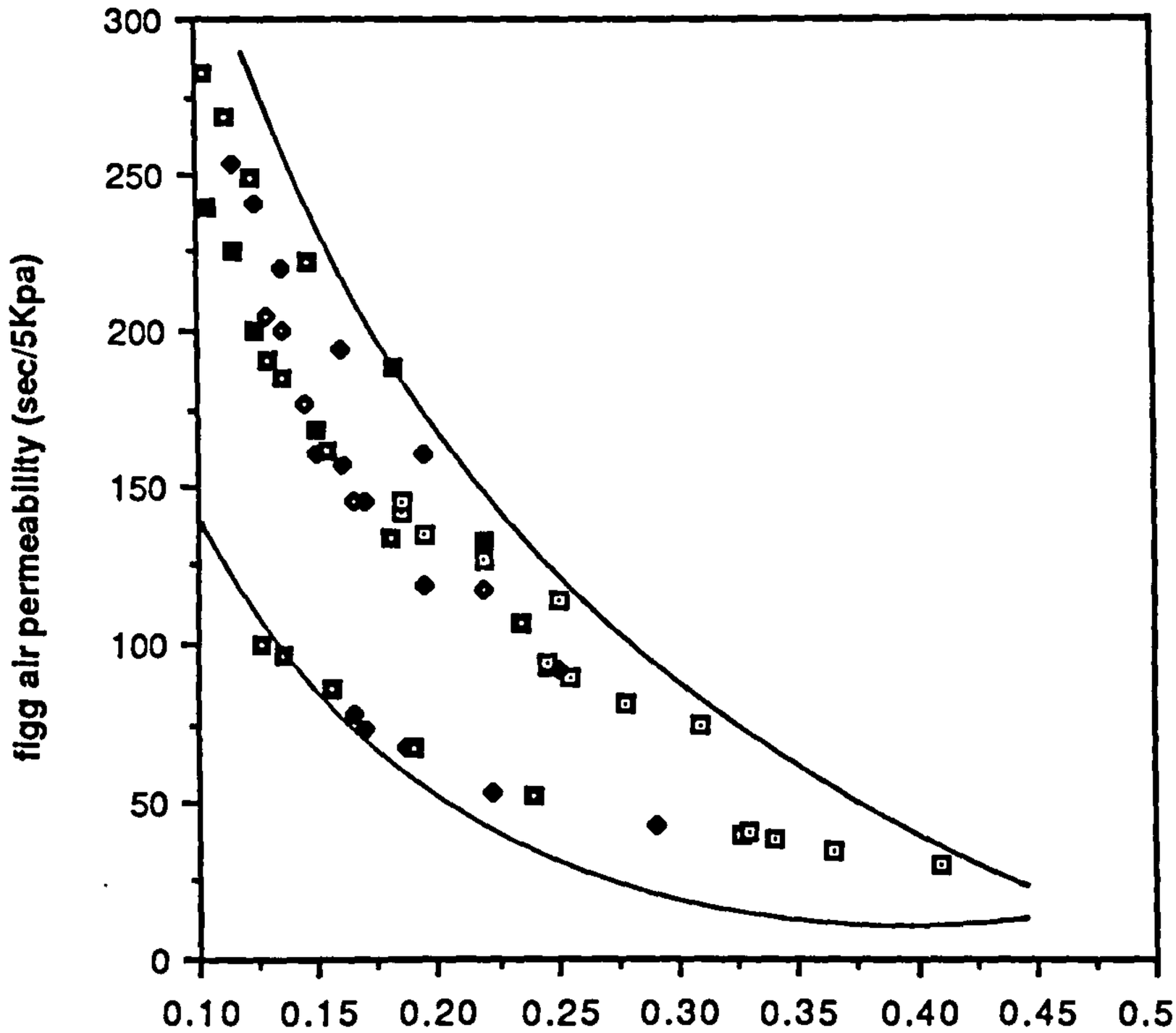

Figure 8.75 Relationship between Figg air permeability and ISAT (Hot curing)

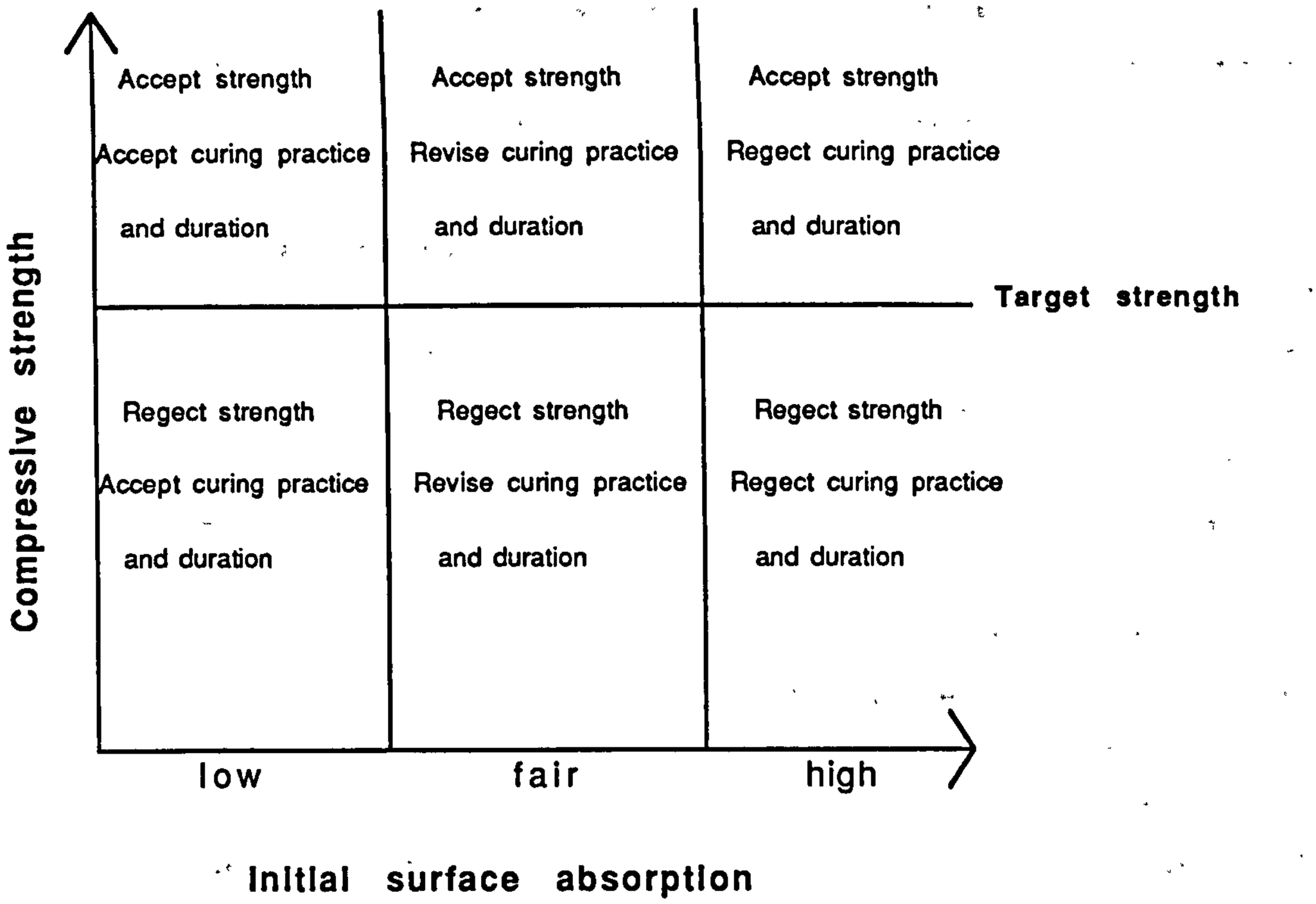

Figure 8.76 Quality control for verifying both mix proportions and curing efficiency

CHAPTER NINE

MICROSTRUCTURAL CHARACTERISTICS AND PERMEABILITY OF PLAIN AND SILICA FUME MORTARS

9.1 Introduction

The main purpose of the work reported in this chapter was to investigate the effect of hot environments on some of the durability related properties of mortars made from plain OPC and various combinations of OPC/CSF mixes. Durability was assessed by means of mercury intrusion porosimetry (MIP) and water and air permeability. In the light of test results, discussion is presented covering the effect of age, curing environment, CSF content suplerplasticizer and the relationship between pore structure and permeability.

The tests were carried out on mortar mixes derived from the C40 grade plain and CSF concrete mixes. Mortars were considered to have a number of advantages over the concrete mixes: they have a more consistent paste matrix which is unintermitted by coarse aggregate; offer easier preparation; and variation in test results between identical specimens expected to be lower than that with concrete specimens.

9.2 Mix proportions

The proportions of these mortar mixes were derived from the plain and CSF concrete mixes grade C40 by leaving out the coarse aggregate fraction and adjusting the amount of mixing water by the amount absorbed from the coarse aggregate at 30 minutes. Details of the mix proportions are given in Table 9.1. Mixing was performed as described in Chapter 6. Section 6.3.2.

9.3 Curing environments

Simulated temperate and hot Iraqi environments were investigated. Details of these curing environments and how they were provided are given in Chapter 6, Section 6.4. In the hot environment temperature and humidity of day and night were 40°C, 15% R.H. and 20°C, 35% R.H. respectively. In the

temperate environment the day and night temperature and humidity were 20°C, 40% R.H. and 18°C, 45% R.H. respectively.

9.4 Mercury intrusion porosimetry test result and discussion

9.4.1 Introduction

Mercury intrusion porosimetry was carried out on more than 200 specimens. Samples were mortars made of OPC and OPC-CSF at various replacement levels. The pore size distribution was determined at ages 7, 28, 56, 90 and 180 days. For each mix at least four samples were tested at each age. See Chapter 6 Section 6.9.8.

The effects of age, curing environment, CSF content and using superplasticizer on the pore structure of OPC and OPC/CSF paste matrices were based on the cumulative pore size distribution. Therefore, it was suggested to highlight the effect of the above measures by means of several parameters which are related to the characteristics of pore structure of hydrated paste matrix. These parameters, which are calculated from the cumulative pore size distribution together with pore volume and pore surface area are the pore surface area (PSA), median pore diameter by volume (MPD-V), median pore diameter by surface area (MPD-A) and average pore diameter (Ave.P.D.).

A full description of the above parameters is given in Chapter 6. Section 6.9.7. The statistical analysis performed on test results shows that the coefficients of variation are within 10%.

Discussion of test results together with their general trend will be based on the pore surface area (PSA) and median pore diameter by volume (MPD-V). PSA is as illustrated previously, a parameter relating to the volumes and sizes of pores; the bigger the (PSA) the greater the number of small pores. On the other hand, the MPD-V relates to the volume of smaller pores in the cement matrix, i.e. the greater the MPD-V, the greater is the volume of large pores.

The effect of research parameters on other pore size distribution test results concerning the MPD-A and Ave.P.D

are in line with the trend shown by PSA and MPD-V. Thus, MPD-A and Ave.P.D results are shown graphically in Appendix 3 but not discussed here.

9.4.2 Effect of Age

The effect of age on the pore structure of plain and CSF mortars can be illustrated by its effect on PSA and MPD-V under temperate and hot environments, which is shown in Figures 9.1-9.4. Test results show that longer hydration periods resulted in finer pore structure revealed by the increase in PSA and reduction in MPD-V. The rate of increase in PSA and reduction in MPD-V is higher at early ages and gradually decreases at later ages. Results also reveal that hydration of CSF mortars and precipitation of hydration products proceeded at a higher rate as compared to the plain OPC ones, yielding finer pore structure at late ages under both curing environments. This higher rate of hydration and hydration products precipitation is believed to be initially caused by the physical properties of CSF particles, i.e. their extreme fineness and large surface area. This effect can be illustrated by the high ability of CSF particles to disperse cement flocs, resulting in higher exposed surfaces of OPC to normal hydration. According to Elken (169) in a typical silica fume mix containing 10% of CSF by weight of cement, there will be at least 50,000 particles for every grain of OPC. At later ages the presence of highly reactive CSF alters the pore structure of the paste matrix dramatically. CSF reacts with the liberated $Ca(OH)_2$ forming a secondary calcium silicate hydrate (C-S-H). The precipitation of these C-S-H dense gels in the capillary pores may possibly result in a dramatic reduction in the volume and percentage of coarse capillary pores. The continuation of hydration brought about by the presence of silica fume (see Section 5.2.1) can result in more and more precipitation of C-S-H gel in the capillary spaces. This eventually will yield a very fine pore structure which leads to more densely packed and less permeable mortars.

The general effect of age on the pore structure was expected both on the basis of the Powers model of hydration (174) and from the general notion that the hydration products occupy more volume than that occupied by the cement grains they replace. When cement and water are mixed together, large water-filled pores exist between the grains of unhydrated cement. OPC hydration yields several products, the predominant one being a poorly crystalline C-S-H gel. The specific volume of the hydration products is greater than that of the unhydrated cement. The hydration products are deposited in the large water-filled pores which exist between the unhydrated cement grains. During hydration the apparent bulk volume of the mix remains essentially constant. As the gel is deposited in the large water-filled spaces it gradually isolates these spaces from their neighbours and after sufficient hydration the large pores become discontinuous.

From the above it is possible to draw several conclusions about the nature and evolution of the pore structure of cement paste. Since the bulk volume of the mix is approximately constant and the specific volume of the hydration products is higher than the unhydrated cement, then the volume of pores must decrease as hydration proceeds. Since the hydration products are deposited in the large initial pores, then the diameter and volume of the large pores must decrease. Since continued hydration produces more gel, then the volume of pores associated with the gels must increase.

The effect of age on the MPD-A and Ave.P.D is shown in Figure A3.1 to !3.4, in Appendix 3.

9.4.3 Effect of curing environment

The effect of temperate and hot curing environments on the pore structure of OPC mortars is illustrated by their effect on the PSA and MPD-V, shown in Figures 9.5 and 9.6 respectively. These figures show that at early ages, mortar mixes cured under a hot environment have higher PSA and lower MPD-V than those cured under temperate environments. This

suggests that high curing temperature accelerates the early age hydration and precipitation of hydration products in the capillary pore spaces, reducing their volume. However, at late-ages hot curing produces lower PSA and greater MPD-V compared with temperate curing. This suggests that higher curing temperature can result in a large number and volume of coarse pores. The test results agree with Goto and Roy test results (101). They found that mortars cured at 60°C contained a greater volume of large pores than those cured at 27°C.

An explanation for this trend is suggested by the proposed model illustrated in Chapter 5 section 5.3.2. The model suggests that high curing temperature may affect the morphology and structure of C-S-H gel fibres. In fact rapid initial hydration appears to form short fibred C-S-H gels which will restrict the development of long-fibred gels. This may obstruct the isolation of the capillary porosity caused by the intermeshing of long gel fibres from adjacent particles. Furthermore, hydrated C-S-H gel will build up in the vicinity of cement grains. This gel may be converted by the effect of heat to crystalline, dense products forming an encapsulating layer which in the course of time retards any subsequent hydration. Therefore rapid initial hydration appears to form products of a poor physical structure.

The effect of curing temperature on the MPD-A and Ave.P.D is shown graphically in Figures A3.5 and A3.6 respectively.

The effect of temperate and hot curing environments on the pore structure of CSF mortars is illustrated in terms of PSA and MPD-V and shown in Figures 9.7 and 9.8 respectively. Test results revealed an advantageous behaviour as far as the hot Iraqi environment is concerned when CSF was partially substituted for OPC in the plain mix. PSA and MPD-V results of CSF mortars show a different trend from those of OPC mortar mixes. High curing temperature results in a significant increase in the PSA with a significant decrease in the MPD-V at both early and late ages. A possible explanation for this behaviour is offered by the model

described in Chapter 5 Section 5.4.2. which suggests that high curing temperature will initially accelerate the normal hydration of OPC grains and activate the pozzolanic reaction between CSF and $Ca(OH)_2$ to take place at an earlier time. This will result in a high rate of deposition of hydration products in the capillary water-filled spaces, reducing their sizes and volumes. This behaviour is revealed by the higher PSA and lower MPD-V at early ages. Because of their high surface area, CSF grains are liable to provide more sites which are favourable for the precipitation of C-S-H gels. Thus the presence of CSF may improve the diffusion of hydration products away from cement grains allowing uniform precipitation and motivate the continuation of hydration. This continuation of hydration may provide the matrix with more C-S-H gel fibres. This will increase the volume and percentage of fine gel pores between the fibre needles. On the other hand the volume and size of coarse capillary pores will be reduced and they may be converted to fine pores as a result of segmentation caused by the intermeshing of gel needles from the adjacent cementitious particles.

The effect of curing temperature on the MPD-A and the Ave.P.D of CSF mortars is shown in Figures A3.7 and A3.8 in Appendix 3.

9.4.4 Effect of CSF content

The effect of CSF content on the pore structure of mortar mixes is again illustrated by their effect on the PSA and MPD-V under temperate and hot environments shown in Figures 9.9 and 9.10 respectively.

Results indicate that regardless of curing environment, partial replacement of OPC with CSF results in significantly greater PSA and smaller MPD-V values, i.e. finer pore structure. Results also indicate that the increase in PSA and the reduction in MPD-V are exponentially related to the percentages of CSF used. An explanation for this behaviour has been given earlier. Briefly the presence of CSF can significantly alter the pore structure of the paste matrix; i.e. increase the volume and percentage of fine

pores at the expense of coarse pores. The higher the amount of CSF up to 15% by weight of OPC, the finer is the pore structure of the paste matrix.

The effect of CSF content on the MPD-A and Ave.P.D is shown in Figures A3.9 and A3.10 respectively.

9.4.5 Effect of superplasticizer

The effect of securing the workability in mortar mix M40/15 by using superplasticizer without adding extra water on the pore structure compared to that in which extra water was used is shown in Figures 9.11 and 9.12. Results indicate that using superplasticizer to control the workability of mix (M40/155) improved the pore structure of the paste matrix *which* had higher PSA and lower MPD-V than the non-superplasticized mortars (M40/15). This better pore structure is possibly caused by the effect of superplasticizer on the dispersion of cementitious particles and the water/cementitious ratio. Good dispersion of cementitious material caused by superplasticizer may result in a more uniform distribution of hydration products. A lower water/cementitious ratio can help in reducing the volume and percentage of initial capillary coarse pores. As a result of both effects, superplasticized mixes had a finer and better segmented pore structure compared with the non-superplasticized mixes.

The effect of superplasticizer on the MPD-A and the Ave.P.D is shown in Figures A3.11 and A3.12 in Appendix 3.

9.4.6 Statistical relationship between pore structure parameter

A statistical analysis was performed on the relationship between the pore structure parameters, i.e. PSA, MPD-V, MPD-A and Ave.P.D. As expected the statistical analysis show that there is a well defined linear relationship between the above parameters. This is confirmed by the graphical presentation of these relationships shown in Figures A3.13 to A3.24 in Appendix 3. Tables 9.2 & 9.3 also show the coefficient of correlation for the linear

relationships. The above proves that these parameters are well related to each other and from measuring or monitoring either of the above parameters one can forecast the behaviour of the othe parameters. Consequently a clear picture can be drawn with less effort and experimental work.

9.4.7 Volume of pores greater than 0.1 micrometer

A comparison was made between the volume of coarse pores in mortars made with OPC and combinations of OPC and CSF. Coarse pores are defined as those having a diameter greater than 0.1 micrometre. The reason for the selection of this value is that research variables, (age, curing environment, CSF content and the use of superplaticizer) were found to influence mainly the volume of coarse pores with a diameter greater than 0.1 micrometre. Moreover Mehta and Manmohan (175) found the durability of related properties such as permeability mainly influenced by the volume of pores greater than a diameter of 0.1 micrometre. As far as permeability is concerned, Mehta and Manmohan classify the pore system of a cement matrix into two groups: the first consists of the harmful pores (pores greater than a diameter of 0.1 micrometre): the second group consists of the harmless pores (pores smaller than a diameter of 0.1 micrometre).

The relationships between age and the relative volume of pores greater than 0.1 micrometre (percent of specimen volume) of OPC and OPC/CSF mortars cured in temperate and hot environments is shown in Figures 9.13 and 9.14. The figures show that the volume of coarse pores decreases rapidly at early ages, but at a slower rate at late ages up to 180 days of age.

The volume of coarse pores of plain OPC mortars cured in hot environment is higher at later ages (from 28 days and onwards) compared to that of those cured in temperate environment (See Figure 9.15). However, OPC/CSF mortars show a completely different trend. The volume of coarse pores of CSF mortars cured in a hot environment is lower than those cured in a temperate environments (see Figure 9.16). An explanation for such a behaviour has been given earlier.

Results also shows that the volume of coarse pores was reduced with increasing CSF replacment percentages (see Figure 9.17). Superplasticized CSF mortar mixes (M40/155) had lower volume of coarse pores compared with the non-superplasticized ones, under both curing environments (See Figure 9.18).

9.5 Water and air permeability

Air and water permeability were determined at ages of 7, 28, 90 and 180 days. Tests were carried out on at least two specimens for each specified age. See Chapter 6 Sections 6.9.9 & 6.9.10.

Results of tests conducted by Hudd (153) showed that the coefficient of permeability k varies with testing time, but k becomes almost constant after 14 days. Therefore a maximum of 14 days was chosen and the value of permeability at 14 days was calculated by application of formulae (6.13 and 6.17) and used for the purpose of comparison between different mortar mixes.

Air permeability was calculated at four pressure heads chosen from the range under which gas flow through specimen is laminar (see Chapter 6. Section 6.9.9.). These pressure heads were 0.2, 0.3, 0.4 and 0.5 MPa. The average permeability values were used for the purpose of comparison between different mortar mixes.

9.5.1 Effect of age

The effect of age on the water and air permeability of plain and CSF mortar mixes cured in temperate and hot environments is shown in Figures 9.19 and 9.20. Generally the test results show that a longer hydration period resulted in lower water and air permeability values. The normal hydration of OPC in the plain mixes together with the pozzolanic reaction in the CSF mixes progressively replaces the original cementitious material with hydration products, principally C-S-H gels. The volume of gels produced by hydration is approximately 2-3 times the volume of the cementitious grains (36). Consequently the gels will not

only replace the original OPC grains in the plain mix and the CSF grains in the CSF mix but also tend to fill the original water filled spaces. This is expected to be accompanied by a continuous decrease in water and air permeability coefficients. The results also show that the permeability of CSF mortar mixes decreases at a higher rate compared with the plain OPC control. This reveals that hydration of OPC/CSF mortar mixes proceeds at a higher rate yielding a higher rate of gel deposition and consequently lower permeability. The reason for this higher rate was explained earlier in section (9.4.2).

The rate of reduction in water and air permeabilities is higher at early ages and gradually decreases at later ages. This is due to the slowing of the hydration process. Water permeability test results on plain mixes agreed with those reported by Powers et al (176).

9.5.2 Effect of curing temperature

The effect of temperate and hot curing temperatures on the water and air permeability of plain OPC mixes is shown in Figure 9.21 and 9.22 respectively. The figures show clearly that high curing temperature reduces the water and air permeability coefficients at early ages (7 days) very rapidly. However, at late-ages (from 28 days and onwards) water and air permeabilities of mortar specimens cured in a hot environments are higher than those of specimens cured under temperate environment. Test results agree with those reported by Goto and Roy (101). An explanation for this behaviour is offered by the model described in Chapter 5, Section (5.3.2) which suggests that rapid initial hydration caused by high curing temperature appears to form products of a poor physical structure which yields a poor matrix with high percentage of coarse pores and most probably a well interconnected pore structure. Since any water or gas flow from outside to inside can only be facilitated by an interconnected network of coarse pores, then permeability is expected to increase.

The effect of curing temperature on the water and air permeability of CSF mortar mixes is shown in Figures 9.23 and 9.24 respectively. The figures show that the effect of high curing temperature on the permeability of CSF mortars seems to be the reverse of that found from examining the plain OPC mixes. Specimens cured under hot environments were found to have early and late-age water and air permeabilities lower than those cured under temperate environments. The reason for such behaviour can be attributed to the change in pore structure caused by CSF under hot environment compared to that which takes place under temperate environment (see Section 9.4.3). More specifically water and air permeability of CSF specimens cured in a hot environment falls due to the lower volume of coarse pores and the higher volume of fine pores compared with those cured in a temperate environment. This is caused by the high rate of hydration influenced by high curing temperature and the continuation of hydration brought about by the presence of CSF (see Chapter 5, Section 5.4.2).

9.5.3 Effect of CSF content

The effect of CSF content (percent by weight of OPC) on the water and air permeability of CSF mortars cured under temperate and hot environments is shown in Figures 9.25 and 9.26 respectively. Test results show that regardless of curing environments, partially replacing OPC with CSF up to 15% weight of OPC can result in a significant reduction in water and air permeabilities. Even a modest amount of CSF resulted in a considerable permeability reduction. Test results agreed with those of Radjy and Loeland, reported by Hustad (177). They found that water permeability reduced by a factor of 10 and 100 at replacement percentages of 5 and 10 percent by weight of OPC.

The significant reduction in water and air permeability caused by the use of CSF as a cementitious material can be explained as follows: the water and air

permeability tests measure the steady-state fluid flow through the mortar samples. Permeability can be lowered either by the presence of blocked pores or by narrower pores or both. The effect of blocked pores on permeability is obvious. However, permeability reduction due to the existence of smaller diameter pores can be explained by flow theory; according to the theory of fluid mechanism (178) smaller pores lower the flow rate even though porosity may be unchanged. The effect of pore diameter on the flow rate can be estimated by the following equation:

$$\text{Head loss} = \frac{4 L F V^2}{2gD} \quad \ldots\ldots\ldots (9.1)$$

where:

L = length of pores

F = Friction coefficient

D = diameter of the pore

V = flow velocity

g = gravity

Since there is a direct relationship between flow rate and permeability this equation can be used to show that finer pore systems exhibit lower flow rates and hence lower permeabilities.

9.5.4. Effect of superplasticizer

The effect of using superplasticizer to secure the workability in mortar mixes (M40/155) without adding extra water on the water and air permeabilities compared to those in which extra water was used is shown in Figures 9.27 and 9.28 respectively. Results show that the superplasticized mortar mixes had lower water and air permeabilities compared with the non-superplasticized ones. This was caused by the effect of superplaticizer on the dispersion of hydration products and water/cementitious ratio explained earlier.

9.5.5 Relationship between permeability and pore structure

The permeability of the cement matrix is not a simple function of its porosity; it depends also on the size distribution and continuity of the pores. Thus although the cement gel has a porosity of 28% its permeability is about 20 to 100 times lower than the permeability of cement paste itself (36). This is because fluids can flow more easily through the coarse capillary pores than through the much smaller gel pores. It follows that the permeability of cement paste is controlled by the coarse pores. An attempt was made to find the relationship between permeability and the volume of coarse pores greater than 0.1 micrometre in diameter.

9.5.5.1 Relationship between water permeability and volume of pores >0.1 micrometre

The relationship between the volume of pores greater than 0.1 micrometer in diameter and the water permeability of OPC and CSF mortars cured in temperate and hot environments is shown in Figures 9.29 and 9.30 respectively. The typical water permeability values recommended by the Concrete Society and published in the permeability report (179) are used for defining the ranges of low, average and high water permeabilities of the Figures above. Figures 9.29 and 9.30 show that regardless of the curing environment mortars exhibiting high permeability values seem to contain volumes of coarse pores (>0.1 micrometer) in excess of 14.5 percent of specimen volume. On the other hand, mortars exhibiting low water permeability values seem to contain volumes of coarse pores (>0.1 micrometre) less than 6.5 percent of specimen volume. Therefore, test results on both OPC and CSF mixes reveal the existence of a critical volume of coarse pores (>0.1 micrometre) below which mortars are expected to show low water permeability and above which mortars are expected to show high water permeability. This critical volume lies between 6.5 and 14.5 percent of specimen volume.

The statistical analysis carried out on the relationship between water permeability and the volume of

coarse pores (>0.1 micrometre) shows that there is a good logarithmic fit between water permeability and the volume of coarse pores. (See Figures 9.31 and 9.32).

9.5.5.2 Relationship between air permeability and volume of coarse pores >0.1 micrometre

The relationship between the coefficient of air permeability and the volume of pores with a diameter greater than 0.1 micrometre in OPC and CSF mixes cured under temperate and hot environments is shown in Figures 9.33 and 9.34 respectively. Once again the typical coefficient of air permeability recommended by the Concrete Society, published in the permeability report (179) was used for identifying the range of low, average and high permeabilities. Due to the limited range of collected data only the low and average air permeability ranges were able to be shown. The Figures above show that regardless of curing environment, mortar mixes exhibiting low air permeability values seem to contain a volume of coarse pores (>0.1 micrometre) less than 4 percent of specimen volume. Although no mortar mixes exhibited high permeability values according to the limits set by the Concrete Society, it is expected that any mortar mix exhibiting air permeability value above 1 x 10^{-12} (metres/second) may contain a volume of coarse pores greater than 17 percent of specimen volume. Thus as far as air permeability is concerned the data suggests a critical volume of coarse pores below which mortar may exhibit low air permeabilities and above which mortars are expected to show high air permeabilities. This critical volume lies between 4 and 17 percent by volume of specimens. Comparing the critical volume of coarse pore for water permeability was earlier found to lie between 6.5 and 14.5 by volume of specimens with the values above for air permeability we can suggest a critical volume of coarse pores lie between 5 and 16% by volume of specimens which could be applicable for both permeabilities.

The statistical analysis performed on the possible relationship between air permeability and volume of coarse

pores of mortars cured in temperate and hot environments reveal a reasonable fit, with correlation coefficients of 98% and 97% respectively. (see Figures 9.35 and 9.36).

Mix	Water	OPC	CSF	Sand
	kg/m³	kg/m³	kg/m³	kg/m³
M40/0	175	300	-	660
M40/5	175	225	16	
M40/10	180	205	32	
M40/15	200	210	46	
M40/155	175	175	46	

Table 9.1: Ingredients of mortar sizes

	PSA	MPD-V	MPD-A	Ave.P.D
PSA	1.0	0.991	0.987	0.959
MPD-V	0.991	1.0	0.995	0.970
MPD-A	0.987	0.995	1.0	0.979
Ave.P.D	0.959	0.970	0.970	1.0

Table 9.2: Correlation coefficients for linear relationships between pore structure parameters of mortars cured under temperate environment

	PSA	MPD-V	MPD-A	Ave.P.D.
PSA	1.0	0.930	0.938	0.897
MPD-V	0.930	1.0	0.993	0.980
MPD-A	0.938	0.993	1.0	0.983
Ave.P.D	0.897	0.980	0.983	1.0

Table 9.3: Correlation coefficient for linear relationships between pore structure parameters of mortars cured under hot environments

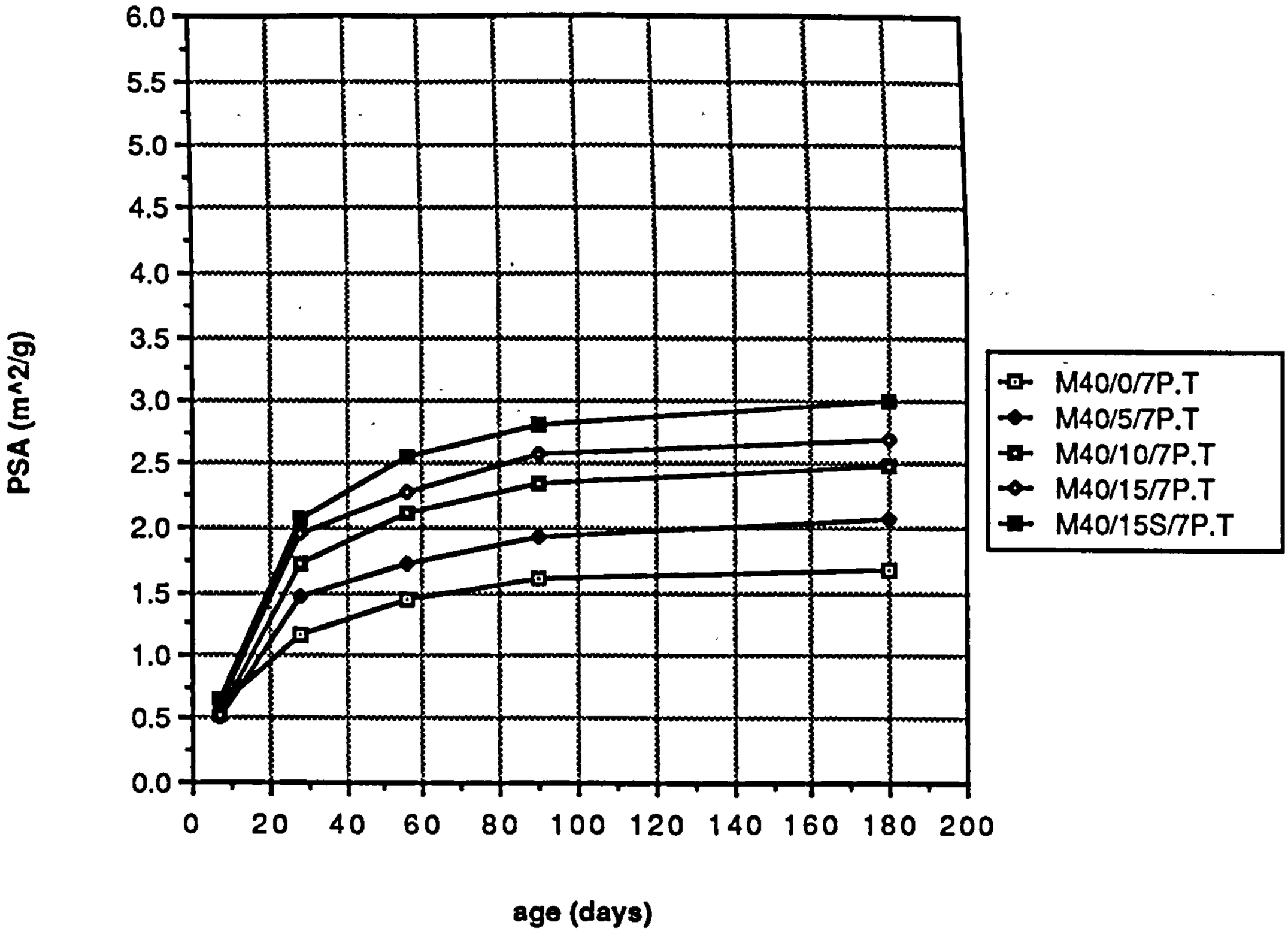

Figure 9.1 Age versus PSA relationships of mortars cured in a temperate environment

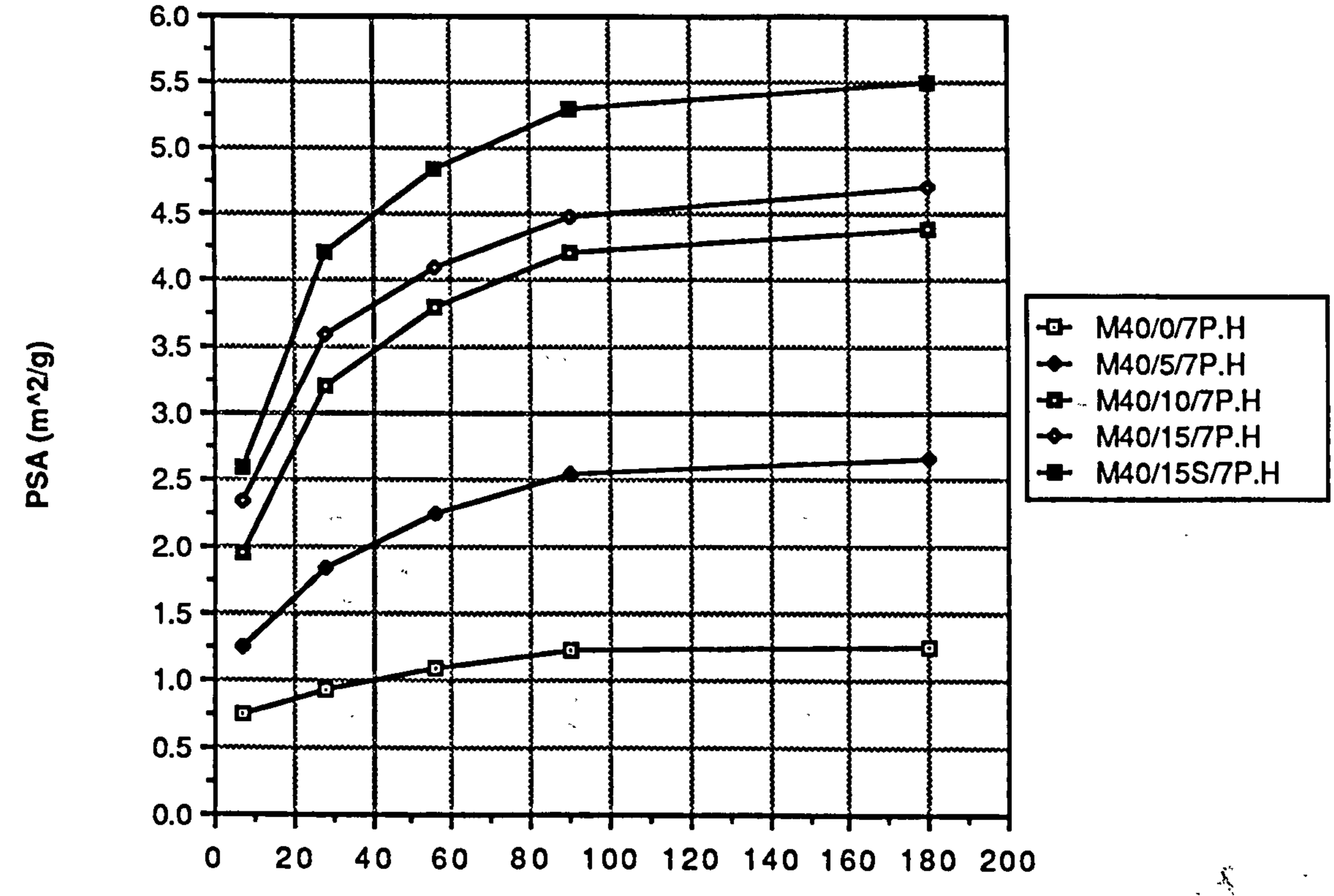

Figure 9.2 Age versus PSA relationship of mortars cured in a hot environment

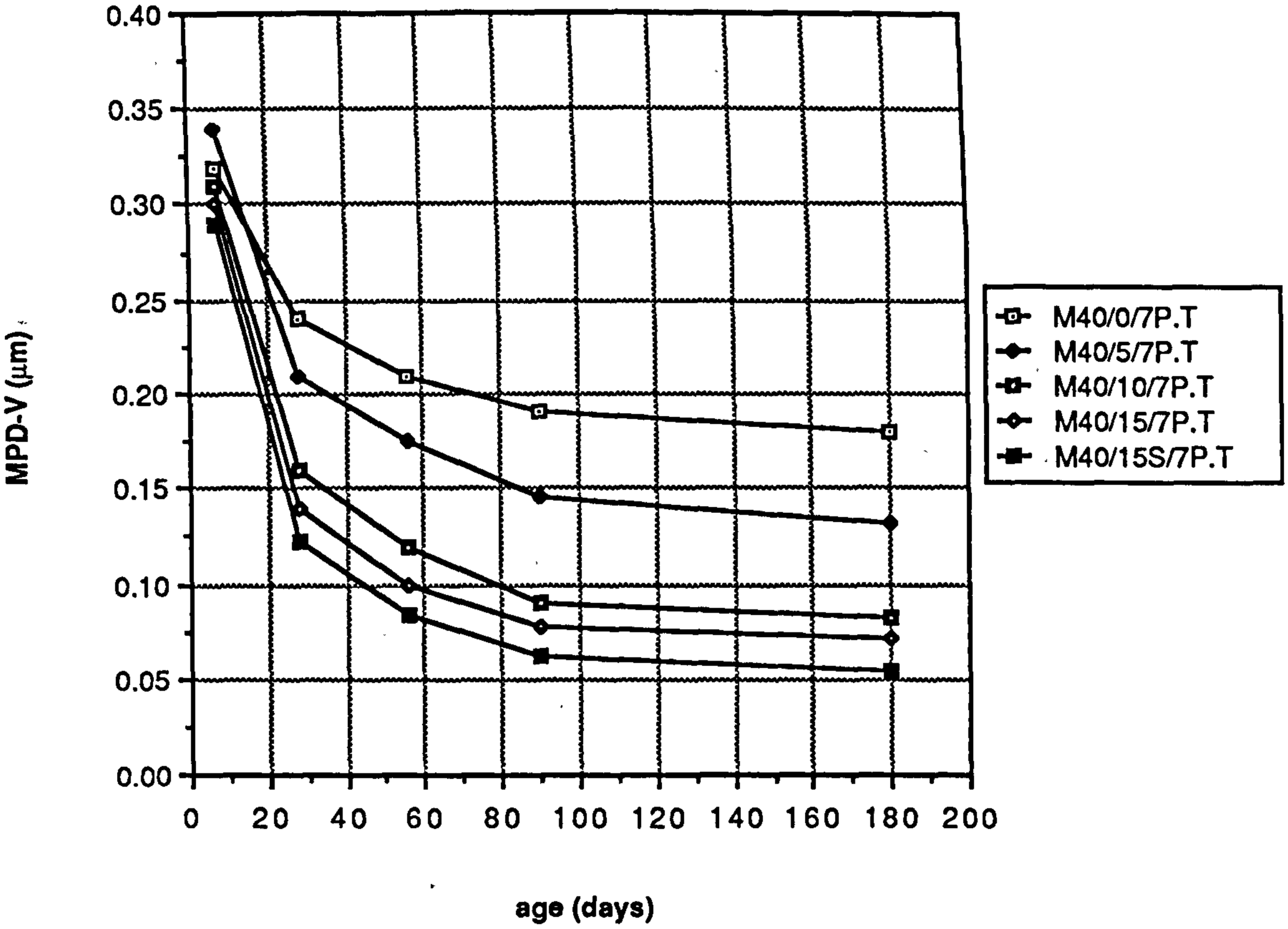

Figure 9.3 Age versus MPD-V relationship of mortars cured in a temperate environment

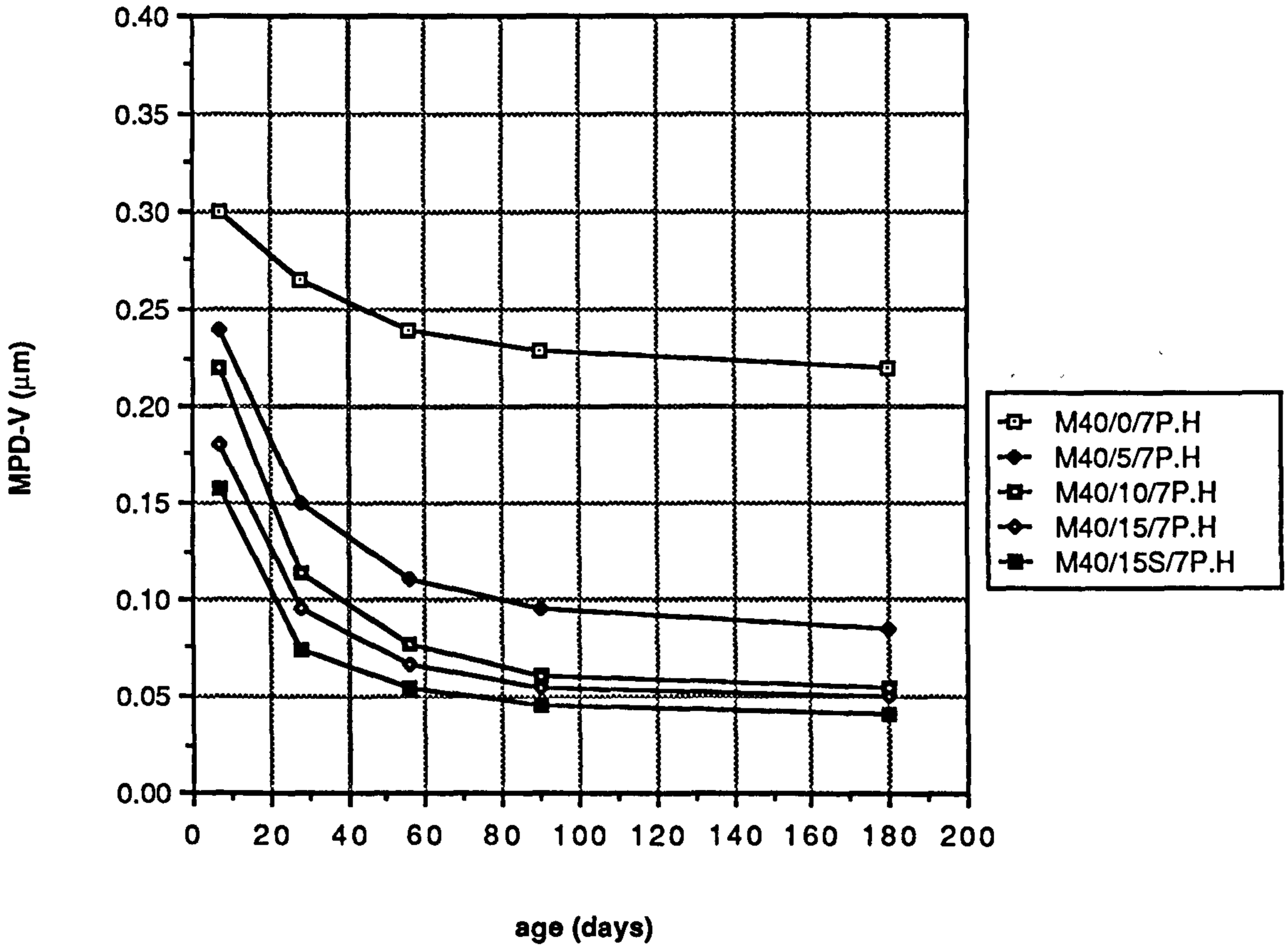

Figure 9.4 Age versus MPD-V relationship of mortars cured in a hot environment

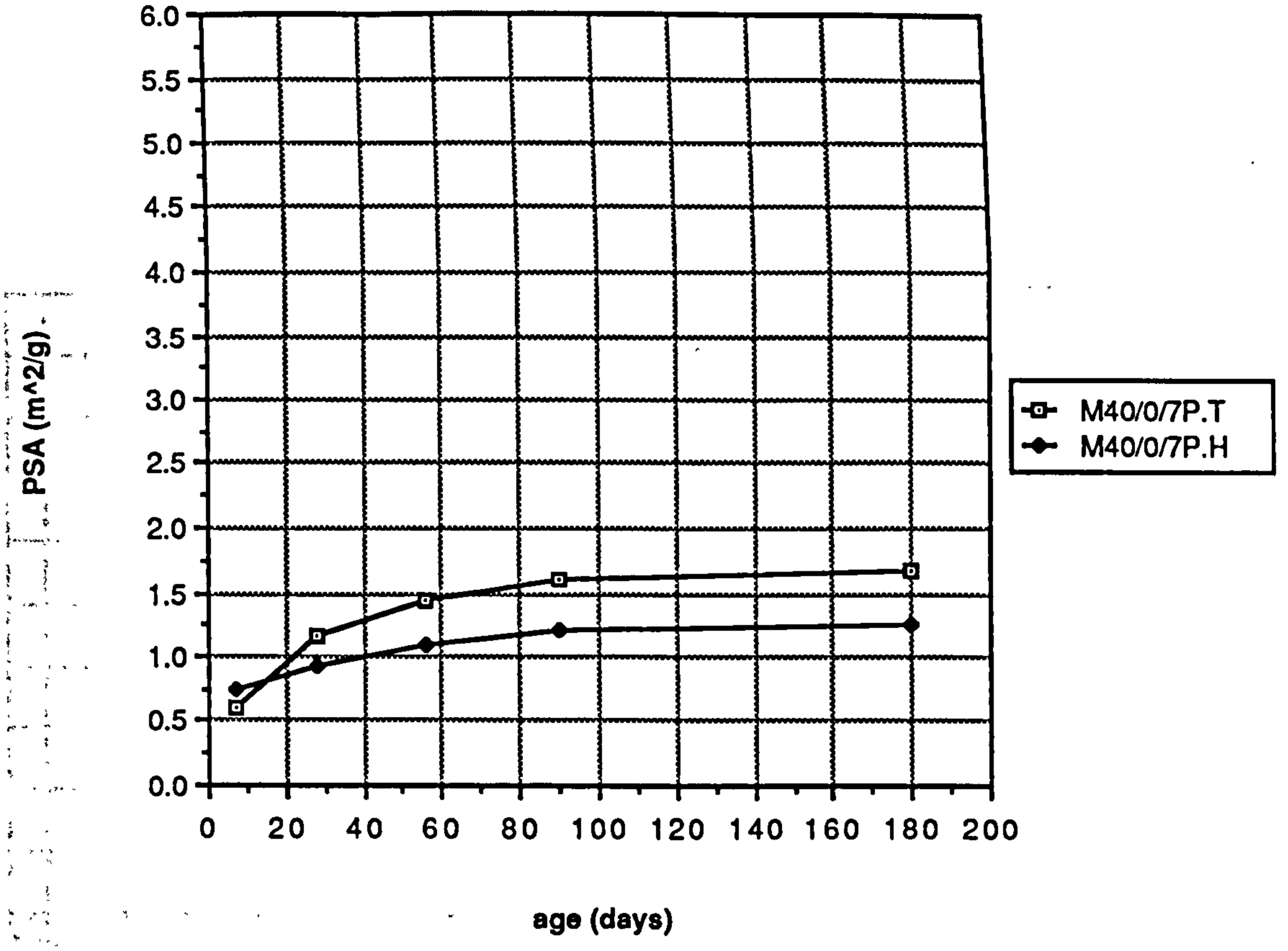

Figure 9.5 Age versus relationship of plain mortars cured in temperate and hot environments

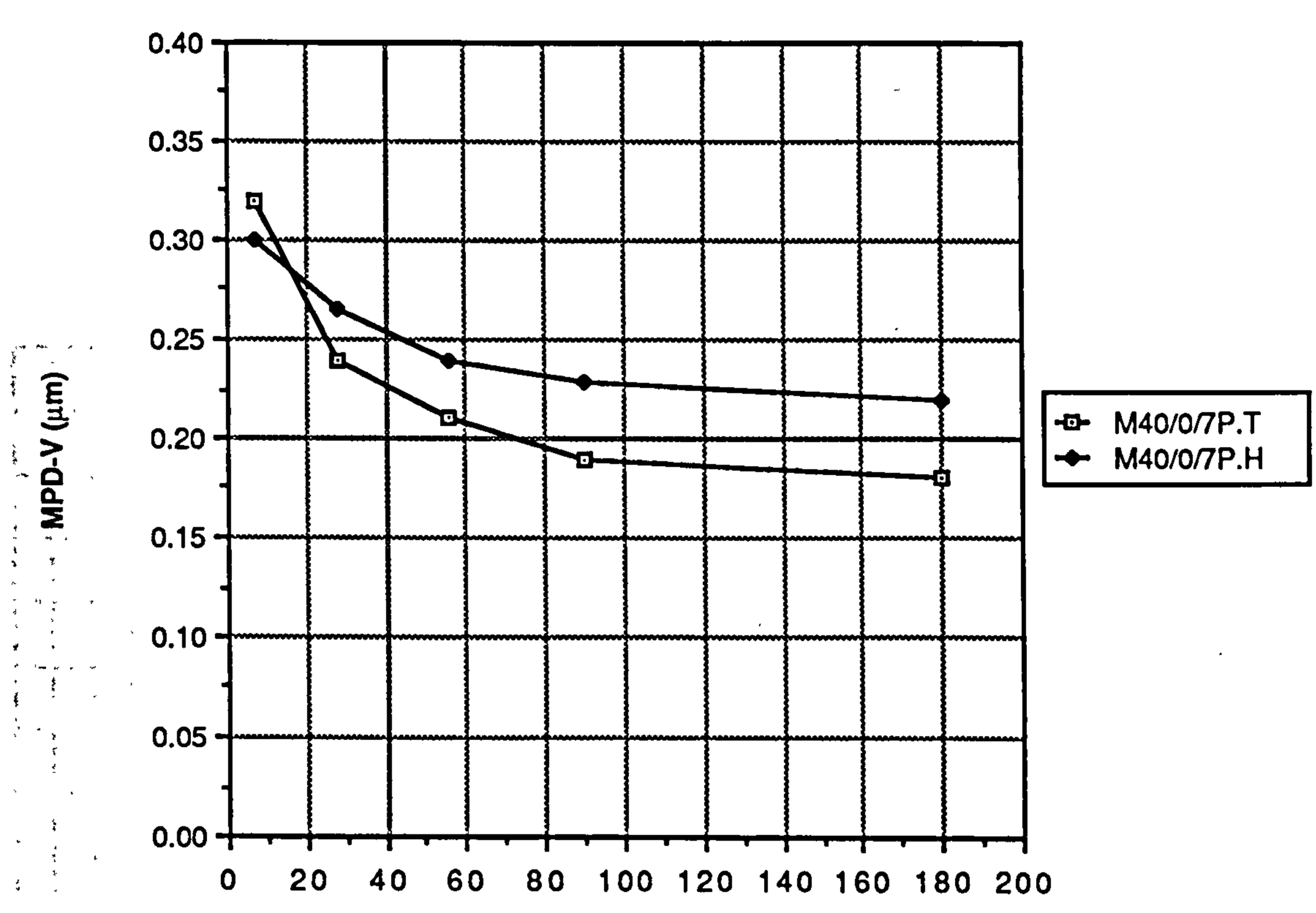

Figure 9.6 Age versus MPD-V relationship of plain mortars cured in hot and temperate environments

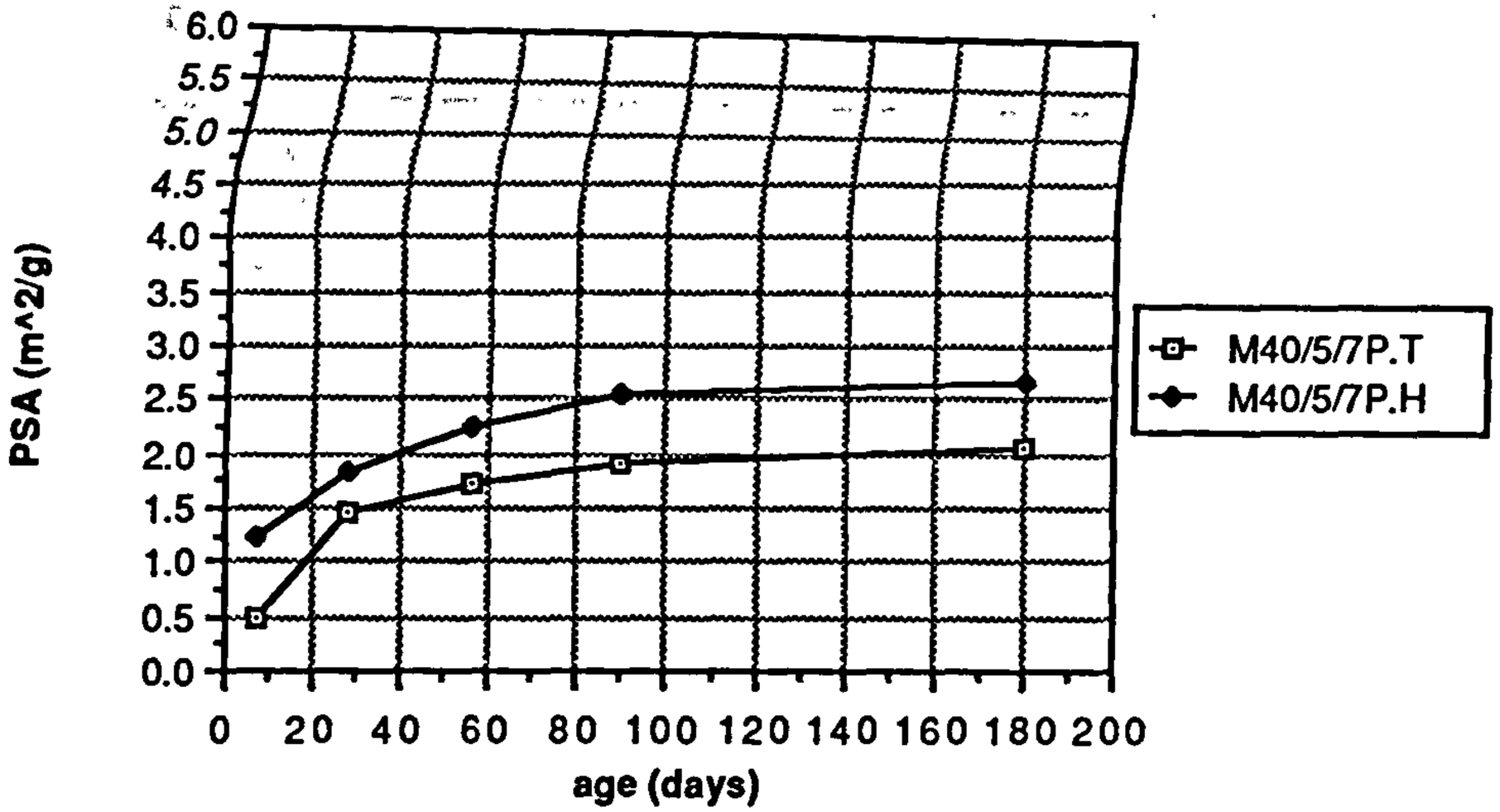

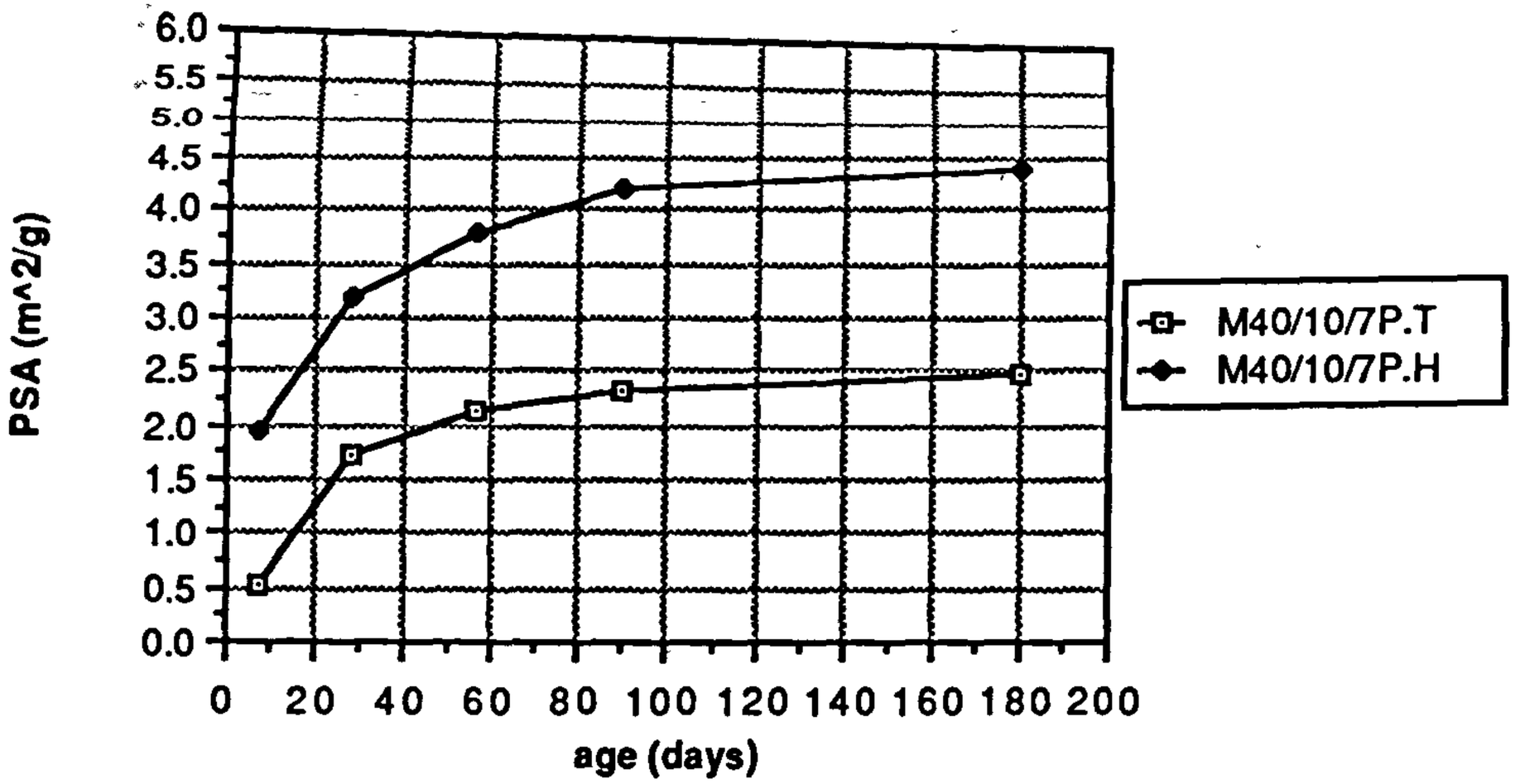

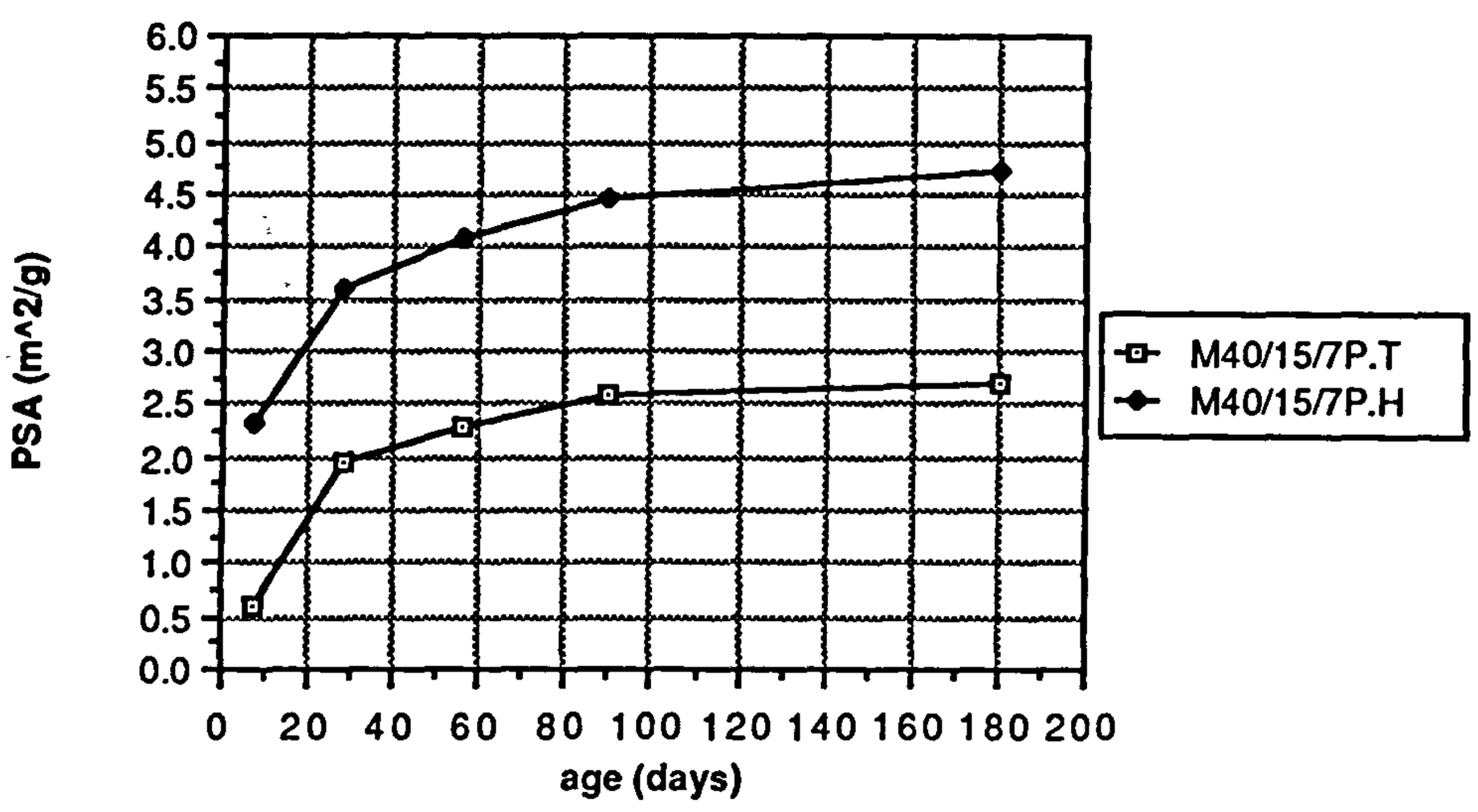

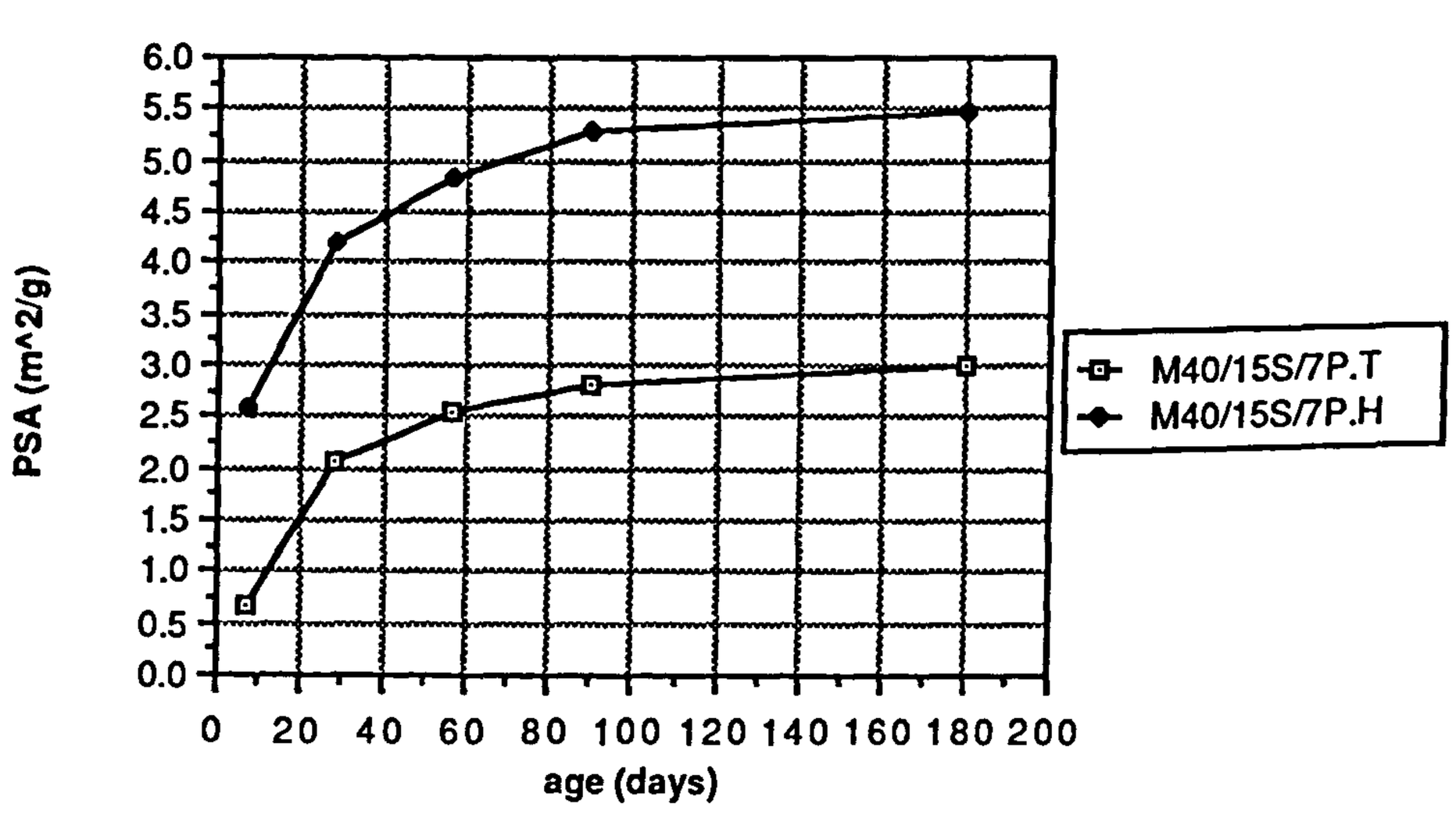

Figure 9.7 Age versus PSA relationship of CSF mortars cured in hot and temperate environments

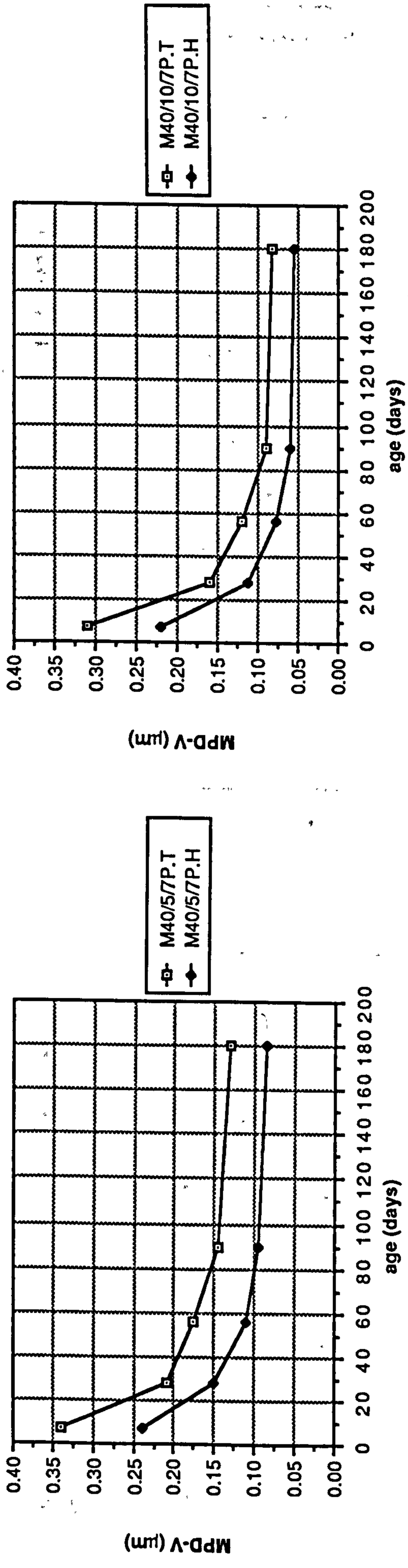

Figure 9.8 Age versus MPD-V relationship of CSF mortars cured in hot and temperate environments

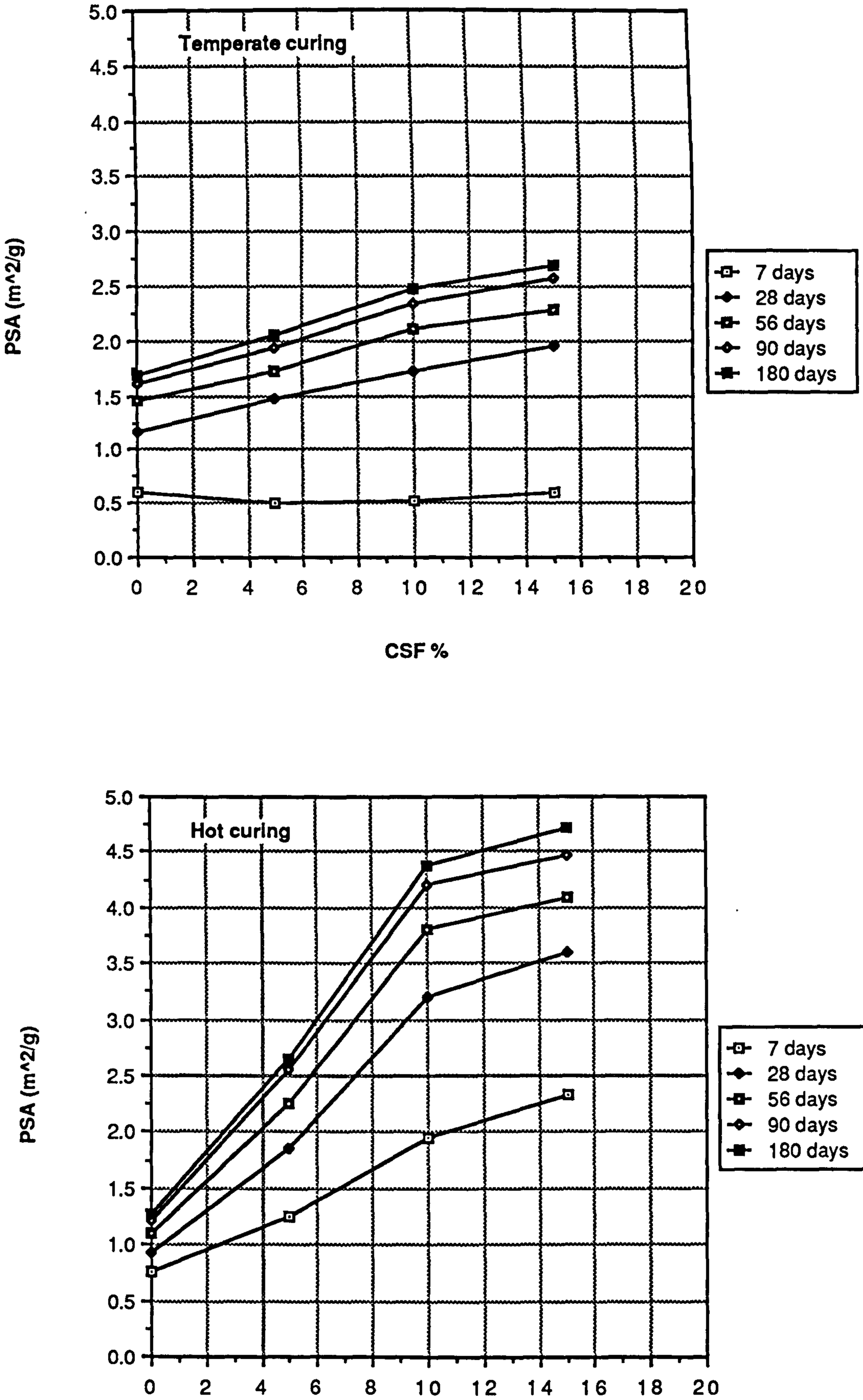

Figure 9.9 Effect of CSF content on the PSA of CSF mortars cured in temperate and hot environments

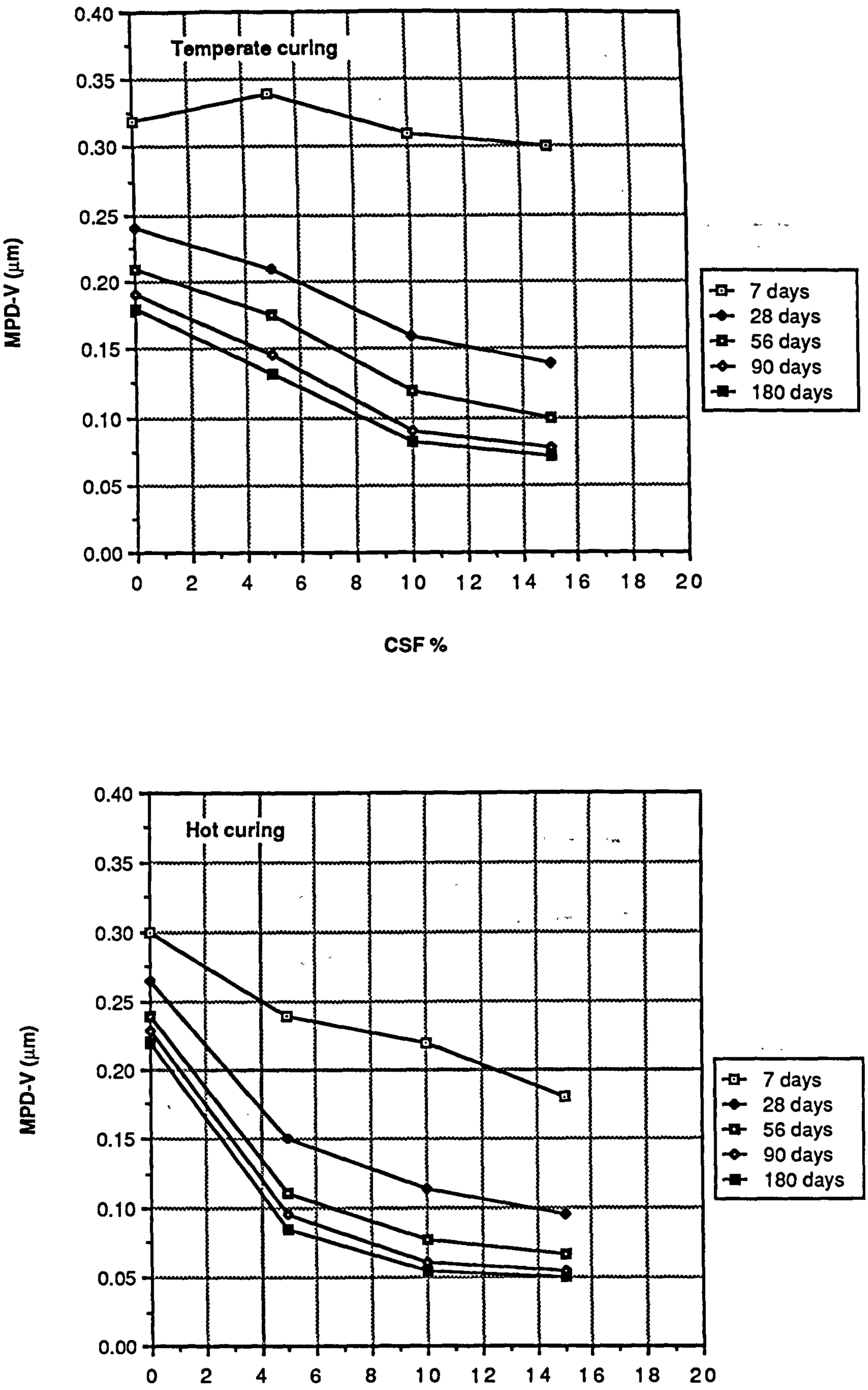

Figure 9.10 Effect of CSF content on the MPD-V of CSF mortars cured in temperate and hot environments

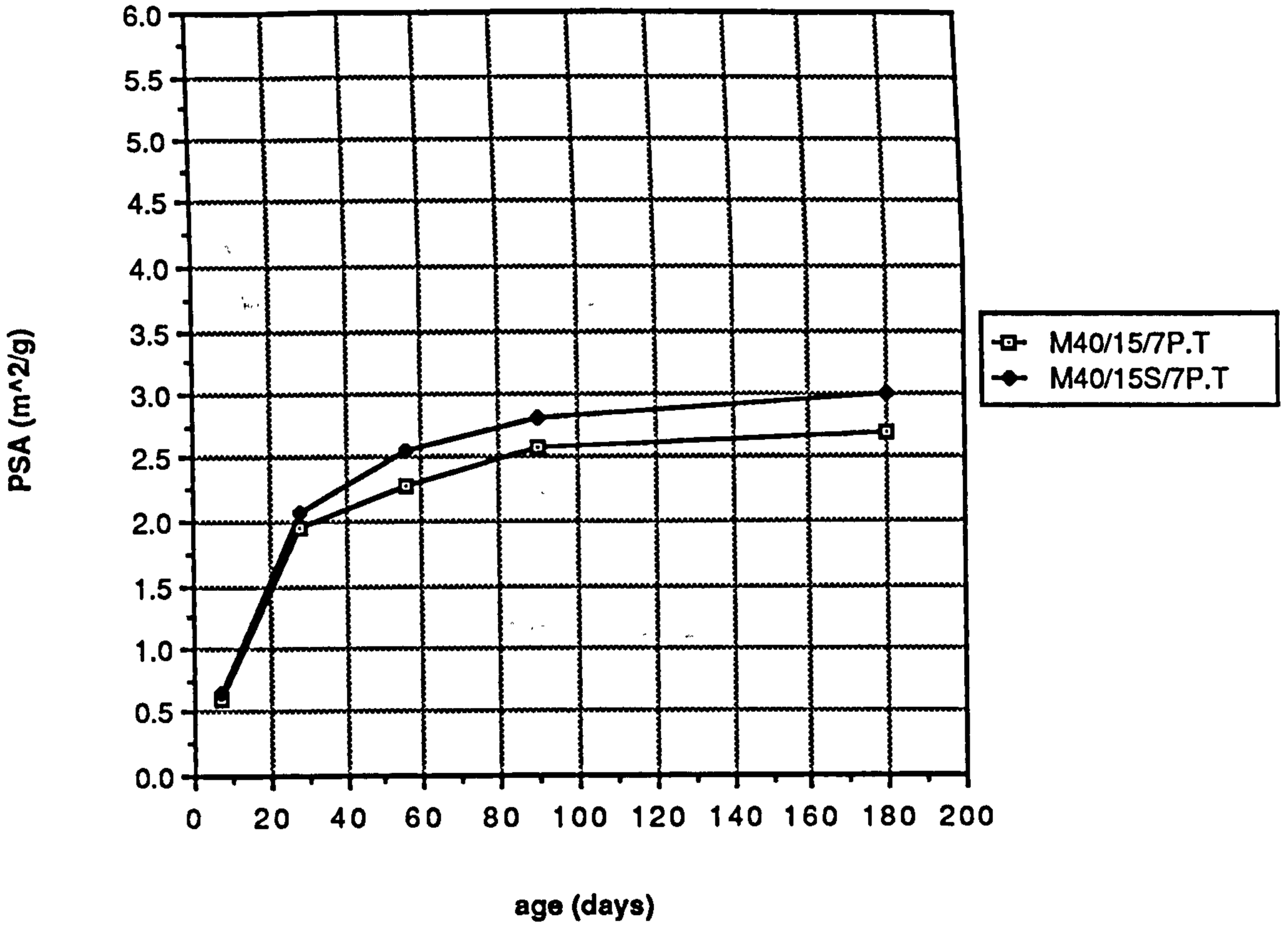

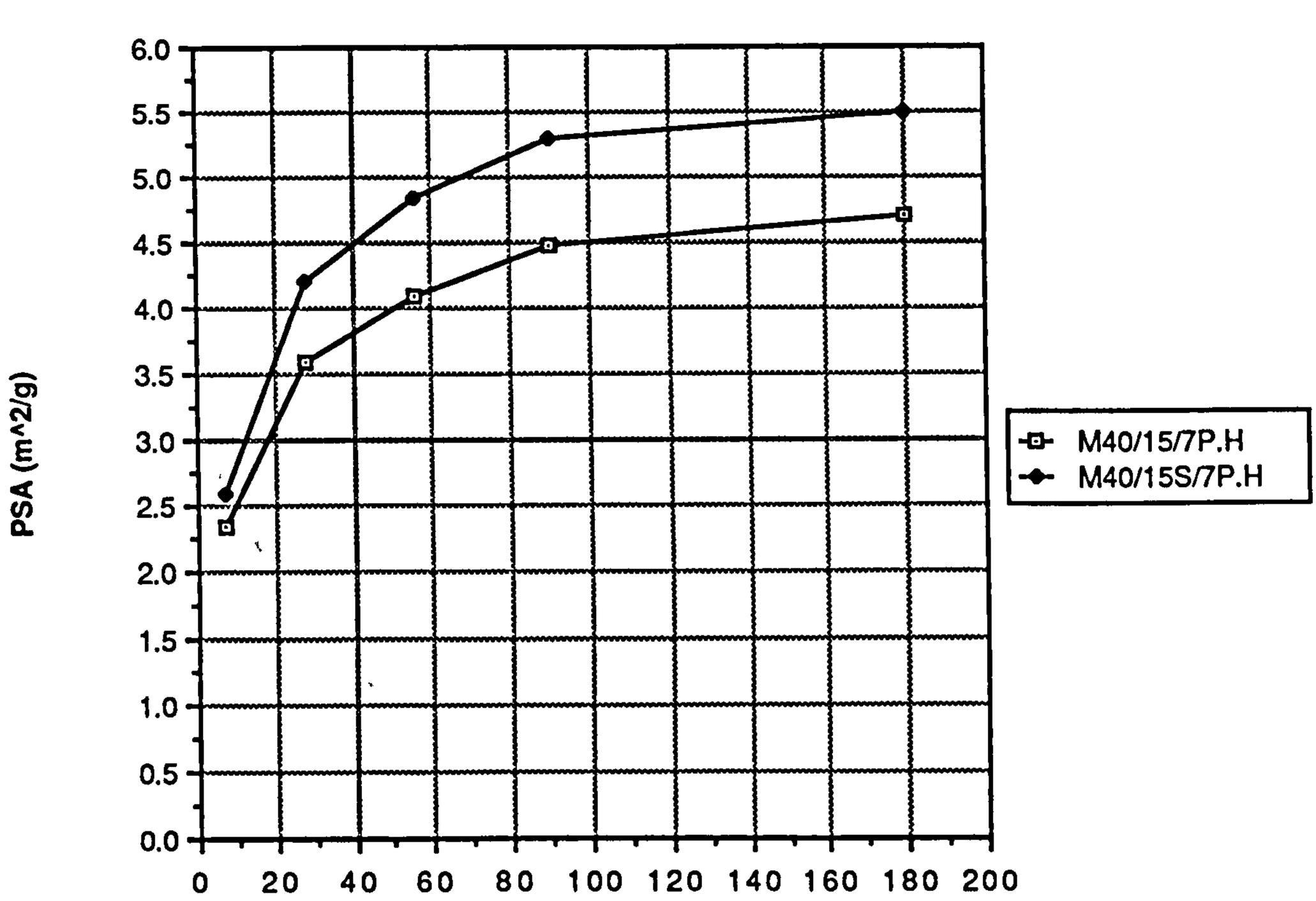

Figure 9.11 Effect of superplasticizer on PSA of mortar mix (M40/15) cured in temperate and hot environments

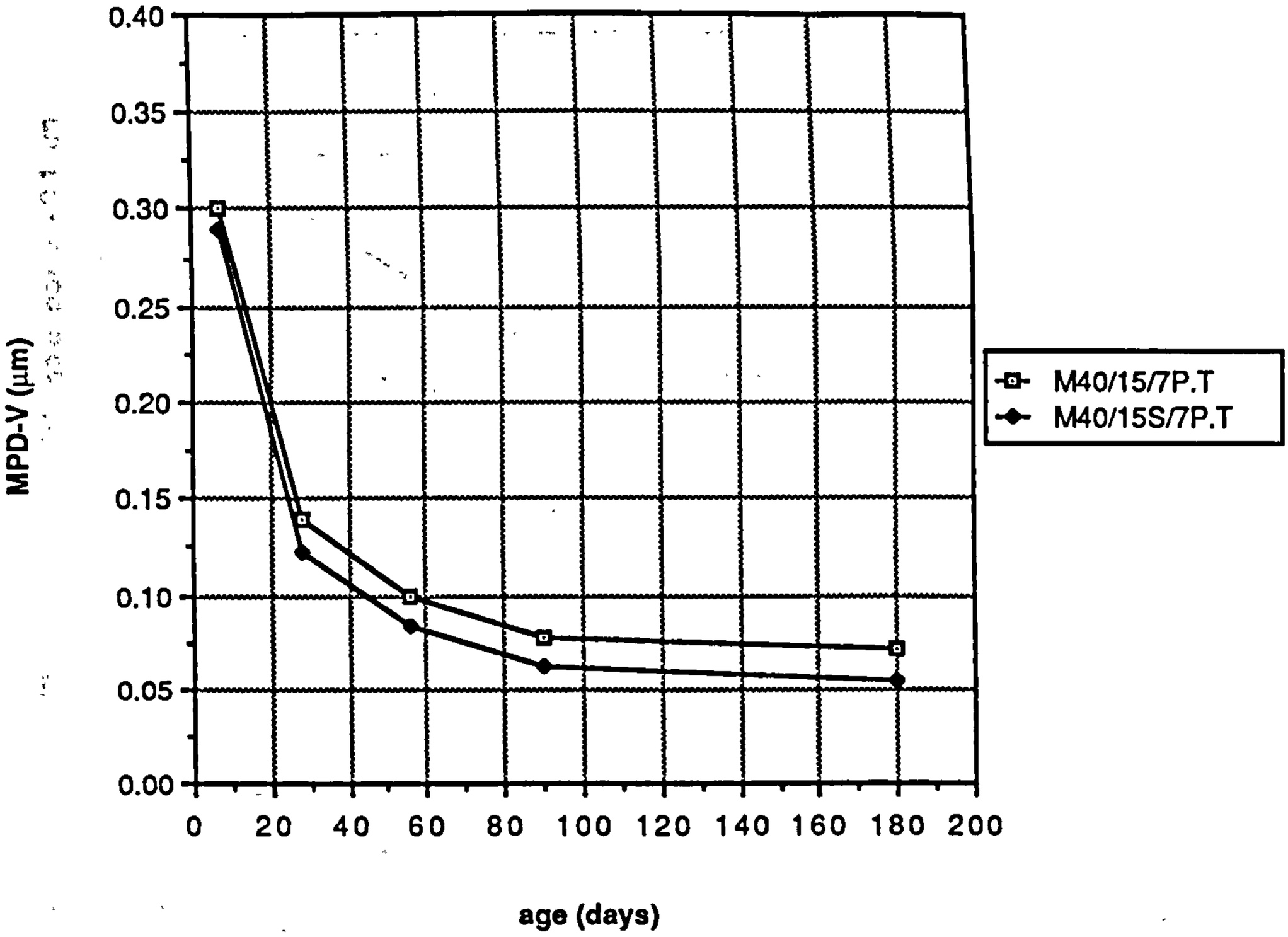

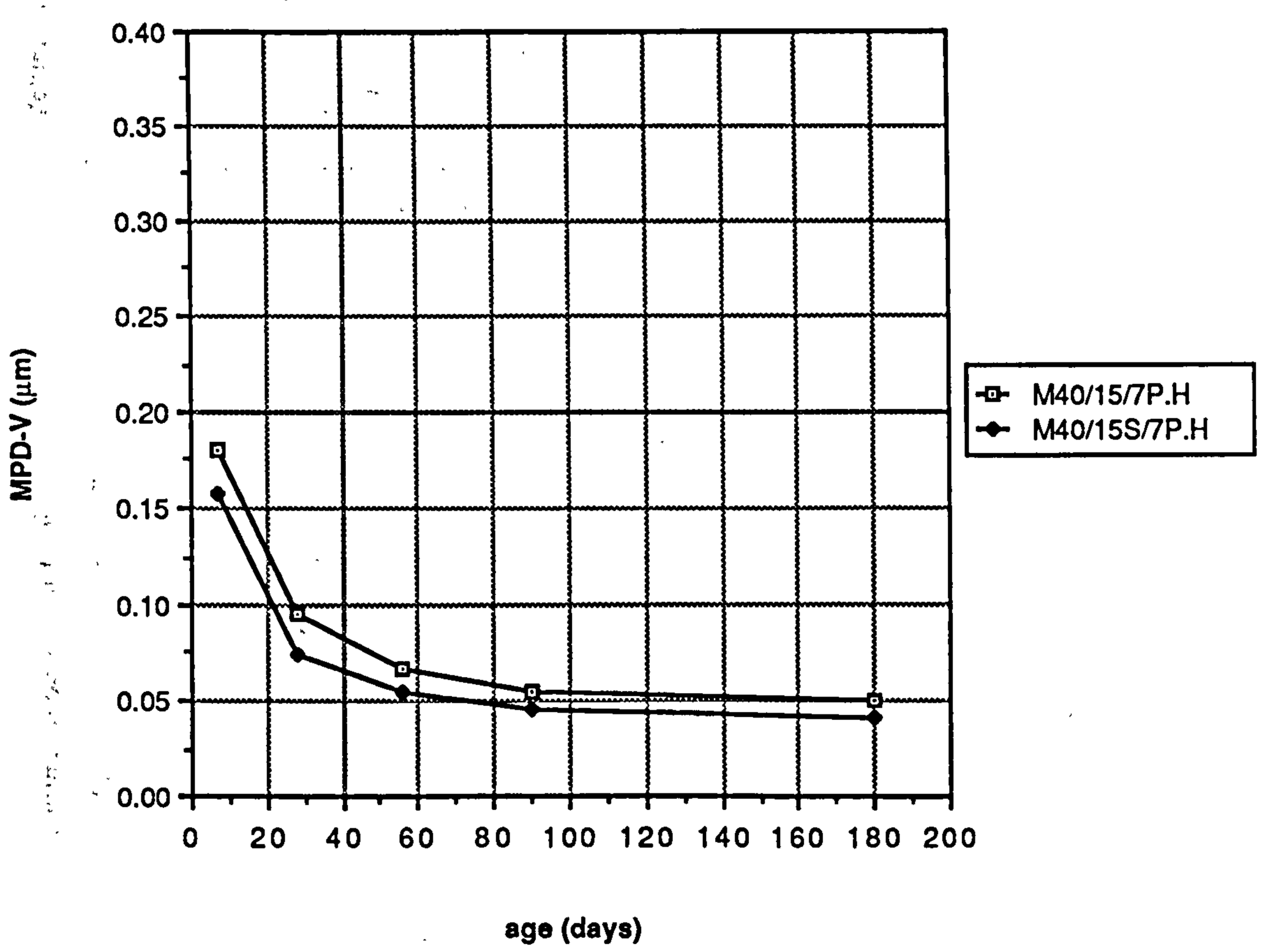

Figure 9.12 Effect of superplasticizer on the MPD-V of CSF mortar mix (M40/15) cured in temperate and hot environments

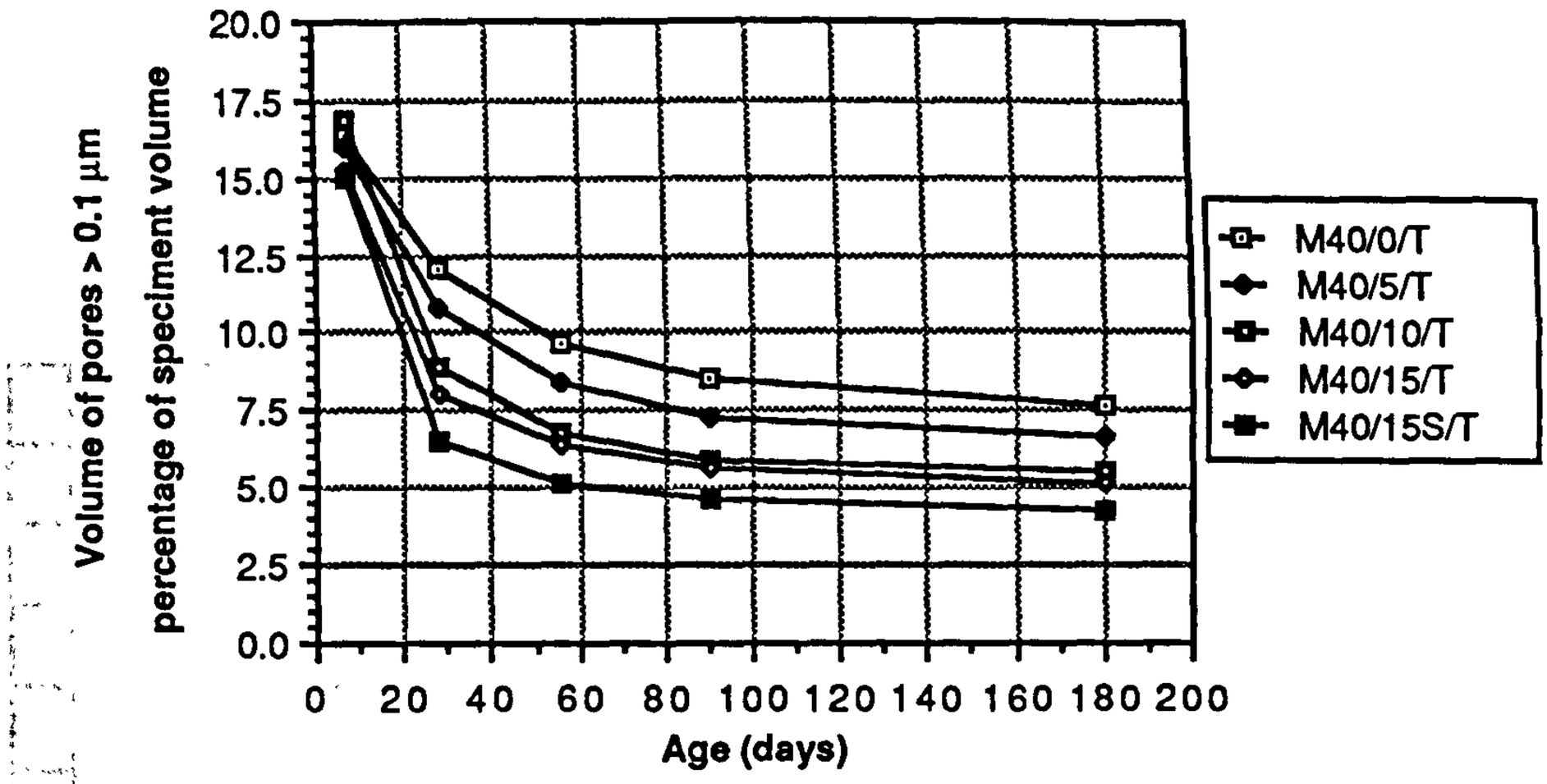

Figure 9.13 Age versus volume of coarse pores (>0.1 µm) relationship of mortars cured in a temperate environment

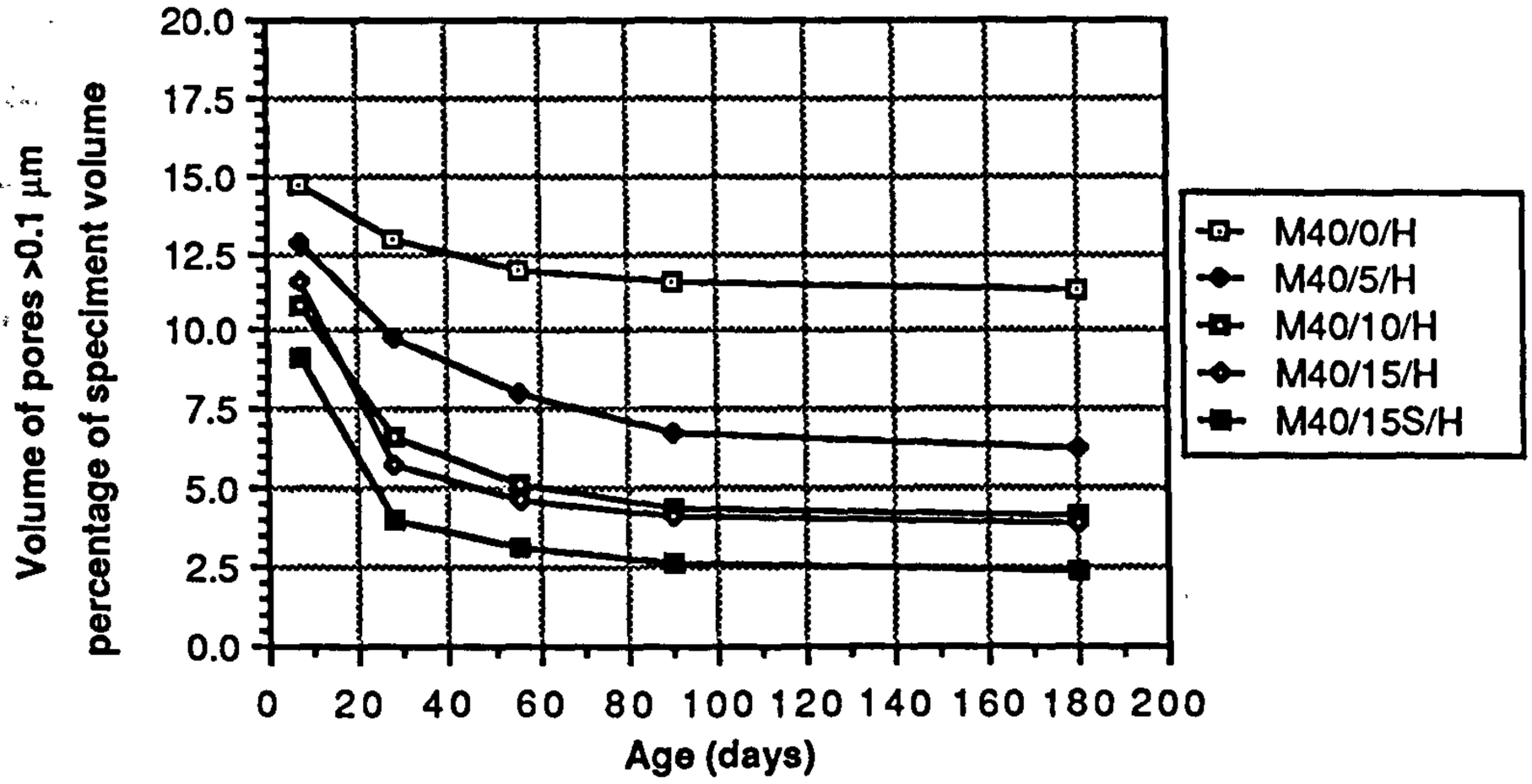

Figure 9.14 Age versus volume of coarse pores (>0.1µm) relationship of mortars cured in a hot environment

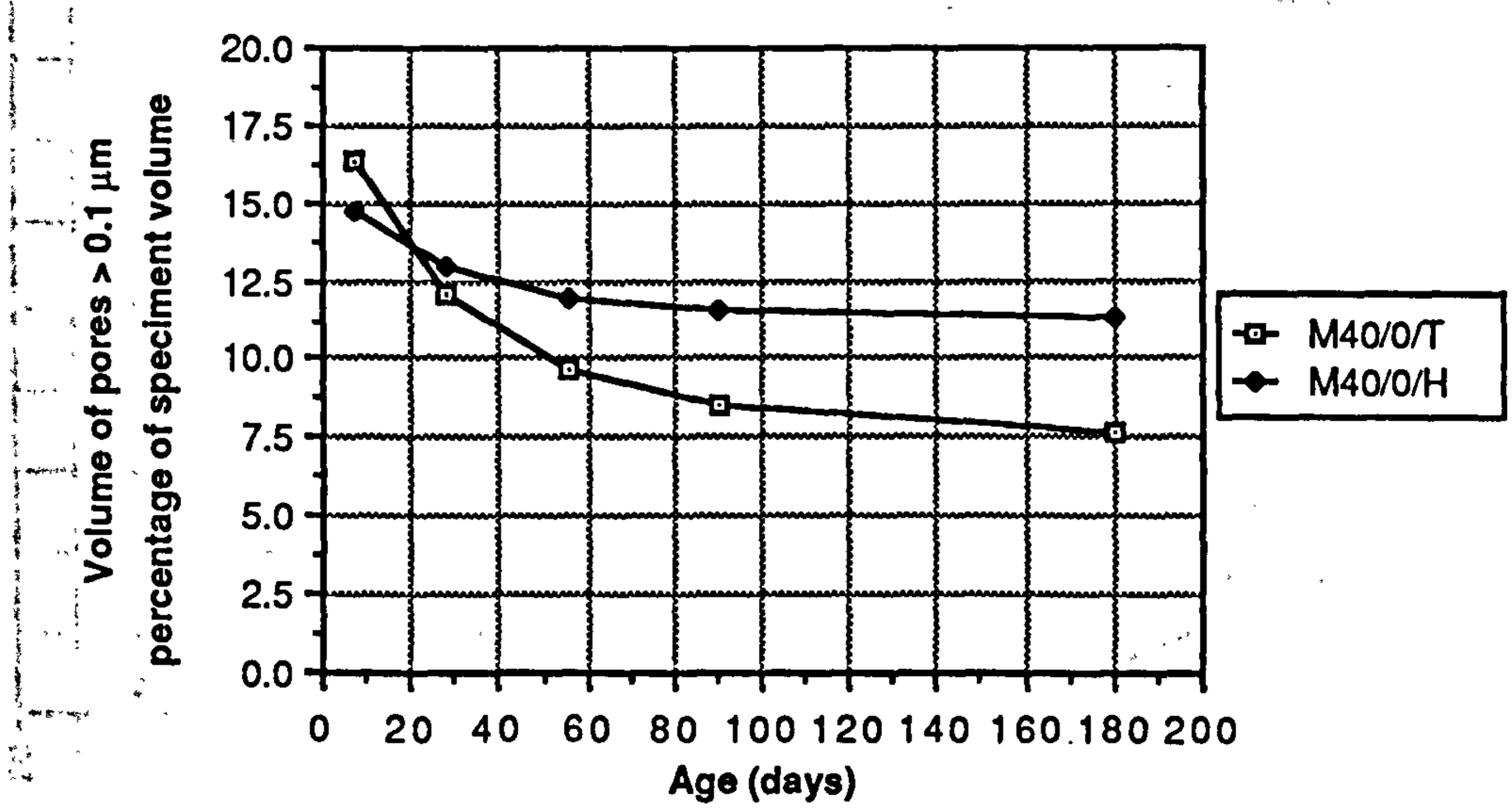

Figure 9.15 Age versus volume of coarse pores (>0.1µm) of plain mortars cured in temperate and hot environments

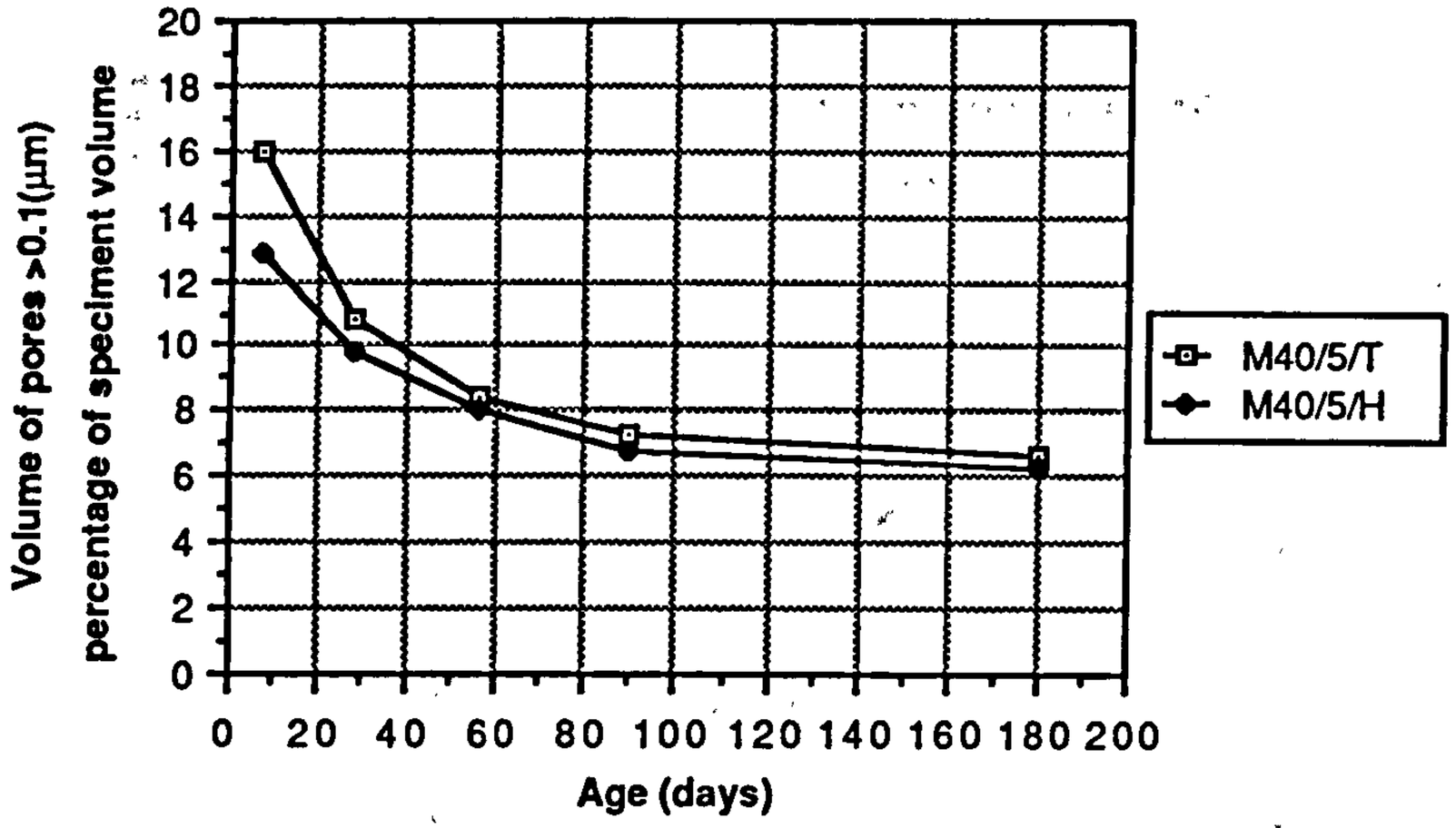

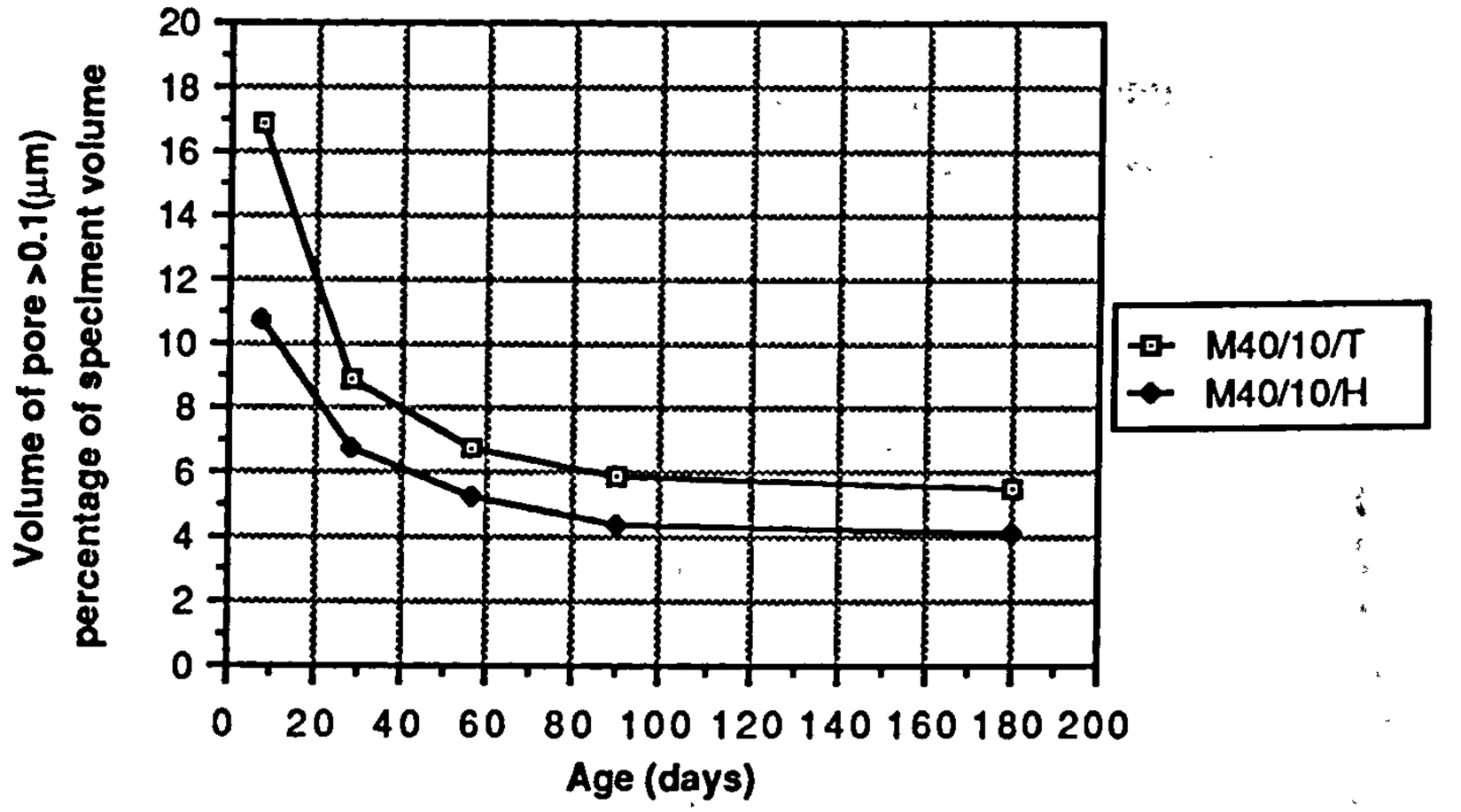

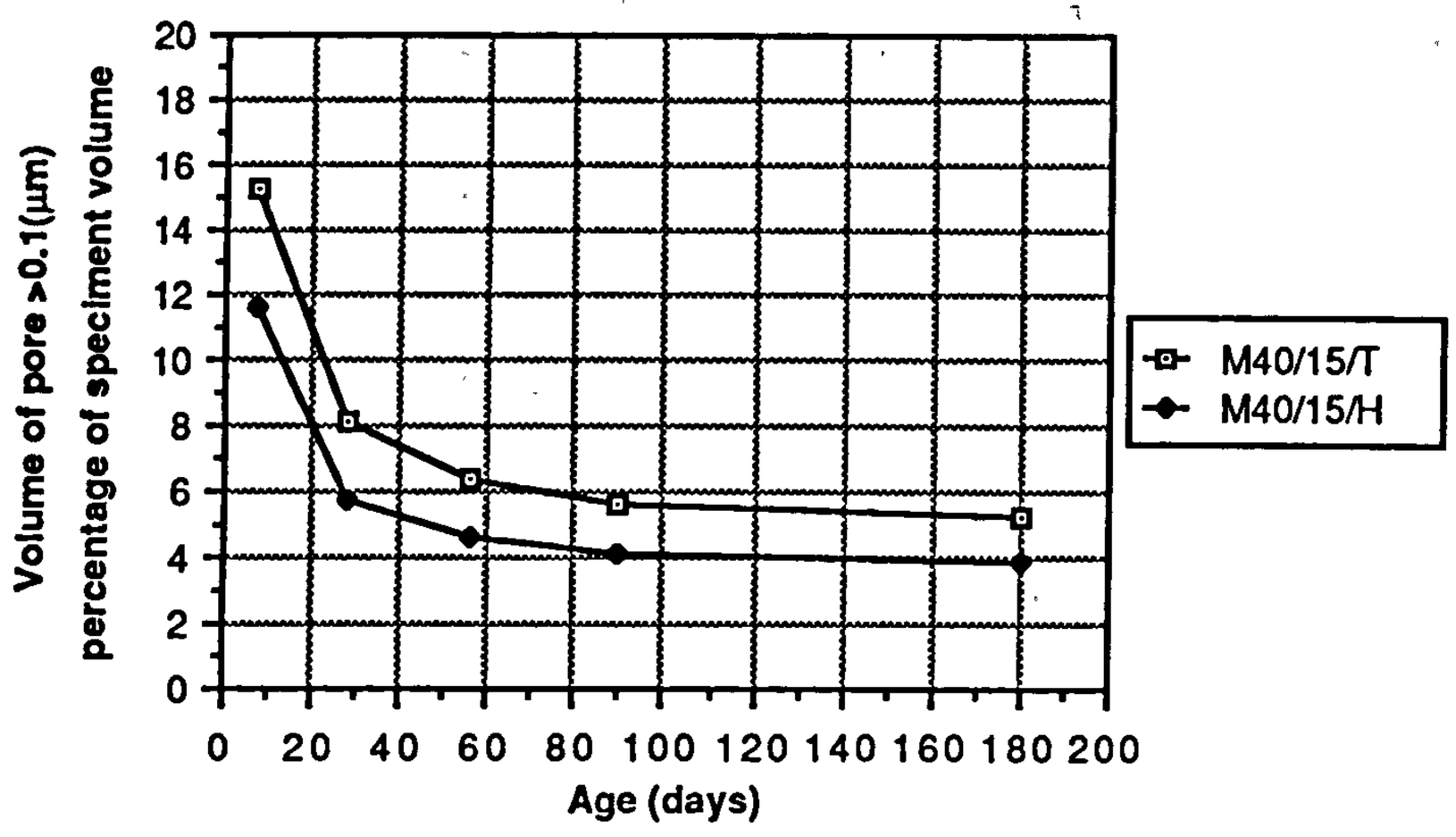

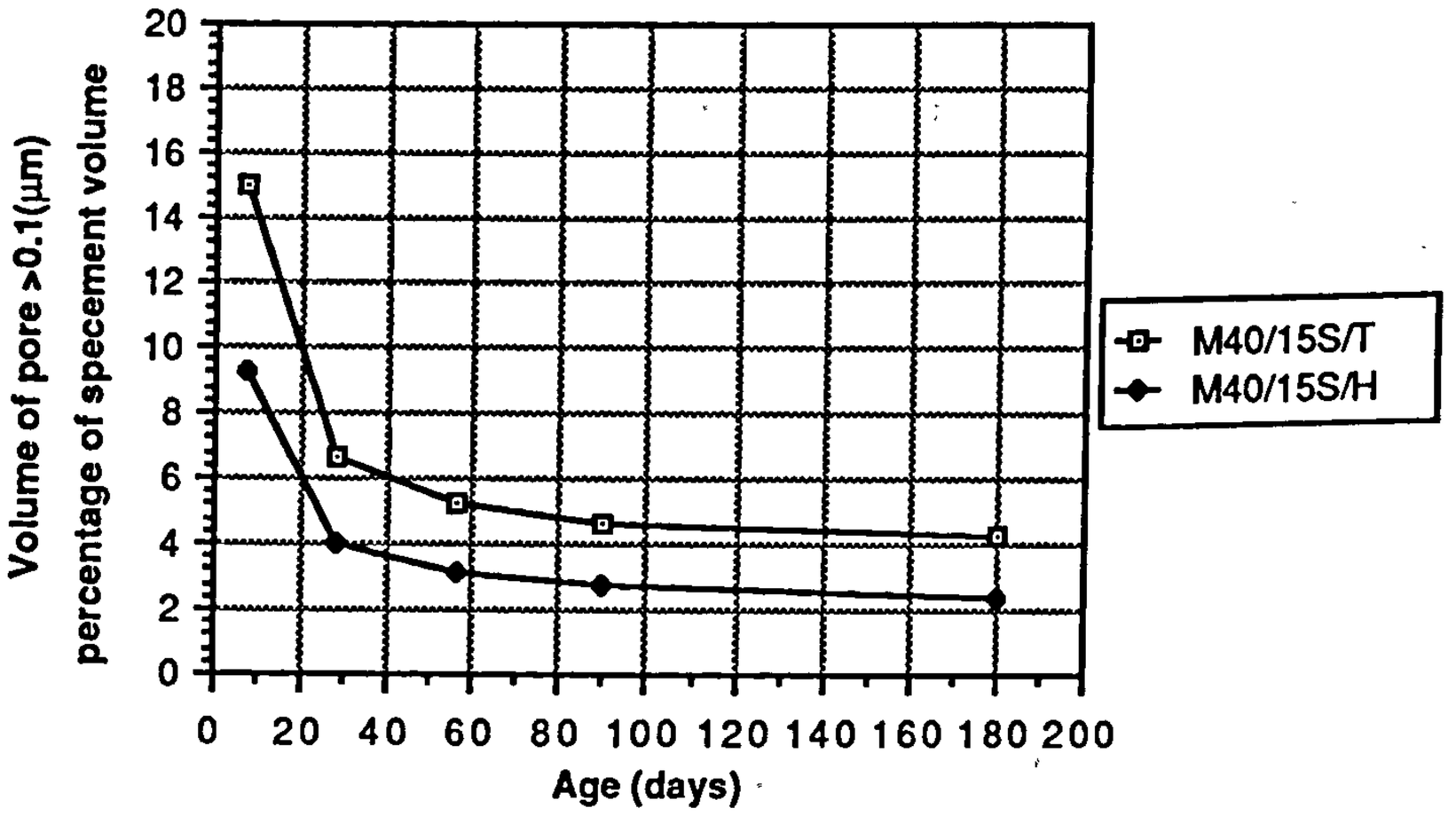

Figure 9.16 Age versus volume of coarse pores (>0.1μm) relationship of CSF mortars cured in temperate and hot environments

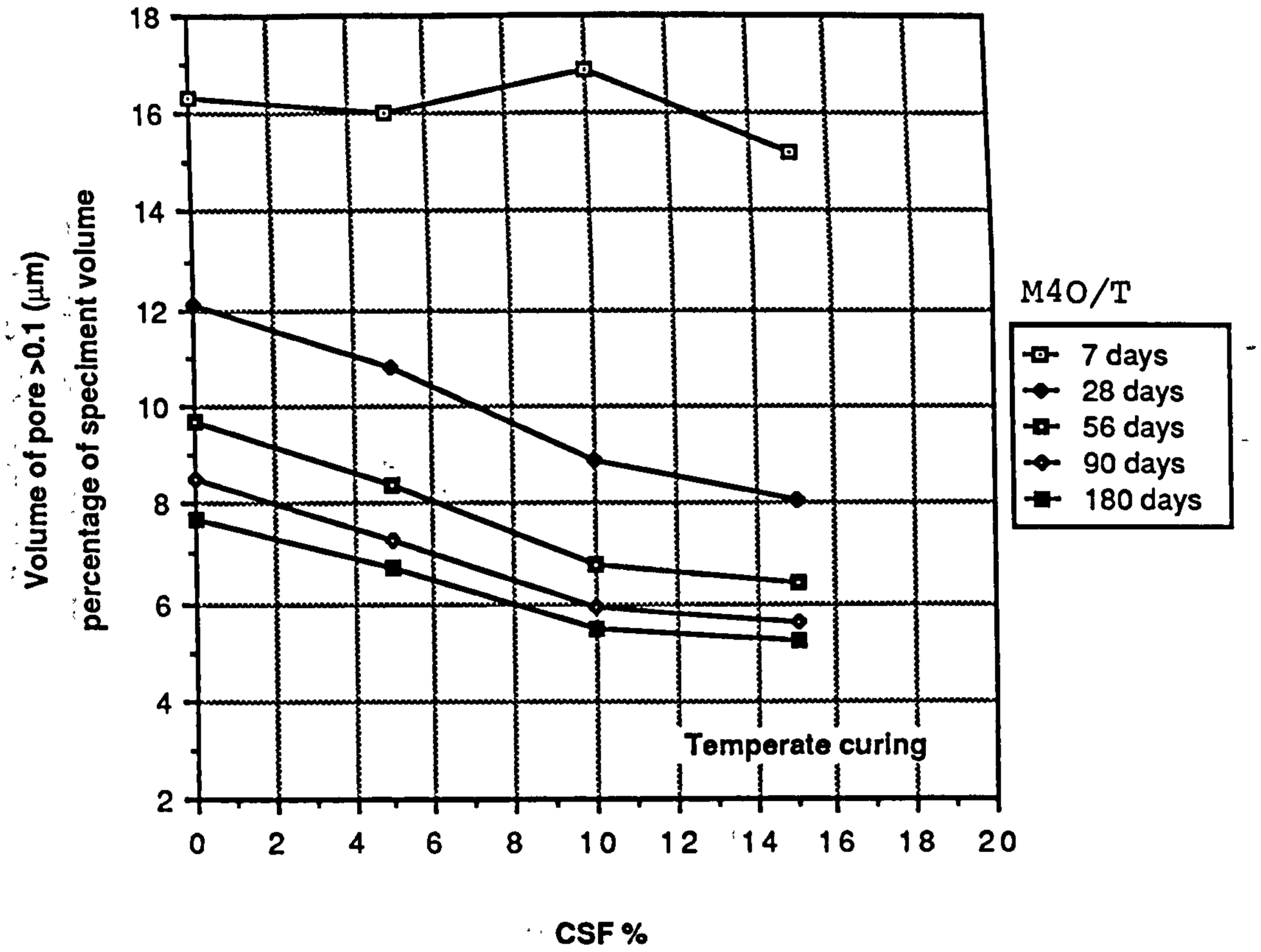

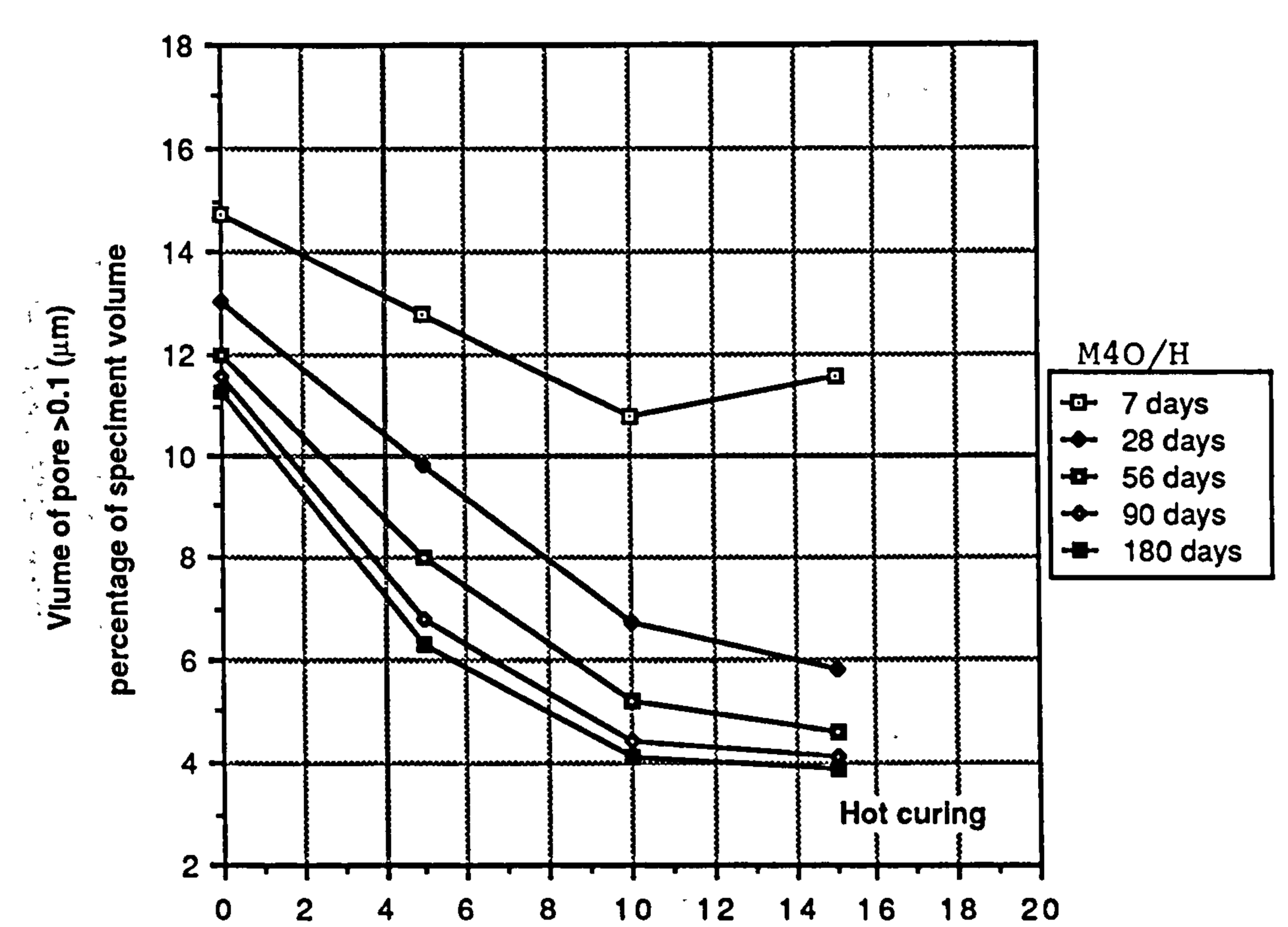

Figure 9.17 Effect of CSF content on the volume of coarse pores in temperate and hot environments

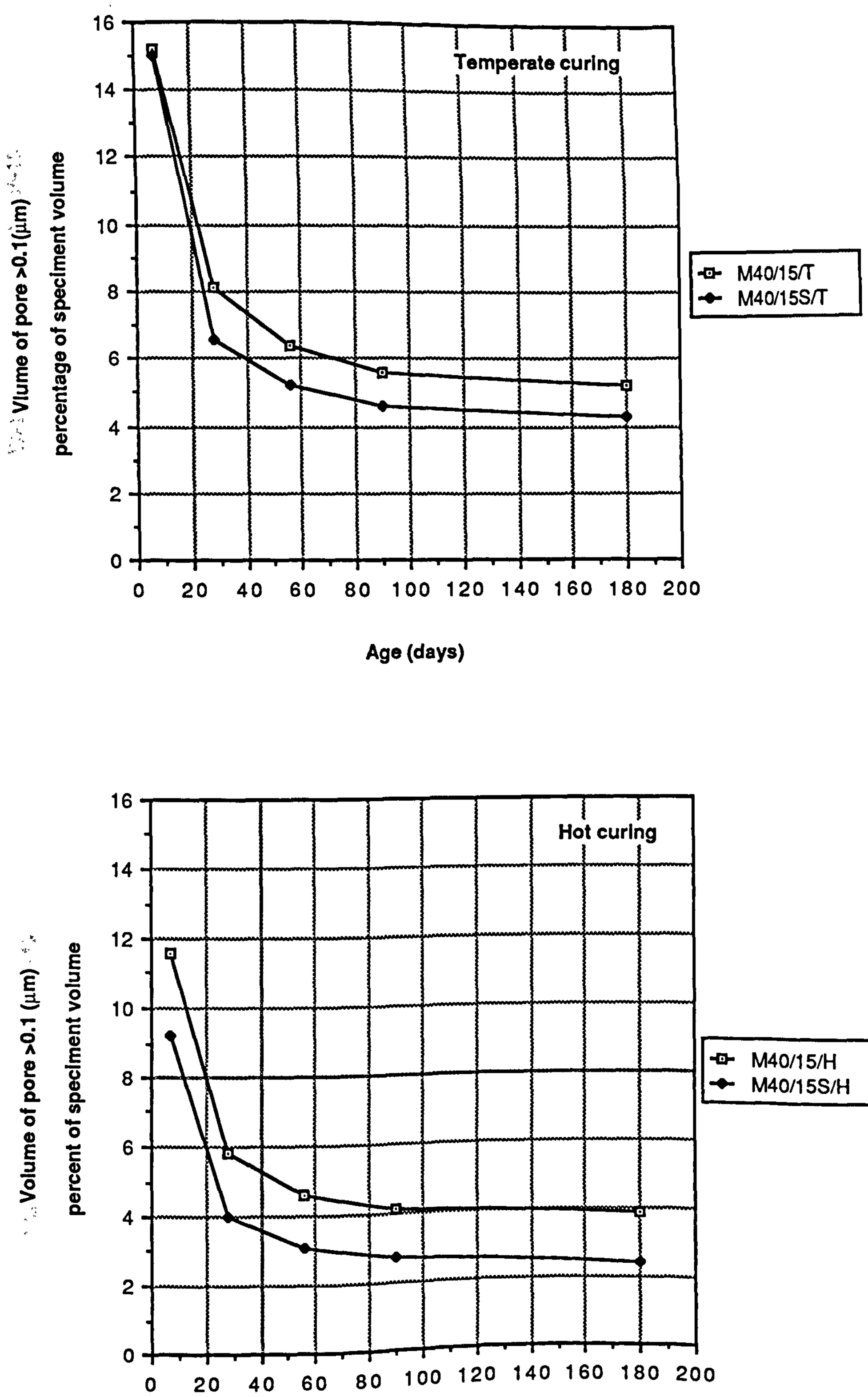

Figure 9.18 Effect of superplasticizer on the volume of coarse pores in temperate and hot environments

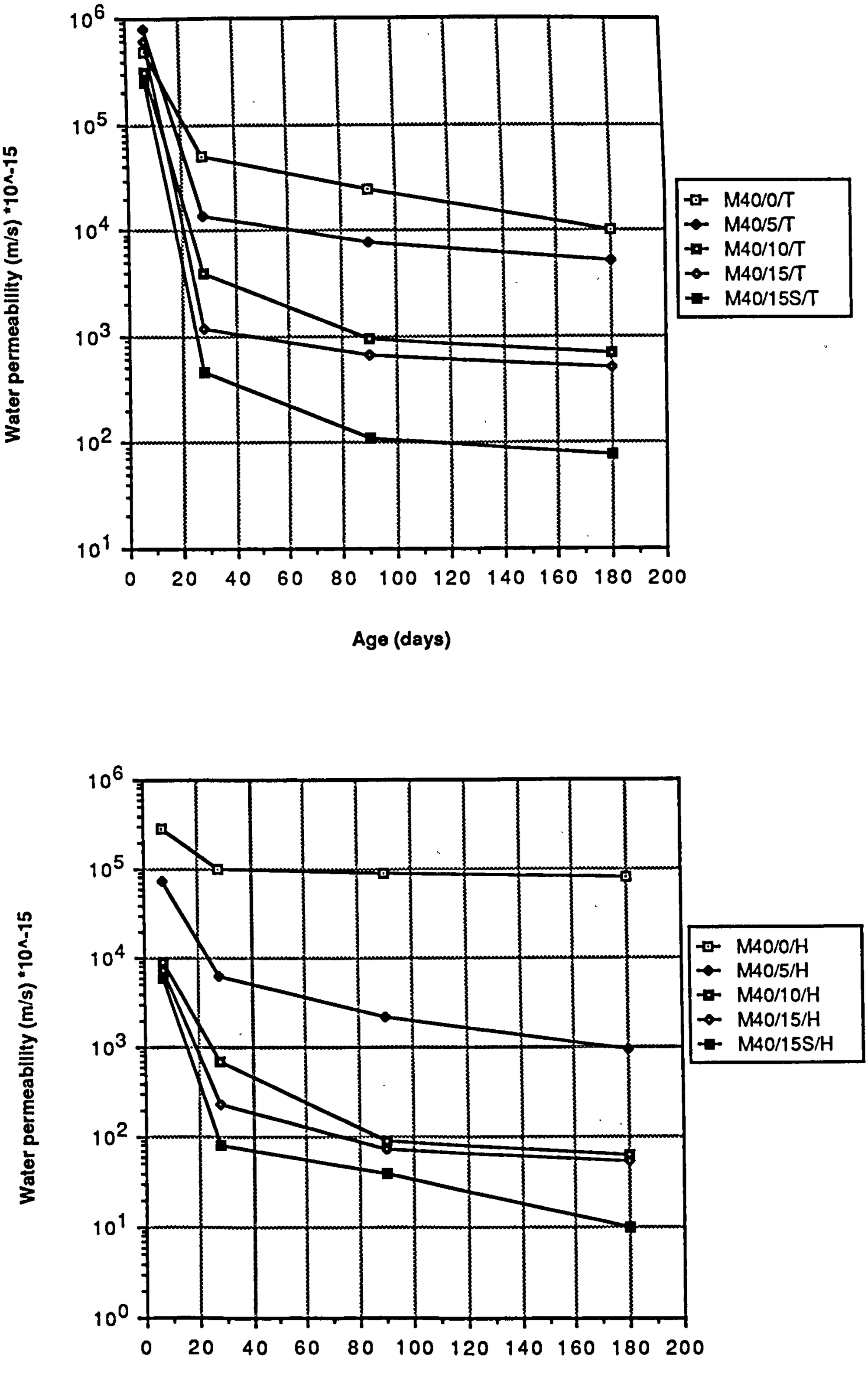

Figure 9.19 Age versus coefficient of water permeability relationship in temperate and hot environments

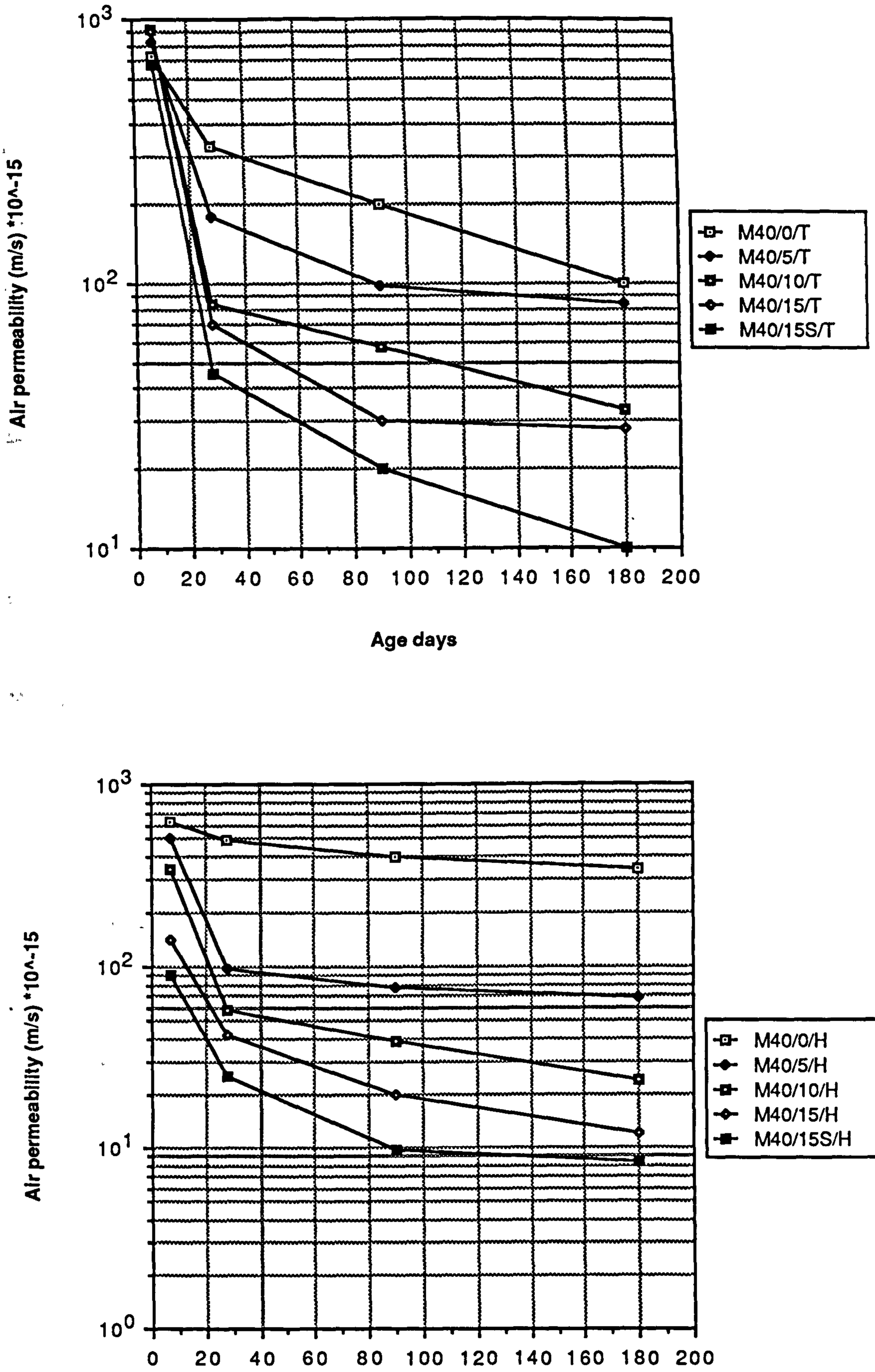

Figure 9.20 Age versus coefficient of air permeability relationship in temperate and hot environments

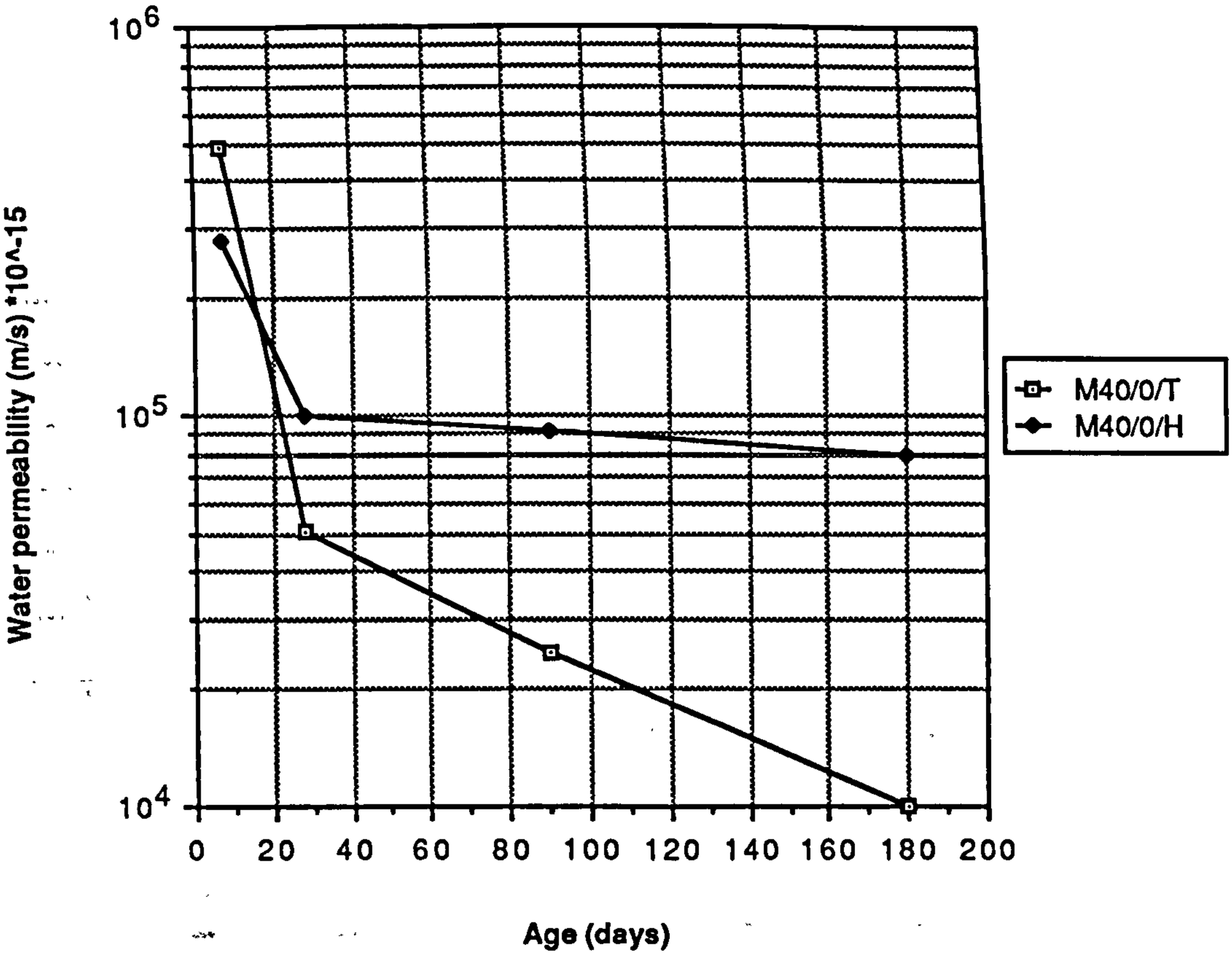

Figure 9.21 Effect of curing environment on the water permeability of plain OPC mortars .

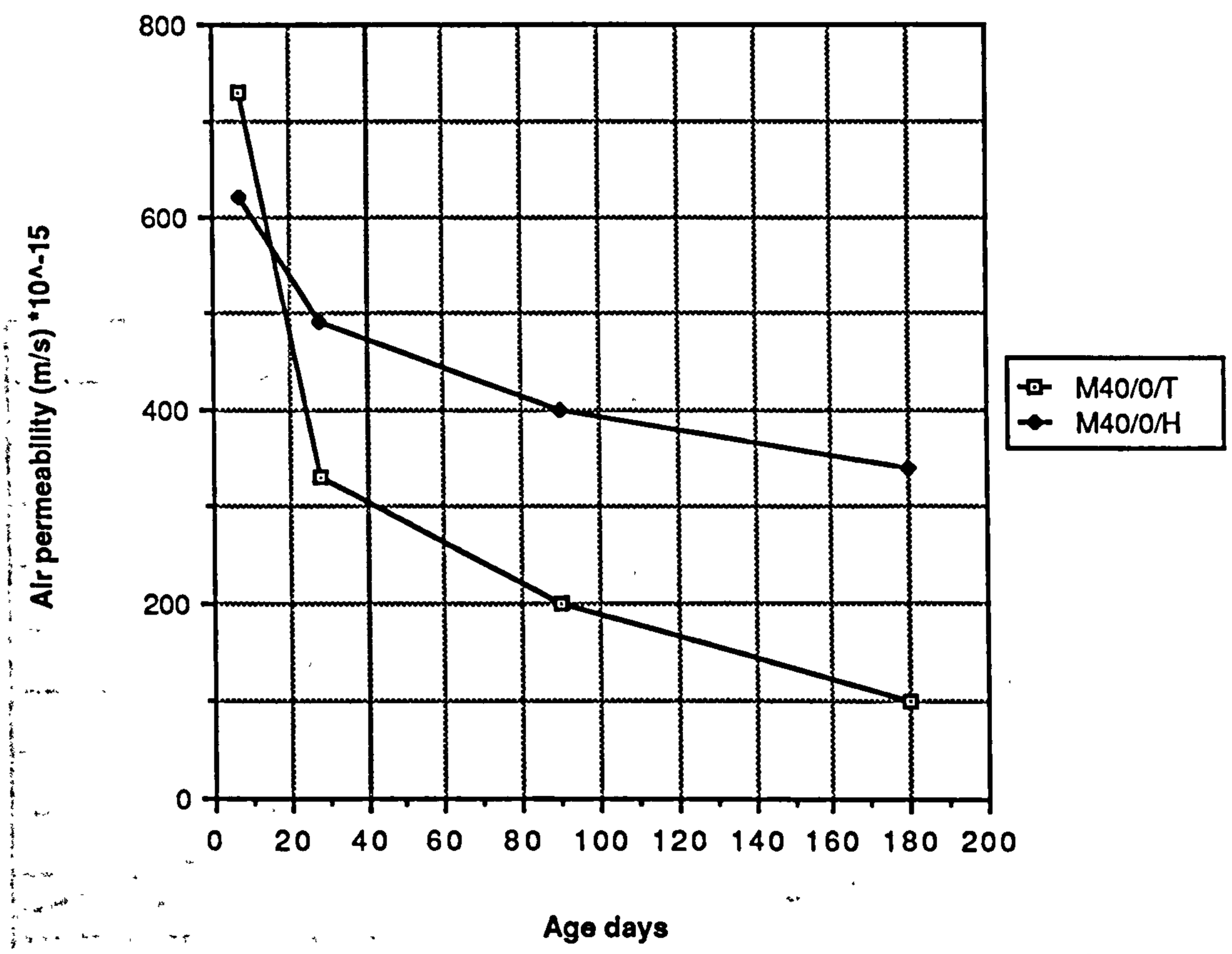

Figure 9.22 Effect of curing environments on the air permeability of plain OPC mortars

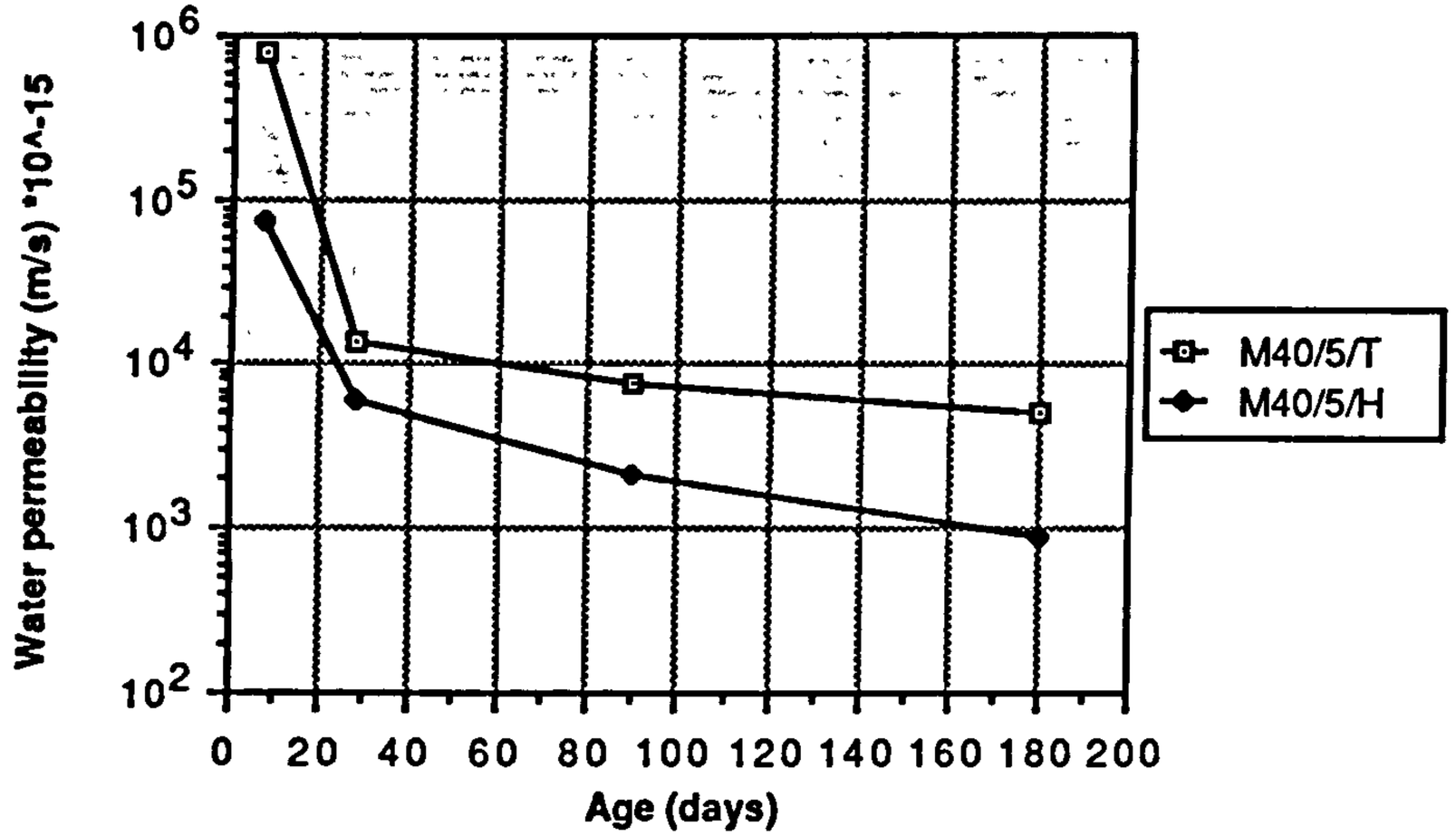

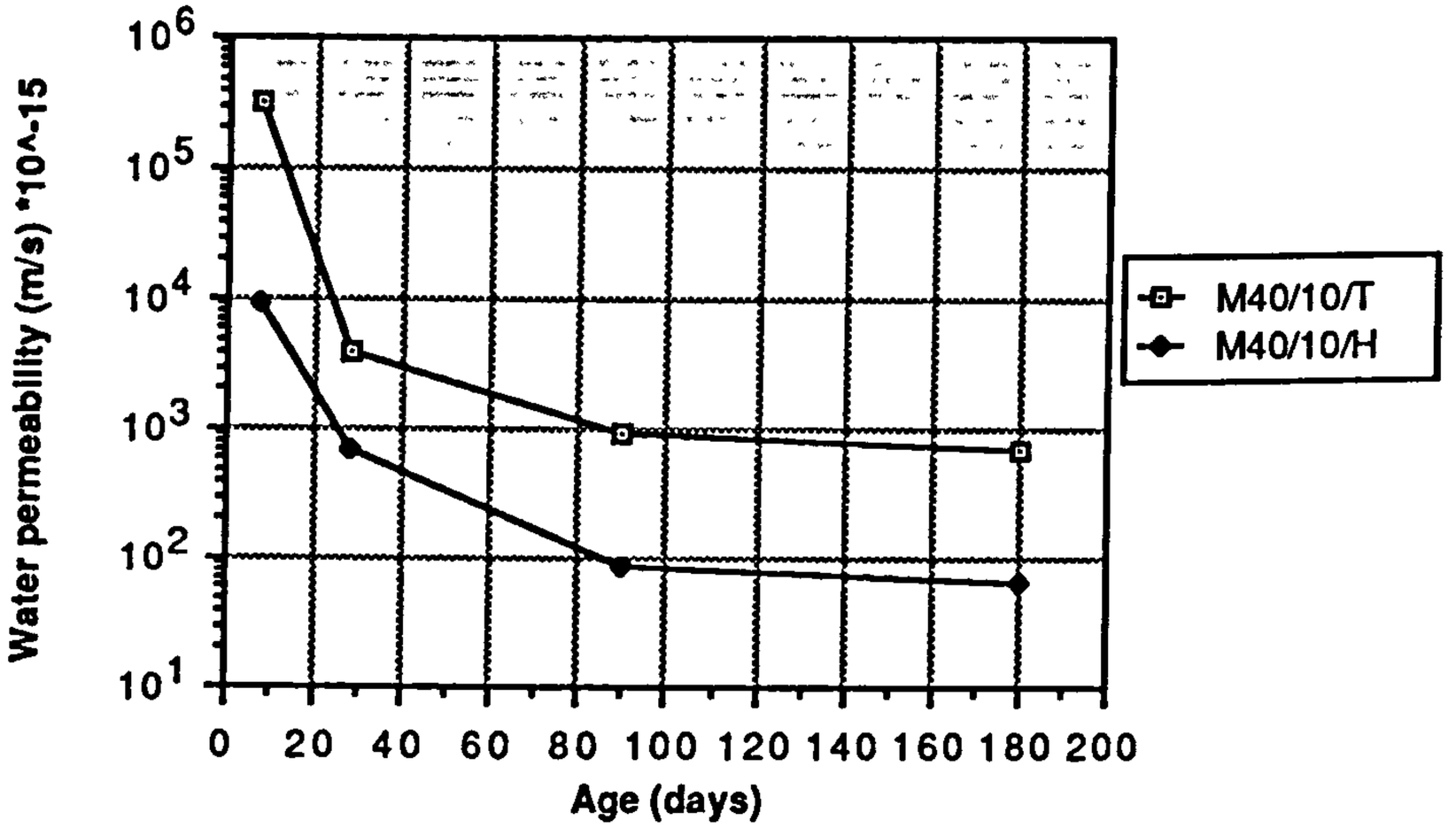

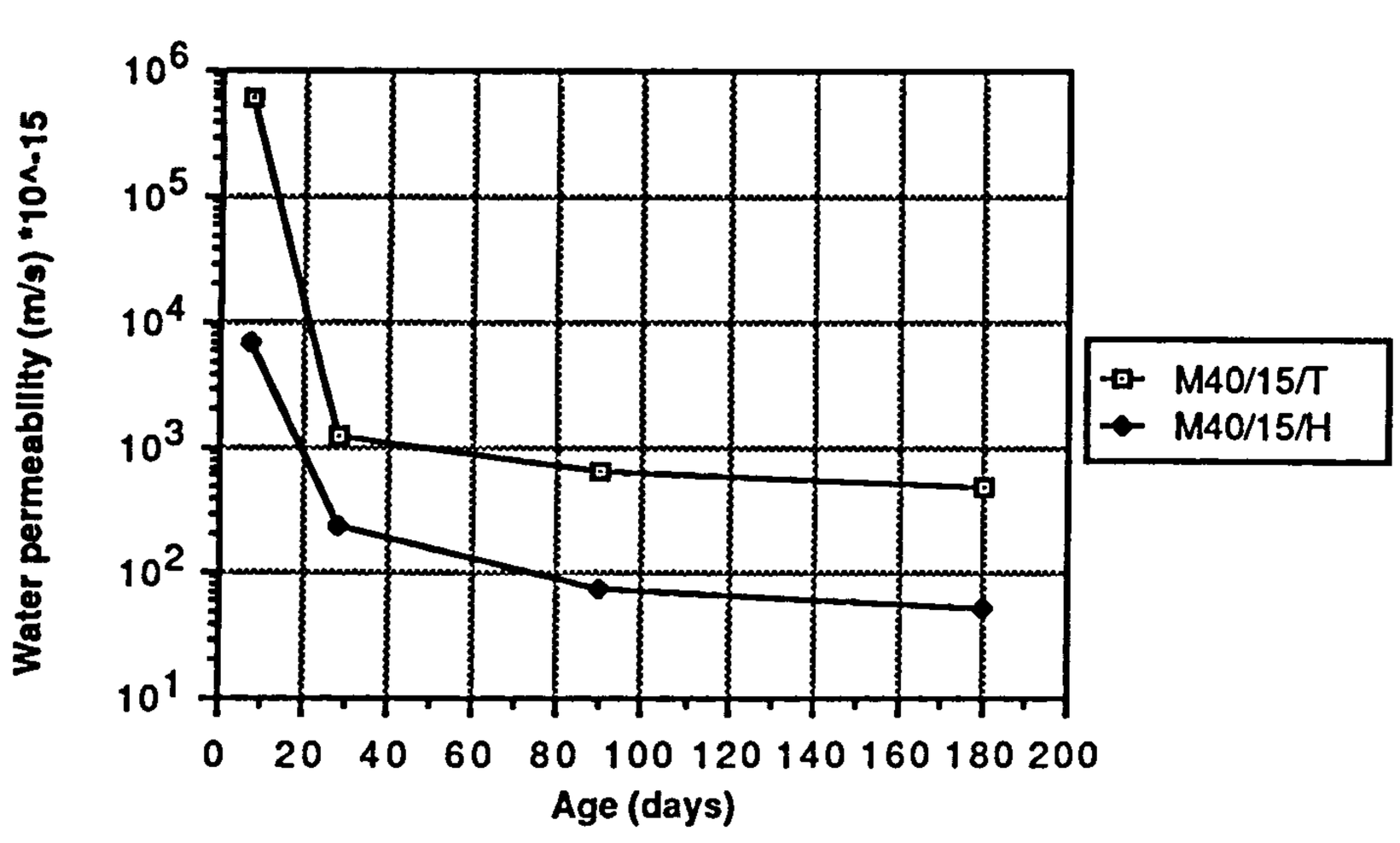

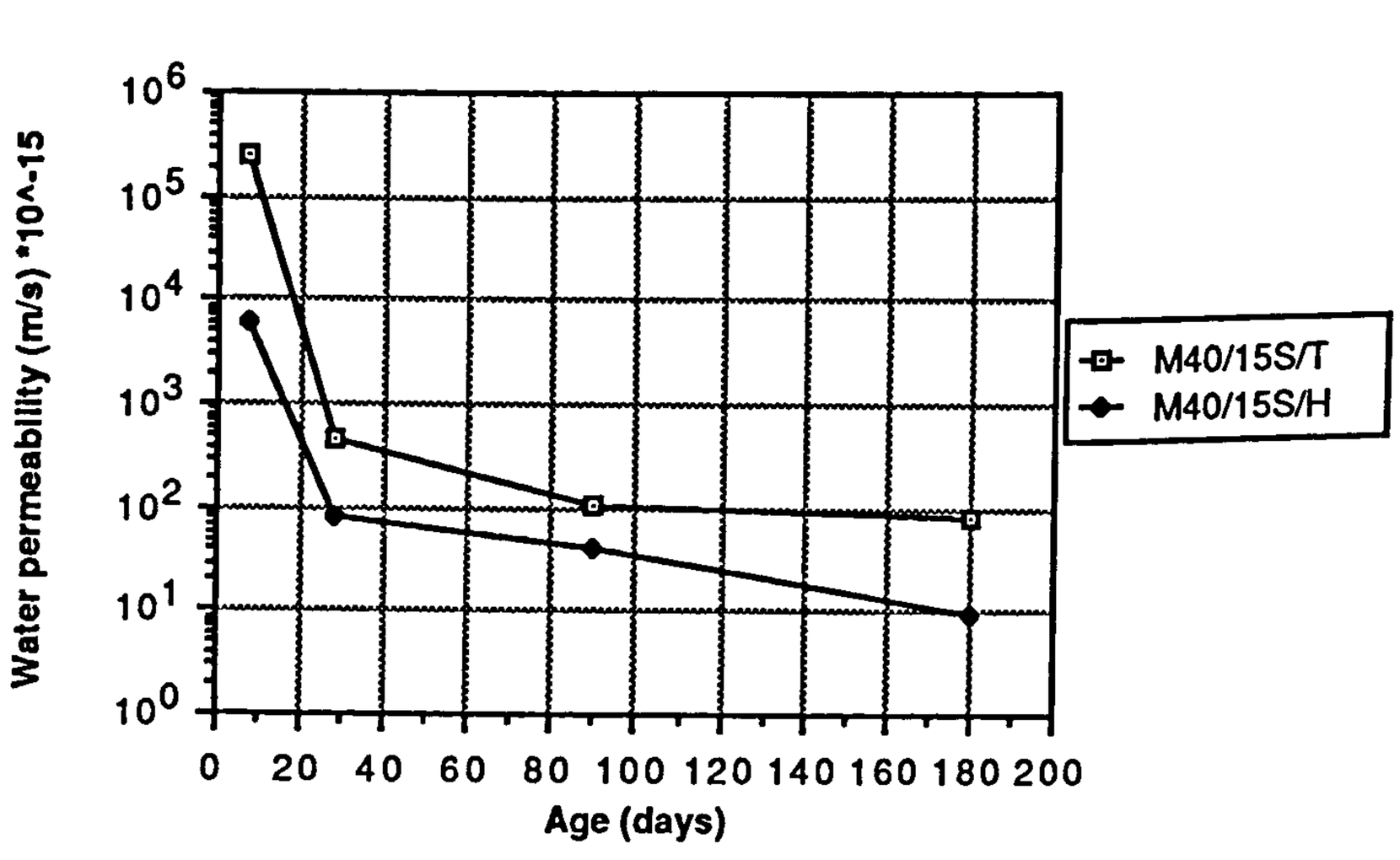

Figure 9.23 Effect of curing environment on the water permeability of CSF mortars

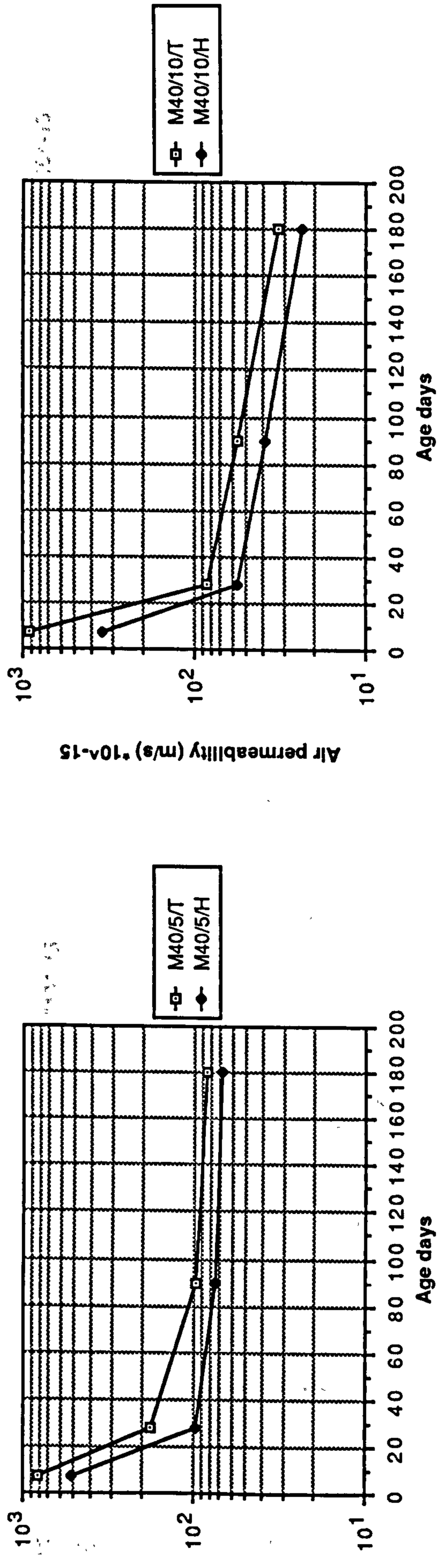

Figure 9.24 Effect of curing environment on the air permeability of CSF mortars

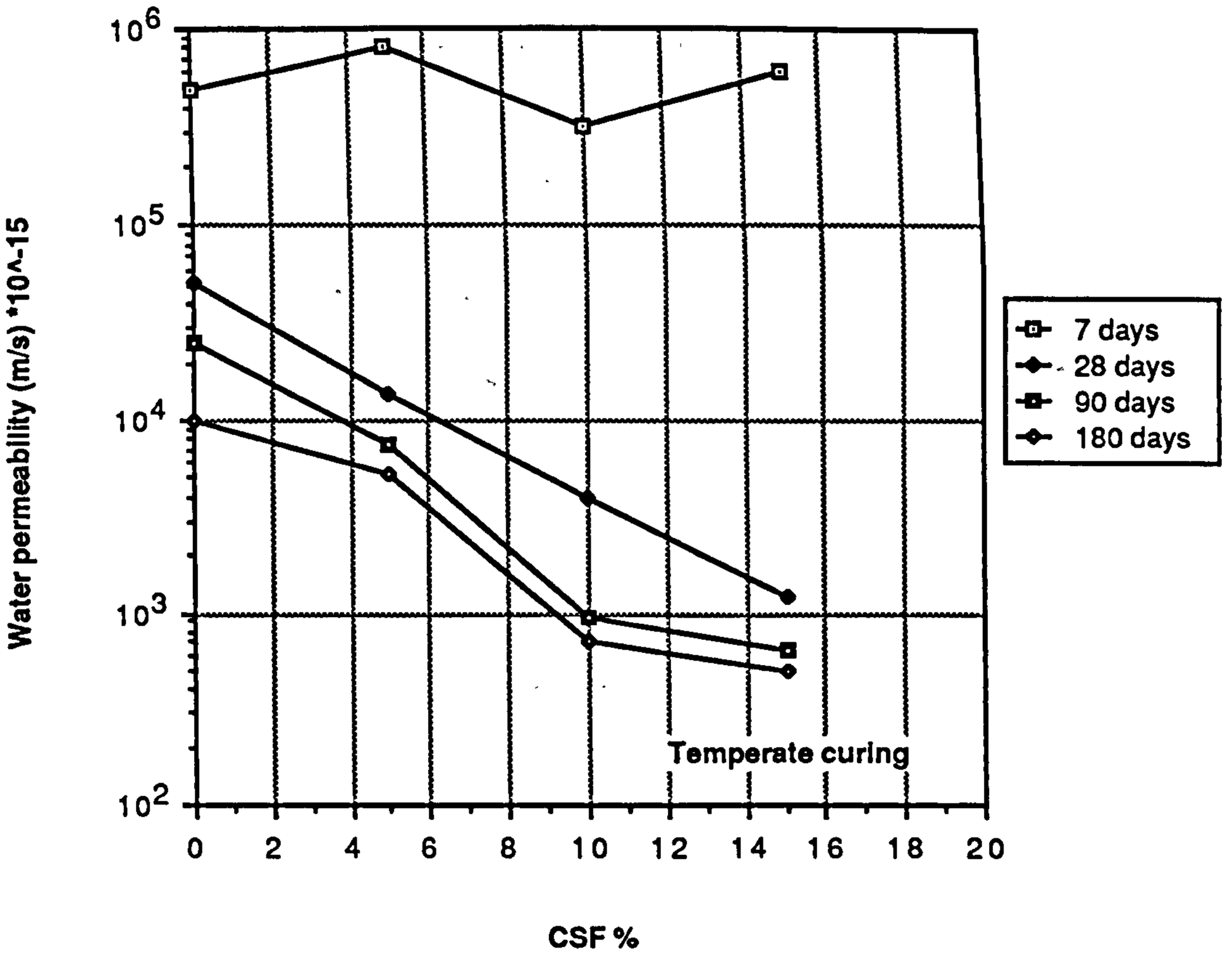

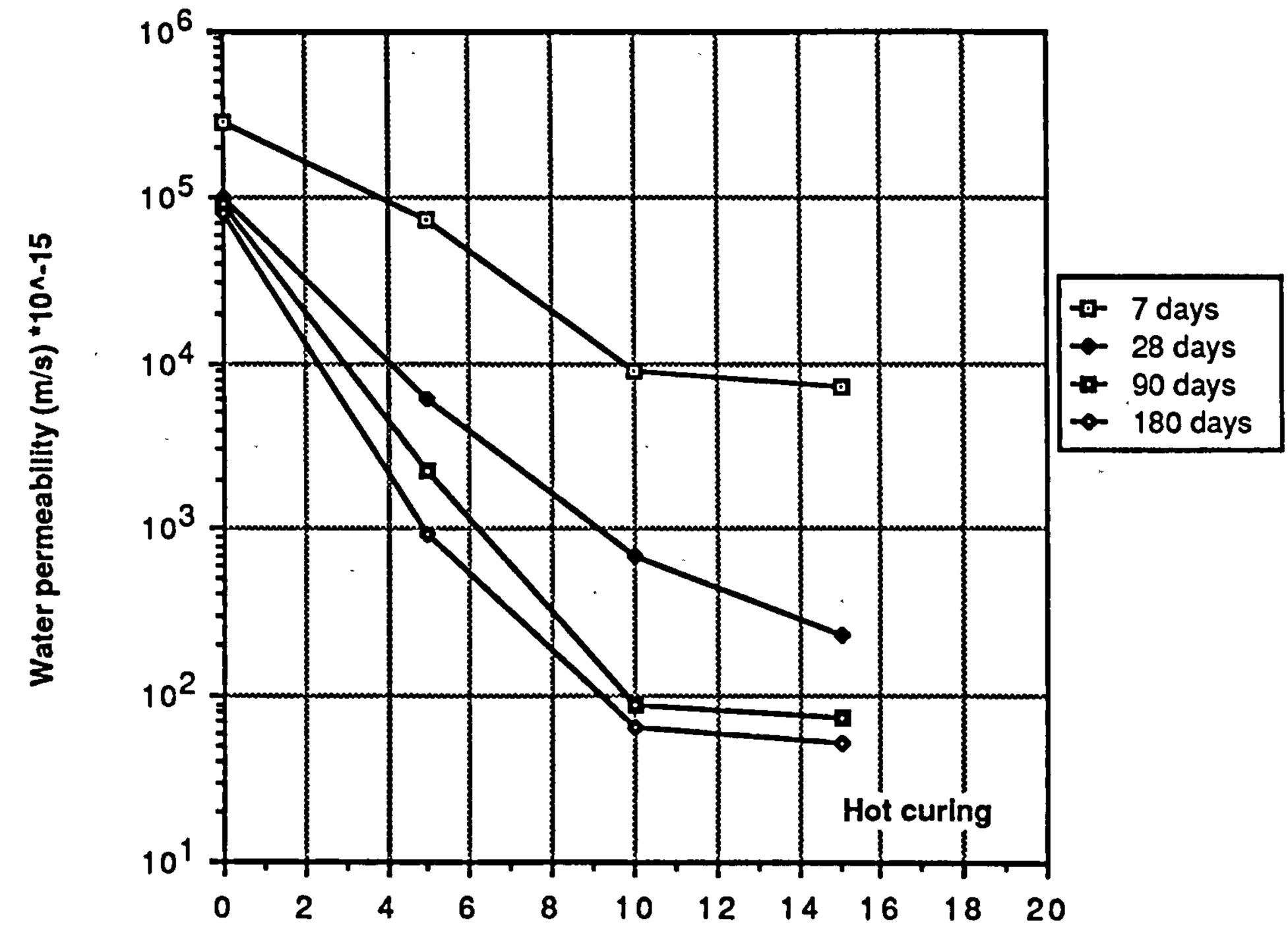

Figure 9.25 Effect of CSF content on the water permeability of CSF mortars cured in temperate and hot environments

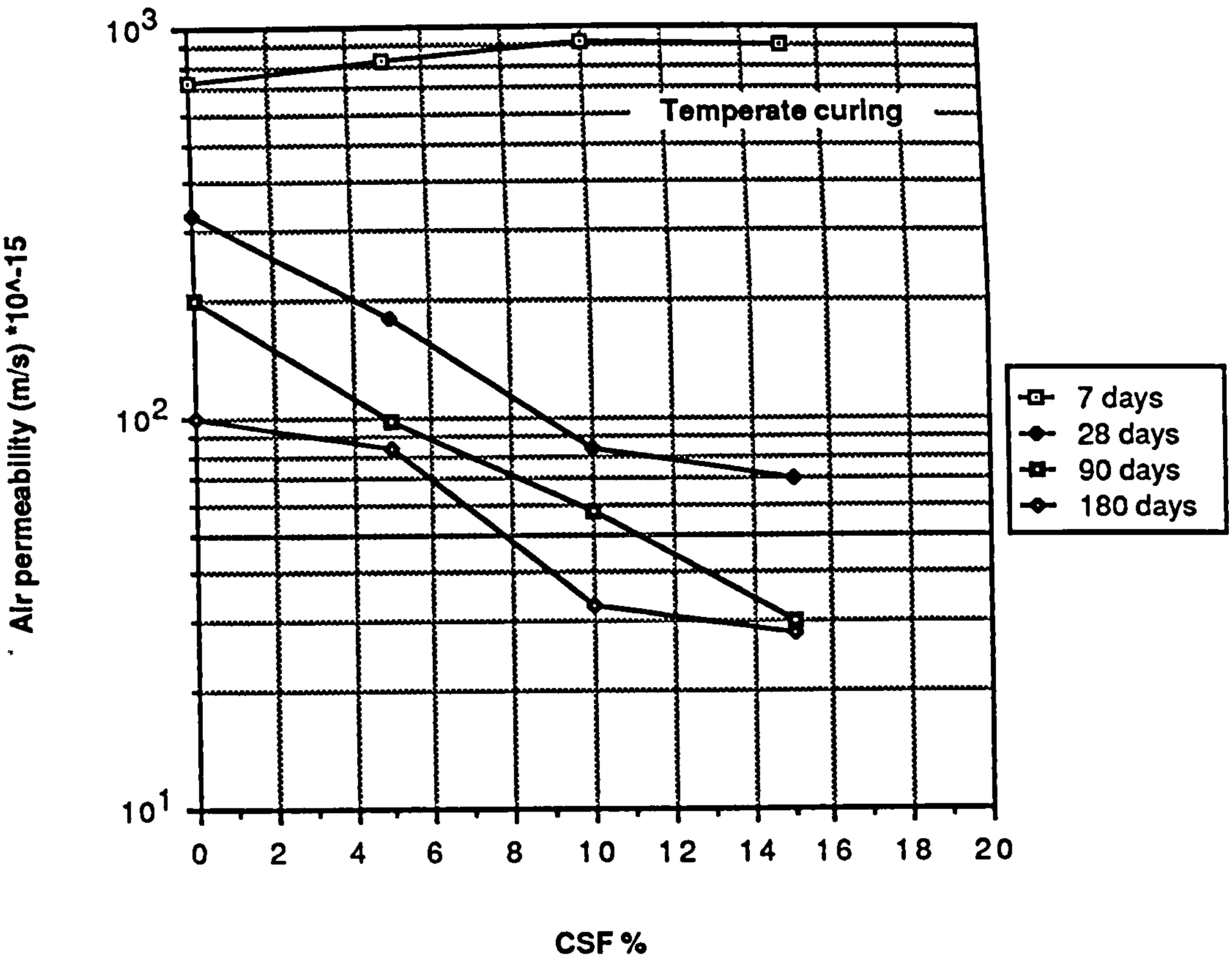

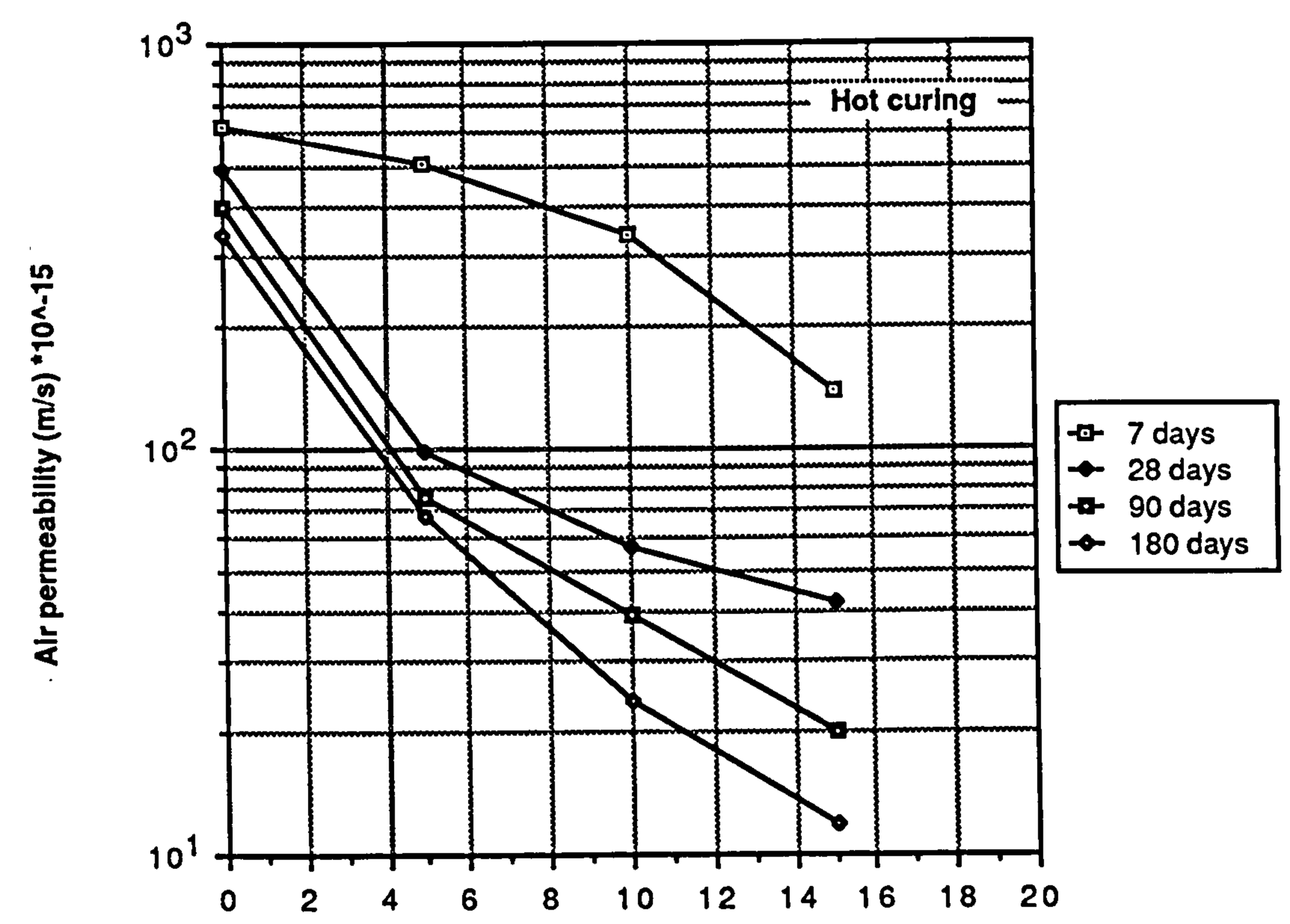

Figure 9.26 Effect of CSF content on the air permeability of CSF mortars cured in temperate and hot environments

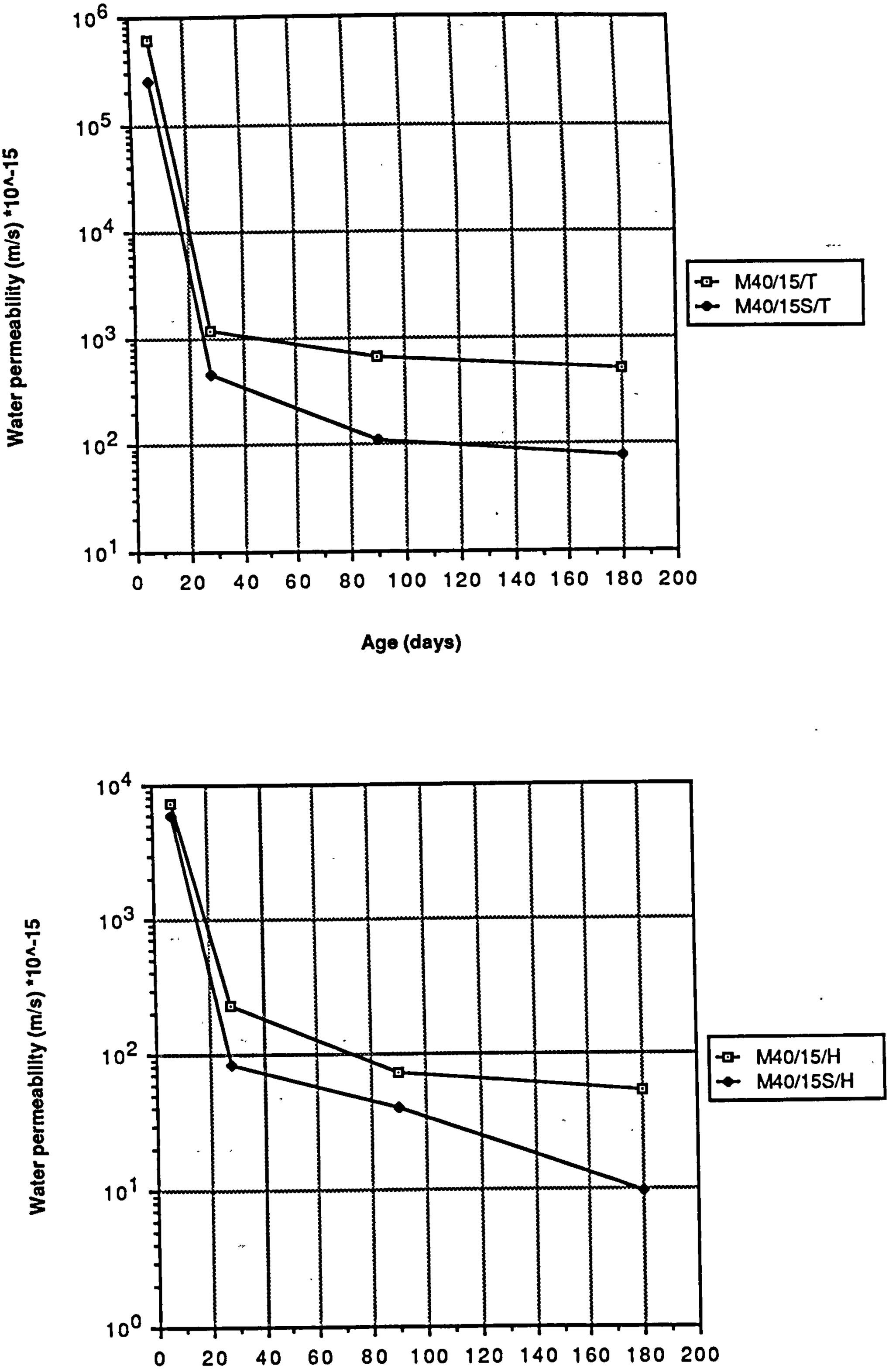

Figure 9.27 Effect of superplasticizer on the water permeability of mortar mix (M40/15) cured in temperate and hot environments

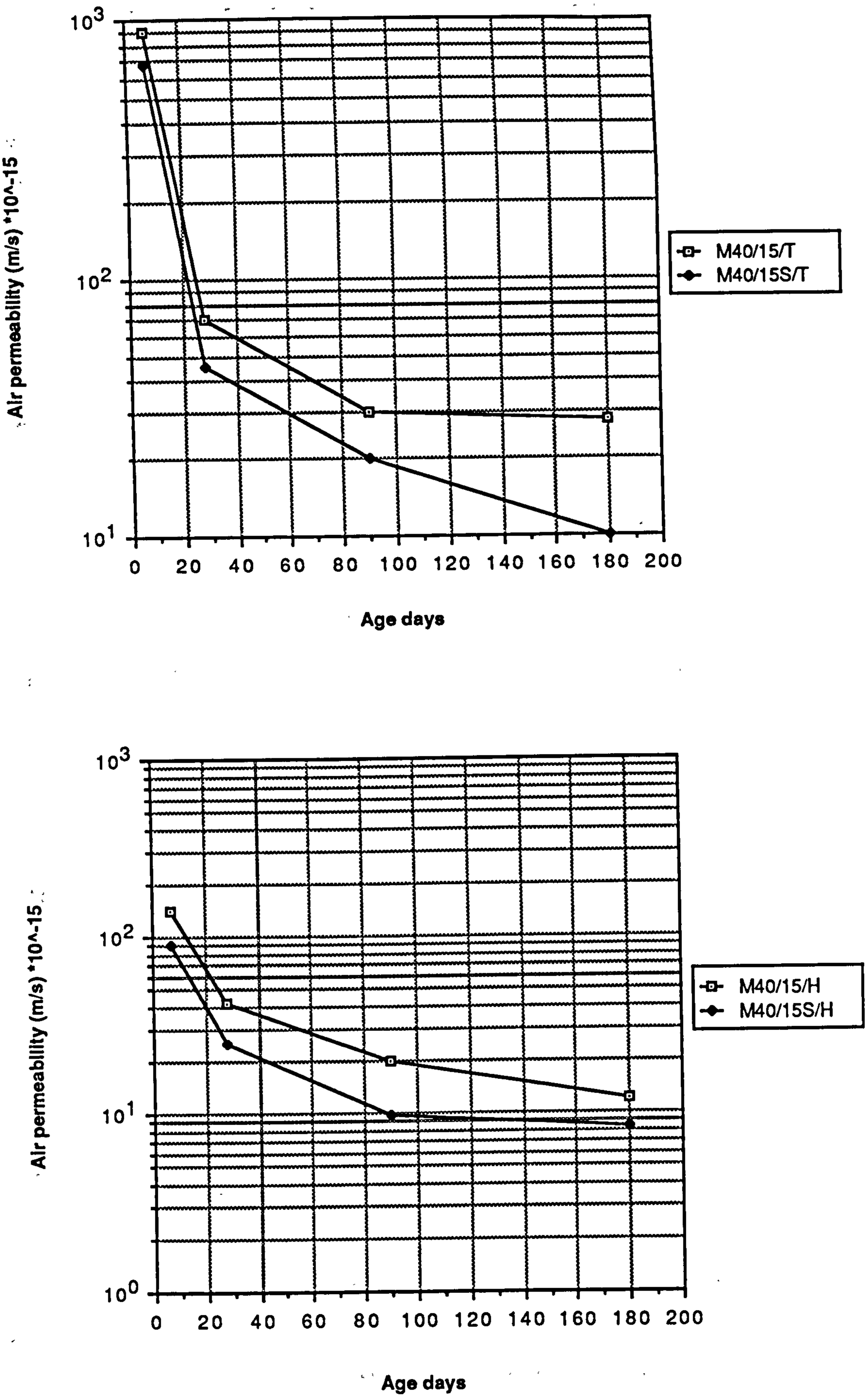

Figure 9.28 Effect of superplasticizer on the air permeability of mortar (M40/15) cured in temperate and hot environments

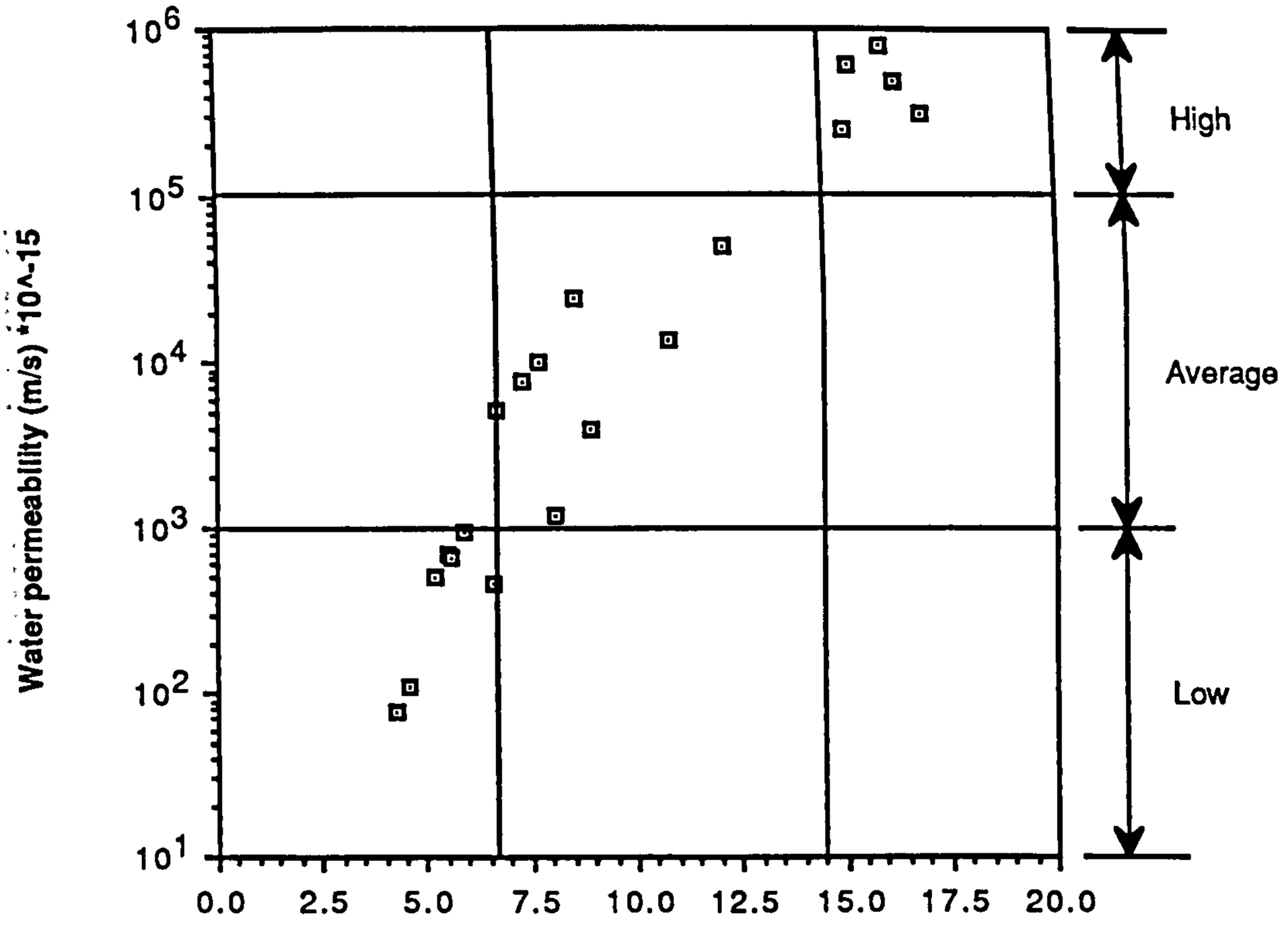

Figure 9.29 Relationship between water permeability and the volume of coarse pores under the effect of temperate curing

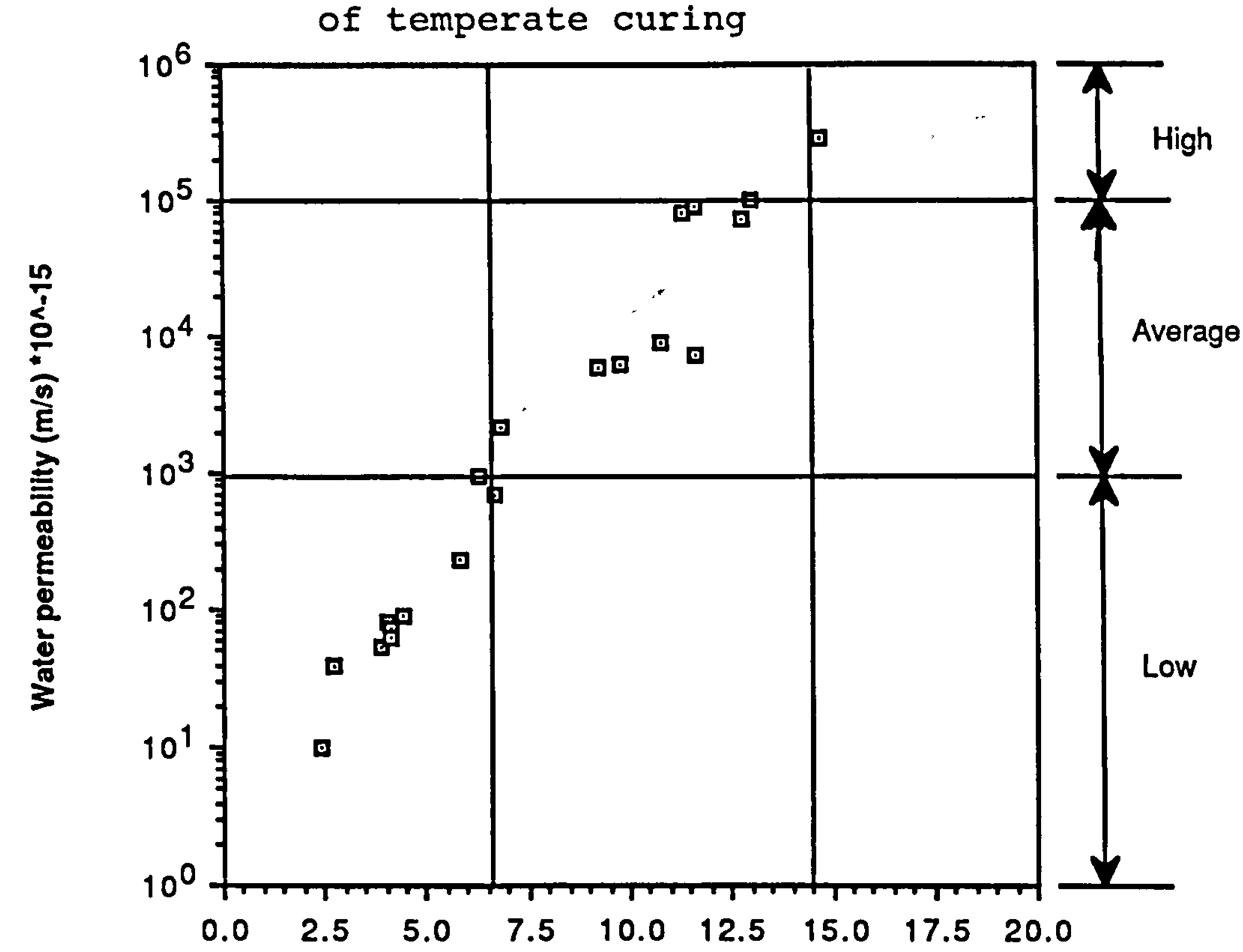

Figure 9.30 Relationship between water permeability and volume of coarse pores under the effect of hot curing

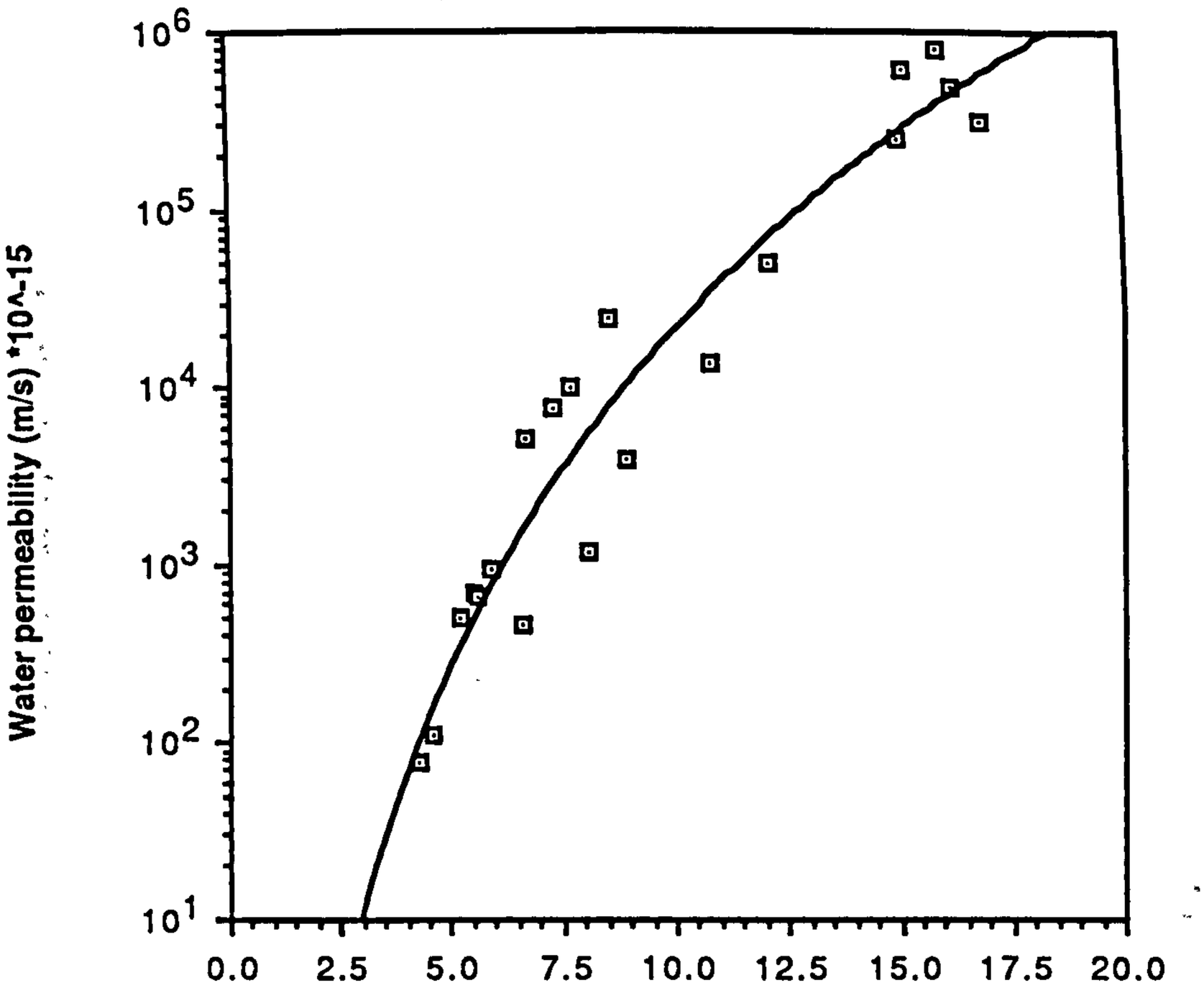

Figure 9.31 Relationship between water permeability and the volume of coarse pores in a temperate environment

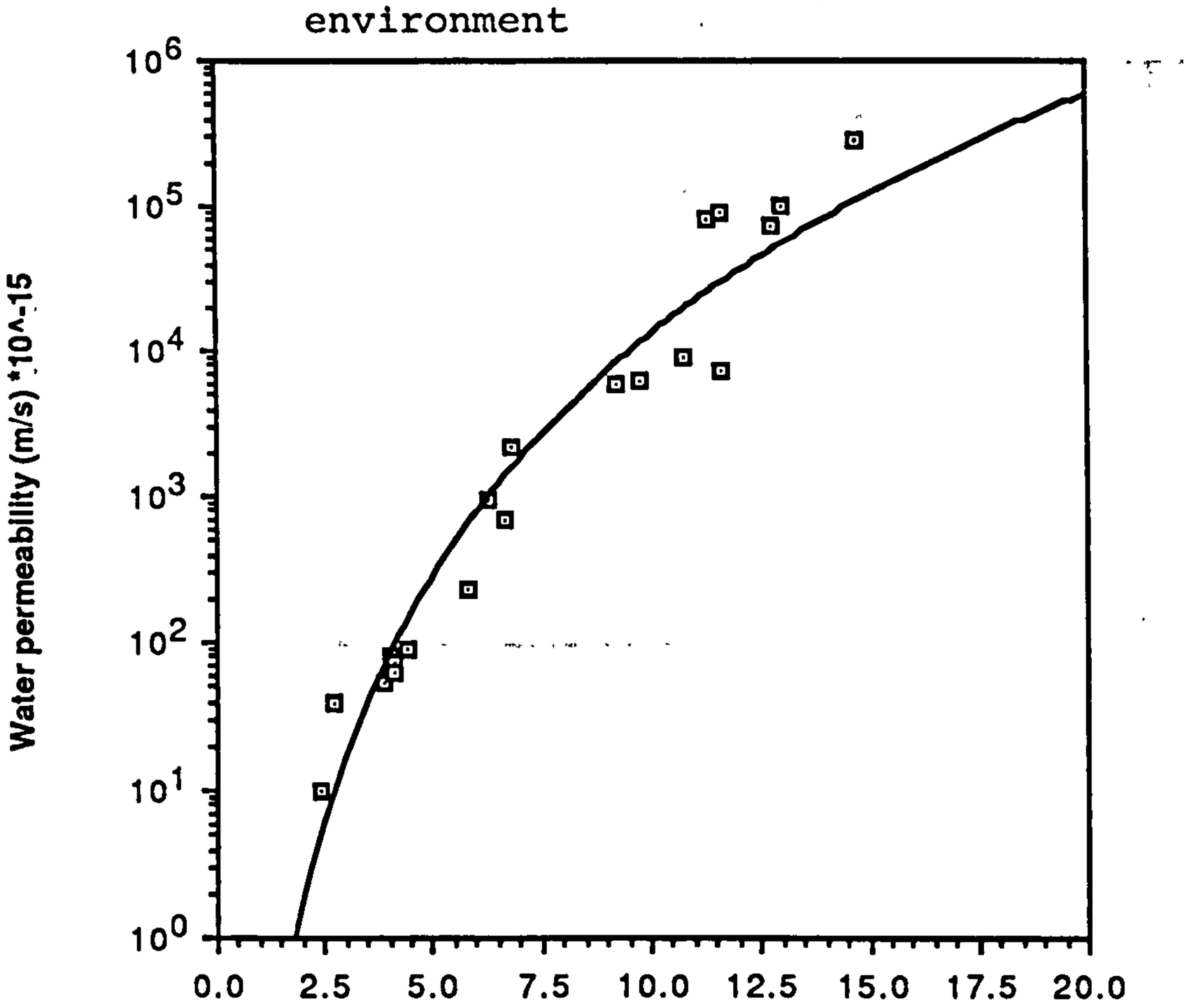

Figure 9.32 Relationship between water permeability and volume of coarse pores in a hot environment

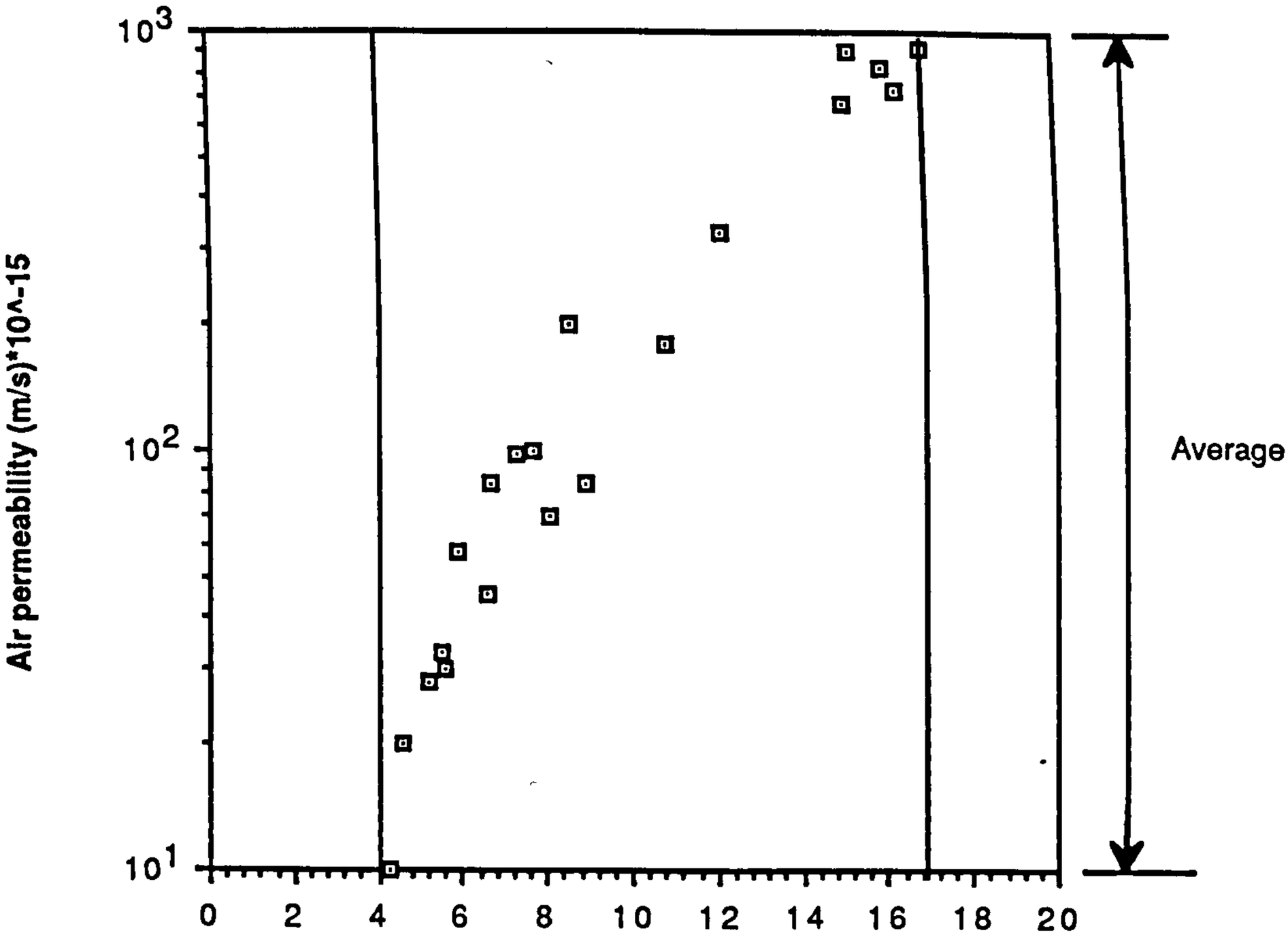

Figure 9.33 Relationships between air permeability and volume of coarse pores in a temperate environment

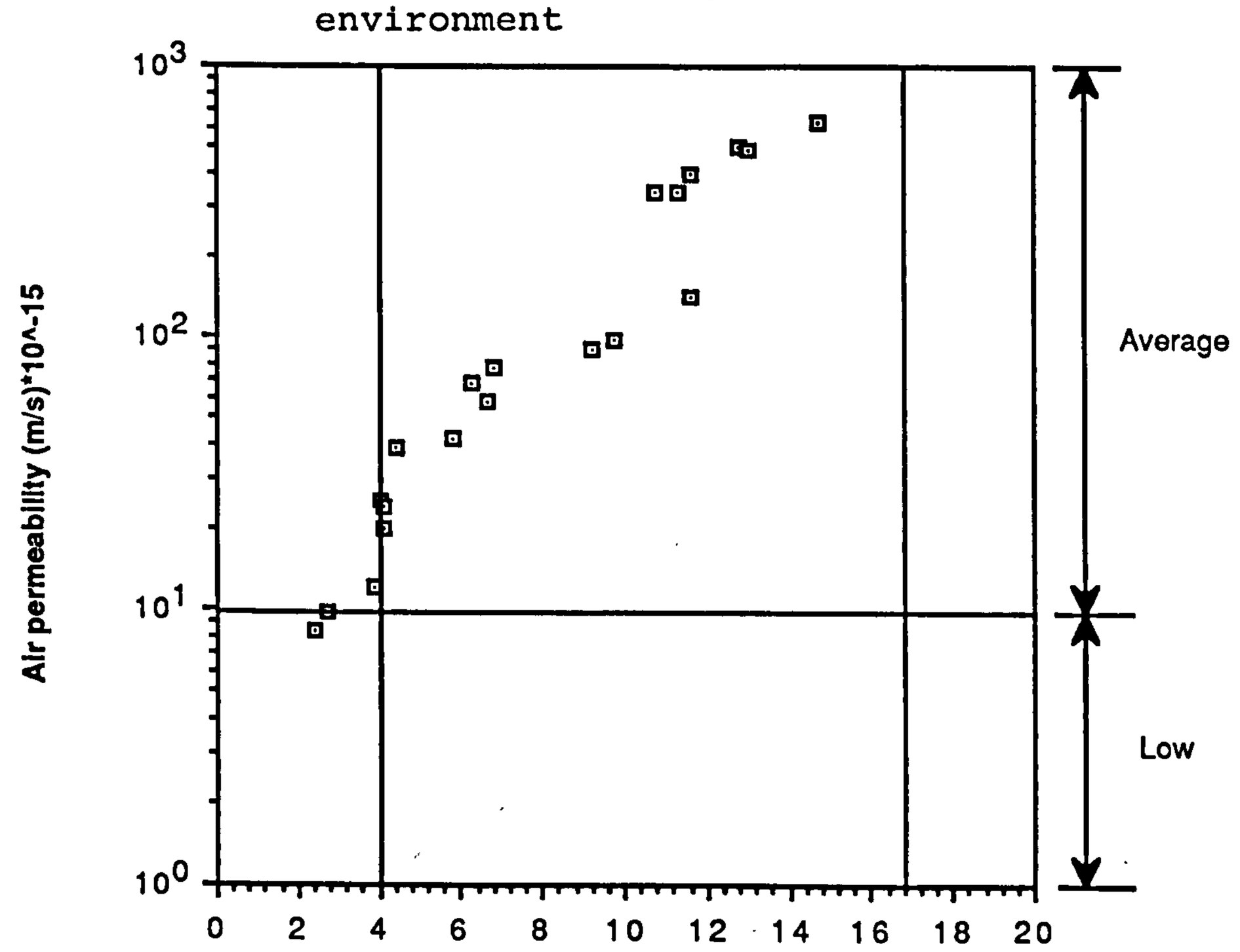

Figure 9.34 Relationship between air permeability and volume of coarse pores in a hot environment

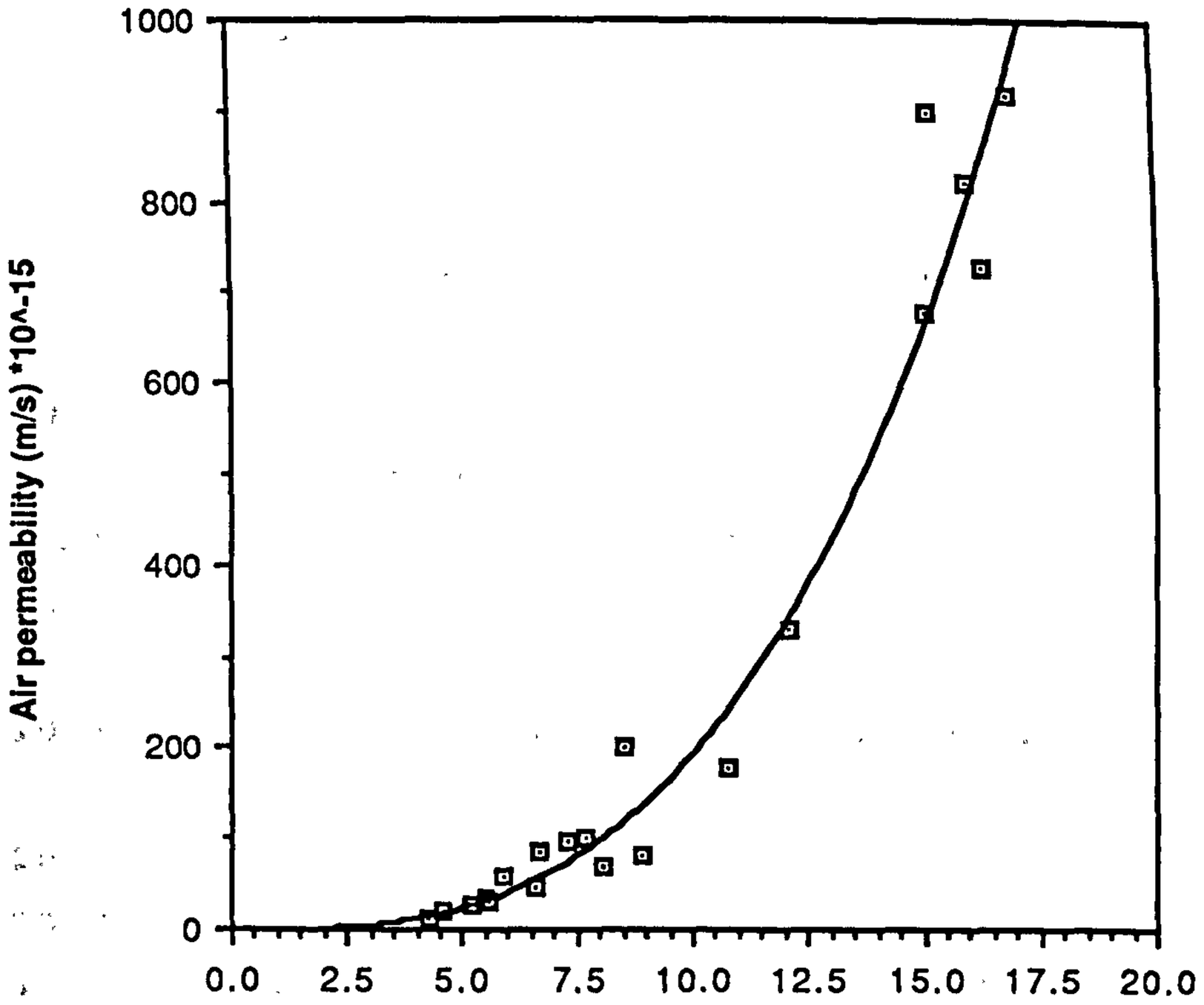

Figure 9.35 Relationship between air permeability and volume of coarse pores in a temperate environment

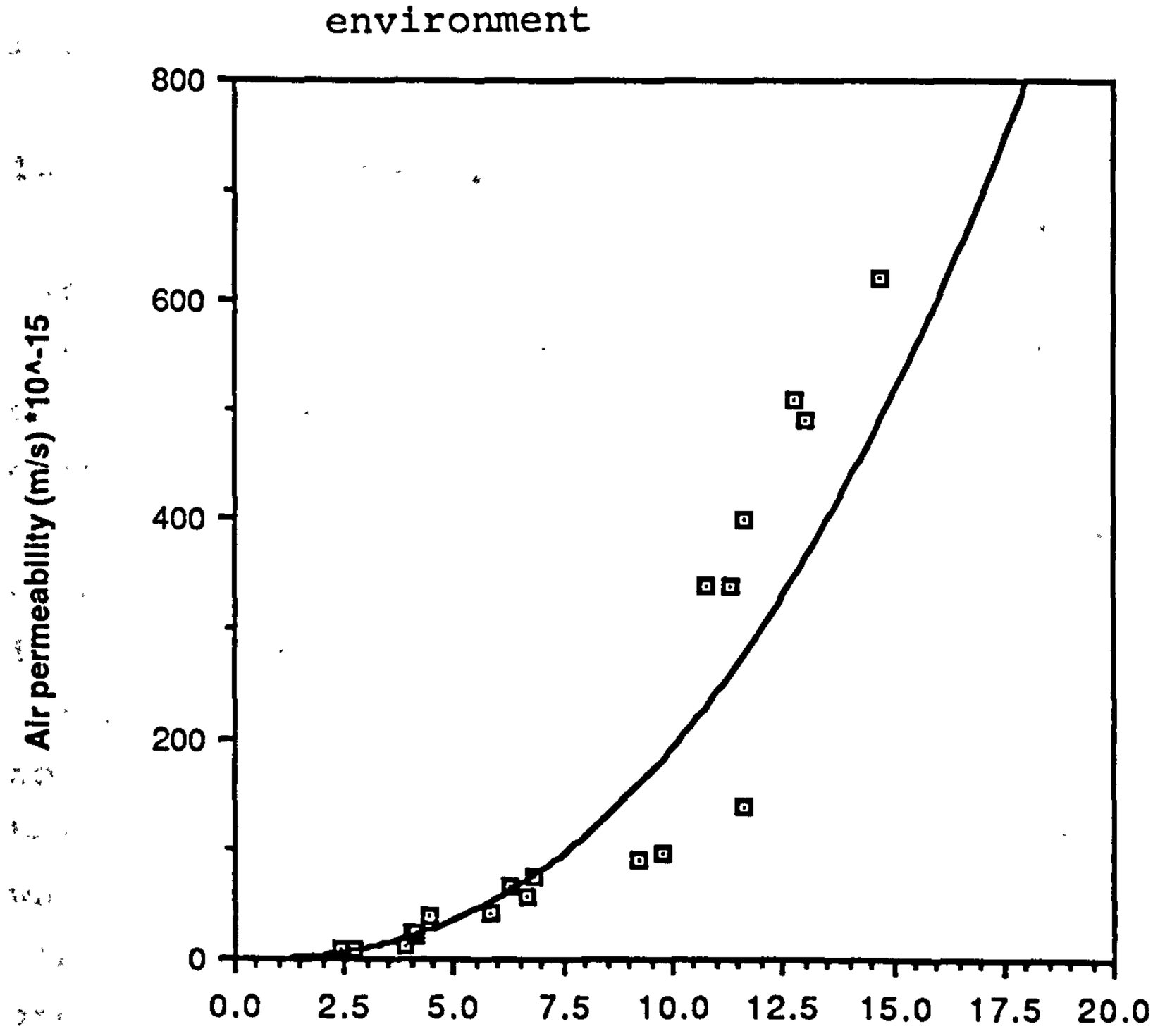

Figure 9.36 Relationship between air permeability and volume of coarse pores in a hot environment

CHAPTER TEN

SULPHATE RESISTANCE OF SILICA FUME MORTARS

10.1 Introduction

The work described in this chapter was designed to examine the sulphate resistance of plain OPC and OPC-CSF mortars cured under temperate and hot environment.

10.2 Mixes used and curing environments

The plain OPC and OPC-CSF mortar mixes used in this investigation are the same as those examined in the permeability and porosity work. Small mortar prisms (40 x 40 40 mm cubes) were chosen to accelerate the attack. The specimens were cured under polythene sheeting for seven days in either a temperate or hot environment. After 7 days they were left exposed to the same environment for another 21 days. At the age of 28 days all specimens were subjected to sulphate attack.

10.3 Test procedure

It has been argued earlier that the accelerated laboratory testing should take into account the type and nature of attack (weakening by leaching disruption by volume change ... etc), the type of laboratory exposure and the criterion of evaluation.

Consequently two types of exposure were created that were considered to be possible in the environments considered in this research (temperate and simulated Iraqi hot climates). In the first exposure, specimens were soaked continuously in sulphate solution. This type of exposure is believed to cause the formation of gypsum and ettringite which result from the reaction between sulphate and hydrated lime and calcium aluminate respectively. These two reactions are accompanied by expansion. This type of attack can take place in either environments. However, for the purpose of this research work and due to the limited resources available this attack was considered only in a temperate environment.

In the second exposure, specimens were soaked in the sulphate solution for 16 hours and then dried in an oven at 50°C for 8 hours. This type of exposure is believed to result in the deposition of salt crystals in the capillary pores as a result of alternate wetting and drying. This type of attack usually take place under hot environment where high temperature and low humidities occur.

For a reliable assessment of sulphate attack to take place, the criterion of evaluation should correspond to the type of exposure and attack. Expansion due to the formation of gypsum and ettringite was expected under the first exposure. Therefore the change in volume calculated as a percent of the original was monitored.

Volume was determined using fluid (magnesium sulphate) displacement method. Mortar specimens were weighed in magnesium sulphate solution recorded as (M_2) and in air immediately after removing them from solution and wiping off any surplus liquid from the surface. This weight was recorded as (M_1). Specimen volume can be calculated from the following equation:

$$V = \frac{M_1 - M_2}{\text{density of } Mg\ SO_4}$$

Deposition of salt crystals in the capillary pores due to the alternate wetting and drying is expected to increase the weight and possible the compressive strength initially due to the filling mechanism, and to result in a reduction in weight at advanced attack stages due to disruption. Therefore the change in weight calculated as a percent of the original was monitored.

10.4 Test results and discussion

10.4.1. Alternate soaking and drying

Under this type of exposure, the change in weight as a percentage of the original was monitored. Results are shown in Figure 10.1.

Results show that mortar mixes M40/0 and M40/5 had shown an increase in weight for the first few weeks then lost

weight. No initial icrease in weight was noticed in mortar mixes M40/10, M40/15 and M40/15S (see Figure 10.1). The Figure also shows that the rate of deterioration expressed by weight loss is high in the plain OPC mortars and is much lower in the CSF mortar mixes. The higher the CSF content the lower is the rate of weight loss and deterioration. The reason for this behaviour can be attributed to the fact that cement paste represents the most sensitive and vulnerable part of mortar that is attacked by sulphate solution. Thus its physical and chemical properties are of vital importance in studying corrosion due to aggressive media. As far as this type of attack is concerned it is the former element, i.e. physical properties of the cement paste, viewed as permeability to the aggressive fluid, which can play the major role in sulphate resistance. The use of CSF was found earlier to reduce the volume and percentage of harmful pores (pores with a diameter greater than 0.1 micrometre), increase the volume and percentages of fine pores (reflected by the pore surface area) and reduce the permeability to fluid quite dramatically. (See Section 9.5)

Using superplasticizer to control the workability in mix M40/15S without adding extra water resulted in a remarkable improvement in sulphate resistance as compared with mortar mix M40/15 (see Figure 10.1). A reason for this is the lower water/cementitious ratio, which results in a finer pore structure and lower permeability.

10.4.2 Continuous soaking

Under this type of exposure and attack, the change in volume as a percentage of the original was monitored. Results are shown graphically in Figure 10.2. The time (in terms of weeks) required to register a 0.5% change in volume is accepted as a failure criterion. For this type of test tests were carried out for a period of up to 30 weeks. Only CSF mortar mixes M40/5 and M40/15 reached the failure limit set above within the testing time. However, CSF mixes M40/10 and M40/15S did not reach the failure limit. Therefore the time (in weeks) required to achieve a volume change of 0.5%

was calculated theoretically by fitting a polynominal curve to the data. The results are shown in Figure 10.3.

The test results show that the sulphate resistance of CSF mortar is higher than that of plain OPC mortar. The higher the CSF content (up to 10%) the higher is the resistance to sulphate attack and formation of expansive gypsum and ettringite products. The reason behind this behaviour is attributed again to the fact stated earlier, that is the cement paste represents the most vulnerable part of the mortar attacked by sulphate solution. As far as this exposure or attack is concerned, it is the chemical properties of the paste matrix which can play the major role in sulphate resistance. This can be illustrated in terms of the C_3A content of the cement or cementitious material used which represents the major contributor to the failure. Thus the improvement in sulphate resistance caused by the use of CSF is attributed to the reduction in C_3A content since there is less cement in the matrix. The other possible factor responsible for improving sulphate resistance is the formation of a dense C-S-H gel produced by the pozzolanic reaction between $Ca(OH)_2$ and CSF. This reaction has two benefits. The first is the removal of free $Ca(OH)_2$ from the matrix and the second is that the impervious C-S-H gel may be deposited on the surface of alumina bearing phases, forming a protective film. This may inhibit the reaction taking place between sulphate and aluminate bearing phases producing obstructive reaction products. No change in volume was noticed initially for up to 6 weeks in mortar mix M40/15. However, with the progress of attack, the resistance of the M40/15 mix was found to be lower than mix M40/5. This is attributed to the presence of hair line surface cracks. The possible reasons behind the presence of these cracks are discussed earlier in Chapter 8. The effect of these cracks was to provide an easy and accessible path for the sulphate solution to penetrate inside the specimens. It is also argued that the initial early age expansion caused by the sulphate reaction was taken up by these cracks, and thus no

change in volume was noticed for the first six weeks of exposure.

The results also show that the resistance of superplasticized CSF mortar mixes is higher than that of the non-superplasticized one. The reason can be attributed not only to the low water/cementitious ratio of the mix but also to the absence of the surface hair cracks noticed on the specimens surface of the non-superplasticized mix.

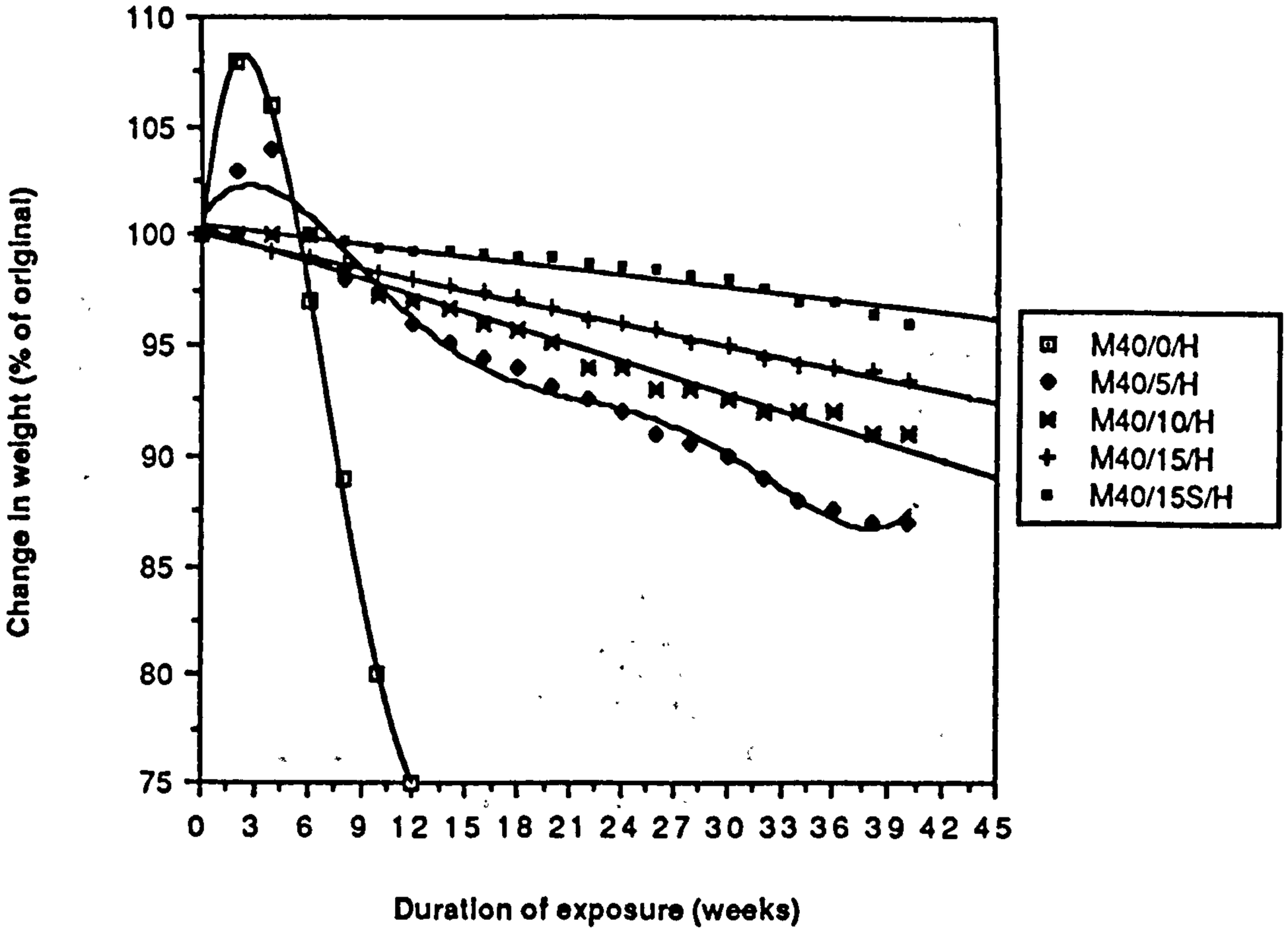

Figure 10.1 Relationship between change in weight of mortar cubes and duration of exposure to magnesium sulphate

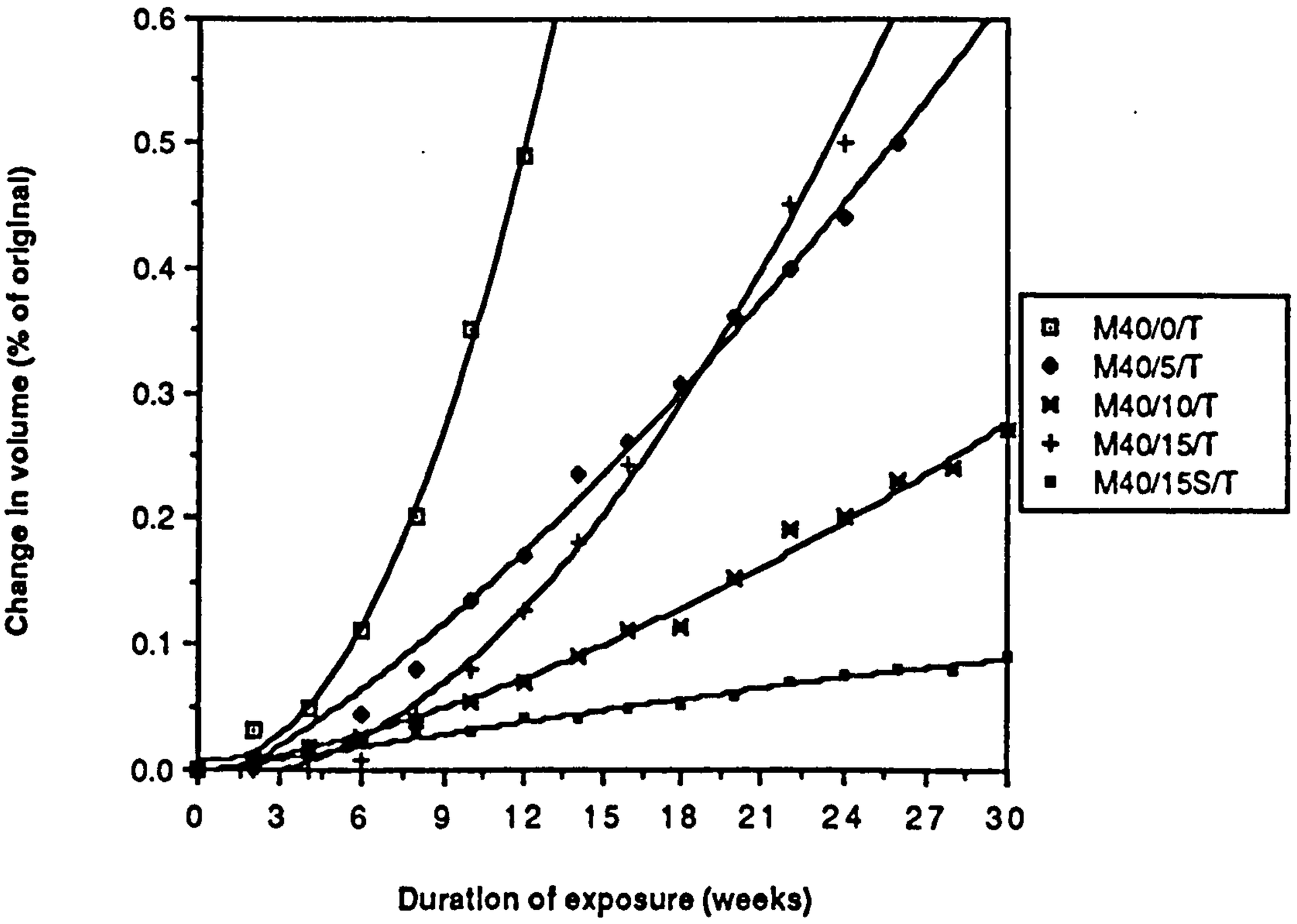

Figure 10.2 Relationship between change in volume of mortar cubes and duration of exposure to magnesium sulphate

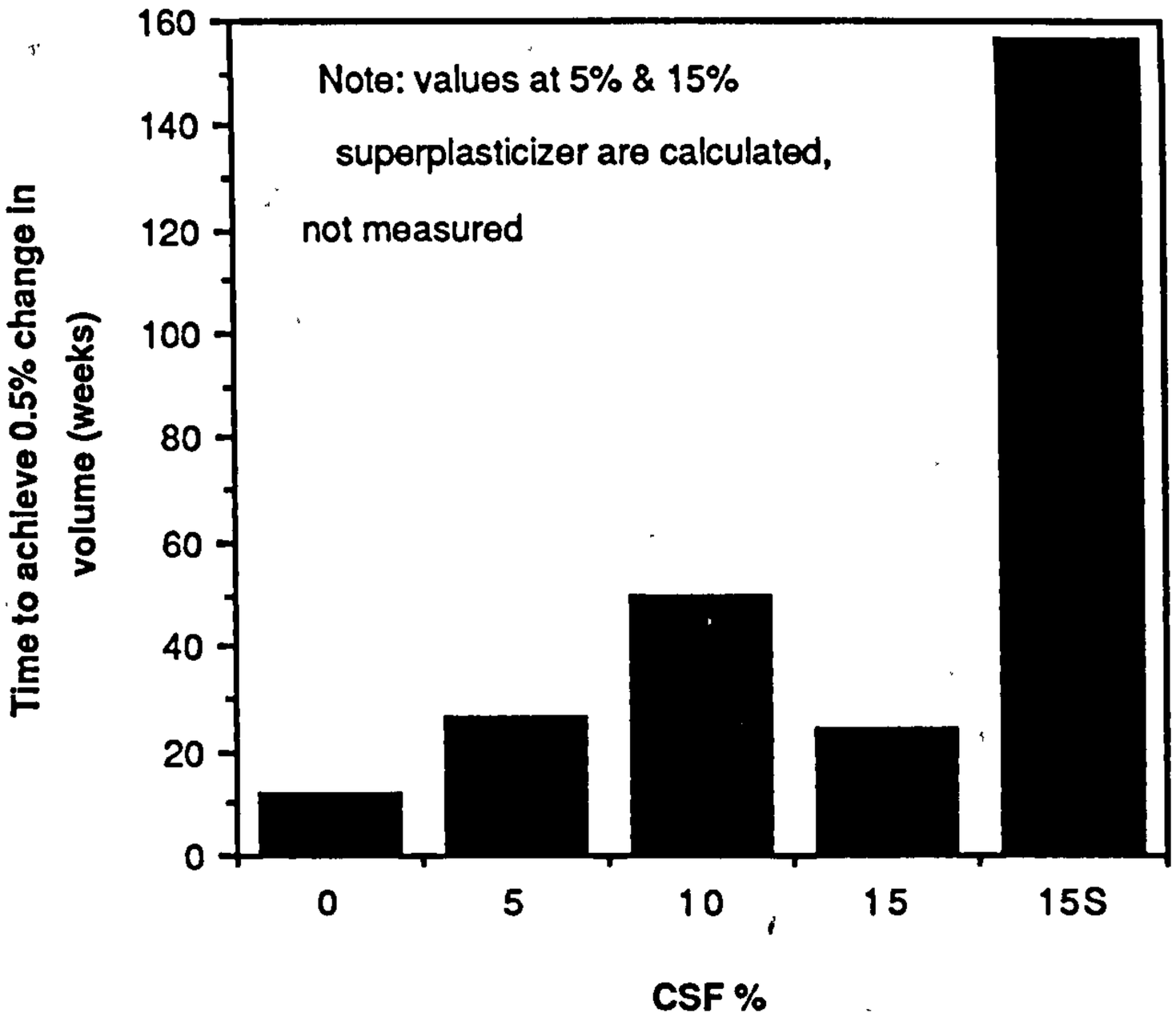

Figure 10.3 Effect of CSF content on sulphate resistance in terms of time (in weeks) to achieve 0.5% change in volume.

CHAPTER ELEVEN

CONCLUSION AND RECOMMENDATIONS FOR FURTHER RESEARCH WORK

11.1 Plastic properties

The test results indicate that concrete mixes containing up to 300 kg/m³ of OPC and 10% of silica fume will not normally have a significantly different water demand for medium workability equivalent to normal OPC mixes of the same total cementitious material. However, richer mixes with higher dosages of CSF required either the use of superplasticizer or an increase in the amount of mixing water to maintain workability. Moreover, the increase in water demand and W/C + CSF ratio for maintaining medium workability was found to be linearly related to the amount of silica fume.

In concrete mixes where superplasticizers were used to secure medium workability, the dosage was independent of OPC content and only dependent on the CSF dosage.

Due to its high surface area and fineness, silica fume tends to make concrete mixes look sticky. However, because of the spherical and smooth nature of the silica fume particles silica fume concrete mixes more workable with vibration. Accordingly, a static workability test method (i.e. slump test) was found to be misleading in identifying their workability, whereas the dynamic workability test such as V.B. test was found to be much better for assessing their workability.

11.2 Relationship between compressive strength, and water/cement + silica fume ratio

The basic inverse relationship between compressive strength and water/cement ratio had changed quantitatively, but not quantitatively when silica fume was added, i.e. using a certain percentage of silica fume resulted in a shift of the strength versus W/C + CSF curve to a higher level without changing the configuration of the curve.

11.3 Cost effectiveness

The economical substitution of CSF for OPC in the control mix depended on the richness of the control mix, the efficiency of CSF, the method of obtaining workability (i.e. adding extra water or using superplasticizer) and the relative cost of CSF to OPC. The optimum substitution of CSF for OPC was in the range of 4 to 10 percent in lean concrete mixes and 4 to 5 percent in rich mixes. CSF is clearly more efficient in lean mixes than in rich mixes. The most economic substitution percentages range in the superplasticized mixes was in the range of 3.5 to 7.5 in lean concrete mixes and 3.5 to 6.0 in rich mixes. Clearly these are lower than the values above due to the fact that any additional saving in OPC quantity and cost of cementitious materials caused by using superplasticizer was diminished by the added high extra cost of superplasticizer.

11.4 Strength, absorption and permeability related properties of plain and CSF concrete mixes

11.4.1 Compressive strength

The CSF concrete mixes had lower early age (3 & 7 days) strength compound to the control plain mixes. However, their late-age (> 28 days) strength is higher than the plain mixes. Results also show that CSF concrete compressive strength continues to increase for a longer period at a higher rate compared to the control plain concretes. The higher late-age compressive strength of CSF concrete was attributed due to the formation of more strength dependent cementitious reaction products, i.e. C-S-H gels. The above confirms the behaviour of CSF mixes hypothesised earlier by the model described in Chapter 5.

The compressive strength of polythene cured specimens was found generally to be lower than the water cured specimens at late-ages, whereas both curing methods yielded a comparable compressive strength at early ages. The difference in the late-age compressive strength between the polythene and water cured concrete specimens was a function of the water cementitious products ratio and the richness of

concrete mixes: The lower the W/C ratio the bigger the difference in compressive strength. In other words partial drying by evaporation and self-dessication was found only in rich mixes with a low water/cementitious ratio.

High curing temperature was found favourable to the early age compressive strength of plain OPC concrete mixes. However, at late-ages the situation was found to reverse. The harmful effect of high curing temperature on the late-age compressive strength was found to be a function of the W/C ratio and the richness of concrete mixes. The lower the W/C ratio the higher is the harmful effect of high curing temperature. CSF concrete specimens cured at elevated curing temperature showed a different trend from the plain OPC concrete mixes. High curing temperature was found favourable to both early and late-age compressive strength. This again confirms the strength hypothesis illustrated in Chapter 5.

In a temperate curing environment, the higher the CSF content (up to 10% by weight of OPC) the higher is the later-age compressive strength. For example, compressive strength of concrete grade C40 was increased by 20% when 10% of CSF was added. However, at a replacement percentage of 15%, CSF concrete mixes exhibited compressive strengths lower than those in which only 10% by weight of OPC was used. This was due to the presence of surface cracks which counteract any improvement expected to take place due to the formation of additional C-S-H gels from the pozzolanic reaction between CSF and $Ca(OH)_2$. In a hot curing environment, the increase in compressive strength of CSF concrete mixes was proportionally related to the CSF content up to 10% by weight of OPC. No reduction in the later-age compressive strength of 15% CSF concrete mixes. This was due to the absence of the above mentioned surface cracks.

The use of superplasticizer to secure workability improved the compressive strength of CSF concrete mixes by around 18% and 10% in temperate and hot environment respectively. This effect is attributed to the effect of efficient dispersion of hydration products and lower water/cementitious ratio.

The initial curing duration up to seven days had a significant effect on compressive strength of plain OPC mixes cured in a temperate environment. However no significant difference was recorded from curing concrete specimens for more than 3 days in a hot curing environments. Test results of CSF concrete mixes show no significant difference in strength between specimens cured initially for 3 and 7 days under temperate environments. Moreover, curing these identical specimens initially beyond one day under hot environment brought about no significant change in the compressive strength.

11.4.2 Absorption and permeability related properties

Absorption and permeability of plain and CSF concrete mixes decreases with age. The rate of reduction is high at early ages and gradually decreases at late ages.

Absorption and permeability of polythene cured specimens was found generally higher than the water cured specimens. However, the difference between water and polythene cured specimens was found to be insignificant in lean and medium concrete mixes but noticeable in rich mixes.

For example, polythene cured Figg air permeability of concrete mix C25/5 was higher than the smae identical mix cured in water by only 5%. However, the difference in Figg air permeability of concrete mix C55/5 between the polythene and water cured was 13%. The same was noticed with ISAT result. The difference between the polythene and water cured lean and rich concrete mixes (C25/5 and C55/5) was 2% and 15% respectively. Therefore, partial drying by evaporation and self-dessication was only prevalent in rich mixes with low water/cementitious ratios.

Plain OPC concrete specimens cured in a hot environment had lower absorption and permeabilities compared to those cured in the temperate conditions at early-age. However, at late-age specimens cured in a higher temperature had higher absorption and permeability characteristics. The results show that the degree to which high curing temperature may affect the absorption and permeability properties seems

to be a function of W/C ratio. CSF concrete mixes were found to behave under hot curing conditions in a different way than that noticed with plain OPC mixes. When compared with specimens cured under temperate environment, hot curing reduces the absorption and permeabilities of CSF specimens at early and later-ages.

For example, the Figg air permeability of CSF concrete mix C40/10 was reduced by the order of 48 and 22 percent at early and later-age respectively. The initial surface absorption of the same mix above was reduced by the order of 37 and 20% at early and later-age respectively.

Regardless of the curing method and environment, the subsurfacecrete permeabilities decreased with increasing percentage of CSF up to 15% by weight of OPC.

For example, the Figg air permeability of CSF mix grade C40 was reduced by 20, 37 and 48% at a CSF replacement percentage of 5, 10 and 15% respectively.

Absorption and surfacecrete permeability decreased with increasing percentage of CSF up to 10% by weight of OPC in a temperate and hot condition.

For example, the ISAT of CSF concrete mix grade C40 cured in a temperate condition was reduced by 16 and 23% at a CSF replacement percentage of 5 and 10% respectively. In a hot environment, ISAT was reduced by 40 and 50% at a CSF replacement percentage of 5 and 10%.

The absorption and surfacecrete permeability of CSF in which 15% of CSF was used were higher than that in which only 10% of CSF was used due to the presence of surface cracks. CSF is more effective in reducing absorption and permeabilities in lean mixes compared to rich mixes.

Superplasticized CSF concrete mixes have lower absorption and permabilities compared to the equivalent non-superplasticized mixes in both temperate and hot environments.

Increasing the initial curing duration up to 7 days produced a significant reduction in the absorption and surfacecrete permeability of plain OPC concrete specimens cured under temperate and hot environments. The same

observation was made with the subsurfacecrete permeabilities of specimens cured under temperate conditions. However, with hot curing, no significant change in the sub-surfacecrete permeability was detected when curing plain concrete specimens beyond three days. CSF concrete mixes show less sensitivity to the initial duration in both temperate and hot curing environments. The effect of initial curing duration on surfacecrete and subsurfacecrete permeabilities and absorption characteristics of plain and CSF concrete mixes show that curing is more important for concrete surface characteristics than the subsurface properties.

Figg air and water permeability test results had higher coefficients of variation when the other non-destructive tests namely ISAT, water absorption and Egg.

The relationships between compressive strength and absorption and permeability properties show that concrete mixes of a comparable compressive strength can exhibit significantly different permeabilities and absorption properties. Thus compressive strength cannot give a complete indication of concrete quality.

11.5 Pore structure and permeability of plain and silica fume mortar mixes

Longer hydration periods resulted in finer pore structure as a result of the precipitation of hydration products in the coarse capillary pores. The hydration of CSF mortars and precipitation of hydration products proceded at higher rate compared to the plain OPC ones yielding a finer pore structure at later ages. This confirms the hypothesis stated earlier on the effect of CSF on pore structure. The effect of age on the pore structure measured by the mercury intrusion porosimetry supports Power model of hydration.

High curing temperature accelerated the early age hydration and precipitation of hydrated products in the capillary pore spaces of plain OPC mortars reducing their sizes and volume. However, at later-ages hot curing seem to result in a larger number and volume of undesirable coarse pores (diameter > 0.1 micrometre).

The volume of coarse pores was increased from 7.5% of specimen volume in a temperate condition to 11% in a hot condition, i.e. the later-age volume of coarse pores was increased by 46% due to high curing temperatures.

High curing temperature affects the pore structure of CSF mortar mixes in a completely different manner. A high curing temperature accelerated the early age hydration and precipitation of hydrated products in the capillary pore spaces reducing their sizes and volume quite rapidly. At later-ages, high curing temperatures did not inhibit the hydration process as it did with the plain OPC mixes. Thus resulted in increasing precipitation of hydration products and eventually finer pore structure with smaller percentages of undesirable coarse pores (diameter >0.1 micrometre). This confirms the hypothesised effect of high curing temperature on the pore structure of CSF mixes.

The refining effect of CSF on the pore structure of mortars was approximately proportionally related to the percentage of CSF of up to 10% by weight of OPC in the control mix.

Superplasticized mortars had a better pore structure compared to the equivalent non-superplasticized mix.

Longer hydration periods resulted in lower water and air permeability values. Permeability of CSF mortar mixes decreases at a higher rate compared with the plain OPC mixes. The rate of reduction in water and air permeability for the mortar mixes is high at early ages and gradually decreases at later ages.

The high curing temperatures reduced the water and air permeability of plain OPC mortars at early ages very rapidly compared to those cured in temperate conditions. However at later-ages water and air permeabilities are higher than those of specimens cured in a temperate environment.

For example the water and air permeability of plain OPC mortars was increased from 1×10^{-11} and 1×10^{-13}(m/s) respectively in a temperate environment to 8×10^{-11} and 3.4×10^{-13} respectively in a hot environment.

The effect of high curing temperature on the permeability of CSF mortars seems to be the reverse of that found with the plain OPC mixes. Specimens cured under hot environment were found to have early and later-age permeabilities lower than those cured under temperate environments.

For example, the water and air permeability of CSF mortar mix (M40/10) was reduced from 7 x 10^{-13} and 3.3 x 10^{-14} (m/s) respectively in a temperate environment to 6.4 x 10^{-14} and 2.4 x 10^{-14} (m/s) respectively in a hot environment.

Regardless of the curing environment, partially replacing OPC with CSF up to 15% by weight of OPC can result in a significant reduction in both water and air permeabilities.

For example, in a hot curing environment the water permeability was reduced from 8 x 10^{-11} (m/s) in the plain OPC mix to 9.3 x 10^{-13}, 6.4 x 10^{-14} and 5.3 x 10^{-14} (m/s) in the CSF mortar mixes M40/5, M40/10 and M40/15 respectively. Air permeability was reduced from 3.4 x 10^{-13} (m/s) in the plain OPC mortar mix to 6.8 x 10^{-14}, 2.4 x 10^{-14} and 1.2 x 10^{-14} (m/s) in the CSF mortar mixes M40/5, M40/10 and M40/15 respectively.

Superplasticized CSF mortars had lower air and water permeabilities compared with the equivalent non-superplasticized mix.

The paste matrix permeability is not a simple function of its bulk porosity; it depends on the distribution and continuity of pores. Moreover, the permeability of paste matrix is controlled by the coarse pores (greater than a diameter of 0.1 micrometer) available. The relationship between water permeability and volume of coarse pores reveals the existence of a critical volume of coarse pores which lies between 6.5 and 15.0 percent of specimens volume. Therefore any mortar mix which has volume of coarse pores lower than 7 percent is expected to have low water permeability characteristics. On the other hand the relationship between air permeability and volume of coarse pores show that

above the critical volume of coarse pores lie between 4 and 17 percent by volume of specimens. On the basis of the above critical coarse pore volumes. a critical volume of coarse pore lies between 5 and 16% by volume of specimen was suggested for both permeabilities.

11.6 Sulphate resistance of plain and CSF mortars

Under the effect of alternate soaking in magnesium sulphate solution and subsequent oven drying plain OPC and CSF mortars with only 5% of CSF show an initial weight gain followed by weight loss. However, no initial weight gain was noticed in the other CSF mortar mixes with higher percentages of CSF. The rate of deterioration is high in the plain OPC mortars and much lower in the CSF mixes. The higher the CSF content the lower the rate of deterioration. The superplasticized CSF mortar mix was superior in improving the resistance to sulphate attack when compared to the non superplasticized mix.

Under the exposure condition of continuous soaking in magnesium sulphate solution, the use of CSF up to 10% by weight of OPC improves sulphate resistance. Increasing the CSF content up to 15% brought no more improvement in sulphate resistance. In fact the resistance of 15% CSF mix was lower than the 5% CSF mix due to the presence of surface cracks.

11.7 Recommendations for further research work

The research work carried out in this thesis has identified several areas where further research is necessary. It is therefore recommended that investigation should be made into the following:

1. Experimental work here revealed the presence of hairline surface cracks in the high content (15% by weight of OPC) silica fume concrete and mortar mixes cured in a temperate environment. These surface cracks were absent in the same identical mixes cured in hot conditions. Although an explanation for this behaviour was provided, further research work is needed to explain fully this behaviour.

2. Due to the limited resources and time available only one method of curing (polythene sheeting) was used for curing specimens in a hot environment. More information is required on the effect of curing methods on the strength and durability related properties of plain and CSF mixes.
3. In this research the effect of climate was investigated by subjecting concrete specimens to two temperature and humidity cycles. It would be of interest to study the effect of temperature and humidity separately to evaluate which parameter is having the greatest effect.
4. More information is required regarding the effect of substitution of OPC in lean and rich mixes with high percentages of CSF (>10%) on the strength and durability properties in both hot and temperate environments.
5. Since steel corrosion is one of the main problems in hot climates, it is of interest to examine directly the resistance of CSF concrete cured under hot environments to steel corrosion.

11.8 Application of OPC/CSF in a hot climate

Concreting and concrete performance in the Middle Eastern environment and more specifically in Iraq, is known to suffer from many problems. In particular high curing temperature has a negative effect on the long-term strength, permeability and durability properties of concrete, and the concurrent presence of high chloride and sulphate concentrate in soil and ground water exerts a complex deterioration effect on concrete structures in contact with them. Using sulphate resisting cement can provide protection against sulphate attack, but would fail to decelerate embedded steel corrosion. On the other hand using normal cement with a high C_3A content would provide adequate protection against steel corrosion, but would fail to provide resistance to sulphate attack. The use of an OPC/CSF blend as an alternative to plain OPC was expected to provide a solution to this problem

and overcome the long-term strength and durability problems in hot environment. Results achieved from this research work have shown that silica fume concrete and mortar mixes have better strength and durability characteristics when compared to the plain OPC mixes cured simultaneously in a simulated hot Iraqi environment. Therefore, this blended OPC/CSF cementitious material is recommended to be used in the Iraqi environment for the construction of both superstructural and substructural concrete element. In addition to all the valuable improvement in strength and more importantly the performance and durability of concrete offered by this material, the acceleration of hydration and hardening of cement can reduce the form stripping time. This can improve the construction scheduled time and reduce the necessary construction time which means some saving in the construction cost can be gained. The high performance and durability of this material can in the long term increase the service life of the building and save money in the maintenance cost.

REFERENCES

1. Aitcin, P.C.
"Condensed silica fume"
University of Sherbrooke, Quebec, Canada.

2. Parker, D.G.
"Microsilica Concrete: Part 1, The Material"
Concrete Society current practice sheet No.104, Concrete, London, Oct 1985, P21-22.

3. Regourd, M., Mortureux, B; Aitcin, P.C. & Pinsonneault, P.
"Microstructure of field concrete containing silica fume". Proc. 4th International conference on Cement Microscopy, March/April 1982, Las Vegas, Nevada, (15A), p.249-260.

4. Carette, G.G. & Malhotra, V.M.
"Mechanical Properties, durability and drying shrinkage of Portland Cement concrete incorporating silica fume". ASTM J. Cement, Concrete, Aggregate, V5,N1, 1983.

5. Sellevold, E.J.
"Review: Microsilica in Concrete". Report No. 08037/EJS/TJJ, Norwegian Building Research Institute, Oslo, 1984.

6. Loland, K.E. & Hustad, T.
"Fresh Concrete and Method of Data Analysis". Report No. STFGS A81031, Cement and Concrete Research Institute, The Norwegian Institute of Technology, Trondheim, June 1981.

7. Sellevold, E.J. & Radjy, F.F.
"Condensed silica fume (Microsilica) in concrete: water demand and strength development". ACI special publication, SP-79, Malhotra, V.M. Ed., American Concrete Institute, Detroit, 1983, p.677-694.

8. Maage, M.
"Modifier Portland Cement". Rep. No. STF65 A83063, Cement and Concrete Research Institute, The Norwegian Institute of Technology.

9. Burge, A.T.
"High strength lightweight concrete with condensed silica fume. ACI spec. pub. SP-79, Malhotra, V.M. Ed. American Concrete Institute, Detroit, 1983, p.731+.

10. British Standard Institution
"BS4550, Sec 3.6; Methods for testing cement: test for setting time". British Standard Institute, London, 1978.

11. Swamy, R.N.
"Cement replacement materials". Concrete Technology and Design Vol.3, Surrey University Press.

12. Pistillia, M.F. Wintersteen, R. and Cechner, R.
"The uniformity and influence of silica fume source on the properties of Portland Cement concrete". Cement, concrete, and aggregate Vol.6, No.2, 1984, p.120-124.

13. William, L.
"Plastic shrinkage". ACI Journal, U28, N8, Feb 1957, p.797-802.

14. Menashi, D.C; Olek, J & Dolch, W.L.
"Effect of the form of silica fume on plastic shrinkage cracking of Portland Cement paste". Third CANMENT/ACI International Conference on fly ash, silica fume, slag and natural pozzolans in concrete. Norway 1989, p.431-443.

15. Cheng, Yi, H and Feldman R.F.
"Hydration reaction in Portland Cement - silica fume blends". Cement and Concrete Research, V15, 1985, p.585-592.

16. Kurdowski, W. and Nocun-Wczelik, W.
"The tricalcium silicate hydration in the presence of active silica". Cement and Concrete Research, V13, 1983, p.341-348.

17. Wu, Z.Q and Young, J.F.
"The hydration of tricalcium silicate in the presence of colloidal silica". J. Mater. Sci. V.19,p3477-3486, 1984.

18. Buke, A.D. & Burkers, J.P.
"Characterization and reactivity of silica fume". Proceedings 3rd International Conference on Cement Microscopy, Houston, March 1981, p.279-285.

19. Malhotra, V.M.
"Mechanical properties and freezing and thawing resistance of non-air entrained and air-entrained condensed silica fume concrete using ASTM Test C666 Procedures A & B Div." Rep. MRP/MSL 84-153 (OP & J), CANMENT, Energy, Mines and Resources, Canada, Ottawa, 1984.

20. Sandvik, M. & Gjorv, O.E.
"Effect of condensed silica fume on the strength development of concrete". 2nd Int. Conf. on fly ash, silica fume, slag and natural pozzolands in concrete ACI, Vol.2, 1980, p.891-901.

21. Malhotra, V.M. & Carette, G.G.
"Silica fume concrete: properties application and limitations". ACI Concrete Int. Design Construction, V5 N5, p40-46, 1983.

22. Popovic, K; Utraincik, V. & Djurekovic, A.
"Improvement of mortar and concrete durability by the use of condensed silica fume". Durability Building Materials, V2, N2, May 1989, p.171-186.

23. Skrastins, J.J. & Zoldners, N.G.
"Ready-mixed concrete incorporating condensed silica fume". ACI spec. publ. SP-79, Malhotra, V.M. Ed. American Concrete Institute, Detroit, 1983, VII, p813-829.

24. Jahren, P.
"Use of silica fume in concrete". ACI spec. Publ. SP-79. Malhotra, V.M. Ed. American Concrete Institute Detroit, 1983, p625-643.

25. Malhotra, V.M. & Carette, G.G.
"Silica fume". Concr. Const. V27, N5, May 1982, p443-446.

26. Wolsiefer, J.
"Ultra high-strength field placeable concrete with silica fume admixture". ACI Concrete Int. Design Constr. V6, N4, p25-31, 1984.

27. Bache, H.H.
"Densified cement ultra-fine particles based material". 2nd Int. Conf. on superplasticizer in concrete, Ottawa, June 1981, p.1-35.

28. Carette, G.G; Malhotra, V.M. & Aitcin, P.C.
"Preliminary data on long-term strength development of condensed silica fume concrete". Third ACI Int. Conf. on the use of fly ash, silica fume, slag and natural pozzolans in concrete". VIII p585-618. Trondhiem, Norway 1989.

29. Aitcin, P.C. & Laplante, P.
"Long-term compressive strength of silica fume concrete". Third ACI Int. Conf. on the use of fly ash, silica fume, slag and natural pozzolans in concrete - VIII, p727-738. Trondheim, Norway, 1989.

30. Johansen, R.
"Long term effects, Rep. STF 65, A81031", Cement and Concrete Research Institute, The Norwegian Institute of Technology, Trondheim, 1983.

31. Carette; G.G. & Malhotra, V.M.
"A note on drying shrinkage of condensed silica fume concrete Div. Rep. MRP/MSL 86-24 (OP&S) CANMENT, Energy Mines and Resources Canada, Ottawa, 1985.

32. Bager, D.H.
"Effect of silica fume on pore structure and drying shrinkage in mortars". Norelisk Betong, V72, p3-4, 1984.

33. Buil, M; Paillere, A.M. & Roussel, B.
"High strength mortars containing condensed silica fume". Cement and Concrete Res., V14, 1984, p693-704.

34. Ravindrarajah, S. & Paramasivam, P.
"Effects of condensed silica fume addition on the properties of mortar". 3rd ACI Int. Conf. on the use of fly ash, silica fume, slag and natural pozzolans in concrete, VIII, P406-419, Norway 1989.

35. Buil, M. & Acker, P.
"Creep of silica fume concrete". Cem. & Concr. Res. V15, 1985, p463-466.

36. Nevill A.M.
"Properties of concrete". Third edition, 1983.

37. Berry, E.E. & Malhotra, V.M.
"Fly ash in concrete". CANMET Spec. Publ. SP85-3, Energy, Mines and Resources. Canada, Ottawa, 1985.

38. Charles-Gibergues, A. Grandet, J. & Oliver, J.P.
"contact zone between cement paste and aggregate". Bond in Concrete, Bartos, P. Ed. London, 1982.

39. Gjorv, O.E.
"Durability of concrete containing condensed silica fume". ACI Spec. Publ. SP-79, Malhotra, V.M. Ed. ACI. Detroit, 1983, p695-708.

40. Maage, M.
"Efficiency factors for condensed silica fume in concrete". 3rd ACI Int. Conf. on the use of fly ash, silica fume, slag and natural pozzolans in concrete, VII, p783-799, Trondheim, Norway 1989.

41. Grutzech, M.W; Roy, D.M. & Wolfe-Confer, D.
"Mechanism of hydration of Portland Cement composite containing ferro silicon dust". Proc. 4th Int. Conf. on cement microscopy, 1982, p193-202.

42. Meland, I.
"Influence of condensed silica fume and fly ash on the heat evolution in cement paste". Proc. Int. Conf. on the use of fly ash, silica fume, slag and other mineral by-products in concrete, 1983, 677+.

43. Huang, C.Y. and Feldman, R.F.
"Hydration reactions in Portland Cement - silica fume blends". Cem. & Concr. Res., V15 p585-592, 1985.

44. Beaudoin, J.J.
"Porosity measurements of some hydrated cementitious systems by high pressure mercury - intrusion - microstructural limitation". Cem. & Concr. Res. 9, p 771, 1979.

45. Day
"Reactions between methanol and Portland Cement Paste". Cement & Concrete Research V11, p.341-349, 1981.

46. Parrott
"Thermogravimetric and sorption studies of methanol exchange in an alite paste". Cement & Concrete Research, V13, 1983, P18-22.

47. Feldman, R.F. & Huang, C.Y.
"Properties of Portland Cement - silica fume pastes. I. Porosity and surface properties". Cem. & Concr. Res. 15 , p765-774, 1985.

48. Feldman, R.F.
"Significance of porosity measurement on blended cement performance". Proc. 1st Int. Conf. on the use of fly ash, silica fume, slag and other mineral by-products in concrete, Vol.1, 1983, p.415+.

49. Feldman, R.F.
"Pore structure change in blended cement caused by mercury intrusion". J. American Ceramic Society, V67, N1, p30-33, 1984.

50. Regourd, M; Mortureux, B; Aitcin, P.C. and Pinsonneault, P.
"Microstructure of field concrete containing silica fume", Proc. 4th Int. Conf. on cement microscopy, 1982, p249-260.

51. Sellevold, E.J; Bager, D.H; Klitgaard-Jensen, E. & Knudsen, J.
"Silica fume-cement paste - hydration and pore structure". Condensed silica fume in concrete, BML 82-610, Norwegian Institute of Technology, Trondheim, 1982, 19pp.

52. Gautefall, O.
"Effect of condensed silica fume on the diffusion of chloride through hardened cement paste". 2nd Int. Conf. on fly ash, silica fume, slag and natural pozzolans in concrete, Madrid, Spain, 1986, V2, p.992-997.

53. Grimaldi, G; Carpio, J. & Raharinaivo, A.
"Effect of silica fume on carbonation and chloride penetration in mortars". 3rd Int. conf. on the use of fly ash, silica fume, slag and natural pozzolans in concrete, VIII, p320-335, Norway 1989.

54. Berke, N.S.
"Resistance of microsilica concrete to steel corrosion, erosion and chemical attack". 3rd Int. Conf. on use of fly ash, silica fume, slag, and natural pozzolans in concrete, VII, p861-879, 1989 Norway.

55. Gautefall, O. & Havdahi, J.
"Effect of condensed silica fume on the mechanism of chloride diffusion into hardened cement paste". 3rd Int. Conf. on use of fly ash, silica fume, slag and natural pozzolans in concrete, VII p849-861, Norway 1989.

56. Vennesland, O. & Gjorv, O.E.
"Silica fume - protection against corrosion of embedded steel". ACI Spec. Publ. SP-79, Vol.2, Malhotra, V.M. Ed. ACI, Detroit, 1983, p719+.

57. Hope, B.B; IP, K.K. & Manning, D.A.
"Corrosion and electrical impedance in concrete". Cement & concrete Res. V15, p525-534.

58. Stanton, T.E.
"Expansion of concrete through reaction between cement and aggregate". Proc. ASCE, V66, p1781+, 1981.

59. Swenson, E.G. & Gillott, J.E.
"Alkali-Carbonate rock reaction". Highway research record, No.45, Highway Research Board, Washington, D.C. 1964, 21pp.

60. Oberholster, R.E. & Westra, P.
"The effectiveness of mineral admixture in reducing expansion due to alkali reaction with Malmesbury group aggregate". Alkali-Aggregate Reaction in concrete Conf. 1981, in Cape Town, p294-299.

61. Olafson, H.
"The effect of finely grained silica dust and fly ash on alkali silica reactivity on high alkali cements". National Bureau of Standard Building Composite Group, Washington, D.C. 1980, 1.

62. Perry, C. & Gillott, J.E.
"The feasibility of using silica fume to control concrete expansion due to alkali-aggregate reactions". Durability of building materials, 3, 1985, p133-146.

63. Regourd, M; Mortureux, B. & Horman, H.
"Used of condensed silica fume as filler in blended cements". Proc. 1st Int. Conf. on the use of fly ash, silica fume, slag and other mineral by-products in concrete, Montebello, Canada, July 1983, p.847.

64. Feldman, R.F. & Huang, C.Y.
"Resistance of mortars containing silica fume to attack by a solution containing chlorides". Cement & Concrete Res. 15, p411-420, 1985.

65. Mather, K.
"Factors affecting sulphate resistance of mortars". 7th Int. Congr. on the Chemistry of Cement. Vol.4, Paris 1980, p580-.

66. Mehta, P.K.
"Durability of low water-cement ratio concrete containing latex or silica fume as admixture". Proc. Rilem-ACI Symp. on Technology of Concrete when pozzolans, slag and chemical admixture are used. Monterrey, Mexico, 1985, p.325.

67. Carlsson, M; Hope, R. and Pedersen, J.
"Use of condensed silica fume (CSF) in concrete". 2nd Int. Conf. on fly ash, silica fume, slag and natural pozzolans in concrete, Madrid, Spain, 1986, U2, p.1013-1030.

68. Yamato, T; Soeda, M; & Emoto, K.
"Chemical resistance of concrete containing condensed silica fume". 3rd Int. Conf. on the use of fly ash, silica fume, slag and natural pozzolans in concrete, VII, p.897, Norway.

69. Fookes, P.G; Pollock, D.J. & Kay, E.A.
"Concrete in Middle East, Parts 1 & 2" Viewpoint publication. 1982.

70. Shirley, D.E.
"Concreting in hot weather"
C & CA publication No. 45-013, construction guide

71. Scanlon, J.M.
"Quality control during hot and cold weather". Concrete Int. Sept. 1979, p.58-65.

72. ACI Committee 308
"Standard practice for curing concrete". ACI (308-81), ACI, Detroit, 11pp.

73. Berhane, Z.
"Evaporation of water from fresh mortars and concrete at different environmental conditions": ACI J. Nov/Dec 1984, p.560-565.

74. Shalon, R. & Ravina, D.
"Studies in concreting in hot countries". Proc. Relim, Symp., on concrete and reinforced concrete in hot countries, B.R.S., Haifa, Vol.1, 1960.

75. Fedration Internationale de la Precontrainte (FIP)
"Concrete construction under extreme climate conditions: hot weather concrete practice". Draft report, 1984.

76. Venuat, M.
"Effect of elevated temperature and pressure on the hydration and hardening of cement". 6th Int. Congress on the Chemistry of Concrete. Moscow, Sept 1974.

77. ACI Committee 305
"Hot weather concreting". ACI 305 R-77, 1977, Revised 1982.

78. Samarai, M; Popovics, S. & Malhotra, V.M.
"Effect of high temperature on the properties of fresh concrete". Transport Res. Rec. 924, 1983, p.42-50.

79. Varshney, R.S. & Coal, M.C.
"Effect of delaying in placing normal concrete and air-entraining concrete". The Indian Concr. J. V48, 1974, March, p.82-89.

80. Klieger, D.
"Effect of mixing and curing temperature on concrete strength". ACI J. V54, N12, June 1958, p1063-1081.

81. Orr, F.M.
"A factorial experiment to investigate the effect of cement temperature and initial mix temperature on the consistency and 28-day strength of concrete". Rilem Symp. on concrete and reinforced concrete in hot countries, B.R.S., Haifa, 1971, Vol.I.

82. Previte, R.W.
"Concrete slump loss". ACI J. U74, N8, 1977, p.381-367.

83. Ramakrishnan, V., Coyle, W.V. & Pande, S.S.
"Workability and strength of retempered superplasticized concrete". Transp. Res. Rec., 720, 1979, p.13-19.

84. Malhotra, V.M.
"Effect of repeated dosage of superplasticizer on workability, strength and durability of concrete". CANMENT, Ottawa, Canada, Rep. MRP-MSL 78-40, Feb. 1978.

85. Ravina, D.
"Retempering of prolonged-mixed concrete with admixture in hot weather". JACI, June 1975, p.291-295.

86. Lerch, W.
"Plastic shrinkage". ACI J. V53, N8, Feb. 1957, p.797-802.

87. ACI Committee 305
"Recommended practice for hot weather concreting". ACI Proc., V68, June 1971, p.489-501.

88. Ravina, D. & Shalon, R.
"Plastic shrinkage cracking". ACI J. U65, N4, 1968, p.282-292.

89. Van Dijk, J.
"Plastic shrinkage cracking of concrete". Proc. Rilem. Symp on concrete and reinforced concrete in hot countries, Haifa, 1971, Vol.I.

90. Ray, Hewn.
"Hot weather concreting". Engineering notebook Civil Engineering ASCE, Sept. 1978, p100-.

91. Helmuth and Verbeck.
"Structural and physical properties of cement paste". Int Symp. on the chemistry of cement, Tokyo, October 1988.

92. Price, W.H.
"Factors influencing concrete strength". ACI J. V47, 1951, p417-432.

93. Abbasi, A.F. & Alam, M.S.
"Compressive strength of concrete in hot weather". Int. J. for housing science and its application, V6, N2, p121-134, 1982.

94. Berhare, Z.
"Compressive strength of mortars in hot-humid environment". Cem & Concr. Res. V13, 1983, p225-231.

95. Jaegermann, C.H. & Glucklick, J.
"Effect of exposure of fresh concrete to high evaporation and elevated temperature on the long-term properties of hardened concrete". Proc. Int. Relim. Symp. on concrete and reinforced concrete in hot countries, B.R.S., Haifa, Vol. II, 1971, p.383-426.

96. PCA Bulletin
"Design and control of concrete mixture". Portland Cement Association, Engineering Bulletin, EB 001.11 T, Skokie, Illinois, USA, 1968.

97. Bloem, D.L.
"Effect of curing conditions on the compressive strength test specimens". NRMCA Publication No.53, National Ready Mixed Concrete Association, Silver Spring, MD, October 1969.

98. Gaynor, R.D; Meininger, R.C. & Shan, T.S.
"Effect of temperature and delivery time on concrete properties". ASTM, STP858, Philadephia, 1985, p68-87.

99. Ridgley, T.
"An investigation into manufacture of high strength concrete in a tropical climate". Proc. Inst. C.E, London, V13, 1959, p.23-24.

100. Mindess, S. & Young, J.F.
"Concrete". Ed. Newmark, V.M. & Hall, W.J. 1981.

101. Goto, S. & Roy, D.M.
"The effect of W/C ratio and curing temperature on the permeability of hardened cement paste". Cement and Concr. Res. V11, 1981, p.575-579.

102. Bakker, R.F.M.
"permeability of blended cement". 1st Int. Conf. on the use of fly ash, silica fume, slag and other mineral by products in concrete, Montebello, Canada, ACI, Sp.79, July 1983, p.584-605.

103. Winslow, D.N. & Diamond, J.
J. of material, V5, N3, 1970, p564-585.

104. Parcevaux, P.
"Pore size distribution of Portland Cement slurries at very early stages of hydration influence of curing temperature and pressure". Cem. & Concr. Res. V14, 1984, p419-430.

105. British Standard Institute, B.S.
"Specification for ready mixed concrete". BS 1926, 1962, p6-7.

106. Ministry of Transport.
"Specification for road and bridge work". H.M.S.O., London, 1969, p91-92.

107. Suroka, I. & Peer, E.
"Influence of cement composition on compressive strength of concrete cast and initially cured at high temperature". Proc. Int. Reilem, Symp. on Concr. & reinforced Concrete in Hot Countries, BRS, Haifa, 1971, Vol.1, p241-258.

108. "Curing of concrete pavements".
Current road problem No I-R revised edition, Highway Research Board, June 1979.

109. Cement and Concrete Association.
"Curing of Concrete". C & CA Note on concrete curing, MSc course, Loughborough University of Technology.

110. Powers, T.C.
"A discussion of cement hydration in relation to curing of concrete". Proc. Highway Res. Bd. Bul. 27, p.178-188, 1947.

111. Copeland, L.E. & Bragg, R.H.
"Self dessication in Portland Cement paste". ASTM Bulletin, Feb. 1955, p.34-39.

112. Powers, T.C. & Brownyard, T.C.
"Studies of the physical properties of hardened Portland Cement paste". J. Am. Concr. Inst. 43, Oct. 1947.

113. Carrier, R.E. & Cady, P.D.
"Evaluation effectiveness of concrete curing compounds". J. of material, V5, N2, June 1970, p.294-302.

114. Abrams, M.S. & Orals, D.L.
"Concrete drying method and their effect on fire resistance". Publication No. Rx181, Portland Cement Association, Skoki, 1965, 32pp.

115. ACI Committee 308
"Standard practice for curing concrete". ACI (308-81) manual of concrete practice, p1-11.

116. Carrier, R.E.
"Curing material". Significance of test and properties of concrete and concrete materials Chapter 44, 1978.

117. Carrier, R.E.
"Concrete curing tests". Concrete International, April 1983, p23-26.

118. Water, T.
"The effect of allowing concrete to dry before it has fully cured". Mag. of concrete Res. July 1955, V7, N22, p79-82.

119. Curing concrete - method and materials
A collection of articles from Concrete Construction Magazine, July 1973.

120. British Standards Institute
BS 8110:Part 1, 1985, Structural use of concrete.

121. Blackledge, G.
"Curing concrete". Man on the job, C & CA Publication 1980.

122. Keeley, C.
"Curing concrete under Middle East conditions". C & CA Publications, TDH 9559, sheet 1-8.

123. Govind, S.
"Curing concrete - correcting defects of concreting". Conf. on Our World in Concrete and Structure v3, Singapore, 1983-84.

124. "Concrete Manual"
8th edition, US Bureau of reclamation, 1981.

125. Birt, J.C.
"Curing concrete - an appraisal of attitudes, practices and knowledge". Construction Industry Research and Information Association, CIRIA, Report 43, 1981, 33pp.

126. ACI Committee 201
"Guide to durable concrete". Am. Concr. Inst. J. Dec. 1977, p573-609.

127. Taylor, A.F.W.
"The chemistry of cement". London and New York Academic Press, Vol.1, 1964, p1-24.

128. Lea, F.M.
"The chemistry of cement and concrete". 3rd edition, London, Edward Arnold (publ) Ltd., 1980.

129. Calleja, J.
Durability. 7th international Congress on The Chemistry of Cement. Vol.1, Principle Report, Paris, 1980, p.vii-2/1 - 2/47.

130. Pommersheim, J. and Clifton, J.
Prediction of Concrete Service Life. Mat. and Struct., Vol.18, No.103, p21-30, 1985.

131. Mather, B.
Effect of sea water on concrete. Highway Res. Rec., No.113, p.33-40. 1966.

132. Nevill, A.M.
Behaviour of concrete in saturated and weak solutions of magnesium sulphate or calcium chloride. J. of Mat. JMLSA, Vol.4, No.4, Dec. 1969, p.781-816.

133. Heller, L. and Ben-Yair, M.
Effect of sulphate solution on normal and sulphate resisting Portland Cement. Journal of Applied Chemistry, Vol.14, Jan.1964, p.20-30.

134. Mehta, P.K.
Mechanism of sulphate attack on Portland Cement - concrete - another look. Cem. and Concr. Res., 1983, Vol.13, p.401-406.

135. Ogawa, K; Uchikawa, H; Takemoto, K. & Yasui, I.
"The mechanism of the hydration in the system C_3S - pozzolana". Cement & Concrete Res. V10, N5, p683-696.

136. British Standards Institution
"BS12:1978 specification for ordinary and rapid-hardening Portland cement". London. 4pp.

137. British Standards Institution
"BS812:Part 1 & 2: sampling and testing of mineral aggregate, sand and filler". British Standards Institute, London 1975.

138. British Standards Institution
"BS882: Aggregate from natural sources for concrete". British Standards Institute, London, 1983.

139. Rixom, M.R.
"Chemical admixture in concrete". London, ed. E & F.N. Spon Ltd., 1978.

140. British Standards Institution
"BS1881:Part 125: Method of mixing and sampling fresh concrete in the laboratory". London, 1986, 6pp.

141. Tazaw, Ei-ich; Yonekura, A. & Tanaka, S.
"Rate of hydration and drying shrinkage of concrete silica fume mortars prepared by double mixing". Third CANMENT ACI Int. Conf. on fly ash, silica fume, slag and natural pozzolans in concrete, VIII, p350-365, Norway, 1989.

142. Pearce, E.A. & Smith, G.G.
"The world weather guide". Pub. Hutchinson, 1984.

143. Buxtehude, W.R.
"World climate". Pub. Thames and Hudson, 1979.

144. Oliver, J.E. & Fairbridge, R.W.
"The Encyclopedia of climatology". Pub. Van Nostrand Reinhold, 1987.

145. Figg, J.W.
"Methods of measuring the air a water permeability of concrete". Mag. of Concr. Res. V25, N85, Dec 1973, p 213-219.

146. British Standards Institution
"BS1881:Part 5: Methods for testing hardened concrete for other than strength". British Standards Institute, London 1970.

147. Hudd, R.W; Austin, S.A. & Robins, P.J.
"A non destructive In-situ permeability test for concrete surfaces". Loughborough University of Technology/Institute of Concrete Technology workshop on measurement of in-situ concrete permeability, 12 December 1989, Loughborough University.

148. British Standards Institution
"BS1881:Part116: method of determination of compressive strength of concrete cubes" London 1983. 6pp.

149. Figg, C.R; Marsden, J.W; & O'Brien, T.P.
"Improvement to the Figg method for detemrining the air permeability of concrete". Mag. of Concrete Research, V36, N129, Dec. 1984, p241-245.

150. J. Figg
"In-situ measurement of concrete permeability, the method, procedure and developments to date". One-day workshop at Loughborough University of Technology, 12 Dec. 1989.

151. A.S. Read
"Figg permeability testing in Hong Kong". One-day workshop at Loughborough University of Technology, 12 Dec. 1989.

152. Montgomery, F.R.
"Concrete surface permeability". Cement & Concr. Association Research Seminar, 30th June-2nd July 1986.

153. Hudd, R.
"Measurement of concrete permeability". PhD thesis 1989, Loughborough University.

154. Levitt, M.
"Concrete quality conference". Proc. Symp. the C & CA, London 1966.

155. Ritter, H.L. & Drake, L.C.
"Pore size distribution in porous materials". Industrial and engineering chemistry, V17, N12, 1945, p782-786.

156. Washburn, E.W.
"Notes on a method of determining the distribution of pore sizes in a porous material". Proc. of National Academy of Science, V7, 1921, p115-116.

157. Orr, C.
"Application of mercury penetration to amterial analysis". Powder Technology, V3, 1970, p117-123.

158. Diamonds, S.
"A critical comparison of mercury porosimetry and capillary condensation pore size distribution of Portland cement pastes". Cem. & Concr. Res. V1, 1971, p531-545.

159. Winslow, D.M. & Diamond, S.
"A mercury porosimetry study of the evaluation of porosity of Portland Cement". J. of materials, JMLSA, V5, N3, 1970, p564-585.

160. Winslow, D.N.
"The validity of high pressure mercury porosimetry", J. of Colloid and Interface Science, V67, N1, 1978, p42-47.

161. Lovelock, P.E.R.
"Laboratory measurement of soil and rock permeability". Institute of Geological Science, London, 1970.

162. American Petroleum Institute
"Recommended Practice for Core Analysis Procedure". A.P.I. Dallas, Pexas, 1960.

163. Newsomne
"Concrete catchwater: a case study". Civil Eng. Dept. L.U.T. 1983.

164. Markestad, A.S.
"The resistance of different cement mortars to sulphate solutions determined by testing ½ inch cube". C & CA Technical Report TRA/383.

165. Mielenz, R.C.
"Significance of accelerated durability testing on concrete". Highway Res. Rec. 1969, N268, pA-34.

166. Mehta, P.K. & Gjorv, O.E.
"New test to sulphate resistance of cement". J. of Testing and Evaluation, V2, N6, Nov. 1974, p510-514.

167. Tuthill, L.H.
"Resistance of hardened concrete to chemical attack". ASTM, Special Publication, No.169-A, 1966.

168. Teychenne, D.C; Franklin, R.E; and Erntroy, H.
"Design of normal concrete mixes". 31pp, Department of the Environment, London, 1975.

169. Microsilica, Technical Bulletin, No.2
Elkem Chemical Limited, 4A Corporation Street, High Wycombe, Bucks, U.K.

170. Barnes, B.D.
"Morphology of the paste - aggregate interface". Lafayette, Indiana, Purdue University 1976, Vol.1, 125pp, JHRP, 76-13.

171. Popovics, S.
"Effect of curing length and final moisture content on the compressive strength of concrete". ACI-J. July-Aug. 1986, p605-657.

172. Nyame, B.R. & Illston, J.M.
"Relationship between permeability and pore structure of hardened cement paste". Mag. of Concrete Research V33, N116, Sept. 1981, p139-146.

173. Payne & Dransfield
"Permeability and its control". 1-day Conference, Concrete Society, London, Dec. 1985.

174. Power, T.C.
"Structure of physical properties of hardened Portland Cement paste". J. of the American Ceramic Society, V41, No.1, p1-6.

175. Mehta and Manmohan
"Pore size distribution and permeability of hardened cement paste". Proc. 7th Int. Congress on Chemistry of Cement, V3, ppVII 1-5, 1980.

176. Powers, T.C; Copeland, L.E; Hayes, J.C; & Mann, H.M.
"Permeability of Portland Cement paste". J. of Am. Concr. Inst. Nov. 1954, p.285-298.

177. Hustad, K.E; Loland, E. and Gjorv, O.E.
"Effect of condensed silica fume on the permeability of concrete". 3rd CANMET/ACI Int. Conf. on fly ash, silica fume, slag and natural pozzolans in concrete, VIII, p307-320, Norway 1989.

178. Fox, J.A.
"An introduction to engineering fluid mechanism", 1983.

179. The Concrete Society
"Permeability of concrete and its control". One-day Conference, Concrete Society, Dec. 12th 1985.

APPENDIX 1

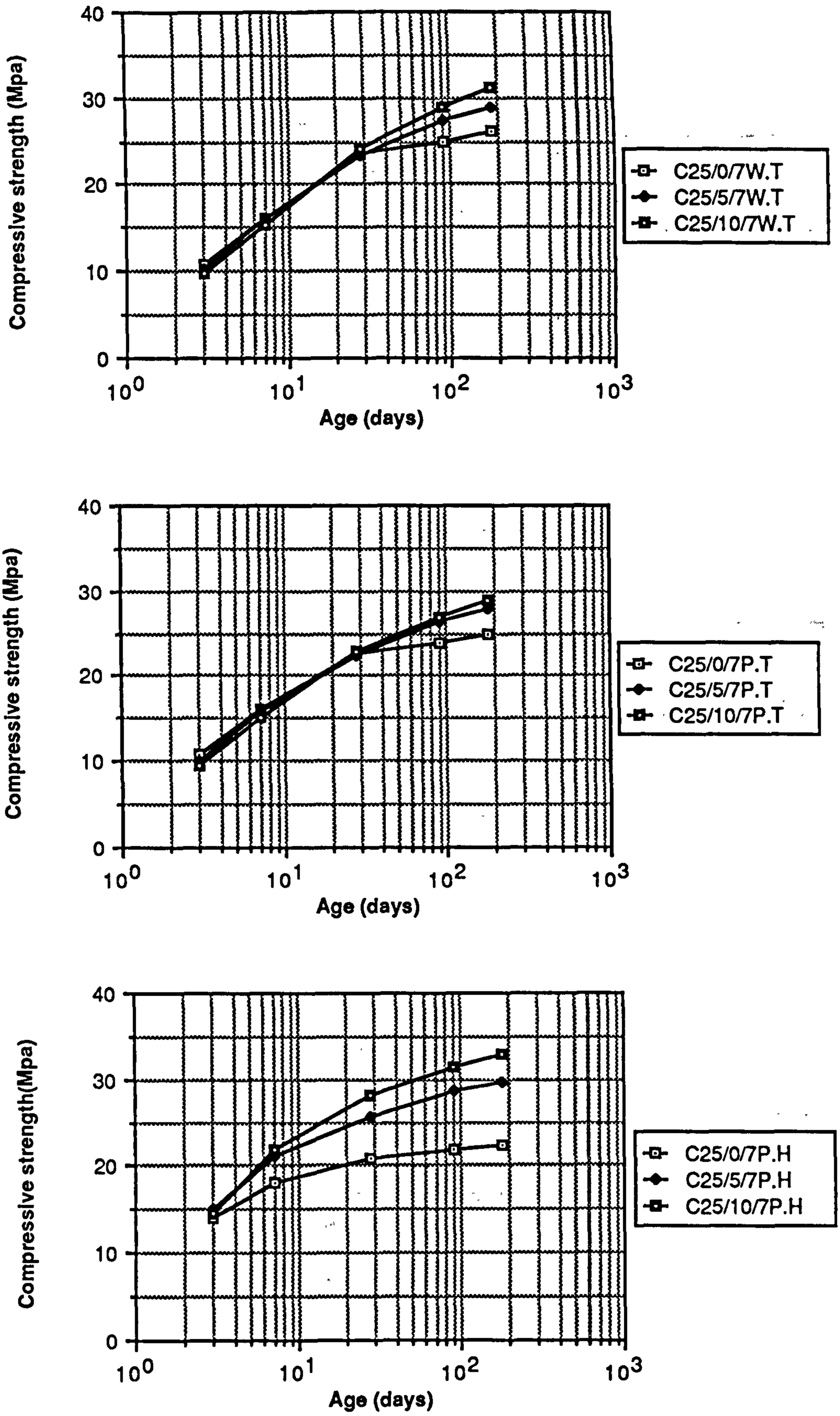

Figure A1.1 Relationship between age and compressive strength of plain and CSF concrete mixes grade C25

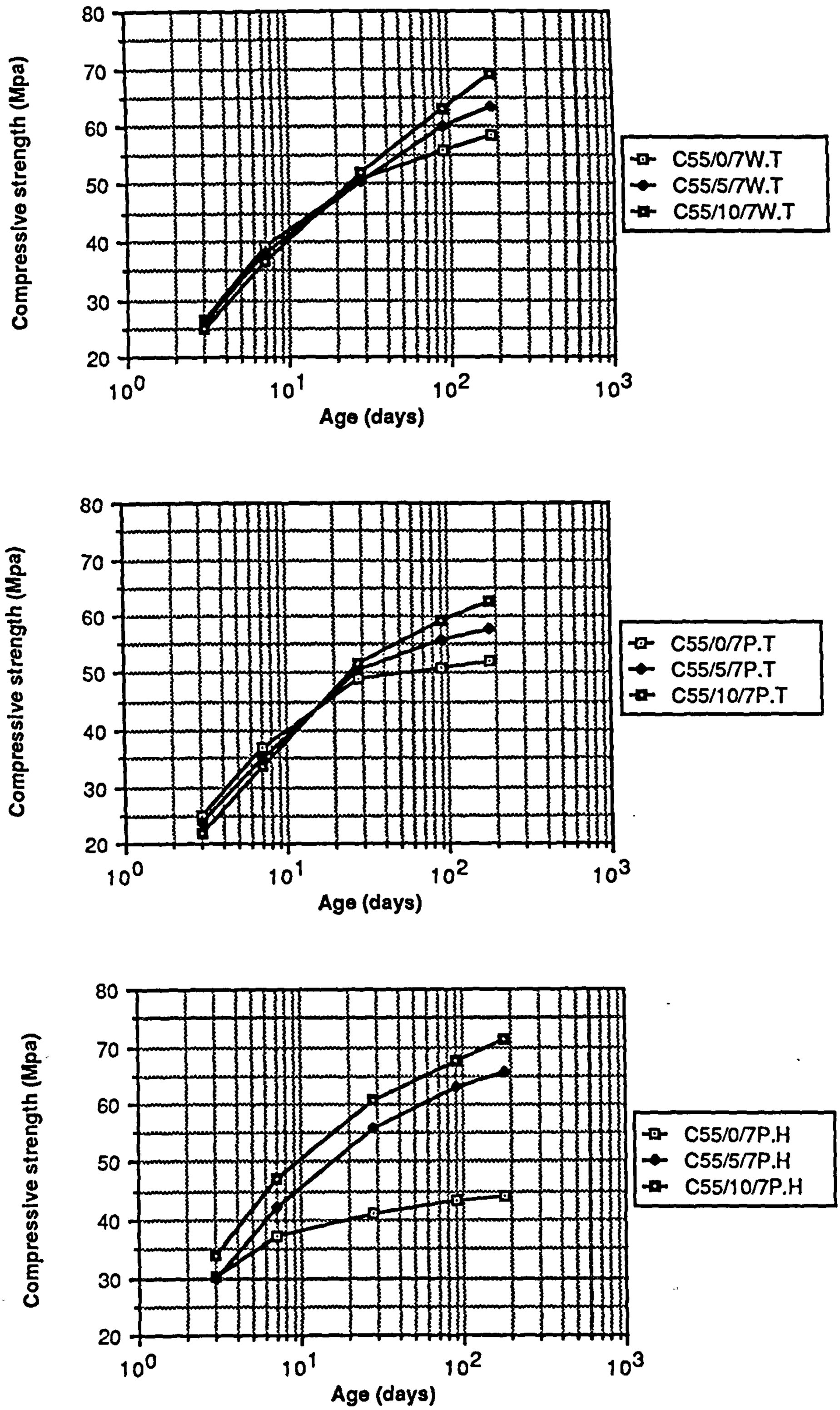

Figure A1.2 Relationship between age and compressive strength of plain and CSF concrete mixes grade C55

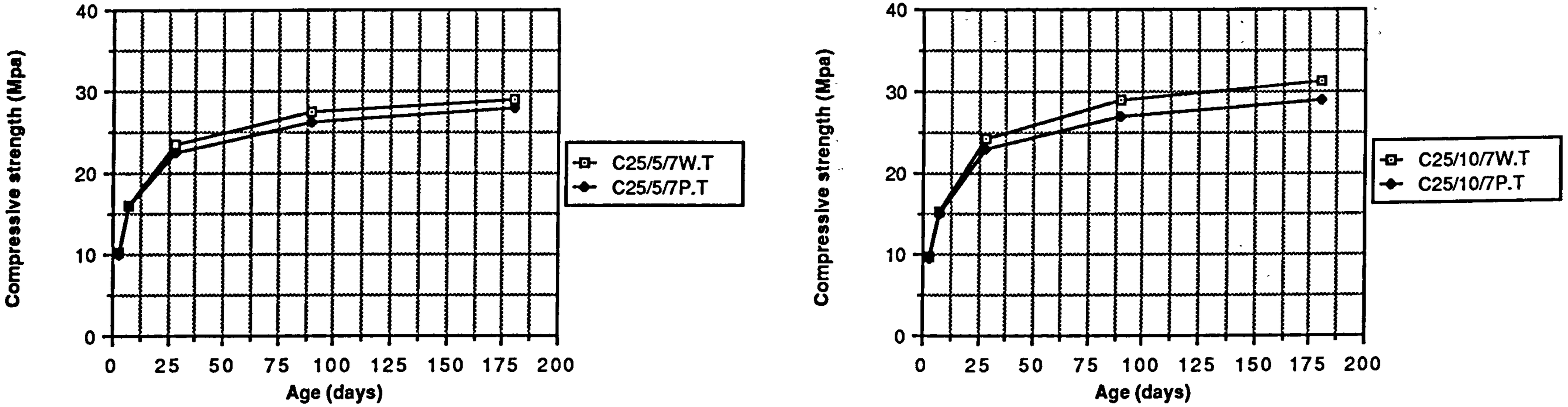

Figure A1.3 Effect of water and polythene curing on the compressive strength of CSF concrete mixes grade C25

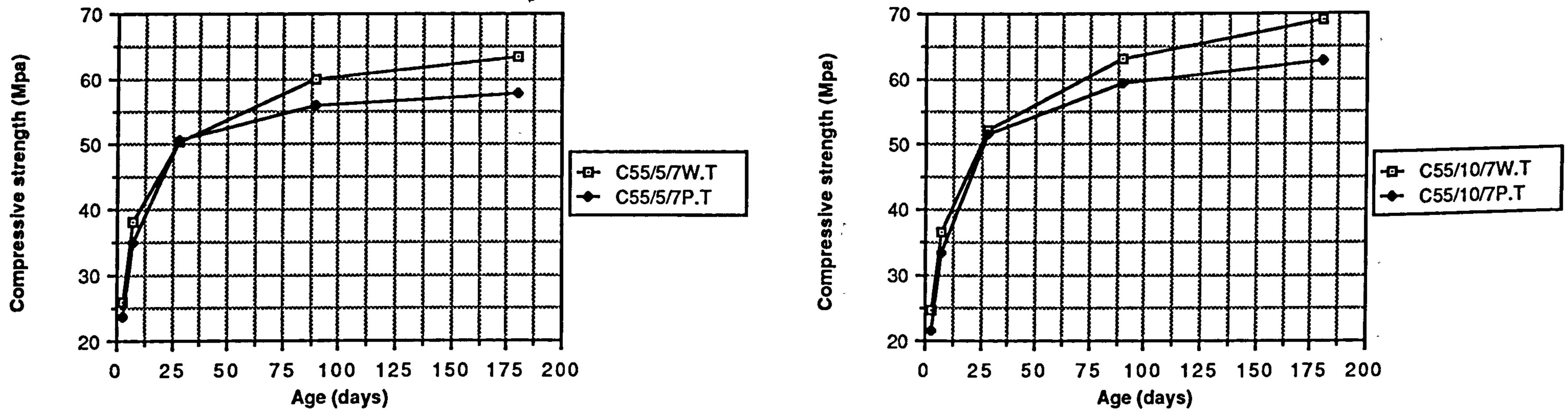

Figure A1.4 Effect of water and polythene curing on the compressive strength of CSF concrete mixes grade C55

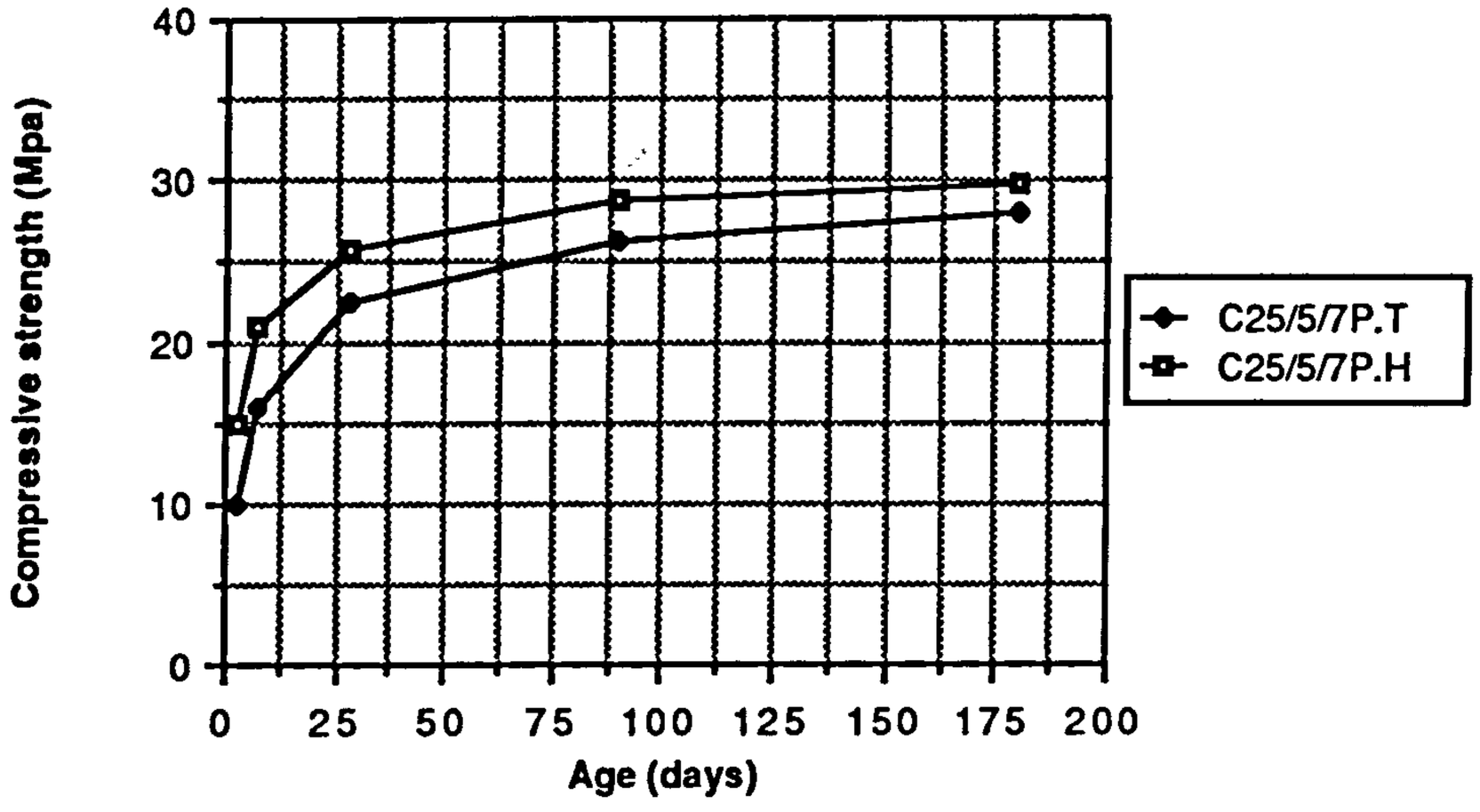

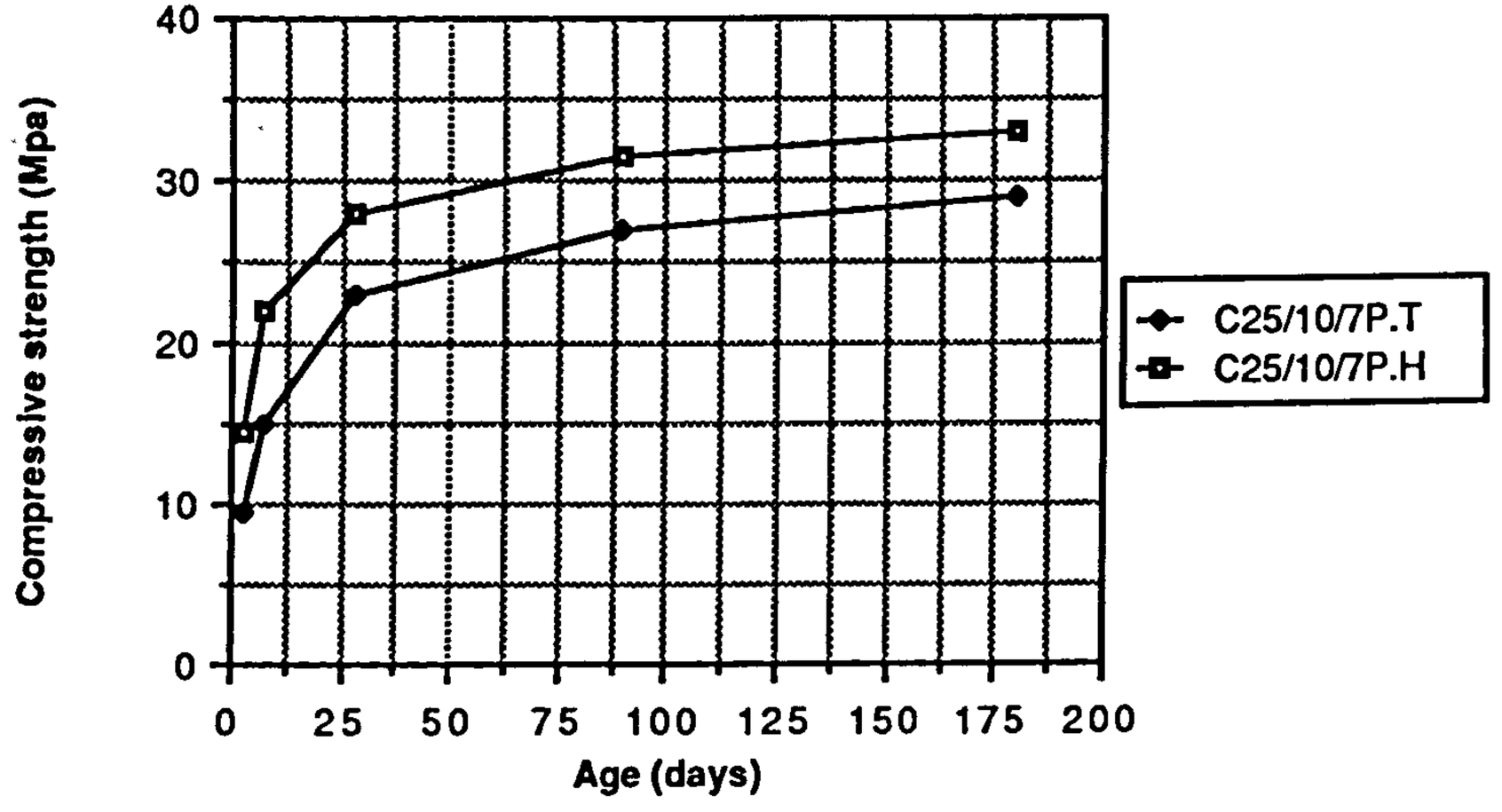

Figure A1.5 Effect of temperate and hot curing on the compressive strength of CSF concrete mixes grade C25

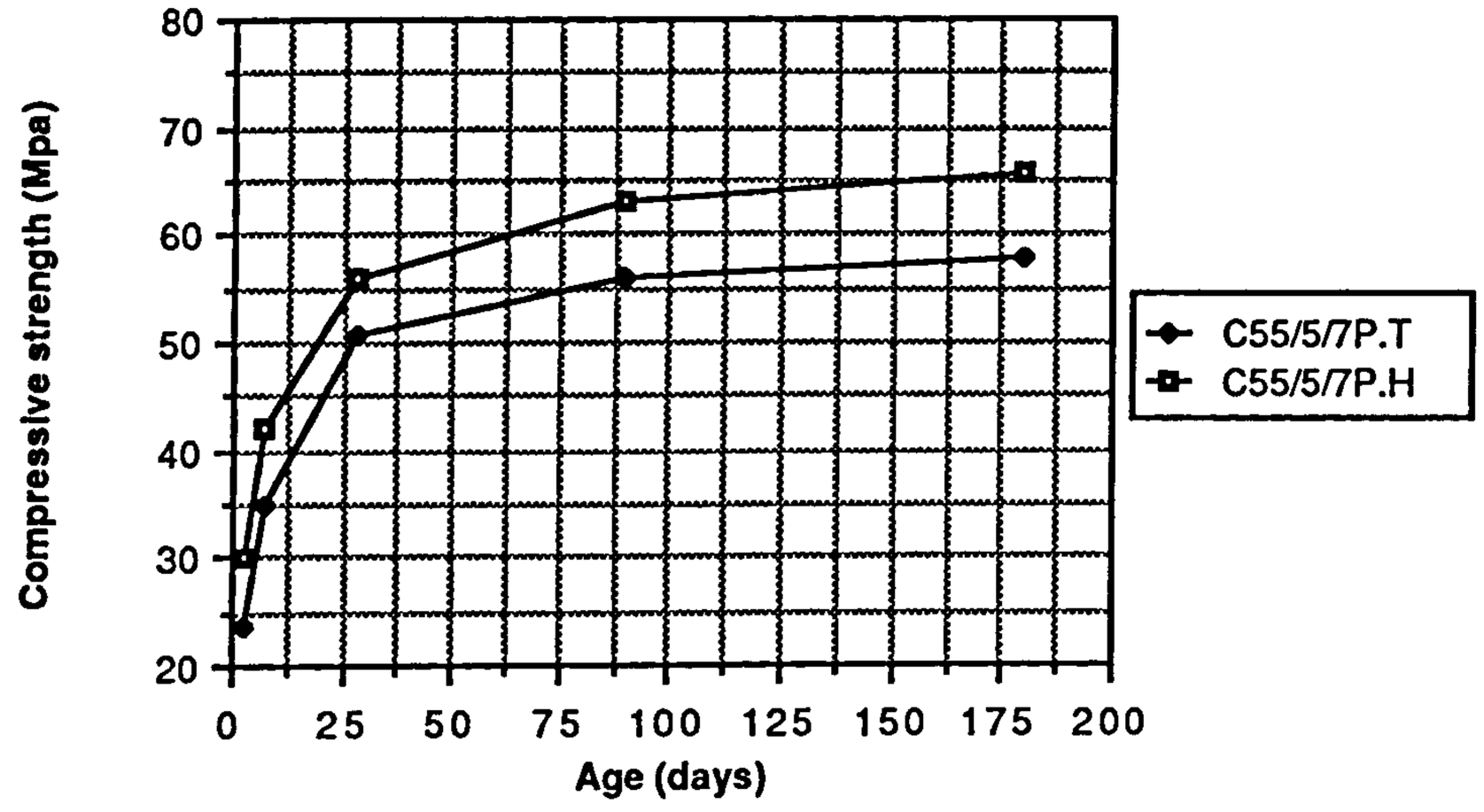

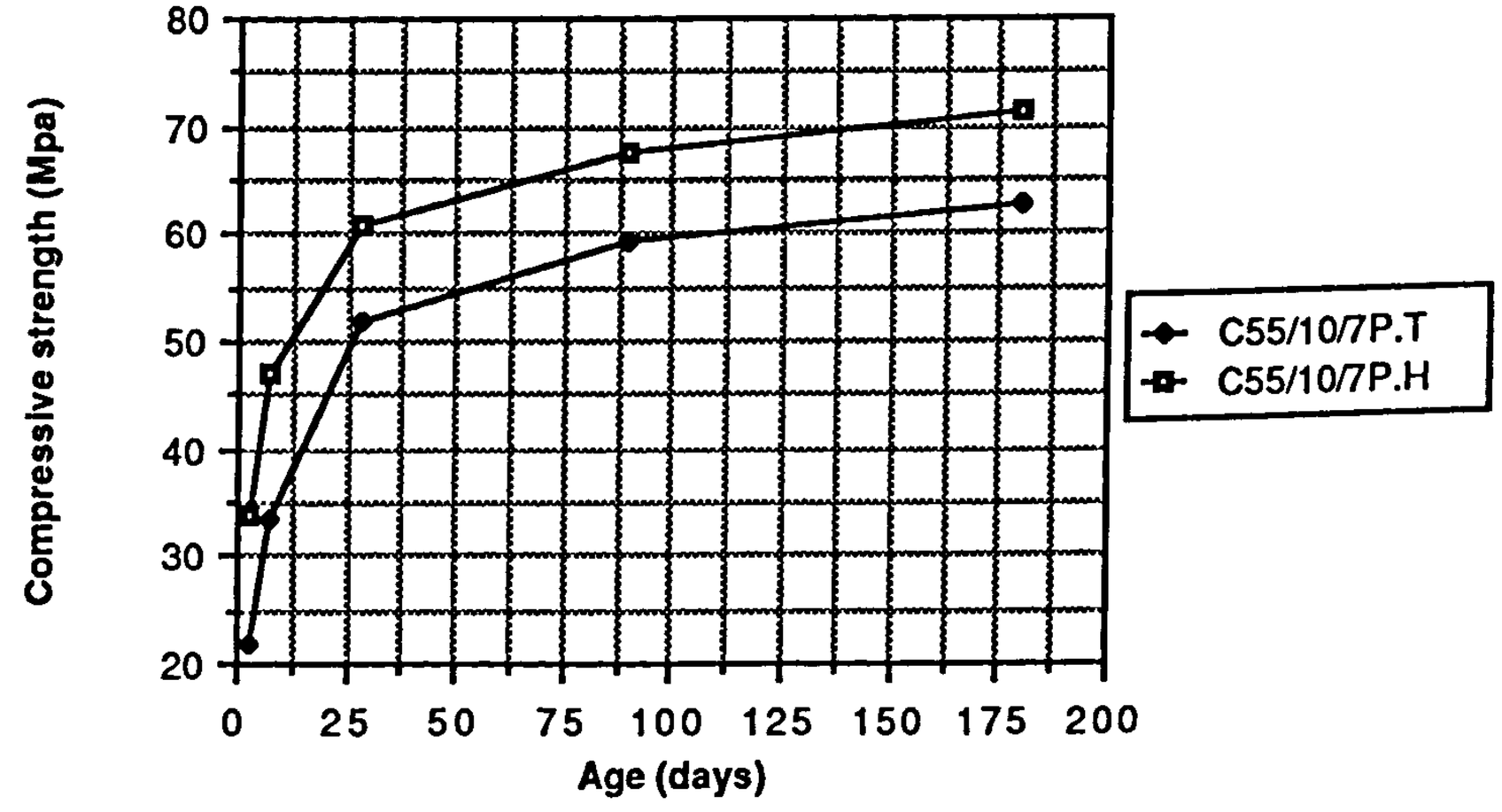

Figure A1.6 Effect of temperate and hot curing on the compressive strength of CSF mixes grade C55

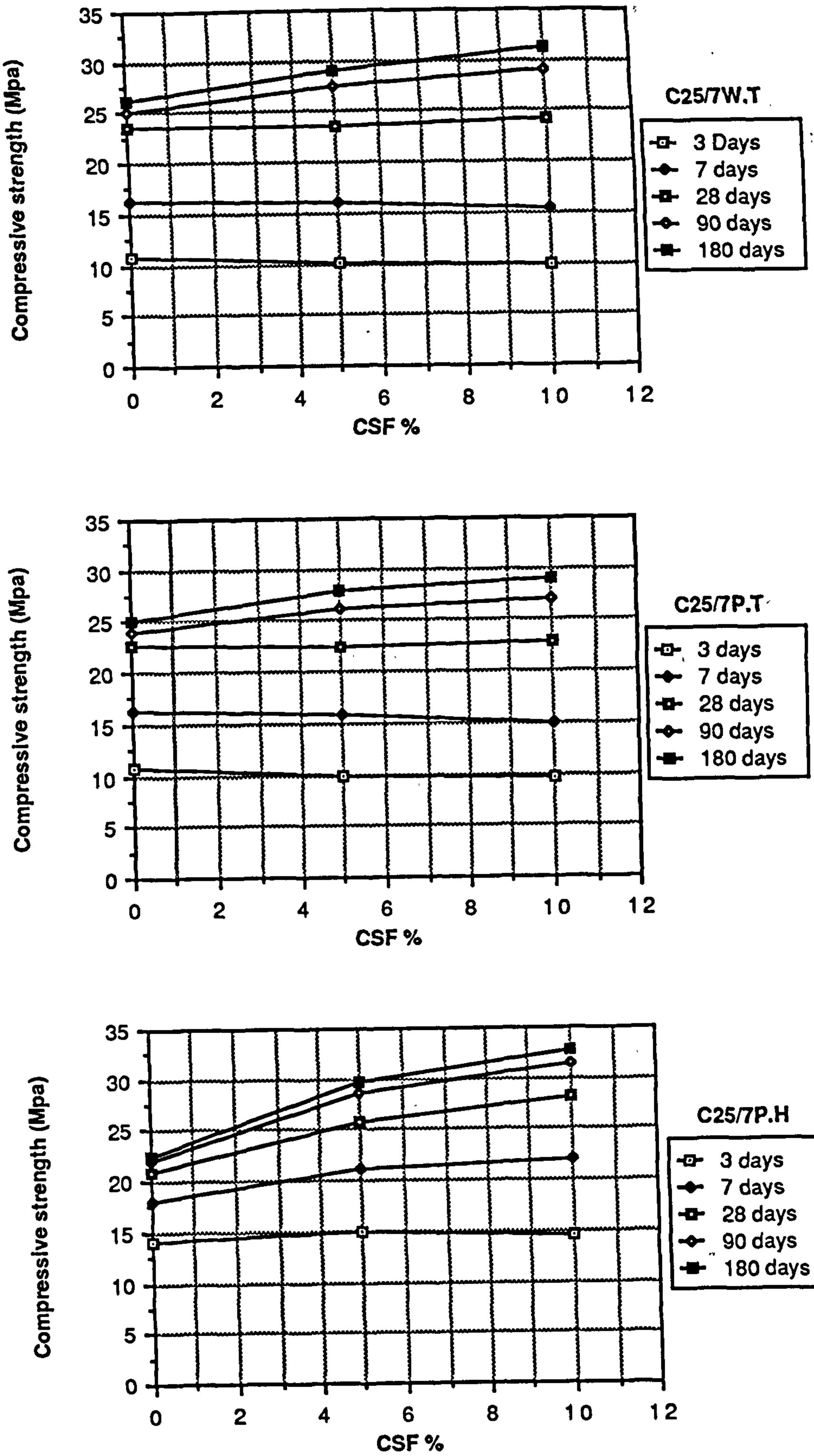

Figure A1.7 Effect of CSF content on the compressive strength of CSF concrete mixes grade C25

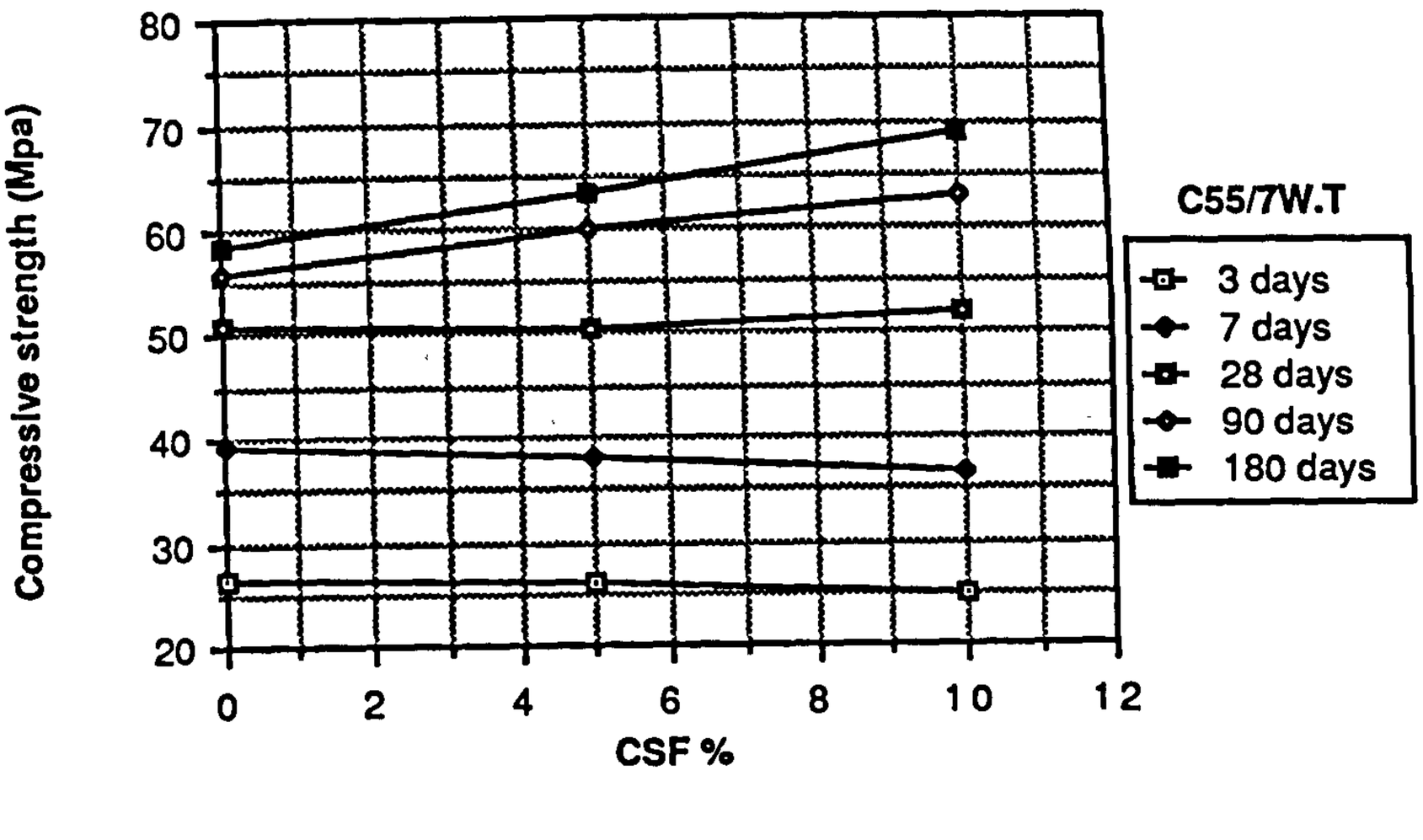

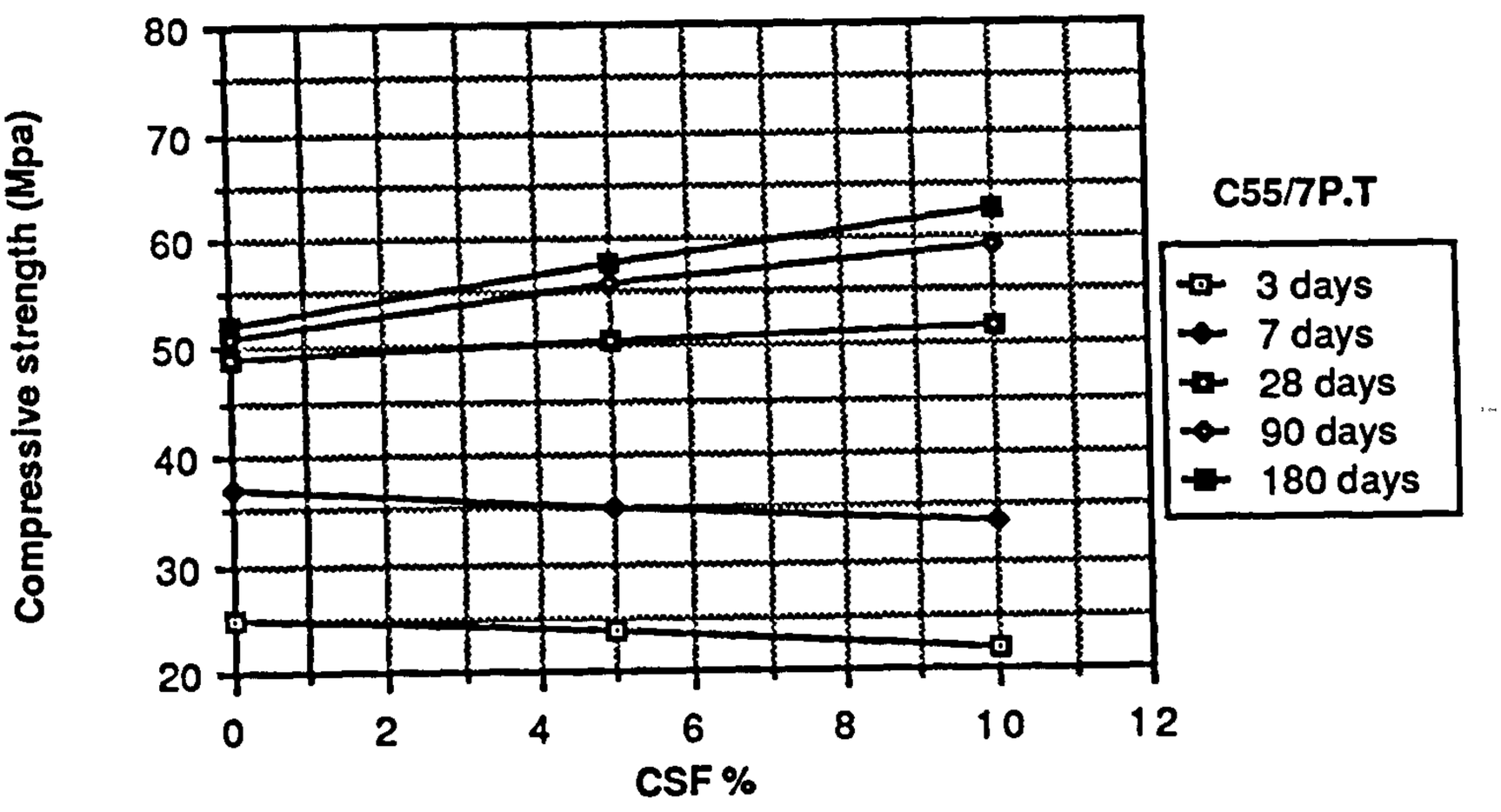

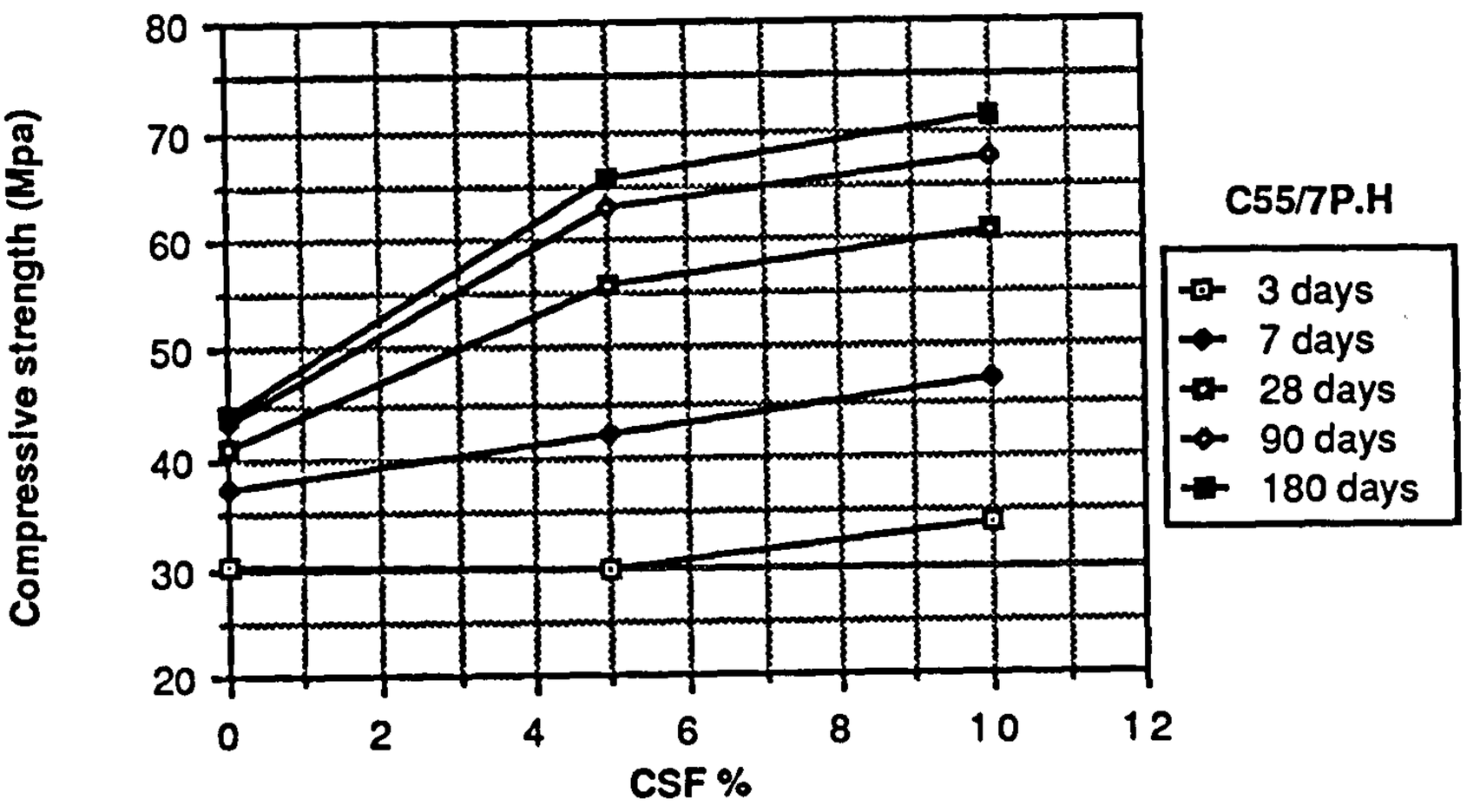

Figure A1.8 Effect of CSF content on the compressive strength of CSF concrete mixes grade C55

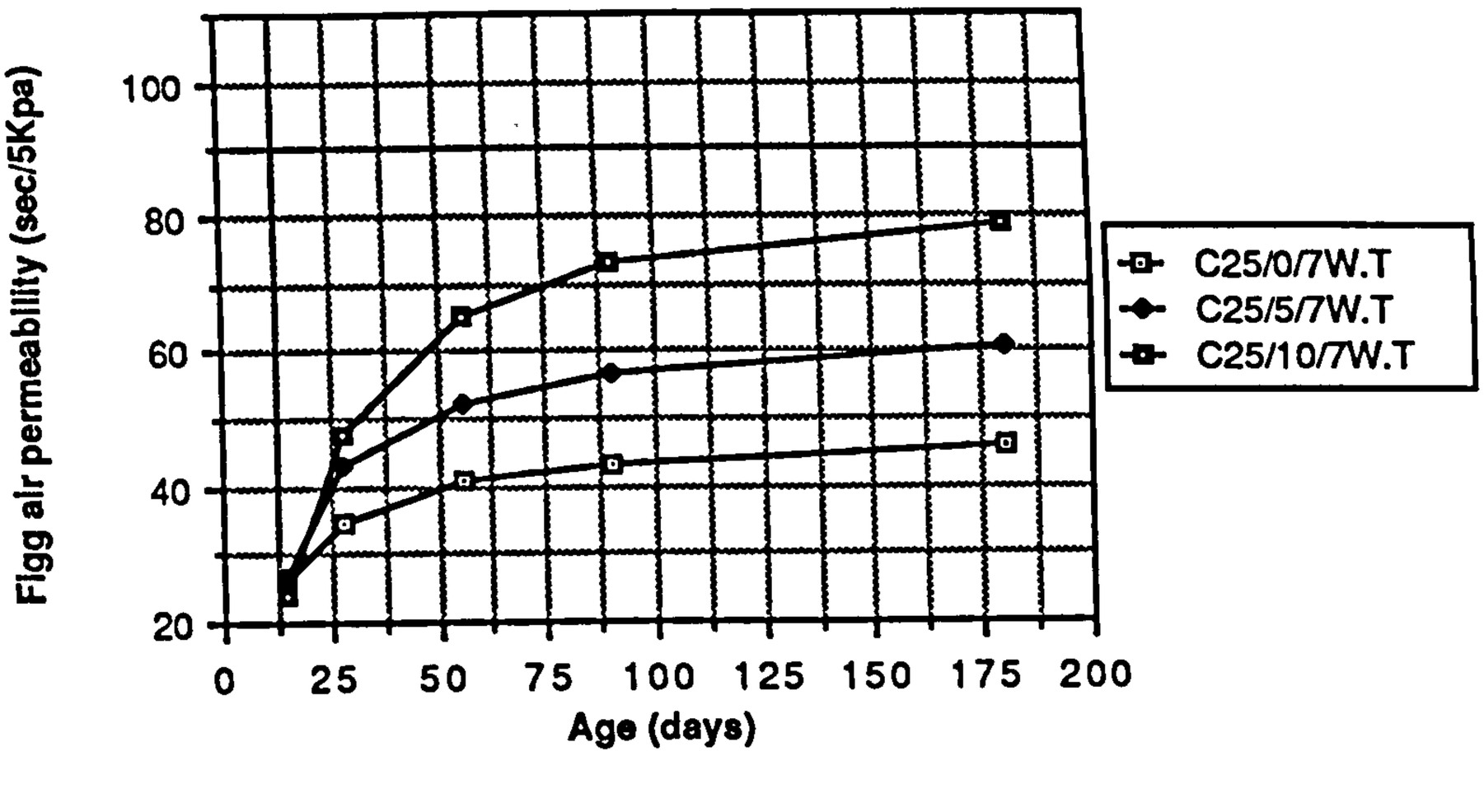

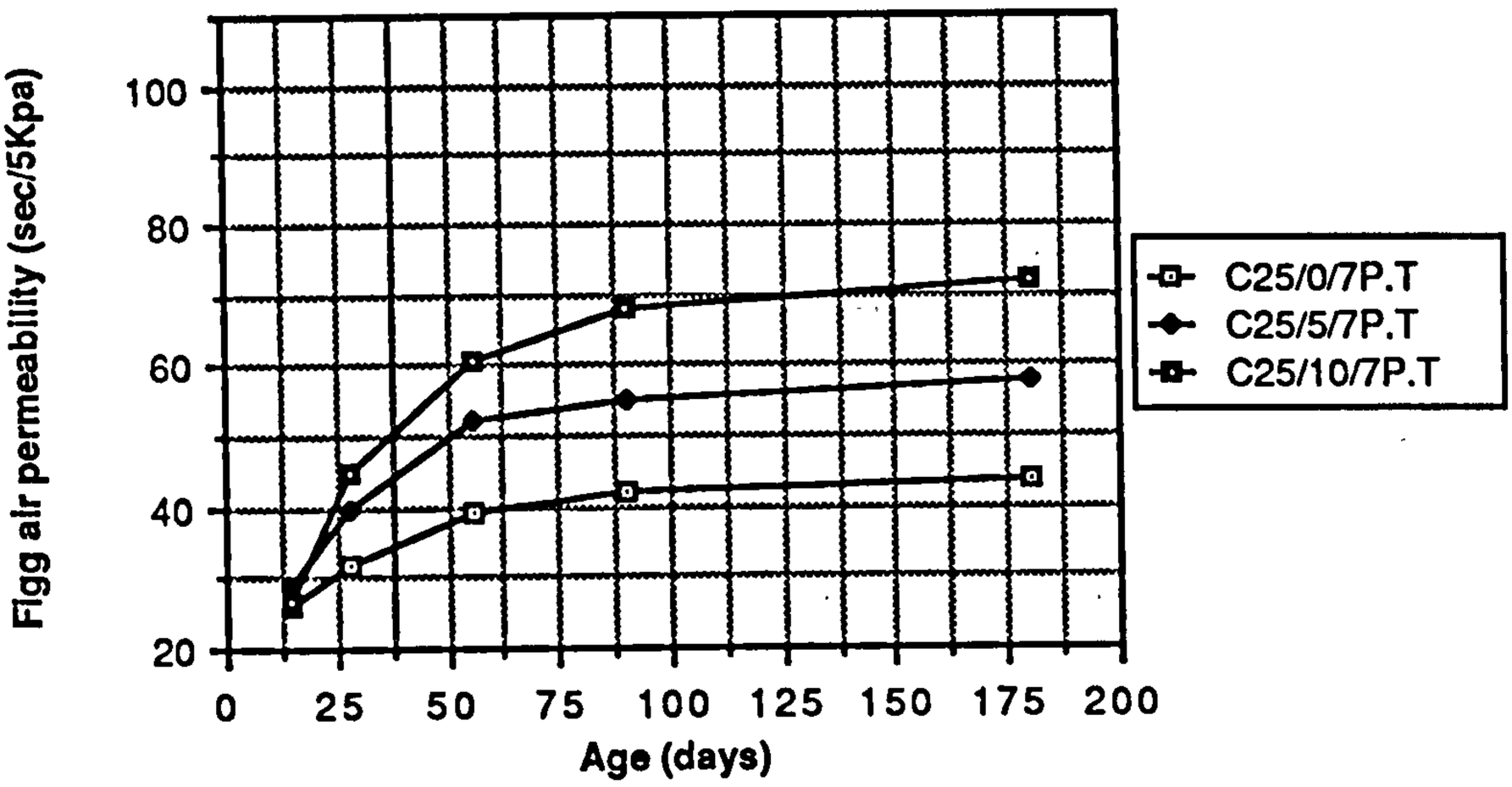

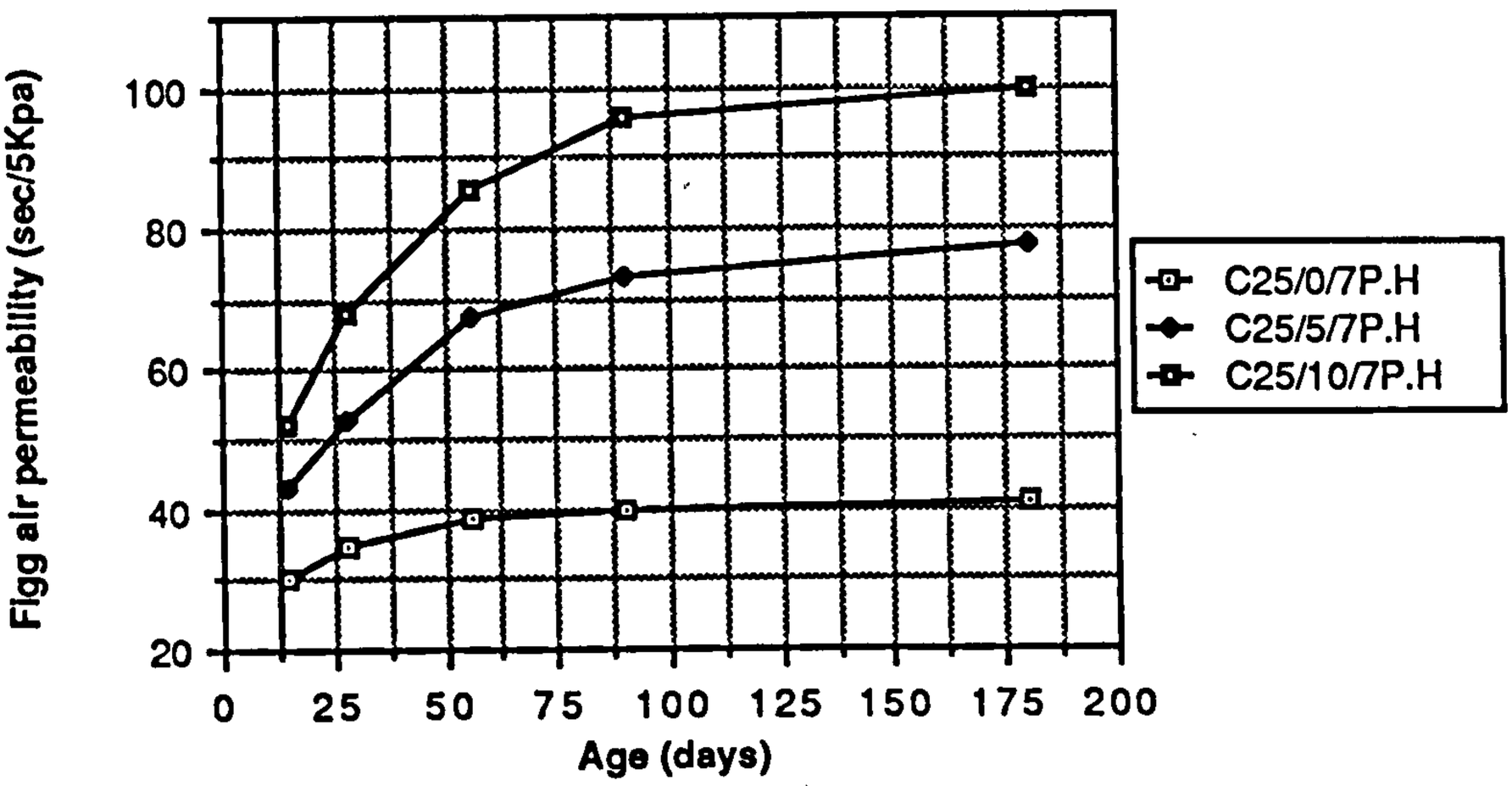

Figure A1.9 Relationship between age and Figg air permeability of plain and CSF mixes grade C25

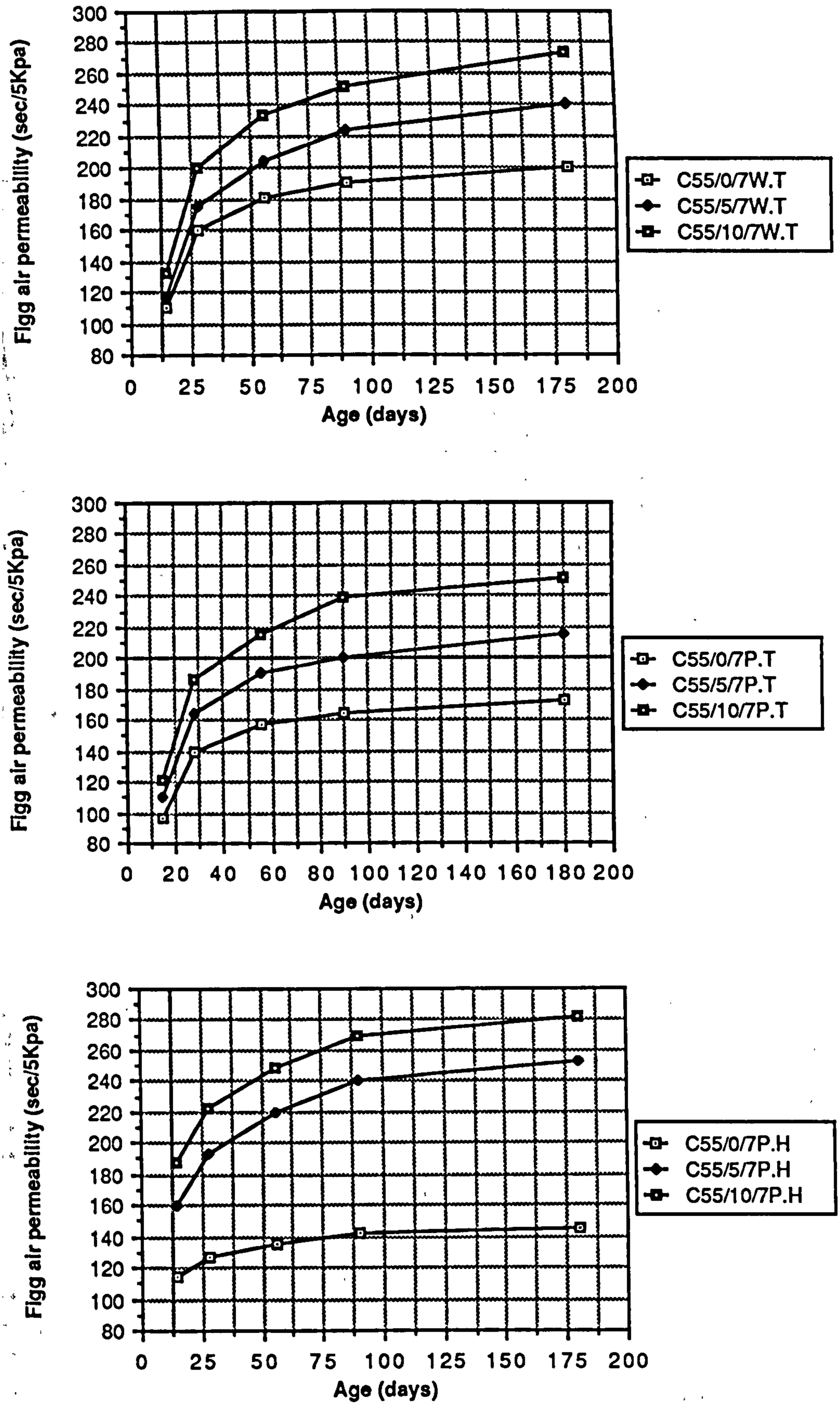

Figure A1.10 Relationship between age and Figg air permeability of CSF concrete mixes grade C55

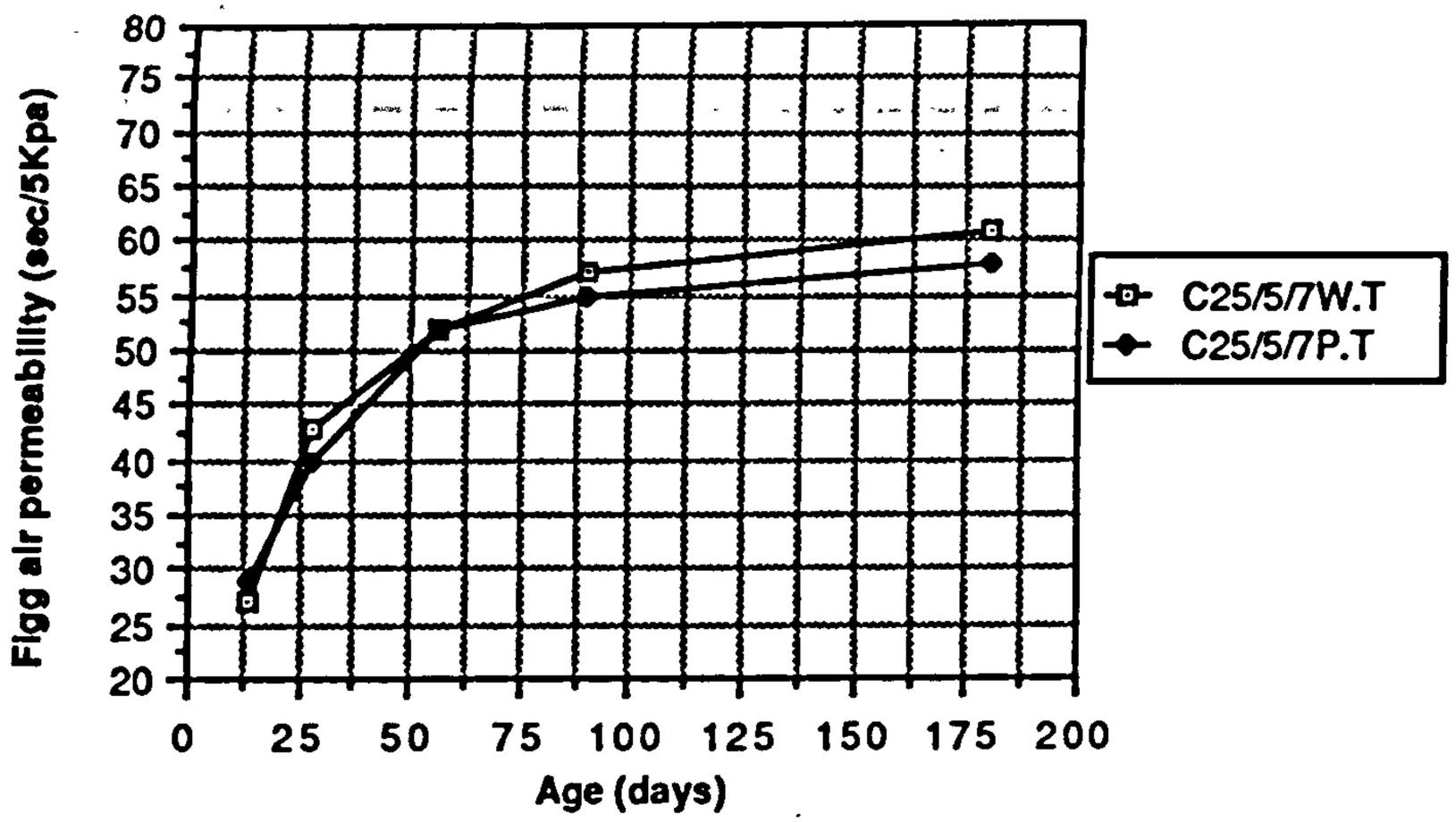

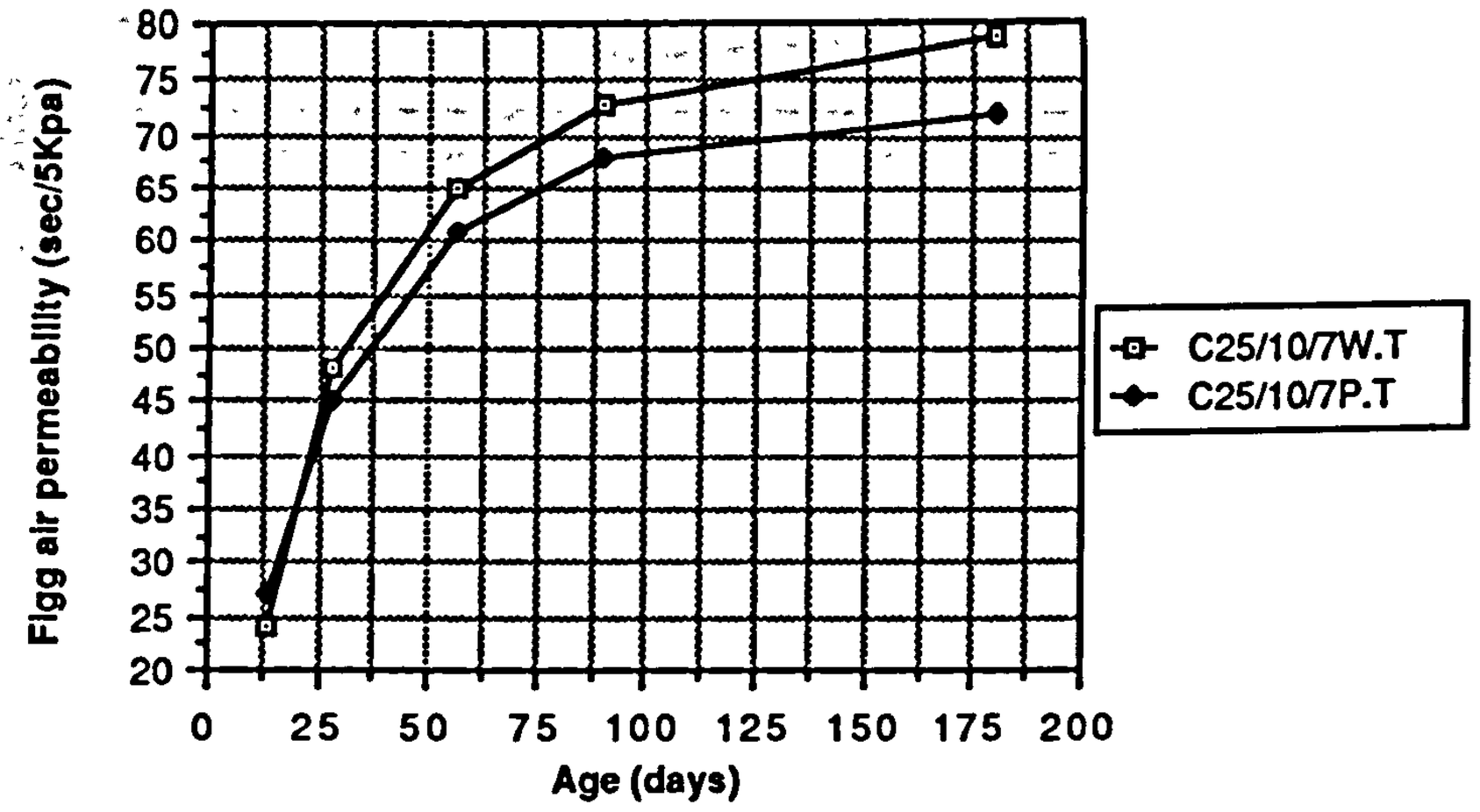

Figure A1.11 Effect of water and polythene curing on Figg air permeability of CSF concrete mixes grade C25

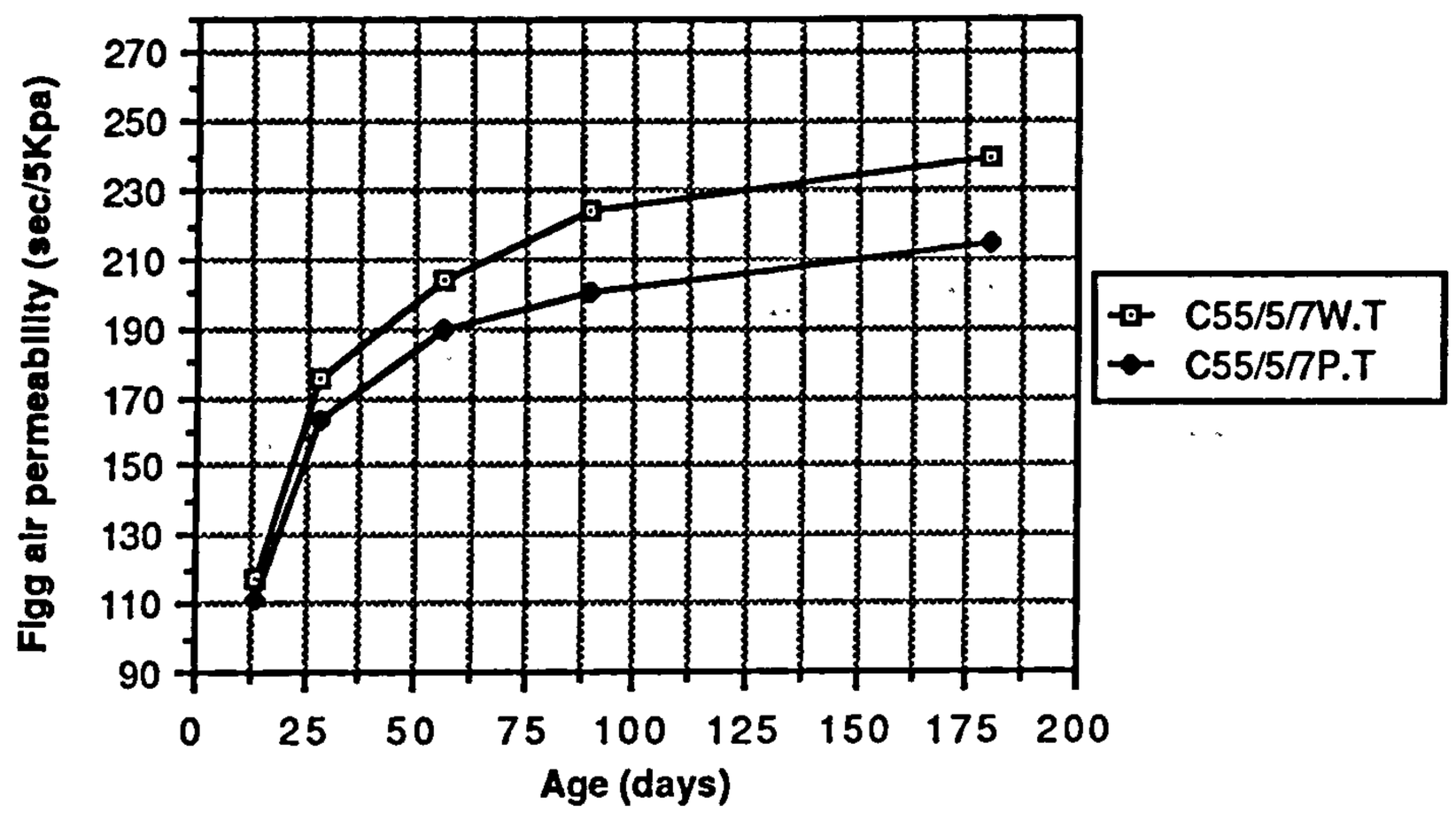

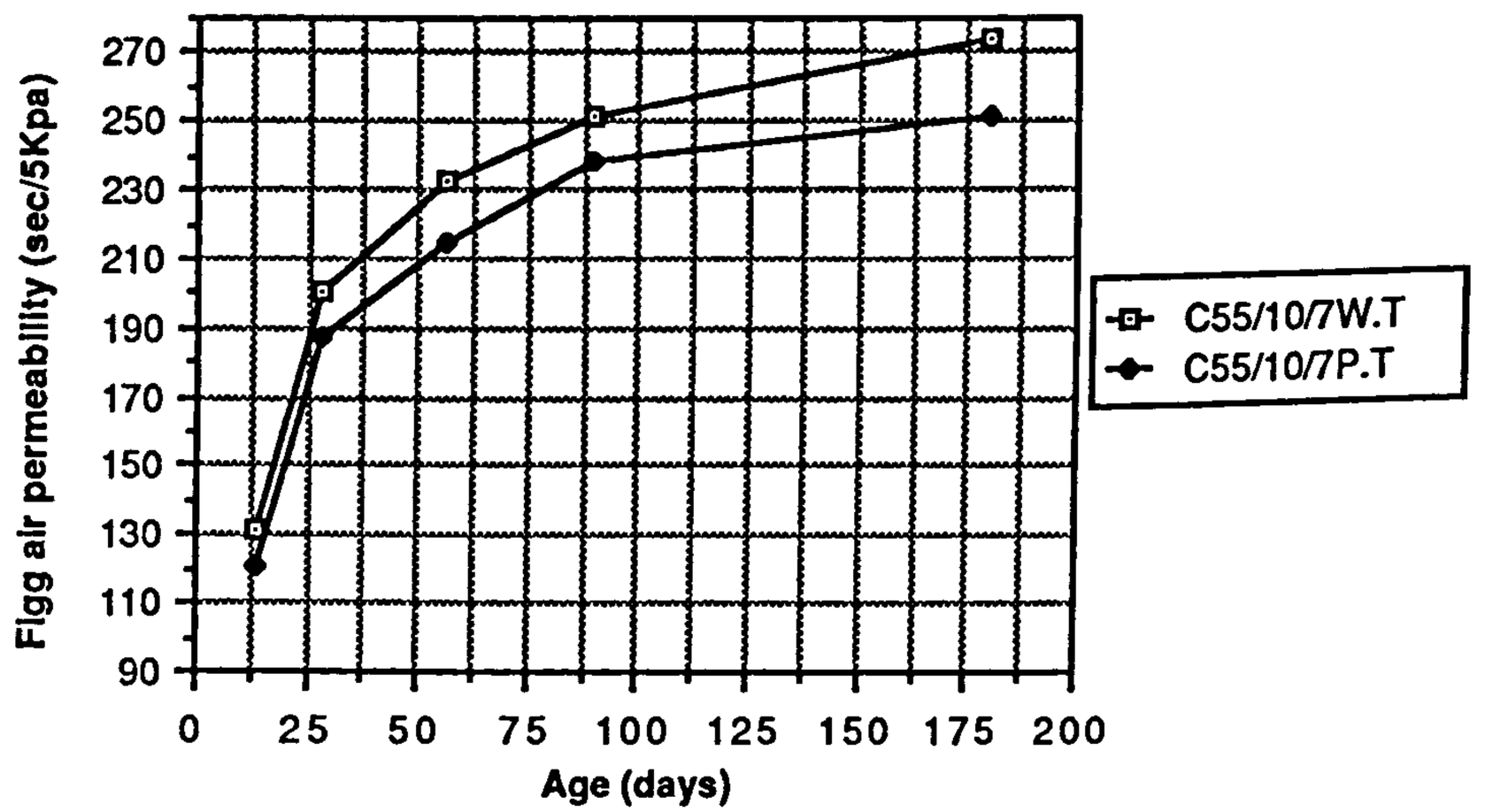

Figure A1.12 Effect of water nad polythene curing on Figg air permeability of CSF concrete mixes grade C55

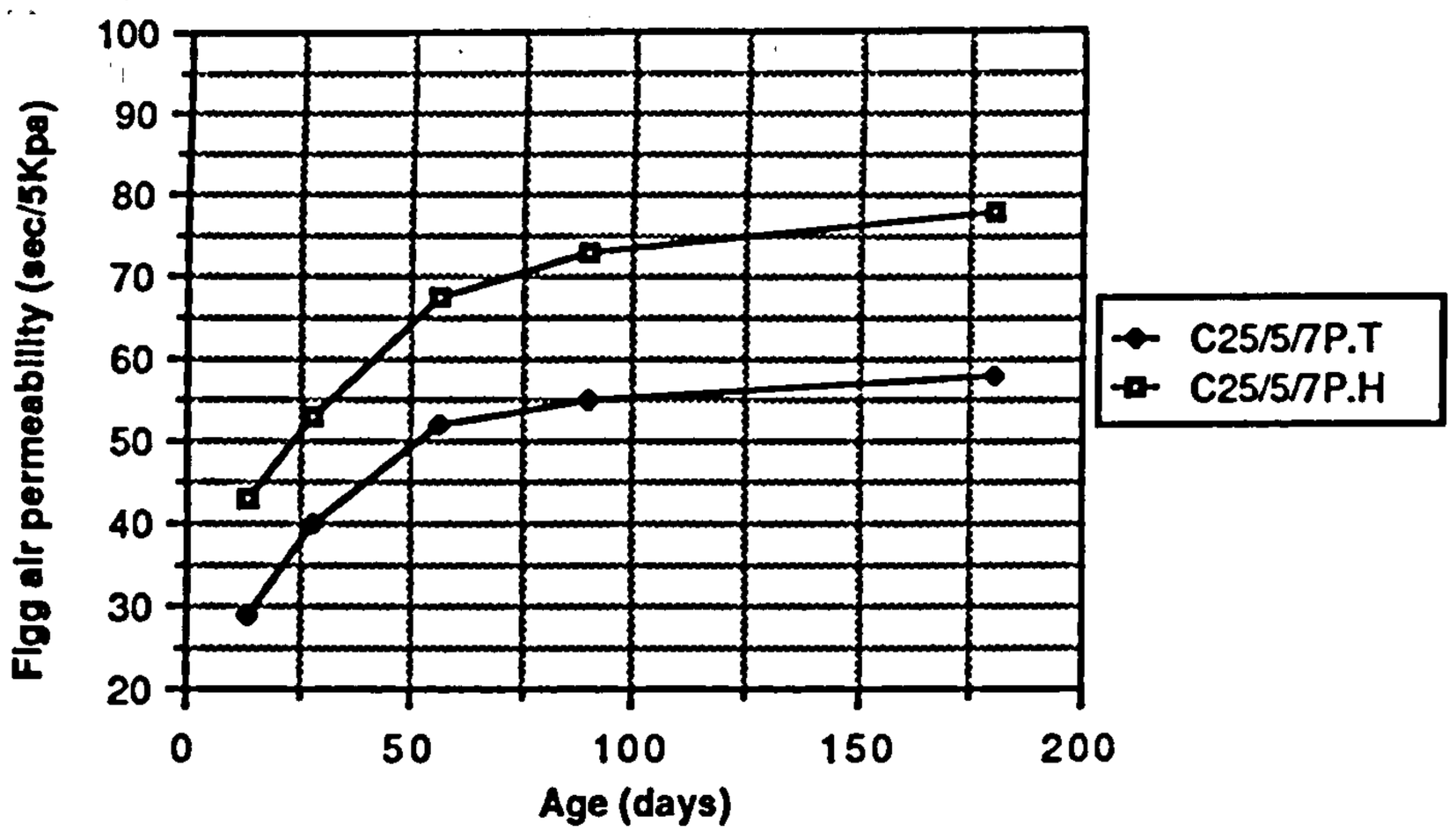

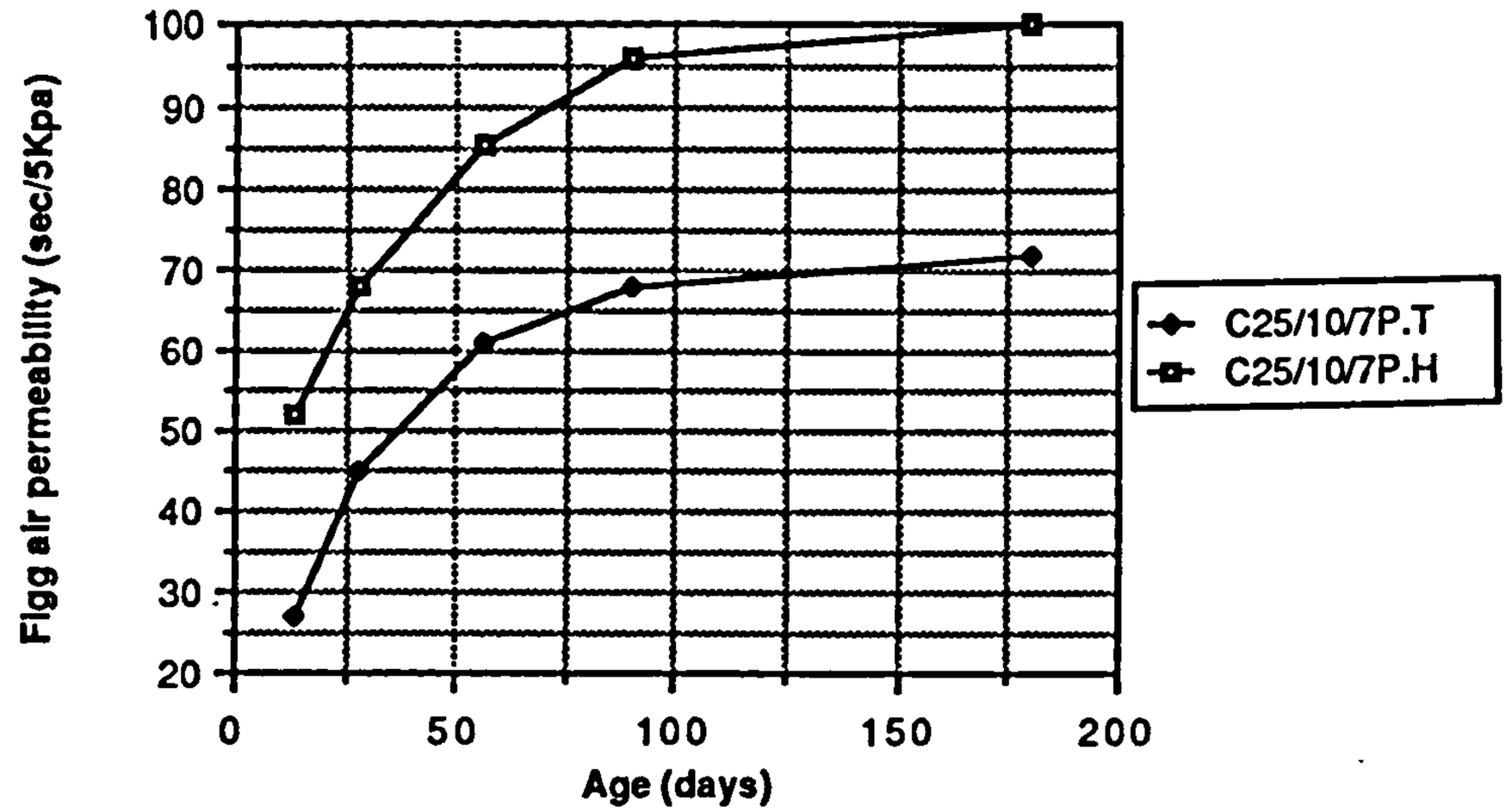

Figure A1.13 Effect of temperate and hot curing on Figg air permeability of CSF concrete mixes grade C25

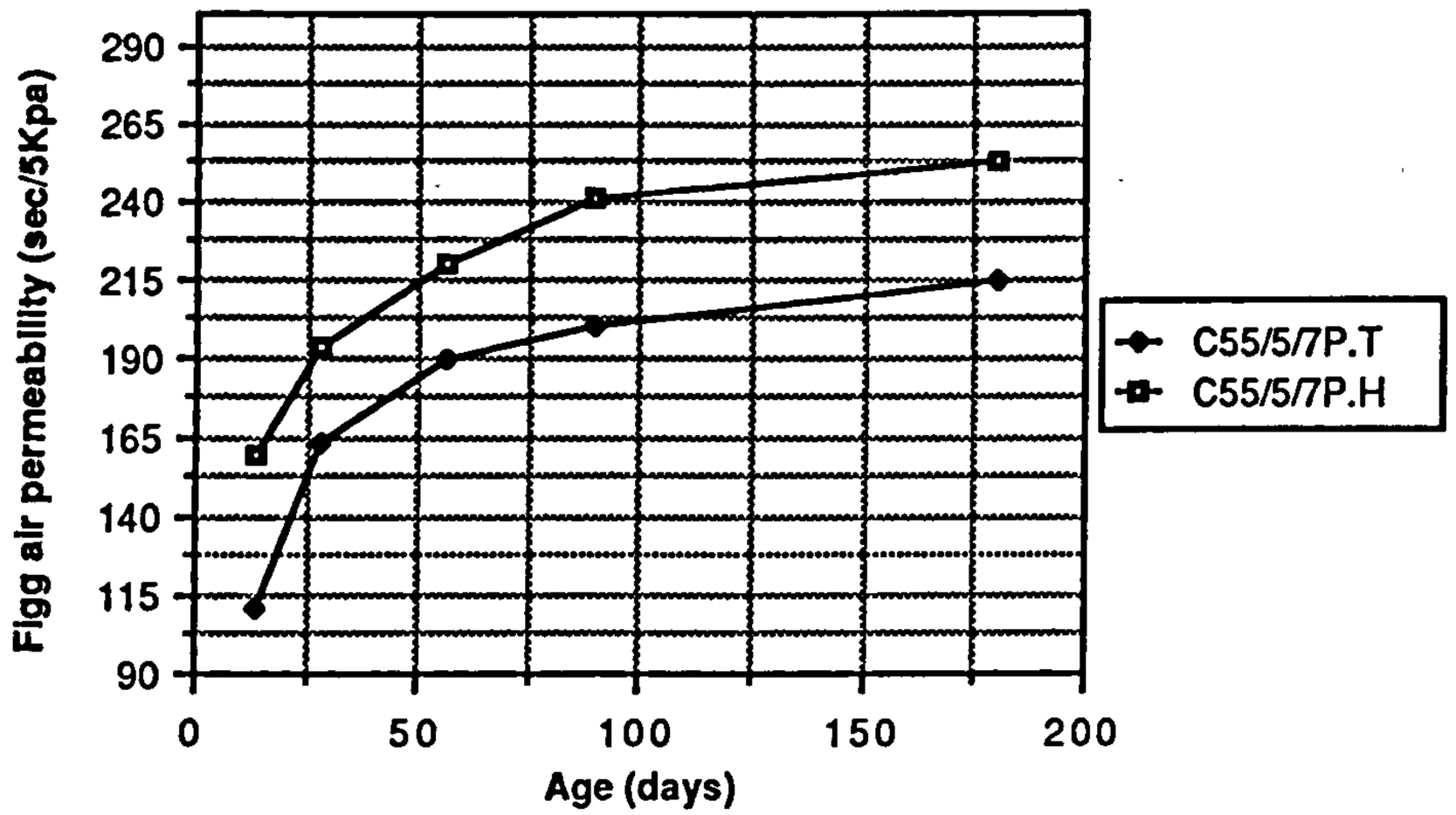

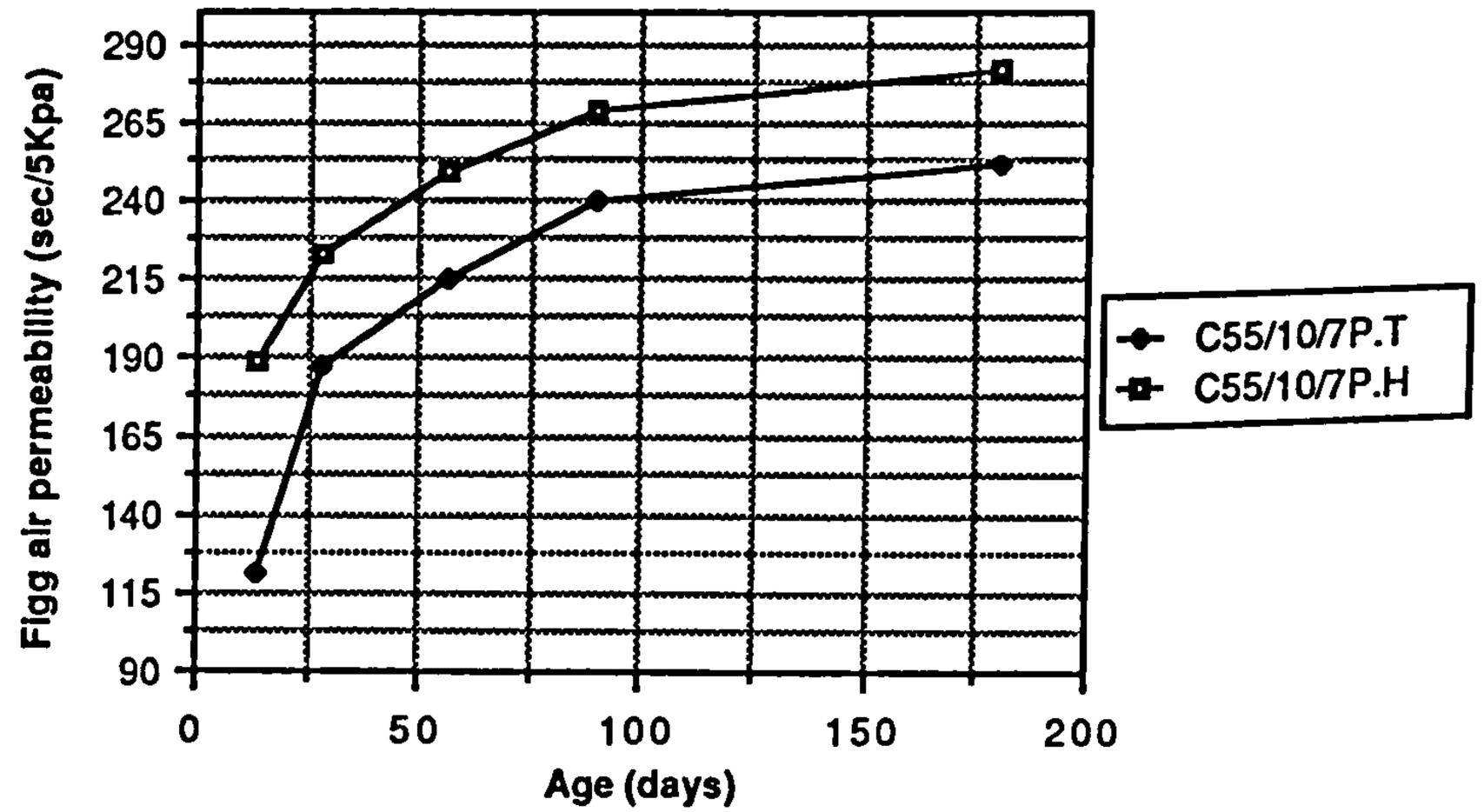

Figure A1.14 Effect of temperate and hot curing on Figg air permeability of CSF concrete mixes grade C55

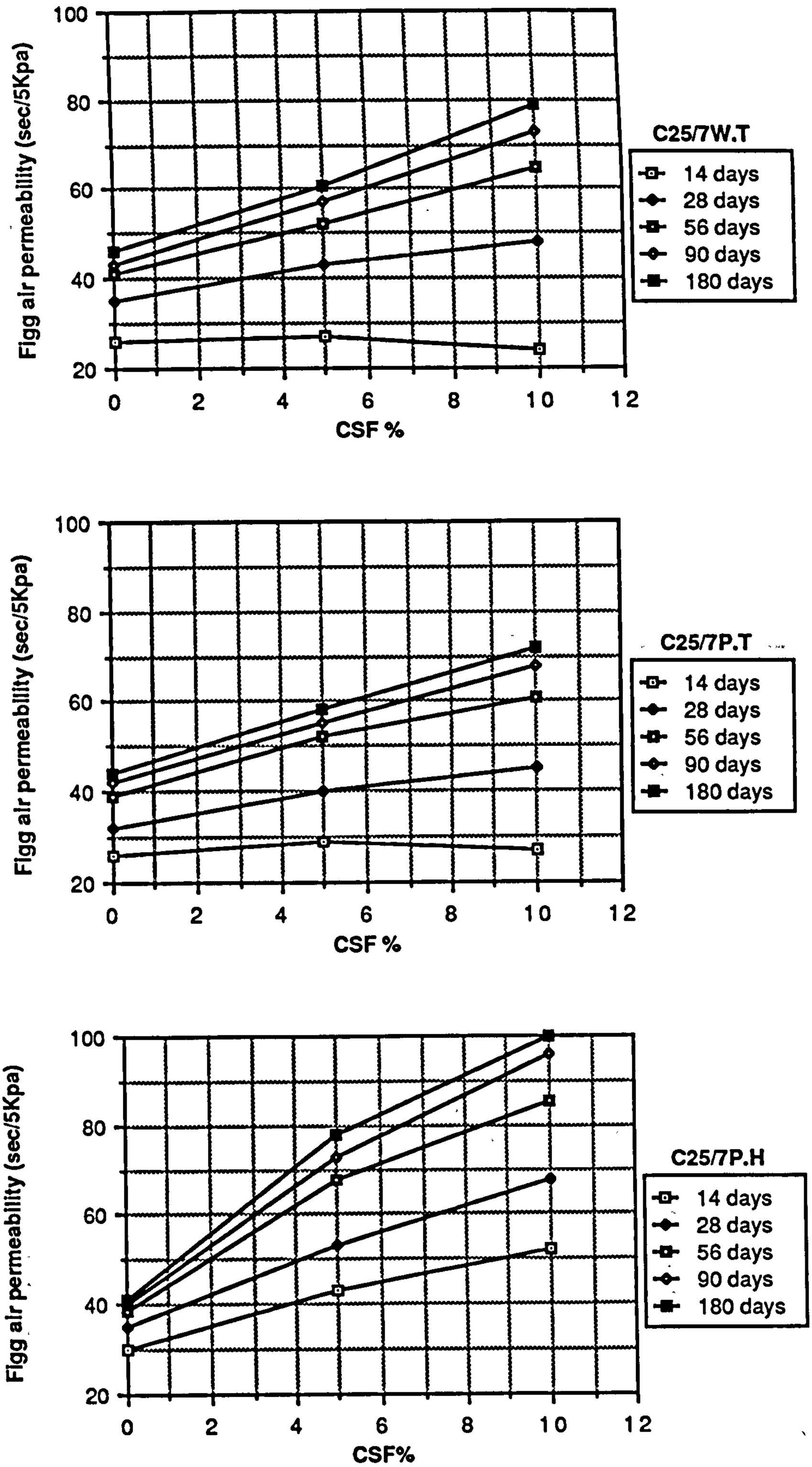

Figure A1.15 Effect of CSF content on Figg air permeability of CSF concrete mixes grade C25

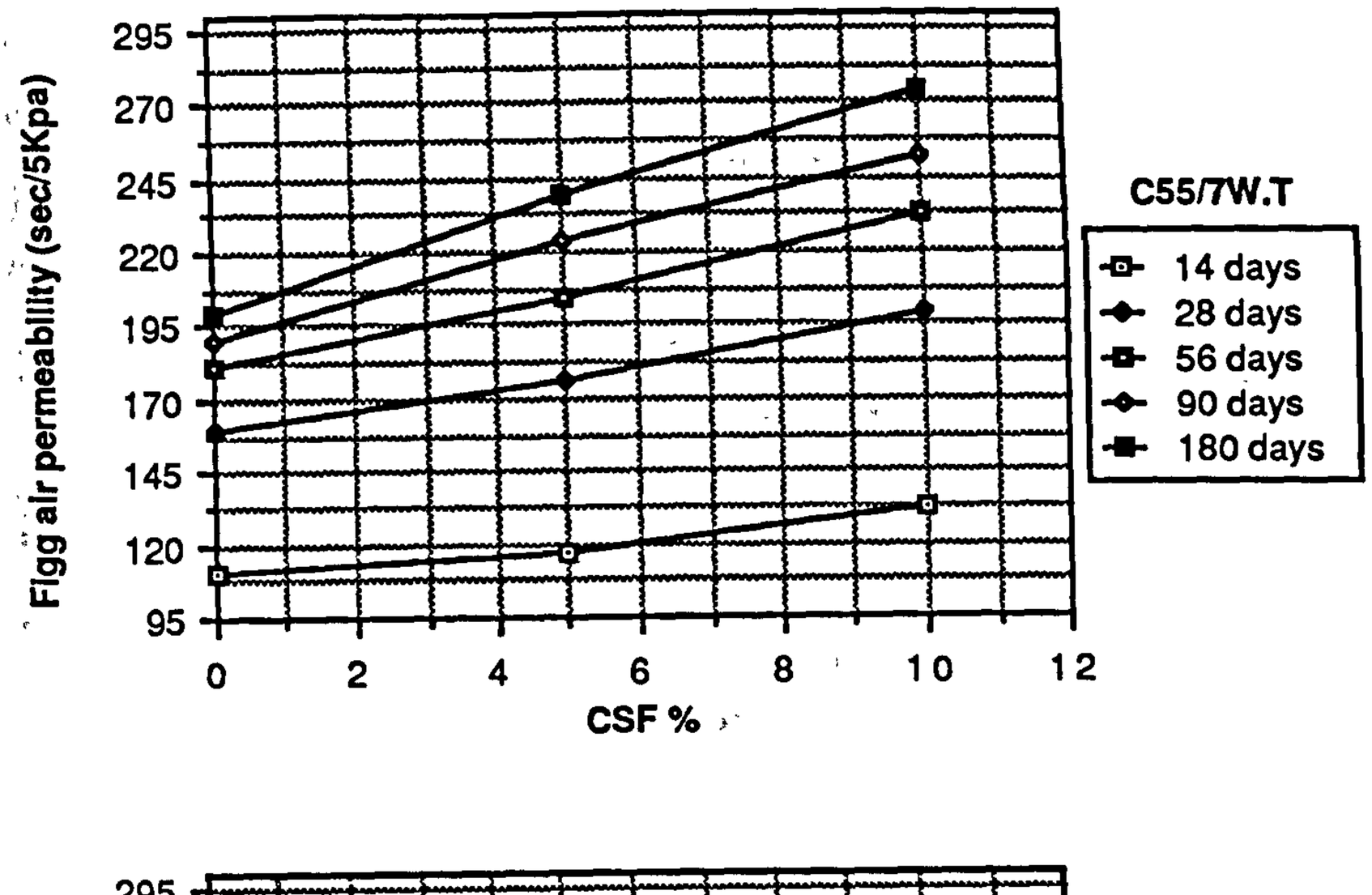

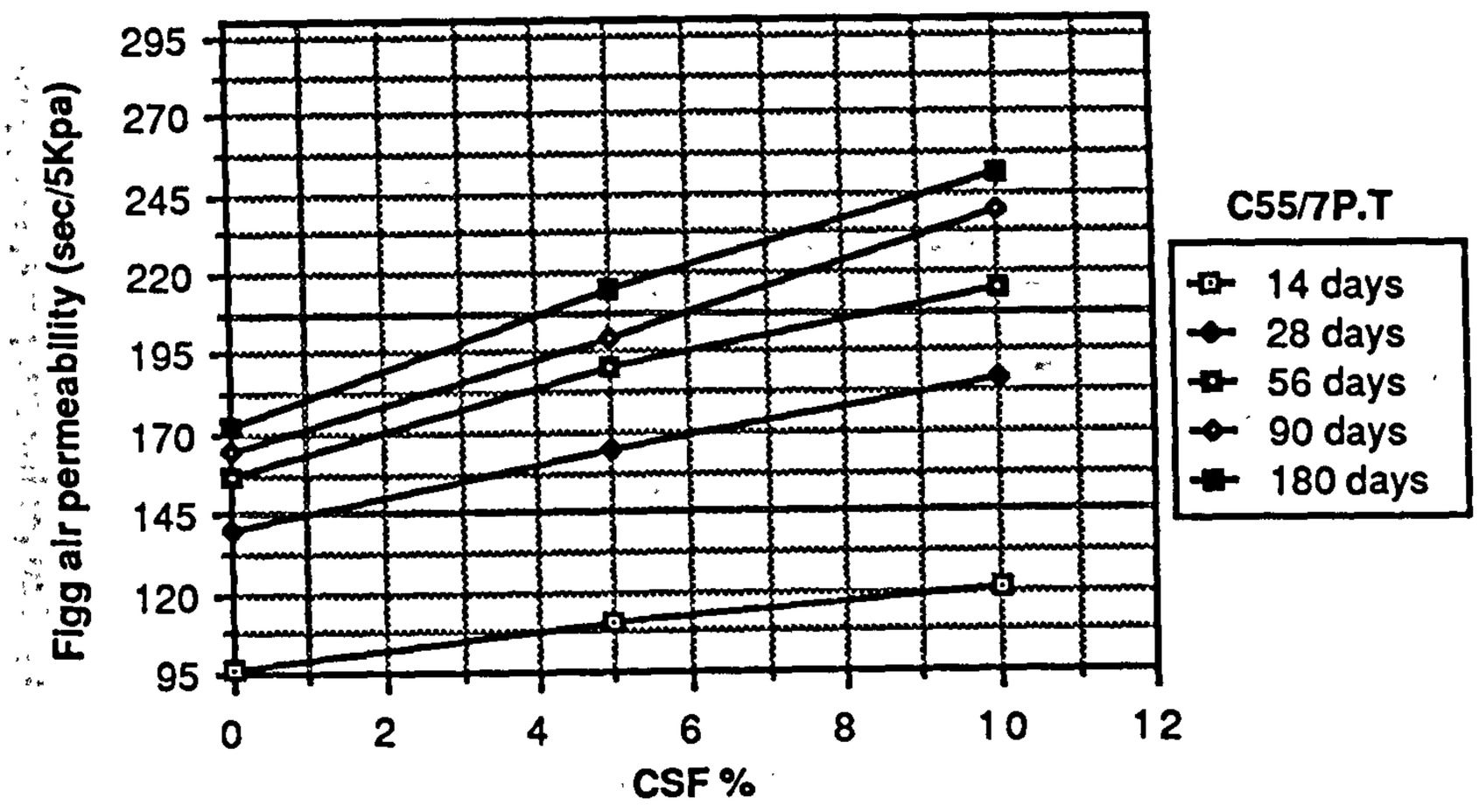

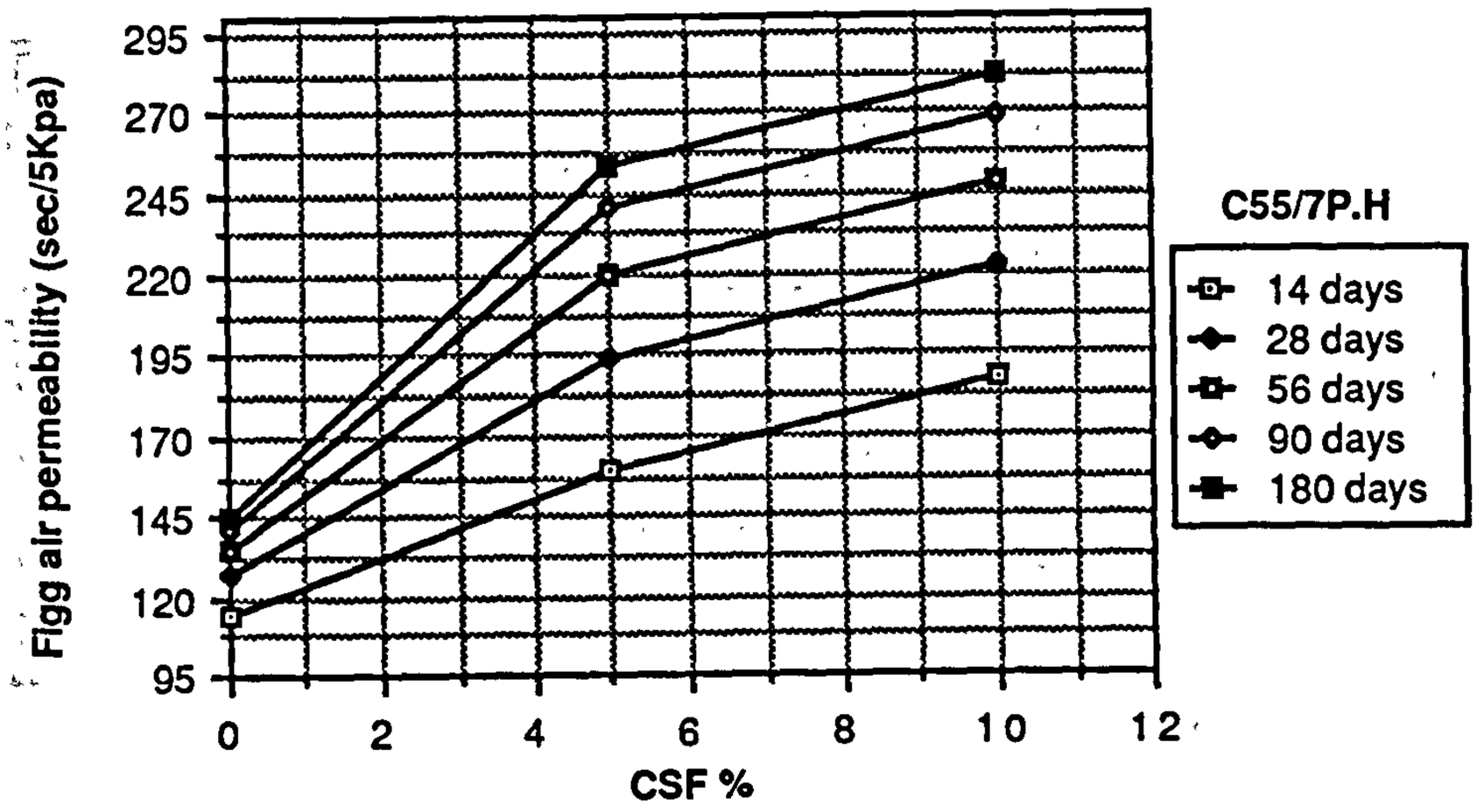

Figure A1.16 Effect of CSF content on Figg air permeability of CSF concrete mixes grade C55

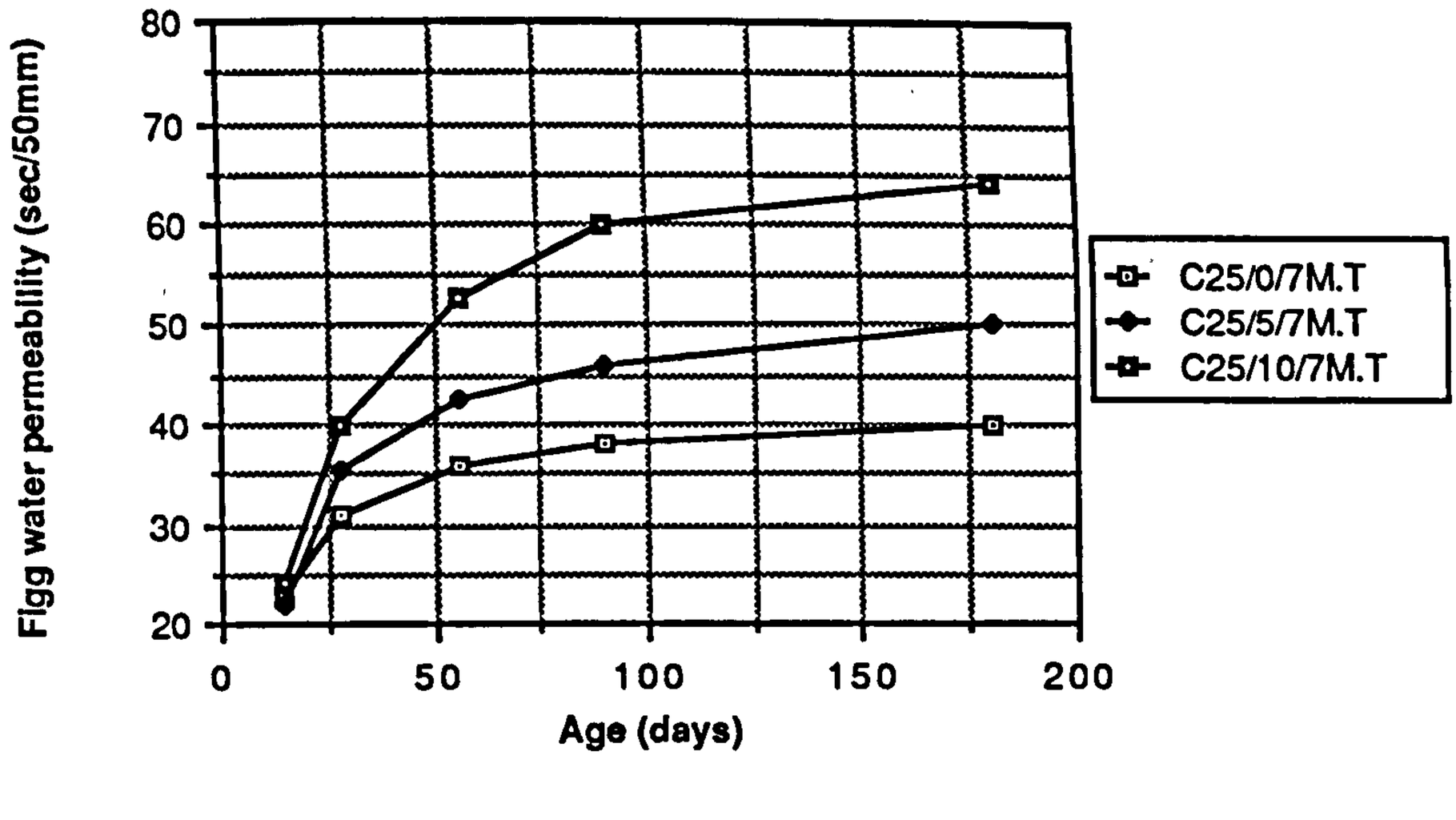

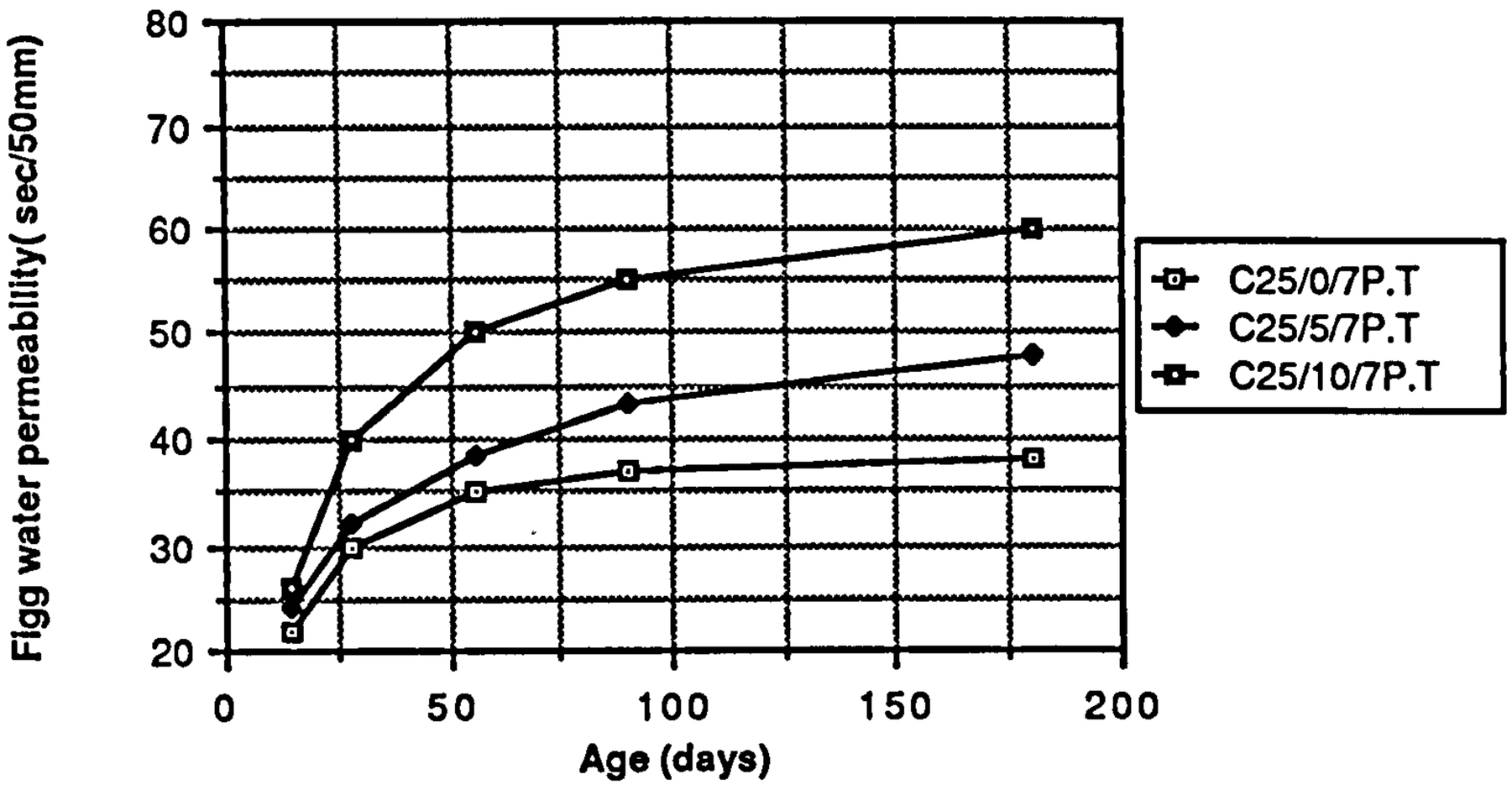

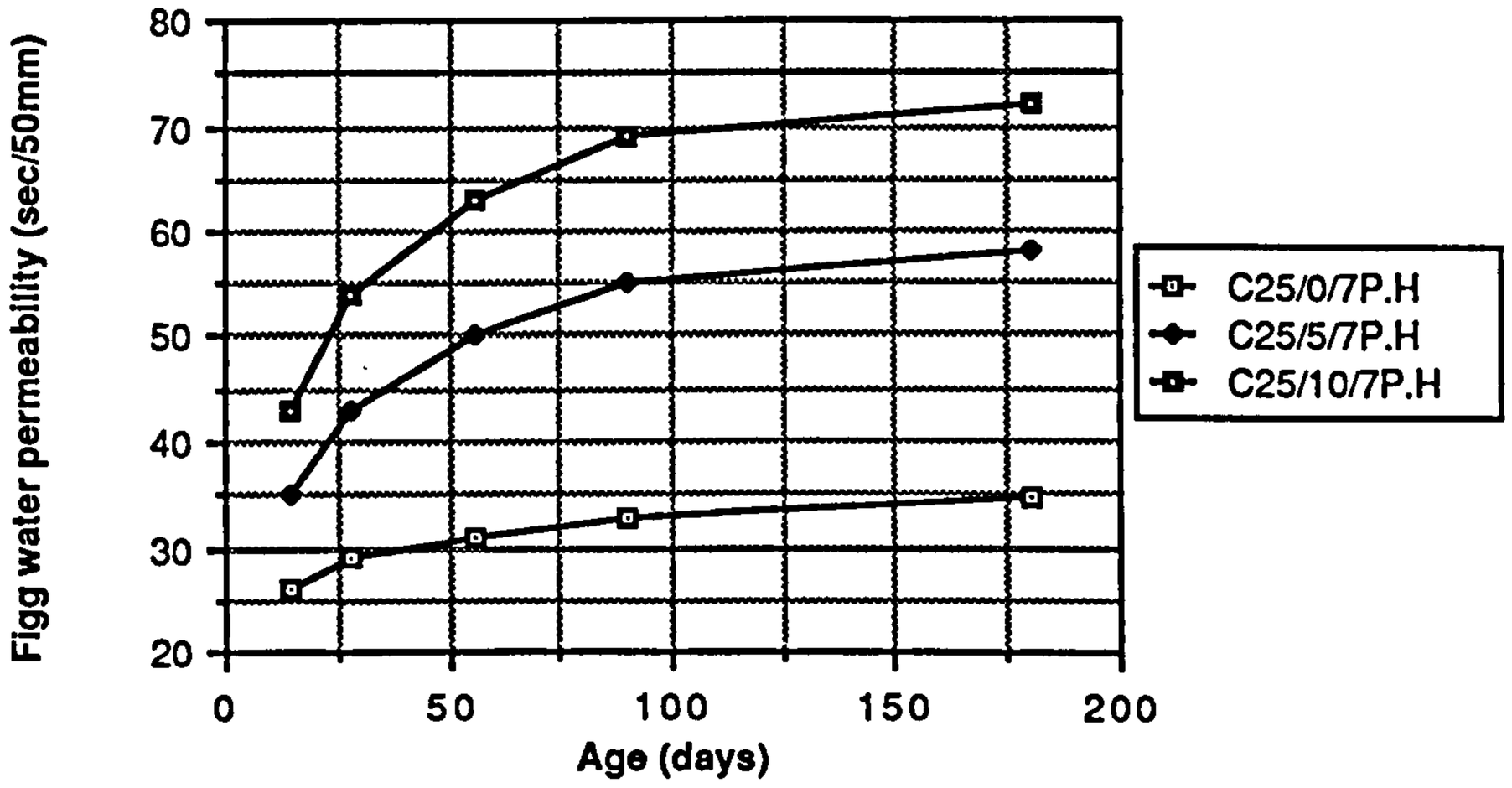

Figure A1.17 Relationship between age and Figg water permeability of CSF concrete mixes grade C25

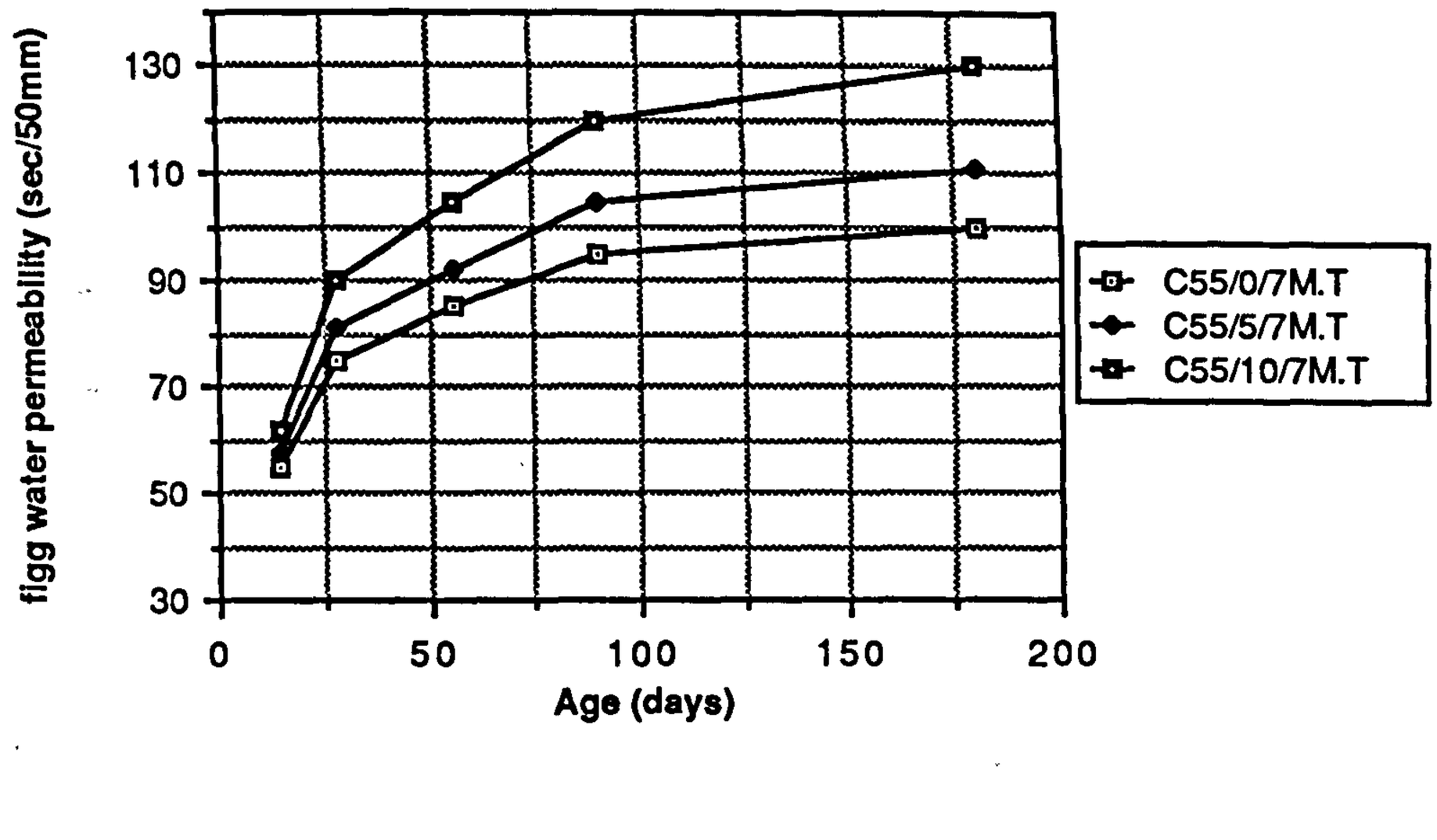

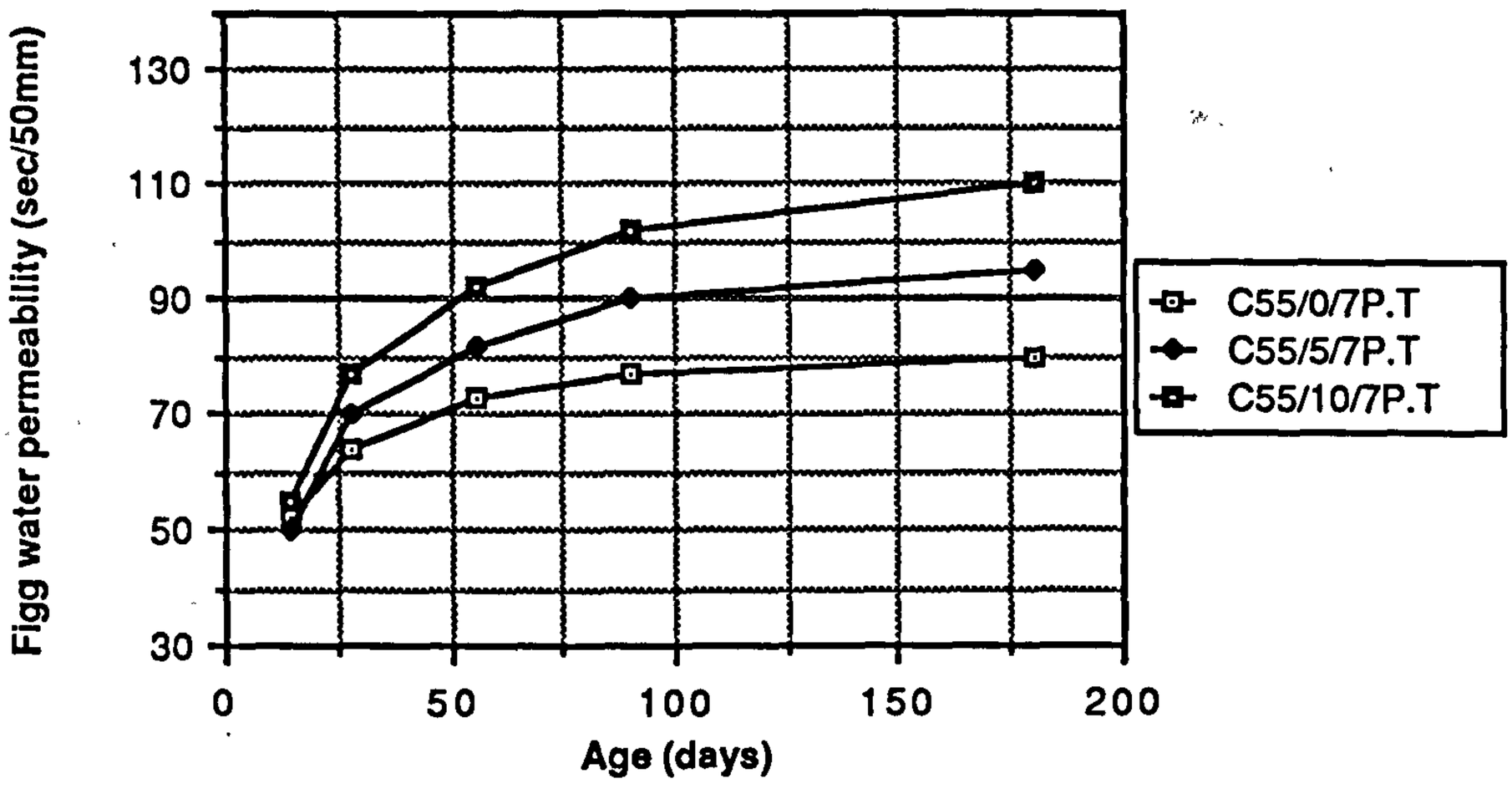

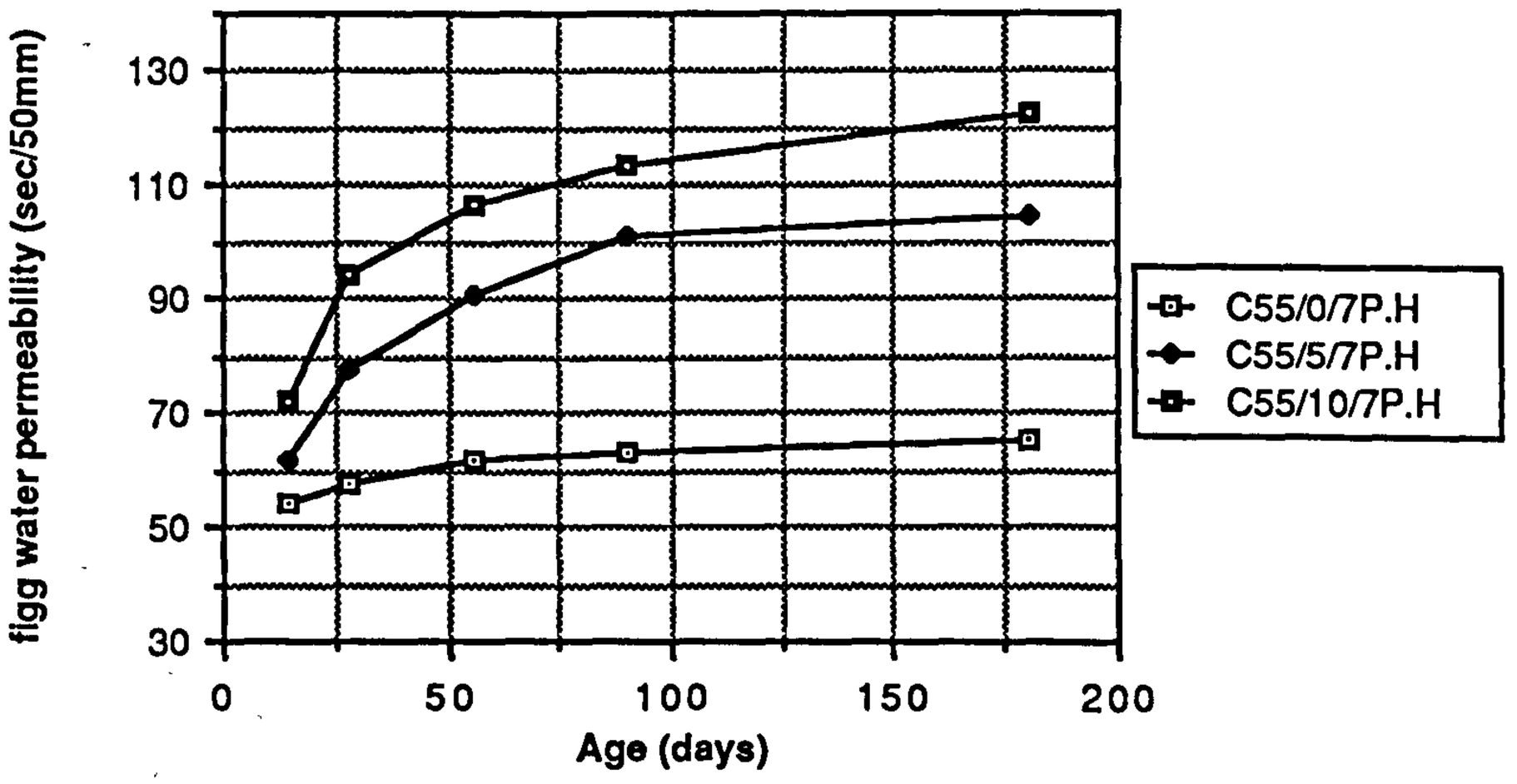

Figure A1.18 Relationship between Age and Figg water permeability of CSF concrete mixes grade C55

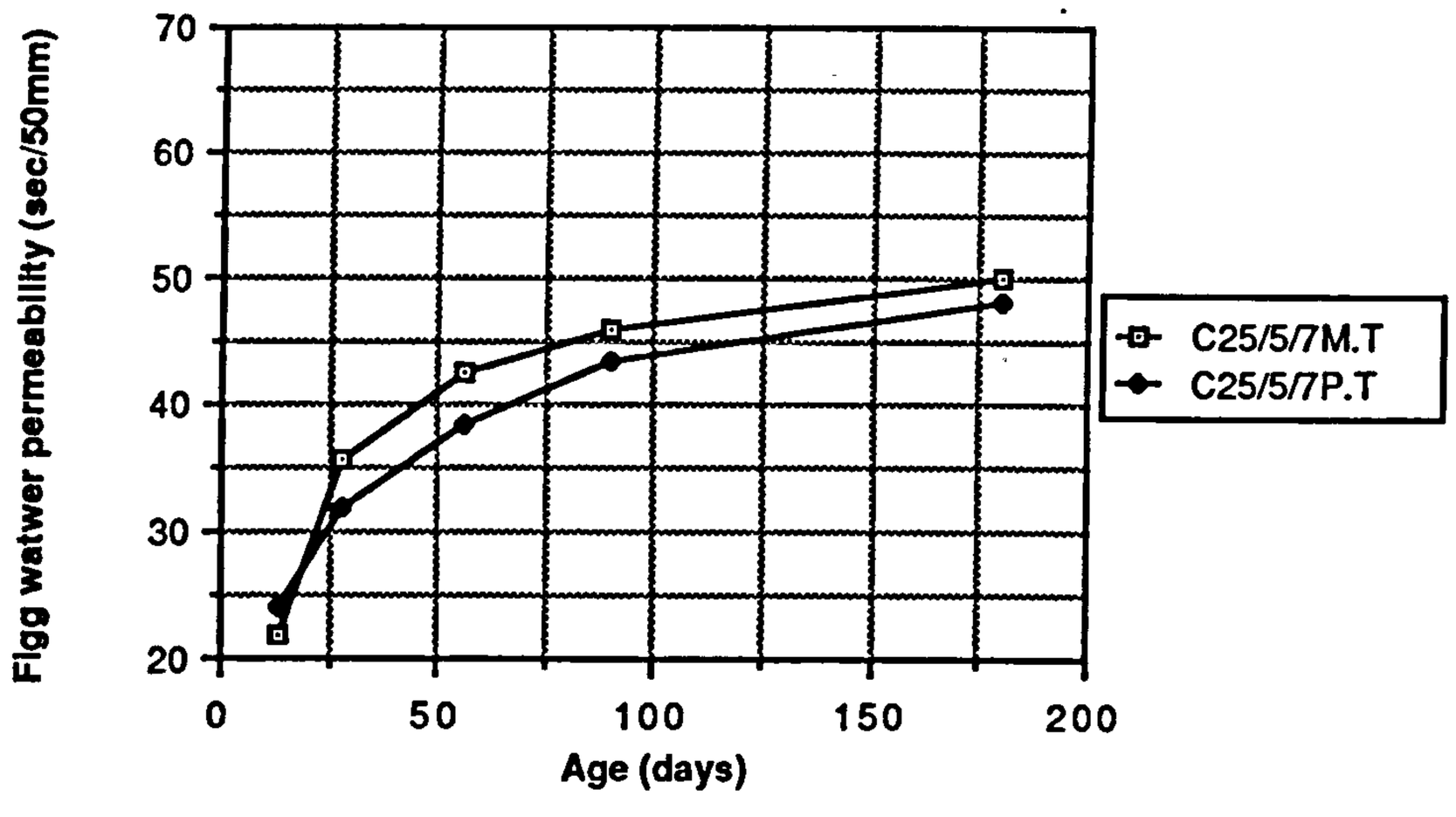

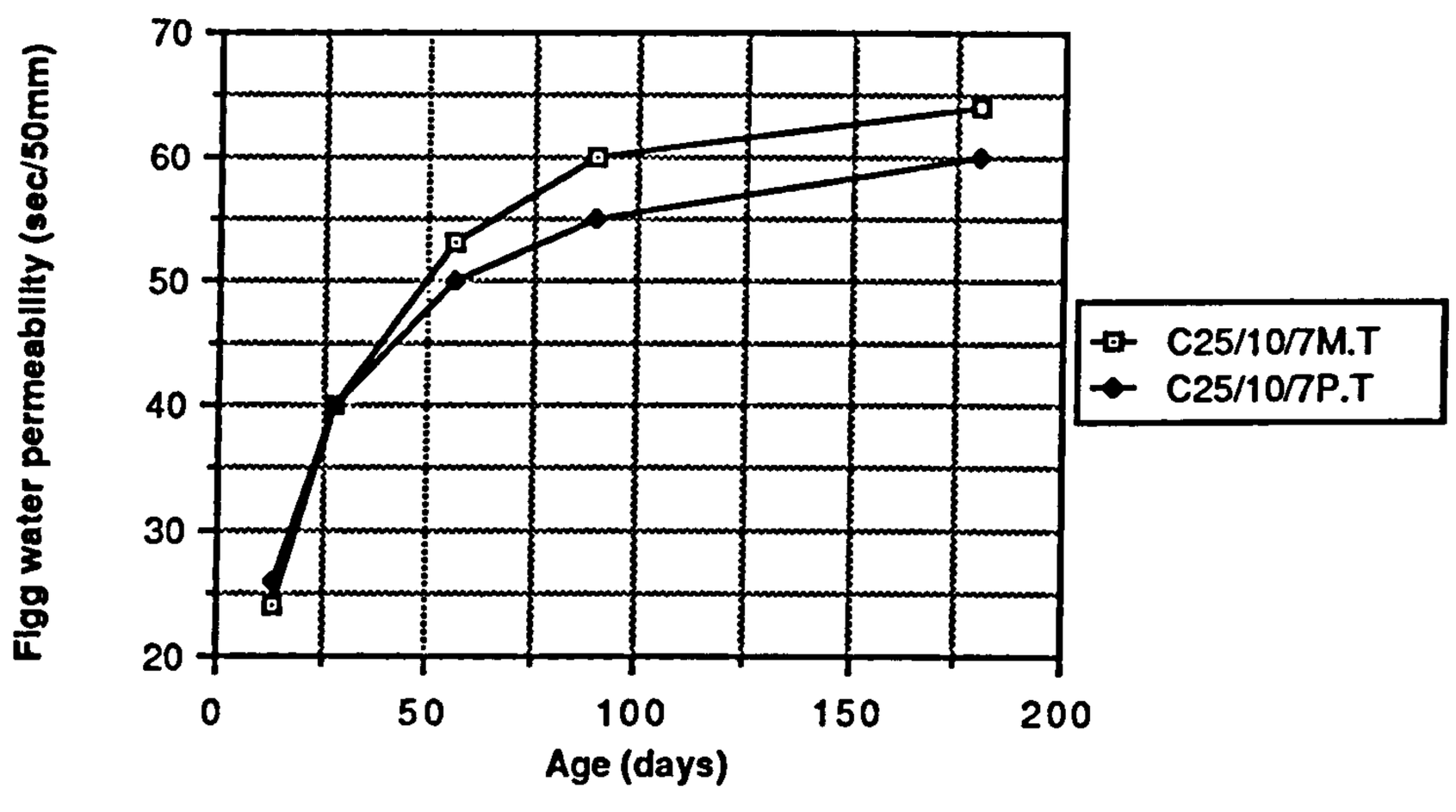

Figure A1.19 Effect of water and polythene curing on Figg water permeability of CSF concrete mixes grade C25

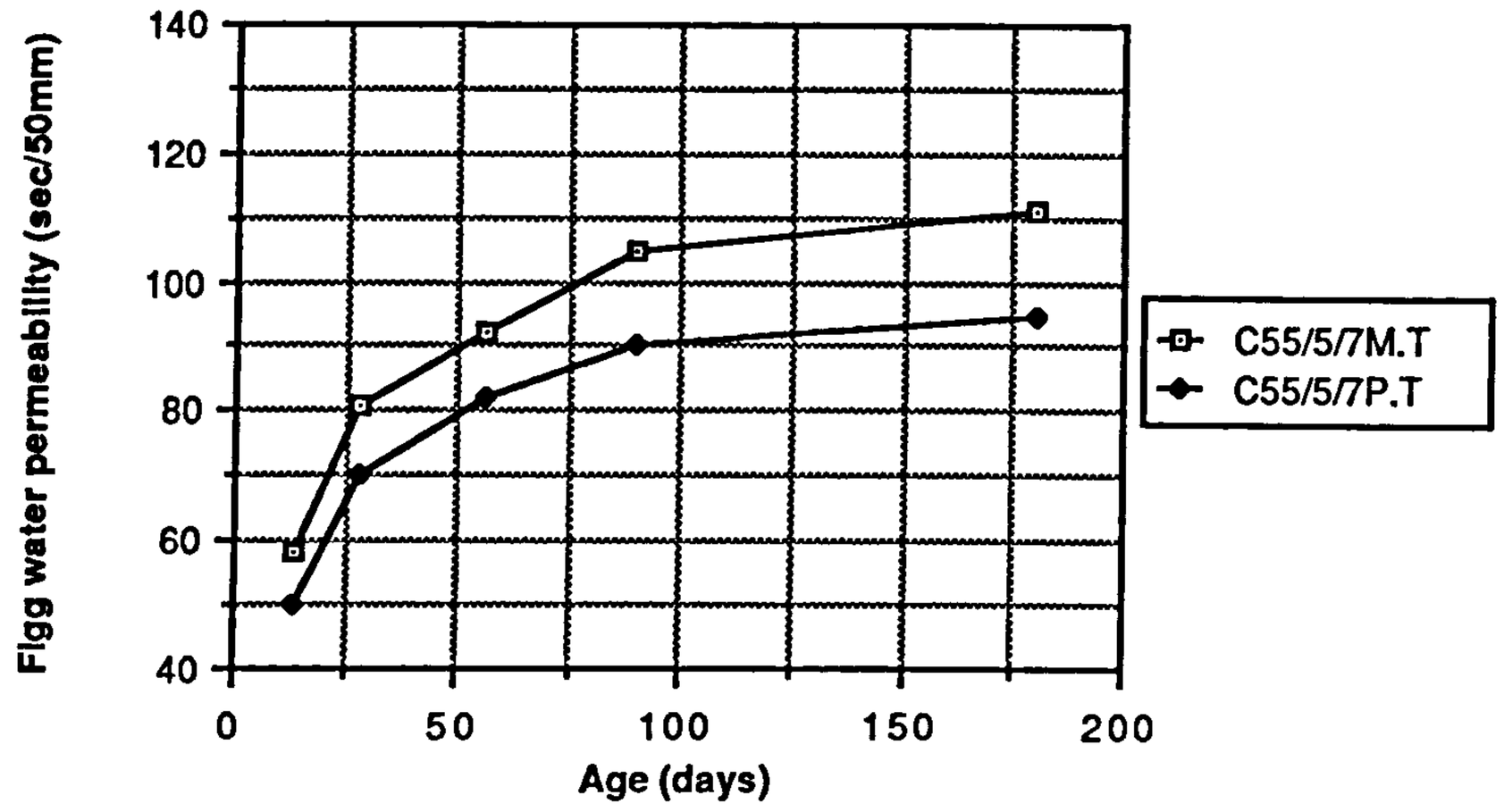

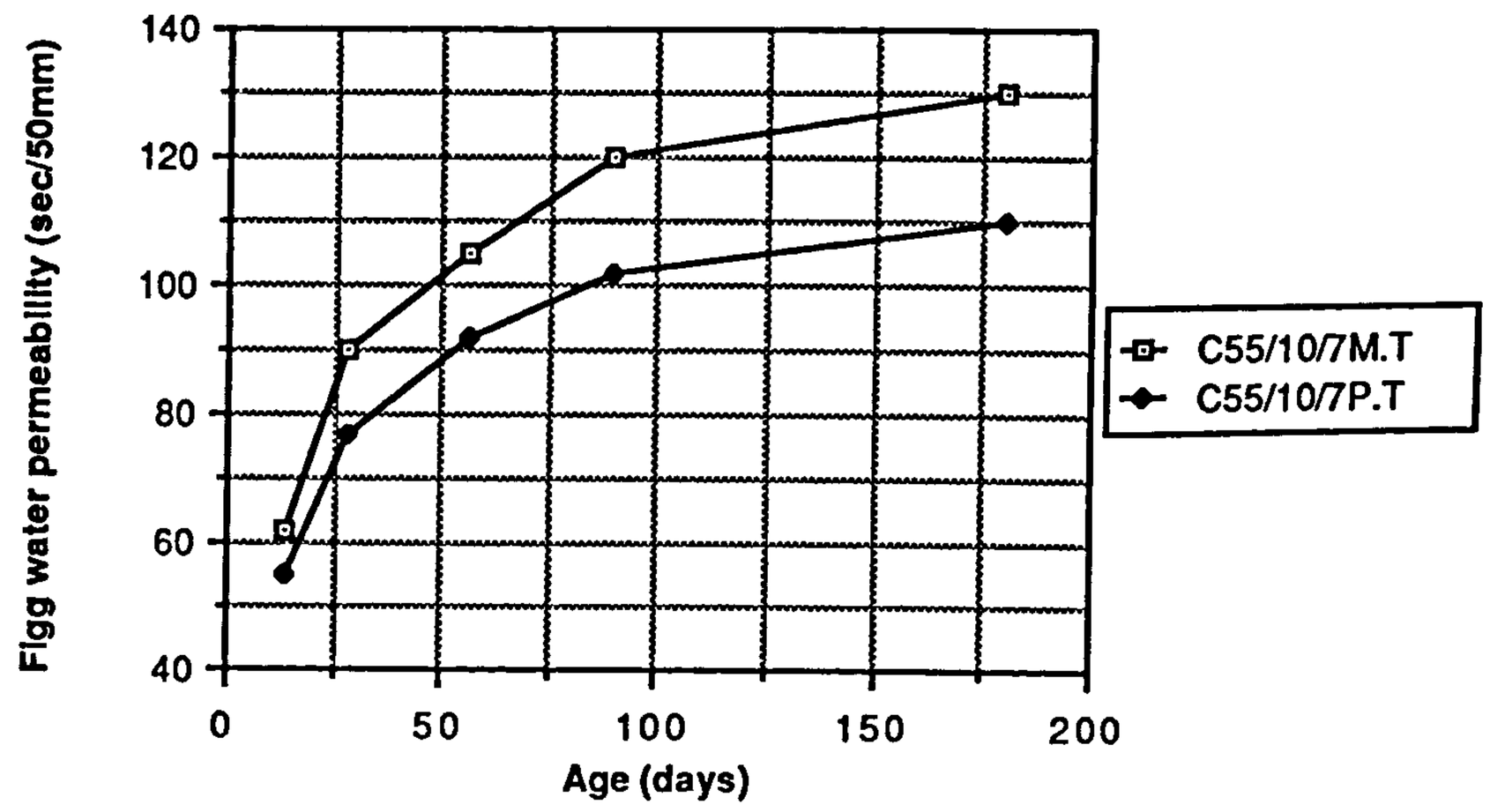

Figure A1.20 Effect of water and polythene curing on Figg water permeability of CSF concrete mixes grade C55

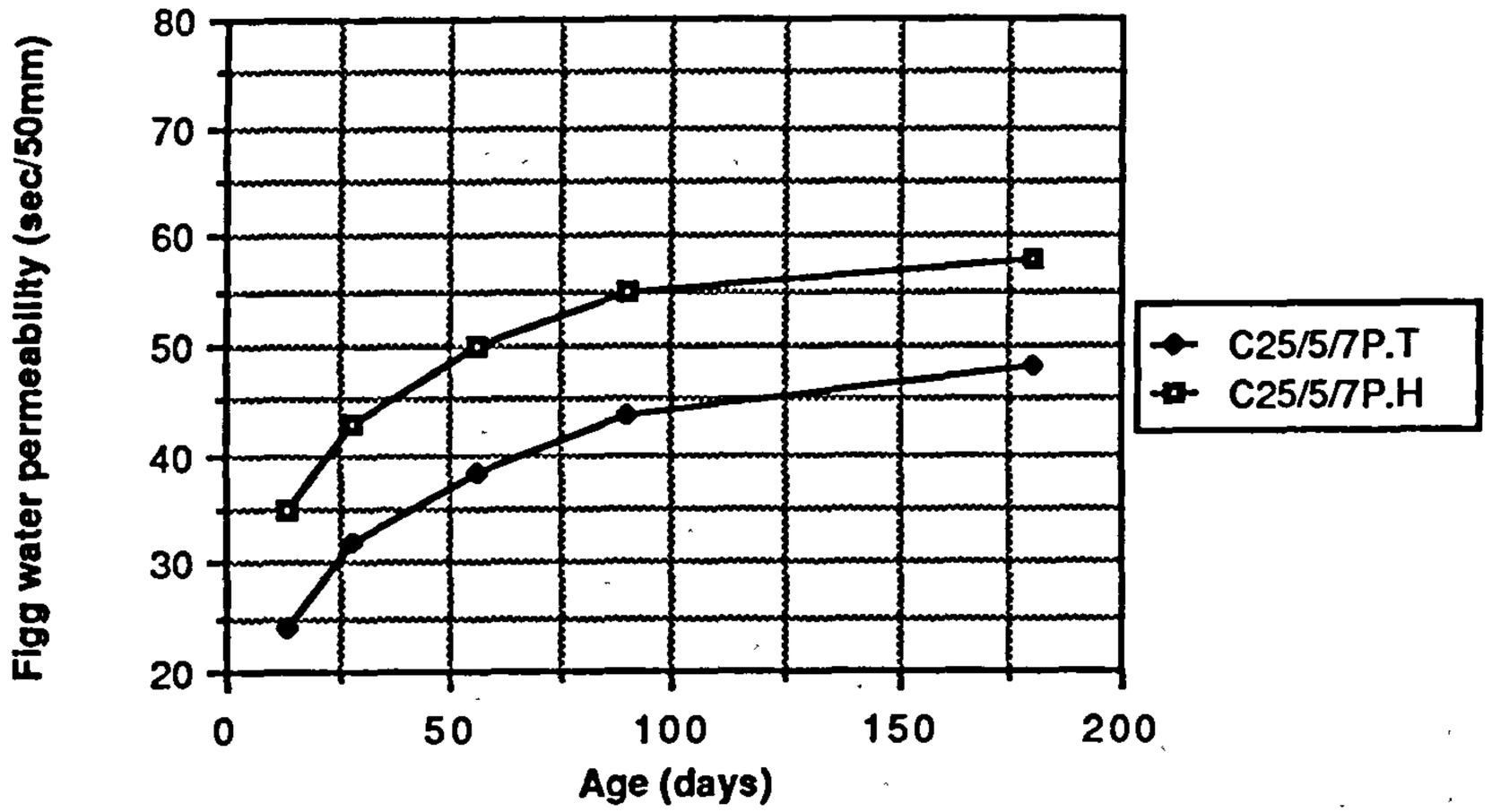

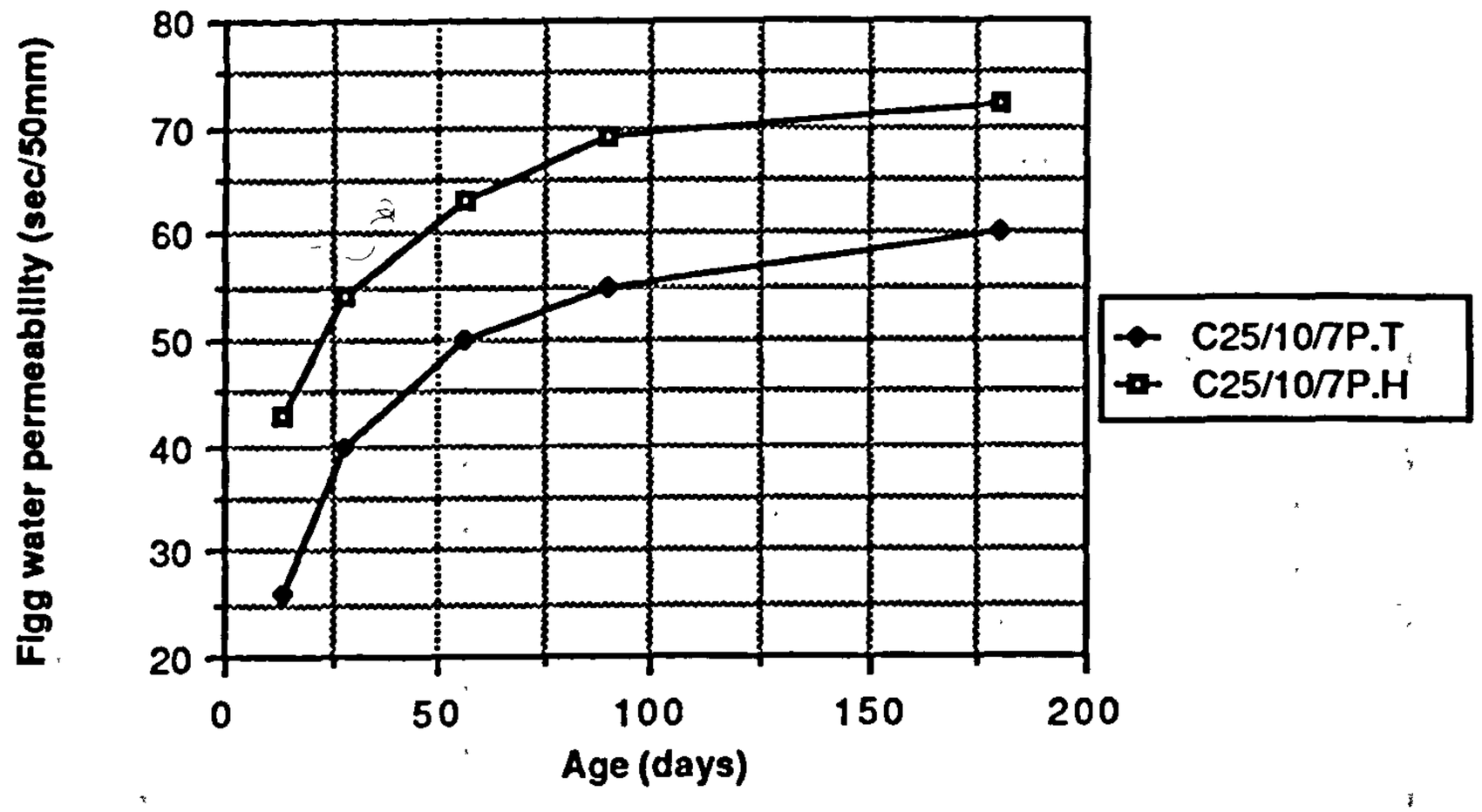

Figure A1.21 Effect of temperate and hot curing on Figg water permeability of CSF concrete mixes grade C25

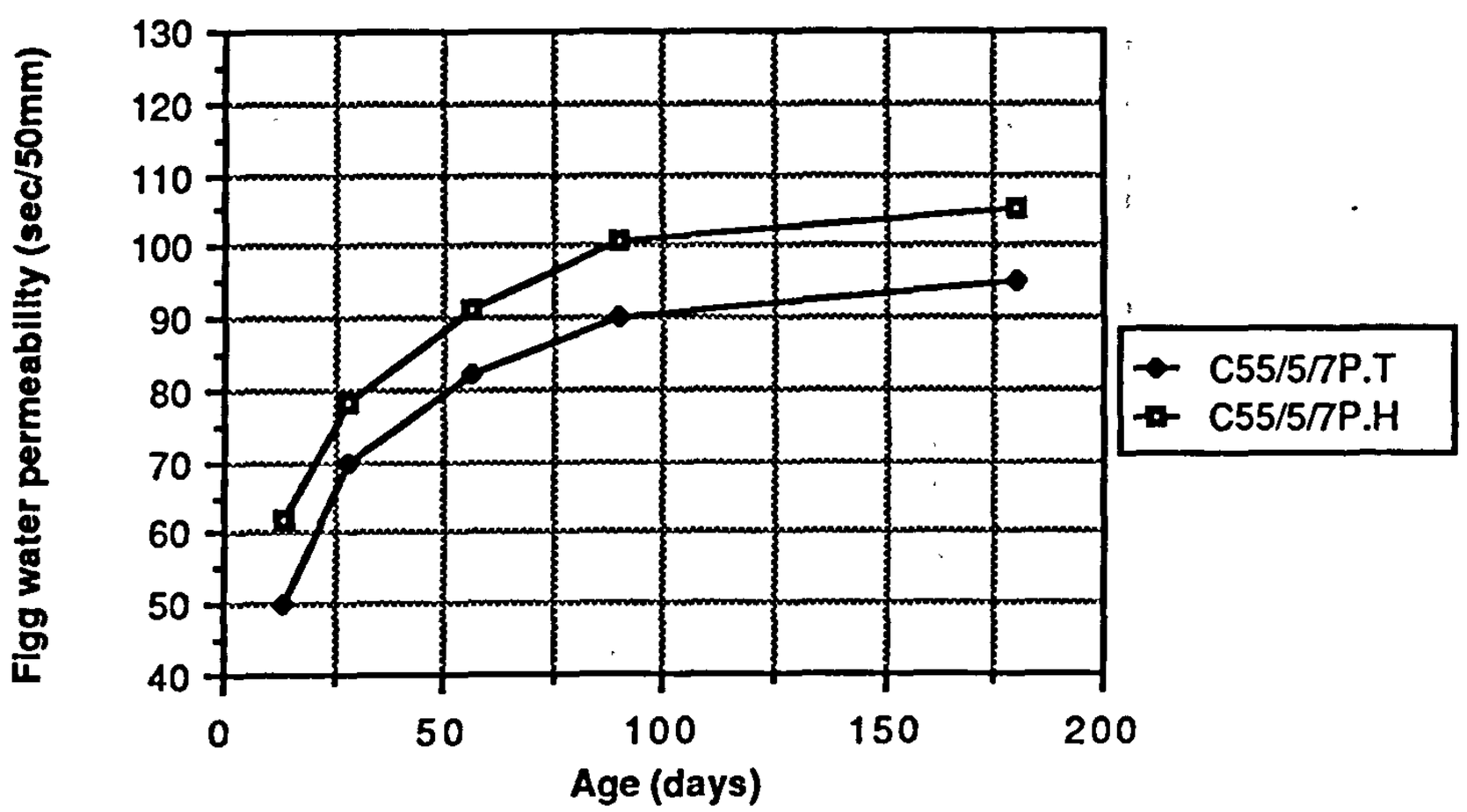

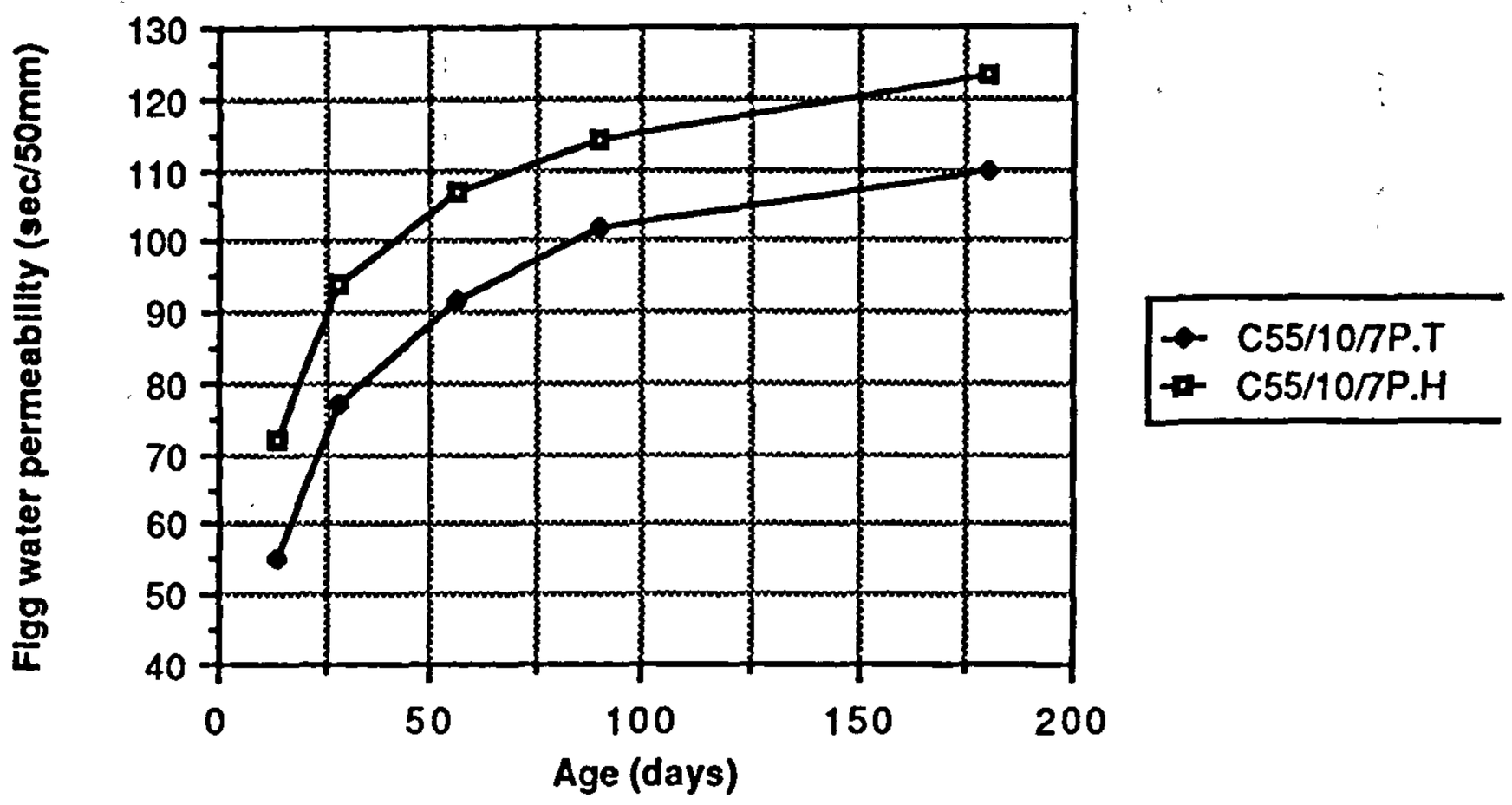

Figure A1.22 Effect of temperate and hot curing on Figg water permeability of CSF concrete mixes grade C55

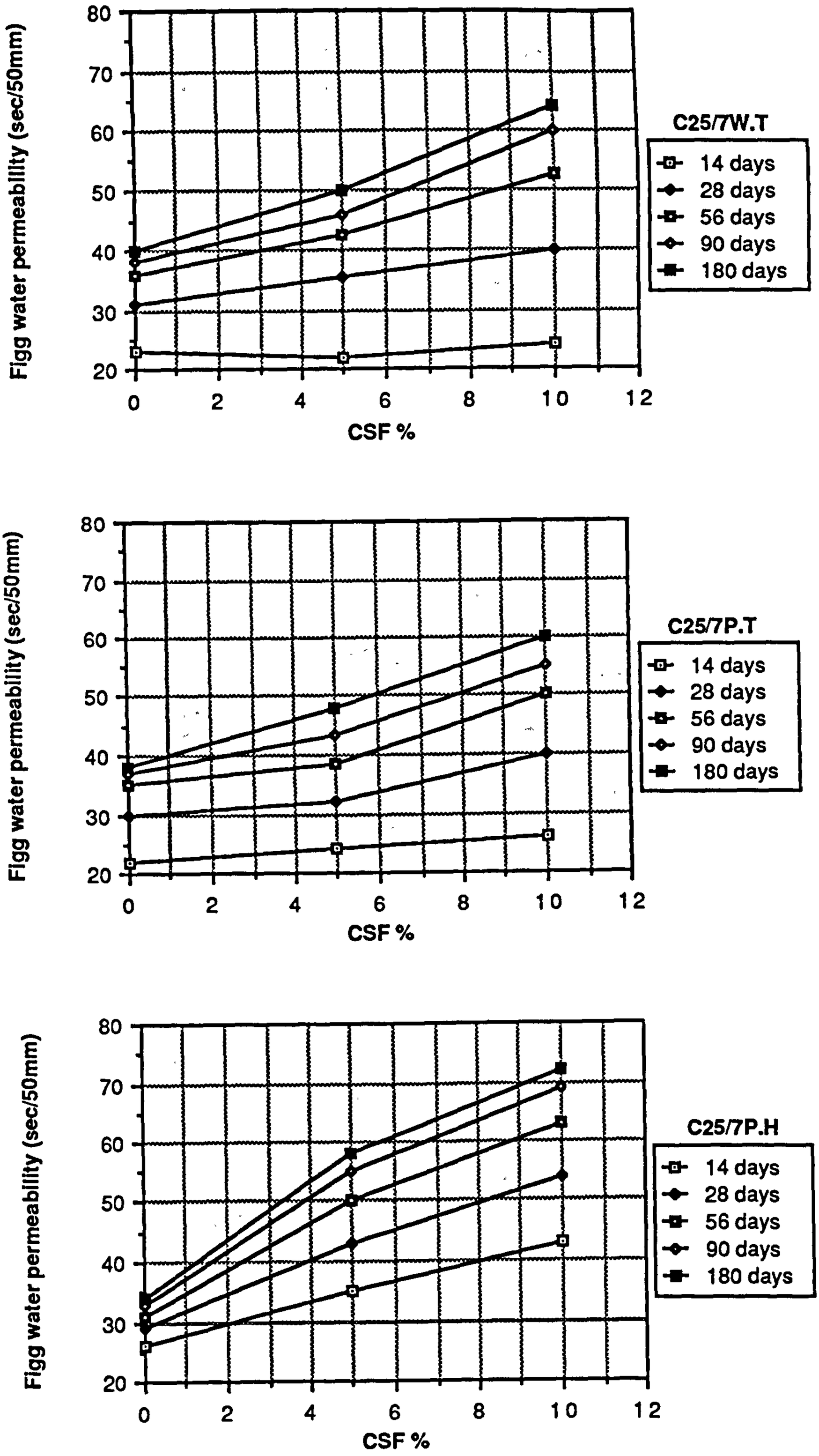

Figure A1.23 Effect of CSF content on Figg water permeability of CSF concrete mixes grade C25

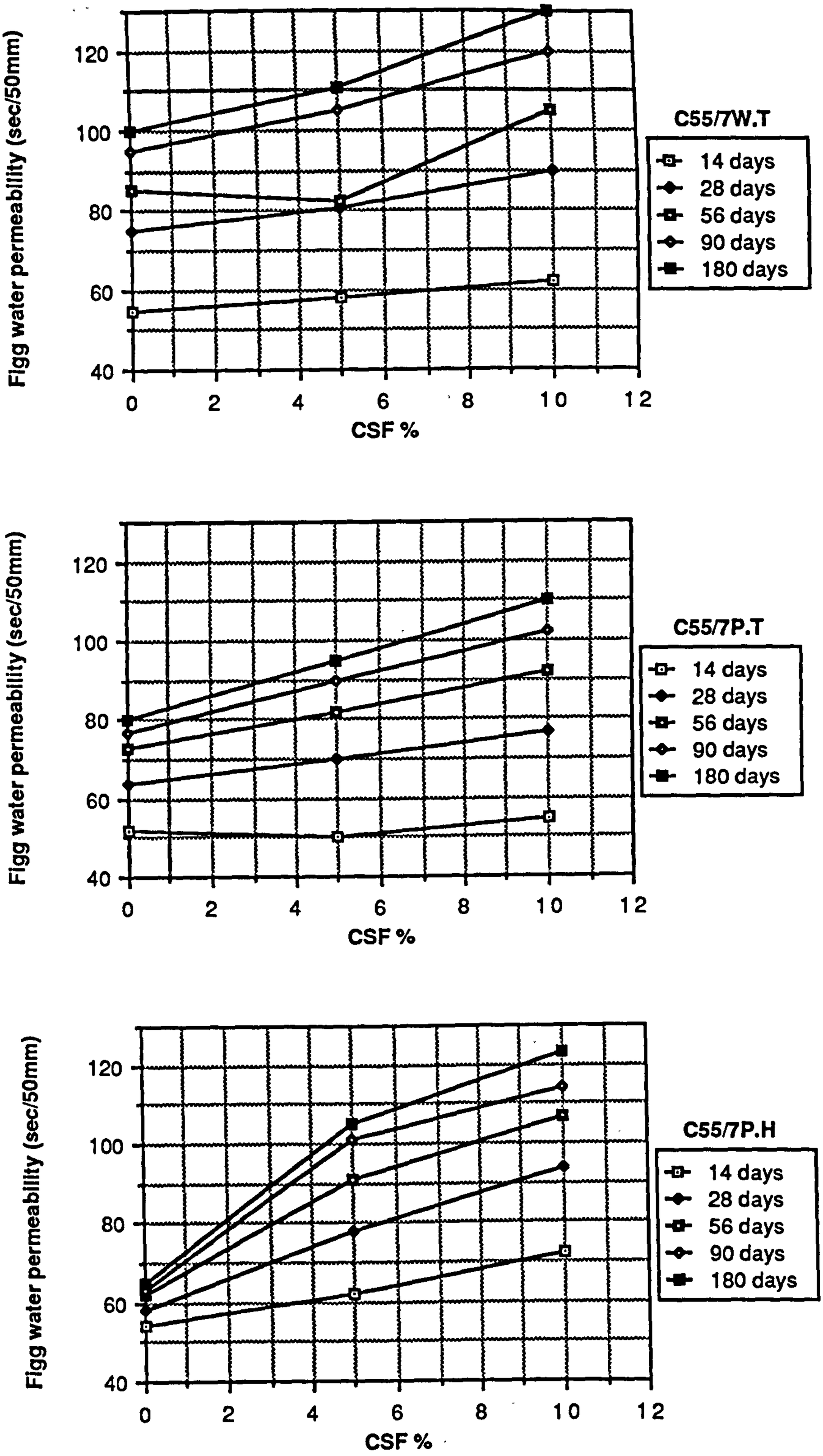

Figure A1.24 Effect of CSF content on the Figg water permeability of CSF concrete mixes grade C55

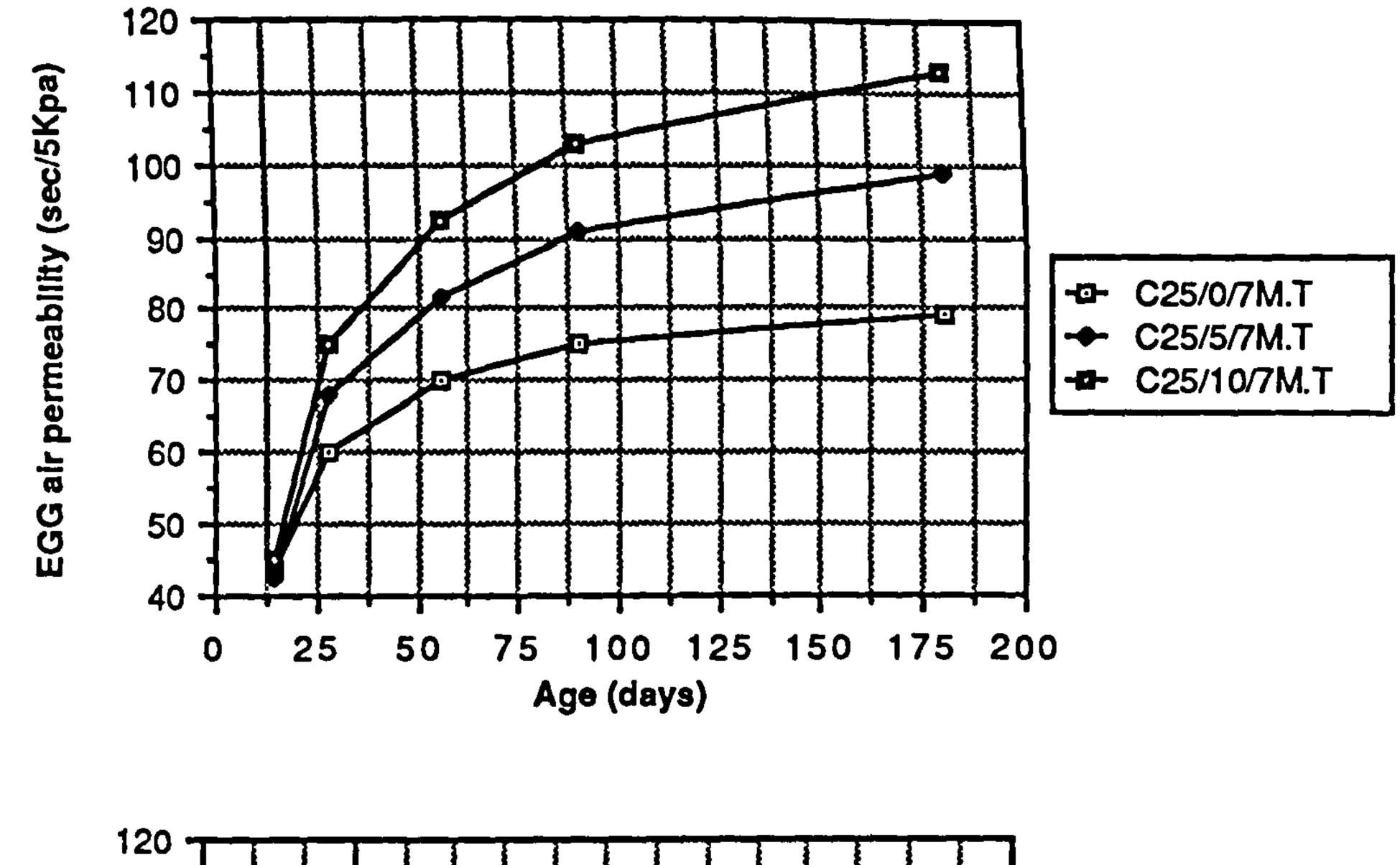

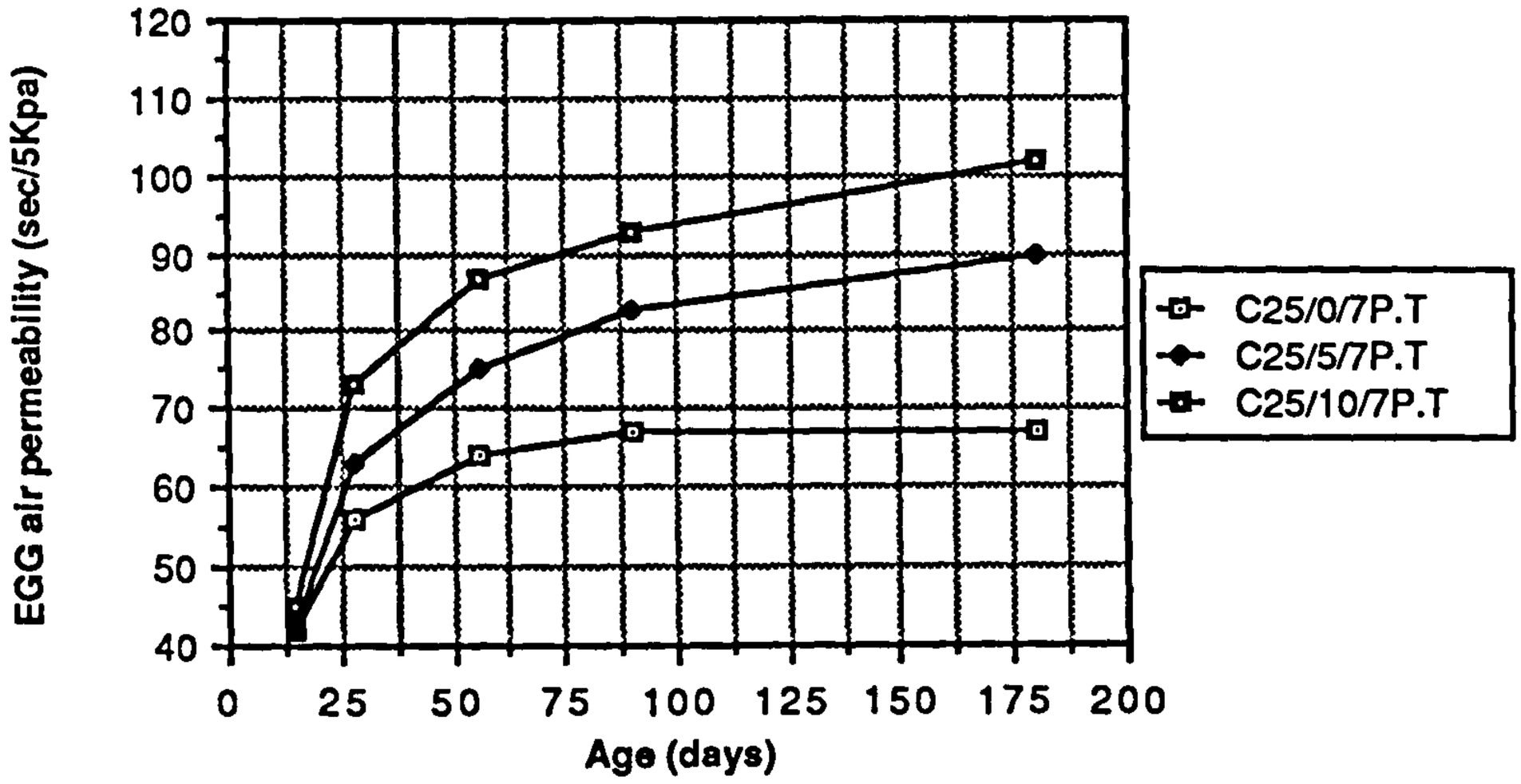

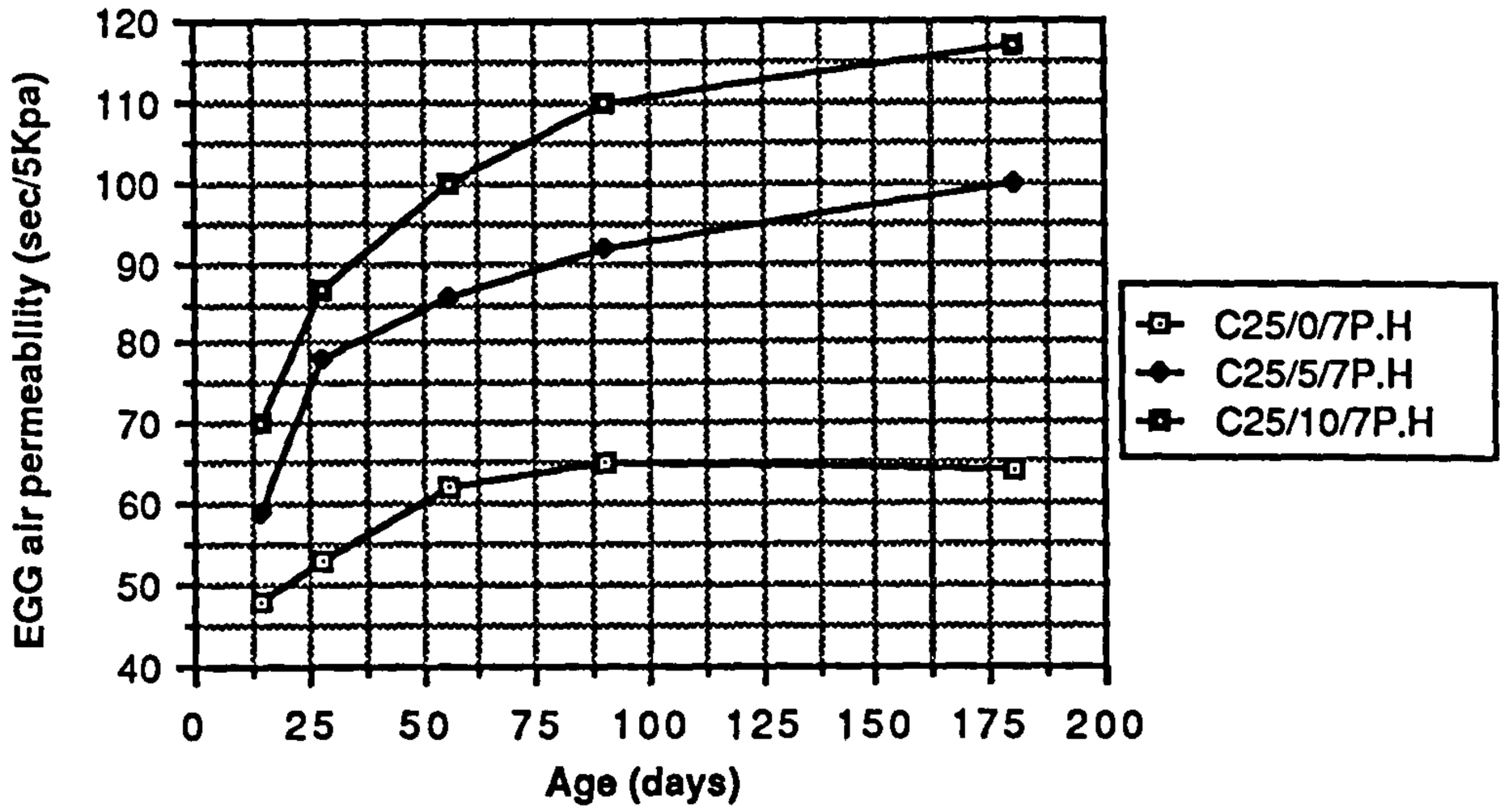

Figure A1.25 Relationship between age and Egg air permeability of CSF concrete mixes grade C25

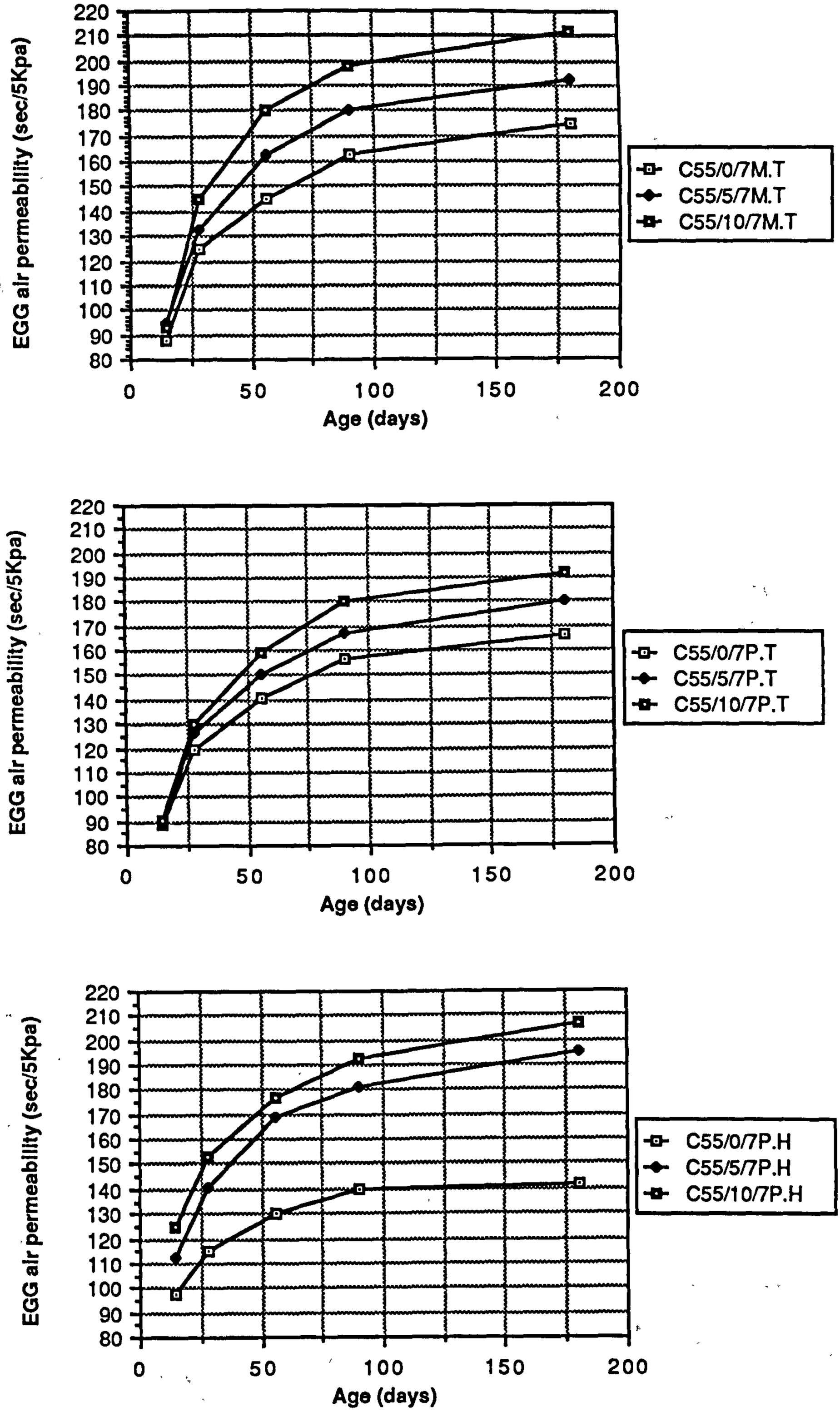

Figure A1.26 Relationship between age and Eff air permeability of CSF concrete mixes grade C55

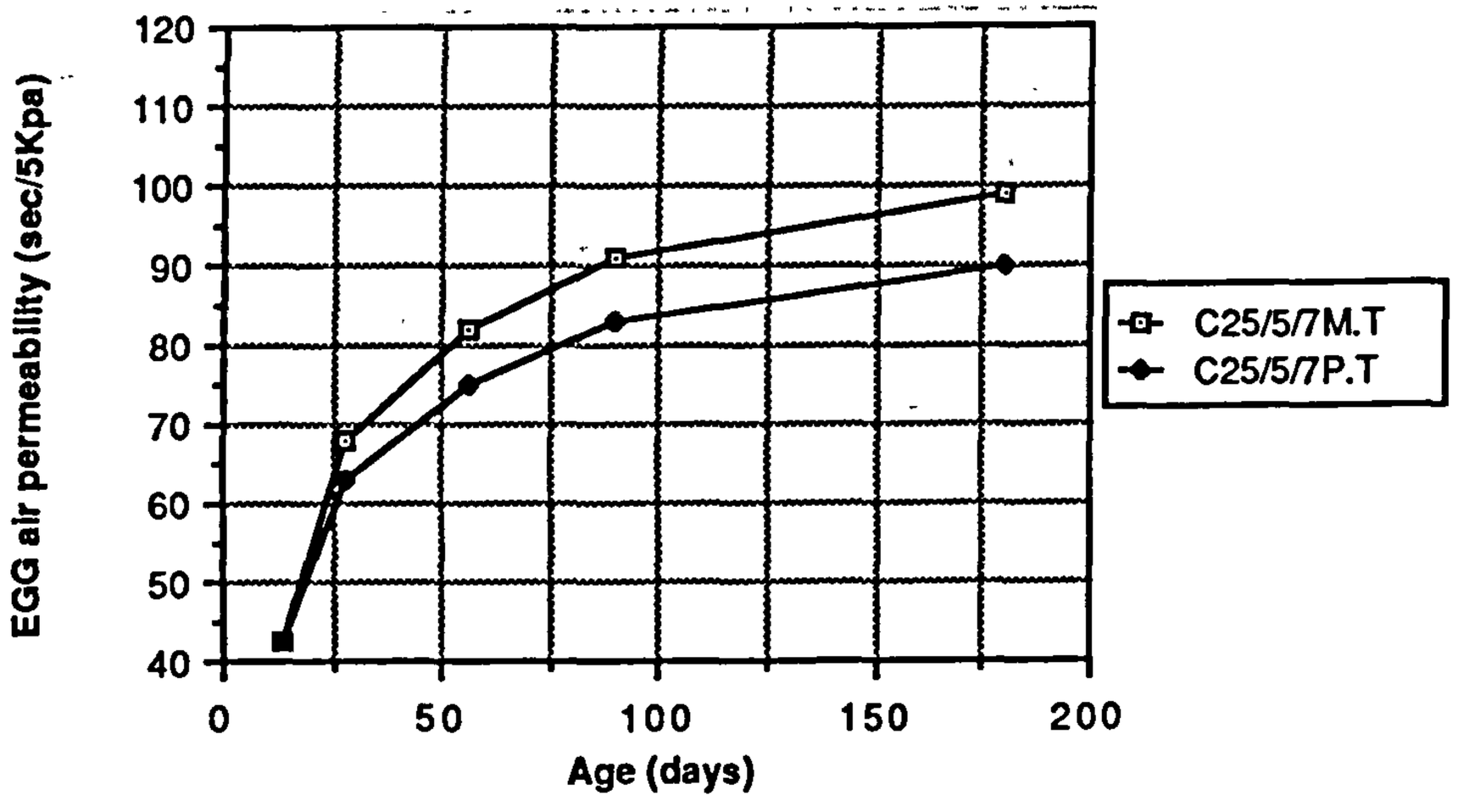

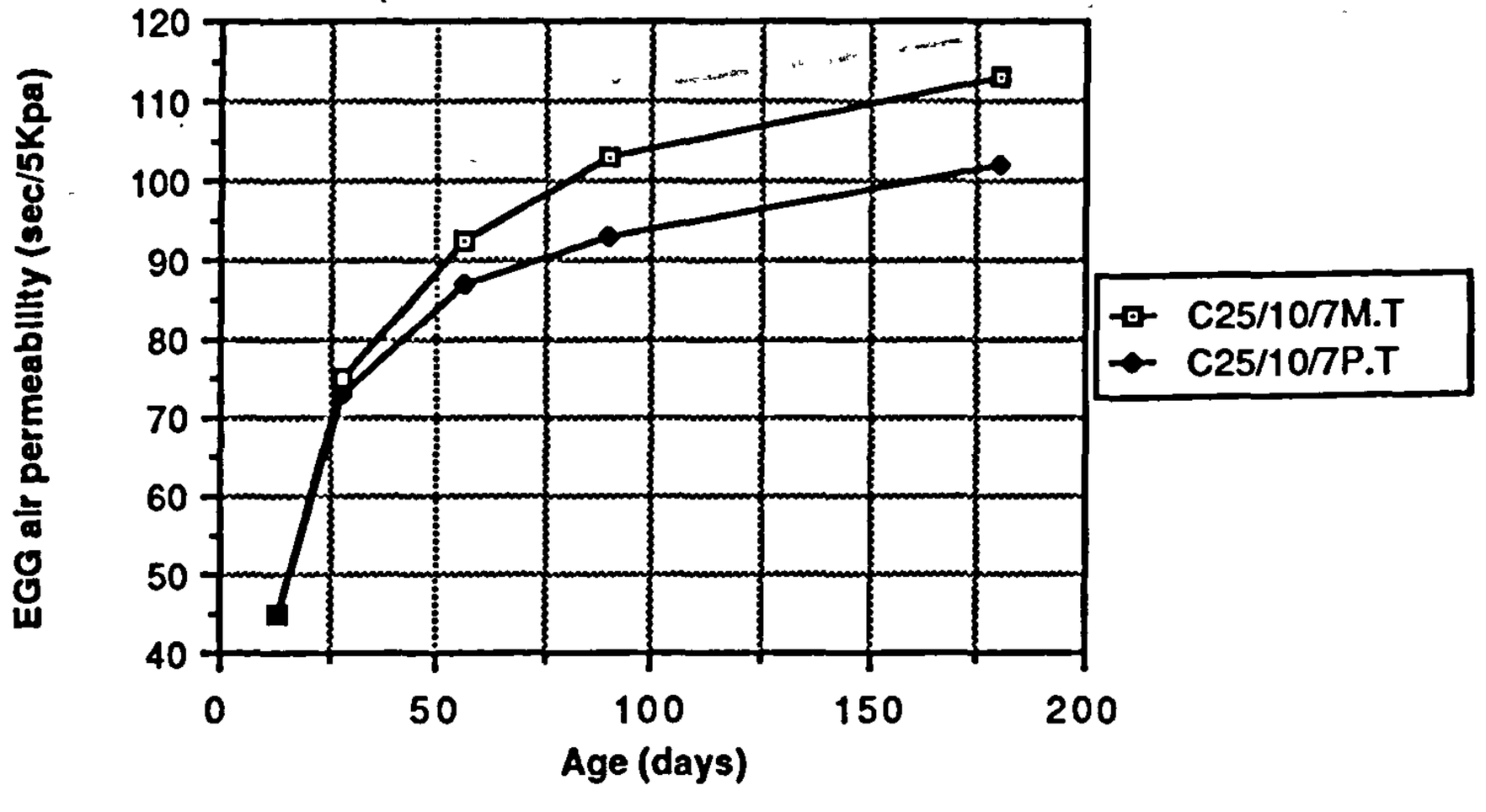

Figure A1.27 Effect of water and polythene curing on Egg air permeability of CSF concrete mixes grade C25

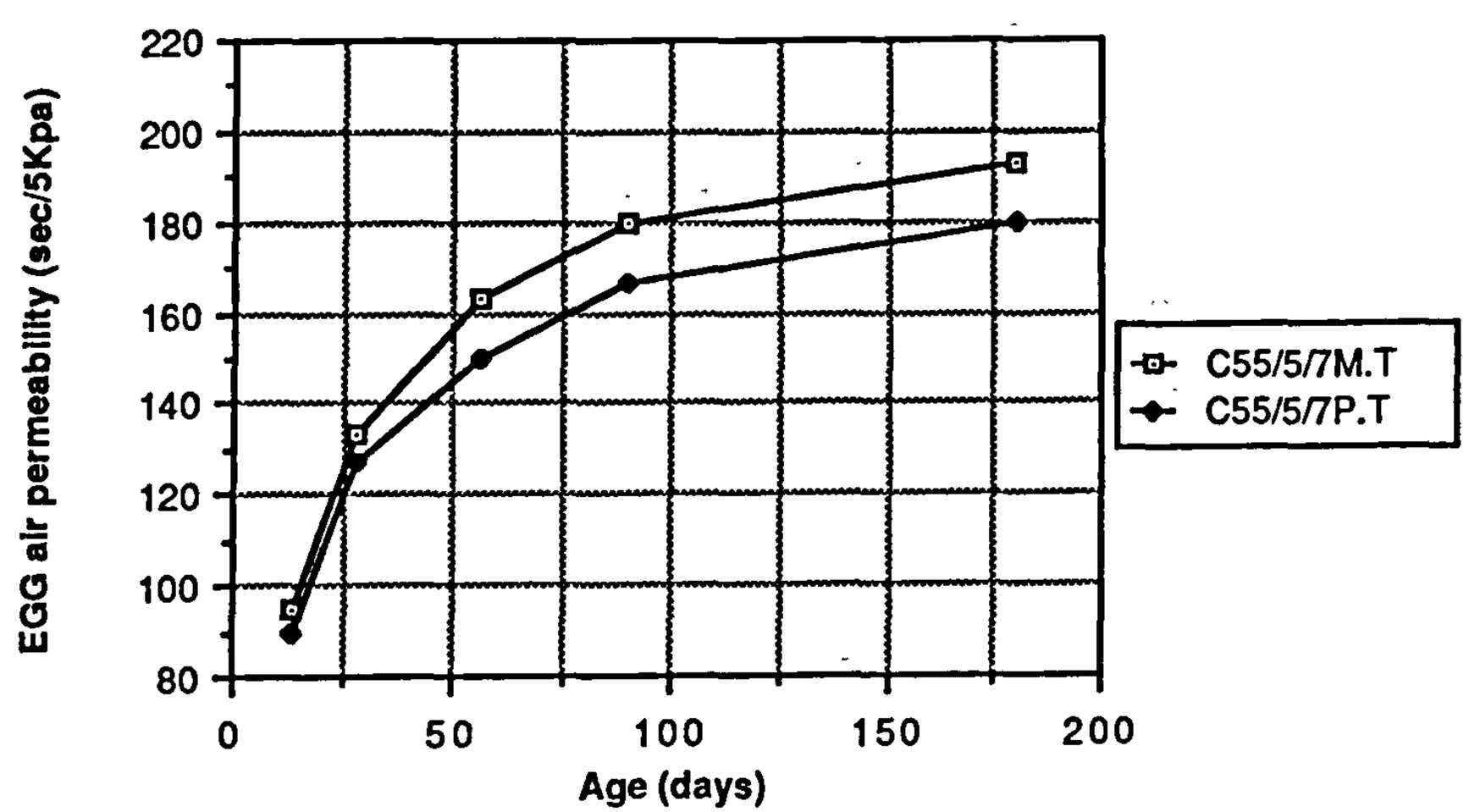

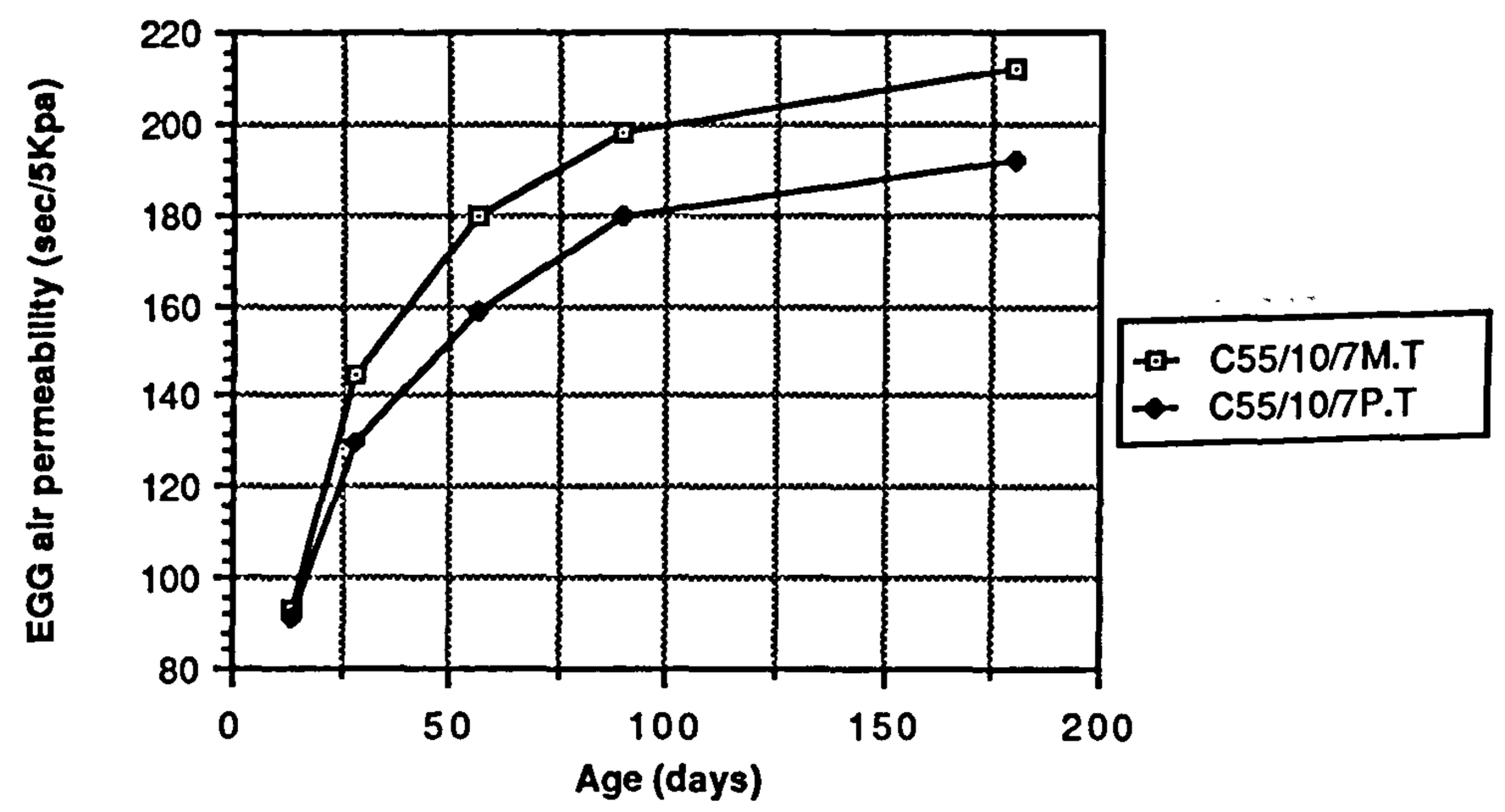

Figure A1.28 Effect of water and polythene curing on Egg air permeability of CSF concrete mixes grade C55

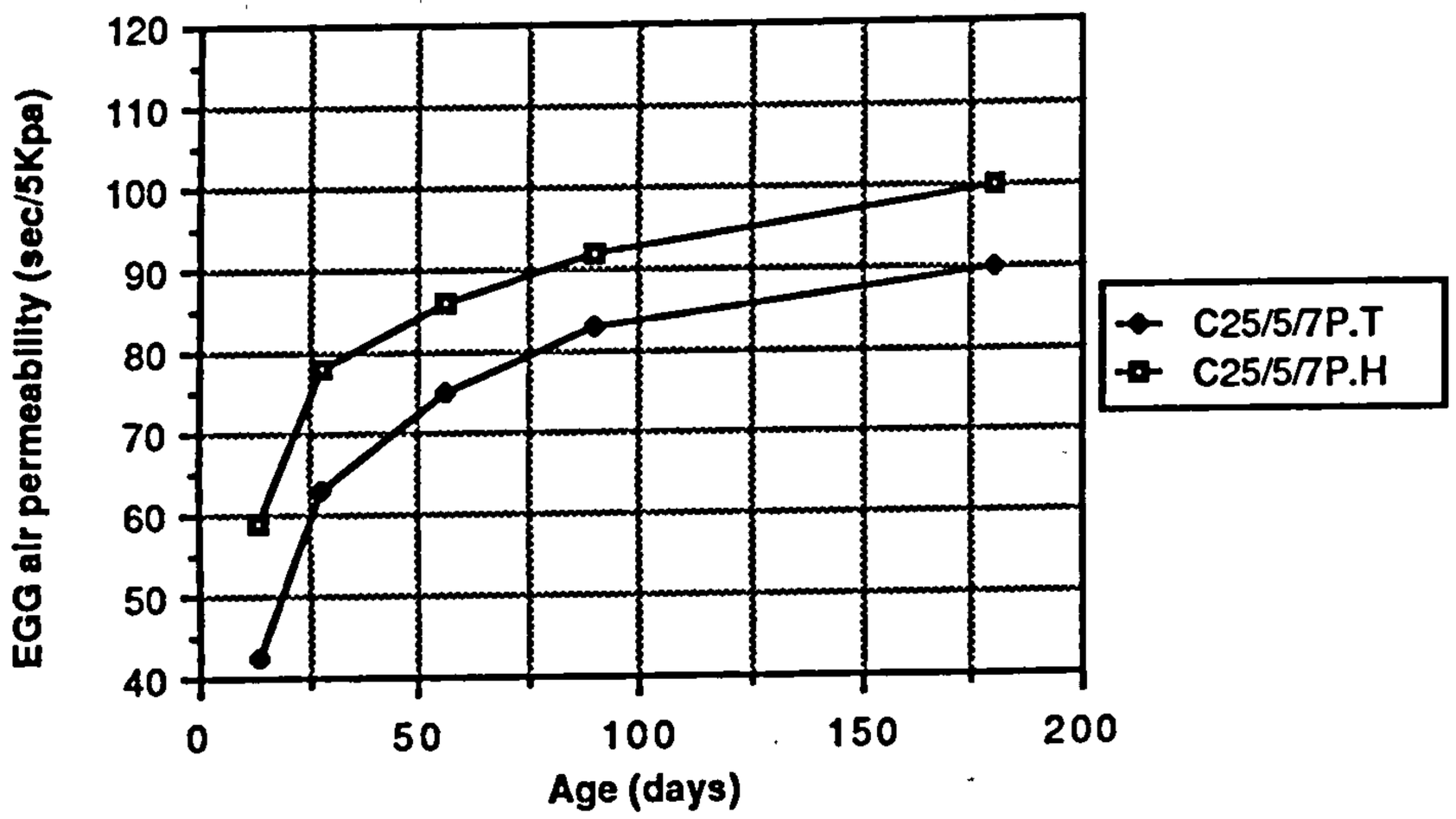

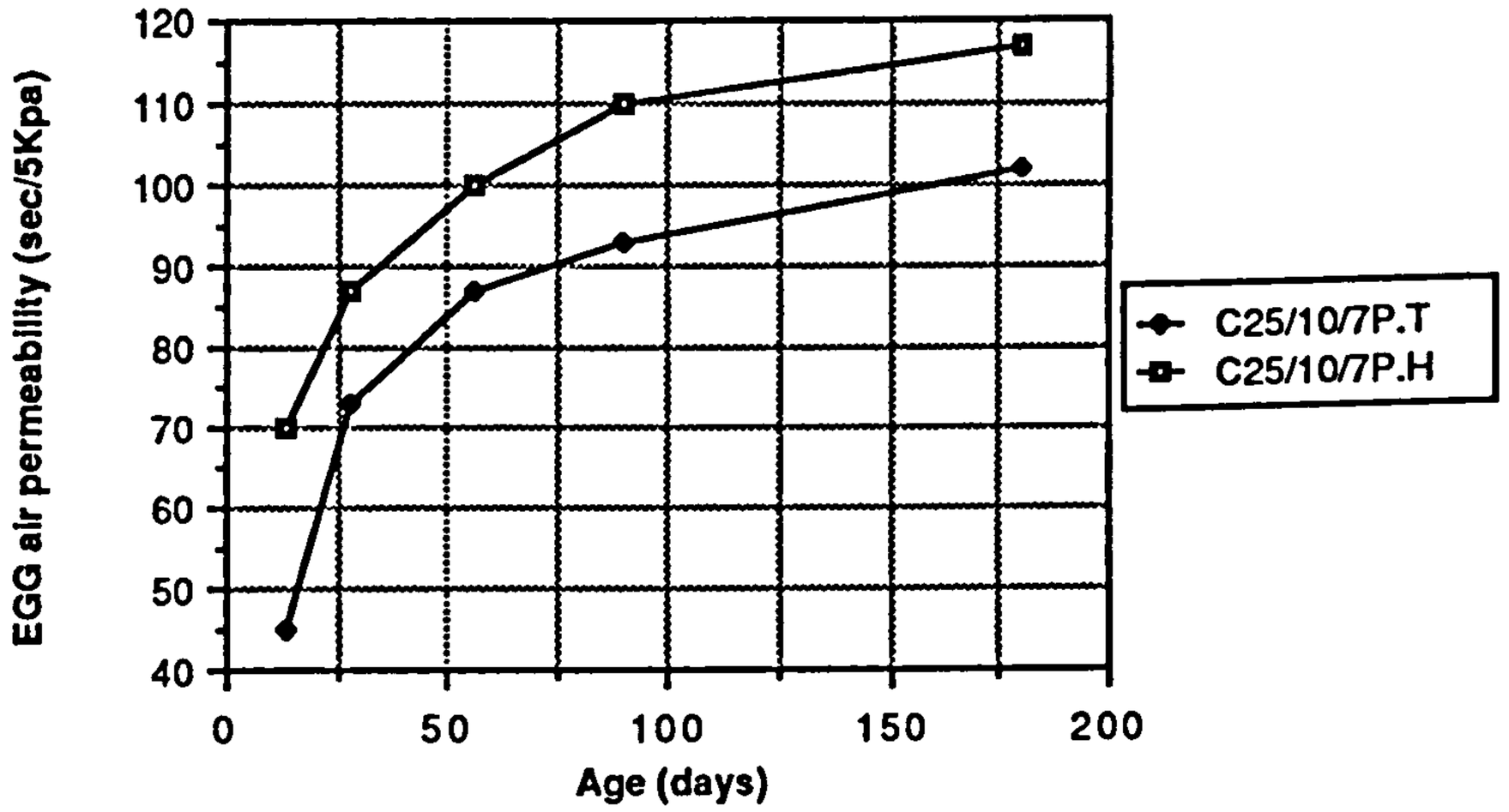

Figure A1.29 Effect of temperate and hot curing on Egg air permeability of CSF concrete mixes grade C25

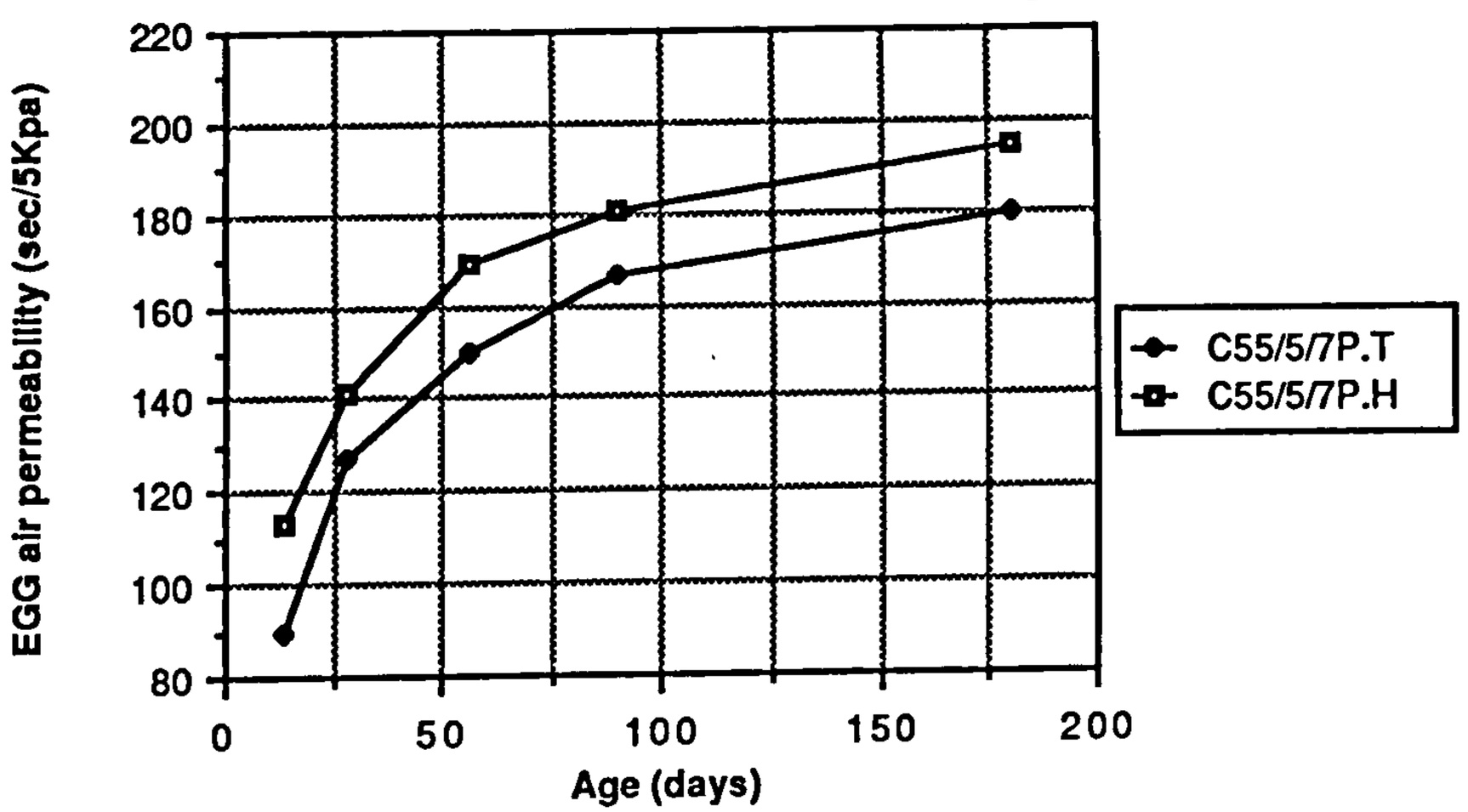

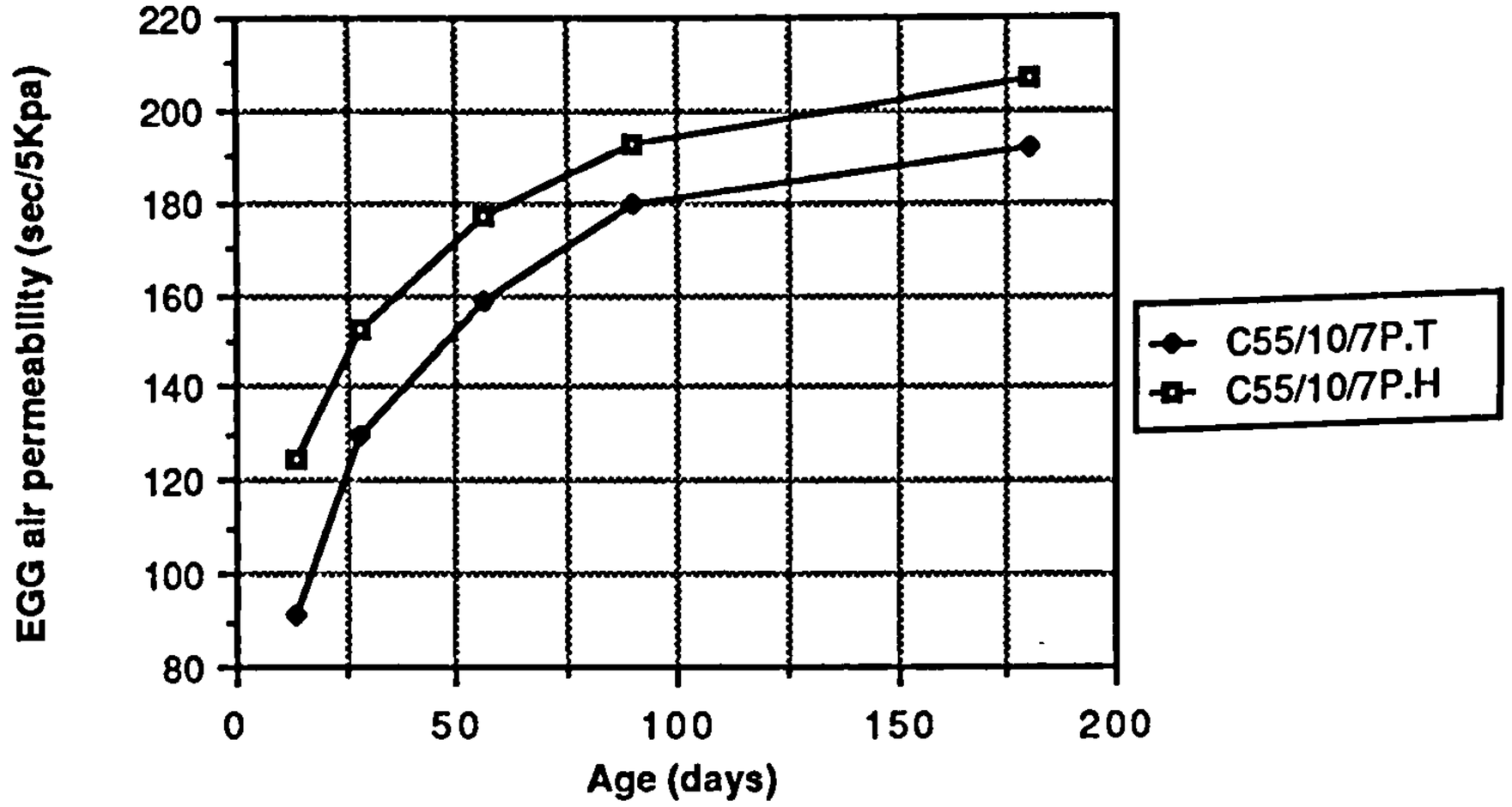

Figure A1.30 Effect of temperate and hot curing on Egg air permeability of CSF concrete mixes grade C55

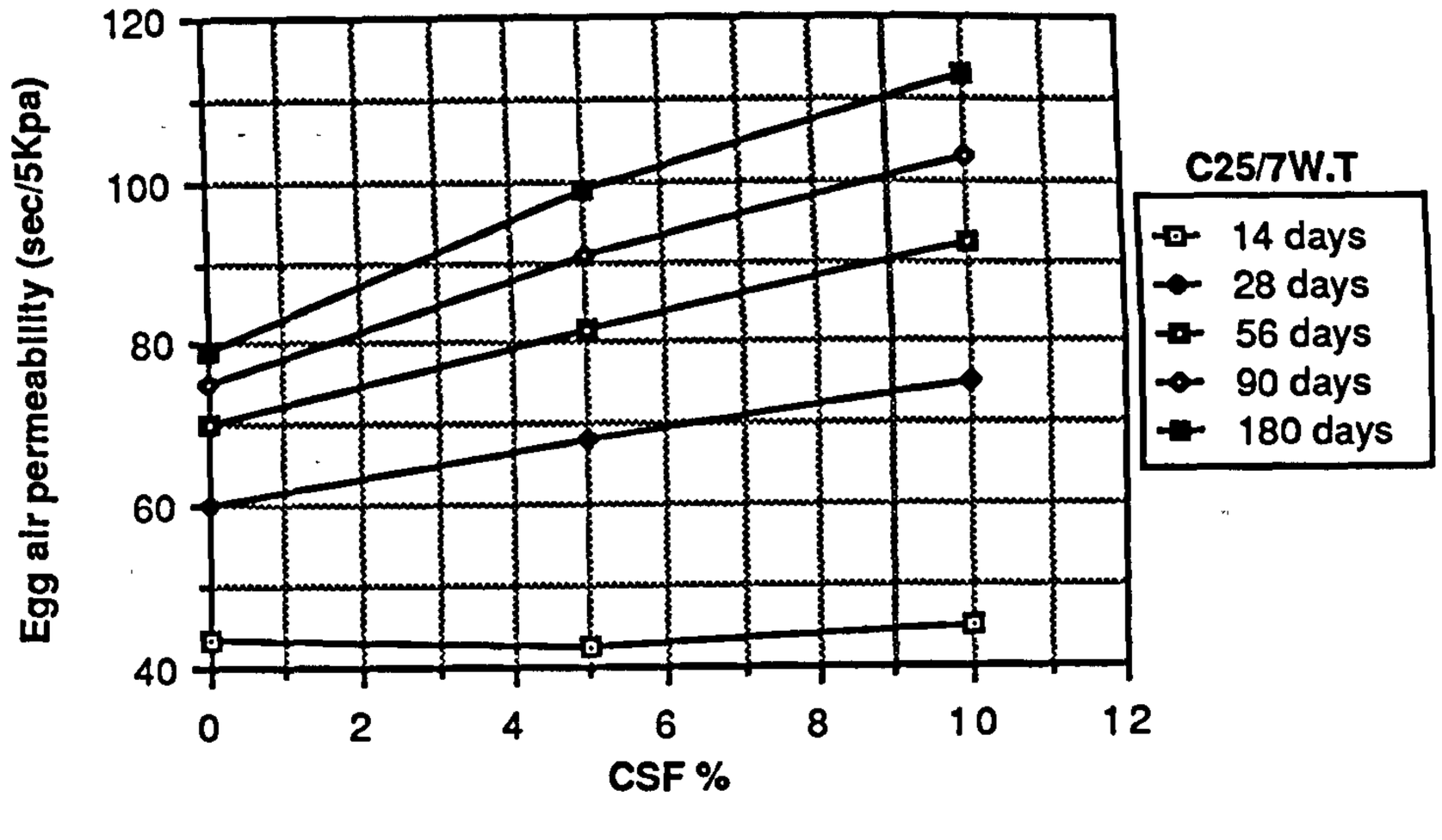

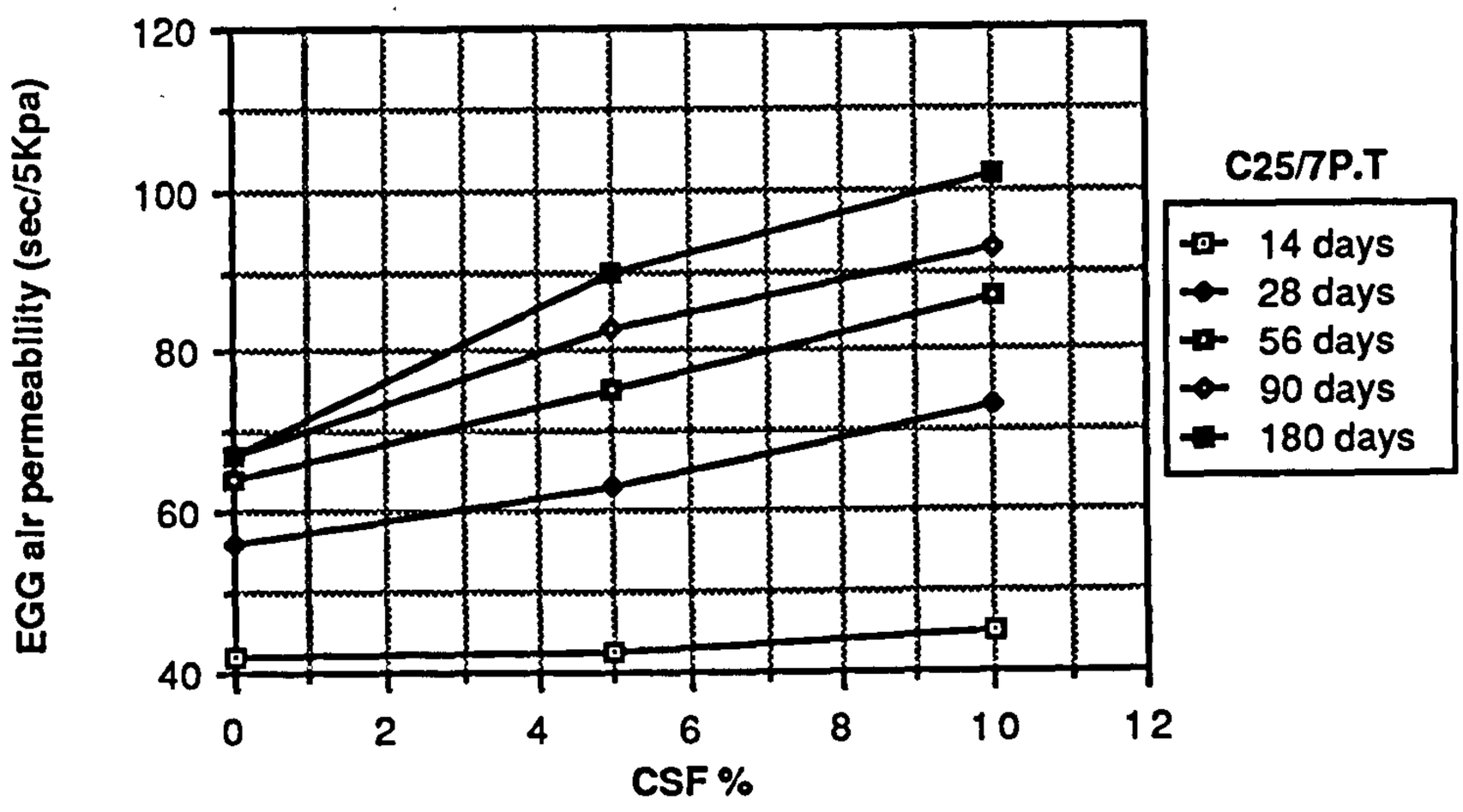

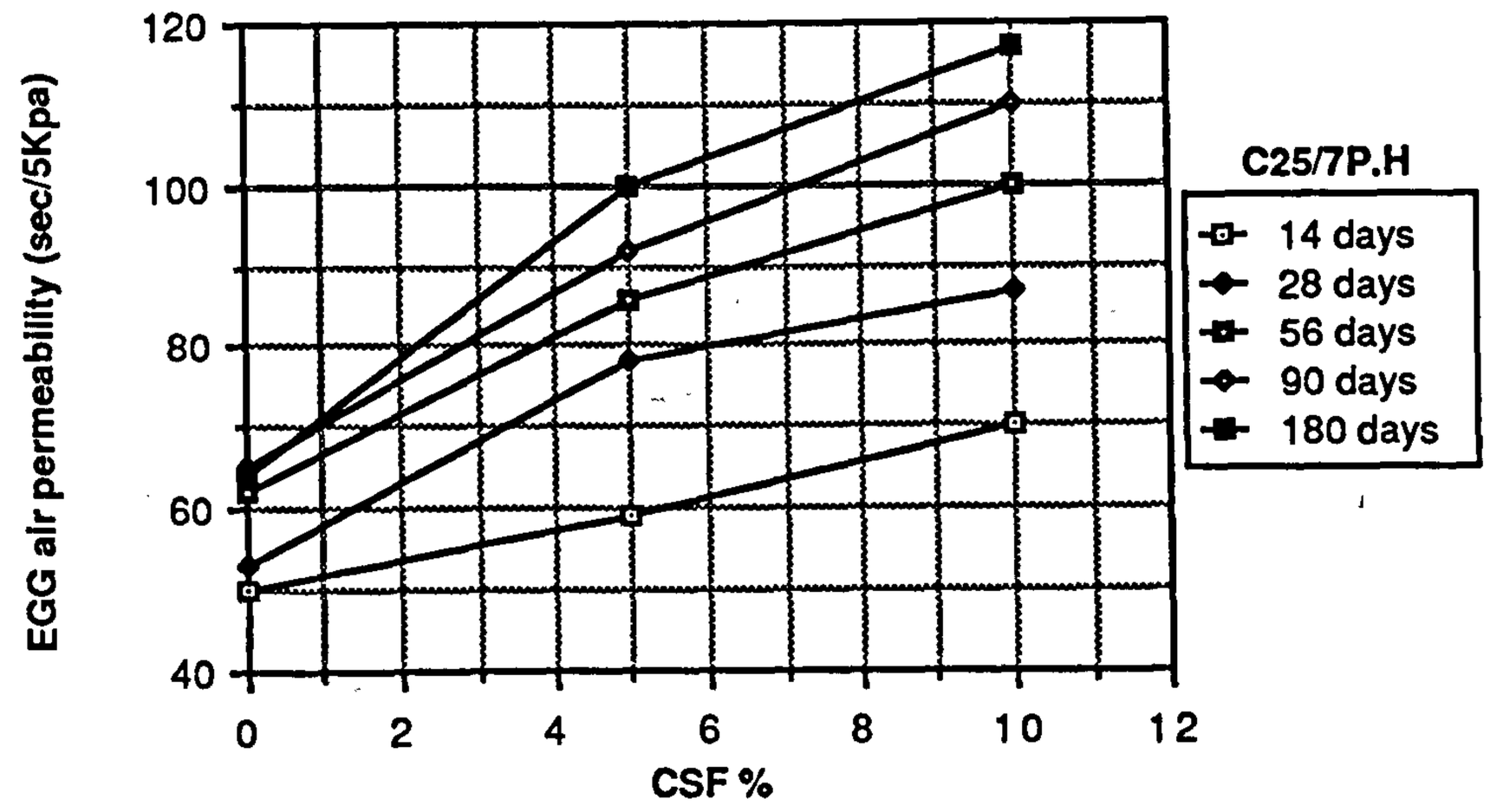

Figure A1.31 Effect of CSF content on Egg air permeability of CSF concrete mixes grade C25

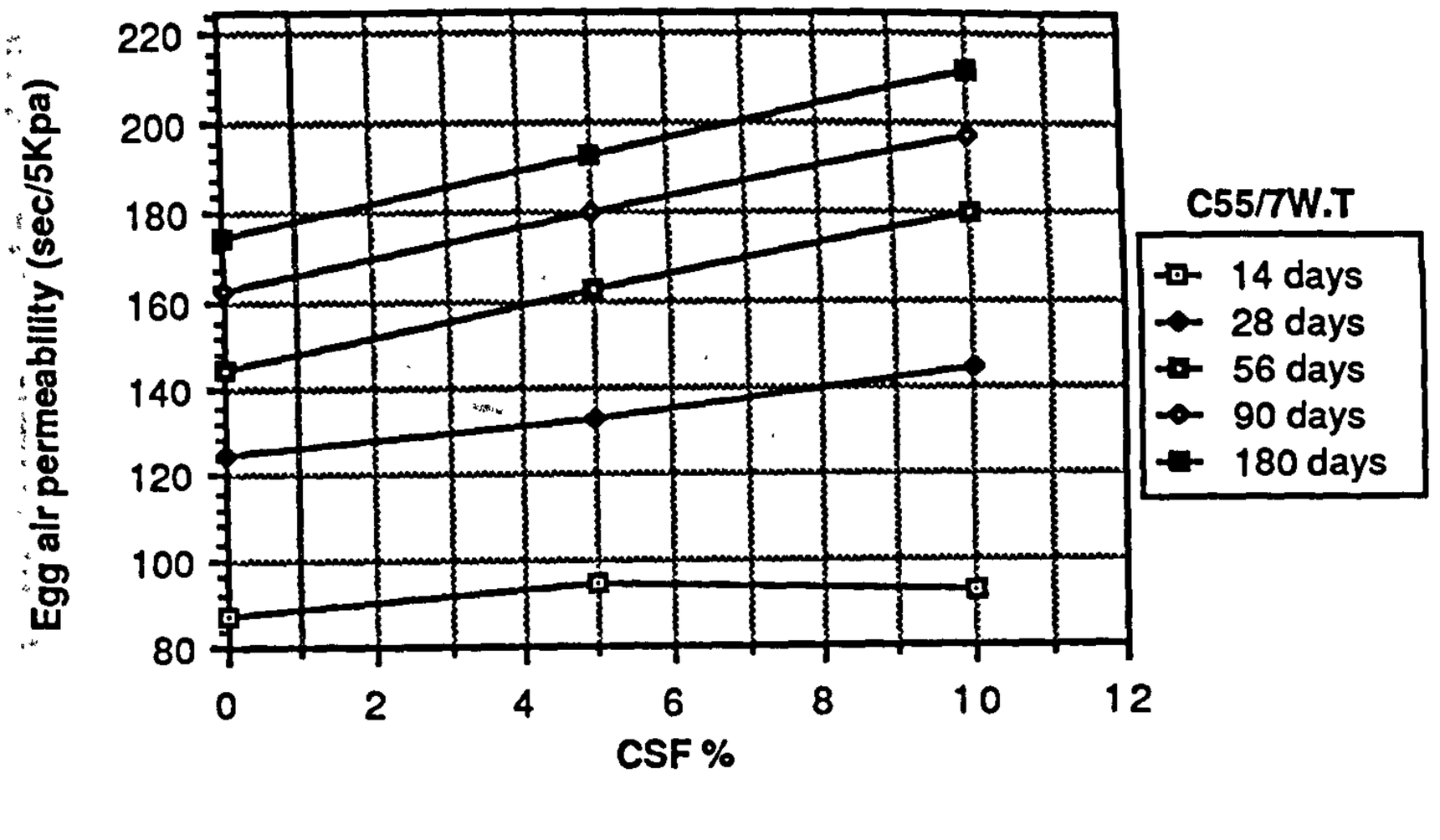

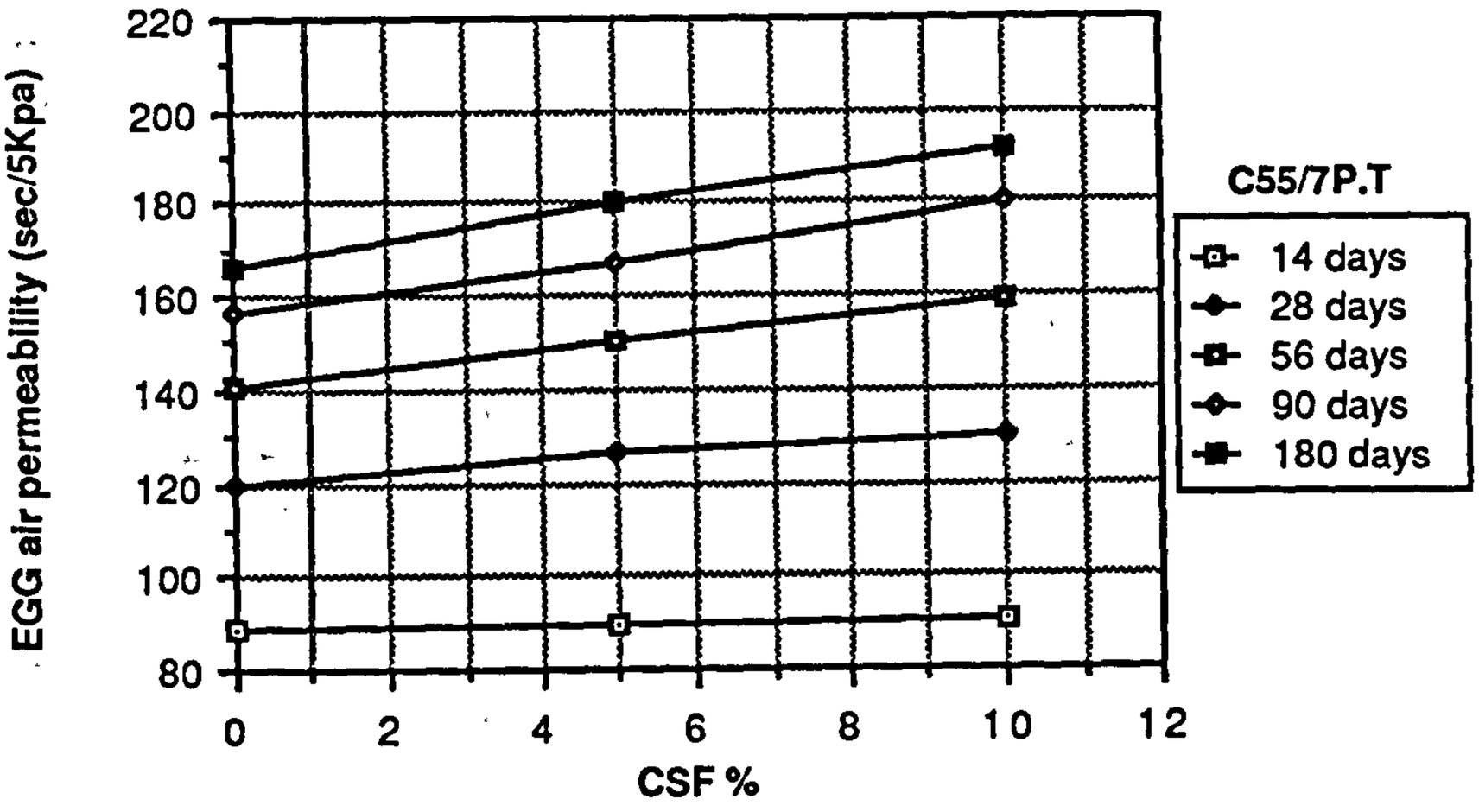

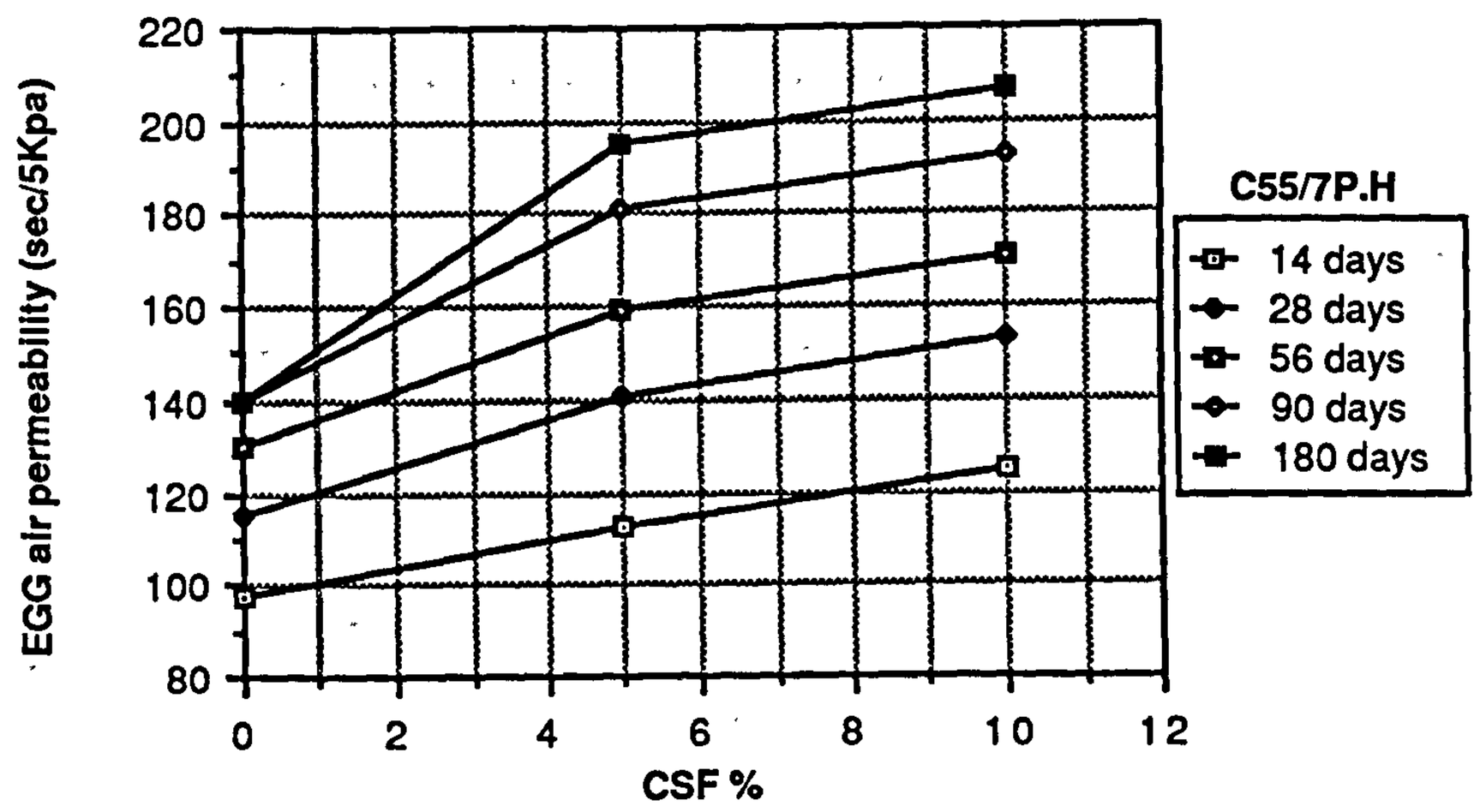

Figure A1.32 Effect of CSF content on Egg air permeability of CSF concrete mixes grade C55

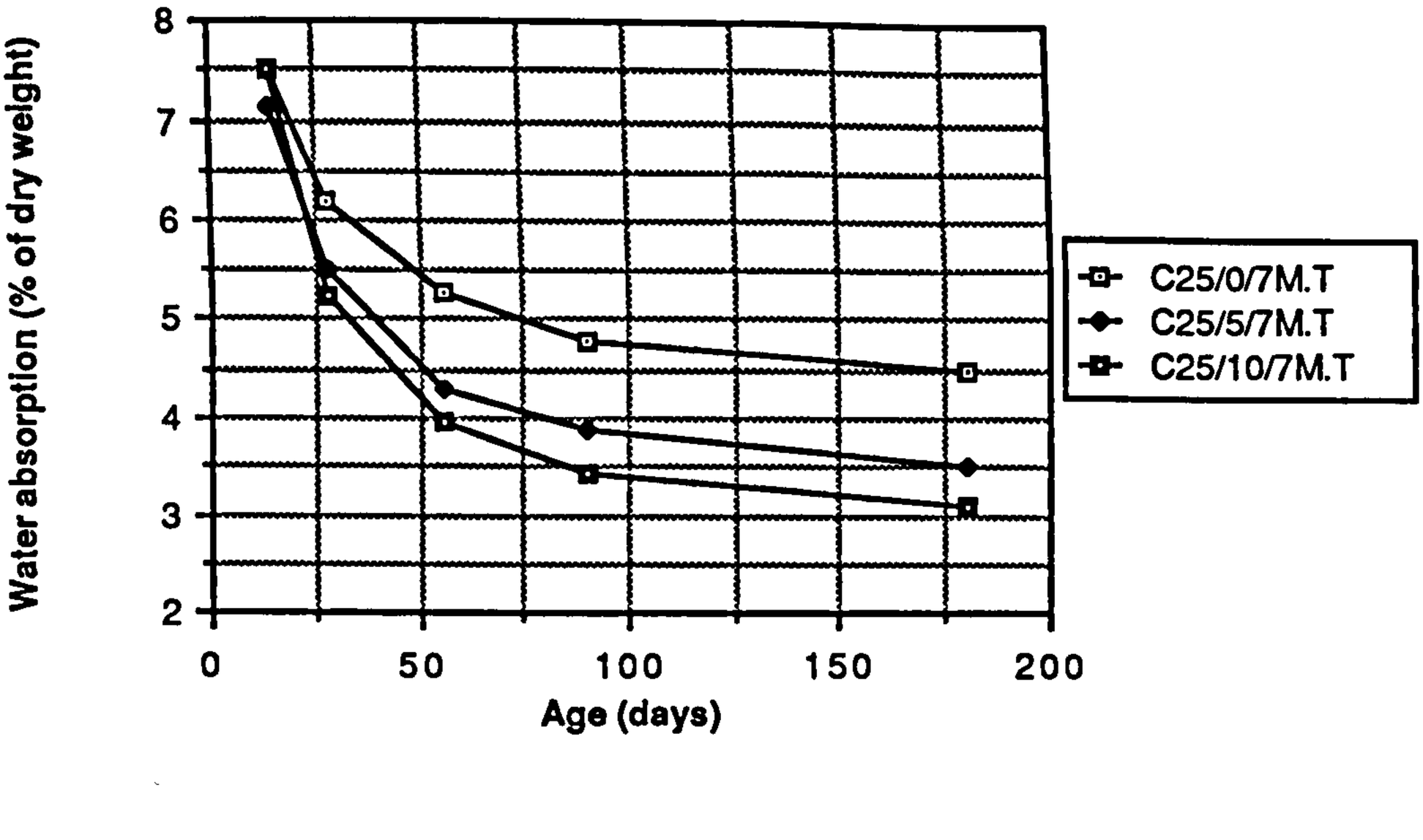

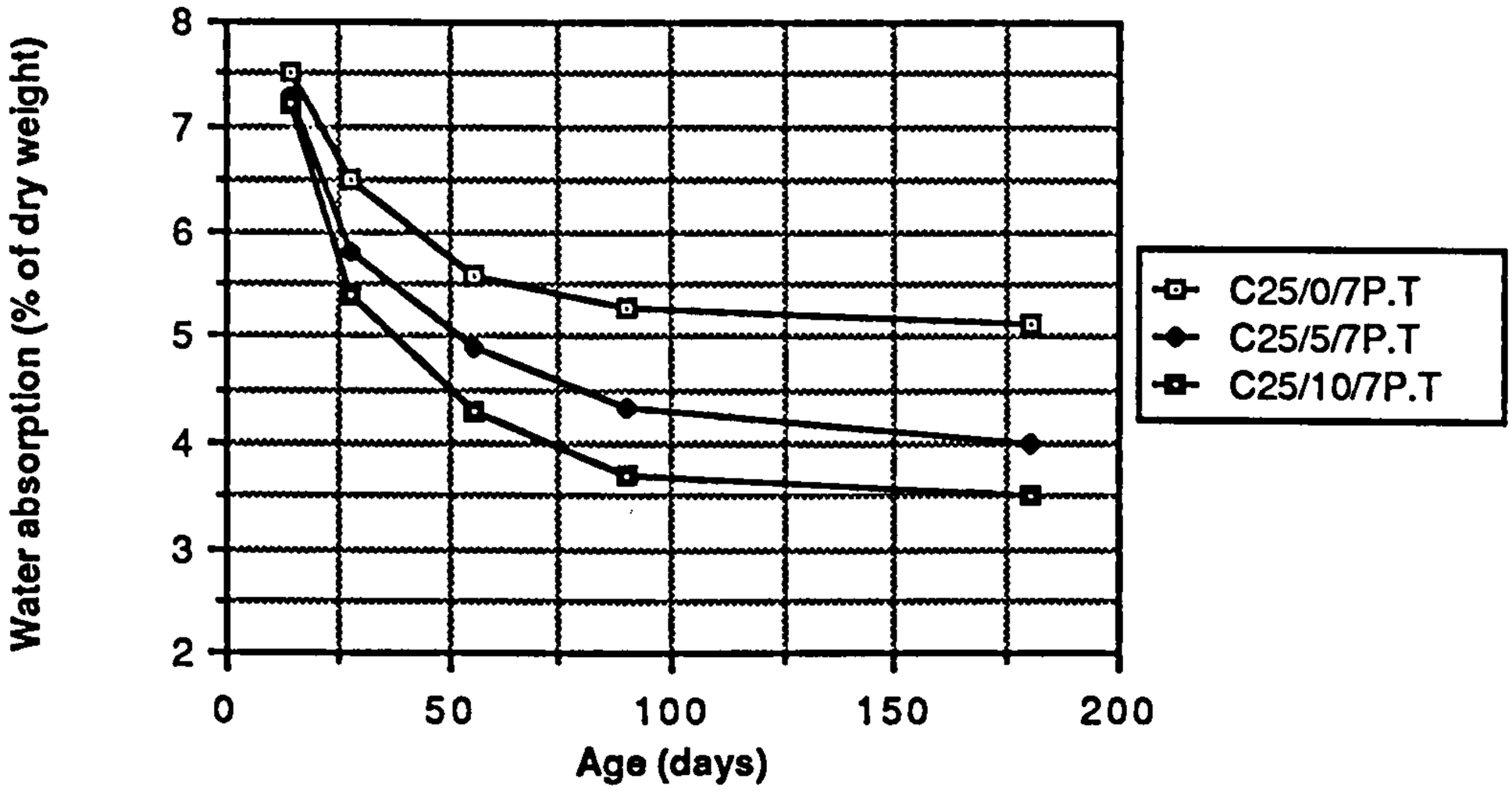

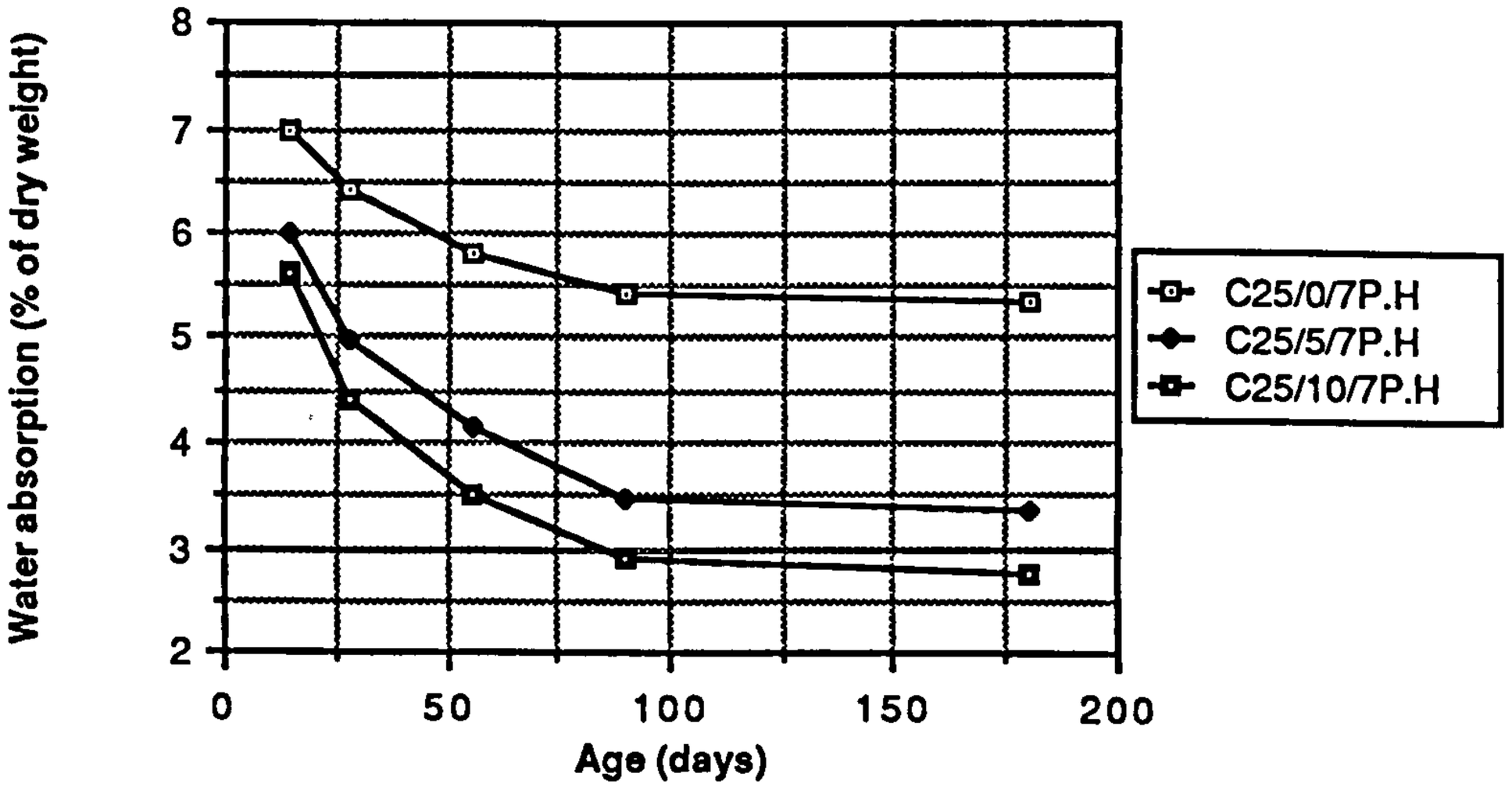

Figure A1.33 Relationship between age and water absorption of CSF concrete mixes grade C25

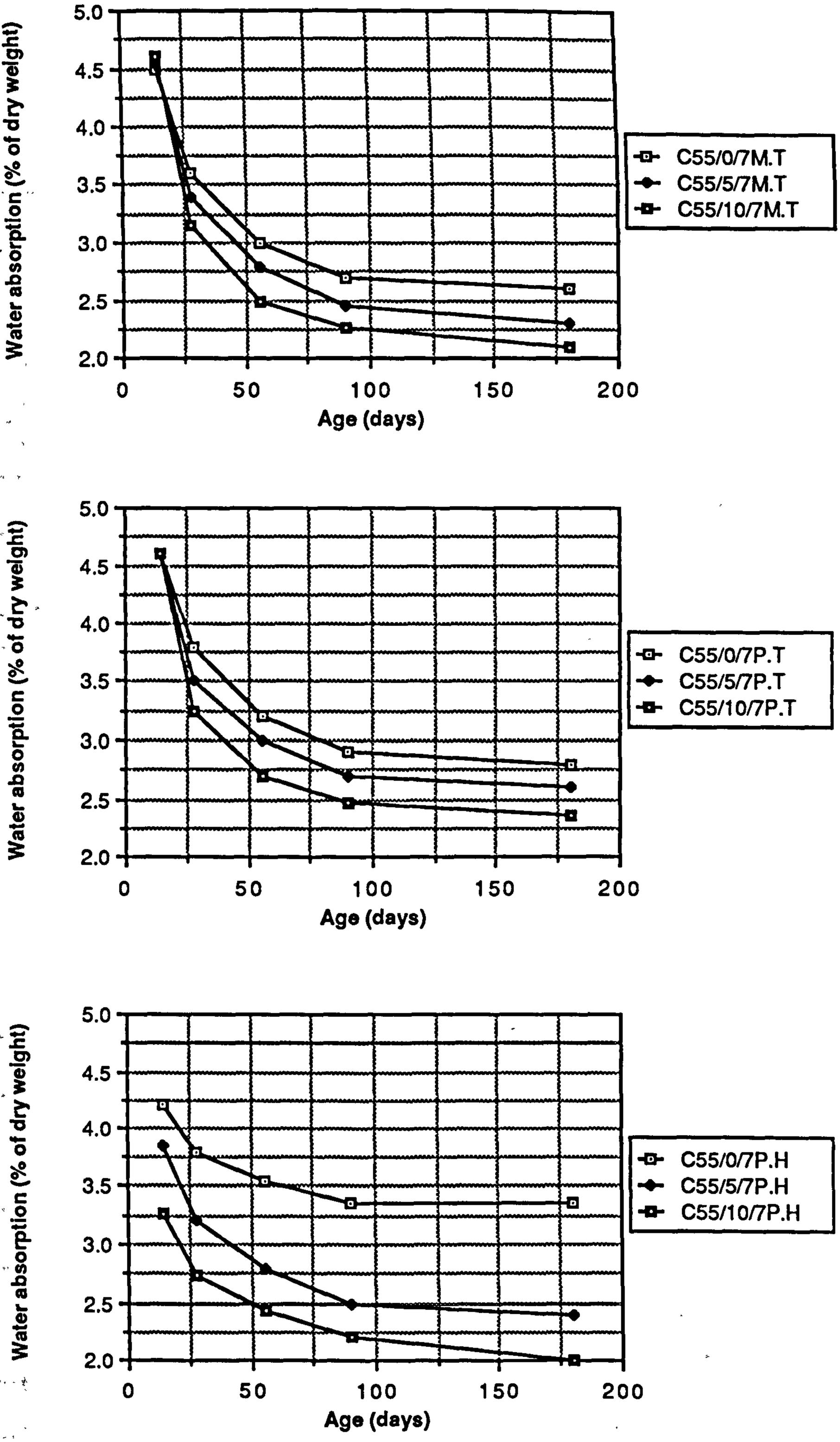

Figure A1.34 Relationship between age and water absorption of CSF concrete mixes grade C55

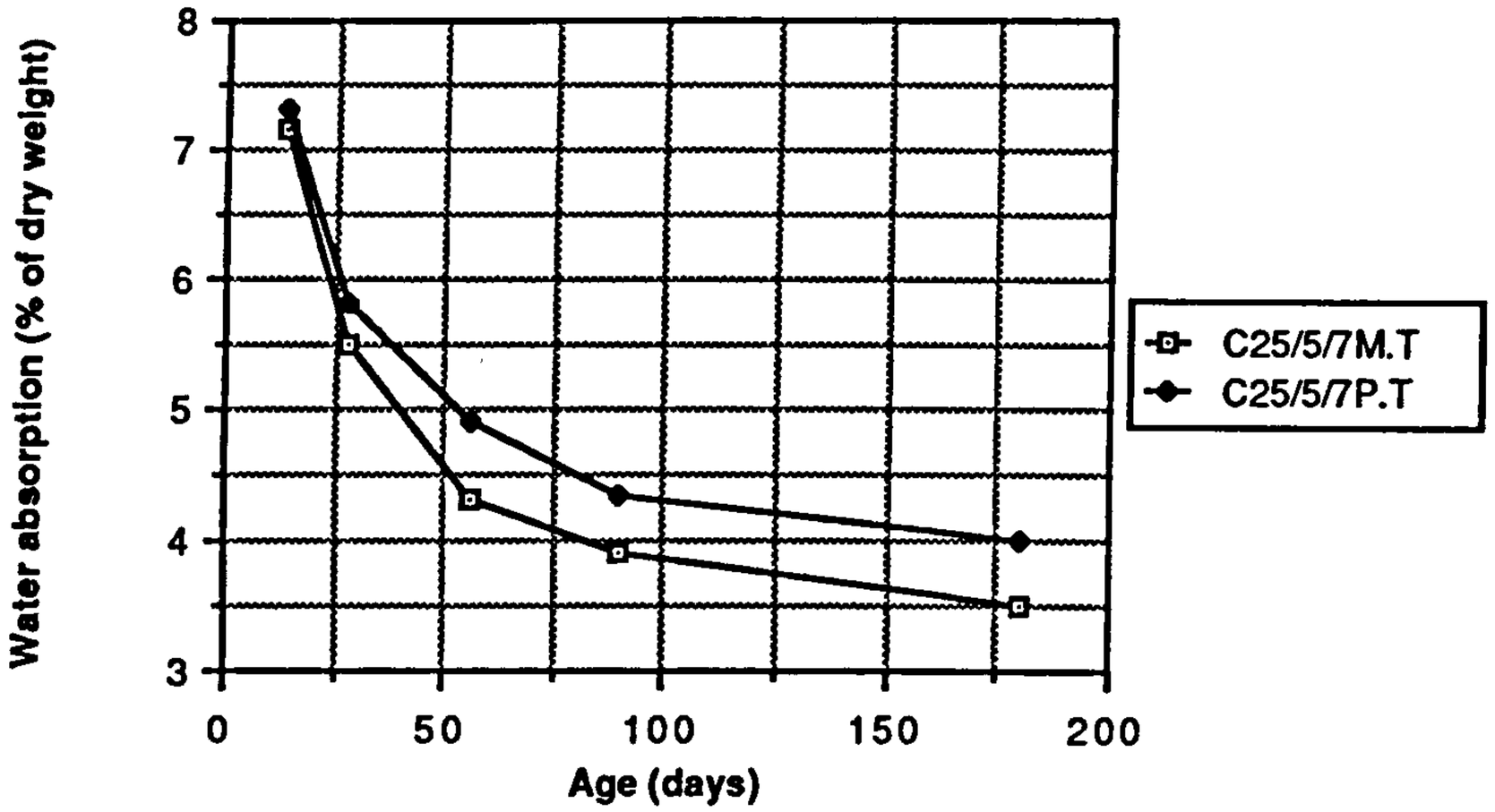

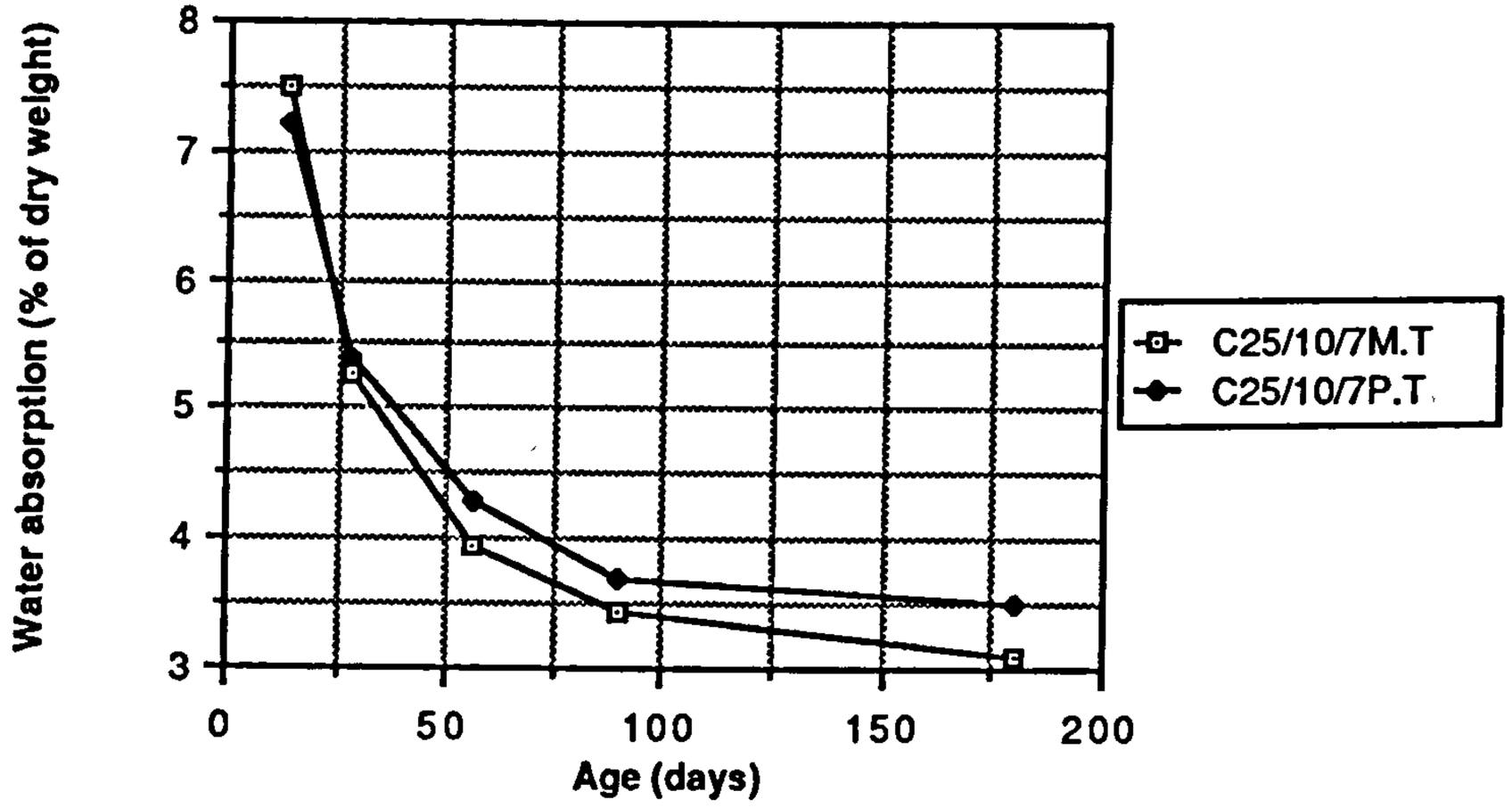

Figure A1.35 Effect of water and polythene curing on water absorption of CSF concrete mixes grade C25

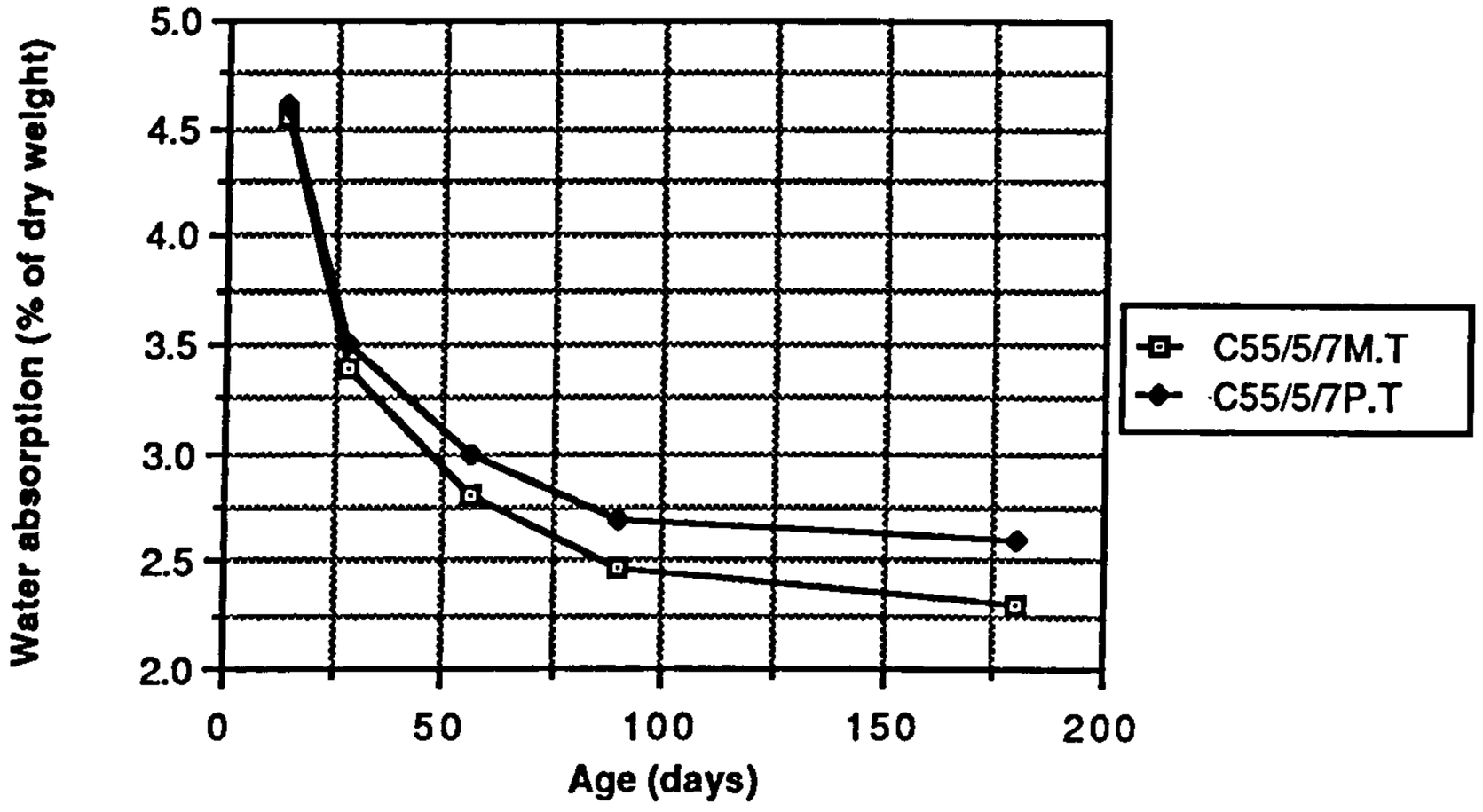

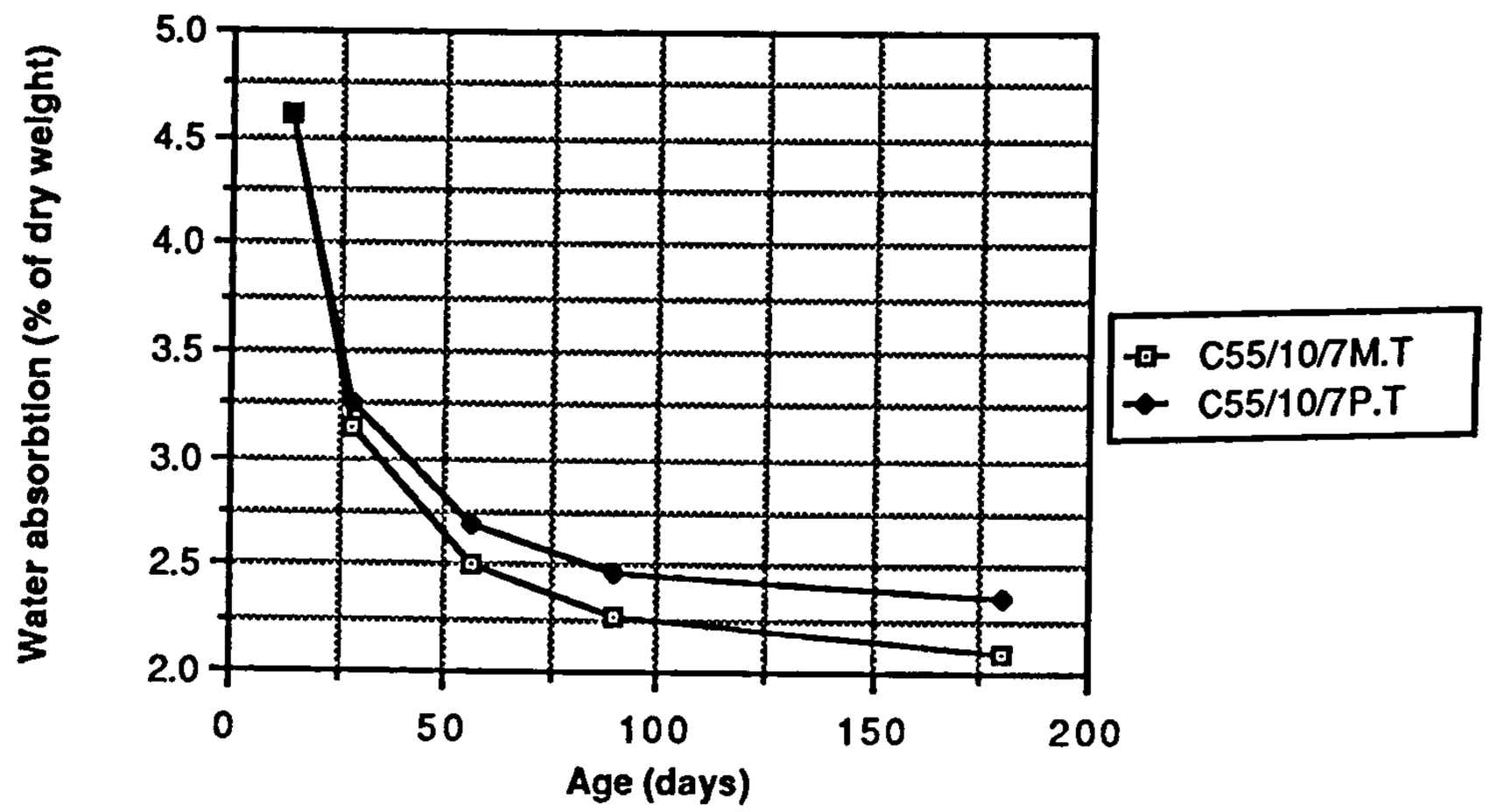

Figure A1.36 Effect of water and polythene curing on water absorption of CSF concrete mixes grade C55

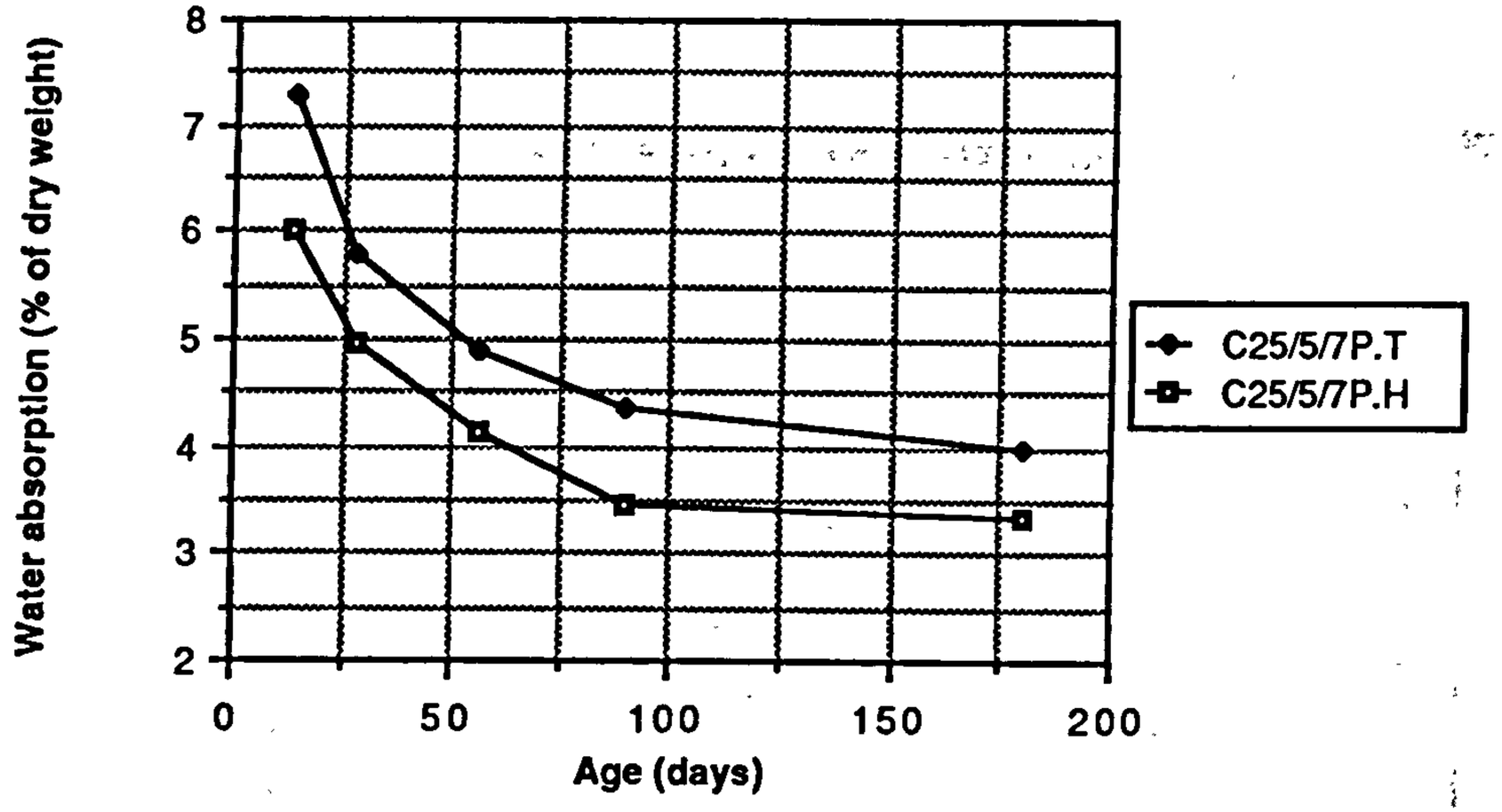

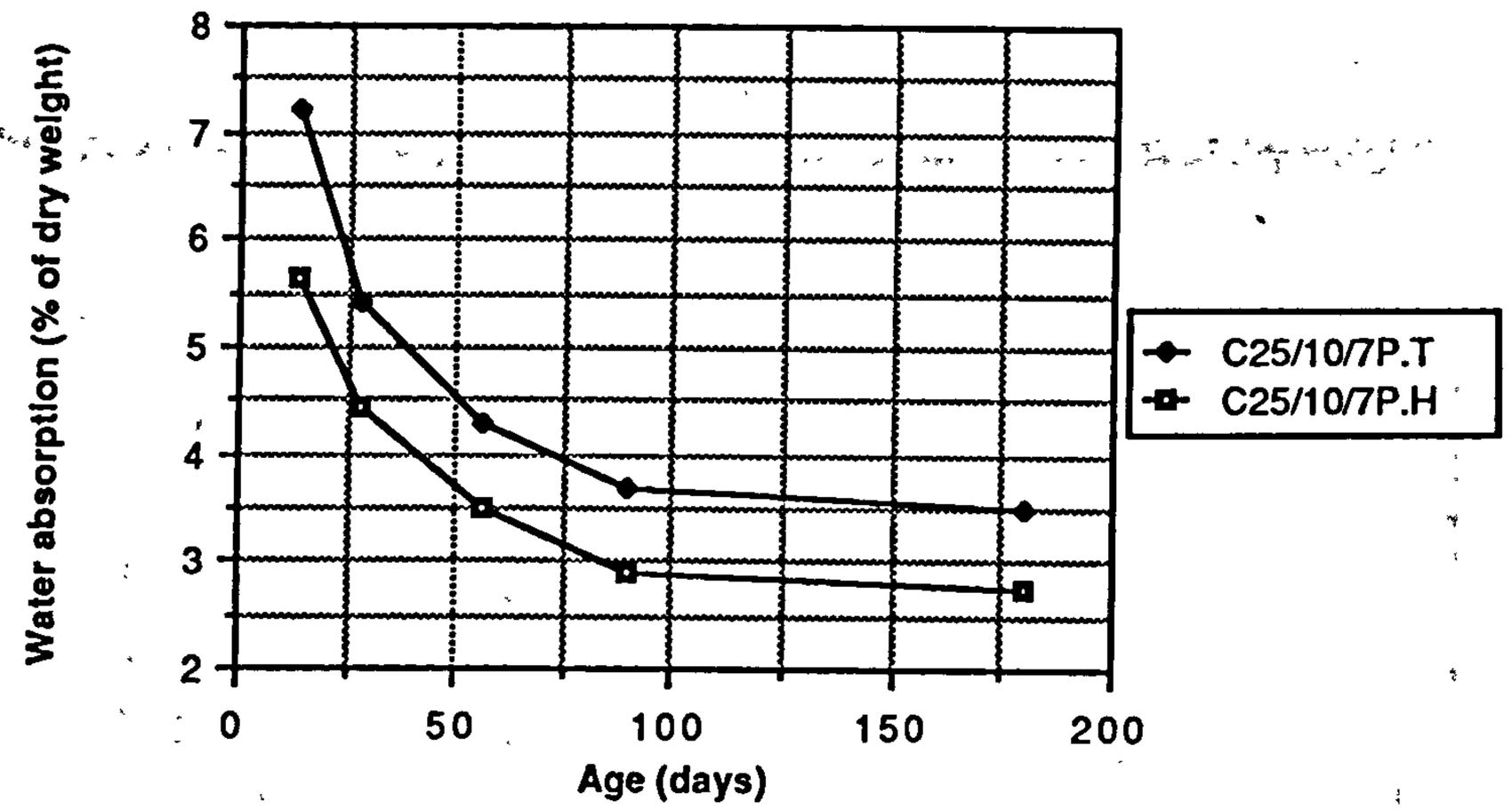

Figure A1.37 Effect of temperate and hot curing on water absorption of CSF concrete mixes grade C25

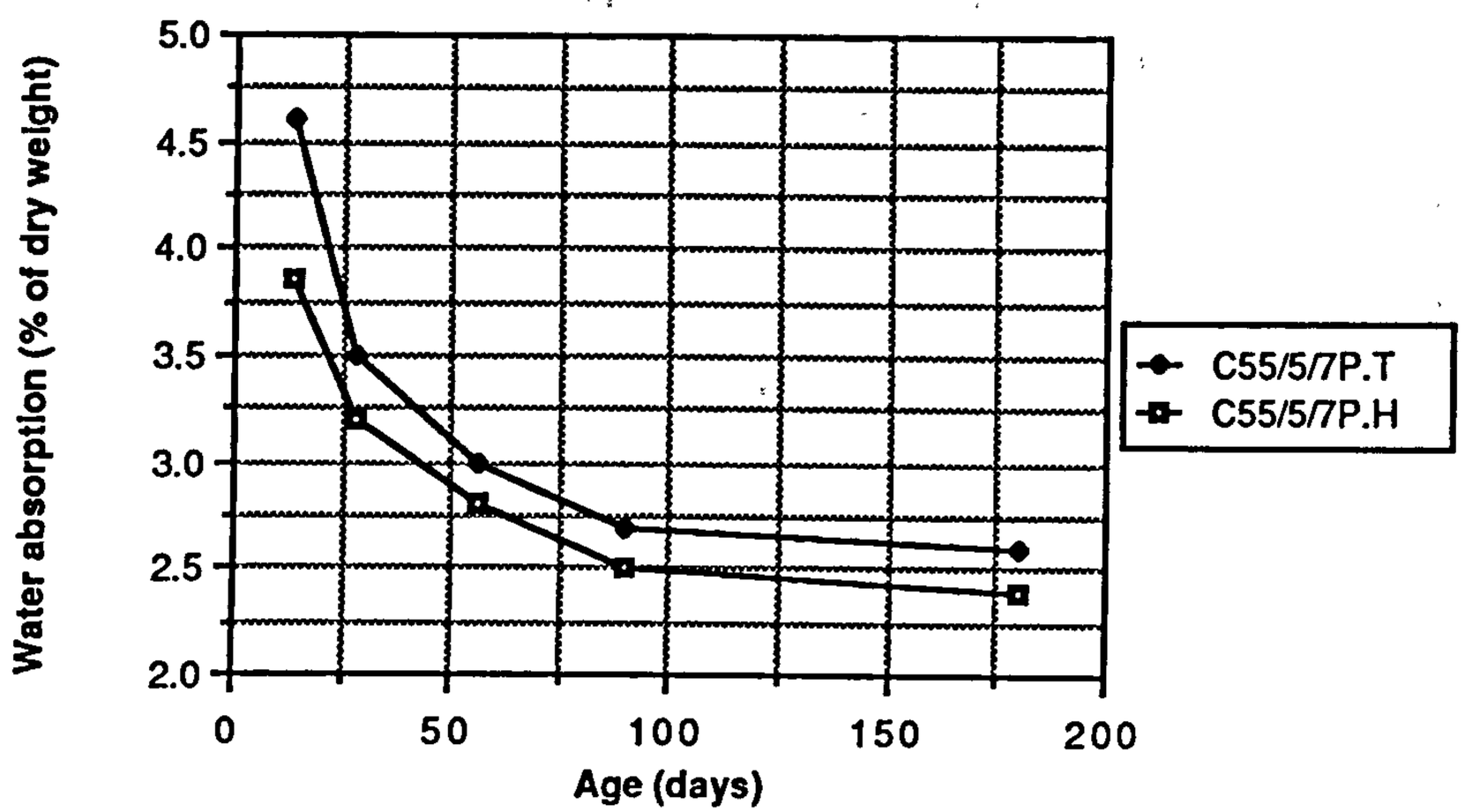

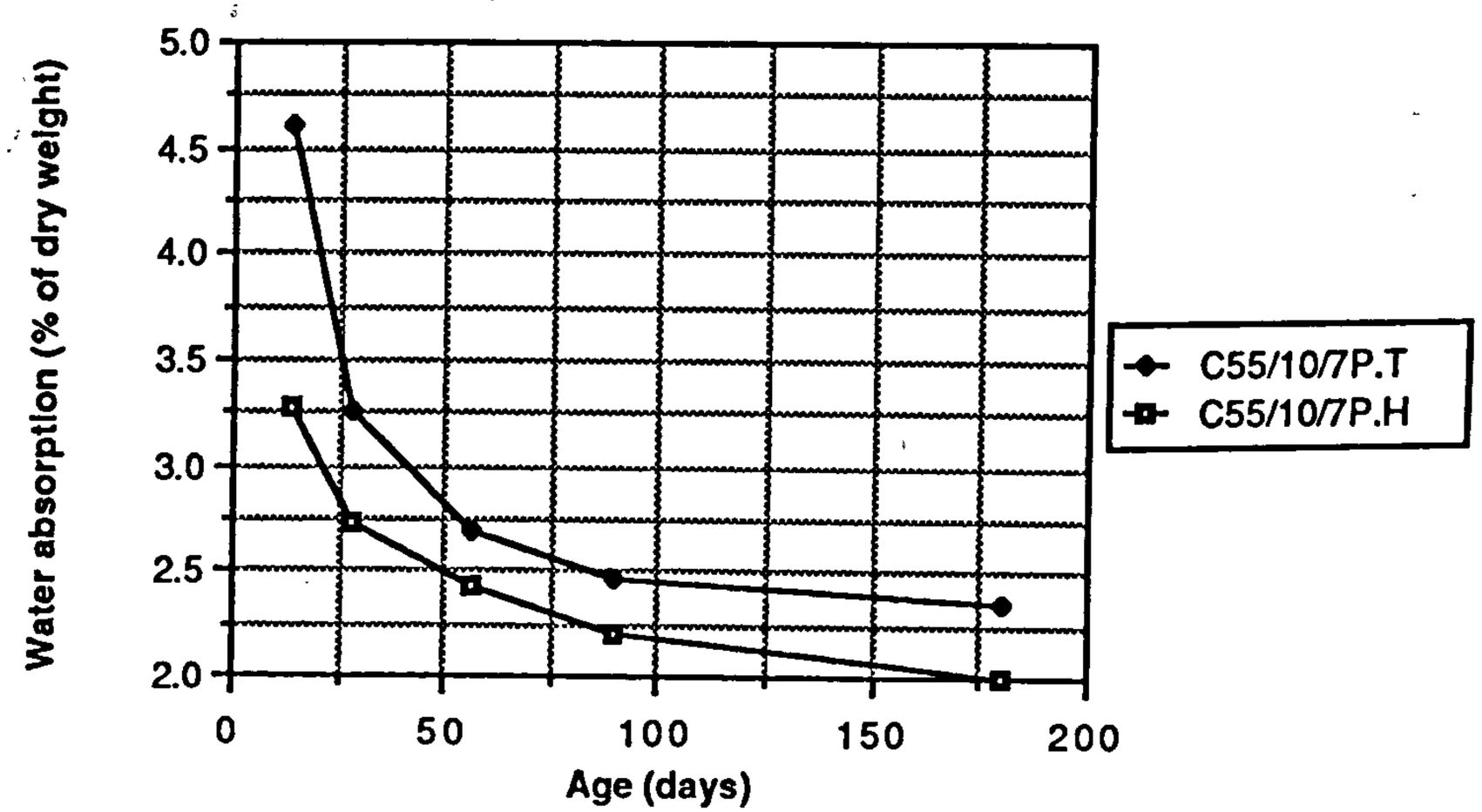

Figure A1.38 Effect of temperate and hot curing on water absorption of CSF concrete mixes grade C55

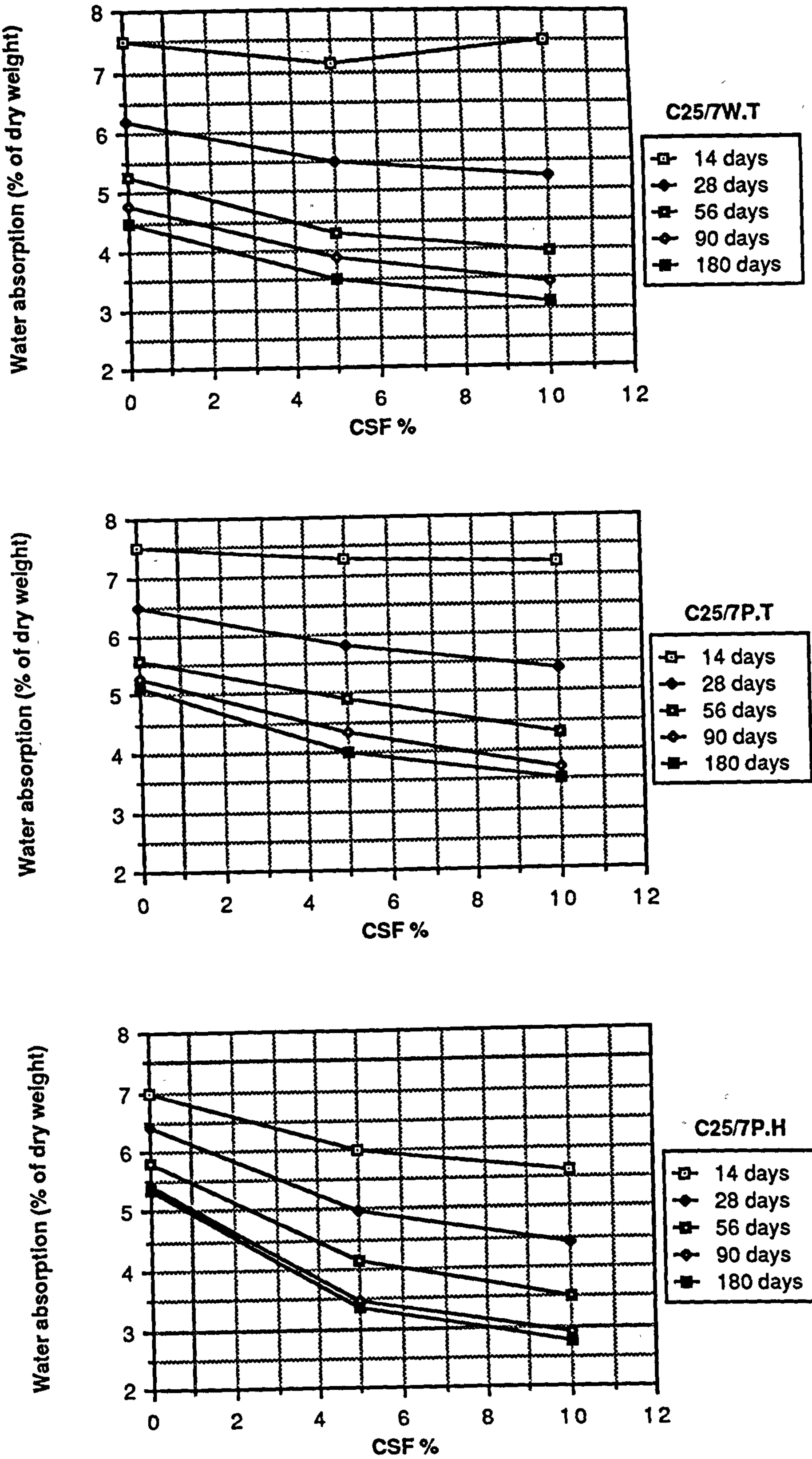

Figure A1.39 Effect of CSF content on water absorption of CSF concrete mixes grade C25

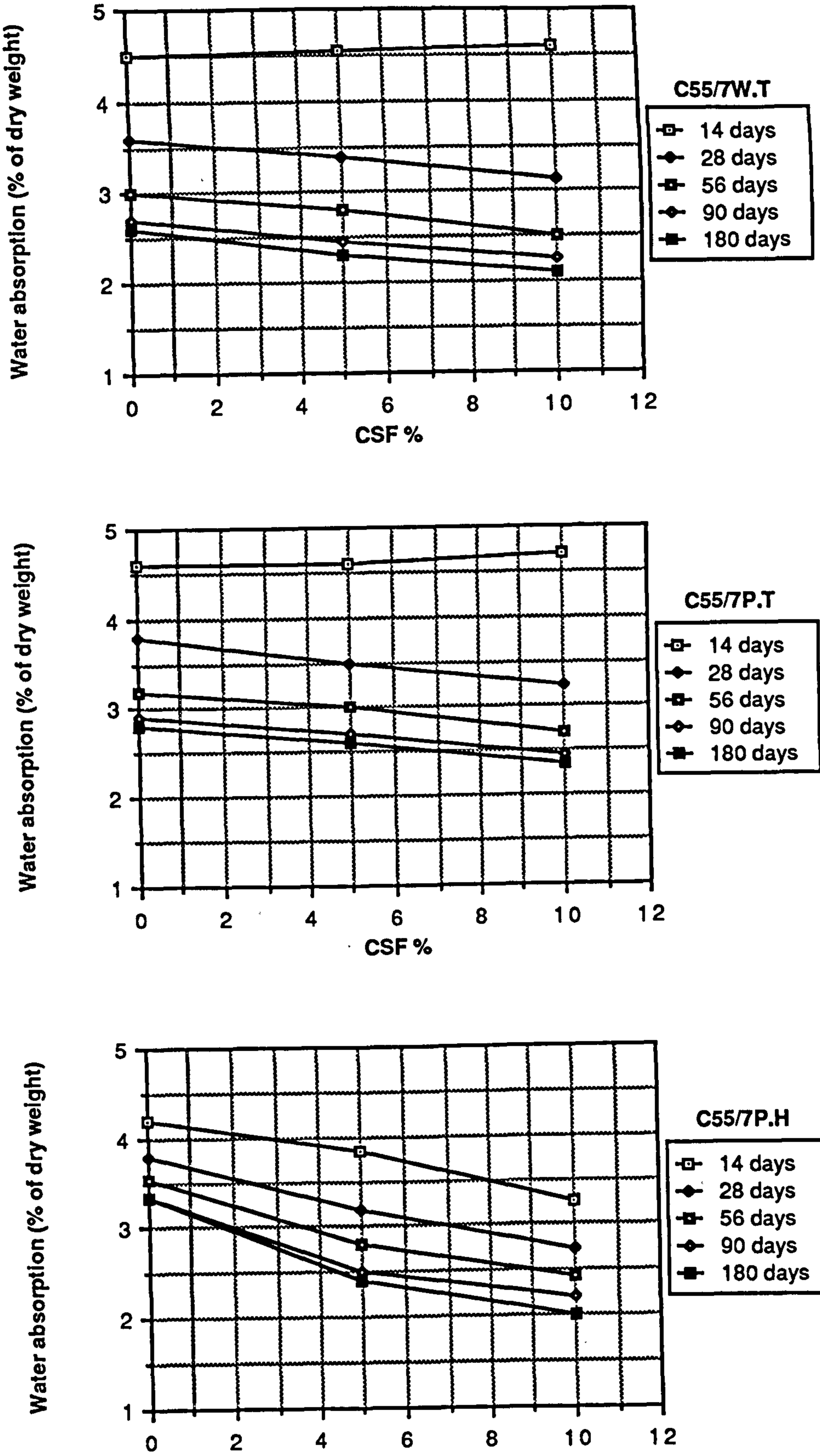

Figure A1.40 Effect of CSF content on water absorption of CSF concrete mixes grade C55

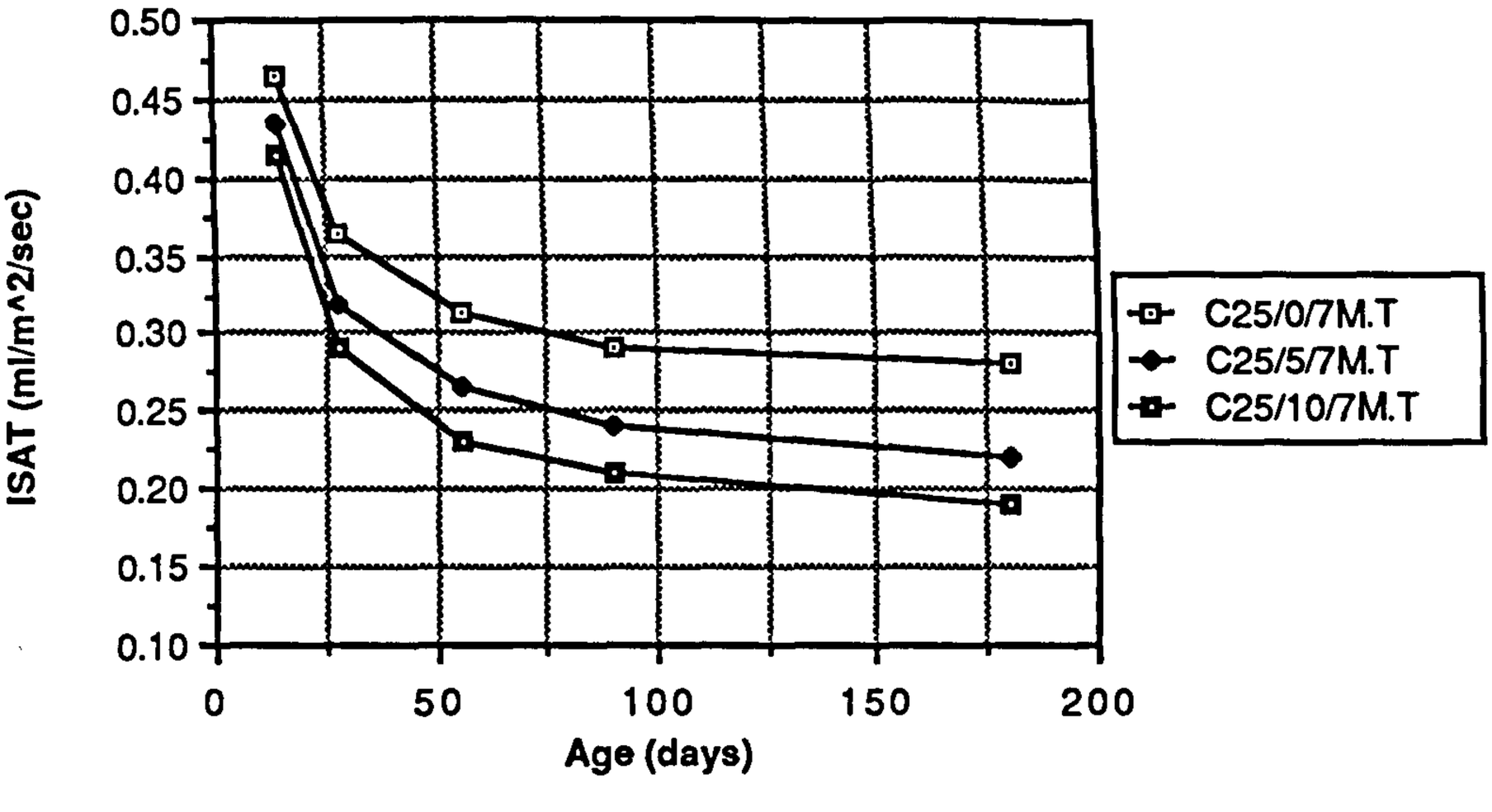

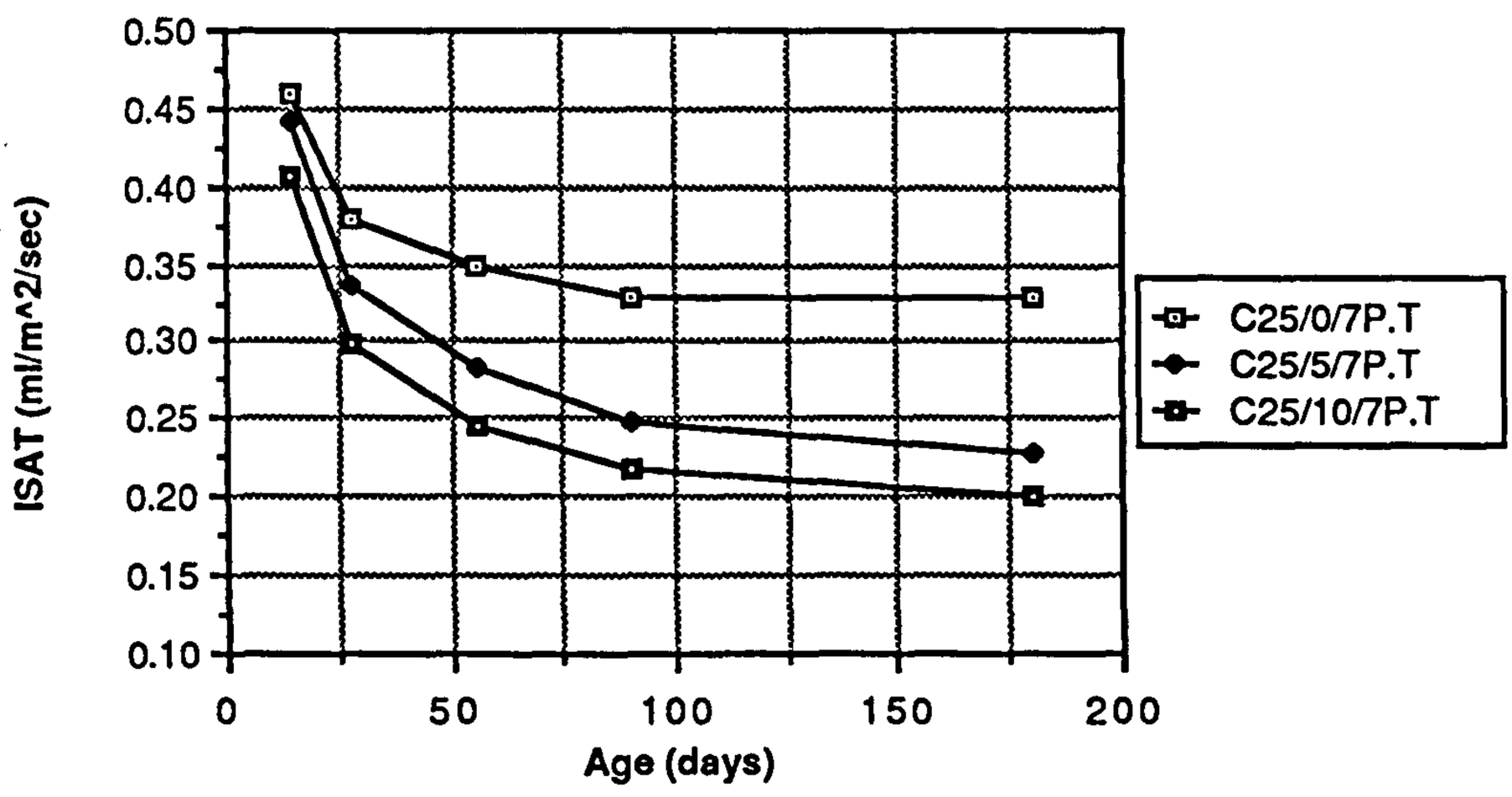

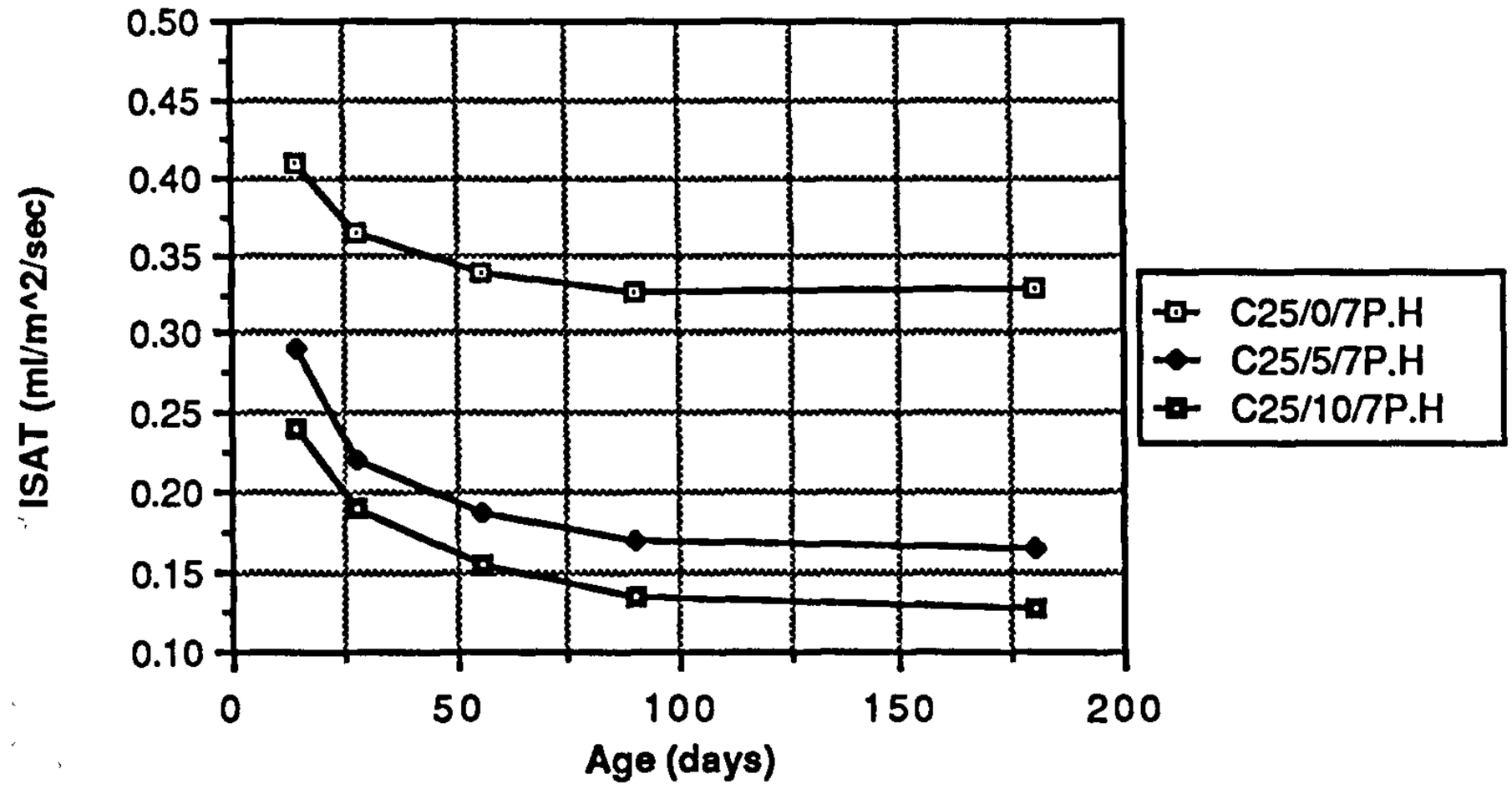

Figure A1.41 Relationship between age and ISAT of CSF concrete mixes grade C25

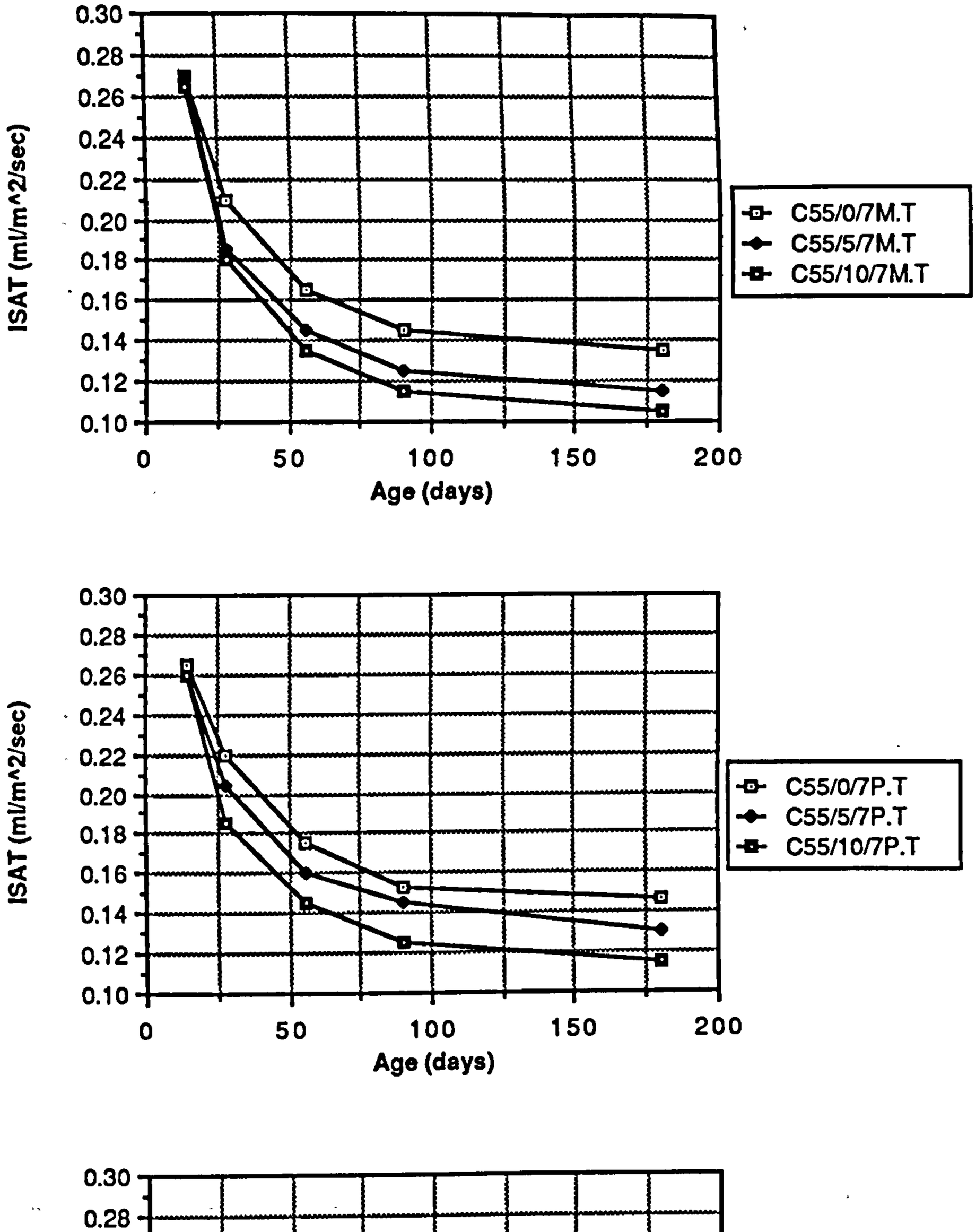

Figure A1.42 Relationship between age and ISAT of CSF concrete mixes grade C55

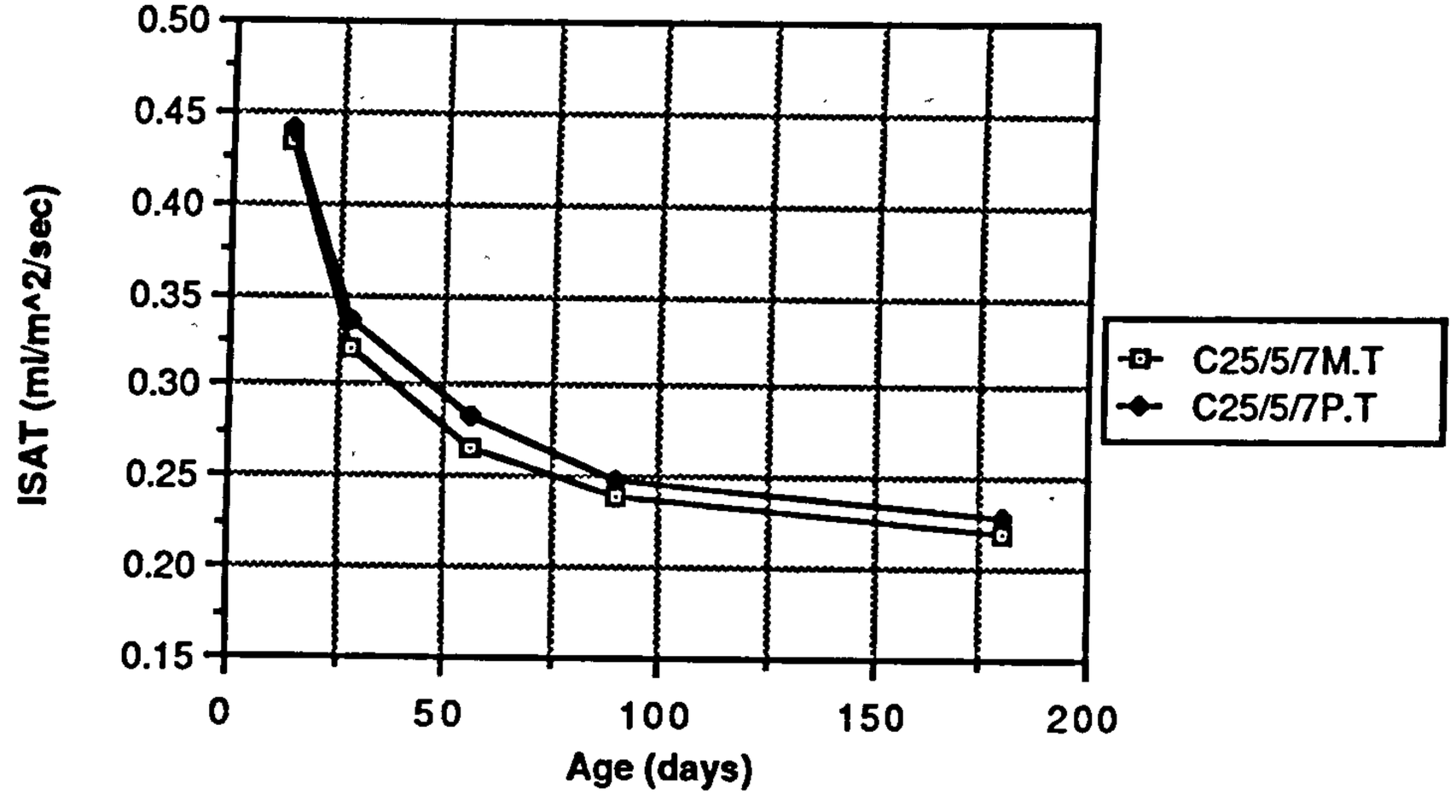

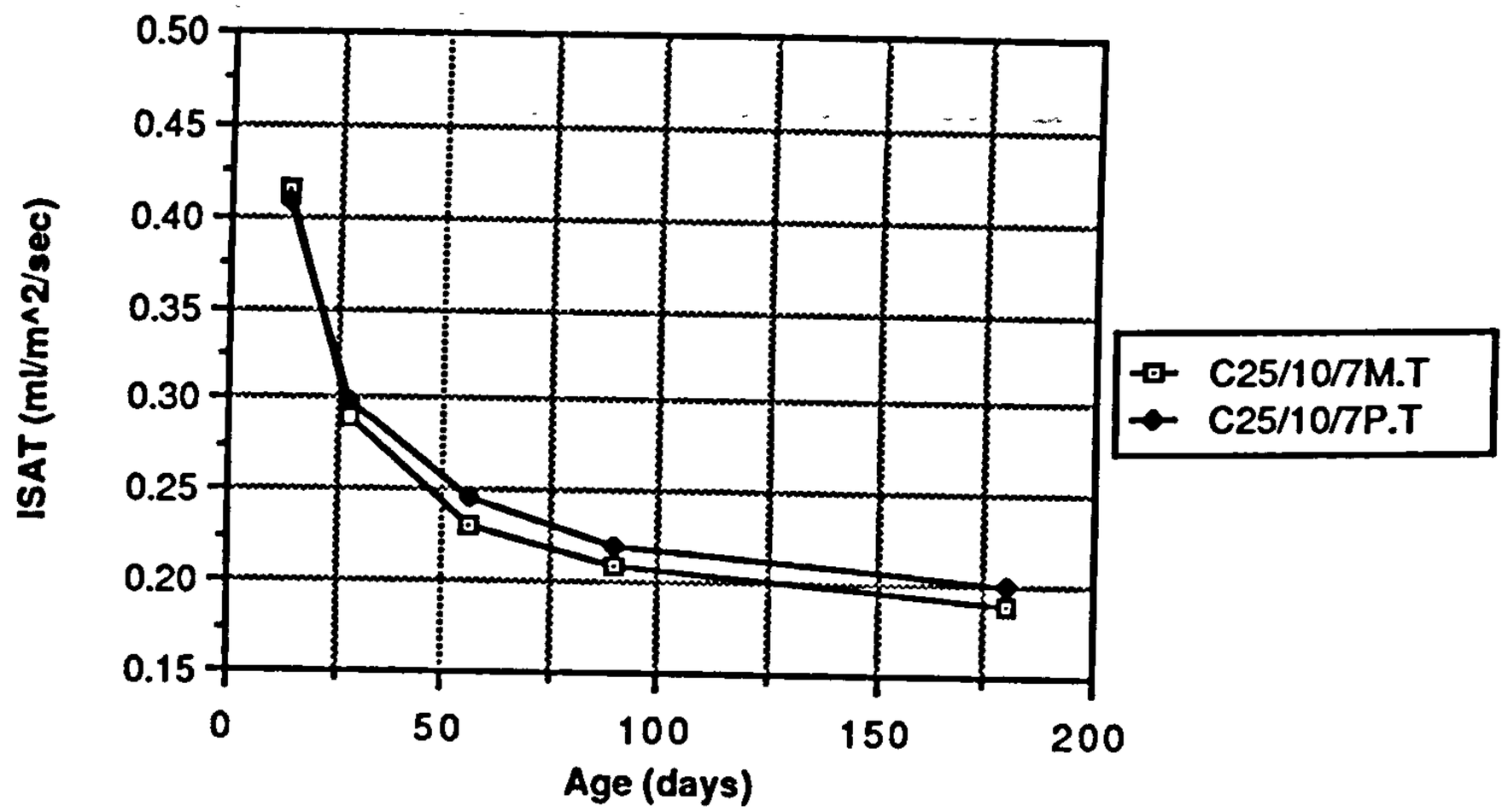

Figure A1.43 Effect of water and polythene curing on ISAT of CSF concrete mixes grade C25

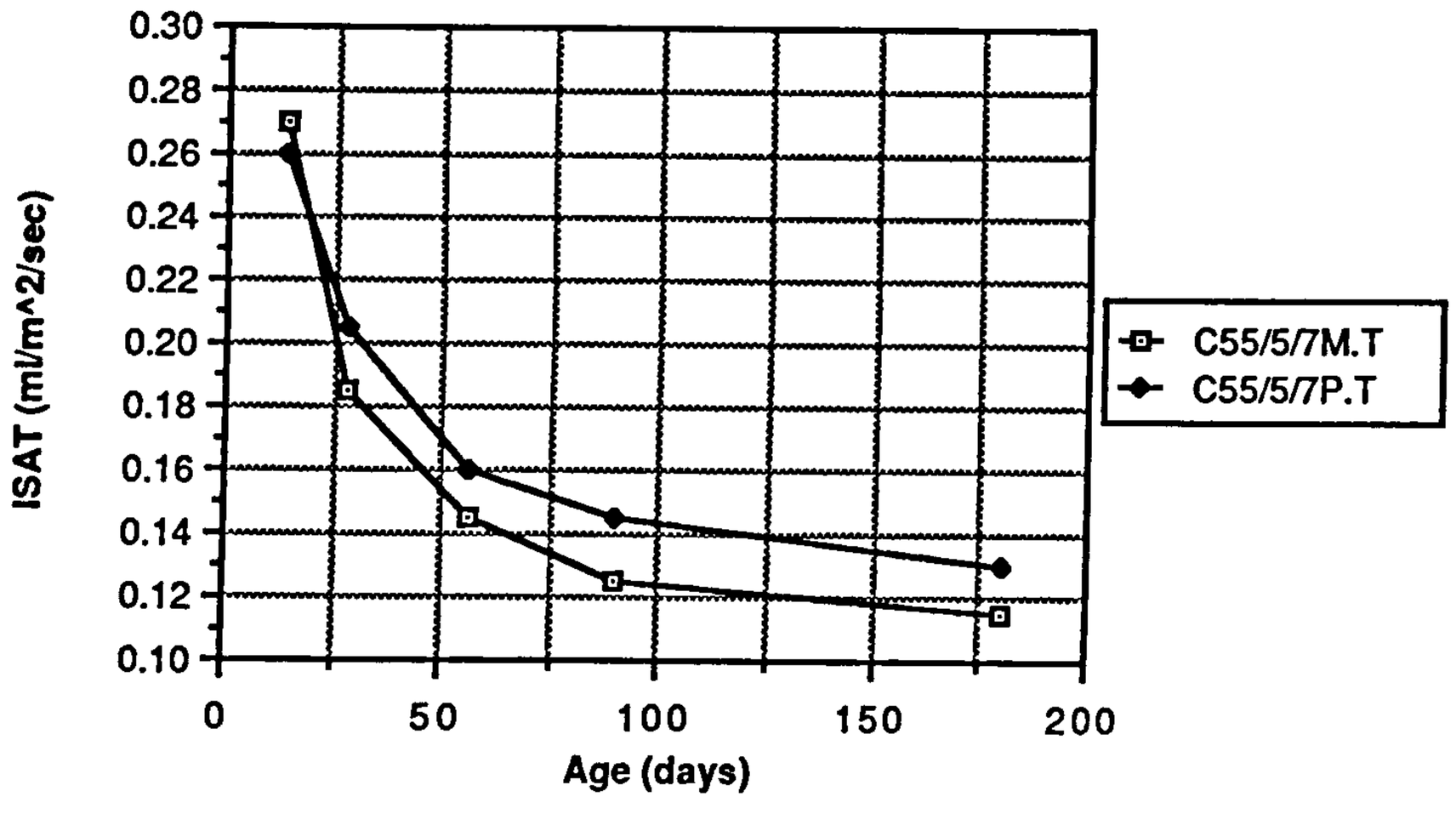

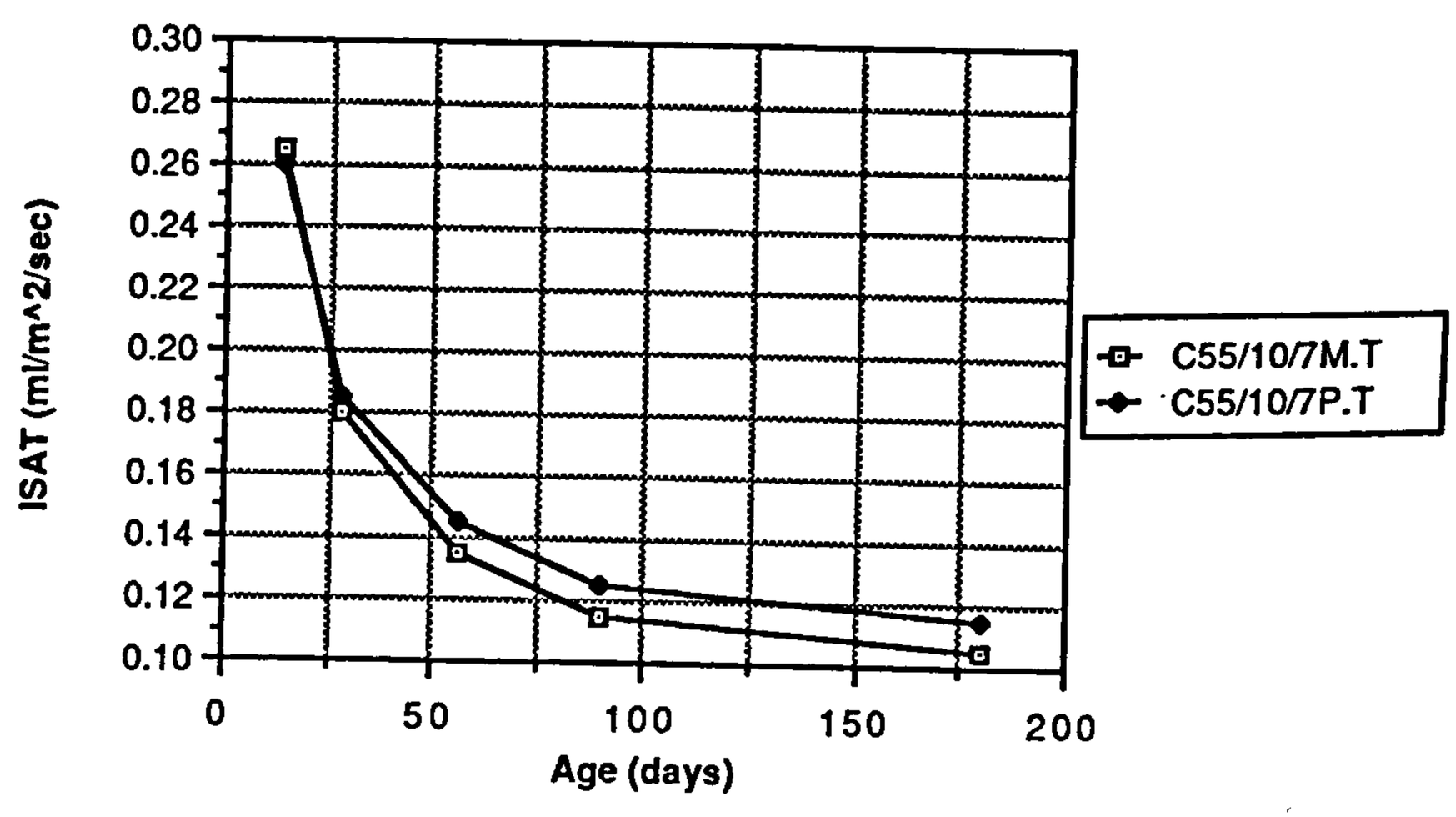

Figure A1.44 Effect of water and polythene curing on ISAT of CSF concrete mixes grade C55

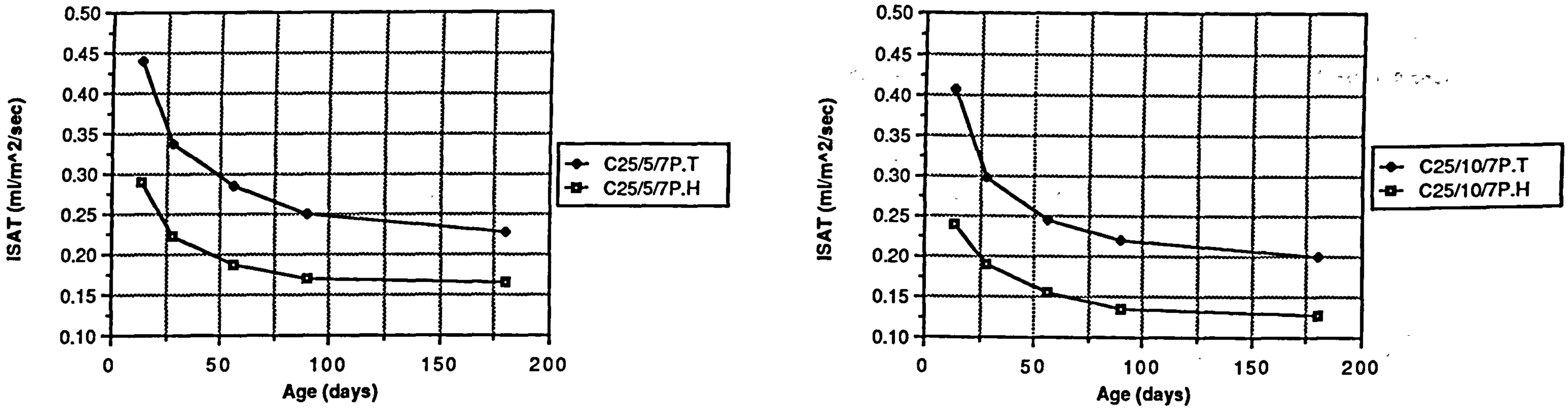

Figure A1.45 Effect of temperate and hot curing on ISAT of CSF concrete mixes grade C25

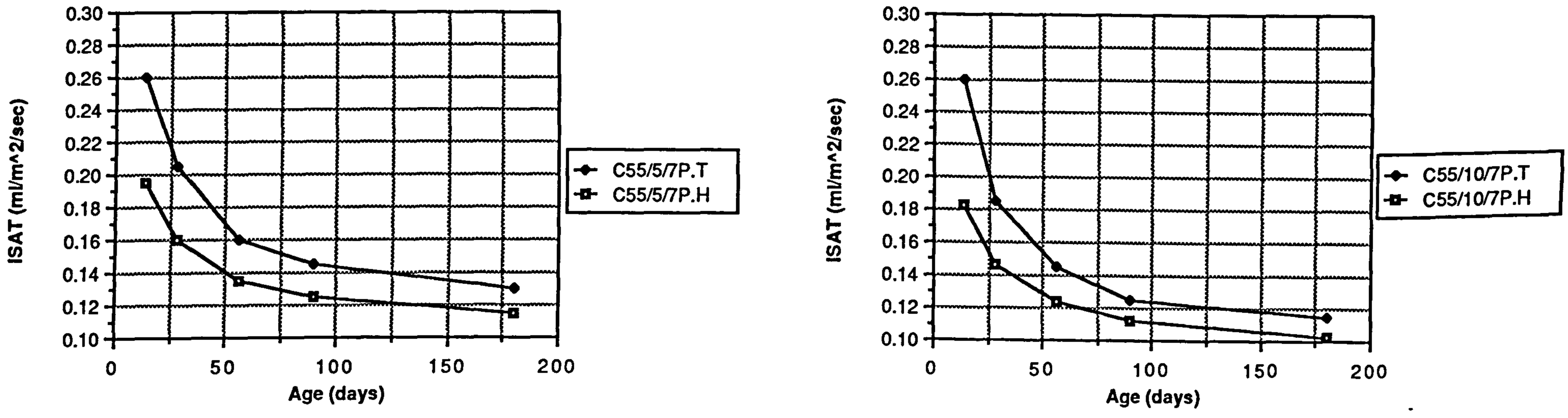

Figure A1.46 Effect of temperate and hot curing on ISAT of CSF concrete mixes grade C55

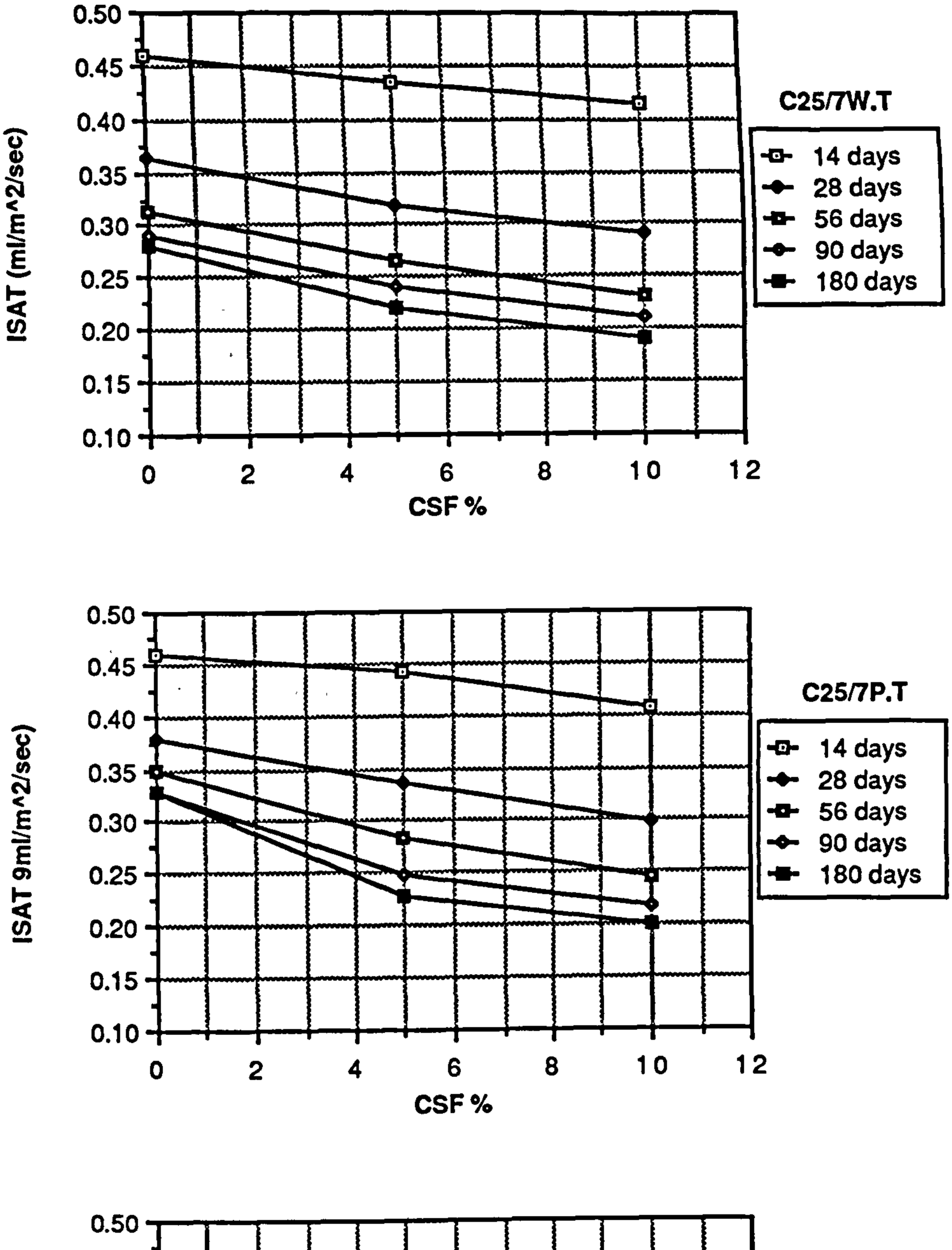

Figure A1.47 Effect of CSF content on ISAT og CSF concrete mixes grade C25

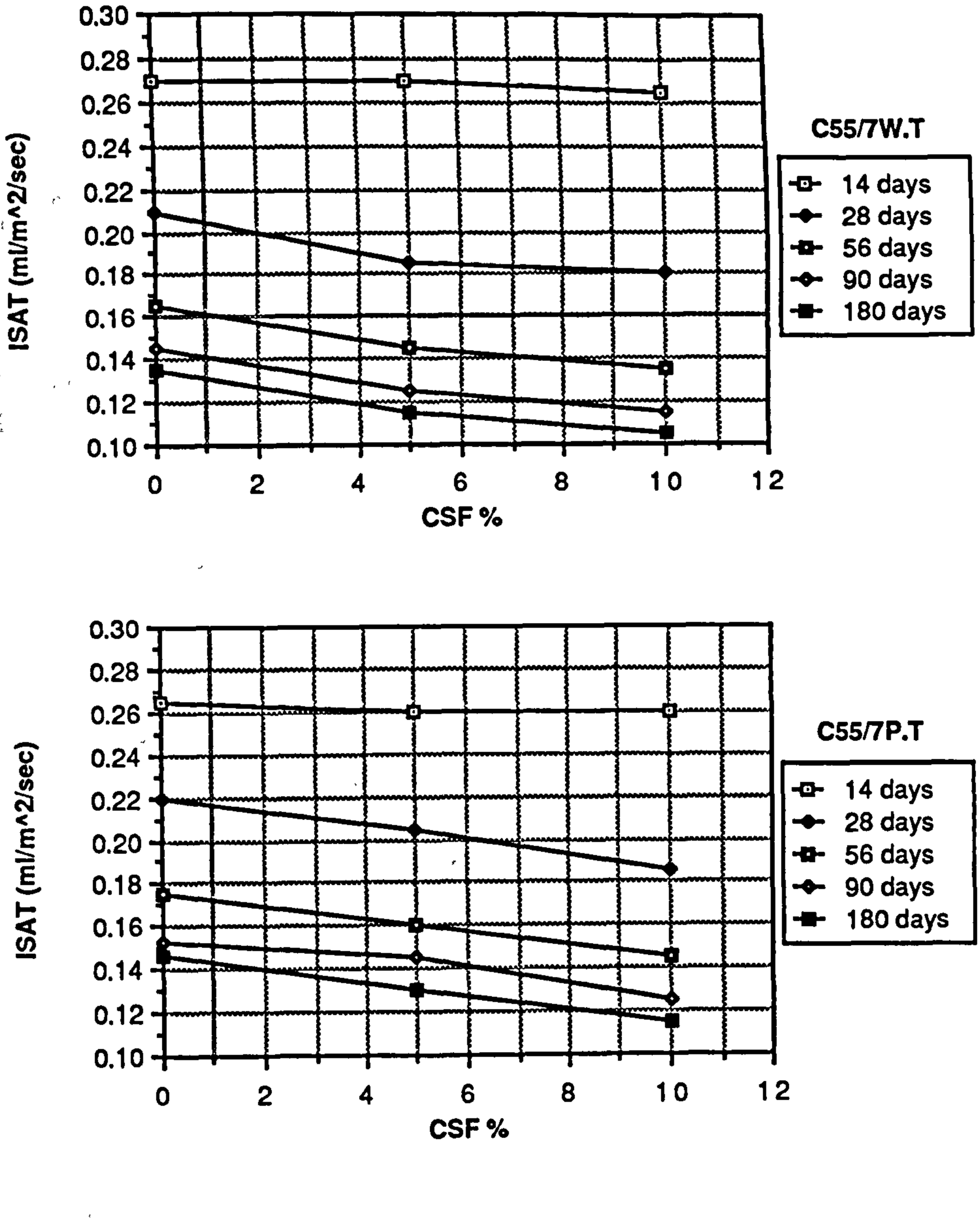

Figure A1.48 Effect of CSF content on ISAT of CSF concrete mixes grade C55

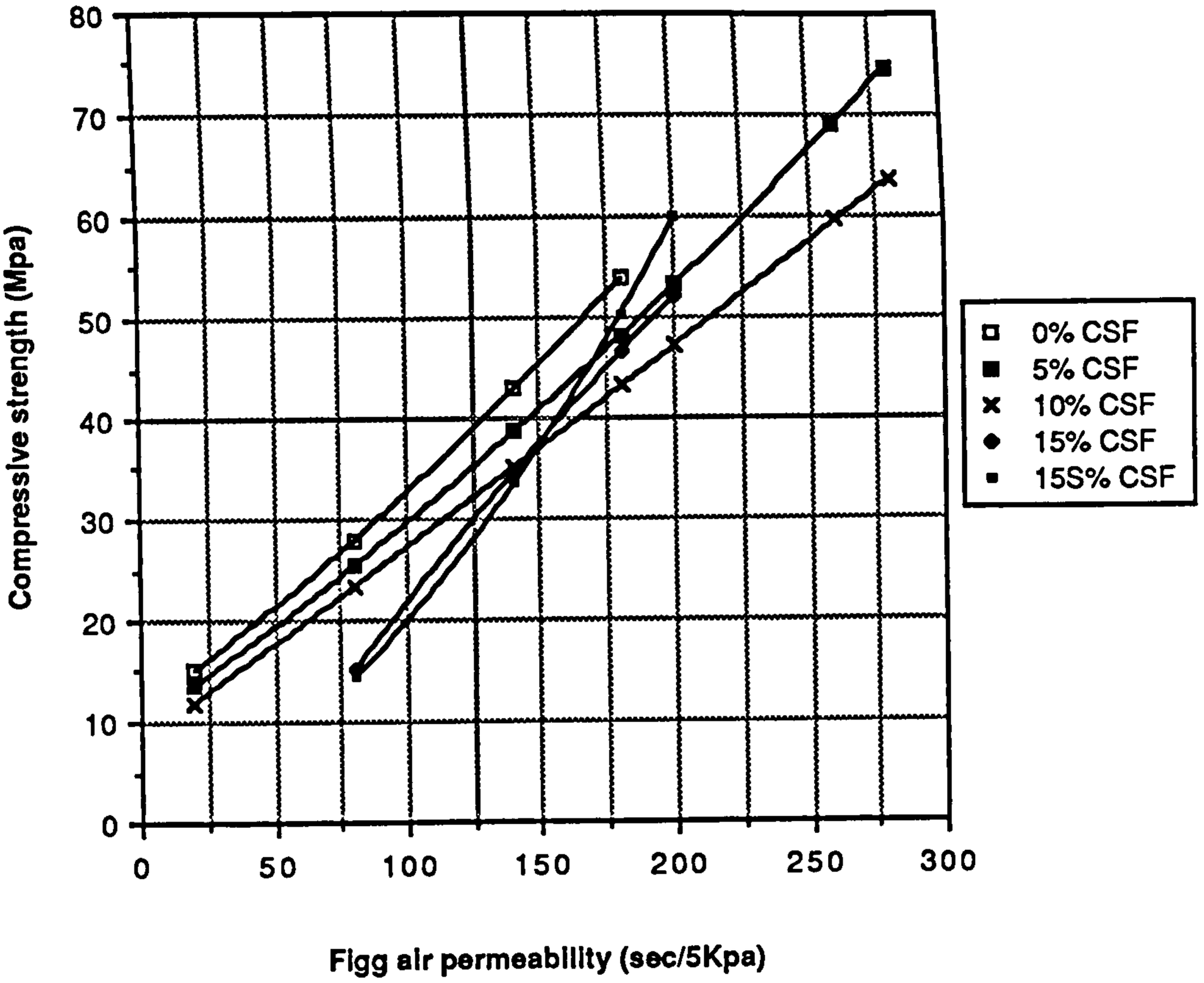

Figure A1.49 Relationship between compressive strength and Figg air permeability (temperate curing)

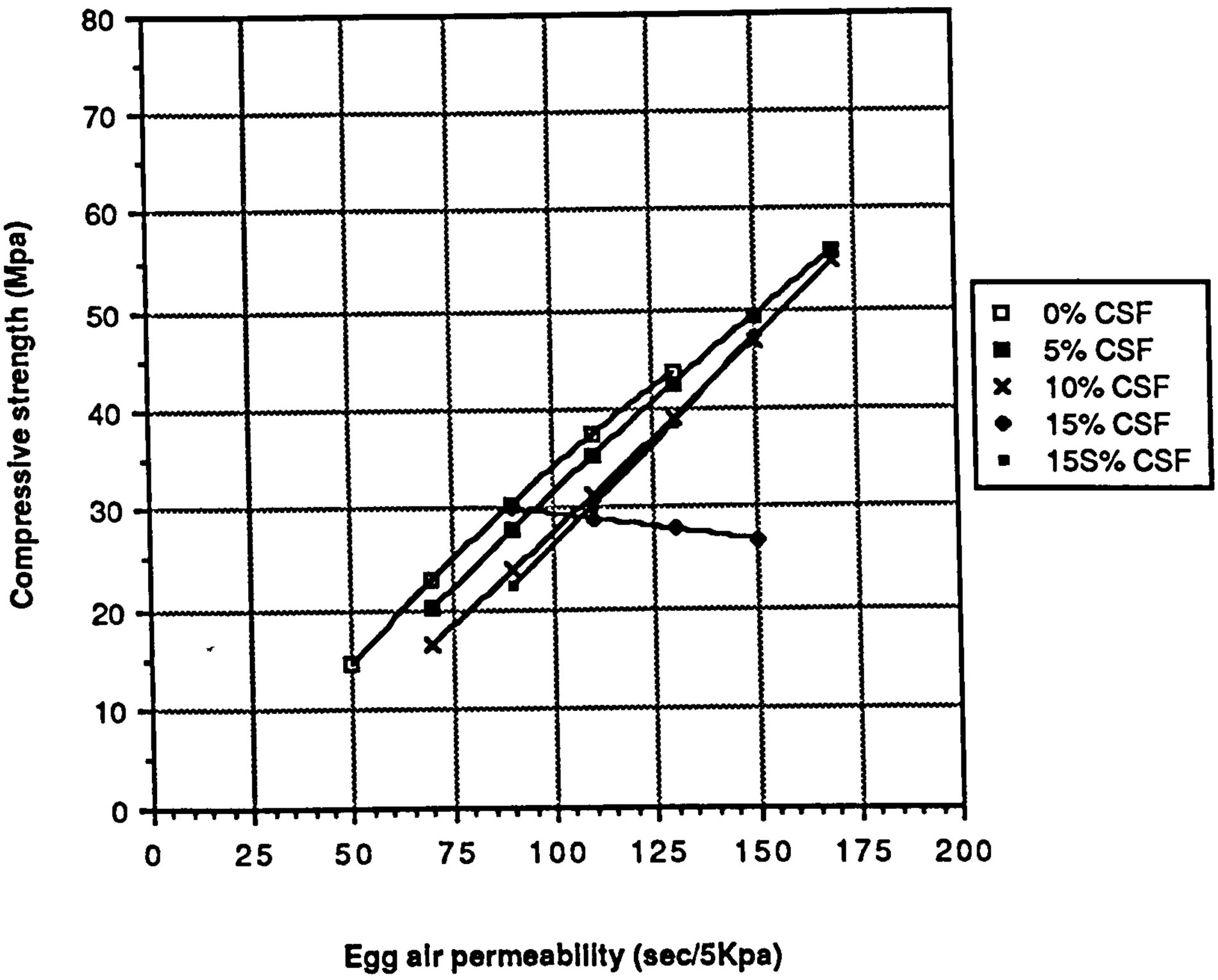

Figure A1.50 Relationship between compressive strength and Egg air permeability (temperate curing)

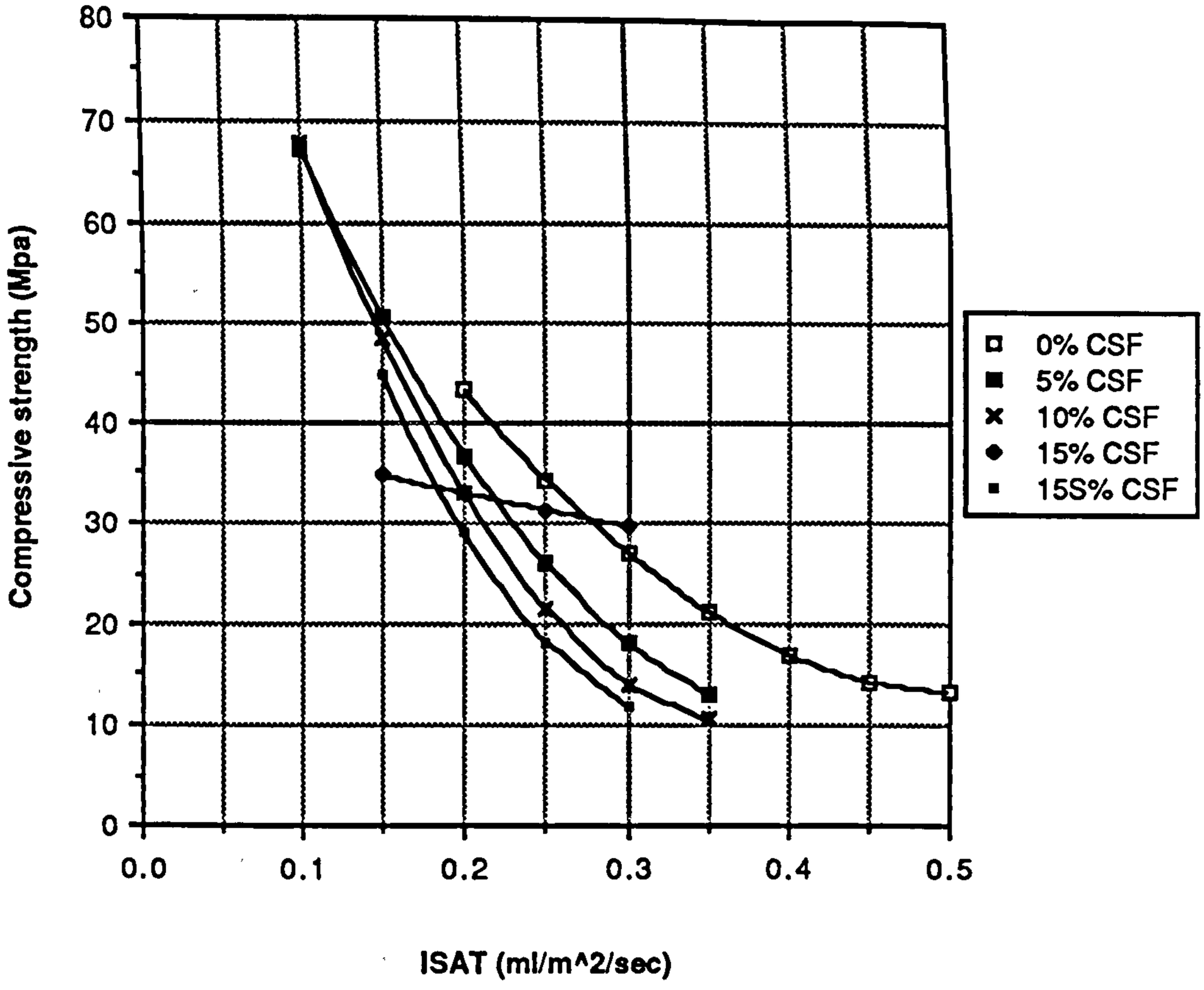

Figure A1.51 Relationship between compressive strength and ISAT (temperate curing)

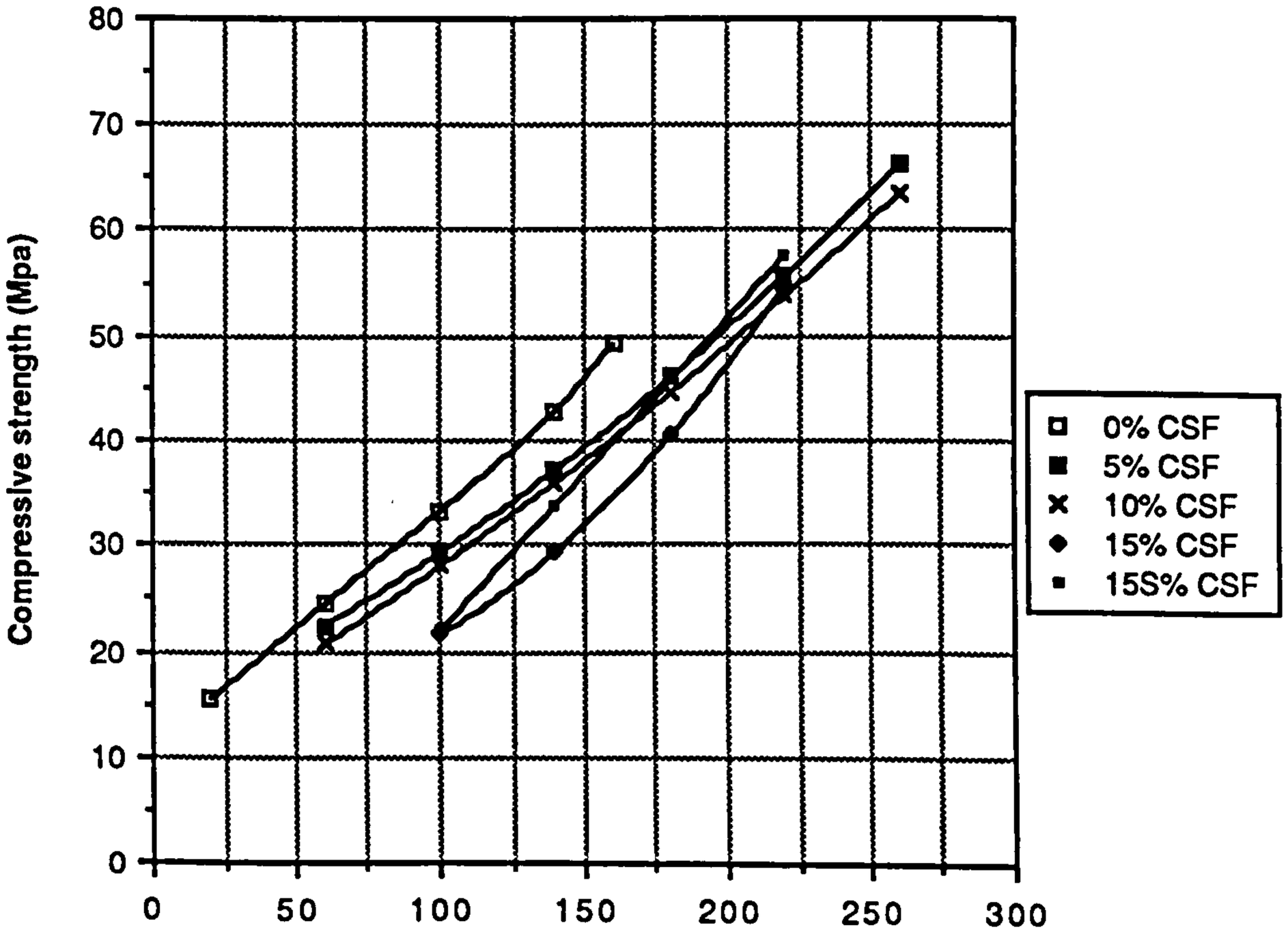

Figure A1.52 Relationship between compressive strength and Figg air permeability (hot curing)

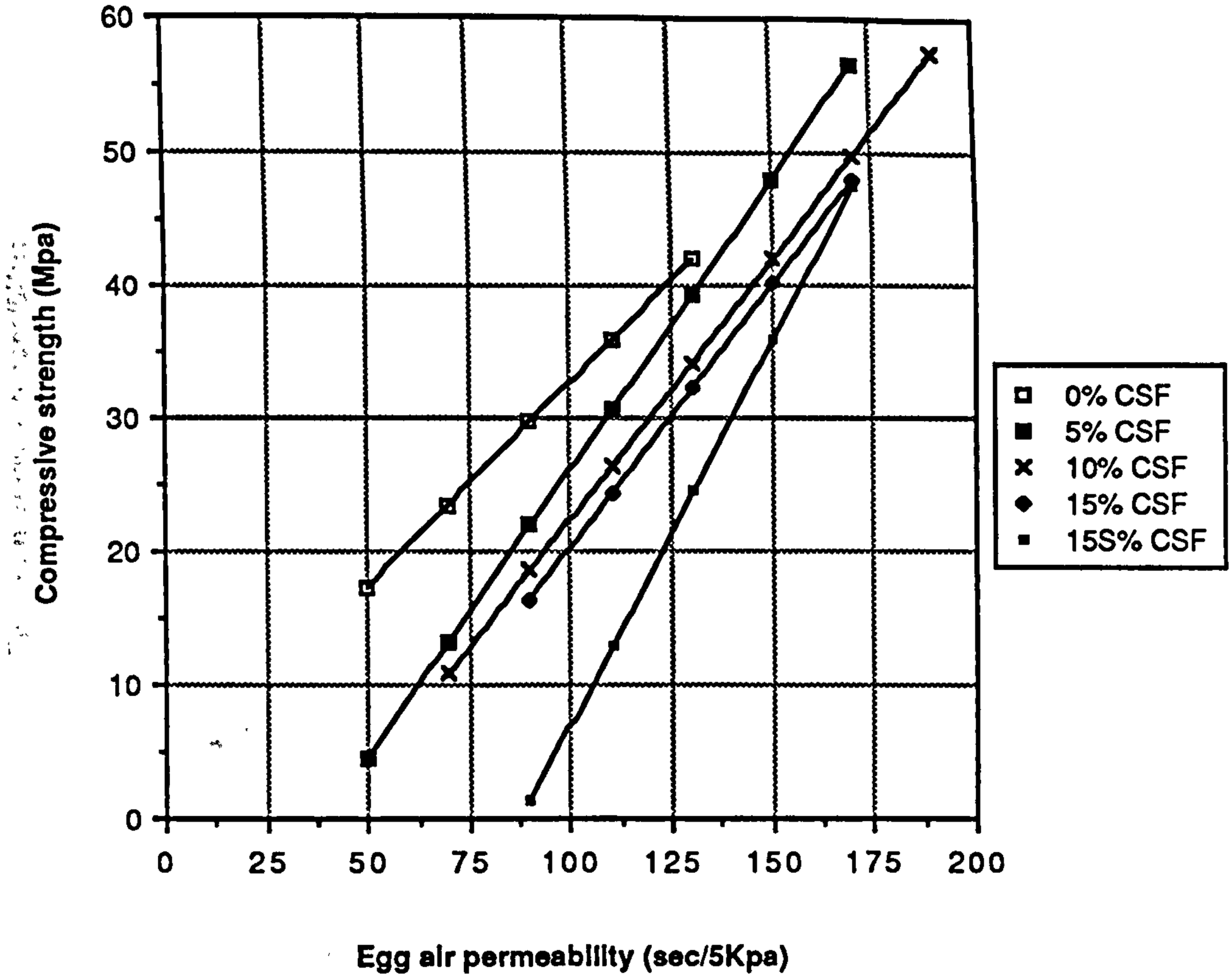

Figure A1.53 Relationship between compressive strength and Egg air permeability (hot curing)

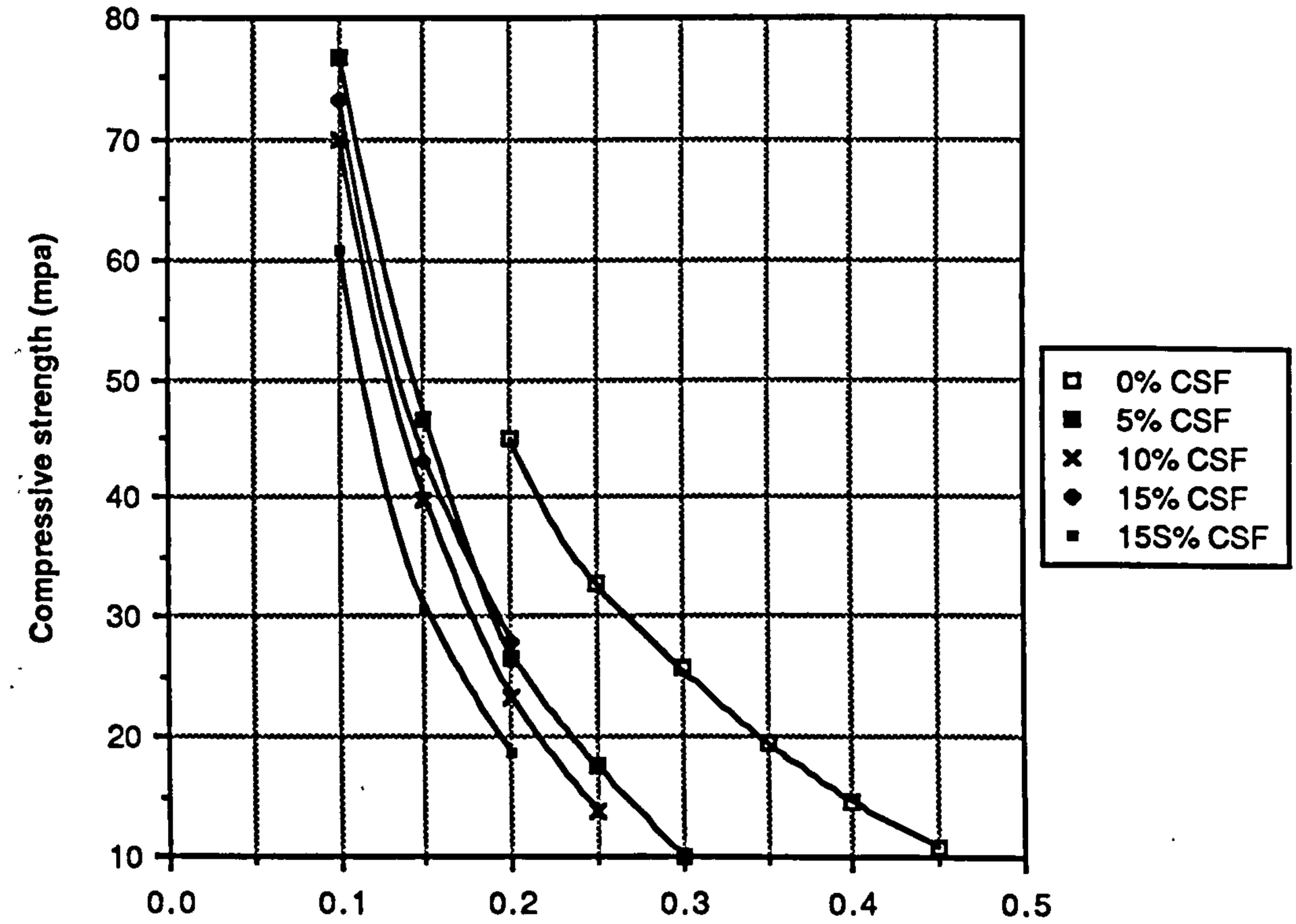

Figure A1.54 Relationship between compressive strength and ISAT (hot curing)

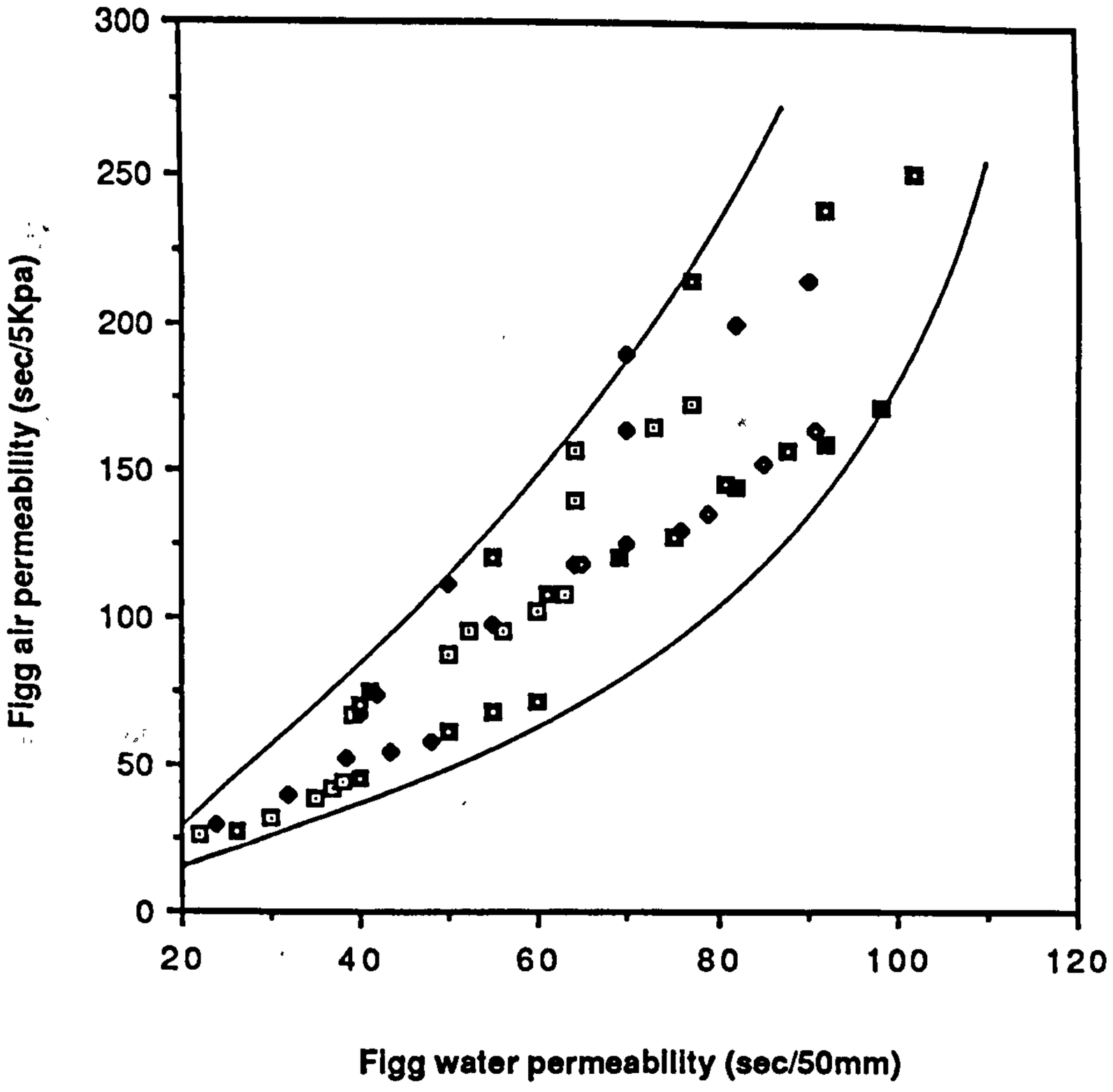

Figure A1.55 Relationship between Figg air permeability and Figg water permeability (temperate curing)

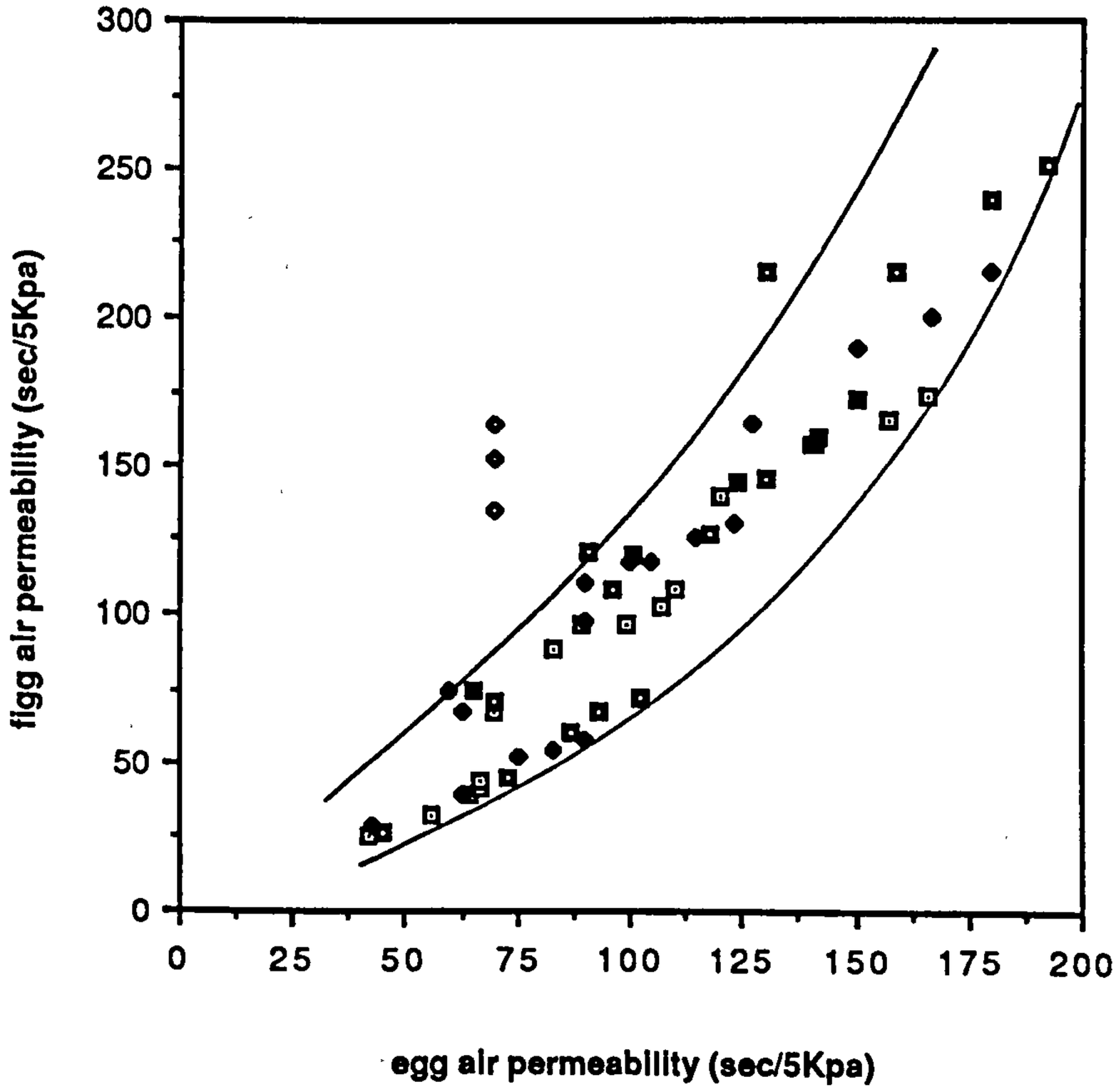

Figure A1.56 Relationship between Figg air permeability and Egg air permeability (temperate curing)

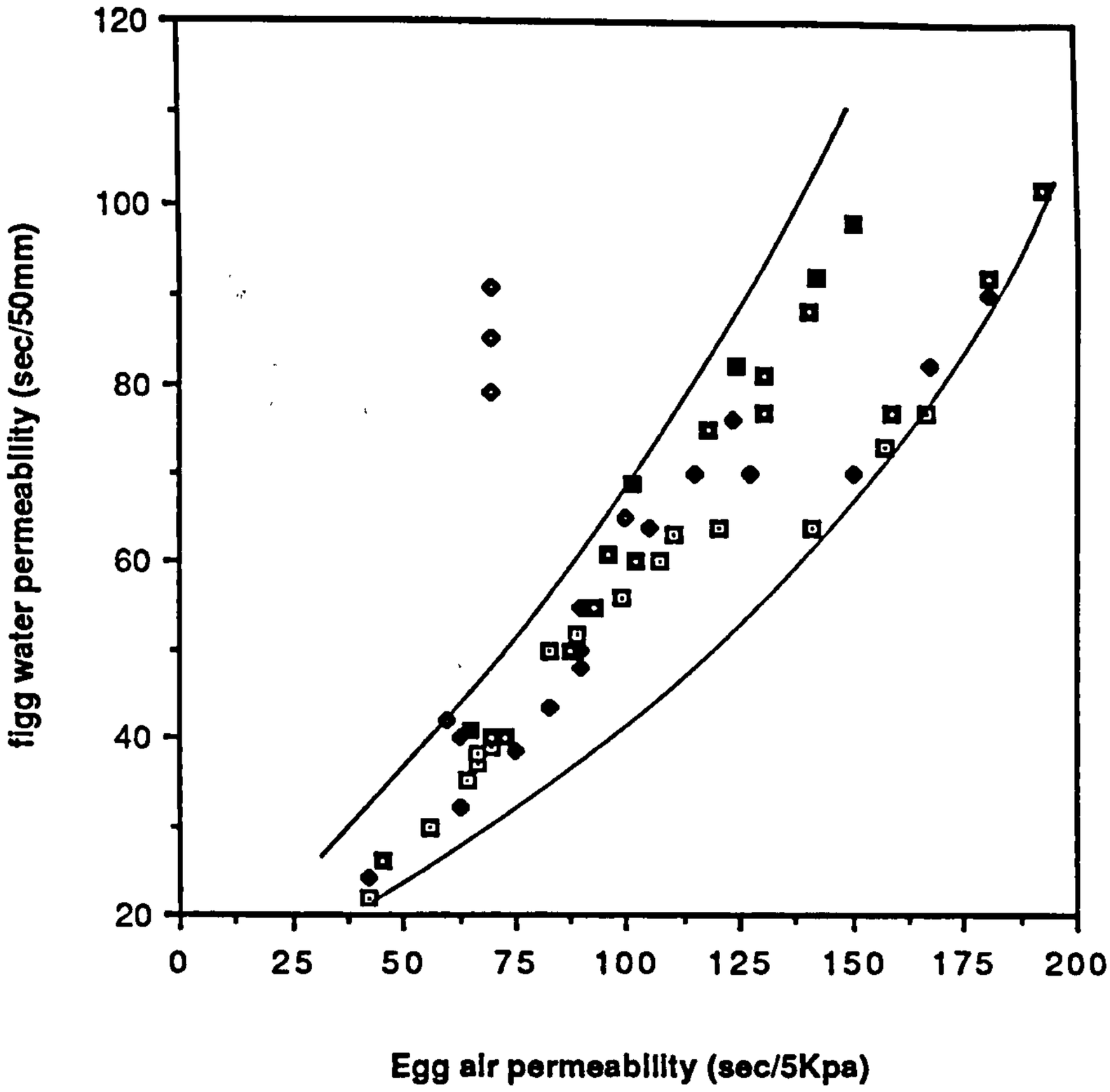

Figure A1.57 Relationship between Figg water permeability and Egg air permeability (temperate curing)

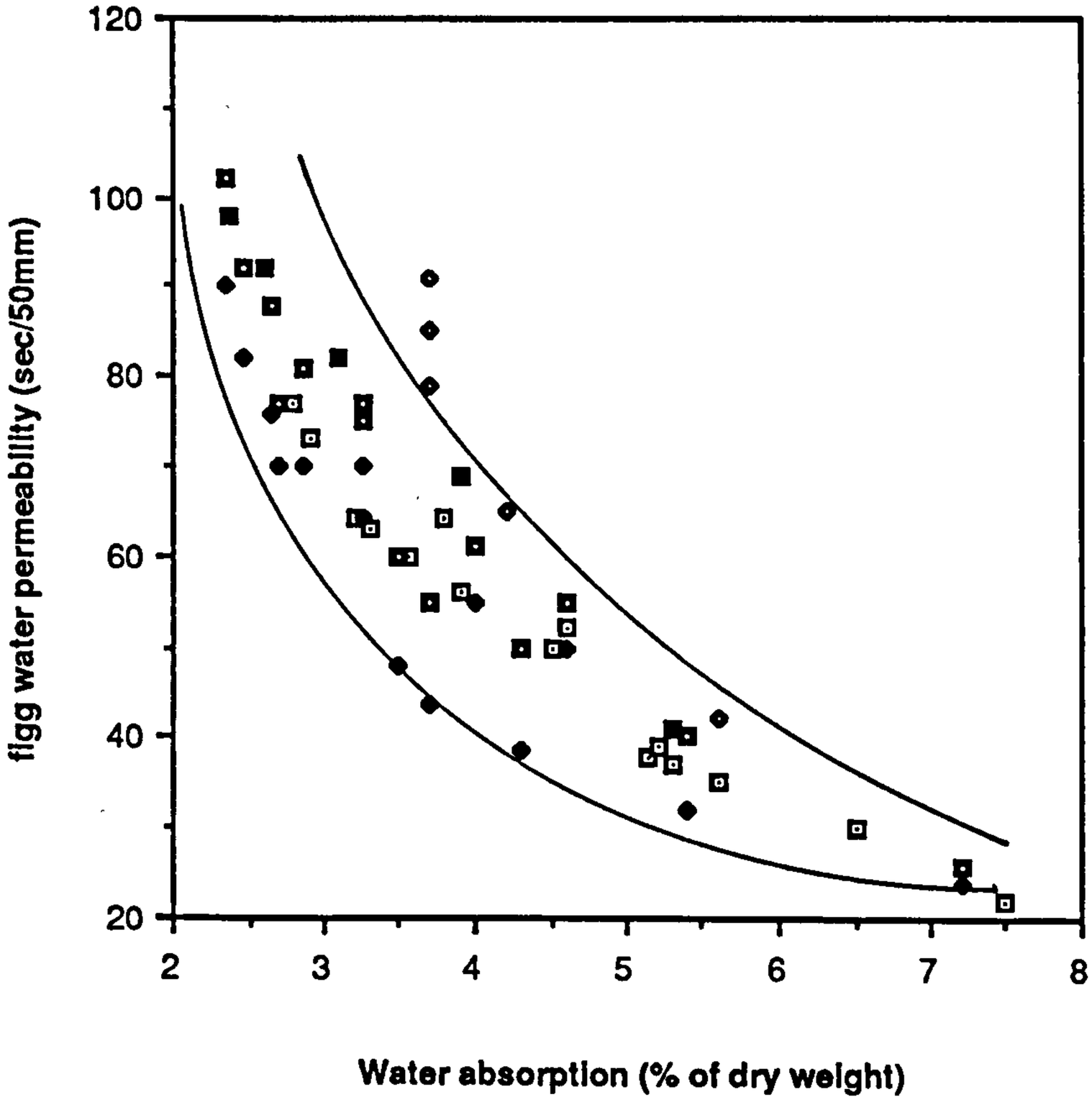

Figure A1.58 Relationship between Figg water permeability and water absorption (temperate curing)

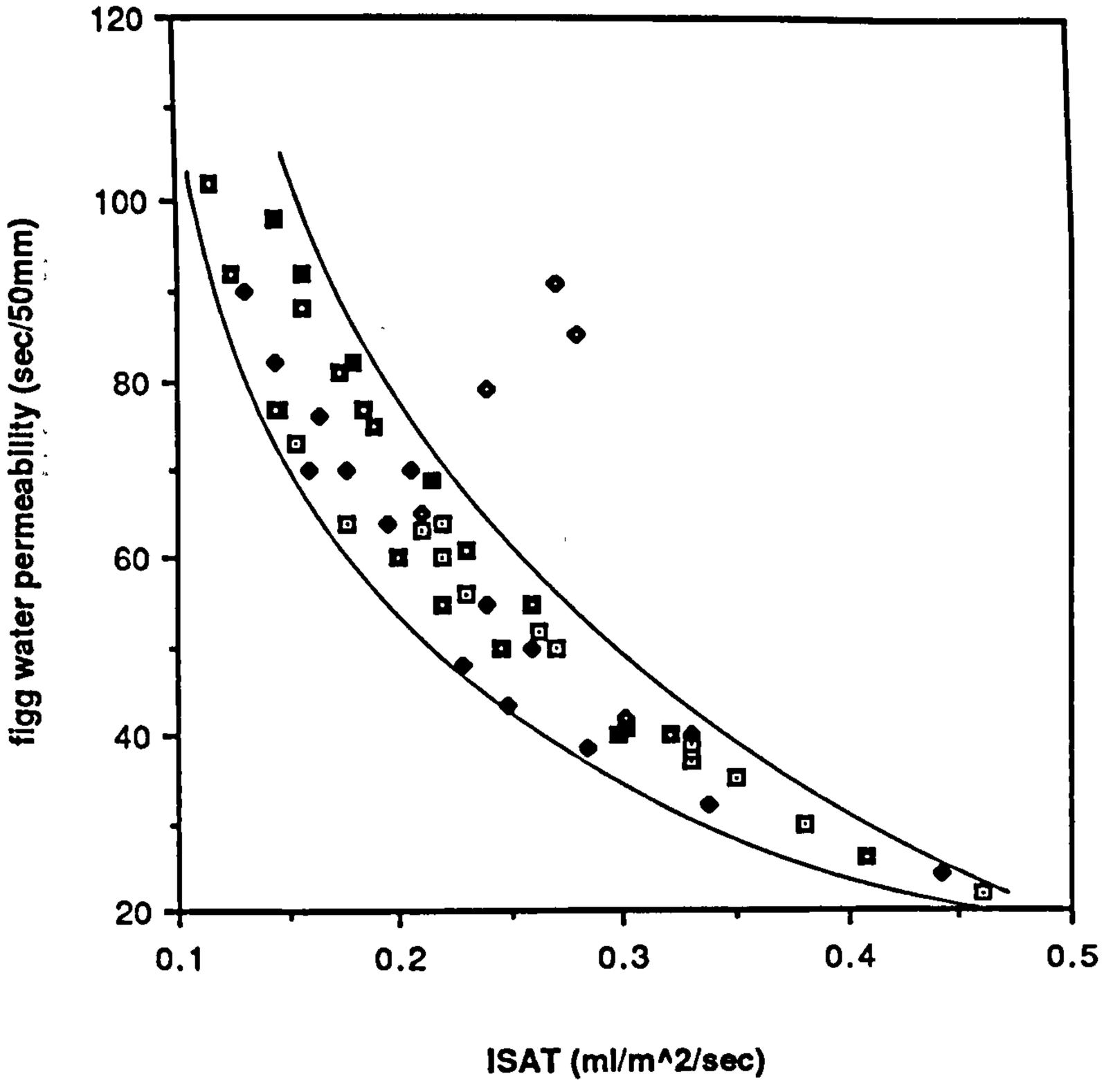

Figure A1.59 Relationship between Figg water permeability and ISAT (temperate curing)

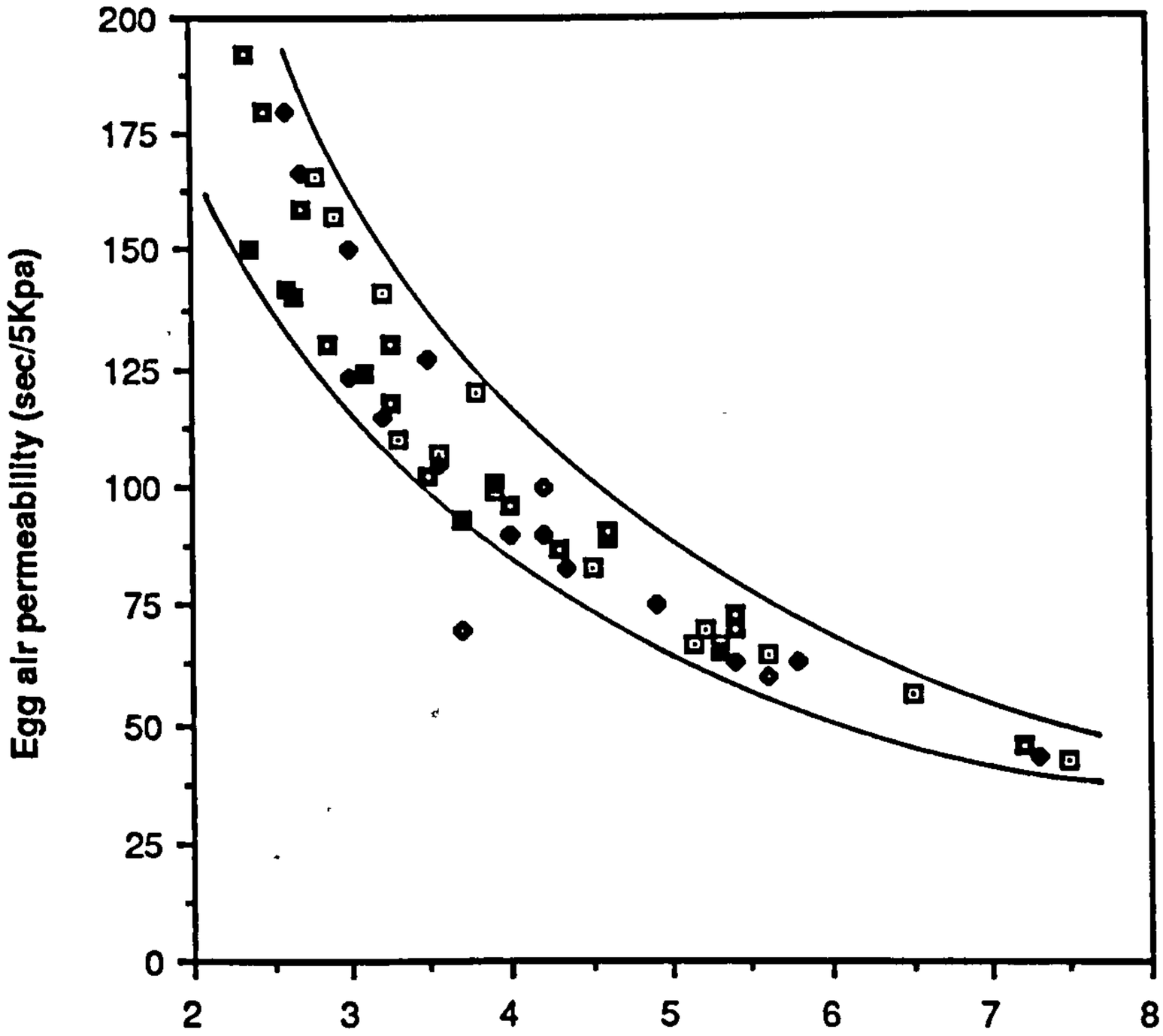

Figure A1.60 Relationship between Egg air permeability and water absorption (temperate curing)

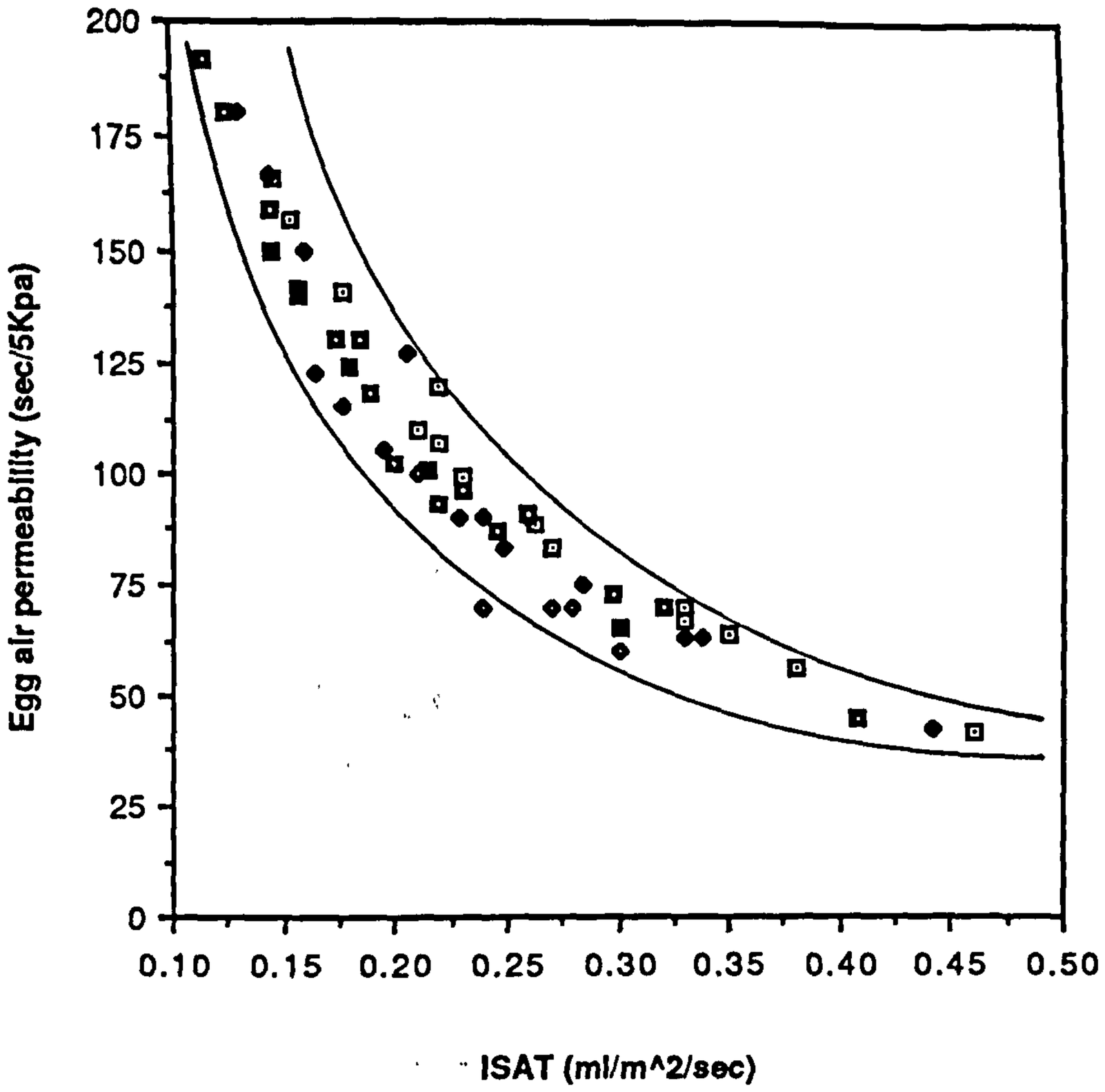

Figure A1.61 Relationship between Egg air permeability and ISAT (temperate curing)

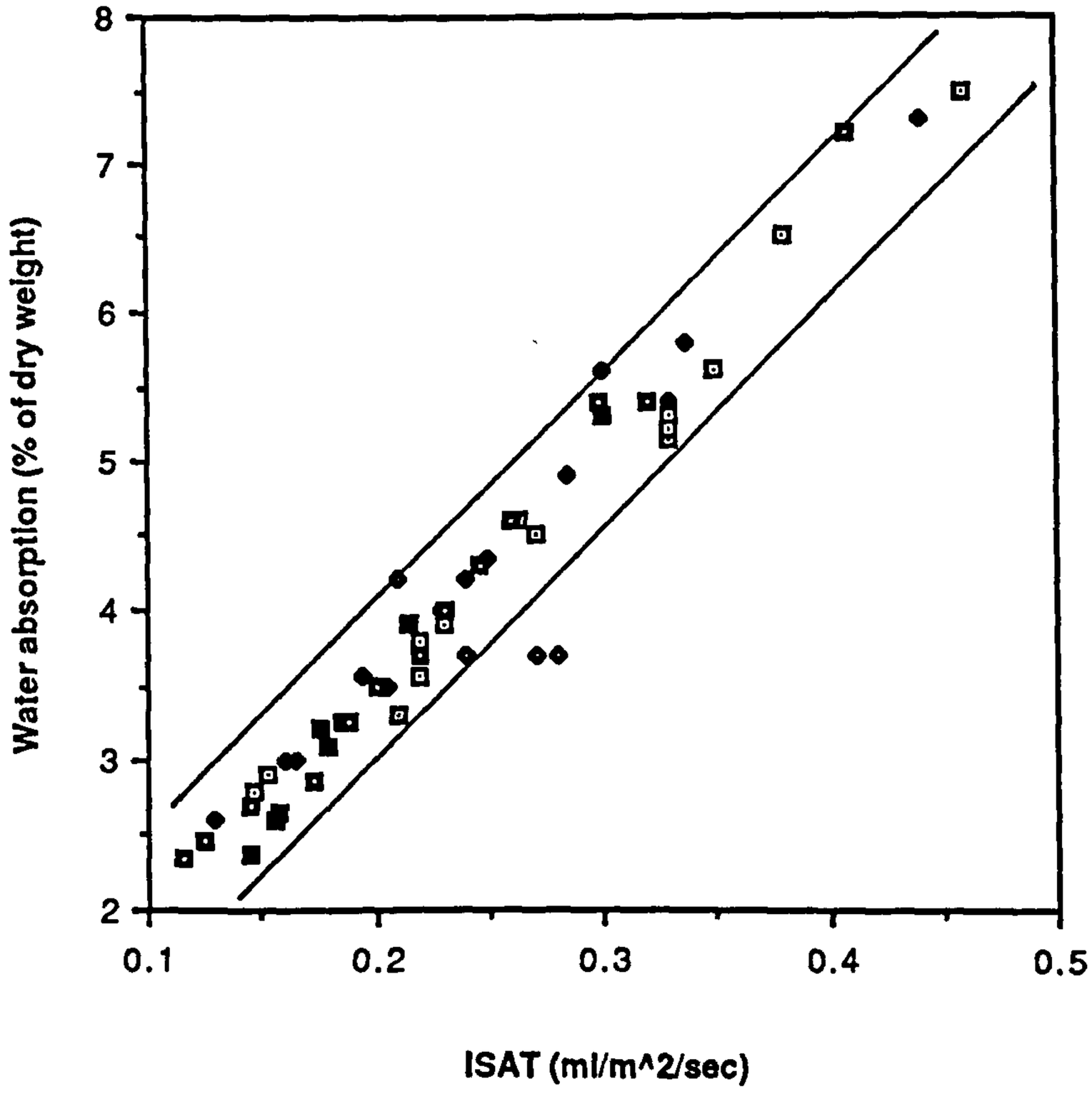

Figure A1.62 Relationship between water absorption and ISAT (temperate curing)

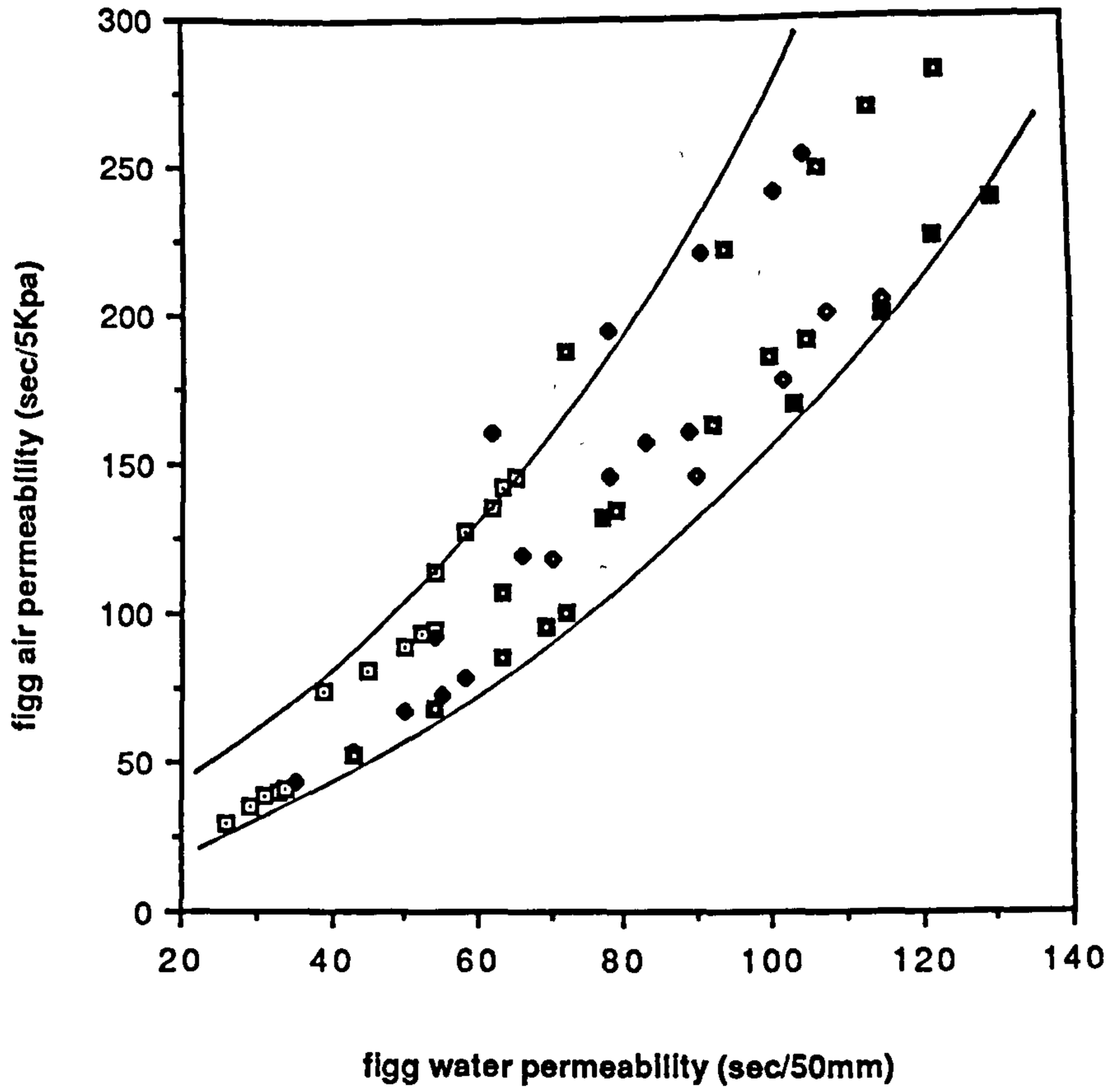

Figure A1.63 Relationship between Figg air permeability and Figg water permeability (hot curing)

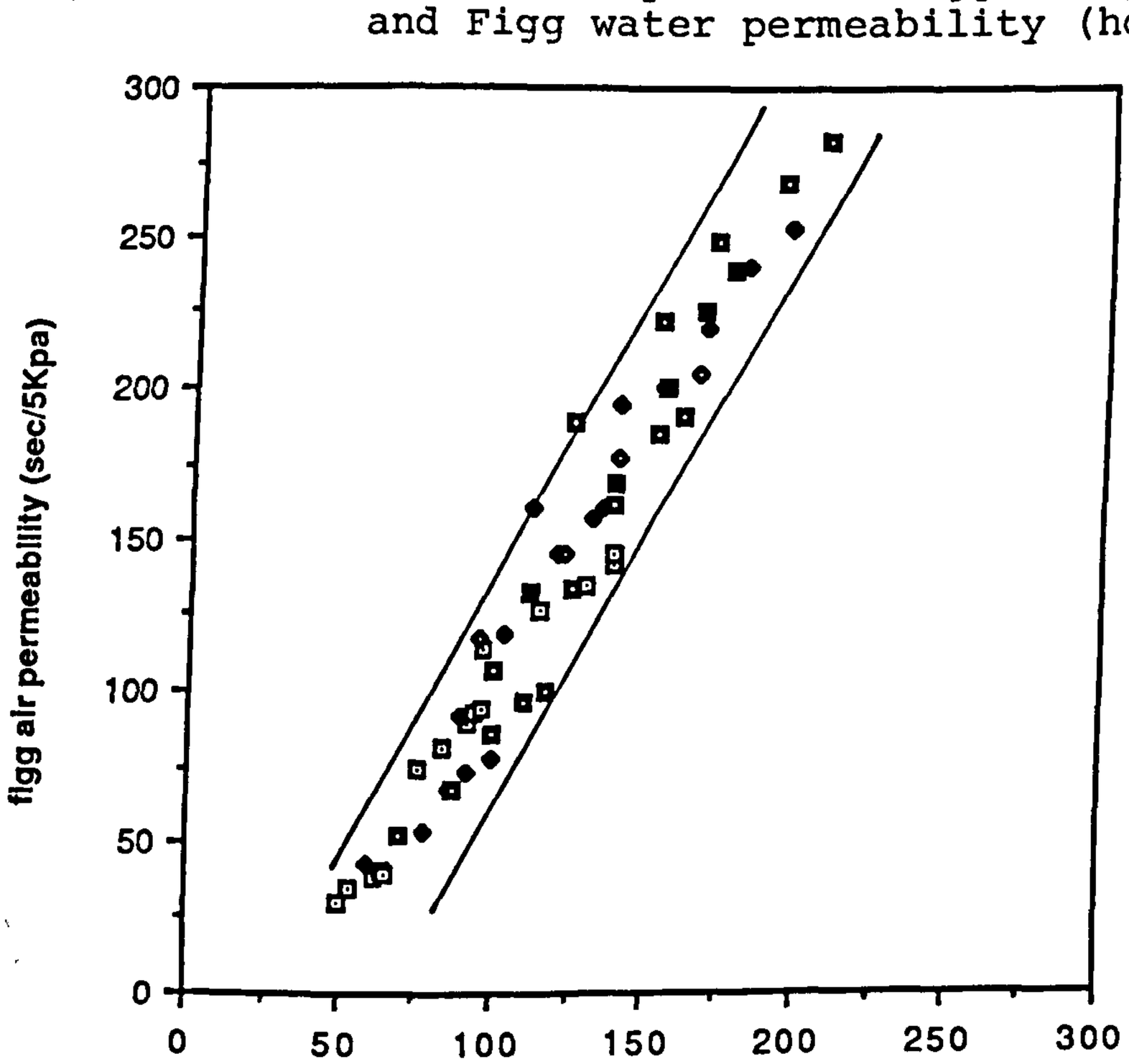

Figure A1.64 Relationship between Figg air permeability and Egg air permeability (hot curing)

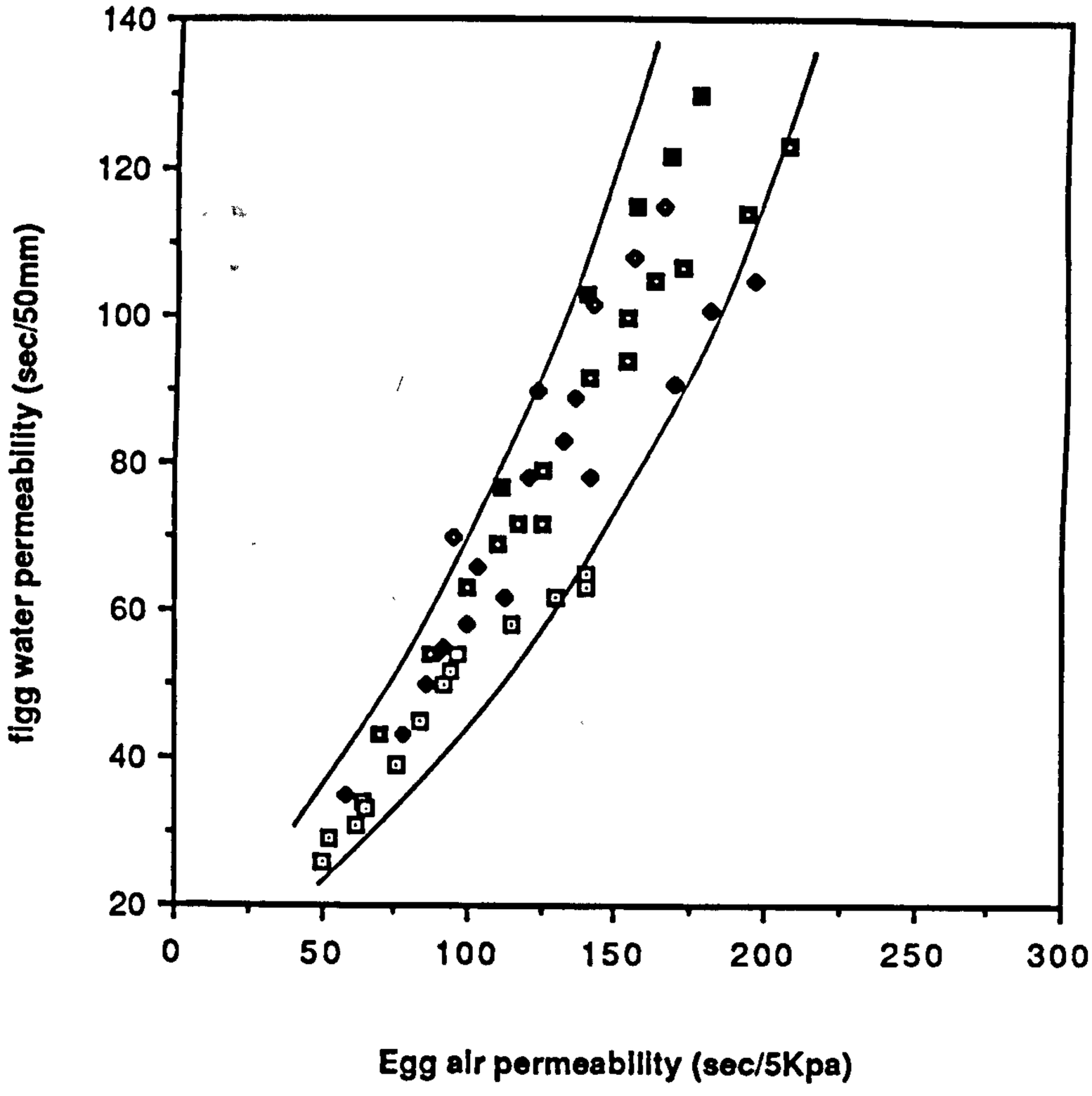

Figure A1.65 Relationship between Figg water permeability and Egg air permeability (hot curing)

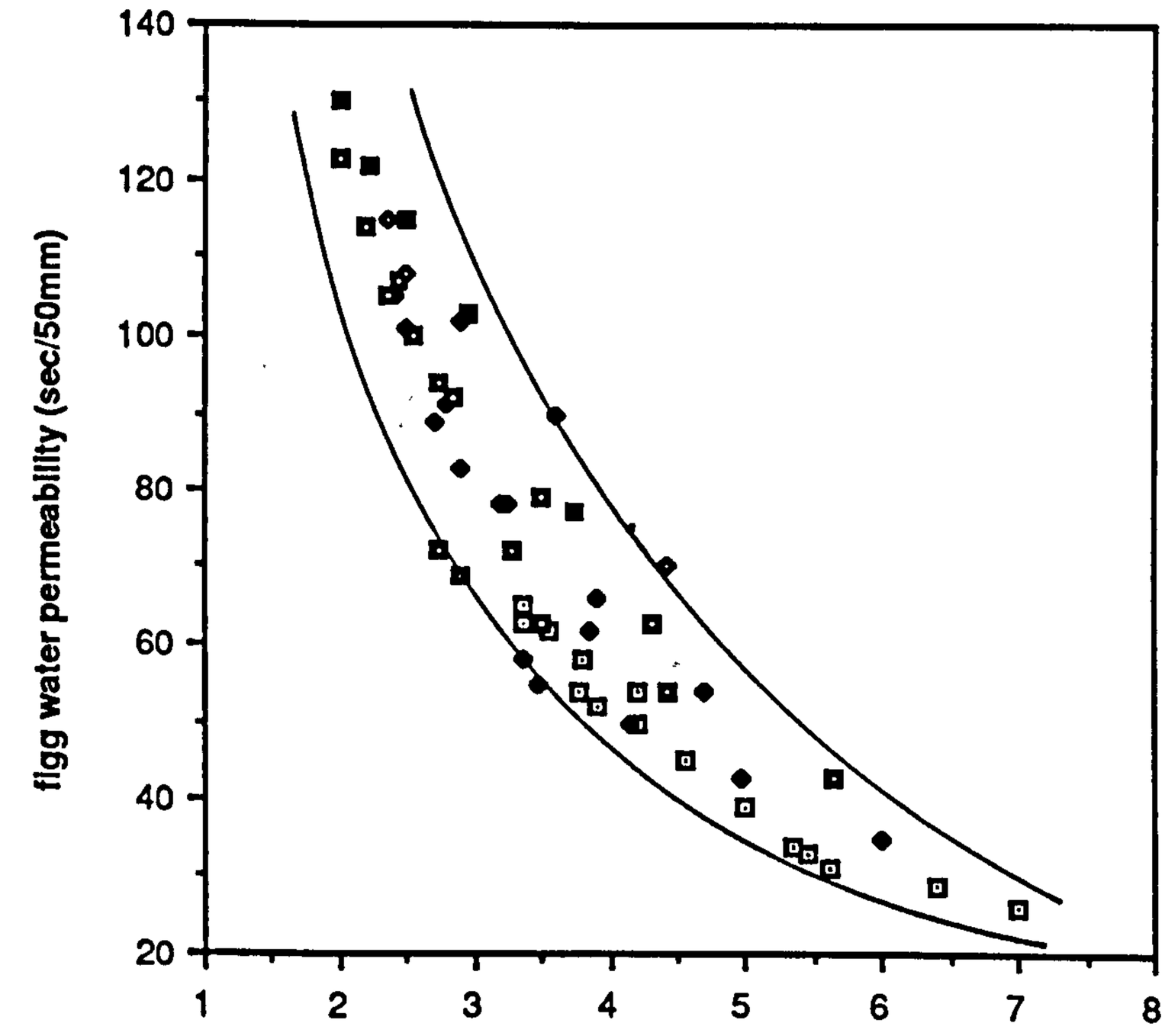

Figure A1.66 Relationship between Figg water permeability and water absorption (hot curing)

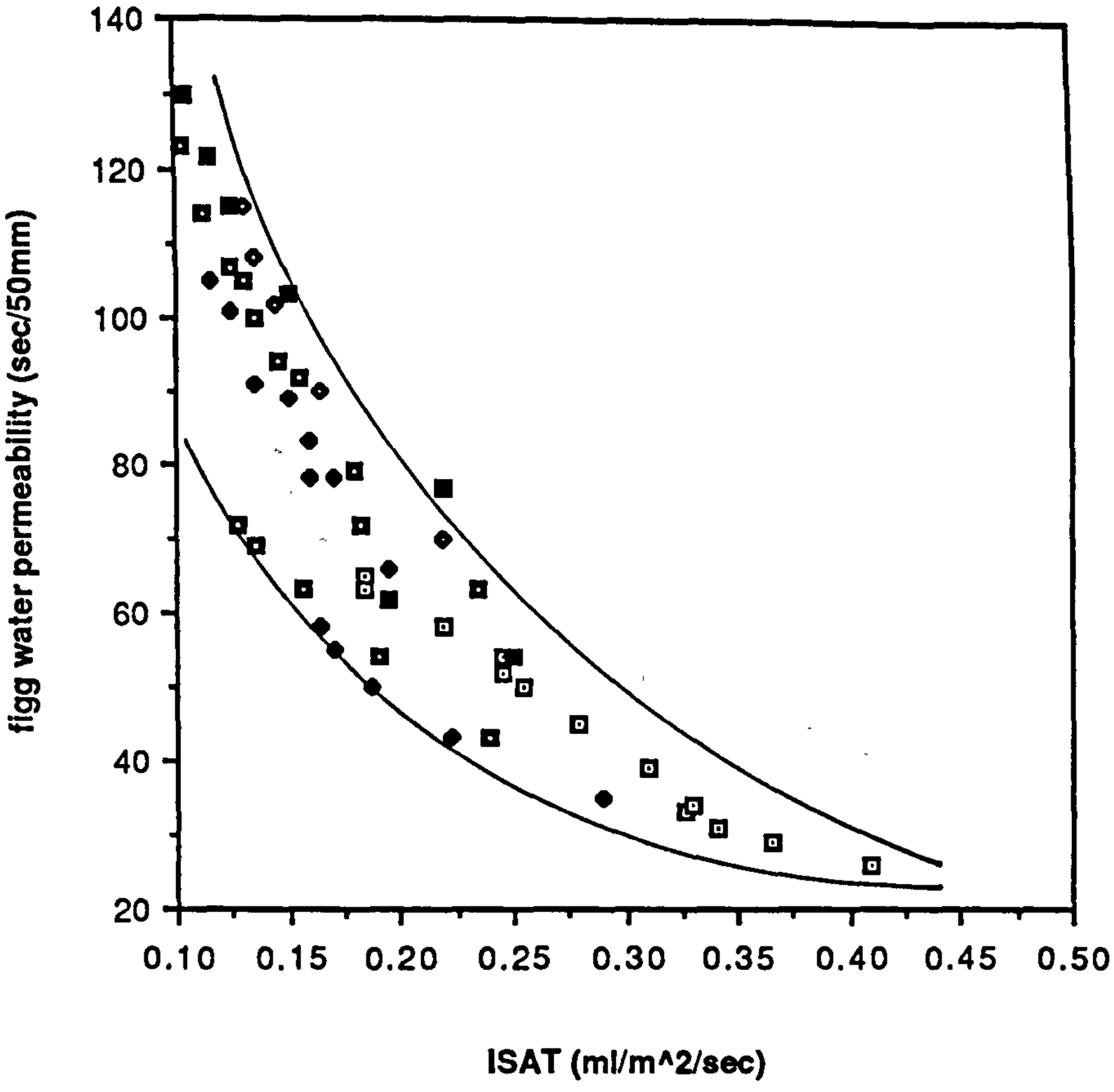

Figure A1.67 Relationship between Figg water permeability and ISAT (hot curing)

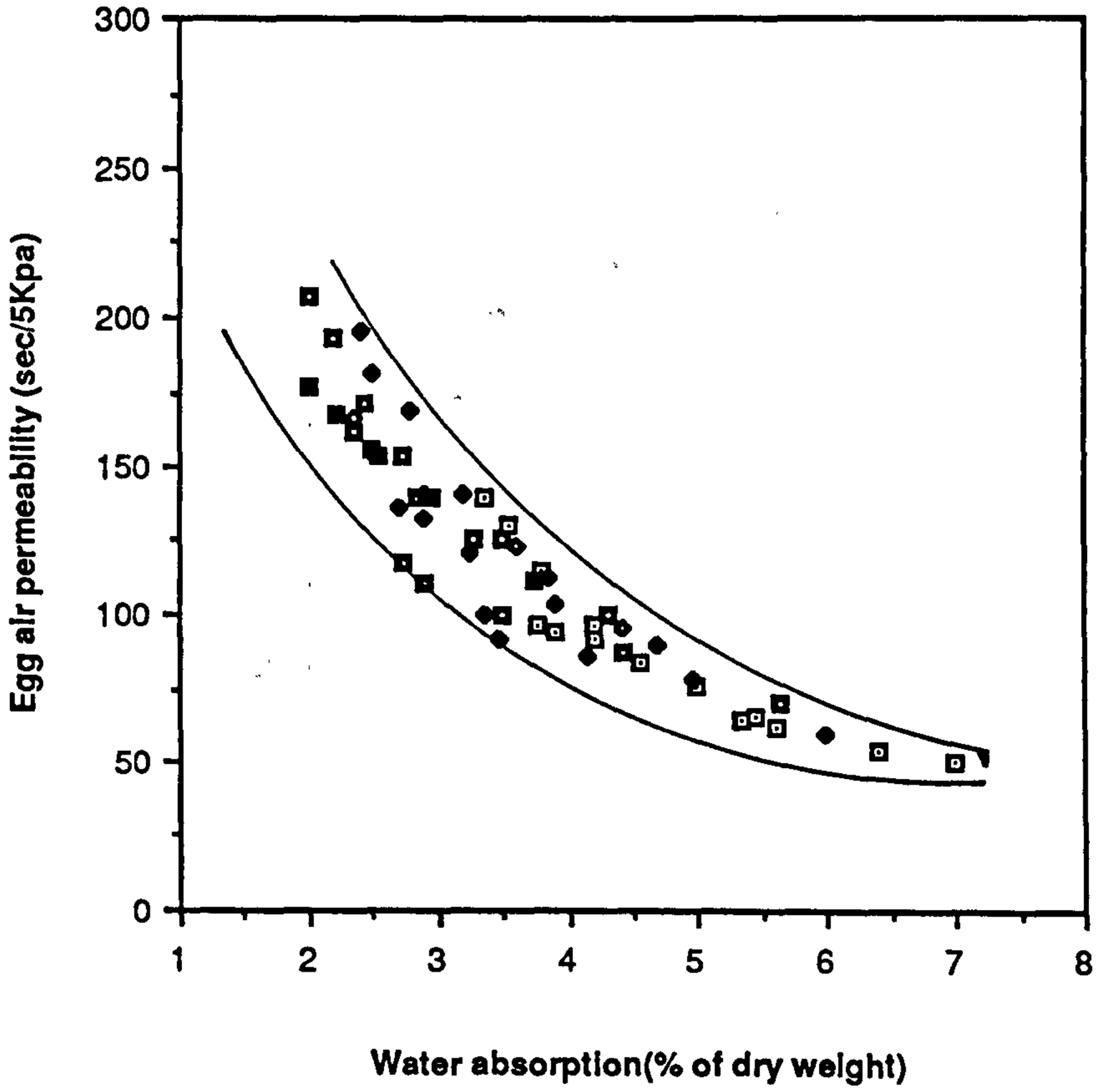

Figure A1.68 Relationship between Egg air permeability and water absorption (hot curing)

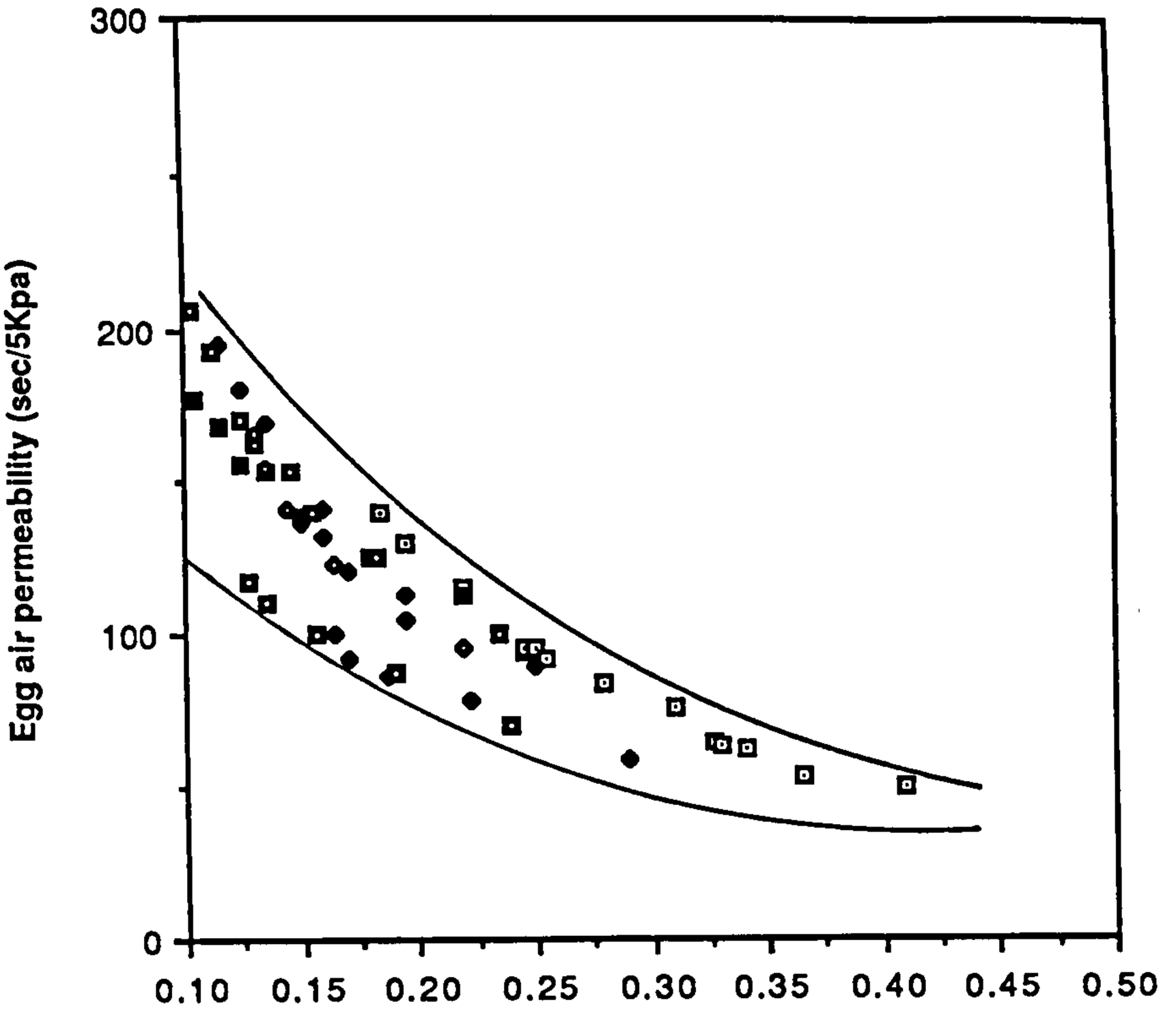

Figure A1.69 Relationship between Egg air permeability and ISAT (hot curing)

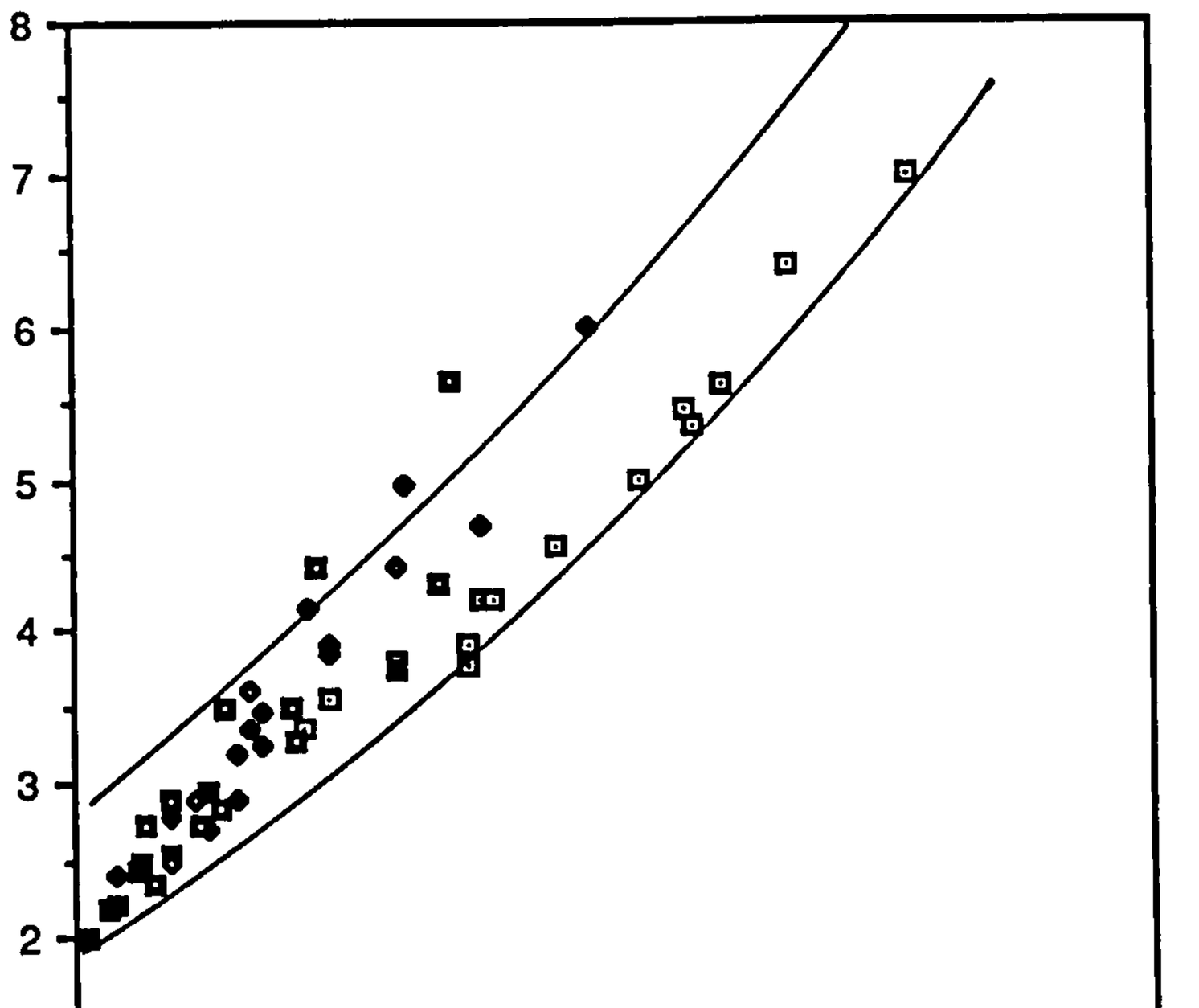

Figure A1.70 Relationship between water absorption and ISAT (hot curing)

APPENDIX 2

Appendix 2

Hydration products of 1 cubic centrimetre of cement require a space 2.1 times the volume of original cement. Thus, not less than 2.1 cu.cm. of water-filled space per cu.cm. of cement is required in the fresh paste simply to provide the room required by the amount of hydration products that can be derived from 1 cu.cm. of cement. A simple calculation will show that this amount of water per unit of cement corresponds to about 0.66 gram of water per gram of cement or, conversely 1.5 gram of cement per gram of water. Out of the basis above, a typical 10% lean (25/10) and rich (C55/10) CSF concrete mixes were considered to find out the amount of water-filled spaces required to provide room for housing hydration products. Simple calculation had shown that the amount of water-filled spaces required for mix C25/10 and C55/10 were 131 kg and 235 kg. Comparing these figures with the amounts of mixing water used which were 185 and 216 kg for (C25/10) and (C55/10) respectively we will find that there is not enough space in the rich mixes for housing all hydration products and eventually hydration will stop utilizing all the cementitious material available even if all the necessary conditions for hydration continuation are provided. Whereas in the lean CSF mix (C25/10) there is an ample space for housing all hydration products - even if a full utilization of cementitious materials is achieved.

Considering the fact that the use of CSF will convert the hexagonal $Ca(OH)_2$ plates to a high surface area dense C-S-H fibres, the spaces required by the hydration products ion the OPC/CSF mixes could be even higher than 2.1 cubic cm. This means that in OPC/CSF mixes more water-filled spaces are required for housing hydration products, a situation which tends to make the situation more critical.

APPENDIX 3

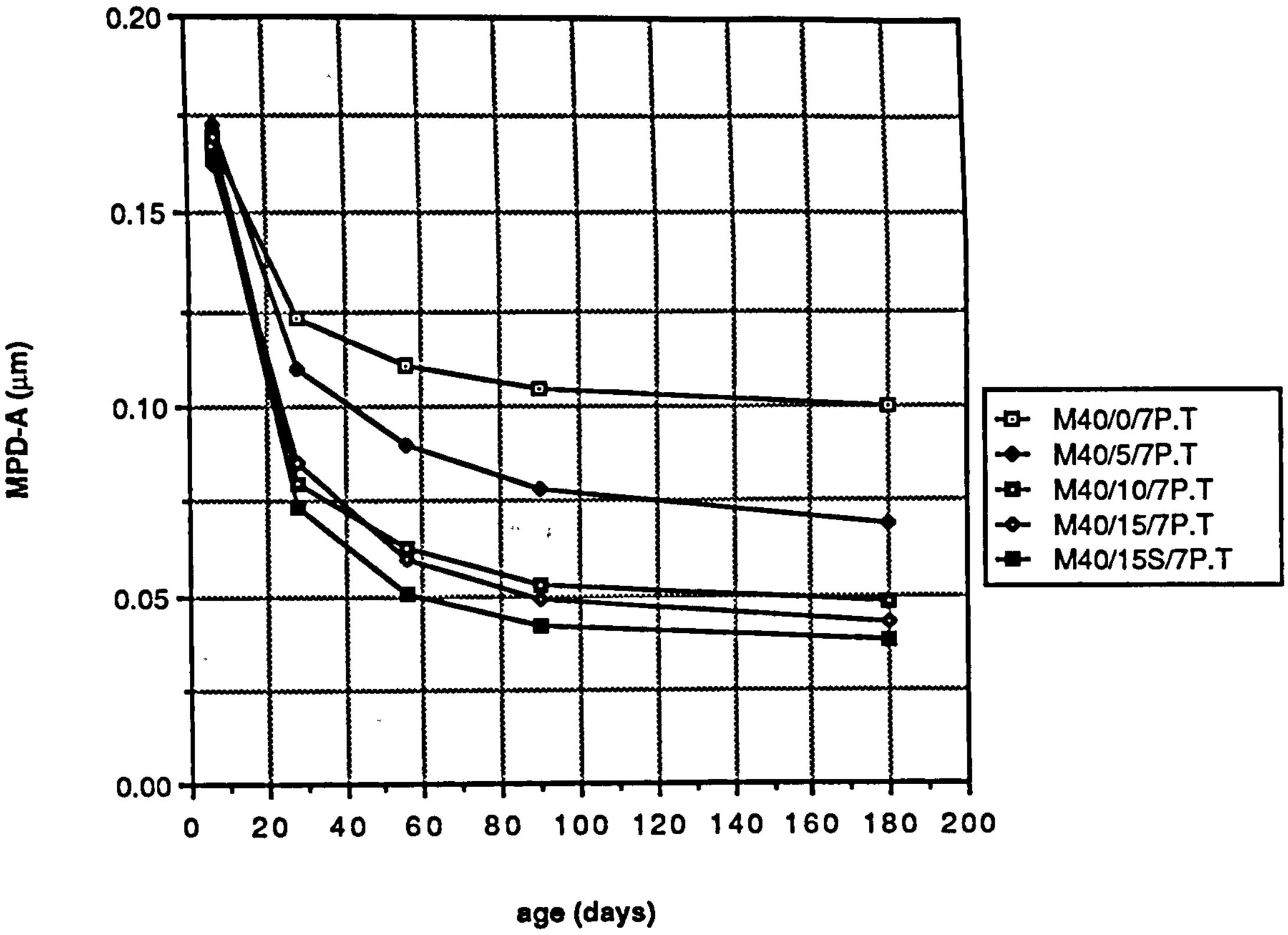

Figure A3.1 Age versus MPD-A relationship of mortar cured in a temperate environment

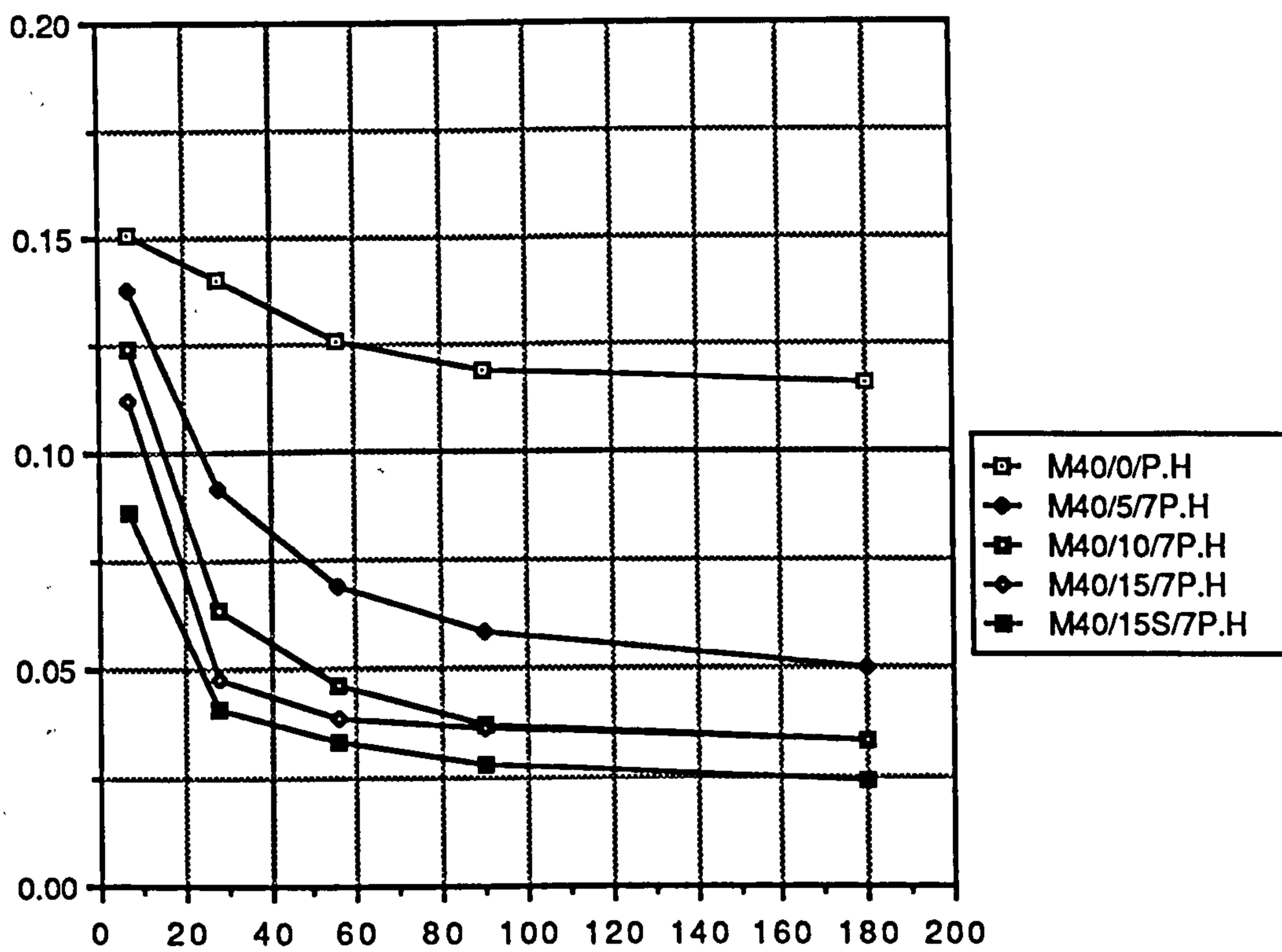

Figure A3.2 Age versus MPD-A relationship of mortars cured in a hot environment

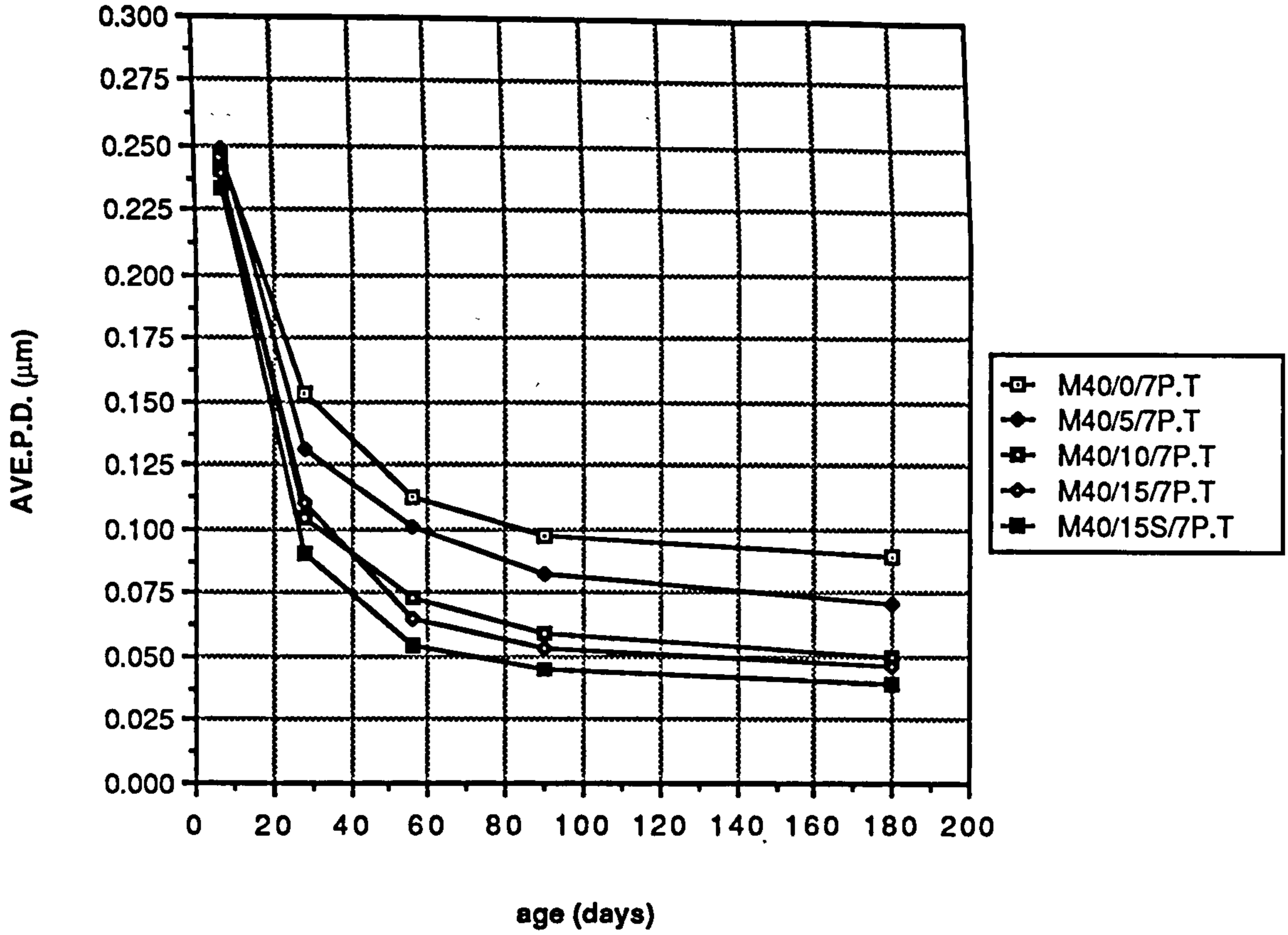

Figure A3.3 Age versus Ave. P.D. relationship of mortars cured in a temperate environment

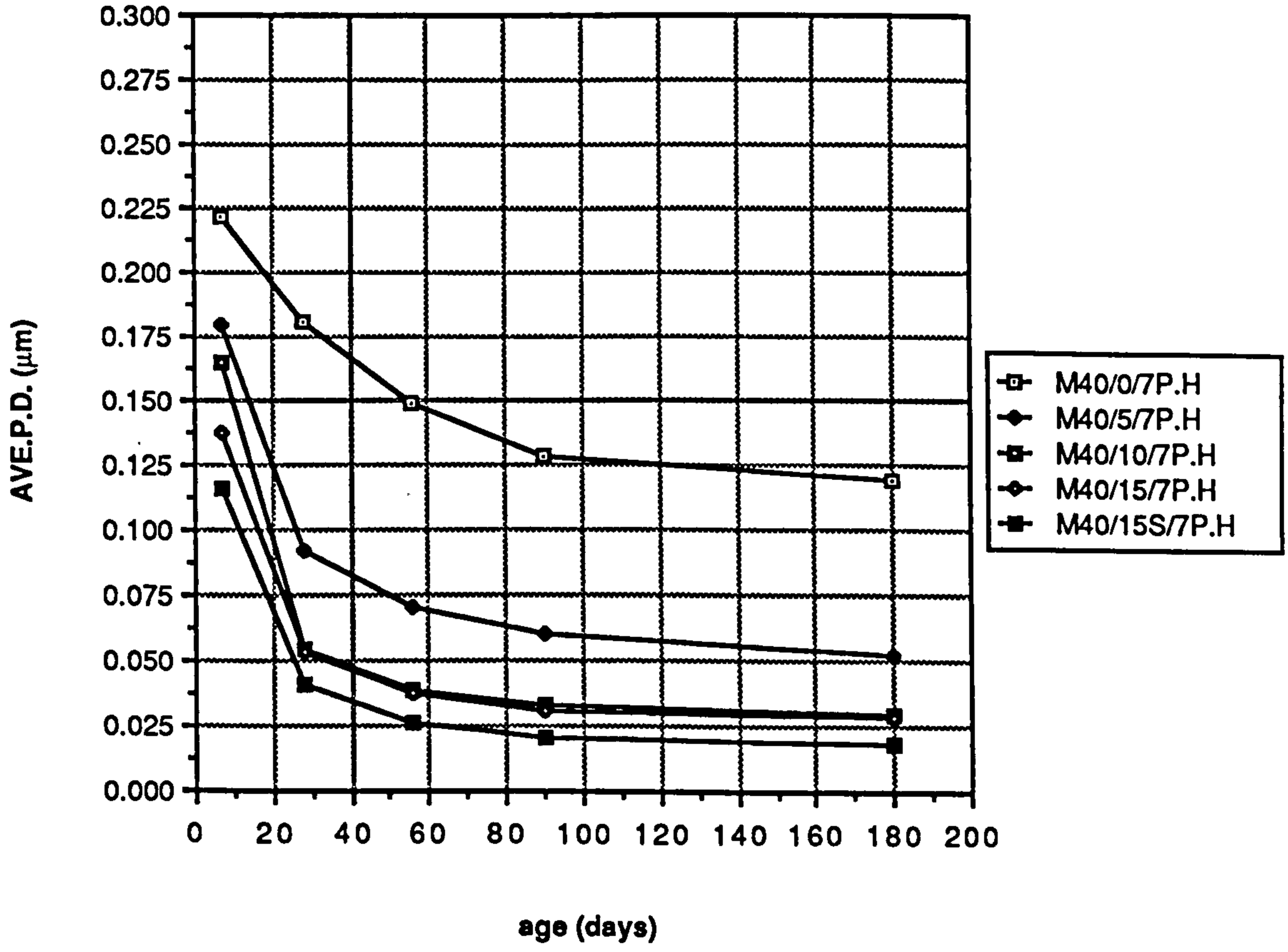

Figure A3.4 Age versus Ave. P.D. relationship of mortars cured in a hot environment

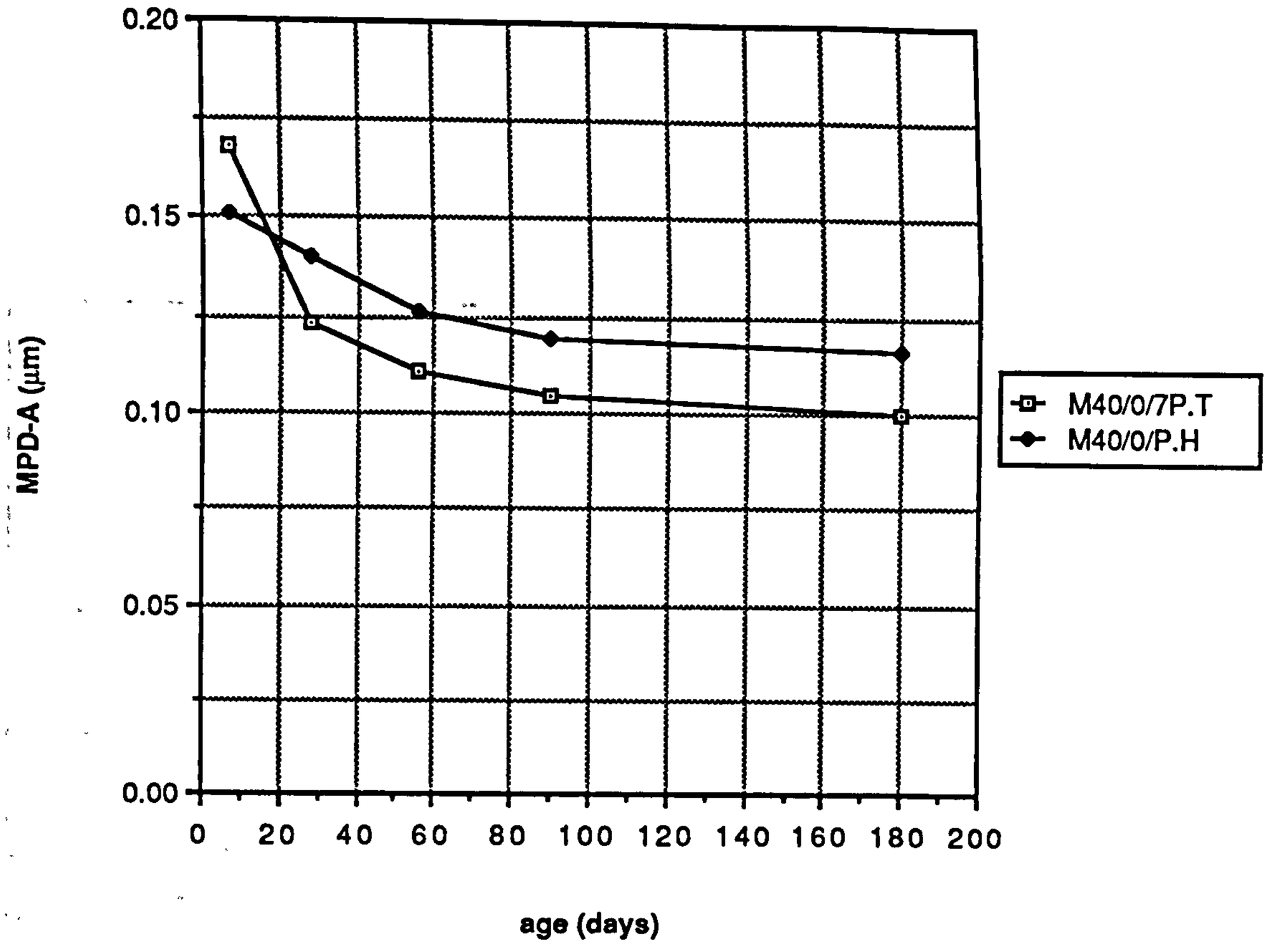

Figure A3.5 Age versus MPD-A relationship of plain mortar cured in a temperate and hot environment

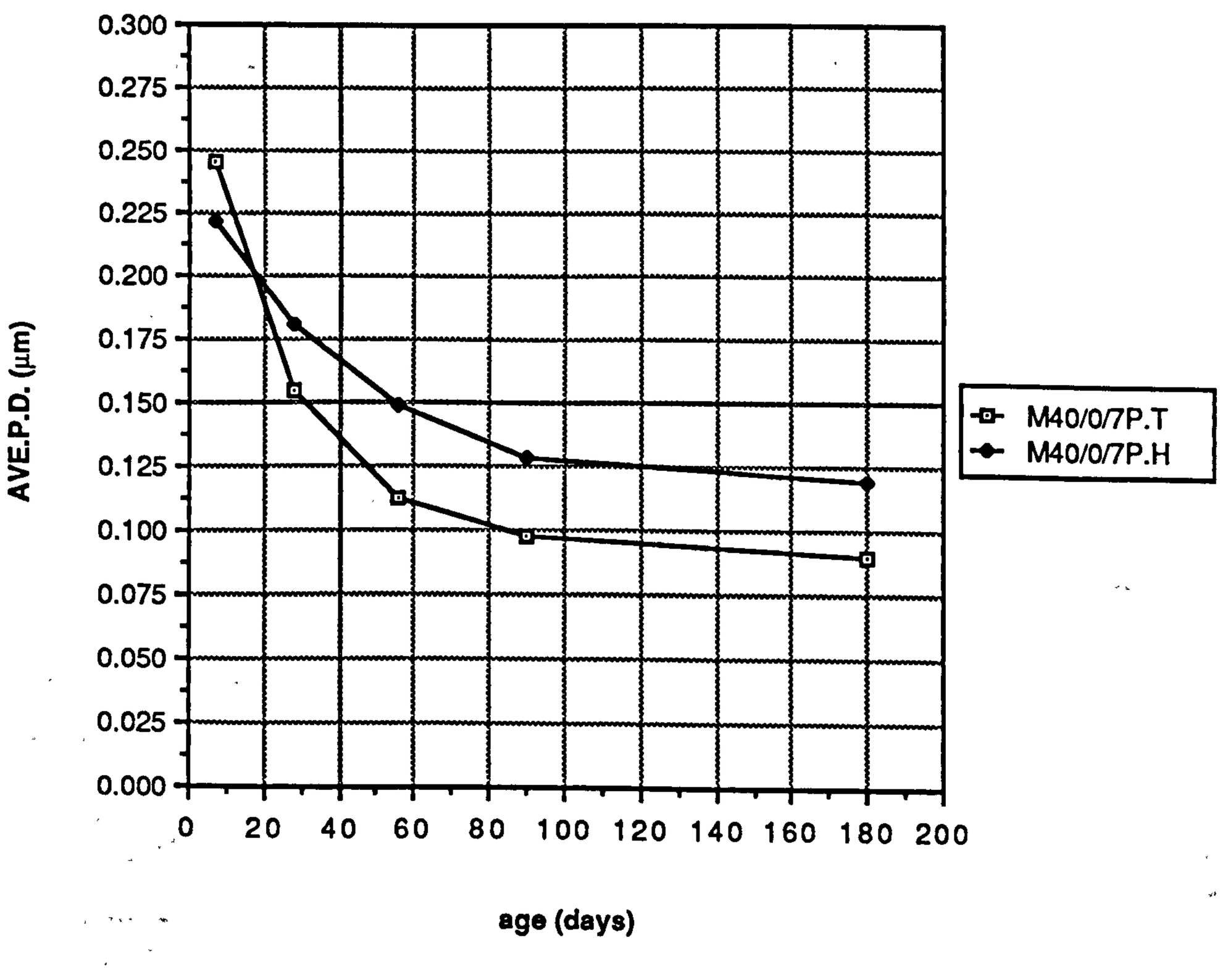

Figure A3.6 Age versus Ave. P.D. relationship of plain mortar cured in a temperate and hot environment

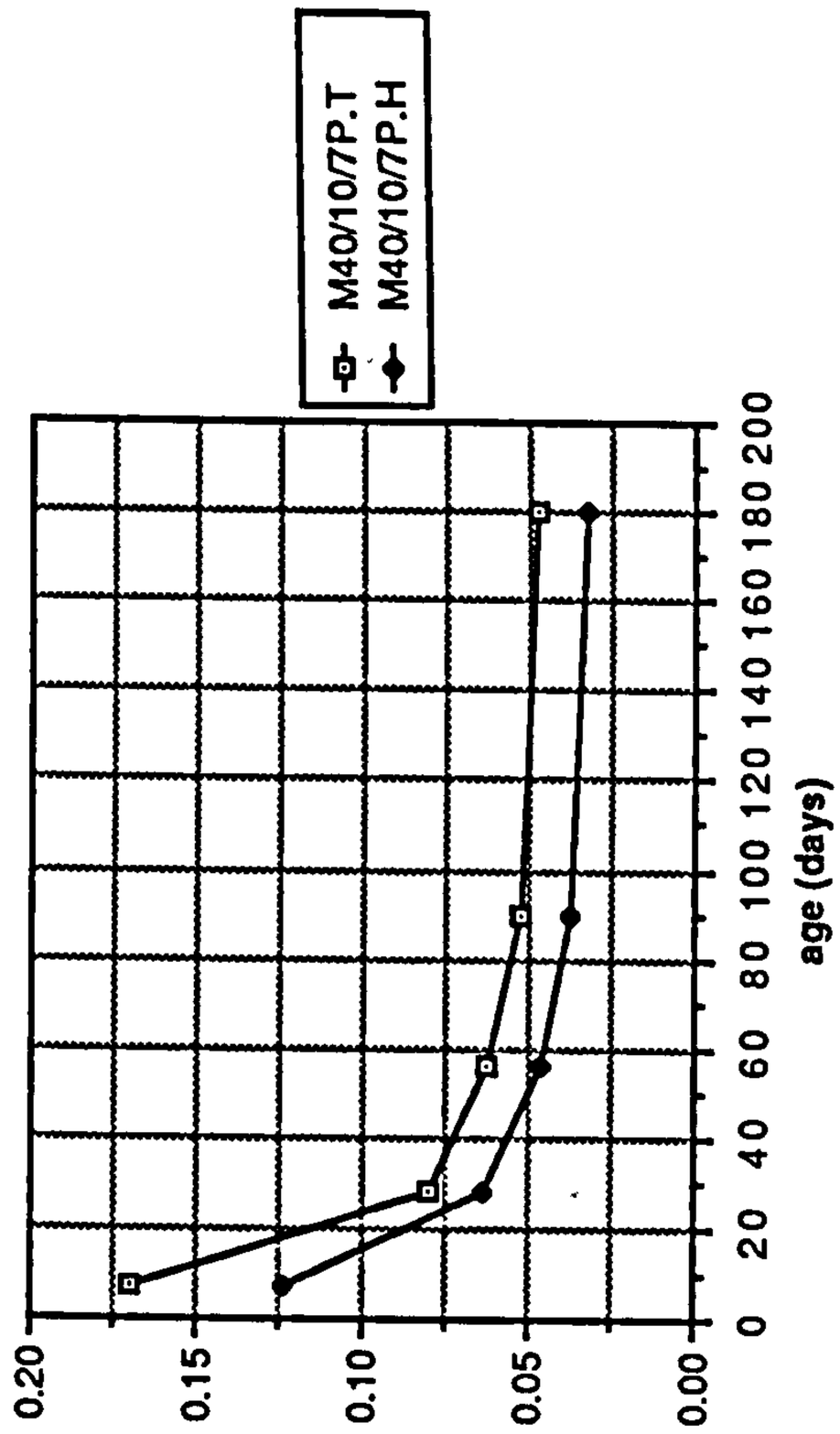

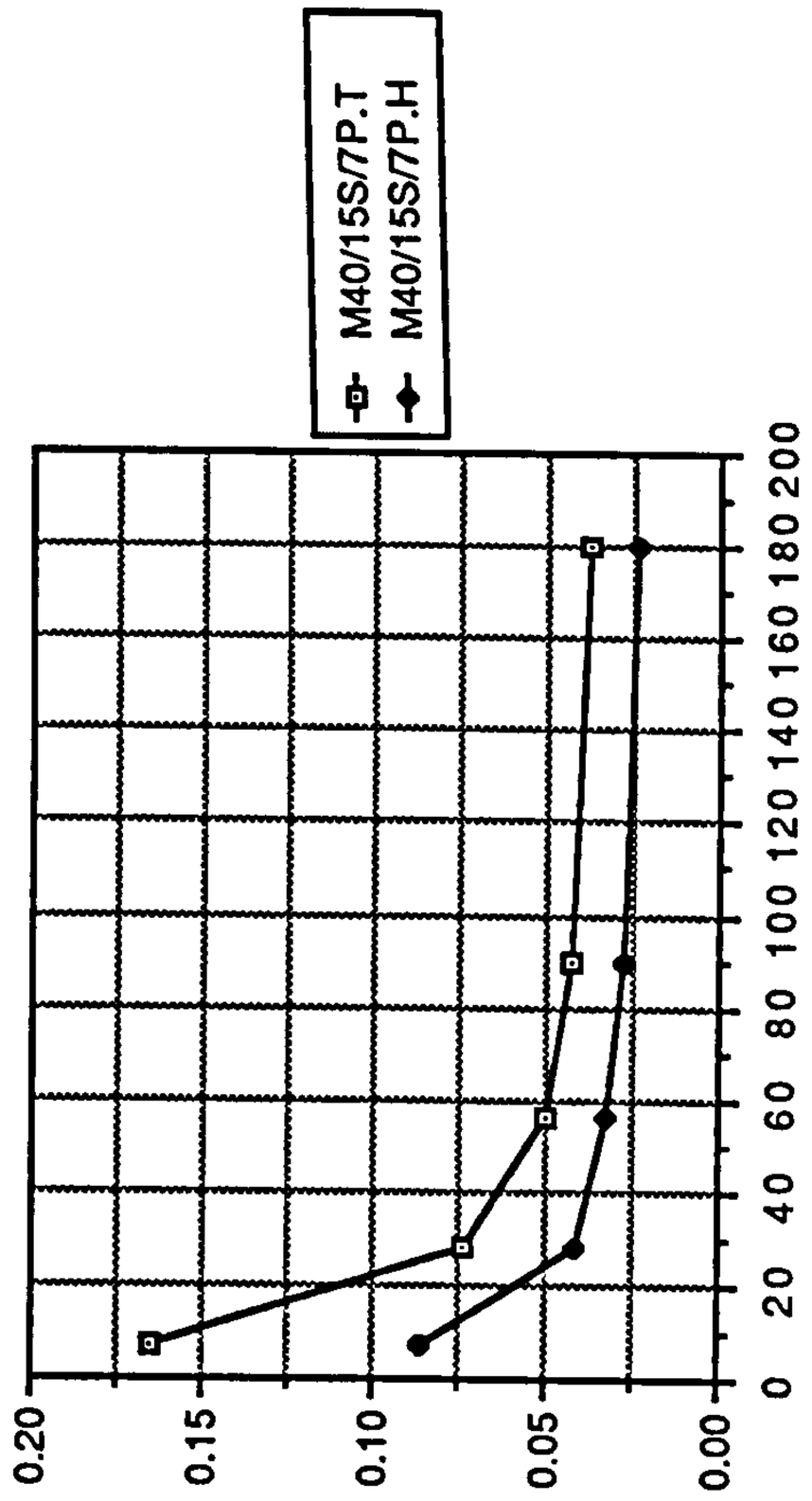

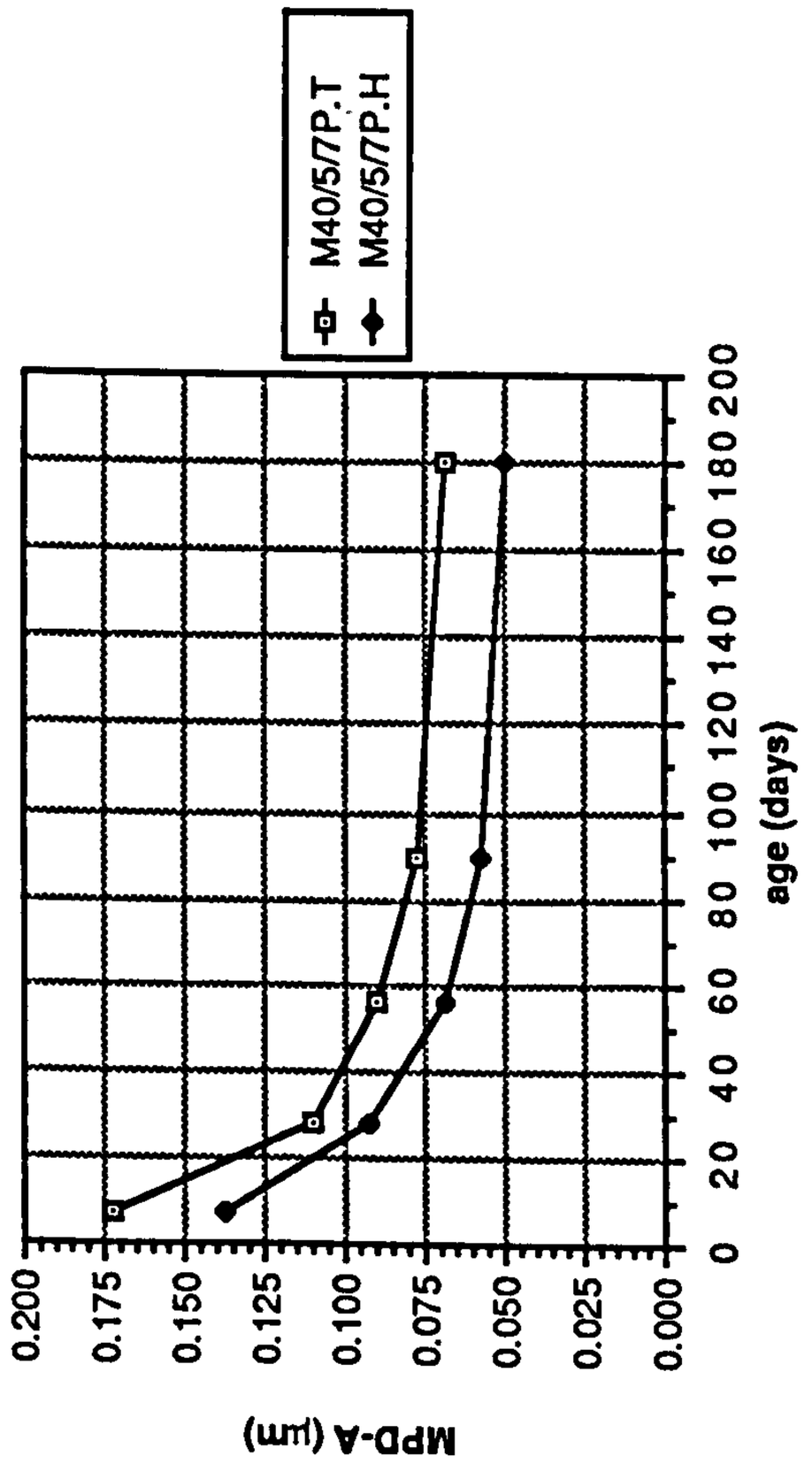

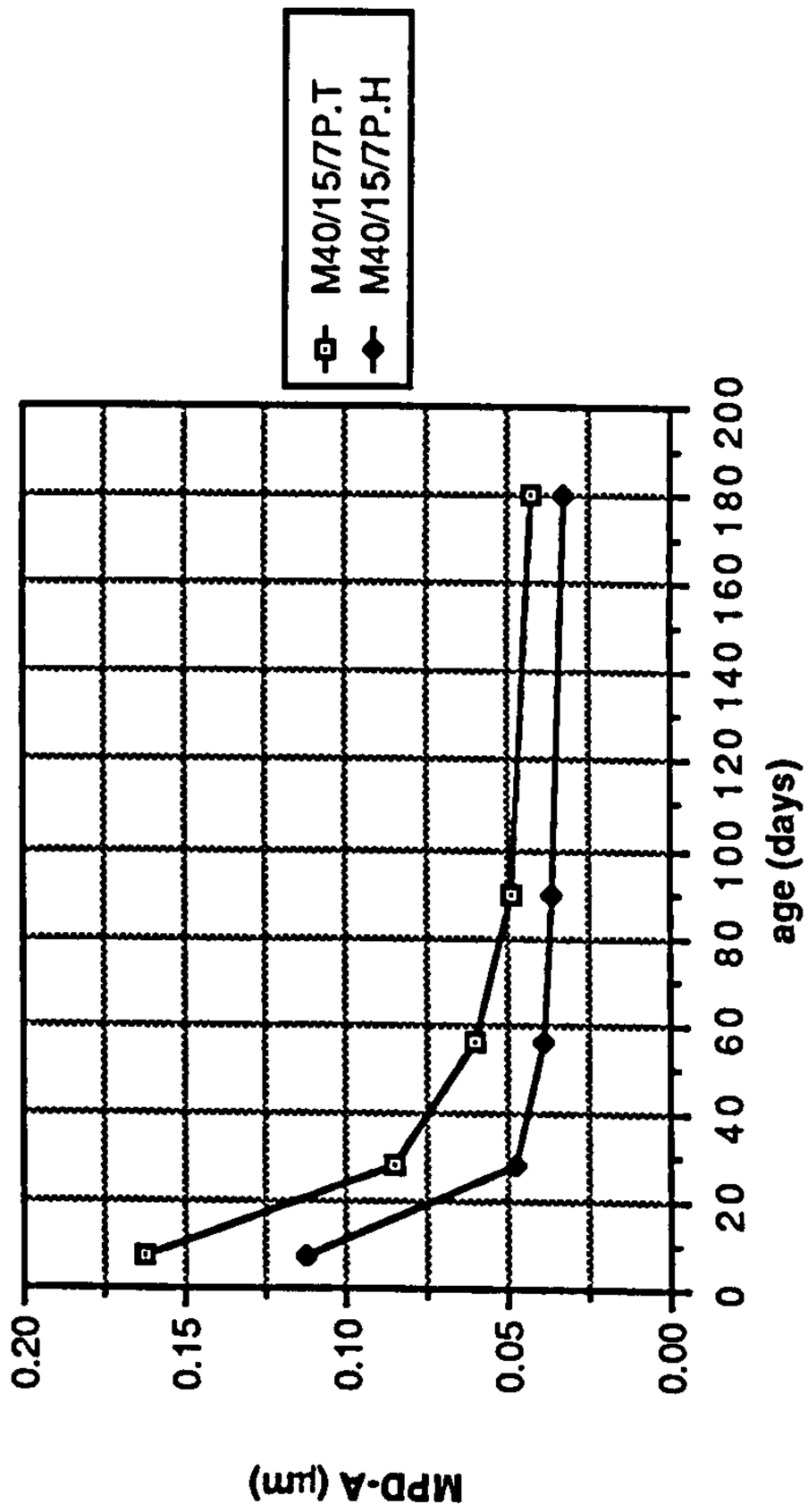

Figure A3,7 Age versus MPD-A relationship of CS mortars cured in a temperate and hot environment

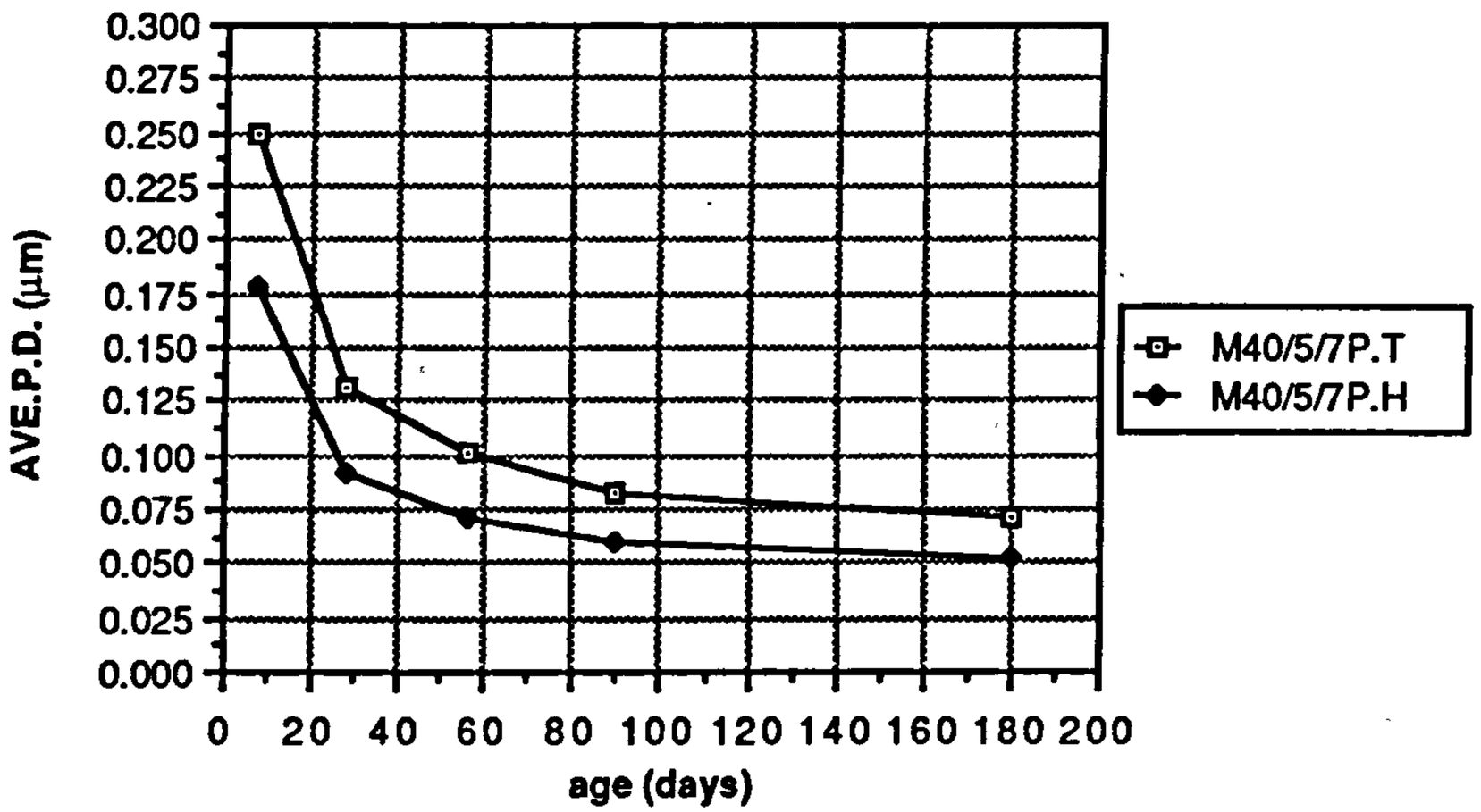

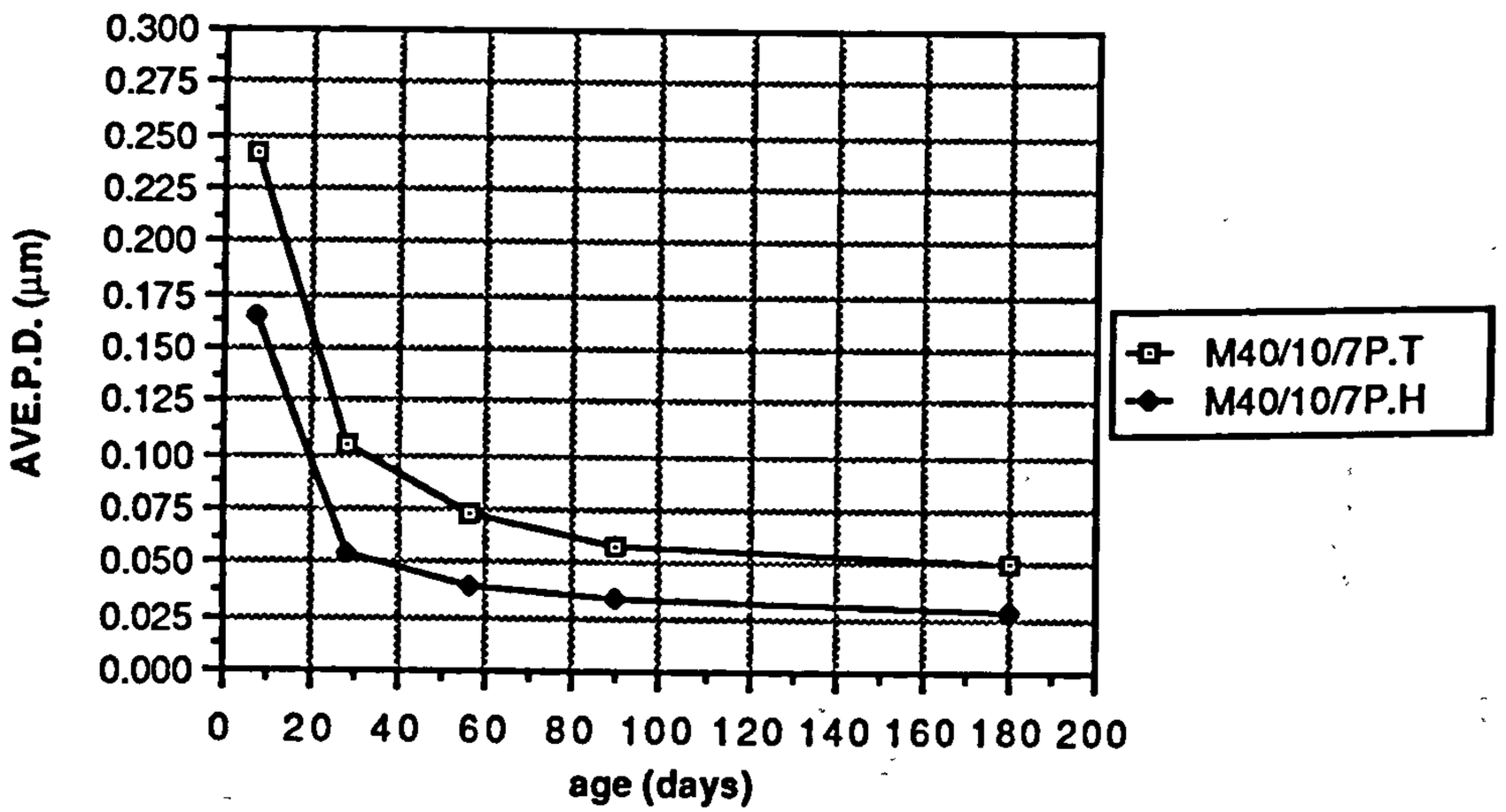

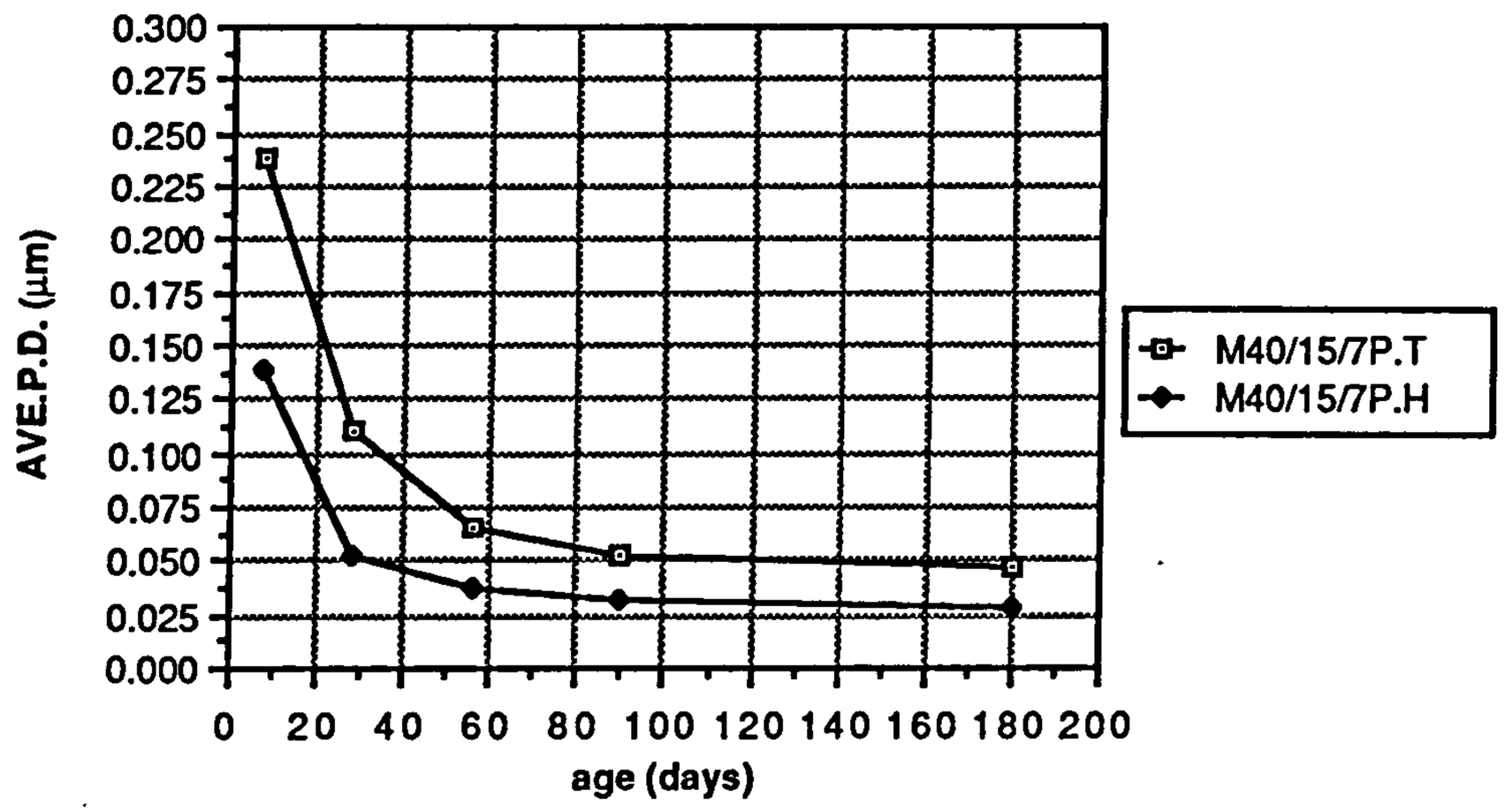

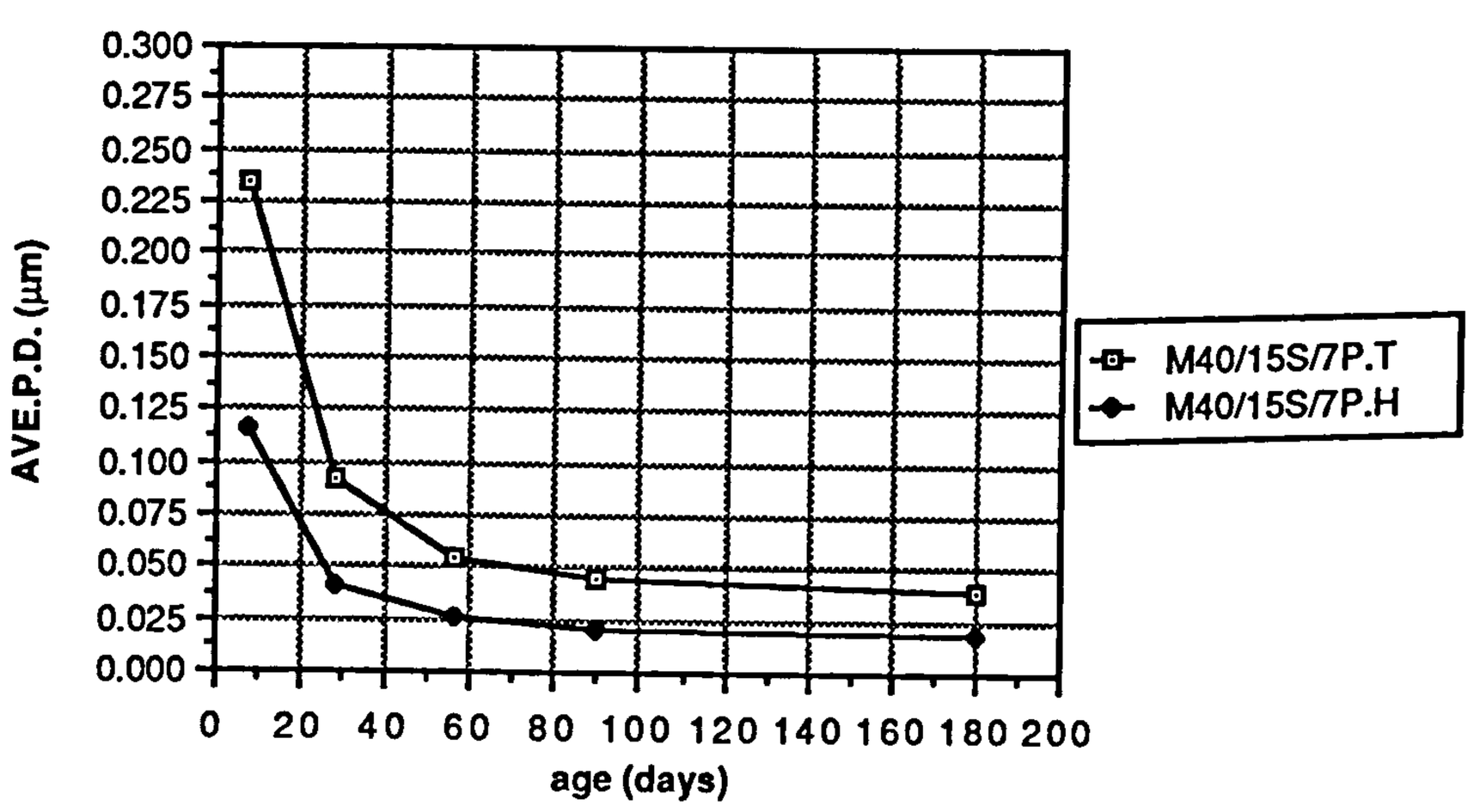

Figure A3.8 Age versus Ave.P.D. relationship of CSF mortars cured in a temperate and hot environment

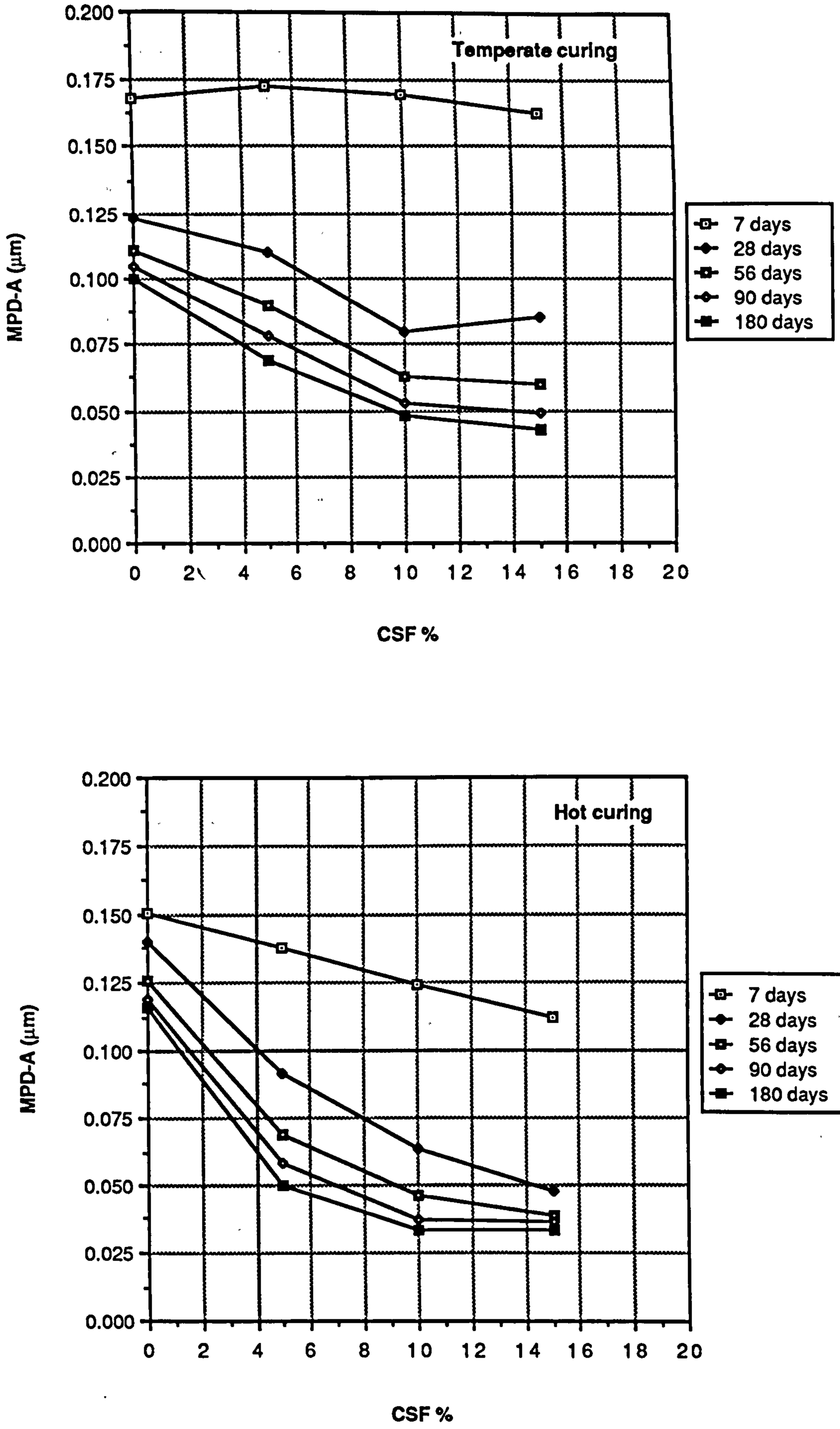

Figure A3.9 Effect of CSF content on the MPD-A of CSF mortars cured in temperate and hot environment

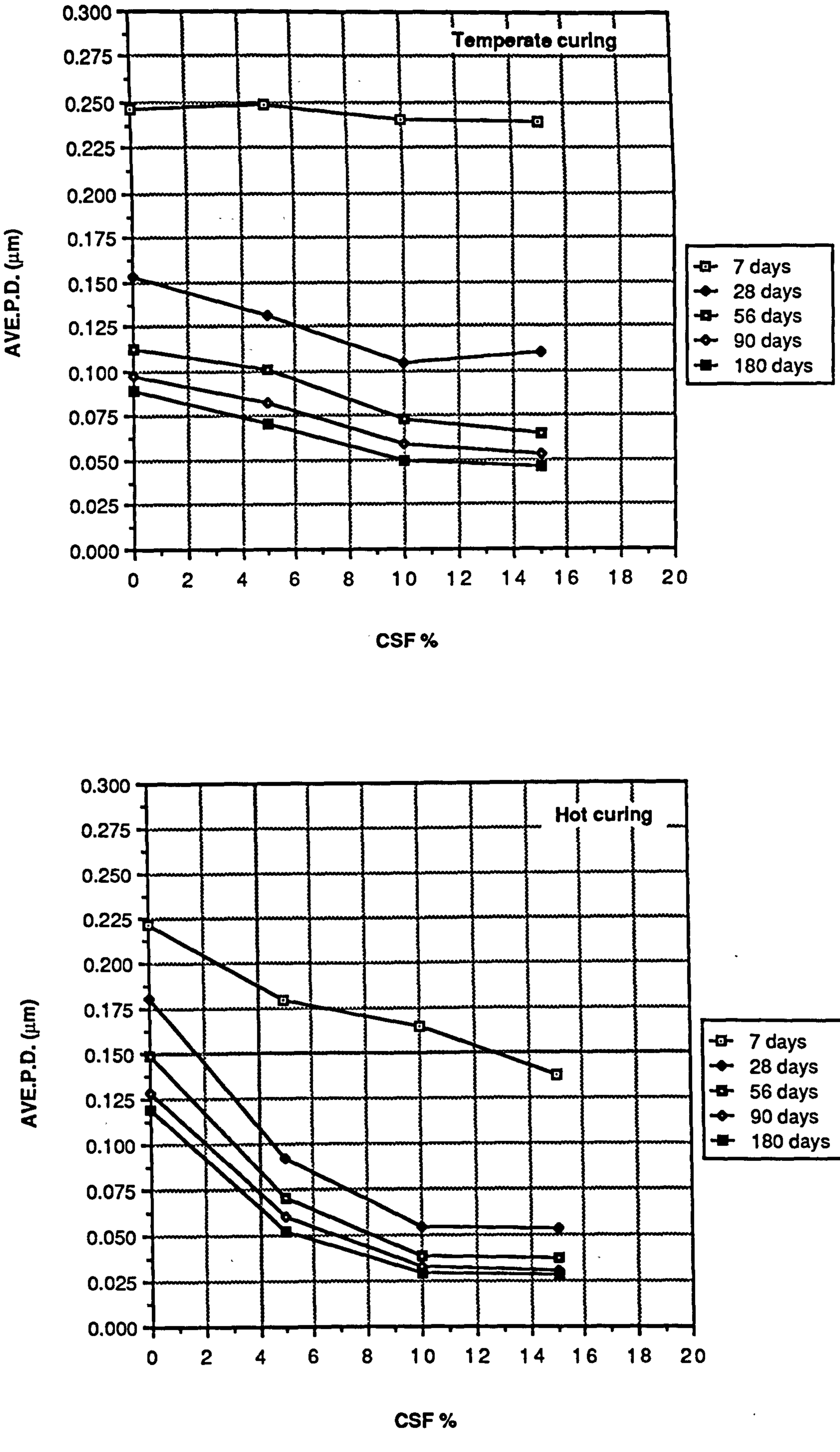

Figure A3.10 Effect of CSF content on the Ave. P.D. of CSF mortars cured in temperate and hot environments

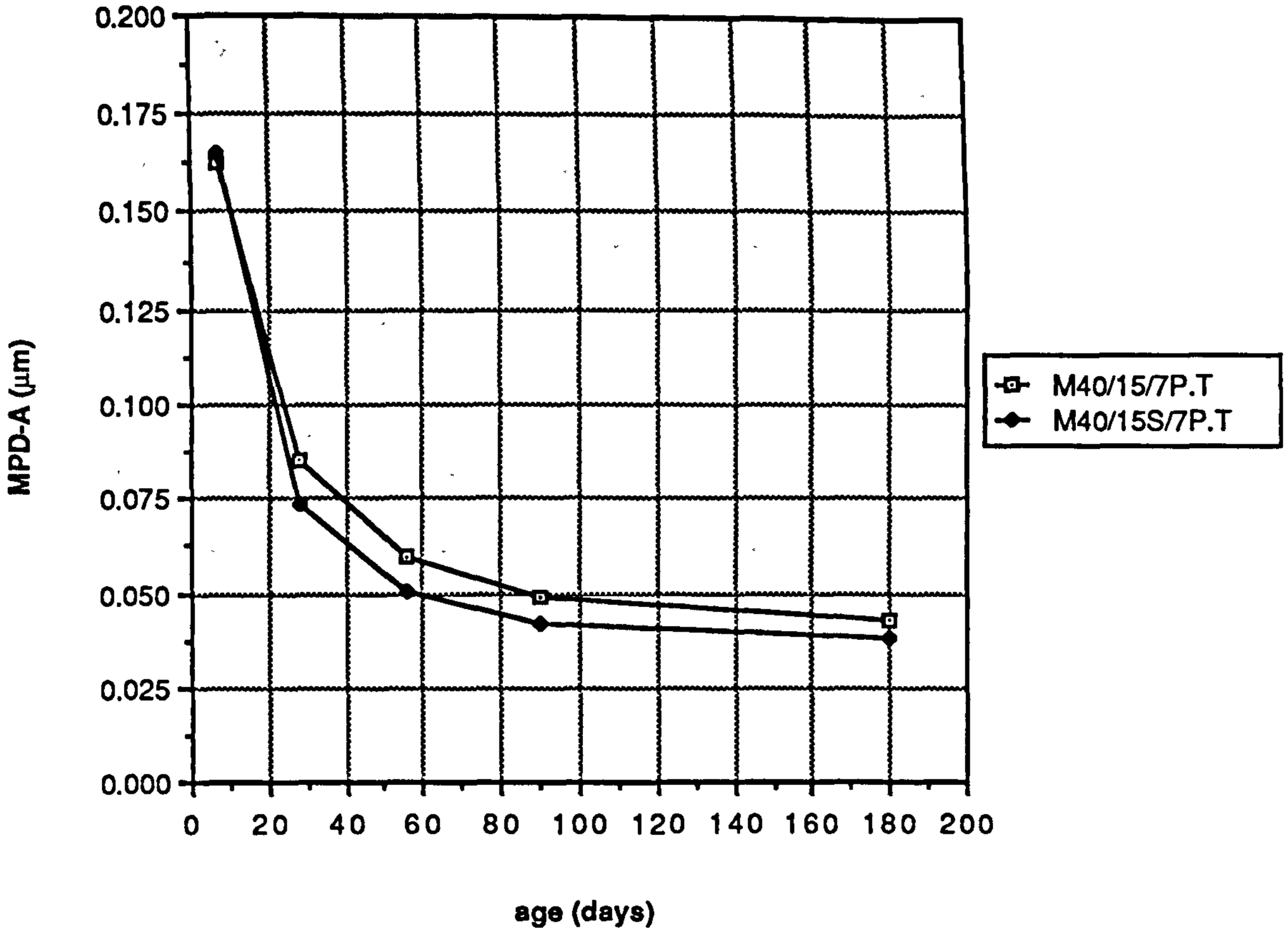

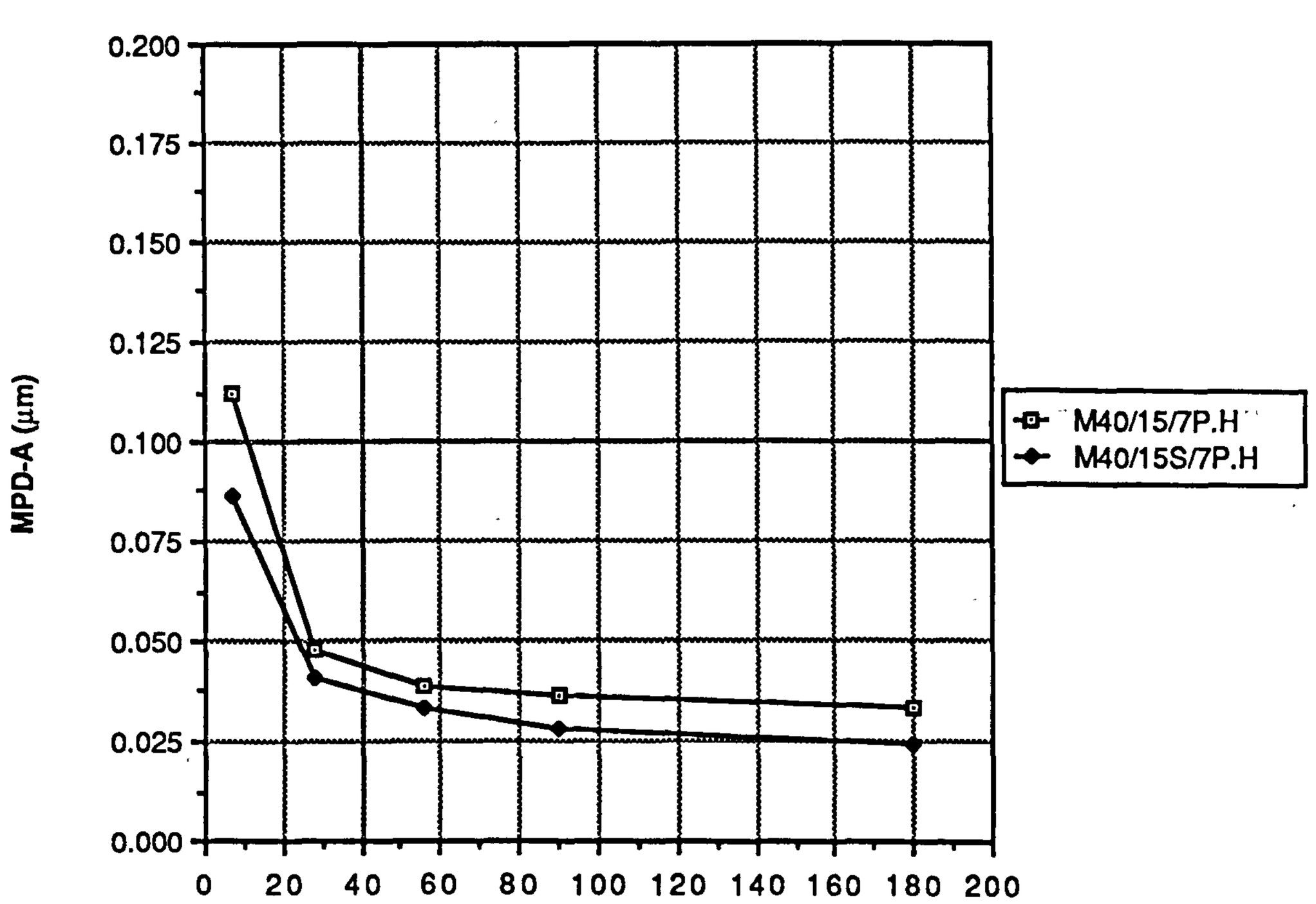

Figure A3.11 Effect of superplasticizer on MPD-A of mortar mix M40/15 cured in temperate and hot environments

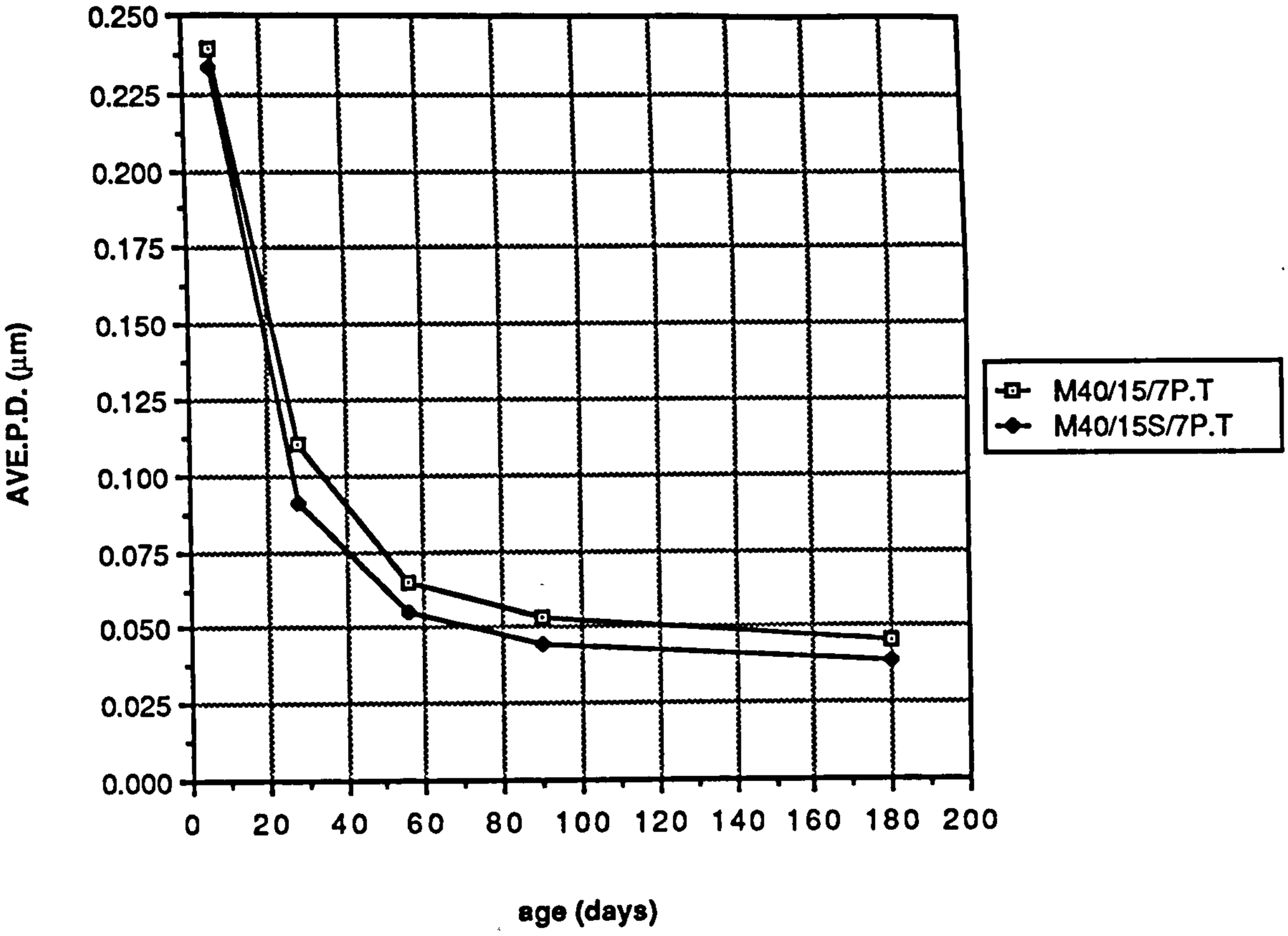

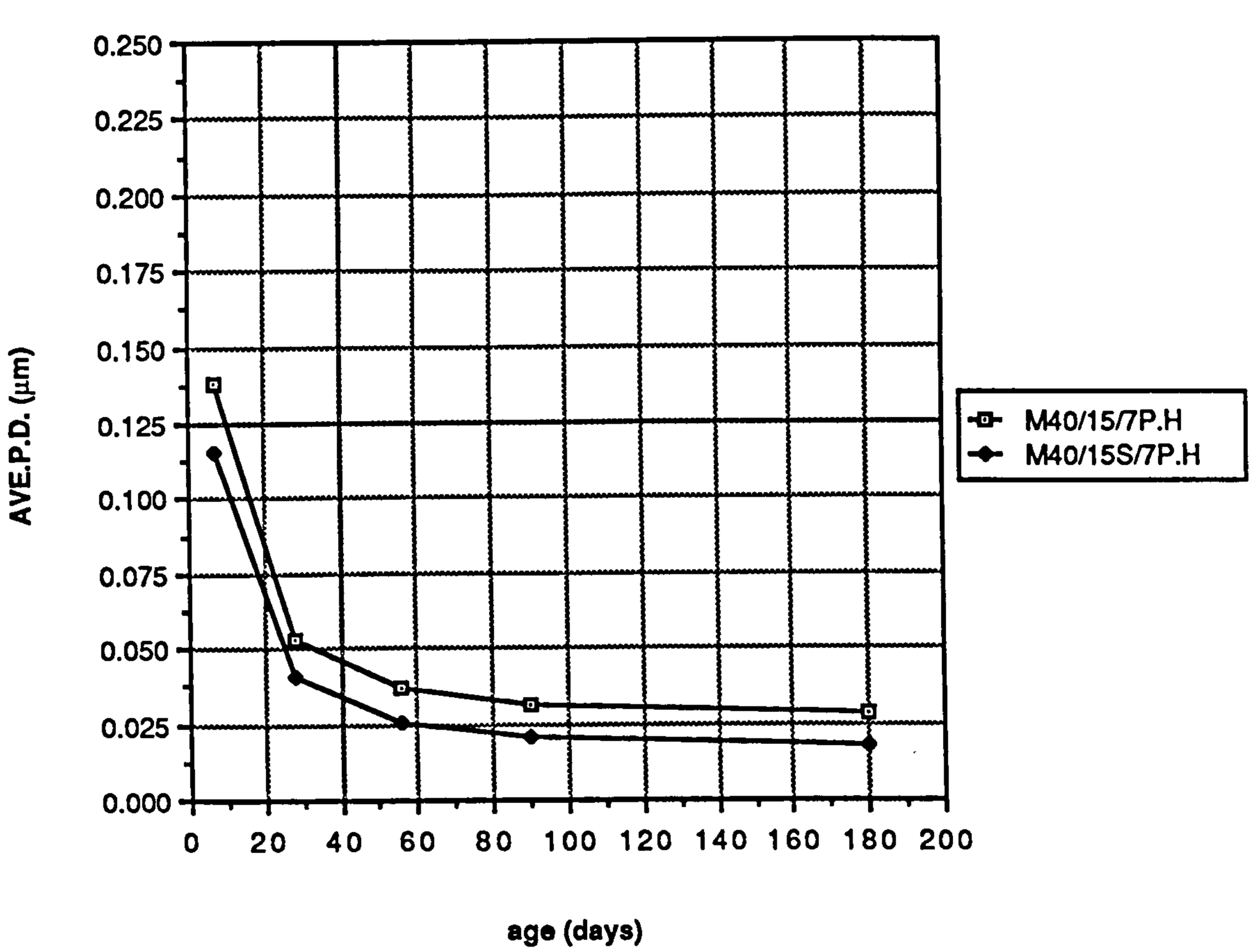

Figure A3.12 Effect of superplasticizer on Ave. P.D. of mortar mix (M40/15) cured in temperate and hot environments

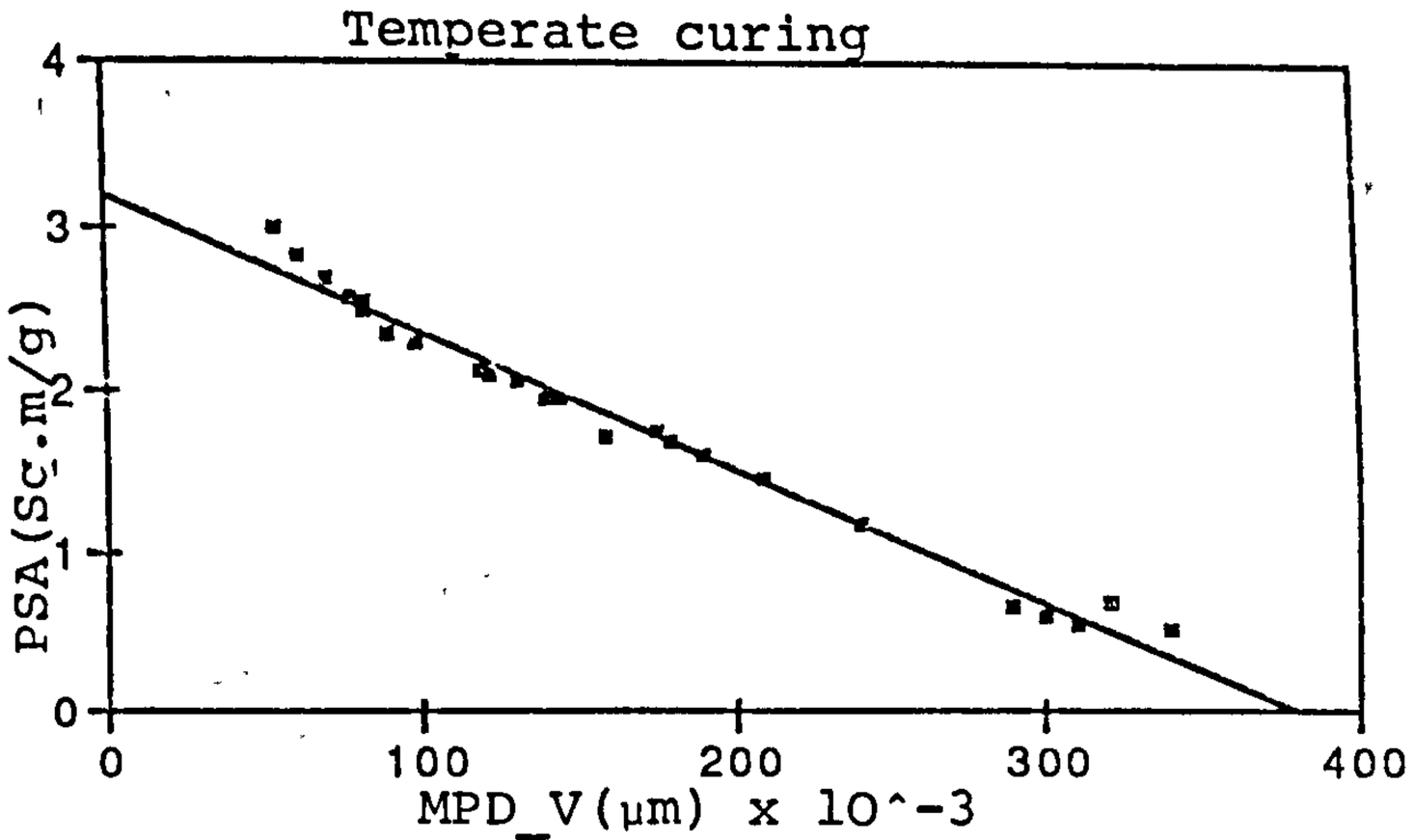

Figure A3.13 Relationship between PSA and MPD_V (temperate curing)

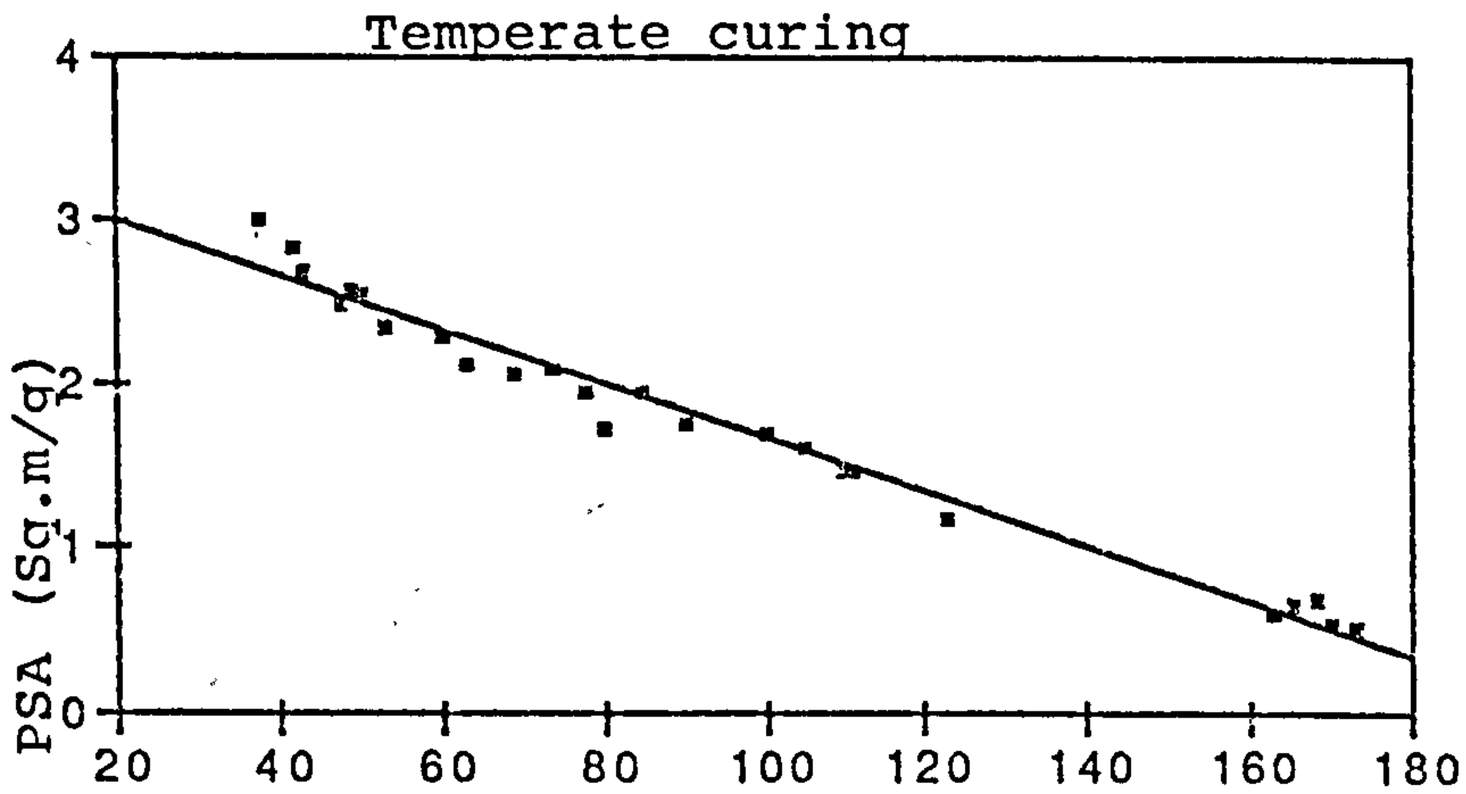

Figure A3.14 Relationship between PSA & MPD_A temperate curing)

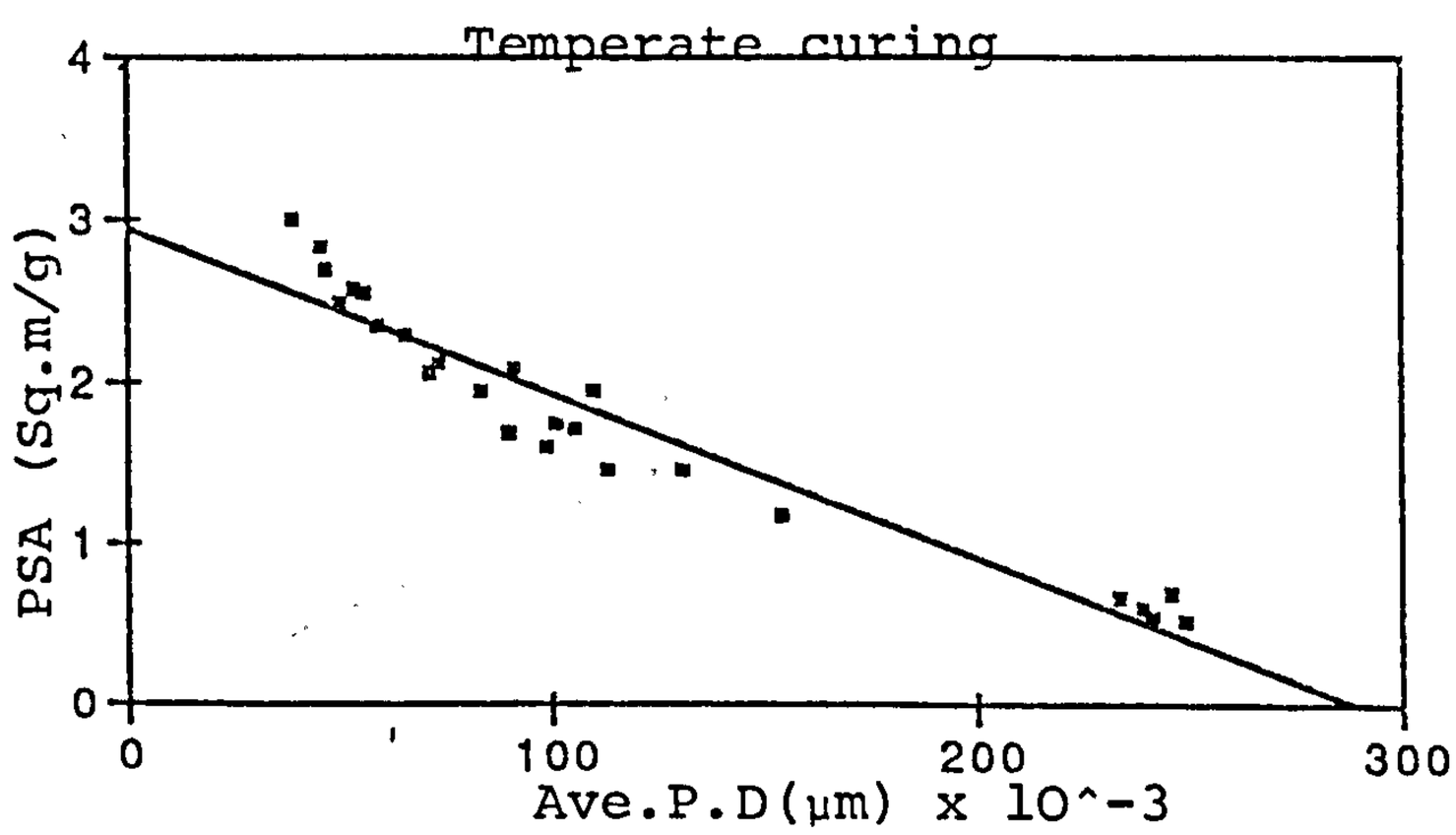

Figure A3.15 Relationship between PSA and Ave.P.D (temperate curing)

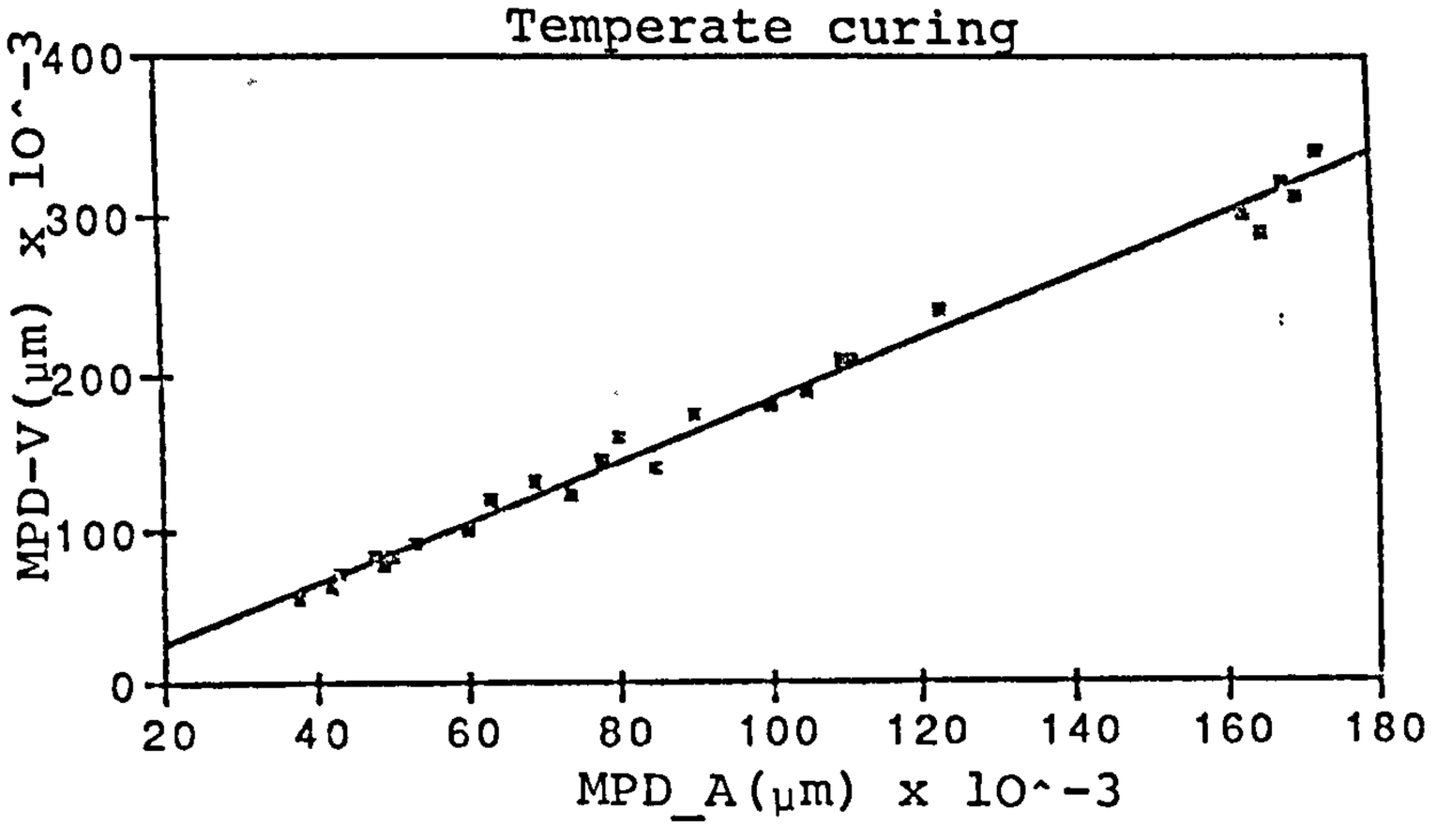

Figure A3.16 Relationship between MPD_V and MPD_A (temperate curing)

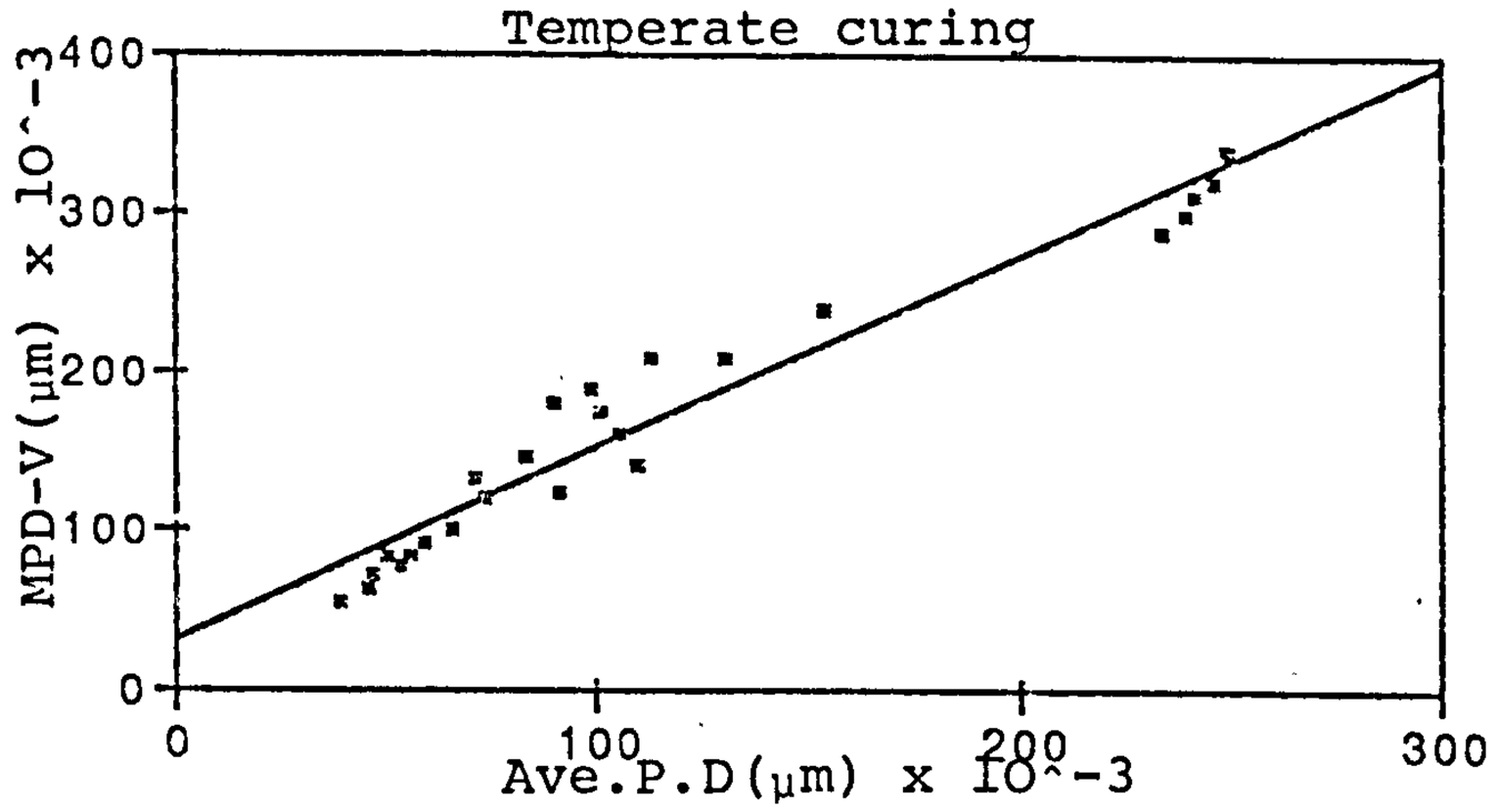

Figure A3.17 Relationship between MPD_V and Ave.P.D(temperate curing)

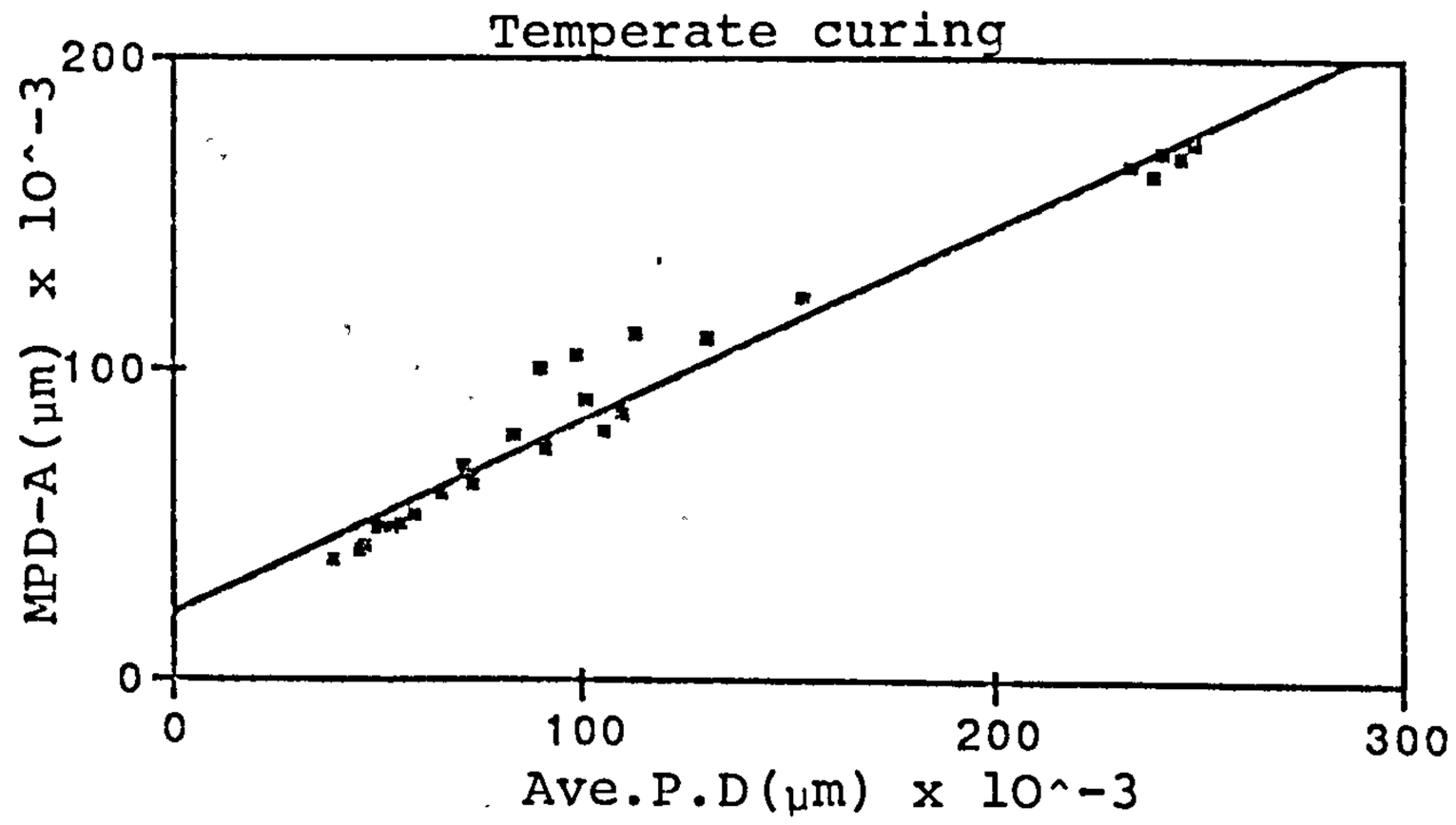

Figure A3.18 Relationship between MPD_A and Ave.P.D (temperate curing)

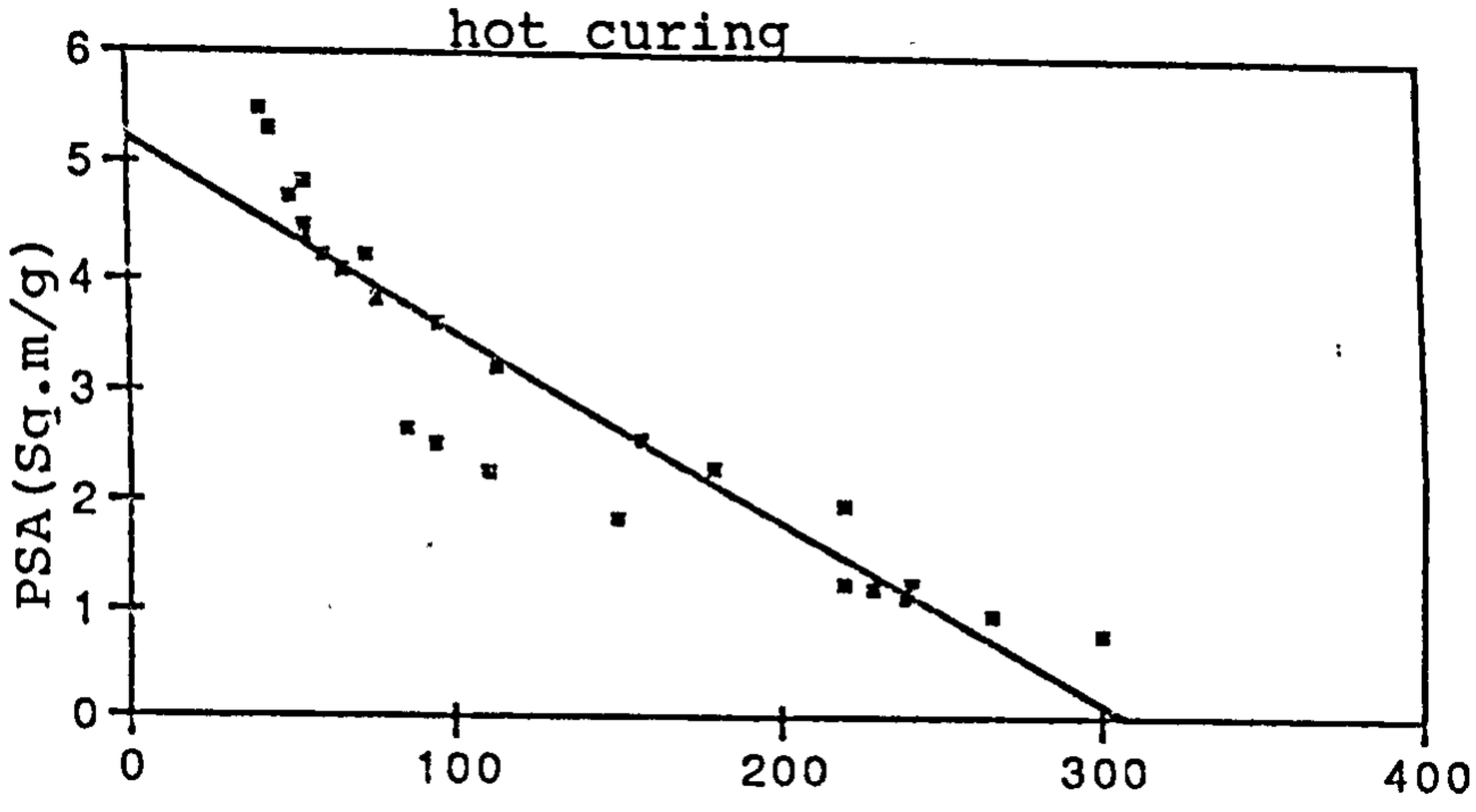

Figure A3.19 Relationship between PSA and MPD-V (hot curing)

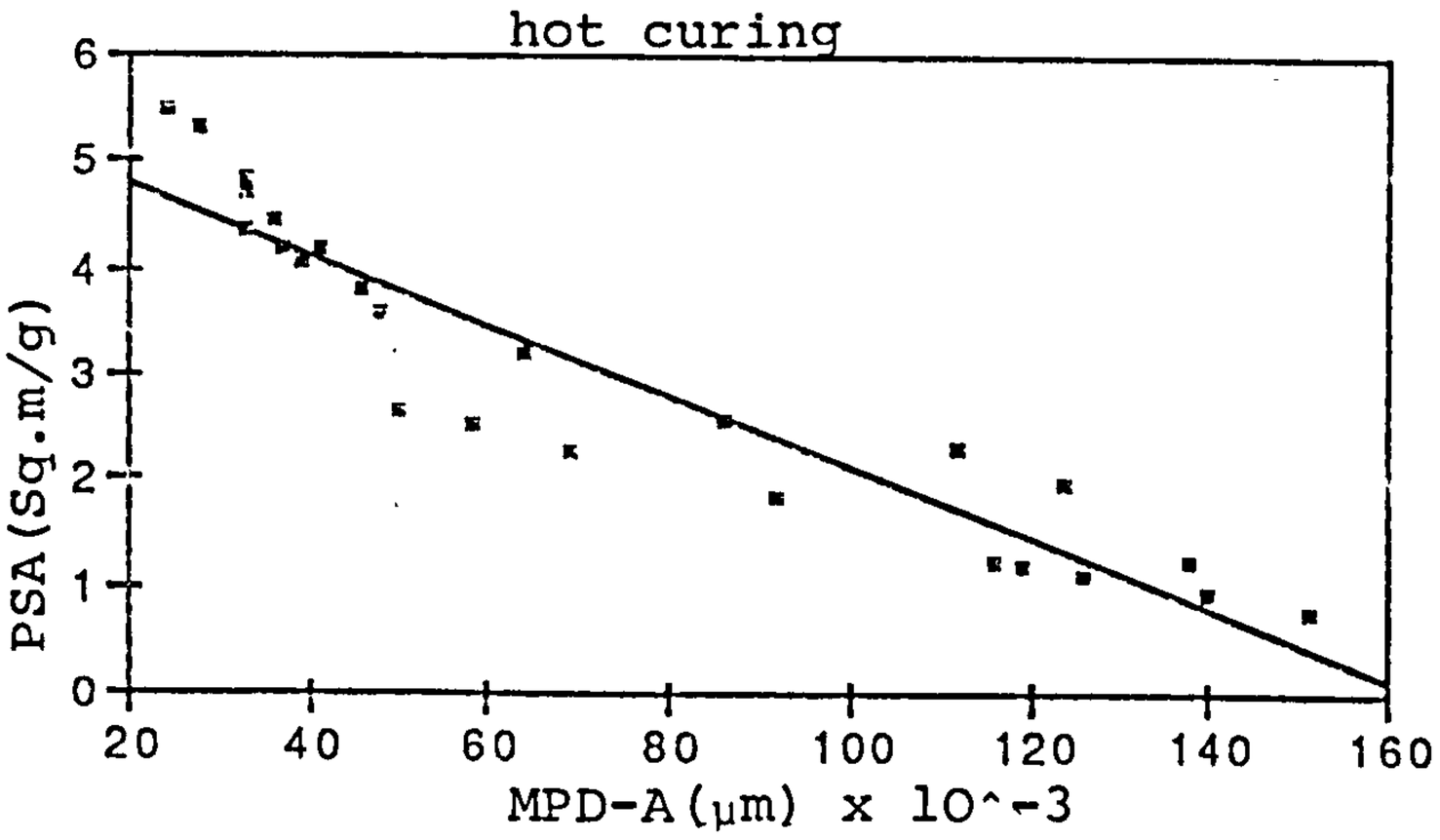

Figure A3.20 Relationship between PSA and MPD-A (hot curing)

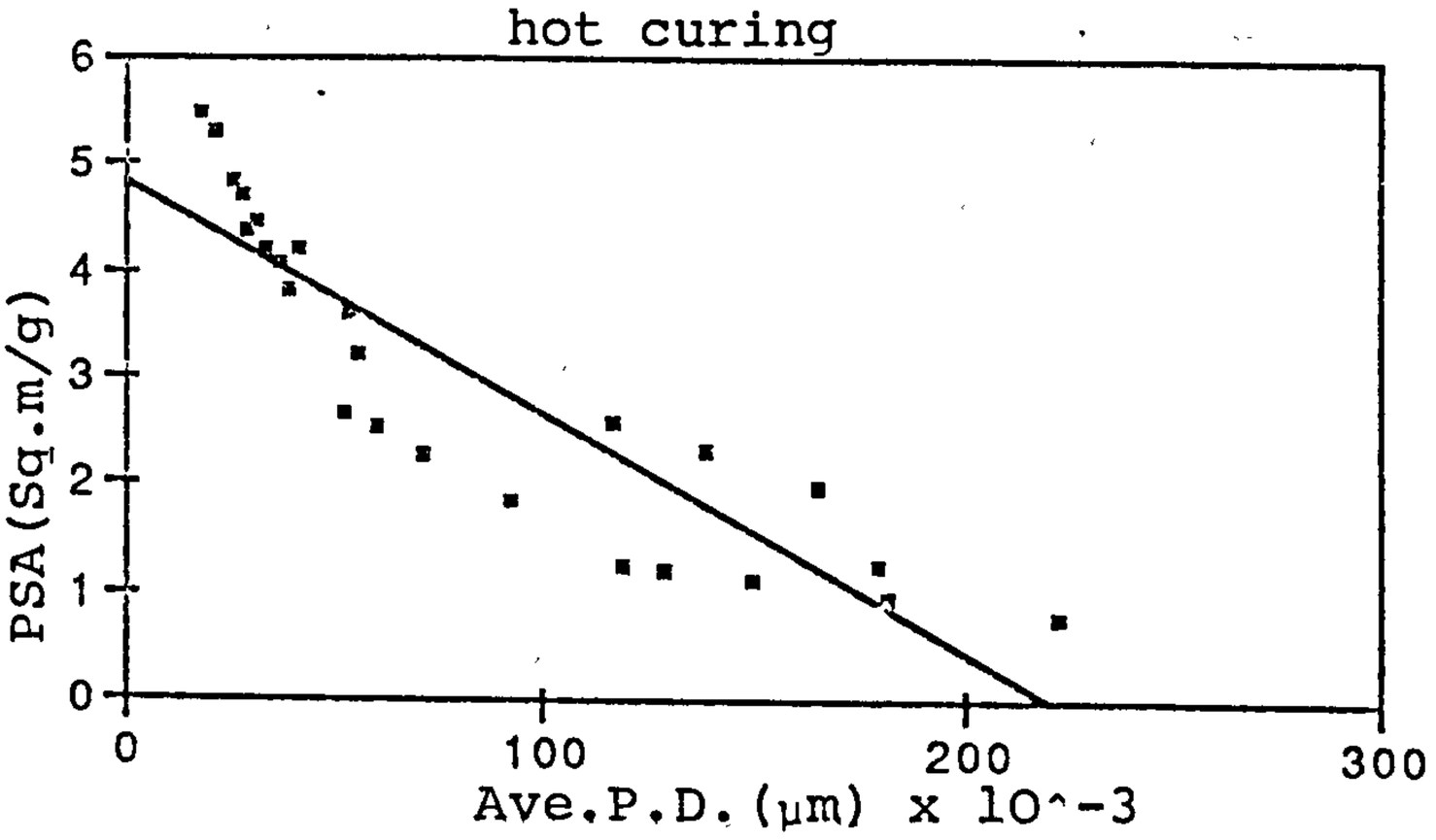

Figure A3.21 Relationship between PSA and Ave.P.D. (hot curing)

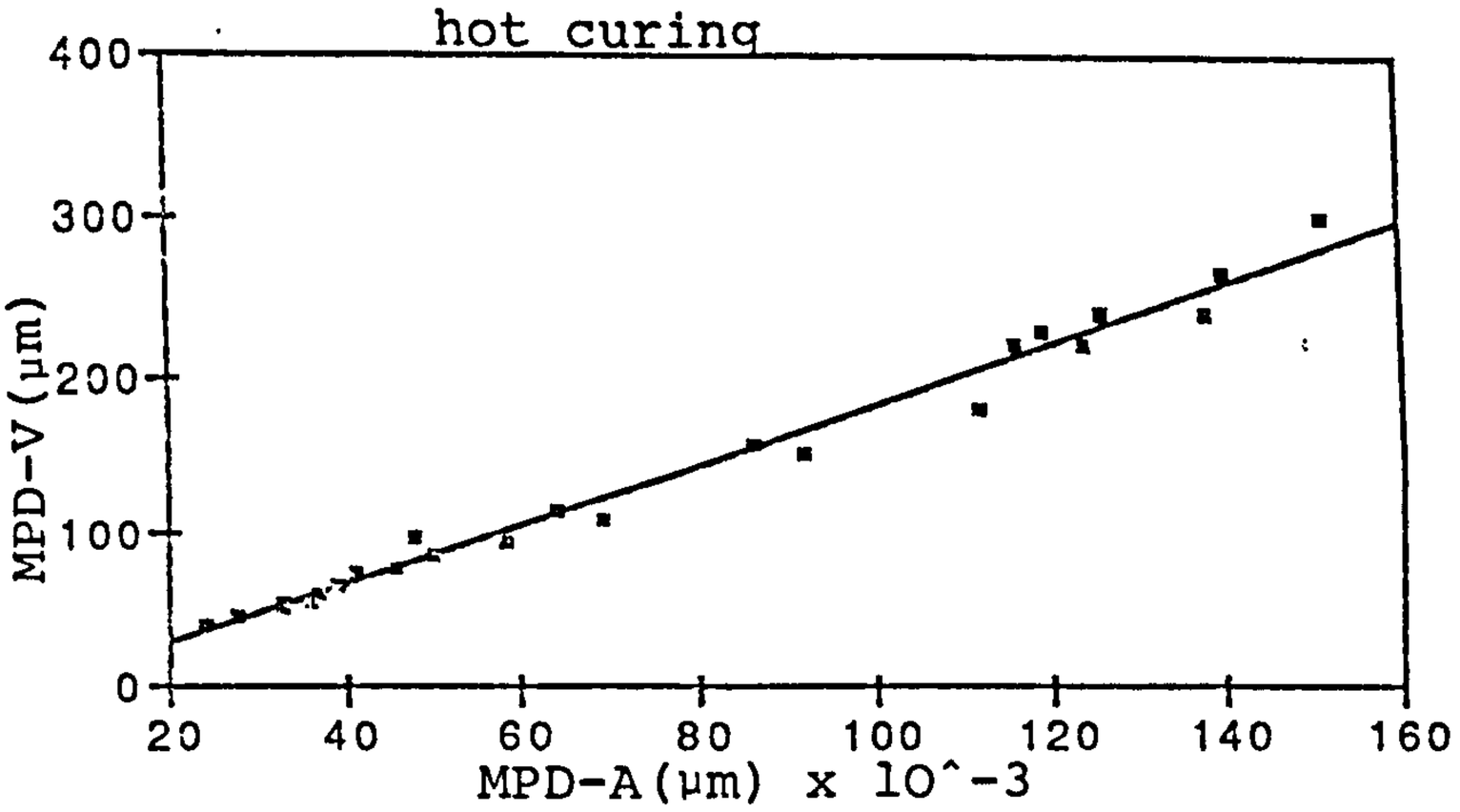

Figure A3.22 Relationship between MPD-V abd MPD-A (hot curing)

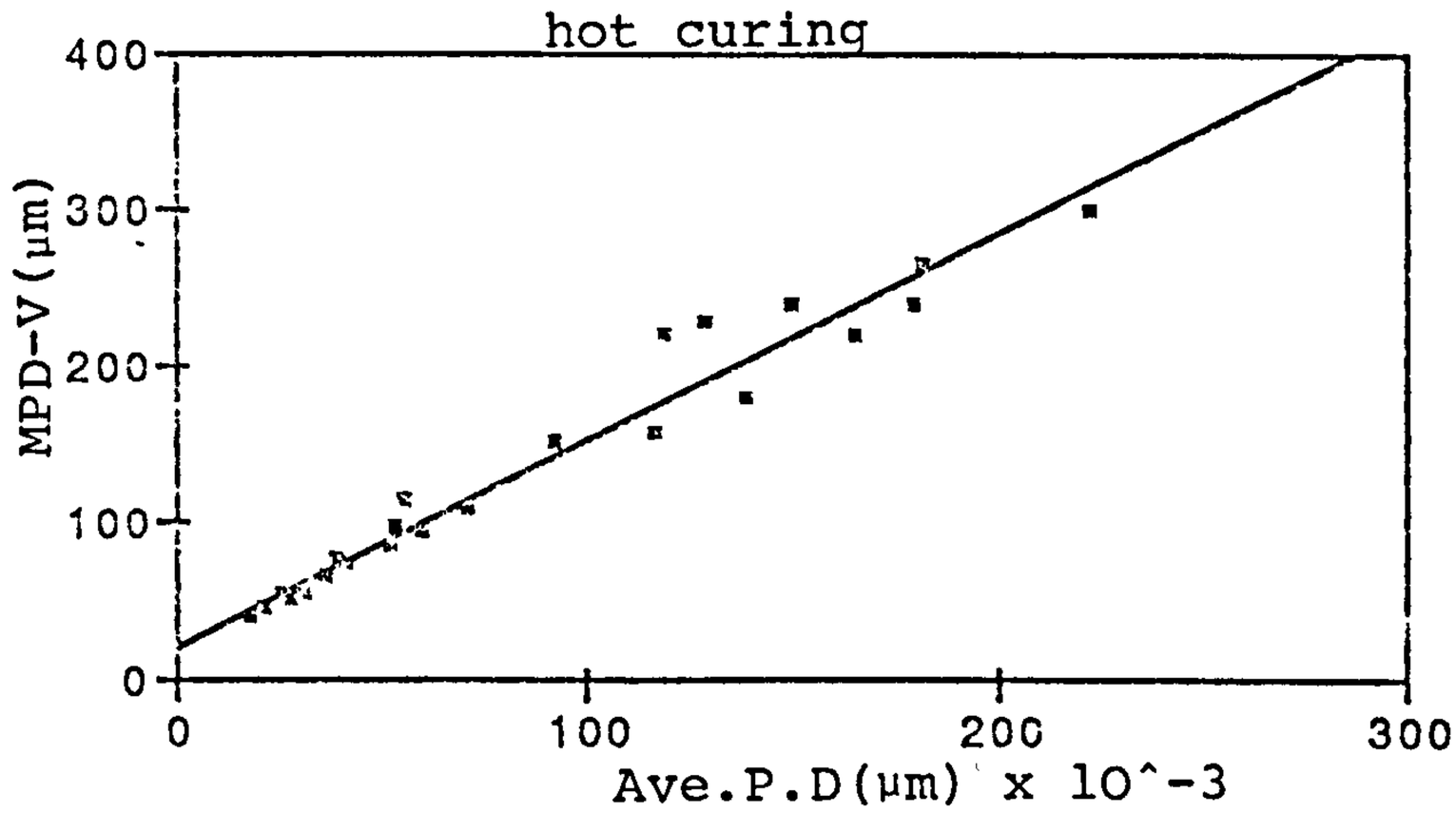

Figure A3.23 Relationship between MPD-V and Ave.P.D (hot curing)

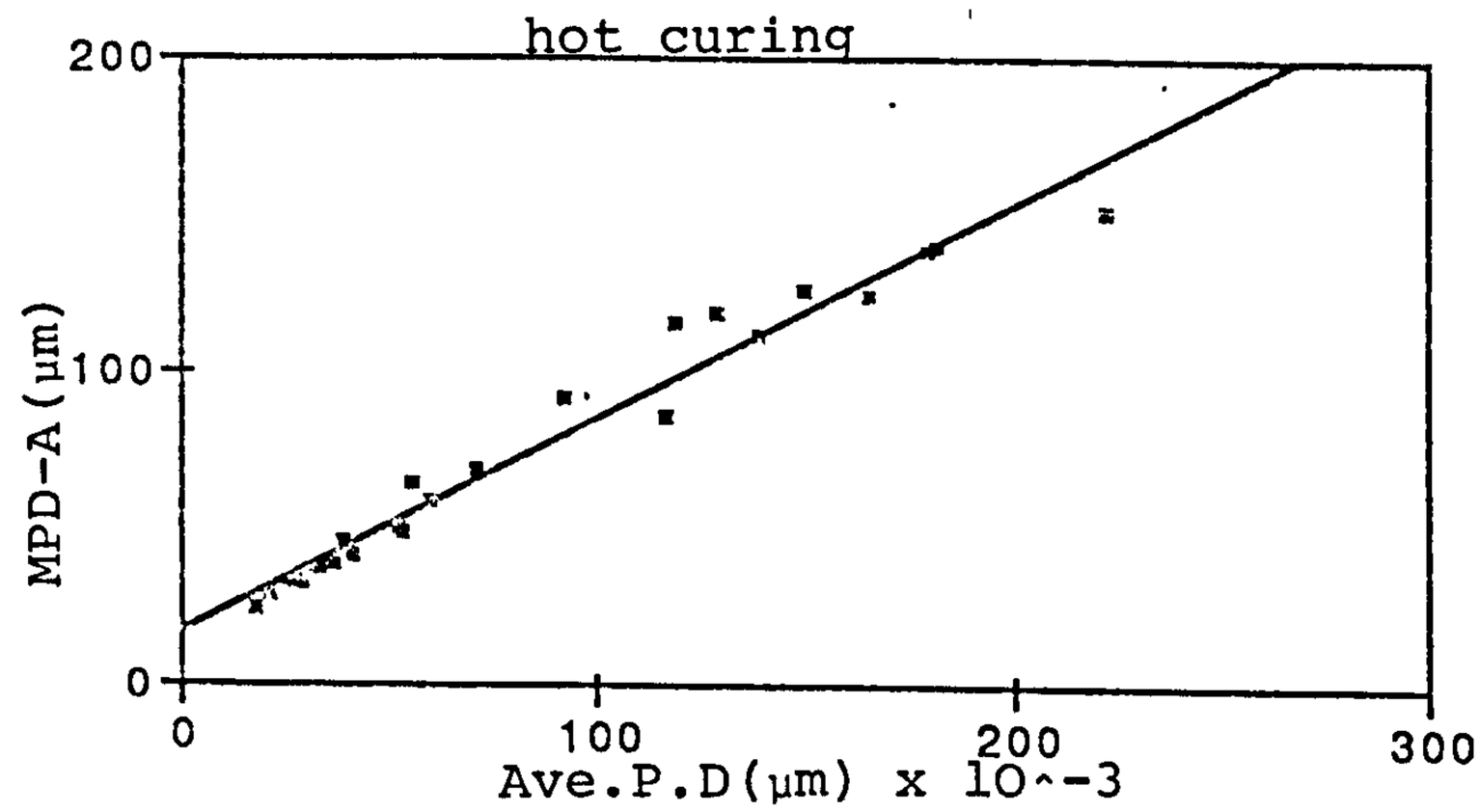

Figure A3.24 Relationship between MPD-A and Ave.P.D (hot curing)